Nanostructure Science and Technology
Series Editor: David J. Lockwood

Ligia Maria Moretto
Kurt Kalcher *Editors*

Environmental Analysis by Electrochemical Sensors and Biosensors

Volume 1: Fundamentals

Springer

Nanostructure Science and Technology

Series Editor:
David J. Lockwood, FRSC
National Research Council of Canada
Ottawa, Ontario, Canada

More information about this series at http://www.springer.com/series/6331

Ligia Maria Moretto • Kurt Kalcher
Editors

Environmental Analysis by Electrochemical Sensors and Biosensors

Fundamentals

Volume 1

Springer

Editors
Ligia Maria Moretto
Department of Molecular Sciences
and Nanosystems
University Ca' Foscari of Venice
Venice, Italy

Kurt Kalcher
Institute of Chemistry
Karl-Franzens Universität
Graz, Austria

ISSN 1571-5744 ISSN 2197-7976 (electronic)
ISBN 978-1-4939-0675-8 ISBN 978-1-4939-0676-5 (eBook)
DOI 10.1007/978-1-4939-0676-5
Springer New York Heidelberg Dordrecht London

Library of Congress Control Number: 2014949384

Printed on acid-free paper

Springer is part of Springer Science+Business Media (www.springer.com)

Foreword

Electrochemical sensors are transforming our lives. From smoke detectors in our homes and workplaces to handheld self-care glucose meters these devices can offer sensitive, selective, reliable, and often cheap measurements for an ever increasing diversity of sensing requirements. The detection and monitoring of environmental analytes is a particularly important and demanding area in which electrochemical sensors and biosensors find growing deployment and where new sensing opportunities and challenges are constantly emerging.

This manual provides up-to-date and highly authoritative overviews of electrochemical sensors and biosensors as applied to environmental targets. The book surveys the entire field of such sensors and covers not only the principles of their design but their practical implementation and application. Of particular value is the organizational structure. The later chapters cover the full range of environmental analytes ensuring the book will be invaluable to environmental scientists as well as analytical chemists.

I predict the book will have a major impact in the area of environmental analysis by highlighting the strengths of existing sensor technology whilst at the same time stimulating further research.

Oxford University
Oxford, UK

Richard G. Compton

Preface

Dear Reader,

We are pleased that you have decided to use *Environmental Analysis* by *Electrochemical Sensors and Biosensors* either as a monograph or as a handbook for your scientific work. The manual comprises two volumes and represents an overview of an intersection of two scientific areas of essential importance: environmental chemistry and electrochemical sensing.

Since the invention of the glass electrode in 1906 by Max Cremer, electrochemical sensors represent the oldest type of chemical sensor and are ubiquitously present in all chemical labs, industries, as well as in many fields of our everyday life. The development of electrochemical sensors exploiting new measuring technologies makes them useful for chemical analysis and characterization of analytes in practically all physical phases - gases, liquids and solids - and in different matrices in industrial, food, biomedical, and enviromental fields. They have become indispensible tools in analytical chemistry for reliable, precise, and inexpensive determination of many compounds, as single shot, repetitive, continuous, or even permanent analytical devices. Environmental analytical chemistry demands highly sensitive, robust, and reliable sensors, able to give fast responses even for analysis in the field and in real time, a requirement which can be fulfilled in many cases only by electrochemical sensing elements.

The idea for this manual was brought to us by Springer. The intention was to build up an introduction and a concise but exhaustive description of the state of the art in scientific and practical work on environmental analysis, focused on electrochemical sensors.

To manage the enormous extent of the topic, the manual is split into two volumes. The first one, covering the basic concepts and fundamentals of both environmental analysis and electrochemcial sensors,

1. gives a short introduction and description of all environments which are subject to monitoring by electrochemical sensors, including extraterrestrial ones, as a particularly interesting and exciting topic;

2. provides essential background information on electroanalytical techniques and fundamental as well as advanced sensor technology;
3. supplies numerous examples of applications along with the concepts and strategies of environmental analysis in all the various spheres of the environment and with the principles and strategies of electrochemical sensor design.

The second volume is more focused on practical applications, mostly complementary to the examples given in volume I, and

1. overviews and critically comments on sensors proposed for the determination of inorganic and organic analytes and pollutants, including emerging contaminants, as well as for the measurement of global parameters of environmental importance;
2. reviews briefly the mathematical background of data evaluation.

We hope that we have succeeded in fulfilling all these objectives by supplying general and specific data as well as thorough background knowledge to make *Environmental Analysis with Electrochemical Sensors and Biosensors* more than a simple handbook but, rather, a desk reference manual.

It is obvious that a compilation of chapters dealing with so many different specialized areas in analytical and environmental chemistry requires the expertise of many scientists. Therefore, in the first place we would like to thank all the contributors to this book for all the time and effort spent in compiling and critically commenting on research, and the data and conclusions derived from it.

Of course, we would like to particularly acknowledge all the people from Springer who have been involved with the process of publication. Our cordial thanks are addressed to Kenneth Howell, who accompanied us during all the primary steps and, later during the process of revision and editing together with Abira Sengupta, was always available and supportive in the most professional and pleasant manner.

Furthermore, we are indebted to a number of our collaborators, colleagues, and friends for kindly providing us literature and ideas, and stimulating us with fruitful discussions. We would also like to thank all the coworkers who did research together with us and under our supervision, as well as all the scientific community working in the field of environmental sensing.

In particular, we would like to express our gratitude to all the persons, especially to our families, who supported us in the period of the preparation of the book.

Last but not least, we will be glad for comments from readers and others interested in this book, since we are aware that some contributions or useful details may have escaped our attention. Such feedback is always welcome and will also be reflected in our future work.

Venice, Italy — Ligia Maria Moretto
Graz, Austria — Kurt Kalcher
December 2013

About the Editors

Ligia Maria Moretto graduated in Chemical Engineering at the Federal University of Rio Grande do Sul, Brazil, and received her Ph.D. in 1994 from the University Ca' Foscari of Venice with a thesis entitled "Ion-exchange voltammetry for the determination of copper and mercury. Application to seawater." Her academic career began at the University of Caxias do Sul, Brazil, and continued at the Research Institute of Nuclear Energy, Sao Paulo, Brazil. In 1996 she completed the habilitation as researcher in analytical chemistry at the University Ca' Foscari of Venice. Working at the Laboratory of Electrochemical Sensors, her research field has been the development of electrochemical sensor and biosensors based on modified electrodes, the study of gold arrays and ensembles of nanoelectrodes, with particular attention to environmental applications. She has published more than 60 papers, several book chapters, and has presented about 90 contributions at international conferences, resulting in more than 1,100 citations. Prof. Moretto collaborates as invited professor and invited researcher with several institutions in Brazil, France, Argentina, Canada, and the USA.

Kurt Kalcher completed his studies at the Karl-Franzens University (KFU) with a dissertation in inorganic chemistry entitled "Contributions to the Chemistry of Cyantrichloride, CINCCI2"; he also received his Ph.D. in 1980 from the same institution. In 1981 he then did postdoctoral work at the Nuclear Research Center in Jülich (Germany) under the supervision of Prof. Nürnberg and Dr. Valenta, and conducted intensive electroanalytical research while he was there. Prof. Kalcher continued his academic career at KFU with his habilitation on chemically modified carbon paste electrodes in analytical chemistry in 1988. Since then, he has been employed there as an associate professor. His research interests include the development of electrochemical sensors and biosensors for the determination of inorganic and biological analytes on the basis of carbon paste, screen-printed carbon,

and boron-doped diamond electrodes, as well as design, automation, and data handling with small analytical devices using microprocessors. He has published around 200 papers and has presented about 200 contributions at international conferences. These activities have resulted in more than 3,100 citations. Prof. Kalcher has received numerous guest professor position offers in Bosnia-Herzegovina, Poland, Slovenia, and Thailand.

Contents of Volume 1

Contents of Volume 2

Part I
Environmental Analysis

Chapter 1
Introduction to Electroanalysis of Environmental Samples

Ivan Švancara and Kurt Kalcher

1.1 Electroanalysis

For lengthy decades, electroanalysis represents the largest area of applied electrochemistry, involving measurements of the electric signals associated with the behaviour and/or transformations of charged species in the solution. From traditional point of view, electroanalysis can be classified as a special area of electrochemistry which is primarily focused on the determination (quantification) of chemical substance(s) in a sample, but also on qualitative characterisation—i.e., identification.

Historically, one can find the first pioneering attempts with potentiostatic electrolysis/electrogravimetry that can be considered as analytical applications within some revolutionary electrochemical experiments (see examples in reference (1)); nevertheless, real electroanalysis began in the first half of the twentieth century with the development of potentiometric and amperometric analytical methods characterized by milestones such as design and physicochemical interpretation of the first real electrochemical sensor, the glass electrode by Cremer and Haber[2,3] and Heyrovský's invention of polarography.[4,5] The latter had launched a tremendous development of techniques with modulated potential ramps,[6–8] followed by invention of the highly effective electrochemical stripping analysis[9,10] and its further extension to the time-dependent potentiometric mode.[11] A wide application of the methods to environmental, pharmaceutical, and medical analyses resulted

I. Švancara (✉)
Department of Analytical Chemistry, Faculty of Chemical Technology, University of Pardubice, CZ-532 10, Pardubice, Czech Republic
e-mail: Ivan.Svancara@upce.cz

K. Kalcher
Institute of Chemistry—Analytical Chemistry, Karl-Franzens-University of Graz, Universitaetsplatz 1, 3000, Graz, Austria
e-mail: kurt.kalcher@uni-graz.at

L.M. Moretto, K. Kalcher (eds.), *Environmental Analysis by Electrochemical Sensors and Biosensors*, DOI 10.1007/978-1-4939-0676-5_1

accompanied by coupling electroanalytical devices to flow systems (amperometric or coulometric detection)[12,13] that contributed to the expansion of electrochemical principles into the realm of analytical separations.

In parallel with these current flow-based measurements (equilibrium) potentiometry held an important position,[14] particularly after introduction of all the various types of ion-sensitive membranes whereas conductometry, oscillometry, and dielectrometry[15] were an occasional choice and nearly the same can be said about some other measurements (e.g. biamperometry and bipotentiometry,[16] chronoamperometry and chronopotentiometry[17]). In the last half century, other techniques were proposed, such as sonovoltammetry,[18] electrochemical impedance spectroscopy (EIS[19]), electrochemiluminescence,[20] spectroelectrochemistry,[21] and scanning electrochemical microscopy (SECM[22]).

Similar to other fields of instrumental analysis, the development and expansion of both electrochemistry and electroanalysis is tightly associated with the progress in instrumentation; some apparatuses over the years are depicted in Fig. 1.1. The first automated electroanalytical analyzer, a polarograph constructed by Heyrovsky and Shikata,[24] was practically also the first automatic analytical device at all. With the rapid technical development after the WW II, various devices had appeared on the market which allowed comfortable voltammetric and potentiometric analyses with a high degree of automatization; companies worth to mention in this context are Tacussel in France, Princeton Applied Research (PAR, later part of EG&G) and Orion in the US, Metrohm in Switzerland and Radiometer in Denmark (see Fig. 1.1c). The first commercial whole blood glucose analyzer was introduced in the US by Yellow Springs Instruments in 1975, it was the legendary Yellow Springs Glucose Analyzer Model 23A based on the first biosensor developed by Leland "Lee" Clark.[25] Nowadays there is the trend for miniaturisation on one hand, as demonstrated by hand-held devices produced by PalmSens or DropSens; on the other we find sophisticated desktop instruments offering the whole landscape of electrochemical techniques such as AutoLab (Metrohm) or BASi (Bioanalytical Systems Inc.) analyzers.

With respect to electrodes potentiometry started with the glass electrode from Cremer in 1906[2]; starting in the 1960s the development of polymer-based membranes had a strong impact on the popularity of ion-sensitive electrodes.

Mercury was the dominant electrode material for current-based measurements in the first half of the twentieth century, which has eventually changed during its second half ending up in some kind of mercuryphobia. Nevertheless, other materials came to the fore as a consequence, such as graphite, glassy carbon, gold plus some other precious metals, and newly also bismuth.

A milestone was the invention of carbon paste by Ralph "Buzz" Adams in 1958,[26] which favoured, due to its heterogeneous paste-like composition, simple and multiple modification of the electrode material even with labile biological components. The first amperometric sensor, the famous "Clark oxygen electrode" was described in by Leland Clark 1954.[27] Currently, new substances have a primary position in electrochemical literature, such as boron-doped diamond or nanostructured materials.

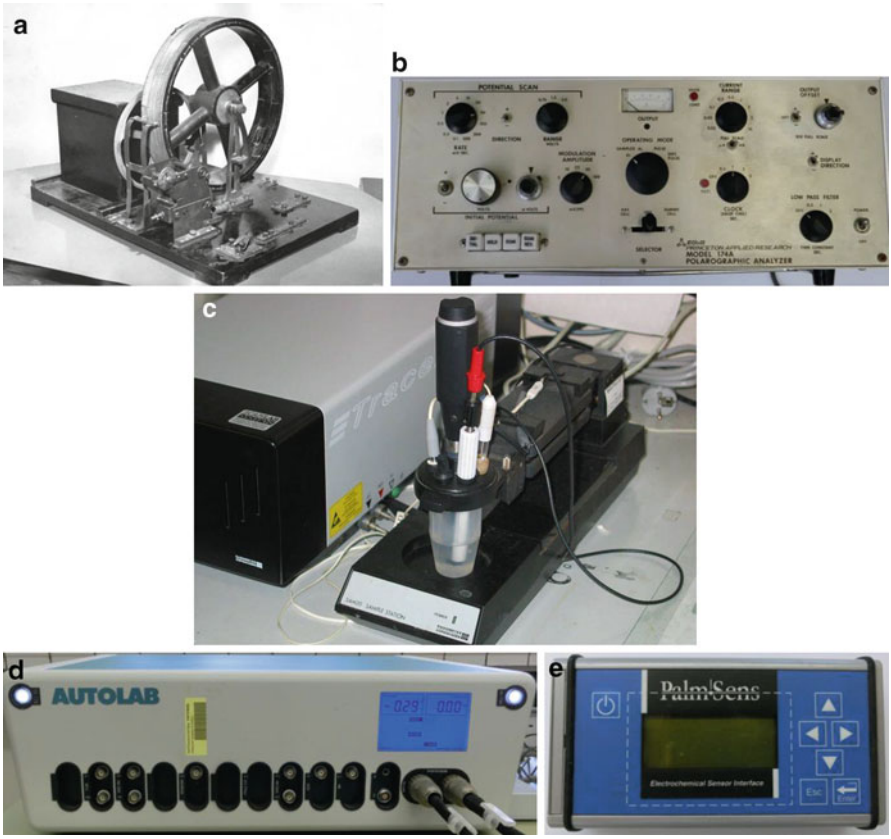

Fig. 1.1 Potentiostat: Original polarographic analyzer by Heyrovský (**a**); Princeton Applied Research Model 164 (**b**); Radiometer TraceLab PSU unit with the electrode stand (**c**); AutoLab Model PSTAT (**d**); handheld device PalmSens (**e**). Photo (**a**) reproduced from reference (23) with permission of Prof. Z. Samec, Heyrovsky Institute, Prague, Czech Republic, photos (**b–e**) by the authors (K. Kalcher and I. Švancara)

1.2 A Glance into Electroanalytical Literature

The extent of electrochemical literature, apart from publications in scientific journals, is very wide, meaning that any surveys or suggestions to be made are always arbitrary and incomplete. Within such a selection,[5,13,16,19,21,22,28–66] one can find extensive book series,[37,40,49] chapters in encyclopedic literature (e.g. reference (33)), fundamental and general textbooks (e.g. references (5, 29, 35, 46–48, 53)), practical guides,[38–41,52,54] and monographs focused on instrumentation,[44,45] electrodes,[5,32,66] analyses[41,55,58] and techniques,[13,16,39,43,51] including new disciplines[11,19,22]. Whereas most of books listed still are available worldwide (e.g. references (29, 35, 45, 66)), other issues and releases have more regional or local character.[56–65]

1.3 Electroanalysis in a Flash

As each field of instrumental analysis, also electrochemical measurements can be evaluated via the respective possibilities and limitations, without need of going into specific details.

1.3.1 Advantages

- Long tradition and highly elaborated theoretical background.
- Relatively simple and inexpensive instrumentation.
- Generally low investment and operational costs.
- High level of diversity in modifying the instrumentation (including electrodes) for special purposes.
- Wide flexibility in practical analysis (of inorganic ions, complexes and molecules, organic substances as well as biologically important compounds, including some microorganisms).
- Excellent performance in trace analysis (high selectivity, extraordinary detection characteristics).
- Applicability in speciation and differentiation analysis.
- Suitable as reference technique/method in evaluations of new procedures for routine analysis.
- Adaptability for field monitoring and similar outdoor employment.
- Good premises for miniaturisation and compatibility with PC controlled systems.
- Wide applicability of new technologies.
- Good compatibility with other analytical instrumentation (detection in flow injection analysis (FIA), high performance liquid chromatography (HPLC), and capillary electrophoresis (CE); combinations with optical and microscopic techniques).
- Adaptability to the principles of green analytical chemistry.
- Widely accessible educational tool for training and practicing of young analysts.

1.3.2 Drawbacks

- Relatively high knowledge required to understand principles and techniques, as well as to interpret data.
- High susceptibility to matrix influences.
- Limited stability of detection/sensing units, requiring frequent (re)calibration.
- Complicated and time-consuming regeneration of some electrodes and detectors.

– Wide diversity of electrode materials, modifiers, and detection techniques differing principally in the properties and performance, thus needing certain orientation.
– Discontinuity of measurement if low detection limits are required (typically, in stripping analysis with pre-concentration).
– Limited application to multicomponent analyses.
– Frequent use of toxic and harmful materials or reagents.
– Particular need for well-trained operators/users.

Amongst electroanalysts, some points gathered in the above-given Pros & Cons—and, especially, those described as disadvantages—may induce certain displeasure. It is quite natural, but the authors of this text have compiled both surveys carefully and being fully convinced about usefulness of such confrontation. Because even an incidental polemics about the individual points seems to be beneficial as it would indicate mainly the liveliness of the field that successfully "struggles for lengthy decades" with other instrumental techniques.

1.4 Electrochemistry and Environmental Analysis

1.4.1 History and Present

First environmental focused analyses can surely be found already within the early era of electrochemical measurements (see references (29, 38–40, 43) and references therein); nevertheless, a more systematic orientation towards the environmental samples began later, in the early 1970s of the twentieth century. In this context, the most renowned groups (or even schools) were the teams of H.W. Nürnberg and P. Valenta in Juelich (Germany) and M. Branica in Zagreb (Croatia). Later S. Van den Berg's group in Great Britain performed extensive—and, in overall scope, unprecedented—marine environmental research, resulting, among others, in a wide palette of ultimate methods for the determination of various metals and metallic species in sea water (e.g., references (67–69) and references therein).

Of similar focus was the scientific interest of the Australian electrochemist T.M. Florence,[70] also known as the inventor of the in-situ plated mercury film electrode, MFE,[71] and of his successor, A.M. Bond.[72,73] In the U.S., the use of stripping voltammetry in environmental analysis and modern trends in electrochemical instrumentation as such were widely popularised by Joseph "Joe" Wang[74–76] whose legendary monograph from the mid-1980s[28] still belongs amongst the top texts in the field. Traditionally strong electrochemistry in the former U.S.S.R also included some scientists active in environmental analysis, such as Kh. Z. Brainina's group.[77,78]

In Europe, H.W. Nürnberg[79,80] had, together with M. Stoeppler,[81] promoted the establishment of a special multidisciplinary project, the "Environmental Specimen Bank (ESB)". Logistically and materially, the ESB program was realised in Juelich

Fig. 1.2 Institute of Applied Physical Chemistry, the Reseach Centre Juelich, in the mid-1990s: Environmental Specimen Bank (E.S.B.) in the front, research labs and offices in the back [photo by the author (I. Svancara)]

(Nord-Rhine Westphalia; see also Fig. 1.2) as a systematic collection of representative environmental samples, their long-time storage (for future generations), and regular control analyses with the aid of AAS, neutron activation analysis, isotope dilution-mass spectrometry, ion chromatography, and electrochemical techniques.

Stripping analysis was used to determine selected metals and metalloids; namely: Zn, Cd, Pb, Cu, Tl, Ni, Co, As, and Se, by employing ASV, AdSV, PSA, or CCSA (see references (82, 83) and references therein).

Nowadays, globally seen, many scientific teams and individuals focus research on environmental analysis, such as in western,[84–99] southern,[100–104] northern[11,98] and middle Europe including countries of former Yugoslavia. [33,51,105–116] In North America, notable activities can be seen across the U.S.A., opening a number of new attractive applications, thanks to a wide employment of chemically modified electrodes,[74,75,117] special flow systems for air analysis (e.g. reference (118)), or decentralised monitoring with portable analysers.[119–122] Interesting applications can be traced up in Latin America; just to pick out a few of the many examples: determination of electrochemically inert Li^+ ions,[123] highly sensitive detection of Hg^{II} at a gold layer-based detector made of a recordable compact disc,[124] or unusual electroanalysis of non-aqueous samples of crude oil.[125]

Also in Africa, some representatives are involved in environmental analysis,[126,127] and the same can be said about the Near[128–130] and the Far East,[131–138]

where the leading position is naturally held by highly populated China (see e.g. reference (131) and references therein).

1.4.2 Main Topics

Undoubtedly, a discipline that includes the identification, quantification, and monitoring of various species in the environment is also one of the largest areas of electroanalysis (see e.g. references (28, 58, 67–83, 99, 119–122, 131, 139–176))

The key topics in environmental analysis and therefore also in electrochemical environmental analysis as can be seen by corresponding review articles in the literature are, apart from certain necessities, also subject to trends and collective behaviours (see e.g. references (68, 70, 75, 77, 81, 140–146) and references therein). In the following survey the most important analytes are summarised:

- *Toxic heavy metals* (mainly Cd, Pb, Cu, and Hg); usually at very low concentration levels and determined by methods of trace analysis, occasionally also with the aid of speciation analysis (e.g.: Cu^{2+} and $[Cu(OH)_m]^{(m-n)-}$, Hg^{2+} and $[HgCl_m]^{(m-n)-}$ or Hg^{II} and Hg-CH_3^+).
- *Metals of strategic importance* (Co, Ni, V, Mn, Cr, Mo, U); in wide concentration ranges, often, in complex matrices of waste waters or originally solid materials; studied due to the occurrence at different valence (Co^{II} vs. Co^{III}, Mn^{II} vs. Mn^{VII}, Cr^{III} vs. Cr^{VI} etc.).
- *Highly toxic metals with less common occurrence* (Tl, In, Ge, Be); monitored mainly in heavily polluted industrial localities.
- *Other metals frequently occurring in the environment* (Fe, Al, Zn); in many cases, studied via chemical speciation in aquatic systems (as hydrated ions $[Me(OH)_m]^{(m-n)-}$).
- *Less common metals* (Sb, Bi, Ti, Nb, Ta, and some rare earths of the Sc and Ac groups); known as minor components of various electronics and industrial catalysts.
- *Precious metals* (Au, Ag); the latter gaining a considerable attention in its new nanoforms applicable as effective disinfectants[151].
- *Platinum metals* (Ru, Rh, Pd, Os, Ir, Pt); a family of catalytically acting species whose impact on the environment is not yet fully understood; see introduction in reference (152) and the next section.
- *Organometallic compounds containing Hg, Pb, Sn, and B*i; all occurring as both naturally and industrially released species.
- *Metalloids* (As and Se); often as the subjects of interest in speciation analysis (As^V, As^{III}, As^{-III}, and As^{ORG} or Se^{IV} and Se^{VI}, respectively).
- *Toxic and harmful anions*, such as nitrogen-based ions (NO_2^-, NO_3^-, N_3^-, NH_4^+, and $N_2H_5^+$), sulphur anions (SO_4^{2-}, SO_3^{2-}, S^{2-}), phosphates (HPO_4^{2-}, $[PO_3]_x$, P^{ORG}); all being applied as fertilizers, industrial explosives, food additives, conserving or water-treatment agents.

- *Gases in air and dissolved in aquatic systems* (O_2, CO_2, NH_3) and gaseous emissions from volcanoes, industry, cars, and firing processes (NO_X, SO_2, Cl_2, HCHO, etc.).
- *Organic pollutants*; namely: polyaromatic hydrocarbons (PAHs) with their NO_2- and NH_2-derivatives, nitroso-amines, and similar potentially carcinogenic compounds, herbicides and pesticides (halogenated aromates, organophosphates, carbamides) and related formulations for agricultural use, synthetic dyes, or industrially applied surfactants.
- *Biologically important compounds*; e.g., compounds of fluorine and iodine, biogenic amines, some antioxidants or plasticizers (e.g. phthalates).

Electrochemical analyses can often be specifically tailored for special applications or uncommon matrices, such as quantification of selected metals in crude oil and petroleum,[125] analysis of industrial plating baths (see e.g. references (146, 147)), or physical characterisation and elemental analysis of solid minerals and rocks.[52,148] Among organic and biological compounds that have attracted attention of environmental analysts in the recent years (see e.g. reference (150)), one can name explosives in soil,[177] newly defined groups of persistent organic pollutants (POPs), including some new types of pesticides, volatile organic compounds (VOCs), cytokinine-based plant hormones or cyanotoxins.[153] Some other "new analytes" of interest have come forth in environmental electroanalysis; mostly, associated with the dynamic progress of new technologies and modern communication systems.[33,120,149,150,178]

During the last four decades, the objectives of environmental electroanalysis have changed significantly. Whereas at the beginning the determination of (total) elements as a laboratory method was in the foreground, this position is now held by very potent multielement techniques, to mention in the first place inductively-coupled plasma mass spectrometry (ICP-MS) which is also gradually replacing less efficient methods, such as atomic absorption spectrometry (AAS). Nevertheless, electrochemical analysis still maintains a niche if its strengths are exploited to its advantage: as a sensing device. The instruments can be made small and mobile, so sensing of elements directly in the field at the point of interest may result in very cost-effective strategies if decisions can be made ad hoc if a sample should be sent to the laboratory for further analysis or if concentrations of noxious substances are below a threshold not worth of further analysis.

Thus, the main strength of electroanalysis is not elemental analysis, but determination of various species, organic and inorganic compounds of toxicological, environmental, and biological importance. The real future of electroanalysis is sensing and detecting compounds which is with other methods difficult to achieve, expensive or labour-intensive. As can be seen with the current literature already, biosensors in all forms, but also other types of special or even specific detectors will be in the central focus of research.

Environmental analysis and electroanalysis of the new millennium reflect also some further trends. At first, there is still a growing influence of green chemistry, resulting soon in the establishment of a new discipline, green analytical

chemistry.[119,154] In close association with the strictly ecological principles, the 2000s saw the rise of "mercuryphobia",[155] which is a phenomenon covering a more intense monitoring of mercury(II) compounds in the environment and, mainly, culminating in aversion against the use of liquid mercury-based electrodes, including traditional configurations of the HMDE, DME, and MFE. It is indisputable that the electroanalysts may miss these highly reliable and flexible detection tools, on the other hand, the respective efforts to find alternate electrode materials have already led to the notable achievements beneficial also for environmental analysis. Herein, one has to quote the invention and a rapid expansion of bismuth-based electrodes and related sensors[156,179] that have been shown to be almost comparable substitutes for the mercury counterparts in many applications while remaining environmentally friendly or, at least, markedly less toxic than mercury and its compounds.

1.4.3 Sampling, Sample Storage, and Pretreatment

Sampling is one of the most crucial points in environmental analytical chemistry. Most mistakes made in this phase cannot be eliminated by the analytical method anymore. The main objectives are to avoid contamination on one hand, and loss of analytes on the other.

Gases can be sampled by standardised procedures and apparatuses; gases themselves can be absorbed in liquids or adsorbed on solid tube-like supports. Particulate matter in gases is precipitated either as a whole in electrofilters or other types of precipitators, or can be fragmented according to particle sizes by cascade impactors.

Liquids/Solutions (mainly various types of water) have to be carefully sampled to avoid contamination; e.g., early analyses of lead in ocean water showed too high results because of contamination of sea water from the boat itself. Water samples are usually filtered through membranes with 0.45 or 0.2 μm pore size to separate liquid and particulate matter. Waters from greater depths are sampled with special deep water sampling devices.

Soils from surfaces are sampled according to the specific top layers; they are usually rather inhomogeneous and often separated into different components (roots, larger stones etc.), homogenised and sieved. Soils from deeper layers are obtained by drilling, where contamination by abrasion of the driller should be observed.

Biological samples may show strong individual variations of analytes due to different dispositions and exposition conditions; apart from this it must be taken into account that organs and even sub-structures of organs can vary strongly in their composition. Such factors must be considered during sampling already. Animal and plant tissues and fluids may suffer from metal contamination when being in contact with metallic instruments; special cutting and operational tools are avail (e.g., from quartz glass or pure titanium).

Storage is a crucial aspect for many samples, particularly when the analytes are present at trace concentrations. The storage container materials must be chosen carefully because they may be permeable for ions, gasses, and water; but also the

surface may adsorb (loss of analyte) or desorb (contamination) constituents or impurities of the material which may cause problems in ensuing analysis.

Biological materials can be stored at low temperatures; at −195 °C (liquid nitrogen as used in specimen banks) or −70 °C (special laboratory freezers) biodegradation processes due to enzymatic or microbial activity are at minimum allowing storage times over years. A temperature around −20 °C (household freezers) is sufficient for short storage times in domains of weeks and months, whereas 4 °C permits only very short-termed storage (hours to a few days). Apart from storage at low temperatures storage after drying is a common procedure; drying can be achieved by elevated temperatures (80–120 °C) with the risk of volatilization of analytes and disintegration of the organic matrix. Lyophilization ("freeze-drying") is often a good alternative.

Sample pretreatment is dependent on the objectives.[161–167] For total element determinations often the organic matrix of biological sample has to be destroyed by oxidation, either by burning or treatment with excited oxygen (oxygen "plasma", dry ashing), or by strongly oxidising liquid agents (wet ashing; nitric acid, perchloric acid, sulphuric acid, hydrogen peroxide).

For the determination of organic compounds or various forms of element compounds (speciation analysis) the desired group(s) of analytes are usually isolated by extraction (Soxhlet, solid phase, liquid–liquid) or by other separation processes (ion exchange, electrophoresis, chromatography) prior to analysis.[143]

Insoluble inorganic environmental samples are dissolved either in acids or bases; if they are still highly resistive to dissolution they are usually digested in various types of molten salts.

1.4.4 Measurements with Electrochemical Sensors

Chemical sensors are simple devices with a more or less specific receptor for the analyte (molecular or ionic recognition) which are yield information about the chemical composition of samples. The chemical information obtained by the receptor is converted into an electric signal by the transducer.[180] Biosensors contain a biological recognition element in the receptor, such as enzymes, nucleic acids, antibodies, cell organelles, whole cells, tissues or even living microorganisms.[181] Environmental samples can be a challenging analytical task because analytes, in general, can be present at concentrations ranging from major to trace constituents. Nevertheless, an overwhelming percentage of studies is dealing with the determination of traces of noxious substances, where the limit of detection can be the crucial point. Measurements can be done discontinuously ("single shot" sensors or repetitive measurements), continuously (over a short period, such as detectors in flow systems) or permanently (over a long period).

An important issue is the calibration of sensors. Often the measured signal depends on the history of use of the sensor as well as on its shelf rest-time. Calibration with standards is a necessary issue in this respect. For validation of

methods the use of certified reference materials (CRMs) is an essential prerequisite. For many cases CRMs are not available with respect to analytes and/or matrix; spiking the sample with analyte and determining recovery rates or the use of matrix-matched standards being often an inadequate substitute for materials with certified concentrations of the analyte.

1.5 Concluding Remarks

Electrochemical sensing devices may constitute good solutions to detect analytes of interest with sufficient precision for numerous environmental samples. With respect to elemental analysis in the laboratory it may be stated that apart from speciation analysis (different oxidation states, complexes etc.) electroanalysis will play only a supplementary role; particularly total element concentrations or isotopic variations is the domain of mass spectrometry, where electrochemical methods often can hardly compete with respect to sample throughput, multi-element determination and detection limits. But, in this context, electrochemical sensors offer the advantage of simplicity and portability combined with inexpensiveness of sensors and instrumentation. The strength of analyses with electrochemical sensors lies definitely more in the area of analytical chemistry of molecules and species which are not directly detectable with ICP-MS or only with sophisticated instrumentation such as liquid chromatography in combination with various types of mass spectrometry. Compared with optical sensors, electroanalytical devices and systems are simpler in many cases because there is no need of a light source, and the signal is an electric entity already (in most cases current or potential) which can be monitored very precisely and can be handled as a direct output of the transducer. Electrochemical sensors are ideal candidates for decentralized testing and screening, and can be easily miniaturised and used simultaneously in arrays; for instance, like electronic noses and tongues; see e.g. references (159, 182, 183) mimicking human sensing organs.

Acknowledgement Herein, I.Š. and K.K. would like to acknowledge the valuable contributions from the research activities of their close colleagues and friends who have collaborated with the authors over the years and whose results are also somehow present in this text.

References

1. Ashok K, Shukla AK, Prem Kumar T (2013) Pillars of modern electrochemistry: a brief history. http://electrochem.cwru.edu/encycl/art-p05-pillars-of-ec.htm. Downloaded 5 May 2013
2. Cremer M (1906) Über die Ursache der elektromotorischen Eigenschaften der Gewebe, zugleich ein Beitrag zur Lehre von polyphasischen Elektrolytketten. Z Biol 47:542
3. Haber F, Klemensiewicz Z (1909) Ueber elektrische. Phasengrenzkraefte. Z Phys Chem 67:385–427
4. Heyrovský J (1922) Electrolysis with a mercury drop cathode (in Czech). Chem Listy XVI:258–264

5. Heyrovský J, Kůta F (1966) Principles of polarography. Academic, New York
6. Kalousek M (1946) Investigation on the reversibility of the dropping mercury electrode by discontinually changeable polarisation voltage (in Czech). Chem Listy 40:149–157
7. Barker GC, Jenkins IL (1952) Square-wave polarography. Analyst 77:685–696
8. Elbei AW (1960) Tast polarography (in German). Fresenius' Z Anal Chem 173:70–73
9. Bruckenstein S, Bixler IW (1965) Chemical stripping analysis. Anal Chem 37:786–790
10. Fogg AG, Wang J (1999) Terminology and convention for electrochemical stripping analysis (technical report). Pure Appl Chem 71:891–897
11. Jagner D (1982) Potentiometric stripping analysis: a review. Analyst (UK) 107:593–599
12. Růžička J, Hansen EH (1975) Flow injection analyses. 1. New concept of fast continuous analysis. Anal Chim Acta 78:145–157
13. Růžička J, Hansen EH (1988) Flow injection analysis, 2nd edn. Wiley, New York
14. Kolthoff IM, Furman NH (1931) Potentiometric titrations. Wiley, New York
15. Pungor E (1965) Oscillometry and conductometry. Pergamon Press, London
16. Vydra F, Štulík K (1971) Biamperometric titrations (in Czech). SNTL, Prague
17. MacDonald DD (1977) Chronopotentiometry. In: Transient techniques in electrochemistry. Springer, Berlin, pp 119–184
18. Compton RG, Eklund JC, Page SD (1994) Voltammetry in the presence of ultrasound: sonovoltammetry and surface effects. J Phys Chem 98:12410–12414
19. Orazem ME, Tribollet B (2011) Electrochemical impedance spectroscopy (EIS). Wiley, New York
20. Knight AW (1999) A review of recent trends in analytical applications of electrogenerated chemiluminescence. Trends Anal Chem 18:47–62
21. Gale RJ (1988) Spectroelectrochemistry: theory and practice. Springer, Berlin
22. Bard AE, Mirkin EV (eds) (2012) Scanning electrochemical microscopy. CRC Press, Boca Raton, FL
23. J. Heyrovsky Institute of Physical Chemistry, homepage (2013) http://www.jh-inst.cas.cz/www/data/dokument/obrazek/539o.jpg. Downloaded 5 May 2013
24. Heyrovsky J, Shikata M (1925) Researches with the dropping mercury cathode. II. The polarograph. Rec Trav Chim Pays Bas 44:496
25. Clark LC, Lyons C (1962) Electrode system for continuous monitoring in cardiovascular surgery. Ann N Y Acad Sci 102:29
26. Adams RN (1958) Carbon paste electrodes. Anal Chem 30:1576
27. Clark LC, Wolf R, Granger D, Taylor Z (1953) Continuous recording of blood oxygen tensions by polarography. J Appl Physiol 6:189–193
28. Wang J (1985) Stripping analysis: principles, instrumentation, and application. VCH Publishers, Deerfield Beach, FL
29. Wang J (1994) Analytical electrochemistry. VCH Publishers, New York
30. Veselý J, Weis D, Štulík K (1978) Analysis with ion-selective electrodes. E. Horwood, Chichester
31. Štulík K, Pacáková V (1987) Electroanalytical measurements in flowing liquids. Ellis Horwood, Chichester
32. Adams RN (1969) Electrochemistry at solid electrodes. Marcel Dekker, New York
33. Kalcher K, Švancara I, Metelka R, Vytřas K, Walcarius A (2006) Heterogeneous electrochemical carbon sensors. In: Grimes CA, Dickey EC, Pishko MV (eds) Encyclopedia of sensors, vol IV. American Scientific Publisher, Stevenson Ranch, pp 283–429
34. Rivas GA et al (eds) (2009) Carbon nanotubes: a new alternative for electrochemical sensors. Nova, Hauppauge, NY
35. Delahay P (1954) New instrumental methods in electrochemistry: theory, instrumentation, and applications to analytical and physical chemistry. Interscience, New York
36. Lingane JJ (1958) Electroanalytical chemistry. Interscience, New York
37. Bard AJ et al (eds) (1966–2013) Electroanalytical chemistry, a series of advances, vol I–XXV. M. Dekker, New York

38. Heyrovský J, Zuman P (1968) Practical polarography. Academic, New York
39. Vydra F, Štulík K, Juláková E (1976) Electrochemical stripping analysis. Ellis Horwood, Chichester
40. Meittes L, Zuman P, Rott A (1976) Handbook series in inorganic electrochemistry (Vol. I + II) & Handbook series in organic electrochemistry (Vol. III + IV). CRC Press, Cleveland, OH
41. Wang J (1988) Electroanalytical techniques in clinical chemistry and laboratory medicine. VCH Publishers, Weinheim
42. Smyth MR, Vos J (eds) (1992) Analytical voltammetry, vol 27, Comprehensive analytical chemistry series. Elsevier, Amsterdam
43. Brainina K, Neiman E (1993) Electroanalytical stripping methods. Wiley, New York
44. Vanýsek P (ed) (1996) Modern techniques in electroanalysis. Wiley, New York
45. Kissinger P, Heineman WR (eds) (1996) Laboratory techniques in electroanalytical chemistry, 2nd edn. CRC Press, Boca Raton, FL
46. Brett CMA, Oliveira Brett MA (1998) Electroanalysis, Oxford chemistry primers series. Oxford University Press, Oxford
47. Monk PMS (2001) Fundamentals of electroanalytical chemistry. Wiley, New York
48. Bard AJ, Faulkner LR (2001) Electrochemical methods: principles and application, 2nd edn. Wiley, New York
49. Bard AJ, Stratmann M et al (eds) (2002–2007) Encyclopedia of electrochemistry, vol I–XI. Wiley, Weinheim
50. Grimes CA, Dickey EC, Pishko MV (eds) (2006) The encyclopedia of sensors, vol I–X. American Scientific Publisher, Stevenson Ranch
51. Mirčeski V, Komorski-Lovrić Š, Lovrić M (2007) Square-wave voltammetry: theory and application. Springer, Heidelberg
52. Scholz F (ed) (2011) Electroanalytical methods: guide to experiments and applications, 2nd edn. Springer, Berlin
53. Compton RG, Banks CE (2011) Understanding voltammetry, 2nd edn. Imperial College Press, London
54. Compton RG, Batchelor-McAuley C, Dickinson EJF (2011) Understanding voltammetry: problems and solutions. Imperial College Press, London
55. Ozkan SA (2012) Method validation. In: Electrochemical methods in pharmaceutical analysis and their validation. HNB Publishing, New York, pp 293–335
56. Neeb R (1969) Inverse polarography and voltammetry (in German). Verlag Chemie, Weinheim
57. Vydra F, Štulík K, Julakova E (1977) Stripping polarography and voltammetry (in Czech). SNTL, Prague
58. Doležal J, Musil J (1977) Polarographic analysis of mineral resources (in Czech). SNTL, Prague
59. Kalvoda R (ed) (1985) Electroanalysis of the environment (in Czech). SNTL, Prague
60. Neeb R, Henze G (1986) Electrochemical analysis (in German). Springer, Berlin
61. Brainina KZ, Neiman E, Slepuschkin VV (1988) Inverse electroanalytical methods (in Russian). Chimiya, Moscow
62. Galus Z (1994) Fundamentals of electroanalytical chemistry (in Polish), 2nd edn. Polish Scientific Publishers, Warsaw
63. Ion A, Banica FG (2002) Electrochemical methods in analytical chemistry (in Roumanian). ARS Docendi, Bucharest
64. Jindra J (2009) History of electrochemistry in Czech lands, 1882–1989 (in Czech). Libri, Prague
65. Kalcher K, Vytřas K, Švancara I, Metelka R (eds) (2005–2012) Sensing in electroanalysis, an annual series of books (in English), vol I–VII. University Press Centre, University of Pardubice, Pardubice
66. Švancara I, Kalcher K, Walcarius A, Vytřas K (2012) Electroanalysis with carbon paste electrodes. CRC Press, Boca Raton, FL

67. Van den Berg CMG, Kramer JR (1979) Determination of complexing capacities of ligands in natural waters and conditional stability constants of the copper complexes by means of manganese dioxide. Anal Chim Acta 106:113–120
68. Achtenberg EP, Van den Berg CMG (1994) Automated voltammetric system for shipboard metal speciation in sea water. Anal Chim Acta 284:463–471
69. Yang RJ, Van den Berg CMG (2009) Metal complexation by humic substances in seawater. Environ Sci Technol 43:7192–7197
70. Florence TM (1989) Electrochemical techniques for trace element speciation in waters. In: Batley GE (ed) Trace element speciation: analytical methods and problems. CRC Press, Boca Raton, FL, pp 77–116
71. Florence TM (1970) Anodic stripping voltammetry with a glassy carbon electrode mercury-plated in situ. J Electroanal Chem 27:273–278
72. Bond AM, Heritage ID, Thormann W (1986) Strategy for trace metal determination in seawater by anodic stripping voltammetry using a computerized multitime-domain measurement method. Anal Chem 58:1063–1066
73. Howell GN, O'Connor MJ, Bond AM (1986) Methylmercury generation in seawater by transmethylation reactions of organolead and organotin compounds with inorganic mercury as monitored by multi-nuclear magnetic resonance and electroanalytical techniques. Aust J Chem 39:1167–1175
74. Wang J (1982) Anodic stripping voltammetry as an analytical tool. Environ Sci Technol 16:104A–109A
75. Wang J (2001) In-situ monitoring electrochemical sensors. In: Ghassemi A (ed) Handbook of pollution control and waste minimization. M. Dekker, New York
76. Wang J (2007) Stripping-based electrochemical metal sensors for environmental monitoring. In: Alegret A, Merkoci A (eds) Chemical sensors. Elsevier, Amsterdam
77. Brainina KZ, Malakhova NA, Stojko NY (2000) Stripping voltammetry in environmental and food analysis. Fresenius J Anal Chem 368:307–325
78. Brainina KZ, Kubysheva IV, Miroshnikova EG et al (2001) Small-size sensors for in-field stripping voltammetric analysis of water. Field Anal Chem Technol 1:260–271
79. Nurnberg HW (1977) Potentialities and applications of advanced polarographic and voltammetric methods in environmental research and surveillance of toxic metals. Electrochim Acta 22:935–949
80. Nurnberg HW (1979) Polarography and voltammetry in studies of toxic metals in man and his environment. Sci Total Environ 12:35–60
81. Stoeppler M, Durbeck HW, Nurnberg HW (1982) Environmental specimen banking: a challenge in trace analysis. Talanta 29:963–972
82. Ostapczuk P, Froning M (1992) Advanced electrochemical techniques for the determination of heavy metals in specimen bank materials. In: Rossbach M, Schladot JD, Ostapczuk P (eds) Specimen banking—environmental monitoring and modern analytical approaches. Springer, Berlin, pp 153–165
83. Ostapczuk P (1993) Present potentials and limitations in the determination of trace elements by potentiometric stripping analysis. Anal Chim Acta 273:35–40
84. Compton RG, Foord JS, Marken F (2003) Electroanalysis at diamond-like and doped-diamond electrodes. Electroanalysis 15:1349–1363
85. Welch CW, Compton RG (2006) The use of nanoparticles in electroanalysis: a review. Anal Bioanal Chem 384:601–619
86. Campbell FW, Compton RG (2010) The use of nanoparticles in electroanalysis: an updated review. Anal Bioanal Chem 396:241–259
87. O'Connor KM, Arrigan DWM, Gy S (1995) Calixarenes in electroanalysis. Electroanalysis 7:205–215
88. Dempsey E, Smyth MR, Richardson DHS (1992) Application of lichen-modified carbon paste electrodes to the voltammetric determination of metal ions in multielement and speciation studies. Analyst (UK) 117:1467–1470

89. Ruíz Barrio MA, Pingarron Corrazón JM (1992) Voltammetric determination of pentachlorophenol with a silica gel-modified carbon paste electrode. Fresenius J Anal Chem 344:34–38
90. Agraz R, Sevilla MT, Hernández L (1995) Voltammetric quantification and speciation of mercury compounds. J Electroanal Chem 390:47–57
91. Estela JM, Tomás C, Cladera A, Cerdà V (1995) Potentiometric stripping analysis: a review. Crit Rev Anal Chem 25:91–141
92. Brett CMA (1999) Electroanalytical techniques for the future: the challenges of miniaturization and of real-time measurements. Electroanalysis 11:1013–1016
93. Marchal V, Barbier F, Plassard R, Faure R, Vittori O (1999) Determination of cadmium in bentonite clay mineral using a carbon paste electrode. Fresenius J Anal Chem 363:710–712
94. Walcarius A (1995) Zeolite-modified electrodes: analytical applications and prospects. Electroanalysis 8:971–986
95. Walcarius A (2001) Electroanalysis with pure, chemically modified, and sol-gel-derived silica-based materials (an overview). Electroanalysis 13:701–718
96. Monien H, Gerlach U, Jacob P (1981) Inverse-voltammetry of some copper-chelates using a carbon paste electrode—determination of copper in drinking water by oxidation of copper dithiooxamide. Fresenius′ Z Anal Chem 306:136–143
97. Meyer S, Kubsch G, Lovric M, Scholz F (1997) Speciation of mercury in two dimictic lakes of North-East Germany during a period of 600 days. Int J Environ Anal Chem 68:347–368
98. Bakker E, Pretsch E (2005) Potentiometric sensors for trace-level analysis. Trends Anal Chem 24:199–207
99. Tercier ML, Buffle J (1993) In-situ voltammetric measurements in natural waters: future prospects and challenges. Electroanalysis 5:187–200
100. Daniele S, Ugo P, Bragato C et al (1996) Use of Nafion(R) coated carbon disk microelectrodes in solution without and with different concentrations of supporting electrolyte. J Electroanal Chem 418:29–34
101. Daniele S, Baldo MA, Bragato C (2008) Recent developments in stripping analysis on microelectrodes. Curr Anal Chem 4:215–228
102. Arduini F, Quintana Calvo J, Amine A, Palleschi G, Moscone D (2010) Bismuth-modified electrodes for lead detection (a review). Trends Anal Chem 29(2010):1295–1304
103. Paneli MG, Voulgaropoulos A (1993) Applications of adsorptive stripping voltammetry in the determination of trace and ultratrace metals. Electroanalysis 5:355–373
104. Economou A, Fielden PR (1993) Adsorptive stripping voltammetry on mercury film electrodes in the presence of surfactants. Analyst (UK) 118:1399–1403
105. Hocevar SB, Ogorevc B (2007) Preparation and characterization of carbon paste microelectrode based on carbon nanoparticles. Talanta 74:405–411
106. Kemula W, Kublik Z (1958) The hanging mercury drop electrode. Anal Chim Acta 18:104–108
107. Stará V, Kopanica M (1989) Chemically modified carbon paste and carbon composite electrodes. Electroanalysis 1:251–256
108. Barek J, Cvačka J, Muck A, Quaiserová V, Zima J (2001) Electrochemical methods for monitoring of environmental carcinogens. Fresenius J Anal Chem 369:556–562
109. Navrátilová Z, Kula P (2003) Clay modified electrodes: present applications and prospects. Electroanalysis 15:837–846
110. Beinrohr E, Tschopel P, Tolg G, Nemeth M (1993) Flow-through anodic stripping coulometry and anodic stripping coulometry with collection for the simultaneous determination of copper, lead, cadmium, and zinc. Anal Chim Acta 273:13–25
111. Labuda J, Vaníčková M, Bučková M, Korgová E (2000) Development in voltammetric analysis with chemically modified electrodes and biosensors. Chem Papers 54:95–103
112. Bobrowski A, Zarebski J (2000) Catalytic systems in adsorptive stripping voltammetry: a review. Electroanalysis 12:1177–1186
113. Kalcher K, Grabec I, Raber G, Cai XH, Tavcar G, Ogorevc B (1995) The vermiculite-modified carbon paste electrode as a model system for preconcentrating mono- and divalent cations. J Electroanal Chem 386:149–156

114. Nović M, Divjak B, Pihlar B, Hudnik V (1996) Influence of the sample matrix composition on the accuracy of the ion chromatographic determination of anions. J Chromatogr A 739:35–42
115. Guzsvány V, Kádár M, Zs P, Bjelica L, Gaál F, Tóth K (2008) Monitoring of photocatalytic degradation of selected neonicotinoid insecticides by cathodic voltammetry with a bismuth film electrode. Electroanalysis 20:291–300
116. Pižeta I, Branica M (1997) Simulation and fitting of anodic stripping voltammetry data for determination of the metal complexing capacity. Anal Chim Acta 351:73–82
117. Murray RW, Ewing AG, Durst RA (1987) Chemically modified electrodes: molecular design for electroanalysis. Anal Chem 59:A379–A390
118. Bonakdar M, Mottola HA (1989) Electrocatalysis at chemically modified electrodes. Detection/determination of redox gaseous species in continuous-flow systems. Anal Chim Acta 224:305–313
119. Wang J (2002) Real-time electrochemical monitoring: toward green analytical chemistry. Acc Chem Res 35:811–816
120. Hart JP, Wring SA (1997) Recent developments in the design and application of screen-printed electrochemical sensors for biomedical, environmental and industrial analyses. Trends Anal Chem 16:89–103
121. Wang J (2002) Portable electrochemical systems. Trends Anal Chem 21:226–232
122. Hart JP, Wring SA (1994) Screen-printed voltammetric and amperometric electro-chemical sensors for decentralized testing. Electroanalysis 6:617–624
123. Teixeira MFS, Bergamini MF, Bocchi N (2004) Lithium ions determination by selective pre-concentration and differential pulse anodic stripping voltammetry using a carbon paste electrode with a spinel-type manganese oxide. Talanta 62:603–609
124. Augelli MA, Muñoz RAA, Richter EM, Junior AG, Angnes L (2005) Chronopotentiometric stripping analysis using gold electrodes, an efficient technique for mercury quantification in natural waters. Electroanalysis 17:755–761
125. Muñoz RAA, Correia PRM, Nascimento AN, Silva CS, Oliveira PV, Angnes L (2007) Electroanalysis of crude oil and petroleum-based fuel for trace metals: evaluation of different microwave-assisted sample decompositions and stripping techniques. Energy Fuels 21:295–302
126. Alemu H, Chandravanshi BS (1998) Electrochemical behavior of N-phenylcinnamohydroxamic acid incorporated into carbon paste electrode and adsorbed metal ions. Electroanalysis 10:116–120
127. Siswana M, Ozoemena KI, Nyokong T (2006) Electrocatalytic behaviour of carbon paste electrode modified with iron(II) phthalocyanine nanoparticles towards the detection of amitrole. Talanta 69:1136–1142
128. Üslu B, Ozkan SA (2007) Solid electrodes in electroanalytical chemistry: present applications and prospects. Comb Chem High Throughput Screen 10:495–513
129. Turyan I, Mandler D (1993) Low-level mercury electrochemical detection. Nature 362:703–704
130. Turyan I, Mandler D (1994) Electrochemical determination of ultralow levels ($<10^{-12}$ M) of mercury by anodic stripping voltammetry using a chemically modified electrode. Electroanalysis 6:838–843
131. Wang S-T, Xu H-D, Li J-H (2002) Environmental electroanalytical chemistry. Fenxi Huaxue (Chinese J Anal Chem) 30:1005–1011
132. Li J, Liu S, Mao X, Gao P, Yan Z (2004) Trace determination of rare earths by adsorption voltammetry at a carbon paste electrode. J Electroanal Chem 561:137–142
133. Hu ZW, Li Z-L, Li R-L, Jiang H-S, Wang E-K, Tian L-Q, Jiang H-H, Xu X-Y, Tian W-Z, Zheng S-H (1997) Study of the fallen ice in Meichun (Xishan, China). Gaoxiao Dizhi Xuebao (Geol J Chin Univ) 3:361–369
134. Watanabe D, Furuike T, Midorikawa M, Tanaka T (2005) Simultaneous determination of copper and antimony by differential pulse anodic stripping voltammetry with a carbon-paste electrode. Bunseki Kagaku (Jpn Analyst) 54:907–912

135. Kamio A, Nagaosa Y (2008) 1-Butyl-3-methylimidazolium hexafluorophosphate ionic liquid as a new solvent for the determination of Pb(II) and Cd(II) by anodic stripping voltammetry after extraction of the iodide complexes. Anal Sci (Jpn) 24:1363–1367
136. Lee Y-K, Kim C-K, Park J-T, Kim K-S, Whang K-J (1985) Potentiometry with carbon paste-based ion-selective electrode for the determination of sulphate. J Korean Air Pollut Res Assoc 1:99–103
137. Chuanuwatanakul S, Punrat E, Panchompoo J, Chailapakul O, Motomizu S (2008) On-line preconcentration and determination of heavy metals by sequential injection-anodic stripping voltammetry by using bismuth film screen-printed carbon electrode. J Flow Injection Anal (Japan) 25:49–52
138. Khoo SB, Guo SX (2002) Rapidly renewable and reproducible mercury film coated carbon paste electrode for anodic stripping voltammetry. Electroanalysis 14:813–822
139. Graabæk AM, Jeberg B (1992) Trace element analysis by computerized stripping potentiometry. Intern Labor 22:33–38
140. Manahan SE (2001–2012) Fundamentals of environmental chemistry, 1–3rd edn. CRC Press, Boca Raton, FL
141. Keith LH, Crummett W, Deegan J Jr, Libby RA, Taylor JK, Wentler G (1983) Principles of environmental analysis. Anal Chem 55:2210–2218
142. Keith LH (1991) Environmental sampling and analysis: a practical guide. Lewis Publishers, Chelsea
143. Arthur CL, Pratt K, Motlagh S, Pawliszyn J, Belardi RP (1992) Environmental analysis of organic compounds in water using solid phase micro extraction. J High Resolut Chromatogr 15:741–744
144. Subramanian G (ed) (1995) Quality assurance in environmental monitoring: instrumental methods. VCH, Weinheim
145. Patnaik P (1997) Handbook of environmental analysis: chemical pollutants in air, water, soil, and solid wastes. CRC Press, Boca Raton, FL
146. Reimann C, De Caritat P (1998) Chemical elements in the environment: factsheets for the geochemists and environmental scientists. Berlin, Springer
147. Sunahara GI (2002) Environmental analysis of contaminated sites. Wiley, New York
148. Grygar T, Marken F, Schroeder U, Scholz F (2002) Electrochemical analysis of solids. A review. Collect Czech Chem Commun 67:163–208
149. Namieśnik J (2003) Trends in environmental analytics and monitoring. In: New horizons and challenges in environmental analysis and monitoring. CEEAM, Gdansk (Poland), pp 260–283
150. Namieśnik J, Szefer P (eds) (2010) Analytical measurements in aquatic environments. CRC Press, Boca Raton, FL
151. Rai M, Yadav A, Gade A (2009) Silver nanoparticles as a new generation of anti-microbials. Biotechnol Adv 27:76–83
152. Locatelli C (2007) Voltammetric analysis of trace levels of platinum group metals: principles and applications. Electroanalysis 19:2167–2175
153. Research Centre for Toxic Compounds in the Environment (RECETOX)—homepage (2013) http://www.recetox.muni.cz/index-en.php. Downloaded 30 May 2013
154. Koel M, Kaljurand M (2010) Green analytical chemistry. RSC, London
155. Navrátil T, Švancara I, Mrázová K, Nováková K, Šestáková I, Heyrovský M, Pelclová D (2011) Mercury and mercury electrodes: the ultimate battle for the naked existence (a consideration). In: Kalcher K, Metelka R, Švancara I, Vytřas K (eds) Sensing in electroanalysis, vol VI. University Press Centre, Pardubice, pp 23–53
156. Yáñez-Sedeño P, Pingarrón JM, Hernández L (2012) Bismuth electrodes. In: De la Guardia M, Garrigues S (eds) Handbook of green analytical chemistry. Wiley, New York, pp 262–268 and 282–284
157. Förstner U, Salomons W (1980) Trace metal analysis on polluted sediments. Part I: assessment of sources and intensities. Environ Technol Lett 1:494–505

158. Salomons W, Förstner U (1980) Trace metal analysis on polluted sediments. Part II: evaluation of environmental impact. Environ Technol Lett 1:506–517
159. Di Natale C, Macagnano A, Davide F, D'Amico A, Legin A, Vlasov Y, Rudnitskaya A, Selezenev B (1997) Multicomponent analysis on polluted waters by means of an electronic tongue. Sensors Actuat B 44:423–428
160. Meloun M, Sáňka M, Němec P, Křítková S, Kupka K (2005) The analysis of soil cores polluted with certain metals using the Box-Cox transformation. Environ Pollut 137:273–280
161. Lagakos SW, Wessen BJ, Zelen M (1986) An analysis of contaminated well water and health effects in Woburn, Massachusetts. J Am Stat Assoc 81:583–596
162. Karstensen KH, Ringstad O, Rustad I, Kalevi K, Jørgensen K, Nylund K, Alsberg T, Ólafsdóttir K, Heidenstam O, Solberg H (1998) Methods for chemical analysis of contaminated soil samples: tests of their reproducibility between Nordic laboratories. Talanta 46:423–437
163. Šulcek Z, Povondra P (1989) Methods of decomposition in inorganic analysis. CRC Press, Boca Raton, FL
164. Matusiewicz H (2003) Wet digestion methods. In: New horizons and challenges in environmental analysis and monitoring. CEEAM, Gdansk, pp 225–259
165. Hoenig M (2005) Dry ashing. In: Worsfold P, Townshend A, Poole C (eds) Encyclopedia of analytical science, vol VIII, 2nd edn, Sample dissolution for elemental analysis. Elsevier Science, London, pp 131–145
166. Twyman RM (2005) Wet digestion. In: Worsfold P, Townshend A, Poole C (eds) Encyclopedia of analytical science, vol VIII, 2nd edn, Sample dissolution for elemental analysis. Elsevier Science, London, pp 146–153
167. Ojeda CB, Rojas FS (2005) Microwave digestion. In: Worsfold P, Townshend A, Poole C (eds) Encyclopedia of analytical science, vol VIII, 2nd edn, Sample dissolution for elemental analysis. Elsevier Science, London, pp 153–165
168. Rajeshwar K, Ibanez JG, Swain GM (1994) Electrochemistry and the environment. J Appl Electrochem 24:1077–1091
169. Wang J (1994) Decentralized electrochemical monitoring of trace metals: from disposable strips to remote electrodes. Analyst (UK) 119:763–766
170. Esteban M, Casassas E (1994) Stripping electroanalytical techniques in environmental analysis. Trends Anal Chem 13:110–117
171. Simonsson D (1997) Electrochemistry for a cleaner environment. Chem Soc Rev 26:181–189
172. Barek J, Fischer J, Navrátil T, Pecková K, Yosypchuk B, Zima J (2007) Nontraditional electrode materials in environmental analysis of biologically active organic compounds. Electroanalysis 19:1967–1986
173. De Marco R, Clarke G, Pejcic B (2007) Ion-selective electrode potentiometry in environmental analysis. Electroanalysis 19:1987–2001
174. Badihi Mossberg M, Buchner V, Rishpon J (2007) Electrochemical biosensors for pollutants in the environment. Electroanalysis 19:2015–2028
175. Zima J, Švancara I, Pecková K, Barek J (2009) Carbon paste electrodes for the determination of detrimental substances in drinking water. In: Lefèbvre MH, Roux MM (eds) Progress on drinking water research. Nova, Hauppauge, NY, pp 1–54
176. Vyskocil V, Barek J (2009) Mercury electrodes-possibilities and limitations in environmental electroanalysis. Crit Rev Anal Chem 39:173–188
177. Wang J (2007) Electrochemical sensing of explosives. Electroanalysis 19:415–423
178. Hart JP, Crew A, Crouch E, Honeychurch KC, Pemberton RM (2004) Some recent designs and developments of screen-printed carbon electrochemical sensors/bio-sensors for biomedical, environmental, and industrial analyses. A review. Anal Lett 37:789–830
179. Švancara I, Prior C, Hočevar SB, Wang J (2010) A decade of bismuth-modified electrodes in electroanalysis. Electroanalysis 22:1405–1420
180. Hulanicki A, Glab S, Ingman F (1991) Chemical sensors: definitions and classification. Pure Appl Chern 63:1247–1250

181. Theavenot DR, Toth K, Durst RA, Wilson GS (1999) Electrochemical biosensors: recommended definitions and classification. Pure Appl Chem 71:2333–2348
182. Krantz-Rülcker C, Stenberg M, Winquist F, Lundström I (2001) Electronic tongues for environmental monitoring based on sensor arrays and pattern recognition: a review. Anal Chim Acta 426:217–226
183. Ampuero S, Bosset JO (2003) The electronic nose applied to dairy products: a review. Sensors Actuat B 94:1–12

Chapter 2
Soil

Kenneth A. Sudduth, Hak-Jin Kim, and Peter P. Motavalli

2.1 Introduction to Soil and Its Characteristics

The pedosphere is the total surficial layer of the earth that consists of soil and which has complex and dynamic interactive linkages with the lithosphere, the hydrosphere, the biosphere, and the atmosphere[1] (Fig. 2.1). Soil covers a large proportion of the 149 million km^2 global land area, but only an estimated 93 million km^2 are biologically productive containing approximately 33 % forest, 32 % pastures and 11 % crop land.[2] Over the pedosphere, variations in soil properties with depth and across landscapes can be accounted for by several interacting factors including physical and chemical weathering, erosion and deposition, and human and natural disturbances and result from the effects of the different factors of soil formation which include parent material, climate, living organisms (e.g., vegetation), topography and time.[3,4] An example of the resulting spatial diversity existing in soils is shown by the fact that the National Cooperative Soil Survey of the United States has identified and mapped over 20,000 different kinds of soil in the United States alone.[5]

Soils can be evaluated at different scales, from the molecular level of individual soil components (e.g., soil clay mineralogy), to individual three-dimensional soil

K.A. Sudduth (✉)
Cropping Systems and Water Quality Research Unit, USDA Agricultural Research Service, Columbia, MO, USA
e-mail: Ken.Sudduth@ars.usda.gov

H.-J. Kim
Department of Biosystems & Biomaterials Science and Engineering, Seoul National University, Seoul, South Korea

P.P. Motavalli
Department of Soil, Environmental, and Atmospheric Sciences, University of Missouri, Columbia, MO, USA

L.M. Moretto, K. Kalcher (eds.), *Environmental Analysis by Electrochemical Sensors and Biosensors*, DOI 10.1007/978-1-4939-0676-5_2

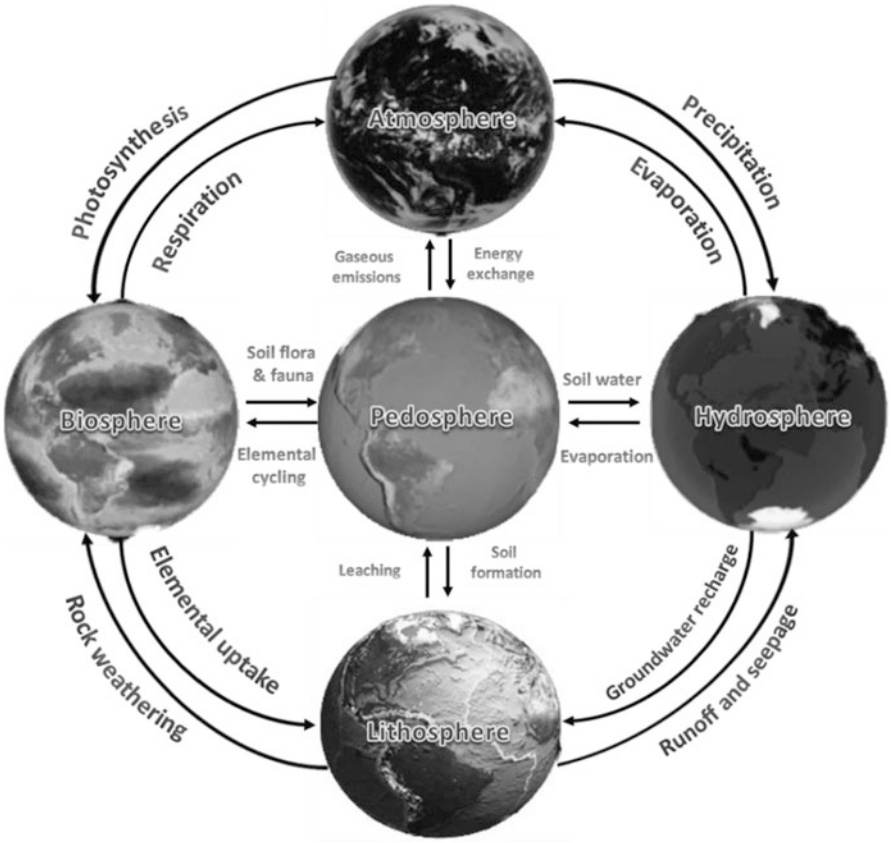

Fig. 2.1 Diagram illustrating the linkage and interactive processes of the pedosphere with other important systems on earth (adapted from reference (1)); Earth images from Exploring Earth (http://www.classzone.com/books/earth_science/terc/content/visualizations/es0102/es0102page01.cfm?chapter_no=visualization) and Utah State Office of Education (http://utahscience.oremjr.alpine.k12.ut.us/sciber99/8th/earth/sciber/surface.htm)

bodies (known as pedons), to large-scale soil toposequences and ultimately to the pedosphere itself[6] (Fig. 2.2). The appropriate tool for measurement of soil properties at each of these scales of soil evaluation may vary (Fig. 2.2) and may be affected by several factors including the objective of the evaluation, technical capabilities for measurement, the observed spatial and temporal variability, and cost.

New tools for assessment of soil physical, biological, and chemical properties are critically needed to better understand the complex processes and spatial and temporal variability that occur in soils at different scales and in interaction with other biotic and abiotic components of terrestrial ecosystems. Increasing pressures for food production, growing human populations, and accelerating environmental degradation require improved soil management, including a better capability to

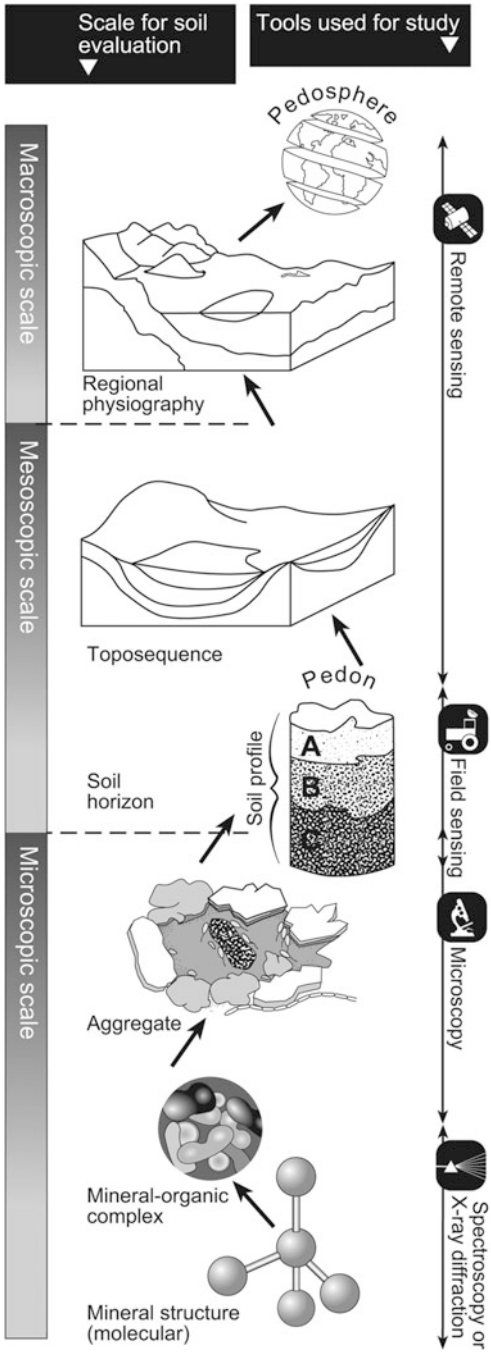

Fig. 2.2 The broad range of scales at which soil sensor-based evaluation can take place and examples of assessment procedures used for evaluation at each scale (adapted from references (6, 7))

more intensively monitor changes in soil properties and processes, to determine how those changes may affect soil, water, and atmospheric systems, and to provide information for decision-makers to select appropriate land use practices. Such improvements may also require concomitant improvements in data quality control procedures and innovative data management, analysis, and presentation techniques for both short-term and long-term use of the collected soil and supporting information.

2.2 The Unique Nature of Soils: A Heterogeneous, Three Phase System

Soil is a diverse natural material that is characterized by solid, liquid, and gas phases that give it unique chemical, physical, and biological properties. The proportion of solids, liquids, and gases in the soil will vary depending on several factors including the composition of the organic and inorganic constituents in the soil and their physical spatial arrangement (i.e., soil structure). In the U.S. Department of Agriculture classification system, the solid mineral components in soil are categorized based on particle diameter into sand (0.50–2 mm), silt (0.002–0.50 mm) and clay (<0.002 mm) particles.[8] Other classification systems for particle size limits may also be used from organizations such as the Canada Soil Survey Committee (CSSC), the International Soil Science Society (ISSS), and the American Society for Testing and Materials (ASTM).[8] Organic and inorganic colloidal material are defined to have particle sizes of <0.001 mm in diameter and these size particles have particular importance environmentally because of their relatively large surface area, charge, mobility, and role in biological activity.[9]

The inorganic components of soils include primary (e.g., quartz) and secondary minerals (e.g., phyllosilicate clays) which are composed primarily of nine chemical elements (i.e., oxygen, silicon, aluminium, iron, carbon, calcium, potassium, sodium, and magnesium). An important characteristic of the secondary soil minerals is their high total surface area ranging from kaolinite with a specific surface area of 7–30 $m^2\ g^{-1}$ to montmorillonite with a specific surface area of 600–800 $m^2\ g^{-1}$. Soil organic matter is the organic fraction of the soil that includes organic materials in all stages of decomposition, including a more stable complex organic fraction known as soil humus. The soil organic matter is primarily composed of carbon, hydrogen, oxygen, nitrogen, sulphur, and other elements that are contained in organic materials (e.g., plant residues) that are added into the soil.

Surface charge develops on soil clays and organic matter due to cation substitutions in the crystalline structures of clay (resulting in permanent negative charge) and loss or gain of hydrogen ions from functional groups of inorganic soil minerals and organic matter with changes in soil pH (resulting in pH-dependent

negative or positive charge). The presence of surface charge in soils is critical for cation and anion exchange processes that allow for retention of ionic species on the soil surfaces in equilibrium with ionic species in the soil solution contained in the soil pores.

In soils, the individual mineral and organic particles often bind together to form aggregates of various sizes ranging from 0.5 to 5 mm in diameter. Factors influencing aggregation include soil faunal (e.g., earthworms) and microbial (e.g., soil fungi) activity producing extracellular polysaccharides and hyphae, root growth and exudation, inorganic binding agents (e.g., calcium), and environmental variables (e.g., drying and wetting).[10] Pores or voids formed due to the geometrical packing of the individual soil particles are known as "intra-aggregate" pores and voids formed by the physical arrangement of aggregates are known as "inter-aggregate" pores.[11] These pores are categorized by size into macropores (>500 μm radius), coarse mesopores (25–500 μm radius), fine mesopores (5–25 μm radius), and micropores (<5 μm radius).[12] Other pore size limits have also been used to distinguish micropores and macropores (e.g., reference (13)). Soil organic matter can also contain pore space and surface area that facilitates the retention of water. The distribution and continuity of these soil pores affect multiple processes in soils including root growth and nutrient uptake, water infiltration, drainage and storage, gaseous exchange in and out of the soil, and chemical retention and transport. Porosity or the proportion of the soil pore volume to the total soil volume is often approximately 50 % in soils (i.e., when the soil bulk density is 1.3 Mg m^{-3}).

The soil pore space itself is filled with varying proportions of gas and water (known as the soil solution) and this environment provides ideal microhabitats for soil biological activity, although the space occupied by living microorganisms represents generally less than 5 % of the overall space in soils[14] (Fig. 2.3). In addition, almost 80–90 % of soil microorganisms are on solid surfaces. Among the factors affecting the ecology, activity and population dynamics of soil microorganisms in soil pores and on soil surfaces are the availability of carbon and energy sources, the presence of mineral nutrients, the amount and potential of soil water, temperature, pore air composition, pH of soil solution, soil oxidation–reduction potential, the area and charge of soil surfaces, the genetics of the microorganisms and the interaction among microorganisms and other soil biological components (e.g., plant roots).[14] Soil has a large and diverse biological population that includes micro- and macro-fauna and flora. For example, the estimated number of bacterial cells in a gram of soil is typically approximately 10^9 and based on DNA reassociation kinetics, the estimated number of distinct genomes in a gram of soil ranges from 2,000 to 18,000.[15]

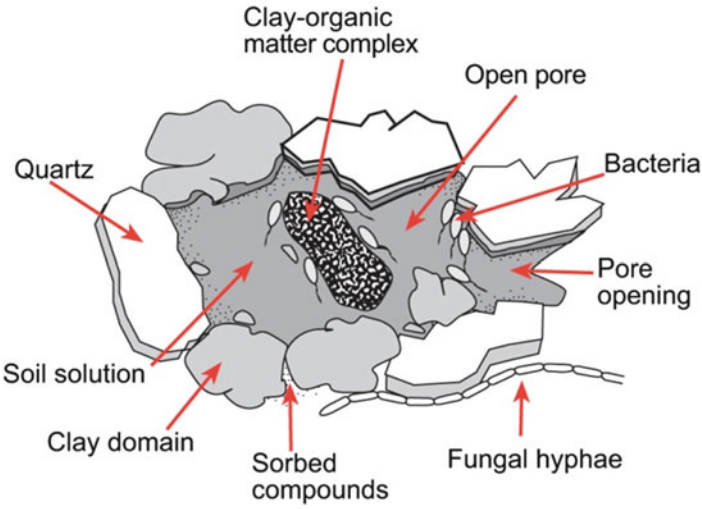

Fig. 2.3 Components and structure of a soil aggregate (adapted from reference (16))

2.2.1 Interactions of Biological, Chemical, and Physical Processes

Several important soil biological, chemical, and physical processes have major effects on the environment and are important for understanding the basis for several important environmental issues including air, soil, and water pollution, climate change, and the fate of pollutants and other materials added to soil. The magnitude and rate of many of these processes are affected by abiotic factors, such as temperature, aeration, soil water content, and soil moisture potential.

2.2.1.1 Buffering

Buffering of soil moisture content and soil temperature relative to air temperature and humidity make soil an ideal medium for plant growth and soil biological activity. The retention of water in soil pores and water's very high specific heat capacity account for the relatively moderate changes in soil temperature compared to changes in air temperature when a soil contains moisture. In addition, the large soil surface area and pore size distribution (i.e., micropores tend to retain more water than macropores) act to reduce soil water loss through evaporation and drainage.

Another type of buffering in soil moderates changes in the chemical composition of the soil solution and ionic species retained on the exchange sites of soil colloids. The process by which charged soil surfaces (i.e., clays, organic matter, sesquioxides, and amorphous minerals) attract and retain ionic species from the soil solution which is bathing the surface is known as adsorption. These sorbed

chemical species are retained at various strengths of retention depending on several factors including the nature and charge of the surface functional groups and the hydrated radius and charge of the sorbed species. These chemical species can also form sparingly soluble precipitates on the soil surfaces. The combined processes of adsorption and precipitation are known as sorption.

The interaction between sorbed chemical species on soil surfaces and chemical species in the soil solution helps to moderate excessive changes in the chemical concentration or activity of chemical species in the soil solution. For example, soil pH is buffered because when H^+ ion is added to the soil solution, some of the H^+ will be sorbed on the soil surfaces and the possible soil pH decrease resulting from that addition of H^+ will be moderated. Similarly, if H^+ is removed from the soil solution, H^+ (and Al^{+3}) will be desorbed from the soil surfaces and the possible soil pH increase due to H^+ removal will be moderated. This chemical solid-solution buffering system in soils affects multiple soil properties and processes including plant nutrient availability, biological activity, and the fate of chemical pollutants. Due to this chemical buffering system, measurement of soil reaction (acidity and alkalinity) for purposes of determining the amount of liming or acidifying material to raise or lower the soil pH for optimizing plant growth must measure both the soil acidity in the soil solution and 'exchangeable acidity' or concentrations of H^+ and Al^{+3} on the exchange sites of the soil surfaces. Similar assessments for determining the amount of phosphorus (P) fertilizer to add to a particular soil to raise the soil solution P level to an optimum level for plant growth must also take into account the soil's P buffering capacity.

2.2.1.2 Filtering and Retention

The capacity of soils to filter and retain organic and inorganic pollutants is an important ecosystem service or function of soils.[17] The filtering process occurs because of the interaction of physical, chemical, and biological processes in soils and is optimized when organic and inorganic pollutants are exposed to soil surfaces and biological activity. Therefore, preferential flow of pollutants through soil channels or cracks, shallow soils, slow infiltration of polluted water into soil causing surface runoff, and sandier-textured soils reduce the amount of potential filtering and retention of pollutants. Optimizing soil filtration is a major objective in the design of septic systems and pollutants from the sewage, such as human enteric viruses, move through soils due to several factors such as rainfall, temperature, soil structure, soil organic matter content, and soil pore water pH.[18]

2.2.1.3 Decomposition and Soil Organic Carbon Dynamics

Decomposition is the process by which organic materials are progressively dissociated and ultimately can be converted into inorganic constituents. This process serves two important ecosystems functions—the mineralization of carbon (C) (e.g.,

from organic C to carbon dioxide) and other elements (e.g., from organic to inorganic forms of nitrogen, phosphorus and sulphur), and the formation of soil organic matter.[19] Decomposition is also the primary process in the biodegradation of pollutants[20] and affects soil efflux of carbon dioxide into the atmosphere, which is an important component of the global carbon balance affecting climate change. The conversion of C and other elements to mineral forms is called mineralization, and the reverse process by which inorganic forms are incorporated into organic forms in microbial biomass is called immobilization.[21]

Decomposition is primarily a biological process that includes the activity of soil organisms, but abiotic factors can also facilitate mass loss of organic materials through fragmentation, physical abrasion, photochemical breakdown and leaching.[22] Among the factors affecting the degree and rate of decomposition are the resource quality of the organic materials, the soil physical/chemical environment (e.g., soil water potentials, oxygen supply, temperature, soil texture and mineralogy, pH) and the physical accessibility of the organic materials to microbial and enzymatic breakdown.[22–24] Due to the higher proportion of organic matter and biological activity in the soil surface horizons, the highest rates of decomposition most often occur in this zone.

Several factors influence soil organic C stabilization by affecting both plant productivity and the activity of the saprotrophic system.[25] These factors include soil temperature, moisture, texture, pH, landscape position, ecosystem type, biological activity, the physicochemical properties of soil organic fractions, soil structure, nutrient availability, and clay mineralogy.[24,26–29] A primary difficulty in assessing the relative importance of these factors in stabilizing soil organic C is the interactive nature of many of these variables. For example, among the effects of changes in soil moisture are changes in biological activity, in chemical solubility and transport, in plant productivity, and in soil temperature. The soil solid phase can adsorb biological molecules, retain them from transport in the environment, and also protect them from biological decomposition.[14] In addition, loss mechanisms of soil organic C are not confined to decomposition, but also include losses due to soil erosion and leaching of dissolved organic C. These latter C loss processes may have relatively greater significance than decomposition among some soils situated in highly erosive or well-drained environments.

2.3 Importance of Soil Analysis

As a major component of terrestrial cycles, soils are a central component for many important agricultural and environmental issues. Soil degradation is a growing problem in the world while increased food production utilizing soil resources is needed to meet a growing world population (Table 2.1). One estimate is that food production will need to double in 30 years since the world's population is expected to reach 9.2 billion by 2050.[31] However, approximately 25 % of all global land resources have been highly degraded or trending to high degradation, resulting in

Table 2.1 Major soil and other resource degradation in different agricultural land use types in developing countries (adapted from reference (30))

Land type	On-site soil degradation	Other resource degradation
Irrigated lands	• Salinization and waterlogging • Nutrient constraints under multiple cropping • Biological degradation (reduced soil organic matter, agrochemicals)	• Nutrient pollution in ground/surface water • Pesticide pollution • Water-borne disease • Water conflicts
High-quality rain-fed lands	• Nutrient depletion • Soil compaction and physical degradation from overcultivation, machinery • Acidification • Removal of natural vegetation, perennials • Soil erosion • Biological degradation (reduced soil organic matter, agrochemicals)	• Pesticide pollution • Deforestation
Densely populated marginal lands	• Soil erosion • Soil fertility depletion • Removal of natural vegetation, perennials • Soil compaction, physical degradation from overcultivation • Acidification	• Loss of biodiversity • Watershed degradation
Extensively managed marginal lands	• Soil erosion from land clearing • Soil erosion from crop/livestock production • Soil nutrient depletion • Weed infestation • Biological degradation from topsoil removal	• Deforestation • Loss of biodiversity • Watershed degradation
Urban and peri-urban agricultural lands	• Soil erosion from poor agricultural practices • Soil contamination from urban pollutants • Overgrazing and compaction	• Water pollution • Air pollution • Human disease vectors

reduced productivity and negative environmental consequences.[32] Examples of soil degradation include loss of soil organic matter, a decline in soil fertility and soil structure, increased erosion, salinity, acidity or alkalinity and the effects of toxic chemicals, pollutants, or excessive flooding.[1]

Society faces diverse environmental challenges that include soil resources and their management as an important component of these challenges. Current soils-related environmental issues that are being extensively researched include: biogeochemical cycling of carbon and nutrient elements such as nitrogen and phosphorus; the fate of trace elements and other inorganic and organic pollutants (e.g., pesticides, biological agents, waste products, industrial chemicals) in soils; soil erosion processes and impacts; soil greenhouse gas emissions; the impacts of climate change on soil resources; and the effects of land use on soil, air, and water quality in urban and rural areas in different regions of the world.

2.4 Issues Related to Soil Assessment and Testing

Soil assessment for improving agricultural production has a long history of development and, more recently, environmental soil testing has become a major focus of effort to monitor and provide information related to environmental contamination.[33] Other uses of soil assessment include geotechnical investigations to assess physical properties of soils for foundations and earthworks and suitability for waste treatment and drainage.

Soil testing could be defined as any physical, chemical, or biological measurement that is performed on a soil, but for agricultural testing the definition of soil testing has been broadened to include soil sampling and processing, soil analysis, interpretation of the results, and management recommendations.[34] Additional important elements in modern soil testing programs have been the use of Global Positioning System (GPS) technology to add geographic references to soil sample information, communication of soil test results to soil testing clients and offering of supporting information and decision tools through use of the World-Wide Web, and improved storage and analysis of historical soil test databases. Environmental soil testing has several of the same features as agricultural soil testing including that the tests have to be rapid, accurate, and reproducible as well as provide some information to interpret the results.[33] However, environmental soil testing often follows standardized procedures that may be officially sanctioned (e.g., by a national agency such as the U.S. Environmental Protection Agency, see http://www.epa.gov/ne/info/testmethods/) and accuracy and reproducibility are a greater priority for agricultural soil testing, which often emphasizes rapid turn-around times and lower cost procedures to allow agricultural managers to make timely decisions.

The development of state-based soil testing programs to support agriculture in the United States relied on extensive research that assisted in the selection of appropriate soil testing methods and extractants, correlated the results of soil tests with plant production to allow for the interpretation of soil test results, and provided field calibration to develop nutrient recommendations for plant production based on soil test results. Several methods have been developed to analyse soil for important soil physical, chemical, and biological properties that might affect agricultural production and soil quality (Table 2.2).

2.4.1 Representative Sampling or Monitoring with Spatial and Temporal Variation

Representative sampling or monitoring of the soil resource is a major component of soil assessment since most soil samples or monitoring points provide information on a small fraction of the total soil volume contained in a field and may only represent certain locations and depths at a specific point in time. If the soil sampling or monitoring strategy is not designed and conducted correctly based on the

Table 2.2 Common soil properties measured and examples of methods used for agricultural and soil quality assessments

Category	Soil property	Methods used[a]
Physical	• Water content	• Time domain reflectometry (TDR)
	• Bulk density	• Core or clod methods
	• Porosity	• Calculation from particle and bulk densities
	• Penetrability	• Penetrometer resistance
	• Wet aggregate stability	• Wet-sieving method
	• Soil moisture potential	• Tensiometer or pressure plates
	• Saturated hydraulic conductivity	• Constant head soil core
	• Particle size distribution	• Pipette method
	• Soil temperature	• Thermocouple thermometry
Chemical	• Soil reaction (acidity and alkalinity)	• pH meter and exchangeable acidity
	• Oxidation-reduction status	• Redox potential using probe and meter
	• Soil salinity and sodicity	• Electrical conductivity and analysis for sodium
	• Surface charge	• Sum of base cations plus exchangeable acidity
	• Soil organic matter	• Total organic carbon by combustion
	• Exchangeable cations	• Atomic absorption (AA) or inductively-coupled plasma emission (ICP) spectrometry
	• Other plant nutrients (e.g. nitrate)	• Spectrophotometry
Biological	• Microbial activity	• Measure soil microbial respiration or enzyme activity
	• Microbial diversity	• Polar lipid fatty acid analysis or molecular biological techniques
	• Active organic carbon	• Potassium permanganate-oxidizable carbon
	• Nitrogen fixation	• Acetylene reduction
	• Nitrogen mineralization	• In-situ ion exchange resins or ex-situ laboratory incubation
	• Greenhouse gas flux	• Open chamber method and gas chromatography

[a]Multiple methods are available for measurement of soil physical, chemical, and biological properties and this table lists some examples of those methods. For more complete discussion of methods of soil analysis, see the Methods of Soil Analysis series published by the Soil Science Society of America

objectives of the soil testing effort and the nature of the targeted soil properties then data and conclusions based on the soil test may be in error or misleading.

An example of an important sampling and monitoring consideration is the selection of the appropriate soil depth and soil depth increments for sampling and monitoring.

A traditional approach in soil sampling for agricultural testing is to take soil samples to the depth of cultivation (also known as the plow layer depth) which is approximately 15–20 cm with conventional tillage. However, the recommended depth for agricultural assessment of soil nitrate nitrogen is deeper, with the preplant soil nitrogen test often recommended to a depth of 60 cm and the pre-sidedress nitrate test (PSNT) to a depth of 30 cm due to the more extensive movement of nitrate in the soil profile. Environmental soil testing may require even deeper testing to determine possible leaching and lateral movement of pollutants, but shallow sampling depths (e.g., 2.5–5 cm) may also be employed in studies related to surface runoff and erosion.

Selected sample depth increments may provide additional information related to vertical variation in soil resources and are often done in uniform increments through the soil profile. Depending on the soil sampling or monitoring objectives, soil depth locations may also be selected based on known morphological differences (i.e., location and width of soil horizons) since these horizons and their different properties may have environmental significance on several processes.

Increasingly for certain soil properties more intensive temporal sampling is being sought to more accurately understand changes in those properties over time due to changes caused by diurnal, seasonal, and disturbance effects. For example, wider time intervals in sampling for assessment of cumulative soil surface greenhouse gas (i.e., carbon dioxide, nitrous oxide, and methane) emissions either over- or under-estimate these emissions compared to shorter time intervals, especially for trace gases such as nitrous oxide.[35]

Similarly, more intensive spatial soil sampling over land areas is being utilized for multiple objectives including precision agricultural management[36] and for assessment of the extent of environmental pollution.[37] More intensive spatial soil sampling provides a better understanding of variations in soil properties across landscapes caused by natural and anthropogenic processes, but the cost of sampling and analysis with the larger number of samples may make this approach cost-prohibitive and requires use of more advanced geostatistical techniques (e.g., reference (38)).

Statistical design and analysis are important components of soil sampling and evaluation, and therefore the selection of the statistical approach and the method for statistical analysis are important to consider prior to sample collection. Fuller discussion of this topic can be found in several texts including references (39) and (40).

2.4.2 Selection of Soil Analytical Methods

The selection of analytical methods for determining soil properties may vary depending on several factors including: the objectives of soil testing; the speed at which the soil analysis must be done; where the soil analysis will occur (i.e., in the field or laboratory); the native properties of the soil; whether the soil can be disturbed; the cost and speed of the analysis; the accuracy and precision of the method; any imposed requirements for standard testing and quality control procedures; the availability of information to interpret the analytical results; the

training of the person doing the analysis; the availability of analytical equipment and reagents; and the necessary time intervals between analyses. As analytical technology and methods have progressed, the capacity and speed of analysis has increased and more options have become available for non-destructive analytical procedures (e.g., remote sensing and proximal sensor technology). These analytical methods have also been linked with GPS and geographic information system (GIS) technologies to geographically reference and store analytical information and provide maps as a basis for management decisions, such as variable rate application of fertilizers in agricultural fields. The possibility of linking the results of analytical methods with other procedures (e.g., with interpretation and management steps) may also influence the selection of a specific analytical method.

A key principle for selection of analytical procedures is to identify methods that provide information on soil properties that are significant to the assessment or management objective or application. For example, selection of an appropriate chemical extractant for measuring plant-available nutrients is a critical element for agricultural soil testing.[41] As a basis of selection of the extractant, the amount of nutrient element (e.g., phosphorus) extracted should have a significant correlation with the amount of nutrient taken up by the plant or with crop performance over a critical period of time, such as the growing season. An environmental testing example is measurement of lead in soils to determine potential health hazards. Total lead contained in the soil can be determined after acid digestion, but this information would not be as significant to assessing the potential health hazard as measuring the bioavailable fraction of lead in the soil through use of dilute acid- or chelate-based soil test extractants.[33]

An associated consideration for selection of analytical methods is whether they have been extensively tested for the specific application and, if it is a new procedure, whether it has been compared to standard methods and incorporates quality control (QC) procedures. Uniform use of extensively-tested methods and QC allows for comparisons of data results collected across different studies and environments over time.

2.4.3 Associated Measurements

The collection of associated measurements (e.g., soil water content, soil temperature, soil bulk density, soil classification) in addition to the primary soil test assessment can provide valuable information for interpretation of the results as well as other applications. For example, measurements of soil carbon including total organic carbon and soil carbon fractions are often done on a weight basis, but simulation modellers of soil carbon dynamics who wish to validate their models may need the results on a volume or area basis. The measurement of soil bulk density allows for conversion of the data results from a weight to volume basis and vice versa. In addition, soil properties (e.g., biological properties) may be influenced by changes in soil temperature and water content and, therefore, these associated measurements are useful for understanding the observed results and again may help in simulation modelling.

2.4.4 Use of Soil Test Databases and Networks

Extensive soil testing information has been collected in the United States since the 1940s but maintenance of records of this information (referred to collectively as the soil testing database) has improved with the spread of computer technology since the 1970s.[42] Private and public soil testing laboratories in the United States analyse and provide recommendations for approximately 3–3.5 million soil samples annually, and therefore a large database of information is generated about soil conditions. For agricultural soil test programs, information accompanying the samples may include client information (e.g., name, address, telephone number), information regarding the soil sample (e.g., type of sample, source of sample, previous crop, previous fertilization, crop to be grown, and yield goal), results of soil or plant analyses, and plant nutrient recommendations.

Traditionally, soil testing databases have been used to examine general trends in soil nutrient levels on county, state, or regional scales and to assess the service performance of the laboratory.[42] This information can also be used by agricultural extension personnel to determine the geographic effectiveness of their efforts at promoting soil testing, identify priority issues, and to re-allocate extension resources. The relative levels of soil plant nutrients among submitted samples can also be evaluated within regions of a state or among states at the national scale, and problems associated with nutrient deficiencies or excess can be identified. For example, comparison of soil test phosphorus results among states has provided information on issues related to regions with possible phosphorus deficiency for crop growth but also on states where excessive soil test phosphorus may be an environmental issue.[43]

Currently geographically referenced soil test information is also being generated at a large-scale on agricultural land with the collection of sensor-based information, such as soil apparent electrical conductivity, in support of precision agriculture management practices. This soil test database is also being stored and could have potential uses for improving long-term management and may have commercial and research value for prediction of crop production and other uses, such as validation of computer simulation models. In addition, large-scale environmental monitoring networks (e.g., the Fluxnet network of sites examining exchanges of carbon dioxide (CO_2), water vapour, and energy between terrestrial ecosystems and the atmosphere; see http://fluxnet.ornl.gov/introduction) are posing many different challenges for existing data management systems such as the transport, storage, quality control and assurance, gap-filling and analysis of large sets of sensor-generated environmental data.[44]

Properly curating and preserving soil test information and providing the appropriate metadata associated with the collected data is especially important for large soil test datasets for which the information may have long-term value for preservation. Therefore, procedures and policies associated with the collected soil test database may need to be formulated prior to initiation of data collection to incorporate established ecoinformatics practices.[45]

2.5 Application of Proximal Soil Sensors

Various sensing methodologies play a key role in soil analysis. Optical, radiometric, mechanical, electrochemical, and other methods are commonly used in standard laboratory analyses. Some of these methods have been adapted for in-field proximal soil sensing (PSS). Proximal soil sensing has been defined as the use of field-based sensors to obtain signals from the soil when the sensor's detector is in contact with or close to (within 2 m) the soil.[46] A comprehensive review of PSS methodologies and applications was recently presented.[47]

Operation of PSS may be either stationary or mobile ("on-the-go"), and each of these two sensor deployment models may present different advantages and disadvantages. Mobile sensors are best suited to providing spatially dense, although often temporally sparse datasets. A major application of mobile PSS, as reviewed by references (48, 49), is to generate the spatially dense data needed in precision agriculture, where crop management inputs such as fertilizers and pesticides are varied spatially according to within-variation in the need for the input. Sensor response time is a key factor due to mobile operation, as are durability and reliability with respect to machine vibration.

Stationary PSS are better able to provide temporally dense data; however, the number of feasible sensing locations is often limited by the cost of multiple sensors and data recording devices. Stationary PSS are often organized in sensor arrays or networks, which may consist of multiple sensor types as well as multiple sensors of the same type. Sensors may be arranged vertically in the soil profile to collect data documenting fluxes from one depth to another or horizontally to provide some degree of spatial coverage. Applications include monitoring temporal changes in soil water content to control irrigation of crops[50] and documenting soil changes at a comprehensive ecological observatory site.[51] Signal-to-noise issues may be a concern if long leads are used in an attempt to connect sensors at multiple locations to the same datalogger. Many newer sensor networks use wireless connectivity to overcome this problem. Stability, durability, and long-term reliability under harsh ambient conditions are important considerations, particularly if sensors are to be deployed for extended periods of time.[52]

A key issue with application of soil sensors is the inherent heterogeneity of the soil mass. In part, this heterogeneity is caused by the three-phase nature of the soil and its significant biological component (see Sect. 2.2). Depending on the properties of interest, PSS data collection may need to be spatially dense, temporally dense, or both. Soil heterogeneity can cause problems for electrochemical measurements. One approach for dealing with heterogeneity is to measure the properties of interest in soil extracts.[53] However, in cases where many sensor measurements are needed to fully characterize the soil, the soil extract approach may be infeasible. Then a detailed understanding of soil heterogeneity is needed for optimal placement of stationary PSS or for developing deployment plans for mobile PSS.[51]

Below we discuss applications of electrochemical sensors to soil analysis, categorized by the type of measurement[54]: voltammetric, conductometric, or potentiometric.

2.5.1 Voltammetric Methods

A particular application of voltammetric methods to soil analysis has been in the detection of heavy metals. Heavy metals, unlike organic wastes, are non-biodegradable and can accumulate in living tissues, causing various diseases and disorders.[55] High levels of toxic elements, such as cadmium (Cd), copper (Cu), zinc (Zn), and lead (Pb) can be found in agricultural soils. They can also be found in stream systems in and around abandoned metalliferous mines due to improper disposal and management of mine wastes.[56] Moreover, rapid industrialization has become an additional source for environmental contamination by heavy metals, which originates from metal plating, mining activities, and paint manufacture. Therefore, monitoring heavy metal levels in the environment and food samples is necessary to efficiently characterize the contaminated sites and minimize the exposure of humans to heavy metal contaminated crops.

Inductively coupled argon plasma (ICP) spectrometry has been the most widely used technique used for metal determination in the environment and food crops, combined with wet or dry ashing procedures for digesting organic matter as a sample pre-treatment process.[57] Yet, such conventional methods are costly and time consuming, thereby limiting the number of samples tested in the field. Therefore, real-time, continuous analytical methods capable of detecting heavy metal ions with high temporal and spatial resolution are desirable. Recent advances in electronic technology have increased the potential for the development of portable electrochemical sensors for in-field monitoring of heavy metals.[58]

Anodic stripping voltammetry (ASV), which involves preconcentration of a metal phase, a solid electrode surface at negative potentials, and selective oxidation of each metal phase species during an anodic potential sweep, has been considered a powerful technique for detecting trace levels of heavy metals in aqueous samples due to its remarkable sensitivity, fast response, and portability.[58,59] Two basic electrode systems, a mercury-film electrode and a hanging mercury drop electrode, have been widely used in the development of ASV. Glassy carbon (GC) electrodes have been commonly used with ASV to support the mercury film, because of their wide potential window and low porosity.[60] However, the use of mercury as an electrode material, historically used in electrochemical methods of analysis for determining Cd, Pb, Cu and Zn, has been recently limited in many countries due to the toxicity of mercury itself, thereby requiring mercury-free electrodes[59,61,62] (see Chap. 16). Several researchers have reported that bismuth, which is an environmentally friendly element with very low toxicity, could be used as an alternative to mercury for ASV analysis.[59,63–65]

2.5.2 Conductometric Methods: Soil EC_a

Electrical conductivity (or its mathematical inverse, resistivity) of a soil solution is strongly correlated with total salt content. Therefore, laboratory methods involving solution or saturated paste conductivity are often used to assess soil salinity. Electrical conductivity measurements of bulk soil (designated as EC_a for apparent electrical conductivity) were also first used to assess salinity.[66] Resistivity and conductivity measurements are also useful for estimating other soil properties, as reviewed by[67] and.[68] Factors that influence EC_a include soil salinity, clay content and cation exchange capacity (CEC), clay mineralogy, soil pore size and distribution, soil moisture content, and temperature.[69,70] For saline soils, most of the variation in EC_a can be related to salt concentration.[71] In non-saline soils, conductivity variations are primarily a function of soil texture, moisture content, bulk density, and CEC.[68] The theoretical basis for the relationship between EC_a and soil physical properties has been described by a model where EC_a was a function of soil water content (both the mobile and immobile fractions), the electrical conductivity of the soil water, soil bulk density, and the electrical conductivity of the soil solid phase.[72] Later, this model was used to predict the expected correlation structure between EC_a data and multiple soil properties.[73]

Because EC_a is a function of a number of soil properties, EC_a measurements can be used to provide indirect measures of these properties if the effects of other soil properties on the EC_a measurement are known or can be estimated. In some situations, the contribution of within-field changes in one factor will be large enough with respect to variation in the other factors that EC_a can be calibrated as a direct measurement of that dominant factor. This direct calibration approach was used to quantify within-field variations in soil salinity under uniform management and where water content, bulk density, and other soil properties were "reasonably homogeneous".[74] In addition, EC_a can be calibrated to the thickness of soil layers with contrasting conductivities. Examples include EC_a regressions for the depth of flood-induced sand deposition[75] and for topsoil depth (TD) above a subsoil argillic horizon.[76–79]

Researchers have related EC_a to a number of different soil properties either within individual fields or across closely related soil landscapes. Examples include soil moisture,[80,81] clay content,[82] and CEC and exchangeable Ca and Mg.[83] Mapping of areas of differing soil texture[75] and soil type[84] have also been reported. In a project relating EC_a to multiple soil properties across a number of locations in the north-central USA, the strongest and most consistent relationships were with clay content.[78,85] When EC_a was evaluated for delineating a number of soil physical, chemical, and biological properties related to yield and ecological potential it was found useful for delimiting distinct zones of soil condition.[86] Although many soil factors affecting EC_a are relatively fixed over time (e.g., clay content), others may exhibit strong seasonal dynamics. For example, a time sequence of EC_a maps was related to temporal changes in available soil nitrogen,[87] suggesting that it might be possible to use EC_a measurements as an indicator of soluble nitrogen gains and

losses in the soil over time. Because soil EC_a integrates texture and moisture availability, two characteristics that both vary over the landscape and also affect productivity, EC_a sensing also shows promise in interpreting crop yield variations, at least in certain soils (e.g., reference (88)).

Soil EC_a has been used to assess soil environmental susceptibility. For example, EC_a was used as an estimator of the partitioning of a triazine herbicide between the soil and soil solution, which could allow mapping soil susceptibility to leaching of the herbicide.[89] Other researchers have applied EC_a data for measuring and mapping contaminant plumes, including seepage from animal waste lagoons[90] and industrial waste landfill leachate.[91]

2.5.2.1 Soil Conductivity Sensors

Two types of mobile, proximal EC_a sensors are commercially available for soil investigations, an electrode-based electrical resistivity (ER) sensor requiring soil contact and a non-contact electromagnetic induction (EMI) sensor. In the EMI approach, nominal measurement depth depends on coil orientation and operating frequency of the instrument, and is also proportional to the spacing between the coils of the sensor.[69] Most EMI instruments used for soil investigation operate at a single frequency; however, many allow multiple measurements by reorienting the sensor, or through the inclusion of multiple receiver coils. An EMI-based EC_a sensor widely used for soil investigation is the EM38 (Geonics Limited, Mississauga, Ontario, Canada), which was initially developed for root-zone salinity assessment.[92] The EM38 is a lightweight bar designed to be carried by hand and provide stationary EC_a readings. It can be operated in two orientations, providing effective measurement depths of approximately 1.5 and 0.75 m. A newer version (EM38-MK2) has multiple receiver coils, and provides simultaneous measurements at two depths. To implement mobile data acquisition, it is necessary for the user to assemble a transport mechanism and data collection system (e.g., references 77 and 93). The EMI approach is also used by the DUALEM sensors (Dualem, Inc., Milton, Ontario, Canada) which provide two or more simultaneous measurements through multiple receiver coils.

The ER sensing approach generally requires a minimum of four electrodes in direct contact with the soil, two to inject an electrical current and two others across which a voltage potential is measured. The measurement depth depends on the spacing between the electrodes. In an early implementation, EC_a was measured with a four-electrode sensor and used to create maps of soil salinity variations in a field.[94] Later, a version of the electrode-based sensor was tractor-mounted for mobile, georeferenced measurements of EC_a.[95] Several commercial sensors implementing the electrode-based approach are manufactured by Veris Technologies, Salina, Kansas, USA. Smaller models use four rolling coulters for electrodes and provide a single measurement, while larger models use six rolling coulters and provide two simultaneous EC_a measurements.[96] Another system, called GEOPHILUS ELECTRICUS, provides five simultaneous measurements.[97]

Operational advantages and disadvantages of each type of commercial proximal EC_a sensor have been summarized.[78] In addition to the widely used proximal EC_a sensors, there are also commercial penetrometer-based EC_a sensors that allow direct measurement of EC_a as a function of depth.[98,99]

2.5.3 Potentiometric Methods: Ion-Selective Electrodes

Most of the potentiometric methods employed in soil analysis are based on the use of an ion-selective electrode (ISE) with glass or a polymer membrane, or an ion-selective field effect transistor (ISFET). The ISFET has the same theoretical basis as the ISE, i.e., both ISEs and ISFETs respond selectively to a particular ion in solution according to a logarithmic relationship between the ionic activity and electric potential. The ISEs and ISFETs require recognition elements, i.e., ion-selective membranes, which are integrated with a reference electrode and enable the chemical response (ion concentration) to be converted into an electrical potential signal.[100] Due to an increased demand for the measurement of new ions, and major advances in the electronic technology required for producing multiple channel ISFETs, numerous ion-selective membranes have been developed in many areas of applied analytical chemistry, e.g., in the analysis of clinical or environmental samples.[101]

2.5.3.1 Issues in ISE/ISFET Application

There are several potential disadvantages of ISE/ISFET sensors, as compared to standard analytical methods. One is chemical interference by other ions, because ion-selective electrodes are not truly specific but respond more or less to a variety of interfering ions. To overcome interference issues, various data processing methods have been used. For example, multivariate calibration models have been proposed to allow cross responses arising from primary and interfering ions to be decoupled, thus allowing accurate determination of individual ion concentrations within mixtures.[102] In some cases, another compound can be added to suppress the interference effect. For example, Ag_2SO_4 can be used to suppress the chloride interference in nitrate sensing.[103]

Another disadvantage is degraded performance over time due to ambient environmental conditions. For example, accuracy can be reduced due to electrode response drift and biofilm accumulation caused by the presence of organic materials and soil microbial activity in environmental samples.[104] In particular, signal drift and biofilm accumulation may be a major concern when considering an in-line management system that includes continuous immersion of ISEs in solution. Particularly for in-situ applications, poor soil-electrode contact is a concern. Although good contact may be attained during installation, the range of environmental conditions encountered during operation, including soil moisture variations

and associated shrinking and swelling of the soil mass, may make it difficult to maintain the required contact. Also, the general challenges associated with environmental sensor measurements must be considered. Temperature variations, excessive moisture, electromagnetic interference, and susceptibility to damage are some of the factors that are more likely to affect field sensor measurements than laboratory measurements.

Application of ISE technology to real-time soil sensing requires continuous determination of individual ion concentrations with acceptable sensitivity and stability. In general, stability and repeatability of response are a concern in the use of an array of multiple ISEs to measure ion concentrations in a series of samples because accuracy of the measurement may be limited by drift in electrode potential over time. The use of a computer-based automatic measurement system would improve accuracy and precision because consistent control of sample preparation, sensor calibration, and data collection can reduce variability among multiple electrodes during replicate measurements.[105] Ideally, an automated sensing system would be able to periodically calibrate and rinse the electrodes and continuously measure ions of interest in the solution, while automatically introducing solutions for calibration and rinsing as well as measurement.

2.5.3.2 Application: Soil Nutrient Sensing

The soil macronutrients, nitrogen (N), phosphorus (P), and potassium (K), are essential for crop growth, and the use of commercial N, P, and K fertilizers has contributed greatly to the increased yield of agricultural crops. However, excessive fertilizer applications can lead to environmental contamination, primarily of surface and ground waters.[106] Ideally, fertilizer application should be adjusted to match the requirements for optimum crop production at each within-field location, because there can be high spatial variability in the N, P, and K levels found within fields.[107,108]

To quantify soil nutrient (i.e., N, P, and K) levels at the spatial scale needed for within-field measurements, on-the-go real-time sensors present an attractive alternative to current manual and/or laboratory methods.[109,110] Mobile sensors could provide measurements at a high spatial density and relatively low cost,[48] and with an overall accuracy potentially higher than that of conventional methods. This occurs because there are two sources of error in soil testing—analysis error due to sub-sampling and analytical determination, and sampling error due to point-to-point variation in soils. With traditional soil testing, analysis error is relatively low; however, sampling error can be substantial since cost limits the sampling intensity. Mobile sensors can provide a spatial sampling intensity several orders of magnitude greater than traditional methods. Therefore, a mobile real-time soil sensor can tolerate much higher analysis errors while providing greater overall accuracy in mapping soil variability. Reviews of soil nutrient sensing by ISE and other methods have been presented.[111,112]

2.5.3.3 Nitrate, Potassium, and Phosphate Membranes and Electrodes

Numerous nitrate ion-selective membranes (Table 2.3) have been described for various environmental applications, such as food, plants, fertilizer, soil, and wastewater. Overall, best results were obtained with PVC ion-selective membranes prepared with quaternary ammonium compounds, such as TDDA or MTDA as the sensing element. These membranes were able to determine nitrate across the concentration range important for N fertilizer application management, i.e., $10 \sim 30$ mg kg^{-1} NO_3. The best membranes also maintained acceptable selectivity levels in mixed solutions, being at least 40 times more sensitive to nitrate than to chloride and bicarbonate.

Valinomycin-based membranes (Table 2.4) have been the predominant choice for potassium sensing in soil and other environmental samples. Considerable research effort has focused on improving the adhesion of the PVC membrane to extend the consistent sensitivity period, and thus, the lifetime of the electrode. Valinomycin ionophores have exhibited strong K selectivity and sensitivity sufficient to quantify variations in the typical range in soil K where additional fertilizer is recommended.[111]

The design of an ionophore for selective recognition of phosphate has been especially challenging for several reasons. Due to the very high hydration energy of phosphate, ion selective membranes have a very poor selectivity for phosphate. The free energy of the phosphate species is very small and the large size of orthophosphate ions prohibits the use of size-exclusion principles for increased selectivity. Reviews[111,113,128] report work on various phosphate sensors, including polymer membranes based on organotin, cyclic polyamine, or uranyl salophene derivatives; protein-based biosensors; and cobalt-based electrodes (Table 2.5). A recurring problem has been the low selectivity response of such membranes toward many anions that may be present in the soil. At present, the best alternative appears to be the solid cobalt electrode, which has exhibited sufficient sensitivity, selectivity, and durability to provide a quantitative measure of phosphates in soil extracts.[141,144,145]

2.5.3.4 Laboratory Prototype Systems for Soil Nutrient Sensing

Ion selective electrodes have historically been used in soil testing laboratories to conduct standard chemical soil tests, especially soil pH measurement. Many researchers in the 1970s and 1980s concentrated on the suitability of ISEs as an alternative to routine soil nitrate testing. More recently, researchers whose end goal was a mobile macronutrient sensing system have reported on laboratory tests of components of such systems.

Nitrate and potassium ion-selective electrodes have been evaluated for use in moistened soils as opposed to soil extracts.[146] Soluble nitrate and K content of moist soil samples could be determined in the laboratory ($r^2 = 0.56 \sim 0.94$) if several limitations such as inconsistent contact between soil and electrode and

Table 2.3 Comparison of nitrate ion-selective membranes

Chemicals used	Performance factors[a]				References
	Sensitivity (mV/decade)	Linear range (M)	Detection limit (M)	Selectivity (log K_{ij})	
Tetradodecylammonium nitrate (TDDA); 2-nitrophenyl octyl ether (NPOE); high-molecular-weight polyvinyl chloride (PVC)	−63.4	$10^{-4} \sim 10^{-1}$		$Cl^- = -2.40$ $HCO_3^- = -3.29$ $HPO_4^{2-} = -3.76$ $SO_4^{2-} = -3.76$ $Ac^- = -3.48$ $Br^- = -0.81$	114
TDDA; dibutylphthalate (DBP); PVC	−56.2		8.3×10^{-7}	$Cl^- = -2.30$ $NO_2^- = -1.15$ $F^- = -3.0$ $HCO_3^- \geq -3.30$	115
Tetraoctylammonium nitrate (TOAN); triooctyl phosphonate (TOP); aliphatic urethane diacrylate Ebecryl 270 and hexanediol diacrylate (HDDA); 2-2′-dimethoxyl phenylacetophenone (Irgacure 651)	−62.6	$2.3 \times 10^{-5} \sim 6 \times 10^{-2}$	1×10^{-5}	$Cl^- = -2.0$	116
Tetraoctylammonium nitrate (TOAN); DBP; PVC Tridodecylmethylammonium nitrate (TDMAN); NPOE; PVC Ttris(4,7-diphenyl-1,10-phenanthroline) nickel(II) nitrate (TDPNN); NPOE; PVC	-54.0 ± 0.6 -56.1 ± 0.9 -55.8 ± 7.1		2.3×10^{-4} 2.8×10^{-4} 7.8×10^{-4}		117
Methyltridodecylammonium nitrate (MTDAN); methyltriphenyl phosphonium bromide; NPOE; PVC	−55.6	$10^{-4} \sim 10^{-1}$		$Cl^- = -1.45$ $HCO_3^- = -2.17$ $SO_4^{2-} = -2.74$	118
Triallydecylammonium nitrate (TDDAN); NPOE; Krynac; dicumyl peroxide (DCP)	−57.7	$1.2 \times 10^{-5} \sim 10^{-1}$	8.8×10^{-6}	$Cl^- = -4.0$ $HCO_3^- = -4.9$ $SO_4^{2-} = -5.0$	119
TDDA; NPOE; PVC	-54.9 ± 1.3	$10^{-4} \sim 10^{-1}$	10^{-5}	$Cl^- = -2.07$ $HCO_3^- = -3.22$ $Br^- = -1.03$	120

[a]Empty cells occur when data for that membrane characteristic were not provided in the reference

Table 2.4 Comparison of potassium ion-selective membranes

Chemicals used	Performance factors[a]				References
	Sensitivity (mV/decade)	Linear range (M)	Detection limit (M)	Selectivity (log K_{ij})	
Valinomycin; Benzophenonetetracarboxylic acid tetra-*n*-undecyl ester (BTCU); High-molecular-weight polyvinyl chloride (PVC)	51.7	$10^{-4} \sim 10^{-1}$		$K^+ > NH_4^+ > H^+ > Na^+ > Li^+ > Ca^{++}$	121
Valinomycin; bis (2-ethylhexyl) sebacate (DOS); PVC; potassium tetrakis(4-chlorophenyl) borate (KTpClPB)	58	$1.8 \times 10^{-5} \sim 10^{-1}$	3×10^{-6}	$Na^+ = -4.2$ $Li^+ = -4.3$	122
Valinomycin; KTpClPB; DOS; Eb270 + HDDA	55.7	$7 \times 10^{-5} \sim 0.1$	4×10^{-5}		116
Valinomycin; DOS; PVC; KTpClPB	51.5 ± 1.41	$10^{-4} \sim 10^{-1}$	10^{-4}	$Na^+ = -2.57$ $NH_4^+ = -1.63$ $Mg^{2+} = -2.94$ $Ca^{2+} = -2.88$	120
Valinomycin; Dioctyl adipate; PVC	54.88 ± 1.137	$10^{-5} \sim 10^{-1}$			123
Valinomycin; Dioctyl adipate; PVC; copolymer VAGH	53 ± 0.6		4×10^{-5}	$Na^+ = -4.0$	124
Cis-bis(15-crown-5 ether); 2-nitrophenyl octyl ether (NPOE); PVC	59		9.5×10^{-7}	$Na^+ = -3.69$ $NH_4^+ = -2.28$ $Li^+ = -4.07$ $Cs^+ = -2.25$	125
Valinomycin; dioctyl adipate; PVC	58–59				126
Valinomycin; bis(2-ethylhexyl) adipate; PVC	56 ~ 59	$10^{-5} \sim 10^{-1}$	$\sim 10^{-6}$	$Na^+ = -3.56$	127

[a]Empty cells occur when data for that membrane characteristic were not provided in the reference

Table 2.5 Comparison of phosphate ion-selective membranes and electrodes

Chemicals used	Performance factors[a]				References
	Sensitivity (mV/decade)	Linear range (M)	Detection limit (M)	Selectivity order	
Measured species: HPO_4^{2-}					
Bis(tribenzyltin) oxide; 2-nitrophenyl octyl ether (NPOE); high-molecular-weight polyvinyl chloride (PVC)	−30.1	$5 \times 10^{-6} \sim 10^{-1}$	10^{-6}	$HPO_4^{2-} > Br^- > NO_3^- > Cl^- > Ac^- > SO_4^{2-}$	129
Bis(guanidinium); HDTODAB; NPOE; PVC	−32.1		10^{-6}		130
Bis(*p*-chlorobenzyl)tin dichloride; Dibutyl sebacate; PVC; *N, N*-dimethylformamide	−33	$2.2 \times 10^{-4} \sim 1.2 \times 10^{-2}$	3.3×10^{-5}	$HPO_4^{2-} > I^- > NO_3^- > Br^- > Cl^-$	131,132
3-decyl-1,5,8-triazacyclodecane-2,4-dione (N3-cyclic amine); dibutyl sebacate; PVC	−29	$10^{-6} \sim 10^{-2}$		$HPO_4^{2-} > Cl^- > NO_3^- > SO_4^{2-}$	133

Measured species: $H_2PO_4^-$					
Bidentate organic tin compound; bis(2-ethylhexyl) sebacate (DOS); PVC	−54.6				134,135
Trialkyl/aryl-tin chloride NPOE; PVC; NaTFPB	−60	$10^{-4} \sim 10^{-1}$	7×10^{-5}		136
Uranyl salophene derivative; NPOE; PVC; tetradecy-lammonium bromide (TDAB)	−59	$10^{-4} \sim 10^{-1}$			137,138
Cobalt rod (99.99 %, 5 mm diameter) coated with Teflon	−55	$10^{-5} \sim 10^{-2}$	5×10^{-6}	$Br^- > Cl^- > SO_4^{2-} = AcO^- > NO_3^-$	139
Cobalt wire (99.99 %, 0.5 mm diameter)	-38 ± 0.5	$10^{-5} \sim 10^{-3}$	10^{-6}	$I^- > Br^- > Ac^- > Cl^- > NO_3^- > SO_4^{2}$	140–143
Cobalt rod (99.95 %, 5 mm diameter) coated with silicone and a plastic body	-32.9 ± 0.9	$10^{-4} \sim 10^{-1}$	10^{-5}	$Ac^- > HCO_3^- > Cl^- > F^- > Br^- > NO_3^-$	144

[a]Empty cells occur when data for that membrane or electrode characteristic were not provided in the reference

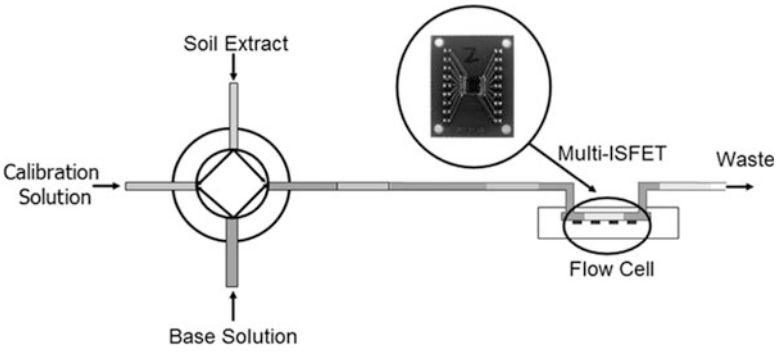

Fig. 2.4 Scheme of an ion-selective field effect transistor (ISFET)—flow injection analysis (FIA) system.[111] The soil extract sample, calibration, and base solutions are sequentially introduced through a flow injection line system with multiple inlets, and are transported to a multi-ISFET chip with outputs that continuously change due to the passage of the sample through the flow cell

potential drift due to continuous measurements were addressed. Plant-available K of 32 agricultural soils as determined by two ISEs (glass and PVC-based) was highly correlated with values from standard laboratory analysis.[147]

A multi-ISFET sensor chip was used to measure soil nitrate in a flow injection analysis (FIA) system using low flow rates, short injection times, and rapid rinsing[114,148] (Fig. 2.4). The multi-ISFET/FIA system successfully estimated soil nitrate-N content in manually prepared soil extracts ($r^2 > 0.90$) while allowing samples to be analyzed within 1.25 s with sample flow rates less than 0.2 mL s^{-1}. Later, a rapid extraction system was designed for in-field real-time measurement of soil nitrates using these ISFETs.[149] Several design parameters affecting nitrate extraction were studied. Nitrate concentration could be determined 2–5 s after injection of the extracting solution when using data descriptors based on the peak and slope of the ISFET nitrate response curve.

A sensor array including three different ISEs based on TDDA-NPOE and valinomycin-DOS membranes and cobalt rod was evaluated using an automated test stand (Fig. 2.5) to simultaneously determine NO_3-N, available K, and available P in Kelowna-soil extracts.[150] The nitrate ISE in conjunction with the Kelowna extractant[103] provided results in close agreement with the standard method. Kelowna-K ISE concentrations were about 50 % lower than those obtained with the standard method due to decreased K extraction by the Kelowna solution. Soil P concentrations obtained with the Kelowna extractant and cobalt P ISEs were about 64 % lower than those obtained by the standard method due both to a lower P extraction by the Kelowna solution, and to lower estimates of P concentrations in the extracts by the cobalt P ISEs. Although P and K concentrations were low, a calibration factor could address this issue because there was a linear relationship between ISE and standard methods ($r^2 = 0.81$ and 0.82 for P and K, respectively). In further evaluation of this system, it was possible to transfer existing calibration equations to new membranes and electrodes.[151] An adjustment for the difference in

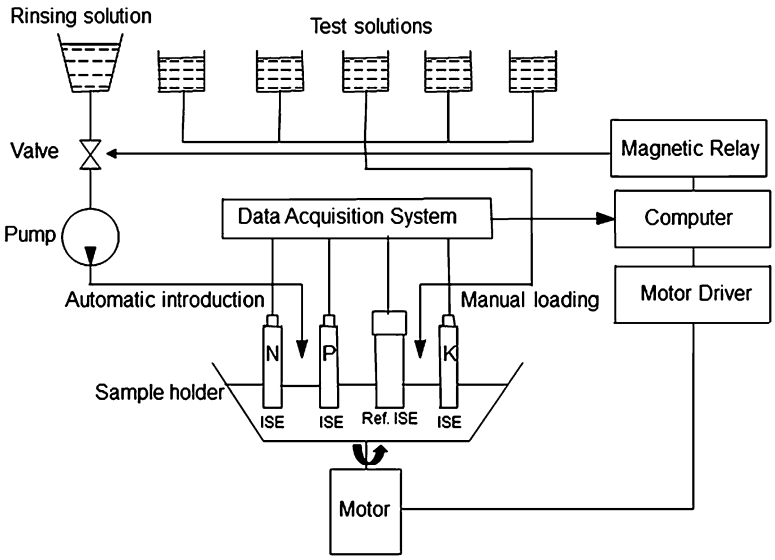

Fig. 2.5 Schematic diagram of a test stand for multiple electrode tests[151]

extraction efficiency between Kelowna and standard extractants yielded linear relationships with near 1:1 slopes between estimates and actual soil N and K values. However, a relatively large offset between calibrated ISE and standard method concentrations for P was said to require further investigation.

2.5.3.5 Field-Mobile Soil Nutrient Sensors

Beginning in the early 1990s, several prototype real-time on-the-go soil nutrient sensing systems were developed using custom-designed soil samplers and commercially available ion-selective electrodes for sensing nitrate and pH in soils. In a laboratory study nitrate level was estimated by ISE with 95 % accuracy after 6 s of measurement.[152] However, a follow-up study where the ISE was integrated into a tractor-mounted system for field measurement encountered several mechanical and electrical problems.[153] The functionality of this automated soil sampler was later improved and evaluated with comprehensive performance testing conducted in five fields. There was strong agreement between measurements of soil nitrate by the extraction system and by standard laboratory instruments (slope = 1.0, $r^2 = 0.94$).[110]

An automated sampling system for soil pH by direct soil measurement (DSM) was based on a flat-surface combination pH electrode in direct contact with moist soil collected by the sampling system.[154] There was a high correlation between the electrode voltage output and soil pH in the laboratory and field ($r^2 = 0.92$ and 0.83, respectively). The system could measure pH while taking soil samples at a pre-selected depth between 0 and 20 cm every 8 s. Based on these results, a

commercial soil pH mapping system was developed by Veris Technologies, Salina, Kansas, USA.[155] Sensor-based mapping of soil pH provided improved accuracy of lime prescription maps[156] and was used to plan variable-rate liming for eight production fields.[157] In this study a field-specific bias in overall error estimates of 0.4 pH units or greater could be reduced to less than 0.3 pH units through site-specific calibration. Additional tests of the same commercial mobile soil pH system on two fields, one with a uniform soil and the other with six different soil types, showed that the real-time system provided more accurate estimates at the 0–7.5 cm depth ($r^2 = 0.75$–0.83) than at the 7.5–15 cm depth ($r^2 = 0.53$–0.79).[158] In addition, the inclusion of EC_a as a covariable improved pH estimates in the field with six different soil types, but not the uniform field.

The DSM approach was investigated for soil K, NO_3, and Na as well as pH, but good results were only obtained for pH.[159] The reason for decreased accuracy for K, NO_3, and Na was hypothesized to be a lower level of variability of the sensed properties in the soil samples tested. Another approach was the agitated soil measurement (ASM)-based integrated system that placed ISEs into a suspension of soil and water.[160,161] The effects of various measurement parameters on sensor performance were investigated and the system was evaluated for on-the-go mapping of soil pH, soluble K, and residual NO_3 under laboratory conditions. Calibration parameters were stable during each test for pH and K electrodes. However, significant drift was observed for the NO_3 electrode. Both accuracy and precision errors were low with good correlations to the reference measurements ($r^2 = 0.67 \sim 0.98$ for means).

2.6 Future Outlook and Considerations

Soil sensing is an area of considerable research interest and activity, as documented in numerous recent reviews.[47,111,112,162] In addition to developments in the sensors themselves, other related advancements are helping further the application of PSS. For example, the ability to extract useful information from the large spatial datasets generated by mobile PSS has improved because of advances in mathematical and statistical methods. Improved electronics and imbedded computer technology, made possible by advancements in the consumer and automotive sectors, have made it possible to readily control and obtain data from sensors. Wireless data transfer from mobile PSS and wireless sensor networks for stationary PSS are now available to facilitate more seamless integration of PSS data with other measurements, computer models, and expert interpretation. These advances in data handling are particularly important when PSS data are combined for analysis across multiple sites, whether for integrated soil nutrient management across fields and farms, or to evaluate environmental changes across a network such as the National Ecological Observatory Network (NEON) in the USA.[51] Each PSS application will require consideration of particular issues. Below we discuss in detail the specific application of soil nutrient sensing.

2.6.1 Considerations in Soil Nutrient Sensing

Soil nutrient sensing is one area where the application of electrochemical sensing technology would seem to be relatively straightforward. As discussed earlier in this chapter, progress has been made on developing ion-selective elements for soil macronutrients. However, automation of the process of obtaining a representative soil sample and creating an extract for analysis requires further work. Approaches that circumvent this step and directly place ISEs in contact with moist soil have generally been unsuccessful except for soil pH. Other ways to increase accuracy, such as sensor fusion (discussed below), may hold promise. Sensor measurements must also be considered within the context of the overall nutrient management system. System issues include how well the sensed value can be calibrated against plant response to applied nutrients and how that information can be integrated into an intelligent fertilizer application system.

2.6.1.1 Sensor Fusion

There are several limitations to current on-the-go nutrient sensing systems. Although electrochemical systems can directly measure soil nutrient levels, there are implementation issues. Direct electrochemical measurement of moist soil, while shown to be viable for pH and perhaps nitrate, seems to be less feasible for the other soil macronutrients. Thus, a complex set of steps is generally needed to acquire a sample from the field, create a soil slurry or extract, and then complete the measurement. Spectroscopic sensing,[111] while less invasive, generally measures soil nutrients indirectly, through correlations with other soil properties. Thus, local calibrations are generally necessary and results have been of variable accuracy.

One potential approach for improved accuracy is sensor fusion, whereby readings from multiple, functionally different sensors are combined to estimate the soil properties of interest. For example, a commercial mobile sensor platform[163] (Fig. 2.6) combined the soil pH sensing system described in reference (155) with soil apparent electrical conductivity (EC_a) sensing. As EC_a provides a strong indication of soil texture variations,[86] the combination of the pH and EC_a data was useful for establishing lime requirements. An NIR reflectance sensor was later added to this multi-sensor platform.[164]

In a laboratory-based example of sensor fusion, both ISE and spectral reflectance data were obtained for 37 surface soil samples from the US states of Missouri and Illinois.[165] Although ISE estimates of P and K were of good accuracy ($r^2 \geq 0.87$), they were further improved ($r^2 \geq 0.95$) by including both ISE and spectral data in the calibration model. The authors attributed the increased accuracy to the ability of the spectral data to provide an estimate of soil texture.

Fig. 2.6 Commercial sensor system integrating soil electrical conductivity and pH mapping (Veris pH manager, Veris Technologies, Salina, Kansas, USA)

2.6.1.2 Sensor Calibration

Widespread adoption of on-the-go soil nutrient sensing may be somewhat limited by the degree to which precise sampling and rapid extraction of the macronutrients in the sample can be achieved in a real-time system. Because extraction efficiency is strongly affected by the extraction time and because the time required for complete extraction may not be feasible in a real-time system, this approach may provide different results as compared to traditional soil testing methods. In this regard, research will be needed to calibrate sensor-based nutrient measurements against plant nutrient response, so that agronomists and growers gain confidence in the applicability of the new methods. Such a calibration might be implemented in the same way that past calibrations to standard laboratory measurements were developed. However, this process would require numerous field experiments with different crops and soil types. An alternative method, whereby sensor measurements were directly calibrated to laboratory nutrient measurements across a broad range of conditions, might be preferable. Although the calibration to plant response would be an indirect one with this approach, it would be considerably less costly and time-consuming.

2.6.1.3 Integration with Fertilizer Application Equipment

Control decisions for variable rate application can be implemented either on-line or off-line. In the on-line, or sensor-based approach, the controlled equipment incorporates onboard sensors and the sensor data are used immediately for automatic control. In the off-line, or map-based approach, data are collected and stored in one operation, and the controlled equipment uses the information in a separate field operation. The map-based approach allows more flexibility in data manipulation and pre-processing but requires multiple field operations. Most systems currently available are map-based, but more on-line systems will likely become available as real-time sensing technologies become more mature. Hybrid systems which rely on a combination of both mapped and real-time data may also come into more widespread use.

Development and implementation of a variable-rate application system presents a number of engineering challenges. Physical connectivity and data flow in such a system can be quite complex (Fig. 2.7). The general system consists of both office tasks and vehicle tasks. Office tasks include interpreting input data, developing management plans, and determining application rate maps. Vehicle tasks include using these application rate maps in conjunction with onboard sensors and actuators to apply fertilizer, chemicals, or inputs in the field, along with any real-time sensing that may be employed. In any given system, the elements shown in this general schematic (Fig. 2.7) may not be present. For example, a system may or may not

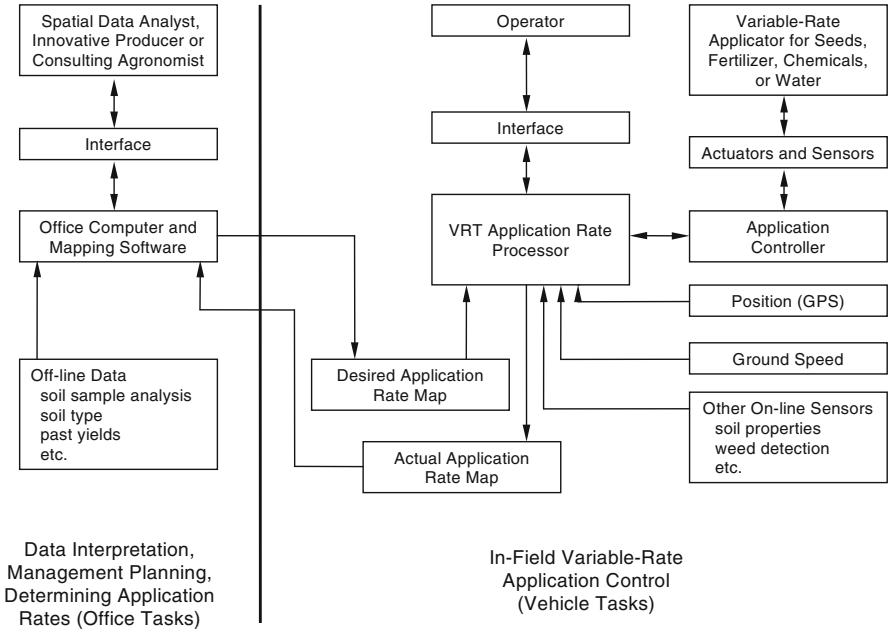

Fig. 2.7 Generalized schematic of data flow in a variable-rate application system

include on-line sensors and may or may not generate an actual application rate map. It is worth noting that the information to drive a map-based system could also come from on-the-go sensor measurements. Decoupling the sensing and application operations might make sense if sensor operating requirements, such as a long delay time for sensing nutrient levels in a soil extract, precluded sensing and application in the same operation.

References

1. Lal R, Kimble J, Follett R (1998) Pedospheric processes and the carbon cycle. In: Lal R, Kimble J, Follett R et al (eds) Soil processes and the carbon cycle. CRC Press, Boca Raton, FL, pp 1–8
2. Targulian VO, Arnold RW (2010) Pedosphere. In: Jorgensen SE (ed) Global ecology: a derivative of encyclopedia of ecology. Academic, Amsterdam, pp 83–88
3. Birkeland PW (1984) Soils and geomorphology. Oxford University Press, New York
4. Wysocki DA, Schoenberger PJ, LaGarry HE (2000) Geomorphology of soil landscapes. In: Sumner ME (ed) Handbook of soil science. CRC Press, Boca Raton, FL, pp E5–E39
5. Natural Resources Conservation Service (2013) Soil formation and classification. U.S. Dept of Agriculture. http://www.nrcs.usda.gov/wps/portal/nrcs/detail/national/soils/?cid = nrcs142p2_054278. Accessed 16 Dec 2013
6. Wilding LP (2000) Pedology. In: Sumner ME (ed) Handbook of soil science. CRC Press, Boca Raton, FL, pp E1–E4
7. Lin H, Bouma J, Wilding LP et al (2005) Advances in hydropedology. Adv Agron 85:1–89
8. Gee GW, Or D (2002) Particle-size analysis. In: Dane JH, Topp GC (eds) Methods of soil analysis: Part 4 physical methods. Soil Science Society of America, Madison, WI, pp 255–293
9. Goldberg S, Lebron I, Suarez DL (2000) Soil colloidal behavior. In: Sumner ME (ed) Handbook of soil science. CRC Press, Boca Raton, FL, pp B195–B263
10. Six J, Bossuyt H, Degryze S et al (2004) A history of research on the link between (micro) aggregates, soil biota, and soil organic matter dynamics. Soil Till Res 79:7–31
11. Cameron KC, Buchan GD (2006) Porosity and pore size distribution. In: Lal R (ed) Encylopedia of soil science, vol 2, 2nd edn. Taylor & Francis, New York, pp 1350–1353
12. Anderson SH, Gantzer CJ, Brown JR (1990) Soil physical properties after 100 years of continuous cultivation. J Soil Water Conserv 45:117–121
13. Clothier BE (2008) Soil pores. In: Chesworth W (ed) Encyclopedia of soil science. Springer, Dordrecht, pp 693–698
14. Nannipieri P, Ascher J, Ceccherini MT et al (2003) Microbial diversity and soil functions. Eur J Soil Sci 54:655–670
15. Dunbar J, Barns SM, Ticknor LO et al (2002) Empirical and theoretical bacterial diversity in four Arizona soils. Appl Environ Microbiol 68:3035–3045
16. Paul EA, Clark FE (1989) Soil microbiology and biochemistry. Academic, San Diego
17. Natural Resources Conservation Service (2011) Soil quality for environmental health. U.S. Dept. of Agriculture. http://soilquality.org/home.html. Accessed 16 Dec 2013
18. Borchardt MA, Bertz PD, Spencer SK et al (2003) Incidence of enteric viruses in groundwater from household wells in Wisconsin. Appl Environ Microbiol 69:1172–1180
19. Swift MJ, Heal OW, Anderson JM (1979) Decomposition in terrestrial ecosystems, vol 5, Studies in ecology. University of California Press, Berkley
20. Miller RM (1996) Biological processes affecting contaminant fate and transport. In: Pepper IL, Gerba CP, Brusseau ML (eds) Pollution science. Academic, New York, pp 77–91

21. Stevenson FJ (1986) Cycles of soil: carbon, nitrogen, phosphorus, sulfur, micronutrients. Wiley, New York
22. Gregorich EG, Janzen HH (2000) Decomposition. In: Sumner ME (ed) Handbook of soil science. CRC Press, Boca Raton, FL, pp C107–C120
23. Anderson JM, Flanagan PW (1989) Biological processes regulating organic matter dynamics in tropical soils. In: Coleman DC, Oades JM, Uehara G (eds) Dynamics of soil organic matter in tropical ecosystem. University of Hawaii, Honolulu, pp 97–123
24. Motavalli PP, Palm CA, Parton WJ et al (1995) Soil pH and organic C dynamics in tropical forest soils: evidence from laboratory and simulation studies. Soil Biol Biochem 27:1589–1599
25. Christensen BT (1996) Matching measurable soil organic matter fractions with conceptual pools in simulation models of carbon turnover: revision of model structure. In: Powlson DS, Smith P, Smith JU (eds) Evaluation of soil organic matter models: using existing long-term datasets, NATO ASI Series I, global environmental change. Springer, Berlin, pp 143–159
26. Boudot JP, Brahim ABH, Chone T (1988) Dependence of carbon and nitrogen mineralization rates upon amorphous metallic constituents and allophanes in highland soils. Geoderma 42:245–260
27. Oades JM (1988) The retention of organic matter in soils. Biogeochemistry 5:35–70
28. Burke IC, Yonker CM, Parton WJ et al (1989) Texture, climate, and cultivation effects on soil organic matter content in U.S. grassland soils. Soil Sci Soc Am J 53:800–805
29. Condron LM, Tiessen H, Trassar-Cepda C et al (1993) Effects of liming on organic matter decomposition and phosphorus extractability in an acid humic Ranker soil from Northwest Spain. Biol Fert Soils 15:279–284
30. Scherr SJ (1999) Soil degradation: a threat to developing country food security by 2020. Food, agriculture and the environment discussion paper 27. International Food Policy Research Institute, Washington
31. Glenn JC, Gordon TJ, Florescu E (2008) The millennium project: state of the future. World Federation of UN Associations, Washington
32. FAO (2011) The state of the world's land and water resources for food and agriculture: managing systems at risk. Earthscan Publications, New York
33. Pierzynski GM, Sims JT, Vance GF (2005) Soils and environmental quality. CRC Press, Boca Raton, FL
34. Melsted SW, Peck TR (1973) The principles of soil testing. In: Walsh LM, Beaton JD (eds) Soil testing and plant analysis. Soil Science Society of America, Madison, WI, pp 13–21
35. Parkin TB (2008) Effect of sampling frequency on estimates of cumulative nitrous oxide emissions. J Environ Qual 37:1390–1395
36. Gebbers R, Adamchuk VI (2010) Precision agriculture and food security. Science 327:828–831
37. Xie Y, Chen T, Lei M et al (2011) Spatial distribution of soil heavy metal pollution estimated by different interpolation methods: accuracy and uncertainty analysis. Chemosphere 82:468–476
38. Lakhankar T, Jones AS, Combs CL et al (2010) Analysis of large scale spatial variability of soil moisture using a geostatistical method. Sensors 10:913–932
39. Webster R, Oliver MA (1990) Statistical methods in soil and land resource survey. Oxford University Press, Oxford
40. Webster R, Oliver MA (2007) Geostatistics for environmental scientists, 2nd edn. Wiley, West Sussex
41. Corey RB (1987) Soil test procedures: correlations. In: Brown J (ed) Soil testing: sampling, correlation, calibration, and interpretation. Soil Science Society of America, Madison, WI, pp 15–22
42. Motavalli PP, Lory JA, Nathan MV et al (2002) Increased access to soil testing databases through the world wide web: opportunities and issues. Commun Soil Sci Plant Anal 33:1157–1171
43. Fixen PE (2002) Soil test levels in North America. Better Crops 86:12–15
44. Porter JH, Hanson PC, Lin C (2012) Staying afloat in the sensor data deluge. Trends Ecol Evol 27:121–129

45. Michener WK, Jones MB (2012) Ecoinformatics: supporting ecology as a data-intensive science. Trends Ecol Evol 27:85–93
46. Viscarra Rossel RA, McBratney AB (1998) Laboratory evaluation of a proximal sensing technique for simultaneous measurement of clay and water content. Geoderma 85:19–39
47. Viscarra Rossel RA, Adamchuk VI, Sudduth KA et al (2012) Proximal soil sensing: an effective approach for soil measurements in space and time. Adv Agron 113:237–282
48. Adamchuk VI, Hummel JW, Morgan MT et al (2004) On-the-go soil sensors for precision agriculture. Comp Electron Agric 44:71–91
49. Sudduth KA, Hummel JW, Birrell SJ (1997) Sensors for site-specific management. In: Pierce FJ, Sadler EJ (eds) The state of site-specific management for agriculture. ASA, CSSA, and SSSA, Madison, WI, pp 183–210
50. Vellidis G, Tucker M, Perry C et al (2008) A real-time wireless smart sensor array for scheduling irrigation. Comp Electron Agric 61:44–50
51. Rundel PW, Graham EA, Allen MF et al (2009) Environmental sensor networks in ecological research. New Phytologist 182:589–607
52. Unger IM, Muzika RM, Motavalli PP et al (2008) Evaluation of continuous in situ monitoring of soil changes with varying flooding regimes. Commun Soil Sci Plant Anal 39:1600–1619
53. Bieganowski A, Ciesla J (2011) Electrochemical measurements in soils. In: Glinski J, Horabik J, Lipiec J (eds) Encyclopedia of agrophysics. Springer, Dordrecht, pp 260–264
54. Brett CMA (2001) Electrochemical sensors for environmental monitoring: strategy and examples. Pure Appl Chem 73(12):1969–1977
55. Wan Ngah WS, Hanafiah MAKM (2008) Removal of heavy metal ions from wastewater by chemically modified plant wastes as adsorbents: a review. Biores Technol 99(10):3935–3948
56. Jung MC (2001) Heavy metal contamination of soils and waters in and around the Imcheon Au–Ag mine, Korea. Appl Geochem 16(11–12):1369–1375
57. Hanrahan G, Patil DG, Wang J (2004) Electrochemical sensors for environmental monitoring: design, development and applications. J Environ Monit 6(8):657–664
58. Cooper J, Bolbot JA, Saini S et al (2007) Electrochemical method for the rapid on site screening of cadmium and lead in soil and water samples. Water Air Soil Pollut 179 (1):183–195
59. Wang J (2005) Stripping analysis at bismuth electrodes: a review. Electroanalysis 17(15–16):1341–1346
60. Wang J, Tian B, Rogers KR (1998) Thick-film electrochemical immunosensor based on stripping potentiometric detection of a metal ion label. Anal Chem 70:1682–1685
61. Banks CE, Hyde ME, Tomcik P et al (2004) Cadmium detection via boron-doped diamond electrodes: surfactant inhibited stripping voltammetry. Talanta 62:279–286
62. McGaw EA, Swain GM (2006) A comparison of boron-doped diamond thin-film and Hg-coated glassy carbon electrodes for anodic stripping voltammetric determination of heavy metals in aqueous media. Anal Chim Acta 575:180–189
63. Kachoosangi RT, Banks CE, Ji X et al (2007) Electroanalytical determination of cadmium (II) and lead(II) using an in-situ bismuth film modified edge plane pyrolytic graphite electrode. Anal Sci 23:283–289
64. Kefala G, Economou A, Voulgaropoulos A et al (2003) A study of bismuth-film electrodes for the detection of trace metals by anodic stripping voltammetry and their application to the determination of Pb and Zn in tapwater and human hair. Talanta 61:603–610
65. Wang J, Lu J, Hocevar SB et al (2000) Bismuth-coated carbon electrodes for anodic stripping voltammetry. Anal Chem 72:3218–3222
66. Rhoades JD, van Schilfgaarde J (1976) An electrical conductivity probe for determining soil salinity. Soil Sci Soc Am J 40:647–651
67. Samouelian A, Cousin I, Tabbagh A et al (2005) Electrical resistivity survey in soil science: a review. Soil Till Res 83:173–193
68. Corwin DL, Lesch SM (2005) Apparent soil electrical conductivity measurements in agriculture. Comp Electron Agric 46:11–43

69. McNeill JD (1992) Rapid, accurate mapping of soil salinity by electromagnetic ground conductivity meters. In: Advances in measurement of soil physical properties: bringing theory into practice. Soil Science Society of America, Madison, WI, pp 209–229
70. Rhoades JD, Corwin DL, Lesch SM (1999) Geospatial measurements of soil electrical conductivity to assess soil salinity and diffuse salt loading from irrigation. In: Corwin DL (ed) Assessment of non-point source pollution in the vadose zone. American Geophysical Union, Washington, DC, pp 197–215
71. Williams BG, Baker GC (1982) An electromagnetic induction technique for reconnaissance surveys of soil salinity hazards. Aust J Soil Res 20:107–118
72. Rhoades JD, Manteghi NA, Shrouse PJ et al (1989) Soil electrical conductivity and soil salinity: new formulations and calibrations. Soil Sci Soc Am J 53:433–439
73. Lesch SM, Corwin DL (2003) Using the dual-pathway parallel conductance model to determine how different soil properties influence conductivity survey data. Agron J 95:365–379
74. Lesch SM, Strauss DJ, Rhoades JD (1995) Spatial prediction of soil salinity using electromagnetic induction techniques: 2. An efficient spatial sampling algorithm suitable for multiple linear regression model identification and estimation. Water Resour Res 31:387–398
75. Kitchen NR, Sudduth KA, Drummond ST (1996) Mapping of sand deposition from 1993 midwest floods with electromagnetic induction measurements. J Soil Water Conserv 51 (4):336–340
76. Doolittle JA, Sudduth KA, Kitchen NR et al (1994) Estimating depths to claypans using electromagnetic induction methods. J Soil Water Conserv 49(6):572–575
77. Sudduth KA, Drummond ST, Kitchen NR (2001) Accuracy issues in electromagnetic induction sensing of soil electrical conductivity for precision agriculture. Comp Electron Agric 31:239–264
78. Sudduth KA, Kitchen NR, Bollero GA et al (2003) Comparison of electromagnetic induction and direct sensing of soil electrical conductivity. Agron J 95:472–482
79. Sudduth KA, Kitchen NR, Myers DB et al (2010) Mapping depth to argillic soil horizons using apparent electrical conductivity. J Environ Eng Geophysics 15:135–146
80. Kachanoski RG, Gregorich EG, Van Wesenbeeck IJ (1988) Estimating spatial variations of soil water content using noncontacting electromagnetic inductive methods. Can J Soil Sci 68:715–722
81. Sheets KR, Hendrickx JMH (1995) Noninvasive soil water content measurement using electromagnetic induction. Water Resour Res 31(10):2401–2409
82. Williams BG, Hoey D (1987) The use of electromagnetic induction to detect the spatial variability of the salt and clay contents of soils. Aust J Soil Res 25:21–27
83. McBride RA, Gordon AM, Shrive SC (1990) Estimating forest soil quality from terrain measurements of apparent electrical conductivity. Soil Sci Soc Am J 54:290–293
84. Anderson-Cook CM, Alley MM, Roygard JKF et al (2002) Differentiating soil types using electromagnetic conductivity and crop yield maps. Soil Sci Soc Am J 66:1562–1570
85. Sudduth KA, Kitchen NR, Wiebold WJ et al (2005) Relating apparent electrical conductivity to soil properties across the north-central USA. Comp Electron Agric 46:263–283
86. Johnson CK, Doran JW, Duke HR et al (2001) Field-scale electrical conductivity mapping for delineating soil condition. Soil Sci Soc Am J 65:1829–1837
87. Eigenberg RA, Doran JW, Nienaber JA et al (2002) Electrical conductivity monitoring of soil condition and available N with animal manure and a cover crop. Agric Ecosys Environ 88:183–193
88. Kitchen NR, Sudduth KA, Drummond ST (1999) Soil electrical conductivity as a crop productivity measure for claypan soils. J Prod Agric 12:607–617
89. Jaynes DB, Novak JM, Moorman TB et al (1995) Estimating herbicide partition coefficients from electromagnetic induction measurements. J Environ Qual 24:36–41
90. Brune DE, Doolittle JA (1990) Locating lagoon seepage with radar and electromagnetic survey. Environ Geol Water Sci 16(3):195–207

91. Yoon GL, Park JB (2001) Sensitivity of leachate and fine contents on electrical resistivity variations of sandy soils. J Hazard Mater B84:147–161
92. Rhoades JD, Corwin DL (1981) Determining soil electrical conductivity-depth relations using an inductive electromagnetic soil conductivity meter. Soil Sci Soc Am J 45:255–260
93. Cannon ME, McKenzie RC, Lachapelle G (1994) Soil salinity mapping with electromagnetic induction and satellite-based navigation methods. Can J Soil Sci 74:335–343
94. Halvorson AD, Rhoades JD (1976) Field mapping soil conductivity to delineate dryland saline seeps with four-electrode technique. Soil Sci Soc Am J 40:571–575
95. Rhoades JD (1993) Electrical conductivity methods for measuring and mapping soil salinity. Adv Agron 49:201–251
96. Lund ED, Christy CD, Drummond PE (1999) Practical applications of soil electrical conductivity mapping. In: Stafford JV (ed) Precision agriculture'99: proceedings of the second European conference on precision agriculture. Sheffield Academic Press, Sheffield, pp 771–779
97. Lueck E, Ruehlmann J (2013) Resistivity mapping with GEOPHILLUS ELECTRICUS—Information about lateral and vertical soil heterogeneity. Geoderma 199:2–11
98. Sudduth KA, Myers DB, Kitchen NR et al (2013) Modeling soil electrical conductivity-depth relationships with data from proximal and penetrating ECa sensors. Geoderma 199:12–21
99. Kweon GY, Lund E, Maxton C et al (2009) Soil profile measurement of carbon contents using a probe-type vis-NIR spectrophotometer. J Biosyst Eng 34:382–389
100. Eggins BR (2002) Chemical sensors and biosensors. Wiley, West Sussex
101. Bakker E (2004) Electrochemical sensors. Anal Chem 76:3285–3298
102. Forster RJ, Regan F, Diamond D (1991) Modeling of potentiometric electrode arrays for multicomponent analysis. Anal Chem 63(9):876–882
103. Van Lierop W (1986) Soil nitrate determination using the Kelowna multiple element extractant. Commun Soil Sci Plant Anal 17(12):1311–1329
104. Cloutier GR, Dixon MA, Arnold KE (1997) Evaluation of sensor technologies for automated control of nutrient solutions in life support systems using higher plants. In Proceedings of the sixth European symposium on space environmental control systems, Noordwijk, the Netherlands
105. Dorneanu SA, Coman V, Popescu IC et al (2005) Computer-controlled system for ISEs automatic calibration. Sensors Actuators B 105:521–531
106. Vadas PA, Kleinman PJA, Sharpley AN (2004) A simple method to predict dissolved phosphorus in runoff from surface-applied manures. J Environ Qual 33:749–756
107. Page T, Haygarth PM, Beven KJ et al (2005) Spatial variability of soil phosphorus in relation to the topographic index and critical source areas: sampling for assessing risk to water quality. J Environ Qual 34:2263–2277
108. Ruffo ML, Bollero GA, Hoeft RG et al (2005) Spatial variability of the Illinois soil nitrogen test: implications for soil sampling. Agron J 97:1485–1492
109. Schirrmann M, Gebbers R, Kramer E et al (2011) Soil pH mapping with an on-the-go sensor. Sensors 11(1):573–598
110. Sibley KJ, Astatkie T, Brewster G et al (2009) Field-scale validation of an automated soil nitrate extraction and measurement system. Precis Agric 10(2):162–174
111. Kim HJ, Sudduth KA, Hummel JW (2009) Soil macronutrient sensing for precision agriculture. J Environ Monit 11:1810–1824
112. Sinfield JV, Fagerman D, Colic O (2010) Evaluation of sensing technologies for on-the-go detection of macro-nutrients in cultivated soils. Comp Electron Agric 70:1–18
113. Buhlmann P, Pretsch E, Bakker E (1998) Carrier-based ion-selective electrodes and bulk optodes. 2. Ionophores for potentiometric and optical sensors. Chem Rev 98:1593–1687
114. Birrell SJ, Hummel JW (2000) Membrane selection and ISFET configuration evaluation for soil nitrate sensing. Trans ASAE 43(2):197–206
115. Nielson HJ, Hansen EH (1976) New nitrate ion-selective electrodes based on quaternary ammonium compounds in nonporous polymer membranes. Anal Chim Acta 85(1):1–16

116. Artigas J, Beltran A, Jimenez C et al (2001) Application of ion selective field effect transistor based sensors to soil analysis. Comp Electron Agric 31(3):281–293
117. Gallardo J, Alegret S, Valle MD (2004) A flow-injection electronic tongue based on potentiometric sensors for the determination of nitrate in the presence of chloride. Sensors Actuators B 101:72–80
118. Miller AJ, Zhen RG (1991) Measurement of intracellular nitrate concentration in Chara using nitrate-selective microelectrodes. Planta 184:47–52
119. Sutton PG, Braven J, Ebdon L et al (1999) Development of a sensitive nitrate-selective electrode for on-site use in fresh waters. Analyst 124:877–882
120. Kim HJ, Hummel JW, Birrell SJ (2006) Evaluation of nitrate and potassium ion-selective membranes for soil macronutrient sensing. Trans ASABE 49(3):597–606
121. Tsukada K, Sebata M, Miyahara Y et al (1989) Long-life multiple-ISFETs with polymeric gates. Sensors Actuators 18(3–4):329–336
122. Knoll M, Cammann K, Dumschat C et al (1994) Microfibre matrix-supported ion-selective PVC membranes. Sensors Actuators B 20(1):1–5
123. Moody GJ, Slater JM, Thomas JDR (1988) Membrane design and photocuring encapsulation of flatpack based ion-selective field effect transistors. Analyst 113:103–108
124. Moody GJ, Thomas JDR, Slater JM (1988) Modified poly (vinyl chloride) matrix membranes for ion-selective field effect transistor sensors. Analyst 113:1703–1707
125. Oh KC, Kang EC, Cho YL et al (1998) Potassium-selective PVC membrane electrodes based on newly synthesized cis-and trans-bis (crown ether)s. Anal Sci 14:1009–1012
126. Sibbald A, Whalley PD, Covington AK (1984) A miniature flow-through cell with a four-function chemfet integrated circuit for simultaneous measurements of potassium, hydrogen, calcium and sodium ions. Anal Chim Acta 159:47–62
127. Bae YM, Cho SI (2002) Response of polymer membranes as sensing elements for an electronic tongue. Trans ASAE 45(5):1511–1518
128. Engblom SO (1998) The phosphate sensor. Biosens Bioelectron 13(9):981–994
129. Liu D, Chen WC, Yang RH et al (1997) Polymeric membrane phosphate sensitive electrode based on binuclear organotin compound. Anal Chim Acta 338:209–214
130. Fibbioli M, Berger M, Schmidtchen FP et al (2000) Polymeric membrane electrodes for monohydrogen phosphate and sulfate. Anal Chem 72(1):156–160
131. Glazier SA, Arnold MA (1988) Phosphate-selective polymer membrane electrode. Anal Chem 60:2540–2542
132. Glazier SA, Arnold MA (1991) Selectivity of membrane electrodes based on derivatives of dibenzyltin dichloride. Anal Chem 63(8):754–759
133. Carey CM, Riggan WB (1994) Cyclic polyamine ionophores for use in a dibasic-phosphate-selective electrode. Anal Chem 66(21):3587–3591
134. Tsagatakis JK, Chaniotakis NA, Jurkschat K (1994) Multiorganyltin compounds—designing a novel phosphate-selective carrier. Helv Chim Acta 77(8):2191–2196
135. Tsagkatakis I, Chaniotakis N, Altmann R et al (2001) Phosphate-binding characteristics and selectivity studies of bifunctional organotin carriers. Helv Chim Acta 84(7):1952–1961
136. Sasaki S, Ozawa S, Citterio D et al (2004) Organic tin compounds combined with anionic additives—an ionophore system leading to a phosphate ion-selective electrode. Talanta 63 (1):131–134
137. Wroblewski W, Wojciechowski K, Dybko A et al (2000) Uranyl salophenes as ionophores for phosphate-selective electrodes. Sensors Actuators B 68(1–3):313–318
138. Wroblewski W, Wojciechowski K, Dybko A et al (2001) Durable phosphate-selective electrodes based on uranyl salophenes. Anal Chim Acta 432:79–88
139. Xiao D, Yuan HY, Li J et al (1995) Surface-modified cobalt-based sensor as a phosphate-sensitive electrode. Anal Chem 67:288–291
140. Chen ZL, De Marco R, Alexander PW (1997) Flow-injection potentiometric detection of phosphates using a metallic cobalt wire ion-selective electrode. Anal Commun 34(3):93–95

141. Chen ZL, Grierson P, Adams MA (1998) Direct determination of phosphate in soil extracts by potentiometric flow injection using a cobalt wire electrode. Anal Chim Acta 363(2–3):191–197
142. De Marco R, Pejcic B, Chen ZL (1998) Flow injection potentiometric determination of phosphate in waste waters and fertilizers using a cobalt wire ion-selective electrode. Analyst 123(7):1635–1640
143. De Marco R, Phan C (2003) Determination of phosphate in hydroponic nutrient solutions using flow injection potentiometry and a cobalt-wire phosphate ion-selective electrode. Talanta 60(6):1215–1221
144. Kim HJ, Hummel JW, Sudduth KA et al (2007) Evaluation of phosphate ion-selective membranes and cobalt-based electrodes for soil nutrient sensing. Trans ASABE 50(2):215–225
145. Engblom SO (1999) Determination of inorganic phosphate in a soil extract using a cobalt electrode. Plant Soil 206(2):173–179
146. Adamchuk VI (2002) Feasibility of on-the-go mapping of soil nitrate and potassium using ion-selective electrodes. Paper 02-1183. American Society of Agricultural and Biological Engineers, St. Joseph, MI
147. Brouder SM, Thom M, Adamchuk VI et al (2003) Potential uses of ion-selective potassium electrodes in soil fertility management. Commun Soil Sci Plant Anal 34:2699–2726
148. Birrell SJ, Hummel JW (2001) Real-time multi ISFET/FIA soil analysis system with automatic sample extraction. Comp Electron Agric 32(1):45–67
149. Price RR, Hummel JW, Birrell SJ et al (2003) Rapid nitrate analysis of soil cores using ISFETs. Trans ASAE 46(3):601–610
150. Kim HJ, Hummel JW, Sudduth KA et al (2007) Simultaneous analysis of soil macronutrients using ion-selective electrodes. Soil Sci Soc Am J 71(6):1867–1877
151. Kim HJ, Sudduth KA, Hummel JW et al (2013) Validation testing of a soil macronutrient sensing system. Trans ASABE 56(1):23–31
152. Thottan J, Adsett JF, Sibley KJ et al (1994) Laboratory evaluation of the ion selective electrode for use in an automated soil nitrate monitoring system. Commun Soil Sci Plant Anal 25(17–18):3025–3034
153. Adsett JF, Thottan JA, Sibley KJ (1999) Development of an automatic on-the-go soil nitrate monitoring system. Appl Eng Agric 15(4):351–356
154. Adamchuk VI, Morgan MT, Ess DR (1999) An automated sampling system for measuring soil pH. Trans ASAE 42(4):885–891
155. Collings K, Christy C, Lund E et al (2003) Developing an automated soil pH mapping system. Paper MC03-205. American Society of Agricultural and Biological Engineers, St. Joseph, MI
156. Lund ED, Collings KL, Drummond PE et al (2004) Managing pH variability with on-the-go pH mapping. In Proceedings of the seventh international conference on precision agriculture. ASA, CSSA, and SSSA, Madison, WI
157. Adamchuk VI, Lund ED, Reed TM et al (2007) Evaluation of an on-the-go technology for soil pH mapping. Precis Agric 8:139–149
158. Staggenborg SA, Carignano M, Haag L (2007) Predicting soil pH and buffer pH in situ with a real-time sensor. Agron J 99:854–861
159. Adamchuk VI, Lund ED, Sethuramasamyraja B et al (2005) Direct measurement of soil chemical properties on-the-go using ion-selective electrodes. Comp Electron Agric 48:272–294
160. Sethuramasamyraja B, Adamchuk VI, Dobermann A et al (2008) Agitated soil measurement method for integrated on-the-go mapping of soil pH, potassium and nitrate contents. Comp Electron Agric 60(2):212–225
161. Sethuramasamyraja B, Adamchuk VI, Marx DB et al (2007) Analysis of an ion-selective electrode based methodology for integrated on-the-go mapping of soil pH, potassium, and nitrate contents. Trans ASABE 50:1927–1935
162. Kuang B, Mahmood HS, Quraishi MZ et al (2012) Sensing soil properties in the laboratory, in situ, and on-line: a review. Adv Agron 114:155–223

163. Christy CD, Collings K, Drummond P et al (2004) A mobile sensor platform for measurement of soil pH and buffering. Paper 041042. American Society of Agricultural and Biological Engineers, St. Joseph, MI
164. Christy CD (2008) Real-time measurement of soil attributes using on-the-go near infrared reflectance spectroscopy. Comp Electron Agric 61:10–19
165. La WJ, Sudduth KA, Chung SO et al (2008) Spectral reflectance estimates of surface soil physical and chemical properties. Paper 084242. American Society of Agricultural and Biological Engineers, St. Joseph, MI

Chapter 3
Water

Eduardo Pinilla Gil

3.1 Introduction

Water is a key matrix to understand and manage environmental phenomena, e.g. pollutant dynamics, geochemical processes or climate studies. Moreover, an adequate supply of good-quality water is a strategic resource for human development and well-being. In this context, accurate and representative analytical information about chemical composition of water is essential for correct assessment, interpretation, and solving of environmental problems. Whereas standardised, lab-based analytical methodologies are still dominant in water analysis, chemical sensors and particularly electrochemical sensors are growing as advantageous alternatives to develop simplified and miniaturised analytical tools applicable for flexible, decentralised measurements capable of providing improved spatial and temporal data resolution that is essential in environmental monitoring. In this chapter, we'll discuss first the fundamental aspects of environmental water chemistry and how this chemistry is linked to relevant chemical substances most often analysed in the context of environmental studies, with special attention to pollutants. Then, we'll summarise main concepts about environmental water analysis with special focus on methodological aspects. Finally, we'll discuss the use of electrochemical sensors for water analysis, including the present status and future prospects about the application of electroanalytical sensing approaches to water component determination and speciation, including relevant inorganic, organometallic and organic substances.

E.P. Gil (✉)
Faculty of Sciences, Department of Analytical Chemistry,
University of Extremadura, Badajoz, Spain
e-mail: epinilla@unex.es

L.M. Moretto, K. Kalcher (eds.), *Environmental Analysis by Electrochemical Sensors and Biosensors*, DOI 10.1007/978-1-4939-0676-5_3

3.2 Water Chemistry: Environmental Relevance

3.2.1 Chemical Processes in Ambient Water

Water, as the universal solvent in the environment, can dissolve in some extent virtually all organic and inorganic substances, but it can also sweep along liquid droplets, coarse and fine particulates, microorganisms and other biological entities. This results in a complex composition that is affected by a dynamic mix of physicochemical and biological interactions. A detailed knowledge of these interactions is advisable for proper development and application of sensor-based analytical methods in this media. Not only water body processes are to be considered, but also the interfacial behaviour of water bodies with the atmosphere (gas exchange) and with solid surroundings (leaching and uptake at soil, sediments, water body bottoms and so on). Moreover, aquatic processes are rarely at equilibrium, so consideration of kinetic aspects in addition to thermodynamic constants is also necessary. Relevant aquatic processes that regulate water composition are visualised in Fig. 3.1; a detailed discussion of these processes is out of the scope of this book, so we'll give only a brief outlook of them with special emphasis on complexation and oxidation-reaction, which are probably the most relevant processes in connexion to environmental analysis of water. The reader is referred to authoritative treatises on Environmental Chemistry as Manahan[1] for a comprehensive discussion about aquatic chemistry.

Gas–liquid–aerosol equilibria in the lower troposphere determine the composition of wet atmospheric precipitation. The most relevant process in the context of precipitation analysis is the solubilisation of airborne gaseous substances and particulates that are in this way deposited to soils and water bodies. For example primary emissions of SO_2 and NO_x are converted to SO_4^{2-} and NO_3^- by atmospheric processes and then swept to the earth's surface by wet deposition as acids (acid rain) or salts (e.g. eutrophicating NH_4HSO_4 and NH_4NO_3).

The most important process related to gas exchange at water surface is O_2 and CO_2 transfer. The atmosphere is the main supply of water-dissolved oxygen when it is consumed by water sinks, especially the microorganism-mediated degradation of organic matter, but the maximum concentration of oxygen in water in equilibrium with air at 25 °C is limited to 8.32 mg/L, so the oxygen content of 1 L of water saturated with oxygen can degrade only 7–8 mg of organic matter. Any significant excess of reducible pollutants can easily cause oxygen depletion representing a main cause of poor water quality. Dissolution in seawater is an important sink for atmospheric CO_2, with evident but not fully understood connexions to climate change.

Another important process in water bodies is gas–liquid–aerosol exchange at water surface. This process transfers matter from ocean surfaces to the atmosphere via marine aerosol generation, a mechanism which generates an estimated mass transfer of $1–3 \times 10^{16}$ g/year[2] affecting physicochemical properties of the lower

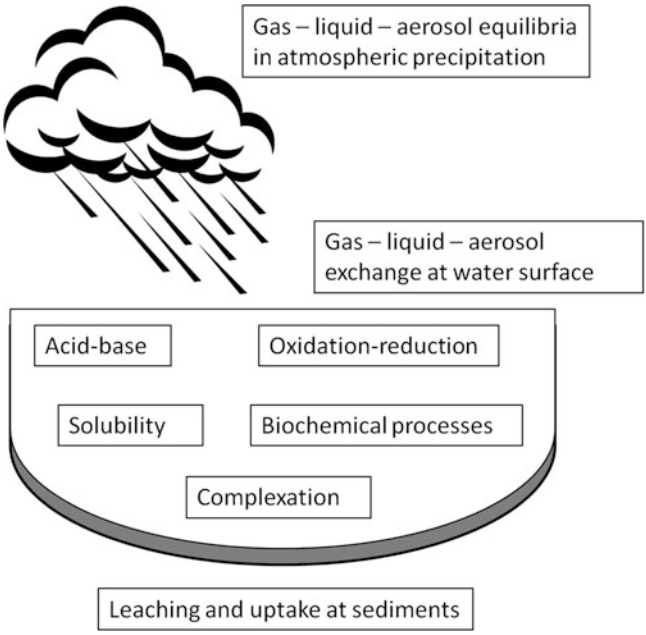

Fig. 3.1 Main physicochemical processes in environmental water

atmosphere and the chemical composition of atmospheric dry and wet precipitation, especially in terms of sea salt-related ions.

Main acid-base parameters in natural water are related with CO_2–HCO_3^-–CO_3^{2-} equilibria, including pH (normal range 6.8 to 7.5), alkalinity (the capacity of water to accept protons), dissolved inorganic carbon content, and the chemistry of calcium and calcium carbonates. pH is a critical parameter in water chemistry, influencing the stability, reactivity and mobility of elements, inorganic and polar organic compounds; for example the pH dependence of dissolved inorganic carbon is closely related to water fertility for photosynthetic and calcifying organisms. The increased accumulation of atmospheric CO_2 in the ocean has produced a shift in the carbonate-system equilibrium, resulting in ocean acidification, a major topic in oceanographic research. It's estimated that surface-ocean pH has decreased by 0.1 pH units since the onset of the industrial revolution, with a prediction of global surface pH reduction of ~0.3–0.5 units by year 2100.[3] The changes in the marine-carbonate system reduce the ocean's capacity to absorb future atmospheric CO_2 emissions limiting its capacity to compensate environmental stress due to atmospheric CO_2 excess.[4] Other important acid-base aquatic chemistry processes are the reactions of hydrated metal ions with OH^- to form polymeric and polymeric hydrolytic species, e.g. Fe(III), Al(III), Cu(II) among others.

As discussed later in this subchapter and in several chapters of this book, direct analytical measurement of metal species is probably the most relevant feature of electroanalytical sensors with respect to other available analytical techniques for

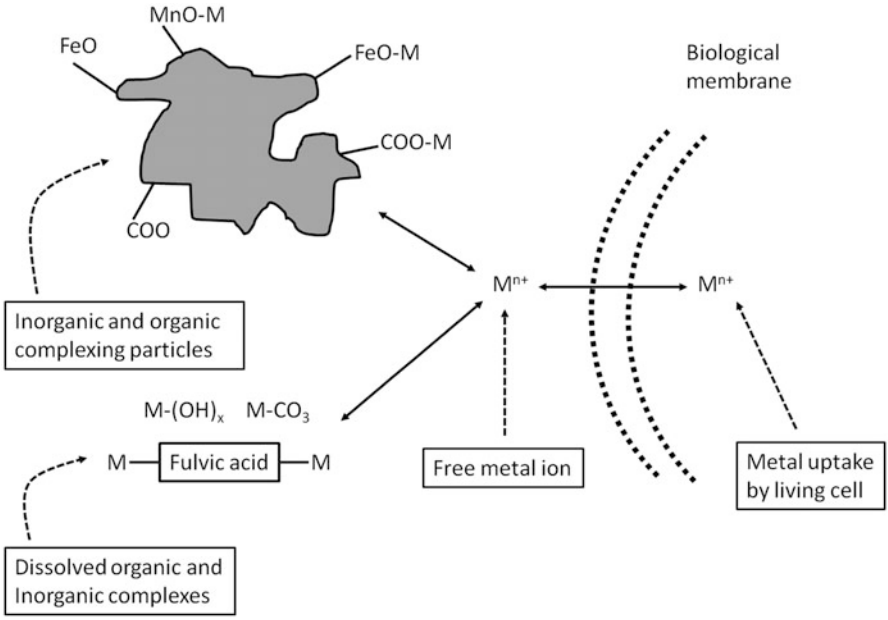

Fig. 3.2 Metal speciation in environmental water

water monitoring. Speciation measurements are largely dependent on the metal complexation state, which is a critical parameter to understand their environmental chemistry in water. Reactions of both ligands and metals have profound effects on physicochemical states. Complexation may cause changes in metal oxidation states (connexion to redox processes), metal solubilisation and insolubilisation (connexion to precipitation processes) and adsorption-desorption on particulate matter, and it's closely related with important biochemical processes as metal bioavailability (living cell uptake) and toxicity,[5,6] as depicted in Fig. 3.2. The classification of the main groups of aquatic ligands published by Buffle and Tercier-Waeber,[7] in relation to the voltammetric properties of their metal complexes, remains as the most rigorous and comprehensive reference in the area (Table 3.1). Complex lability is especially relevant in the context of metal speciation in water by electroanalytical techniques, describing the ability of complexes to maintain equilibrium with the free metal ion, M^{n+}, within the context of an ongoing interfacial process in which a particular species, usually M^{n+}, is consumed.[8] Diffusion coefficients of complexes (D_{ML}), particle radius (r), length of macromolecules (l) and molecular weight (M_w) inform about complex mobility. Other important properties of water complexes shown in Table 3.1 are their thermodynamic stability and the tendency of complexants and complexes to adsorb on electrodes.

Reduction and oxidation (redox) reactions affect the behaviour of many elements and chemical constituents in environmental aquatic media and interfaces with the atmosphere, the sediments—soil phases and the living organisms. The redox

Table 3.1 Voltammetrically relevant properties of the major types of natural complexants and their complexes with trace metals in natural systems

Complexant type	Information related to mobility of complexes	"Effective" complex lability	Thermodynamic stability of complexes	Adsorption of complexants and complexes on electrodes
1. Inorganic anions (CO_3^{2-}, Cl^-, SO_4^{2-}, F^-, etc.) except OH^- and S^{2-}	D_{ML} close to D_M	High	Weak	No
2. OH^-, S^{2-}, polysulphides				
Soluble M complexes	D_{ML} close to D_M	Sometimes labile	Strong	Sometimes
Colloidal species	$1 < r < 500$ nm	Low or nil	Strong	Often
3. Clay colloids	$r > 10$ nm, often aggregated	Low	Intermediate	Weak or nil
4. Fe(III) oxyhydroxide	$1 < r < 500$ nm, often aggregated	Low	Intermediate to strong	Intermediate to strong
5. Mn(IV) oxides		Low	Strong	
6. Fibrillar polysaccharides	l = 10–1,000 nm, often aggregated	High	Low	Possible
7. Soil-derived fulvics (FA) and humics (HA)	$0.5 < r < 5$ nm, partly aggregated. Typically for FA: D_{ML} (0.5–3) × 10^{-10} m^2/s	From fully labile (high M/L; pH < 7) to fully inert (low M/L; pH ≥ 7)	From low (high M/L; pH < 7) to very high (low M/L; pH ≥ 7)	Usually strong
8. Small specific organic complexants possibly released by organisms	$M_w < 1{,}000$		Weak to strong	

Based on reference[7] with permission
D_{ML} = diffusion coefficient of metal ion M complex with ligand L; DM = diffusion coefficient of metal ion M; r = particle radius; l = length of macromolecule; Mw = molecular weight

potential, defined by the Nernst equation and representing all corresponding redox pairs contained in the solution when chemical equilibrium is established, is limited by water oxidation and reduction. Oxidation of water (O^{2-}/O_2 gas) can give a maximum value of about +1,200 mV (O_2 saturated media), whereas the minimum potential for the reduction process (H^+/H_2 gas) is −800 mV, but actual environmental conditions, where O_2 or H_2 saturation is not attained, give redox potentials in the range of +600 to −500 mV. Redox status of water bodies is mainly controlled by oxygen concentration, so the typical situation is a stratified system with oxidising conditions near the surface and reducing conditions near the anoxic bottom, and there is also a close

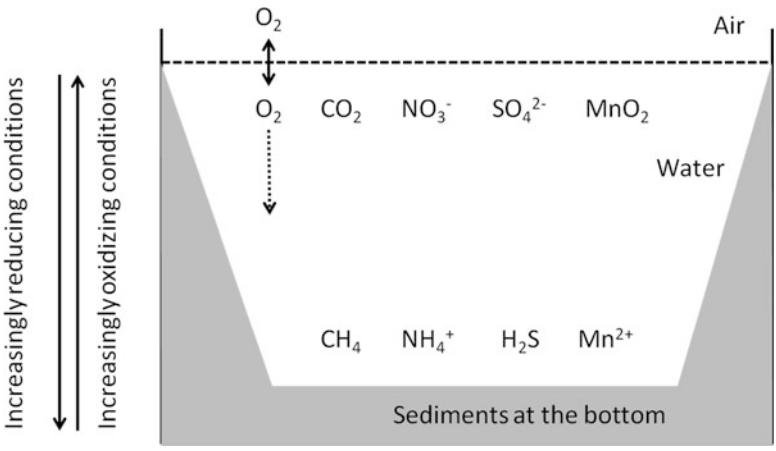

Fig. 3.3 Chemical species depending on oxidising and reducing conditions within water bodies

relationship between redox potential and pH. Oxidised and reduced forms of environmental water constituents are correspondingly dominant along the water column as depicted in Fig. 3.3. It's important to stress that many of the most important redox reactions are catalysed by microorganisms.

3.2.2 Water Pollution

Waterborne toxic chemicals are nowadays an issue of pressing concern in developed and developing countries. Along the water cycle, rainwater washes atmospheric pollutants to the earth's surface. Natural and anthropogenic substances in soil are leached to streams and groundwater. As an example, the European Environmental Agency estimates that about 25 % of all groundwater bodies across Europe are in poor chemical status.[9] High levels of different chemicals, e.g. nitrate in groundwater bodies, are the most frequent cause of bad status, as a consequence of a range of pressures driven by human activities in different economic sectors. Large amounts of treated and untreated wastewater and even solid wastes are discharged to rivers and to the oceans, the final deposit of most persistent pollutants. The sediments deposited in lakes, canals, reservoirs and estuaries are local (and often only temporary) deposits for many of the contaminants present in water effluents. Metals within estuary sediment deposits are frequently bioavailable to microorganisms and subject to remobilisation within the water column, aquatic ecosystem and food chains. The main sources of chemical constituents in ambient water can be classified as naturally occurring and derived from human activities. Sources of naturally occurring substances include geochemical factors as rock weathering, soil leaching and climate. Typical industrial and human dwelling sources are mining (extractive industries, including oil

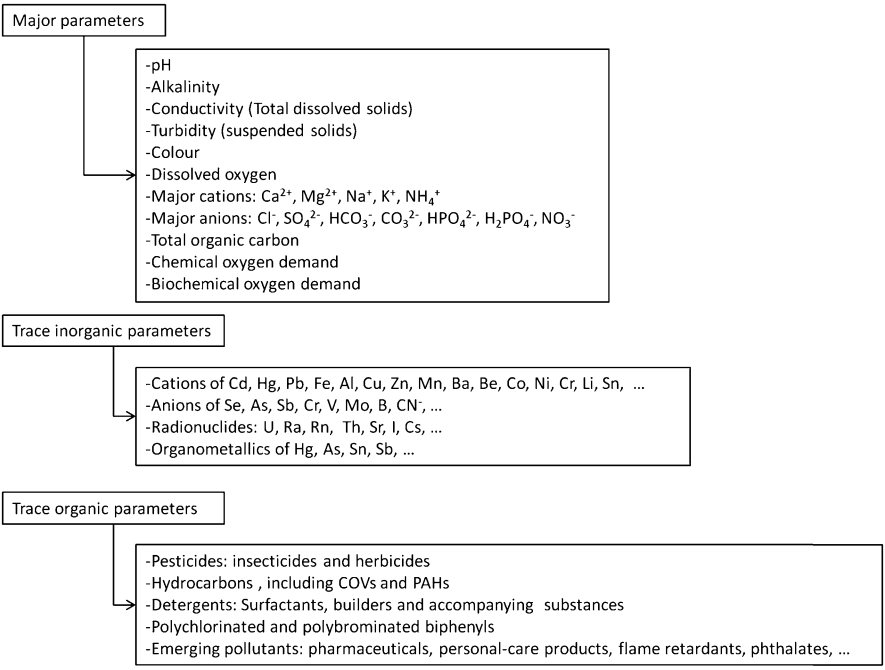

Fig. 3.4 Main analytical parameters in environmental water monitoring

exploration and extraction), shipping, manufacturing and processing industries, water treatment and sewage (including a number of contaminants of emerging concern), solid wastes, urban runoff and fuel leakages. Agricultural, livestock and aquaculture activities generate manures, fertilisers and pesticides. Public health and recreational activities imply chemical treatments with potential impact on green areas and artificial water bodies.

In the frame of environmental monitoring, water contaminants can be conveniently classified according to their chemical nature, but physical state (dissolved species or suspended and colloidal matter) is also relevant for sampling design. The main chemical categories of water pollutants relevant to environmental analysis are summarised in Fig. 3.4. Major parameters inform about the overall chemical status of water, so they are generally measured for screening and routine monitoring purposes. Extensive information about the environmental significance of these parameters can be found in environmental chemistry textbooks and monographs. Many chemical substances belonging to the trace inorganic and organic parameter categories are considered to be significant menaces for human and environmental health even at low concentrations, so they are classified as priority pollutants by international organism and environmental agencies. As detailed in Table 3.2, environmental quality standards and drinking water guidelines have been published for many of these substances, establishing protection thresholds at trace or ultra trace levels that give a clear picture of how dangerous are these pollutants, and also

Table 3.2 Drinking water parametric values and Environmental Quality Standards, for selected priority water pollutants at trace levels (regulated values under 100 ng/mL)

Class and name of substance	Potential health effect from long-term exposure, (1) and (2)	Common sources in drinking water, (1) and (2)	US EPA DW-MCL (1)	WHO DW-PV (2)	EU DW-PV (3)	EU AA-EQS Inland surface waters (4)	EU MAC-EQS Inland surface waters (4)
Trace elements and compounds							
Antimony	Increase in blood cholesterol; decrease in blood sugar	Discharge from petroleum refineries; fire retardants; ceramics; electronics; solder	6	20	5.0	n.a.	n.a.
Arsenic	Skin damage or problems with circulatory systems, and may have increased risk of cancer	Erosion of natural deposits; runoff from orchards, runoff from glass and electronics production wastes	10	10	10	n.a.	n.a.
Bromate	Increased risk of cancer	By-product of drinking water disinfection	10	10	10	n.a.	n.a.
Cadmium	Kidney damage	Corrosion of galvanised pipes; erosion of natural deposits; discharge from metal refineries; runoff from waste batteries and paints	5	3	5.0	0.09[a]	0.6[a]
Chromium	Allergic dermatitis	Discharge from steel and pulp mills; erosion of natural deposits	100	50	50	n.a.	n.a.
Lead	Infants and children: delays in physical or mental development; children could show slight deficits in attention	Corrosion of household plumbing systems; erosion of natural deposits	15	10	10	7.2	

	span and learning abilities. Adults: kidney problems; high blood pressure						
Mercury	Kidney damage	Erosion of natural deposits; discharge from refineries and factories; runoff from landfills and croplands	2	6	1.0	0.05	0.07
Nickel	Lack of evidence	Released from taps and fittings		70	20	20	n.a.
Selenium	Hair or fingernail loss; numbness in fingers or toes; circulatory problems	Leaching from ore-processing sites; discharge from electronics, glass and drug factories	50	40	10	n.a.	n.a.
Thallium	Hair loss; changes in blood; kidney, intestine or liver problems	Leaching from ore-processing sites; discharge from electronics, glass and drug factories	0.5	n.a.	n.a.	n.a.	n.a.
Hydrocarbons and polycyclic aromatic hydrocarbons							
Benzene	Anaemia; decrease in blood platelets; increased risk of cancer	Discharge from factories; leaching from gas storage tanks and landfills	5	10	1	10	50
Benzo[a]pyrene	Reproductive difficulties; increased risk of cancer	Leaching from linings of water storage tanks and distribution lines	0.2	0.7	0.01	0.05	0.1
Pesticides					0.5		
Alachlor	Eye, liver, kidney or spleen problems;	Runoff from herbicide used on row crops	2	20	0.1	0.3	0.7

(continued)

Table 3.2 (continued)

Class and name of substance	Potential health effect from long-term exposure, (1) and (2)	Common sources in drinking water, (1) and (2)	US EPA DW-MCL (1)	WHO DW-PV (2)	EU DW-PV (3)	EU AA-EQS Inland surface waters (4)	EU MAC-EQS Inland surface waters (4)
	anaemia; increased risk of cancer						
Aldicarb	Acetylcholinesterase inhibition	Groundwater in the vicinity of application areas	n.a.	10	0.1	n.a.	n.a.
Aldrin and dieldrin	Affects central nervous system and the liver	Pest treatment and wood protection		0.03	0.1 each	0.01	n.a.
Atrazine	Cardiovascular system or reproductive problems	Runoff from herbicide used on row crops	3	100	0.1	0.6	2
Carbofuran	Problems with blood, nervous system or reproductive system	Leaching of soil fumigant used on rice and alfalfa	40	7	0.1	n.a.	n.a.
Chlordane	Liver or nervous system problems; increased risk of cancer	Residue of banned termiticide	2	0.2	0.1	n.a.	n.a.
Chlorpyrifos	Inhibition of cholinesterase activity	Broad-spectrum organophosphorus insecticide	n.a.	30	0.1	0.03	0.1
2,4-Dichlorophenoxyacetic acid	Kidney, liver or adrenal gland problems	Runoff from herbicide used on row crops	70	30	0.1	n.a.	n.a.
Endrin	Liver problems	Residue of banned insecticide	2	0.6	0.1	0.01	
Isoproturon	Appears to be a tumour promoter	Runoff from herbicide use	n.a.	9	0.1	0.3	1
Lindane	Liver or kidney problems	Runoff/leaching from insecticide used on cattle, lumber, gardens	0.2	2	0.1	0.02	0.04
Simazine	Blood problems	Runoff from herbicide use	4	2	0.1	1	4

Trihalomethanes			80				
Bromodichloromethane	Liver, kidney or central nervous system problems; increased risk of cancer	By-product of drinking water disinfection	0	60	100[b]	n.a.	n.a.
Bromoform	Liver, kidney or central nervous system problems; increased risk of cancer	By-product of drinking water disinfection	0	100	100[b]	n.a.	n.a.
Chloroform	Liver, kidney or central nervous system problems; increased risk of cancer	By-product of drinking water disinfection	70	300	100[b]	2.5	n.a.
Dibromochloromethane	Liver, kidney or central nervous system problems; increased risk of cancer	By-product of drinking water disinfection	60	100	100[b]	n.a.	n.a.
Other organic compounds							
Acrylamide	Nervous system or blood problems; increased risk of cancer	Added to water during sewage/wastewater treatment	n.a.	0.5	0.1	n.a.	n.a.
Carbon tetrachloride	Liver problems; increased risk of cancer	Discharge from chemical plants and other industrial activities	5	4	n.a.	12	n.a.
1,2-Dichloroethane	Increased risk of cancer	Discharge from industrial chemical factories	5	30	3	10	n.a.
Dichloromethane	Liver problems; increased risk of cancer	Discharge from drug and chemical factories	5	20	20	n.a.	n.a.
Di(2-ethylhexyl)-phthalate (DEHP)	Reproductive difficulties; liver problems; increased risk of cancer	Discharge from rubber and chemical factories	6	8	n.a.	1.3	n.a.
Hexachlorobenzene	Liver or kidney problems; reproductive difficulties; increased risk of cancer	Discharge from metal refineries and agricultural chemical factories	1	n.a.	n.a.	0.01	0.05

(continued)

Table 3.2 (continued)

Class and name of substance	Potential health effect from long-term exposure, (1) and (2)	Common sources in drinking water, (1) and (2)	US EPA DW-MCL (1)	WHO DW-PV (2)	EU DW-PV (3)	EU AA-EQS Inland surface waters (4)	EU MAC-EQS Inland surface waters (4)
Hexachlorobutadiene	Possible human carcinogen	Discharge from chemical plants and other industrial activities	n.a.	0.6	0.1	0.1	0.6
Pentachlorophenol	Liver or kidney problems; increased cancer risk	Discharge from wood preserving factories	1	9	0.1	0.4	1
Tetrachloroethene	Liver problems; increased risk of cancer	Discharge from factories and dry cleaners	5	40	10	10	n.a.
Trichloroethene	Liver problems; increased risk of cancer	Discharge from metal degreasing sites and other factories	5	20	10	10	n.a.
Trichlorobenzenes	Changes in adrenal glands	Discharge from textile finishing factories	70	n.a.	n.a.	0.4	n.a.

All data in ng/mL

Sources:

(1) US EPA National Primary Drinking Water Regulations, 2009 (http://water.epa.gov/drink/contaminants/). *DW-MCL* drinking water maximum contaminant level

(2) World Health Organization Guidelines for Drinking-water Quality, 4th Ed, 2011. *DW-PV* drinking water parametric value

(3) European Directive 98/83/EC on the quality of water intended for human consumption. *DW-PV* drinking water parametric value

(4) European Directive 2008/105/EC on environmental quality standards (EQS) in the field of water policy. *AA* annual average, *MAC* maximum allowable concentration

[a]Depending on water hardness classes, data given for class 3 (medium hardness), 50 to <100 mg $CaCO_3$/L

[b]Total trihalomethanes

showing how difficult are the analytical challenges for an accurate and representative measurement of these parameters in the frame of pollution assessment activities. Further analytical requirements in terms of sensitivity and selectivity can be needed if chemical speciation (e.g. for trace element like As, Cr, Hg or Se) is required. Table 3.2 is not exhaustive since a number of contaminants have different regulations depending on the regulation source; the reader is referred to the documents cited in Table 3.2 footnote for detailed information.

Among the trace elements listed in Table 3.2, the toxic heavy metals cadmium, lead and mercury are the most worrying elemental pollutants in ambient water. They are emitted from different sources including industrial waste disposal, landfill leaching and fossil fuel burning. Atmospheric emissions can be transported to long distances, especially in the case of mercury, before wet or dry deposition to enter the water cycle. Mining is a localised but significant route for heavy metal transport to water streams and groundwater, with abandoned mines representing a particular threat.[10] Mining tailing dam failures have been the cause of severe episodes of water contamination by heavy metals, e.g. well-studied cases in Aznalcóllar, Spain,[11] or Baia Mare, Romania[12]; the subject has been reviewed by Rico et al.[13] Some metalloids, notably arsenic, are also relevant pollutants in the aquatic environment. Arsenic has attracted much attention since recognition in the 1990s of its wide occurrence in well water in Bangladesh, the largest poisoning of a population in history with millions of people exposed.[14] Biotransformation of trace elements in the aquatic environment can produce more toxic species as in the case of Hg (II) conversion to methylmercury CH_3Hg^+ and the volatile dimethylmercury $(CH_3)_2Hg$. These organic forms biomagnify in the aquatic food chains due to affinity to living tissue media, so the concentration factor from water to fish may exceed 10^3. Like mercury, arsenic may be converted to more toxic methyl derivatives as methyl arsenic and dimethylarsinic acids, but also to the relatively nontoxic arsenobetaine, which is the main form of arsenic found in fish tissues. Organotin compounds are also of concern in the aquatic system due to long-term use of tributyltin and other derivatives as antifouling agents for boats and ships; this use is presently banned in many countries.

The nutrient elements phosphorus, nitrogen and potassium present in sewage and runoff from heavily fertilised fields are relevant water pollutants due to their contribution to eutrophication of freshwater and coastal marine ecosystems. Eutrophication produces nuisance algal blooms, poor water clarity and extensive hypoxic areas. As a clear example of this phenomenon, it has been recently described that Lake Erie experienced in 2011 the largest harmful algal bloom in its recorded history, with peak intensity over three times greater than any previously observed bloom.[15] Long-term trends in agricultural practices were correlated with increasing phosphorus loading to the western basin of the lake, and these trends, coupled with meteorological conditions in spring 2011, produced record-breaking nutrient loads.

Other inorganic substances relevant as potential water pollutants, especially in the vicinity of specifically related industrial activities, are acids (also derived from acid rain) and bases, cyanide, ammonia, hydrogen sulphide, nitrite, sulphite and perchlorate. Some radionuclides can be found in water, from both natural and

anthropogenic sources. The most concerning radionuclide in drinking water is radium, but a number of fission-product radioisotopes from nuclear power production and nuclear weapon tests can be also detected. A recent example is the accident at the Fukushima nuclear power plant in March 2011, where fluvial discharges of radiocaesium from contaminated watersheds by fallout have been reported.[16] The distribution and inorganic speciation of iodine-129 in seawater offshore Fukushima after the nuclear accident have been also described by Hou et al.[17]

A wide range of organic compounds have been identified as relevant water pollutants. Main categories include hydrocarbons and polycyclic aromatic hydrocarbons, detergents and detergent builders, pesticides, polychlorinated and polybrominated biphenyls and trihalomethanes. Table 3.2 gives some details about environmental and health significance of representative individual compounds, with indication of regulated levels in water. The list is not exhaustive since there is no universal agreement about the establishment of guideline values for several substances, so the reader is referred to original sources to obtain specific information on known facts about organic pollutants in ambient water. WHO Guidelines for Drinking-water Quality,[18] and US EPA National Primary Drinking Water Regulations[19] can be cited as references on this subject. Steroid sex hormones, pharmaceuticals and personal care products, illicit drugs, flame retardants and perfluorinated compounds are considered emerging environmental contaminants of particular concern in wastewater and sewage sludge, as many of them display endocrine-disrupting properties.[20] Due to their physicochemical properties, they tend to accumulate in sewage sludge during wastewater treatment, so the common practice of spreading sewage sludge over agricultural land can constitute a source of many important xenobiotic compounds.

Nanoparticles (NP) and especially engineered nanoparticles (ENP) can be considered as another class of emerging pollutants in water systems and in all environmental compartments. Nanotechnology has gained a great deal of public interest because of the needs and applications of nanomaterials in many areas including industry, agriculture, business, medicine and public health. Environmental exposure to nanomaterials is inevitable as they are increasingly becoming part of our daily life. Manufactured nanomaterials enter the environment through atmospheric emissions and solid or liquid waste streams from production facilities. In addition, nanomaterials in paints, fabrics and personal and health care products, including sunscreens and cosmetics, enter the environment proportional to their use. Emitted nanomaterials will ultimately deposit on land and water surface, having the potential to contaminate soil and migrate into surface and ground waters. Particles in solid wastes, wastewater effluents, direct discharges or accidental spillages can be transported to aquatic systems by wind or rainwater runoff.[21] Scientific uncertainties remain about the environmental risks associated with the widespread use and production of ENP, but potential (eco)toxicity is under active research, based on the type of base material, size, shape and coatings. Some models have been developed to study the release of ENPs to the environment throughout the whole life cycle of ENP and ENP-containing products. Sewage sludge, wastewater and waste incineration of products containing ENP have been identified as major

vehicles through which ENPs end up in the environment.[22] Besides knowing the amounts of ENP released into the environment, it is equally important to investigate in what form ENPs are released, but there are only a limited number of analytical methods that can be directly applied to ENP characterisation and quantification in aqueous samples, so a great analytical challenge is open, also for electroanalytical sensors. The main analytical problems concerning environmental aqueous NP suspensions are[23] low concentrations (especially of ENP); high concentration of the matrix; difficulties in sample preparation, artefacts and sample stability; polydispersity and lack of reference and standard materials for calibration and validation.

3.3 Environmental Water Analysis

Environmental water analysis is a complex task, so all the stages of the analytical process shall be carefully planned and executed to obtain relevant and timely data to fit the monitoring objectives. Individual aspects that need to be considered include sampling design, selection and pretreatment of sampling materials, sample transport and storage, sample pretreatment, data quality assurance and data interpretation. Some of these aspects can be eluded by the strong "lab-to-field" trend currently ongoing in environmental analytical chemistry. In situ or on site measurement avoids problems due to contamination during sampling and storage, instability of analyte species during transport and storage prior to measurement (through processes associated with aggregation, re-equilibration of gaseous components and precipitation) and adsorption/desorption of analytes on container walls.

Systematic sampling design is essential to select adequate scales of spatial and temporal resolution to reach the desired objective within the frame fixed by available resources. Spatial and time scales usually managed in water environmental monitoring, with typical examples of applications, are given in Table 3.3 to show the wide variability of analytical demands that environmental analysts are expected to face. Water bodies' chemical monitoring design must account on surface, volume and temporal dynamics. It's important to collect relevant data on emission sources to reduce monitoring costs, because they give a good basis for choosing proper sampling locations, and optimising the number of sampling sites and the appropriate sampling frequencies. Detailed guidance on sampling strategies for environmental water bodies is available, e.g. from the European Water Framework Directive technical work.[25]

Water sampling equipment range from atmospheric wet and bulk deposition devices, as discussed in detail by Krupa,[26] to a variety of recipients for surface and deep water collection, including depth-stratified sampling.[27] Proper pretreatment of sample recipients is essential to prevent contamination or losses through adsorption on recipient walls. Passive sampling technology is increasingly used as an useful alternative to traditional sampling with many significant advantages, including simplicity, low cost, no need for expensive and complicated equipment, no power

Table 3.3 Spatial and temporal scales in environmental water monitoring

Scales	Size	Example
Spatial domains		
Global	<10,000 km	Hydrosphere, ocean
Meso	>100 km	Sea, major lake, ice sheet
Intermediate	>1 km	Watershed, river, lake, glacier
Field	>1 m	Pond, well, fountain, rain event, pipe discharge
Macro	>1 mm	Raindrop, hailstone
Temporal domains		
Geologic	>10,000 years	Antarctic ice sheet-stratified analysis
Generation lifetime	20–100 years	Acid rain, heavy metal wet deposition, eutrophication
Annual	>1 year	Groundwater quality
Seasonal	>4 months	Pesticides and fertilisers in agriculture field runoff
Daily	>24 h	Drinking water quality
Hourly	>60 min	River water monitoring (on-site)
Instantaneous	<1 s	River water monitoring (in situ)

Modified from reference (24)

requirements, unattended operation and the ability to produce accurate results.[28,29] The use of passive samplers has been explored as a tool for regulatory monitoring of trace metals in surface water.[30] Active biomonitoring is being explored as an integrative sampling strategy for hydrophobic micropollutants in continental waters.[31] Once extracted from natural status, significant changes can take place in water samples within hours due to the dynamic chemical and biochemical nature of water samples, so sample transport and storage before analytical measurements must be carried out following recommended protocols to prevent significant changes in sample composition. This includes critical parameters as type and material of sample containers and methods of preservation.[32]

About sample pretreatment, the first and probably the most critical step in environmental sample processing is the separation of liquid and particulate phases, usually accomplished by filtering. Analyte partitioning into the dissolved, colloidal and particulate states has a profound effect on analytical results. Gaillardet et al.[33] characterised the dissolved state as below 1 nm, and colloids are operationally defined as between 1 or several nanometres to 0.20–0.45 μm and particulates or suspended matter as >0.45 μm. The most important consideration is the separation of colloidal material that involves removing material more than 90 times finer than what is commonly removed using conventional filtering methods. Removing this colloidal material would involve the utilisation of ultracentrifugation techniques or the repeated filtering of samples in order to clog and thereby reduce the pore size of ordinary membranes.[34] Matrix interferences from soluble species are generally managed by separation techniques as coprecipitation, solvent extraction and solid-phase extraction (SPE) by chelating resins.[27] Conducting polymers have been also identified as useful alternatives for solid-phase extraction (SPE) or

microextraction (SPME) of environmental pollutants from water samples. Large surface area, the ability to establish p–p interactions and excellent chemical, mechanical and thermal stability make conducting polymers very attractive as SPE or SPME sorbents for extraction or isolation of trace amounts of compounds.[35] Separation is usually associated with a significant grade of analyte preconcentration.

Quality data assurance is presently ensured in most laboratories by the use of field blanks, sample replicates, clean sampling and analytical equipment and clean analytical facility protocols. The use of appropriate certified reference materials (CRMs) and laboratory intercomparison to test accuracy is today a standard in environmental water monitoring, after great efforts made along the last two decades. CRMs for trace elements in water are widely available, including the most priority pollutants Cd, Pb, Ni and Hg at the concentration levels usually encountered in the frame of environmental monitoring activities. Hg-certified CRMs are challenging, due to known difficulties in stabilising mercury ions in water matrices, especially at very low levels. On the opposite, no real matrix CRMs for organic compounds in water are presently available in the market; the technical problems associated to the production and storage of homogeneous and stable CRMs of this type have been recently reviewed by Ricci et al.[36] So quality assurance for trace organic analysis in environmental water samples mainly rely on inter-laboratory comparisons, with several large-scale examples reported in recent years.[27,37]

Regarding data interpretation, chemometric tools are increasingly used to manage the growing availability of complex chemical data sets obtained from environmental water networks monitoring units and experimental campaigns. Trace and some major pollutants can be linked to specific sources, so analytical results can be additionally used for pollution source assignment and apportionment.[38–40] Modelling of the chemical evolution of water bodies and the dispersion of pollutants from individual and diffuse sources (e.g. after chemical spills) is also an increasingly important aspect of environmental monitoring and assessment[41] that relies on the measured analytical data of major and trace chemical parameters.

3.4 Electrochemical Sensors in Water Analysis

Specific chapters of this book give a detailed description of the wide range of electrochemical sensors available for many different environmental applications, so only a short discussion will be given in this subchapter about the present status of electrochemical sensing in environmental water analysis. We'll present an overview about the main features and applicability of the most relevant electroanalytical techniques, some outstanding trends about instrumental and technological aspects and a brief comment on standardised methods.

3.4.1 Electroanalytical Techniques

A wide range of electroanalytical strategies are available for water analysis, including direct measurements of analytes by conductometry, amperometry, potentiometry, voltammetry and stripping chronopotentiometry. Additionally, the greatly expanding field of electrochemical biosensors, based on conductometric, amperometric and potentiometric measurements, is opening new perspectives for water analysis. They measure signals generated by electro-active species that are produced or consumed by the action of the biological elements (e.g. enzymes), and also by interfacial changes caused by molecular recognition (e.g. antibodies).

Conductometric sensors are an inexpensive and robust class of electrochemical sensors, widely used as the base of standard methods for total dissolved ions monitoring in water samples (see Chap. 4 vol 2). The ability of an aqueous solution to conduct a current, its electrical conductivity, depends on the presence of ions, their total concentration, mobility and valence, and on the temperature. By contrast with many organic molecules, most inorganic compounds dissociate in aqueous solution, so conductivity can be regarded as a non-specific measure for their concentration in water. The conductometric response is unspecific because the measured signal derives from the combined responses of all ion concentrations and their corresponding specific ionic conductivities, so direct conversion of conductivity measurements to ionic concentration cannot be easily derived. The main applicability of simple conductometric measurements in environmental applications is the detection of abnormal variations in dissolved ion content, highly useful as a screening tool to identify and assess contamination episodes. Coupling of conductometric detectors with ion chromatography, often with assistance of online suppression of eluent conductivity, greatly enhances its analytical performance. Many standardised methods are described for monitoring major cations (e.g. Li^+, Na^+, K^+, Mg^{2+}, Sr^{2+}, Al^{3+}, NH_4^+) and anions (e.g. F^-, Cl^-, Br^-, HCO_3^-, NO_3^-, SO_4^{2-}, PO_4^{3-}) in ambient water. A recent review of applications, including methods for trace organic ions in wastewater, has been published by Trojanowicz.[42] Capillary electrophoresis with contact and contactless conductometric detection provides an alternative way for the same applications, with the additional benefits of miniaturisation and simplification of the equipment. The fundamentals of electrochemical detection in capillary electrophoresis, including a detailed description of conductometric sensors, have been published by Kubán and Hauser,[43] and applications to water samples have been reviewed.[44,45] Mai et al.[46] have developed a portable capillary electrophoresis instrument with automated injector and contactless conductivity detection with application to inorganic ion detection within 16 s in wastewater samples, with detection limits below 1 μM. A range of conductometric biosensors have been developed for water monitoring. A recent example of this approach is a bacterial biosensor for trichloroethylene (TCE) detection based on a three-dimensional carbon nanotube bioarchitecture.[47] The bacterial biosensor was successfully applied to the determination of TCE in spiked

groundwater samples and in six water samples collected at an urban industrial site contaminated with TCE.

Amperometric measurements at a fixed potential have a long tradition of applicability in water analysis, both in static and flowing systems. Aside to the well-known amperometric sensors for dissolved oxygen (see Chap. 3 volume 2), amperometric methods have been developed for a wide range of water pollutants.[45] Amperometric biosensors based on inhibition of the enzyme acetylcholinesterase by pesticides have been developed and applied to environmental water with sub-ppb detection limits.[48] The main approach used to measure AChE inhibition is based on the amperometric detection of thiocholine, which is the enzymatic reaction product of acetylthiocholine and is oxidised at constant potential at the electrochemical transducer. Whole-cell amperometric biosensors are typically based on the measurement of oxygen consumption or production during respiration/photosynthesis processes, consumption or production of specific compounds in the course of analyte metabolisation or induction or inhibition of a specific enzyme activity. This type of biosensors has been applied to the measurement of relevant water parameters as the biochemical oxygen demand (BOD) (see Chap. 2 vol 2), pesticides (see Chap. 13 vol 2) and heavy metals (see Chap. 5 vol 2).[49]

Potentiometric measurements by ion-selective electrode potentiometry (ISE) or ion-selective field effect transistors (ISFET), stripping voltammetry (SV) and stripping chronopotentiometry (SCP) are analytical techniques capable of giving not only the total concentration of analytes in water samples, but also metal speciation information, since they are sensitive to the free metal fraction. This capability is especially useful for the study of metal distribution and transfer among environmental compartments in water, as previously commented in this subchapter (Fig. 3.1). It's important to stress that SV and SCP are dynamic techniques, whereas ISE and ISFET are equilibrium techniques. For more details on potentiometric measurements, see Chap. 9 vol 2.

ISE measurements are attractive in environmental water analysis due to their simple measurement principle, low energy requirements and portability, making them very suitable for in situ and on-site applications. Briefly, ISEs are based on equilibrium partition of the test ion between an ionic hydrophobic liquid, or solid, membrane and the test solution. The resulting equilibrium or steady-state membrane potential is measured and related to the free metal ion concentration. Operation of ISEs is however challenging due to a range of experimental problems, including electrode fouling, signal drift on continuous exposure to sample medium, electrode dissolution causing a high surface excess of analyte, electrode carryover of the analyte and electrode instability caused by passivation.[50] Aside to common routine applications for pH and major ion (e.g. NO_3^-, F^-, NH_4^+) determination, a differential capability of ISEs is their response to free metal ion activity, a critically important parameter for trace metal bioavailability and toxicity assessment in environmental waters, as previously mentioned. In this field, a clear shift is observed in recent years from liquid filled to solid contact ISEs, which can be produced as miniaturised disposable sensors by screen printing or other microfabrication technologies, as recently reviewed by Zuliani and Diamond.[51] Examples of

application to trace element determination at required detection levels in real environmental waters (e.g. to fulfil the heavy metal monitoring requirements of the European Water Framework Directive, see Table 3.2) are scarce. The determination of cadmium at 1 ng/mL level in simulated seawater, after preconcentration on a bismuth-coated electrode, has been described.[52] The combination of screen-printed solid-contact Pb^{2+} ISE and solid contact reference electrodes has been recently demonstrated as suitable for use in disposable sensing devices for environmental monitoring of lead in the nanomolar range.[53] The potentiometric measurements correlated well with data determined using inductively coupled plasma mass spectrometry (ICP-MS) in a number of real river water samples. Microfabricated ISE devices have been also used in lab-on-a-chip systems for pH, nitrate and phosphate determination.[54] Potentiometric measurements are well suited for flow detection schemes, so a range of instrumental strategies and applications have been described for flow analysis, capillary electrophoresis and microfluidic systems,[45] and also for liquid chromatography,[42] but none of them have been yet commercialised.

The advantage of the ISFET sensors includes reduced drift and noise due to stray currents as a result of the lower impedance compared to an ISE. A number of applications have been described for the determination of environmental water parameters, notably long-term unattended pH measurements in the open ocean.[55] Precise seawater-pH data (better than 0.002 pH units) with good spatial and temporal coverage are particularly critical to appreciate ocean-acidification phenomena and their consequences on the marine carbonate system.[56]

Potentiometric biosensors based in both ISE and ISFET for water analysis have been widely developed in the last few years, with recent research leading to nanomaterial-based devices. New nanoparticle (NP)-based signal amplification and coding strategies for bioaffinity assays are in use, along with molecular carbon-nanotube (CNT) wires for achieving efficient electrical communication with redox-enzyme and nanowire-based label-free DNA sensors.[57]

Stripping voltammetry (SV) is the most sensitive electroanalytical technique available for trace analysis in environmental water. The usual configurations include anodic stripping voltammetry (ASV) or adsorptive stripping voltammetry (AdSV) techniques with differential pulse (DPASV), or square wave (SWASV) sweeps. A vast number of SV methods have been described for the determination of virtually all organic and inorganic analytes of interest in environmental water samples. ASV is the dominant mode for inorganic species, but there are also many examples of AdsV approaches by analyte complexation and adsorption. Some degree of sample pretreatment is usually needed for total concentration measurements, to destroy complex species and avoid interfering signals at the working electrode. Sample digestion can be tuned depending on the organic load of the sample, from mild treatments as UV or ultrasonic irradiation for natural water to microwave treatment or even total digestion by acids in wastewater or polluted river water. As representative examples of these strategies, Alves et al.[58] have described the simultaneous electrochemical determination of arsenic, copper, lead and mercury in unpolluted fresh waters using a vibrating gold microwire electrode,

after UV digestion; Cukrov et al.[59] studied the spatial distribution of dissolved and total trace metals (zinc, cadmium, lead and copper) in the Krka River, Croatia, by DPASV on a hanging mercury drop electrode (HMDE), after acid digestion with HNO_3. Jakuba et al.[60] described the speciation of zinc in acidified ocean water samples, by anodic stripping voltammetry on a mercury film electrode. Organic compounds are almost exclusively determined by AdsV. The main experimental problem encountered for trace organic analysis by AdsV in environmental waters arises from interferences caused by organic components in the water matrix, so a limited number of applications to real samples are described in the literature. A good example of potentialities and limitations is exemplified in a paper describing the development and evaluation of a sequential injection method to automate the determination of methyl parathion in river water by square wave adsorptive cathodic stripping voltammetry, exploiting the concept of monosegmented flow analysis to perform in-line sample conditioning and standard additions.[61]

A known feature of SV measurements is the minimum disturbance that collecting the analytical signal causes on the sample, since analytical currents are produced by phenomena occurring at the electrode-solution interface without affecting the bulk volume of the sample. These properties, aside with low cost, low energy consumption and ease of miniaturisation, make these techniques especially suitable for in situ and on-site analytical measurements in water samples, a very valuable advantage in environmental monitoring. Moreover, careful adjustment of electrode design, deposition potential and potential waveforms applied to undisturbed or minimally disturbed samples allow the measurement of voltammetric responses from species with different degrees of lability, dependent on the nature of physicochemical processes and chemical reactions in solutions, enabling the identification and quantification of, e.g. oxidation states, complexation states or matrix-bounded elemental ions in solution. The correct interpretation of the results requires not only the knowledge of equilibrium parameters but also the kinetic features of the interconversion of metal complex species. Diffusion and/or kinetic fluxes of the various metal species in solution, both depending on the time scale of the analytical technique and on the intrinsic characteristics of the complexing species (see Table 3.2), influence the signal. As a dynamic analytical sensor, SV is characterised by its (1) response time, which is determined by the thickness of the diffusion layer, and its (2) accumulation time. The signal resulting from the accumulation step represents an integration of all fluctuations in the test medium during this time period.[62]

The use of SV for metal speciation in environmental water has been the subject of intensive research for decades, as reviewed by Pesavento et al.[63] and recently by Mota et al.[64] (see Chap. 5 vol 2). The most straightforward approach is probably ASV. In this mode, the kinetically labile metal species M^{n+} are reduced during the deposition step to M(0), on the working electrode surface. The deposited M(0) is stripped back to the solution by oxidation during an anodic sweep, and the resultant current is measured. The stripping process is strongly affected by solutes giving adsorptive interferences. Kinetically labile species are determined, so the ASV-labile metal ion can be correlated with bioavailability. For speciation purposes

the metal M^{n+} is added to titrate the ligands L present in the sample and information on complexing capacity is obtained in this way, as discussed in detail by Pesavento et al.[63] Competitive ligand exchange-adsorptive stripping voltammetry (CLE-AdSV) is another widely applied SV approach to determination of metal speciation.[65] The technique involves reaction of M^{n+} with an added ligand, L_{ad}, followed by detection of the resulting ML_{ad} complexes by adsorptive accumulation and subsequent reduction of the metal. The measurement is made after a competing equilibrium has been established between L_{ad} and any ambient, naturally occurring, M^{n+} ligand (L). The added ligand is usually one which forms rather stable complexes with the target metal. Finally, absence of gradient and Nernstian equilibrium stripping (AGNES) is an SV technique designed for the determination of the concentration of free metal ions M^{n+} by two sequential steps: (1) application of a potential program (e.g. a step at a fixed potential) generating a known concentration gain between the outer and inner concentrations of the metal at the working electrode surface together with null gradients of the concentration profiles and (2) determination of the concentration of reduced metal inside the amalgam in a stripping step.[66]

Stripping chronopotentiometry (SCP) is methodologically analogue to SV, but the accumulation step is followed by chronopotentiometric measurements with chemical (usually a chemical oxidant) or electrochemical (electric current) force. Within the specific field of metal speciation in water samples, SCP has been empirically proved to be less sensitive than SV to the adsorption of species on the electrode surface in the presence of important quantities of organic matter and mostly insensitive to electrochemical irreversibility, especially at a microelectrode. Moreover, it's free from induced metal ion adsorption interferences and offers greater resolution than corresponding SV measurements.[67] Stripping chronopotentiometry at scanned deposition potential, SSCP, has been shown to be a powerful tool for determination of the distribution of metal dissociation rate constants for heterogeneous ligands, as demonstrated for Cu(II) and Pb(II) complexes with fulvic acids.[68] The applications of SCP to environmental analysis, including the determination of total concentrations of elements, element speciation analyses and theoretical and experimental methods for the study of heavy metal complexation/speciation in the environment, have been reviewed by Serrano et al.[69]

3.4.2 Instrumental and Technological Trends

Electroanalytical instrumentation for environmental water analysis has experienced an impressive progress in recent years, with significant advances on the most relevant aspects for environmental monitoring sensors: cost, portability, assay time, fast personnel training, minimal or absent sample preparation, sensitivity, dynamic range and specificity. Main trends are focused on devices for in situ measurements in large water bodies (lakes, seas and open oceans), miniaturised lab-on-a-chip instruments for decentralised monitoring, including remote sensing, and new electrode technologies for improved sensing performance.

In situ detection of water pollutants, and specifically of metal species, has been the objective of many instrumental developments during the last two decades with the goal of avoiding sample perturbations due to sampling, sample storage and handling, the major limitations of conventional approaches to trace-metal speciation. As discussed in detail by Hanrahan et al.,[70] the development and application of in situ electrochemical devices require proper attention to major issues. They include reversibility of electrochemical processes (to avoid carryover), long-term stability (surface fouling by surface active substances in organic-rich natural waters or in wastewater, drift), specificity (overlapping signals caused by co-existing compounds) and changes in natural conditions (such as oxygen or convection) that may affect the sensor response. Calibration for in situ measurements is affected by different factors and needs careful attention to minimise inaccuracies.[71] In waters and sediments, pH, temperature and ionic strength may vary with depth. The temperature dependence of voltammetric currents is typically 3–8 %/°C (depending on the analyte, the technique and experimental conditions used). Strong pH and ionic strength gradients may also occur in estuaries, the top layers of fresh or seawater or at the sediment–water interface. They may influence significantly not only metal speciation but also the rate of electron transfer at the electrode and thus the measured signals.

A number of submersible instruments have been proposed, as the voltammetric in situ profiling system (VIP) developed by the group of Buffle in Geneva. This instrument, equipped with a gel-integrated microelectrode (GIME), was applied, e.g. for the SWASV measurement of depth-concentration profiles of Cu(II) and Pb (II) in Swiss lakes.[71] Wang and co-workers proposed in situ voltammetric equipment for seawater, based on the coupling of gold surfaces, potentiometric stripping operation and ultramicroelectrode technology.[70] The remote sensor assembly consisted of gold-fibre, silver and platinum working, reference and counter electrodes, respectively, operated in the stripping potentiometric mode. A modified electrochemical cell comprising a mercury-coated platinum disk microelectrode was applied for in situ measurement of the labile fractions of lead and copper.[72] Several examples of unattended and remote in situ voltammetric monitoring and/or profiling of trace elements in water columns and sediments have been reviewed.[73]

Electroanalytical techniques are very suitable for inclusion in lab-on-a-chip instruments, thanks to the miniaturisation potential of detectors and associate electronics. Lab chip and electrochemical sensing-based portable monitoring systems, based on micro-electromechanical system (MEMS) and polymer micromachining techniques, appear well suited to complement standard analytical methods for a number of environmental monitoring applications.[54] In addition, this type of portable system could save time, reagents and sample when installed at contaminated sites. A compilation of micro-sensors for the measurement of priority pollutants targeted in the EU Water Framework Directive, including conductometric, amperometric and voltammetric devices, has been published by Namour et al.[74] The lack of ruggedness of the receptor towards environmental conditions in the long term has been identified as the main factor limiting micro-sensor applications in ambient water.

About electrode design and fabrication oriented to environmental water monitoring, the increasing availability of screen-printed technology is probably the most outstanding progress in recent years. Screen-printed platforms with carbon, gold and bismuth working electrodes (both bare and modified with diverse organic and inorganic layers) have been the base for multiple developments in environmental analysis. Applications to water samples, mainly focused on trace element detection, have generated promising methodologies for the portable sensing of toxic pollutants in water. The main developments and applications of screen-printed electrodes in environmental assays, including applications to a wide set of organic and inorganic water pollutants, have been recently reviewed by Li et al.[75] A step further in the screen-printed progress for water analysis has been the recent development of wearable screen-printed electrochemical sensors on underwater garments comprising the synthetic rubber neoprene, for determining the presence of environmental pollutants (phenols and heavy metals) and security threats (trace explosives as trinitrotoluene) in marine environments.[76,77] Neoprene is an attractive substrate for thick-film electrochemical sensors for aquatic environments and offers high-resolution printing with no apparent defects. The neoprene-based sensor has been evaluated for the voltammetric detection of trace heavy metal contaminants and nitroaromatic explosives in seawater samples. The introduction of molecularly imprinted polymers in working electrode designs is another promising trend to improve the performance of electrochemical sensors in environmental water applications.[78]

3.4.3 Standardised Methods

As summarised in Table 3.4, some electroanalytical methods have been certified by standardisation bodies for the chemical characterisation of ambient water samples, mostly in the class of inorganic substances. Conductometric detection is used in direct method for ionic constituents and also as chromatographic detector for individual cations and anions. Total, inorganic and organic carbon in water can be also assayed by conductometric detection. Amperometric detection has been certified for dissolved oxygen and cyanide. ISE potentiometry is used for standardised measurements of a set of ions and also for the evaluation of water oxidation-reduction potential. Voltammetric detection is the base for diverse methodologies oriented to the determination of trace elements including the most relevant elemental pollutants.

Table 3.4 Selected examples of standard electrochemical method for environmental water characterisation, classified by electroanalytical techniques

Method type and code	Analytes	Samples	Standardisation body
Conductometric detection			
ISO 7888:1985	Conductivity (ionic constituents)	Surface waters, process waters in water supply and treatment plants, and wastewaters	ISO
ISO 14911:1998	Li^+, Na^+, NH_4^+, K^+, Mn^{2+}, Ca^{2+}, Mg^{2+}, Sr^{2+} and Ba^{2+}	Water and wastewater	ISO
ISO 10304-1:2007	Bromide, chloride, fluoride, nitrate, nitrite, phosphate and sulphate	Water	ISO
ISO 10304-3:1997	Iodide, sulphite, thiocyanate and thiosulphate	Water	ISO
ISO 10304-4:1997	Chlorate, chloride and chlorite	Water with low contamination	ISO
ASTM D5904-02 (2009)	Total carbon, inorganic carbon and organic carbon	Raw water, drinking water and wastewater	ASTM
EPA 314.0	Perchlorate	Drinking water	USEPA
Amperometric detection			
ISO 5814:2012	Dissolved oxygen	Drinking waters, natural waters, wastewaters and saline waters	ISO
ASTM D7237-10	Cyanide	Natural water, saline waters and wastewater effluents	ASTM
Potentiometric detection			
ISO 6778:1984	Ammonium	Water, wastewater and sewage	ISO
ISO 15682:2000	Chloride	Water and wastewater	ISO
ISO 10359-1:1992	Fluoride	Lightly polluted water	ISO
ISO 10523:2008	pH	Rain, drinking and mineral waters, bathing waters, surface and ground waters, municipal and industrial wastewaters and liquid sludge	ISO
ASTM D4658-09	Sulphide	Water	ASTM
ASTM D1498-08	Oxidation-reduction potential	Water	ASTM
Voltammetric detection			
DIN 38406-16:1990-03	Zinc, cadmium, lead, copper, thallium, nickel and cobalt	Water, wastewater and sludge	DIN

(continued)

Table 3.4 (continued)

Method type and code	Analytes	Samples	Standardisation body
DIN 38406-17:2009-10	Uranium	Surface water, raw water and drinking water	DIN
ASTM D3557-12	Cadmium	Water and wastewater	ASTM
ASTM D3559-08	Lead	Water and wastewater	ASTM
EPA 7063	Arsenic	Drinking water, natural surface water, seawater, and domestic and industrial wastewater	USEPA
EPA 7472	Mercury	Drinking water, natural surface water, seawater, and domestic and industrial wastewater	USEPA
EPA 7198	Hexavalent chromium	Natural and wastewater	USEPA

ISO: International Organization for Standardization; DIN: German Institute for Standardization
ASTM: ASTM International, formerly American Society for Testing and Materials
USEPA: United States Environmental Protection Agency

3.5 Conclusions and Outlook

There are today increasing demands of chemical knowledge about ambient water, as a consequence of intensive environmental water research, stricter regulations for environment protection and growing public concern. Analytical challenges immediately derived for these requirements are evident. The location and the density of monitoring points will need to be adapted to provide adequate spatial and temporal coverage (surveillance monitoring) and to capture the effect of individual and diffuse pressures, including "in situ" and on-site monitoring. This will require further effort on sensor miniaturisation and simplification, towards the so-called geosensor networks concept.[79] Furthermore, more substances will need to be monitored in a more systematic manner, in particular those listed as priority substances and emerging, poorly characterised contaminants, e.g. nanoparticles. From a technical perspective, the main challenges will comprise developing new and greener analytical methods, based on robust and simple techniques and capable of transmitting data wirelessly. Developing information systems for managing an increasing volume of data coming from different producers and controlling measurement uncertainty will be also important tasks. These requirements can be conveniently referred under the screening and monitoring emerging tools (SMET) concept,[80] to designate tools that differ from classical spot sampling and laboratory analysis. They can be used directly on-site or in situ, and they often enable a quicker water quality assessment than classical laboratory analysis. Different types of SMET are expected to measure time-weighted average concentrations of pollutants,

provide rapid on-site or online analysis or detect potentially harmful conditions through biological or chemical detectors. Electrochemical sensors have already demonstrated their capability to address the aforementioned challenges, so they will undoubtedly play an outstanding and increasingly important role to fulfil these desired analytical requirements for ambient water monitoring.

References

1. Manahan SE (2010) Environmental chemistry, 9th edn. CRC, Boca Raton, FL
2. Gong SL, Barrie L, Lazare M (2002) Canadian aerosol module (CAM): a size-segregated simulation of atmospheric aerosol processes for climate and air quality models 2. Global sea-salt aerosol and its budgets. J Geophys Res 107:AAC13-1–AAC13-14
3. Caldeira K, Wickett ME (2005) Ocean model predictions of chemistry changes from carbon dioxide emissions to the atmosphere and ocean. J Geophys Res Oceans 110:1–12
4. Canadell JG, Le Quéré C, Raupach MR et al (2007) Contributions to accelerating atmospheric CO_2 growth from economic activity, carbon intensity, and efficiency of natural sinks. Proc Natl Acad Sci U S A 104:18866–18870
5. Nowack B, VanBriesen JM (eds) (2005) Biogeochemistry of chelating agents. American Chemical Society, Washington, DC
6. van Leeuwen HP, Town RM, Buffle J, Cleven RFMJ, Davison W, Puy J, Van Riemsdijk WH, Sigg L (2005) Dynamic speciation analysis and bioavailability of metals in aquatic systems. Environ Sci Technol 39:8545–8556
7. Buffle J, Tercier-Waeber ML (2000) In situ voltammetry: concepts and practice for trace analysis and speciation. In: Buffle J, Horvai G (eds) In situ monitoring of aquatic systems. Chemical analysis and speciation. IUPAC series on analytical and physical chemistry of environmental systems, vol 6. Wiley, Chichester, pp 279–405
8. van Leeuwen HP, Cleven RFMJ, Buffle J (1989) Voltammetric techniques for complexation measurements in natural aquatic media. Role of the size of macromolecular ligands and dissociation kinetics of complexes. Pure Appl Chem 61:255–274
9. EEA (2012) European waters—current status and future challenges. European Environment Agency, Copenhagen
10. EA (2008) Abandoned mines and the water environment, Science report from the Environment Agency. Environment Agency, Bristol
11. Olías M, Cerón JC, Moral F, Ruiz F (2006) Water quality of the Guadiamar River after the Aznalcóllar spill (SW Spain). Chemosphere 62:213–225
12. László F (2006) Lessons learned from the cyanide and heavy metal accidental water pollution in the Tisa river basin in the year 2000. In: Durga G, Kambourova V, Simenoova F (eds) Management of intentional and accidental water pollution. NATO security through science series C: environmental security. Springer, Heidelberg, pp 43–50
13. Rico M, Benito G, Díez-Herrero A (2008) Floods from tailings dam failures. J Hazard Mater 154:79–87
14. Smith AH, Lingas EO, Rahman M (2000) Contamination of drinking-water by arsenic in Bangladesh: a public health emergency. Bull World Health Organ 78:1093–1103
15. Michalak AM, Anderson EJ, Beletsky D et al (2013) Record-setting algal bloom in Lake Erie caused by agricultural and meteorological trends consistent with expected future conditions. Proc Natl Acad Sci U S A 110:6448–6452
16. Ueda S, Hasegawa H, Kakiuchi H, Akata N, Ohtsuka Y, Hisamatsu S (2013) Fluvial discharges of radiocaesium from watersheds contaminated by the Fukushima Dai-ichi Nuclear Power Plant accident, Japan. J Environ Radioact 118:96–104

17. Hou X, Povinec PP, Zhang L et al (2013) Iodine-129 in seawater offshore Fukushima: distribution, inorganic speciation, sources, and budget. Environ Sci Tech 47:3091–3098
18. WHO (2011) Guidelines for drinking-water quality, 4th edn. WHO Press, Geneva, Switzerland
19. EPA (2009) National primary drinking water regulations. http://water.epa.gov/drink/contaminants/index.cfm#List. Accessed 4 May 2013
20. Díaz-Cruz MS, García-Galán MJ, Guerra P et al (2009) Analysis of selected emerging contaminants in sewage sludge. Trends Anal Chem 28:1263–1275
21. Ray PC, Yu H, Fu PP (2009) Toxicity and environmental risks of nanomaterials: challenges and future needs. J Environ Sci Health C Environ Carcinog Ecotoxicol Rev 27:1–35
22. Gottschalk F, Nowack B (2011) The release of engineered nanomaterials to the environment. J Environ Monit 13:1145–1155
23. Delay M, Frimmel F (2012) Nanoparticles in aquatic systems. Anal Bioanal Chem 402:583–592
24. Artiola JF (2004) Monitoring surface waters. In: Artiola JF, Pepper IL, Brusseau ML (eds) Environmental monitoring and characterization. Elsevier, Amsterdam
25. WFD-CIS (2003) Guidance document 7. Monitoring under the Water Framework Directive. Office for Official Publications of the European Communities, Luxembourg
26. Krupa SV (2002) Sampling and physico-chemical analysis of precipitation: a review. Environ Pollut 120:565–594
27. Sohrin Y, Bruland KW (2011) Global status of trace elements in the ocean. Trends Anal Chem 8:1291–1307
28. Esteve-Turrilas FA, Pastor A, Yusá V, de la Guardia M (2007) Using semipermeable membrane devices as passive samplers. Trends Anal Chem 26:703–712
29. Zabiegala B, Kot-Wasik A, Urbanowicz M, Namiesnik J (2010) Passive sampling as a tool for obtaining reliable analytical information in environmental quality monitoring. Anal Bioanal Chem 396:273–296
30. Allan IJ, Knutsson J, Guigues N, Mills GA, Fouillac AM, Greenwood R (2008) Chemcatcher®and DGT passive sampling devices for regulatory monitoring of trace metals in surface water. J Environ Monit 10:821–829
31. Besse JP, Geffard O, Coquery M (2012) Relevance and applicability of active biomonitoring in continental waters under the Water Framework Directive. Trends Anal Chem 36:113–127
32. Artiola JF, Pepper IL, Brusseau ML (2004) Monitoring and characterization of the environment. In: Artiola JF, Pepper IL, Brusseau ML (eds) Environmental monitoring and characterization. Elsevier, Amsterdam
33. Gaillardet J, Viers J, Dupré B (2004) Trace elements in river waters. In: Holland HD, Turekian KK (eds) Treatise on geochemistry. Elsevier, Amsterdam, pp 225–272
34. Rose S, Shea JA (2007) Environmental geochemistry of trace metal pollution in urban watersheds. In: Sarkar D, Datta R, Hanningan R (eds) Developments in environmental science, vol 5. Elsevier, Amsterdam, Chapter 6
35. Li X, Wang Y, Yang X, Chen J, Fu H, Cheng T (2012) Conducting polymers in environmental analysis. Trends Anal Chem 39:163–179
36. Ricci M, Kourtchev I, Emons H (2012) Chemical water monitoring under the Water Framework Directive with certified reference materials. Trends Anal Chem 36:47–57
37. Ademollo N, Patrolecco L, Polesello S, Valsecchi S, Wollgast J, Mariani G, Hanke G (2012) The analytical problem of measuring total concentrations of organic pollutants in whole water. Trends Anal Chem 36:71–81
38. Kowalkowski T, Zbytniewski R, Szpejna J, Buszewski B (2006) Application of chemometrics in river water classification. Water Res 40:744–752
39. Zhou F, Guo H, Liu Y, Jiang Y (2007) Chemometrics data analysis of marine water quality and source identification in Southern Hong Kong. Mar Pollut Bull 54:745–756
40. Zhang Y, Guo F, Meng W, Wang XQ (2009) Water quality assessment and source identification of Daliao river basin using multivariate statistical methods. Environ Monit Assess 152:105–121

41. Zhao L, Chen Z, Lee K (2011) Modelling the dispersion of wastewater discharges from offshore outfalls: a review. Environ Rev 19:107–120
42. Trojanowicz M (2011) Recent developments in electrochemical flow detections—a review: Part II. Liquid chromatography. Anal Chim Acta 688:8–35
43. Kubán P, Hauser PC (2009) Fundamentals of electrochemical detection techniques for CE and MCE. Electrophoresis 30:3305–3314
44. Solínová V, Kasicka V (2006) Recent applications of conductivity detection in capillary and chip electrophoresis. J Sep Sci 29:1743–1762
45. Trojanowicz M (2009) Recent developments in electrochemical flow detections—a review: Part I. Flow analysis and capillary electrophoresis. Anal Chim Acta 653:36–58
46. Mai TD, Pham TTT, Pham HV, Saíz J, Ruiz CG, Hauser PC (2013) Portable capillary electrophoresis instrument with automated injection and contactless conductivity detection. Anal Chem 85:2333–2339
47. Hnaien M, Lagarde F, Bausells L, Errachid A, Jaffrezic-Renault N (2011) A new bacterial biosensor for trichloroethylene detection based on a three-dimensional carbon nanotubes bioarchitecture. Anal Bioanal Chem 400:1083–1092
48. Liu S, Zheng Z, Li X (2013) Advances in pesticide biosensors: current status, challenges, and future perspectives. Anal Bioanal Chem 405:63–90
49. Lagarde F, Jaffrezic-Renault N (2011) Cell-based electrochemical biosensors for water quality assessment. Anal Bioanal Chem 400:947–964
50. de Marco R, Clarke G, Pejcic B (2007) Ion-selective potentiometry in environmental analysis. Electroanalysis 19:1987–2001
51. Zuliani C, Diamond D (2012) Opportunities and challenges of using ion-selective electrodes in environmental monitoring and wearable sensors. Electrochim Acta 84:29–34
52. Chumbimuni-Torres KY, Calvo-Marzal P, Wang J, Bakker E (2008) Electrochemical simple matrix elimination for trace-level potentiometric detection with polymeric membrane ion-selective electrodes. Anal Chem 80:6114–6118
53. Anastasova S, Radu A, Matzeu G, Zuliani C, Mattinen U, Bobacka J, Diamond D (2012) Disposable solid-contact ion-selective electrodes for environmental monitoring of lead with ppb limit-of-detection. Electrochim Acta 73:93–97
54. Jang A, Zou Z, Lee KK, Ahn CH, Bishop PL (2011) State-of-the-art lab chip sensors for environmental water monitoring. Meas Sci Technol 22:1–18
55. Martz TR, Connery JG, Johnson KS (2010) Testing the Honeywell Durafet® for seawater pH applications. Limnol Oceanogr Methods 8:172–184
56. Rérolle VMC, Floquet CFA, Mowlem MC et al (2012) Seawater-pH measurements for ocean-acidification observations. Trends Anal Chem 40:146–157
57. Farré M, Kantiani L, Pérez S, Barceló D (2009) Sensors and biosensors in support of EU directives. Trends Anal Chem 28:170–185
58. Alves GMS, Magalhaes JMCS, Salaün P, van den Berg C (2011) Simultaneous electrochemical determination of arsenic, copper, lead and mercury in unpolluted fresh waters using a vibrating gold microwire electrode. Anal Chim Acta 703:1–7
59. Cukrov N, Cmuk P, Mlakar M, Omanovic D (2008) Spatial distribution of trace metals in the Krka River, Croatia: an example of the self-purification. Chemosphere 72:1559–1566
60. Jakuba RW, Moffet JW, Saito MA (2008) Use of a modified, high-sensitivity, anodic stripping voltammetry method for determination of zinc speciation in the North Atlantic Ocean. Anal Chim Acta 614:143–152
61. dos Santos LBO, Masini JC (2008) Square wave adsorptive cathodic stripping voltammetry automated by sequential injection analysis: potentialities and limitations exemplified by the determination of methyl parathion in water samples. Anal Chim Acta 606:209–216
62. Sigg L, Black F, Buffle J et al (2006) Comparison of analytical techniques for dynamic trace metal speciation in natural freshwaters. Environ Sci Tech 40:1934–1941

63. Pesavento M, Alberti G, Biesuz R (2009) Analytical methods for determination of free metal ion concentration, labile species fraction and metal complexation capacity of environmental waters: a review. Anal Chim Acta 631:129–141
64. Mota AM, Pinheiro JP, Simões Gonçalves ML (2012) Electrochemical methods for speciation of trace elements in marine waters. Dynamic aspects. J Phys Chem A 116:6433–6442
65. van Leeuwen HP, Town RM (2005) Kinetic Limitations in Measuring Stabilities of Metal Complexes by Competitive Ligand Exchange-Adsorptive Stripping Voltammetry (CLE-AdSV). Environ Sci Technol 39:7217–7255
66. Galcerán J, Companys E, Puy J, Cecilia J, Garces JL (2004) AGNES: a new electroanalytical technique for measuring free metal ion concentration. J Electroanal Chem 566:95–109
67. Town RM, van Leeuwen HP (2004) Depletive stripping chronopotentiometry: a major step forward in electrochemical stripping techniques for metal ion speciation analysis. Electroanalysis 16:458–471
68. Town RM (2008) Metal binding by heterogeneous ligands: kinetic master curves from SSCP waves. Environ Sci Technol 42:4014–4021
69. Serrano N, Diaz-Cruz JM, Ariño C, Esteban M (2007) Stripping chronopotentiometry in environmental analysis. Electroanalysis 19:2039–2049
70. Hanrahan G, Patil DG, Wang J (2004) Electrochemical sensors for environmental monitoring: design, development and applications. J Environ Monit 6:657–664
71. Buffle J, Tercier-Waeber ML (2005) Voltammetric environmental trace metal analysis and speciation: from laboratory to in situ measurements. Trends Anal Chem 24:172–191
72. Baldo MA, Daniele SD, Ciani I, Bragatto C, Wang J (2003) Remote stripping analysis of lead and copper by a mercury-coated platinum microelectrode. Electroanalysis 16:360–366
73. Tercier-Waeber ML, Taillefert M (2008) Remote in situ voltammetric techniques to characterize the biogeochemical cycling of trace metals in aquatic systems. J Environ Monit 10:30–54
74. Namour P, Lepot M, Jaffrezic-Renault N (2010) Recent trends in monitoring of european water framework directive priority substances using micro-sensors: a 2007–2009 review. Sensors 10:7947–7978
75. Li M, Li YT, Li DW, Long YT (2012) Recent developments and applications of screen-printed electrodes in environmental assays—a review. Anal Chim Acta 734:31–44
76. Malzahn K, Windmiller JR, Valdés-Ramírez G, Schöning MJ, Wang J (2011) Wearable electrochemical sensors for in situ analysis in marine environments. Analyst 136:2912–2917
77. Windmiller JR, Wang J (2013) Wearable electrochemical sensors and biosensors: a review. Electroanalysis 25:29–46
78. Suryanarayanan V, Wu CT, Ho KC (2010) Molecularly imprinted electrochemical sensors. Electroanalysis 22:1795–1811
79. Nittel S (2009) A survey of geosensor networks: advances in dynamic environmental monitoring. Sensors 9:5664–5678
80. Graveline N, Maton L, Lückge H, Rouillard J, Strosser P, Palkaniete K, Rinaudo JD, Taverne D, Interwies E (2010) An operational perspective on potential uses and constraints of emerging tools for monitoring water quality. Trends Anal Chem 29:378–384

Chapter 4
Atmosphere

Andrea Gambaro, Elena Gregoris, and Carlo Barbante

The atmosphere is the receiver of many by-products of our society, such us products of combustion of fossil fuels and industrial manufacturing. The studies on chemical pathways of trace atmospheric species are often complexes since the life cycles of such species are linked to an elaborate system of chemical and physical processes. As a result, it is possible that a perturbation in the concentration of one species leads to significant changes in quantity and lifetimes of other trace species; the feedback could also amplify or damp the original perturbation. Trace species can exhibit an enormous range of spatial and temporal variability, depending on their lifetime in the atmosphere. Relatively long-lived species are usually uniformly distributed: in this case strategically located sampling sites around the globe could be adequate to characterize their spatial distribution and temporal trend. As species lifetimes become shorter, their spatial and temporal distributions become more variable.

The Earth's atmosphere is composed primarily of the gases N_2 (78 %), O_2 (21 %) and Ar (1 %); their abundance is controlled by the biosphere over geologic timescales, through uptake and release from crustal material and degassing of the interior. The later most abundant constituent of the atmosphere is water vapour; it is found mainly in the lower layer (troposphere) and its concentration is highly variable, reaching 3 % of concentration. The remaining gaseous constituents (trace gases) represent less than 1 % of the atmosphere. Trace gases play a crucial role in the Earth's radioactive equilibrium and in the chemical properties of the atmosphere. Besides gases, the atmosphere, whether in urban or remote areas, contains significant concentrations of "particulate matter" or aerosol. By "particulate matter" we refer to any substance, except pure water, that exists as a liquid or solid in the atmosphere under normal conditions and is of microscopic or

A. Gambaro (✉) • E. Gregoris • C. Barbante
Institute for the Dynamics of Environmental Processes-CNR, Venice 30123, Italy

Department of Environmental Sciences, Informatics and Statistics-University Ca' Foscari of Venice 30123, Italy
e-mail: gambaro@unive.it

L.M. Moretto, K. Kalcher (eds.), *Environmental Analysis by Electrochemical Sensors and Biosensors*, DOI 10.1007/978-1-4939-0676-5_4

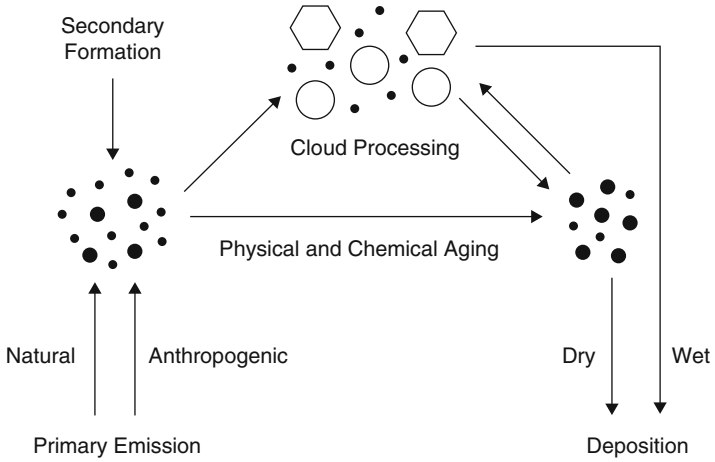

Fig. 4.1 Atmospheric cycling of aerosol (reproduced from reference[2] with permission from John Wiley and Sons)

submicroscopic size larger than molecular dimensions.[1] Among atmospheric constituents, particulate matter is unique in its complexity. Atmospheric particles affect a great variety of processes such as solar radiation scattering, visibility, climate and health effects. Moreover the atmospheric particles play an important role in the transport of chemical compounds both at local and remote scales. Atmospheric particles are classified by their size, shape and composition. They can be the result of primary emission that means they are directly emitted from sources or can be produced in the atmosphere by physical processes or chemical reactions (secondary formation, Fig. 4.1). The properties of such particles can be modulated by atmospheric processes, like condensation, evaporation and coagulation. Particles can persist in the environment from minutes to weeks after their release or formation, and can travel meters to thousands of kilometres; the typical removing mechanisms are wet or dry deposition.

There are three distinct modes into which airborne particles can typically be divided, based on their size, that are the following:

1. Transient nuclei mode: These particles are typically less than ca. 100 nm in diameter; they are formed by the condensation of less volatile materials and subsequently grow by condensation processes. Their formation can occur both in hot combustion gases and within the atmosphere itself from chemical reactions of gases.
2. Accumulation mode: Particles in the transient nuclei mode can grow both by condensation of low-volatility materials and through coagulation, reaching the state of "accumulation mode" that consists of particles between ca. 100 nm and 2 μm in diameter. The accumulation mode is so called because particle removal mechanisms are the less efficient in this regime, causing particle to be accumulated.

3. Coarse particle mode: The coarse particles are usually formed by mechanical action at high temperatures, crustal erosion, road dust resuspension and sea salts, being the fine fraction of a mixture of primary and secondary aerosol, principally emitted from anthropogenic sources (combustion, high-temperature industrial activities, automotive traffic, etc.).

Therefore, detailed information on the aerosol mass distribution and on its chemical composition is essential to identify their sources as well as to assess the environmental and health risks.[3]

Estimations of global emissions, as reported by many authors, have shown that natural and anthropogenic sources can contribute to the principal dimensional classes (coarse, fine and ultrafine)[4,5] of atmospheric particulate matter (PM). About 10–20 % of the aerosols can be characterized as anthropogenic on a global scale,[1] but these values may drastically change due to local scenarios, human activities and the prevailing particle cut-off.

A condition of "air pollution" may be defined as a situation in which substances that result from anthropogenic activities are present at concentrations sufficiently high above their normal ambient levels to produce a measurable effect on humans, animals, vegetation or materials.[1]

4.1 Gaseous Constituents

4.1.1 Sulfur Oxides

Sulfur oxides in the atmosphere are usually present as sulfurous anhydride or sulfur dioxide (SO_2) and sulfuric anhydride or sulfur trioxide (SO_3). Sulfur dioxide is a colourless, irritating, non-flammable, very soluble gas. It is one of the most aggressive and dangerous pollutants; it derives from the oxidation of sulfur during combustion processes. Health effects of sulfur oxides are prevalently linked to respiratory system pathologies, but in high concentration they can cause asphyxiation.

The most used analytical technique for SO_2 monitoring is based on fluorescence. Excitation of sulfur dioxide molecules by ultraviolet radiation (UV) in the 190–230 nm region gives an emitting fluorescent radiation, whose wavelength and intensity are directly proportional to the concentration of sulfur dioxide. The main interfering compound is represented by polycyclic aromatic hydrocarbons: to eliminate their effect, the analyzers are equipped with a permeation device which selectively removes hydrocarbon molecules from the gas sample.[6]

4.1.2 Nitrogen Oxides

The most important nitrogen oxides, from an environmental point of view, are the so-called NO_x that indicates the sum of nitrous oxide or nitrogen monoxide

Table 4.1 Typical analytical techniques used to analyze gaseous components of atmosphere

Compound	Analytical method
Sulfur oxides	Fluorescence
Nitrogen oxides	Chemiluminescence
Ozone	Spectrophotometry

(NO) and nitric oxide or nitrogen dioxide (NO_2). NO is produced during high-temperature combustion processes and comes principally from motor vehicle exhaust and stationary sources. NO_2 derives from the oxidation of NO in the atmosphere and represents an intermediate in the production of several secondary pollutants as ozone. Nitrogen dioxide is highly oxidant and toxic: it can irritate the lungs and lower resistance to respiratory infections.

Nitrogen oxides are usually analyzed by a chemiluminescence technique. In this method a gas-phase reaction between nitrogen monoxide and ozone produces excited NO_2 molecules (NO_2*). Excited molecules emit light, as they return to the ground state: the intensity of the emission peak at 1,200 nm is linearly proportional to the concentration of nitrogen monoxide (NO). The chemiluminescent reaction occurs only between NO and ozone; therefore it is necessary to convert nitrogen dioxide (NO_2) to nitric oxide (NO). For this purpose, the analyzer contains a molybdenum converter, heated at 315 °C: the sample gas flow intercepts a switching valve, that periodically deviates it to the converter before entering the reaction chamber. In these conditions, the analyzer measures the concentration of NO_x, as the sum of NO and NO_2. NO_2 concentration is obtained by the difference between NO_x and NO concentrations.[7]

4.1.3 Ozone

Ozone is a toxic gas, consisting of unstable molecules formed by three oxygen atoms (O_3); these molecules are easily broken releasing molecular oxygen (O_2) and an extremely reactive oxygen atom ($O_3 \rightarrow O_2 + O$). Because of these properties, ozone is an energetic oxidant, able to react both with organic and inorganic materials. Ozone is present for more than 90 % in the stratosphere (10–50 km of altitude) where it is produced by the solar ultraviolet radiation action. In the stratosphere it protects us against UV radiation generated by the sun. As a result of the atmospheric circulation it can be transported to a small extent also in the lower atmosphere (troposphere), but it can also be produced as result of photochemical reactions from primary pollutants. Health effects of excessive exposure to ozone involve mainly the respiratory tract.

Ozone (O_3) is often analyzed by a spectrophotometric method. The sample is irradiated by UV light that is partially adsorbed by ozone. The decrease of light intensity is registered by the detector and the ozone concentration is calculated following the Lambert-Beer law. Since that calculus requires a reference state, the

analyzer is equipped with a device that removes O_3, giving the reference and a valve that permits the analyzer to shift from the measure and the reference mode. In Table 4.1 a summary of the typical analytical techniques used to analyze gas in atmosphere is reported.[8]

4.2 Atmospheric Aerosol

The principal chemical components of particulate matter (PM) are the following: sulfate, nitrate, ammonium, mineral dust, sea salt, organic compounds and black or elemental carbon; an example of the relative contribution of PM components is represented in Fig. 4.2.

- Sulfate—a secondary component, usually originated from atmospheric oxidation of SO_2.
- Nitrate—product from the neutralization of nitric acid vapour by ammonia in the form of ammonium nitrate (NH_4NO_3) or by the displacement of hydrogen chloride from sodium chloride by nitric acid vapour, forming sodium nitrate ($NaNO_3$).
- Ammonium—usually present in the form of ammonium sulfate ($(NH_4)_2SO_4$) or nitrate (NH_4NO_3).
- Sodium and chloride—typical of coastal area, these components are coming from sea salt.
- Elemental carbon—originated during high-temperature combustion of fossil and biomass fuels.
- Organic carbon—carbon present in the form of organic compounds: could be either primary, originated from traffic or industrial processes, or secondary, resulting from the oxidation of volatile organic compounds.
- Mineral components—the coarse fraction is rich in aluminium, silicon, iron and calcium.
- Water may also be present within water-soluble components, such as ammonium sulfate, ammonium nitrate and sodium chloride. These chemicals are able to take up water from the atmosphere at high relative humidity, thereby turning from crystalline solids into liquid droplets.

In addition to the main components, many minor chemicals are present in aerosol particles. Their concentration can be very low, but they have physical and chemical characteristics that lead up to a great interest about their detection:

- Trace metals—lead, cadmium, mercury, nickel, chromium and zinc.
- Trace organic compounds—although the total mass of organic compounds can constitute an important fraction of the whole mass of particles, the contribute of each individual organic compound can be very small.[9]

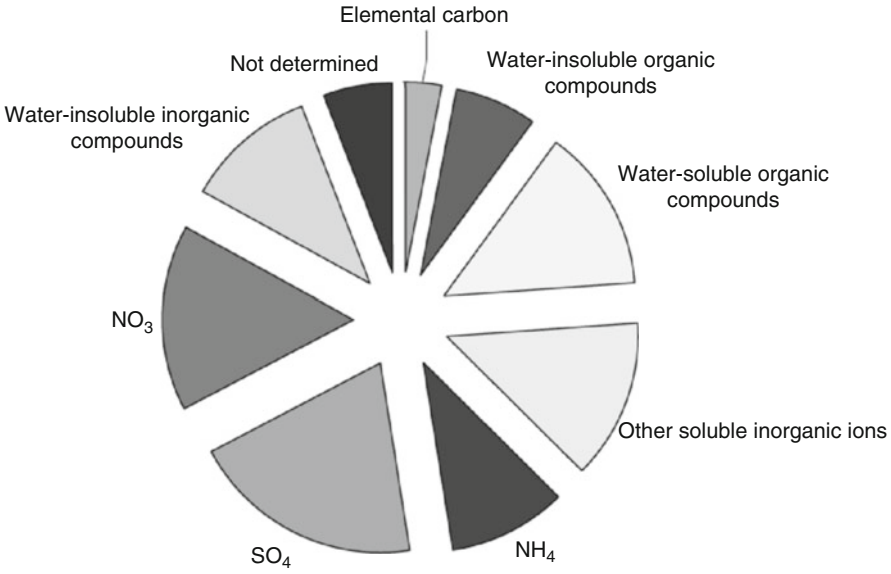

Fig. 4.2 Chemical balance on element constituents of aerosol mass in Italy (reproduced from (10) with permission from Elsevier)

4.3 Inorganic Aerosol

In the last few years much attention has been given to the evaluation of the elemental content of airborne particulate matter due to their detrimental effects on human health. Many epidemiological studies have revealed that the degree of adverse respiratory effects depends on the physical and chemical properties of atmospheric aerosol.[11–13] The particulate matter with an aerodynamic diameter <10 μm (PM_{10}) constitutes the inhalable fraction of aerosol, while the particulate matter with an aerodynamic diameter <2.5 μm ($PM_{2.5}$) could have more serious toxic effects as it constitutes the breathable fraction of the aerosol. Under this framework, European Commission (EC) legislation requires that member states monitor the PM_{10} and the lead concentration in atmosphere.[14] Furthermore the EC has recently proposed the monitoring of other toxic elements such as arsenic, cadmium and nickel in atmospheric particulate.[15]

Major and trace elements in particulate matter can be classified as natural (Na, Mg, K, Ca, Si, Al, Mn, etc.) or anthropogenic (V, Cr, Mn, Ni, Cu, Zn, Cd, Pb, etc.). The principal anthropogenic emission sources are attributed to fossil fuels: Cr, Mn and Sb are good markers for this source as they are present in coal, while V, Ni and Pb are emitted by fuel oil combustion. Industrial processes and non-ferrous mineral extraction are important sources for Cd, Zn, Cu and Hg, while elements like Ni, Zn, Pb and Cu are emitted during industrial processing of iron, cast iron and steel.

Since the atmospheric particulate samples are often constituted of minute quantities of dust (fractions of milligrams) collected onto large cellulose filters, total sample digestion is widely used for trace element analysis. Various methods using microwave-assisted digestion with different acid mixtures and different heating programs are described in the literature.[16–19] Yet in the total digestion of aerosol samples, elements contained in the cellulose material as impurities, as well as the large amounts of chemicals required, could give high blank levels and matrix effects during analysis. Therefore a careful quality control and optimization of the analytical procedure are crucial. Improvements in analytical techniques, together with the increase in awareness of ultraclean procedures, have drawn on reliable information about trace element concentrations in the different size ranges of airborne particles. No matter how much air is drawn through a filter and despite occasionally high particle loadings in the atmosphere, the amount of sample available for chemical analysis is small.

Several analytical techniques can be used to quantify metals in the aerosol. X-ray fluorescence (XRF) and proton-induced X-ray emission (PIXE) spectroscopy quantify the concentrations of elements with atomic numbers ranging from 11 (sodium) to 92 (uranium). In addition to providing a large number of chemical concentrations, neither XRF nor PIXE requires sample preparation or extensive operator time after they are loaded into the analyzer. Filters remain intact after analysis and can be used for additional analyses by other methods. Inductively coupled plasma (ICP) and instrumental neutron activation analysis (INAA) are as commonly applied to aerosol samples as XRF and PIXE. ICP requires destroying the filter, and INAA wads up the filter and makes it radioactive. These analyses are useful in certain applications owing to lower detection limits for some species used in source apportionment studies. Atomic absorption spectrophotometry (AAS) is useful for few elements, but it requires a too great dilution of the sample to be an effective technique when many different elements are to be measured. Ionic species, that are soluble in water, are important constituents of secondary aerosol, and can often be used to distinguish among pollution sources, as in the case of soluble potassium for wood smoke. Several simple ions, such as sodium, magnesium, potassium and calcium, are best quantified by ICP-optical emission spectrometry (ICP-OES). Generally lower elemental limits of detections are obtained using a microwave digestion procedure associated with an inductively coupled plasma mass spectrometry (ICP-MS) determination.

Polyatomic ions, such as sulfate, nitrate, ammonium and phosphate, must be quantified by other methods such as ion chromatography (IC). Ion analysis methods require filters to be extracted in deionized distilled water and then filtered to remove the insoluble residue. The extraction volume needs to be as small as possible, lest the solution become too dilute to detect the desired constituents (Table 4.2).

Table 4.2 Typical analytical techniques used to analyze inorganic components of atmosphere

Analytical method	Characteristics
X-ray fluorescence (HRF)	No sample preparation
Proton-induced X-ray emission (PIXE)	Non-destructive
Inductive coupled plasma (ICP)	Destructive
	Low detection limit
Instrumental neutron activation analysis (INAA)	Makes the filter radioactive
	Low detection limit
Atomic adsorption spectroscopy (AAS)	Useful only for few elements
Inductive coupled plasma-optical emission spectrometry (ICP-OES)	Useful for simple ions (Na, Mg, K, Ca)
Inductive coupled plasma-mass spectrometry (ICP-MS)	Low detection limit

4.4 Organic Aerosol

In the lower atmosphere the main components of PM are the following: highly water-soluble inorganic salts, insoluble mineral dust and carbonaceous material, including soluble and insoluble organic compounds and elemental carbon. A complete characterization of the organic fraction of PM is extremely difficult because of the high variability of physical properties and reactivity associated to both natural and anthropogenic particles. The best knowledge on the effects of organic compounds on climate and health can be achieved by the study of the distribution, lifetime and removal mechanisms. As atmospheric organic compounds are present in both the gaseous and condensed phases, the investigation of the gas-particle partitioning of such compounds becomes crucial.[20]

The most studied organic compounds in the aerosol are the persistent organic compounds (POPs) as polychlorinated dibenzo-*p*-dioxins and furans (PCDD/Fs), polychlorinated biphenyls (PCBs), polychlorinated naphthalenes (PCNs), polybrominated diphenyl ethers (PBDEs) and polycyclic aromatic hydrocarbons (PAHs).

If compared with other environmental compartments, the atmospheric burden of POPs is relatively small, but air is considered the most important vehicle for their global redistribution. POPs can persist in the environment for a long time; they are affected by long-range transport and their presence has been discovered in remote environments such as Arctic[21,22] and Antarctica.[23–25]

Gas chromatography-mass spectrometry (GC-MS) is the most common analytical technique used to identify and quantify organic compounds in atmospheric aerosol. The usefulness of GC resides in the very wide range of compounds that can be separated on a single column and on the easy online coupling to mass spectrometry (generally electron-impact quadrupole). This method has been precious in revealing that PM contains a very large number of different organic compounds.

Because of the convenience of GC methods, liquid chromatography (LC) has seldom been used for the study of organic aerosols. LC methods employ a very wide

Table 4.3 Typical analytical techniques used to analyze organic components of atmosphere

Compound	Analytical method
POPs	GC-MS
MAs	GC-MS after derivatization
	HPLC-MS and other detectors

range of different kinds of columns and solvents with different compositions, while using GC methods a single column and a change in temperature can give a good separation of compounds. On the other hand GC-MS appears capable of accounting for only about 25 % of organic compounds in several locations; so LC-MS should be considered a good alternative for those compounds that cannot be identified by GC methods, like water-soluble organic compounds (WSOCs) in the aerosol.[20]

Recently a lot of studies are focusing on biomass burning evaluation in aerosol. Important WSOCs from biomass burning are the monosaccharide anhydrides (MAs), and the most important tracer compound among them is levoglucosan (1,6-anhydro-β-D-glucopyranose) with small amounts of galactosan (1,6-anhydro-β-D-galactopyranose) and mannosan (1,6-anhydro-β-D-mannopyranose). Even though the MAs and, in particular, the levoglucosan content in organic aerosols have been the topic of many studies, a diversity between the methodologies for the chemical analysis has been observed.

Various chromatographic techniques have been used for MA analysis including gas chromatography-mass spectrometry (GC-MS) after derivatization and high-performance liquid chromatography (HPLC) by various detectors,[26–28] among which high-resolution mass spectrometry was included (Table 4.3).[29] Schkolnik and Rudich,[30] in a review on detection and quantification in atmospheric aerosols, report that GC with mass spectrometer as detector is the most commonly used method for levoglucosan quantification, despite requiring long preparation time and dry conditions. Recently alternative methods using HPLC with mass spectrometric detection have been proposed, and great efforts have been directed toward simple, fast, precise, accurate and possibly direct analytical methods. Engling et al.[31] report a high-performance anion-exchange chromatography method with pulsed amperometric detection for the determination of anhydrosugars in smoke aerosol that requires minimal sample preparation. Dixon and Baltzell[26] investigating HPLC with aerosol charge detection for the analysis of the main MAs in atmospheric aerosols reported for levoglucosan a limit of detection (LOD) lower than the lowest LODs listed by Garcia et al.[32] using electrophoretic microchip with pulsed amperometric detection (CE-PAD) and by Schkolnik et al.[30] using ion-exclusion HPLC and spectroscopic detection but higher than electrospray ionization (ESI-MS) and high-performance anion-exchange chromatography (HPAEC) with pulsed amperometric detection (PAD). A recent work determined phenolic compounds (PCLCs) in atmospheric aerosols at trace levels using liquid chromatography electrospray ionization tandem mass spectrometry (HPLC/(-)ESI-MS/MS).[33]

4.5 Conclusions

The atmosphere is a very complex mixture of chemicals. Some of them, both in gaseous and in particulate phase, can affect environment, climate and human health, so the development of newer and more specific techniques that permit to quantify pollutants in a fast and accurate way is very important. Among the gaseous constituents of atmosphere, sulfur oxides, nitrogen oxides and ozone are the most commonly monitored: for these chemicals European Regulations established spectrophotometric, luminescence and chemiluminescence techniques, respectively, because of their velocity and convenience. For monitoring purpose electrochemical sensors are likewise used; in addition to an accurate and rapid determination, the miniaturization of the sensors gives the possibility to obtain portable devices, very useful for in situ determinations. Despite the atmosphere is mainly composed by gases, it is very important to consider also the particulate matter in the environmental and health risk assessment. The predominant chemical components of PM are sulfate, nitrate, ammonium, sea salt, mineral dust and organic and elemental carbon; minor chemicals are trace metals and trace organic compounds. Different analytical techniques can be employed to investigate the inorganic part of aerosol: metals are historically analyzed by electrochemical stripping analysis using anodic stripping voltammetry (ASV) that gives simplicity, inexpensive, portability and accurate determination to the metal detection (see Chap. 10 vol 1 and Chap. 5 vol 2). Depending on the purpose of the analysis metals can be alternatively determined with X-ray fluorescence (XRF), proton-induced X-ray emission (PIXE) spectroscopy, inductive coupled plasma (ICP), instrumental neutron activation analysis (INAA) or atomic absorption spectroscopy (AAS). Several simple ions are best quantified by ICP-OES (optical emission spectrometry) or ICP-MS (mass spectrometry), while polyatomic ions must be analyzed by ion chromatography (IC). The most studied organic chemicals in aerosol are the persistent organic compounds (POPs), usually identified by gas chromatography-mass spectrometry (GC-MS). Immunosensors for the quantification of POPs have also been developed (see Chap. 13). Liquid chromatography (LC) can be useful for the determination of water-soluble organic compounds (WSOCs), including the monosaccharide anhydrides (MAs), which are biomass-burning markers in atmosphere. To quantify MAs several techniques have been improved: GC-MS after derivatization and high-performance liquid chromatography (HPLC) coupled with various detectors.

References

1. Seinfeld JH, Pandis SN (2006) Atmospheric chemistry and physics: from air pollution to climate change, 2nd edn. Wiley, New York
2. Poschl U (2005) Atmospheric aerosols: composition, transformation, climate and health effects. Angew Chem Int Ed 44:7520–7540

3. Harrison RM, Shi JP, Xi S et al (2000) Measurement of number, mass and size distribution of particles in the atmosphere. Philos Trans R Soc Lond A 358(1775):2567–2580
4. Chung SH, Seinfeld JH (2002) Global distribution and climate forcing of carbonaceous aerosols. J Geophys Res 107:509–512
5. Liao H, Seinfeld JH, Adams PJ et al (2004) Global radiative forcing of coupled tropospheric ozone and aerosols in a unified general circulation model. J Geophys Res 109, D16207
6. EN-14212 (2012) Ambient air—standard method for the measurement of the concentration of sulphur dioxide by ultraviolet fluorescence. European Regulations
7. EN-14211 (2012) Ambient air—standard method for the measurement of the concentration of nitrogen dioxide and nitrogen monoxide by chemiluminescence. European Regulations
8. EN-14625 (2012) Ambient air - Standard method for the measurement of the concentration of ozone by ultraviolet photometry. European Regulations
9. Colbeck I (2008) Environmental chemistry of aerosols. Blackwell, London
10. Zappoli S, Andracchio A, Fuzzi S et al (1999) Inorganic, organic and macromolecular components of fine aerosol in different areas of Europe in relation to their water solubility. Atmos Environ 33(17):2733–2743
11. Englert N (2004) Fine particles and human health: a review of epidemiological studies. Toxicol Lett 149:235–242
12. Pope CA III (1996) Adverse health effects of air pollutants in a nonsmoking population. Toxicology 111:149–155
13. Schwartz J, Dockery DW, Neas LM (1996) Is daily mortality associated specifically with fine particles? J Air Waste Manag Assoc 46:927–939
14. EC (European Commission) (1998) No. 57/98, 98/C360/04. Official Journal of European Communications C360/99, 23 Nov 1998
15. EC (European Commission) (2003) Commission of the European Communities, COM(2003) 423 final, 16 July 2003
16. Karanasiou AA, Thomaidis NS, Eleftheriadis K et al (2005) Comparative study of pretreatment methods for the determination of metals in atmospheric aerosol by electrothermal atomic absorption spectrometry. Talanta 65:1196–1202
17. Yang KX, Swami K, Husain L (2002) Determination of trace metals in atmospheric aerosols with a heavy matrix of cellulose by microwave digestion-inductively coupled plasma mass spectroscopy. Spectrochim Acta B 57:73–84
18. Pekney NJ, Davidson CI (2005) Determination of trace elements in ambient aerosol samples. Anal Chim Acta 540:269–277
19. Fernández Álvarez F, Ternero Rodríguez M, Fernández Espinosa AJ et al (2004) Physical speciation of arsenic, mercury, lead, cadmium and nickel in inhalable atmospheric particles. Anal Chim Acta 524:33–40
20. Jacobson MC, Hansson H-C, Noone KJ et al (2000) Organic atmospheric aerosols: review and state of the science. Rev Geophys 38(2):267–294
21. Hung H, Blanchard P, Halsall CJ et al (2005) Temporal and spatial variabilities of atmospheric polychlorinated biphenyls (PCBs), organochlorine (OC) pesticides and polycyclic aromatic hydrocarbons (PAHs) in the Canadian Arctic: results from a decade of monitoring. Sci Total Environ 32(1–3):119–144
22. Polkowska Z, Cichala-Kamrowska K, Ruman M (2011) Organic pollution in surface waters from the Fuglebekken Basin in Svalbard, Norwegian Arctic. Sensors 11(9):8910–8929
23. Dickhut RM, Cincinelli A, Cochran M et al (2012) Aerosol-mediated transport and deposition of brominated diphenyl ethers to Antarctica. Environ Sci Technol 46(6):3135–3140
24. Klanova J, Matykiewiczova N, Macka Z et al (2008) Persistent organic pollutants in soils and sediments from James Ross Island, Antarctica. Environ Pollut 152(2):416–423
25. Negri A, Burns K, Boyle S et al (2006) Contamination in sediments, bivalves and sponges of McMurdo Sound, Antarctica. Environ Pollut 143(3):456–467

26. Dixon RW, Baltzell G (2006) Determination of levoglucosan in atmospheric aerosols using high performance liquid chromatography with aerosol charge detection. J Chromatogr A 1109:214–221
27. Palma P, Cappiello A, De Simoni E et al (2004) Identification of levoglucosan and related stereoisomers in fog water as a biomass combustion tracer by ESI-MS/MS. Ann Chim-Rome 94:911–919
28. Cappiello A, De Simoni E, Fiorucci C et al (2003) Molecular characterization of the water-soluble organic compounds in fog water by ESIMS/MS. Environ Sci Technol 37:1229–1240
29. Dye C, Yttri KE (2005) Determination of monosaccharide anhydrides in atmospheric aerosols by use of high-performance liquid chromatography combined with high-resolution mass spectrometry. Anal Chem 77:1853–1858
30. Schkolnik G, Rudich Y (2006) Detection and quantification of levoglucosan in atmospheric aerosols: a review. Anal Bioanal Chem 385(1):26–33
31. Engling G, Carrico CM, Kreidenweis SM et al (2006) Determination of levoglucosan in biomass combustion aerosol by high-performance anion-exchange chromatography with pulsed amperometric detection. Atmos Environ 40:S299–S311
32. Garcia CD, Engling G, Herckes P et al (2005) Determination of levoglucosan from smoke samples using microchip capillary electrophoresis with pulsed amperometric detection. Environ Sci Technol 39:618–623
33. Zangrando R, Barbaro E, Zennaro P et al (2013) Molecular markers of biomass burning in arctic aerosols. Environ Sci Technol 47(15):8565–8574

Chapter 5
Biosphere

Adela Maghear and Robert Săndulescu

5.1 Chemical and Electrochemical Sensors in Living World

Living world offers a lot of examples of sensors consisting in biological receptors (proteins, nucleic acids, signaling molecules) located everywhere, in the cell (nucleus, mitochondria, cell membrane), in all the tissues, in organs, or even in the circulating bloodstream. Muscular and nervous activities are accompanied by electrical currents which can be measured by electrocardiography or electroencephalography, for example. The transmission of the nervous stimuli represents in fact a true electrochemical process, during which an electrical current is carried all along the neuronal axon to the synapse, where a chemical entity (acetylcholine, adrenaline, etc.) is released. This chemical species passes through the synapse space where it is discharged to the next neuron, generating a new electrical current, in picoseconds, or even in a shorter time. In fact, the whole metabolism, cell division, growth and apoptosis, immune response by antibody synthesis, or even pathologic processes like inflammation are controlled by an outstanding network of receptors and signaling molecules in a sensor-actuator manner. This extremely important feature is common to all living organisms, from microorganisms like viruses and bacteria, to the plant and animal world. In other words, one can say that electrochemistry is surrounding and controlling us in every moment.

Mitochondria are the power plants of the living cell; their most important roles are to produce the energy of the cell, adenosine triphosphate (ATP) (i.e., phosphorylation of adenosine diphosphate (ADP) by a chain of reactions known as the citric acid cycle or the Krebs cycle) through respiration, and to regulate the cellular metabolism (Fig. 5.1).[1]

A. Maghear (✉) • R. Săndulescu
Faculty of Pharmacy, Analytical Chemistry Department, "Iuliu Haţieganu" University of Medicine and Pharmacy, 4 Louis Pasteur St., Cluj-Napoca 400349, Romania
e-mail: rsandulescu@umfcluj.ro

L.M. Moretto, K. Kalcher (eds.), *Environmental Analysis by Electrochemical Sensors and Biosensors*, DOI 10.1007/978-1-4939-0676-5_5

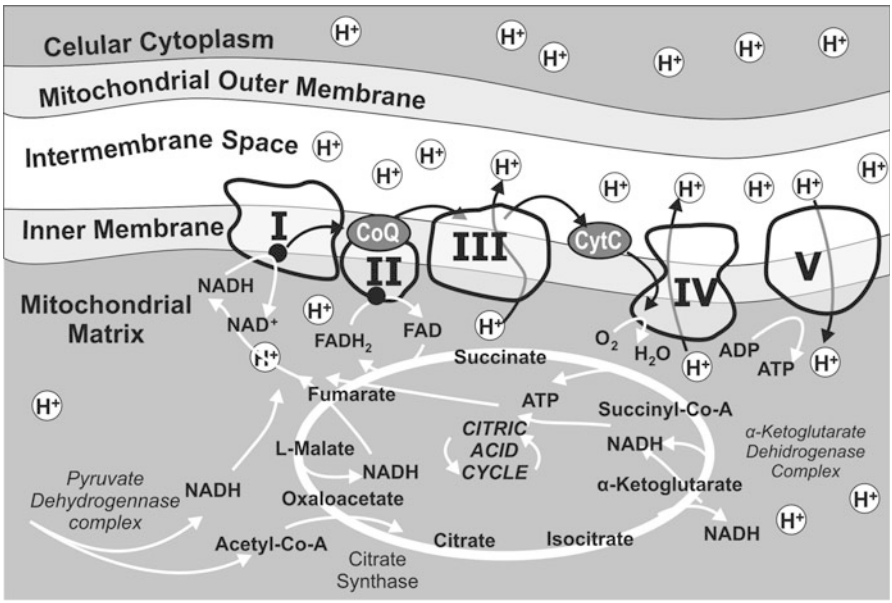

Fig. 5.1 Mitochondrial tricarboxylic acid (TCA) cycle or Krebs cycle

The outer protein-phospholipidic mitochondrial membrane contains a large number of integral proteins called porins, which form channels that allow relatively small molecules (5,000 Da or less in molecular mass) to freely diffuse from one side of the membrane to the other.[2] Larger proteins are transferred by the protein of the outer membrane called translocase which binds a signaling sequence at their N-terminus, and actively moves them across the membrane.[3]

The intermembrane space situated between the outer membrane and the inner membrane has the same composition as the cytosol, because the outer membrane is freely permeable to small molecules. Large proteins (cytochrome *c*) must have a specific signaling sequence to be transported across the outer membrane.[4]

The inner mitochondrial membrane contains proteins[2] that perform the redox reactions of oxidative phosphorylation, generate ATP in the matrix (ATP synthase), regulate the metabolite passage into and out of the matrix by specific transport, and allow the protein passage across the inner membrane (inner membrane translocase), the protein fusion, and fission.

The production of ATP is achieved by glucose, pyruvate, and NADH oxidation in the presence of oxygen (aerobic respiration). In the absence or in the presence of limited amounts of oxygen, the glycolytic products will be metabolized by anaerobic fermentation using alternative substrates such as nitrite.[5]

Pyruvate produced by glycolysis is actively transported across the inner mitochondrial membrane into the matrix where it is oxidized and combined with coenzyme A to form CO_2, acetyl-CoA, and NADH.

During Krebs cycle acetyl-CoA is oxidized to carbon dioxide. The reduced cofactors (three molecules of NADH and one molecule of $FADH_2$) that result from the Krebs cycle are a source of electrons for the electron transport chain, and the molecule of guanosine triphosphate (GTP) is converted to ATP.[1]

Protein complexes in the inner membrane (NADH dehydrogenase, cytochrome c reductase, and cytochrome c oxidase) transfer the redox energy from NADH and $FADH_2$ to O_2 in several steps via the electron transport chain. The released energy is used to pump H^+ into the intermembrane space. Electrons may also reduce oxygen, forming reactive oxygen species such as superoxide, which is a cause of oxidative stress associated with the aging process.[6]

A strong electrochemical gradient occurs across the inner membrane, as the proton concentration increases in the intermembrane space. The protons can return to the matrix through the ATP synthase complex, their energy being used to synthesize ATP from ADP and inorganic phosphate.[1]

Living organisms developed outstanding and very complex networks of biological sensors distributed all over, from single cells and tissues to specialized organs like the eyes, ear, skin, nasal mucous, or tongue. The skin-sensitive fibers are in fact the dendrites of the sensitive neurons that emerge from spinal ganglions and receive external signals like pressure, coldness, or heat. These signals are sent to and from the brain through efferent and afferent neurons. Transmission of nerve impulses constitutes the most convincing example of electrochemistry in the living world.

Neurons do not touch each other; a gap called a *synapse* or *synaptic cleft* separates the axon of one neuron and the dendrites of the next neuron. All the signals must cross the synapse to continue on its path through the nervous system. In the brain, the nervous impulse is carried across synapses by electrical conduction, while in other parts of the body impulses are carried across synapses by an electrochemical process. When an impulse comes, the membrane at the end of the axon depolarizes, opening the gated ion channels, and calcium ions are allowed to enter the cell. The presence of calcium ions determines the release into the synapse of a chemical species called neurotransmitter which moves across the synapse and binds to specific receptors (different proteins serve as receptors for different neurotransmitters) on the postsynaptic neuron membrane that is about to receive the impulse.

Excitation or inhibition depends on the neurotransmitter and the receptor. For example, if the neurotransmitter causes the opening of the Na^+ channels, the neuron membrane becomes depolarized and the impulse is carried through that neuron. If the K^+ channels open, the neuron membrane becomes hyperpolarized and inhibition occurs.

When a neuron is not stimulated its membrane is polarized; the outside of the membrane containing Na^+ ions is positively charged while the electric charge on the inside of the membrane containing K^+ ions, negatively charged proteins, and nucleic acid molecules is negative. The neuron is inactive and polarized until a stimulus comes. Then, the Na^+/K^+ pumps on the membrane pump the Na^+ back outside the membrane and the K^+ back inside.

When a stimulus occurs, the neuron is depolarized; the gated ion channels on the resting neuron's membrane open suddenly and allow the Na^+ that was outside the membrane enter the cell, which becomes positively charged. Polarization is removed and the threshold level is reached. When the stimulus goes above the threshold level, more gated ion channels open allowing more Na^+ inside the cell. Like this, complete depolarization of the neuron is achieved, an action potential is created, and the stimulus will be transmitted.

Once the inner space of the cell is occupied by Na^+, the Na^+ gates close and the K^+ gated ion channels of the cell membrane open allowing K^+ to move to the outside space. Thus, the electrical balance (the repolarization of the membrane) is restored, but at this time the repolarized membrane has Na^+ on the outside and K^+ on the inside.

The membrane potential when K^+ gates finally close is lower than the resting potential, and the membrane is hyperpolarized because the neuron has slightly more K^+ on the outside than it has Na^+ on the inside. After the impulse has passed through the neuron, the action potential is over, and the cell membrane returns to the resting potential.

The Na^+/K^+ pumps will return the ions to their rightful side of the neuron's cell membrane; the neuron returns to its normal polarized state and stays in the resting potential until another impulse occurs. During this period called refractory period, the neuron does not respond to any incoming stimulus.

Signals are sent along the neuronal axon as electrochemical waves (called action potentials) producing cell-to-cell signals where axon terminals make synaptic contact with other cells. Synapses may be electrical or chemical, the last ones being much more common and diverse in functions.[7,8] The neuron that sends the signals is called presynaptic neuron, and the one that receives the signals is called postsynaptic neuron. In the presynaptic area are located numerous microvesicles containing chemical molecules, called neurotransmitters. When the presynaptic terminal is electrically stimulated, the contents of the vesicles are released into the synaptic cleft. The neurotransmitter binds to the receptors located in the postsynaptic membrane, which will be activated. As a consequence, the resulting effect on the postsynaptic cell can be excitatory, inhibitory, or modulatory, depending on the type of receptor (Fig. 5.2). For example, the release of the neurotransmitter acetylcholine at a synaptic contact between a motor neuron and a muscle cell induces rapidly the muscle contraction, the entire synaptic transmission process taking only a fraction of a millisecond.[7]

Over a hundred neurotransmitters are known nowadays, many of them having multiple types of receptors. Among the well-known neurotransmitters are monoamines (dopamine, norepinephrine, epinephrine, histamine, serotonin), amino acids (glutamate, aspartate, D-serine, gamma-aminobutyric acid (GABA), glycine), peptides (somatostatin, P substance, opioid peptides like endorphins), and some others, such as acetylcholine, adenosine, anandamide, nitric oxide, hydrogen sulfide, and carbon monoxide.[9]

Acetylcholine (Ach) can be found in the central nervous system, neuromuscular junctions, spinal cord, and preganglionic and motor neurons. Neurological and

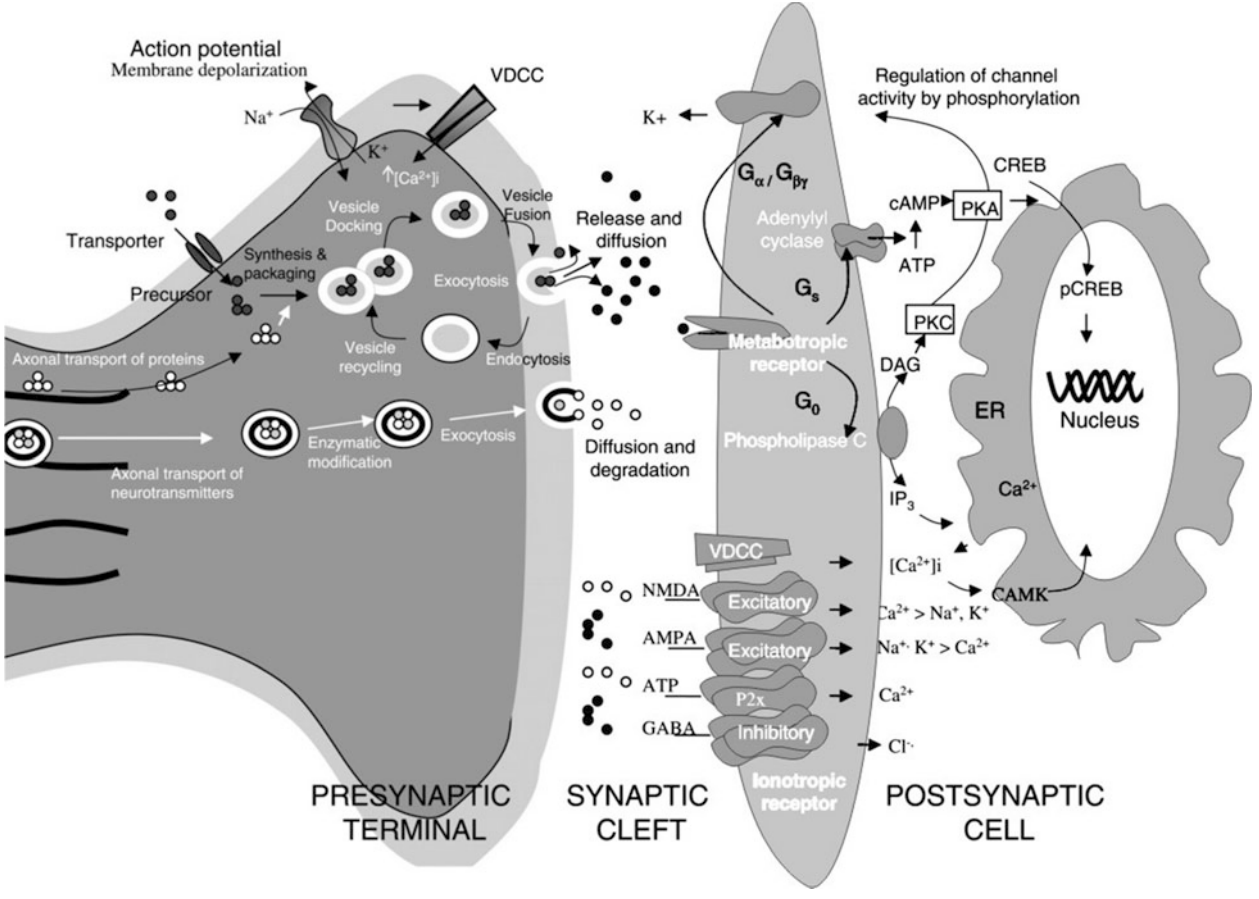

Fig. 5.2 Synaptic nervous transmission

neuropsychiatric diseases, such as Alzheimer's disease, Parkinson's disease, progressive dementia, and schizophrenia, may occur due to acetylcholine accumulation in nervous tissue without being metabolized. This fact explains the considerable interest for its determination in vitro and in vivo, but unfortunately, Ach is neither easily oxidizable/reducible, nor possesses structural characteristics (electroreactive, chromophore, or fluorophore groups) in order to allow a sensitive detection by electrochemical, spectrophotometric, or fluorometric methods. Sattarahmady et al. investigated the electrocatalytic oxidation of Ach by cyclic voltammetry, steady-state polarization measurements, and chronoamperometry on a nickel nanoshells-carbon microparticles-Nafion nanocomposite.[10] The nanocomposite-based Ach biosensor showed a sensitivity of 48.58 ± 0.52 mA M^{-1} cm^{-2} and a limit of detection of 49.33 nM. The same group reported the electrocatalytic oxidation of Ach on two different copper-based transducers, a copper microparticle-modified carbon paste electrode (CPE) and a copper nanoparticle-modified CPE.[11]

Generally, synapses use more than one neurotransmitter, in most cases a fast-acting small-molecule neurotransmitter, such as GABA or glutamate, together with one or more neurotransmitters with slower acting modulatory like peptides.[7,8]

Receptors can be divided into two main types: chemically gated ion channels and second messenger systems. When a chemically gated ion channel is activated, it allows specific types of ions to flow across the membrane, the effect on the target cell being excitatory or inhibitory, depending on the ion type. When a second messenger system is activated, a chain of molecular interactions starts inside the target cell, resulting in a wide variety of complex effects (i.e., the increase or decrease of the cell sensitivity to stimuli).

Both glutamate and GABA have several widely occurring receptor types, but all of them are excitatory or modulatory for glutamate and inhibitory for GABA.[12]

Axonal transport occurs along the cellular cytoskeleton, which is the neuron structural support, allowing the cell to grow or change in size and shape over time. There are three major components of the neuronal cytoskeleton: microtubules, actin, and intermediate filaments. Neurons are uniquely dependent on the microtubule-based transport and the deficits in axonal transport contribute to pathogenesis (neurodegenerative diseases, like amyotrophic lateral sclerosis). The motor, cytoskeletal, and adaptor proteins involved in the axonal transport, in the disruption of axonal transport, and the pathways that may cause neuronal dysfunction and death are described in a review by Chevalier-Larsen and Holzbaur.[13]

An electrochemical strategy to investigate the 1,4-naphthoquinone effect on voltage-gated potassium channels was recently reported by Rodríguez-Fernández et al.[14] Naphthoquinone (NQ) was tested on voltage-gated ion channels expressed in *Xenopus laevis* oocytes by cyclic voltammetry. A typical two-stage mono-electronic reduction mechanism was observed in dimethylsulfoxide (DMSO), while a one-stage bielectronic reduction process was found in physiological supporting electrolyte ND-96 (NaCl, 96 mM; KCl, 2 mM; $CaCl_2$, 1.8 mM; $MgCl_2$, 1 mM; and HEPES buffer, 5 mM; pH adjusted to 7.0 with NaOH). The structural features, such as aromaticity and substituents, prone to hydrogen

bond formation of NQs, are important, together with the NQ interactions with some channel residues which favors their reduction process in the protein surroundings.

5.2 Electrochemical Sensors for Flora and Fauna on Earth

Biosphere comprises all living organisms on earth; this is why it represents the most dynamic and fragile "sphere" of our planet, being strongly influenced by all other "spheres," soil, water, and air. Terrestrial flora and fauna are the main components of the biosphere, but it can be considered that microorganisms (bacteria, viruses, etc.) and human community have their particular features and should be treated separately. Human community brings its main contribution to the pollution of all spheres through industrial and domestic activity, but in the same time one of its main concerns is fighting against environmental pollution by coordinated actions.

Biosphere represents also the most complex and heterogeneous sphere by comparison with air, water, and soil, which are relatively "homogeneous," and, therefore, it makes it difficult to characterize. The great variety of living organisms (microorganisms, plants, animals) makes the assessment of both normal and abnormal "composition" of this sphere almost impossible. So each case should be treated separately and set in the general context of the biosphere and the whole environment. The normal behavior and environmental conditions for a particular living species, plant or animal, in relation with other environmental factors (soil, air, or water) represent an interesting topic. Another topic consists in either the environmental factors or pollutants that affect or damage the living species, or in how the environment is affecting particular species. Some important features here are the continuous deforestation (especially in equatorial areas, such as Amazonia) and desertification caused by intensive agriculture which seriously affect terrestrial atmosphere. Another worrying matter is represented by carbon dioxide emissions caused by the intensive cattle livestock and the so-called greenhouse effect (taking into consideration the important amount of CO_2 that a single cow "produces" per year).

Two different approaches describe the electrochemical sensors for vegetal and animal organisms: sensors able to detect the presence, the movement, and the number of organisms in a given environment, or sensors able to detect a large variety of normal or pathologic parameters in living organisms.

The representative techniques currently applied for an efficient, specific, rapid detection of viruses are described by Caygill et al.[15] Among them, electrochemical biosensors based on amperometric, potentiometric, and impedance measurements, optical biosensors that use surface plasmon resonance, optical fibers and piezoelectric biosensors based on microcantilevers, and recently the use of nanoparticles and novel nanomaterials as alternate recognition surfaces have been widely applied.

Cheran et al.[16] reported the current techniques employed for the transduction and processing of cellular signals, both for single-cell behavior and populations of cells. Electrochemical methodology (transistor and impedance methods), optical (light addressable potentiometry), and vibrational methods (transverse acoustic wave

methodology and Kelvin nanoprobe) were employed for examining populations of neurons, smooth muscles, and human red blood cells on a substrate in a label-free manner.

The use of microtechnology to develop new micro-fabricated electrode structures able to manipulate sub-micrometer particles by means of a nonuniform AC electric field was described by Abonnenc et al.[17] The microchip could integrate manipulation of living cells under software control without affecting the viability of living organisms, and allowed their recovery after having performed complex operations, offering like this a powerful tool for the development of new diagnostic and therapeutic protocols.

The sensors able to detect a great variety of normal or pathologic parameters in living organisms are designed for three main types of pollutants: chemical, microbiological, and genetic.

Some examples in this way are the electrochemical microsensors for Cd(II) and Pb(II) detection in plants[18]; the real-time electrochemical detection of extracellular nitric oxide in tobacco cells as a potent regulator of major processes including germination, root growth, stomatal closure, flowering, and adaptive responses to biotic and abiotic stresses[19]; a DNA electrochemical biosensor based on 2,6-pyridinedicarboxylic acid film and gold nanoparticles on the glassy carbon electrode (GCE) for electrochemical impedance spectroscopic detection of the sequence-specific DNA related to the PAT transgene in transgenic plants[20]; or an electrochemical sensor array for monitoring the proliferation effects of *Cissus populnea* plant extracts on TM4 Sertoli.[21] Some organisms, such as blue-green algae (cyanobacteria), can produce and deliver in water toxic metabolic products for the aquatic organisms and humans, which can be detected and quantified by a phycocyanin sensor.[22]

Environmental monitoring based on whole-organism bioassays and biological early warning systems (BEWS) is lately considered to replace standard expensive chemical analysis. The tests must accomplish some basic conditions like to be simple, based on standardized protocols, predictive, low cost, and applicable to species, populations, and communities. They also need to be sensitive to a wide range of chemicals with minimal matrix effects.[23]

Whole-organism bioassays are based on the measurement of the biological response (acute or chronic toxicity) of a test organism to contaminants present in a water sample (e.g., drinking, ground, surface, or wastewater effluent) in a standardized test usually conducted in the laboratory.[24] Several test species covering most of the different trophic levels in freshwater and/or estuarine/marine environments may be employed, the use of multiple test species and trophic levels being usually recommended because each species shows specific sensitivity to different chemicals or classes of compounds.[24,25]

The usually measured parameters are bioluminescence, metabolic status, or growth, when microorganisms at the base of the trophic chain, such as *Vibrio fischeri* or *Pseudomonas putida*, are used.[26]

Other parameters, like the reduction in photosynthetic activity (by measuring fluorescence) or the growth rate inhibition, can be considered if phototrophic

organisms, such as green algae (*Selenastrum capricornutum* or *Pseudokirchneriella subcapitata*), are employed. The use of dormant organism technology (e.g., algae or daphnid *Daphnia magna*) allows a simplified, rapid, and cost-effective test without the inconvenience of cell cultures, which are much more expensive.[27,28] Thus, the detection of specific effects of herbicides which can affect either photosynthesis systems I or II[29] can be achieved.

Chronic toxicity testing using invertebrates is usually based on growth rate or survival of amphipods (e.g., *Hyalella azteca* or *Gammarus*), chironomid larvae (*Chironomus riparius*), daphnids, oysters (*Crassostrea gigas*), and many other organisms under controlled conditions.[26,30] Bigger organisms such as fish are used for risk assessment, larval/embryonic development rate, fish lethality, or growth rate being the toxicity endpoints used in these assays.[24]

Biomonitoring using BEWS is based on the toxicological response of an organism to a contaminant or mixture of contaminants.[31] Many organisms, including fish species,[32,33] daphnia, midge larvae, microorganisms (e.g., algae and bacteria),[34] bivalve mollusks (e.g., various species of mussels), or even combinations of these test organisms[35] have been used as BEWS.

BEWS applications include monitoring of drinking water intakes, water distribution systems, wastewater effluents, effluents from contamination sites,[36,37] or river basin monitoring,[38] and provide a rapid evaluation of water quality and toxicity that cannot be achieved through other analytical methods.

Generally, BEWS consist of a living organism, a sensing element to detect changes in the test organism, and a processing element to translate the signal from the sensing element into a warning response system. The species commonly used are the rainbow trout (*Oncorhynchus mykiss*) or the bluegill (*Lepomis macrochirus*).[39] The secondary sensing system is composed of electrodes immersed close to the fish to monitor changes in electrical voltage associated with gill muscle activity.[32] Swimming and positioning behavior, or the ability to swim against current and ventilation frequency, are regularly employed.[33,39] Algal monitors are based on fluorescence, oxygen production measurements, and growth rate monitoring and can detect the effects from herbicides or other toxicants that interact with chlorophyll photosynthetic systems.[34] Measurements based on respiration, pumping, and heart rates of bivalve mollusks, such as the freshwater zebra mussel (*Dreissena*) or the marine blue mussel (*Mytilus edulis*),[40] have been tested, even though valve closure or movement responses are defense mechanisms used by bivalves to avoid stress such as contaminated water.[41] Behavioral changes of *Tubificids* worms have also been undertaken.[42]

The exploitation of BEWS depends on the data treatment and coordination of response measures to pollution events in order to mitigate their environmental impact,[43] but also on the improvement in data transfer and on personal computers, the use of online chemical monitoring systems (e.g., SAMOS) being a crucial factor.

A particular category of electrochemical sensors is the sensors able to detect the great variety of normal or pathologic parameters of living organisms. They can be designed either for analytical laboratory conditions, like any other type of sensor, or to be used in vivo, like implantable sensors. In the latter case, issues like their size,

shape, biocompatibility, and lifetime are crucial and will be discussed together with some examples of implantable sensors recently reported in scientific literature.

A broad variety of pharmaceuticals relying on nanoparticles has been reported for both drug delivery and diagnosis tasks.[44] Pharmaceutical products gave rise to new opportunities in directions such as topical and transdermal delivery owing to their ability to penetrate through human tissues, implantable release systems for tissue engineering applications, and ophthalmic delivery in which drug release can be externally controlled by stimuli-responsive nanocomponents.[45–49]

Microdialysis is known as a powerful sampling technique that makes it possible to continuously monitor the concentrations of biological molecules and other substances both in vivo and in vitro.[50] Microdialysis sampling was first applied in the area of neuroscience research,[51] and then it has been extensively employed for other pharmaceutical applications, such as the investigation of the transdermal delivery of drugs,[52] tissue pharmacokinetics,[53] and regional metabolism of drugs in tissues.[54,55] Microdialysis probes have been placed in virtually every tissue and organ in the body, including the liver,[56,57] heart,[58,59] skin,[54,60] blood,[61,62] placenta,[63] stomach,[64,65] and ear.[66]

The mechanism of microdialysis sampling was also explored. Therefore, the probe containing a dialysis membrane with a specific molecular mass cutoff, implanted in the physiological region of interest, is perfused with a fluid that is similar in ionic strength and composition to the extracellular fluid being sampled. Small molecules in the extracellular fluid can diffuse across the membrane based on their concentration gradient and are then transported to the analysis system. In this way, the compounds in the perfusate that are not present in the extracellular fluid can be delivered directly to the physiological site of interest.[50] Therefore, compounds from a single tissue site can be both delivered and recovered. This was proved to be very useful for looking at site-specific release of neurotransmitters,[50] observing regional metabolism of neuropeptides,[67,68] or comparing the metabolism of antineoplastic agents in tumor vs. healthy tissue.[69]

For neurochemical studies, probes are generally composed of stainless steel and are implanted into the specific brain region of interest using a guide cannula. Typical probes used for rat brain studies are normally 15 mm long with a diameter between 200 and 500 μm. The dialysis membrane, from 1 to 4 mm in length, is located at the end of the concentric cannula.[50]

A probe designed for blood sampling was first described by Telting-Diaz et al.[70] and consisted of two pieces of fused silica tubing attached to the dialysis membrane. This probe was so flexible that it could bend when the animal moved, minimizing any blood vessel damage. Online microdialysis–biosensor systems need low sample volumes (μL) if high temporal resolution is required.[50] Also, high sensitivity and specificity for the analyte(s) of interest in the presence of other endogenous electroactive analytes are mandatory.[71] A flow-through biosensor was reported for direct coupling to continuous low-flow microdialysis. Analyte selectivity for glucose and lactate could be achieved by using immobilized oxidoreductase enzymes followed by amperometric detection of hydrogen peroxide.[72]

Online microdialysis sampling coupled to biosensors was reported for analytes such as ascorbate,[73] glucose, lactate,[74,75] and glutamate.[74,76,77] The simultaneous monitoring of glucose and lactate in rats under hypoxic conditions was also achieved.[78] An online system for multianalyte in vivo monitoring was described by Yao et al. and consisted of a triple-enzyme electrode that selectively detected glucose, L-lactate, and pyruvate without significant cross-reactivity.[79] Similar flow injection-based online systems were reported for L-glutamate, acetylcholine, dopamine,[80] and D-/L-lactic acid.[81]

An online system for glucose and lactate to monitor ischemic events in freely moving rats was also developed. The analytes were monitored by flow injection analysis with enzyme-based amperometric detection.[82] Glucose monitoring was achieved in an awake rabbit using a flow-through sensor with chemiluminescence detection.[83] Online monitoring of glucose and lactate from rat brain was also performed following ischemia and reperfusion. In this case, the sensor employed methylene green adsorbed on single-walled carbon nanotubes for detection.[84]

Few studies have used carbon nanotube sensors in biological samples. By reducing the size of the electrodes, as many are based on larger GCEs or CPEs, so they are compatible with tissue implantation or the size of cells; more applications can be found in this direction. Due to the fact that dopamine and other catecholamines are not expected to be present at high levels in plasma or urine, studies should focus on examining tissue from the nervous system or investigating release from cells. Moreover, the low basal levels of dopamine (10 nM) and other neurotransmitters make sensitivity a particular challenge.[85]

Another concern for in vivo use of carbon nanotube-based sensors is their toxicity. Even carbon nanotube toxicity has not yet been fully characterized; many present studies find that CNTs aggregate together, generally in the liver, spleen, and lung tissue. CNT aggregates might have similar carcinogenic properties to asbestos fibers.[86–88]

The extracellular recording of bioelectric signals was proved to be widely achieved by microelectrode electrophysiology. By replacing the traditional electrode conductors with highly flexible electroconductive polymers, non-cytotoxic and biostable all-polymer microelectrode arrays able to reliably capture action potentials and local field potentials from acute preparations of heart muscle cells and retinal whole mounts, in vivo epicortical and epidural recordings, as well as during long-term in vitro recordings from cortico-hippocampal cocultures could be achieved.[89]

By using organic conjugated polymers that use both electrons and ions as charge carriers of the nervous system, a series of novel communication interfaces between electronic components and biological systems was developed. An organic electronic ion pump made of the polymer–polyelectrolyte system poly (3,4-ethylenedioxy thiophene):poly(styrenesulfonate) able to translate electronic signals into electrophoretic migration of ions and neurotransmitters was described.[90] Therefore, it was demonstrated how spatiotemporally controlled delivery of ions and neurotransmitters can be used to modulate intracellular Ca^{2+} signaling in neuronal cells in the absence of convective disturbances. In this way, the amplitude and frequency of Ca^{2+} responses can be strictly controlled due to the

electronic control of delivery, which can be used to generate temporal patterns mimicking naturally occurring Ca^{2+} oscillations. By developing an electrophoretic chemical transistor, an analog of the traditional transistor used to amplify and/or switch electronic signals, the further control of the ionic signals was enabled. Finally, the organic electronic ion pump could be used in a new "machine-to-brain" interface by modulating brainstem responses in vivo.[90]

In spite of its disadvantages, platinum has been used for nonenzymatic detection of blood glucose. One of the drawbacks of the platinum electrode is its catalytic activity for the electrochemical oxidation of glucose drops which can be seriously affected by the chloride ion present in physiological fluids.[91,92] On the other hand, amino acids,[93,94] biochemicals like ascorbic acid, creatinine, epinephrine, and urea[94] in blood can destroy the platinum electrode. In this way, if blood proteins occupy the catalytic sites on the platinum surface, the detection of glucose on platinum will be deteriorated.[96] Due to the fact that glucose oxidation can be inhibited by many biochemicals and amino acids in blood,[95] this can lead to a loss of sensitivity when glucose is detected with platinum.[96]

A system for continuous estimation of blood glucose in fish was developed by Yonemori et al.[97] The eyeball scleral interstitial fluid (EISF) was used as the site of sensor implantation and the relationship between EISF and blood glucose concentrations was evaluated, revealing that blood glucose concentrations were closely correlated with the EISF glucose concentration. A needle-type enzyme sensor for implantation in the fish sclera using a flexible wire electrode was then prepared. The sensor provided a rapid response, good linearity, and reproducibility. Continuous glucose monitoring could be carried out by implanting this needle-type glucose sensor onto the eye. An accurate glucose monitoring could be achieved for over 160 min.

A hybrid biological fuel cell (HBFC) comprising a microbial anode for lactate oxidation and an enzymatic cathode for oxygen reduction was developed and then tested in a marine environment. A laboratory-cultivated *Shewanella oneidensis* DSP-10 was fixed on a carbon felt electrode via a silica sol–gel process in order to catalyze anodic fuel cell processes. The cathode electrocatalyst consisted of bilirubin oxidase, fixed to a carbon nanotube electrode using a heterobifunctional cross-linker, and then stabilized with a silica sol–gel coating. The HBFC maintained a reproducible open-circuit voltage >0.7 V for 9 days in laboratory settings and sustained electrocatalytic activity for >24 h in open environment tests.[98]

A chitosan-modified carbon fiber microelectrode for in vivo detection of serotonin was described. It was demonstrated that chitosan has the ability to reject physiological levels of ascorbic acid interferences and facilitate selective and sensitive detection of in vivo levels of serotonin. In vivo results demonstrated that the chitosan-modified electrode could measure serotonin produced in the zebrafish intestine with high spatial and temporal resolution. A serotonin concentration of 30.8 ($\pm$3.4) nM could be recorded in vivo with the implanted chitosan-modified microelectrode in normal physiological conditions. Due to its inherent biocompatibility and remarkable adherence, chitosan was proved to be an excellent coating for use in implantable sensors, able to selectively detect and monitor levels of in vivo neurotransmitters.[99]

5.3 Sensors for Monitoring Agriculture, Food, and Drug Quality

In order to provide accurate information on crop, soil, climate, and environmental conditions, modern agricultural management relies strongly on many different techniques.[100] For more information on soil and agricultural analysis, see Chap. 2.

5.3.1 Remote Spectral Sensing

An important tool in this direction is the remote spectral sensing of crops, which refers to imagery taken from above a field where the incident electromagnetic radiation is generally sunlight.[101] The difference in color, texture, or shape of the contacted bodies is due to the amount of the reflected, absorbed, and transmitted energy of a specific wavelength.[100] The ratio of reflected energy to incident energy, known as spectral reflectance, is measured as a function of wavelength[102] and its recorded images represent a spectral signature, which is unique to plant species and conditions.[100] Food quality and food contaminants could be detected in food industry by using remote spectral sensing.[103–106] A sensor system that measures induced fluorescence or scattered reflectance is used in food-processing plants when an artificial light source is needed to illuminate the food as it passes on a conveyor belt.[100] The wavelengths measured in food quality cover generally the ultraviolet (10–400 nm), visible (400–750 nm), and near-infrared range (750–2,500 nm).[103] Some studies used also three-dimensional hyperspectral images for accurate detection.[107–111]

5.3.2 The Electronic Nose

Each plant releases a specific volatile organic compound (VOC) as a result of its everyday biological processes and the quantity of this compound represents an indicative of crop and field conditions. VOCs can be affected by the different environmental conditions, but also by insects or plant diseases. Electronic noses are used in agriculture to detect crop diseases, identify insect infestations, and monitor food quality. The electronic nose generally contains two components: an array of gas sensors with a broad and partly overlapping selectivity and an electronic pattern recognition system with multivariate statistical data processing tools.[100] The electronic nose is typically able to compare the profile of VOCs released by healthy plants/fruits with diseased plants/fruits.[100] In the food industry the electronic nose was used to assess the freshness/spoilage of fruits and vegetables during the processing and packaging process.[112,113] The detection of VOCs that indicate fruit ripeness and/or compounds that trigger fruit ripening, such as

ammonia,[114,115] ethanol,[115] ethylene,[115,116] and *trans*-2-hexenal[117] was also achieved. Even they are in preliminary stages of feasibility, studies reported the monitoring of the changes in the aroma profile during storage of apples,[118] to assess the postharvest quality of peaches, pears, bananas,[118–120] and nectarines[118,120] and to detect spoilage in potatoes.[121] Electronic noses were also used to determine the coverage area of pheromone traps set to capture insect herbivores[122–124] or to identify early stages of insect infestations by detecting VOCs secreted by plants that have been attacked.[125–127]

5.3.3 Electrochemical Sensors

The direct measurement of soil chemistry through tests such as pH or nutrient content represents an important application of electrochemical sensors. Due to the importance of soil testing results in obtaining optimal crop production yields and quality food, two types of electrochemical sensors were employed to measure the activity of selected ions (H^+, K^+, NO_3^-, Na^+, etc.) in the soil: ion-selective electrodes and ion-selective field effect transistors. These two types of sensors were also used to monitor the uptake of ions by plants, thus enabling farmers to design fertilization strategies that optimize production.[100] Ion-selective sensors were applied in nitrogen monitoring in soil and crops, such as potatoes,[128,129] and vegetables for fertilization management.[130,131] The investigation of plant metabolism and nutrition, and also the toxicological effects that heavy metals have on plants,[132–135] could also be achieved with these sensors by measuring concentrations of ions, such as iodide, fluoride, chloride, sodium, potassium, and cadmium, in plants or soils. Electrochemical sensors also found their applications in the greenhouse industry.[100] Systems that inject liquid fertilizers based upon ion-specific concentration measurements[136,137] which automatically ensure that the nutrient demand of the plants is satisfied were also developed.[100]

5.3.4 Biosensors

Rapid detection of target chemicals or pathogens in the agricultural field by minimally skilled personnel[138–140] is the main target in nowadays biosensor development.[100] The main bioprobes include nucleic acids (DNA/RNA), proteins, enzymes, antibodies, and phages.[141,142,145] Due to their robust structures and their resistance to heat (up to 80 °C) and chemicals, such as acid, alkali, and organic solvents,[143] filamentous and lytic phages have attracted the interest of researchers as biomolecular recognition elements.[144–146] Also, due to their three-dimensional recognition surface, phages can provide multiple binding sites and hence a strong binding to target pathogens.[100] Therefore, they found their application in the detection of food-borne pathogens.[147–165]

Acoustic wave devices represent an important family of highly sensitive transducers.[100] Phage-based magnetoelastic (ME) biosensors composed of an ME resonator that is coated with genetically engineered phages able to bind specifically with target pathogens[166,167] were described. The mechanism of the ME biosensors has been also explained: the biosensor oscillates with a characteristic resonance frequency under an applied alternating magnetic field and when it comes in contact with the target pathogen, binding occurs.[115] As a result, the mass of the resonator increases and this leads to a decrease in the biosensor's resonance frequency.[1] Various pathogens, such as *S. typhimurium*, *B. anthracis* spores, and *E. coli*,[168–174] could be detected using ME biosensors. Recent studies demonstrated that ME biosensors were able to directly detect bacteria on a fresh food surface without the use of a sampling process (water rinse/stomaching).[175]

Enzyme-based biosensors are said to be very promising tools for highly sensitive and discriminative detection of many chemical threat agents and food contaminants. Organophosphate neurotoxins which have been extensively used as insecticides in agriculture have been detected using biosensors with two types of mechanism approaches[100]: (1) inhibition of particular enzymes such as acetyl or butyryl cholinesterases,[176–179] and (2) organophosphate neurotoxins direct hydrolysis using different hydrolases.[180–184] For more information about biosensors see Chaps. 11, 12 and 13.

5.3.5 *Wireless Sensor Networks*

Wireless sensor networks have been developed to enable new precision in agricultural practice.[100]

Even in their earliest stages of development, wireless sensor networks include already radio-frequency transceivers; soil, water, ion, and VOC sensors; global positioning sensors; microcontrollers; and power sources.[185] See Chap. 14 of second volume for VOC sensors.

The development of this technology aims to provide revolutionary means for observing, assessing, and controlling agricultural practices.[100]

Food represents a very important environmental factor with great impact on "life quality" and, therefore, the need of analytical methods for the assessment of normal constituents, degradation products by alteration, genetic modifications, or chemical (pesticides, hormones, antibiotics, etc.) and biological contaminants.

The great variety of food contaminants and residues at very low concentrations, their various physicochemical features, and the complexity of the food matrix make food analysis a challenging task. Gas chromatography and high-performance liquid chromatography which are commonly employed in food analysis are relatively slow, expensive, and time consuming, and require extensive sample preparation and qualified operators.[186]

Biosensors have demonstrated a great potential for the detection of a large variety of chemical compounds.[187] The high selectivity of the biorecognition

molecule for the target component, the low production cost, the ability to detect analytes in a complex sample matrix with minimal pretreatment, and the potential for miniaturization are the main advantages that recommend biosensors for the specific and rapid detection of biological and chemical components in food, environmental, clinical, and pharmaceutical sector.[187–190]

The microfabrication technologies developed in the last decade have transformed the analytical chemistry research field due to the large surface-to-volume ratios of miniaturized systems, which enhance molecular diffusion and heat transfer, using very small liquid volumes and performing very rapid analyses.[191–193] Microfluidic analytical devices, known as lab-on-a-chip (see Chap. 21) or micro total analysis systems (μTAS), include microfluidic chips as well as non-fluidic miniaturized systems, such as sensors and arrays (biochips), developed for multi-analyte screening in food.[194] Microfluidics technology involves fluid control and small-scale analysis, making possible the integration of multiple steps, multiplexing and parallelization of analyses on a single device, and the achievement of microfluidic analytical systems capable to provide high-throughput and large-scale analysis.[191,195]

Generally, microfluidic analytical devices are made of silica-based materials with channel sizes ranging from 10 to 200 μm, but low-cost disposable microfluidic devices from materials such as polymers or even paper have lately been developed.[196] The most important advantages of microfluidic analytical devices are the low volume of samples and reagents reducing the cost of analysis and the amount of generated waste, the large surface-to-volume ratio, the mass and heat transfer enhancement, short analysis time, portability, allowing on-site analysis, disposability and low cost of fabrication, and integration of multiple processes which allows assay automation and improves analytical performances even when used by unskilled operators.[191,193,197] These devices achieve all the requirements that the food industry and quality control authorities are looking for to maintain the quality and safety of food throughout the entire food chain. Food sample analysis concerning the integration of nanotechnology applications in capillary electrophoresis microchips was reported by Escarpa et al.[198] The rapidly growing number of publications on microfluidics demonstrates the huge interest for microfluidic applications in the field of food and environmental analysis, biotechnology (e.g., fermentation processes in the pharmaceutical and food industry) for online process monitoring and analysis,[199] and homeland security. Microfluidic devices are extensively developed in health care industry for point-of-care diagnostic, high-throughput clinical analysis, and drug screening in pharmaceuticals.[200] The use of biorecognition elements (such as enzymes, antibodies, and DNA) for specific analysis from the sample matrices, and the application of nanotechnology in the detection mechanism of the analytical devices, could be achieved in real sample analysis.

In the same perspective, drugs and pharmaceutical formulations constitute a special issue, especially if we define the internal environment, opposite to the external environment. Detailed aspects will be discussed later (Chap. 9, second volume).

5.4 Future Aspects and Developments

Supposing that plants, just like other forms of life, communicate with other plants and beneficial insects by producing certain chemicals, researchers are trying to develop sensors able to detect the release of particular chemicals in very low concentrations, ignoring other chemicals released by the plant. These new sensors would not only allow farmers to save money, but the decrease in the pesticide concentration would make farmlands more environmentally adequate.

References

1. Voet D, Voet JG, Pratt CW (2012) Fundamentals of biochemistry, 4th edn. Wiley, New York
2. Alberts B, Johnson A, Lewis J, Raff M, Roberts K, Walter P (2002) Molecular biology of the cell. Garland Science, New York
3. Herrmann JM, Neupert W (2000) Protein transport into mitochondria. Curr Opin Microbiol 3 (2):210–214
4. Chipuk JE, Bouchier-Hayes L, Green DR (2006) Mitochondrial outer membrane permeabilization during apoptosis: the innocent bystander scenario. Cell Death Differ 13 (8):1396–1402
5. Stoimenova M, Igamberdiev AU, Gupta KJ, Hill RD (2007) Nitrite-driven anaerobic ATP synthesis in barley and rice root mitochondria. Planta 226(2):465–474
6. Huang K, Manton KG (2004) The role of oxidative damage in mitochondria during aging: a review. Front Biosci 9:1100–1117
7. Kandel ER, Schwartz JH, Jessel TM (eds) (2000) Principles of neural science, 4th edn. McGraw-Hill, New York
8. Hormuzdi SG, Filippov MA, Mitropoulou G, Monyer H, Bruzzone R (2004) Electrical synapses: a dynamic signaling system that shapes the activity of neuronal networks. Biochim Biophys Acta 1662(1–2):113–137
9. Rang HP, Dale MM, Ritter JM, Moore PK (2003) Pharmacology, 5th edn. Churchill Livingstone, Edinburgh
10. Sattarahmady N, Heli H, Moosavi-Movahedi AA (2010) An electrochemical acetylcholine biosensor based on nanoshells of hollow nickel microspheres-carbon microparticles-Nafion nanocomposite. Biosens Bioelectron 25:2329–2335
11. Heli H, Hajjizadeh M, Jabbari A, Moosavi-Movahedi AA (2009) Copper nanoparticles-modified carbon paste transducer as a biosensor for determination of acetylcholine. Biosens Bioelectron 24:2328–2333
12. Marty A, Llano I (2005) Excitatory effects of GABA in established brain networks. Trends Neurosci 28(6):284–289
13. Chevalier-Larsen E, Holzbaur ELF (2006) Axonal transport and neurodegenerative disease. Biochim Biophys Acta 1762:1094–1108
14. Rodríguez-Fernández T, Ugalde-Saldívar VM, González I, Escobar LI, García-Valdés J (2012) Electrochemical strategy to scout 1,4-naphthoquinones effect on voltage gated potassium channels. Bioelectrochemistry 86:1–8
15. Caygill RL, Blair GE, Millner PA (2010) A review on viral biosensors to detect human pathogens. Anal Chim Acta 681:8–15
16. Cheran LE, Cheung SL, Wang XM, Thompson M (2008) Probing the bioelectrochemistry of living cells. Electrochim Acta 53:6690–6697

17. Abonnenc M, Altomare L, Baruffa M, Ferrarini V, Guerrieri R, Iafelice B, Leonardi A, Manaresi N, Medoro G, Romani A, Tartagni M, Vulto P (2005) Teaching cells to dance: the impact of transistor miniaturization on the manipulation of populations of living cells. Solid-State Electron 49:674–683
18. Krystofova O, Trnkova L, Adam V, Zehnalek J, Hubalek J, Babula P, Kizek R (2010) Electrochemical microsensors for the detection of cadmium(II) and lead(II) ions in plants. Sensors 10:5308–5328
19. Besson-Bard A, Griveau S, Bedioui F, Wendehenne D (2008) Real-time electrochemical detection of extracellular nitric oxide in tobacco cells exposed to cryptogein, an elicitor of defense responses. J Exp Bot 59(12):3407–3414
20. Yang J, Yang T, Feng Y, Jiao K (2007) A DNA electrochemical sensor based on nanogold-modified poly-2,6-pyridinedicarboxylic acid film and detection of PAT gene fragment. Anal Biochem 365(1):24–30
21. Osibote E, Noah N, Sadik O, Dennis McGee D, Modupe Ogunlesi M (2011) Electrochemical sensors, MTT and immunofluorescence assays for monitoring the proliferation effects of *Cissus populnea* extracts on Sertoli cells. Reprod Biol Endocrinol 9:65
22. Svrcek C, Smith DW (2004) Cyanobacteria toxins and the current state of knowledge on water treatment options: a review. J Environ Eng Sci 3(3):155–185
23. Allan IJ, Vrana B, Greenwood R, Mills GA, Roig R, Gonzalez C (2006) A "toolbox" for biological and chemical monitoring requirements for the European Union's Water Framework Directive. Talanta 69:302–322
24. Keddy CJ, Greene JC, Bonell MA (1995) Review of whole-organism bioassays: soil, freshwater sediment, and freshwater assessment in Canada. Ecotoxicol Environ Saf 30:221–251
25. Gabrielson J, Kuhn I, Colque-Navarro P, Hart M, Iversen A, McKenzie D, Mollby R (2003) A microplate based microbial assay for risk assessment (MARA) and (eco)toxic fingerprinting of chemicals. Anal Chim Acta 485:121–130
26. Farré M, Barceló D (2003) Toxicity testing of waste water and sewage sludge by biosensors, bioassays and chemical analysis. Trends Anal Chem 22:299–310
27. Persoone G, Marsalek B, Blinova I, Torokne A, Zarina D, Manusadzianas L, Nalecz-Jawecki G, Tofan L, Stepanova N, Tothova L, Kolar B (2003) A practical and user-friendly toxicity classification system with microbiotests for natural waters and wastewaters. Environ Toxicol 18:395–402
28. Pascoe D, Wenzel A, Janssen CR, Girling AE, Juttner I, Fliedner A, Blockwell SJ, Maund SJ, Taylor EJ, Diedrich M, Persoone G, Verhelst P, Stephenson RR, Crossland NO, Mitchell GC, Pearson N, Tattersfield L, Lay JP, Peither A, Neumeier B, Velletti AR (2000) The development of toxicity tests for freshwater pollutants and their validation in stream and pond mesocosms. Water Res 34:2323–2329
29. Eulaffroy P, Vernet G (2003) The F684/F735 chlorophyll fluorescence ratio: a potential tool for rapid detection and determination of herbicide phytotoxicity in algae. Water Res 37:1983–1990
30. Schafer H, Hettler H, Fritsche U, Pitzen G, Roderer G, Wenzel A (1994) Biotests using unicellular algae and ciliates for predicting long-term effects of toxicants. Ecotoxicol Environ Saf 27:64–81
31. Kramer KJM, Botterweg L (1991) Aquatic biological early warning systems: an overview. In: Jeffrey D, Madden B (eds) Bioindicators and environmental management. Academic, London
32. Baldwin IG, Kramer KJM (1994) Biological early warning systems (BEWS). CRC, Boca Raton
33. Baldwin IG, Harman MMI, Neville DA, George SG (1994) Performance characteristics of a fish monitor for detection of toxic substances—II. Field trials. Water Res 28:2201–2208

34. Kuster E, Dorusch F, Vogt C, Weiss H, Altenburger R (2004) On line biomonitors used as a tool for toxicity reduction evaluation of in situ groundwater remediation techniques. Biosens Bioelectron 19:1711–1722
35. Gerhardt A, Schmidt S, Hoss S (2002) Measurement of movement patterns of *Caenorhabditis elegans* (Nematoda) with the multispecies freshwater Biomonitor® (MFB)—a potential new method to study a behavioral toxicity parameter of nematodes in sediments. Environ Pollut 120:513–516
36. De Bisthoven LJ, Gerhardt A, Soares AMVM (2004) Effects of acid mine drainage on larval *Chironomus* (Diptera, Chironomidae) measured with the multispecies freshwater Biomonitor®. Environ Toxicol Chem 23:1123–1128
37. Gerhardt A, de Bisthoven LJ, Soares AMVM (2004) Macroinvertebrateresponse to acid mine drainage: community metrics and on-line behavioural toxicity bioassay. Environ Pollut 130:263–274
38. Gerhardt A, Clostermann M (1998) A new biomonitor system based on magnetic inductivity for freshwater and marine environments. Environ Int 24:699–701
39. Van der Schalie WH, Shedd TR, Widder MW, Brennan LM (2004) Response characteristics of an aquatic biomonitor used for rapid toxicity detection. J Appl Toxicol 24:387–394
40. Borcherding J, Jantz B (1997) Valve movement response of the mussel *Dreissena polymorpha* the influence of the pH and turbidity on the acute toxicity of pentachlorophenol under laboratory and field conditions. Ecotoxicology 6:153–165
41. Tran D, Ciret P, Ciutat A, Durrieu G, Massabuau JC (2003) Estimation of potential and limits of bivalve closure response to detect contaminants: application to cadmium. Environ Toxicol Chem 22:914–920
42. Leynen M, Van den Berckt T, Aerts JM, Castelein B, Berckmans D, Ollevier F (1999) The use of Tubificidae in a biological early warning system. Environ Pollut 105:151–154
43. Van der Schalie WH, Shedd TR, Knechtges PL, Widder MW (2001) Using higher organisms in biological early warning systems for real-time toxicity detection. Biosens Bioelectron 16:457–465
44. Torchilin VP (2006) Multifunctional nanocarriers. Adv Drug Deliv Rev 58:1532–1555
45. Papakostas D, Rancan F, Sterry W, Blume-Peytavi U, Vogt A (2011) Nanoparticles in dermatology. Arch Dermatol Res 303:533–550
46. Medeiros SF, Santos AM, Fessi H, Elaissari A (2011) Stimuli-responsive magnetic particles for biomedical applications. Int J Pharm 403:139–161
47. Ganta S, Devalapally H, Shahiwala A, Amiji M (2008) A review of stimuli-responsive nanocarriers for drug and gene delivery. J Control Release 126:187–204
48. Bajpai AK, Shukla SK, Bhanu S, Kankane S (2008) Responsive polymers in controlled drug delivery. Prog Polym Sci 33:1088–1118
49. Domingo C, Saurina J (2012) An overview of the analytical characterization of nanostructured drug delivery systems: towards green and sustainable pharmaceuticals: a review. Anal Chim Acta 744:8–22
50. Nandi P, Lunte SM (2009) Recent trends in microdialysis sampling integrated with conventional and microanalytical systems for monitoring biological events: a review. Anal Chim Acta 651:1–14
51. Bourne JA (2003) Intracerebral microdialysis: 30 years as a tool for the neuroscientist. Clin Exp Pharmacol Physiol 30:16–24
52. Holovics HJ, Anderson CR, Levine BS, Hui HW, Lunte CE (2008) Investigation of drug delivery by iontophoresis in a surgical wound utilizing microdialysis. Pharm Res 25:1762–1770
53. Kim A, Suecof LA, Sutherland CA, Gao L, Kuti JL, Nicolau DP (2008) In vivo microdialysis study of the penetration of daptomycin into soft tissues in diabetic versus healthy volunteers. Antimicrob Agents Chemother 52:3941–3946

54. Bielecka-Grzela S, Klimowicz A (2003) Application of cutaneous microdialysis to evaluate metronidazole and its main metabolite concentrations in the skin after a single oral dose. J Clin Pharm Ther 28:465–469
55. Lanckmans K, Clinckers R, Van Eeckhaut A, Sarre S, Smolders I, Michotte Y (2006) Use of microbore LC-MS/MS for the quantification of oxcarbazepine and its active metabolite in rat brain microdialysis samples. J Chromatogr B 831:205–212
56. Richards DA, Silva MA, Murphy N, Wigmore SJ, Mirza DF (2007) Extracellular amino acid levels in the human liver during transplantation: a microdialysis study from donor to recipient. Amino Acids 33:429–437
57. Davies MI, Lunte CE (1996) Simultaneous microdialysis sampling from multiple sites in the liver for the study of phenol metabolism. Life Sci 59:1001–1013
58. Gilinsky MA, Faibushevish AA, Lunte CE (2001) Determination of myocardial norepinephrine in freely moving rats using in vivo microdialysis sampling and liquid chromatography with dual-electrode amperometric detection. J Pharm Biomed Anal 24:929–935
59. Price KE, Vandaveer SS, Lunte CE, Larive CK (2005) Tissue-targeted metabonomics: metabolic profiling by microdialysis sampling and microcoil NMR. J Pharm Biomed Anal 38:904–909
60. Ault JM, Riley CM, Meltzer NM, Lunte CE (1994) Dermal microdialysis sampling in vivo. Pharm Res 11:1631–1639
61. Huang H, Zhang Y, Yang R, Tang X (2008) Determination of baicalin in rat cerebrospinal fluid and blood using microdialysis coupled with ultra-performance liquid chromatography-tandem mass spectrometry. J Chromatogr B 874:77–83
62. Lin LC, Hung LC, Tsai TH (2004) Determination of (−)-epigallocatechin gallate in rat blood by microdialysis coupled with liquid chromatography. J Chromatogr A 1032:125–128
63. Ward KW, Pollack GM (1996) Use of intrauterine microdialysis to investigate methanol-induced alterations in uteroplacental blood flow. Toxicol Appl Pharmacol 140:203–210
64. Woo KL, Lunte CE (2008) The direct comparison of health and ulcerated stomach tissue: a multiple probe microdialysis sampling approach. J Pharm Biomed Anal 48:85–91
65. Woo KL, Lunte CE (2008) The development of multiple probe microdialysis sampling in the stomach. J Pharm Biomed Anal 48:20–26
66. Zhu T, Cheung BWY, Cartier LL, Giebink GS, Sawchuk RJ (2003) Simultaneous intravenous and intramiddle-ear dosing to determine cefditoren influx and efflux clearances in middle ear fluid in freely moving chinchillas. J Pharm Sci 92:1947–1956
67. Freed AL, Cooper JD, Davies MI, Lunte SM (2001) Investigation of the metabolism of substance P in rat striatum by microdialysis sampling and capillary electrophoresis with laser-induced fluorescence detection. J Neurosci Methods 109:23–29
68. Kostel KL, Lunte SM (1997) Evaluation of capillary electrophoresis with postcolumn derivatization and laser-induced fluorescence detection for the determination of substance P and its metabolites. J Chromatogr B 695:27–38
69. McLaughlin KJ, Faibushevich AA, Lunte CE (2000) Microdialysis sampling with online microbore HPLC for the determination of tirapazamine and its reduced metabolites in rats. Analyst 125:105–110
70. Telting-Diaz M, Scott DO, Lunte CE (1992) Intravenous microdialysis sampling in awake, freely-moving rats. Anal Chem 64:806–810
71. Zhang M, Mao L (2005) Enzyme-based amperometric biosensors for continuous and on-line monitoring of cerebral extracellular microdialysate. Front Biosci 10:345–352
72. Rhemrev-Boom MM, Jonker MA, Venema K, Tiessen R, Korf J, Jobst G (2001) Online continuous monitoring of glucose or lactate by ultraslow microdialysis combined with a flow-through nanoliter biosensor based on poly(m-phenylenediamine) ultra-thin polymer membrane as enzyme electrode. Analyst 126:1073–1079
73. Miele M, Fillenz M (1996) In vivo determination of extracellular brain ascorbate. J Neurosci Methods 70:15–19

74. Boutelle MG, Fellows LK, Cook C (1992) Enzyme packed bed system for the on-line measurement of glucose, glutamate, and lactate in brain microdialysate. Anal Chem 64:1790–1794
75. Kaptein WA, Zwaagstra JJ, Venema K, Korf J (1998) Continuous ultraslow microdialysis and ultrafiltration for subcutaneous sampling as demonstrated by glucose and lactate measurements in rats. Anal Chem 70:4696–4700
76. Berners MOM, Boutelle MG, Fillenz M (1994) Online measurement of brain glutamate with an enzyme/polymer-coated tubular electrode. Anal Chem 66:2017–2021
77. Miele M, Berners M, Boutelle MG, Kusakabe H, Fillenz M (1996) The determination of the extracellular concentration of brain glutamate using quantitative microdialysis. Brain Res 707:131–133
78. Jones DA, Ros J, Landolt H, Fillenz M, Boutelle MG (2000) Dynamic changes in glucose and lactate in the cortex of the freely moving rat monitored using microdialysis. J Neurochem 75:1703–1708
79. Yao T, Yano T, Nishino H (2004) Simultaneous in vivo monitoring of glucose, L-lactate, and pyruvate concentrations in rat brain by a flow-injection biosensor system with an on-line microdialysis sampling. Anal Chim Acta 510:53–59
80. Yao T, Okano G (2008) Simultaneous determination of L-glutamate, acetylcholine and dopamine in rat brain by a flow-injection biosensor system with microdialysis sampling. Anal Sci 24:1469–1473
81. Nanjo Y, Yano T, Hayashi R, Yao T (2006) Optically specific detection of D- and L-lactic acids by a flow-injection dual biosensor system with on-line microdialysis sampling. Anal Sci 22:1135–1138
82. Gramsbergen JB, Skjoth-Rasmussen J, Rasmussen C, Lambertsen KL (2004) Online monitoring of striatum glucose and lactate in the endothelin-1 rat model of transient focal cerebral ischemia using microdialysis and flow-injection analysis with biosensors. J Neurosci Methods 140:93–101
83. Li B, Zhang Z, Jin Y (2001) Chemiluminescence flow sensor for in vivo on-line monitoring of glucose in awake rabbit by microdialysis sampling. Anal Chim Acta 432:95–100
84. Lin Y, Zhu N, Yu P, Su L, Mao L (2009) Physiologically relevant online electrochemical method for continuous and simultaneous monitoring of striatum glucose and lactate following global cerebral ischemia/reperfusion. Anal Chem 81:2067–2074
85. Jacobs CB, Peairs MJ, Venton BJ (2010) Review: carbon nanotube based electrochemical sensors for biomolecules. Anal Chim Acta 662:105–127
86. Poland CA, Duffin R, Kinloch I, Maynard A, Wallace WAH, Seaton A, Stone V, Brown S, MacNee W, Donaldson K (2008) Carbon nanotubes introduced into the abdominal cavity of mice show asbestos-like pathogenicity in a pilot study. Nat Nanotechnol 3:423–428
87. Fraczek A, Menaszek E, Paluszkiewicz C, Blazewicz M (2008) Comparative in vivo biocompatibility study of single and multi-wall carbon nanotubes. Acta Biomater 4:1593–1602
88. Takagi A, Hirose A, Nishimura T, Fukumori N, Ogata A, Ohashi N, Kitajima S, Kanno J (2008) Induction of mesothelioma in p53+/− mouse by intraperitoneal application of multi-wall carbon nanotube. J Toxicol Sci 33:105–116
89. Blau A, Murr A, Wolff S, Sernagor E, Medini P, Iurilli G, Ziegler C, Benfenati F (2011) Flexible, all-polymer microelectrode arrays for the capture of cardiac and neuronal signals. Biomaterials 32:1778–1786
90. Larsson KC, Kjäll P, Richter-Dahlfors A (2012) Organic bioelectronics for electronic-to-chemical translation in modulation of neuronal signaling and machine-to-brain interfacing. Biochim Biophys Acta 1830:4334–4344
91. Giner J, Malachesky PA (1969) Proceedings of the artificial heart program conference, U.S. Department of Health Education and Welfare. p. 839
92. Skou EM (1973) Inhibition of electrochemical oxidation of glucose at platinum at pH 7.4 by chloride ions. Acta Chem Scand 27:2239–2241

93. Gebhardt U, Luft G, Richter GJ, Von Sturm F (1978) Development of an implantable electrocatalytic glucose sensor. Bioelectrochem Bioenerg 5:607–624
94. Gough DA, Anderson FL, Giner J, Golton CK, Soeldner SJ (1978) Effect of coreactants on electrochemical glucose oxidation. Anal Chem 50:941–944
95. Vassilyev YB, Khazova OA, Nikolaeva NN (1985) Kinetics and mechanism of glucose electrooxidation on different electrode-catalysts: Part I. Adsorption and oxidation on platinum. J Electroanal Chem 196:105–125
96. Park S, Boo H, Chung TD (2006) Electrochemical non-enzymatic glucose sensors. Anal Chim Acta 556:46–57
97. Yonemori Y, Takahashi E, Ren HF, Hayashi T, Endo H (2009) Biosensor system for continuous glucose monitoring in fish. Anal Chim Acta 633:90–96
98. Strack G, Luckarift HR, Sizemore SR, Nichols RK, Farrington KE, Wu PK, Atanassov P, Biffinger JC, Johnson GR (2013) Power generation from a hybrid biological fuel cell in seawater. Bioresour Technol 128:222–228
99. Özel RE, Wallace KN, Andreescu S (2011) Chitosan coated carbon fiber microelectrode for selective in vivo detection of neurotransmitters in live zebrafish embryos. Anal Chim Acta 695:89–95
100. Li S, Simonian A, Chin BA (2010) Sensors for agriculture and the food industry. Electrochem Soc Interface 19:41–46
101. Scotford IM, Miller PCH (2005) Applications of spectral reflectance techniques in northern European cereal production: a review. Biosyst Eng 90:235–250
102. Govender M, Chetty K, Bulcock H (2007) A review of hyperspectral remote sensing and its application in vegetation and water resource studies. Water SA 33:145–152
103. Bin Omar AF, Bin MatJafri MZ (2009) Optical sensor in the measurement of fruits quality: a review on an innovative approach. Int J Comp Electr Eng 1(5):557–561
104. Katayama K, Komaki K, Tamiya S (1996) Prediction of starch, moisture, and sugar in sweet potato by near infrared transmittance. Hort science 31:1003–1006
105. Garrido A, Sanchez MT, Cano G, Perez D, Lopez C (2001) Prediction of neutral and acid detergent fiber content of green asparagus stored under refrigeration and modified atmosphere conditions by near-infrared reflectance spectroscopy. J Food Quality 24:539–550
106. Pedro AMK, Ferreira MMC (2005) Nondestructive determination of solids and carotenoids in tomato products by near-infrared spectroscopy and multivariate calibration. Anal Chem 77:2505–2511
107. Ariana DP, Lu RF (2010) Evaluation of internal defect and surface color of whole pickles using hyperspectral imaging. J Food Eng 96:583–590
108. Ariana DP, Lu RF, Guyer DE (2006) Near-infrared hyperspectral reflectance imaging for detection of bruises on pickling cucumbers. Comput Electron Agric 53:60–70
109. Lu RF (2003) Detection of bruises on apples using near-infrared hyperspectral imaging. T ASAE 46:523–530
110. Lu RF, Peng YK (2006) Hyperspectral scattering for assessing peach fruit firmness. Biosyst Eng 93:161–171
111. Kim MS, Chen YR, Mehl PM (2001) Hyperspectral reflectance and fluorescence imaging system for food quality and safety. T ASAE 44:721–729
112. Deisingh AK, Stone DC, Thompson M (2004) Applications of electronic noses and tongues in food analysis. Int J Food Sci Technol 39:587–604
113. Casalinuovo IA, Di Pierro D, Coletta M, Di Francesco P (2006) Application of electronic noses for disease diagnosis and food spoilage detection. Sensors 6:1428–1439
114. Pinheiro C, Rodrigues CM, Schafer T, Crespo JG (2002) Monitoring the aroma production during wine-must fermentation with an electronic nose. Biotechnol Bioeng 77:632–640
115. Ivanov P, Llobet E, Vergara A, Stankova M, Vilanova X, Hubalek J, Gracia I, Cane C, Correig X (2005) Towards a micro-system for monitoring ethylene in warehouses. Sens Actuators B 111:63–70

116. Baratto C, Faglia G, Pardo M, Vezzoli M, Boarino L, Maffei M, Bossi S, Sberveglieri G (2005) Monitoring plants health in greenhouse for space missions. Sens Actuators B 108:278–284
117. Herrmann U, Jonischkeit T, Bargon J, Hahn U, Li QY, Schalley CA, Vogel E, Vogtle F (2002) Monitoring apple flavor by use of quartz microbalances. Anal Bioanal Chem 372:611–614
118. Brezmes J, Llobet E, Vilanova X, Orts J, Saiz G, Correig X (2001) Correlation between electronic nose signals and fruit quality indicators on shelf-life measurements with pinklady apples. Sens Actuators B 80:41–50
119. Llobet E, Hines EL, Gardner JW, Franco S (1999) Non-destructive banana ripeness determination using a neural network-based electronic nose. Meas Sci Technol 10:538–548
120. Brezmes J, Fructuoso MLL, Llobet E, Vilanova X, Recasens I, Orts J, Saiz G, Correig X (2005) Evaluation of an electronic nose to assess fruit ripness. IEEE Sens J 5:97–108
121. Costello B, Ewen RJ, Gunson HE, Ratcliffe NM, Spencer-Phillips PTN (2000) The development of a sensor system for the early detection of soft rot in stored potato tubers. Meas Sci Technol 11:1685–1691
122. Baker TC, Haynes KF (1989) Field and laboratory electroantennographic measurements of pheromone plume structure correlated with oriental fruit moth behaviour. Physiol Entomol 14:1–12
123. Sauer AE, Karg G, Koch UT, Dekramer JJ, Milli R (1992) A portable EAG system for the measurement of pheromone concentrations in the field. Chem Senses 17:543–553
124. Schutz S, Weissbecker B, Hummel HE (1996) Biosensor for volatiles released by damaged plants. Biosens Bioelectron 11:427–433
125. Purnamadjaja AH, Russell RA (2007) Guiding robots behaviors using pheromone communication. Autonomous Robots 23:113–130
126. Henderson WG, Khalilian A, Han YJ, Greene JK, Degenhardt DC (2010) Detecting stink bugs/damage in cotton utilizing a portable electronic nose. Comput Electron Agric 70:157–162
127. Weerakoon K, Chin BA (2010) Detecting insect infestation using a carbon/polymer based sensor array system. ECS Trans 33:85–89
128. Vitosh ML, Silva GH (1994) A rapid petiole sap nitrate-nitrogen test for potatoes. Commun Soil Sci Plan 25:183–190
129. Errebhi M, Rosen CJ, Birong DE (1998) Calibration of a petiole sap nitrate test for irrigated. "Russet Burbank" potato. Commun Soil Sci Plan 29:23–35
130. Warncke DD (1996) Soil and plant tissue testing for nitrogen management in carrots. Commun Soil Sci Plan 27:597–605
131. Kubota A, Thompson TL, Doerge TA, Godin RE (1997) A petiole sap nitrate test for broccoli. J Plant Nutr 20:669–682
132. Rashed MN (1995) Trace element determination in warm-climate plants by atomic absorption spectroscopy and ion selective electrodes. J Arid Environ 30:463–478
133. Rieger M, Litvin P (1998) Ion selective electrodes for measurement of sodium and chloride in salinity experiments. J Plant Nutr 21:205–215
134. Brouder SM, Thom M, Adamchuck VI, Morgan MT (2003) Potential uses of ion selective potassium electrodes in soil fertility management. Commun Soil Sci Plan 34:2699–2726
135. Plaza S, Szigeti Z, Geisler M, Martinoia E, Aeschlimann B, Gunther D, Pretsch E (2005) Potentiometric sensor for the measurement of Cd2+ transport in yeast and plants. Anal Biochem 347:10–16
136. Gieling TH, Van Straten G, Janssen HJJ, Wouters H (2005) ISE and CHEMFET sensors in greenhouse cultivation. Sens Actuators B 105:74–80
137. Gutierrez M, Alegret S, Caceres R, Casadesus J, Marfa O, Del Valle M (2007) Application of a potentiometric electronic tongue to fertigation strategy in greenhouse cultivation. Comput Electron Agric 57:12–22
138. Cass AEG (1990) Biosensors: a practical approach. Oxford University Press, New York

139. Ivnitski D, Abdel-Hamid I, Atanasov P, Wilkins E (1999) Biosensors for detection of pathogenic bacteria. Biosens Bioelectron 14:599–624
140. Jones C, Patel A, Griffin S, Martin J, Young P, O'Donnell K, Silverman C, Porter T, Chaiken I (1995) Current trends in molecular recognition and bioseparation. J Chromatogr A 707:3–22
141. Chambers JP, Arulanandam BP, Matta LL, Weis A, Valdes JJ (2008) Biosensor recognition elements. Curr Issues Mol Biol 10:1–12
142. Leonard P, Hearty S, Brennan J, Dunne L, Quinn J, Chakraborty T, O'Kennedy R (2003) Advances in biosensors for detection of pathogens in food and water. Enzyme Microb Technol 32:3–13
143. Brigati JR, Petrenko VA (2005) Thermostability of landscape phage probes. Anal Bioanal Chem 382:1346–1350
144. Sorokulova IB, Olsen EV, Chen IH, Fiebor B, Barbaree JM, Vodyanoy VJ, Chin BA, Petrenko VA (2005) Landscape phage probes for Salmonella typhimurium. J Microbiol Methods 63:55–72
145. Petrenko VA, Vodyanoy VJ (2003) Phage display for detection of biological threat agents. J Microbiol Methods 53:253–262
146. Petrenko VA, Smith JP (2000) Phages from landscape libraries as substitute antibodies. Protein Eng 13:589–592
147. Neufeld T, Schwartz-Mittelmann A, Biran D, Ron EZ, Rishpon J (2003) Combined phage typing and amperometric detection of released enzymatic activity for the specific identification and quantification of bacteria. Anal Chem 75:580–585
148. Neufeld T, Schwartz-Mittelmann A, Buchner V, Rishpon J (2005) Electrochemical phagemid assay for the specific detection of bacteria using Escherichia coli TG-1 and M13KO7 phagemid in a model system. Anal Chem 77:652–657
149. Yemini M, Levi Y, Yagil E, Rishpon J (2007) Specific electrochemical phage sensing for Bacillus cereus and Mycobacterium smegmatis. Bioelectrochemistry 70:180–184
150. Yang LMC, Diaz JE, McIntire TM, Weiss GA, Penner RM (2008) Direct electrical transduction of antibody binding to a covalent virus layer using electrochemical impedance. Anal Chem 80:5695–5705
151. Yang LMC, Tam PY, Murray NJ, McIntire TM, Overstreet CM, Weiss GA, Penner RM (2006) Virus electrodes for universal biodetection. Anal Chem 78:3265–3270
152. Mejri MB, Baccar H, Baldrich E, Del Campo FJ, Helali S, Ktari T, Simonian A, Aouni M, Abdelghani A (2010) Impedance biosensing using phages for bacteria detection: generation of dual signals as the clue for in-chip assay confirmation. Biosens Bioelectron 26:1261–1267
153. Jia YF, Qin M, Zhang HK, Niu WC, Li X, Wang LK, Li X, Bai YP, Cao YJ, Feng XZ (2007) Label-free biosensor: a novel phage-modified light addressable potentiometric sensor system for cancer cell monitoring. Biosens Bioelectron 22:3261–3266
154. Banaiee N, Bodadilla-del-Valle M, Bardarov S, Riska PF, Small PM, Ponce-De-Leon A, Jacobs WR, Hatfull GF, Sifuentes-Osornio J (2001) Luciferase reporter mycobacteriophages for detection, identification, and antibiotic susceptibility testing of *Mycobacterium tuberculosis* in Mexico. J Clin Microbiol 39:3883–3888
155. Turnbough CL (2003) Discovery of phage display peptide ligands for species-specific detection of Bacillus spores. J Microbiol Methods 53:263–271
156. Goodridge L, Chen JR, Griffiths M (1999) The use of a fluorescent bacteriophage assay for detection of *Escherichia coli* O157:H7 in inoculated ground beef and raw milk. Int J Food Microb 47:43–50
157. Goodridge L, Chen JR, Griffiths M (1999) Development and characterization of a fluorescent bacteriophage assay for detection of *Escherichia coli* O157:H7. Appl Environ Microb 65:1397–1404
158. Edgar R, McKinstry M, Hwang J, Oppenheim AB, Fekete RA, Giulian G, Merril C, Nagashima K, Adhya S (2006) High-sensitivity bacterial detection using biotin-tagged phage and quantum-dot nano-complexes. Proc Natl Acad Sci U S A 103:4841–4845
159. Souza GR, Christianson DR, Staquicini FI, Ozawa MG, Snyder EY, Sidman RL, Miller JH, Arap W, Pasqualini R (2006) Networks of gold nanoparticles and bacteriophage as biological sensors and cell-targeting agents. Proc Natl Acad Sci U S A 103:1215–1220

160. Nanduri V, Balasubramanian S, Sista S, Vodyanoy VJ, Simonian AL (2007) Highly sensitive phage-based biosensor for the detection of beta-galactosidase. Anal Chim Acta 589:166–172
161. Liu FF, Luo ZF, Ding X, Zhu SG, Yu XL (2009) Phage-displayed protein chip based on SPR sensing. Sens Actuators B 136:133–137
162. Balasubramanian S, Sorokulova IB, Vodyanoy VJ, Simonian AL (2007) Lytic phage as a specific and selective probe for detection of *Staphylococcus aureus*—a surface plasmon resonance spectroscopic study. Biosens Bioelectron 22:948–955
163. Zhu HY, White IM, Suter JD, Fan XD (2008) Phage-based label-free biomolecule detection in an opto-fluidic ring resonator. Biosens Bioelectron 24:461–466
164. Olsen EV, Sorokulova IB, Petrenko VA, Chen IH, Barbaree JM, Vodyanoy VJ (2006) Affinity-selected filamentous bacteriophage as a probe for acoustic wave biodetectors of *Salmonella typhimurium*. Biosens Bioelectron 21:1434–1442
165. Fu L, Li S, Zhang K, Cheng ZY, Barbaree J (2007) Detection of *Bacillus anthracis* spores in water using biosensors based on magnetorestrictive microcantilever coated with phage. Proc SPIE 6556:655619
166. Johnson ML, LeVar O, Yoon SH, Park JH, Huang S, Kim DJ, Cheng Z, Chin BA (2009) Dual-cathode method for sputtering magnetoelastic iron-boron films. Vacuum 83:958–964
167. Johnson ML, Wan JH, Huang SC, Cheng ZY, Petrenko VA, Kim DJ, Chen IH, Barbaree JM, Hong JW, Chin BA (2008) A wireless biosensor using microfabricated phage-interfaced magnetoelastic particles. Sens Actuators A 144:38–47
168. Huang S, Yang H, Lakshmanan RS, Johnson ML, Wan JK, Chen IH, Wikle HC, Petrenko VA, Barbaree JM, Chin BA (2009) Sequential detection of Salmonella typhimurium and Bacillus anthracis spores using magnetoelastic biosensors. Biosens Bioelectron 24:1730–1736
169. Lakshmanan RS, Guntupalli R, Hu J, Kim DJ, Petrenko VA, Barbaree JM, Chin BA (2007) Phage immobilized magnetoelastic sensor for the detection of *Salmonella typhimurium*. J Microbiol Methods 71:55–60
170. Lakshmanan RS, Guntupalli R, Hu J, Petrenko VA, Barbaree JM, Chin BA (2007) Sens Actuators B 126:544
171. Wan JH, Johnson ML, Guntupalli R, Petrenko VA, Chin BA (2007) Detection of *Bacillus anthracis* spores in liquid using phage-based magnetoelastic microresonators. Sens Actuators B 127:559
172. Wan JH, Shu HH, Huang SC, Fiebor B, Chen IH, Petrenko VA, Chin BA (2007) Phage-based magnetoelastic wireless biosensors for detecting Bacillus anthracis spores. IEEE Sensors J 7:470–477
173. Shen W, Lakshmanan RS, Mathison LC, Petrenko VA, Chin BA (2009) Phage coated magnetoelastic micro-biosensors for real-time detection of Bacillus anthracis spores. Sens Actuators B 137:501–506
174. Lu QZ, Lin HL, Ge ST, Luo SL, Cai QY, Grimes CA (2009) Wireless, remote-query, and high sensitivity escherichia coli O157:H7 biosensor based on the recognition action of Concanavalin A. Anal Chem 81:5846–5850
175. Li S, Li Y, Chen H, Horikawa S, Shen W, Simonian A, Chin BA (2010) Direct detection of *Salmonella typhimurium* on fresh produce using phage-based magnetoelastic biosensors. Biosens Bioelectron 26:1313–1319
176. Palleschi G, Bernabei M, Cremisini C, Mascini M (1992) Determination of organophosphorus insecticides with a choline electrochemical biosensor. Sens Actuators B 7:513–517
177. Kulys J, D'Costa EJ (1991) Printed amperometric sensors based on TCNQ and cholinesterase. Biosens Bioelectron 6:109–115
178. Starodub NF, Kanjuk NI, Kukla AL, Shirshov YM (1999) Multi-enzymatic electrochemical sensor: field measurements and their optimization. Anal Chim Acta 385:461–466
179. Compagnone D, Bugli M, Imperiali P, Varallo G, Palleschi G (1998) Determination of heavy metals using electrochemical biosensors based on enzyme inhibition. In: Nikolelis DP, Krull UJ, Wang J, Mascini M (eds) Biosensors for direct monitoring of environmental pollutants in field. Kluwer Academic Publishers, Dordrecht

180. Rainina EI, Efremenco EN, Varfolomeyev SD, Simonian AL, Wild JR (1996) The development of a new biosensor based on recombinant *E. coli* for the direct detection of organophosphorous neurotoxins. Biosens Bioelectron 11:991–1000
181. Simonian AL, Wild JR (2006) Detection and remediation of organophosphate contamination. In: Amass S, Bhunia AK, Chaturvedi A, Dolk D, Peeta S, Atallah M (eds) The science of homeland security, vol 1. Purdue University Press, West Lafayette
182. Viveros L, Paliwal S, McCrae D, Wild J, Simonian A (2006) A fluorescence-based biosensor for the detection of organophosphate pesticides and chemical warfare agents. Sens Actuators B 115:150–157
183. Zourob M, Simonian AL, Wild JR, Mohr S, Goddard N (2007) Optical leaky waveguide biosensors for the detection of organophosphorus pesticides. Analyst 132:114–120
184. Ramanathan M, Simonian AL (2007) Array biosensor based on enzyme kinetics monitoring by fluorescence spectroscopy: application for neurotoxins detection. Biosens Bioelectron 22:3001–3007
185. Wang N, Zhang NQ, Wang MH (2006) Wireless sensors in agriculture and food industry—recent development and future perspective. computers and electronics in agriculture. Comput Electron Agric 50:1–14
186. Atalay YT, Vermeir S, Witters D, Vergauwe N, Verbruggen B, Verboven P, Nicolaï BM, Lammertyn J (2011) Microfluidic analytical systems for food analysis. Trends Food Sci Technol 22:386–404
187. Tombelli S, Minunni M, Mascini M (2007) Aptamers-based assays for diagnostics, environmental and food analysis. Biomol Eng 24:191–200
188. Schubert-Ullrich P, Rudolf J, Ansari P, Galler B, Führer M, Molinelli A, Baumgartner S (2009) Commercialized rapid immunoanalytical tests for determination of allergenic food proteins: an overview. Anal Bioanal Chem 395:69–81
189. Tran DT, Janssen KP, Pollet J, Lammertyn E, Anné J, Van Schepdael A, Lammertyn J (2010) Selection and characterization of DNA aptamers for egg white lysozyme. Molecules 15:1127–1140
190. Velusamy V, Arshak K, Korostynska O, Oliwa K, Adley C (2010) An overview of foodborne pathogen detection: in the perspective of biosensors. Biotechnol Adv 28:232–254
191. Li PCH (2006) Microfluidic Lab-on-a-chip for chemical and biological analysis and discovery. Taylor & Francis, New York
192. Manz A, Harrison DJ, Verpoorte EMJ, Fettinger JC, Paulus A, Lüdi H, Widmer HM (1992) Planar chips technology for miniaturization and integration of separation techniques into monitoring systems: capillary electrophoresis on a chip. J Chromatogr A 593:253–258
193. Stone HA, Stroock AD, Ajdari A (2004) Engineering flows in small devices. Microfluidics toward a lab-on-a-chip. Annu Rev Fluid Mech 36:381–411
194. Raz SR, Bremer MGEG, Giesbers M, Norde W (2008) Development of a biosensor microarray towards food screening, using imaging surface plasmon resonance. Biosens Bioelectron 24:552–557
195. Melin J, Quake SR (2007) Microfluidic large-scale integration: the evolution of design rules for biological automation. Annu Rev Biophys Biomol Struct 36:213–231
196. Martinez AW, Phillips ST, Whitesides GM, Carrilho E (2010) Diagnostics for the developing world: microfluidic paper-based analytical devices. Anal Chem 82(1):3–10
197. Squires TM, Quake SR (2005) Microfluidics: fluid physics at the nanoliter scale. Rev Mod Phys 77:977–1026
198. Escarpa A, González MC, Gil MAL, Crevillén AG, Hervás M, García M (2008) Microchips for CE: breakthroughs in real-world food analysis. Electrophoresis 29:4852–4861
199. Schemberg J, Grodrian A, Römer R, Gastrock G, Lemke K (2010) Application of segmented flow for quality control of food using microfluidic tools. Phys Status Solidi A 207(4):904–912
200. Dittrich PS, Tachikawa K, Manz A (2006) Micro total analysis systems. Latest advancements and trends. Anal Chem 78:3887–3907

Chapter 6
Extraterrestrial

Kyle M. McElhoney, Glen D. O'Neil, and Samuel P. Kounaves

Electrochemical sensors, especially ion-selective electrodes (ISEs), are ideally suited for analyses of extraterrestrial environments where comparatively little is known about the aqueous geochemistry: they have remarkably high sensitivity over a wide dynamic range and are available for a wide range of organic and inorganic cations and anions. In addition, ISEs require very little power, have low mass, and can withstand dramatic swings in temperature and pressure without loss of function. Analyses in extraterrestrial environments offer unique challenges caused by the preflight preparations and storage of the sensors, the long cruise to the planetary body, and the harsh environmental conditions in which they must be performed. Currently, only a single set of electrochemical analyses of another planet has been performed, but several new instruments are being developed which will potentially provide insight into the scientific questions surrounding the chemistry and biology of other planetary bodies in our solar system.

Even though the Viking spacecraft in 1976 moistened the soil samples to observe gases released as part of the life detection experiments, the first true and comprehensive wet chemical analysis performed on another planet was by the 2007 Phoenix Mars Scout Lander. Using an array of electrochemical sensors in four identical Wet Chemistry Laboratory (WCL) units that were part of the Microscopy, Electrochemistry, and Conductivity Analyzer (MECA) instrument package, it measured the concentration of anions and cations released by the addition of water to the martian soil. The main objectives of the Phoenix mission were to verify the presence of water, assess the habitability of the soil, and characterize the climate and geology of Mars. Previous landed missions have included Viking Landers 1 and 2, Pathfinder, the Mars Exploration Rovers (MER) Spirit and Opportunity, and currently the Mars Science Lab (MSL) Curiosity. Although these missions contributed to our understanding of Mars' history, its geology,

K.M. McElhoney • G.D. O'Neil • S.P. Kounaves (✉)
Department of Chemistry, Tufts University, Medford, MA, USA
e-mail: samuel.kounaves@tufts.edu

L.M. Moretto, K. Kalcher (eds.), *Environmental Analysis by Electrochemical Sensors and Biosensors*, DOI 10.1007/978-1-4939-0676-5_6

mineralogy, and climatology, Phoenix and the WCL made discoveries that have given us a new view of the aqueous chemistry and geochemistry, the knowledge of what happens when water and soil come into contact.

The WCL beaker contained 11 plasticized PVC-based membrane ion-selective electrodes (including two pH electrodes) for cations and anions, 4 solid pellet crystal ion-selective electrodes for halides, an iridium oxide pH electrode, 3 electrodes for chronopotentiometry of halides, and individual electrodes for determining heavy metals by anodic stripping voltammetry, conductivity, cyclic voltammetry of redox species, and an electrode for the oxidation-reduction potential. The ion-selective electrodes used on Phoenix were designed specifically for the demands of the mission. In the traditional configuration, an ion-selective membrane is used to separate the sample and reference solutions. However, this configuration is not suitable for prolonged analysis. In place of the reference solution, a hydrogel impregnated with a salt solution was used in order to increase durability. This chapter discusses the challenges of performing electrochemical analyses in an extraterrestrial environment such as Mars, with an emphasis on sensor development, characterization, and calibration, while addressing lessons learned from the Phoenix mission, and looking to the future of electrochemical analyses of other planetary bodies.

6.1 Introduction

Humans have observed the stars and planets since prehistoric times and wondered about their significance and composition. After observations and conjectures by early philosophers such as Democritus in the fourth century BCE, understanding of our solar system rapidly accelerated during the sixteenth–nineteenth centuries starting with Copernicus' discoveries of Jupiter's four largest moons and the rings of Saturn, followed by Galileo's study of lunar mountains and his suggestion that other worlds may also have Earth-like surfaces. These initial observations were astronomical, made by optical and later radio telescopes. In the mid-twentieth century though, the politically driven "Space Race" accelerated the quest to physically reach these other worlds. Following those successes, human and robotic missions to the Moon as well as robotic missions to other planetary bodies have revolutionized our understanding of our solar system. Starting with the first successful rendezvous with another planet (Mariner 2 at Venus in 1962) and first successful landing (Venera 7 on Venus in 1970), robotic landed missions have provided a great deal of knowledge about these nearby but alien environments through a combination of visual images and physical measurements, supporting a variety of geological, chemical, and meteorological investigations.

The first successful landing on Mars was made by the two NASA Mars Viking 1 and 2 landers in 1976. Included in the payload were a gas chromatograph, mass spectrometer, X-ray fluorimeter, and three life detection instruments. Additional surface missions in 1997 (Pathfinder/Sojourner Rover) and 2004 (Opportunity and

Spirit rovers) included mainly X-ray spectrometers and imagers. It was not until 2007 with the launch of the Phoenix Mars lander mission that the first electroanalytical measurement system was delivered to the martian surface. Here we present the historical context of the first electroanalyses on Mars, an overall description of the electrochemically based sensors that were part of the Phoenix Wet Chemistry Laboratory (WCL), the results of the martian soil analyses and their implications, the most recent Earth-based experiments, and a preview of the next-generation electroanalytical instruments currently in development for upcoming missions to Mars and beyond.

6.1.1 *Historical Development of Electroanalytical Instruments for Mars*

By the early 1990s the evidence pointed to a Mars that was most likely wet and warm sometime in its past history. Though much data had been collected by previous missions via elemental analyses using either X-ray or optical spectroscopy, little or nothing was directly known about the soluble salts in the soil or parameters such as pH or conductivity. Such knowledge is critical in understanding the biological potential of Mars for supporting indigenous life in the past or present, and also for assessing hazards that might be encountered by future human explorers. This prompted proposals to develop instrumentation that could investigate the aqueous geochemistry of the martian soil. The idea was to reconstitute the ancient wet environment by adding water to the soil and measuring the ionic species in the solution. The limitation was that whatever technique was to be used had to be preferably rugged, and of low mass, volume, and power. Electrochemical sensors appeared ideal for such an endeavor.

The first reported development and demonstration of an electrochemically based analyzer for martian regolith (soil) was as part of the Mars Aqueous Chemistry Experiment (MACE) program at Lockheed Martin Astronautics (LMA) in Denver, Colorado, as an in-house study of the feasibility of a chemical reaction investigation for future Mars missions.[1] Among its goals were to determine the reactions between Martian surface materials and liquid water; investigate the unusual oxidation capabilities of Martian soil discovered by Viking; and explore for evidence of chemical and physical modifications of the surface to understand weathering processes. To accomplish its goals, MACE included ion-selective electrodes (ISE) for a variety of cations/ions (e.g., Na^+, K^+, Mg^{2+}, Ca^{2+}, Cl^-, Br^-, NO_3^-) and electrodes for redox potential and conductivity.

The Wet Chemistry Laboratory (WCL) was first proposed in 1997 to NASA's Office of Human Exploration and Development of Space as a payload on the 2001 Mars Surveyor Program (MSP'01) Lander, as part of the Mars Environmental Compatibility Assessment (MECA) instrument package. The purpose of the MSP'01 WCL was to determine the total dissolved solids, redox potential, and

pH, and to detect potentially dangerous heavy metal ions, emitted hazardous gases, and the soil's corrosive potential. The WCL was chosen by NASA in 1998 to be designed, built, and flight qualified for the 2001 mission.[2] The MSP'01 Lander was canceled in May 2000 due to the loss of NASA's two 1998 Mars-bound spacecraft, the Mars Climate Orbiter and Mars Polar Lander. In the summer of 2002 the WCL was proposed as part of the Microscopy, Electrochemistry, and Conductivity Analyzer (MECA) instrument package for the 2007 Phoenix Mars Scout Lander (MECA). The Phoenix, including WCL, was selected by NASA on August 4th, 2003, as the first Mars Scout Mission. It was launched on August 4th, 2007, and landed on the northern polar planes of Mars on May 25th, 2008.[3,4]

6.2 The Phoenix Wet Chemistry Laboratory (WCL) Electroanalytical Sensor Array

The MECA instrument package on board the Phoenix lander included four identical Wet Chemistry Laboratories (WCL), whose objective was to address the mission goals of understanding the aqueous chemical reactivity of the soil and identify potential chemical energy sources available to support past or present life. The WCL has been previously described in detail[2,5] and is only briefly reviewed here. Figure 6.1 shows an individual WCL unit and as part of the MECA package on Mars during its first sol (day) of operation. To accomplish its objectives, each WCL included an upper "actuator" and a lower "beaker" assembly. The actuator consisted of a 25 mL titanium tank that contained deionized water plus ionic species at ~10^{-5} M concentrations for the initial sensor calibrations, a drawer that would accept ~1 cm^3 of soil through a screened funnel from the robotic arm, and a stirrer motor for stirring the soil/solution mixture. The actuator also included a reagent

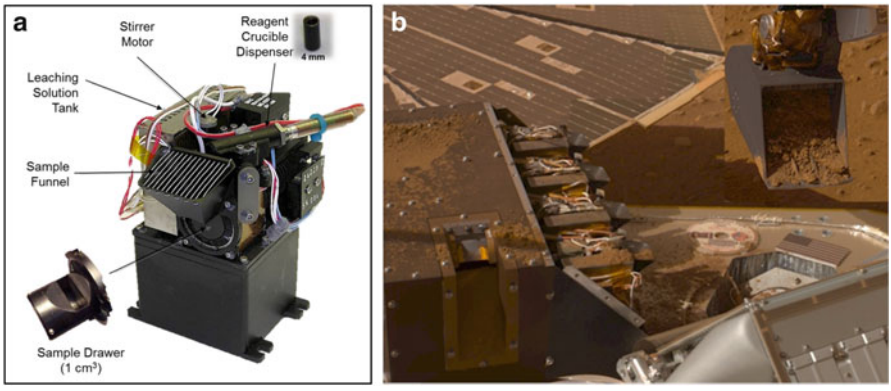

Fig. 6.1 An individual Wet Chemistry Laboratory (WCL) (**a**) and as part of MECA on Mars (**b**). *Courtesy of NASA JPL and S. P. Kounaves*

dispenser that held five "crucibles" for a second calibration reagent, an acid, and three crucibles packed with $BaCl_2$ for the titrimetric determination of SO_4^{2-}.

The lower "beaker" contained an array of sensors which included ion-selective electrodes (ISEs) for the determination of Na^+, NH_4^+, K^+, H^+, Mg^{2+}, Ca^{2+}, SO_4^{2-} (via Ba^{2+} titration), and NO_3^-/ClO_4^-; solid pellet ISEs for the determination of Cl^-, Br^-, and I^-; an iridium oxide electrode and two H^+ ISEs for the determination of pH between 0 and 12 with an accuracy of ±0.5 pH units; a 564 element 12 μm Au disk microelectrode array (MEA) for anodic stripping voltammetry (ASV); a set of 1 mm Ag disk electrodes for the determination of halides by chronopotentiometry (CP); a 1 mm Pt disk electrode for redox acid/base chemistry by CP; a concentric two-carbon-ring electrode for solution electrical conductivity; a 250 μm Au disk electrode for cyclic voltammetry (CV), within a potential window of ±1,000 mV and accuracy of ±1 mV, to identify and analyze for possible reversible and irreversible redox couples; and a 1 mm Pt disk electrode for determination of the oxidation-reduction potential (E_h) between ±1,000 mV with an accuracy of 20 mV.[5] Each beaker also contained two Li^+ ISEs that served as reference electrodes. The only electrodes present in duplicate were the solid pellet Cl^- electrode, along with a set of Ag electrodes for CP halide determination and the Li^+ electrodes for a total of 23 electrodes in each beaker.

The most important consideration for the WCL beaker assembly was to ensure that all of the electrochemical sensors would arrive on Mars in the same condition they left Earth. The sensors had to survive a prolonged prelaunch stay on the flight deck at Cape Canaveral, Florida; significant physical stress during launch; a 9-month cruise to Mars at subzero temperatures; entry to the martian atmosphere; landing on the surface; and exposure to extreme temperature swings and radiation during the time on the planet. Prior to launch significant preflight characterization and testing were performed in order to understand the demands of spaceflight on the WCL and each of the sensors.[5] Each sensor was rigorously characterized before and after the series of stress tests, which included operation at ~7 mbar (the expected pressure at the landing site), standard accelerated aging cycles, shock and vibration tests, and long periods (>8 months) of cold storage.

Using elemental analyses to determine that the surface materials contain elements such as sulfur, chlorine, magnesium, or calcium provides little or no information about the identity of ionic species, especially their oxidation state. Using a simple array of electrochemical sensors, the Phoenix WCL analyses on the other hand made startling new discoveries providing new scientific insights into the aqueous geochemistry and history of the Mars, its potential for supporting microbial life, its chemistry, and its atmospheric chemistry. An instrument which can easily identify and quantify ion components in an aqueous solution is the only way to fully understand the geochemistry, habitability, and potential human toxicity, not only of Mars, but also of other planetary environments, including the oceans of Europa.

6.2.1 Ion-Selective Electrodes

Ion-selective electrodes are potentiometric sensors which are routinely used on Earth for a variety of laboratory, environmental, and clinical analyses.[6,7] ISEs are sensitive, selective, and inexpensive; have dynamic ranges that are typically greater than five orders of magnitude; are robust enough for field-based research; and are available for nearly 100 cations and anions.[8] ISEs are prepared by separating two solutions (an internal reference and the external sample) by a chemically selective membrane. These membranes were traditionally made from glass, but are now commonly constructed from plasticized polyvinyl chloride (PVC). The potential difference measured across the PVC membrane originates from selective partitioning of an ion from the sample solution into the membrane via a complexing ligand referred to as an ionophore.[9] This partitioning results in a potential gradient across the membrane that is measured by the internal and external reference electrodes. Its magnitude is given by the Nernst equation (see Chap. 9):

$$E = E_i^o + \frac{2.303RT}{zF}\log(a_i) \tag{6.1}$$

where E is the measured potential, E^0 is a collection of potentials relating to the various electronic connections within the sensor, reference electrode, and voltmeter, R is the ideal gas constant, T is absolute temperature, z is the charge of the ion involved in the complex, F is Faraday's constant, and a_i is the activity of ion i in solution. Note that this equation is only valid for a solution containing only ion i. When multiple ions are present in solution, the measured potential is a function of both logarithmic activity of the primary and interfering ions, and can be described by the Nikolsky-Eisenman equation:

$$E = E_i^0 + \frac{2.303RT}{zF} log\left(a_i + \sum K_{i,j}^{pot} a_j^{z_i/z_j}\right) \tag{6.2}$$

The subscripts i and j in Eq. (6.2) refer to the primary and interfering ions, respectively, and $K_{i,j}^{pot}$ is the potentiometric selectivity coefficient. $K_{i,j}^{pot}$ varies for each interfering ion, and depends upon the precise membrane composition. The lower the value of $\log K_{i,j}^{pot}$, the more highly the interfering ion is discriminated. (For a detailed review of ion-selective electrodes, including selectivity theory and a detailed account of ISE response, see Chap. 9.)

For the WCL Mars data the following equations were used in order to account for temperature differences between Earth and Mars during calibration and use:

$$S_M = S_E\left({}^{T_M}/_{T_E}\right) \tag{6.3}$$

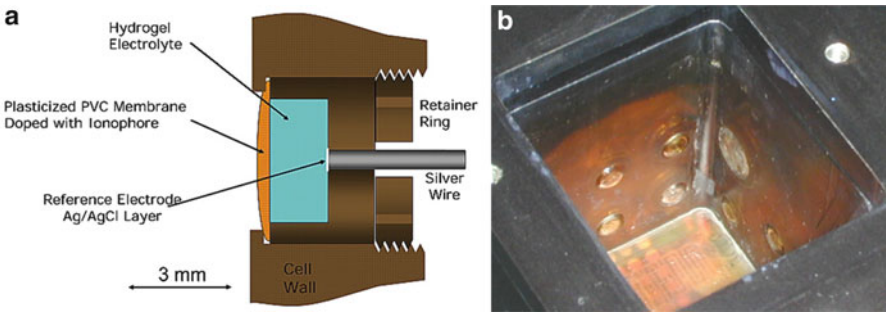

Fig. 6.2 (**a**) Schematic of a hydrogel ion-selective electrode used onboard NASA's 2007 Lander Phoenix. (**b**) Placement of electrodes along the WCL beaker wall. *Courtesy of NASA JPL and S. P. Kounaves*

$$E_i = E_C - S_M \log(a_i) \tag{6.4}$$

where S_M and S_E are the calibration slopes determined on Mars and Earth, respectively; T_M and T_E are the temperatures at which the calibration was carried out on Mars and Earth, respectively; E_I is the calibrant intercept; E_C is the stable calibrant potential; and a_i is the activity of the calibrant ion. The validity of the above relationships was confirmed during preflight characterization of the electrodes.

The ISEs deployed on Phoenix were designed to cope with the difficult conditions associated with long-term analysis at a harsh and remote location. The sensors were required to be robust; have long lifetimes; survive preflight testing and characterization; and have large dynamic ranges suitable for analysis of an environment that had yet to be studied. For these reasons, a configuration was chosen where the aqueous inner-filling solution was replaced by the polymeric hydrogel poly (hydroxymethyl acrylate) (poly-HEMA) (Fig. 6.2), as described by Cosofret et al.[10] The hydrogel was conditioned in an electrolyte solution containing a chloride salt to complete the interface with a Ag|AgCl electrode placed in contact with the gel. The hydrogel enabled extremely robust sensors because the material is able to freeze/thaw without large physical deformations, and can be effectively rehydrated given enough conditioning time.

6.2.2 *Other Electroanalytical Electrodes*

The electrodes used for electrical conductivity (EC), oxidation-reduction potential (E_h), cyclic voltammetry (CV), chronopotentiometry (CP), and anodic stripping voltammetry (ASV) were all solid state, and thus did not require the same design considerations as the membrane ISEs. The electrodes were polished and tested after fabrication, then calibrated and characterized, and remained as is until their use on Mars.[5]

Electrical conductivity is a measure of how well a solution is able to carry charge. This is largely a property of the dissolved ionic species in solution and temperature. The EC probes onboard Phoenix consisted of two concentric activated carbon electrodes, separated by a layer of insulating epoxy. The inner electrode was a 3 mm diameter disk, while the outer electrode was a 0.7 mm thick ring. EC was used to estimate the ionic strength (μ) of the solution and to calculate activity. Prior to flight, the EC of solutions, which were of varying ionic strengths and made from ionic species assumed to be present in the martian regolith, was measured and the resulting calibrations were used to calculate ionic strength using the relationship

$$\mu = 7 \times 10^{-6} EC^{1.0733} \tag{6.5}$$

This was an empirically derived relationship, and assumed that the species present in the preflight calibration solutions were similar to those found on Mars.

The results of the 1976 Viking biology experiments suggested that the martian soil probably contained one or more oxidants and thus might result in water/soil solutions with high oxidation-reduction potentials (E_h). The E_h was measured using a 1.0 mm Pt disk electrode. When a normal hydrogen reference electrode (NHE) is used, positive potentials correspond to the presence of oxidizing species (electron donors), while negative potentials are related to reducing species (electron acceptors).

In cyclic voltammetry (CV) a triangularly changing potential is applied to an electrode while the current is monitored. CV can be used to identify redox couples and, depending on conditions, can sometimes be used to constrain the identity of the redox species by using the peak potential (E_p).[11] On Phoenix, the potential was scanned between ± 1 V. In the WCL a standard three-electrode cell was employed, with a 250 μm Au disk serving as the working electrode, a Cl^- ISE as the reference, and a 1.0 mm Pt disk as the counter. A gold working electrode was selected based on its broad applicability towards organic and inorganic redox active compounds. The minimum scan rate achievable was 333 mV/s due to constraints caused by the large scan window and the hardware buffer limit of 4,094 bytes, which ultimately limited the number of data points to 2015. In order to accommodate all possible current windows, each experiment needed to be run six times at different gain settings.

Anodic stripping voltammetry (ASV) is primarily used for the detection of heavy metal ions in solution. ASV is performed by applying a cathodic potential for a fixed amount of time and reducing a metal ion onto the working electrode surface. The deposited heavy metal is then oxidized during an anodic potential scan. The resulting peak current is proportional to both the metal ion concentration and the deposition time. Very low detection limits can be achieved using ASV because of the effective preconcentration of analyte on the electrode. The WCL contained a 564-element array of 12 μm Au microelectrodes for ASV. The array of microelectrodes are attractive for remote analysis due to their very low capacitive charging currents, small size, rugged construction, low noise, and spherical diffusion with increased current signal. Unfortunately, just before launch the ASV

software was found to be problematic and thus ASV was never successfully performed for any martian soil samples.

Chronopotentiometry is the measurement of the potential at a working electrode as a function of applied current. The current can be applied as a step or a ramp (both of which were used on Phoenix). A three-electrode cell was employed in WCL, with a 1.0 mm Ag disk as the working electrode. The reference and counter were the same as used for CV. The CP was primarily used for the determination of halides present in the soil. In the presence of halides, the silver surface will oxidize to form an insoluble salt at the surface of the electrode. The reaction at the silver electrode is

$$Ag + X^- \rightarrow AgX + e^- \tag{6.6}$$

where X^- is a halide anion (Cl^-, Br^-, or I^-). The concentration of X^- (C^*) in solution can be determined using the Sand equation:

$$C^* = \frac{2i\tau^{1/2}}{nFAD^{1/2}\pi^{1/2}} \tag{6.7}$$

where i is the applied current, τ is the transition time, n is the number of electrons transferred, F is Faraday's constant, A is the electrode area, and D is the diffusion coefficient of X^-. When the current applied to the working electrode is sufficient to cause a redox reaction at the surface, the potential will adjust to maintain the applied current. As the concentration of X^- at the electrode surface decreases, the potential required to drive the reaction will increase. When the concentration of X^- at the electrode surface drops to zero, the potential will rapidly decrease causing an inflection point in the E vs. t curve.

For mixtures of halides the measured potential and transition time can be used to determine the identity of the species in solution. The measured potential is related to the standard potential of the redox couple, while the transition time indicates concentration. In the Phoenix experiments the transition order was iodide, bromide, and chloride, which is inversely related to the K_{sp} of each silver salt.

6.2.3 The WCL Custom Reference Electrode Configuration

The typical reference electrode serves two main functions in electrochemical cells: it produces a constant potential independent of ions in the sample, and, along with the working electrode, completes the flow of current in the electrochemical circuit.[11] Conventional reference electrodes based on liquid junctions are able to accomplish these functions by separating the sample solution from a reference solution. They rely on slow leakage of ions from the inner solution into the sample in order to complete the circuit. This type of arrangement has several drawbacks, which make their use for long-term remote monitoring impossible: the slow diffusion of ions from the inner solution would cause sample contamination and

an increase in conductivity; liquid junctions typically require frequent maintenance; inner solutions need to be changed and refilled and can only be used in an upright position in situations where bubbles might form internally and block the junction.

Two Li^+ ISEs were used as reference half cells in the WCL to mitigate the risks of the unknown composition of the martian soil and the need for stability. To maintain their potential, the leaching solution contained 1 mM $LiNO_3$ as a reference electrolyte.[5] This choice assumed that there would be significantly less than 1 mM Li^+ present in the martian soil and that interfering cations would not be a problem due to the high selectivity of the lithium ionophore. However, the presence of 1 mM NO_3^- limited its detection to levels >1 mM. In the case that both Li^+ ISEs failed, a solid-pellet Cl^- ISE would then act as the reference electrode. Since the concentration of Cl^- in the regolith could be significant, a correction could be made using the Cl^- concentration obtained from the CP experiments, which can measure Cl^- concentration without calibration.

6.3 Results from the Phoenix WCL

After landing successfully on Mars, the Phoenix payload underwent a series of system checks to ensure that all of the instrumentation had arrived in proper working order.[12] Before any electrochemical analyses could be performed, the beaker chamber needed to be equilibrated with the martian atmosphere by repeatedly opening and closing the sample drawer (referred to as "burping"). Once the pressure was equilibrated, the first leaching solution (TS20) was added to the beaker. TS20 contained 10^{-5} M of Na^+, NH_4^+, K^+, Ca^{2+}, Mg^{2+}, Ba^{2+}, HCO_3^-, 5×10^{-5} M Cl^-, and 1×10^{-3} M NO_3^-. A simple two-point calibration was subsequently performed by adding a solid pellet of salts, which increased the concentrations to 3×10^{-5} M, 1.5×10^{-4} M, and 1.09×10^{-3} M, respectively. After about an hour the potential of the electrodes had stabilized and ~1 cm^3 of martian soil was then delivered to the beaker. Figure 6.3 shows the real-time monitoring of the ISE potentials during the analysis sequence. In total, three samples, one from the surface (Rosy Red) and two from the top of the ice table approximately 5 cm in depth (Sorceress 1 and Sorceress 2), were successfully added and analyzed in three of the four WCLs.

The wet chemistry laboratory onboard Phoenix provided the first wet chemical measurement of soluble species in the martian soil.[12,13] The ionic species and their concentrations in the soil were found to be similar to those generally observed on Earth; thus the martian soil at the Phoenix site is considered to be habitable for any putative martian microbes.[14] Preliminary data analyses showed the monovalent cations, Na^+ and K^+, to be present at relatively low concentrations: ~1.4 mM and ~0.4 mM, respectively. The concentrations of the Ca^{2+} and Mg^{2+} ions at 0.75 and 6.4 mM were consistent with a saturated Ca/Mg carbonate-buffered system.[12] Chloride was also measured, and was found to be present at 0.40 mM.

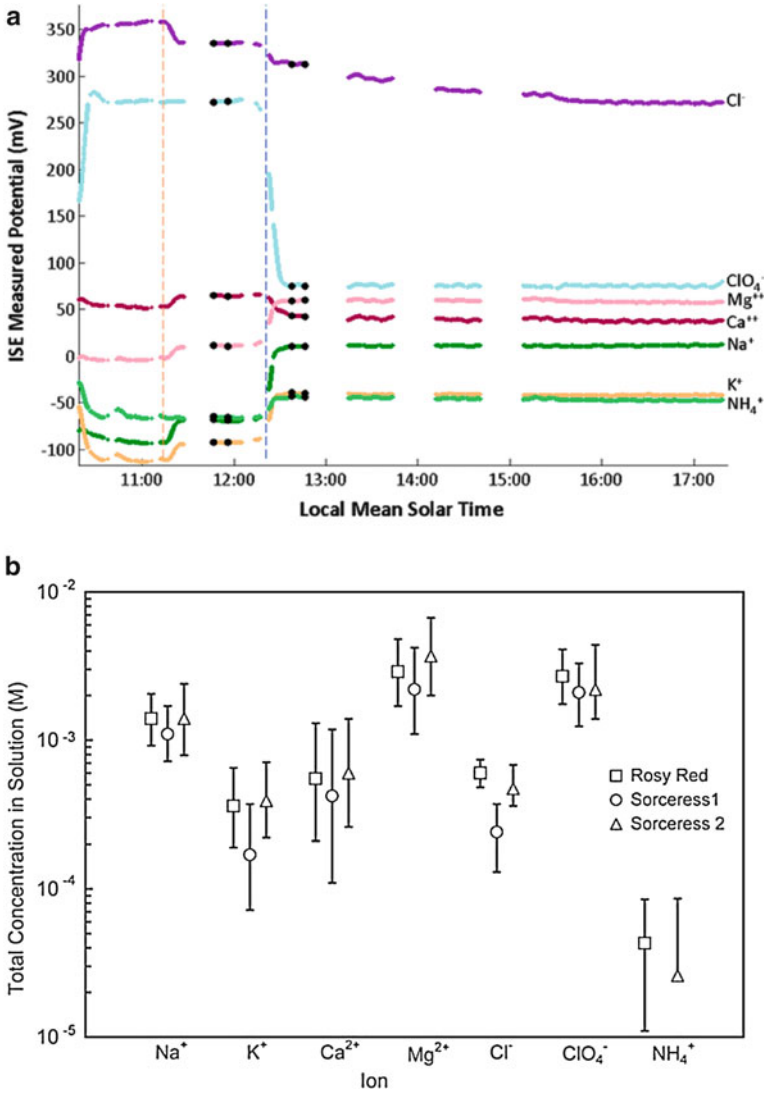

Fig. 6.3 (**a**) Potential vs. time traces recorded for the ISEs for the Sol-30 (Rosy Red) sample on Mars. The *two vertical lines* indicate the addition of the calibrant crucible and the sample. (**b**) Concentrations of cations and anions in solution containing 25 mL leaching solution and 1 g of martian regolith for three of the WCL units. *Reprinted with permission from* reference (12)

6.3.1 The Discovery of Perchlorate and Its Parent Salts Using the Perchlorate and Calcium ISEs

One of the most significant discoveries made by Phoenix was the high concentration of perchlorate (ClO_4^-) in all three of the soil samples analyzed, roughly 2.5 mM in the 25 mL solution, equivalent to ~0.6 wt% in the soil.[12,13] The ClO_4^- was measured by the ISE originally intended for NO_3^-, but whose membrane actually responds selectively according to the Hofmeister lipophilicity series ($ClO_4^- > I^- > Br^- > NO_3^- > NO_2^- > HCO_3^- > Cl^-$). Thus, the 3 orders of magnitude response can only be due to ClO_4^-. Perchlorate when heated is a strong oxidizing agent, and is used on Earth in a variety of products, including solid rocket propellants, fireworks, explosives, and automotive airbag systems. It also occurs naturally and has been found in a variety of arid regions, though its discovery in the McMurdo Dry Valleys of Antarctica has provided conclusive evidence that its terrestrial presence is ubiquitous.[15,16] On Mars, the presence of ClO_4^- is a tracer for liquid water because the ClO_4^- ion is highly soluble and relatively unreactive at ambient temperatures. The presence of ClO_4^- has widespread implications for Mars' geological history and future human exploration. In addition, the identity of the ClO_4^- parent salt cation has significant implications for the planet's ancient and modern history of water.[17]

The initial findings from the WCL had suggested that the ClO_4^- was likely present as either Ca^{2+} or $Mg(ClO_4)_2$.[12,13] The ISE data has been recently reanalyzed and indicates that the parent salts include a major fraction of $Ca(ClO_4)_2$.[17] The signal from the Ca^{2+} ISE for Sol 30 (Fig. 6.4a) shows a negative exponential response after addition of the soil sample, in contrast to the expected positive exponential response given the amount of $CaCO_3$ in the soil.[18] However, due to the presence of ClO_4^- in the sample, the Ca^{2+} sensor suffers from anion interference, resulting in a negative bias of the signal.[19]

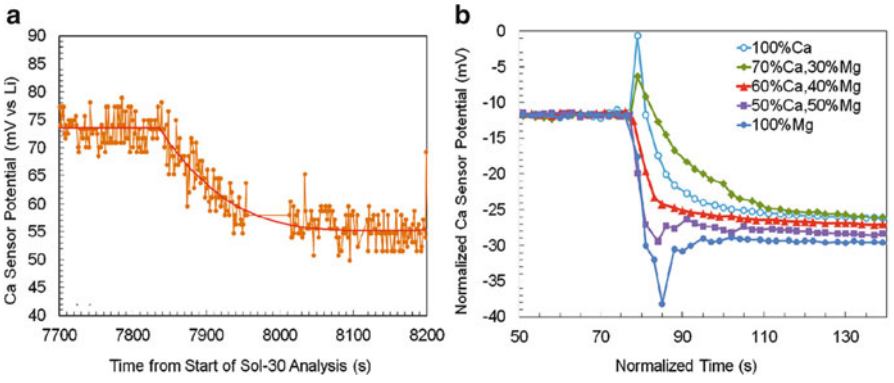

Fig. 6.4 Determination of perchlorate parent salts using Ca^{2+} ISE response. (**a**) Data from WCL on Sol 30. (**b**) Ca^{2+} ISE response with various ratios of Ca/Mg. *Reprinted with permission from* reference (17)

Laboratory experiments using various ratios of $Ca(ClO_4)_2$ to $Mg(ClO_4)_2$ in a Mars simulant show that when the ClO_4^- parent salt is 100 % $Ca(ClO_4)_2$, an initial potential spike is observed (Fig. 6.4b, light blue open circles), mainly due to the rapid detection of Ca^{2+} by the Ca^{2+}-selective ionophore. After a short time, the potential decreases to an equilibrium value ~23 mV below the calibration standard. When the ClO_4^- parent salt is 100 % $Mg(ClO_4)_2$ (Fig. 6.4b, dark blue closed circles), the potential shows a sharp decrease immediately after soil addition followed by a subsequent stabilization to the equilibrium value. In order to match the curve observed with WCL on Mars, an ~3:2 mixture of Ca/Mg is necessary. The existence of a soluble Ca^{2+} salt means that there has not been sufficient liquid water for the Ca^{2+} to react and precipitate with the known higher levels of sulfates that are globally present. The implication of this is that the Phoenix landing site (and most likely most of the martian surface) has been severely arid for perhaps for the past three billion years.[17]

6.3.2 *Determination of Soluble Sulfate by Titration Using a Barium ISE*

Another goal of the Phoenix WCL was to determine the presence and levels of soluble sulfate that had been suggested by previous Mars missions. Because no suitable ISE was available for the direct determination of SO_4^{2-}, the detection of SO_4^{2-} was accomplished by using a Ba^{2+} ISE to monitor the concentration of Ba^{2+} (added as $BaCl_2$) used to precipitate the SO_4^{2-} in the soil/solution mixture.[20] In the presence of sulfate, the soluble Ba^{2+} immediately precipitates due to the highly selective and rapid formation of $BaSO_4$. As the precipitation occurs there is a decrease in the measured amount of Ba^{2+} and increase in the amount of Cl^-.

The slow and more accurate determination of the sulfate by titration was fortuitous. It was noticed early on that the Cl^- in the first two WCL units slowly increased during the analysis. Initially this was thought to be due to a slow release of Cl^- from the added soil. However, during the Sol 96 analysis no sample was added to the WCL, but the same increase in Cl^- was present. It thus became clear that there was a slow and constant titration of the solution with the barium in the reagent crucibles. The increase in Cl^- was also independently confirmed by chronopotentiometry. Figure 6.5 shows the results of this unintended titration.

The amount of SO_4^{2-} in solution was determined by taking the change in Cl^- concentration and dividing it by 2, or

$$\left[SO_4^{2-}\right]_T = \frac{1}{2}\Delta[Cl^-] \tag{6.8}$$

where $[Cl^-]$ is taken immediately after the sample addition response until an increase is seen in the Ba^{2+}, indicating that no more SO_4^{2-} is being precipitated by the Ba^{2+}.

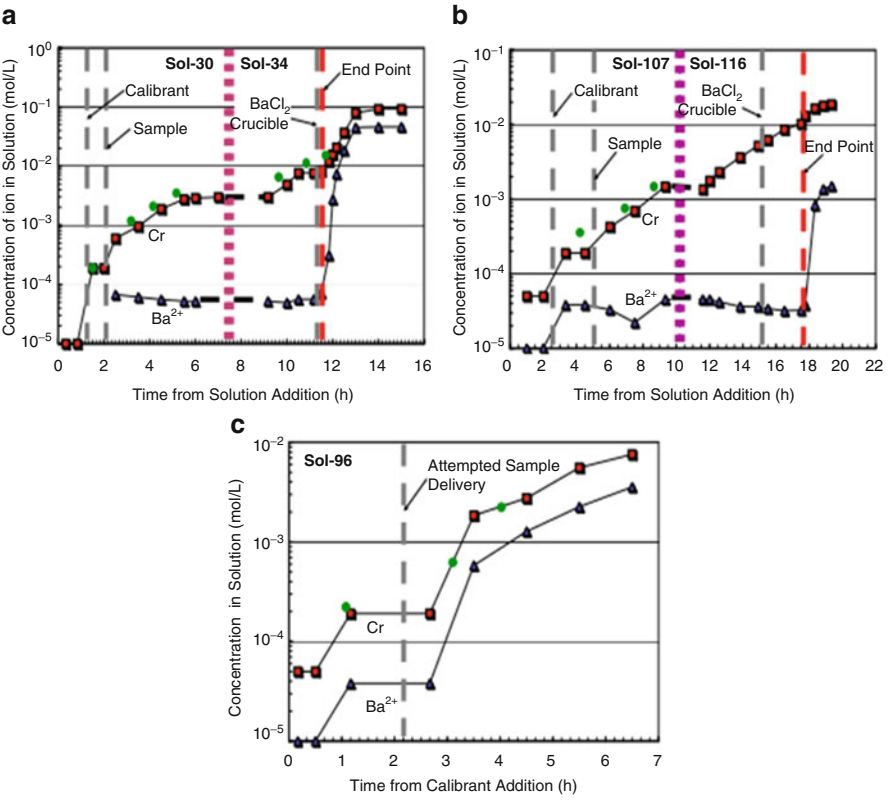

Fig. 6.5 Determination of SO_4^{2-} by the Ba^{2+} ISE (filled triangle), Cl^- ISE (filled square), and CP electrode (filled circle). Response of the Ba^{2+} and Cl^- ISEs in (**a**) cell 0 to the soil sample on Sols 30 and 34; (**b**) cell 2 to the soil sample on Sols 107 and 116; and (**c**) to the failed soil delivery on Sol 96 in cell 3 (i.e., the blank). *Reprinted with permission from* reference (20)

The results from the Ba^{2+} and Cl^- electrodes in the two working WCL units indicated that there was 4.8 (±1.5) mM (equivalent to 1.2 (±0.5) wt% soluble SO_4^{2-} in the soil) for the Rosy Red sample, and 5.9 (±1.5) mM SO_4^{2-} (equivalent to 1.4 (±0.5) wt% soluble SO_4^{2-} in the soil) for the Sorceress 2 sample.[20]

6.3.3 Determination of pH for the Soil/Water Mixture

The pH of the martian regolith was measured using two polymer-based membrane ISEs and an iridium oxide electrode. Measurement of pH of the martian regolith was seen as a critical objective for the mission, which is why this measurement was performed in triplicate. The dynamic range of the polymer-based pH ISEs as determined preflight was $1 < pH < 9$, while the dynamic range of the iridium

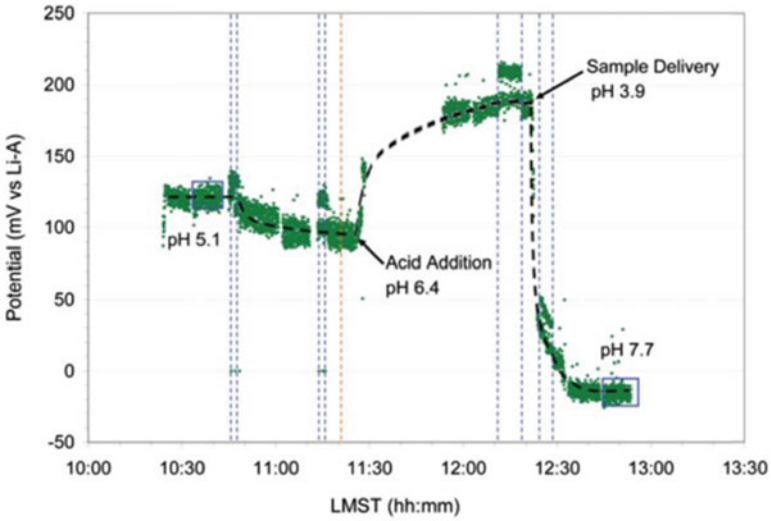

Fig. 6.6 Determination of the pH of the martian soil (Sorceress 1). Pairs of *dashed blue lines* represent opening and closing of sample drawer. *Orange line* represents addition of calibrant acid. *Blue boxes* represent intervals used for the determination of pH before opening of the sample drawer (~LMST 10:35) and after sample delivery (~LMST 12:50). LMST is the local mean solar time. *Reprinted with permission from* reference (12)

oxide electrode was $1 < \text{pH} < 12$.[5] Here, we discuss the preflight calibration and how the measurement was obtained on the surface of Mars.

Prior to flight each pH sensor was calibrated with four standard pH buffers saturated with ambient air as well as with 0.5 % CO_2. In order to correctly identify the contributions of the martian soil apart from the atmospheric contributions towards pH, the leaching solutions were pH buffered by equilibration with a gas that was predicted to be similar to the martian atmosphere (0.8 % CO_2, 94.2 % N_2, and 5 % He at 1,000 mbar pressure). The leaching solutions delivered on Mars to each WCL were expected to have a pH of 5.06 ± 0.04 at the analysis temperatures expected on Mars.[5]

Figure 6.6 shows the response of a polymeric membrane pH electrode towards the Sorceress 1 sample. The early part of the green curve confirms that after equilibration with the martian atmosphere the pH was indeed within the expected range. This measurement served as the initial calibration point for the pH sensors. As the cell was burped, the pH increased to 6.4, in line with the P_{CO2} of 8.4 mbar as measured by the Meteorological Station (MET) aboard Phoenix. When the calibration standard was added, the pH decreased to 3.9, confirming that the pH electrodes were functioning properly. Accounting for atmospheric P_{CO2} and the temperature of approximately 8 °C (Rosy Red) and 6 °C (Sorceress 1), at the time of sample delivery, the pH was determined to be 7.7 (±0.3) for the pH 1 sensor for the Rosy Red sample, and 7.6 (±0.3) and 7.6 (±0.3) for pH 1 and 2 for the Sorceress 1 sample. An average of these values yields a pH for the martian soil/solution mixture of approximately 7.7.[12] This was a major finding, showing that the martian soil was alkaline and would be a habitable soil for Earth-like organisms.

6.3.4 Determination of the Redox Potential

The oxidation-reduction potential (E_h) was measured to determine the presence of any species capable of oxidative electron transfer. In general, the redox potential of a solution can be calculated using the Nernst equation:

$$E_h = E^o - \frac{RT}{nF} ln \frac{a_{red}}{a_{ox}} - \frac{mRT}{nF} ln[a_{H^+}] \tag{6.9}$$

where E°, R, T, n, F, and a all have their usual meanings (see Chap. 9) and m is the number of moles of protons transferred. As Eq. (6.9) predicts, at constant pH the measured E_h is a function of the relative amounts of reduced and oxidized species present in solution.

The E_h of martian soil as measured in the Rosy Red beaker was 253 ± 6 mV at pH 7.7 ± 0.1, which suggests a slightly oxidizing environment.[21] The plausible identity of the oxidizing species was investigated using laboratory measurements of martian simulants. Figure 6.7 shows the overlay of E_h measured in WCL (black circles) compared with simulant data with added 16 ppm oxygen (as calcium peroxide—grey triangles) and 10 ppm ferrous iron (as ferrous sulfate—grey crosses). The ferrous iron was found to be thermodynamically unstable at pH 7.7, so thus any iron was likely present as a near-insoluble ferric species. The data

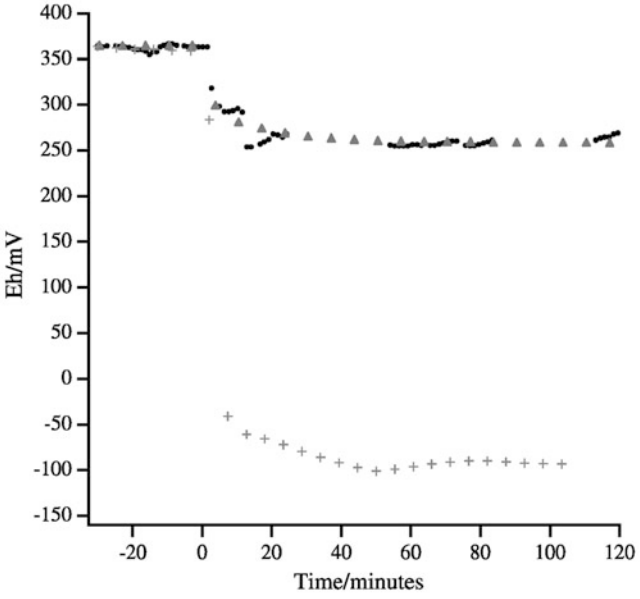

Fig. 6.7 E_h of Mars simulant salt mixtures containing 10 ppm ferrous iron (*grey crosses*) and 16 ppm peroxide (*grey triangles*). The data are overlaid with the measured WCL data collected from the Rosy Red beaker. *Reprinted with permission from* reference (21)

suggests that the measured E_h may be due to low levels of oxidants such as metal peroxides.[21]

6.4 Future Directions for Planetary Electroanalytical Instrumentation

Currently on Mars, the rover Curiosity (also known as the Mars Science Laboratory, MSL) is busy refining our understanding of the martian surface. Although there are several complex science instruments aboard the rover, there are no electrochemical sensors. Future characterization of martian chemistry and geochemistry requires in situ wet chemical analysis of the regolith. Currently under development in our group with the support of NASA and JPL are two instrument payloads that build upon the successes of the Phoenix mission while incorporating new sensor technologies and measurement protocols. A discussion of these instruments is presented below with a focus placed on the electrochemical sensors that are under development.

6.4.1 The Next-Generation WCL: CHEMSENS

The NASA supported development of the in situ ***Chem****ical Analysis Laboratory and* ***Sens****or Array* (CHEMSENS) is based on the Phoenix WCL and will provide for real-time investigation of the soil on Mars and similar planetary settings. Though the Phoenix mission is viewed as highly successful and is still providing results years after the end of the mission, it was clear that improvements could be made for future missions. These included (1) the number of individual WCL units, (2) an increased number of sensors in the array, and (3) sensor redundancy. Incorporating these improvements resulted in a scalable payload of "mini-WCL" units with a movable gantry for sample delivery and various actuator assemblies. This will allow for a payload of a few or a hundred WCL units to be incorporated into a lander or rover.

While decreasing the overall size of the WCL unit from accommodating 1 cc of soil and 25 mL of leaching solution to 1 cc of soil and roughly 8 mL of leaching solution, the number of sensors was increased by a factor of greater than 3. In order to achieve this goal while increasing the number of sensors, the overall size of the sensors needed to be miniaturized. ISEs in the WCL beaker had an outer diameter (O.D.) between 6 and 7 mm. Along with the conductivity sensors (O.D. ~10 mm) the ISEs took up the greatest amount of space in the WCL. Figure 6.8 shows a prototype of the CHEMSENS beaker where there is room for 15 sensors per beaker wall and the actuator assembly and delivery is accomplished by the XY gantry above the beaker.

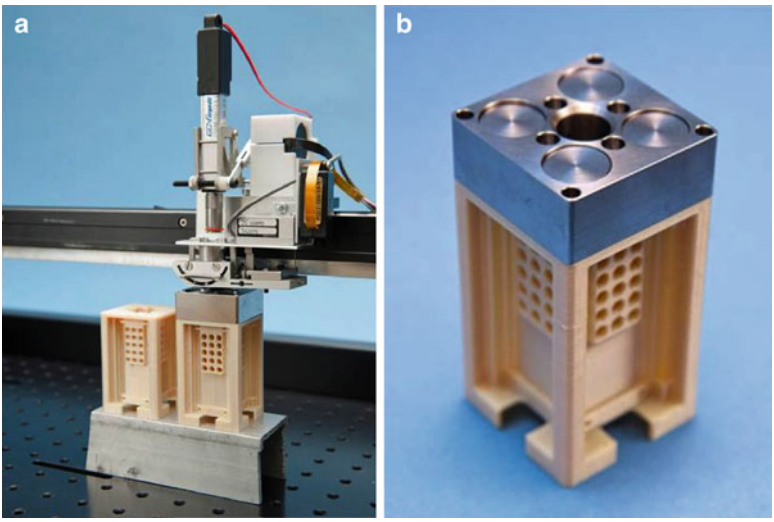

Fig. 6.8 Prototype of the CHEMSENS beaker and actuator assembly (**a**). Each beaker has been fabricated to accommodate 15 sensors per wall across 3 walls and an empty wall for the incorporation of other electrochemical sensors such as pH, conductivity, CV, and CP. The actuator assembly is on an XY gantry that will deliver sample (after external delivery to sample cup), dispense calibration solutions, and weigh samples. A close-up of the beaker (**b**) shows the leaching solution reservoirs, with four equal volume reservoirs (*larger circles*). *Courtesy of Draper/Tufts*

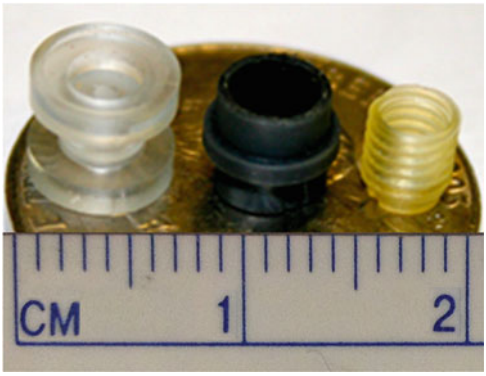

Fig. 6.9 A comparison of the sensor housing used in WCL and developed for CHEMSENS. The sensor housing on the *left* is similar to that used during the Phoenix mission housed in the WCL beakers. The *middle* housing was an initial prototype, and the housing on the *right* is the current housing used for the ISEs for the CHEMSENS project. *Courtesy of McElhoney/Tufts*

The main task and challenge of the sensor development was the miniaturization of the ISEs. When the active area of the internal reference element reservoir (pHEMA) was decreased, the sensors lost their ability to operate for more than a few days, if at all. Keeping the reservoir O.D. of ~3 mm, the membrane diameter was then decreased from 6 to 7 mm to ~4 mm (Fig. 6.9). When performing studies

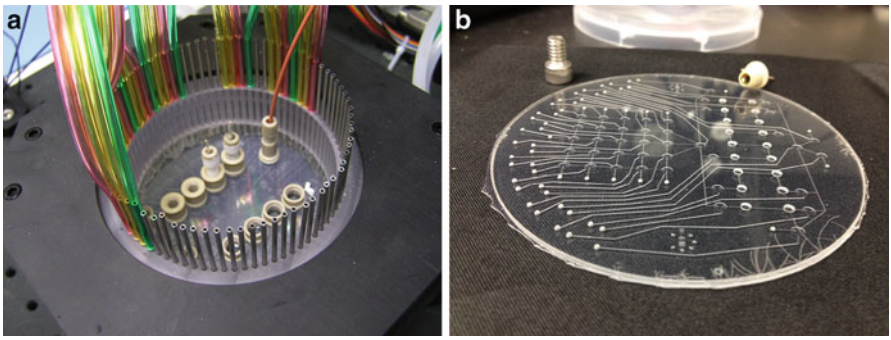

Fig. 6.10 The NERNST setup showing full assembly (**a**) and chip (**b**). *Courtesy of NASA JPL*

with the pHEMA, leaching of the electroactive components occurred much faster than for the large O.D. ISEs. To counteract the loss of ionophore, a previous method incorporating porous carbon was utilized.[22] Doping the porous carbon with a plasticized ionophore mixture allowed any ionophore that leached out of the ion-selective membrane (ISM) to be replaced from the reservoir, driven by the equilibrium between the two phases. This allowed for continuous monitoring of solutions in constant contact with solution for >50 days.[23]

6.4.2 *A Microfluidic Wet Chemical Analysis System: NERNST*

Another approach being developed in our laboratory in collaboration with researchers at NASA's Jet Propulsion Laboratory is a microfluidic total analysis system for analysis of martian regolith (Fig. 6.10). The system, called NERNST, provides a more detailed chemical picture of the martian surface material by allowing the manipulation of reagents and increasing the number of measurements. A microfluidic system offers several very attractive advantages for in situ planetary analysis: it requires very little power; can be effectively miniaturized to have a small footprint; and uses extremely small amounts of reagents. In addition, the analyses generally do not suffer as a result of miniaturization.

The NERNST concept applies several lessons learned from the Phoenix mission in order to provide a more robust, sensitive, and accurate measurement of the martian regolith. With NERNST, a sample of martian soil is first mixed with water off-chip in a sample extraction hub, and then the sample leachate (the water separated from the soil-water mix) is pumped on-chip for analysis. The sample can then be manipulated (with acid/base, $BaCl_2$, etc.) and measured multiple times with multiple electrodes in order to provide a deeper understanding of the soluble chemistry of the soil sample.

The advantages of using this microfluidic configuration lies in the ability to more closely perform a classical laboratory-based wet chemical analysis. For instance, with NERNST the electrodes can be calibrated over their entire dynamic range prior to sample analysis, and then spot-checked randomly throughout the analysis time. This is typical laboratory procedure, but was not available on Phoenix due to the beaker and experiment design. A second advantage is that reagents can be added to small aliquots of the sample solution without permanently altering the stock sample.

Automated wet chemical analysis systems such as CHEMSENS and NERNST can be used in conjunction with electroanalytical sensors, not only to reduce the mass, cost, and power consumption of the instrument, but also to provide a very detail picture of the aqueous geochemistry of samples in remote extreme environments. The direction of such devices points to evermore sophisticated robotic systems that could one day provide basically the same chemical analyses as a sophisticated terrestrial analytical laboratory.

References

1. Clark BC, Mason L, Thompson P (1995) Mars aqueous chemistry experiment (MACE), NASA technical report CR-201925. Lockheed Martin Astronautics, Denver, CO
2. Kounaves SP et al (2003) Mars Surveyor Program'01 Mars Environmental Compatibility Assessment wet chemistry lab: a sensor array for chemical analysis of the Martian soil. J Geophys Res 108:5077. doi:10.1029/2002JE001978
3. Smith PH et al (2008) Introduction to special section on the phoenix mission: landing site characterization experiments, mission overviews, and expected science. J Geophys Res 113: E00A18. doi:10.1029/2008JE003083
4. Smith PH et al (2009) H_2O at the phoenix landing site. Science 325:58–61
5. Kounaves SP, Hecht MH, West SJ et al (2009) The MECA wet chemistry laboratory on the 2007 Phoenix Mars scout lander. J Geophys Res 114:E00A19. doi:10.1029/2008JE003084
6. Bakker E, Bühlmann P, Pretsch E (1997) Carrier-based ion selective electrodes and bulk optodes. 1. General characteristics. Chem Rev 97:3083–3132
7. Bakker E, Pretsch E (2007) Modern potentiometry. Angew Chem Int Ed 46:5660–5668. doi:10.1002/anie.200605068
8. Bühlmann P, Pretsch E, Bakker E (1998) Carrier-based ion selective electrodes and bulk optodes. 2. Ionophores for potentiometric and optical sensors. Chem Rev 98:1593–1688
9. Buck RP, Lindner E (1998) Studies of potential generation across membrane sensors at interfaces and through bulk. Acc Chem Res 31:257–266. doi:10.1021/ar9700623
10. Cosofret VV, Erdosy M, Johnson TA et al (1995) Microfabricated sensor arrays sensitive to pH and K+ for ionic distribution measurements in the beating heart. Anal Chem 67:1647–1653. doi:10.1021/ac00106a001
11. Bard AJ, Faulkner LR (2001) Electrochemical methods: fundamentals and applications, 2nd edn. Wiley, New York, NY
12. Kounaves SP, Hecht MH, Kapit J et al (2010) Wet chemistry experiments on the 2007 phoenix Mars scout lander mission: data analysis and results. J Geophys Res 115:E00E10. doi:10.1029/2009JE003424
13. Hecht MH, Kounaves SP, Quinn RC et al (2009) Detection of perchlorate and the soluble chemistry of martian soil at the phoenix lander site. Science 325:64–67

14. Stoker CR, Zent A, Catling DC et al (2010) Habitability of the phoenix landing site. J Geophys Res 115:E00E20. doi:10.1029/2009JE003421
15. Kounaves SP, Stroble ST, Anderson RM et al (2010) Discovery of natural perchlorate in the Antarctic Dry Valleys and its global implications. Environ Sci Technol 44:2360–2364. doi:10.1021/es9033606
16. Catling DC, Claire MW, Zahnle KJ et al (2010) Atmospheric origins of perchlorate on Mars and in the Atacama. J Geophys Res 115:E00E11. doi:10.1029/2009JE003425
17. Kounaves SP, Chaniotakis NA, Chevrier VF et al (2013) Identification of the perchlorate parent salts at the Phoenix Mars landing site and possible implications. Icarus 232:226–231
18. Boynton WV, Ming DW, Kounaves SP et al (2009) Evidence for calcium carbonate at the Mars Phoenix landing site. Science 325:61–64
19. Bühlmann P, Amemiya S, Yajima S, Umezawa Y (1998) Co-Ion interference for ion selective electrodes based on charged and neutral ionophores: a comparison. Anal Chem 70:4291–4303
20. Kounaves SP, Hecht MH, Kapit J et al (2010) Soluble sulfate in the martian soil at the Phoenix landing site. Geophys Res Lett 37. doi: 10.1029/2010GL042613
21. Quinn RC, Chittenden JD, Kounaves SP, Hecht MH (2011) The oxidation-reduction potential of aqueous soil solutions at the Mars Phoenix landing site. Geophys Res Lett 38:L14202. doi:10.1029/2011GL047671
22. Vamvakaki M, Chaniotakis NA (1996) Solid-contact ion selective electrode with stable internal electrode. Anal Chim Acta 320:53–61. doi:10.1016/0003-2670(95)00524-2
23. McElhoney K, O'Neil GD, Chaniotakis NA, Kounaves SP (2012) Stability and lifetime of potassium solid-contact ion selective electrodes for continuous and autonomous measurements. Electroanalysis 24:2071–2078. doi:10.1002/elan.201200264

Part II
Fundamental Concepts of Sensors and Biosensors

Chapter 7
Electrochemical Sensor and Biosensors

Cecilia Cristea, Veronica Hârceagă, and Robert Săndulescu

7.1 General Sensor Concept

From the basic researches of the electrochemistry parents, Volta, Galvani, Sir Humphry Davy, and Faraday, a long period of silence followed in this interdisciplinary field that ends only at the beginning of the twentieth century with the invention of the glass electrode by M. Cremer and the discovery of polarography by J. Heyrovsky. That was the moment when modern electrochemistry was born. The research boom, which leads to the elaboration of the most well-known electrochemical methods and main types of electrodes, continues even today. Electrochemical methods (potentiometry, voltamperometry, and conductimetry) experienced a huge development due to their multiple advantages that they offer, mainly the high sensitivity that allows detection of concentrations in the range of 10^{-8}–10^{-10} M especially for differential pulse, square wave voltammetry, and stripping techniques.

At the same time the major disadvantage of the electrochemical methods became obvious: lack of selectivity. Practically, all the electroactive species can be reduced or oxidized from a sample or from a matrix and the simultaneous detection in the same sample is possible only in the case when two species possess redox potentials sufficiently separated in the investigated domain of potential. The reduced selectivity was the main issue that pointed the researchers' attention towards the delicate area of the electrode surface, where essential phenomena take place and trigger the race that still continues today having the goal of increasing the selectivity (specificity) for certain analytes. A new domain has been born, the field of modified electrochemical sensors. There are several possibilities today to modify the electrode material or its surface; the general strategies of electrochemical sensor technology will be discussed later.

C. Cristea • V. Hârceagă • R. Săndulescu (✉)
Analytical Chemistry Department, Faculty of Pharmacy, "Iuliu Haţieganu" University of Medicine and Pharmacy, 4 Louis Pasteur St., 400349 Cluj-Napoca, Romania
e-mail: rsandulescu@umfcluj.ro

L.M. Moretto, K. Kalcher (eds.), *Environmental Analysis by Electrochemical Sensors and Biosensors*, DOI 10.1007/978-1-4939-0676-5_7

According to IUPAC[1] a chemical sensor is "a device that transforms chemical information, originating from a chemical reaction of the analyte or from a physical property of the investigated system, ranging from the concentration of a specific sample component to total composition analysis, into an analytically useful signal."

Generally, chemical sensors contain two basic functional units connected in series: a chemical (molecular) recognition system, named *receptor*, which transforms the chemical information into a measurable form of energy, and a physicochemical *transducer* capable of transforming the energy carrying the chemical information about the sample into a useful analytical signal.[1]

A modern sensor system generally incorporates besides the receptor and the transducer other two key components: a sample delivery unit and a data processor.[2]

The receptor part of the chemical sensors is based on three various basic principles of stimulus: *physical*, where no chemical reaction takes place (e.g., measurement of absorbance, refractive index, conductivity, temperature or mass change); *chemical*, in which a chemical reaction with participation of the analyte gives rise to the analytical signal; and *biochemical*, in which a biochemical process is the source of the analytical signal (e.g., enzyme amperometric sensors, microbial potentiometric sensors, or immunosensors).[1] The last category consists of the well-known biosensors and they can be differentiated according to the biological elements used as receptor, namely enzymes, nucleic acids, aptamers, antibodies, organelles, membranes, cells, tissues, or even whole organisms.

The main function of the receptor is to provide the sensor with a high degree of selectivity for the analyte to be measured. While most chemical sensors are more or less selective (specific) for a particular analyte, some are, by design and construction, only class specific, e.g., sensors or biosensors for phenolic compounds, or whole-cell biosensors used to measure the biological oxygen demand.

The second part of a sensor, the transducer, serves to transfer the signal from the output domain of the recognition system into an output signal (usually electric) which is then amplified by the electronics and converted into useful data.[3]

According to the operating principle of the transducer, chemical sensors may be classified in optical, electrochemical, electrical, mass-sensitive, magnetic, and thermal sensors or sensors based on other physical properties such as radioactivity. The transducer part is responsible for the sensitivity of the device.

1. Optical devices transform changes of optical phenomena, which are the result of an interaction of the analyte with the receptor part. This group may be further subdivided according to the type of optical properties which have been applied in the chemical sensors: absorbance, reflectance, luminescence, and fluorescence, refractive index including the surface plasmon resonance effect, the optothermal effect, and light scattering.
2. Electrochemical devices transform the effect of the electrochemical interaction which takes place between the analyte (or the generated species from the interaction of the analyte and a biological compound) and the electrode into an exploitable electric signal (current or potential). Such effects may be stimulated

electrically or may result in a spontaneous interaction at zero-current conditions. The following subgroups may be distinguished:

- Voltammetric sensors, including amperometric devices, in which a current is measured in direct or alternating current mode. This subgroup may include sensors based on chemically inert electrodes, chemically active electrodes, and modified electrodes. In this group are included also sensors with and without (galvanic sensors) external current source.
- Potentiometric sensors, in which the potential of the indicator electrode (ion-selective electrode, redox electrode, metal/metal oxide electrode) is measured against a reference electrode.
- Chemically sensitized field effect transistor in which the effect of the interaction between the analyte and the active coating is transformed into a change of the source-drain current. The interactions between the analyte and the coating are, from the chemical point of view, similar to those found in potentiometric ion-selective sensors.
- Potentiometric solid electrolyte gas sensors, differing from classical potentiometric sensors because they work with high-temperature solid electrolytes and are usually applied for gas-sensing measurements.

3. Electrical devices based on measurements, where no electrochemical processes take place, but the signal arises from the change of electrical properties caused by the interaction with the analyte. This group can be subdivided into metal oxide semiconductor sensors, organic semiconductor sensors, electrolytic conductivity sensors, and electric permittivity sensors.
4. Mass-sensitive devices transform the mass change at a specially modified surface into a change of a property of the support material. The mass change is caused by accumulation of the analyte. This group has two subgroups: piezoelectric devices and surface acoustic wave devices.
5. Magnetic devices based on the change of paramagnetic properties of a gas being analyzed. These are represented by certain types of oxygen monitors.
6. Thermometric devices based on the measurement of the heat effects of a specific chemical reaction or adsorption which involve the analyte. Examples of this group are the so-called catalytic sensors. The devices based on measuring optothermal effects can alternatively be included in this group.
7. Other physical properties as for example X-, β-, or I^--radiation may form the basis for a chemical sensor in case they are used for determination of chemical composition.[1]

Among the different classes of transducers employed in sensor and biosensor construction, the electrochemical transducers are the most used ones. They occupy the first position as far as their disponibility on the market is concerned and they have already demonstrated their practical utility. Electrochemistry has superior properties in comparison to other measurement systems because of the rapid, simple, and sensitive characteristics.[4]

The transducer part of an electrochemical sensor is also called a detector, sensor, or electrode, but the term transducer is preferred to avoid confusion.

In case of electrochemical sensors with respect to homogeneous monolithic electrodes, the electrode material fulfilled both roles, as receptor and transducer, but later the run for more selective surfaces has focused the attention of electrochemists to the electrode surface, which is in fact the receptor and is responsible for the sensor's selectivity.

In addition to the classifications of sensors according to the operation principle of the receptor or the transducer part, they can also be classified based on the analyte to be measured: sensors for pH, for metal ions, or for oxygen or other gases, or based on the mode of application: for use in vivo, for process monitoring, etc.

Taking into consideration the abovementioned criterions, attention must be paid to avoid confusion between the terms biosensor and chemical and physical sensors. A biosensor, which by definition incorporates a biological compound, can be used to monitor either biological or non-biological matrices. Chemical sensors, which incorporate a non-biological specificity-conferring part, although used for monitoring biological processes, such as the in vivo pH or oxygen sensors, are strictly speaking not biosensors. Similarly, physical sensors used in a biological environment, even electrically based, such as in vivo pressure or blood flow sensors, are also excluded from the class of biosensors.[5]

7.2 Comparison with Biological Sensors

All living organisms contain biological sensors with functions similar to those of the electrochemical devices described above. Generally speaking a sensor, either electrochemical or biological, is a device which receives and responds to a signal when activated.

Most of the biological sensors are specialized cells that are sensitive to a stimulus that can be light, motion, temperature, magnetic field, gravity, humidity, moisture, vibration, pressure, electrical field, sound, and other physical aspects of the external environment, physical aspects of the internal environment (stretch, motion of the organism), environmental molecules (toxins, nutrients, pheromones), internal metabolic milieu (glucose level, oxygen level, osmolality), internal signal molecules (hormones, neurotransmitters, cytokines), and differences between proteins of the organism itself and of the environment or alien creatures.

Starting from this similarity the word receptor or bioreceptor, used for the recognition system of a chemical sensor or biosensor, comes from the sensing systems present in living organisms or systems where the actual recognition is performed by a cell receptor.

Also the term sensitivity can be used for both electrochemical and biological sensors having the same meaning. It indicates how much the sensor's output changes when the measured quantity of the stimulus changes.

Having very similar operating mode and design there are even electrochemical sensors described in the scientific literature called electronic nose[6] or electronic tongue.[7,8]

Nowadays, the term biological sensor is used extensively in the scientific literature. Apart from its meaning as sensing organ in living organisms some authors use it to define sensors that measure a biological component either in vivo or in vitro or for sensors that contain in their structure a biological component as receptor, actually the biosensors.[9]

7.3 The Importance of Sensors in Analytical Chemistry

Electrochemical sensors are an important domain of modern analytical chemistry. Understanding sensor devices requires some knowledge of a variety of academic areas. This leads to a very interdisciplinary field populated by physicists, chemists, engineers, biologists and biochemists, materials scientists, electrochemists, and others.

There are many examples of the topics of application of sensors including pharmaceutics, medicine, analytical sciences, synthetic chemistry, biotechnology, materials sciences, and (bio)molecular engineering.

Electrochemical sensors and detectors are very attractive for on-site monitoring of priority pollutants, as well as for addressing other environmental needs. Such devices satisfy many of the requirements for on-site environmental monitoring and have already made a significant impact also on decentralized analysis. Electrochemical sensors can be used for process line monitoring across a range of simultaneous measurement points, bundling different levels of information into the decision-making process.

The possibility of miniaturization and the use of these devices at the so-called point of care or point of action is a strong driver for innovation. This is of great importance especially for biological samples because they generally are available in small amounts and tissue damage must be minimized in case of in vivo monitoring.

A special advantage of sensors for analytical purposes is the possibility of automatization and mass production of miniaturized devices.

Electrochemical sensors have major advantages over traditional analytical methods, which will certainly lead to their even more pronounced use in the near future. They are attractive analytical devices due to their inherent sensitivity and selectivity towards electroactive species, sometimes even due to specificity, accurate and short response times, adaptability, and simplicity of preparation. They are compact, portable, and easy to use; they have a high benefit/cost ratio and present quickness in data collection.

However, many sensors described in the recent literature still display a few drawbacks when compared to other analytical methods. The most difficult problems

to overcome are electrochemical interferences in complex sample matrices. Anyway this can be still optimized through different design techniques.

The choice of a suitable working principle and design as well as the layout and constituent materials of a sensor package depends very much on the requirements of sensitivity, selectivity, portability, multivariant or single-use detection, and the specific field of application.[10]

7.4 General Strategies of Electrochemical Sensor Technology

In order to construct a successful sensor or biosensor a number of conditions must be met:

1. The receptor must be highly specific for the purpose of the analysis, be stable under normal storage conditions, and show a low variation between assays.
2. The reaction should be as independent as manageable of physical parameters such as stirring, pH, and temperature. This will allow analysis of samples with minimal pretreatment. If the reaction involves cofactors they should, preferably, also be co-immobilized with the receptor.
3. The response should be rapid, accurate, precise, reproducible, and linear over the concentration range of interest, without dilution or preconcentration. It should also be free from electrical or other transducer-induced noise.
4. The method should be sensitive and have limits of detection and quantification adequate to the concentration of the analyte, which is in many cases very low.
5. The complete sensor should be inexpensive, small, portable, automated, and capable of being used by semiskilled operators.
6. For rapid measurements of analytes it is desirable that the sensor can provide in situ real-time results.
7. In case of biosensors for invasive monitoring in clinical situations, the device must be tiny and biocompatible, having no toxic or antigenic effects. Furthermore, the sensor should not be prone to inactivation or proteolysis.[11]

The systematic strategy for designing sensors should consider five features: (1) the detected or measured parameter, (2) the working principle of the transducer, (3) the physical and chemical/biochemical model, (4) the practical application, and (5) the available technology and materials for sensor fabrication.

The selection of materials and fabrication techniques is crucial for an adequate sensor function and the performance of a sensor often ultimately depends upon these factors. Consequently, future developments in sensor design will inevitably focus upon the technology of new materials. Materials used in electrochemical sensors are classified as (1) materials for the electrode and supporting substrate (metals: platinum, gold, silver, and stainless steel; carbon-based materials: graphite, carbon black, and carbon fibre; new mixed materials; or organic electroconductive

polymers or salts); (2) materials for improved sensitivity and selectivity (especially nano-sized materials: nanoparticles and carbon nanotubes); (3) materials for the immobilization of biological recognition elements (multifunctional agents: glutaraldehyde and hexamethyl diisocyanate or alternatively non-conductive polymers: polyacrylamide and polyphenol); and (4) biological elements (enzymes, antibodies, antigens, mediators, and cofactors); the last two are applicable for electrochemical biosensors.[12]

Nanomaterials are acquiring a big impact on the development of electrochemical sensors as they bring new possibilities for developing novel electrochemical assays. Nanomaterials can be divided into two categories concerning their utility: nanoscale materials for electrode construction or modification and nanomaterials as tracers for biomolecules. Modified electrodes with nano-sized materials offer the advantages of better sensitivity and selectivity and shorter response time. Nanomaterials have been widely used as biomolecule tracers for electrochemical bio-sensing. Nanoparticles are very stable (compared to enzyme labels); they offer high sensitivity (thousands of atoms can be released from one nanoparticle) and a wide variety of them are available on the market. Nanoparticles are used nowadays as electrochemical labels or as vehicles containing several hundreds or thousands of electroactive labels, pushing the detection limits down to several hundreds of biomolecules.[13]

One of the most important steps in case of constructing electrochemical biosensors is the optimal immobilization of the biocomponent at the surface of the electrode. This optimum immobilization should assure a maximum quantity of bioreceptor immobilized or, more appropriately, a maximum number of functional reactive active sites immobilized in a unity of immobilization substrate as well as its stability and its efficacy.

General strategies of electrochemical sensor technology will cover the development and discovery of new biological molecules and systems, aspects of immobilization and stabilization, micro- and nano-fabrication technologies, challenges associated with measuring signals generated by bio-sensing systems, issues associated with integrating technologies to produce a functioning bio-sensing system, technical interfacing challenges such as sample introduction and handling through to aspects of commercialization, and adoption of bio-sensing technology into chosen markets.

7.5 Current Trends and Future Prospects

The requirements and regulations in the fields of environmental protection, control of biotechnological processes, and certification of food and water quality are becoming increasingly urgent. At the same time stricter requirements regarding human and animal health have led to a rising number of clinical and veterinary tests. Therefore, there is a need in developing highly sensitive, fast, and economic methods for detection, quantification, and monitoring analysis. The elaboration of

electrochemical sensors is probably one of the most promising ways to solve some problems concerning sensitive, fast, simple, cost-effective, and repetitive measurements with miniaturized and portable devices.

The developed sensors are mainly used in the following three ways:

1. As "off-line" detectors, when samples are taken from the investigated medium and injected in the measuring chamber of the sensor which reads the concentration of the analyte of interest.
2. As "in vivo" detectors, when the sensor is implanted in a living organism and continuously reads the concentration of the analyte of interest.
3. As "online" detectors, when sensors that measure the concentration of the analyte of interest are integrated into a flow line system.[14]

The area of electrochemical sensor research is very active and fruitful. It must be emphasized that most of the challenges in this field remain in the area of selectivity. This may be overcome by their integration into more complex analytical systems that combine online sampling and separation steps or the use of modified electrodes with highly selective chemical or biological recognition layers. However, in cases where direct detection in unmodified samples is possible, the high analysis speed and the capability of detecting extremely small volumes and low concentrations without significantly perturbing the sample remain highly attractive characteristics of electrochemical sensors.[15]

On the other hand, nowadays, the general demands required for analytical systems are extended to multianalyte sensing. Thus, tremendous efforts are focusing on the development of multianalyte assays with the advantages of short analysis time, simplified analytical procedure, decreased sampling volume, improved test efficiency, and reduced cost as compared to parallel single-analyte assays. In this context modified sensors could be promising analytical tools.[16]

The trend of using novel materials in electrochemical sensing systems for improved selectivity and sensitivity is constantly increasing, with their success largely due to the continuous design and development that meets the needs of modern electrochemical (bio)sensor technology. Materials ranging from carbon composites, beads or microspheres, molecular imprinted polymers, or quantum dots are playing an important role in these sensing systems. Nanomaterials (e.g., nanoparticles and CNTs) are the core of an emerging technological revolution. The main advantages of these materials are unique thermal, mechanical, electronic, and biological properties not found in conventional materials. Combining these outstanding properties with their remarkable recognition capabilities has resulted in systems with significantly improved performance for analytical applications. Most of the exceptional characteristics of nanomaterials are linked to their surface properties (area, roughness, energetic characteristics, and electron distributions) which enable improved interactions with many chemical and biological entities. These characteristics result in improved stability and selectivity of nanomaterials, and finally of the whole electrochemical sensor device.[17]

The electrochemical sensors are adaptable also to flow injection systems that have the advantages of high sample throughput.[18]

One of the main challenges faced nowadays by the analytical chemist is the development of methods that respond to the growing need to perform rapid "in situ" analyses. The advancement in miniaturization and microfabrication technology has led to the development of sensitive and selective electrochemical devices for field-based and *in situ* environmental monitoring. Electrochemical sensing devices have a major impact upon the monitoring of priority pollutants by allowing the instrument to be taken to the sampling site (rather than the traditional way of bringing the sample to the laboratory). Such devices can perform automated chemical analyses in complex matrices and provide rapid, reliable, and inexpensive measurements of a variety of inorganic and organic pollutants.[19]

Some other expectations of the nowadays practice is the development of analytical devices that are able to monitor in real time in vivo parameters. In this case electrochemical biosensors have played an important significant role in the transition towards point-of-care diagnostic devices. Such electrical devices are extremely useful for delivering the diagnostic information in a fast, simple, and low-cost fashion in connection with compact (handheld) analyzers. Such modern electrochemical bioaffinity, DNA, or immunosensors have been developed with remarkable sensitivity essential for early cancer detection.[20]

One of the most important driving forces for research in many areas of modern analytical chemistry is miniaturization, simplification, automation, and computerized instrumentation of the whole analytical procedure, the so called lab-on-a-chip or micro total analysis (μTAS) technology. The speed for generating the results (high throughput), the amount of information (simultaneous or multiparametric), and the autonomy (portability) are obvious advantages. Other characteristics of miniaturized systems are the simplicity of use and the cost efficiency, combined with small reagent consumption and small waste generation. Recent advances in electrochemical sensor technology include the introduction of microfabrication and ultramicroelectrodes. Although exciting to contemplate, electrochemical or other types of "chips" have not been widely accepted yet in the commercial area. So far these techniques have neither demonstrated the compelling, cost-effective benefits required to displace current technology or workflow nor have they shown the ease of use needed to induce users to change. The major benefit claims of minimum sample requirement and solvent and reagent savings from these approaches seem however encouraging.[21]

Another reason to consider electrochemical sensors as attractive alternative in modern analytical chemistry is the possibility of mass production, the flexibility of the design, and the simplicity of manufacturing especially if we think of screen-printed electrodes.

Originally the biological recognition element in case of electrochemical biosensors was assumed to be isolated from a living system, but now there are prospects of synthesizing this component or employing genetically modified enzymes to increase some specific features of the biorecognition-based assays such as sensitivity, selectivity, and stability. In order to improve these experimental parameters genetic engineering should emphasize two main fields for biosensors—genetically transformed cells and genetically engineered receptor molecules.

Genetic modification already showed the potential for selection of enzyme variants that are specific for a range of individual compounds. Even more novel gene fusions have also resulted in more sensitive biosensors.[22]

Transferability of the analytical data is related to the appropriate analytical validation in order to provide robust and standard operational procedures for practical use in routine analytical work or in control programs. In case of electrochemical sensors the validation step is still a hurdle to be overcome that requires additional further works.[23]

Sensor science generates thousands of new publications each year. Undoubtedly, the development of sensor applications, in the course of these last years, is and has to remain multidisciplinary with research and engineering opportunities straddling across chemical engineering, biology, chemistry, physics, materials, processing science, surface science, information science, and other engineering disciplines, so the innovative ideas described in the scientific literature will reach the marketplace in the future.

References

1. Hulanicki A, Glab S, Ingman F (1991) Chemical sensors. Definitions and classification. Pure Appl Chem 63(9):1247–1250
2. Potyrailo RA, Mirsky VM (2009) Introduction to combinatorial methods for chemical and biological sensors. In: Potyrailo RA, Mirsky VM (eds) Combinatorial methods for chemical and biological sensors. Springer, New York, NY
3. Chaubey A, Malhotra BD (2002) Mediated biosensors. Biosens Bioelectron 17:441–456
4. Wang J (1999) Amperometric biosensors for clinical and therapeutic drug monitoring: a review. J Pharm Biomed Anal 19:47–53
5. Thevenot DR, Toth K, Durst RA, Wilson GS (2001) Electrochemical biosensors: recommended definitions and classification. Biosens Bioelectron 16:121–131
6. Stella R, Barisci JN, Serra G, Wallace GG, Rossi D (2000) Characterisation of olive oil by an electronic nose based on conducting polymer sensor. Sensor Actuator B Chem 63(1–2):1–9
7. Peris M, Escuder-Gilabert L (2009) A 21st century technique for food control: electronic nose. Anal Chim Acta 638(1):1–15
8. Woertz K, Tissen C, Kleinebudde P, Breitkreutz J (2011) Taste sensing systems (electronic tongues) for pharmaceutical applications. Int J Pharm 417(1–2):256–271
9. Kang YR, Park EJ, Kim JH, Min NK, Kim SW (2010) Development of bio-nanowire networks using phage-enabled assembly for biological sensor application. Talanta 81(4–5):1425–1430
10. Luttge R (2011) Chapter 6 chemical and biological sensors at component and device level. In: Luttge R (ed) Microfabrication for industrial applications. Elsevier, Amsterdam, pp 179–198
11. Grieshaber D, MacKenzie R, Voros J, Reimhult E (2008) Electrochemical biosensors - sensor principles and architectures. Sensors 8:1400–1458
12. Zhang S, Wright G, Yang Y (2000) Materials and techniques for electrochemical biosensor design and construction. Biosens Bioelectron 15(5–6):273–282
13. Pumera M, Sanchez S, Ichinose I, Tang J (2007) Electrochemical nanobiosensors. Sensor Actuator B Chem 123(2):1195–1205
14. Castillo J, Gáspár S, Leth S, Niculescu M, Mortari A, Bon□idean I, Soukharev V, Dorneanu SA, Ryabov AD, Csöregi E (2004) Biosensors for life quality: design, development and applications. Sensor Actuator B Chem 102:179–194
15. Bakker E (2004) Electrochemical sensors. Anal Chem 76:3285–3298

16. Wu J, Zhang Z, Fu Z, Ju H (2007) A disposable two-throughput electrochemical immunosensor chip for simultaneous multianalyte determination of tumor markers. Biosens Bioelectron 23(1):114–120
17. Scida K, Stege PW, Haby G, Messina GA, Garcia CD (2011) Recent applications of carbon-based nanomaterials in analytical chemistry: critical review. Anal Chim Acta 691:6–17
18. Junqueira JRC, Araujo WR, Salles MO, Paixao TRLC (2013) Flow injection analysis of picric acid explosive using a copper electrode as electrochemical detector. Talanta 104:162–168
19. Hanrahan G, Patil DG, Wang J (2004) Electrochemical sensors for environmental monitoring: design, development and applications. J Environ Monit 6:657–664
20. Wang J (2006) Electrochemical biosensors: towards point-of-care cancer diagnostics. Biosens Bioelectron 21(10):1887–1892
21. Rios A, Zougagh M, Avila M (2012) Miniaturization through lab-on-a-chip: Utopia or reality for routine laboratories? A review. Anal Chim Acta 740:1–11
22. Campas M, Prieto-Simon B, Marty JL (2009) A review of the use of genetically engineered enzymes in electrochemical biosensors. Semin Cell Dev Biol 20:3–9
23. Farre M, Kantiani L, Perez S, Barcelo D (2009) Sensors and biosensors in support of EU directives. Trends Anal Chem 28(2):170–185

Chapter 8
Electrochemical Sensors in Environmental Analysis

Cecilia Cristea, Bogdan Feier, and Robert Sandulescu

8.1 The Importance of Environmental Analysis

Monitoring the environment for contaminants is nowadays closely related with our whole planet and human health. Due to the large variety of pollutants and required environmental analyses, the need for rapid, sensitive, decentralized analysis is continuously increasing. Electrochemical sensors could be well suited for this need but also could complement standard analytical techniques validated for some environmental analysis. When speaking about environmental analysis it should be underlined that this includes atmospheric analysis, groundwater and surface water analysis, ocean monitoring, soil analysis, and agriculture, food, and even pharmaceuticals monitoring.

With the development of industries, mining, and large-scale agriculture the number of pollutants threatening the environment, with effects on human and animal health, has increased a lot. The immune system can be attacked by many chemicals, with potentially severe adverse effects on the human health. In Western European countries, pesticides, together with other chemicals, have been implicated in the increasing prevalence of diseases associated with alterations of the immune response, such as hypersensitivity reactions, autoimmune diseases, and even cancer. Xenobiotics may initiate, facilitate, or exacerbate pathological immune processes, resulting in immunotoxicity by induction of mutations in genes coding for immunoregulatory factors, modifying immune tolerance and activation pathways.[1] The development of medicine at the cellular and molecular scale has allowed a better understanding of the mechanism by which these pollutants harm the leaving cells, leading to better protocols for avoiding work-related intoxications, increasing demands for environmental protection, and decreasing accepted limits for all the

C. Cristea • B. Feier • R. Sandulescu (✉)
Analytical Chemistry Department, Faculty of Pharmacy, "Iuliu Haţieganu" University of Medicine and Pharmacy, 4 Louis Pasteur St., 400349 Cluj-Napoca, Romania
e-mail: rsandulescu@umfcluj.ro

L.M. Moretto, K. Kalcher (eds.), *Environmental Analysis by Electrochemical Sensors and Biosensors*, DOI 10.1007/978-1-4939-0676-5_8

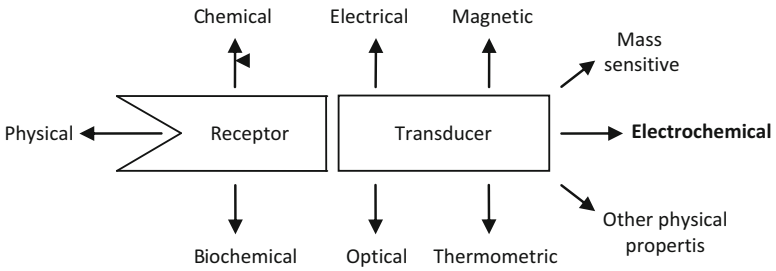

Fig. 8.1 Sensor classes

pollutants. For example, a concentration of lead in the blood of 60 μg/dl was considered safe in the 1960s, the acceptable concentration being reduced to 25 μg/dl in 1985 and to 10 μg/dl in 1991. Despite these changes, subclinical effects of lead exposure have been reported at concentration less than 10 μg/dl.[2] This continuous increase in the level of exigence regarding the environmental analyses demands a continuous improvement of the analytical methods and the development of new ones.

Table 8.1 presents the admitted concentrations in drinking water as recommended by the World Health Organization,[3–5] sources of pollution, possible toxic effects,[6–8] and some analytical methods and their LOD for some of the pollutants discussed in this work.

The main purpose of this chapter is to present the potential use of electrochemical sensors and biosensors in environmental monitoring.

8.2 General Definitions of Electrochemical (Bio)sensors

A chemical sensor is a device that transforms chemical information into an analytically useful signal (see previous chapter). Sensors contain two basic functional units: a receptor, at which the chemical information is transformed into a form of energy which may be measured by the transducer, which is capable of transforming the energy carrying the chemical information about the sample into a useful analytical signal (Fig. 8.1). The transducer does not show selectivity; thereby in order to increase this property a modification of the receptor is needed.[9]

Electrochemical sensors transform the effect of the electrochemical interaction which takes place between the analyte and the electrode surface into an analytical signal (current or potential). The abovementioned electrochemical reaction may be electrically stimulated or may result in a spontaneous interaction at zero-current conditions.[9]

Electrochemical sensors can be classified as voltamperometric and potentiometric sensors, chemically sensitized field effect transistors, and potentiometric solid electrolyte gas sensors (10) (see also the previous chapter).

Table 8.1 Main pollutants, their toxic effects, sources of pollution, and detection methods

Pollutant	Drinking water standards (μg/l)	Toxic effects	Sources of pollution	LOD and detection method
Heavy metals				
Pb	10	Toxic effects on the central nervous, renal, hematopoietic, and immune system	Paint, dust, gas, drinking water	1 μg/l by AAS; practical quantification limit in the region of 1–10 μg/l
Cd	3	Toxic effects on the bone and renal systems, carcinogenic	Batteries, paint, plastics, cigarettes	0.01 μg/l by ICP-MS; 2 μg/l by flame AAS
Cr	50	Carcinogenicity and allergenicity	Paints, fungicides, the ceramic and glass industry, chrome plating	0.05–0.2 μg/l (total Cr) by AAS
Cu	2,000	Hepatic cirrhosis, renal, neurological, gastrointestinal problems	Electrical wiring, pipes, fungicides, algicides, insecticides, fertilizers	0.02–0.1 μg/l by ICP-MS; 0.3 μg/l by ICP-optical emission spectroscopy; 0.5 μg/l by flame AAS
Hg	1	Lungs, central and peripheral nervous system, gastrointestinal tract, kidney disorders	Dental medicine, batteries, paints, explosives, photography, paper and insecticide manufacture, seafood	0.05 μg/l by cold vapor AAS; 0.6 μg/l by ICP; 5 μg/l by flame AAS
As	10	Neuropathy, seizures, cirrhosis, anemia, leukopenia, hyperkeratosis, multiple cancers	Pesticides, mining, microelectronics, fossil fuel combustion, homeopathic remedies	0.1 μg/l by ICP-MS; 2 μg/l by hydride generation AAS or flame AAS
Sb	5	Abdominal pain, epistaxis, pneumoconiosis, cardiomyopathy, skin spots	Textile industry, in alloys, glass manufacture, metallurgy, welding	0.01 μg/l by electrothermal AAS; 0.1–1 μg/l by ICP-MS; 0.8 μg/l by graphite furnace AAS; 5 μg/l by hydride generation AAS
Ni	20	Contact dermatitis, asthma, conjunctivitis, gastrointestinal distress, hepatic effects, cancers	Stainless steel, electroplating, rechargeable batteries, magnetic	0.1 μg/l by ICP-MS; 0.5 μg/l by flame AAS; 10 μg/l by ICP-AES

(continued)

Table 8.1 (continued)

Pollutant	Drinking water standards (μg/l)	Toxic effects	Sources of pollution	LOD and detection method
			tapes, plastic and rubber industries	
Anions				
NO_3^-/NO_2^-	50,000 (nitrate); 500 (nitrite)	Methemoglobinemia, shortness of breath, hepatotoxicity; nitrite may also be the origin of certain cancers through the formation of nitrosamide and nitrosamine compounds	Fertilizers, explosives, ink, tanning manufacture, petroleum refiner, meat preservatives, vegetable juice, industrial salts	0.005–0.01 mg/l (nitrite) and 0.01–1 mg/l (nitrate) by spectrometric techniques; 0.022 mg/l (nitrate) and 0.035 mg/l (nitrite) by ion chromatography; 0.1 mg/l (nitrate) and 0.05 mg/l (nitrite) by LC
CN^-	50 (total), 10 (free)	Irritative or corrosive chemical dermatitis, memory problems, neuropsychiatric symptoms, weakness, increased hemoglobin and lymphocyte, thyroid dysfunction	Mining, metal extraction, rubber, plastic, pharmaceutical manufacturing, metal polishing and hardening	1.9 μg/l by UV–Vis spectrophotometry, 0.26 μg/l by CE, 0.05 μg/l by amperometry, 0.36 μg/l by voltammetry
Pesticides				
2,4-Dichloro phenoxy acetic acid (2,4-D)	0.1 (class), 0.5 (total)	Severe eye and dermal irritation, neurotoxicity, and hepatic dysfunction	The use as a systemic herbicide for control of broad-leaved weeds, including aquatic weeds	0.1 μg/l by gas–liquid chromatography with electrolytic conductivity detection
Chlordane		Peripheral and central neurologic manifestations, skin rash, hepatic dysfunction	The use as a broad-spectrum insecticide, used mainly to destroy termites by subsurface injection into soil	0.014 μg/l by GC with ECD
Endrin		Peripheral and central neurologic manifestations, skin rash, hepatic dysfunction	The use as a broad-spectrum foliar insecticide used against a wide range of agricultural pests and as a rodenticide	0.002 μg/l by GC with ECD

Halogenated organic compounds				
Chloroform	300	Profound CNS, cardiovascular, gastrointestinal, hepato-renal, dermal, carcinogen toxic effects	Used widely in industry: solvents, chemical intermediates, propellants, fumigants, degreasers, paint and varnish remover	0.1–0.2 μg/l by purge-and-trap and liquid–liquid extraction in combination with a chromatographic system; 0.1 μg/l by GC-ECD; 2.2 μg/l by GC-MS
Vinyl chloride	0.3			0.01 μg/l by GC-ECD or GC-FID with MS for confirmation
Carbon tetrachloride	4			0.1–0.3 μg/l by GC-ECD or GC-MS
Hexachloro butadiene	0.6			0.01 μg/l by GC-MS; 0.18 μg/l by GC with ECD
Phenols				
Pentachloro phenol	9	Confusion, lethargy, tachycardia, hypotension, metabolic acidosis, hepatic and renal injury, swelling and hypalgesia of the skin	Manufacture of phenolic resins, plastics, explosives, fertilizers, paints, pharmaceuticals, paper, phenolic disinfectants	0.005–0.01 μg/l by GC with ECD
Mono- and polynuclear aromatic hydrocarbons				
Benzene	10	Highly toxic, profound CNS and bone narrow toxic effects, risks for leukemia	In degreasing operations, printing, electronics and rubber manufacture, paints, solvents and intermediates for chemical synthesis	0.2 μg/l by GC with photoionization detection and confirmation by MS

(continued)

Table 8.1 (continued)

Pollutant	Drinking water standards (µg/l)	Toxic effects	Sources of pollution	LOD and detection method
Toluene	700	Psychiatric change, cognitive dysfunction, fatigue, myopathy, nephrotoxicity, teratogen	Gasoline, paints, adhesives, inks, solvents	0.13 µg/l by GC with FID; 6 µg/l by GC-MS
Styrene	20	Profound CNS, cardiovascular, gastrointestinal, hepato-renal, dermal, carcinogen toxic effects	Plastics and resins manufacture, naturally present in some foods	0.3 µg/l by GC with photoionization detection and confirmation by MS
Benzo[a]pyrene	0.7	Carcinogenesis, dermal effects, photosensitivity, reduced lung function	Combustion of the fossil fuel, wood, seafood and agricultural products, roasted coffee, tea, smoking	0.01 µg/l by GC-MS and reversed-phase HPLC with a fluorescence detector
Nitrated compounds (nitro phenols)				
Trifluralin	20	Headache, nausea, weakness, fever; hypo- or hypertension; tachycardia, tachypnea; hepatic, mutagenic, carcinogenic effects	Used as a herbicide	0.05 µg/l by GC with nitrogen–phosphorus detection
Pharmaceuticals				
Antibiotics, anti-inflammatory/analgesics, lipid regulators, beta-blockers, cancer therapeutics, diuretics, antiepileptics, steroids, and related hormones	No regulations	Development of antibiotic-resistant bacteria, genotoxic effects, endocrine-disrupting effects, changes in the reproductive health of humans, including declining male fertility, birth defects, breast and testicular cancer	Excretion and disposal of pharmaceuticals and their metabolites in wastewater from human use, industries, hospitals, farms, pharmacies, household waste	Concentrations of pharmaceuticals in surface water and groundwater sources impacted by wastewater discharges are typically less than 100 ng/l and concentrations in treated drinking water are usually well below 50 ng/l, detected by GC–MS with or without derivatization and LC–MS or LC–MS–MS

The advantages of electrochemical sensors that could be exploited in environmental monitoring are the following:

1. The development of miniaturized sensors and of portable instrumentation allows the use of electrochemical sensors for in situ and flow system environmental monitoring.
2. Each chemical species and element has its own associated oxidation/reduction potential; therefore by applying this potential in voltamperometric sensors certain selectivity and specificity could be gained.
3. The selectivity can be also improved by the judicious choice of electrode material or by its modification.
4. High sensitivity and low detection limits can be obtained, due to performant electrochemical instrumentation and the possibility of accumulation of the species at the electrode surface.

Electrical sensors differ from electrochemical ones by the fact that no electrochemical processes take place, the signal being the result of the change of electrical properties caused by the interaction of the analyte as described in the previous chapter.

Biosensors are based on the same principles as the chemical sensors. They could be defined as analytical devices that associate a biological recognition element (i.e., enzymes, nucleic acid, antibodies, organelles, membranes, cells, tissues, or even whole organisms) that are immobilized at the surface of a transducer (made on carbon-based materials, platinum, gold, magnetic nanoparticles, silicon, glass, etc.). Another definition of a biosensor establishes that it is an integrated device that consists of a biological recognition species in direct contact with a transduction element. Therefore, biosensors can be categorized according to the biological recognition element (immuno, enzymatic, DNA, and whole-cell biosensors) or the signal transduction method (optical, mass-based, electrochemical, and thermal biosensors). To summarize, a biosensor combines a biological recognition element with a suitable transduction method such that a meaningful signal can be realized when binding or some reaction occurs between that element and a target species.

The implementation of several techniques in environmental analysis leads to reducing and/or eliminating the amounts of toxic discharges into the environment. It could be observed that there is a constant need to develop techniques and devices that can detect and monitor the environmental pollutants in a sensitive and selective manner to enable effective remediation. Due to their integrated nature, biosensors are ideal for environmental monitoring and detection as they can be portable and able to provide selective, sensitive, and fast responses in real time.[11]

In fact, during the last 20 years, biosensors were successfully applied in many fields of the environmental analysis, especially due to a variety of enzymes produced by bacteria, plants, or animals. Another reason is their catalytic property and the possibility of modifying the substrate specificity through genetic engineering.

Recent trends and challenges in research and development of sensors and biosensors consist in increasing the selectivity and sensitivity, particularly in the detection of species of environmental significance such as organic contaminants,

organophosphate nerve agents, polyaromatic hydrocarbons (PAH), polyphenols, pesticides, pharmaceuticals, and heavy metals as inorganic pollutants.

An innovative direction in the development of sensors is devoted nowadays to the modification of the electrode surface. Normally, the electrochemical methods and the electrochemical sensors are not very selective. In order to increase the selectivity of several methods and of electrodes, modification of their surfaces was performed. Even though the modified electrodes are in the early stages of their development their modified interfaces represent a great promise for environmental monitoring.

In environmental analysis modified electrodes could be useful due to the acceleration of the electron transfer reaction, accumulation of pollutants at the surface of the electrodes, permselective transport, incorporation of antibodies or small proteins (affibodies, aptamers, and mARN), incorporation of whole bacteria or cells in membranes attached to the electrodes, use of modified porous electrodes, flow analysis, and coupling electrochemistry with electrophoresis or chromatographic techniques.[12,13] The electrodes can be modified by formation of films at their surface, by using membranes, by adsorption, by layer-by-layer deposition, by monolayer, by covalent grafting, etc. (see corresponding topics in Chap. 3). Compared to other analytical methods electrodes present the advantage of being easily modifiable, allowing modification of the surface of the electrode by physical, chemical, or electrochemical processes.

8.3 Advantages and Disadvantages of Electrochemical Sensors and Their Importance in Environmental Analysis

Electrochemical sensors present many advantages as follows: very good sensitivity which allows low LODs and LOQs; fast analytical response making them useful for flow analysis and alert systems; simplicity offering practically an unlimited choice of electrode materials, geometries, and configurations; ease of use (simple and low-cost equipment, possibility to be integrated as detection module in various analytical systems, few analytical steps, it does not request specialized personnel); miniaturization and automation (useful in environmental and biomedical applications); and mass fabrication, meaning low cost and development of single-use disposable sensors, very important especially in the medical field where contamination is a major issue.

Biosensors are attractive analytical devices for environmental and biomedical analysis featuring other additional advantages: detection of the key substrate is very often made without prior separation; the sensitivity could arrive at ng/ml; high selectivity, and sometimes even specificity; high benefit/cost ratio; simple use; and the rapid data collection. The main advantages and drawbacks of first, second, and

third generations of amperometric biosensors will be described in a dedicated subchapter.

However, the major disadvantages of electrochemical sensors have to be mentioned: low or lack of selectivity, low reproducibility, and difficult validation of the analytical method. The most difficult problems to overcome for biosensors are reduced stability, rapid loss of enzyme activity, limited lifetime of biosensors, electrochemical interferences from complex sample matrices, bioincompatibility, and biofouling in case of in vivo measurements.[14,15]

In comparison to other instrumental methods of chemical analysis, electroanalytical instrumentation is relatively easy to miniaturize. The main trends in modern electroanalysis include development of chemical and biochemical sensors based on progress in chemical and biochemical methods of molecular recognition and development of measuring devices of a large integration scale, including sensor arrays. This is accompanied by the use of new materials, including nanomaterials and nanostructures, as well as the introduction of flow systems.[16]

The main classes of pollutants which will be described in several chapters are presented here briefly comparing the results of electrochemical sensors to other analytical methods.

8.3.1 Electrochemical Detection of Polyphenols

Phenols, widely used in industry, represent one of the most common organic water pollutants, being extremely toxic even at low concentrations. It is worth mentioning that phenol is relevant in environmental research, because it has been chosen frequently as a model pollutant and many data are available on its removal from wastewater treatments.[17] Besides being toxic, phenol is also a refractory compound, its removal from wastewater being difficult.[18]

Among the carbon-based electrodes, used to replace the mercury electrode, modification of the electrode surface to improve its performance was made by the addition of carbon nanotubes, magnetic or metallic nanoparticles, thin films, etc. The literature reports the use of biosensors incorporating tyrosinase (polyphenol oxidase) for the detection of phenols in aqueous and in organic medium.[19]

Organic phase enzyme electrodes (OPEEs) have attracted considerable interest for their applications in environmental and clinical monitoring. The use of organic solvents facilitates, indeed, the detection of compounds poorly soluble in water, prevents microbial contamination, and may circumvent side reactions leading to enzyme deactivation or electrode fouling. Among the various enzymes successfully applied to the fabrication of OPEEs, polyphenol oxidase (PPO) was widely used because Kazandjian and Klibanov demonstrated, 30 years ago, the possibility for this enzyme to work in chloroform.[20] Thanks to its excellent activity in both aqueous and organic solvents, this enzyme which catalyzes the oxidation of phenols and *o*-diphenols to *o*-quinone constitutes a convenient enzyme model for the concept and the development of new procedures of OPEE construction.

Cristea et al.[19] developed an amperometric biosensor using a hydrophilic polypyrrole film electrogenerated from a new bispyrrolic derivative containing a long hydrophilic spacer in which the polyphenol oxidase was entrapped. The amperometric detection of catechol was carried out in anhydrous chloroform at −0.2 V versus Ag/AgCl. Owing to its cross-linking structure and its partially hydrophilic character, the polymer film constitutes an attractive host matrix for biosensor construction. The immobilization of PPO was performed by electropolymerization of a monomer/enzyme mixture deposited on a glassy carbon electrode surface following the "adsorption step procedure." For this purpose, a controlled potential of 0.8 V versus Ag/AgCl was applied at glassy carbon electrodes, modified by PPO-monomer coatings, with different ratios of enzyme/monomer. The electroanalytical parameters of the biosensor strongly depended on its configuration and on the hydration state of the enzyme matrix. Nevertheless, it should be noted that this optimized biosensor sensitivity (15.6 mA/M cm^2) remained lower than those previously reported for PPO electrodes based on sol–gel or organohydrogel composites (27.5–785 mA/M cm^2) and also exhibited broader linearity ranges.[19]

Compared to solid electrodes (like glassy carbon or other carbon-based materials) the screen-printed electrode (SPE)-based electrochemical biosensors appear to be an attractive and suitable option for more sensitive and selective determinations of phenolic compounds. Enzymes have been widely used in the preparation of biosensors for the determination of phenol derivatives and have allowed the measurement to be performed at a low operation potential to significantly reduce interference.

In the construction of a biosensor one of the most important aspects that affect the performances of enzymatic biosensors is the effective immobilization of the enzyme on the electrode surface. Hence, most research in this area has focused on the development of approaches that retain the biochemical activity of an enzyme while minimizing denaturation of the enzyme and its leakage into solution. One approach is to immobilize the enzyme through the entrapment method. As immobilizing agents, polyazetidineprepolymer (PAP) and polyvinyl alcohol photopolymer have been successfully used to immobilize enzymes on the surface of SPEs. The efficiency of the constructed SPEs was confirmed by Fusco et al. by using them successfully for phenolic analysis.[21–23] Electrodeposition is another simple method to immobilize an enzyme onto an electrode surface. The detection of phenol using SPEs modified with MWCNTs without their entrapment in a polymeric film or any other matrix was achieved through the electrodeposition of PPO with the addition of a Bi^{3+} precursor onto the electrode.[24] Other research reported a biosensor for the detection of 1,2-diaminobenzene (DAB) by electropolymerization of PPO, DAB, and a mediator complex on a screen-printed Pt electrode.[25] The analytical results for DAB demonstrated that the mediator-modified enzymes showed improved electron-transfer rates compared to that of the native enzyme. Recently, other efficient immobilization techniques have been developed. The combination of magnetic nanoparticles with bioimmobilization, separation, and detection could provide unique capabilities and improve the performances of the biosensors. Magnetic nickel or gold nanoparticles were used as an immobilization

platform to construct disposable biosensors with the highest performance for the determination of bisphenol A. A comparison between biosensors based on Fe_3O_4 and AuNPs was made by Alkasir et al.[26] Other simple and versatile noncovalent methods through supermolecular interactions that could also be used to construct biosensors are presented in an interesting review by Li et al.[27]

Enzyme-based biosensors have been used also for the detection of phenolic estrogens. The detection principle was based on the ability of tyrosinase to catalyze the oxidation of phenolic estrogens to *o*-diphenol and *o*-quinone. Using this principle tyrosinase-carbon paste electrodes have been used for the detection of phenol, catechol, bisphenol A, genistein, quercetin, nonylphenol, and diethylstilbestrol with detection levels in the micromolar range.[11] Optical and amperometric biosensors based on estrogen receptors have also been developed.

Polychlorinated biphenyls (PCBs) are related to immunological abnormalities, reproductive dysfunction, increased thyroid volume, and liver and thyroid disorders, interfering with the endogenous hormone systems and referred to as endocrine-disrupting chemicals. Immunosensors for the detection of PCBs were constructed by immobilizing an anti-PCB antibody within a conducting polymer matrix. The specific binding between PCB and its antibody was monitored electrochemically down to ng ml^{-1} levels. Biosensors for PCBs and for aromatic amines using DNA have also been constructed. In this case, the analytical signal is represented by the reduction of the anodic peak of guanine in the presence of increasing concentrations of the organic compounds.[28,29]

Nitrophenols, commonly used in the manufacture of wood preservatives, explosives, pesticides, dyes, plasticizers, and pharmaceuticals, are toxic and biorefractory compounds, and are classified as priority pollutants, dangerous for the environment, both in the USA, in UESEPA list, and in EU countries. *p*-Nitrophenol (PNP) is used in the manufacture of acetaminophen, one of the most popular analgesics, pesticides, and dyes, but is a carcinogen, mutagen, and cyto- and embryotoxic compound, which led the European Commission to set for it a limit of 0.1 ppb in drinking water. In order to detect selectively, sensitively, and rapidly this compound in the field, whole-cell biosensors were developed using different bacteria.[30] *Moraxella* sp. is able to specifically degrade PNP to hydroquinone, a more electroactive compound than PNP, so a microbial biosensor for PNP was constructed. By using a modified carbon paste electrode with *Moraxella* sp. the electrochemical oxidation current of phenol to hydroquinone was measured and directly correlated to the concentration of *p*-nitrophenol. In another microbial biosensor, the authors took advantage of the fact that *Moraxella* sp. consumes oxygen to oxidize *p*-nitrophenol to hydroquinone. So, by measuring the oxygen concentration with a Clark oxygen electrode the *p*-nitrophenol concentration was estimated.[31] Similar biosensors were fabricated with *Arthrobacter* sp.[32,33]

A very difficult process is the treatment of water contaminated with *p*-nitrophenols. The presence of the nitro group in their structure gives them a strong chemical stability and resistance to microbial degradation. Therefore, reducing the concentration of these compounds in wastewater by adsorption is an environmentally important task besides their detection. Activated carbons are effective adsorbents for

the organic compounds[34]; however, they are expensive and hardly recyclable. There are of low cost and widely available adsorbents, such as zeolites, biosorbents, and clays that are in trend in this field of research. Recent studies suggest that modified clays are effective adsorbents for phenolic compounds and nitrophenolic derivatives.[35] The work of Tertiş et al. presents a combined procedure of the electrochemical reduction with the adsorption on active carbon (A + R), with the goal to reduce the concentrations of 4-NP and 2,6-DNP from synthetic solutions, and to find if there are some improvements by using this combined procedure instead of simple procedures (electrochemical reduction (R) or adsorption on active carbon (A)).[36,37]

8.3.2 Electrochemical Detection of Pesticides

A pesticide is any substance used to kill, repel, or control certain forms of plant or animal life that are considered to be pests. Due to their toxicity, pesticides, especially organophosphate pesticides (OPs), can lead to cholinergic dysfunction, which affects the health of both humans and animals. Because of their extensive use in agriculture, human beings are exposed daily to low levels of pesticide residues through their food, and because of the pesticides used in a variety of settings including homes, schools, hospitals, and workplaces an uncertainty still remains regarding possible health effects related to this long-term and low-level exposure. Over 98 % of sprayed insecticides and 95 % of herbicides reach a destination other than their target species. As a result, the development of new analytical methods for the determination of these compounds in a wide variety of samples is currently a high-interest research area.

Monitoring the amount of pesticides in water and soil is an effective way to detect the abuse of pesticides in agriculture. Because pesticides can inhibit the activity of many enzymes, such as acetylcholinesterase (AChE), butyrylcholinesterase (BChE), organophosphate hydrolase (OPH), and tyrosinase (Tyr), various inhibition biosensor systems emerged in recent years as promising alternatives for in situ detection of pesticides.[26] Modern methods for the detection of pesticides usually involve liquid or gas chromatography coupled to mass spectrometric detection (HPLC–MS, GC–MS), requiring an appropriate sample preparation (as seen in Table 8.1). However, optical and electrochemical detection methods were also developed for this purpose.

Neurotoxic organophosphorus (OP) compounds are commonly used as pesticides. Due to their high toxicity, rapid and sensitive field detection of these compounds has developed fast. Biosensors made with organophosphate hydrolase are generally designed to detect amperometrically the electroactive group produced after the enzymatic cleavage, or to detect potentiometrically the pH change that occurs during the cleavage. Sahin et al. developed a new amperometric dual-enzyme electrochemical assay that enabled the detection of a broad class of OP compounds using the enzyme OPH combined with horseradish peroxidase (HRP). The assay was applied to the detection of dichlofenthion, which does not yield an

electroactive product and is not a commonly investigated OPH substrate. After optimization of the pH of the solution, the analytical characteristics of the dual enzyme were found to be limit of detection (LOD) 24 μM (7.6 ppm) and sensitivity 0.095 ± 0.024 nA/μM for dichlorofenthion.[38]

8.3.3 *Electrochemical Detection of Polycyclic Aromatic Hydrocarbons (PAHs)*

Polycyclic aromatic hydrocarbons (PAHs) are a class of over several hundred individual compounds defined to be composed of two or more fused aromatic rings. PAHs are classified as probable human carcinogen and show carcinogenic activity and endocrine disrupting activity in mammals. The incomplete combustion of organic materials and the atmospheric photochemical reactions of PAHs lead to the formation of many kinds of substituted PAHs, such as nitrated PAHs (NPAHs), hydroxylated PAHs (OH-PAHs), and amino-PAHs (APAHs). Diesel and petrol engines, industrial processes, coal combustion, and cigarette smoke are sources of PAHs and their derivatives, but they have also been found in carbon black and photocopier toners, fly ash, and exhaust emissions from waste incineration plants. Automobiles are also a source of atmospheric PAHs and NPAHs. PAHs and their derivatives need to be monitored in time, which is necessary to assess the quality of air and to spot the source of pollutants.[39]

In addition to the frequency with which PAHs occur in the environment, proof of their mutagenicity and carcinogenicity led to some of them being selected as priority pollutants (e.g., 16 PAHs) by the US Environmental Protection Agency (EPA). The World Health Organization (WHO) added 17 more making a total of 33 PAHs under its regulation.[39]

Sensitive, rapid, simple, and accurate analytical methods have been developed to determine PAHs and their derivatives in the atmospheric particles. Extensively used are GC and coupled methods like GC-FTD, GC-MS, and HPLC-FL as highly efficient separation tools have been used for analyzing all kinds of samples.[40] The direct determination of traces of PAHs and their derivatives by modem chromatographic techniques is still difficult. There are some limitations associated with the insufficient sensitivity of these techniques and also problems related to matrix interference. For instance in the case of samples of atmospheric particulates, extraction methods of PAHs and their derivatives include traditional Soxhlet extraction, ultrasonic extraction, supercritical fluid extraction, microwave-assisted extraction, and accelerated solvent extraction.[40]

The compounds containing five or more aromatic rings are known as “heavy” PAHs, whereas those containing less than five rings are named “light” PAHs. It is now known that heavy PAHs are more stable and toxic than the other group.[41] Another example of possible PAH contamination in food is due to traffic, i.e., crops or livestock close to urban roads could be exposed to PAHs and nitro-PAHs

(derivates from PAHs). Other food products, such as seafood and fish, can be exposed to PAHs present in water and sediments and the PAH content depends on the ability of the aquatic organisms to metabolize them (e.g., bivalve mollusks accumulate more PAHs than vertebrate fish, which metabolize these compounds very rapidly).[39]

The electrochemical oxidation behavior and the oxidation mechanism for 1-hydroxypyrene (1-OHP) were investigated at a disposable SPE.[42]

PAHs are always found as a mixture of individual compounds with similar molecular structure, similar electron density, and a lack of side groups. Therefore, an immunosensor based on SPEs was developed for PAH detection using a co-exposure competition assay. The immunosensor displayed cross-reactivities of varying degrees towards 16 important PAH compounds.[43]

8.3.4 Electrochemical Detection of Heavy Metals

Heavy metals have been persistently monitored all over the world because of their toxicity, even at low concentrations. Therefore, simple and inexpensive sensing devices are needed for in situ monitoring. Common toxic metal ions, such as Pb(II), Cd(II), Hg(II), and As(III), are especially important because they are neurotoxic (e.g., Pb(II) and Hg(II)), easily absorbed by the human body, and accumulate in the environment and in living organisms. Elements as lead, cadmium, and mercury are not biodegradable, and hence can accumulate in the environment, which results in contaminated food and water. Therefore, the World Health Organization (WHO) and the Environmental Protection Agency (EPA) have strictly defined the concentration limits of these metal ions that are allowed in drinking water.[3]

Historically, electrochemical stripping analysis, commonly using anodic stripping voltammetry (ASV), has been widely recognized as a powerful technique for heavy-metal detection because of the simplicity of the instrument as well as its moderate cost and portability. Moreover, the ASV technique combined with SPEs can handle all scenarios that require rapid, inexpensive, sensitive, and accurate determination in the field of environmental monitoring. Most studies of heavy-metal determination using SPEs show that mercury, gold, silver, bismuth, or other materials that modify the surface of SPEs can improve selectivity or sensitivity.[11]

Being easily automatable, electrochemical flow detection has been used in many fields of research, like environmental and agricultural monitoring, and food and health control. Flow systems are particularly advantageous in stripping voltammetric analysis since they enhance the mass transport, improving the preconcentration step. There is an interest for graphite felt electrodes for application in flow electroanalysis, this material having a high surface area (616 cm^2 cm^{-3}) and a good conductivity and presenting good hydrodynamic properties.[44,45] Using the unmodified or modified graphite felt as a working electrode, copper(II) and zinc (II), two cations essentials for the homeostasis of the human body, but both toxic if found in excess, were detected in food supplements[46,47] and tap water.[46] A special flow electrochemical cell was designed for this purpose (Fig. 8.2).

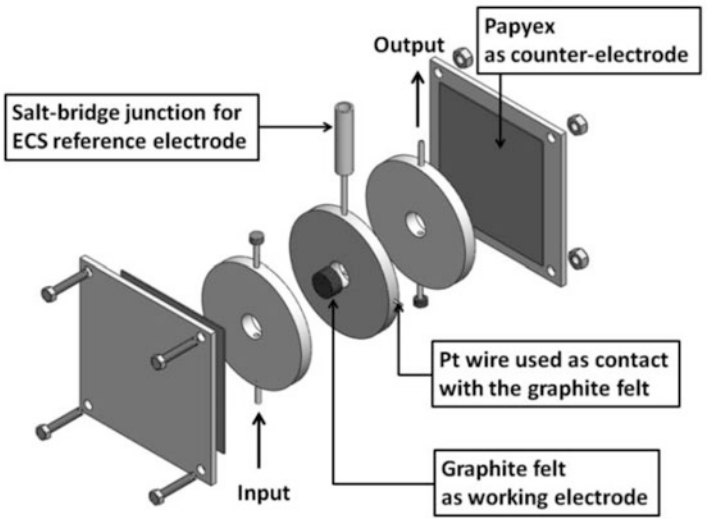

Fig. 8.2 SolidWorks image of the electrochemical flow cell[46]

8.3.5 Pharmaceuticals

Categorized as emerging organic pollutants, pharmaceuticals and personal-care products have been the focus of global environmental researchers' attention since the late 1990s. Pharmaceuticals have caused concerns due to their extensive human and veterinary consumption, excretion or washing off their hosts after their intended usages, and their entry into the environment through effluents of wastewater treatment plants, as well as surface-water runoffs and soil leaching after agricultural applications of manure or treated sludge. As pharmaceuticals were designed to correct, enhance, or protect a specific physiological or endocrine condition, their target effects in humans and/or farm stocks are well understood and documented. However, there is limited knowledge about their unintended effects in the environment. Sample preparation followed by GC or HPLC separation, and qualitative and quantitative analysis using detectors, has become the standard approach for detection of pharmaceuticals in environmental matrices.[48]

Due to the fact that for the moment there are no regulations regarding the loading of pharmaceuticals in water, air, or soil and the accumulation of pharmaceuticals in living organisms that induce toxic effects, there are only some recommendations made by scientists.[49–51]

The literature data present some examples of sensors for the detection of several antibiotics and antihypertensive and anti-inflammatory drugs currently used in urban areas. The detection of antibiotic residues in environmental samples through the use of various disposable electrochemical sensors has proved the capacity of these sensors for fast, low-cost, and sensitive detection. Tetracyclines, as an important class of antibiotics, were investigated on gold SPEs using cyclic voltammetry

and flow injection analysis.[52] Another sensor employing a screen-printed eight-electrode-based immunoarray for the detection of sulfonamide antibiotics was developed using magnetic beads as a solid phase, which allowed the rapid extraction of sulfonamides in complex matrices.[53] The combination of the antibody-based assays, magnetic bead separation, and screen-printed array transduction is an attractive aspect of this research that has the potential to be used in the development of a high sample throughput screening system.

Steroid hormone drugs and their (semi)synthetic analogues manufactured from steroids of plant origin or by total synthesis are among the most important groups of drug materials. Steroid hormones like estradiol, estrone, estriol, progesterone, testosterone, and hydrocortisone are present in the human and animal organism. Electroanalytical methods have never played an important role in determination of steroid hormones even though they are used in important quantities as such or in combination with other active compounds for topic use (antibiotics mainly). These methods are still considered as nonselective and non-stable indicating methods.[54] Few studies used mercury as dropping[55] or hanging[56] electrodes. The voltammetric determination of finasteride in tablets and the assay of danazol in capsules by square-wave adsorptive stripping voltammetry were already reported. A modern approach is the development of drug-selective electrodes, e.g., a modified carbon paste-based electrode for the selective potentiometric determination of estradiol valerate in formulations.[57]

Seventeen different therapeutic classes of pharmaceuticals were detected in raw urban wastewater and effluents from an activated sludge system after a usual treatment adopted for urban wastewaters worldwide prior to final discharge into surface water bodies.[58]

This analysis showed that the highest amounts discharged into the effluent were represented by one antihypertensive, several beta-blockers, and analgesics/anti-inflammatory agents, while the highest risk was posed by antibiotics and several psychiatric and analgesics/anti-inflammatory drugs.

8.4 Other Sensor Methods and Non-sensor Laboratory Methods

A short comparison with other sensor methods (optical sensors, surface plasmon resonance) and non-sensor laboratory methods (high-performance gas and liquid chromatography, capillary electrophoresis, AAS, mass spectrometry, etc.) is made below.

8.4.1 Optical Sensors

An optical sensor is a device that converts light rays into electronic signals. Optical sensors have many applications in environmental control, national defense, and commercial markets such as medical diagnostics and process control. Because of the various fields of applications for optical sensors the challenges to the design and to optimization of an optical sensor for a particular use require knowledge of optical, material, and environmental properties that affect sensor performance. The wavelength range of the optical signal, the interaction between electromagnetic radiation and target, the effect of the medium on the propagation of the light, methods to enhance the optical signal, and materials used to generate, focus, and collect optical radiation are all important aspects of optical sensors.

Environmental analysis represents a challenge for optical sensors. Usually the matrices to be analyzed are complex, so the sensors need to be specific for one substance or a class of substances. In order to increase the selectivity, an optical immunosensor system consisting of a disposable low-cost sensor chip including a fluidic system and a base unit for the optical readout was developed by Meusel et al.[59] Near-infrared (NIR)-fluorescence markers (Cy5) were excited by an evanescent wave generated on the surface of the sensor chip. The combination of both fluorescence measurements and evanescent wave excitation provides extremely sensitive detection. The assay was applied to determine the herbicide 2,4-dichlorophenoxyacetic acid (2,4-D) in the relevant concentration range. Within an assay time of 15 min only, the analyte 2,4-D could be determined in a linear concentration range covering three orders of magnitude.[59]

Another example is an optical sensor for Zn(II) detection developed by incorporating 4-(2-pyridylazo)resorcinol (PAR) in a sol–gel thin film. The sensor was coupled to a multicommutated flow system and applied to the direct determination of Zn(II) in injectable insulins. Optical transduction was based on the use of a dual-color LED and a photodiode. The sensor showed optimum response at pH 5.5 with maximum absorbance at 500 nm. A linear response was obtained for Zn(II) in the concentration range of 5.0–25.0 μg l^{-1}, with a limit of detection of 2.0 μg l^{-1} and a sampling frequency of 16 samples h^{-1}.[60]

The surface-enhanced Raman spectroscopic (SERS) effect, even though discovered in the late 1970s, has received an increased interest only in the last few years. Extensive research efforts have been devoted to the investigation and determination of the sources of enhancement. The experimental observations related to SERS, and the origins of the enormous Raman enhancement, are believed to be the result of several mechanisms. It has been shown that electromagnetic interactions between the molecule and the substrate provide the dominant enhancement in the SERS process. These electromagnetic interactions are divided into two major classes: (a) interactions that occur only in the presence of a radiation field and (b) interactions that occur even without a radiation field.[61]

This technique has been applied for the detection of heavy metals,[62] PAH,[63] viruses,[64] and PCBs.[65]

8.4.2 Surface Plasmon Resonance (SRP) Sensors

Optical immunosensors (including fiber-optic and evanescent wave biosensors) are based on the measurement of the absorption or emission of light by the immunoreactants. The interactions between light and immunoreactants can be measured as changes in absorbance, luminescence, polarization, or refractive index. SPR is one of the most attractive optical-signal transducers, which allows real-time monitoring of biochemical interactions without the need for labeling the reagents. The most notable attraction in SPR-based sensors is the highly specific detection of small molecules with extraordinarily low detection limits for a wide variety of analytes in complex matrices.

SPR is a surface-sensitive optical technique for monitoring biomolecular interactions occurring in the very close vicinity of a transducer (gold) surface, and that has given it a great potential for studying surface-confined affinity interactions without rinsing out unreacted agents or reactants in excess in sample solutions. Ever since its introduction in the early 1990s, SPR plays a central role in the research of biomaterial characterization, kinetics of antibody–analyte interactions leading to ligand-fishing, drug discovery, and the detection of a variety of chemical and biological substances.[66]

Several examples of SPR sensors applied in the detection of environmental samples are presented below. A simple and versatile miniaturized surface plasmon resonance (SPR) immunosensor enabling parallel analysis of multiple analytes or multiple samples of an analyte was investigated for the detection of a low-molecular-weight (lmw) toxin, 2,4-dichlorophenoxyacetic acid (2,4-D). A specially designed multi-microchannel SPR sensor module, integrating an optical-prism coated with an array of thin Au films, a multi-microchannel plate (eight channels), and a flow cell, was fabricated. The sensing surface was generated simply by physical adsorption of a protein conjugate of 2,4-D, and an indirect competitive immunoassay principle was applied for the quantification of 2,4-D. Multiple 2,4-D samples were analyzed in a single step and a low detection limit of 0.1 ppb 2,4-D was established. The competence of the portable SPR immunosensor for selective detection of 2,4-D despite the presence of various structurally resembling interferents was demonstrated in river water. The independent all-in-one sensor module highly favored shelf-storage between multiple determinations, and reusability of the same multi-microchannel flow module for more than 35 days with intermittent storage (4–8 °C) was confirmed. The LOD of 2,4-D could be enhanced further by introducing a simple avidin–biotin interaction-based sandwich immunoassay, with which the sensor signal was multiplied by a factor of ca. 10 with a detection limit of 0.008 ppb. The miniature SPR sensor used for simultaneous analysis of multiple samples with good reusability and storage ability was an important impact on the advancement of biosensor technology.[67]

A portable SPR optical biosensor device was described as a direct immunosensing system for the determination of organic pollutants in natural water samples by Mauriz et al.[68] The investigated compounds were organochlorine

(DDT), organophosphorus (chlorpyrifos), and carbamate (carbaryl) pesticides. The lowest limit of detection (LOD) was obtained for DDT with 20 ng l^{-1}, while 50 ng l^{-1} and 0.9 μg l^{-1} were achieved for chlorpyrifos and carbaryl, respectively. Matrix effects were evaluated for the carbaryl immunoassay in different water types with detection limits within the range of carbaryl standards in distilled water (0.9–1.4 μg l^{-1}). This portable SPR-sensor system is already a product on the market, commercialized by the company SENSIA, SL (Spain). The size and the electronic configuration of the device allow its portability and utilization at contaminated locations.[68]

Another SPR-based immunosensor for DDT, its metabolites, and analogues in real water samples was developed by Mauriz et al.[69] Low limits of detection (LODs), in the sub-nanogram per liter range, were attained for DDT-selective (15 ng l^{-1}) and DDT group-selective immunoassays (31 ng l^{-1}). The SPR analysis of DDT proved to be three times more sensitive than colorimetric ELISAs without the need of labeling combined with a much shorter time of response. This SPR biosensor portable platform (β-SPR) is also commercialized by the SENSIA company.

Another portable SPR immunosensor designed for on-site determination of low-molecular-weight compounds by immunosensing was developed with the dimensions of 16 cm × 9 cm × 6 cm with four sensing microchannels. Highly sensitive and selective analysis of benzo[a]pyrene and 2-hydroxybiphenyl was realized by using an indirect competitive immunoreaction based on SPR detection. The sensitivity of the compact, portable SPR sensor to ppb levels of the two compounds was equivalent to that obtained with a conventional SPR apparatus.[70]

8.4.3 Chromatographic and Other Spectral Methods

Besides sensors, other analytical methods involved in environmental analyses are chromatography and spectral methods. Using the two most common techniques for analyzing drugs in environmental samples, gas and liquid chromatography coupled with mass spectrometry or tandem mass spectrometry (GC–MS, GC–MS/MS and LC–MS, LC–MS/MS), the presence of several drugs was investigated in environmental samples (β-blockers and β-agonists, drugs commonly found in the environment) by Caban et al.[71] All the results confirmed that GC–MS analyses are much less sensitive to the complexity of sample matrices than LC–MS, so GC–MS measurements appear to be a very good alternative to LC–MS methods for determining pharmaceutical residues in environmental samples.

A group of nine specific pharmaceuticals from aqueous environmental samples (flubendazole, propiconazole, pipamperone, cinnarizine, ketoconazole, miconazole, rabeprazole, itraconazole and domperidone) was also analyzed with LC–ESI/MS/MS by Van De Steene et al.[72]

A synoptic table with other analytical techniques used in environmental analysis is presented in Table 8.1.

8.5 Future Aspects

There are several electrochemical sensors, biosensors, and immunosensors employed in environmental analysis even though they are limited in solving all the environmental needs. Recent trends in this field involve the use of arrays in monitoring a wide range of inorganic and organic pollutants, of other biological recognition materials, innovations in the microelectronic industry, and of micro- and disposable sensors.

Online and flow-injection systems have also been adapted for the monitoring of several pollutants. Recent developments in nanomaterials area also improved the characteristic of the sensors.

As seen in Fig. 8.3, the research in the field of electrochemistry is focused on the development of new electrode materials in order to improve the performances of the electrodes, on the miniaturization of the electrodes in order to make them more portable and more suitable for incorporation in online and microfluidics systems, and on the development of new types of biosensors, more specific, more stable, better fitted for real samples.

Another way to increase sensor specificity is offered by antibodies used as biological recognition element, but they have also some limitations due to the complexity of the assay that must be developed for each analyte. The development of sensor arrays to create multianalyte detection systems could be interesting not only in environmental but also in diagnostic and therapy monitoring.

The immobilization of receptors is a crucial step in the development of biosensors including methods like entrapment in conductive polymeric films, clays, sol–gel, or hydrogel matrices increasing their mechanical stability and resistance to a wide range of chemicals and thermal shocks. The electrochemical transducers can be planar or three dimensional involving electrodes that could be printed on inert support (to form a disposable electrochemical cell) or expanded in a special design flow cell (e.g., modified graphite felt). Microsized electrodes can also be grouped in microarrays.

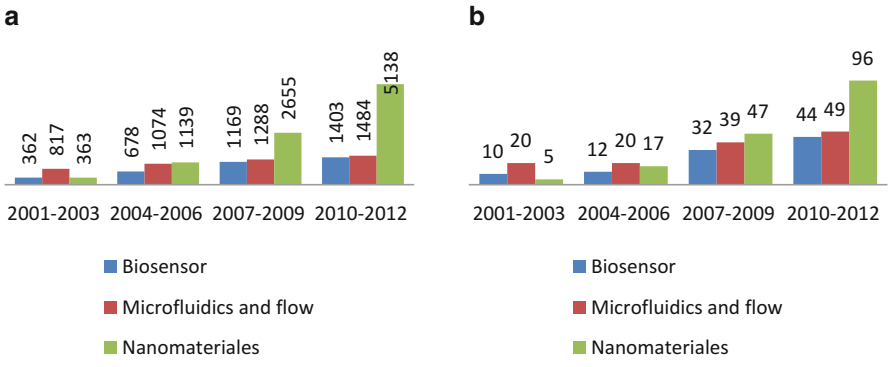

Fig. 8.3 Articles published on ScienceDirect in the field of electroanalysis with reference to general (**a**) and to environmental analysis (**b**)

A wide range of cell-based biosensors (with bacteria, yeast, algae, and tissue culture cells) were reported also in the literature for potential environmental applications. Genetically modified microorganisms capable to detect the presence of toxic metals like lead, mercury or zinc, chlorinated compounds, organic peroxides, nitrate, or ammonia were used in the development of biosensors.

Other interests in the field of new sensors for environmental analysis are the development of electronic nose and tongue.

Electronic noses (e-noses) and *electronic tongues* are devices already used in pharmaceutical formulations, in different areas of food industry (oil, tee, wine, dairy discrimination taste or smells), as well as in medicine. Applications in the field of environmental analysis start to emerge.

Electronic tongue systems for remote environmental monitoring applications have been presented in several applications. A new approach in the chemical sensor field consists in the use of an array of nonspecific sensors coupled with a multivariate calibration tool which may form a node of a sensor network. The proposed arrays were made up of potentiometric sensors based on polymeric membranes, and the subsequent cross-response processing was based on a multilayer artificial neural network model as proposed by Mimendia et al.[73] who described environmental monitoring of ammonium as a pollutant plus alkaline ions at different measuring sites in the states of Mexico and Hidalgo (Mexico), and monitoring of heavy metals (Cu^{2+}, Pb^{2+}, Zn^{2+}, and Cd^{2+}) in open-air waste streams and rivers.

Another example presents the first study and development of an electronic tongue analytical system for the monitoring of stable species of nitrogen compounds: nitrate, nitrite, and ammonium in water. The electronic tongue was composed of an array of 15 potentiometric poly(vinyl chloride) membrane sensors sensitive to cations and anions plus an artificial neural network (ANN) response model. The building of the ANN model was performed in a medium containing sodium, potassium, and chloride as interfering ions, thus simulating real environmental conditions.[74] Different types of electronic tongues were described and evaluated for monitoring purposes by Krants-Rulcker et al.[75] More specifically, the performance of multielectrode arrays used for voltammetric analysis of aqueous samples was described by showing how an "electronic tongue" could be used to monitor the quality of water in a production plant for drinking water. It was pointed out that the concepts of "electronic noses" and "electronic tongues" often predict a quality of a sample rather than giving exact information about concentrations of individual species.

Polypyrrole (PPy)-based electronic noses (ENs) for the determination of some toxic and nontoxic substances, such as ammonia, nitrogen oxides, carbon monoxide, sulfur dioxide, hydrogen sulfide, methane, oxygen, hydrogen, alcohols, phenol, benzene, and water vapors were successfully applied to samples ranging from water and beverages to wastewaters and sewage effluents.[76]

In this light, future advances in the field of electroanalysis with impact on environmental analysis and on pollution control should focus on the development of specific and stable recognition elements, portable devices, microarrays, miniaturization of commercially available sensors, use of nanotechnologies in the

fabrication of the sensors, smart sensors connected to users through friendly interfaces, etc. The current technologies offer the premises for a rapid development of this field.

References

1. Corsini E, Sokooti M, Galli CL, Moretto A, Colosio C (2013) Pesticide induced immunotoxicity in humans: a comprehensive review of the existing evidence. Toxicology 307:123–135
2. Ahamed M, Siddiqui MKJ (2007) Low level lead exposure and oxidative stress: current opinions. Clin Chim Acta 383:57–64
3. World Health Organisation (2011) Guidelines for drinking-water quality, 4th edn. http://whqlibdoc.who.int/publications/2011/9789241548151_eng.pdf
4. World Health Organisation (2012) Pharmaceuticals in drinking-water. http://whqlibdoc.who.int/publications/2012/9789241502085_eng.pdf
5. World Health Organisation (2012) Tackling antibiotic resistance from a food safety perspective in Europe. http://www.euro.who.int/__data/assets/pdf_file/0005/136454/e94889.pdf
6. Shannon MW, Borron SW, Burns MJ (2007) Haddad and Winchester's clinical management of poisoning and drug overdose, 4th edn. Saunders, An imprint of Elsevier, Philadelphia, PA
7. Flomenbaum NE, Howland MA, Goldfrank LR, Lewin NA, Hoffman RS, Nelson LS (2006) Goldfrank's toxicologic emergencies, 8th edn. McGraw-Hill, New York, NY
8. Dart RC (ed) (2004) Medical toxicology. Lippincott Williams & Wilkins, Philadelphia, PA
9. Hulanicki A, Glab S, Ingman F (1991) Chemical sensors. Definitions and classification. Pure & Appl Chem 63:1247–1250
10. Brett CMA (2001) Electrochemical sensors for environmental monitoring. Strategy and examples. Pure & Appl Chem 73:1969–1977
11. Wanekaya AK, Chenb W, Mulchandani A (2008) Recent biosensing developments in environmental security. J Environ Monit 10:703–712
12. Wang J (1995) Electrochemical sensors for environmental monitoring: a review of recent technology. http://www.clu-in.org/download/char/sensr_ec.pdf
13. Nikolelis DP, Krull UJ, Wang J, Mascini M (eds) (1997) Biosensors for direct monitoring of environmental pollutants in field. Kluwer Academic Publishers, Dordrecht
14. Castillo J, Gáspár S, Leth S, Niculescu M, Mortari A, Bon□idean I, Soukharev V, Dorneanu SA, Ryabov AD, Csöregi E (2004) Biosensors for life quality: design, development and applications. Sens Actuators B:Chem 102:179–194
15. Chaubey A, Malhotra BD (2002) Mediated biosensors. Biosens Bioelectron 17:441–456
16. Llorent-Martinez EJ, Ortega-Barrales P, Fernandez-de Cordova ML, Ruiz-Medina A (2011) Trends in flow-based analytical methods applied to pesticide detection: a review. Anal Chim Acta 684:30–39
17. Busca G, Berardinellia S, Resinia C, Arrighi L (2008) Technologies for the removal of phenol from fluid streams: a short review of recent developments. J Hazard Mater 160:265–288
18. Bajaj M, Gallert C, Winter J (2008) Biodegradation of high phenol containing synthetic wastewater by an aerobic fixed bed reactor. Biores Tech 99:8376–8381
19. Cristea C, Mousty C, Cosnier S, Popescu IC (2005) Organic phase PPO biosensor based on hydrophilic films of electropolymerized polypyrrole. Electrochim Acta 50:3713–3718
20. Kazandjian RZ, Klibanov AM (1985) Regioselective oxidation of phenols catalyzed by polyphenol oxidase in chloroform. J Am Chem Soc 107:5448–5450
21. Fusco MD, Tortolini C, Deriu D, Mazzei F (2010) Laccase-based biosensor for the determination of polyphenol index in wine. Talanta 81:235–240

22. Tortolini C, Fusco MD, Frasconi M, Favero G, Mazzei F (2010) Laccase-polyazetidine prepolymer-MWCNT integrated system: biochemical properties and application to analytical determinations in real samples. Microchem J 96:301–307
23. Ibarra-Escutia P, Gomez JJ, Calas-Blanchard C, Marty JL, Ramirez-Silva MT (2010) Amperometric biosensor based on a high resolution photopolymer deposited onto a screen-printed electrode for phenolic compounds monitoring in tea infusions. Talanta 81:1636–1642
24. Merkoci A, Anik U, Cevik S, Cubukcu M, Guix M (2010) Bismuth film combined with screen-printed electrode as biosensing platform for phenol detection. Electroanalysis 22:1429–1436
25. Akyilmaz E, Kozgus O, Türkmen H, Cetinkaya B (2010) A mediated polyphenol oxidase biosensor immobilized by electropolymerization of 1,2-diamino benzene. Bioelectrochemistry 78:135–140
26. Alkasir RSJ, Ganesana M, Won YH, Stanciu L, Andreescu S (2010) Enzyme functionalized nanoparticles for electrochemical biosensors: a comparative study with applications for the detection of bisphenol A. Biosens Bioelectron 26:43–49
27. Li M, Li YT, Li DW, Long YT (2012) Recent developments and applications of screen-printed electrodes in environmental assays - a review. Anal Chim Acta 734:31–44
28. Centi S, Marrazza G, Mascini M (2007) Procedure 25PCB analysis using immunosensors based on magnetic beads and carbon screen-printed electrodes in marine sediment and soil samples. Comprehensive Anal Chem 49:179–184
29. Centi S, Marrazza G, Mascini M (2007) Coupling of screen-printed electrodes and magnetic beads for rapid and sensitive immunodetection: polychlorinated biphenyls analysis in environmental samples. Comprehensive Anal Chem 49:585–602
30. Mulchandani P, Hangarter CM, Lei Y, Chen W, Mulchandani A (2005) Amperometric microbial biosensor for p-nitrophenol using *Moraxella* sp.-modified carbon paste electrode. Biosens Bioelectron 21:523–527
31. Mulchandani P, Lei Y, Chen W, Wang J, Mulchandani A (2002) Microbial biosensor for *p*-nitrophenol using *Moraxella* sp. Anal Chim Acta 470:79–86
32. Lei Y, Mulchandani P, Chen W, Wang J, Mulchandani A (2004) *Arthrobacter* sp. JS443 based whole cell amperometric biosensor for p-nitrophenol. Electroanalysis 16:2030–2034
33. Lei Y, Mulchandani P, Chen W, Wang J, Mulchandani A (2003) A Microbial biosensor for p-nitrophenol using *Arthrobacter* sp. Electroanalysis 15:1160–1164
34. Tertiş MC, Jitaru M, Ionescu F (2009) Equilibrium study on adsorption processes of 4-nitrophenol and 2,6-dinitrophenol onto granular activated carbon. Studia Univ Babes-Bolyai, Chemia 54:213–222
35. Tchieda VK, Tonle YK, Tertis MC, Ngameni E, Jitaru M (2010) Adsorption of 2,4 dinitrophenol and 2,6 dinitrophenol onto organoclays and inorganic-organic pillared clays. Environ Eng Manag J 9:953–960
36. Tertiş MC, Jitaru M, Silaghi-Dumitrescu L (2010) Combined procedure for nitrophenols removal. Rev Chimie (Bucharest) 61:360–363
37. Tertiş MC, Jitaru M, Coman V, Filip M, Lowy DA (2009) Electrochemical reduction-adsorption procedure for the removal of nitrophenol contaminants from aqueous media. Studia Univ Babes-Bolyai, Chemia (Special issue 1):151–162
38. Sahin A, Dooley K, Cropek DM, West AC, Banta S (2011) A dual enzyme electrochemical assay for the detection of organophosphorus compounds using organophosphorus hydrolase and horseradish peroxidase. Sens Actuators B:Chem 158:353–360
39. Pandey SK, Kim KH, Brown RJC (2011) A review of techniques for the determination of polycyclic aromatic hydrocarbons in air. Trends in Analytical Chemistry 30:1716–1739
40. Liu L, Liu Y, Lin J, Tang N, Hayakawa K, Maeda T (2007) Development of analytical methods for polycyclic aromatic hydrocarbons (PAHs) in airborne particulates: a review. J Environ Sci 19:1–11
41. Plaza Bolaños P, Garrido Frenich A, Martinez Vidal JL (2010) Polycyclic aromatic hydrocarbons in food and beverages. Analytical methods and trends. J Chromatogr A 1217:6303–6326

42. Honeychurch KC, Hart JP, Kirsch N (2004) Voltammetric, chromatographic and mass spectral elucidation of the redox reactions of 1-hydroxypyrene occurring at a screen-printed carbon electrode. Electrochim Acta 49:1141–1149
43. Fahnrich KA, Pravda M, Guilbault GG (2003) Disposable amperometric immunosensor for the detection of polycyclic aromatic hydrocarbons (PAHs) using screen-printed electrodes. Biosens Bioelectron 18:73–82
44. Nasraoui R, Floner D, Paul-Roth C, Geneste F (2010) Flow electroanalytical system based on cyclam-modified graphite felt electrodes for lead detection. J Electroanal Chem 638:9–14
45. Nasraoui R, Floner D, Geneste F (2010) Improvement in performance of a flow electrochemical sensor by using carbamoyl-arms polyazamacrocycle for the preconcentration of lead ions onto the electrode. Electrochem Commun 12:98–100
46. Feier B, Floner D, Cristea C, Bodoki E, Sandulescu R, Geneste F (2012) Flow electrochemical analyses of zinc by stripping voltammetry on graphite felt electrode. Talanta 98:152–156
47. Feier B, Floner D, Cristea C, Sandulescu R, Geneste F (2013) Development of a novel flow sensor for copper trace analysis by electrochemical reduction of 4-methoxybenzene diazonium salt. Electrochem Commun 31:13–15
48. Hao C, Zhao X, Yang P (2007) GC-MS and HPLC-MS analysis of bioactive pharmaceuticals and personal-care products in environmental matrices. Trends in Analytical Chemistry 26:569–580
49. Mompelat S, Le Bot B, Thomas O (2009) Occurrence and fate of pharmaceutical products and by-products, from resource to drinking water. Environ Int 35:803–814
50. Santos LHMLM, Araujo AN, Fachini A, Pena A, Delerue-Matos C, Montenegro MCBSM (2010) Ecotoxicological aspects related to the presence of pharmaceuticals in the aquatic environment. J Hazard Mater 175:45–95
51. Kummerer K (2009) The presence of pharmaceuticals in the environment due to human use – present knowledge and future challenges. J Environ Manag 90:2354–2366
52. Masawat P, Slater JM (2007) The determination of tetracycline residues in food using a disposable screen-printed gold electrode (SPGE). Sens Actuators B:Chem 124:127–132
53. Centi S, Stoica AI, Laschi S, Mascini M (2010) Development of an electrochemical immunoassay based on the use of an eight-electrodes screen-printed array coupled with magnetic beads for the detection of antimicrobial sulfonamides in honey. Electroanalysis 22:1881–1888
54. Görög S (2011) Advances in the analysis of steroid hormone drugs in pharmaceuticals and environmental samples (2004-2010). J Pharm Biomed Anal 55:728–743
55. Alvarez-Lueje A, Brain-Isasi S, Nuñez-Vergara LJ, Squella JA (2008) Voltammetric reduction of finasteride at mercury electrode and its determination in tablets. Talanta 75:691–696
56. Alghamdi AH, Belal FF, Al-Omar MA (2006) Square-wave adsorptive stripping voltammetric determination of danazol in capsules. J Pharm Biomed Anal 41:989–993
57. Batista IV, Lanza MRV, Dias ILT, Tanaka SMCN, Tanaka AA, Sotomayor MDPT (2008) Electrochemical sensor highly selective for estradiol valerate determination based on a modified carbon paste with iron tetrapyridinoporphyrazine. Analyst 133:1692–1699
58. Verlicchi P, Al Aukidy M, Zambello E (2012) Occurrence of pharmaceutical compounds in urban wastewater: removal, mass load and environmental risk after a secondary treatment - a review. Sci Total Environ 429:123–155
59. Meusel M, Trau D, Katerkamp A, Meier F, Polzius R, Cammann K (1998) New ways in bioanalysis – one-way optical sensor chip for environmental analysis. Sens Actuators B:Chem 51:249–255
60. Jerónimo PCA, Araújo AN, Montenegro MCBSM (2004) Development of a sol-gel optical sensor for analysis of zinc in pharmaceuticals. Sens Actuators B:Chem 103:169–177
61. Vo-Dinh T (1995) SERS chemical sensors and biosensors: new tools for environmental and biological analysis. Sens Actuators B:Chem 29:183–189
62. Eshkeiti A, Narakathu BB, Reddy ASG, Moorthi A, Atashbar MZ, Rebrosova E, Rebros M, Joyce M (2012) Detection of heavy metal compounds using a novel inkjet printed surface enhanced Raman spectroscopy (SERS) substrate. Sens Actuators B:Chem 171–172:705–711

63. Péron O, Rinnert E, Lehaitre M, Crassous P, Compère C (2009) Detection of polycyclic aromatic hydrocarbon (PAH) compounds in artificial sea-water using surface enhanced Raman scattering (SERS). Talanta 79:199–204
64. Ravindranath SP, Wang Y, Irudayaraj J (2011) SERS driven cross-platform based multiplex pathogen detection. Sens Actuators B:Chem 152:183–190
65. Yuan J, Lai Y, Duan J, Zhao Q, Zhan J (2012) Synthesis of a β-cyclodextrin-modified Ag film by the galvanic displacement on copper foil for SERS detection of PCBs. J Coll Interface Sci 365:122–126
66. Shankaran DR, Gobi KV, Miura N (2007) Recent advancements in surface plasmon resonance immunosensors detection of small molecules of biomedical, food and environmental interest. Sens Actuators B:Chem 121:158–177
67. Kim SJ, Gobi V, Iwasaka H, Tanaka H, Miura N (2007) Novel miniature SPR immunosensor equipped with all-in-one multi-microchannel sensor chip for detecting low-molecular-weight analytes. Biosens Bioelectronics 23:701–707
68. Mauriz E, Calle A, Montoya A, Lechuga LM (2006) Determination of environmental organic pollutants with a portable optical immunosensor. Talanta 69:359–364
69. Mauriz E, Calle A, Manclús JJ, Montoya A, Hildebrandt A, Barceló D, Lechuga LM (2007) Optical immunosensor for fast and sensitive detection of DDT and related compounds in river water samples. Biosens Bioelectronics 22:1410–1418
70. Kawazumi H, Gobi KV, Ogino K, Maeda H, Miura N (2005) Compact surface plasmon resonance (SPR) immunosensor using multichannel for simultaneous detection of small molecule compounds. Sens Actuators B:Chem 108:791–796
71. Caban M, Migowska N, Stepnowski P, Kwiatkowski M, Kumirska J (2012) Matrix effects and recovery calculations in analyses of pharmaceuticals based on the determination of β-blockers and β-agonists in environmental samples. J Chromatogr A 1258:117–127
72. Van De Steene JC, Mortier KA, Lambert WE (2006) Tackling matrix effects during development of a liquid chromatographic-electrospray ionization tandem mass spectrometric analysis of nine basic pharmaceuticals in aqueous environmental samples. J Chromatogr A 1123:71–81
73. Mimendia A, Gutiérrez JM, Leija L, Hernández PR, Favari L, Muñoz R, del Valle M (2010) A review of the use of the potentiometric electronic tongue in the monitoring of environmental systems. Environ Model Software 25:1023–103
74. Nuñez L, Cetó X, Pividori MI, Zanoni MVB, del Valle M (2013) Development and application of an electronic tongue for detection and monitoring of nitrate, nitrite and ammonium levels in waters. Microchem J 110:273–279
75. Krantz-Rülcker C, Stenberg M, Winquist F, Lundström I (2001) Electronic tongues for environmental monitoring based on sensor arrays and pattern recognition: a review. Anal Chim Acta 426:217–226
76. Ameer Q, Adeloju SB (2005) Polypyrrole-based electronic noses for environmental and industrial analysis. Sens Actuators B:Chem 106:541–552

Chapter 9
Potentiometric Sensors

Eric Bakker

9.1 Introduction

In environmental analysis, potentiometry is important for the detection of redox potential and as an analytical tool for the measurement of a variety of ionic and ionizable species. In both cases, the open circuit potential of a two-electrode cell is observed where an inert metal electrode or an ion-selective electrode (also called indicator electrode) is measured against a suitable reference electrode.

In both cases, the response is dependent on the activity, a, which is related to molar concentration, c, by the activity coefficient, f, as follows:

$$a_j = f_j c_j \tag{9.1}$$

Note that single ion activity coefficients cannot be rigorously assessed experimentally. Potentiometric measurements in cells without liquid junctions where a cation-selective indicator electrodes is measured against an anion-selective electrode gives information on the mean activity coefficient:

$$\log f_{\pm} = \frac{|z_-|}{|z_+| + |z_-|}\log f_+ + \frac{|z_+|}{|z_+| + |z_-|}\log f_- \tag{9.2}$$

For ionic species, the mean activity coefficient is a function of the ionic strength of the solution, which is determined from all molar cation and anion concentrations as follows:

E. Bakker (✉)
Department of Inorganic and Analytical Chemistry, University of Geneva,
Quai E.-Ansermet 30, 1211 Geneva, Switzerland
e-mail: eric.bakker@unige.ch

L.M. Moretto, K. Kalcher (eds.), *Environmental Analysis by Electrochemical Sensors and Biosensors*, DOI 10.1007/978-1-4939-0676-5_9

$$I = \frac{1}{2}\sum_j {z_j}^2 c_j \tag{9.3}$$

where z_j is the charge of each ion that is summed. A 0.10 M $CaCl_2$ solution, for example, has an ionic strength of $0.5 \times (2^2 \times 0.10\ \text{M} + (-1)^2 \times 0.20\ \text{M}) = 0.30\ \text{M}$. The activity coefficient is a measure of the interionic interactions of ions in an electrolyte and can be reasonably well predicted for dilute solutions with the Debye–Hückel theory and its modifications. Activity coefficients tend to decrease with increasing ionic strength in solutions of practical relevance in environmental analysis (typically up to 1 M).

Mean activity coefficients may be described on the basis of the extended Debye–Hückel theory by a semiempirical relationship such as[1]:

$$\log f_\pm = -\frac{A\left|z_+ z_-\right|\sqrt{I}}{1 + B\sqrt{I}} + CI \tag{9.4}$$

where A is a constant (A = 0.5108) that is a function of temperature in Kelvin ($A \propto T^{-3/2}$). This relationship uses just two fittable parameters, $B(\propto T^{-1/2})$ and C (with an unspecified dependence on temperature). Depending on the electrolyte in question, this equation is reasonably adequate for ionic strengths up to 1 M by using published values for B and C.[1]

Splitting the mean activity coefficient into the relevant single ion activity coefficients requires the use of an appropriate convention. Complex conventions such as that based on the hydration theory of Stokes, Robinson, and Bates are more precise for fundamental studies. However, routine analytical applications may be better served by the simplified Debye–Hückel convention, which is formulated quite naturally as[2]:

$$\log f_+ = \left|\frac{z_+}{z_-}\right| \log f_\pm \tag{9.5}$$

$$\log f_- = \left|\frac{z_-}{z_+}\right| \log f_\pm \tag{9.6}$$

Consequently, for a given ionic strength and nature of electrolyte single ion activity coefficients for most situations of practical relevance may be estimated with reasonable precision (Fig. 9.1).

In potentiometric analysis, the indicator electrode is intrinsically responsive to single ion activities. It is the potential at the reference electrode that introduces a non-thermodynamic assumption (liquid junction potential) to the measurements. This term can be kept small and corrected by calculation if needed. In pH measurements, one uses the practical determination of pH, which uses the output of a calibrated combination pH electrode (normally with the bridge electrolyte at the reference electrode containing 3 M KCl) as the accepted pH value of the solution. In essence, any uncertainty in potential arising at the reference electrode is ascribed to

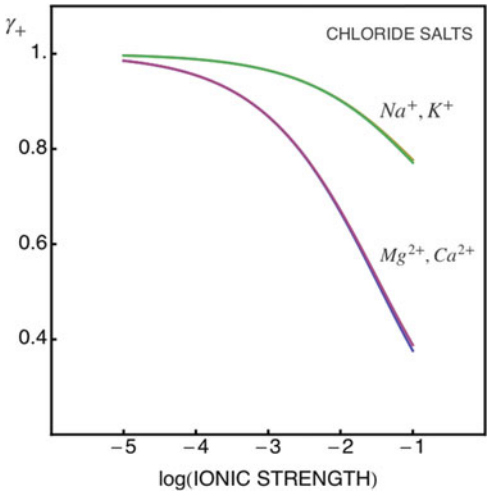

Fig. 9.1 Shows calculated single ion activity coefficients (γ) for the common cations sodium, potassium, magnesium, and calcium as their chloride salts as a function of solution ionic strength

the pH readout. While this not strictly thermodynamically correct, the typical error in solutions of moderate pH amounts to ca. 2 mV (0.03 pH units) and allows one to properly trace measurements with standard procedures. On the other hand, measurements of other ions are traditionally reported in terms of ion activity or molar ion concentration. For these purposes, one either calculates and corrects for liquid junction potentials arising at the reference electrode, calibrates in solutions of similar background electrolyte, or employs a dilution step with a total ionic strength adjustment buffer (TISAB) before measurement. The latter two steps can also be used to minimize uncertainties in activity coefficients.

In the following, we will more closely examine the detection of redox potential before focusing this book chapter on the principles of potentiometric ion sensors.

9.1.1 Measurement of Redox Potential

The detection of redox potential of a solution is important in environmental analysis to judge the redox state of the system so that one can predict the possible direction of oxidation–reduction reactions. Electron acceptors such as oxygen, nitrate and sulfate are consumed by the biological oxygen demand of organic carbon. Chemical reduction can occur indirectly by the chemical reduction of oxidized pollutants via formation of hydrogen. Direct chemical oxidation of organics are possible via Fe (O) oxidation/reduction reactions.[3]

The detection of potentiometric redox potential involves the use of an inert electrode such as platinum that is measured against a suitable reference electrode. Since the measurement is carried out under zero current conditions, the rate of oxidation and reduction at the electrode must be identical. The current amplitude of

the cathodic and anodic component of this process is also called the exchange current and is written as i_0:

$$i_0 = \left|i_{cathodic}\right| = \left|i_{anodic}\right| \tag{9.7}$$

Potentiometric measurement of the redox potential is therefore only meaningful if the solution contains a redox couple that gives rise to a reversible exchange current density at the inert electrode surface. Unfortunately, this is not always the case in environmental systems where electron transfer reactions are often sluggish or irreversible. A key challenge in this regard is the heterogeneous nature of the electron transfer reaction in potentiometry, which does not adequately reflect the homogeneous reaction conditions often found in natural waters. For electron transfer to occur at an inert metal electrode such as platinum, an activation barrier must be overcome that depends on the reaction of interest. Recent work has aimed at reducing such barriers by the use of modified electrode materials, for example a mixture of different nanoparticle coatings on the electrode surface.[4] Other researchers have made use of molecular mediators that more closely mimic the reactivity in natural waters.[5] Clearly, the determination of redox potential by potentiometry is not always straightforward and the observed values do not necessarily reflect the desired reactivity of the system.

For systems containing a reversible redox couple, one can relate the observed potential to activities by the Nernst equation for redox reactions. The half-reaction is always written as a reduction, as in:

$$Fe^{3+} + e \rightarrow Fe^{2+} \tag{9.8}$$

So that we can arrive at the Nernst equation as follows:

$$E = E^0_{Fe^{3+}/Fe^{2+}} - \frac{RT}{F}\ln\frac{a_{Fe^{2+}}}{a_{Fe^{3+}}} \tag{9.9}$$

An environmentally relevant half reaction for the reduction of iron(III) is:

$$Fe(OH)_3 + 3H^+ + e \rightarrow Fe^{2+} + 3H_2O \tag{9.10}$$

In which case the Nernst equation is written as

$$E = E^{0'}_{Fe(OH)_3/Fe^{2+}} - \frac{RT}{nF}\ln\frac{c_{Fe^{2+}}}{c_{Fe(OH)_3}\left(c_{H^+}\right)^3} \tag{9.11}$$

where n is the number of electrons transferred in Eq. (9.10), which is here $n = 1$. For this example, we have written the potential as a function of concentrations instead of activities, in which case the formal potential $E^{0'}$ value must be used. Note that the potential E corresponds to the one at the inert indicator electrode, which is not

identical to the observed cell potential since there are other potential contributions to the measurement, in particular at the reference electrode. Since for historical reasons, all half reactions are referenced to the hydrogen ion/hydrogen gas couple (standard conditions, 1 M of $a_{H}{}^{+}$ and 1 bar of P_{H2}), the potential at the reference electrode must be corrected to that of the standard hydrogen electrode with established values (see below). An inconvenience of this historical approach is that the hydrogen ion/hydrogen gas couple is not necessarily the optimum reference to judge the direction of a reaction in natural waters. Consequently, a positive reduction potential does not mean that the environment is oxidizing (it wants be reduced itself), but that the reaction as written would be spontaneous if the oxidation would involve the conversion of hydrogen gas to hydrogen ions at a pH of 0 and at atmospheric pressure.

As well known, there exists an equivalence between electrode potentials and the Gibb's free energy of reaction:

$$\Delta G = -nFE \tag{9.12}$$

In which case a negative free energy, as with positive potentials, means that the reaction is spontaneous as written. As above, one again needs to be aware that any half reaction written as in Eq. (9.10) is referenced to the hydrogen standard half reaction, which is not directly translatable to an environmental system. To do this, one needs to identify the potential of the relevant half reaction (as for the solute we intend to study the reactivity of) and correct the values accordingly.

9.1.2 The Nernst Equation for Ion-Selective Electrodes

Ion-selective electrodes (ISEs) are measured under zero current conditions in a two-electrode setup, see Fig. 9.2. The indicator electrode (ion-selective electrode) is treated as the cathode, while the reference electrode acts as the anode.

The potential difference measured between the indicator and reference electrode at zero current is also called the electromotive force and is the sum of all potential differences in the cell as schematically shown in Fig. 9.3. One aims to keep all potentials independent of the sample composition with the exception of the potential at the interface between sample and membrane.

Under ideal conditions, the potential change at the ISE membrane is proportional to the change in the logarithmic ion activity, see Fig. 9.4. This ideal relationship is known as the Nernst Equation for ion-selective electrodes, which is written for the electrochemical cell as

$$E_I = K_I + E_J + \frac{RT}{z_I F} \ln a_I \tag{9.13}$$

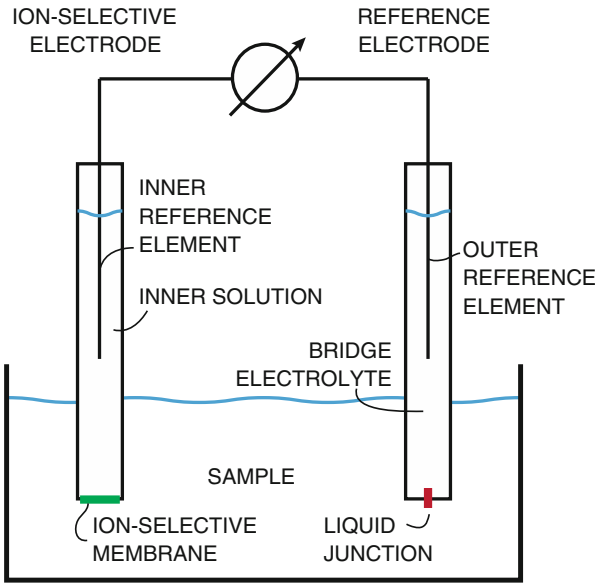

Fig. 9.2 Two-electrode electrochemical cell used for potentiometry with ion-selective electrodes

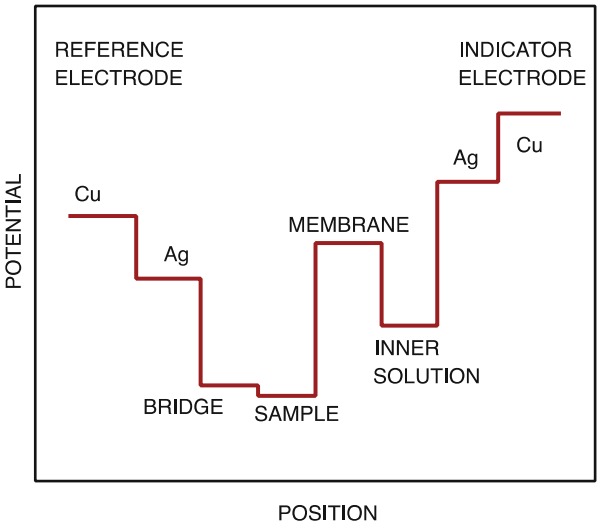

Fig. 9.3 The observed cell potential is the sum of all potential changes in the cell. All but the one at the sample–membrane phase boundary are ideally independent of sample composition

where R is the universal gas constant, T the absolute temperature, F the Faraday constant, z_I the charge of the primary ion I^zI, K_I is an experimentally determined constant potential value, and E_J is the liquid junction potential at the reference electrode (between sample and bridge electrolyte). At room temperature (298 K), Eq. (9.13) can be rewritten in simplified form to:

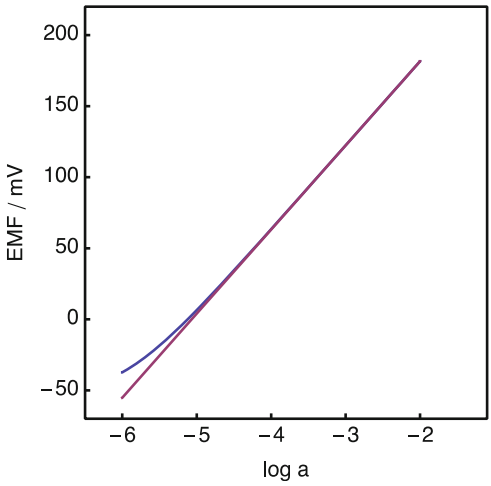

Fig. 9.4 The observed potential at zero current ideally depends on the logarithmic sample ion activity in a linear fashion, described by the Nernst equation (9.13) for ion-selective electrodes (*red trace*). *Blue trace*: behavior of a real electrode, giving deviations near the detection limit

$$E_I = K_I + E_J + \frac{s}{z_I} \log a_I \tag{9.14}$$

where s is the Nernstian slope of 59.18 mV, which is divided by the charge of the primary ion as shown. For this slope to be observed, the membrane must be ideally permselective to the primary ion and the potential at the reference electrode must be indifferent to sample composition changes. This is only approximately achieved because the liquid junction potential at the reference electrode, E_J, introduces an extra-thermodynamic assumption to the measurement.[2] Unlike the discussion on redox potential above, we are here not concerned with absolute potentials and we simply aim for K_I in Eq. (9.14) to be indifferent of the sample composition.

In practice, ISEs may obey this equation when the ion-selective membrane interacts reversibly with the specific ion of interest. Moreover, this partitioning process should have no substantial effect on the chemical composition of the ion-selective membrane[6]: a_I in the membrane must remain constant to observe a Nernstian response. A silver chloride-based membrane, for example, exhibits a Nernstian slope to chloride ion activity only if the membrane surface is unaltered by other, less soluble halides. Other membrane materials behave in analogous manner.

The sensitivity of potentiometry as analytical technique is mainly dependent on the charge z of the analyte. For monovalent or divalent cations, for example, a tenfold concentration change will give +59.2 mV or +29.6 mV change in the observed potential. Anionic analytes have negative z values and will give negative potential changes. Figure 9.4 shows a typical calibration curve for a monovalent ion-selective electrode.

ISEs assess free, and not total ion concentrations/activities. This experimental distinction between free and complexed forms of the analyte makes them very useful, e.g., for bioavailability and speciation studies.

In routine blood analysis of electrolytes, where ion-selective electrodes are used nearly universally, very small concentration changes are sometimes determined with direct potentiometry. This requires potential stabilities and reproducibilities on the order of 10–100 μV, which is achieved in temperature controlled flow-through cells and with frequent, automated recalibrations between measurements.[7] In batch mode benchtop analyses with ISEs and in environmental monitoring applications,[8] such a high precision is often not achieved. Precision and accuracy is mainly limited by variations in the liquid junction potential between the calibration and sample phases and by interferences from other sample ions, temperature fluctuations, and, if concentrations rather than activities are desired, variations in activity coefficients.

Such possible experimental biases can be minimized in benchtop analysis by adding an ionic strength adjusting solution to the sample prior to measurement. Of course, ion-selective electrodes are also routinely integrated into automatic titration instruments where they make up very convenient endpoint indicators. In these cases, the accuracy and precision of the cell potential readings influences the accuracy of the analytical measurement to a much smaller extent than in direct potentiometry.

9.1.3 Modes of Measurement

Information on the sample composition is obtained by a number of different measurement protocols.[9]

9.1.3.1 Direct Potentiometry

In direct potentiometry, the observed potential E_I is related to the primary ion activity in the sample with the Nernst equation:

$$a_I = 10^{(E_I - K_I)z_I/s} \tag{9.15}$$

The electrode slope s and the constant potential term K_I are determined by calibration.

This protocol is the most rapid and yields information on the ion activity, which is relevant to ecotoxicology and reactivity. Excellent precision is achieved by one point calibration after each measurement point and by careful temperature control, and is routinely used in controlled environments such as clinical analysis.

9.1.3.2 Standard Addition After Ionic Strength Adjustment

In standard addition potentiometry, the sample is diluted with a total ionic strength adjusting buffer (abbreviated as TISAB). This brings about a known electrolyte background to the sample, and hence keeping activity coefficients in the sample constant. It also reduces changes in the liquid junction potential at the reference electrode. Known increments of ion standard are added to the sample and the potential changes are used to determine the original ion concentration.

This method is advisable if ion concentrations, rather than activities, are to be determined and if the sample matrix is of unknown or variable composition.

9.1.3.3 Endpoint Detection

An ion-selective electrode can be used as an endpoint detector in a volumetric titration and may give precise results on the concentration of titrated analyte. With good selectivity and measuring range, the ISE response may reflect the entire change in logarithmic ion activity in the course of the titration. If so, it can also be used to obtain thermodynamic characteristics of the analyte, such as binding constants with the titrant. This approach is routinely used in the determination of sample acidity and alkalinity as well as water hardness.

9.1.4 Selectivity and Detection Limit

If a sample contains other ions of the same charge sign of the primary ion (analyte ion), they may displace the primary ion from the ion-selective membrane. If this occurs, a deviation from the Nernst equation is observed. For interfering ions of the same charge as the primary ion, an expanded Nernst equation may be used to describe this behavior:

$$E = K_I + \frac{s}{z_I} \log \left(a_I + \sum_{j \neq I} K_{I,j}^{pot} a_j \right) \tag{9.16}$$

where $K_{I,j}^{pot}$ is the selectivity coefficient. This equation is known as the *Nicolsky equation*, after Boris P. Nicolsky (1900–1990) who developed this equation for glass electrodes. The selectivity coefficient shown in Eq. (9.16), $K_{I,j}^{pot}$, is effectively a weighting factor for any interfering ion activity, a_j. Figure 9.5 illustrates the expected calibration curve of a primary ion for membranes of variable selectivity. Smaller selectivity coefficients and more dilute interfering ions give lower levels of interference and hence lower detection limits.

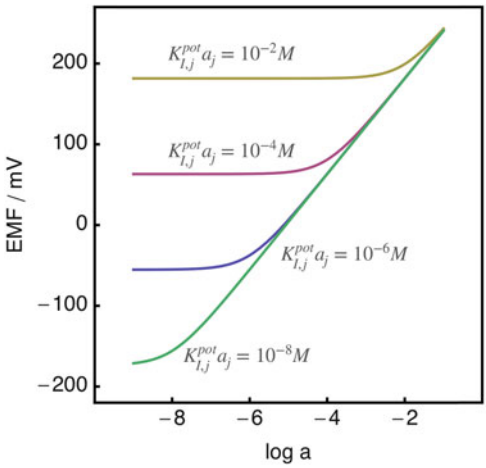

Fig. 9.5 The level of interference increases with increasing value of the selectivity coefficient, see Eq. (9.16)

If the primary and interfering ions have different charges, expanded equations must be used to describe the potential change.

The previously accepted the so-called *Nicolsky–Eisenman* equation, written as

$$E = K_I + \frac{s}{z_I}\log\left(a_I + \sum_{j\neq I} K^{pot}_{I,j} a_j^{z_I/z_j}\right) \tag{9.17}$$

has been shown to give inconsistent results with errors of up to 8 mV (0.14 logarithmic concentration units) and should not be used to describe the mixed ion response if high accuracy is desired.[2,6] Instead, for any combination of monovalent and divalent ions in the sample, the following modified equation has instead been established:

$$E = K_I + \frac{s}{z_I}\log\left[\frac{1}{2}\sum_{j(z_J=1)}\left(K^{pot}_{Ij}\right)^{1/z_I} a_j + \sqrt{\left(\frac{1}{2}\sum_{j(z_J=1)}\left(K^{pot}_{Ij}\right)^{1/z_I} a_j\right)^2 + \sum_{j(z_J=2)}\left(K^{pot}_{Ij}\right)^{2/z_I} a_j}\right] \tag{9.18}$$

The summations are grouped according to the charge of each ion and include the primary ion (for which case $K_{\mathrm{I,I}}{}^{\mathrm{pot}} = 1$).

As Fig. 9.6 illustrates for the case of a monovalent primary and divalent interfering ion, Eq. (9.17) predicts a stronger level of interference in mixed solutions than the self-consistent equation (9.18).

Equation (9.18) may be used to predict the experimental error originating from competing interfering ions. For the example shown in Fig. 9.6 one obtains the anticipated error as shown in Fig. 9.7. The graph shows that reliable measurements must be performed well above the detection limit.

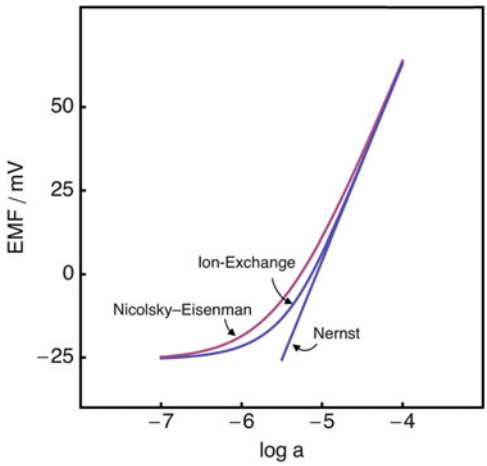

Fig. 9.6 Potentiometric responses in mixed solutions (here for a monovalent cation as primary ion and a divalent ion as interfering background) may be described with Eq. (9.18). The previously used semiempirical Nicolsky–Eisenman Eq. (9.17) is only an approximation

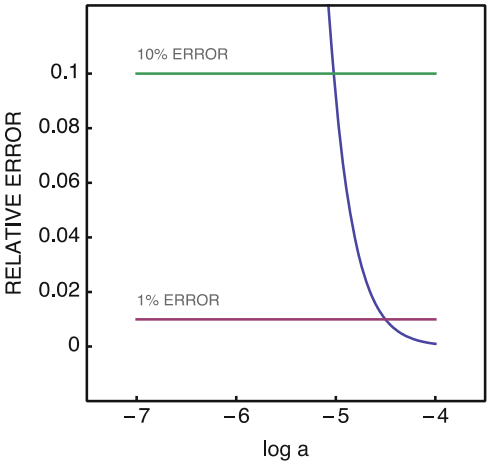

Fig. 9.7 Anticipated relative error of the data shown in Fig. 9.6, calculated from Eq. (9.18). *Bottom line*: 1 % error. *Top line*: 10 % error mark

In potentiometry, the lower detection limit is defined as the intersection of the two extrapolated linear portions of the calibration curve, as illustrated in Fig. 9.8.

The lower detection limit may be understood as the point in the calibration curve where a substantial deviation from the Nernst slope is observed. If the calibration curve is accurately described with Eq. (9.16) or (9.18), and one type of interfering ion J^{zJ} dominates, the detection limit is given by:

$$a_I(LDL) = K_{I,j}^{pot} a_j^{z_I/z_j} \tag{9.19}$$

The power term of the interfering ion activity may be quite important and only give intuitive predicted detection limits for primary and interfering ions of the same

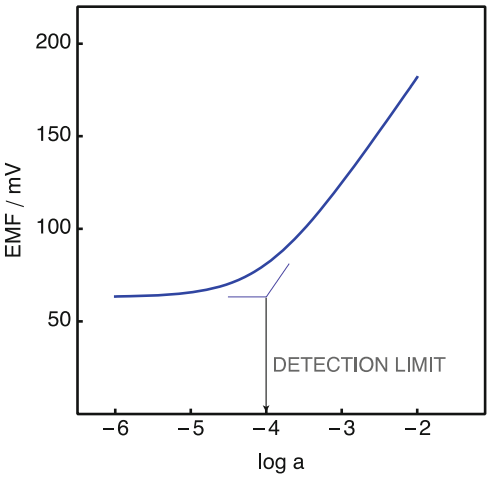

Fig. 9.8 In potentiometry, the detection limit is given as the intersection of the extrapolated linear sections of the calibration curve, in units of analyte activity. This definition differs from most other analytical methods that base the detection limit on a multiple of the background noise

charge. For example, if primary and interfering ions have the same charge, and the interfering ion level is at 1.0 mM, a selectivity coefficient of $\log K_{I,J}^{pot} = -3$ is required to reach a micromolar detection limit. On the other hand, a 1.0 mM calcium ion background as interfering ion would require a selectivity coefficient of $\log K_{I,Ca}^{pot} = -4.5$ in order to reach this micromolar detection for a monovalent primary ion. If sodium is the interference at the same millimolar level, one needs just $\log K_{Ca,Na}^{pot} = 0$ for the same detection limit.

As the detection limit anticipated on the basis of simple thermodynamic displacement (ion-exchange) becomes on the order of micromolar or lower, counterdiffusion ion fluxes may become important (see below for more detail). For a well conditioned membrane electrode with an optimized inner solution composition or a suitable solid contact material the following relationship may be used to estimate the kinetic detection limit if all ions are monovalent.[10]

$$c_I(LDL) = \left(q c_R^m \sum_{j \neq I} K_{I,j}^{pot} a_j \right)^{1/2} \tag{9.20}$$

where c_R^m is the molar ion-exchanger concentration in the membrane and the permeability ratio q (typically on the order of 10^{-3}) is given by:

$$q = \frac{D_m \delta_{aq}}{D_{aq} \delta_m} \tag{9.21}$$

where D and δ are the diffusion coefficient and diffusion layer thicknesses in the indicated phases.

9.1.5 Response Time of Potentiometric Sensors

If a planar ion-selective electrode responds in an ideal fashion to analyte concentration changes in the sample, the composition of the membrane phase remains unchanged. The response time for such membranes depends solely on the time required for the boundary concentrations in the diffusion layer to equilibrate with the sample bulk. An exact solution from diffusion equations is available; the following approximate equation is normally more convenient for practical use[11]:

$$E(t) = E(\infty) + \frac{RT}{z_j F} \ln \left\{ 1 - \left(1 - \frac{a_j^{aq}(0, t = 0)}{a_j^{aq*}} \right) \frac{4}{\pi} e^{-t/\tau'} \right\} \tag{9.22}$$

where the time constant τ' is given by:

$$\tau' = \frac{(\delta^{aq})^2}{2D_j^{aq}} \tag{9.23}$$

According to Eq. (9.22), the response time depends strongly on the diffusion layer thickness and is longer when going from a concentrated to a more dilute sample solution. This is illustrated in Fig. 9.9.

The response behavior can also be visualized by numerical simulation. For this purpose, the concentration at the membrane surface is treated as a reflection and the concentration at a fixed distance (diffusion layer thickness) is kept constant and equal to the concentration in the sample bulk. Figure 9.10 shows the simulated response times upon a tenfold concentration change in the sample bulk. As the gradients flatten with increasing amounts of time, the rate of equilibration of the surface concentration with the sample bulk slows with time. Since the potential is a

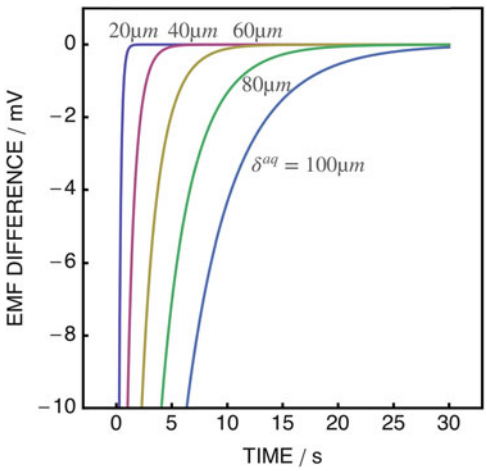

Fig. 9.9 Response time of an ideally responding ion-selective electrode (membrane concentration does not change) upon a tenfold concentration increase in the sample (monovalent ion, total potential change of 59.2 mV). Calculated according to Eq. (9.22) with $D_j^{aq} = 10^{-5} cm^2 s^{-1}$ and the indicated aqueous diffusion layer thicknesses

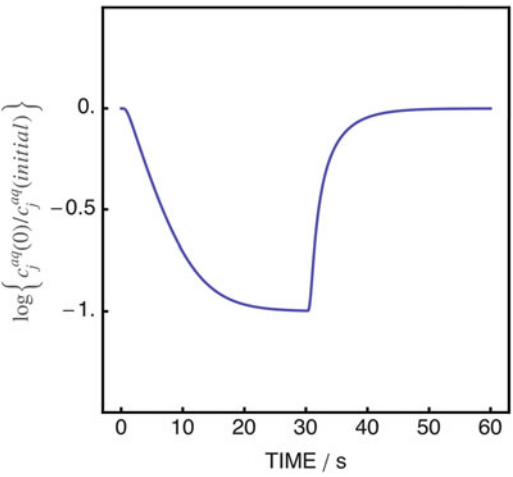

Fig. 9.10 Simulated logarithmic concentration changes at the electrode surface. The values on the y-axis are proportional to the open circuit potential (multiply by the Nernstian slope)

function of the logarithmic surface concentration, these small absolute concentration changes translate into relatively large potential changes. The response time is therefore comparatively long. For the change to higher concentrations, the logarithmic response function of the membrane electrode is less sensitive to small deviations at higher concentration, and the response time becomes faster than for the previous case, see Fig. 9.10.

9.2 Reference Electrodes and Liquid Junction Potentials

9.2.1 Reference Electrodes

For more than a century, the reference electrode in most electrochemical measurements has been composed of an electrode of the second kind in contact with a solution of defined electrolyte composition that is brought in contact with the sample solution of interest through a liquid junction. In cases where the reference electrolyte is chemically incompatible with the sample or may result in contamination, an intermediate salt bridge is placed between the reference electrolyte and the sample solution.

Established electrodes of the second kind include the silver/silver chloride element and the mercury/calomel element. Both require a defined chloride concentration in the contacting aqueous solution in order to give a stable potential at the reference electrode. The half reactions and associated reduction potentials are given as

$$AgCl(s) + e \rightarrow Ag(s) + Cl^{-}(aq) \tag{9.24}$$

with $E^0_{AgCl/Ag} = 0.222V$ and, in 3 M KCl, $E_{AgCl/Ag} = 0.210V$
and

$$\frac{1}{2}Hg_2Cl_2(s) + e \rightarrow Hg(l) + Cl^-(aq) \tag{9.25}$$

with $E^{0'}_{Hg_2Cl_2/Hg} = 0.280V$ and in saturated KCl at room temperature, the reduction potential is $E_{SCE} = 0.241V$.

An overwhelming number of ion-selective electrodes today use a Ag/AgCl element rather than a calomel element. This is mainly driven by the mandate to reduce the usage of mercury, but Ag/AgCl elements are also more suited for applications at higher temperatures.

The solubility of AgCl in 3 M KCl is not negligible (around 1 mM due to the formation of higher silver chloride complexes) and temperature dependent. Simple AgCl coated wire reference elements are therefore not suited for conditions where the electrode is exposed to high and varying temperatures. For that purpose, a cartridge design containing excess AgCl particles is preferred to achieve temperature stability.

With membrane electrodes, the backside of the membrane is typically an aqueous electrolyte in contact with the same type of reference element. The standard reduction potentials for the two elements are therefore the same and inconsequential to the overall measured potential. The cell potential is mainly dictated by the chloride activity in the two reference compartment, the membrane potential and the liquid junction potential.

In pH measurements, the liquid junction potential forms part of the practical definition of pH if a 3 M KCl bridge electrolyte is used. Simply defining the output of a calibrated pH measurement as the practical pH makes the measurements traceable, although substantial systematic deviations of up to 15 mV from the Nernst function can be observed in strongly acidic or basic solutions (see below).

With other ion-selective electrodes, the liquid junction potential can be estimated and corrected with the equations given below, the calibration can be performed in a similar electrolyte background, or the electrolyte background can be adjusted by adding a buffer electrolyte (TISAB). In some cases, a liquid junction is not necessary, such as with potentiometric gas sensing probes and in some dynamic electrochemistry approaches.

9.2.2 The Diffusion Potential

When an electrolyte assumes a concentration gradient, the anion may exhibit a different mobility (diffusion coefficient) than the cation. At zero current, however, the net transport rate of the two types of ions must be equal. This is accomplished by the buildup of a so-called diffusion potential. This potential accelerates through

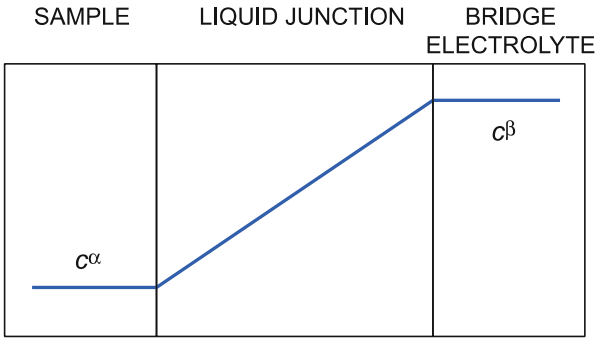

Fig. 9.11 Schematic presentation of a dilution junction. The same electrolyte is considered throughout the junction, but it is more concentrated in one compartment than in the other

electrical migration the slower ion and decelerates the faster one in order for both to attain the same rate of mass transport. If diffusion potentials are relevant, they form part of the overall cell potential. Diffusion potentials are especially important to understand with liquid junctions at reference electrodes. A bridge electrolyte is placed in contact with the sample solution by means of a porous liquid junction made of a chemically inert material without ion-exchanger properties (typically a ceramic frit, a capillary or a gel). In this contact zone, electrolyte concentration gradients will take place, hence resulting in a liquid junction potential that assures the deceleration of the faster diffusion ion and the acceleration of the slower one in order to arrive at an equal transport rate of both ions. We consider here first the dilution junction, in which an electrolyte encounters a concentration gradient. The same type of treatment is then expanded to two electrolyte solutions of any composition in contact with each other, resulting in the Henderson equation.

9.2.2.1 The Dilution Junction

The simplest case of a liquid junction consists of a single electrolyte at a different concentration in the sample solution and bridge electrolyte, see Fig. 9.11.

The potential change across this liquid junction can be directly obtained from the Nernst–Planck equation. The following equation describes the *dilution junction potential* as:

$$E_J = \frac{RT}{F}\frac{(D_M - D_A)}{(D_A + D_M)}\ln\frac{c^\beta}{c^\alpha} \tag{9.26}$$

where α marks the sample solution and β the bridge electrolyte, and D is the diffusion coefficient for the cation M and anion A as indicated. This equation may equally be given as a function ion mobilities u (for values see Table 9.1)[2]:

$$E_J = \frac{RT}{F}\frac{(u_M - u_A)}{(u_A + u_M)}\ln\frac{c^\beta}{c^\alpha} \tag{9.27}$$

Table 9.1 Single ion mobilities at infinite dilution in aqueous solutions at 25 °C [2]

Ion mobility	$u/10^{-4} cm^2 s^{-1} V^{-1}$
H^+	37.6
K^+	8.00
Na^+	5.47
Li^+	4.24
NH_4^+	8.00
Ag^+	6.82
Mg^{2+}	2.90
Ca^{2+}	3.22
Ba^{2+}	3.49
OH^-	20.6
Cl^-	8.11
I^-	8.16
NO_3^-	7.58
OAc^-	4.38
SO_4^{2-}	4.24

Table 9.2 Liquid junction potentials for selected electrolytes at tenfold concentration change across the junction, at 25 °C

Ion	E_J (mV) for $c^\beta/c^\alpha = 10$
HCl	−38.2
KCl	0.4
NaCl	11.5
LiCl	18.6
NH_4Cl	0.4
KOH	26.1
KI	0.6
KNO_3	−1.6
NaOH	34.3
NaOAc	−6.6
$LiNO_3$	16.7
LiOAc	1.0
$AgNO_3$	3.1

From Eq. (9.27) with mobility data from Table 9.1

This equation holds for any gradient across the junction and the concentration profiles do not have to be linear as shown in Fig. 9.11.

Table 9.1 shows typical values of ion mobilities[2] and Table 9.2 predicted liquid junction potentials for a tenfold concentration change across the dilution junction using this equation. Clearly, cations and anions of similar mobility predict the smallest junction potentials, with KCl, KNO_3 and LiOAc particularly attractive for practical use.

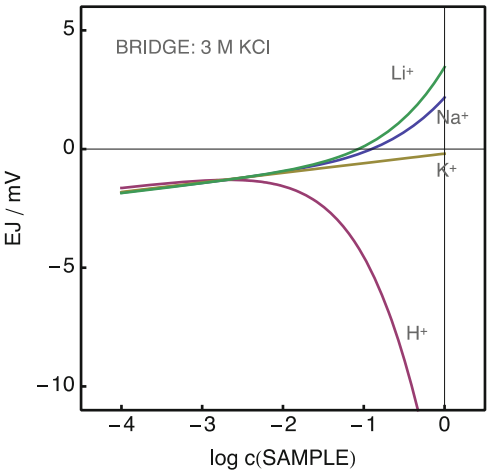

Fig. 9.12 Calculated liquid junction potentials according to the Henderson equation for a 3 M KCl bridge electrolyte and various sample concentrations. The counterion in the sample is chloride

9.2.2.2 The Henderson Equation

If one considers a sample solution and bridge electrolyte of any desired composition, one must make assumptions about the concentration gradient within the liquid junction in order to arrive at simplified expressions. While it is possible to numerically simulate these profiles on the basis of the Nernst–Planck equation,[12] for practical purposes it is perfectly acceptable to use the *Henderson equation* as approximation. It assumes linear concentration gradients across the junction and is written as:

$$E_J = \frac{\sum_j z_j u_j \left(c_j^{\beta} - c_j^{\alpha}\right)}{\sum_j u_j z_j^2 \left(c_j^{\beta} - c_j^{\alpha}\right)} \frac{RT}{F} \ln \left\{ \frac{\sum_j u_j z_j^2 c_j^{\beta}}{\sum_j u_j z_j^2 c_j^{\alpha}} \right\} \tag{9.28}$$

where the summations involve all ions in the two contacting electrolytes, with negative values for z_j if anions are involved. As above, with liquid junctions at reference electrodes, phase α denotes the sample solution and phase β the bridge electrolyte.

Figures 9.12 and 9.13 show liquid junction potentials calculated according to Eq. (9.5) with the ion mobilities given in Table 9.1. A 3 M KCl bridge electrolyte exhibits small liquid junction potentials, although strongly acidic samples give larger values. A bridge electrolyte of 1 M LiOAc gives somewhat inferior results but may be preferable if either potassium or chloride give rise to chemical interference.

Table 9.3 gives specific values for the liquid junction potential for the indicated electrolytes in the bridge and sample solution. Even for the equitransferent (similar mobility of anion and cation) bridge electrolytes KCl, KNO_3, NH_4NO_3 and LiOAc, the liquid junction potential accounts for a few millivolts, depending on the specific sample composition.

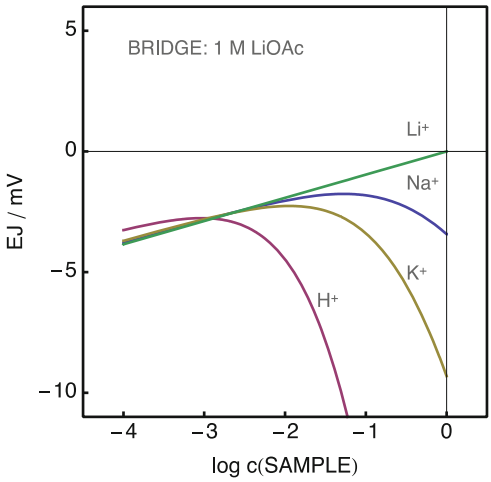

Fig. 9.13 Calculated liquid junction potentials according to the Henderson equation for a 1 M LiOAc bridge electrolyte and various sample concentrations. The counterion in the sample is acetate. The curve for protons is not realistic owing to the basicity of the acetate ion

Table 9.3 Liquid junction potentials for selected electrolytes in the sample and bridge electrolyte, at 25 °C

Bridge	Sample	E_J (mV)
3 M KCl	1 M $CaCl_2$	−0.28
3 M KCl	1 mM $CaCl_2$	−1.35
3 M KCl	1 M HCl	−16.3
3 M KCl	1 mM NaCl	−1.42
3 M KCl	H_2O (pH 7)	−2.80
3 M KCl	0.1 M NaCl	−0.13
3 M KCl	0.1 M Li_2SO_4	−0.44
0.1 M KCl	0.1 M NaCl	4.39
1 M LiOAc	0.1 M NaCl	−1.82
1 M KNO_3	0.1 M NaCl	3.74
1 M LiOAc	1 M HCl	−40.7
1 M KNO_3	1 M HCl	−27.6
1 M NaCl	H_2O (pH 7)	−2.80

From Eq. (9.28) with mobility data from Table 9.1

9.2.2.3 The Liquid Junction

For the liquid junction potential to be well defined and stable with time, one must avoid contamination of the sample or bridge electrolyte by mixing from the other side of the junction. Junction materials are therefore chemically inert porous materials that block convective mixing between the two compartments. They need to be chemically inert not to introduce surface charges that may act as ion-exchangers and hence result in undesired Donnan exclusion potentials.

Contamination of the bridge electrolyte is further avoided by slight pressurization of that compartment. In laboratory use this is simply accomplished

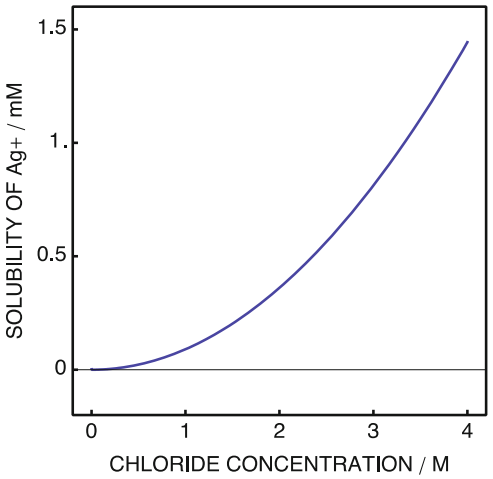

Fig. 9.14 Solubility of silver(I) in aqueous solution as a function of the chloride concentration. The solubility reaches millimolar levels at concentrations typical for bridge electrolytes owing to the formation of chloride complexes of high stoichiometry

hydrostatically by providing for a bridge electrolyte filling sufficiently above the air–water interface and placed at atmospheric pressure. In more demanding conditions, the bridge electrolyte can be pressurized in some designs or simply replaced with a polymeric (hydrogel) electrolyte in direct contact with the sample (no junction material).

The solubility of AgCl in 3 M or saturated KCl is much higher than expected based on the solubility product of AgCl ($K_{sp} = 1.8 \times 10^{-10}$) . This is due to the formation of complexes of the type $[AgCl_n]^{1-n}$, with n from 1 to 4. For zero ionic strength, for example, log β_n values can be 3.2 (n = 1), 5.1 (n = 2), 5.0 (n = 3). While for 4 M KCl, a value of 5.7 (n = 4) has been reported.[13] Figure 9.14 shows the solubility of silver ions as a function of chloride concentration using just the latter number. The solubility rises to over 1 mM at 4 M KCl.

Consider now a 3 M KCl bridge electrolyte in contact with a sample solution that is much more dilute in chloride. Figure 9.14 makes it clear that AgCl must precipitate in the junction material as less chloride is available to form the higher chloride complexes. This has important implications for the storage and handling of reference electrodes and combination electrodes using liquid junctions, as prolonged contact with dilute solutions will result in eventual blockage of the junction material.

9.2.3 Liquid Junction-Free Reference Electrodes

If one aims to design a reference electrode that does not require a liquid junction, the potential of the reference element in direct contact with the sample must be indifferent of sample composition.

Recently, Kakiuchi put forward a promising concept using ionic liquid membranes[14]. The principle is easily understood. The ionic liquid phase is allowed to locally equilibrate with the sample solution. If the ionic liquid electrolyte is denoted as $R_1^+R_2^-$, one may write for the partitioning equilibrium between the ionic liquid phase (IL) and water:

$$R_1^+(IL) + R_2^-(IL) \rightleftharpoons R_1^+(aq) + R_2^-(aq) \tag{9.29}$$

The key assumption is that the electrolyte has a sufficiently high affinity for the ionic liquid phase that other sample ions may not undergo ion-exchange reactions.

Since the electrolyte under study makes up the ionic liquid phase, one may accept that the activity of cation and anion in the ionic liquid is constant. We also consider that neither cation or anion are intrinsically present in the sample solution so that we may assume $a_{R_1^+}^{aq} \approx a_{R_2^-}^{aq}$. In the absence of ion-exchange, the potential at the sample–ionic liquid phase boundary is constant because it depends essentially on the ion activity of the ionic liquid that originates from self-dissolution of the material. The potential at this reference electrode is then only dependent on the nature of the ionic liquid and independent of the sample composition. The elegant and principally convincing concept put forward by Kakiuchi may not be appropriate for cases where chemical contamination of the sample solution by the ionic liquid cannot be accepted.

Ionic liquids with higher water solubility will contaminate the sample more quickly and will also result in an earlier operational loss of the reference electrode because of completely dissolving the electrode. Since the ionic liquid membrane consists of the electrolyte and solubility is on the order of millimolar, one expects a dramatically longer lifetime in comparison with traditional reference electrodes on the basis of KCl electrolytes of similar dimensions.

9.3 Ion-Selective Electrodes

9.3.1 Key Examples of Ion-Selective Electrodes

Table 9.4 summarizes ion-selective electrodes of practical importance. They are classified according to analyte, with the membrane type and brief information on the major ingredient indicated in the second and third column. The last column shows information on ion selectivity by giving logarithmic selectivity coefficients over the indicated potentially interfering ions. For references, see Table 9.4 and reference (15)

Table 9.4 Selected potentiometric sensors (see also reference (15))

Analyte	Membrane electrode	Composition	Logarithmic selectivity coefficient log $K_{I,j}^{pot}$ over j	Reference
H^+	Glass	72.2 % SiO_2, 6.4 % CaO, 21.4 % Na_2O	Na^+: −11; K^+: −11	
H^+	Ionophore	Tri-*n*-dodecylamine	Na^+ −10.4; K^+: −9.8; Ca^{2+}: < −11.1	16
H^+	Ionophore	Chromoionophore I	Na^+: −10.9; K^+: −10.5; Ca^{2+}: < −11.2	17
Li^+	Ionophore	14-crown-4 with decalino subunit	Na^+: −3.1; K^+: −3.6; NH_4^+: −3.8 Ca^{2+}: < −5.0	18
Na^+	Glass	11 % Na_2O, 18 % Al_2O_3, 71 % SiO_2	K^+: −2; Ag^+: +2.6; NH_4^+: −4.2; H^+: 1–2.5	
Na^+	Ionophore	*t*-Butyl-calix[4]arene tetramethylester	K^+: −2.5; Li^+: −2.9; H^+: 2.0	19
Na^+	Ionophore	Calix[4]arene crown-4	Li+: −2.8 K^+: −5.0 NH_4^+: −4.4 Mg^{2+}:−4.5; Ca^{2+}: −4.4	20
K^+	Ionophore	Valinomycin	Na^+: −4.5; Mg^{2+}: −7.5 Ca^{2+}: −6.9	21
K^+	Ionophore	BME-44	Na^+: −3.3	22
NH_4^+	Ionophore	Nonactin/Monactin	Li^+: −2.9; Na^+: −2.3; K^+: −1.1; Mg^{2+}:−4.0; Ca^{2+}: −4.0	23
Mg^{2+}	Ionophore	Double armed diaza-crown ether	Li^+: −3.7; Na^+: −3.2; K^+: −1.4; NH_4^+: −2.0; Ca^{2+}: −2.5	24
Ca^{2+}	Ionophore	ETH 129	Na^+: −8.3; K^+: −10.1; Mg^{2+}: −9.3	25
Ca^{2+}	Ionophore	ETH 1001	H^+: −4.4; Na^+: −6.1; K^+: −6.6; Mg^{2+}: −4.4	26
Cu^{2+}	Ionophore	Cu^{2+}-9	Zn^{2+}: −3.0; Pb^{2+}: −2.7; Ni^{2+}: −3.0; Cd^{2+}: −2.7; Ag^+: −0.1; Hg^{2+}: −2.0;	27
Cu^{2+}	Ionophore	*N*,*N*,*N*′*N*′-tetracyclohexyl-3-thiaglutaric diamide	H^+: −0.7; Na^+: < −5.7; Ag^+: 3.5; Ca^{2+}: −4.7; Zn^{2+}: −1.95; Cd^{2+}: −3.5; Pb^{2+}:−1.8	28
Ag^+	Solid-state	Ag_2S polycrystalline membrane	Cu^{2+}: −6; Pb^{2+} : −6 to −9; H^+: −5; Hg^{2+}: −2	
Ag^+	Ionophore	Methylenebis (diisobutyldithiocarbamate)	Na^+: −8.7; K^+: −8.2; Ca^{2+}: −11.0; Cu^{2+}: −10.5; Pb^{2+}: −10.3	29
Zn^{2+}	Ionophore		Li^+, Na^+: −2.7; K^+: −2.5; NH_4^+: −3.1; Ca^{2+}: −2.8; Cd^{2+}: −3.6; Pb^{2+}: −2.1	30

(continued)

Table 9.4 (continued)

Analyte	Membrane electrode	Composition	Logarithmic selectivity coefficient log $K_{I,j}^{pot}$ over j	Reference
Hg^{2+}	Ionophore		Hg^{2+}:−3; Ag^{+}: 0.0; Fe^{3+}: −3.4; Zn^{2+}: −2.9; Pb^{2+}: −2.6, Cu^{2+}: −2.7	[31]
Pb^{2+}	Ionophore	ETH 5435	Na^{+}:−6.3; K^{+}: −6.3; Ca^{2+}: −12.3; Cu^{2+}: −3.7; Cd^{2+}:−5.4	[32]
F^{-}	Solid-state	Single LaF_3 crystal	OH^{-}: −1; Br^{-}: −4; F^{-}: −4; HCO_3^{-}: < −3	
Cl^{-}	Ionophore	In(III) Porphyrin	I^{-}: 0.9; SCN^{-}: 1.4; Sal^{-}: 2.2; NO_2^{-}: 0.3; NO_3^{-}: −3.8	[33]
Cl^{-}	Ionophore	Mercuracarborand[3]	SCN^{-}: 1.9; Sal^{-}: −2.3; Br^{-}: 1.3; I^{-}: 4.1; NO_3^{-}: −4.3	[34]
Cl^{-}	Ionophore	2,7-di-tert-butyl-9,9-dimethyl-4,5-xanthenediamine	Sal^{-}: +1.8; SCN^{-}: +1.6; NO_3^{-}: +0.7; HCO_3^{-}: −2.6	[35]
I^{-}	Solid-state	50 mol% Ag_2S, 50 mol% AgI	Cl^{-}: −4; Br^{-}: −7; SCN^{-}: −4; S^{2-}: >10	
I^{-}	Ionophore	Mercuracarborand[3]	Cl^{-}: −4.1; NO_3^{-}: −7.6	[36]
S^{2-}	Solid-state	Ag_2S polycrystalline membrane	Br^{-}: −25; I^{-}: −18; Cl^{-}: −30	
HSO_3^{-}	Ionophore	Guanidinium derivative	ClO_4^{-}: −2.2; Cl^{-}: < −3.0; Sal^{-}: −2.3	[37]
CO_3^{2-}	Ionophore	Tweezer-type ionophore	Cl^{-}, Br^{-}: −6.5; Sal^{-}: −1; ClO_4^{-}: −1.8; NO_3^{-}: −4.2;	[38]
SCN^{-}	Ionophore	Mn(III) porphyrin	ClO_4^{-}: −2.0; I^{-}: −2.3; NO_3^{-}: −3.6 NO_2^{-}: −3.0; Cl^{-}: −3.4; HCO_3^{-}: −5.1	[39]
NO_2^{-}	Ionophore	Cobalt(III) cobyrinate	SCN^{-}: 0.2; Cl^{-}: −3.7; I^{-}: −2.2; ClO_4^{-}: −2.2	[40]
NO_2^{-}	Ionophore	Cobalt(III) phthalocyanine	SCN^{-}: −1.0; I^{-}: −1.6; NO_3^{-}: −3.1; Cl^{-}: −3.5; Br^{-}: −2.9	[41]
$H_2PO_4^{-}$	Ionophore	Uranyl salophene	F^{-}: −0.4; NO_3^{-}: −1.6; Cl^{-}: −2.1	[42]
Salicylate	Ionophore	Sn(IV) phthalocyanine	ClO_4^{-}: −3.3; SCN^{-}: −2.9; Cl^{-}: −4.8; OAc^{-}: −3.4	[43]

9.3.2 Glass Electrodes

The most widely used ISE is clearly the pH glass membrane electrodes that has been, since their humble beginnings over 100 years ago, developed into reliable sensors. They exhibit a wide dynamic measurement range, high selectivity, and good temperature resistance. The pH response of glass electrodes originates from a hydrated surface layer that contains SiO^- ion-exchanger sites that are selective the hydrogen ions. pH glass electrodes often display extraordinary potentiometric selectivities for H^+ over other cations which is largely due to the favorable equilibrium for the primary reaction occurring within the hydrated layer of the glass:

$$SiO^- + H^+ \rightleftharpoons SiOH$$

There are still active debates about the response mechanism of the pH glass electrode since some regard the mechanism as dependent on an adsorption process rather than simple ion-exchange, but there is agreement that the recognition process occurs in the surface layer of the glass, not in its interior.

A variety of optimized glass compositions exists that are suited for a range of applications. The classical sodium oxide containing glass has been largely replaced by lithium glass. High content of Li_2O favors a low membrane resistance and low alkali error (and a larger measuring range). Today, glass electrodes can be manufactured that are small, have extremely large measuring ranges of pH 0–14, and show low resistances even with the relatively thick membranes required to achieve acceptable robustness. In the early years of pH glass electrode developments, researchers tended to blow their own glass electrodes akin to Christmas tree bulbs. These electrodes were very fragile and had to be handled with care. Today, glass membrane thicknesses may exceed 1 mm and are mechanically robust. Glasses with very high (ca. wt-30 %) Li_2O content, however, can crystallize rather easily and can therefore not be handled by a glass blower. Moreover, they have shorter lifetimes, corrode more easily, and are not suited for high temperature applications. This last step is important for situations where pH electrodes must be sterilized before use. A variety of more rugged, extremely stable high temperature glasses are commercially available for this reason. They exhibit emf response over a reduced pH range but function reliably at high temperature without the need for intermittent calibration.

Since pH glass membrane electrodes are used in a variety of applications, manufacturers of pH electrodes have devoted significant effort in designing *combination pH electrodes* (containing pH and reference electrode in a single body) in many shapes and sizes, for use in NMR test tubes, with flat surfaces for paper and cheese pH measurements, pressure resistant electrodes for reactor applications, and a wide variety of laboratory pH electrodes. Beyond the type, size and shape of the pH sensitive glass, an essential component of the combination pH electrode is the reference electrode. Depending on the application of the pH electrode, one can

choose from refillable electrolytes in single and double junction designs, and low viscosity maintenance-free solid polymers and gel electrolytes that can sustain high external pressures. In addition, available junction materials range from simple ceramic frits, flat, circular ceramic frits for surface pH applications, Teflon sleeve junctions, free diffusion liquid junctions, and hole junctions for polymeric electrolytes. Some reference electrolytes can be pressurized in special chambers, while others are factory pre-pressurized or sustain high pressures without additional treatment. The excellent reliability, lifetime, and analytical performance of pH glass electrodes–reference combinations set a very high standard that few if any other ISEs can match.

Some specialized glass formulations have been found to be sensitive to ions other than H^+ as well.[15] Glass membranes with a high content of Na^+, for example, are known to be more Na^+ responsive. Since they are still selective for H^+, they can be only be used to assess Na^+ activities in samples that are far from acidic. A different class of glass electrodes, chalcogenide and jalpaite glasses, has been found to respond to a variety of heavy metal ions, including lead, cadmium, and copper, with some of them exhibiting extremely low detection limits for environmental analysis.[44]

The main limitations of glass membrane electrodes in certain applications are their tendency to be fouled by strongly adsorbing proteins, and by the limited number of ions that can be sensed potentiometrically with glass membranes. Indeed, glass membranes cannot be utilized to sense anions, and thus do not provide a generic approach for ion sensing. While adsorption problems can be reduced with repetitive washing cycles, difficulties in manufacturing miniaturized versions of glass electrodes to be used in conjunction with other types of ISEs in sensor arrays has motivated significant research on different pH selective materials. Most notable are pH electrodes based on polymeric membranes doped with amine functional ionophores and solid state iridium oxide membrane materials.[45]

With pH electrodes, one expects the cell potential to be near zero at pH 7. The two reference elements in the cell exhibit an asymmetry with respect to the chloride concentration in the contacting electrolyte solutions: the outer reference element is typically in contact with 3 M KCl, while the inner electrolyte contains on the order of tens of millimolar of chloride salt. Not considering the junction potential, one may write for the ideal cell potential:

$$E_{cell} = s\log\left[\frac{a_{H^+}(sample)}{a_{H^+}(inner\ solution)}\right] + s\log\left[\frac{a_{Cl^-}(outer\ reference)}{a_{Cl^-}(inner\ solution)}\right] \tag{9.30}$$

Consequently, the solution pH at the backside of the pH electrode must be somewhat acidic to achieve the desired cell potential at a sample pH of 7.

9.3.2.1 Liquid Junction Potentials in pH Measurements

Commercial pH electrodes are typically purchased as the so-called combination electrode where the reference electrode is integrated into the pH electrode body. A liquid junction potential develops in the contact zone between the sample solution and the reference electrolyte. If one considers a typical reference electrolyte of 3 M KCl in contact with a sample containing 10 mM KCl with varying concentrations of HCl or KOH, one obtains the liquid junction potentials from the Henderson equation as presented in Fig. 9.15.

The liquid junction potential adds to the membrane potential, so the potential readings are too high at high pH and too low at low pH. If the pH electrode is calibrated between pH 4 and 10 and one does not correct for the liquid junction potential, one expects an acid error of up to 0.25 pH units and an alkaline error up to 0.15 pH units. These considerations are with a perfectly selective pH electrode.

In addition to these challenges, pH membrane electrodes may exhibit deviations from Nernstian behavior in alkaline and acid media. This depends on the glass composition and is established by the manufacturer. Alkaline error arises from ion-exchange with other (alkaline) cations, while acid error originates from acid extraction into the glass gel layer. These processes are analogous to ionophore-based membranes, which are treated in some detail below.

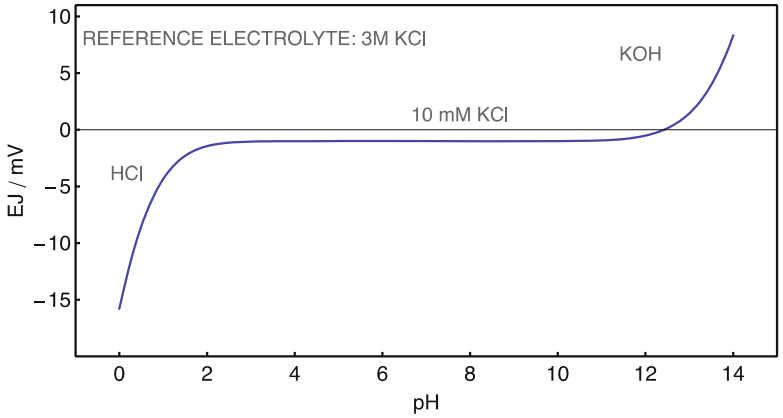

Fig. 9.15 Liquid junction potentials for a 10 mM KCl solution with added appropriate concentrations of HCl or KOH to arrive at the indicated pH values. This potential arises at the reference electrode and results, on the basis of the practical definition of pH, in a deviation from the Nernstian pH response behavior and is often erroneously associated with measurement error (alkaline and acid error)

9.3.3 Solid State Membrane Electrodes

ISEs based on solid-state membrane materials use sparingly soluble inorganic salts as the membrane matrix.[46] They must exhibit ion conducting properties to properly function in potentiometry. Interesting examples of this family of electrodes include the silver precipitate-based membranes. Pressed pellets of silver sulfide (Ag_2S) are known to respond to silver ions. This membrane is also sensitive to sulfide ions because any change in the sample sulfide activity affects the available silver activity at the surface of the electrode membrane according to the following dissolution equilibrium:

$$Ag_2S(s) \rightleftharpoons 2Ag^+(aq) + S^{2-}(aq)$$

This electrode shows a very high selectivity to both silver and sulfide (both ions cannot be simultaneously present in solution in large quantities because of the small solubility product of Ag_2S). The only substantial interferent is the mercury(II) ion owing to the extremely low K_{sp} for HgS. The pressed pellet requires periodic polishing to remove surface adsorbates and other precipitates, but shows otherwise very long lifetimes. This principle has been extended to other silver salts, especially silver halides. Silver sulfide pellets doped with CuS will respond to Cu^{2+} because of the larger dissolution equilibrium of CuS relative to Ag_2S. A silver sulfide pellet doped with AgBr will be bromide selective, and so on. The selectivity observed with such silver halide precipitates follows exactly the solubility product of the respective silver salt. Consequently, the following sequence is always observed for any given silver precipitate membrane:

$$S^{2-} > I^- > Br^- > Cl^- \tag{9.31}$$

A silver chloride precipitate membrane in prolonged contact with an I^- containing solution will, therefore, eventually become an iodide sensitive electrode since all surface bound chloride will exchange with iodide. This process can take some time in dilute solutions, however, during which the electrode remains essentially responsive to chloride. Unfortunately, silver precipitate membranes are not always suitable for practical measurements because thiol containing molecules (for example with proteins containing cysteines) may foul the surface of the ion-selective membrane and the AgCl may dissolve because silver ions are complexed by protein amine or other functional groups.

Chloride measurements in complex samples are therefore normally not performed with AgCl-based membranes. Analytical properties similar to pressed pellet membranes have also been observed with silver salts embedded in a silicone membrane, with ionophore-based silver-selective liquid membranes, and with silver/silver halide wires. The latter class is usually less preferred for practical measurements since any exposed metal may induce some redox species cross-sensitivity

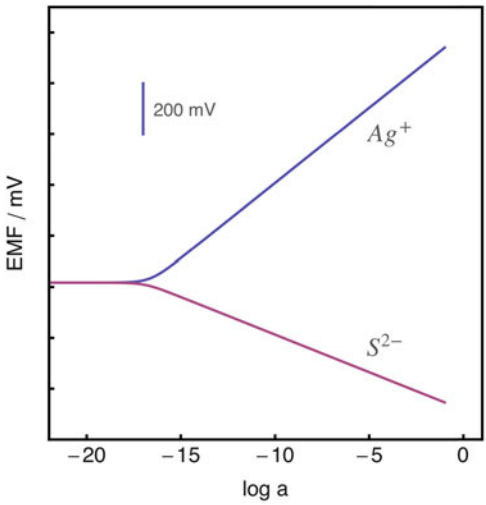

Fig. 9.16 Calculated changes in the boundary potential (emf) at zero current for a Ag_2S membrane as a function of changing silver (*top trace*) and sulfide ion activity changes in the sample (*bottom trace*). The potential at very low activities is dictated by the self-dissolution of Ag_2S (protonation of sulfide is suppressed with a solution of high pH). The exhibited detection limit can only be attained in practice by the use of ion buffers in the sample

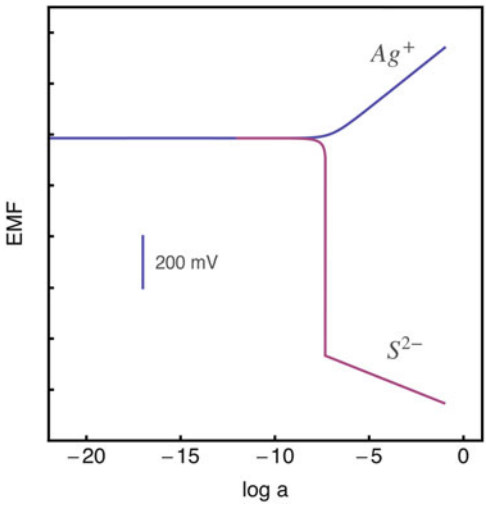

Fig. 9.17 Calculated changes in the boundary potential (emf) at zero current for a Ag_2S membrane as a function of changing silver (*top trace*) and sulfide ion activity changes in the sample (*bottom trace*). In contrast to Fig. 9.16, a membrane impurity results in the release of a 100 nM concentration of silver ions at the membrane surface. The exhibited response functions are observed in the absence of an ion buffer in the sample

of the electrode, which does usually not occur with membrane-based indicator electrodes.

With Ag_2S based membranes thermodynamics predict extremely low detection limits down to 10^{-17} M or so, see Fig. 9.16. This can be achieved in sulfide solutions at elevated pH where the dissolved silver is extremely small. Note that this is in essence a thermodynamic cycle and one can equally state that the electrode is responsive to the abundant sulfide ion (the silver activity is calculated from the sulfide concentration and the known solubility product). However, if no such ion buffer is present and one aims to measure low total concentrations, one often finds the behavior shown in Fig. 9.17, which has been attributed to the presence of

halides or other impurities in the membrane that results in increased dissolution of silver and hence of a poorer than expected detection limit.

Another solid-state membrane of extremely high selectivity and applicability is the single crystal LaF_3 membrane electrode.[47] The crystal is doped with europium to lower its electrical resistance and it acts as an effective pure F^- conductor. When used as an ion-selective electrode material, a large measuring range of about six orders of magnitude is observed (10^{-6} to 1 M F^-), with Nernstian response slopes. The only significant interferent is hydroxide due to the low solubility of $La(OH)_3$. Such electrodes are typically used under strict pH control between 5 and 6 to avoid hydroxide interference at higher pH and the formation of HF at lower pH, which would decrease the activity of F^-. Suitable ionic strength adjustment buffers for fluoride measurements typically also contain complexing agents such as citrate to remove cations such as aluminum and iron from the sample that have a tendency to complex fluoride. The LaF_3 electrode has an extremely long lifetime under normal use. Its main disadvantage is its cost due to the necessity of using a polished single crystal.

9.3.4 Ion-Exchanger Membranes

Liquid or solvent polymeric membranes must exhibit ion-exchanger properties to properly function. It was mentioned above that the concentration of analyte in the membrane phase must remain reasonably invariant in the course of an experiment[6,29]. In the absence of lipophilic ion-exchanger, however, a concentration increase of an electrolyte in the sample would lead to a proportional increase in the organic phase. Therefore, such a process would not lead to a change in the phase boundary potential since the activity ratio in the organic and aqueous is constant.[48]

Consequently, liquid membranes are routinely doped with a salt of a lipophilic ion, for example, tridodecylmethylammonium chloride for anion-selective electrodes and potassium tetrakis(4-chlorophenyl)borate for cation-selective electrodes. Numerous other ion-exchangers have been reported in the literature, but their main function tends to be the same.[2] Before use, the liquid membrane is allowed to condition in a solution that contains a high concentration of the cation or anion to be measured. During this conditioning period, the hydrophilic counterion of the ion-exchanger in the membrane is replaced with the analyte ion of interest. The selectivity of such membranes is a direct function of the free energy of hydration of the measured ions. For anion-selective membranes (containing the anion salt of a quaternary ammonium ion, for example), the observed selectivity sequence always follows the so-called Hofmeister sequence:

$$R^- > ClO_4^- > I^- > NO_3^- > Br^- > Cl^- > F^- \tag{9.32}$$

where R^- denotes an organic anion. By analogy, the selectivity sequence for ion-selective membranes incorporating a cation-exchanger is:

$$R^+ > Cs^+ > Rb^+ > K^+ > Na^+ > Li^+ \tag{9.33}$$

For this reason, ion-exchanger based ISEs have historically been used for the detection of perchlorate and nitrate, as well as a range of lipophilic organic ions including many drugs and cationic/anionic surfactants. Anion exchanger-based membrane electrodes are routinely used to assess nitrate in environmental and laboratory samples. While there is some interference from bicarbonate, calibration in samples with very similar background electrolytes can minimize such effects.

The above listed selectivity sequences are thermodynamic sequences that are not always observed under practical measuring conditions. If a strongly interfering ion is present but relatively dilute (typically at less than 10^{-4} M levels), its effect on the cell potential is often much smaller than predicted on the basis of the Nicolsky equation and its modifications.[49] Such low concentrations result in a mass transport limited ion exchange, even if thermodynamically favored. For short exposure times, therefore, the electrode can often still reliably be used to assess the analyte. After prolonged contact with a sample containing a strong interferent, the electrode does eventually recondition by ion-exchange and fails to respond to the primary analyte. These effects have historically been exploited for sensing applications in samples for which no thermodynamic selectivity was available. It requires careful reconditioning between measurements and is not recommended if an intrinsically better selectivity can be achieved with another ISE. This effect may explain why some manufacturers offer ion-exchanger based ISEs for a variety of ions, even though the starting membrane compositions are essentially identical.

9.3.5 Ion-Selective Membranes Containing Ionophores

9.3.5.1 Neutral Ionophores

Lipophilic, electrically neutral ionophores are also called ion carriers because of their capability of selectively transporting ions across artificial membranes. They are chemical components that are key to achieving high selectivity with liquid or polymer membrane based ISEs.

Neutral carrier-based membranes require the addition of a lipophilic ion-exchanger for proper functioning. This ion-exchanger forms the counterion of the complexed analyte ion in the membrane. Its concentration should not be too large in order to allow for a substantial concentration of unbound ionophore in the membrane. For instance, a cation-selective membrane may contain the ionophore and the lipophilic tetraphenylborate derivative cation-exchanger potassium tetrakis(4-chlorophenyl)borate, while anion-selective membranes may be doped with tridodecylmethylammonium chloride as anion-exchanger in addition to the ionophore.

While ionophore-free ion-exchanger based membranes always show the same selectivity pattern that follows the hydration energies of the ions (see above), ionophore-based membranes exhibit selectivities that can be very different. This is because of the formation of strong complexes between the analyte ion and the ionophore in the membrane. Values of logarithmic complex formation constants can vary widely. They have been reported to be up to about 12 for monovalent and about 25 for divalent ions.[50] Sensor selectivity is dictated by the free energy of transfer of the ions from the aqueous to the membrane phase, the complex formation constants between the extracted ions and the ionophore, and the concentrations of ionophore and lipophilic ion-exchanger in the membrane.

Hydration energies are still important since ion extraction process is involved and it is typically more difficult to design ISEs for hydrophilic ions than it is for hydrophobic ones. On the other hand, it is often a difficult to design selective receptors for large, bulky ions. Consequently, ionophore-based ISEs for potassium and calcium were realized early on, while selective sensors for magnesium, lithium, sodium, and small anions such as chloride, carbonate, and phosphate have been developed more recently or are still topics of current research.[51] Ionophore-based ISEs for bulky anions such as perchlorate are not really known.

Table 9.4 summarizes typical membrane compositions of the corresponding ISEs and observed selectivity coefficients. Observed selectivities can be extremely high and explain the significant success that such sensors have enjoyed for practical measurement applications.

Ionophores may be developed on the basis of a variety of recognition principles. They include simple crown ethers, bis-crown ionophores, crowns with bulky side groups to prohibit intermolecular sandwich formation, non-cyclic amide and thioamide ionophores, basket shaped calix[4]arene and calix[6]arene ionophores, calixarenes with crown bridges, thiocarbamates, lipophilic amine bases as H^+-ionophores, guanidinium derivatives, multitopic hydrogen bond forming ionophores for selective anion recognition, metalloporphyrins, cobyrinates, and phthalocyanines with different metal centers and a variety of axial ligands, and aromatic trifluoroacetyl derivatives for the recognition of hydrophilic nucleophiles.[51] Some of these ionophores are electrically charged in their uncomplexed form.

To function in ion-selective membranes as desired, ionophores should be sufficiently lipophilic so that they are retained within the hydrophobic membrane phase to ensure a long lifetime of the sensor. This is most often achieved by adding long alkyl chains, cyclohexyl or adamantyl substituents to the molecular backbone. They should have a polar moiety or a set of polar functional groups responsible for the ion recognition process.[6,51] The remainder of the ionophore molecule should contain hydrophobic regions that are compatible with the surrounding membrane matrix. The historical argument that an ionophore molecule must also exhibit a certain mobility within the membrane (recall the term "ion carrier") has been largely disproved by the comparable analytical performance of a number of membrane materials where the ionophore is covalently anchored onto the polymeric backbone. It seems beneficial, however, to at least either have mobile ionophores or mobile ion-exchanger to guarantee an acceptably low membrane resistance.

Table 9.5 Optimum composition of ionophore-based membranes[52]

Charge of cation		Complex stoichiometry		Ratio
z_I	z_J	n_I	n_J	c_R^m/L_T
2	2	1	2	1.41
2	2	2	3	0.77
2	2	3	4	0.54
2	1	1	1	1.62
2	1	2	2	0.73
2	1	3	3	0.46
1	1	1	2	0.71

Giving a predicted optimal selectivity for the analyte ion I with respect to the interfering cation J

Membrane selectivities for a given ionophore may vary substantially. Membranes of relatively high polarity are normally preferred for the development of divalent-ion selective electrodes and many anion-selective electrodes, while non-polar membranes are often more suited for monovalent cations. Many other parameters may also influence selectivity, including the tendency to form ion pairs, the availability of functional groups on the plasticizer that can compete with the ionophore, and variations of complex stoichiometries of the ionophore in different solvent environments. Optimization of ISE selectivity is therefore still done empirically.

If the complex stoichiometries are known, optimum molar concentration ratios between ionophore and lipophilic ion-exchanger may be predicted from thermodynamic analysis.[52] Table 9.5 shows the optimum concentration ratios for a number of assumed complex stoichiometries and charges of the two compared ions. Some ionophores are capable of forming mixed complexes and the optima also depend on the relative binding strength of the resulting complexes. The tabulated values should be used as first guesses only and the selectivity should be evaluated for a range of ion-exchanger concentrations.

9.3.5.2 Determination of Selectivity Coefficients

Experimental protocols for the determination of selectivity coefficients have been laid out by IUPAC. One distinguishes two main methods, the separate solutions method (SSM) and the fixed interference method (FIM).[53]

As the name implies, the separate solutions method involves the measurement of the cell potential in a solution containing only the salt of the analyte (primary ion I), followed by that in a solution containing only the salt of the interfering ion, J. One then obtains the selectivity coefficient for any activity as follows:

$$\log K_{I,J}^{pot} = \frac{z_I}{s}(E_J - E_I) + \log \frac{a_I^{aq}}{\left(a_J^{aq}\right)^{z_I/z_J}} \tag{9.34}$$

With the fixed interference method, a calibration curve for the primary ion in a fixed interfering ion background is determined. The lower detection limit is then determined and related to the selectivity coefficient as follows:

$$a_I(LDL) = K_{I,J}^{pot} a_J^{z_I/z_J} \tag{9.35}$$

While these two methods have been applied for many decades in the field, they exhibit the important drawback that no effort is made to guarantee or even determine a Nernstian response slope to the interfering ion. Such a Nernstian slope is required for Eq. (9.34) or (9.35). If the membrane is very selective towards the analyte ion, one may not be able to achieve this condition easily and experimental selectivity coefficients may deviate orders of magnitude from the thermodynamic values.[29]

To address this important problem, improved methods have been proposed to eliminate the bias originating from an incomplete ion-exchange at the sample–membrane interface. In one such method, the membrane is conditioned with a discriminated ion, not the analyte ion.[29] This results in complete ion-exchange at elevated concentrations and allows one to obtained unbiased selectivity coefficients. The procedure is analogous to the Hulanicki effect discussed above,[49] and therefore requires high sample concentrations in order to avoid concentration polarizations. Other methods include the use of chelators or precipitation reactions in the sample to keep the concentration of the primary ion in the sample very low. Membranes exhibiting a strong inward flux of primary ions have also successfully been used to determine unbiased selectivity coefficients.[54]

9.3.6 *Electrically Charged Ionophores*

Most ionophores used in ion-selective electrodes today are electrically neutral in their uncomplexed form, see above. In the membrane, the following complexation equilibrium exists between ionophore L and a (monovalent) anion A^-:

$$nL(m) + A^-(m) \rightleftharpoons AL_n^-(m) \tag{9.36}$$

For this reason, membranes containing neutral ionophores must also contain a lipophilic ion-exchanger whose charge is opposite that of the analyte ion. It then dictates via electroneutrality condition the concentration of the jL_n^+ complex in the membrane.

On the other hand, ionophores exist that are electrically charged in their uncomplexed form (such as many metalloporphyrins and phthalocyanines). An additional electrical charge on the coordinating functional group of the ionophore may be attractive to strengthen the complex with additional coulombic forces and are promising for designing ionophores for anion recognition.

Functional ISEs may be fabricated with membranes that contain just the salt of a charged ionophore, since the ionophore has both ionophoric and ion-exchanger properties. However, it can be shown that the corresponding sensing selectivities are then often less than ideal.[55] Consider for example a membrane with a charged ionophore selective for a monovalent anion. The concentration of uncomplexed ionophore in the membrane is ordinarily small and dictated by the dissociation constant of the complex:

$$AL(m) \rightleftharpoons L^{+}(m) + A^{-}(m) \tag{9.37}$$

If the ISE membrane were to be conditioned in a solution of an interferent whose complex with the ionophore is weaker, the concentration of uncomplexed ionophore in the membrane would be larger since the dissociation constant is now also larger. If both ions are present, an intermediate situation would be observed: a higher interfering ion level would lead to a higher concentration of uncomplexed ionophore in the membrane. This dependence between sample composition and uncomplexed ionophore concentration is not ideal since it favors the formation of the complex with a more weakly binding analyte.

Instead, optimum selectivities may be achieved by incorporating an ion-exchanger into the membrane that has the same charge as the analyte, and which forms the counterion of the uncomplexed ionophore L^{+}. That concentration is then independent of the nature of extracted sample ion. One predicts that the ISE selectivity is now dependent on the binding selectivity of the charged ionophore in the same manner as for membranes containing neutral ionophores.[55]

Other ionophores, especially of the metalloporphyrin types, show peculiar super-Nernstian response slopes. One may understand these by the occurrence of hydroxide anion bridges binding two such metalloporphyrins together[56]:

$$2L^{+}(m) + OH^{-}(m) \rightleftharpoons LOHL^{+}(m) \tag{9.38}$$

On the other hand, the ionophore still binds to A^{-} as shown in Eq. (9.37) above.

The non-Nernstian response slope is explained by a competition between OH^{-} and A^{-} as a function the sample composition. As the concentration of A^{-} increases in the course of a calibration curve, it results in a decreased concentration of dimer and in an increase of L^{+} concentration. This stabilizes A^{-} more (lower activity of the free ion in the membrane) with increasing sample concentration and results in a larger response slope than expected from the Nernst equation.

9.3.7 Selectivity Optimization

The selectivity coefficient should be as small as possible for optimal selectivity. With ionophore-based membrane electrode, the membrane composition can have a direct influence on the resulting selectivity and used for optimization purposes.

Much of this optimization is empirical since the complex stoichiometries and complex formation constants within the membrane phase are not a priori known. Nonetheless, effective models have been developed that show how the selectivity coefficient can be tuned for a given set of binding parameters.[52,57]

For monovalent ions giving a 1:1 stoichiometry in the membrane, one can show that the concentration of uncomplexed ionophore at the membrane side of the phase boundary, $c_L^m(j)$, in the presence of the indicated ion j, follows the following relationship:

$$c_L^m(j) = \frac{-1 - \beta_{jL} c_R^m + \beta_{jL} L_T + \sqrt{4\beta_{jL} L_T + \left(-1 - \beta_{jL} c_R^m + \beta_{jL} L_T\right)^2}}{2\beta_{jL}} \tag{9.39}$$

where c_R^m the ion-exchanger concentration and L_T the ionophore concentration and β_{jL} is the complex formation constant. This equation can be formulated for the primary ion, I, and the interfering ion, J, to predict the E^0 value for each ion as:

$$E_I^0 = \Delta_{aq}^m \phi_I^0 + s\log\left(\frac{1 + \beta_{nI} c_L^m(I)}{c_R^m}\right) \tag{9.40}$$

and

$$E_J^0 = \Delta_{aq}^m \phi_J^0 + s\log\left(\frac{1 + \beta_{nJ} c_L^m(J)}{c_R^m}\right) \tag{9.41}$$

which are used to obtain the selectivity coefficient with the expression

$$\log K_{I,J}^{pot} = z_I\left(E_J^0 - E_I^0\right)/s \tag{9.42}$$

The resulting graphs are shown for the indicated parameters in Fig. 9.18. For ions of the same charge, optimum selectivity is observed at a concentration of ion-exchanger below that of the ionophore. If complex formation constants are weak, best selectivity is expected at an ion-exchanger concentration that is as low as practical.

If complexes are stable (uncomplexed ions may be neglected), and the ion-exchanger concentration is lower than that of the ionophore, the selectivity coefficient simplifies to:

$$\log K_{IJ}^{pot} = \frac{z_I \Delta\Delta_{aq}^m \phi_{J,I}^0}{s} + \log\frac{\beta_{JL}}{\beta_{IL}} \tag{9.43}$$

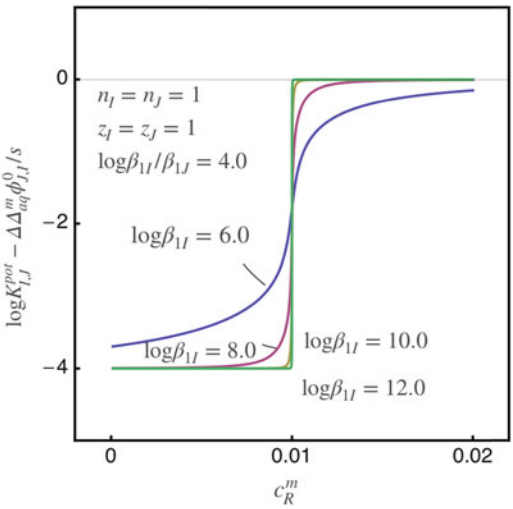

Fig. 9.18 Logarithmic selectivity coefficient changes as a function of the lipophilic ion-exchanger concentration in the membrane, calculated for monovalent primary and interfering ions and a 1:1 stoichiometry with the ionophore whose concentration is $L_T = 10$ mM

while for an excess ion-exchanger, the relationship reduces to:

$$\log K^{pot}_{IJ} = \frac{z_I \Delta\Delta^m_{aq}\phi^0_{J,I}}{s} \tag{9.44}$$

Clearly, the second relationship reflects the Hofmeister selectivity sequence (ions of higher lipophilicity are preferred over more hydrophilic ones), while the former predicts a selectivity that is additionally dictated by the binding constants between the ions and the ionophore.

Other cases of varying ion charge and complex stoichiometry can be computed and optimal molar membrane concentration ratio of ion-exchanger to ionophore are shown in Table 9.5.[52]

9.3.8 The ISE Detection Limit

Most analytical techniques compare the signal from a dilute solution to a multiple of the background signal uncertainty to characterize the detection limit. For historical reasons, the detection limit of ISEs has been based on a significantly different definition than other techniques. It is traditionally defined as the intersection of the two extrapolated linear segments of the calibration curve.[53]

According to the general protocol to determine the detection limit, the background potential in the absence of primary ions is equated to primary ion activity predicted from the Nernst equation at the same potential. If one assumes that the background potential is dictated by the potentiometric response to an interfering

ion, j, that has quantitatively displaced the primary ion, I, from the membrane phase boundary, one may formulate this detection limit as:

$$a_I(LDL) = \sum_j K_{I,j}^{pot} \left(a_j\right)^{z_I/z_j} \tag{9.45}$$

Here, multiple interfering ions have been semiempirically summed. In some cases, Eq. (9.45) predicts phenomenally low detection limits that are not readily observed in practice. As a case in point, a membrane with a selectivity coefficient of $K_{Ag,H}^{pot} = 10^{-10}$ measured in pure water ($a_H \approx 10^{-7} M$) should give a detection limit on the order of $10^{-17} M$.

If the solution contains an ion buffer, i.e., a large excess of a labile species that maintains, at equilibrium, a defined activity of the free ion, the detection limit may correspond to that given by Eq. (9.45). Such examples have been repeatedly given in the field, with nominal detection limits even going down to the single molecule level.[2,25]

9.3.9 Membrane Concentration Changes and Kinetic Detection Limit

If, on the other hand, the sample solution is very dilute in primary ion, mass transfer properties may become important. We can understand the extent of ion-exchange with the following equation, written here for monovalent ions as[32]:

$$\frac{c_I^m}{c_I^m(I)} = \frac{a_I}{a_I + K_{I,J}^{pot} a_J} \tag{9.46}$$

The left side shows the mole fraction of primary ion I in the membrane phase boundary relative to its concentration when ion-exchange is absent. This ratio is a direct function of membrane selectivity and sample composition. The effect of ion-exchange on the detection limit of the corresponding electrode is shown in Fig. 9.19. Based on simple ion-exchange, half of the primary ions have been displaced at the detection limit.

However, this ion-exchange results in a concentration gradient across the membrane because the perturbation only occurs at the outer membrane side. This gradient results in a counterdiffusion flux, with competing ions being transported inward, in direction of the inner solution, while primary ions are expelled out of the membrane. Since potentiometry is sensitive to the activity at the membrane surface, this can result in a bias that introduces an important error in the measurement. It often defines the lower limit of detection with highly selective membranes.

At steady-state, we expect a linear concentration gradient across the aqueous diffusion layer (of constant thickness δ^{aq}) and across the whole of the membrane

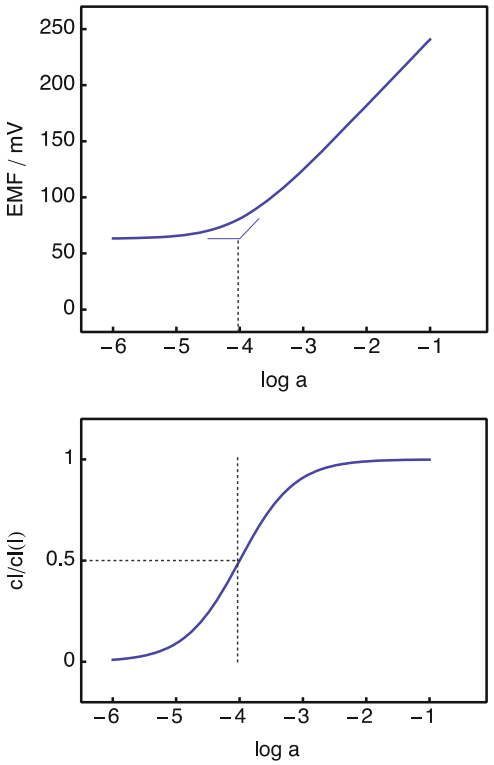

Fig. 9.19 Calculated response functions and associated membrane phase boundary concentration changes of primary ion. The detection limit is attained at a mole fraction of 50 % when half of the primary ions have been displaced by interfering ones of the same charge

(thickness δ^m), as illustrated in Fig. 9.20. The ion flux from the membrane to the interface and from the interface to the sample solution must be equal. We can therefore write with Fick's first law of diffusion:

$$D_{jL}^{m}\frac{c_{jL}^{m}(0)-c_{jL}^{m}(\delta^m)}{\delta^m}=D_j^{aq}\frac{c_j^*-c_j^{aq}(0)}{\delta^{aq}} \tag{9.47}$$

The ion concentration at the sample side of the phase boundary is now found as:

$$c_j^{aq}(0)=c_j^*-q\left(c_{jL}^{m}(0)-c_{jL}^{m}(\delta^m)\right) \tag{9.48}$$

with the permeability ratio

$$q=\frac{\delta^{aq}D_{jL}^{m}}{\delta^m D_j^{aq}} \tag{9.49}$$

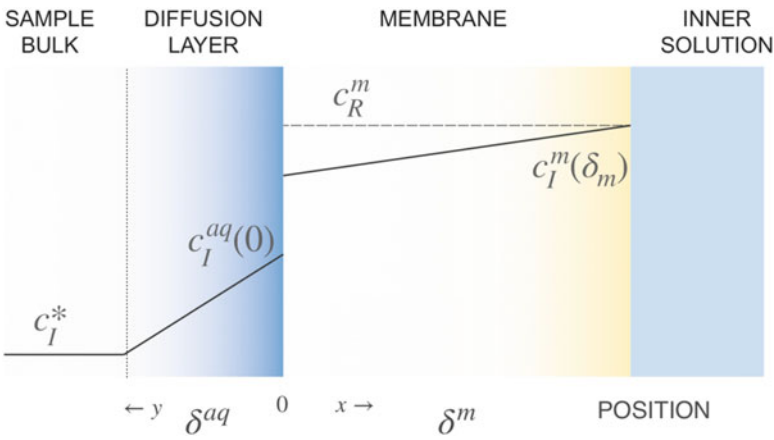

Fig. 9.20 Representation of steady-state concentration gradients and their notations for the description of the dynamic detection limit that is dictated by zero-current ion fluxes across the membrane and aqueous diffusion layer

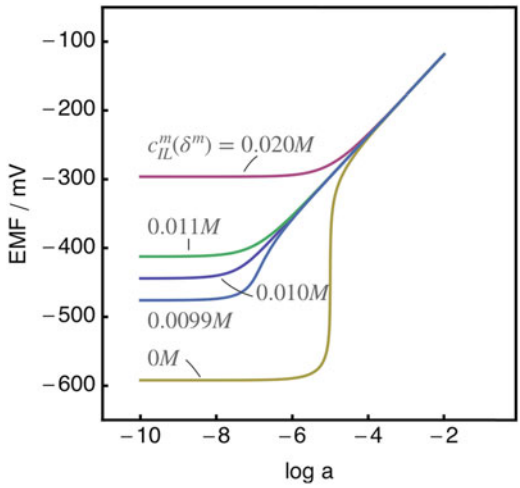

Fig. 9.21 Steady-state potentiometric response curves as a function of the analyte concentration at the inner membrane side, calculated according to Eq. (9.50) with $c_R^m = 0.010M$, $q = 0.001$ and $K_{I,J}^{pot} c_J = 10^{-10}$

If monovalent primary and interfering ions are considered, the aqueous surface concentration imposed by transmembrane counterdiffusion fluxes may be described as:

$$c_I^{aq}(0) = \frac{1}{2}\left(c_I^* - K_{IJ}^{pot} c_J + q c_{IL}^m(\delta^m) - q c_R^m \right. \\ \left. + \left\{ 4K_{IJ}^{pot} c_J \left(c_I^* + q c_{IL}^m(\delta^m)\right) + \left(c_I^* - K_{IJ}^{pot} c_J + q\left(c_{IL}^m(\delta^m) - c_R^m\right)\right)^2 \right\}^{1/2}\right) \tag{9.50}$$

The strong influence of the inner solution composition on the resulting calibration curves is shown in Fig. 9.21. A very high detection limit can be obtained in practice with concentrated and lipophilic electrolytes that result in substantial electrolyte extraction into the back side of the membrane (here, $c_{IL}^{m}(\delta^{m}) = 0.02M$). The predominant mode of transport is then co-diffusion with its counterion.

A very strong inward gradient is observed for $c_{IL}^{m}(\delta^{m}) = 0M$. This polarizes the surface concentrations to much smaller values, resulting in a so-called super-Nernstian potential change at a critical concentration. Predominant mode of transport is counter-diffusion with an interfering ion of the same charge sign as the primary ion.

The two above mentioned effects become less pronounced as the inner membrane concentration approaches that of the ion-exchanger. The lowest detection limit without a super-Nernstian slope region is found at an inner primary ion concentration equal to the ion-exchanger concentration (0.01 M) at the inner membrane side. This optimal detection is significantly higher than that predicted by Eq. (9.45) for the classical detection limit, 10^{-10} M.

The optimal detection limit attainable when ion fluxes are relevant is calculated from Eq. (9.50) with a sample bulk concentration of $c_I^{*} = 0$, an inner membrane concentration of

$$c_I^{m}(\delta^{m}) = c_R^{m}, \text{ and } qc_R^{m} \gg K_{IJ}^{pot} c_J \text{ as:}$$

$$c_I^{aq}(LDL) = c_I^{aq}(0) = \left\{ qc_R^{m} K_{IJ}^{pot} c_J \right\}^{1/2} \tag{9.51}$$

For a given selectivity and background electrolyte, the operational detection limit can be minimized by reducing the ion-exchanger concentration and permeability ratio q, which is a function of the diffusion layer thicknesses and ion mobilities.

While the concentration profiles indicated on the previous pages reflect idealized steady-state behavior, in real situations the membrane is exposed to a range of sample compositions. Consequently, the membrane gradients will change as a function of the solution composition.[58] The potential at the detection limit, therefore, will depend on the prior history of the electrode.

These processes are illustrated by numerical simulation, see Fig. 9.22. Here, the membrane does not exhibit ion-exchange with interfering ions before exposure to a sample containing no analyte ions at all. The observed potential change is initially rapid, similar to that of a regular concentration step (blue trace), but a drift is subsequently observed. This drift reflects the slow changes in membrane concentration until the steady-state is reached. In practice, such drifts can be avoided by keeping to solution concentrations well above the detection limit. They are also minimized by preconditioning the membrane in a solution close to the desired sample composition.

More recent work has introduced all solid state configurations to avoid the need for optimizing the inner solution for each desired sample composition. So far, the lowest detection limits have been achieved with ion-selective membranes containing a poly(octylthiophene) layer between the membrane and contacting

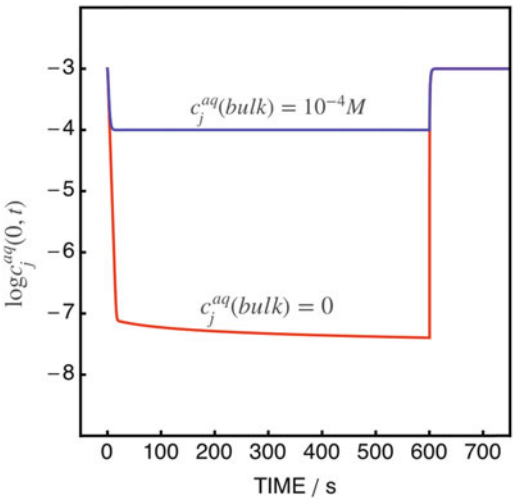

Fig. 9.22 Medium term drift of an ionophore-based membrane at the detection limit (*red trace*), where the sample bulk concentration is changed from 1 mM to 0 at time 0. At 600 s, the sample bulk concentration is returned to 1 mM. *Blue trace*: corresponding simulation where the concentration is changed to just 0.1 mM, showing no such drift

Table 9.6 Optimal detection limits of selected potentiometric sensors[60]

Primary ion	Molar detection limit
Na^+	3×10^{-8}
K^+	5×10^{-9}
NH_4^+	2×10^{-8}
Cs^+	8×10^{-9}
Ca^{2+}	10^{-10}
Ag^+	3×10^{-11}
Pb^{2+}	6×10^{-11}
Cd^{2+}	1×10^{-10}
Cu^{2+}	2×10^{-9}
ClO_4^-	2×10^{-8}
I^-	2×10^{-9}

electrode.[59] The light sensitivity of such underlayers places some limits on their environmental applicability and requires shielding the electrode from direct sunlight. Table 9.6 gives the detection limits for a number of recently reported ion-selective electrodes when measured in samples without primary ion buffer, see reference (60).

9.4 Dynamic Electrochemistry with Ion-Selective Electrodes

While this book chapter focuses on the topic potentiometric sensors, ion-selective membrane electrodes can also be interrogated by dynamic electrochemistry techniques.[61] This allows one to gain additional information from the sample for

speciation analysis, to achieve in-situ localized titrations, sample accumulation for lower limits of detection, or calibration-free sensing.

Ion fluxes to or from the membrane can be imposed by an applied current. If mass transport of the ions is by diffusion only, one essentially imposes the magnitude of the concentration gradient at the membrane surface. For ion fluxes in direction of a planar membrane, the diffusion layer will increase with the square root of time because the ions need to be sourced deeper and deeper from the solution as they are lost by transfer into the sensing membrane. At a certain point in time, and depending on the current amplitude, the imposed ion flux can no longer be maintained and a different electrochemical process must start to maintain the imposed current. As these membranes are sensitive to surface concentration changes we may be able to observe this depletion event by a potential change. The analytical signal does not depend on the magnitude of the potential, but on the time at which the event takes place, also called the transition time. Consequently, one can use a simplified electrochemical setup (simpler reference electrode design) to make such measurements. The transition time τ is dependent on the concentration of the transferred ion with the Sand equation, written as

$$\tau = \pi D_j^{aq} \left(\frac{z_j F A c_I^{*,aq}}{2i} \right)^2 \tag{9.52}$$

The time of the depletion event is given by the ability of the solution to maintain an imposed flux, which bears some analogy to the mechanisms of bio-uptake and ecotoxicology in environmental systems. This class of sensors therefore gives information on the concentration of kinetically available species in solution.[62] The technique is also promising for effecting localized titrations to assess information on total acidity or alkalinity (the latter is detectable by a controlled current release of hydrogen ions from a pH sensitive membrane electrode).[63]

Controlling the interfacial potential at a membrane electrode allows one to impose a thermodynamic condition to extract ions from the sample solution into the sensing phase or vice versa. While this can be exploited in voltammetric sensors, the strategy is perhaps most promising for sensors that work on the principle of ion transfer stripping voltammetry. In essence, a suitable potential is applied for some fixed period (typically a few minutes) that results in the extraction of the ion of interest from the sample phase. The potential is then scanned or pulsed to values where this ion is stripped off, resulting in a peak-shaped current. The accumulation step can result in lower detection limits (typically in the low nanomolar concentration range) and the stripping peak potential gives information on the nature of the stripped ion. Recent progress in this direction has involved the use of a thin layer sensing film deposited on top of a solid electrolyte with a conducting polymer intermediate layer.[64] The extraction of anions from the sample is then coupled to the oxidation of conducting polymer, resulting in a current. Stripping is effected by re-reduction of the polymer.

If one elects to reduce the sample thickness to that of the diffusion layer, one can design an electrochemical ion sensing system that exhaustively extracts selected ions from the sample under potential control. The current associated with this extraction decays with time as the ions are depleted, and is integrated over time to arrive at the removed charge. With Faraday's law we arrive at a direct relationship between this charge and the amount of removed ions. With fixed dimensions of the cell the concentration is then inferred. This principle has been pioneered on liquid receiving phases[65] and more recently adapted to ion-selective membranes,[66] which allows further miniaturization and the design of single use calibration free sensing systems.

References

1. Meier PC (1982) 2-Parameter Debye-Huckel approximation for the evaluation of mean activity-coefficients of 109 electrolytes. Anal Chim Acta 136:363–368
2. Morf WE (1981) In the principles of ion-selective electrodes and of membrane transport. Elsevier, New York
3. DeLaune RD, Reddy KR (2005) Redox potential. In: Hillel D (ed) Encyclopedia of soils in the environment. Elsevier, Amsterdam, pp 366–371
4. Noyhouzer T, Valdinger I, Mandler D (2013) Enhanced potentiometry by metallic nanoparticles. Anal Chem 85:8347–8353
5. Bergren AJ, Porter MD (2005) Electrochemical amplification using selective self-assembled alkanethiolate monolayers on gold: a predictive mechanistic model. J Electroanal Chem 585:172–180
6. Bakker E, Bühlmann P, Pretsch E (1997) Carrier-based ion-selective electrodes and bulk optodes. 1. General characteristics. Chem Rev 97:3083–3132
7. Jacobs E, Ancy JJ, Smith M (2002) Multi-site performance evaluation of pH, blood gas, electrolyte, glucose, and lactate determinations with the GEM Premier 3000 critical care analyzer. Point Care J Near-Patient Test Technol 1:135–144
8. Müller B, Reinhardt M, Gächter R (2003) High temporal resolution monitoring of inorganic nitrogen load in drainage waters. J Environ Monit 5:808–812
9. Lindner E, Pendley BD (2013) A tutorial on the application of ion-selective electrode potentiometry: an analytical method with unique qualities, unexplored opportunities and potential pitfalls. Anal Chim Acta 762:1–13
10. Bakker E, Pretsch E (2001) Potentiometry at trace levels. Trends Anal Chem 20:11–19
11. Morf WE, Lindner E, Simon W (1975) Theoretical treatment of the dynamic response of ion-selective membrane electrodes. Anal Chem 47:1596–1601
12. Morf WE, Pretsch E, De Rooij NF (2007) Computer simulation of ion-selective membrane electrodes and related systems by finite-difference procedures. J Electroanal Chem 602:43–54
13. Fritz JJ (1985) Thermodynamic properties of chloro-complexes of silver chloride in aqueous solution. J Solution Chem 14:865–879
14. Kakiuchi T, Yoshimatsu T, Nishi N (2007) New class of Ag/AgCl electrodes based on hydrophobic ionic liquid saturated with AgCl. Anal Chem 79:7187–7191
15. Cammann K (1996) Das Arbeiten mit Ionenselektiven Electroden, 3rd edn. Springer, Berlin
16. Schulthess P, Shijo Y, Pham HV, Pretsch E, Ammann D, Simon W (1981) A hydrogen ion-selective liquid-membrane electrode based on tri-n-dodecylamine as neutral carrier. Anal Chim Acta 131:111–116
17. Cosofret VV, Nahir TM, Lindner E, Buck RP (1992) New neutral carrier-based H+ selective membrane electrodes. J Electroanal Chem 327:137–146

18. Suzuki K, Yamada H, Sato K, Watanabe K, Hisamoto H, Tobe Y et al (1993) Design and synthesis of highly selective ionophores for lithium ion based on 14-crown-4 derivatives for an ion-selective electrode. Anal Chem 65:3404–3410
19. Diamond D, Svehla G, Seward EM, McKervey MA (1988) A sodium ion-selective electrode based on methyl p-t-butylcalix[4]aryl acetate as the ionophore. Anal Chim Acta 204:223–231
20. Yamamoto H, Shinkai S (1994) Molecular design of Calix[4]arene-based sodium-selective electrodes which show remarkably high 105.0–105.3 sodium/potassium selectivity. Chem Lett 23:1115–1118
21. Pioda LAR, Stankova V, Simon W (1969) Highly selective potassium ion responsive liquid-membrane electrode. Anal Lett 2:665–674
22. Tóth K, Lindner E, Horváth M, Jeney J, Bitter I, Agai B et al (1989) Novel bis-crown-ether derivatives for potassium sensors. Anal Lett 22:1185
23. Ghauri MS, Thomas JDR (1994) Evaluation of an ammonium ionophore for use in poly(vinyl chloride) membrane ion-selective electrodes: solvent mediator effects. Analyst 119:2323–2326
24. Suzuki K, Watanabe K, Matsumoto Y, Kobayashi M, Sato S, Siswanta D et al (1995) Design and synthesis of calcium and magnesium ionophores based on double-armed diazacrown ether compounds and their application to an ion sensing component for an ion-selective electrode. Anal Chem 67:324–334
25. Schefer U, Ammann D, Pretsch E, Oesch U, Simon W (1986) Neutral carrier based calcium(2+)-selective electrode with detection limit in the sub-nanomolar range. Anal Chem 58:2282–2285
26. Ammann D, Güggi M, Pretsch E, Simon W (1975) Improved calcium ion-selective electrode based on a neutral carrier. Anal Lett 8:709–720
27. Ren K (1989) A liquid-state copper(II) ion-selective electrode containing a complex of Cu (II) with salicylaniline. Talanta 36:767–771
28. Szigeti Z, Bitter I, Toth K, Latkoczy C, Fliegel DJ, Guenter D et al (2005) A novel polymeric membrane electrode for the potentiometric analysis of Cu2+ in drinking water. Anal Chim Acta 532:129–136
29. Bakker E (1997) Determination of unbiased selectivity coefficients of neutral carrier-based cation-selective electrodes. Anal Chem 69:1061–1069
30. Lindner E, Horvath M, Toth K, Pungor E, Bitter I, Agai B et al (1992) Zinc selective ionophores for potentiometric and optical sensors. Anal Lett 25:453–470
31. Szcepaniak W, Oleksy J (1986) Liquid-state mercury(II) ion-selective electrode based on N-(O, O-diisopropylthiophosphoryl)thiobenzamide. Anal Chim Acta 189:237–243
32. Ceresa A, Bakker E, Hattendorf B, Gunther D, Pretsch E (2001) Potentiometric polymeric membrane electrodes for measurement of environmental samples at trace levels: new requirements for selectivities and measuring protocols, and comparison with ICPMS. Anal Chem 73:343–351
33. Park SB, Matuszewski W, Meyerhoff ME, Liu YH, Kadish KM (1991) Potentiometric anion selectivities of polymer membranes doped with indium(III)-porphyrins. Electroanalysis 3:909–916
34. Badr IHA, Diaz M, Hawthorne MF, Bachas LG (1999) Mercuracarborand "Anti-Crown Ether"-based chloride-sensitive liquid/polymeric membrane electrodes. Anal Chem 71:1371–1377
35. Xiao KP, Bühlmann P, Nishizawa S, Amemiya S, Umezawa Y (1997) A chloride ion-selective solvent polymeric membrane electrode based on a hydrogen bond forming ionophore. Anal Chem 69:1038–1044
36. Malon A, Radu A, Qin W, Qin Y, Ceresa A, Maj-Zurawska M et al (2003) Improving the detection limit of anion-selective electrodes: an iodide electrode with a nanomolar detection limit. Anal Chem 75:3865–3871
37. Hutchins RS, Molina P, Alajarin M, Vidal A, Bachas LG (1994) Use of a guanidinium ionophore in a hydrogen sulfite-selective electrode. Anal Chem 66:3188–3192

38. Choi YS, Lvova L, Shin JH, Oh SH, Lee CS, Kim BH et al (2002) Determination of oceanic carbon dioxide using a carbonate-selective electrode. Anal Chem 74:2435–2440
39. Brown DV, Chaniotakis NA, Lee IH, Ma SC, Park SB, Meyerhoff ME et al (1989) Mn(III)—porphyrin-based thiocyanate-selective membrane electrodes: characterization and application in flow injection determination of thiocyanate in saliva. Electroanalysis 1:477–484
40. Stepanek R, Krautler B, Schulthess P, Lindemann B, Ammann D, Simon W (1986) Aquocyanocobalt(III)-hepta(2-phenylethyl)-cobyrinate as a cationic carrier for nitrite-selective liquid-membrane electrodes. Anal Chim Acta 182:83–90
41. Li J-Z, Pang X-Y, Yu R-Q (1994) Substituted cobalt phthalocyanine complexes as carriers for nitrite-sensitive electrodes. Anal Chim Acta 297:437–442
42. Wojciechowski K, Wroblewski W, Brzozka Z (2003) Anion buffering in the internal electrolyte resulting in extended durability of phosphate-selective electrodes. Anal Chem 75:3270–3273
43. Li J-Z, Pang X-Y, Gao D, Yu R-Q (1995) Salicylate-selective electrode based on lipophilic tin (IV)phthalocyanine. Talanta 42:1775–1781
44. Zirino A, De Marco R, Rivera I, Pejcic B (2002) The influence of diffusion fluxes on the detection limit of the jalpaite copper ion-selective electrode. Electroanalysis 14:493–498
45. Marzouk SAM, Ufer S, Buck RP, Johnson TA, Dunlap LA, Cascio WE (1998) Electrodeposited iridium oxide pH electrode for measurement of extracellular myocardial acidosis during acute ischemia. Anal Chem 70:5054–5061
46. Pungor E, Toth K (1973) Precipitate-based ISEs. Pure Appl Chem 34:105–138
47. Frant MS, Ross JW (1966) Electrode for sensing fluoride ion activity in solution. Science 154:1553–1555
48. Bühlmann P, Yajima S, Tohda K, Umezawa K, Nishizawa S, Umezawa Y (1995) Studies on the phase boundaries and the significance of ionic sites of liquid membrane ion-selective electrodes. Electroanalysis 7:811–816
49. Maj-Zurawska M, Sokalski T, Hulanicki A (1988) Interpretation of the selectivity and detection limit of liquid ion-exchanger electrodes. Talanta 35:281–286
50. Mi Y, Bakker E (1999) Determination of complex formation constants of lipophilic neutral ionophores in solvent polymeric membranes with segmented sandwich membranes. Anal Chem 71:5279–5287
51. Buhlmann P, Pretsch E, Bakker E (1998) Carrier-based ion-selective electrodes and bulk optodes. 2. Ionophores applied in potentiometric and optical sensors. Chem Rev 98:1593–1687
52. Eugster R, Gehrig PM, Morf WE, Spichiger UE, Simon W (1991) Selectivity-modifying influence of anionic sites in neutral-carrier-based membrane electrodes. Anal Chem 63:2285–2289
53. Guilbault GG, Durst RA, Frant MS, Freiser H, Hansen EH, Light TS et al (1976) Recommendations for nomenclature of ion-selective electrodes. Pure Appl Chem 48:127–132
54. Ceresa A, Pretsch E (1999) Determination of formal complex formation constants of various Pb2+ ionophores in the sensor membrane phase. Anal Chim Acta 395:41–52
55. Schaller U, Bakker E, Spichiger UE, Pretsch E (1994) Ionic additives for ion-selective electrodes based on electrically charged carriers. Anal Chem 66:391–398
56. Amemiya S, Bühlmann P, Umezawa Y (1998) A phase boundary potential model for apparently "Twice-Nernstian" responses of liquid membrane ion-selective electrodes. Anal Chem 70:445–454
57. Meier PC, Morf WE, Läubli M, Simon W (1984) Evaluation of the optimum composition of neutral-carrier membrane electrodes with incorporated cation-exchanger sites. Anal Chim Acta 156:1–8
58. Ion AC, Bakker E, Pretsch E (2001) Potentiometric Cd^{2+}-selective electrode with a detection limit in the low ppt range. Anal Chim Acta 440:71–79
59. Chumbimuni-Torres K, Rubinova N, Radu A, Kubota LT, Bakker E (2006) Solid contact potentiometric sensors for trace level measurements. Anal Chem 78:1318–1322
60. Bakker E, Pretsch E (2007) Modern potentiometry. Angew Chem Int Ed 46:2–11

61. Bakker E (2014) Enhancing ion-selective polymeric membrane electrodes by instrumental control. Trends Anal Chem 53:98–105
62. Ghahraman Afshar M, Crespo GA, Bakker E (2012) Direct ion speciation analysis with ion-selective membranes operated in a sequential potentiometric/time resolved chronopotentiometric sensing mode. Anal Chem 84:8813–8821
63. Crespo GA, Ghahraman Afshar M, Bakker E (2012) Direct detection of acidity, alkalinity, and pH with membrane electrodes. Anal Chem 84:10165–10169
64. Kim Y, Rodgers PJ, Ishimatsu R, Amemiya S (2009) Subnanomolar ion detection by stripping voltammetry with solid-supported thin polymeric membrane. Anal Chem 81:7262–7270
65. Yoshizumi A, Uehara A, Kasuno M, Kitatsuhi Y, Yoshida Z, Kihara S (2005) Rapid and coulometric electrolysis for ion transfer at the aqueouslorganic solution interface. J Electroanal Chem 581:275–283
66. Grygolowicz-Pawlak E, Bakker E (2010) Thin layer coulometry with ionophore based ion-selective membranes. Anal Chem 82:4537–4542

Chapter 10
Controlled Potential Techniques in Amperometric Sensing

L.M. Moretto and R. Seeber

10.1 Galvanic, Potentiometric, and Electrolytic Cells

Thermodynamics should strictly govern every reliable measurement supposedly performed in equilibrium conditions, as it is the case of potentiometry, in such a way that a measure that is not in agreement with thermodynamics is actually of poor meaning, if any. On the other hand, if an external power source controls the occurrence of a redox process at an electrode, as it happens in the controlled potential techniques, thermodynamics tries to manage what is going on, though not always successfully. Sometimes it happens that it does, sometimes that the system "runs after" equilibrium conditions, only approaching them more or less closely.

For this reason, by passing from a potentiometric cell, in which current absolutely does not flow, and much time is given to the electrode/solution system to achieve the equilibrium, to an electrolytic cell, which is at the basis of the controlled potential techniques, everything becomes more complex. Nernst's equation often only constitutes a point of reference, and the arising of different over voltages should be considered. Electrode thermodynamics is the basis from which electrode kinetics, with a series of phenomena differently overlapping with each other, emerges: a photograph evolves to a movie, even far from being just a series of subsequent photographs. Furthermore, the consumption of electroactive species at the electrode also implies that mass transfer to the electrode has to be taken into account.

L.M. Moretto
Department of Molecular Sciences and Nanosystems, University Ca' Foscari of Venice, Dorsoduro 2137, 30123 Venice, Italy
e-mail: moretto@unive.it

R. Seeber (✉)
Department of Chemical and Geological Sciences, University of Modena and Reggio Emilia, Via G.Campi, 183-41125 Modena, Italy
e-mail: renato.seeber@unimore.it

L.M. Moretto, K. Kalcher (eds.), *Environmental Analysis by Electrochemical Sensors and Biosensors*, DOI 10.1007/978-1-4939-0676-5_10

In principle, an electrolytic cell, similarly to a potentiometric cell, can be illustrated starting from a galvanic one. In a true galvanic cell spontaneous redox or even physical processes take place; the aim is to transform the free energy change (ΔG) accompanying the conversion of reactants into products in useful (electrical) work (w_u). The yield of transformation tends to one only if the current flowing (i) tends to zero, i.e., occurs through equilibrium states: a thermodynamically reversible process. E_{eq} is called "electromotive force" and is given by the potential difference between the two electrodes at open circuit: $E_{eq} = E_{eq,cathode} - E_{eq,anode}$ once assuming a spontaneous positive sign for the cathode, the electrode at which a spontaneous reduction occurs. Actually, the system cannot evolve through equilibrium states: the current flowing lowers the yield due to the Joule effect.

As electroanalysts, we are much more interested to the shift to a potentiometric cell of what is only formally a galvanic one, as described in detail in Chap. 9. One electrode is at a fixed potential (reference electrode) and the other electrode (indicator electrode) assumes a potential indicating that of the solution. No current flows, the aim being no more that of collecting energy (work) from the cell reaction, but rather that of performing a thermodynamic measurement on a solution: the system is under equilibrium conditions.

On the other hand, if a (continuous) voltage generator is connected in opposition to the galvanic cell, it slows down the rate of the cell reaction as far as the voltage supplied, ΔV, is lower than E_{eq} of the cell; when $\Delta V = -E_{eq}$, the process is stopped ($i = 0$). Further increase of $|\Delta V|$ reverses the process: it is forced to a non-spontaneous sense in an electrolytic cell. These different situations are sketched in Fig. 10.1. The *minus* sign in front of E_{eq} indicates that the voltage source is "in opposition" to the cell, ΔV being intrinsically negative in order to reflect what required by the Kirchhoff's principle.

10.2 From the Two-Electrode to the Three-Electrode Cell

Two electrodes are involved in the electrolytic cell reported in Fig. 10.2: the so-called working electrode (WE) and the auxiliary (AE) or counter electrode. The denominations suggest that we are interested in what happens at one of the two electrodes, namely the WE. In a similar cell the following relationship holds:

$$-\Delta V = E_{eq} + \eta + iR_s = E + iR_s \tag{10.1}$$

where ΔV, in Volt, is the potential difference that should be applied (in opposition) to the cell in order to make the current intensity i, in A per unit area, flow through: $E = E_{anode} - E_{cathode}$, both E_{anode} and $E_{cathode}$ being obviously different from the relevant equilibrium values, even in respect to sign; η is the sum of the absolute values of the shifts of the anodic and cathodic actual potentials with respect to the relevant equilibrium values $[E_{anode} - E_{cathode} - (E_{eq,cathode} - E_{eq,anode})]$. In other words, η is the sum of the anodic and the opposite of the cathodic overvoltages

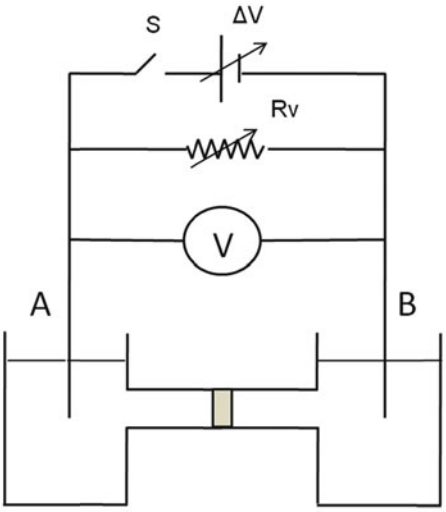

Fig. 10.1 Sketch of the three different circuits accounting for: (1) a working galvanic cell when S, an ON/OFF switch, is open, for finite values of the variable resistance, $Rv - A$ is the (positive) cathode and B is the (negative) anode; (2) a potentiometric cell when S is open and $Rv \rightarrow \infty$; (3) an electrolytic cell when S is closed and $|\Delta V| > E_{eq} - A$ is the (positive) anode and B is the (negative) cathode. V high input impedance voltmeter. The ΔV dc potential generator is such that electrodes with similar signs of those of the galvanic cell are connected

Fig. 10.2 Scheme of a two-electrode electrolytic cell with relevant circuit

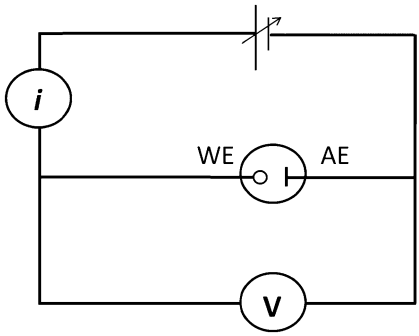

necessary to render E_{anode} and $E_{cathode}$ positive and negative enough, respectively, to make the i current flow: $\eta = \eta_{anode} - \eta_{cathode}$; iR_s accounts for the ohmic drop in solution, R_s, in Ohm, being the resistance of the solution between anode and cathode. Let's evidence that $E_{eq,anode}$, $E_{cathode}$, and $\eta_{cathode}$ are intrinsically negative:

$$E_{anode}(> 0) = -E_{eq,anode} + \eta_{anode} \tag{10.2}$$

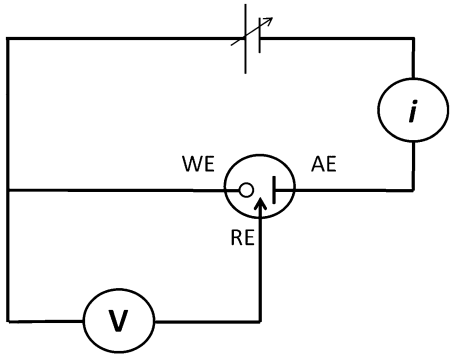

Fig. 10.3 Three-electrode cell with relevant circuit

$$E_{cathode}(<0) = -E_{eq,cathode} + \eta_{cathode} \tag{10.3}$$

In Eq. (10.1) ΔV, i and E_{eq} are known quantities, R_s can be computed independently, or made, as discussed hereafter, small enough to render the iR_s term negligible as a first approximation. However, since the interest lies in knowing either E_{anode} or $E_{cathode}$, depending on which one is WE, we need knowing $E_{WE} = E_{eq,WE} + \eta_{WE}$; however, we only know η, i.e., the sum of the over voltages of WE and AE.

Apart from the artifact to minimize η_{AE} by using AE large enough to make the density current as low as possible,[1] which is a rough, poorly satisfactory approach, accurate knowledge of the WE potential requires the use of a three-electrode circuit (see Fig. 10.3).

ΔV is applied between WE and AE, and the current flowing is correspondingly measured; however, the potential difference between WE and a suitable reference electrode (RE) is measured in an additional circuit, in which current is prevented from flowing by the high impedance voltmeter (V). This voltmeter measures the potential difference between WE and RE corresponding to the current passing in the "primary" circuit. Well-known poorly polarizable electrodes, such as saturated calomel electrode or Ag/AgCl are used as the RE. Figure 10.4a shows a typical three-electrode single compartment cell for amperometric tests.

Although the three-electrode circuit actually furnishes adequate measures in most situations, the electric field generated in the solution by the WE-AE system induces different values of Φ, the "inner" or Galvani's potential, in the different points of the solution. This implies that a potential difference exists between WE

[1] as it will be clear in the following, the extent of overvoltage depends on the current density, rather than on the overall current. Just two examples to account for this fact: in the case of "charge transfer overvoltage" the electrode kinetics is accounted for by kinetic constants and by the concentrations at the electrode, that in no way depend on the electrode area. Similarly, as to the "concentration overvoltage," once more the finite values of the concentration gradient and, consequently, of the concentration flux, are the sources of the relevant overvoltage, rather than the concentration flow rate, i.e., at the whole electrode surface.

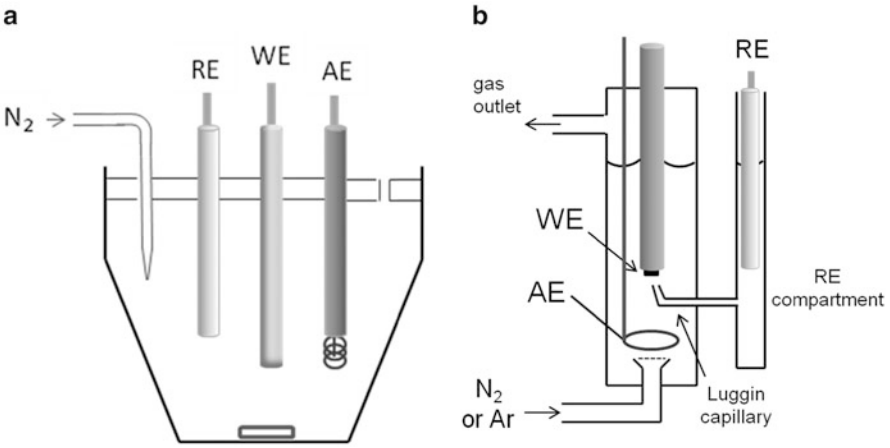

Fig. 10.4 (**a**) Typical three-electrode single compartment cell; (**b**) two-compartment cell with the Luggin capillary for the RE

and RE ascribable to an ohmic drop in solution: iR_u, the so-called uncompensated ohmic drop. Partial solution to this drawback is achieved by inserting the RE electrode into a compartment containing the solvent with the supporting electrolyte that ends with a capillary (Luggin capillary) positioned as close as possible to the WE surface. No current flows between the end of the capillary and RE inside the relevant compartment and, consequently, no change in Φ arises between the two points: the residual iR_u drop is then between the WE surface and the end of the capillary. This term may be further minimized by instrumental artifacts such as positive feedback or current interrupt, or by suitably correcting the actual WE potential by the term iR_u, once R_u has been computed by a conductivity bridge. Such a "refinement" is necessary whenever high currents are involved (see, for example linear sweep voltammetry at high potential scan rates) or particularly high accuracy is required in the WE potential estimate. A sketch of an effective cell possessing the adequate WE-AE geometry, with a Luggin capillary that can be suitably positioned, is shown in Fig. 10.4b. The geometry of the WE-AE system, in fact, should be suitable to assure uniform potential on the WE surface, and the AE surface area must be much wider than that of WE, in order to minimize the AE polarization.

The instrument devoted to manage the experiment employing a three electrode circuit is called "potentiostat." It fixes the potential between WE and RE at a selected value, either constant or variable with time according to the chosen potential waveform, through the imposition of a suitable voltage between WE and AE. Actually, a more or less complex circuit based on operational amplifiers achieves this goal by different approaches. Details on the instrumentation for electroanalysis are found in the reference books suggested at the end of the chapter.

The extent of occurrence of non-spontaneous oxidation or reduction induced by suitable polarization of WE imposes a distinction between two main cases. First,

we deal with the case in which the charge spent due to a small current intensity at a WE with small area does not change significantly the composition of the solution: the current as a function of time or of applied potential has only the role to give account of how the electroactive species responds to the potential applied to WE. This may induce charge transfer from the electrode to the analyte according to different energy pathways, generating species more or less stable, even possibly oxidizable in their turn, etc. A number of possible electrode mechanisms may be activated, only acting, in any cases, on a tiny quantity of electroactive species.[2,3] Most important from an electroanalytical point of view: reliable highly repeatable and reproducible responses are sought, that are characterized by a (possibly linear) dependence of the current intensity on the analyte concentration in solution.

10.3 Electrode Thermodynamics and Kinetics

The user of electrochemical methods of analysis may just aim at collecting information about the electrochemical characteristics of a sample, in order to perform qualitative or quantitative analyses of one or more species. He/she does not necessarily need making the electrochemical thermodynamic and kinetic black box as white as it has to be for an electrochemical researcher. However, in order to suitably choose and exploit the techniques offered by the instrument's menu, the

[2] The knowledge of the operative electrode mechanism is of fundamental importance in a variety of situations, from analytical to industrial applications of electrochemical methods. In electroanalysis the current at a given time or potential is taken as an estimate of the concentration of the electroactive species in solution. A linear relationship between current intensity and concentration represents the case of choice. However, not always linearity is induced by the underlying electrode mechanism, nor the relationship should be forced to linearity, once repeatability and reproducibility are carefully verified.

[3] In the spectroscopic absorption measurements, the interaction of the radiation with matter causes alteration of the probe, namely of the intensity of the exiting radiation. However, the "flux of photons" that immediately afterwards crosses the samples is not affected by what happened to the previous photons: the probe is unaltered and in the case of most, though not all spectroscopies, also the sample does not undergo any changes as a consequence of the measurement. In voltammetric measurements the probe, viz. the electrode, also interacts with the sample, which is essentially unaltered; it is however possible that the probe is "modified" by the occurrence of the interaction: the effect of the modification may persist, inducing changes in the behavior of the probe afterwards. From these drawbacks the "history" of the electrode becomes one of the most meaningful limits of the voltammetric techniques. Polarography at dropping mercury electrode minimizes the history of the probe, since the electrode is periodically a new one, at a frequency that can minimize the effects of poisoning adsorption or other events altering the electroactive surface. Subsequent drops may be figured as the flux of photons, even if it is evident that the total absence of "history" proper of radiations is anyway far from being achieved, owing to the finite length of the life time of each drop. In solid electrodes, the history is the cause of eventual poor repeatability, or even of poor reliability, of the responses.

box should be lit a bit up, and basic concepts should be necessarily acquired. This is true for any analytical techniques, but even more for the electrochemical ones, which most often require not to be "passive" in front of the results obtained by only "pushing the button."

At the very beginning of this chapter it was anticipated that, at variance with potentiometry, controlled potential techniques only incidentally deal with equilibrium situations. Noteworthy, in any cases, equilibrium is meant to possibly exist between the electrode and the closest layer of solution. The reversible character of the electrode process:

$$O^z + ne \rightleftharpoons R^{z'} \tag{10.4}$$

is expressed by the observance of the Nernst's law under the form:

$$E = E^{0'} + \frac{R_g T}{nF} \ln \frac{C_O(x=0)}{C_R(x=0)} \tag{10.5}$$

n indicates the number of exchanged electrons (e) and both the oxidized and reduced species, O and R bearing z and z' charge, respectively, are soluble and stable in solution[4] (uncomplicated reversible charge transfer process)[5]; $E^{\circ\prime}$ is the formal potential of the O/R redox couple, linked to the standard potential E° by the relationship $E^{\circ\prime} = E^\circ + (R_g T/nF)\, ln\, \gamma_O/\gamma_R$[6], γ_O and γ_R being the activity coefficients of O and R, respectively; R_g is the molar gas constant, F is the Faraday constant = 96485.34 Coulomb, T is the absolute temperature, C_O and C_R the

[4] For the sake of simplicity, along the whole chapter, unless otherwise specified, this simple process will be considered. Different mechanisms are often operative in electrode reactions of analytical interest; however, the treatment of these cases requires too much room for a book devoted to the issue of electroanalysis for environmental studies. On the other hand, the simplest mechanism constitutes the basis for the more complex ones. References to specific literature are found in the books of general interest that are listed at the end of the chapter. Noteworthy, a reduction reaction is considered, but negative sign is given in the following to the corresponding cathodic current [see from Eq. (10.5) onwards]. Such a choice is opposite to the "polarographic convention." Electroanalysis was born thanks to the diffusion of amperometric techniques at Hg electrodes, at which reductions are for the very most part studied. It was then spontaneous to assign positive values to the most often encountered currents, so that this habit still survives, despite the subsequent diffusion of electrodes at which oxidations, i.e., flow of anodic currents, are induced.

[5] Bare electrodes, i.e., electrodes in which the interface with the solution consists of a metal such as Pt or Au, or of C, such as glassy carbon, are considered in this chapter. The diffusion of modified electrodes, which will be dealt with in different chapters of the book, offers a variety of solutions and of situations. In principle, everything becomes more versatile, more powerful, and more flexible and, as it often happens in similar cases, also more complex.

[6] In the very well-known relationship $a = \gamma C$, γ represents the activity coefficient. Throughout the whole chapter we make reference either to the activity, e.g., in the frame of rigorous thermodynamic issues, or to the concentration, e.g., when dealing with transfer of mass.

concentration of O and R species, respectively, and x represents the distance from the electrode surface. From here onwards, E indicates the potential of a single electrode, either assumed spontaneously or imposed.

Equation (10.5) derives from the general expression that holds for any equilibrium:

$$\sum\nolimits_i \nu_i \mu_i = 0 \tag{10.6}$$

though, actually, since the reaction deals with charged species, it should be expressed by electrochemical potentials, $\overline{\mu}_i$:

$$\sum\nolimits_i \nu_i \overline{\mu}_i = 0 \tag{10.7}$$

where

$$\overline{\mu}_i = \mu_i + z_i F \Phi_i^{s,M} \tag{10.8}$$

$\overline{\mu}_i$ is hence given by the sum of a chemical, μ_i, and of an electrical, $z_i F \Phi_i^{s,M}$, component. z_i is the electrical charge of the charged species, ν_i the relevant stoichiometric coefficient in the reaction considered, and Φ the Galvani's or inner potential of the solution (s) or metal (M) phase in which the charged species i-th is considered.

The chemical potential for the i species, i.e., O or R in the solution, and e in the metal phase, is defined by the well-known relationship:

$$\mu_i = \mu_i^0 + R_g T \ln a_i = \left(\frac{dG}{dn_i}\right)_{p,T,n_{j\neq i}} \tag{10.9}$$

Analogously, the electrochemical potential may be defined as:

$$\overline{\mu}_i = \left(\frac{d\overline{G}_i}{dn_i}\right)_{p,T,n_{j\neq i}} \tag{10.10}$$

In explicit terms:

$\mu_O^s = \mu_O^{0,s} + R_g T \, ln \, a_O^s$, $\mu_R^s = \mu_R^{0,s} + R_g T \, ln \, a_R^s$, $\mu_e^M = \mu_e^{0,M}$ (the activity of electrons is accounted for by the inner potential of the phase); $\mu_O^{0,s}$, $\mu_R^{0,s}$ and $\mu_e^{0,M}$ are the standard chemical potential of O and R species in solution and of e in the metal phases, respectively. a_i is the activity of the species i, and G and $\overline{G}_i$ indicate the chemical and electrochemical free energy of the system, respectively. $\overline{\mu}_i$ indicates the

electrochemical potential of O and R in solution and of e in the metal phase, in accord with Eq. (10.8). It follows that it also holds[7]:

$$\overline{\mu}_e^M = \mu_e^{0,M} - F\phi^M \tag{10.11}$$

From the equations above, in particular from Eqs. (10.7) and (10.8), the equilibrium condition is expressed by:

$$\sum \nu_i \mu_i = -F \sum \nu_i z_i \Phi_i^{s,M} \tag{10.12}$$

A definition of the electrode potential E may be drawn out by properly expressing the right hand side term of Eq. (10.12), in terms of difference in electrical energy content between products and reagents ($n = z - z'$):

$$z' F\Phi^s - \left(zF\Phi^s + nz_e F\Phi^M\right) = nF\left(\Phi^M - \Phi^s\right) = nF\Delta\Phi = nFE \tag{10.13}$$

Equation (10.13) expresses the electrode potential, E, as the difference between the inner potential of the metal, Φ^M, and that of the solution, Φ^s.

Equation (10.12) may be hence expressed as:

$$\sum\nolimits_i \nu_i \mu_i = -nFE \tag{10.14}$$

and

$$\sum\nolimits_i \nu_i \mu^\circ{}_i = -nFE^0 \tag{10.15}$$

From Eqs. (10.1)–(10.15) it follows that:

$$E = E^0 + \frac{R_g T}{nF} ln \frac{a_O}{a_R} \quad \text{(Nernst equation)} \tag{10.16}$$

that strictly resembles Eq. (10.5), however expressed as a function of activities instead of concentrations; zero distance from the electrode may be meant.

Indeed, while potentiometry refers to a static system, in which no reaction takes place, the current flow in controlled potential techniques is the cause of occurrence of a redox reaction: the electrode potential is imposed by an external source and eventually changes with time. Considering what happens at WE, reversibility

[7] The electrochemical potential of electrons in a given phase, $\overline{\mu}_e^\alpha$, is the Fermi level or Fermi energy. The Fermi level represents the average energy of available electrons in phase α, related, similarly to any charged species, to the chemical potential of electrons in that phase, $\mu_e^{0,\alpha}(=\mu_e^{0,\alpha})$, and the inner potential of α. In a solution phase, it may be computed from the electrochemical potentials of the oxidized and reduced species. For example, for a solution containing Fe(III) and Fe(II): $\overline{\mu}_e^\alpha = \overline{\mu}_{Fe(III)}^\alpha - \overline{\mu}_{Fe(II)}^\alpha$.

requires that the ratio between the activities/concentrations of the species involved in the half-reaction is in perfect agreement with the electrode potential, according to Eq. (10.5). On the other hand, it is well known from basic thermodynamics that a reversible process is requested to occur through equilibrium states. This is an ideal condition, only possible for systems that, in principle, cover a finite length path across states far from each other by subsequent infinitesimal quantities, e.g., through infinitesimal changes in composition. This is something not belonging to the real world. The so-called reversible, though real processes, occur with a rate slow enough not to shift the system as a whole "too much away from" equilibrium states, expressed in our case by the Nernst's equation. Otherwise, different degrees of non-reversibility are proper of the process. It is evident that reversible or non-reversible behavior will be exhibited in dependence both of intrinsic properties of the redox couples and of the experimental conditions adopted, e.g., fast or slow changes of WE potential, requiring more or less speed in reaching a new equilibrium state.

Getting to the point, by considering the actual occurrence of a charge transfer at the electrode, different situations may occur: (1) reversible charge transfer; (2) totally irreversible charge transfer; (3) quasi-reversible charge transfer. In the first case, as above discussed, equilibrium conditions hold and the charge transfer occurs at such a rate to make the concentrations of the two species at the electrode be in agreement with Nernst's law:

$$\frac{C_O(x=0)}{C_R(x=0)} = exp\left[\frac{nF}{R_gT}\left(E - E^{0'}\right)\right] \tag{10.17}$$

We don't care for the moment of possible changes of $C_O(x=0)$ and $C_R(x=0)$, x indicating the distance from the electrode; they are fixed to a constant value, not taking into account any steps that condition their values, the charge transfer step itself included. The mass transport processes to/from the electrode are assumed to occur at an infinite rate: they will be only considered in a further step.

As it is common practice in basic kinetics, expressions are formulated in which the overall rate is the vector sum, i.e., the scalar difference, between the rate of the forward (reduction, in the present case) and the backward (oxidation) reaction rates:

$$v = k_{h,f}C_O(x=0) - k_{h,b}C_R(x=0) \tag{10.18}$$

where subscript h accounts for the heterogeneous nature of the charge transfer. $k_{h,f}$ and $k_{h,b}$ are kinetic constants, expressed in s^{-1}, function of the activation electrochemical free energies for forward and backward reaction, respectively; their units account for a rate referred to unit (electrode surface) area rather than to unit volume.

As discussed above, the difference of the electrochemical potentials, i.e., of the molar electrochemical free energy, between products and reactants defines the thermodynamics of the process. To account for the kinetics, the analogous energy

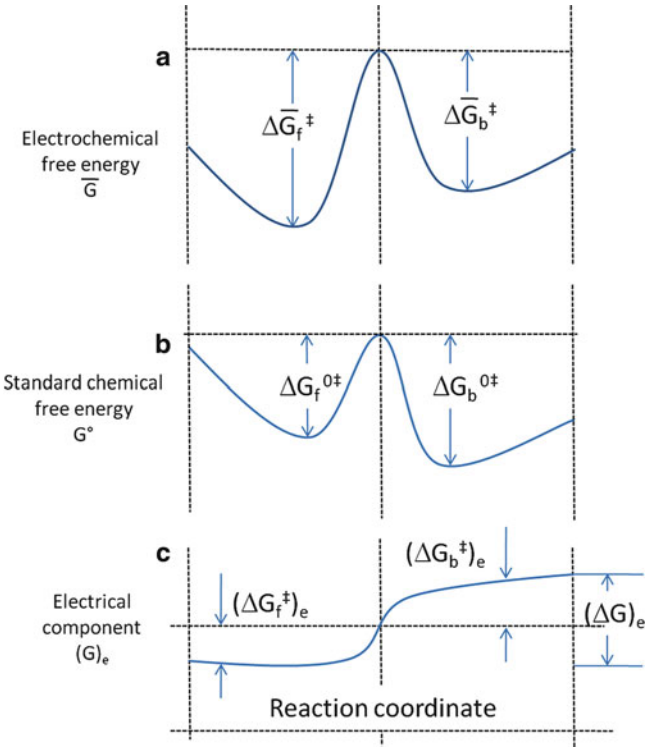

Fig. 10.5 Plots of molar electrochemical free energy and relevant chemical and electrical components along the reaction pathway

content of every intermediate state, in particular of the transition state, should complete the energy plot, presented in Fig. 10.5.[8]

Noteworthy, similarly to the thermodynamic equilibrium between electrode and redox species in solution, also the kinetics of the charge transfer process is not only a function of pressure and temperature, as it happens in the case of the "usual" chemical reactions: the electrode potential, expressed as $\Phi^M - \Phi^s = \Delta\Phi\ (=E)$, i.e., the difference between the inner potential of the electrode and of the solution, respectively, plays a fundamental role. From a thermodynamic point of view, it may impose any

[8] The term "reaction coordinate," reported qualitatively in the plots, assumes however quantitative meaning—with a precise quantity and relevant units—once the reaction path is followed through a quantity suitable to describe its progress. This quantity may be related, for instance, to (1) the bond length if a bond breaks or forms, e.g., in the reduction of iodine to iodide ions or oxidation in the opposite direction, respectively; (2) the angle formed by two atoms of one or two ligands and the metal in a complex, when passing, for instance, from a (regular) square planar coordination (90°) to a (regular) tetrahedral (109°) coordination by changing the oxidation state of the metal/complex; (3) the shortening of the bond length between the metal and one atom of the ligand set once the metal or complex are oxidized, and so on.

value to the C_O/C_R ratio, acting on the energy levels of reactants and products; in a kinetic context, it may favor, slow down, stop, and even reverse the direction of the charge transfer, modifying the activation energy of forward and backward reactions. The "chemical" and the "electrical" components of $\overline{\mu}$, i.e., μ and ϕ terms, should be added to each other, point by point, along the "reaction coordinate" abscissa, to account for the energy content of the system evolving from reactants to products or vice versa. This means that the plot (**a**) in Fig. 10.5 results from the sum of plots (**b**) and (**c**). In correspondence to the minima of plot (**a**) one finds the molar electrochemical free energy content of reactants and products, respectively, which define the thermodynamics of the system; for intermediate values of the abscissa the energy content along the reaction path is found. In particular, making reference to the relative maximum of the curve, i.e., to the transition state, the activation energies for forward and backward reactions, respectively, are expressed by:

$$\Delta\overline{G}_f^{\#} = \Delta G_{c,f}^{0\#} + \beta nF\Delta\Phi \tag{10.19}$$

and

$$\Delta\overline{G}_b^{\#} = \Delta G_{c,b}^{0\#} - (1-\beta)nF\Delta\Phi \tag{10.20}$$

where β is the so-called symmetry factor, accounting for the distribution of the inner potential along the reaction path, $\Delta\overline{G}_f^{\#}$ and $\Delta\overline{G}_b^{\#}$ are the forward and backward activation energy, respectively, and $\Delta G_{c,f}^{0\#}$ and $\Delta G_{c,b}^{0\#}$ the corresponding chemical energy components. The transition state, from an electrical energy point of view, is not far from half way, which means that $0.3 \leq \beta \leq 0.7$, resulting often quite close to 0.5.

Let's define the chemical components of forward and backward kinetic constants, respectively, as inferred from plot (**b**) in Fig. 10.5:

$$k_{c,f} = \frac{k_B T}{h} exp\left[-\frac{\Delta G_{c,f}^{0\#}}{R_g T}\right] \tag{10.21}$$

and

$$k_{c,b} = \frac{k_B T}{h} exp\left[-\frac{\Delta G_{c,b}^{0\#}}{R_g T}\right] \tag{10.22}$$

where k_B and h are the Boltzmann and Planck constants, respectively. The electrical component of the activation energy should be also taken into account in order to express the dependence on the electrode potential of the heterogeneous kinetic constants for forward and backward reactions, respectively:

$$k_{h,f} = \frac{k_B T}{h} exp\left[-\frac{\Delta\overline{G}_f^{\#}}{R_g T}\right] = k_{c,f} exp\left[-\frac{\beta nF\Delta\Phi}{R_g T}\right] \tag{10.23}$$

and

$$k_{h,b} = \frac{k_B T}{h} exp\left[-\frac{\Delta \overline{G}_b^{\#}}{R_g T}\right] = k_{c,b}\, exp\left[\frac{(1-\beta) nF \Delta \Phi}{R_g T}\right] \tag{10.24}$$

Equations (10.18), (10.23), and (10.24), together with Faraday's law ($Q = n\ F\ n_{mol}$, Q = moles of Coulombs used and n_{mol} = number of moles reacted) give everything required for writing explicitly Eq. (10.25). The Coulombs spent per unit area in a unitary time length express the current density:

$$i(t) = nF\left[-k_{h,f} C_O(x=0,t) + k_{h,b} C_R(x=0,t)\right] \tag{10.25}$$

Noteworthy, C_O and C_R not only depend on the distance from the electrode, x, which is the source of the perturbation possibly inducing a charge transfer, but also on time, t, indicating the time elapsed from the start of the electrode polarization. C_O and C_R will be explicitly considered as functions of both x and t variables from here onwards.

Equation (10.25) evolves to different possible forms of the Butler–Volmer equation, which predicts the dependence on the potential of the density current, O and R concentrations at the electrode being supposed not to change in dependence of the flux of current, i.e., of charge. A first one makes use of $k_{h,s}$, the standard heterogeneous kinetic constant, i.e., the kinetic constant of both forward and backward reaction at $E = E^{\circ\prime}$:

$$i(t) = nFk_{h,s}\left\{-C_O(0,t)\, exp\left[-\frac{\beta nF\left(E-E^{0'}\right)}{R_g T}\right] + C_R(0,t)\, exp\left[\frac{(1-\beta) nF\left(E-E^{0'}\right)}{R_g T}\right]\right\} \tag{10.26}$$

An alternative form makes use of i_0, i.e., the so-called "exchange current," flowing with equal intensity in the two opposite senses at $E = E_{eq}$, η expressing the charge transfer overvoltage, i.e., the distance between the applied and the equilibrium potential of WE:

$$i(t) = i_0\left\{-exp\left[-\frac{\beta nF\eta}{R_g T}\right] + exp\left[\frac{(1-\beta) nF\eta}{R_g T}\right]\right\} \tag{10.27}$$

$k_{h,s}$ and i_0 can only be computed by extrapolation; they are the higher, the higher the reversibility degree of the charge transfer. For a totally irreversible charge transfer a finite potential range can be identified within which both $k_{h,f}$ and $k_{h,b}$ assume negligible values. No similar range exists for a quasi-reversible charge transfer.

Figure 10.6 shows the plot of the cathodic and anodic components of the current, together with the relevant sum, for two different reversibility degrees.

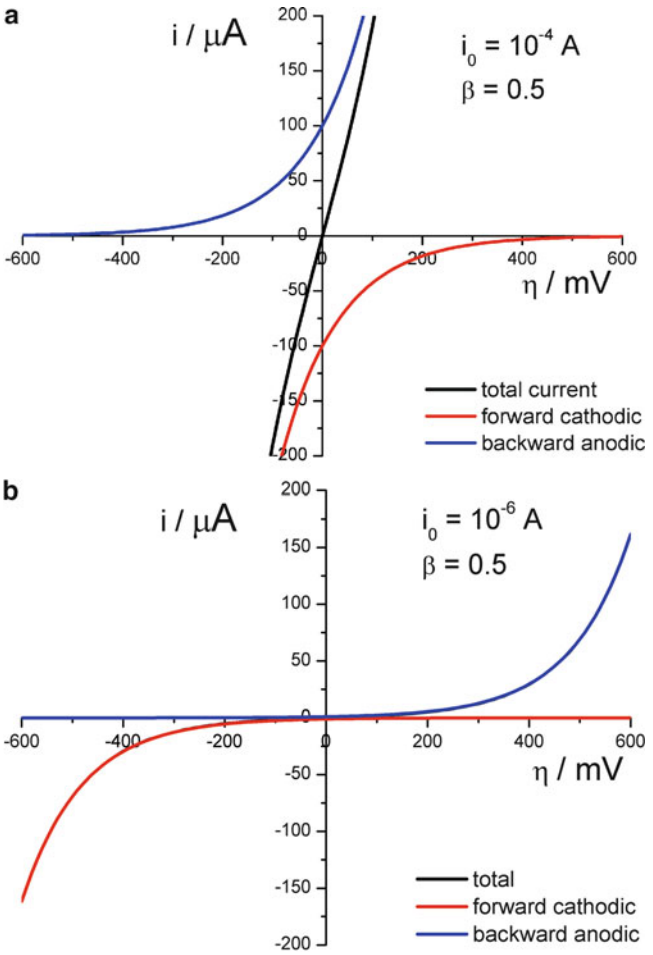

Fig. 10.6 Total currents with relevant cathodic and anodic components, i.e., forward and backward currents, respectively, as a function of the overvoltage for two different reversibility degrees, as simply computed by the Butler–Volmer expression in Eq. (10.27); in plot (**b**) the total current coincides with the anodic (*red line*) or cathodic (*blue line*) component, for positive and negative values of η, respectively

As evidenced at the beginning of the treatment of the electrode kinetics, the Butler–Volmer equation only accounts for the kinetics of the charge transfer, once supposing that the supply of electroactive species at the electrode occurs at infinite rate, i.e., assuming that infinite rate of mass transfer is operative. This is out of the reality: a finite rate characterizes the mass transport. As a consequence of the charge transfer, in fact, mass transfer of reactant and product to and from the electrode surface, respectively, is induced.

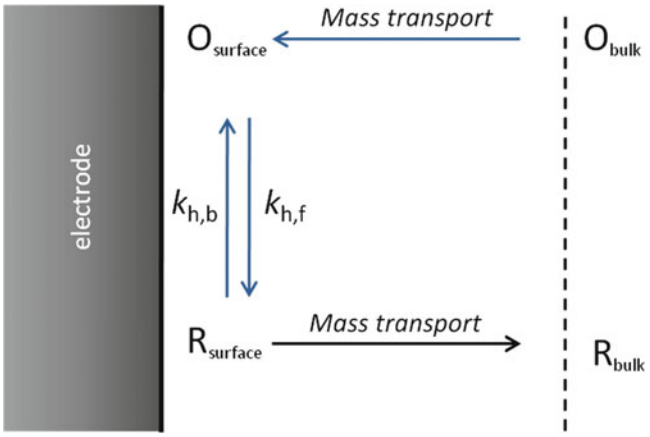

Fig. 10.7 Scheme for a reduction reaction at an electrode surface—uncomplicated charge transfer involving species both soluble in the solution phase

In the considered electrode process three formally distinct steps concur to make the process proceed as a whole:

1. Electron transfer at the electrode that induces
2. *O* transport to the electrode
3. concomitant *R* transport away from the electrode.

These three steps are schematically represented in Fig. 10.7. Noteworthy, this simple scheme only accounts for the case of a bare electrode surface. Much more numerous and more complex steps account for even the simplest electrode process occurring at differently modified electrodes. Other chapters in this book describe the proposed modifications, to which a true renaissance of electroanalysis has to be ascribed. It is obvious that the comprehension of what happens at similar complex electrode systems requires knowing how to deal with the simplest ones.

Figure 10.8 sketches the three different mass transport mechanisms at a planar electrode: diffusion, migration and convection, respectively.

One-dimensional mass transfer is operative once the geometries of WE and of the cell are suitable, as described below for pure diffusion. In the case that all three mass transfer processes are operative, it is accounted for by the Nernst–Planck equation. The first term accounts for diffusion, the second one for migration, and the third one for convection:

$$J(x,t) = -D\frac{\partial C(x,t)}{\partial x} - \left(\frac{zFDC}{R_gT}\right)\frac{\partial \varnothing(x,t)}{\partial x} + C(x,t)V(x,t) \qquad (10.28)$$

where J is the flux of the diffusing species, in mol cm^{-2} s^{-1} when D, the relevant diffusion coefficient, is expressed in cm^2 s^{-1} and C in mol cm^{-3}. V accounts for the velocity of the volume element of the solution moving in the x direction.

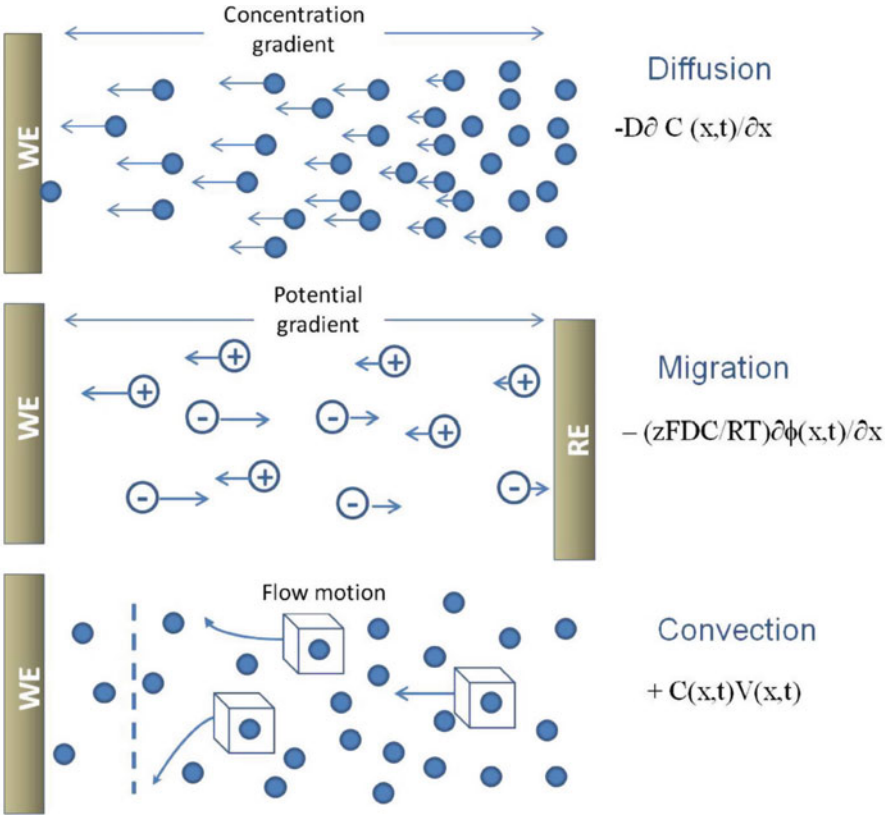

Fig. 10.8 Mechanisms of mass transport at a planar electrode. Adapted from (Wang 2000). The mathematical expressions for the contributions of the three different mass transfer mechanisms to the total flux of the electroactive species are given

In particular, most of the amperometric techniques tend to make the analysis of the relevant responses as easy as possible by operating under suitable experimental conditions, so that diffusion constitutes the largely predominant mass transfer mechanism. Diffusion accounts for the intrinsic capability of O to move inside the solution under the driving force of the relevant concentration gradient, modulated by the diffusion coefficient D_o. Migration is minimized by addition of an inert salt (supporting electrolyte), most inert as possible with respect to the chemical system in solution, as well as to the polarized WE, within an as wide as possible potential window. The supporting electrolyte is present at a high enough concentration—typically not less than 50 to 100 times the electroactive species—to assure electroneutrality everywhere inside the solution, hence to compensate the excess of negative (or positive) charge arising in the layer adjacent to the electrode as a consequence of the charge transfer. Convection arises by movement of the solution with respect to the electrode or vice versa. In some techniques (see below) convection does occur, however under precisely controlled conditions; otherwise, it is

prevented from occurring by avoiding any movement of the solution and of the electrode.

Disks with ca. 2 or 3 mm diameter constitute conventional electrodes for amperometric measurements[9]. Despite the low surface area, the laws governing semi-infinite linear diffusion can be applied as quite a good approximation. This leads to consider diffusion along a single direction, orthogonal to the electrode surface: the diffusional system is supposed not to suffer from edge effects (see Chap. 15). Furthermore, the walls of the cell are far enough from the electrode surface—actually 1 mm is a well sufficient distance—not to be reached by the perturbation arising at the electrode (see below).

Fick's I and II laws account for the concentration values at different times, at different distances from the electrode, once suitable boundary conditions are established.

$$J_O(x,t) = -D_O\left(\frac{\partial C_O}{\partial x}\right)_{x,t} \text{ Fick's I law for electroactive species } O \qquad (10.29)$$

$$\left(\frac{\partial C_O}{\partial t}\right)_{x,t} = D_O\left(\frac{\partial^2 C_O}{\partial x^2}\right)_{x,t} \text{ Fick's II law for electroactive species } O \qquad (10.30)$$

Fick's I law expresses the flux of diffusing species across a unit area orthogonal to the diffusion direction, hence parallel to the electrode, at a distance x from the electrode at a time t; for $x = 0$ the flux is related to the current density by the relationship, derived once more from Faraday's law:

$$i(t) = nF\,J_O(0,t) \qquad (10.31)$$

Fick's II law gives account for the instantaneous change in concentration of the diffusing species in a volume with dx thickness and unitary cross sectional area perpendicular to the diffusion direction, as expressed by the difference between the relevant entrance and exit fluxes.

The following (initial and) boundary conditions allow the solution of the "boundary value problem" for a reversible charge transfer involving stable soluble species (the so-called "uncomplicated charge transfer process"):

[9] Distinction should be made between the value of the geometrical and the electrochemical (active) areas of an electrode. The meaning of geometric area is obvious. The electrochemical area should be computed on the basis of the response to a benchmark species in one of the techniques discussed in the following. Once the diffusion coefficient of the species chosen, typically one partner of a reversible redox couple, such as the hexacyanoferrate anions in water or bis(cyclopentadienyl)iron (II)—ferrocene—in organic solvent, is known, the ratio between the measured current and the expected current density constitutes a reliable estimate of the electrochemical area. The dependence of this area value on the exact nature of the electroactive species may be discarded as a first approximation, once poisoning of the electrode and the occurrence of unknown complex electrode mechanisms can be excluded.

$$O^z + ne^- \rightleftharpoons R^{z'}$$

The proper Fick's II law expressions for species O and R are:

$$\frac{\partial C_O(x,t)}{\partial t} = D_O \frac{\partial^2 C_O(x=0,t))}{\partial x^2} \text{ and } \frac{\partial C_R(x,t)}{\partial t} = D_R \frac{\partial^2 C_R(x=0,t)}{\partial x^2}, \text{ respectively.}$$

Indicating with ${C_O}^b$ and ${C_R}^b$ the initial ($t=0$) O and R concentrations, respectively, which also coincide with the concentrations in the "bulk" of the solution—actually at a large enough distance from the electrode surface (see below)—the following initial conditions hold:

$$\begin{matrix} t=0 \\ x \geq 0 \end{matrix} \begin{cases} C_O(x,0) = C_O^b \\ C_R(x,0) = C_R^b \ (= 0 \text{ for the case of species } O \text{ only present intially in the solution}) \end{cases} \tag{10.32}$$

and the two boundary conditions:

$$\begin{matrix} t>0 \\ x \to \infty \end{matrix} \begin{cases} C_O(x,t) = C_O^b \\ C_R(x,t) = C_R^b \ (= 0 \text{ for the case of species } O \text{ only present intially in the solution}) \end{cases} \tag{10.33}$$

$$\begin{matrix} t>0 \\ x=0 \end{matrix} \begin{cases} -D_O \dfrac{\partial C_O(0,t)}{\partial x} = D_R \dfrac{\partial C_R(0,t)}{\partial x} \left(= \dfrac{i(t)}{nF} \right) \\ \dfrac{C_O(0,t)}{C_R(0,t)} = exp\left[\dfrac{nF}{R_g T} \Big(E(t) - E^{0'} \Big) \right] \end{cases} \tag{10.34}$$

The flux of electrons at the unitary area electrode, *i(t)*, may be obtained by:

$$i(t) = nFJ_O(0,t) = -nFD_O \frac{\partial C_O(0,t)}{\partial x} = -nFJ_R(0,t) = nFD_R \frac{\partial C_R(0,t)}{\partial x} \tag{10.35}$$

Let's recall the assumption of a negative sign for a cathodic current. For a quasi-reversible charge transfer:

$$O^z + ne \overset{k_{h,s};\beta}{\rightarrow} R^{z'}$$

the Butler–Volmer expression substitutes for the Nernst's equation:

$$D_O \frac{\partial C_O(0,t)}{\partial x} = k_{h,f} C_O(0,t) - k_{h,b} C_R(0,t) \tag{10.36}$$

In a quasi-reversible charge transfer $k_{h,f}$ and $k_{h,b}$ are both significantly different from 0, while $k_{h,b} = 0$ in a totally irreversible reduction, over a potential range significantly different from zero.

More complex equations hold for electrode mechanisms in which events additional to diffusion take place, such as chemical reactions in charge of the reactant or of the product, adsorptions at the electrode, etc. It is noteworthy that the boundary condition $x \to \infty$ can be, in practical calculations, substituted by $x = 6\sqrt{D_O t}$ where t is the time length of the experiment[10]. Such a distance defines the "diffusion layer," *viz*. the layer of solution within which the concentration of electroactive species significantly differs from that in the "bulk". This means that for a species possessing $D = 10^{-5}$ cm^2 s^{-1}, which is a typical value for common systems in aqueous solvent, an experiment as long as 10 s allows meaningful expansion of the perturbation arising at the electrode not further than 0.6 mm. It is hence clear that the request of "semi-infinite diffusion" is actually much less urgent than it seemingly is.

The solution of the proper boundary value problem allows the calculation of the so-called concentration profiles for the species involved in the process. The concentration profile consists of the plot of the concentration at different distances from the electrode surface (x independent variable for C dependent variable), at different times (t independent variable). The gradient of the concentration at the electrode allows the computation of the current.

The solution of the boundary value problems is far from being easy also in the simplest cases and numerical solutions are required sooner or later along the solution path. Actually, a variety of numerical finite difference methods for the simulation of the responses have been introduced for a long time. More or less sophisticated transformations of space and time domains are necessary for fast and accurate calculation of the evolving concentration profiles. This is particularly urgent when dealing with specific events coupled to the charge transfer, such as fast chemical reactions, as well as for particular geometries of WE. Examples of more complex geometries are given not only by the dropping or hanging Hg electrodes, which are characterized by spherical shape with quite small radius, but also by (solid) microelectrodes, and by micro- and nano-electrode arrays, which will be dealt with in specific chapters of this book.

Variable t is connected to the potential imposed to the electrode, $E(t)$, which may assume different values over time, depending on the amperometric technique considered. The "potential wave form," $E(t)$, in fact, univocally defines the denomination and the characteristics of the specific technique.

Quite importantly, by considering the different responses relative to reversible and non-reversible charge transfers, a few basic kinetic considerations have to be done, that "join" the Butler–Volmer equation to a finite rate mass transfer, specifically consisting of pure diffusion. The starting point has been already evidenced: in the reversible case the equilibrium between electrode and redox system in solution

[10] The reason for this choice lies in the approximation to 1 of the values of the error function, erf (x), that accounts for the concentration profile of a species undergoing pure diffusion, with 0 concentration at the electrode; in particular, if $C_O(0,t) = 0$ for $t > 0$, $C_O(x,t) = C_O^b \; erf[x/(2(D_o t)^{1/2})]$. It follows that $C_O(6\sqrt{D_O t}, t) = 0.99998\, C_O^b$

is ideally reached instantaneously, while in the non-reversible cases the equilibrium is attained by the system at a finite rate. Whatever expression for the conversion rate, i.e., for the current flowing (see boundary conditions above) is considered, forward and backward rates depend on the concentrations of the species at the electrode. Assuming that diffusion is the only operative mass transfer, the process as a whole consists of two steps, in series to each other (see Fig. 10.7): the diffusion precedes the charge transfer. It is well known that the rate of an overall process depends only on the rate of the first step when it is much slower than the second one. When the second step is the lower one, the rates of both steps condition the overall rate. This means that when the equilibrium at the electrode is reached at a rate much higher than diffusion, the process is "diffusion controlled" and the responses of whatever technique appear as those of a reversible charge transfer: Nernst's equation is obeyed. In the case of a charge transfer rate comparable or even slower than diffusion, both steps, i.e., diffusion and electron transfer, condition the current/potential response obtained.

Clear distinction should be made between non-reversibility due to charge transfer, as considered throughout the whole present chapter, and "apparent" non-reversibility, due to lowering or even vanishing of C_R concentration in the diffusion layer, due to more or less fast irreversible chemical reaction following the charge transfer, i.e., in charge of R species. Also in this case the backward charge transfer reaction is prevented from occurring, owing to the concentration term of the kinetic expression, rather than to the kinetic constant. However, the intrinsic different nature of the electrode mechanism, which affects the relevant proper equations, implies differently shaped responses and different trends of the relevant characteristics, diagnostic of the operative mechanism, at varying experimental conditions. The vague resemblance of the responses obtained with some amperometric techniques often induces non experts in electrochemistry to mismatch the two actually quite different situations.

10.4 Amperometric Techniques

First of all, the meaning of the terms amperometry and voltammetry should be pointed out, owing to more and more widely diffused mismatch. Amperometry (= measurement of a current) simply indicates whatever technique in which a current is measured. It is measured as a function of an independent variable that, in electroanalysis/electrochemistry is reasonably the corresponding electrode potential or time; in principle, however, all possible experimental variables are plausible. Measuring a current as a function of temperature, or of pressure, or even of the gravity force, constitutes in all cases an amperometric measurement.

As a more sound example, chronoamperometry, in which time is the independent variable, is of fundamental importance in order to achieve information about the actual diffusion control or, rather, to conclude that adsorption or kinetic events precede or occur in parallel to the charge transfer. On the other hand, in

amperometric measurements at constant potential under mixed diffusion and convection conditions, as it happens in the case of rotating disk electrode (see below), time is not a meaningful variable: unless the concentration of electroactive species changes, the current assumes a constant value that represents the measured quantity. Similar measurements are at the basis of amperometric titrations, indicating any cases in which the appearance or increase of an electroactive species, as well as its decrease or disappearance caused by any possible events, is monitored by measuring the relevant anodic or cathodic current flow. This can be effectively performed at fixed or at varying potential, recording in the latter case a whole current/potential curve. Similarly, in a number of different studies it is profitable to make use of voltammetric techniques: the current is measured as a function of the potential of the electrode, which varies with time according to different waveforms, described hereafter: the potential waveform univocally defines the relevant voltammetric technique.

10.4.1 Chronoamperometry

The simplest waveform employed in amperometric techniques is shown in Fig. 10.9a. The WE potential is initially at a value at which no redox process takes place (E_i), and "suddenly" assumes a value at which it does occur (E_f). In a chronoamperometric test the current is recorded as a function of the time spent since the application of E_f. "Suddenly" does not express what actually happens, since a (short) delay is introduced by the electronic components of the potentiostat, as well as by the very high values that the current intensity would have to assume, actually tending to ∞, which implies that the iR term also tends to ∞.

E_f may assume a value at which O is converted to R at different rates. One has to keep in mind that this conversion occurs limitedly to O species at the electrode, i.e., for $x = 0$: the concentration values that, in a way or another, are conditioned by E_f are those adjacent to the electrode surface. The expression "in a way or another" intends to distinguish between reversible and non-reversible charge transfers: in the former case the Nernst's equation holds, in the latter a Butler–Volmer relationship is valid.

The solution of the boundary value problem outlined above for the reversible charge transfer occurring under semi-infinite linear diffusion conditions, leads to the following equation for the current density in chronoamperometry:

$$i(t) = -\frac{nFD_O^{1/2}}{\pi^{1/2}t^{1/2}(1 + \xi\Theta)} \tag{10.37}$$

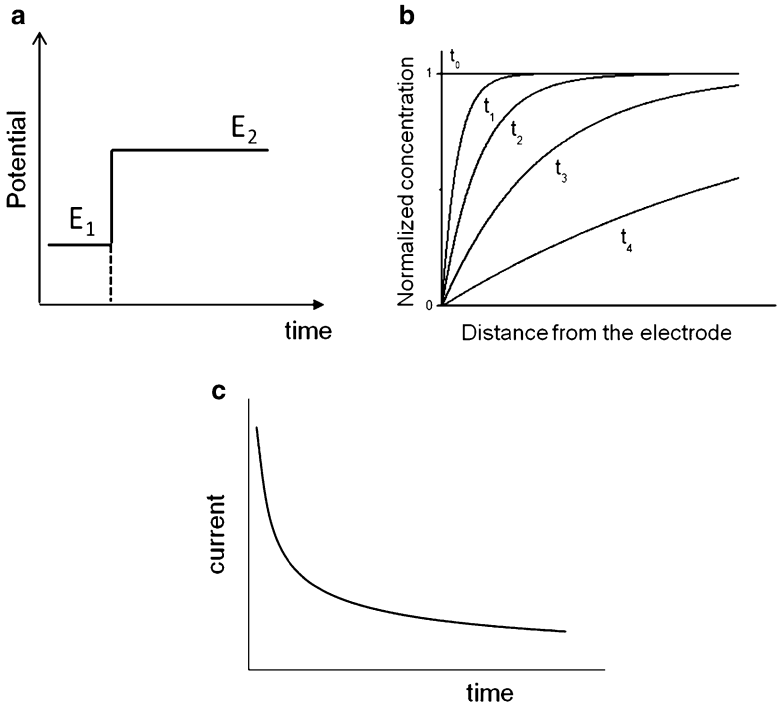

Fig. 10.9 Chronoamperometry at a potential corresponding to $C_O(0,t) = 0$: (**a**) perturbation signal; (**b**) concentration profiles at increasing times; (**c**) signal recorded: $i = f(t)$ according to Cottrell's equation; normalization in (**b**) is performed by dividing $C_O(x,t)$ by C_O^b with respect to the bulk concentration, which is quite common practice

where

$$\xi = \left(\frac{D_O}{D_R}\right)^{1/2} \tag{10.38}$$

and

$$\Theta = exp\left[\frac{nF}{R_g T}\left(E-, E^{0'}\right)\right] = \frac{C_O(0,t)}{C_R(0,t)} \tag{10.39}$$

At a negative (for a reduction) enough potential the concentration of electroactive species at the electrode becomes equal to 0, due to either thermodynamic or kinetic reasons, for a reversible or non-reversible charge transfer, respectively. Under similar conditions the dependence of the current density on time is given in any cases by the Cottrell equation:

$$i(t) = -nFC_O^b D_O^{1/2} \pi^{-1/2} t^{-1/2} \tag{10.40}$$

Although Eq. (10.40) holds not only for uncomplicated charge transfer processes, in some cases chemical reactions coupled to the charge transfer, e.g., the occurrence of a preceding chemical reaction, or of catalytic regeneration of the electroactive species, or even of adsorption phenomena, etc., significantly alter the expression. Figure 10.9b reports the evolution with time of concentration profiles for the electroactive species once $C_O(0,t) = 0$: the variation with time of the concentration gradient at the electrode accounts for the i vs. t curve in Fig. 10.9c.

The time window useful in chronoamperometry, over which the theoretical equations are obeyed, deserves some comments. We point out here, but it is actually true in all experimental situations, that the measured current intensity (i_t) is given by the sum of three contributions: (1) the faradic current (i_F), due to electrons passing from the electrode to the solution or vice versa; (2) the capacitive current (i_c), only flowing in correspondence to a change of the potential responsible for the charging/discharging of the electrode/solution double layer; (3) the background current (i_b).

$$i_t = i_F + i_c + i_b \tag{10.41}$$

The last term (i_b), accounting for the electroactivity of any species present in solution different from that of interest, is, obviously, completely different from one case to another; it contributes to the so-called "noise," meant as the opposite of informative signal, and can be differently subtracted from the overall signal. i_c strongly depends on the geometry of the cell, in particular of WE, of AE and of their reciprocal disposition. Apart from specific studies devoted to the investigation of the nature of the electrode/solution double layer, i_c constitutes a serious trouble; in analytical studies, such a current component also constitutes noise, i.e., an undesired, disturbing signal component. In the case of a chronoamperometric experiment carried out in a cell with suitable geometry, i_c assumes significant values in the first few tens of microseconds after the imposition of E_f. This means that reliable data are collected only after that the charging of the double layer has for the very most part occurred. On the opposite, at times ranging from 0.5 to few seconds, once more depending on the cell geometry, the diffusion layer becomes relatively wide, the concentrations of the species within are low, and the relevant profiles are stretched out. This implies that edge effects arise, progressively inducing diffusion parallel to the electrode. The cause lies in the high gradient value between the concentrations in correspondence to the peripheral portion of the conducting surface and that to the adjacent insulating material constituting the electrode assembly. Diffusion to the electrode with a partial radial character becomes operative[11], owing to the creation of a finite concentration gradient parallel to the electrode surface. The flux at the electrode results consequently higher than predicted by the pure linear diffusion, and correspondingly higher

[11] It is evident from the foregoing that a contribution to diffusion parallel to the planar electrode becomes more and more significant at decreasing the radius of the disk; the diffusional process tends asymptotically to a pure radial one, when the radius tends to zero. Such a kind of diffusion will be treated in detail in this book in the frame of microelectrodes (Chap. 15).

currents flow. In addition, similar stretched out profiles are poorly "stable" and undesired convection phenomena may easily arise. In respect to similar deviations from purely linear diffusion, it is noteworthy that it is quite common to record currents at longer times. In quite a different situation the solution is also stirred (even by a magnetic bar), which implies, however, the adoption of experimental conditions that do not aim at fitting those of chronoamperometry. In both cases similar measurements are only expected to lead to reliable data, e.g., in the frame of a calibration procedure, once the experimental conditions are carefully controlled and reproducible.

The theoretical chronoamperometric curves for different electrode mechanisms have been developed in the 1960s and 1970s, taking care of a number of different situations.

Low amount of theoretical, and maybe even less amount of experimental work has been made on double potential step chronoamperometry that, similarly to cyclic voltammetry (see below) is classified as a "reversal technique": after the forward step potential, WE is polarized at a value at which the electrogenerated species is reoxidized to the starting one. Such a technique is quite effective in studies of electrode reaction mechanisms. As an example, very accurate quantitative data about the kinetics accounting for the stability of electrogenerated species can be gained. However, the issue of how the data should be treated in order to obtain similar information about different homogeneous kinetics coupled to the charge transfer is far beyond the scope of the present book.

The Cottrell's equation indicates that the current is at any time proportional to the bulk concentration of the electroactive species, which potentially makes chronoamperometry a technique suitable for quantitative determinations. Actually, it is not so often directly used to this purpose, due to low sensitivity at times not short enough and poor selectivity exhibited in many situations. However, it is at the basis of a not so often used, maybe underestimated technique, namely the voltammetry with periodical renewal of the diffusion layer. This technique very often furnishes comparable information in respect to the more sophisticated voltammetry making use of the rotating disk electrode, requiring a much less sophisticated experimental setup. Although different initial conditions hold, the responses of pulse techniques described in the following are also based on chronoamperometric decays.

10.4.2 Voltammetry at Electrode with Periodical Renewal of the Diffusion Layer

This technique clearly reflects what acquired in the 1940s and 1950s by polarography with the dropping mercury electrode. Objections are possible to our decision not to treat this last technique, i.e., the direct current (dc) "dropping mercury electrode (dme) polarography" or "dc polarography" or even "polarography" for short, that can be actually considered at the origin of electroanalysis. After the end

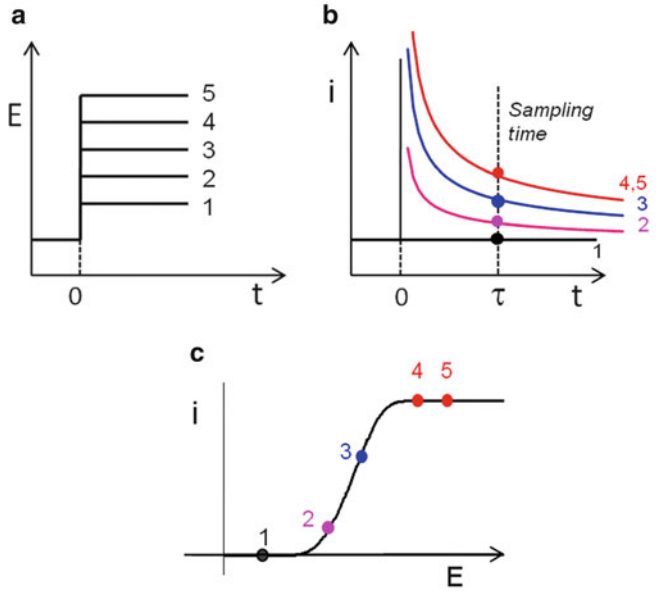

Fig. 10.10 Voltammetry with periodical renewal of the diffusion layer: (**a**) perturbation waveform; (**b**) sequence of chronoamperometric signals recorded at each potential step; (**c**) *i* vs. *E* response

of the II World War the Czech and Russian extraordinary electrochemical schools devoted attention to the Hg electrode. The virtues of Hg are claimed in another chapter of this book (see Chap. 16). The side effects that dramatically limit its use are also evidenced, so much so that the massive use of Hg is nowadays so poorly diffused to (hopefully) legitimate our choice. This notwithstanding, some points about the use of Hg will be necessarily dealt with in this chapter, on the occasion of the discussion of "stripping techniques."

Voltammetry at electrode with periodical renewal of the diffusion layer simply consists in recording different chronoamperometric curves at progressively varying the potential, and sampling the current at a constant time from the start of each single current decay curve. The sampling time should be not so short to include capacitive currents and short enough to lead to best sensitivity, simultaneously. The sampled current values as a function of the potential variable constitute the measured quantities.

Since each curve at a given potential requires initial conditions of unperturbed concentration profiles for the species, different ways to renew the diffusion layer between two subsequent steps have been proposed. In principle, every curve is recorded at a constant potential; potential step values between two subsequent curves should be small enough to allow easy interpolation of the *i* values collected. The result is an S-shaped *i* vs. *E* voltammetric curve. Figure 10.10 reports the waveform and the relevant response obtained; only a few chronoamperometric curves and relevant sampled currents are shown for clarity.

As mentioned in the introduction of the amperometry techniques, the voltammetry with periodical renewal of the diffusion layer is particularly effective in monitoring a process differently involving an electroactive species, e.g., in the already mentioned amperometric titrations, in the determination of the stability of a species, etc. In particular cases, also simple chronoamperometry, i.e., at a fixed, suitably chosen potential, may be effective to this purpose. Noteworthy, it will be clear in the following that the much more widely diffused linear potential scan and cyclic voltammetric techniques are not always suitable to substitute for voltammetry with periodical renewal of the diffusion layer to the purpose of monitoring electroactive species during their transformation. Voltammetry with periodical renewal of the diffusion layer, as well as the voltammetry at rotating disk electrode, only allows the estimation of the concentrations of both partners of a redox couple, on the basis of the ratio between the anodic and cathodic limiting currents.

A few considerations should be made on similar voltammetric curves, reflecting what derived for dc conventional polarography. They once more look very much closely after the observations that can be made with reference to the voltammetric curves recorded at a rotating disk electrode (see below). Curves 4 and 5 in Fig. 10.10b are overlapped to each other, since the evolution of the relevant concentration profiles is the same: past a given potential, the concentration of electroactive species at the electrode approaches 0 very closely. Correspondingly, points 4 and 5 in the i vs. E curve (Fig. 10.10c) indicate equal current values: a "limiting current" has been reached. For a reversible charge transfer, the Nernst's equation indicates that an E value 120/n mV more negative than $E^{\circ\prime}$ corresponds to $C_O(x=0)=C_O^b/100$; a further, poorly meaningful tenfold decrease of the concentration results from further 60 mV, and so on. In the non-reversible case a similar correspondence between applied potential and $C_O(x=0)$ cannot be univocally defined; however, a high enough overvoltage causes, also in this case, that $C_O(x=0)$ tends to 0. The current does not increase anymore and a limiting current has been once more reached; its value does not depend on the reversibility degree of the charge transfer.

The following equation, accounting for the analytically interesting linear dependence of the limiting current density on the bulk concentration of the electroactive species, can be written:

$$i_L = -knFD_O^{1/2}\pi^{1/2}C_O^b \tag{10.42}$$

where k depends on the sampling time.

Furthermore, only for the case of a reversible uncomplicated charge transfer, the potential corresponding to a current equal to one half the limiting value is expressed by:

$$E_{1/2,r} = E^{0'} + \frac{R_gT}{nF}\ln\left(\frac{D_O}{D_R}\right)^{1/2} \tag{10.43}$$

$E_{1/2,r}$, which will be encountered also when dealing with different voltammetric techniques in the following parts of this chapter, is most often a very good approximation of the thermodynamic quantity, E°. It should be emphasized that a dynamic technique may be invaluable tool for evaluating this parameter, for example whenever one partner of the redox couple is not stable enough to make a potentiometric measurement, but it is over the much shorter time scale of a potentiodynamic measurement.

10.4.3 Rotating Disk Electrode (RDE) Voltammetry

Rotating a disk electrode at a controlled frequency, f, constitutes an effective way to induce controlled mass transfer by convection. Actually, convection is operative in the solution as far as a given distance from the electrode is reached; at lower distance, the solution progressively tends to rotate more and more jointly with the electrode. The result consists of the obtainment, in this region, of a solution that is progressively quiescent with respect to the electrode, unperturbed by convection: the mass transfer progressively shifts from a convective to a diffusive character. Figure 10.11a shows an example of concentration profiles that arise in such a system when laminar flux regime is attained—turbulent flux, inducing uncontrolled convection, has to be carefully avoided, by using well suitable experimental setups. A good approximation in accounting for the mass transfer to/from the electrode consists in assuming linear trends of the concentration both in the region closest to the electrode, where the mass transfer is assumed to be diffusive (so-called "Nernst's layer") and outside this layer, far enough from the electrode, where a constant value is imposed by convection. The thickness of the diffusion layer (δ_0), actually computed by extrapolation of the linear trends in the above cited layers, depends on the rotational speed, according to the equation:

$$\delta_0 = 1.61 D_O^{1/3} \nu^{1/6} \omega^{-1/2} \tag{10.44}$$

where ν is the kinematic viscosity of the solution, expressed in $cm^2\ s^{-1}$, ω the angular velocity, in rad s^{-1} ($=2\pi f$) and δ_0 is expressed in cm.

The equation of the current/potential curve closely resembles that of the analogous, though not identical pattern, observed at an electrode with periodical renewal of the diffusion layer. For a reversible uncomplicated charge transfer the current intensity is proportional to the concentration of the electroactive species at any potential values. Independently of the nature of the charge transfer, in correspondence to the limiting (plateau) value, it is given by the Levich equation, which furnishes the linear relationship of analytical significance between current intensity density and concentration in solution:

$$i_L = -0.62 n F D_O^{2/3} \nu^{-1/6} \omega^{1/2} C_O^b \tag{10.45}$$

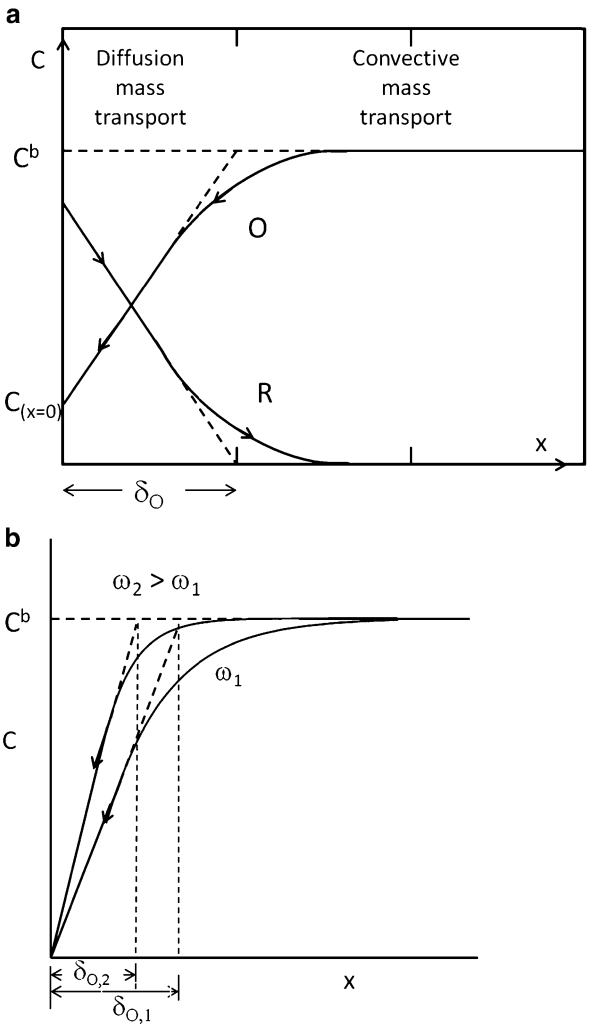

Fig. 10.11 (**a**) Concentration profiles in laminar flow regime; (**b**) concentration profiles of the electroactive species at different rotational speed; stagnant is intended with respect to the rotating electrode disk

Technical/mechanical requirements are urgent, becoming more and more pressing as the rotational speed increases. The rod of insulating material embedding the electrode disk should be aligned with the disk itself and its walls should be regularly cylindrical in shape in order to avoid undesired vibration. Furthermore, the surface of the disk, as well as of the surrounding insulating portion of the device, should be very smooth: as above cited the regime of the flux has to be laminar, turbulent flow creating unacceptable irregularity in convection. Usual rotational speeds are in the range 100 to 10,000 rpm.

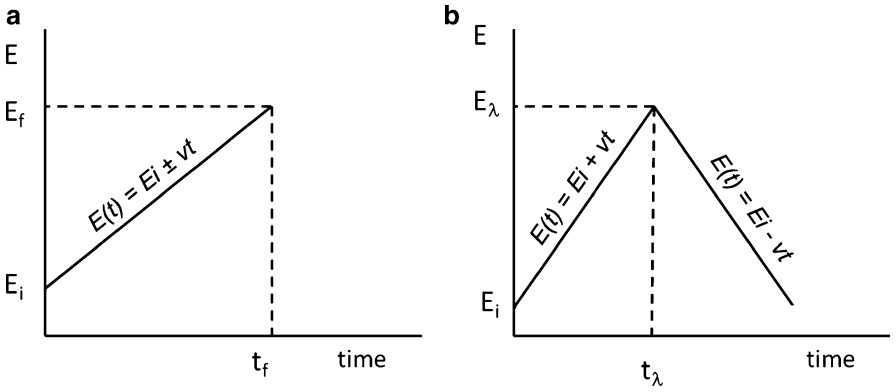

Fig. 10.12 (**a**) LSV and (**b**) CV potential waveforms; *v* indicates the potential scan rate

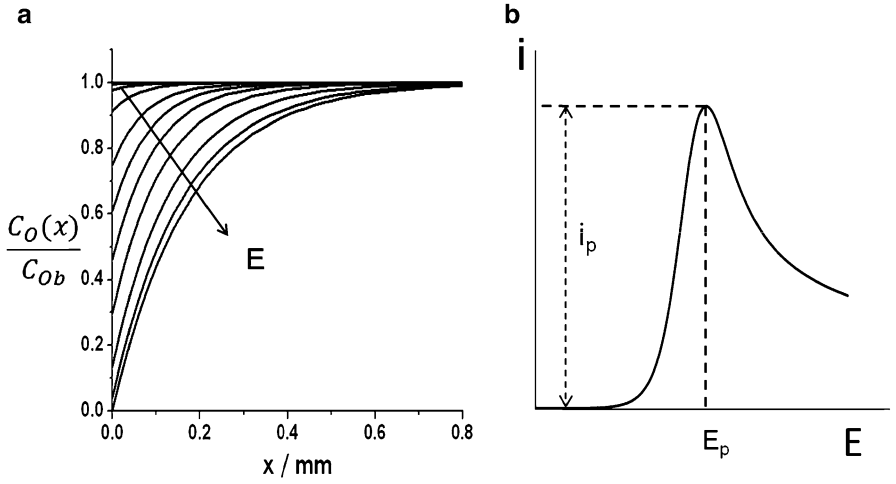

Fig. 10.13 (**a**) Evolution, with potential increasing, of the concentration profiles of the electroactive species; (**b**) voltammetric curve in LSV

10.4.4 Linear Sweep and Cyclic Voltammetry

Linear sweep voltammetry (LSV), with the corresponding "reversal technique," cyclic voltammetry (CV), are definitely the most frequently used voltammetric techniques. This is true when a qualitative approach to the study of the redox characteristics of a solution is pursued, as well as when a quantitative study of the electrode mechanism and even the evaluation of the relevant thermodynamic and kinetic parameters are faced, and also when electroanalytical quantitative information are sought. The potential waveforms for LSV and for CV, with the relevant equations expressing the time dependence of *E*, are shown in Fig. 10.12.

The typical *i vs*. *E* LSV voltammetric curve for an uncomplicated charge transfer consists of a peak-shaped curve (Fig. 10.13b). Such a trend of the current may be

accounted for the occurrence of two counteracting phenomena acting on the concentration gradient at the electrode. The increase of the applied potential causes, on its own, an increase of the concentration gradient due to the decrease of electroactive species concentration at the electrode, till the 0 value is reached. As previously discussed, this is due to the requirement of the Nernst's equation for reversible processes or to the increase of the electrode charge transfer forward rate for non-reversible ones. On the other hand, at increasing time, expansion of the diffusion layer occurs that, on its own, leads to a decrease of the gradient. The former effect prevails till a given potential (relative maximum in the i vs. E curve, i.e., the peak potential, E_p), while the latter effect prevails beyond that point. A typical LSV curve, together with the relevant evolution of the concentration profile of the electroactive species at different potentials of the sweep, for an uncomplicated reversible charge transfer, is reported in Fig. 10.13.

For an uncomplicated (diffusion controlled) reversible charge transfer process, the solution of the Fick's II law differential equation system, with the appropriate initial and boundary conditions, leads to the following relationships for the meaningful quantities of the curve:

$$i_p = -0.4463nFC_O^b\left(\frac{nFvD_O}{R_gT}\right)^{1/2} \tag{10.46}$$

where v is the potential sweep rate ($= \partial E/\partial t$). Eq. (10.46) is the so-called Randles–Sevčik equation that, at 25 °C, can be written as:

$$i_p = -\left(2.69 \times 10^5\right)n^{3/2}C_O^bD^{1/2}v^{1/2} \tag{10.47}$$

$$E_p = E_{1/2} - 1.11\frac{R_gT}{nF} = E_{1/2} - \frac{28.5}{n}\text{mV, at } 25^\circ\text{C} \tag{10.48}$$

$$\left|E_p - E_{p/2}\right| = 2.2\frac{R_gT}{nF} = \frac{56.5}{n}\text{mV, at } 25^\circ\text{C} \tag{10.49}$$

For an uncomplicated totally irreversible charge transfer the solution of the corresponding boundary value problem leads to:

$$i_p = -0.4954nFC_O^b\left(\frac{\alpha n_aFvD_O}{R_gT}\right)^{1/2} \tag{10.50}$$

where the meaning of α, to a first approximation, may be identified with that of the symmetry factor (β) and n_a is the number of electrons exchanged in the slowest step of the charge transfer process, resulting equal to 1 in the very most part of cases:

$$E_p = E^{0'} - \frac{R_gT}{(\alpha n_aF)}\left[0.780 + ln(D_Ob)^{1/2} - ln\, k_{s,h}\right] \tag{10.51}$$

where $b = \frac{\propto n_a F v}{R_g T}$

$$\left|E_p - E_{\frac{p}{2}}\right| = -\frac{47.7}{(\propto n_a)}\text{mV at } 25^\circ\text{C} \tag{10.52}$$

The solution of the boundary value problems for the different electrode mechanisms has been carried out by semi-numerical method and by a variety of finite difference numerical techniques. The particular cases of the modified electrodes represent a very complex issue. They require approaches that vary not only as a function of the nature of the modifier, but also of the specific modification, since the mathematics should accounts for the thickness and structure of it. Hence, the problem to solve depends on the exact nature and peculiar experimental conditions under which the modification has been created.

It should be evidenced that, in addition to the faradic component, not only the background, but even the capacitive current should be taken into account. In LSV and CV experiments the electrode potential, in fact, varies continuously, implying a continuous change in the charge of the electrode/solution interface that induces the flow of capacitive current: it is the higher the faster the change in charge, i.e., the higher the potential scan rate.

Looking at the i_p expressions for either reversible or totally irreversible charge transfers, the analytically most meaningful datum lies in the linear dependence of the current, in particular of the peak current, on the bulk concentration of the analyte, at a fixed potential sweep rate.

On the other hand, the linear dependence of the (peak) current on the square root of the potential scan rate constitutes a further notable feature of a diffusion controlled process. It should be evidenced that increasing the scan rate requires the charge transfer to be faster and faster in order to meet with the requirement of equilibrium, as expressed by the Nernst's law: a decreasing "apparent degree" of the reversibility of the process may be observed, since the higher the scan rate the more difficult the achievement of equilibrium. In other words, it may happen that a process that leads to responses typical of a diffusion controlled, reversible charge transfer, does not behave in the same way at high enough scan rates: it may appears as a quasi-reversible charge transfer. It is hence clear that the reversibility degree, as it appears from a given response, is a function also of the potential scan rate, so much so that a "family" of processes with different intrinsic non-reversibility degree may exhibit equal shape at different potential scan rates. All these processes are characterized by equal value of the dimensionless parameter ψ, which depends on the ratio between $k_{h,s}$ and v:

$$\psi = \frac{\left(\frac{D_O}{D_R}\right)^{\propto/2} k_{h,s}}{\left[\frac{\pi D_O n F v}{R_g T}\right]^{1/2}} \tag{10.53}$$

What happens in CV by reversing the potential scan direction in correspondence to a suitably chosen switching potential, E_λ, strongly depends on the exact nature of

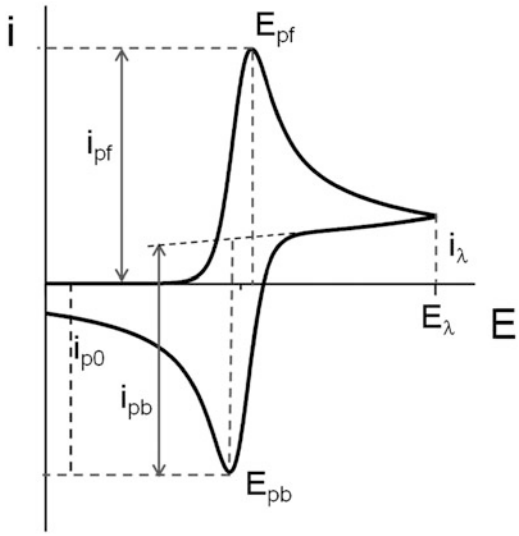

Fig. 10.14 Cyclic voltammogram of a reversible uncomplicated charge transfer process

the operative mechanism, which makes CV such a powerful diagnostic technique. If the product of the charge transfer only undergoes diffusion away from the electrode, a backward current peak is recorded, characterized by net current flow in the opposite direction. An anodic current peak is recorded, relative to reoxidation of *R* species, previously formed by reduction of *O* species in the forward potential scan. The height of this peak should be computed by properly taking into account for the background; the following semi-empirical relationship (see Fig. 10.14 for the meaning of the quantities) is suitable to this purpose:

$$\frac{i_{p,b}}{i_{p,f}} = \frac{\left(i_{p,b}\right)_0}{i_{p,f}} + \frac{0.485 i_\lambda}{i_{p,f}} + 0.086 \tag{10.54}$$

The typical characteristic features of the forward/backward peak system for an uncomplicated reversible charge transfer are given by:

$$E_{p,b} - E_{p,f} = 57/\text{nmV at } 25^\circ\text{C} \tag{10.55}$$

$$\left|i_{p,b}/i_{p,f}\right| = 1 \tag{10.56}$$

$$E_{1/2,r} = \left(E_{p,f} + E_{p,b}\right)/2 \tag{10.57}$$

The symmetry of the response, as expressed by the two last expressions above, is also valid for a quasi-reversible charge transfer when $\alpha n_a = 0.5$. On the other hand, the characteristics of the responses relative to quasi-reversible charge transfers are intermediate between those of fully reversible and irreversible charge transfers. In Fig. 10.14 a typical CV response is shown.

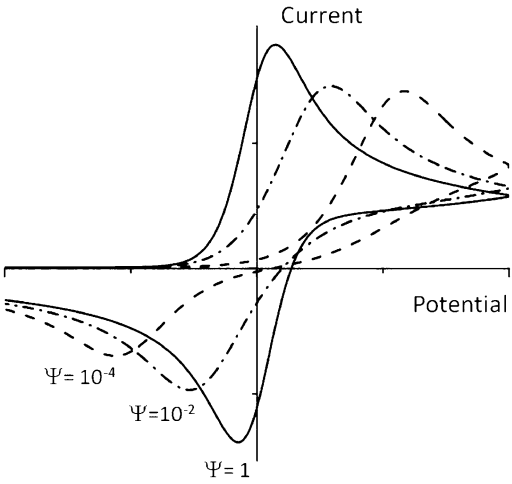

Fig. 10.15 Effect of the dimensionless parameter Ψ on CV responses; $\alpha = 0.5$

As a reversal technique, CV may allow an estimate of the thermodynamic quantity E° even in those cases in which the oxidized or the reduced partner of the O/R redox couple is unstable, i.e., when, once formed by reduction or oxidation of the stable starting partner present in solution, the product (rapidly) decays by a chemical reaction. CV tests at increasing potential scan rates give the species lesser and lesser time to decay. It may well happen that, at high enough rates, a unity value is reached by the backward to forward peak height ratio, so that $E_{1/2,r}$, excellent experimental approximation to E°, can be computed by Eq. (10.57).

On the other hand, if the charge transfer is totally irreversible, the starting species cannot be regenerated via an opposite electrode charge transfer, so that no faradic current flows once reversing the potential scan direction.

Figure 10.15 reports theoretical CV responses for different Ψ values, the highest value identifying a reversible charge transfer. As already noticed, according to Eq. (10.53), the transition to a lower Ψ value may occur either for different systems, for a decrease of the intrinsic reversibility degree of the charge transfer or, for a given process, as the consequence of the increase of the potential scan rate. Attention should be paid to peak broadening due to uncompensated ohmic drop between WE and RE. It may cause an effect seemingly coincident with a quasi-reversible character of the charge transfer. The current, hence the iR_u term, increases at increasing the potential scan rates, which contributes to mimic the increase of the apparent irreversibility degree of the process. It is interesting to notice that the effect of iR_u lies in an actual E applied that results lower, to an iR_u extent, with respect to that measured by the voltmeter: the i vs. E response is spread out over a wider potential range, which means peaks broadening.

More complex mechanisms can be suitably studied by LSV and CV tests. We address the interested reader to specific textbooks, or original articles indicated therein, suggested at the end of this chapter.

10.4.5 Pulse Techniques

Pulse techniques typically derive from polarography, i.e., voltammetry with Hg electrode. Since we choose not to discuss such a polarographic technique, we limit our exam to the evolution of pulse techniques applied to different electrodes. The term "pulse" indicates that the current responses exploit the application to the electrode of a (short) potential impulse. The obvious presence of capacitive currents at the first milliseconds of each pulse constitutes a feature common to any pulse techniques. This is a point that should be kept in mind when going through the operative conditions for similar wave forms.

Potential step techniques, e.g., using a staircase wave form, such as the so-called Barker staircase voltammetry have been proposed more than 40 years ago as sensitive tools in respect to electroanalytical techniques involving continuously varying potential. The most distinctive feature of these techniques lies in the fact that, since the double layer charge varies only in a very short time length after any change of the applied potential, a purely faradic current can be easily sampled. The samplings occur just before each potential change; the step duration is as short as possible, compatible with the minimization of the capacitive current.

10.4.5.1 Differential Pulse Voltammetry (DPV)

It has been already emphasized that, in the case of all amperometric techniques, the overall current flowing is given by the sum of three components: the faradic, the capacitive, and the background ones. On the other hand, as already evidenced, but necessarily underlined here, in voltammetric studies the capacitive and background components "pollute" the information brought by the faradic current which is the only one of interest in electroanalytical, as well as in mechanistic studies. In other words, i_c and i_b tend to hide the useful information brought by i_F. The aim of the pulse techniques and, specifically, of the differential pulse voltammetry (DPV), is to minimize the contribution of both i_c and i_b to the measured signal. The potential waveform typical of DPV is reported in Fig. 10.16: a potential pulse of short duration is applied after that the electrode has been hold for a much longer time at a potential at which the charge transfer occurs at a lower rate. In the case of dme the drop falls at the end of the pulse.

This technique, in fact, was first proposed for the dme. The necessity to apply the potential step at an approximately constant, wide enough surface area requires long enough times for the drop to grow, since the constant flux of Hg from the capillary causes a constant increase of the volume and a lower and lower increment of the surface area. The "dropping Hg" origin of the technique is seemingly the "cause" of the asymmetry in the periodic wave. However, DPV survives, and well, also when using solid electrodes, with respect to the square wave voltammetry (SWV) that will be discussed in the following section, in which the asymmetry of the wave is removed. As it is suggested from Fig. 10.16, the DPV response consists of a

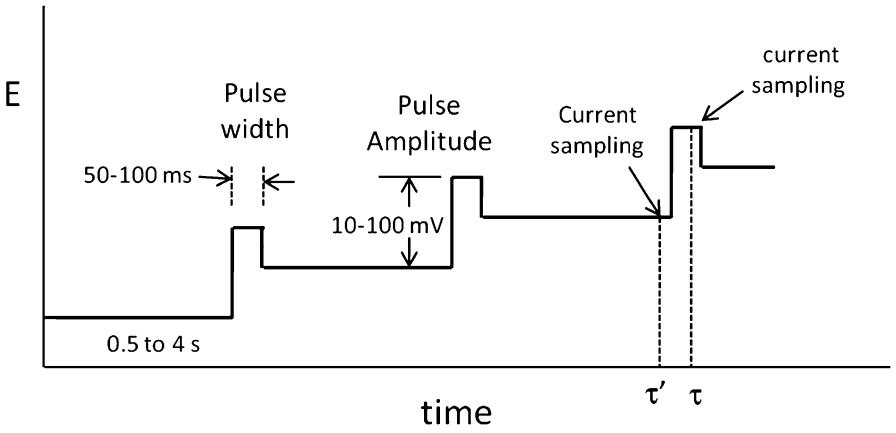

Fig. 10.16 Potential waveform for DPV [adapted from Bard AJ, Faulkner LR (2001)]

difference of currents plotted against the potential, namely the mean value between the potentials at which the two currents are sampled. The first current value is taken just before the application of the impulse and the second one just before the end of the impulse, which is long enough to allow the charging current to become negligible. The duration of the impulse (pulse width), t_p in Eq. (10.58), is anyway not higher than 100 ms, in order not to imply decrease of sensitivity. Additional parameters to set are: "potential impulse" (ΔE_i), typically of 5–50 mV; "potential step," i.e., the potential difference between two subsequent periods, principally conditioning the time necessary to perform the experiment and the density of data on the potential axis; "rest time," i.e., the time spent at the lower potential of a given period, typically from 0.5 to few seconds. The difference between the two sampled currents maximizes the "cleaning up" of the signal from capacitive and background components, enhancing the weight of the pure faradic one. The residual small charging current still flowing at the sampling point in the impulse, in fact, is not significantly different from that just before the application of the impulse. The same consideration holds for the background currents, due to the proximity (5–50 mV) of the two potentials. On the other hand, in correspondence to a faradic current increase, i.e., to the actual signal, this component does significantly change. This implies that the difference between the two overall currents minimizes the contribution of the charging and background "noise" with respect to the informative faradic contribution. The faradic component is hence evidenced by the difference, similarly to what a derivative operator does. It is noteworthy that the look of the DPV curve is quite similar to that of a first derivative of the corresponding S-shaped voltammetric curve, e.g., obtained by a RDE or by an electrode with periodical renewal of the diffusion layer or even by dme polarographic curve. It is actually different in respect to the underlying equation describing it, due to the difference in the waveform and, correspondingly, to the physical phenomena occurring.

The value of the waveform parameters are conditioned by the choice addressed to privilege either sensitivity (higher potential step value) or resolution (lower

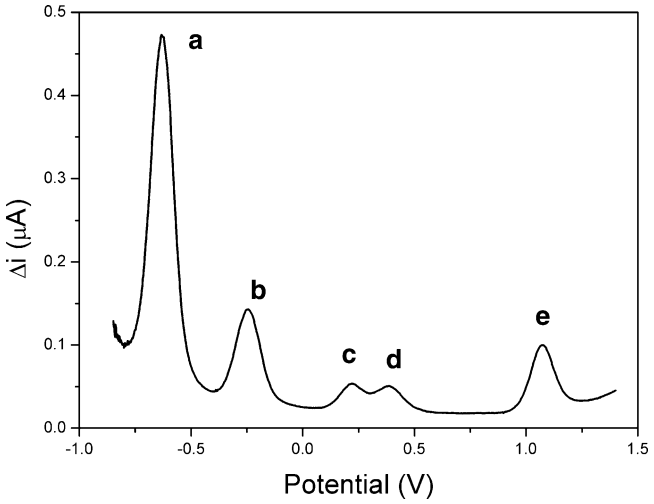

Fig. 10.17 Differential pulse voltammogram recorded for the oxidation of the cations methylviologen (**a**), $Ru(NH_3)_6^{2+}$ (**b**), α-metil ferrocene methanol (**c**), ferrocenylmethyltrimetylammonium (**d**), and $Ru(bpy)_3^{2+}$ (**e**) immobilized at a glassy carbon electrode. Supporting electrolyte 0.1 M phosphate buffer, pH 7. ΔE_i 25 mV, scan rate 10 mV/s

potential step value). Multivariate optimization of the parameter constitutes effective approach, once the response typical quantities to optimize are suitably defined.

The resulting response, in terms of Δi *vs.* E, presents a relative maximum of height expressed by:

$$\Delta i_p = -\frac{nFD_O^{1/2}C_O^*}{\pi^{1/2}t_p^{1/2}}\left(\frac{1-\sigma}{1+\sigma}\right) \tag{10.58}$$

where

$$\sigma = \exp\frac{-nF\Delta E_i}{2R_gT} \tag{10.59}$$

The value of Δi_p is linearly dependent on the concentration of the analyte in solution. The corresponding peak potential is given by the expression:

$$E_p = E_{1/2,r} - \frac{\Delta E_i}{2} \tag{10.60}$$

for a sweep towards negative potentials, i.e., $\Delta E_i < 0$.

Figure 10.17 reports an example of DPV in the determination of five analytes immobilized on a glassy carbon electrode; the high resolution power of the technique is well evident from the very sharp peaks recorded.

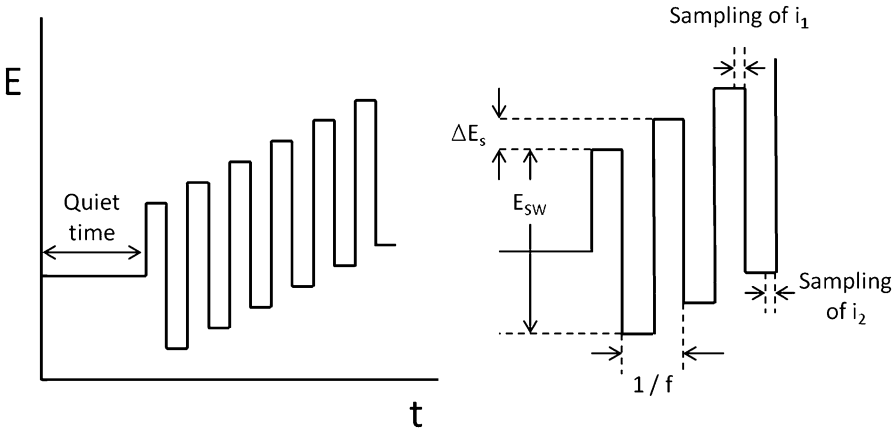

Fig. 10.18 SWV waveform and indication of the meaning of the relevant parameters

10.4.5.2 Square Wave Voltammetry (SWV)

SWV has found experimental applications in more recent times with respect to the previously described voltammetric techniques. Figure 10.18 illustrates the relevant waveform, which corresponds to a sequence of symmetrical square pulses at progressively increasing potentials. It can be viewed as the superimposition of a square wave and a staircase waveform, where the half-period of the square wave is coincident with the step duration of the staircase. The current response is once more given by a difference of two current values, i_1 and i_2, respectively, sampled immediately before the end of two subsequent square wave half-periods. The advantages sought are the same as those for DPV, consisting of an increased signal to noise ratio, i.e., of enhancement of the faradic with respect to capacitive and background currents. The following parameters account for the characteristics of the waveform: E_{sw} defines the amplitude ($5 \div 250$ mV) of the square wave; f identifies the frequency ($8 \div 250$ Hz), and τ is the period $= 1/f$. It follows that $\Delta E_s/\tau$, where ΔE_s is the potential difference between two successive steps of the underlying staircase, defines the "continuous" potential scan rate, which can typically reach as high values as a few V s^{-1}. ΔE_s values typically vary from 1 to 40 mV.

A typical SWV response in terms of Δi is reported in Fig. 10.19. The same figure also shows the plots of the individual i_1 and i_2 values, which may be however more useful in studies of electrode mechanisms rather than in electroanalysis. For an uncomplicated, reversible charge transfer:

$$\Delta i_p = -nF\pi^{-1/2} D_O^{1/2} \Delta\phi_p f^{1/2} C_O^b \tag{10.61}$$

where $\Delta\phi_p$ is a dimensionless parameter that depends on the square wave amplitude and on the step height of the underlying staircase. Noteworthy, the relative maximum of the current occurs at a potential corresponding to $E_{1/2,r}$.

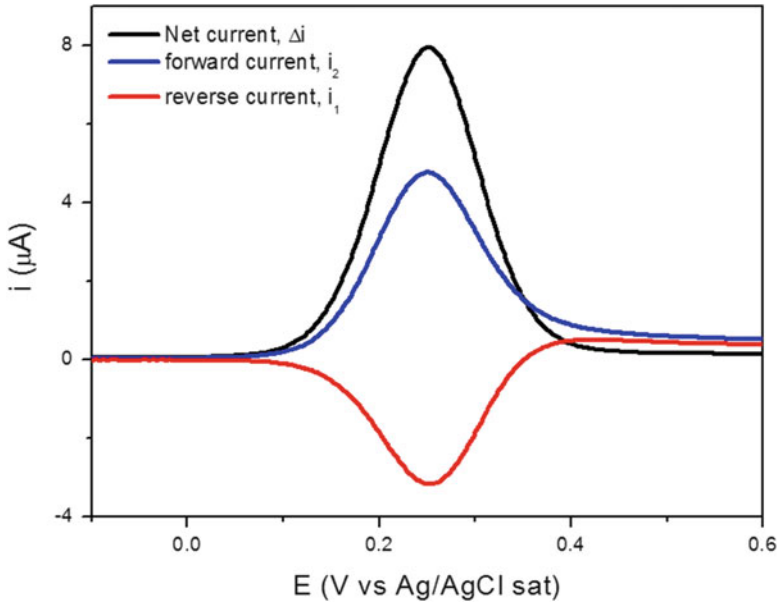

Fig. 10.19 SWV difference response, together with forward and backward components, recorded at a glassy carbon electrode in 1×10^{-4} M, $[Fe(CN)_6]^{4-}$ 0.05 M KNO_3 solution; $E_{SW} = 25$ mV, $f = 25$ Hz, $\Delta E_s = 2$ mV. The forward response corresponds to an anodic process

In addition to the increase of sensitivity at increasing E_{sw} and f, a remarkable characteristic of SWV, of particular interest in electroanalysis, lies in the possibility to use quite high potential variation rates. This implies the feasibility of a high number of measurements in a short time, which allows one to follow an evolving system or to perform analyses over a flux system at a high frequency. This notwithstanding, SWV not always performs better than DPV, particularly in the case of electrode modified by coatings that exhibit structural modifications, requiring relaxation, at the potentials of two subsequent steps. Actually, SWV at high frequency may present drawbacks also in the case of the common electrode materials. The high frequency square wave, in fact, implies the presence of very high frequencies in the potential applied to the WE: we are shifting from a direct current technique to an alternating current one, which would actually require a much more complex treatment of the resulting responses.

10.4.6 Stripping Techniques

A number of so-called "stripping techniques" have been proposed and effectively developed in the "mercury era." It has been already claimed in this chapter that, luckily or not, it is over... Stripping techniques are nowadays barely applied to thin

Hg film electrodes and, much more frequently, to bare or to modified electrodes. Hg thin film electrodes can be differently prepared. Typically, either by reduction of Hg salts onto a bare electrode, or simply by dipping a Au electrode in Hg, so that a layer of Hg–Au amalgam forms, on which pure Hg adheres. On the other hand, other elements are proposed to substitute Hg, such as in the bismuth film electrodes, as well as other modified electrodes where stripping techniques can be successfully applied. Similar electrode materials will be discussed in Chap. 16. Different stripping techniques have been formulated for determination of species of various natures.

10.4.6.1 Anodic Stripping Voltammetry (ASV)

ASV is the most widely diffused stripping technique, resulting most effective in the determination of metals, in particular of "heavy metals."

The technique consists in reducing the cation or the mixture of different cations to the zero valence state, either to form amalgam with Hg or to deposit them onto the solid metal electrode surface. The deposition occurs under precisely controlled experimental conditions, activating carefully controlled stirring of the solution for an exactly measured time length. The geometry of the cell (see Fig. 10.4 as an example) should be suitable to allow for best control of stirring, hence of hydrodynamics of the experiment. After this first step, occurring at a negative enough potential, a sweep to more positive values leads to reoxidation and re-dissolution of the metals to the relevant cations. The waveform used may be simply a Linear Sweep or, for better sensitivity, a Differential Pulse or a Square Wave potential excitation. The determination of the concentration occurs via the traditional methods, based on the use of a calibration curve or by standard additions.

Figure 10.20a sketches the two steps constituting the anodic stripping procedure: the preconcentration/deposition step and the oxidation/dissolution one, respectively. Figure 10.20b presents a typical ASV response, where three metals, Zn, Cd and Cu, are contemporary determined.

10.4.6.2 Cathodic Stripping Voltammetry (CSV)

Similarly to ASV, the analysis by CSV consists of two stages, the preconcentration and stripping steps, respectively. For example, for the analysis of the anion A^{n-} at a Hg film electrode, these steps can be schematically written as:

$$A^{n-} + nHg \rightarrow (Hg_nA)_e + ne^- \quad \text{pre-concentration step}$$
$$(Hg_nA)_e + ne^- \rightarrow A^{n-} + nHg \quad \text{stripping step}$$

The $(Hg_nA_n)_e$ species is on the electrode, i.e., insoluble in the solution phase. The amount of precipitate onto the electrode is proportional to the A^{n-} concentration in solution and determines the current intensity of the response due to the

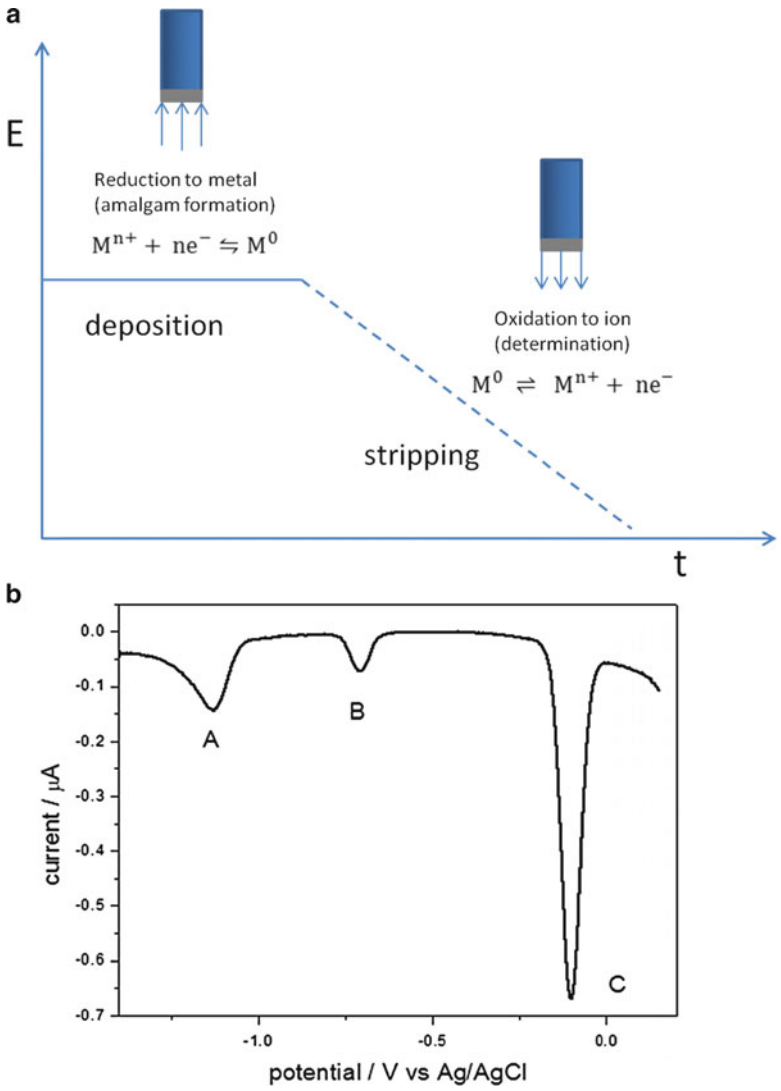

Fig. 10.20 (**a**) Scheme of the anodic stripping procedure and (**b**) relevant differential pulse voltammogram recorded at a Hg electrode for the anodic stripping of 0.1 mM Zn (A), 0.1 mM Cd (B), and 1 mM Cu (C), in 0.1 M KNO_3. Experimental parameters: reduction time: 30 s, potential scan from −1.3 to 0 V, ΔE_i: 25 mV; potential scan rate: 10 mV/s

reduction involved in the stripping step. By proper calibration, the peak current gives the value of A^{n-} concentration in solution. Similar conditions as for ASV should be respected for both steps, except for the obvious difference that the first step occurs by polarization at positive potentials and the subsequent potential scan is toward more negative values.

10.4.6.3 Adsorptive Stripping Voltammetry (AdSV)

In general, AdSV exploits the accumulation of electroactive species at the electrode by adsorption on the surface. The direct adsorption can be selective, or may occur in charge of an adduct between the analyte and a species deliberately added to the solution. An interesting application of similar stripping technique deals with the analysis of trace elements. A simple procedure is adopted in which, similarly to the other stripping techniques, a first step consists in the analyte preconcentration at the electrode. In the simplest general case, adsorption of the analyte onto the electrode surface occurs. In the case of metal ions, the addition of a suitable ligand to the solution causes adsorption of the relevant complex, by following such a procedure, AdSV opens the possibility of the application of stripping techniques to the determination of a wide series of metals. Of particular interest are those metals that cannot be determined directly or by preconcentration of the ion itself, due to the occurrence of irreversible electrode reactions or lack of amalgam formation at mercury film electrodes, respectively. Similar metals are, for example, cobalt, nickel, chromium, antimony. The presence in solution of a ligand or a set of ligands is required that, in presence of the metal ion analyte, form a sparingly soluble complex that adsorbs on the electrode in the preconcentration step. The subsequent scan, typically to negative potential values, exploits the reduction of the complex that usually dissociates into the ligand and the metal in lower oxidation state. The response is directly related to the surface concentration of the complex through an adsorption isotherm that provides the relationship between the surface and bulk concentrations. The steps for the AdSV analysis of a metal M^{n+} that forms a complex with a ligand L can be schematically represented as:

$$
\begin{aligned}
M^{n+} + mL &\rightarrow ML_{n(acq)} \\
ML_{n(acq)} &\rightleftharpoons ML_{n(ads)} \quad \text{preconcentration step} \\
ML_{n(ads)} + xe^- &\rightarrow M^{(n-x)+} + mL \quad \text{stripping step}
\end{aligned}
$$

10.4.6.4 Potentiometric Stripping Analysis (PSA)

PSA is relatively scarcely diffused, but offers an excellent option in the analysis in complex matrices, as it can be the case of environmental samples. PSA is similar to ASV, but differs in the way how the deposited metals are stripped from the electrode. After the preconcentration step at a controlled potential, the potentiostatic control is disconnected and the metal is reoxidized by an oxidizing agent present in solution, such as Hg(II) or oxygen, or by the application of a constant anodic current to the electrode. The potential spontaneously assumed by the indicator electrode—WE in the previous step—is monitored as a function of time. The experimental conditions are set in a way that the rate of reoxidation of the metal is constant during the stripping process and is determined either by the constant anodic current imposed or by the diffusion of the oxidant from the solution to the electrode surface. In the latter case, the mass transport of the oxidant is

facilitated by stirring the solution. When the oxidation potential of a given metal is reached by the electrode, the potential variation slows down, and a sharp time step at a constant potential, due to the depletion of that metal from the electrode, is recorded. The distance between two consecutive flex points in the potential vs. time curve, the so-called "stripping time," is directly proportional to the metal concentration in solution, while the potential of the flex coincides with the formal redox potential that characterizes the nature of the metal. A careful calibration procedure ascribes high performance to the technique.

A main advantage of PSA lies in the use of non de-aerated samples, and in a low susceptibility to interfering effects, since the potential corresponding to the time transition represents a highly selective parameter.

10.4.7 Electrolysis: Coulometry

When dealing with all the previously described techniques, we emphasized that the small electrode area implies the flow of a low current intensity; hence, such a small electric charge is spent that a negligible variation in the solution composition occurs. This is the reason why, in this respect, voltammetric techniques may be compared to the spectroscopic ones. On the contrary, to a number of different purposes, reduction or oxidation of a significant amount of the electroactive species, i.e., of the analyte, may constitute the goal of the electroanalytical operation.

Not considering the case of electrolysis carried out to massive, even industrial preparative purposes, the nature of the final products of an electrode process occurring at a given fixed potential may be a prerequisite to an analytical procedure. Two fundamental quantities relative to the analyte under exam may be determined by exhaustive coulometry: once the concentration is known, the overall number of electrons involved in the electrode process is computed, and vice versa. The Faraday's law links the charge spent to both these quantities. The end of the electrolysis can be established when the background current is reached, as computed in independent tests under the same experimental conditions, but in absence of the analyte. Voltammetric curves recorded at different stages of the electrolysis allow one to monitor its occurrence, depending on the operative electrode mechanism. To this purpose, let's recall what mentioned in respect to the adequacy of voltammetry with periodical renewal of the diffusion layer or voltammetry at RDE and to inadequacy of CV. At whatever starting potential, this last technique, in fact, changes the ratio of oxidized to reduced species concentrations close to the electrode.

It is evident that experimental conditions deeply different from those of the voltammetric techniques should be adopted in more or less exhaustive electrolysis. In particular, obvious advantages derive from the use of large area WEs, which leads to high currents, i.e., to high values of charge spent in a given time, hence to shorter times required in order to complete the test, and hence to minimized

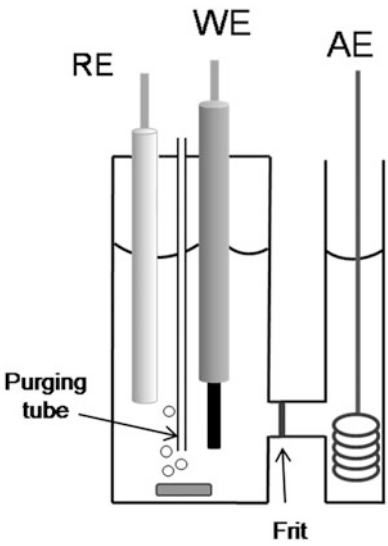

Fig. 10.21 Typical configuration of a H-shaped cell for coulometric test

undesired parallel events. For the same reason, the solution is stirred to speed up the mass transfer, activating convection.

On the other hand, in parallel to the finite quantities of transformed species at WE, e.g., by reduction, a corresponding amount of species is transformed, by oxidation, at AE. Mixing of the products of the two electrode process should be prevented from occurring, since they can react with each other in solution or, in turn, undergo oxidation at WE and reduction at AE, respectively. A separation of the solutions in which WE and AE are located is necessary to prevent mixing, though allowing transfer of ions, usually of the supporting electrolyte, in order to keep the inner circuit of the electrolysis cell closed. A septum of suitable porosity is usually employed, in the frame of a so-called H-shaped cell (see an example in Fig. 10.21). RE is also often separated from WE by a porous disk, in order to avoid reciprocal pollution.

Suggested Fundamental References for Useful Integration

1. Adams RN (1969) Electrochemistry at solid electrodes, vol XII, Monographs in electroanalytical chemistry and electrochemistry. Dekker, New York
2. Bard AJ, Faulkner LR (2001) Electrochemical methods, 2nd edn. Wiley, New York
3. Bond AM (1980) Modern polarographic methods in analytical chemistry. Dekker, New York
4. Bontempelli G, Magno F, Mazzocchin GA, Seeber R (1989) Linear sweep and cyclic voltammetry. Ann Chim (Rome) 79:103–216
5. Brett CMA, Oliveira Brett MA (1993) Electrochemistry: principles, methods, and applications. Oxford Science, Oxford
6. Brett CMA, Oliveira Brett AM (1998) Electroanalysis. Oxford Science, Oxford
7. Britz D (2005) Digital simulation in electrochemistry, Lect Notes Phys 666. Springer, Berlin
8. Delahay P (1954) New instrumental methods in electrochemistry. Wiley, New York

9. Denbigh K (1981) The principles of chemical equilibrium, IVth edn. Cambridge University Press, Cambridge, UK
10. Estela JM, Tomas C, Cladera A, Cerda V (1995) Potentiometric stripping analysis – a review. Crit Rev Anal Chem 25:91–141
11. Feldberg SW (1969) Digital Simulation: a general method for solving electrochemical diffusio-kinetic problems. In: Bard AJ (ed) Electroanalytical chemistry series, vol 3. Dekker, New York, pp 199–296
12. Galus Z (1976) Fundamentals of electrochemical analysis, Ellis Horwood Series in Analytical Chemistry, Ellis Horwood series in analytical chemistry. Wiley, New York, NY
13. Heyrovsky J, Kuta J (1966) Principles of polarography. Academic, New York, NY
14. Jagner D, Granelli A (1976) Potentiometric stripping analysis. Anal Chim Acta 83:19–26
15. Kissinger P, Heinemann WR (1996) Laboratory techniques in electroanalytical chemistry, second edition, revised and expanded. CRC Press
16. Koryta J, Dvorak J, Bohackova V (1970) Electrochemistry. Meuten & Co, London
17. Macdonald DD (1977) Transient techniques in electrochemistry. Plenum, New York, NY
18. Matsuda H, Ayabe Y (1955) Zur theorie der randles-sevcikschen kathodenstrahl-polarographie. Z Elektrochem 59:494–503
19. Monk PMS (2001) Fundamentals of electro-analytical chemistry. Wiley, England
20. Nicholson RS, Shain I (1964) Theory of stationary electrode polarography. Single scan and cyclic methods applied to reversible, irreversible, and kinetic systems. Anal Chem 36:706–723
21. Nicholson RS (1965) Theory and application of cyclic voltammetry for measurement of electrode reaction kinetics. Anal Chem 37:1351–1355
22. Rieger PH (1994) Electrochemistry. Chapmann & Hall, New York, NY
23. Rossiter BW, Hamilton JF (eds) (1986) Physical methods of chemistry, vol II electrochemical methods, 2nd edn. Wiley, New York, NY
24. Scholz F (ed) (2002) Electroanalytical methods. Guide to experiments and application. Springer, Berlin
25. Seeber R, Terzi F (2011) The evolution of amperometric sensing from the bare to the modified electrode systems. J Solid State Electr 15:1523–1534
26. Southampton Electrochemistry Group (1985) Instrumental methods in electrochemistry. Ellis Horwood, Cambridge
27. Vassos BH, Ewing GC (1983) Electroanalytical chemistry. Wiley, New York, NY
28. Vetter KJ (1967) Electrochemical kinetics: theoretical and experimental aspects. Academic, New York, NY
29. Wang J (2000) Analytical electrochemistry, 2nd edn. Willey, New York, NY

Chapter 11
Biosensors on Enzymes, Tissues, and Cells

Xuefei Guo, Julia Kuhlmann, and William R. Heineman

11.1 Overview of Biosensors

The first electrochemical biosensor for glucose was developed by Leland C. Clark in 1962. This enzymatic biosensor for glucose had glucose oxidase immobilized on the surface of an amperometric oxygen electrode and directly quantified the concentration of glucose in a sample. Driven by its huge success, fundamental and applied research has greatly expanded the concept of a biosensor since then. Today, biosensors are widely used in biomedical, industrial, and environmental analysis. According to IUPAC, a biosensor is "*a device that uses specific biochemical reactions mediated by isolated enzymes, immunosystems, tissues, organelles or whole cells to detect chemical compounds usually by electrical, thermal or optical signals*." An electrochemical biosensor is a biosensor with electrochemistry as the transducer, including current, potential, conductivity, and impedance. Electrochemical biosensors offer accuracy, precision, sensitivity, selectivity, rapidity, portability, and ease of operation for on-site environmental analysis without sample preparation. Thus, electrochemical biosensors are considered to be a promising sensing tool, which complements traditional analytical techniques such as gas and liquid chromatography.

There are three main functional steps of an electrochemical biosensor, as illustrated in Fig. 11.1. The first step is the molecular recognition, which is ideally specific to the target analyte. The second step is the signal transduction: the conversion of the molecular interaction into a measurable electrical signal, such as current, potential, or conductivity. The final step of the sensing procedure is converting the measured signal into a readable output.

Numerous biosensors based on enzymes have been developed due to the success of the enzymatic biosensor for glucose. Research on enzyme-based biosensors

X. Guo • J. Kuhlmann • W.R. Heineman (✉)
Department of Chemistry, University of Cincinnati, Cincinnati, OH 45221-0172, USA
e-mail: HEINEMWR@ucmail.uc.edu

L.M. Moretto, K. Kalcher (eds.), *Environmental Analysis by Electrochemical Sensors and Biosensors*, DOI 10.1007/978-1-4939-0676-5_11

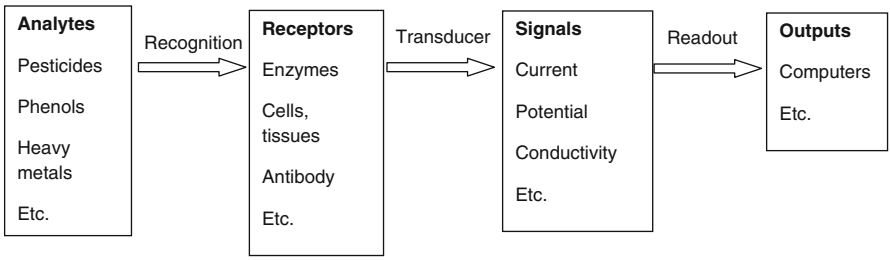

Fig. 11.1 Scheme for electrochemical biosensors

focuses on choice of enzymes, immobilization, electrochemistry, and sensor configurations. In addition to purified enzymes, many researchers have also used whole cells and tissue slices as recognition elements. The types of cells used include eukaryotes (e.g., epithelial cells) as well as prokaryotes (e.g., *E. coli*). In addition to that, some researchers even have used whole-tissue slices. There are many environmental applications for these types of sensors, ranging from the detection of organic compounds like pesticides to inorganic analytes like heavy metals. There are several excellent reviews addressing different aspects of electrochemical biosensors for environmental applications.[1–8] This section covers the principles and research of electrochemical biosensors based on enzymes, cells, and tissues during the recent 10 years.

11.2 Immobilization of Bioelements

One key step in the development of biosensors is the stable immobilization of the biological component onto the surface of the working electrode. This process strongly affects the performance of the biosensor in terms of sensitivity, selectivity, stability, response time, and reproducibility.[8] The immobilization methods that are generally employed include physical adsorption at a solid surface, covalent binding, electrostatic force, and entrapment within a membrane, surfactant matrix, polymer, or microcapsule (Fig. 11.2). Each immobilization method has advantages and drawbacks. Adsorption and electrostatic attraction are simple techniques with limited loss of enzyme activity. However, they suffer from weak interaction and desorption of the enzyme resulting from changes including temperature, pH, and ionic strength. Another drawback is nonspecific adsorption of other proteins or substances, which competes with enzyme adsorption. Covalent linking is a technique that offers high stability, but often shows high loss of enzyme activity. Enzymes are bound onto the transducer surface or onto a thin membrane fixed onto the transducer, which can either be an inorganic material (e.g., controlled pore glass) or a natural (e.g., cellulose) or synthetic polymer (e.g., nylon). Entrapment is the easiest approach to physically entrap several types of enzymes

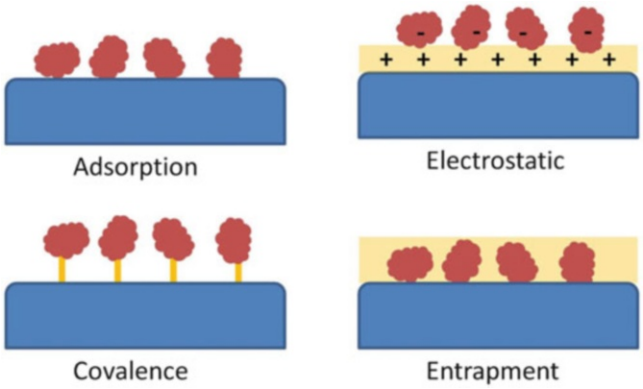

Fig. 11.2 Main immobilization methods for biosensors

in three-dimensional gels or polymers on the sensor surface. However, this method requires high concentrations of monomers and enzymes.

Efforts have been focused on investigation of various immobilization techniques. Self-assembled monolayer (SAM)[9–11] and layer-by-layer (LBL) deposition[12] have been explored for enzymatic biosensors. In these immobilization techniques, enzymes are randomly immobilized, which can lower enzyme activity. Thus, research has been conducted to achieve oriented and site-specific immobilization of biological recognition components. One of the strategies is to create affinity bonds between an activated support and a specific group of the protein sequence. Electrode surfaces have been modified by lectins, (strept)avidin, sugars, and metal chelates. Correspondingly, affinity tags (carbohydrate residues, biotin, histidine, cysteine) are present or genetically engineered at a specific location in the protein sequence without affecting the activity or the folding of the proteins.[5] Ivanov et al. have site-specifically immobilized acetylcholine esterase (AChE) on a hybrid polymer membrane with integrated multi-wall carbon nanotubes (MWCNTs).[13]

These strategies have been developed to immobilize cells and tissues on transducers in a way that allows maintaining long-term viability of the biocatalyst as well as function of the biosensor through flow of nutrients and oxygen, diffusion of analyte, and complete retention of the cells and tissues. While many immobilization methods are focused on retaining the viability of the cells and tissues, it should also be mentioned that non-live cells and tissues are used as well. In those cases, they represent a mere source of biorecognition element and allow omission of the extraction and purification steps before immobilization.[14] The initial method of immobilization used by Rechnitz et al.[15,16] was the entrapment of cells and tissue slices between two semipermeable membranes that were placed on top of the transducer. Although this method has been widely used with various types of membranes (e.g., Teflon, polycarbonate, cellulose),[17–19] it can suffer from slow response times,[20,21] as the diffusion path through the membranes can be very long, thus restricting mass transport. Other entrapment methods that have been developed include the use of organic and inorganic polymers like gelatin,[14,22–26] alginate,[27,28]

agar,[29,30] polyvinyl alcohol (PVA),[31] and sol-gels.[32,33] Gelatin films were demonstrated to have strong adhesion to biological tissues and are usually prepared by mixing gelatin with cell suspension or tissue homogenates that are dispersed on the working electrode or membrane covering the electrode, and then cross-linked with glutaraldehyde (GA). The introduction of the cross-link into the gelatin makes these films insoluble and therefore increases the number of potential applications.[34] In other studies, the gelatin-tissue homogenate was treated with sulfite to complex the inherent enzyme (bioimprinting), which was then cross-linked to the membrane of a Clark oxygen electrode. The addition of the bioimprinting step resulted in an improved operational stability of the biosensor.[14] One tactic to reduce the long response times was the use of conductive polymers, which function as an entrapment matrix as well as the transducer. In 2009 Jha et al.[35] reported the use of polystyrene sulfonate-polyaniline (PSS-PANI) conducting polymer to immobilize lyophilized *Brevibacterium ammoniagenes* cells on platinum wire electrodes to detect urea and achieve a response time of 3 min. Furthermore, they used potentiostatic electropolymerization and suggested that this is one of the safest techniques for immobilization of live cells because it is not as harsh as other polymerization methods. A similar strategy was published by Shitanda et al.,[36,37] who added MWCNTs to a mixture of *Chlorella vulgaris* cells and sodium alginate solution, and screen-printed it on a screen-printed carbon electrode (SPCE) that was used as an oxygen electrode. They reported that the addition of the MWCNTs resulted in a two-times increase in current increment for the detection of water toxicity through measuring the inhibition of photosynthetic oxygen evolution.

A very different approach to reduce the response time was done by Wang et al.[38] who developed an adaption of a modified carbon paste electrode (MCPE), where banana pulp was mixed with graphite powder and mineral oil to form a mixed biocatalyst-carbon electrode. In this configuration the carbon electrode is both the biocatalyst and the transducer, which has the advantage of a close proximity between the catalyst and the sensing element as well as the lack of diffusion layer. This method has since been widely used for immobilization of cells[39–44] and other tissue homogenates.[45–48]

11.3 Biosensors Based on Enzymes

Enzymatic electrochemical biosensors are based on immobilized enzymes, whose products can be electrochemically measured after degradation of the substrate at the surface of the biosensor. Many different types of enzymatic biosensors have been developed for environmental monitoring of pesticides, phenols, heavy metals, nitrate, formaldehyde and sulfur oxide, etc. Commonly used enzymes include but are not limited to organophosphorus hydrolase (OPH), AChE, butyrylcholinesterase (BChE), horseradish peroxidase (HRP), tyrosinase (phenol oxidases), nitrate reductase, nitrite reductase, formaldehyde dehydrogenase (FDH), and sulfite oxidase (SO).

11.3.1 Mechanisms

With the help of enzymes, electroactive products are generated or converted at the surface of biosensors, and the concentration of electroactive products is directly or indirectly (inhibition) related with target analyte concentration. Direct detection of environment-related analytes by enzymatic biosensors is relatively straightforward. For example, metalloenzyme OPH, which is able to cleave P–O, P–F, P–S, and P–CN bonds, catalyzes the hydrolysis of a wide range of organophosphate (OP) compounds, releasing an acid and an alcohol that can be detected by potentiometry[49] and amperometry[50] (Fig. 11.3). In the case of fluorine-containing organophosphates, OPH selectively hydrolyzes the P–F bond of fluorine and the hydrolysis products change solution pH.[51] Thus, direct, selective, rapid, and simple determination of organophosphate pesticides has been achieved by integrating OPH with electrochemical techniques.

Biosensors based on AChE and BChE employ a popular and sensitive detection scheme that indirectly monitors pesticides based on pesticide inhibition of electrochemical signals. AChE preferentially hydrolyzes acetyl esters, such as acetylcholine (ACh), whereas BChE hydrolyzes butyrylcholine. Both enzymes convert substrates to electroactive thiocholine and acids. Pesticides firmly bind to AChE and BChE forming a stable complex that disables their enzymatic activity by covalent binding with serine groups of the enzymes. The binding between enzymes and pesticides hinders the enzymatic degradation of substrate such as ACh and lowers the electrochemical signal. The change of electrochemical signal is thus related with concentration of pesticides indirectly (Fig. 11.4). Amperometry has been widely used to monitor the oxidation of thiocholine.[52–60] The amperometric detection of pesticides by indirectly inhibiting AChE generates very sharp, rapid, and reproducible electric signals that are proportional to the thiocholine concentration. Potentiometry[9, 61] and conductance[62] have also been monitored due to generation of acetic acid.

Several other biosensors for pesticide and toxic metal monitoring are also based on the inhibition of enzymes such as urease for heavy metals,[63,64] tyrosinase for benzoic acid, thiourea and 2-mercaptoethanol,[65] alcohol dehydrogenase for cyanides and heavy metal salts, amino oxidase for plant growth regulators, aldehyde dehydrogenase for fungicides, cytochrome c for cyanides, catalase for heavy metals, and peroxidase for cyanides and heavy metals.[66] Thus, biosensors based on the inhibition of enzymes, suffer from false-positive results. Despite lack of selectivity, this type of biosensor is powerful when rapid toxicity screening is required.

Phenolic compounds have been detected by several types of enzymes including tyrosinase, laccase, and HRP. Tyrosinase and laccase are the main two existing forms of polyphenol oxidase (PPO). The reaction mechanism of PPO is different from HRP. PPO is a copper-containing enzyme and is widely distributed throughout microorganisms, plants, and animals. PPO first binds with oxygen and is then reduced by phenolic compounds to highly reactive *o*-quinones.[1] These reactions

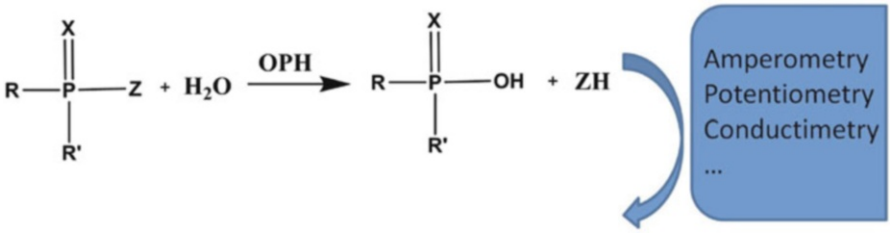

Fig. 11.3 Reaction and sensing scheme for OPH-catalyzed hydrolysis of organic organophosphorus. X is oxygen or sulfur; R is an alkoxy group; R′ is an alkoxy or phenyl group; and Z is a phenoxy, a thio moiety, a cyanide, or a fluorine group

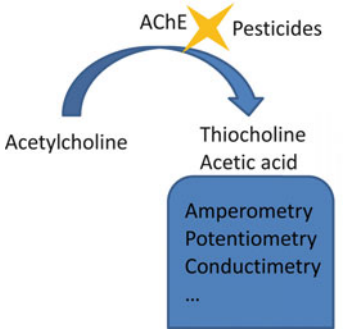

Fig. 11.4 Sensing scheme of inhibition-based biosensor for pesticides with ACh as substrate

can be monitored by various kinds of electrochemical detection techniques such as detection of oxygen consumption[67] and direct reduction of generated *o*-quinone.[68] On the other hand, immobilized HRP is oxidized by hydroperoxide and then reduced by phenolic compounds at the electrode surface. The first reaction involves a two-electron oxidation of the native peroxidase by H_2O_2 (or organic hydroperoxides). This reaction results in the formation of an intermediate, compound-I, containing oxyferryl iron. In the next reaction, compound-I loses one oxidizing equivalent upon one-electron reduction and forms compound-II. In the third step, the enzyme is returned to its native resting state.[69] For HRP-based biosensors, H_2O_2 concentration should be high enough to not limit the total reaction.[70] Nevertheless, the sensing schemes of phenolic compounds by tyrosinase, laccase, and HRP are similar. With help from the enzyme, phenolic compounds are mainly converted into quinones or free radical products, which are electroactive and can be electrochemically reduced on the electrode surface. The current from reduction is proportional to the concentration of phenolic compound in the solution.

It should be noted that tyrosinase can be inhibited by many different compounds such as carbamate and dithiocarbamate pesticides, diuron, atrazines, desisopropylatrazine, chlorophenols, and thioureas.[71] Based on this characteristic, tyrosinase has been used to develop enzymatic biosensors for the detection of many pesticides with a similar sensing mechanism with AChE and BChE (Fig. 11.4). Despite the

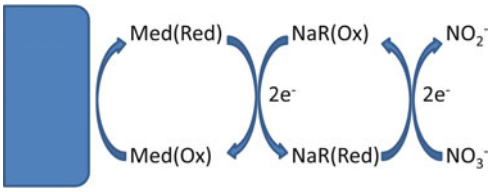

Fig. 11.5 Sensing scheme for nitrate biosensor with nitrate reductase (NaR) and mediator

poor specificity, biosensors for pesticides based on tyrosinase have higher tolerance for organic solvents and have been operated with an organic phase.[72]

Nitrate reductases (NaR) with an iron–sulfur center are used for nitrate conversion. Generally, nitrate is enzymatically reduced and NaR is in the oxidized form, which can be electrochemically reduced. However, the direct electron transfer between an enzyme and an electrode is strongly limited due to the fact that (1) the distance between the electrode surface and the redox active site of the enzyme, which is normally inside the globular protein, is large and (2) the orientation of donor to acceptor sites depends on the method of the immobilization of the enzyme at the electrode.[73] Thus, low molar mass redox mediators including quinones, metal complexes, ferricyanide, derivatives of ferrocene, and organic redox dyes[74] have been used to facilitate the electron transfer between electrode and enzyme (Fig. 11.5).

Detecting formaldehyde by FDH shares a similar mechanism with the nitrate biosensor. Formaldehyde diffuses into the liquid phase constraining FDH on the surface of the electrode. FDH oxidizes formaldehyde to formic acid, while NAD^+ is reduced to NADH. The reaction is monitored by the oxidization of NADH using electrochemical mediators including quinones. FDH from *P. putida,*[75] NAD^+- and/or glutathione-dependent formaldehyde dehydrogenase,[76] and dye-linked formaldehyde dehydrogenase from *H. zavarzinii strain ZV 580* have been used.[77] The amperometric biosensor detects formaldehyde directly from the gas phase without prior accumulation or sampling steps. The sensitivity of the formaldehyde dehydrogenase biosensor is determined by the efficiency of the electron transfer from the mediator to the working electrode.

Similarly, a biosensor for sulfur dioxide has been designed based on the enzyme sulfite oxidase with cytochrome *c* as the electron acceptor.[78] Initially, sulfur dioxide, which is present in the gas phase, dissolves in the thin buffer layer that covers the surface of the biosensor where it is converted to sulfite ions. When sulfite is oxidized to sulfate, the active sites in the enzyme are reduced. The reduced form is then oxidized by cytochrome *c*. The reduced form of cytochrome *c* is monitored by electrochemical methods leading to the analytical signal.

Biosensors based on single-type enzymes usually lack specificity and stability. For example, the presence of a high concentration of H_2O_2 causes inhibition of HRP. Moreover, H_2O_2 is unstable in solution. To improve the detection of enzymatic biosensors, multienzyme systems have been developed.[79] OPH has also been combined with the inhibited AChE strategy to produce a multienzyme biosensor with the unique ability to monitor pesticide mixtures and discriminate between

different pesticide classes.[80] OPH and HRP have been combined for sensitive detection of dichlofenthion.[81] To solve poor specificity of AChE and BChE, genetic engineering of cholinesterase enzymes has been studied to obtain more specific enzymes.[82]

11.3.2 Environmental Applications

Various enzymatic biosensors have been developed and used for environmental monitoring. Pesticides are the most abundant pollutants present in water, atmosphere, soil, plants, and food. Indirect inhibition biosensors based on AChE and BChE for pesticides are highly sensitive and responsive to pesticides at the ppb level.[54,58,83–85] Some literature reports limits of detection (LOD) down to 10^{-13} M.[86,87] Besides sensitivity, another advantage of this system lies in the ability to work with small amounts or volumes of samples, protecting the operator's health. However, since AChE is inhibited by neurotoxins, which include not only OP pesticides but also carbamate pesticides and many other compounds, these analytical tools are not selective and cannot be used for quantification of either an individual or a class of pesticides. For example, heavy metals and arsenic have been detected[63,64,82,88–90] using the inhibition mode with poor selectivity. However, sensors based on inhibition are suitable as screening tools for providing a rapid response and signaling the existence of contaminated samples. Besides poor selectivity, this system suffers from irreversible response, and a multistep protocol (involving a substrate addition and incubation). To solve this problem, enzymes have been immobilized onto cheap disposable supports such as screen-printed electrodes.[52,58,61,83,91,92]

Direct, sensitive, selective, and rapid biosensors have been developed based on OPH, organophosphorus acid hydrolase (OPAA), and parathion hydrolase (PH).[93] Schöning and co-workers developed a silicon-based capacitive field-effect pH sensor, which can detect 2 μM of paraoxon.[94] The same group prepared amperometric and potentiometric biosensor chips by thin-film techniques and integrated them in a flow-injection analysis (FIA) system, which can detect different OP pesticides at the low μM concentration range.[95] Recently, mesoporous carbon and carbon black-modified electrodes have been used to develop an amperometric biosensor based on OPH. With increased sensitivity, the biosensor can detect as low as 0.12 μM (36 ppb) paraoxon.[96]

Sensitive detection of other pollutants is achieved by various enzymatic biosensors. Integration of tyrosinase and redox polymers assures efficient catechol recycling between the enzyme and the polymer-bound redox sites leading to a detection limit of 10 nM for catechol.[97] Nitrate biosensors based on NaR usually employ a cofactor or mediator, such as NADH and Azure A, by either adding to the measurement solution or immobilizing.[98,99] Based on this sensing mechanism, nitrate biosensors can detect as low as 0.2 μM.[100] The nitrate biosensor from the

Nitrate Elimination Company, Inc. (NECi) is one of those commercially available biosensors for environmental applications. However, dissolved oxygen is still a concern for cathodic reduction of nitrate and efforts have been made to reduce interference from oxygen reduction for nitrate biosensors.[101] An electrochemical biosensor based on FDH can detect formaldehyde directly from the gas phase without prior accumulation and sampling steps with a sensitivity of 0.39 μA/ppm.[77] Formaldehyde can also be oxidized by alcohol oxidase (AOX) and a continuous fluidized bed bioreactor has been designed to enable an effective bioconversion of formaldehyde in air.[102]

11.3.3 Trends

Nanotechnology, miniaturization, and especially biotechnology are growing areas that will lead to new biosensing strategies. Nanomaterials including conducting polymer nanowires, carbon nanotubes, and nanoparticles have been incorporated into the design of biosensors constituting an exciting and recent approach to improve the performance of biosensors. Carbon nanotubes (CNTs) have excellent electrical, mechanical, and structural properties and can enhance the electron transfer of biomolecules.[58,87,103–105] It has been demonstrated that single-walled carbon nanotubes (SWCNTs) can enhance the stability of enzymatic biosensors.[106] Metal nanoparticles can enhance the electron transfer between the redox center in proteins and an electrode surface[53–55] and show promise for detection of enzyme inhibitors. AChE has been immobilized in graphene nanocomposites[107] and encapsulated in liposomes.[59] Vastarella and co-workers combined formaldehyde dehydrogenase and CdS nanocrystals.[108] An amperometric biosensor for the highly selective and sensitive determination of methyl parathion (MP) was developed by coupling OPH-loaded quantum dots to CNT/Au nanoparticles (NPs).[109] By dual-signal amplification (large amount of enzymes and synergistic effect of NPs towards enzymatic catalysis), an LOD of 1 ng/mL was achieved. Since sensors based on inhibition suffer from irreversible response, and a multistep protocol, enzymes have been immobilized onto screen-printed electrodes.[52,58,61,83,91,92] Table 11.1 is a representative summary of enzyme-based electrochemical biosensors for pesticides and phenols reported in the past 10 years.

11.4 Biosensors Based on Cells and Tissues

While enzymatic biosensors have gained increasing popularity over the past decades, researchers also focused on the development of whole cell- and tissue-based biosensors. One of the first studies that reported the use of living cells as biocatalytic elements for biosensors was published in 1978 by G.A. Rechnitz

Table 11.1 Representative summary of enzyme-based electrochemical biosensors for pesticides and phenols reported in the past 10 years (2003–2013)

Analyte	Electrochemical method	Bioelement	Immobilization	Linear range[a]	LOD[a]	Reference
Anatoxin	Amperometry	Engineered AChE	Entrapment	n.r.	0.5 nM	110
Aldicarb	Potentiometry	AChE, BChE	Covalence	10^{-7} to 10^{-5} M	2×10^{-7} M	111
Trichlorfon				10^{-7} to 10^{-5} M	1.5×10^{-7} M	
Coumaphos				10^{-8} to 10^{-6} M	5×10^{-9} M	
Methiocarb				10^{-7} to 10^{-5} M	8×10^{-7} M	
Carbaryl	Amperometry	AChE	Adsorption	0.01–0.4 μM 1–5 μM	3 nM	56
Carbaryl	Amperometry	AChE	Adsorption	0.002–2 μg/mL	0.7 ng/mL	107
Carbaryl	Amperometry	AChE	Adsorption	0.1–30 μM	6.0×10^{-8} M	57
Methyl parathion				3.5–200 μM	5.0×10^{-7} M	
Carbaryl, monocrotophos, methyl, parathion	Voltammetry	AChE	Entrapment	n.r.	n.r.	112
Chlorpyrifos	Voltammetry	AChE	Covalence	10^{-10} to 10^{-7} M	1.58×10^{-10} M	113
Chlorpyrifos	Amperometry	AChE	Entrapment	10^{-8} to 10^{-6} M	4 nM	114
Chlorpyrifos-oxon, Chlorfenvinphos, azinphos	Amperometry	Genetically modified AChE	Entrapment	n.r.	1 nM	115
Dichlorvos	Potentiometry	BChE	Covalence	0.1–100 ng/mL	0.05 ng/mL	116
Dichlorvos	Amperometry	AChE	LBL	0.25–1.5 μM 1.75–10 μM	0.86 μg/L	59
Dichlorvos, diazinon, araoxon, parathion,	Amperometry Potentiometry	OPH	Covalence	1–100 μM	0.1 μM	95
Dichlorvos, monocrotophs, parathion	Amperometry	AChE	Adsorption	n.r.	4–7 μg/mL	52
Dimethoate	Amperometry	AChE	Adsorption	0.01 to 10 μM	2 nM	117

DZN-oxon	Amperometry	AChE, ChoX	Entrapment	10^{-10} to 10^{-6} M	1.2×10^{-9} M	[118]
Methyl parathion	Voltammetry	AChE	Electrostatic	10^{-12} to 5×10^{-7} M	7.5×10^{-13} M	[87]
Methyl parathion Acepthate	Voltammetry	AChE	Entrapment	0.1 to 0.5 ppb 50–750 ppb	0.08 ppb 87 ppb	[85]
Malathion	Voltammetry	AChE	Adsorption	0.1–20 ng/mL	0.03 ng/mL	[119]
Malathion, chlorpyrifos, monocrotophos, endosulfan	Amperometry	AChE	Covalence	0.1–50 nM	0.1, 0.1 nM,1 nM,10 nM	[120]
Methyl parathion	Voltammetry	AChE	Entrapment	0.005–4.5 μg/mL	2 ng/mL	[121]
Methyl parathion	Amperometry	AChE	Covalence	0.005–0.3 μg/mL 0.3–4 μg/mL	0.6 ng/mL	[60]
Methyl parathion	Photoelectrochemistry	AChE	Entrapment	0.001 to 1 μg/mL	0.4 ng/mL	[122]
Methyl parathion, chlorpyrifos	Voltammetry	AChE	Covalence	10^{-11} to 10^{-6} M	10^{-12} M	[123]
Methyl parathion	Amperometry	OPH	Covalence	5–1,000 ng/mL	1 ng/mL	[109]
Monocrotophos	Amperometry	AChE	Adsorption	1–1,000 pg/mL 1–10 ng/mL	0.8 pg/mL	[55]
Monocrotophos	Amperometry	AChE	Covalence	0.001–15 μg/mL	0.3 ng/mL	[124]
Monocrotophs	Amperometry	AChE	Entrapment	0.05–10 ppb	0.05 ng/mL	[84]
Monocrotophos, metasystox, lannate	Potentiometry	AChE	Entrapment	0–10 ppb	n.r.	[61]
OPs	Chronoamperometry	AChE	Covalence	10^{-5} to 10^{-9} M	10^{-9} M	[125]
Paraoxon	Amperometry	AChE	Covalence	10^{-10} to 10^{-7} g/L	7×10^{-11} g/L	[53]
Paraoxon	Amperometry	AChE	Affinity	10^{-11} to 10^{-8} g/L	1.4×10^{-12} g/L	[13]
Paraoxon	Amperometry	AChE, ChoX	Covalence	10^{-9} to 10^{-5} M	10^{-10} M	[126]
Paraoxon	Amperometry	AChE	Entrapment	0.035–1.38 ppm	0.035 ppm	[127]
Paraoxon	Amperometry	AChE	Electrostatic	10^{-12} to 10^{-8} M	0.4 pM	[86]
Paraoxon	Amperometry	AChE, ChE	NA	5 pM to 0.5 nM	2 pM	[92]
Paraoxon	Amperometry	AChE	Electrostatic	0.1 pM	0.1 pM to 5 nM	[10]

(continued)

Table 11.1 (continued)

Analyte	Electrochemical method	Bioelement	Immobilization	Linear range[a]	LOD[a]	Reference
Paraoxon	Amperometry	BChE	Covalence	15.8–1,800 nM	15.8 nM	[128]
Paraoxon	Amperometry	OPH	Covalence	0.5–8.5 μM	0.01 μM/L	[106]
Paraoxon	Amperometry	OPH	Entrapment	2–10 μM	0.15 μM	[104]
Paraoxon	Chronoamperometry	OPH	Entrapment	2–20 μM	2 μM	[105]
Paraoxon	Potentiometry	OPH	Covalence Entrapment Adsorption	2–50 μM	2 μM	[94]
Trichlorfon	Amperometry	AChE, ChO	Covalence	0.05–500 μg/L	0.003–700 μg/L	[9]
Resorcinol	Voltammetry	LDH	Entrapment	0–5 mmol/L	n.r.	[129]
DFP	Potentiometry	OPAA	Covalence	20 μM	20 μM to 5 mM	[51]
Diuron, atrazine, DIA, DEA	Conductance	Tyrosinase	Covalence	2–2,330 ppb	1 ppb	[71]
Parathion	Amperometry	PH	Covalence	1–1,000 ng/mL	1 ng/mL	[130]
Catechol, Phenol	Amperometry	Tyrosinase	Entrapment	10 nM to 5 mM	10, 100 nM	[97]
Catechol	Voltammetry	Tyrosinase	Entrapment	60–800 μM	6 μM	[131]
Catechol	Amperometry	Tyrosinase	Entrapment	2.5–140 μM	0.05 μM	[132]
Catechol	Amperometry	PPO	Entrapment	1.25–150 μg/L	1.25 μg/L	[133]
Catechol	Amperometry	HRP	LBL	6–120 μM	0.7 μM	[70]
Catechol	Amperometry	HRP	LBL	6–48 μM	0.6 μM	[12]
Phenol	Amperometry	Tyrosinase	Entrapment	0.5–30 μM	0.3 μM	[134]

[a]n.r. = not reported

et al.[15] They reported the development of a sensor for L-glutamine through entrapment of *Sarcina flava* cells between two membranes mounted on a potentiometric ammonia gas electrode. The biosensor used the inherent glutaminases of the bacterial cells and exhibited excellent sensitivity for L-glutamine over other amino acids in solution with an effective lifetime of over 2 weeks. This exceeded the performance of an enzymatic biosensor for glutamine using immobilized glutaminase III,[135] which had an effective lifetime of only 12 h. One year later, they showed that slices of porcine kidney tissue could also be used as a biocatalytic layer to detect L-glutamine and likewise exhibited improved stability compared to a biosensor based on the purified enzyme.[16] While those biosensors were developed to detect L-glutamine, these two studies laid the groundwork for the development of whole cell- and tissue-based biosensors for many applications (e.g., environmental, biological, pharmaceutical). These biosensor concepts have since been applied to a variety of important analytes using cells and tissues from almost any biological kingdom (e.g., Animalia, Plantae, Fungi) and with different electrochemical transducers (e.g., amperometry, potentiometry, voltammetry). In general, they can be divided into constitutive and inducible systems, where constitutive systems show a decrease in signal intensity with increasing analyte concentration, while inducible systems show an increase. The main drawback of constitutive systems is the potential for false-positive results, as a decrease in signal could also be due to issues with the cells or tissues slices.[136] Furthermore, these biosensors can be subdivided into biocatalysts, where an analyte induces a certain chemical change after it has been recognized and bound, and affinity-based systems, which are non-catalytic and in which the binding is usually irreversible.[137]

One of the reasons for the increased interest in these biosensors is the aforementioned higher catalytic stability of cell- and tissue-based biosensors as compared to enzymatic biosensors. When whole cells and tissue slices are used, the inherent enzymes remain in their native environment, which contains necessary cofactors and reactants that support their function and stability. On the other hand purified enzymes used for enzymatic biosensors can easily lose their activity, since they are lacking this necessary environment. Biosensors based on cells and tissues are generally much cheaper and easier to prepare, since no additional and usually costly extraction and purification of the enzyme are necessary. Although the sensitivity of cell and tissue sensors has been lower than that of enzymatic sensors,[138,139] some more recent studies suggested that these biosensors could exhibit higher sensitivities as they exploit the whole subcellular machinery of living cells, which could amplify a response to an analyte through signaling cascades.[140]

One of the drawbacks of these biosensors can be the lack of selectivity as the cells and tissues contain a variety of different enzymes and thus may respond to multiple analytes simultaneously. This downside could be overcome by incubation with inhibitors or inducers that selectively cancel or select certain enzymatic functions. Another problem could be the lack of recognition element within available and practical cells or tissues to detect a certain analyte. However, with the development of recombinant methods, researchers have been able to genetically engineer bacterial cells to introduce specific enzymatic functions to an

organism.[141,142] This has the added benefit that bacterial or yeast cells are usually more stable, can withstand the often harsh immobilization methods, and can be stored for longer time periods than other cell or tissue types, thus making the biosensor more stable.

When constructing biosensors from cells and tissues there can be several factors that can affect the performance of the sensor. The amount of cells immobilized, the type of membrane used, the degree of polymerization, and the amount of cross-linking agent can also influence the performance of the biosensor. Additionally, the pH, composition, and temperature of the solution tested can influence the biosensor performance dramatically. Even small changes in pH can reduce the enzymatic activity, which is often a function of pH, or even irreversibly destroy the cells or tissues. Furthermore, the composition of the solution is important as certain compounds could inhibit the enzymatic function.

While most biosensors use pure cell cultures or tissues, some biosensor applications use cells that are not purified. One example would be the use of aerobic return-activated sludge from waste waters as a source for sulfur-oxidizing bacteria (SOB). The SOB can attach to elemental sulfur, which collects in an electrochemical flow cell, as it is very insoluble, and use it as an energy source for carbon fixation by producing sulfuric acid in the presence of oxygen. The pH and the conductivity of the effluent are monitored continuously and once they are constant, the system is stable for at least 30 days and can be used to detect toxic substances like endocrine-disrupting compounds (EDCs),[143] heavy metals,[144,145] or oxidized contaminants.[146] When the SOB are exposed to toxic compounds, the sulfur oxidation is inhibited and the pH of the effluent increases while the conductivity decreases, thus indicating water toxicity. Similarly to this approach, some studies use mediator-less microbial fuel cells (MFC) inoculated with activated return sludge to measure the biochemical oxygen demand (BOD) as an indicator for organic matter.[147–149] In these studies the bacterial cells grew inside the MFC as biofilms. Table 11.2 is a representative summary of cell- and tissue-based electrochemical biosensors for environmental monitoring reported in the past 10 years.

11.5 Conclusions and Outlook

Biosensors based on enzymes have high sensitivity and selectivity. A variety of microbial biosensors have also been developed. However, it still remains a great challenge to develop a rapid, inexpensive but sensitive method for real samples. Compared to enzymatic biosensors, development of a highly satisfactory microbial biosensor is still hampered because they suffer from long response time, low sensitivity, and poor selectivity. The trends for the development of biosensors lie in miniaturization of the devices, nanotechnology, and biotechnology. Disposable screen-printed sensors have been developed for industrial wastes or natural water.[52,58,61,83,91,92] Metal nanoparticles can enhance the electron transfer between redox center in proteins and electrode surface[53–55] and show promise for detection

Table 11.2 Representative summary of cell- and tissue-based electrochemical biosensors for environmental monitoring reported in the past 10 years (2003–2013)

Analyte	Electrochemical method	Bioelement	Immobilization	Linear range[a]	LOD[a]	Reference
Cu^{2+}	Amperometry	*Saccharomyces cerevisiae*	Entrapment	1.6–6.4 ppm and 0.05–0.35 ppm	2.1 ppm and 0.0067 ppm	142
Fe^{2+}, $S_2O_3^{2-}$	Amperometry	*Acidithiobacillus ferrooxidans*	Entrapment	Up to 2.5 mM Fe^{2+}	90 μM Fe^{2+}	18
Fe^{2+}	Amperometry	*Leptospirillum ferrooxidans*	Entrapment	Up to 2.1 mM	2.4 μM	19
Nalidixic acid (NA), 2-amino-3-methylimidazo [4,5-f]quinoline (IQ)	Amperometry	*Escherichia coli, Salmonella typhimurium*	Cells added to electrochemical micro-chambers	n.r.	10 μg/mL NA	21
Phenolic compounds	Amperometry	*Pseudomonas putida*	Entrapment	0.1–1 μM phenol	n.r.	26
Phenol	Amperometry	*Helianthus tuberosus*	Entrapment	0.002–0.010 μM	n.r.	23
Phenolic compounds	Amperometry	*Agaricus bisporus*	Entrapment	20–200 μM phenol	20 μM phenol	24
SO_3^{2-}	Amperometry	*Malva vulgaris*	Entrapment	0.2–1.8 mM	0.2 mM	25
Atrazine, 3-(3,4-dichlorophenyl)-1,1-diethylurea (DCMU), toluene, benzene	Amperometry	*Chlorella vulgaris*	Entrapment	2–20 μM atrazine	0.05 μmol/L atrazine	28
Phenolic compounds	Amperometry	*Musa Cavendish*	Entrapment	10–40 μM phenol	n.r.	22
Biochemical oxygen demand (BOD)	Amperometry	Activated sludge cultures	Entrapment	n.r.	n.r.	27
Surfactants	Amperometry	*Comamonas testosteroni*	Entrapment	n.r.		29

(continued)

Table 11.2 (continued)

Analyte	Electrochemical method	Bioelement	Immobilization	Linear range[a]	LOD[a]	Reference
					0.25 mg/L OP-10	
Zn^{2+}, Cd^{2+}	Amperometry	*Chlorella vulgaris*	Entrapment	0.1–1,000 ppb	0.01 ppb	[150]
Biochemical oxygen demand (BOD)	Amperometry	Activated sludge cultures containing sulfur-oxidizing bacteria	Entrapment	Up to 100 ppm	0.035 ppm	[31]
p-Nitrophenyl phosphate (p-NPP)	Amperometry	*Chlorella vulgaris*	Entrapment	n.r.	n.r.	[151]
Atrazine, 3-(3,4-dichlorophenyl)-1,1-diethylurea (DCMU)	Amperometry	*Chlorella vulgaris*	Entrapment	n.r.	1 μmol/L atrazine	[36, 37]
p-Nitrophenol (PNP)	Amperometry	*Moraxella sp.*	Entrapment	Up to 20 μM (2.78 ppm)	20 nM (2.78 ppb)	[39]
γ-Hexachlorocyclohexane (γ-HCH), its isomers, and degradation products	Amperometry	*Escherichia coli*	Adsorption	2–45 ppt	2 ppt	[152]
Phenol, 2,4-dihydroxybenzophenone (DHBP), nonylphenol, toluene, ethanol	Amperometry	*Escherichia coli*	–	1.6–16 ppm phenol	1.6 ppm phenol	[153]
Catechol, phenol, resorcin, orcinol, *p*-cresol, pyrogallol, L-dopa	Amperometry	*Lactobacillus acidophilus*	Entrapment	0.5–5.0 mM catechol	n.r.	[154]
p-Nitrophenol (PNP)	Amperometry	*Arthrobacter sp.*	Entrapment	Up to 0.05 mM (6.95 ppm)	0.2 μM (28 ppb)	[155]
Phenol	Amperometry	*Pseudomonas putida*	Entrapment	8–40 μM	7 μM	[156]
p-Aminophenol	Amperometry	*Salmonella typhimurium*	Adsorption	n.r.	1.2 μM	[157]

$Cr_2O_7^{2-}$	Amperometry	*Acidithiobacillus ferrooxidans*	Entrapment	Up to 0.4 mM $Cr_2O_7^{2-}$	0.41 μM	[158]
Cholinesterase	Amperometry	*Arthrobacter globiformis*	Entrapment	Up to 0.2 mM	0.08 μM	[159]
Phenol, L-tyrosine, L-DOPA	Amperometry	*Pseudomonas putida*	Entrapment	0.1–1.0 μM phenol	n.r.	[160]
Ethanol	Amperometry	*Candida tropicalis*	Entrapment	0.5–7.5 mM	n.r.	[161]
Paraoxon, methyl parathion	Amperometry	*Arthrobacter sp.*	Entrapment	Up to 5 μM	10 nM paraoxon	[162]
Zn^{2+}, Co^{2+}, Cu^{2+}	Potentiometry	*Pseudomonas sp., Bacillus cereus, Escherichia coli*	Entrapment	n.r.	0.05 mg/L Co^{2+}	[30]
Ni^{2+}	Potentiometry	*Bacillus sphaericus*	Entrapment	0.002–0.04 ppb	n.r.	[163]
β-Lactam antibiotics	Potentiometry	*Pseudomonas Aeruginosa*	Entrapment	0.1–11 mM	n.r.	[164]
Cu^{2+}	Voltammetry	*Tetraselmis chuii*	Entrapment	0.050–1.0 μM	0.00046 μM	[40]
Cu^{2+}	Voltammetry	*Circinella sp.*	Entrapment	0.5–10 μM	0.054 μM	[41]
Pb^{2+}	Voltammetry	*Phormidium sp.*	Entrapment	0.01–4.0 ppm	0.025 μM	[42]
Pb^{2+}	Voltammetry	*Rhizopus arrhizus*	Entrapment	0.1–12.5 μM	0.005 μM	[43]
Cu^{2+}	Voltammetry	*Rhodotorula mucilaginosa*	Entrapment	0.0064–0.64 ppm	n.r.	[44]
Pb^{2+}	Voltammetry	*Pennisetum setosum*	Entrapment	0.02–0.08 ppm	0.01 ppm	[46]
Pb^{2+}	Voltammetry	*Musa sp.*	Entrapment	1–20 ppm	0.1 ppm	[72]
Methyl parathion	Voltammetry	*Escherichia coli*	Entrapment	2–80 μM	0.5 μM	[165]
Biodegradable organic matter (biochemical oxygen demand (BOD))	Microbial fuel cell (MFC)	Activated sludge	Adsorption	n.r.	n.r.	[147]
Biodegradable organic matter (biochemical oxygen demand (BOD))	Microbial fuel cell (MFC)	Anaerobic sludge	Adsorption	1–25 g/L glucose	25 mg/L glucose	[148]

(continued)

Table 11.2 (continued)

Analyte	Electrochemical method	Bioelement	Immobilization	Linear range[a]	LOD[a]	Reference
Biodegradable organic matter (biochemical oxygen demand (BOD))	Microbial fuel cell (MFC)	Wastewater biofilm	Adsorption	17–183 mg O_2/L BOD	n.r.	149
3,5-Dichlorophenol, Hg^{2+}	Conductometry	*Escherichia coli*	Entrapment	n.r.	n.r.	20
Cd^{2+}, Zn^{2+}, methyl paraoxon	Conductometry	*Chlorella vulgaris*	Entrapment	n.r.	10 ppb	166
Cd^{2+}, Zn^{2+}, paraoxon-methyl	Conductometry	*Chlorella vulgaris*	Entrapment	0.01–1 ppm Cd^{2+}	10 ppb Cd^{2+}	167
Cd^{2+}	Conductometry	*Chlorella vulgaris*	Entrapment	n.r.	1 ppb	168
Cd^{2+}, Pb^{2+}, Co^{2+}, Ni^{2+}	Conductometry	*Chlorella vulgaris*	Entrapment	n.r.	n.r.	32
Cd^{2+}, Co^{2+}, Ni^{2+}, Pb^{2+}, Zn^{2+}	Conductometry	*Chlorella vulgaris*	Entrapment	0.001–10 ppm Cd^{2+}	1 ppb Cd^{2+}	33
Cd^{2+}	Conductometry	*Chlorella vulgaris*	Covalent	n.r.	1 ppb	169
Diuron, aminomethylphosphonic acid (AMPA)	Conductometry	*Dunaliella tertiolecta*	Covalent	n.r.	n.r.	170
Urea	Resistance	*Brevibacterium ammoniagenes*	Entrapment	0–75 mM	n.r.	35
Gold nanoparticle (AuNP), AgNP, single-walled carbon nanotubes (SWCNT), CdO	Impedance	Human lung fibroblasts, rainbow trout gill epithelial cells	Adsorption	n.r.	n.r.	171
Acrylonitrile, aldicarb, ammonia, As^{3+}, azide, Cu^{2+}, cyanide, fenamiphos, fluoroacetate, Hg^{2+}, methamidophos, methyl parathion, nicotine, paraquat, pentachlorophenate (PCP), phenol, Tl^{3+}, toluene	Impedance	Rainbow trout gill epithelial cells	Adsorption	n.r.	9.4 μM PCP	172

Phenol, 1,1,2-trichloroethane, cyanide, lindane, pentachlorophenate (PCP)	Impedance	Bovine pulmonary artery endothelial cells, bovine lung microvessel endothelial cells	Adsorption	n.r.	n.r.	[173]
Hg^{2+}, 2,4,6-trinitrotoluene (TNT), 1,3,5-trinitrobenzene (TNB), 2-amino-4,6-dinitrotoluene (2-ADNT)	Impedance	*Spodoptera frugiperda*	Adsorption	n.r.	n.r.	[174]
Hg^{2+}, 1,3,5-trinitrobenzene (TNB)	Impedance	Fibroblast cells	Adsorption	n.r.	n.r.	[175]
Hg^{2+}, As^{3+}	Impedance	Mouse spinal cord or frontal cortex networks	Adsorption	n.r.	10 ppm	[176]
Cd^{2+}, Hg^{2+}	Impedance	*Escherichia coli*	Cells fixed onto surface of indium-tin-oxide (ITO) glass with and without nanobeads (NBs) and/or polyelectrolyte multilayers (PEM)	1×10^{-12} to 1×10^{-3} M	1×10^{-12} M	[177]
Bisphenol-A, nonylphenol, estradiol, diethylstilbestrol, tributyltin	Conductometry, potentiometry	Sulfur-oxidizing bacteria	Adsorption	5–200 ppb	n.r.	[143]
Cr^{6+}	Conductometry, potentiometry	Sulfur-oxidizing bacteria	Adsorption	n.r.	5 ppb	[144]
Cr^{6+}	Conductivity, potentiometry	Sulfur-oxidizing bacteria	Adsorption	n.r.	n.r.	[145]
Nitrite, nitrate, perchlorate, dichromate	Conductometry, potentiometry	Sulfur-oxidizing bacteria	Adsorption	5–50 ppb	n.r.	[146]

[a]n.r. = not reported

of enzyme inhibitors. With a better understanding of the genetic information of microbes, more specific enzymes and proteins have been expressed on the cell surface. In this format, the microbes can serve as an enzyme support matrix and faster response and highly sensitive biosensors can be developed.

References

1. Mukherjee S, Basak B, Bhunia B, Dey A, Mondal B (2013) Potential use of polyphenol oxidases (PPO) in the bioremediation of phenolic contaminants containing industrial wastewater. Rev Environ Sci Bio 12(1):61–73. doi:10.1007/s11157-012-9302-y
2. Van Dyk JS, Pletschke B (2011) Review on the use of enzymes for the detection of organochlorine, organophosphate and carbamate pesticides in the environment. Chemosphere 82(3):291–307. doi:10.1016/j.chemosphere.2010.10.033
3. Karim F, Fakhruddin ANM (2012) Recent advances in the development of biosensor for phenol: a review. Rev Environ Sci Bio 11(3):261–274. doi:10.1007/s11157-012-9268-9
4. Liu SQ, Zheng ZZ, Li XY (2013) Advances in pesticide biosensors: current status, challenges, and future perspectives. Anal Bioanal Chem 405(1):63–90. doi:10.1007/s00216-012-6299-6
5. Andreescu S, Marty JL (2006) Twenty years research in cholinesterase biosensors: from basic research to practical applications. Biomol Eng 23(1):1–15. doi:10.1016/j.bioeng.2006.01.001
6. Amine A, Mohammadi H, Bourais I, Palleschi G (2006) Enzyme inhibition-based biosensors for food safety and environmental monitoring. Biosens Bioelectron 21(8):1405–1423. doi:10.1016/j.bios.2005.07.012
7. Almeida MG, Serra A, Silveira CM, Moura JJG (2010) Nitrite biosensing via selective enzymes – a long but promising route. Sensors 10(12):11530–11555. doi:10.3390/S101211530
8. Sassolas A, Blum LJ, Leca-Bouvier BD (2012) Immobilization strategies to develop enzymatic biosensors. Biotechnol Adv 30(3):489–511. doi:10.1016/j.biotechadv.2011.09.003
9. Snejdarkova M, Svobodova L, Evtugyn G, Budnikov H, Karyakin A, Nikolelis DP, Hianik T (2004) Acetylcholinesterase sensors based on gold electrodes modified with dendrimer and polyaniline – a comparative research. Anal Chim Acta 514(1):79–88. doi:10.1016/j.aca.2004.03.019
10. Wang Y, Zhang S, Du D, Shao YY, Li ZH, Wang J, Engelhard MH, Li JH, Lin YH (2011) Self assembly of acetylcholinesterase on a gold nanoparticles-graphene nanosheet hybrid for organophosphate pesticide detection using polyelectrolyte as a linker. J Mater Chem 21(14):5319–5325. doi:10.1039/C0jm03441j
11. Cancino J, Razzino CA, Zucolotto V, Machado SAS (2013) The use of mixed self-assembled monolayers as a strategy to improve the efficiency of carbamate detection in environmental monitoring. Electrochim Acta 87:717–723. doi:10.1016/j.electacta.2012.09.080
12. Yang SM, Chen ZC, Jin X, Lin XF (2006) HRP biosensor based on sugar-lectin biospecific interactions for the determination of phenolic compounds. Electrochim Acta 52(1):200–205. doi:10.1016/j.electacta.2006.04.059
13. Ivanov Y, Marinov I, Gabrovska K, Dimcheva N, Godjevargova T (2010) Amperometric biosensor based on a site-specific immobilization of acetylcholinesterase via affinity bonds on a nanostructured polymer membrane with integrated multiwall carbon nanotubes. J Mol Catal B-Enzym 63(3–4):141–148. doi:10.1016/j.molcatb.2010.01.005
14. Teke M, Sezginturk MK, Dinckaya E, Telefoncu A (2008) Two biosensors for phenolic compounds based on mushroom (Agaricus bisporus) homogenate: comparison in terms of some important parameters of the biosensors. Prep Biochem Biotechnol 38(1):51–60. doi:10.1080/10826060701774346

15. Rechnitz GA, Riechel TL, Kobos RK, Meyerhoff ME (1978) Glutamine-selective membrane electrode that uses living bacterial cells. Science 199(4327):440–441
16. Rechnitz GA, Arnold MA, Meyerhoff ME (1979) Bio-selective membrane electrode using tissue. Nature 278:466–467
17. Lei Y, Mulchandani P, Chen W, Mulchandani A (2005) Direct determination of p-nitrophenyl substituent organophosphorus nerve agents using a recombinant Pseudomonas putida JS444-modified clark oxygen electrode. J Agr Food Chem 53(3):524–527
18. Zlatev R, Magnin JP, Ozil P, Stoytcheva M (2006) Bacterial sensors based on Acidithiobacillus ferrooxidans part I. Fe^{2+} and $S_2O_3^{2-}$ determination. Biosens Bioelectron 21 (8):1493–1500. doi:10.1016/j.bios.2005.07.007
19. Stoytcheva M, Zlatev R, Magnin JP, Ovalle M, Valdez B (2009) Leptospirillum ferrooxidans based Fe2+ sensor. Biosens Bioelectron 25(2):482–487. doi:10.1016/j.bios.2009.08.019
20. Bhatia R, Dilleen JW, Atkinson AL, Rawson DM (2003) Combined physico-chemical and biological sensing in environmental monitoring. Biosens Bioelectron 18(5–6):667–674. doi:10.1016/s0956-5663(03)00012-5
21. Ben-Yoav H, Biran A, Pedahzur R, Belkin S, Buchinger S, Reifferscheid G, Shacham-Diamand Y (2009) A whole cell electrochemical biosensor for water genotoxicity bio-detection. Electrochim Acta 54(25):6113–6118. doi:10.1016/j.electacta.2009.01.061
22. Ozcan HM, Sagiroglu A (2010) A novel amperometric biosensor based on banana peel (Musa cavendish) tissue homogenate for determination of phenolic compounds. Artif Cells Blood Substit Immobil Biotechnol 38(4):208–214. doi:10.3109/10731191003776744
23. Odaci D, Tımur S, Telefoncu A (2004) Immobilized jerusalem artichoke (Helianthus tuberosus) tissue electrode for phenol detection. Artif Cells Blood Substit Biotechnol 32 (2):315–323. doi:10.1081/bio-120037836
24. Topcu S, Sezginturk MK, Dinckaya E (2004) Evaluation of a new biosensor-based mushroom (Agaricus bisporus) tissue homogenate: investigation of certain phenolic compounds and some inhibitor effects. Biosens Bioelectron 20(3):592–597. doi:10.1016/j.bios.2004.03.011
25. Sezgintürk MK, Dinckaya E (2005) Direct determination of sulfite in food samples by a biosensor based on plant tissue homogenate. Talanta 65(4):998–1002. doi:10.1016/j.talanta.2004.08.037
26. Timur S (2003) Detection of phenolic compounds by thick film sensors based on Pseudomonas putida. Talanta 61(2):87–93. doi:10.1016/s0039-9140(03)00237-6
27. Kumlanghan A, Kanatharana P, Asawatreratanakul P, Mattiasson B, Thavarungkul P (2008) Microbial BOD sensor for monitoring treatment of wastewater from a rubber latex industry. Enzyme Microb Tech 42(6):483–491. doi:10.1016/j.enzmictec.2008.01.012
28. Shitanda I, Takada K, Sakai Y, Tatsuma T (2005) Compact amperometric algal biosensors for the evaluation of water toxicity. Anal Chim Acta 530(2):191–197. doi:10.1016/j.aca.2004.09.073
29. Taranova LA, Fesay AP, Ivashchenko GV, Reshetilov AN, Winther-Nielsen M, Emneus J (2004) Comamonas testosteroni strain TI as a potential base for a microbial sensor detecting surfactants. Appl Biochem Microbiol 40(4):404–408
30. Gruzina TG, Zadorozhnyaya AM, Gutnik GA, Vember VV, Ulberg ZR, Kanyuk NI, Starodub NF (2007) A bacterial multisensor for determination of the contents of heavy metals in water. J Water Chem Technol 29(1):50–53. doi:10.3103/s1063455x07010080
31. Wang J, Zhang Y, Wang Y, Xu R, Sun Z, Jie Z (2010) An innovative reactor-type biosensor for BOD rapid measurement. Biosens Bioelectron 25(7):1705–1709. doi:10.1016/j.bios.2009.12.018
32. Durrieu C, Guedri H, Berezhetskyy A, Chovelon J-M (2007) Whole cell algal biosensors for urban waters monitoring. Novatech 7(3):1507–1514
33. Berezhetskyy AL, Durrieu C, Nguyen-Ngoc H, Chovelon J-M, Dzyadevych SV, Tran-Minh C (2007) Conductometric biosensor based on whole-cell microalgae for assessment of heavy metals in wastewater. Biopolym Cell 23(6):511–518

34. Matsuda S, Iwata H, Se N, Ikada Y (1999) Bioadhesion of gelatin films crosslinked with glutaraldehyde. J Biomed Mater Res 45(1):20–27
35. Jha SK, Kanungo M, Nath A, D'Souza SF (2009) Entrapment of live microbial cells in electropolymerized polyaniline and their use as urea biosensor. Biosens Bioelectron 24 (8):2637–2642. doi:10.1016/j.bios.2009.01.024
36. Shitanda I, Takamatsu S, Itagaki M, Watanabe K (2008) Screen-printed algal biosensor with flow injection analysis system for toxicity test. Paper presented at the ECS transactions, Honolulu, HI, USA
37. Shitanda I, Takamatsu S, Watanabe K, Itagaki M (2009) Amperometric screen-printed algal biosensor with flow injection analysis system for detection of environmental toxic compounds. Electrochim Acta 54(21):4933–4936. doi:10.1016/j.electacta.2009.04.005
38. Wang J, Lin MS (1988) Mixed plant tissue carbon paste bioelectrode. Anal Chem 60 (15):1545–1548
39. Mulchandani P, Hangarter CM, Lei Y, Chen W, Mulchandani A (2005) Amperometric microbial biosensor for p-nitrophenol using Moraxella sp.-modified carbon paste electrode. Biosens Bioelectron 21(3):523–527. doi:10.1016/j.bios.2004.11.011
40. Alpat SK, Alpat Ş, Kutlu B, Özbayrak Ö, Büyükışık HB (2007) Development of biosorption-based algal biosensor for Cu(II) using Tetraselmis chuii. Sensor Actuat B Chem 128 (1):273–278. doi:10.1016/j.snb.2007.06.011
41. Alpat S, Cadirci B, Yasa I, Telefoncu A (2008) A novel microbial biosensor based on Circinella sp. modified carbon paste electrode and its voltammetric application. Sensor Actuat B Chem 134(1):175–181. doi:10.1016/j.snb.2008.04.044
42. Yüce M, Nazir H, Dönmez G (2010) An advanced investigation on a new algal sensor determining Pb(II) ions from aqueous media. Biosens Bioelectron 26(2):321–326. doi:10.1016/j.bios.2010.08.022
43. Yüce M, Nazir H, Dönmez G (2010) Using of Rhizopus arrhizus as a sensor modifying component for determination of Pb(II) in aqueous media by voltammetry. Bioresour Technol 101(19):7551–7555. doi:10.1016/j.biortech.2010.04.099
44. Yüce M, Nazir H, Dönmez G (2010) A voltammetric Rhodotorula mucilaginosa modified microbial biosensor for Cu(II) determination. Bioelectrochem 79(1):66–70. doi:10.1016/j.bioelechem.2009.11.003
45. Ramos JA, Bermejo E, Zapardiel A, Pérez JA, Hernández L (1993) Direct determination of lead by bioaccumulation at a moss-modified carbon paste electrode. Anal Chim Acta 273 (1–2):219–227
46. Ouangpipat W (2003) Bioaccumulation and determination of lead using treated-Pennisetum-modified carbon paste electrode. Talanta 61(4):455–464. doi:10.1016/s0039-9140(03)00316-3
47. Mojica E-RE, Gomez SP, Micor JRL, Deocaris CC (2006) Lead detection using a pineapple bioelectrode. Philipp Agricult Sci 89(2):134–140
48. Mojica E-RE, Vidal JM, Pelegrina AB, Micro JRL (2007) Voltammetric determination of lead (II) ions at carbon paste electrode modified with banana tissue. J Appl Sci 7 (9):1286–1292
49. Mulchandani P, Mulchandani A, Kaneva I, Chen W (1999) Biosensor for direct determination of organophosphate nerve agents. 1. Potentiometric enzyme electrode. Biosens Bioelectron 14(1):77–85. doi:10.1016/S0956-5663(98)00096-7
50. Wang J, Chen L, Mulchandani A, Mulchandani P, Chen W (1999) Remote biosensor for in-situ monitoring of organophosphate nerve agents. Electroanal 11(12):866–869. doi:10.1002/(Sici)1521-4109(199908)11:12<866::Aid-Elan866>3.3.Co;2-T
51. Simonian AL, Grimsley JK, Flounders AW, Schoeniger JS, Cheng TC, DeFrank JJ, Wild JR (2001) Enzyme-based biosensor for the direct detection of fluorine-containing organophosphates. Anal Chim Acta 442(1):15–23. doi:10.1016/S0003-2670(01)01131-X

52. Dou JF, Fan FQ, Ding AZ, Cheng LR, Sekar R, Wang HT, Li SR (2012) A screen-printed, amperometric biosensor for the determination of organophosphorus pesticides in water samples. J Environ Sci 24(5):956–962. doi:10.1016/S1001-0742(11)60864-4
53. Marinov I, Ivanov Y, Gabrovska K, Godjevargova T (2010) Amperometric acetylthiocholine sensor based on acetylcholinesterase immobilized on nanostructured polymer membrane containing gold nanoparticles. J Mol Catal B Enzym 62(1):67–75. doi:10.1016/j.molcatb.2009.09.005
54. Liu T, Su HC, Qu XJ, Ju P, Cui L, Ai SY (2011) Acetylcholinesterase biosensor based on 3-carboxyphenylboronic acid/reduced graphene oxide-gold nanocomposites modified electrode for amperometric detection of organophosphorus and carbamate pesticides. Sensor Actuat B Chem 160(1):1255–1261. doi:10.1016/j.snb.2011.09.059
55. Wu S, Lan XQ, Zhao W, Li YP, Zhang LH, Wang HN, Han M, Tao SY (2011) Controlled immobilization of acetylcholinesterase on improved hydrophobic gold nanoparticle/Prussian blue modified surface for ultra-trace organophosphate pesticide detection. Biosens Bioelectron 27(1):82–87. doi:10.1016/j.bios.2011.06.020
56. Song YH, Zhang M, Wang L, Wan LL, Xiao XP, Ye SH, Wang JR (2011) A novel biosensor based on acetylecholinesterase/prussian blue-chitosan modified electrode for detection of carbaryl pesticides. Electrochim Acta 56(21):7267–7271. doi:10.1016/j.electacta.2011.06.054
57. Xue R, Kang TF, Lu LP, Cheng SY (2012) Immobilization of acetylcholinesterase via biocompatible interface of silk fibroin for detection of organophosphate and carbamate pesticides. Appl Surf Sci 258(16):6040–6045. doi:10.1016/j.apsusc.2012.02.123
58. Ivanov AN, Younusov RR, Evtugyn GA, Arduini F, Moscone D, Palleschi G (2011) Acetylcholinesterase biosensor based on single-walled carbon nanotubes-Co phtalocyanine for organophosphorus pesticides detection. Talanta 85(1):216–221. doi:10.1016/j.talanta.2011.03.045
59. Guan HN, Zhang FL, Yu J, Chi DF (2012) The novel acetylcholinesterase biosensors based on liposome bioreactors-chitosan nanocomposite film for detection of organophosphates pesticides. Food Res Int 49(1):15–21. doi:10.1016/j.foodres.2012.07.014
60. Gong JM, Guan ZQ, Song DD (2013) Biosensor based on acetylcholinesterase immobilized onto layered double hydroxides for flow injection/amperometric detection of organophosphate pesticides. Biosens Bioelectron 39(1):320–323. doi:10.1016/j.bios.2012.07.026
61. Dutta K, Bhattacharyay D, Mukherjee A, Setford SJ, Turner APF, Sarkar P (2008) Detection of pesticide by polymeric enzyme electrodes. Ecotox Environ Safe 69(3):556–561. doi:10.1016/j.ecoenv.2007.01.004
62. Suwansa-Ard S, Kanatharana P, Asawatreratanakul P, Limsakul C, Wongkittisuksa B, Thavarungkul P (2005) Semi disposable reactor biosensors for detecting carbamate pesticides in water. Biosens Bioelectron 21(3):445–454. doi:10.1016/j.bios.2004.11.005
63. Zhylyak GA, Dzyadevich SV, Korpan YI, Soldatkin AP, Elskaya AV (1995) Application of urease conductometric biosensor for heavy-metal ion determination. Sensor Actuat B Chem 24(1–3):145–148. doi:10.1016/0925-4005(95)85031-7
64. Berezhetskyy AL, Sosovska OF, Durrieu C, Chovelon JM, Dzyadevych SV, Tran-Minh C (2008) Alkaline phosphatase conductometric biosensor for heavy-metal ions determination. IRBM 29(2–3):136–140. doi:10.1016/j.rbmret.2007.12.007
65. Deng Q, Dong SJ (1996) Amperometric biosensor for tyrosinase inhibitors in a pure organic phase. Analyst 121(12):1979–1982. doi:10.1039/An9962101979
66. Evtugyn GA, Budnikov HC, Nikolskaya EB (1998) Sensitivity and selectivity of electrochemical enzyme sensors for inhibitor determination. Talanta 46(4):465–484. doi:10.1016/S0039-9140(97)00313-5
67. Canofeni S, Disario S, Mela J, Pilloton R (1994) Comparison of immobilization procedures for development of an electrochemical Ppo-based biosensor for on line monitoring of a depuration process. Anal Lett 27(9):1659–1669

68. Onnerfjord P, Emneus J, Markovarga G, Gorton L, Ortega F, Dominguez E (1995) Tyrosinase graphite-epoxy based composite electrodes for detection of phenols. Biosens Bioelectron 10(6–7):607–619. doi:10.1016/0956-5663(95)96937-T
69. Ruzgas T, Csoregi E, Emneus J, Gorton L, MarkoVarga G (1996) Peroxidase-modified electrodes: fundamentals and application. Anal Chim Acta 330(2–3):123–138. doi:10.1016/0003-2670(96)00169-9
70. Yang SM, Li YM, Jiang XM, Chen ZC, Lin XF (2006) Horseradish peroxidase biosensor based on layer-by-layer technique for the determination of phenolic compounds. Sensor Actuat B Chem 114(2):774–780. doi:10.1016/j.snb.2005.07.035
71. Anh TM, Dzyadevych SV, Van MC, Renault NJ, Duc CN, Chovelon JM (2004) Conductometric tyrosinase biosensor for the detection of diuron, atrazine and its main metabolites. Talanta 63(2):365–370. doi:10.1016/j.talanta.2003.11.008
72. Wang J, Dempsey E, Eremenko A, Smyth MR (1993) Organic-phase biosensing of enzyme-inhibitors. Anal Chim Acta 279(2):203–208. doi:10.1016/0003-2670(93)80318-F
73. Kirstein D, Kirstein L, Scheller F, Borcherding H, Ronnenberg J, Diekmann S, Steinrucke P (1999) Amperometric nitrate biosensors on the basis of Pseudomonas stutzeri nitrate reductase. J Electroanal Chem 474(1):43–51. doi:10.1016/S0022-0728(99)00302-2
74. Mellor RB, Ronnenberg J, Campbell WH, Diekmann S (1992) Reduction of nitrate and nitrite in water by immobilized enzymes. Nature 355(6362):717–719. doi:10.1038/355717a0
75. Hammerle M, Hall EAH, Cade N, Hodgins D (1996) Electrochemical enzyme sensor for formaldehyde operating in the gas phase. Biosens Bioelectron 11(3):239–246. doi:10.1016/0956-5663(96)88410-7
76. Ben Ali M, Korpan Y, Gonchar M, El'skaya A, Maaref MA, Jaffrezic-Renault N, Martelet C (2006) Formaldehyde assay by capacitance versus voltage and impedance measurements using bi-layer bio-recognition membrane. Biosens Bioelectron 22(5):575–581. doi:10.1016/j.bios.2006.01.019
77. Achmann S, Hermann M, Hilbrig F, Jerome V, Hammerle M, Freitag R, Moos R (2008) Direct detection of formaldehyde in air by a novel NAD(+)- and glutathione-independent formaldehyde dehydrogenase-based biosensor. Talanta 75(3):786–791. doi:10.1016/j.talanta.2007.12.015
78. Hart JP, Abass AK, Cowell D (2002) Development of disposable amperometric sulfur dioxide biosensors based on screen printed electrodes. Biosens Bioelectron 17(5):389–394. doi:10.1016/S0956-5663(01)00308-6
79. Serra B, Benito B, Agui L, Reviejo AJ, Pingarron JM (2001) Graphite-teflon-peroxidase composite electrochemical biosensors. A tool for the wide detection of phenolic compounds. Electroanal 13(8–9):693–700. doi:10.1002/1521-4109(200105)13:8/9<693::Aid-Elan693>3.0.Co;2-3
80. Simonian AL, Rainina EI, Wild JR (1997) A new approach for discriminative detection of organophosphate neurotoxins in the presence of other cholinesterase inhibitors. Anal Lett 30 (14):2453–2468
81. Sahin A, Dooley K, Cropek DM, West AC, Banta S (2011) A dual enzyme electrochemical assay for the detection of organophosphorus compounds using organophosphorus hydrolase and horseradish peroxidase. Sensor Actuat B Chem 158(1):353–360. doi:10.1016/j.snb.2011.06.034
82. Bontidean I, Ahlqvist J, Mulchandani A, Chen W, Bae W, Mehra RK, Mortari A, Csoregi E (2003) Novel synthetic phytochelatin-based capacitive biosensor for heavy metal ion detection. Biosens Bioelectron 18(5–6):547–553. doi:10.1016/S0956-5663(03)00026-5
83. Arduini F, Ricci F, Tuta CS, Moscone D, Amine A, Palleschi G (2006) Detection of carbamic and organophosphorous pesticides in water samples using a cholinesterase biosensor based on Prussian Blue-modified screen-printed electrode. Anal Chim Acta 580(2):155–162. doi:10.1016/j.aca.2006.07.052

84. Wu S, Zhang LL, Qi L, Tao SY, Lan XQ, Liu ZG, Meng CG (2011) Ultra-sensitive biosensor based on mesocellular silica foam for organophosphorous pesticide detection. Biosens Bioelectron 26(6):2864–2869. doi:10.1016/j.bios.2010.11.029
85. Raghu P, Swamy BEK, Reddy TM, Chandrashekar BN, Reddaiah K (2012) Sol-gel immobilized biosensor for the detection of organophosphorous pesticides: a voltammetric method. Bioelectrochemistry 83:19–24. doi:10.1016/j.bioelechem.2011.08.002
86. Liu GD, Lin YH (2006) Biosensor based on self-assembling acetylcholinesterase on carbon nanotubes for flow injection/amperometric detection of organophosphate pesticides and nerve agents. Anal Chem 78(3):835–843. doi:10.1021/Ac051559q
87. Dong J, Fan X, Qiao F, Ai S, Xin H (2013) A novel protocol for ultra-trace detection of pesticides: combined electrochemical reduction of Ellman's reagent with acetylcholinesterase inhibition. Anal Chim Acta 761:78–83, doi: S0003-2670(12)01719-9 [pii] 10.1016/j.aca.2012.11.042
88. Liu JX, Xu XM, Tang L, Zeng GM (2009) Determination of trace mercury in compost extract by inhibition based glucose oxidase biosensor. T Nonferr Metal Soc 19(1):235–240. doi:10.1016/S1003-6326(08)60258-7
89. Sanllorente-Mendez S, Dominguez-Renedo O, Arcos-Martinez MJ (2012) Development of acid phosphatase based amperometric biosensors for the inhibitive determination of As(V). Talanta 93:301–306. doi:10.1016/j.talanta.2012.02.037
90. Soldatkin OO, Kucherenko IS, Pyeshkova VM, Kukla AL, Jaffrezic-Renault N, El'skaya AV, Dzyadevych SV, Soldatkin AP (2012) Novel conductometric biosensor based on three-enzyme system for selective determination of heavy metal ions. Bioelectrochem 83:25–30. doi:10.1016/j.bioelechem.2011.08.001
91. Andreescu S, Barthelmebs L, Marty JL (2002) Immobilization of acetylcholinesterase on screen-printed electrodes: comparative study between three immobilization methods and applications to the detection of organophosphorus insecticides. Anal Chim Acta 464 (2):171–180. doi:10.1016/S0003-2670(02)00518-4
92. Wang J, Timchalk C, Lin YH (2008) Carbon nanotube-based electrochemical sensor for assay of salivary cholinesterase enzyme activity: An exposure biomarker of organophosphate pesticides and nerve agents. Environ Sci Technol 42(7):2688–2693. doi:10.1021/Es702335y
93. Trojanowicz M (2002) Determination of pesticides using electrochemical enzymatic biosensors. Electroanal 14(19–20):1311–1328. doi:10.1002/1521-4109(200211)14:19/20<1311::Aid-Elan1311>3.0.Co;2-7
94. Schoning MJ, Arzdorf M, Mulchandani P, Chen W, Mulchandani A (2003) A capacitive field-effect sensor for the direct determination of organophosphorus pesticides. Sensor Actuat B Chem 91(1–3):92–97. doi:10.1016/S0925-4005(03)00071-6
95. Schoning MJ, Krause R, Block K, Musahmeh M, Mulchandani A, Wang J (2003) A dual amperometric/potentiometric FIA-based biosensor for the distinctive detection of organophosphorus pesticides. Sensor Actuat B Chem 95(1–3):291–296. doi:10.1016/S0925-4005(03)00426-X
96. Lee JH, Park JY, Min K, Cha HJ, Choi SS, Yoo YJ (2010) A novel organophosphorus hydrolase-based biosensor using mesoporous carbons and carbon black for the detection of organophosphate nerve agents. Biosens Bioelectron 25(7):1566–1570. doi:10.1016/j.bios.2009.10.013
97. Yildiz HB, Castillo J, Guschin DA, Toppare L, Schuhmann W (2007) Phenol biosensor based on electrochemically controlled integration of tyrosinase in a redox polymer. Microchim Acta 159(1–2):27–34. doi:10.1007/s00604-007-0768-1
98. Adeloju SB, Sohail M (2011) Azure a mediated polypyrrole-based amperometric nitrate biosensor. Electroanal 23(4):987–996. doi:10.1002/elan.201000386
99. Sohail M, Adeloju SB (2009) Fabrication of redox-mediator supported potentiometric nitrate biosensor with nitrate reductase. Electroanal 21(12):1411–1418. doi:10.1002/elan.200804542

100. Adeloju SB, Sohail M (2011) Polypyrrole-based bilayer nitrate amperometric biosensor with an integrated permselective poly-ortho-phenylenediamine layer for exclusion of inorganic interferences. Biosens Bioelectron 26(11):4270–4275. doi:10.1016/j.bios.2011.04.002
101. Plumeré N (2013) Interferences from oxygen reduction reactions in bioelectroanalytical measurements: the case study of nitrate and nitrite biosensors. Anal Bioanal Chem 405:3731–3738
102. Sigawi S, Smutok O, Demkiv O, Zakalska O, Gayda G, Nitzan Y, Nisnevitch M, Gonchar M (2011) Immobilized formaldehyde-metabolizing enzymes from Hansenula polymorpha for removal and control of airborne formaldehyde. J Biotechnol 153(3–4):138–144. doi:10.1016/j.jbiotec.2011.03.026
103. Campbell JK, Sun L, Crooks RM (1999) Electrochemistry using single carbon nanotubes. J Am Chem Soc 121(15):3779–3780
104. Deo RP, Wang J, Block I, Mulchandani A, Joshi KA, Trojanowicz M, Scholz F, Chen W, Lin YH (2005) Determination of organophosphate pesticides at a carbon nanotube/organophosphorus hydrolase electrochemical biosensor. Anal Chim Acta 530(2):185–189. doi:10.1016/j.aca.2004.09.072
105. Choi BG, Park H, Park TJ, Kim DH, Lee SY, Hong WH (2009) Development of the electrochemical biosensor for organophosphate chemicals using CNT/ionic liquid bucky gel electrode. Electrochem Commun 11(3):672–675. doi:10.1016/j.elecom.2009.01.006
106. Pedrosa VA, Paliwal S, Balasubramanian S, Nepal D, Davis V, Wild J, Ramanculov E, Simonian A (2010) Enhanced stability of enzyme organophosphate hydrolase interfaced on the carbon nanotubes. Colloids Surf B 77(1):69–74. doi:10.1016/j.colsurfb.2010.01.009
107. Wang K, Liu Q, Dai L, Yan JJ, Ju C, Qiu BJ, Wu XY (2011) A highly sensitive and rapid organophosphate biosensor based on enhancement of CdS-decorated graphene nanocomposite. Anal Chim Acta 695(1–2):84–88. doi:10.1016/j.aca.2011.03.042
108. Vastarella W, Nicastri R (2005) Enzyme/semiconductor nanoclusters combined systems for novel amperometric biosensors. Talanta 66(3):627–633. doi:10.1016/j.talanta.2004.12.007
109. Du D, Chen WJ, Zhang WY, Liu DL, Li HB, Lin YH (2010) Covalent coupling of organophosphorus hydrolase loaded quantum dots to carbon nanotube/Au nanocomposite for enhanced detection of methyl parathion. Biosens Bioelectron 25(6):1370–1375. doi:10.1016/j.bios.2009.10.032
110. Devic E, Li DH, Dauta A, Henriksen P, Codd GA, Marty JL, Fournier D (2002) Detection of anatoxin-a(s) in environmental samples of cyanobacteria by using a biosensor with engineered acetylcholinesterases. Appl Environ Microb 68(8):4102–4106. doi:10.1128/Aem.68.8.4102-4106.2002
111. Ivanov AN, Evtugyn GA, Lukachova LV, Karyakina EE, Budnikov HC, Kiseleva SG, Orlov AV, Karpacheva GP, Karyakin AA (2003) New polyaniline-based potentiometric biosensor for pesticides detection. IEEE Sens J 3(3):333–340. doi:10.1109/Jsen.2003.814647
112. Du D, Chen SZ, Cai J, Zhang AD (2008) Electrochemical pesticide sensitivity test using acetylcholinesterase biosensor based on colloidal gold nanoparticle modified sol-gel interface. Talanta 74(4):766–772. doi:10.1016/j.talanta.2007.07.014
113. Ion AC, Ion I, Culetu A, Gherase D, Moldovan CA, Iosub R, Dinescu A (2010) Acetylcholinesterase voltammetric biosensors based on carbon nanostructure-chitosan composite material for organophosphate pesticides. Mat Sci Eng C-Mater 30(6):817–821. doi:10.1016/j.msec.2010.03.017
114. Zamfir LG, Rotariu L, Bala C (2011) A novel, sensitive, reusable and low potential acetylcholinesterase biosensor for chlorpyrifos based on 1-butyl-3-methylimidazolium tetrafluoroborate/multiwalled carbon nanotubes gel. Biosens Bioelectron 26(8):3692–3695. doi:10.1016/j.bios.2011.02.001
115. Alonso GA, Istamboulie G, Noguer T, Marty JL, Munoz R (2012) Rapid determination of pesticide mixtures using disposable biosensors based on genetically modified enzymes and artificial neural networks. Sensor Actuat B Chem 164(1):22–28. doi:10.1016/j.snb.2012.01.052

116. Ding JW, Qin W (2009) Current-driven ion fluxes of polymeric membrane ion-selective electrode for potentiometric biosensing. J Am Chem Soc 131(41):14640–14641. doi:10.1021/Ja906723h
117. Du D, Wang MH, Cai J, Zhang AD (2010) Sensitive acetylcholinesterase biosensor based on assembly of beta-cyclodextrins onto multiwall carbon nanotubes for detection of organophosphates pesticide. Sensor Actuat B Chem 146(1):337–341. doi:10.1016/j.snb.2010.02.053
118. Shimomura T, Itoh T, Sumiya T, Mizukami F, Ono M (2009) Amperometric biosensor based on enzymes immobilized in hybrid mesoporous membranes for the determination of acetylcholine. Enzyme Microb Tech 45(6–7):443–448. doi:10.1016/j.enzmictec.2009.08.007
119. Du D, Ding JW, Tao Y, Chen X (2008) Application of chemisorption/desorption process of thiocholine for pesticide detection based on acetylcholinesterase biosensor. Sensor Actuat B Chem 134(2):908–912. doi:10.1016/j.snb.2008.06.040
120. Chauhan N, Pundir CS (2011) An amperometric biosensor based on acetylcholinesterase immobilized onto iron oxide nanoparticles/multi-walled carbon nanotubes modified gold electrode for measurement of organophosphorus insecticides. Anal Chim Acta 701 (1):66–74. doi:10.1016/j.aca.2011.06.014
121. Gong JM, Wang LY, Zhang LZ (2009) Electrochemical biosensing of methyl parathion pesticide based on acetylcholinesterase immobilized onto Au-polypyrrole interlaced network-like nanocomposite. Biosens Bioelectron 24(7):2285–2288. doi:10.1016/j.bios.2008.11.012
122. Gong JM, Wang XQ, Li X, Wang KW (2012) Highly sensitive visible light activated photoelectrochemical biosensing of organophosphate pesticide using biofunctional crossed bismuth oxyiodide flake arrays. Biosens Bioelectron 38(1):43–49. doi:10.1016/j.bios.2012.04.040
123. Viswanathan S, Radecka H, Radecki J (2009) Electrochemical biosensor for pesticides based on acetylcholinesterase immobilized on polyaniline deposited on vertically assembled carbon nanotubes wrapped with ssDNA. Biosens Bioelectron 24(9):2772–2777. doi:10.1016/j.bios.2009.01.044
124. Du D, Chen SZ, Song DD, Li HB, Chen X (2008) Development of acetylcholinesterase biosensor based on CdTe quantum dots/gold nanoparticles modified chitosan microspheres interface. Biosens Bioelectron 24(3):475–479. doi:10.1016/j.bios.2008.05.005
125. Crew A, Lonsdale D, Byrd N, Pittson R, Hart JP (2011) A screen-printed, amperometric biosensor array incorporated into a novel automated system for the simultaneous determination of organophosphate pesticides. Biosens Bioelectron 26(6):2847–2851. doi:10.1016/j.bios.2010.11.018
126. Ciucu AA, Negulescu C, Baldwin RP (2003) Detection of pesticides using an amperometric biosensor based on ferophthalocyanine chemically modified carbon paste electrode and immobilized bienzymatic system. Biosens Bioelectron 18(2–3):303–310. doi:10.1016/S0956-5663(02)00173-2
127. Sinha R, Ganesana M, Andreescu S, Stanciu L (2010) AChE biosensor based on zinc oxide sol-gel for the detection of pesticides. Anal Chim Acta 661(2):195–199. doi:10.1016/j.aca.2009.12.020
128. Du D, Wang J, Wang LM, Lu DL, Smith JN, Timchalk C, Lin YH (2011) Magnetic electrochemical sensing platform for biomonitoring of exposure to organophosphorus pesticides and nerve agents based on simultaneous measurement of total enzyme amount and enzyme activity. Anal Chem 83(10):3770–3777. doi:10.1021/Ac200217d
129. Di JW, Cheng JJ, Xu QA, Zheng HI, Zhuang JY, Sun YB, Wang KY, Mo XY, Bi SP (2007) Direct electrochemistry of lactate dehydrogenase immobilized on silica sol-gel modified gold electrode and its application. Biosens Bioelectron 23(5):682–687. doi:10.1016/j.bios.2007.08.002
130. Sacks V, Eshkenazi I, Neufeld T, Dosoretz C, Rishpon J (2000) Immobilized parathion hydrolase: an amperometric sensor for parathion. Anal Chem 72(9):2055–2058. doi:10.1021/Ac9911488

131. Tembe S, Inamdar S, Haram S, Karve M, D'Souza SF (2007) Electrochemical biosensor for catechol using agarose-guar gum entrapped tyrosinase. J Biotechnol 128(1):80–85. doi:10.1016/j.jbiotec.2006.09.020
132. Tan YY, Kan JQ, Li SQ (2011) Amperometric biosensor for catechol using electrochemical template process. Sensor Actuat B Chem 152(2):285–291. doi:10.1016/j.snb.2010.12.021
133. Tan YY, Guo XX, Zhang JH, Kan JQ (2010) Amperometric catechol biosensor based on polyaniline-polyphenol oxidase. Biosens Bioelectron 25(7):1681–1687. doi:10.1016/j.bios.2009.12.007
134. Zejli H, de Cisneros JLHH, Naranjo-Rodriguez I, Liu BH, Temsamani KR, Marty JL (2008) Phenol biosensor based on Sonogel-Carbon transducer with tyrosinase alumina sol-gel immobilization. Anal Chim Acta 612(2):198–203. doi:10.1016/j.aca.2008.02.029
135. Guilbault GG, Shu FR (1971) An electrode for the determination of glutamine. Anal Chim Acta 56(3):333–338
136. Eltzov E, Marks RS (2011) Whole-cell aquatic biosensors. Anal Bioanal Chem 400 (4):895–913. doi:10.1007/s00216-010-4084-y
137. Turner APF (1989) Current trends in biosensor research and development. Sensors Actuat 17 (3–4):433–450
138. D'Souza SF (2001) Immobilization and stabilization of biomaterials for biosensor applications. Appl Biochem Biotechnol 96:225–238
139. D'Souza SF (2001) Microbial biosensors. Biosens Bioelectron 16:337–353
140. Ding L, Du D, Zhang X, Ju H (2008) Trends in cell-based electrochemical biosensors. Curr Med Chem 15(30):3160–3170
141. Su L, Jia W, Hou C, Lei Y (2011) Microbial biosensors: a review. Biosens Bioelectron 26 (5):1788–1799. doi:10.1016/j.bios.2010.09.005
142. Tag K, Riedel K, Bauer H-J, Hanke G, Baronian KHR, Kunze G (2007) Amperometric detection of Cu2+ by yeast biosensors using flow injection analysis (FIA). Sensors Actuat B Chem 122(2):403–409. doi:10.1016/j.snb.2006.06.007
143. Van Ginkel SW, Hassan SH, Oh SE (2010) Detecting endocrine disrupting compounds in water using sulfur-oxidizing bacteria. Chemosphere 81(2):294–297. doi:10.1016/j.chemosphere.2010.05.056
144. Oh S-E, Hassan SHA, Van Ginkel SW (2011) A novel biosensor for detecting toxicity in water using sulfur-oxidizing bacteria. Sensors Actuat B Chem 154(1):17–21. doi:10.1016/j.snb.2010.01.052
145. Gurung A, Oh SE, Kim KD, Shin BS (2012) Semi-continuous detection of toxic hexavalent chromium using a sulfur-oxidizing bacteria biosensor. J Environ Manage 106:110–112. doi:10.1016/j.jenvman.2012.04.010
146. Van Ginkel SW, Hassan SH, Ok YS, Yang JE, Kim YS, Oh SE (2011) Detecting oxidized contaminants in water using sulfur-oxidizing bacteria. Environ Sci Technol 45 (8):3739–3745. doi:10.1021/es1036892
147. Chang IS, Jang JK, Gil GC, Kim M, Kim HJ, Cho BW, Kim BH (2004) Continuous determination of biochemical oxygen demand using microbial fuel cell type biosensor. Biosens Bioelectron 19(6):607–613. doi:10.1016/s0956-5663(03)00272-0
148. Kumlanghan A, Liu J, Thavarungkul P, Kanatharana P, Mattiasson B (2007) Microbial fuel cell-based biosensor for fast analysis of biodegradable organic matter. Biosens Bioelectron 22(12):2939–2944. doi:10.1016/j.bios.2006.12.014
149. Peixoto L, Min B, Martins G, Brito AG, Kroff P, Parpot P, Angelidaki I, Nogueira R (2011) In situ microbial fuel cell-based biosensor for organic carbon. Bioelectrochem 81(2):99–103. doi:10.1016/j.bioelechem.2011.02.002
150. Chong KF, Loh KP, Ang K, Ting YP (2008) Whole cell environmental biosensor on diamond. Analyst 133(6):739–743. doi:10.1039/b719881g
151. Ionescu RE, Abu-Rabeah K, Cosnier S, Durrieu C, Chovelon J-M, Marks RS (2006) Amperometric algal chlorella vulgaris cell biosensors based on alginate and polypyrrole-alginate gels. Electroanalysis 18(11):1041–1046. doi:10.1002/elan.200603506

152. Anu Prathap MU, Chaurasia AK, Sawant SN, Apte SK (2012) Polyaniline-based highly sensitive microbial biosensor for selective detection of lindane. Anal Chem 84 (15):6672–6678. doi:10.1021/ac301077d
153. Neufeld N, Biran D, Popovtzer R, Erez T, Ron EZ, Rishpon J (2006) Genetically engineered pfabA pfabR bacteria: an electrochemical whole cell biosensor for detection of water toxicit. Anal Chem 78(14):4952–4956
154. Sagiroglu A, Paluzar H, Ozcan HM, Okten S, Sen B (2011) A novel biosensor based on Lactobacillus acidophilus for determination of phenolic compounds in milk products and wastewater. Prep Biochem Biotechnol 41(4):321–336. doi:10.1080/10826068.2010.540607
155. Lei Y, Mulchandani P, Chen W, Wang J, Mulchandani A (2003) A microbial biosensor for p-nitrophenol using arthrobacter Sp. Electroanalysis 15(14):1160–1164
156. Kırgöz ÜA, Odacı D, Timur S, Merkoçi A, Pazarlıoğlu N, Telefoncu A, Alegret S (2006) Graphite epoxy composite electrodes modified with bacterial cells. Bioelectrochemistry 69 (1):128–131. doi:10.1016/j.bioelechem.2005.11.002
157. Buchinger S, Grill P, Morosow V, Ben-Yoav H, Shacham-Diamand Y, Biran A, Pedahzur R, Belkin S, Reifferscheid G (2010) Evaluation of chrono-amperometric signal detection for the analysis of genotoxicity by a whole cell biosensor. Anal Chim Acta 659(1–2):122–128. doi:10.1016/j.aca.2009.11.027
158. Zlatev R, Magnin JP, Ozil P, Stoytcheva M (2006) Bacterial sensors based on Acidithiobacillus ferrooxidans part II. Cr(VI) determination. Biosens Bioelectron 21(8):1501–1506. doi:10.1016/j.bios.2005.07.004
159. Stoytcheva M, Zlatev R, Valdez B, Magnin JP, Velkova Z (2006) Electrochemical sensor based on Arthrobacter globiformis for cholinesterase activity determination. Biosens Bioelectron 22(1):1–9. doi:10.1016/j.bios.2005.11.013
160. Timur S, Seta LD, Pazarlioğlu N, Pilloton R, Telefoncu A (2004) Screen printed graphite biosensors based on bacterial cells. Process Biochem 39(11):1325–1329. doi:10.1016/s0032-9592(03)00265-6
161. Akyilmaz E, Dinckaya E (2005) An amperometric microbial biosensor development based on Candida tropicalis yeast cells for sensitive determination of ethanol. Biosens Bioelectron 20 (7):1263–1269. doi:10.1016/j.bios.2004.04.010
162. Lei Y, Mulchandani P, Chen W, Wang J, Mulchandani A (2004) Whole cell-enzyme hybrid amperometric biosensor for direct determination of organophosphorous nerve agents with p-nitrophenyl substituent. Biotechnol Bioeng 85(7):706–713. doi:10.1002/bit.20022
163. Verma N, Singh M (2006) A Bacillus sphaericus based biosensor for monitoring nickel ions in industrial effluents and foods. J Autom Methods Manag Chem 2006:1–4. doi:10.1155/JAMMC/2006/83427
164. Kumar S, Kundu S, Pakshirajan K, Dasu VV (2008) Cephalosporins determination with a novel microbial biosensor based on permeabilized Pseudomonas aeruginosa whole cells. Appl Biochem Biotechnol 151(2–3):653–664. doi:10.1007/s12010-008-8280-6
165. Kumar J, D'Souza SF (2011) Microbial biosensor for detection of methyl parathion using screen printed carbon electrode and cyclic voltammetry. Biosens Bioelectron 26 (11):4289–4293. doi:10.1016/j.bios.2011.04.027
166. Durrieu C, Chouteau C, Barthet L, Chovelon JM, Tran-Minh C (2004) A bi-enzymatic whole-cell algal biosensor for monitoring waste water pollutants. Anal Lett 37(8):1589–1599. doi:10.1081/al-120037589
167. Chouteau C, Dzyadevych S, Durrieu C, Chovelon JM (2005) A bi-enzymatic whole cell conductometric biosensor for heavy metal ions and pesticides detection in water samples. Biosens Bioelectron 21(2):273–281. doi:10.1016/j.bios.2004.09.032
168. Chouteau C, Dzyadevych S, Chovelon JM, Durrieu C (2004) Development of novel conductometric biosensors based on immobilised whole cell Chlorella vulgaris microalgae. Biosens Bioelectron 19(9):1089–1096. doi:10.1016/j.bios.2003.10.012

169. Guedri H, Durrieu C (2008) A self-assembled monolayers based conductometric algal whole cell biosensor for water monitoring. Microchim Acta 163(3–4):179–184. doi:10.1007/s00604-008-0017-2
170. Durrieu C, Guedri H, Fremion F, Volatier L (2011) Unicellular algae used as biosensors for chemical detection in Mediterranean lagoon and coastal waters. Res Microbiol 162 (9):908–914. doi:10.1016/j.resmic.2011.07.002
171. Hondroulis E, Liu C, Li CZ (2010) Whole cell based electrical impedance sensing approach for a rapid nanotoxicity assay. Nanotechnology 21(31):315103. doi:10.1088/0957-4484/21/31/315103
172. Brennan LM, Widder MW, Lee LE, van der Schalie WH (2012) Long-term storage and impedance-based water toxicity testing capabilities of fluidic biochips seeded with RTgill-W1 cells. Toxicol In Vitro 26(5):736–745. doi:10.1016/j.tiv.2012.03.010
173. Curtis TM, Widder MW, Brennan LM, Schwager SJ, van der Schalie WH, Fey J, Salazar N (2009) A portable cell-based impedance sensor for toxicity testing of drinking water. Lab Chip 9(15):2176–2183. doi:10.1039/b901314h
174. Luong JHT, Habibi-Rezaei M (2003) Insect cell-based impedance biosensors: a novel technique to monitor the toxicity of environmental pollutants. Environ Chem Lett 1(1):2–7. doi:10.1007/s10311-002-0001-8
175. Xiao C, Luong JHT (2003) On-line monitoring of cell growth and cytotoxicity using electric cell-substrate impedance sensing. Biotechnol Prog 19(3):1000–1005
176. O'Shaughnessy TJ, Gray SA, Pancrazio JJ (2004) Cultured neuronal networks as environmental biosensors. J Appl Toxicol 24(5):379–385. doi:10.1002/jat.1026
177. Souiri M, Gammoudi I, Ouada HB, Mora L, Jouenne T, Jaffrezic-Renault N, Dejous C, Othmane A, Duncan AC (2009) Escherichia coli-functionalized magnetic nanobeads as an ultrasensitive biosensor for heavy metals. Procedia Chem 1(1):1027–1030. doi:10.1016/j.proche.2009.07.256

Chapter 12
DNA Biosensors

Filiz Kuralay and Arzum Erdem

12.1 Introduction

Deoxyribonucleic acid (DNA) is the largest, well-defined, and naturally occurring molecule that may be considered as the most important molecule of life.[1,2] It encodes heritage information and instructs the biological synthesis of proteins and enzymes through the process of replication and transcription of genetic information in living organisms and many viruses. The genetic information is encoded as a sequence of nucleotides named as guanine (G), adenine (A), thymine (T), and cytosine (C). It is important to understand the structural properties of DNA, the origin of some diseases, the mutation of genes, and the action mechanism of some antitumor and antivirus drugs to design new and more efficient DNA-targeted drugs. Furthermore, the detection of DNA sequences is of widespread interest in many fields including clinical, forensic, pharmaceutical, and environmental studies (pollution, pathogen classification, etc.), bioterrorism, and food applications.[3–6]

The classical methods on DNA detection are time-consuming and labor-intensive.[7–9] However, wide-scale genetic testing requires the development of fast, inexpensive, and sensitive miniaturized devices. Thus, biosensors offer a promising alternative for faster, cheaper, and simpler detection protocols for nucleic acid analysis. These biosensors commonly rely on the immobilization of double-stranded DNA (dsDNA), single-stranded DNA (ssDNA), or an oligonucleotide

F. Kuralay
Ege University, Faculty of Pharmacy, Analytical Chemistry Department,
Bornova 35100, Izmir, Turkey

Ordu University, Faculty of Arts and Sciences, Department of Chemistry, 52200, Ordu, Turkey

A. Erdem (✉)
Faculty of Pharmacy, Analytical Chemistry Department, Ege University,
Bornova 35100, Izmir, Turkey
e-mail: arzum.erdem@ege.edu.tr; arzume@hotmail.com

L.M. Moretto, K. Kalcher (eds.), *Environmental Analysis by Electrochemical Sensors and Biosensors*, DOI 10.1007/978-1-4939-0676-5_12

(ODN) probe onto a transducer surface for hybridization with its complementary target sequence. Even though DNA is a relatively simple molecule, finding the complementary sequence that contains the desired information and distinguishing between perfect and imperfect matches are very challenging tasks. The two major requirements needed for a successful full-match DNA hybridization are high specificity and high sensitivity.

Electrochemical transducers have received considerable attention in DNA detection. Electrochemical DNA biosensors have been widely developed for chemical, biochemical, medical, agricultural, and environmental monitoring because of their compact size, real-time analysis, nearly reagentless operation, simple pretreatment protocols, low cost of construction, and simplicity of use.[10–12]

Electrochemical nucleic acid sensing protocols based on different modes of nucleic acid interaction possess an enormous potential for environmental analysis. Modern electrochemical DNA biosensors and bioassays for environmental monitoring offer remarkable sensitivity, compatibility with modern microfabrication technologies, inherent miniaturization, low cost (disposability), minimal power requirements, and independence of sample turbidity or optical pathway. Such devices are thus extremely attractive for environmental monitoring in a simpler, faster, and cheaper manner compared to traditional methods. In addition, electrochemistry offers innovative routes for monitoring systems with the signal-generating element and for amplifying electrical signals. Advances in technology have led us to face important developments in DNA-based environmental analysis. This chapter details the importance and applications of electrochemical biosensors in the field of environmental control and monitoring. The general description of electrochemical DNA biosensors is given, and the applications of these biosensors based on different electrochemical techniques using various electrode materials for environmental analysis are discussed in detail considering monitoring of pollutants that interact with the immobilized DNA layer and detection of sequences related to microbial or viral pathogens based on nucleic acid hybridization.

12.2 Electrochemical DNA Biosensors

A biosensor is an analytical device having a biologically active material either intimately connected to or integrated within a transducer.[13–16] Biosensors have been widely developed as the tools for chemical, biochemical, medical, agricultural, and environmental monitoring because of their compact size, nearly reagentless operation, simple pretreatment protocols, low cost of construction, real-time analysis, and simplicity of use. A biosensor can simply be classified in several types according to the transducer that is used. Among these types electrochemical biosensors, which are rapid, easy to handle, and of low cost, have emerged as the most commonly used biosensors since they have been found to overcome most of the

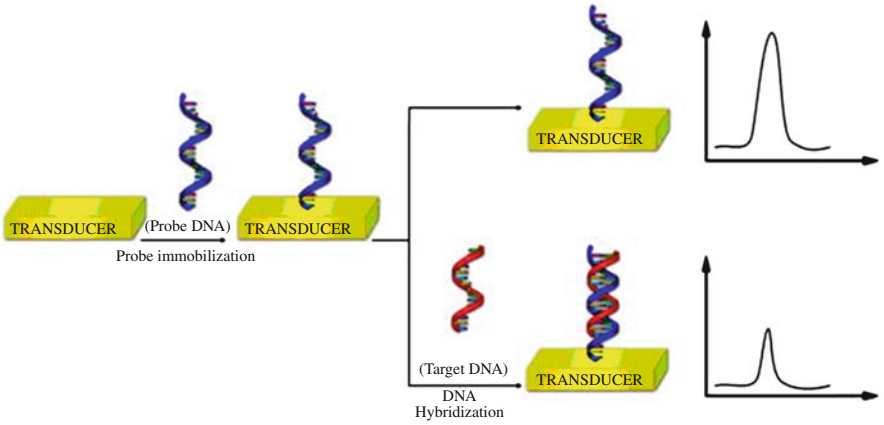

Fig. 12.1 A general configuration of an electrochemical DNA biosensor

disadvantages, which inhibit the use of other types of biosensors.[17,18] An electrochemical biosensor is a self-contained integrated device, which is able to provide specific quantitative or semiquantitative analytical information using a biochemical receptor which is retained in direct and spatial contact with the transduction element.[19] Voltammetric and amperometric sensors rely on the fact that during a bio-interaction process, electrochemical species such as electrons are consumed or generated producing an electrochemical signal, which can in turn be measured by an electrochemical detector. Biosensors based on the electrochemical transducers have the advantage of being economic and present fast response. Electrochemistry offers straightforward preparation of electrodes enabling high selectivity, specificity, and stability. Furthermore, electrochemical devices are capable of operating in complex, high-ionic strength media and are highly amenable to miniaturization. Also, the possibility of automation allows their application in a wide range of samples.[20]

Biosensors provide promising alternative routes for faster, cheaper, and simpler DNA assays compared to traditional DNA detection methods. Even though DNA is a well-defined molecule, finding the sequence that contains the desired information is a challenging task.[21,22]

Major types of DNA biosensors are electrochemical, optical, acoustic, and piezoelectric. Among these types, as mentioned above, electrochemical DNA biosensors have the potential of offering highly sensitive analytical tools. Figure 12.1 shows a general configuration of an electrochemical DNA biosensor. Simply molecular recognition events rely on the changes in the electrochemical responses before and after the hybridization event. The detection of DNA sequences shows that signal transduction can be based on electrogenerated chemiluminescence, potentiometry, and voltammetry which are all capable of detecting the analyte DNA at attomole levels.[23,24]

12.3 Applications of Electrochemical DNA Biosensors

Electrochemical biosensors have received considerable interest in specific DNA detection. The first reports about the electrochemistry of DNA were published by the end of the 1950s and in the beginning of the 1960s by Palecek.[1,2] These reports were based on electrochemical reduction and oxidation signals of DNA due to the electroactive DNA bases.

Electrochemical DNA sensing has been achieved by three types of approaches, including the use of a DNA probe having an electrochemical signal part, the use of an electrochemical DNA target, and the monitoring of the change in electrochemical characteristics of the surface associated with hybridization.[22] The progress on electrochemical DNA sensing methods has increased with the help of technological advances.

The interaction between DNA and some metal complexes or intercalating ligands were reported by many researchers. The voltammetric characterization of lawsone-copper (II) ternary complexes and their interactions with dsDNA was studied by Babula et al.[25] These complexes presented significant prooxidant properties, which may contribute to their cytotoxicity. The interaction of copper (II) complexes of D-gluconic acid with dsDNA was investigated by Tabassum et al. and found to be covalent bond formation.[26] The hybridization indicator performance of ferrocenylnaphthalene diimide was examined based on its binding mode for dsDNA in the threading intercalation.[27] Also, an electrochemical gene-detecting method based on ferrocenylnaphthalene diimide as the electrochemical hybridization indicator coupled with an immobilized DNA probe was studied by Takenaka et al.[28] DNA damage studies related to DNA detection have arisen another attention. The binding of small molecules to DNA was described by intercalation, particularly, in the presence of planar aromatic compounds, such as ethidium bromide or acridine dyes.[29–32] Redox indicators can hold important place in DNA detection. Some compounds interacting with DNA can produce their own redox signals based on binding to DNA.

Many electrochemical works deal with the interactions of DNA with redox indicators, which are used in the determination of a specific DNA sequence. Kelly et al.[33] demonstrated the interaction of DNA duplexes with methylene blue which bound reversibly to sites in the DNA on gold surfaces. Echinomycin (Echi) and cobalt-phenanthroline ($[Co(phen)_3]^{3+}$) were reported for gold electrodes.[34] In order to minimize the nonspecific adsorption of oligonucleotides, the thiol-derivatized oligonucleotides were immobilized onto a gold electrode in the presence of 6-mercapto-1-hexanol. Jelen et al. investigated the interaction of Echi with DNA by cyclic voltammetry (CV) in combination with a hanging mercury drop electrode (HMDE).[35] $[Co(phen)_3]^{3+}$ was used as an electrochemical indicator of DNA hybridization at carbon paste electrodes by Erdem et al.[36] Osmium tetroxide complexes were commonly used as electroactive markers for DNA hybridization at mercury and carbon electrodes by Palecek and his group.[37–40] These complexes were applied as indicators of DNA hybridization, reacting preferentially

with ssDNA and distorted DNA regions. Moreover, DNA–osmium adducts were determined. The interaction of dsDNA and ssDNA with a ruthenium complex and methylene blue (MB) was examined on a carbon paste electrode by Erdem et al.[41] The structure of DNA was determined according to the changes at the voltammetric peaks of the ruthenium–bipyridine complex and methylene blue.[41] Erdem et al. used MB as the indicator for DNA hybridization related to the hepatitis B virus (HBV).[42] An electrochemical gene sensor was developed by using a ferrocene-modified oligonucleotide.[43] In the study of Nakayama et al.,[43] complementary ODN to the target DNA was immobilized onto a gold electrode through the specific chemisorption of phosphorothioates, and DNA sensing was achieved using the well-known ferrocene oxidation. Synthesis and characterization of ferrocene-labeled oligodeoxynucleotides were described by Beilstein and Grinstaff.[44] Electrochemically active probes containing a redox-active group which were prepared by covalent linkage of a ferrocenyl group to the 5′-aminohexyl-terminated synthetic oligonucleotides were used for the investigation of DNA hybridization.[45]

The development of double surface techniques in combination with magnetic separation and DNA sensor systems has attracted another attention in DNA sensing technology.[46–49] The use of magnetic beads offers the convenience of efficient magnetic separation. Wang et al. have studied the attachment of biotinylated oligonucleotide probes onto streptavidin-coated magnetic beads, followed by the hybridization event, dissociation of the DNA hybrid from beads, and potentiometric stripping measurements with a graphite pencil electrode.[46] DNA hybridization with magnetic beads based on the enhanced accumulation of purine nucleobases in the presence of copper ions was also investigated.[47] Zhao et al. characterized DNA-modified gold electrodes by scanning tunneling microscopy (STM), Raman spectroscopy, in situ UV/Vis reflection spectroscopy, X-ray photoelectron spectroscopy (XPS), and alternating current (AC) impedance measurements. The bases and phosphate groups of the DNA backbone interacted with gold electrode surfaces.[48] Voltammetric determination of DNA with a silver electrode at low overpotentials was carried out. In the study of Zhao et al.,[49] the voltammetric response of DNA was attributed to the redox reaction of purine bases.

The number of studies on self-assembled monolayers (SAMs) has grown over the past years. SAMs are molecular layers formed on a surface when it is immersed in a solution containing molecules that specifically interact with the surface. Due to the efficiency and simplicity of the self-assembly technique, the immobilization of thiol- or disulfide-modified DNA on gold electrodes was reported in the literature.[50–52] SAMs at mercury electrodes were also reported by Ostatna and Palecek.[53] Specific DNA sequence detection in clinical samples (undiluted and untreated human serum and urine samples) were performed on a ternary interface involving hexanedithiol (HDT) co-immobilized with the thiolated capture probe (SHCP) on gold surfaces, followed by the incorporation of 6-mercapto-1-hexanol (MCH) as the diluent.[23,24]

The amalgamation of electrochemistry with nanomaterials, which offer enhanced electrocatalytic activities, increased surface areas, and facile electron transfer provides noteworthy advantages over conventional sensing paradigms.

The power and scope of nanomaterials can be greatly enhanced by combining them with biological recognition reactions and electrical processes. Different applications of nanostructured materials have been performed in biosensing, nanomedicine, forensic, nanoelectronics, solar energy, photovoltaics applications, and environmental monitoring. Thus, the development of nanomaterials has been one of the important challenges in the preparation of electrochemical DNA biosensors like in many life sciences. In recent years, the number of studies for electrochemical DNA detection at nanomaterial-based platforms has increased gradually in the numerous types of electrochemical DNA biosensors.[1–100]

The performance of glassy carbon electrodes (GCE) and pencil graphite electrodes (PGE) modified with multiwalled carbon nanotubes (MWCNTs) was compared for electrochemical monitoring of DNA hybridization based on the changes at the guanine signal by Erdem et al.[54] MWCNT-PGEs were tested for direct electrochemical detection of specific DNA hybridization related to *hepatitis B* virus (HBV). Ye et al.[55] used a screen-printed carbon electrode (SPCE) modified with MWCNTs for the detection of calf thymus ssDNA by alternative current (AC) impedance spectroscopy. DNA-partly wrapped single-walled carbon nanotubes (SWCNTs) were used for DNA detection by Zhang et al.[56] The DNA immobilization onto MWCNT-based platform was studied for label-free detection of *influenza* virus (type A) by Tam et al.,[57] and the hybridization of the DNA probe with its target DNA was detected using the changes of the conductance on the surface of sensors leading to a change in the output signal of the system. Enzyme-based detection of DNA hybridization (nucleic acid sequences related to the *breast cancer BRCA1* gene) using an MWCNT-modified GCE was monitored by the amperometric response of α-naphthol in a study of Wang et al.[58] Erdem et al. reported a sensitive and selective assay for the label-free electrochemical detection of DNA hybridization based on the changes in the guanine oxidation signal by using MWCNT–streptavidin conjugate-modified PGEs in combination with differential pulse voltammetry (DPV) and EIS techniques.[59]

Chang et al.[60] studied DNA hybridization using gold nanoparticles based on the assembly of alternating DNA and poly(dimethyldiallylammonium chloride) multilayer films by layer-by-layer electrostatic adsorption.[60] Electrochemical detection of DNA hybridization based on silver-enhanced gold nanoparticle DNA probes was performed. The assay relied on the electrostatic adsorption of target oligonucleotides using a glassy carbon electrode.[61] Electrochemical sensing of DNA was achieved based on the oxidation signals of silver and guanine by using disposable pencil graphite electrodes as reported in a study of Karadeniz et al.[62]; the surface was modified by passive adsorption using amino-linked oligonucleotides attached onto the surface of silver nanoparticles.

The use of electroactive polymers as a DNA immobilization platform or as reporters of DNA hybridization was described in the literature.[63–80] The immobilization of DNA using a polymer film is very simple, and the adsorption or covalent binding method can be applied simultaneously. The characterization of a biofunctional electroactive polymer, poly(5-hydroxy-1,4-naphthoquinone) (juglone)-co-5-hydroxy-3-thioacetic acid-1,4-naphthoquinone, used for direct

electrochemical detection of DNA hybridization was reported by Piro et al.[63] Such a bifunctionalized polymer could act as a reagentless sensor, with the quinone group as the transducer between the biomolecule and the electrode, and the carboxylic function as the binding site. Pyrolytic graphite electrodes with adsorbed poly(4-vinylpyridine) (PVP) and an attached Ru(II) complex with 2,2′-bipyridine ligands ($[Ru(bpy)_3]^{2+}$) gave reversible voltammetric responses and facilitated the fabrication of reusable DNA biosensors. These electrodes responded to poly (guanylic) acid and DNA caused by catalytic oxidation of guanine moieties in these polynucleotides.[64]

Polypyrrole (PPy) is one of the most commonly used conducting polymers in design of advanced electrochemical biosensors.[65] The dielectric method was applied to distinguish between polymers containing different dopants and to monitor their ion exchange occurring when PPy was used for DNA adsorption.[66] Biosensing of DNA based on the electrochemical response of ferrocenyl groups grafted to polypyrrole was also studied by Korri-Youssoufi and Makrouf.[67] The preparation of a polypyrrole nanofiber-modified pencil graphite electrode and its usage as electrochemical DNA biosensor was investigated in the presence of methylene blue by Özcan et al.[68] DNA-immobilized PPy–polyvinyl sulfonate film at indium tin oxide (ITO) was studied for Mycobacterium tuberculosis by monitoring oxidation of guanine and redox indicators, methylene blue and a ruthenium complex.[69]

Polyaniline (PANI) has been used for the preparation of DNA biosensors. A DNA hybridization biosensor based on PANI electrochemically deposited onto a Pt disc electrode was fabricated by Arora et al. using biotin–avidin as indirect coupling agents to immobilize 5'-biotin end-labeled probes to detect the complementary target, using both direct electrochemical oxidations of guanine and methylene blue.[70] A PANI–polyvinyl sulfonate (PVS) film was also fabricated using electrochemically entrapped calf thymus dsDNA for the detection of organophosphorus pesticides.[71]

A poly(cyclopentadithiophene) matrix modified with DNA covalently fixed to the surface was designed to study the redox and ion-exchange properties in surface-tethered DNA-conducting polymers. The voltammetric investigations showed an improvement in conductivity, originating from the DNA modification.[72] Fang et al. investigated a label-free electrochemical method for the detection of DNA–peptide nucleic acid (PNA) hybridization using a ferrocene-functionalized polythiophene transducer and ssPNA probes on a nanogold-modified electrode.[73] A poly-L-lysine/single-walled carbon nanotube-modified carbon paste electrode was prepared as electrochemical DNA biosensor. The well-dispersed carboxylic group-functionalized single-walled carbon nanowires were dripped onto the carbon paste electrode surface, and poly-L-lysine films were subsequently electropolymerized by using cyclic voltammetry.[74] The positively charged chitosan (CS) and negatively charged DNA were alternately adsorbed onto the surface of pyrolytic graphite (PG) electrodes, forming $(CS/DNA)_n$ layer-by-layer films by Liu and Hu.[75] Poly(vinylferrocenium) (PVF^+)-modified PGEs were used for the detection of DNA hybridization based on the changes of the oxidation signals of the

polymer, guanine, and adenine using differential pulse voltammetry (DPV) as reported by Kuralay et al.[76] Also PVF^+-modified Pt and Au electrodes were prepared for biosensing of DNA.[77,78] Zinc oxide nanoparticle-PVF^+- and tin oxide nanoparticle-PVF^+-modified single-use sensor technologies were developed and examined for monitoring DNA hybridization by Erdem's group in collaboration with Sinag's group.[79,80]

The detection of drug–DNA interaction is among the important aspects of biological studies in drug discovery and pharmaceutical development processes. Wang et al. studied the interaction of the antitumor drug daunomycin with calf thymus dsDNA in solution and at the carbon paste electrode (CPE) surface. As a result of an intercalation process between this drug and dsDNA, the daunomycin response decreased.[81] The interactions of the anticancer drugs epirubicin (EPR) and mitoxantrone (MTX) with calf thymus dsDNA and calf thymus ssDNA were studied electrochemically with a CPE by Erdem and Ozsoz.[78,79] Consequently, the signals for EPR and MTX which bound to DNA through intercalation were found to decrease in the order of bare CPE, ssDNA-modified CPE, and dsDNA-modified CPE. Electrochemical investigations of the interaction between the anticancer drug mitomycin C (MC) and DNA in a novel drug-delivery system were performed by Karadeniz et al.[84]; the magnitude of guanine oxidation was monitored before and after interaction between MC and dsDNA.

Electrochemical methods not only facilitate the development of DNA biosensors which have led to a lot of advantages mentioned above but also different possibilities in the fields, such as contemporary nucleic acid research, DNA–protein interactions, DNA damage, highly sensitive nucleic acid determination, effect of surface charge on the structure and properties of DNA adsorbed at the surface, highly sensitive detection of impurities in DNA samples, etc. Electrochemical research on DNA is a vast field requiring more researchers with some knowledge both in electrochemistry and biochemistry of nucleic acids.

12.4 Electrochemical DNA Biosensors for Environmental Analysis

Technological and industrial development has in many different opportunities increased the life quality of human beings, but on the other hand, this development causes a serious danger in the pollution of the environment by various chemicals that are used and released afterwards from the processes. Monitoring pollutants in water, soil, and air is a very challenging task for the environment and also for the public health. Concerns on increasing costs and sample loads have pushed researchers for the development of alternative methods for the detection of potentially harmful pollutants in the environment that will need the requirement for extensive monitoring programs. Reliable devices for measurements of environmental samples are very important for public health, improving the quality of the environment and

facilitating technological advances. Analyses of important pollutants in air, water, soil, and plant tissues are extremely demanded in a fast, simple, easy, sensitive, and low-cost way. Well-known traditional techniques in this important field are mainly chromatographic methods which have still some drawbacks.[85] Hence, biosensors appear as alternative devices with an advantage of the ability to work in very dirty environments with high sensitivity, selectivity, and simplicity. Detection of hazardous industrial chemicals, toxic heavy metals, pesticides, phenols, surfactants, pathogenic bacteria, hormones, and antibiotics has been performed with different types of biosensors. Nucleic acid biosensors with a known sequence of bases or complex structures of DNA or RNA were used as promising analytical devices for the detection of environmental pollution and toxicity. These biosensors enable to do real-time analysis with a wide range of physical, chemical, and biological entities as receptors that can detect chemical species, such as pollutants, even simply as commercial devices. Electrochemical DNA biosensors that are commonly based on the affinity of ssDNA for its complementary strand can be used in environmental analysis with a view of developing portable, low-cost analytical devices.[17,86]

Biosensors have been reported for various environmental analyses including global environmental monitoring, agricultural monitoring, ground water screening, and ocean monitoring.[87,88] Enzyme, antibody, cell, and DNA-based biosensors can be used for environmental monitoring in case that they offer increased sensitivity, stability, and shelf life. Most commonly, electrochemical DNA biosensors have offered promising attention among the other types of biosensors. Many efforts have been made during recent years to develop various types of DNA biosensors as a general pollutant indicator for environmental analysis. These biosensors generally monitor the interaction of pollutants in water, food, soil, and plant samples with the binding affinities with the immobilized DNA layer. The presence of pathogenic microorganisms, carcinogens, and mutagenic pollutants can change the electrochemical signal of DNA bases, or intercalation can occur. In some cases positively charged compounds can bind to the DNA via electrostatic interaction.[85,89,90] The general configuration is summarized in Fig. 12.2.

A disposable electrochemical biosensor was developed by Chiti et al. for the determination of toxic polycyclic aromatic amines (1,2-diaminoanthraquinone, 2-anthramine and acridine orange) based on the intercalative or electrostatic interaction of aromatic amines on dsDNA- or ssDNA-immobilized screen-printed electrodes (SPEs).[90] The changes in the anodic signal of guanine (decrease in guanine peak area) were monitored using chronopotentiometric analysis after 2 min accumulation time. If the analyte was electroactive, it gave an additional oxidation peak in this study. The anodic signal of the guanine base was strongly influenced by structural or conformational modifications of the DNA layer accrued from DNA–analyte association. As a result, the variation in the oxidative signal of guanine was taken as an index of the molecular recognition in the study. The formed biosensor was also tested with wastewater samples. The results were compared with the results of classical genotoxicity tests. The detection limits were found as 0.05 μM for 1,2-diaminoanthraquinone and acridine orange, 0.2 μM for 2-anthramine, and 5 μM for 2-naphthylamine, respectively.

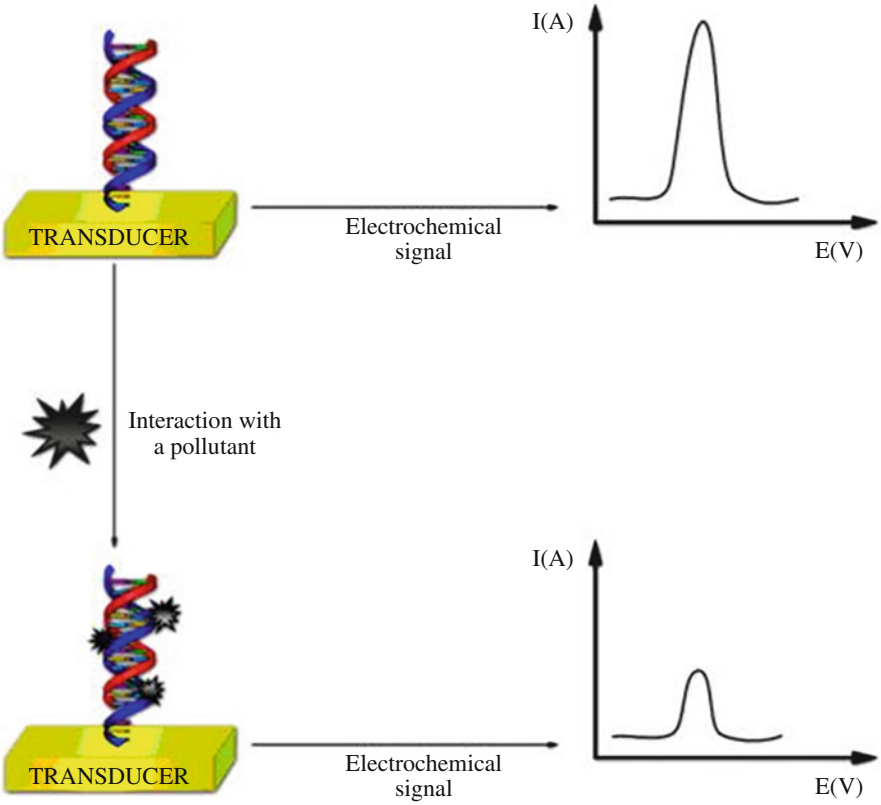

Fig. 12.2 General configuration of an electrochemical DNA biosensor for environmental analysis

Lucarelli et al.[91] reported a disposable carbon SPE that was used for wastewater sample analysis based on electrochemical DNA biosensing. Calf thymus DNA had been immobilized onto an SPE at a fixed potential, and the oxidation signal of guanine was monitored in the study by using square wave voltammetry (SWV). The DNA-immobilized electrode was dipped into the wastewater sample solution and then the oxidation signal of guanine residues after interaction was monitored. The presence of potentially toxic compounds was indicated according to the changes in the electrochemical signal of guanine. The results showed a good correlation with a commercial toxicity test which gave a more complex response than the prepared DNA biosensor since the metabolic activity of the bacterial cell was involved in the commercial test (Toxalert® 100). The determination of 2-anthramine and bisphenol A in the wastewater sample could be carried out in 8 min.

Another disposable biosensor for the detection of low-molecular-weight compounds (toxins and pollutants) was developed using the affinity for DNA on graphite SPEs.[85] The determination of low-molecular-weight compounds with affinity for DNA was measured by their effect on the oxidation signal of the guanine

peak of calf thymus DNA immobilized on the electrode with chronopotentiometric analysis yielding the following detection limits: 0.3, 0.2, and 10 mg L^{-1} for daunomycin, polychlorinated biphenyls (PCBs), and aflatoxin B1, respectively. The applicability of this environmental sensor to river water samples was also demonstrated.

Bettazzi et al.[92] used an electrochemical low-density DNA array in combination with polymerase chain reaction (PCR) in order to investigate the presence of hazelnut major allergens, Cor a 1.04 and Cor a 1.03, in foodstuff. Unmodified PCR products were captured at the electrode interface via sandwich hybridization with surface-tethered probes and biotinylated signaling probes. The resulting biotinylated hybrids were coupled to a streptavidin–alkaline phosphatase conjugate and then exposed to an α-naphthyl phosphate solution. Differential pulse voltammetry (DPV) was used to detect the α-naphthol signal with detection limits as 0.3 and 0.1 nmol L^{-1} for Cor a 1.03 and Cor 1.04, respectively. The results are comparable with the ones obtained with classical ELISA tests.

An electrochemical biosensor for the specific detection of short DNA sequences from the *Escherichia coli* (*E. coli*) pathogen was suggested by Wang et al.[93] The biosensor relied on the immobilization of the 25-mer oligonucleotide probe from the *E. coli lacZ* gene onto a screen-printed carbon electrode (SPCE). The hybridization event was monitored via chronopotentiometric detection of the $Co(bpy)_3^{3+}$ indicator. The biosensor detected 300 and 50 ng mL^{-1} of *E. coli* DNA target with 20 and 30 min of hybridization time, respectively. Untreated environmental water samples were also used in order to present the applicability of the biosensor.

Another electrochemical DNA biosensor for the detection of toxicants in water and wastewater samples was designed by Mascini's group.[94] It was prepared by immobilizing double-stranded calf thymus DNA on disposable screen-printed carbon electrodes. The determination of the genotoxic compounds 4-nitroquinoline-*N*-oxide (4-NQO), 2-aminoanthracene (2-AA), and *N*-methyl-*N*-nitro-nitrosoguanidine (MNNG) was reported by observing a decrease in the guanine oxidation peak area as an indicator evaluated from the SWV data. The obtained results were also compared with some toxicity tests and a commercial luminescence test with bacteria, Toxalert® 100.[94]

Wang et al.[95] reported an electrochemical biosensor for the detection of short DNA fragments (38-mer) specific to the deadly waterborne pathogen *Cryptosporidium* with the DNA probe immobilized on a carbon paste electrode (CPE). The hybridization event was monitored with chronopotentiometry using $Co(phen)_3^{3+}$ as an indicator with short hybridization periods (3 min) resulting in a well-defined hybridization signal at μg mL^{-1} concentrations of *Cryptosporidium* targets and ng/mL detection limits with longer periods (20–30 min). The suitability for the direct detection of the spiked *Cryptosporidium* DNA target was also tested in untreated drinking and river water samples.[95]

Toxic aromatic amines which constitute a very important class of environmental pollutants can be easily detected by electrochemical DNA biosensors. The electrochemical biosensing strategy was developed by Wang's group[96] based on the intercalative behavior of aromatic amines onto an immobilized dsDNA layer

followed by potentiometric stripping quantification of the accumulated species. The extent and rate of the accumulation were strongly dependent upon the structure of the aromatic amines. Nanomolar detection limits were obtained after 10 min of accumulation. Applicability to river and groundwater samples was also demonstrated for the electrochemical monitoring of 2-anthramine.[96]

Another electrochemical DNA biosensor for the detection of hydrazine compounds was developed by exposure of dsDNA-modified carbon paste electrodes to the compounds which resulted in a diminution of the guanine peak due to the formation of N^7-methylguanine.[97] The biosensor relied on monitoring changes in the intrinsic anodic response of the surface-confined DNA resulting from its interaction with hydrazine compounds and required no label or indicator. Short reaction times (1–10 min) were sufficient for monitoring part-per-billion levels of different hydrazines, and the applicability to river and groundwater samples was also demonstrated.[97]

DNAzymes which are single strands of DNA with catalytic activity have attracted recent interest in environmental monitoring. Arrays coated with ultrathin DNA/enzyme films were evaluated to estimate relative rates of genotoxic bioactivation of benzo[*a*]pyrene (BP) for different enzymes simultaneously.[98] Specifically, cytochrome (cyt) P450cam, cyt P40 1A2, and myoglobin in the array were activated with H_2O_2 to metabolize BP to genotoxic metabolites. DNA damage by the metabolites was detected by increases in SW voltammetric oxidation peaks using $Ru(bpy)_3^{2+}$ as a catalyst. The ability of the arrays to generate and detect metabolite-based DNA damage for the enzymes has offered an approach to identify and characterize enzymes involved in genotoxicity of pollutants.

An electrochemical DNAzyme biosensor for the detection of a heavy metal ion, lead (Pb^{2+}), was developed by Shen et al.[99] based on $Ru(NH_3)_6^{3+}$ as the electrochemical signal transducer. A specific DNAzyme upon its binding to Pb^{2+} was immobilized onto an Au electrode via thiol–Au interaction. The DNAzyme was hybridized to a complementary substrate strand that had an overhang, which in turn hybridized to the DNA–Au bio-bar code. Consequently, the DPV signals of $Ru(NH_3)_6^{3+}$ provided quantitative measures of the concentrations of Pb^{2+} in the study with a detection limit of 1 nM.

Erdem's group developed carbon nanotube-modified disposable sensors for electrochemical monitoring of DNA hybridization related to *Microcystis* spp. (MYC) following two strategies: (1) label-free and (2) indicator-based method.[100] DNA was immobilized on multiwalled carbon nanotube (MWCNT)-based screen-printed graphite electrodes (SPEs). MYC-DNA hybridization was monitored by following two strategies by measuring either the guanine oxidation signal or the reduction signal of cobalt-phenanthroline $Co(phen)_3^{3+}$. The voltammetric results were found in a good agreement with the ones recorded by electrochemical impedance spectroscopy.

12.5 Conclusions and Outlook

Wide-scale genetic testing requires the development of easy-to-use, fast, inexpensive, miniaturized analytical devices. Classical methods for detecting nucleic acids are too slow and labor-intensive. Thus, biosensors offer a promising alternative for faster, cheaper, and simpler DNA assays. These biosensors commonly rely on the immobilization of double-stranded DNA (dsDNA), single-stranded DNA (ssDNA), or a single-stranded oligonucleotide probe onto an electrochemical transducer surface for a sequence-selective hybridization with its complementary target sequence. Even though DNA is a relatively simple molecule, finding the sequence that contains the desired information and distinguishing between perfect and imperfect matches are very challenging tasks. Two major requirements are needed for successful nucleic acid hybridization: high specificity and high sensitivity. Electrochemical transducers have received considerable attention in connection to the detection of DNA.

This chapter reviews the importance and applications of electrochemical DNA biosensors in the field of environmental monitoring and control. The general description of electrochemical DNA biosensors is given herein, and also the applications of these biosensors based on different electrochemical techniques using various electrode materials for environmental analysis are discussed in detail considering monitoring of various pollutants that interact with DNA immobilized onto sensor surfaces in order to detect sequence-selective nucleic acid hybridization related to microbial or viral pathogens.

Biosensing technologies based on electrochemical DNA biosensors have provided many advantages for environmental analysis: they are low-cost, fast, easy, powerful, portable, sensitive, selective, and reliable devices for the detection of potential contaminants. To monitor the pollutants in an effective way with these kinds of technologies will lead to a better protection of the environment and hence of the public health.

Acknowledgments A.E. would like to express her gratitude to the Turkish Academy of Sciences (TUBA) as the associate member of TUBA for its partial support. The authors would like to thank Serdar Şanlı for his technical assistance.

References

1. Palecek E (2002) Past, present and future of nucleic acids electrochemistry. Talanta 56:809–819
2. Palecek E (2002) Preface. Talanta 56:807
3. Erdem A, Ozsoz M (2002) Electrochemical DNA biosensors based on DNA-drug interactions. Electroanalysis 14:965–974
4. Lucarelli F, Marrazza G, Turner APF, Mascini M (2004) Carbon and gold electrodes as electrochemical transducers for DNA hybridization sensors. Biosens Bioelectron 19:515–530
5. Cagnin S, Caraballo M, Guiducci C, Martini P, Ross M, SantaAna M, Danley D, West T, Lanfranchi G (2009) Overview of electrochemical DNA biosensors: new approaches to detect the expression of life. Sensors 9:3122–3148

6. Erdem A, Muti M, Karadeniz H, Congur G, Canavar E (2012) Electrochemical biosensors for screening of toxins and pathogens. In: Nikolelis PD (ed) NATO science for peace and security series A: chemistry and biology: portable chemical sensors:weapons against bioterrorism. Springer, Dordrecht, The Netherlands
7. Wang J (2000) From DNA biosensors to gene chips. Nucliec Acids Res 28:3011–3016
8. Gooding JJ (2002) Electrochemical DNA hybridization biosensors. Electroanalysis 14:1149–1156
9. Wang J (2002) Electrochemical detection for microscale analytical systems: a review. Talanta 56:223–231
10. Iuni-Iui Z, Hong C, Ruifu Y (1997) DNA based biosensors. Biotechnol Adv 15:43–58
11. Wang J (2005) Nanomaterial-based electrochemical biosensors. Analyst 130:421–426
12. Palecek E, Fojta M, Tomschik M, Wang J (1998) Electrochemical biosensors for DNA hybridization and DNA damage. Biosens Bioelectron 13:621–628
13. Erdem A (2007) Nanomaterial-based electrochemical DNA sensing strategies. Talanta 74:318–325
14. Wang J, Palecek E, Nielsen PE, Rivas G, Cai X, Shiraishi H, Dontha N, Luo D, Farias PAM (1996) Peptide nucleic acid probes for sequence-specific DNA biosensors. J Am Chem Soc 118:7667–7670
15. Erdem A (2012) Nanomaterials based sensor development towards electrochemical sensing of biointeractions. In: Vaseashta A, Braman E, Susmann P (eds) Technological innovations in sensing and detection of chemical, biological, radiological, nuclear threats and ecological terrorism, NATO science for peace and security series A: chemistry and biology. Springer, Dordrecht, The Netherlands
16. Karadeniz A, Kuralay F, Abaci S, Erdem A (2011) The recent electrochemical biosensor technologies for monitoring of nucleic acid hybridization. Curr Anal Chem 7:63–70
17. Odenthal KJ, Gooding JJ (2007) An introduction to electrochemical DNA biosensors. Analyst 2007:603–610
18. Gerard M, Chaubey A, Malhotra BD (2002) Application of conducting polymers to biosensors. Biosens Bioelectron 17:345–359
19. Thevenot DR, Klara T, Durst RA, Wilson GS (2001) Electrochemical biosensors: recommended definitions and classification. Biosens Bioelectron 16:121–131
20. Chaubey A, Malhotra BD (2002) Mediated biosensors. Biosens Bioelectron 17:441–456
21. Wang J (2005) Electrochemical nucleic acid biosensors. Perspectives in Bioanalysis 1:175–194
22. Millan KM, Mikkelsen SR (1993) Sequence-selective biosensor for DNA based on electroactive hybridization indicators. Anal Chem 65:2317–2323
23. Campuzano S, Kuralay F, Jesús Lobo-Castañón M, Bartošík M, Vyavahare K, Palecek E, Haake DA, Wang J (2011) Ternary monolayers as DNA recognition interfaces for direct and sensitive electrochemical detection in untreated clinical samples. Biosens Bioelectron 26:3577–3583
24. Kuralay F, Campuzano S, Haake D, Wang J (2011) Highly sensitive disposable nucleic acid biosensors for direct bioelectronic detection in raw biological samples. Talanta 85:1330–1337
25. Babula P, Vanco J, Krejcova L, Hynek D, Sochor J, Adam V, Trnkova L, Hubalek J, Kizek R (2012) Voltammetric characterization of lawsone-copper (II) ternary complexes and their interactions with dsDNA. Int J Electrochem Sci 7:7349–7366
26. Tabassum S, Mathur S (2005) Synthesis, characterization, solution stability studies, electrochemistry, and DNA-binding behavior of Cu (II) complexes of D-gluconic acid. J Carbohydr Chem 24:865–887
27. Takenaka S, Uto Y, Takagi M, Kondo H (2005) Enhanced electron transfer from glucose oxidase to DNA-immobilized electrode aided by ferrocenyl naphthalene diimide, a threading intercalator. Chem Lett 27:989–990
28. Takenaka S (2005) Threading intercalators as redox indicators. Perspect Bioanal 1:345–367

29. Fojta M, Kubicarova T, Palecek E (2000) Electrode potential-modulated cleavage surface-confined DNA by hydroxyl radicals detected by an electrochemical biosensor. Biosens Bioelectron 15:107–115
30. Zhu N, Zhang A, Wang Q, He P, Fang Y (2004) Electrochemical detection of DNA hybridization using methylene blue and electro-deposited zirconia thin films on gold electrodes. Anal Chim Acta 17:163–168
31. Navorro AE, Spinelli N, Chaix C, Moustrou C, Mandrand B, Brisset H (2004) Supported synthesis of ferrocene modified oligonucleotides as new electroactive probes. Bioorg Med Chem Lett 14:2439–2441
32. Tang TC, Huang HJ (1999) Electrochemical studies of the intercalation of ethidium bromide to DNA. Electroanalysis 11:1185–1190
33. Kelly OS, Barton JK, Jackson NM, Lill MG (1997) Electrochemistry of methylene blue bound to a DNA-modified electrode. Bioconjugate Chem 8:31–37
34. Karadeniz H, Gulmez B, Erdem A, Ozsoz M, Palecek E (2006) Echinomycin and cobalt-phenanthroline as redox indicators of DNA hybridization at gold electrodes. Front Biosci 11:1870–1877
35. Jelen F, Erdem A, Palecek E (2002) Cyclic voltammetry of echinomycin and its interaction with double-stranded and single-stranded DNA adsorbed at the electrode. Biogeosciences 55:165–167
36. Erdem A, Meric B, Kerman K, Dalbastı T, Ozsoz M (1999) Detection of interaction between metal complex indicator and DNA by using electrochemical biosensor. Electroanalysis 11:1372–1376
37. Kizek R, Havran L, Fojta M, Palecek E (2002) Determination of nanogram quantities of osmium-labeled single stranded DNA by differential pulse stripping voltammetry. Biogeosciences 55:119–121
38. Billova S, Kizek R, Palecek E (2002) Differential pulse adsorptive stripping voltammetry of osmium-modified peptides. Biogeosciences 56:63–66
39. Havran L, Fojta M, Palecek E (2004) Voltammetric behavior of DNA modified with osmium tetroxide 2,2′-bipyridine at mercury electrodes. Biogeosciences 63:239–243
40. Yosypchuk B, Fojta M, Havran L, Heyrovsky M, Palecek E (2006) Voltammetric behavior of osmium-labeled DNA at mercury meniscus-modified solid amalgam electrodes. Detecting DNA hybridization. Electroanalysis 18:186–194
41. Erdem A, Kerman K, Meric B, Ozsoz M (2001) Methylene blue as a novel electrochemical indicator. Electroanalysys 13:219–223
42. Erdem A, Kerman K, Meric B, Akarca US, Ozsoz M (2000) Novel hybridization indicator methylene blue for the electrochemical detection of short DNA sequences related to the hepatitis B virus. Anal Chim Acta 422:139–149
43. Nakayama M, Ihara T, Nakano K, Maeda M (2002) DNA sensors using a ferrocene-oligonucleotide conjugate. Talanta 56:857–866
44. Beilstein AE, Grinstaff MW (2001) Synthesis and characterization of ferrocene-labeled oligodeoxynucleotides. J Organomet Chem 3:637–639
45. Ihara T, Maruo Y, Takenaka S, Takagi M (1996) Ferrocene-oligonucleotide conjugates for electrochemical probing of DNA. Nucleic Acids Res 24:4273–4280
46. Wang J, Kawde AN, Erdem A, Salazar M (2001) Magnetic bead-based label-free electrochemical detection of DNA hybridization. Analyst 126:2020–2024
47. Wang J, Kawde AN (2002) Amplified label-free electrical detection of DNA hybridization. Analyst 127:383–386
48. Zhao YD, Pang DW, Hu S, Wang ZL, Cheng JK, Qi YP, Dai HP, Mao BW, Tian ZQ, Lou J, Lin ZH (1999) DNA-modified electrodes Part 3: spectroscopic characterization of DNA-modified gold electrodes. Anal Chim Acta 388:93–101
49. Fan C, Song H, Hu X, Li G, Zhu J, Xu X, Zhu D (1999) Voltammetric response and determination of DNA with a silver electrode. Anal Biochem 271:1–7

50. Ozkan D, Erdem A, Kara P, Kerman K, Gooding JJ, Nielsen PE, Ozsoz M (2002) Electrochemical detection of hybridization using peptide nucleic acids and methylene blue on self-assembled alkanethiol monolayer modified gold electrodes. Electrochem Commun 4:796–802
51. Sanchez-Pomales G, Santiago-Rodriguez L, Rivera-Velez NE, Cabrera CR (2007) Control of DNA self-assembled monolayers surface coverage by electrochemical desorption. J Electroanal Chem 611:80–86
52. Degefa TH, Kwak J (2008) Electrochemical impedance sensing of DNA at PNA self assembled monolayer. J Electroanal Chem 612:37–41
53. Ostatna V, Palecek E (2006) Self-assembled monolayers of thiol-end-labeled DNA at mercury electrodes. Langmuir 22:6481–6484
54. Erdem A, Papakonstantinou P, Murphy H (2006) Direct DNA hybridization at disposable graphite electrodes modified with carbon nanotubes. Anal Chem 78:6656–6659
55. Ye Y, Ju H (2005) Rapid detection of ssDNA and RNA using multiwalled carbon nanotubes modified screen-printed carbon electrode. Biosens Bioelectron 21:735–741
56. Zhang X, Jiao K, Liu S, Hu Y (2009) Readily reusable electrochemical DNA hybridization biosensor based on the interaction of DNA with single-walled carbon nanotubes. Anal Chem 81:6006–6012
57. Tam PD, Hieu NV, Chien ND, Le AT, Tuan MA (2009) DNA sensor development based on multi-wall carbon nanotubes for label-free influenza virus (type A) detection. J Immunol Methods 31:118–124
58. Wang J, Kawde AN, Jan MR (2004) Carbon-nanotube-modified electrodes for amplified enzyme-based electrical detection of DNA hybridization. Biosens Bioelectron 20:995–1000
59. Erdem A, Karadeniz H, Caliskan A (2011) Dendrimer modified graphite sensors for detection of anticancer drug Daunorubicin by voltammetry and electrochemical impedance spectroscopy. Analyst 136:1041–1045
60. Chang Z, Chen M, Fan H, Zhao K, Zhuang S, He P, Fang Y (2008) Multilayer membranes via layer-by-layer deposition of PDDA and DNA with Au nanoparticles tags for DNA biosensing. Electrochim Acta 53:2939–2945
61. Cai H, Wang Y, He P, Fang Y (2002) Electrochemical detection of DNA hybridization based on silver-enhanced gold nanoparticle label. Anal Chim Acta 469:165–172
62. Karadeniz H, Erdem A, Caliskan A, Pereira CM, Pereira EM, Ribeiro JA (2007) Electrochemical sensing of silver tags labelled DNA immobilized onto disposable graphite electrodes. Electrochem Commun 9:2167–2173
63. Piro B, Haccoun J, Pham MC, Tran LD, Rubin A, Perrot H, Gabrielli C (2005) Study of the DNA hybridization transduction behavior of a quinone-containing electroactive polymer by cyclic voltammetry and electrochemical impedance spectroscopy. J Electroanal Chem 557:155–165
64. Mugweru A, Rusling JF (2001) Catalytic square-wave voltammetric detection of DNA with reversible metallopolymer-coated electrodes. Electrochem Commun 3:406–409
65. Ramanavicius A, Ramanaviciene A, Malinauskas A (2006) Electrochemical sensors based on conducting polymer-polypyrrole. Electrochim Acta 51:6025–6037
66. Saoudi B, Despas C, Chehimi M, Jammul N, Delemar M, Bessiere J, Walcarius A (2000) Study of DNA adsorption on polypyrrole: interest of dielectric monitoring. Sens Actuat 62:35–42
67. Korri-Youssoufi H, Makrouf B (2001) Electrochemical biosensing of DNA hybridization by electroactive ferrocene functionalized polypyrrole. Synthetic Met 119:265–266
68. Özcan A, Şahin Y, Özsöz M, Turan S (2007) Electrochemical oxidation of ds-DNA on polypyrrole nanofiber modified pencil graphite electrode. Electroanalysis 19:2208–2216
69. Prabhakar N, Singh H, Malhotra BD (2008) Nucleic acid immobilized polypyrrole-polyvinylsulphonate film for Mycobacterium tuberculosis detection. Electrochem Commun 10:821–826

70. Arora K, Prabhakar N, Chand S, Malhotra BD (2007) Ultrasensitive DNA hybridization biosensor based on polyaniline. Biosens Bioelectron 23:613–620
71. Prabhakar N, Sumana G, Arora K, Singh H, Malhotra BD (2008) Improved electrochemical nucleic acid biosensor based on polyaniline-polyvinyl sulphonate. Electrochim Acta 53:4344–4350
72. Cougnon C, Gautier C, Pilard JF, Casse N, Chenais B (2008) Redox and ion-exchange properties in surface-tethered DNA-conducting polymers. Biosens Bioelectron 23:1171–1174
73. Fang B, Jiao S, Li M, Qu Y, Jiang X (2008) Label-free electrochemical detection of DNA using ferrocene-containing cationic polythiophene and PNA probes on nanogold modified electrodes. Biosens Bioelectron 23:1175–1179
74. Jiang C, Yang T, Jiao K, Gao H (2008) A DNA electrochemical sensor with poly-L-lysine/single-walled carbon nanotubes films and its application for the highly sensitive EIS detection of PAT gene fragment and PCR amplification of NOS gene. Electrochim Acta 53:2917–2924
75. Liu Y, Hu N (2007) Loading/release behavior of $(chitosan/DNA)_n$ by layer-by-layer films toward negatively charged anthraquinone and its application in electrochemical detection of natural DNA damage. Biosens Bioelectron 23:661–667
76. Kuralay F, Erdem A, Abacı S, Özyörük H, Yıldız A (2009) Poly(vinylferrocenium) coated disposable pencil graphite electrode for DNA hybridization. Electrochem Commun 11:1242–1246
77. Kuralay F, Erdem A, Abacı S, Özyörük H, Yıldız A (2009) Characterization of redox polymer based electrode and electrochemical behavior for DNA detection. Anal Chim Acta 643:83–89
78. Kuralay F, Erdem A, Abacı S, Özyörük H, Yıldız A (2008) Electrochemical biosensing of DNA immobilized poly(vinylferrocenium) modified electrode. Electroanalysys 20:2563–2570
79. Yumak T, Kuralay F, Erdem M, Sinag A, Erdem A, Abaci S (2011) Preparation and characterization of zinc oxide nanoparticles and their sensor applications for electrochemical monitoring of nucleic acid hybridization. Colloids Surf B 86:397–403
80. Erdem M, Kuralay F, Erdem A, Abaci A, Yumak T, Sinag A (2010) Tin oxide nanoparticles enriched polymer modified single-use sensors developed for electrochemical monitoring of label-free DNA hybridization. Talanta 82:1680–1686
81. Wang J, Ozsoz M, Cai X, Rivas G, Shiraishi H, Grant DH, Chicharro J, Palecek E (1998) Interactions of antitumor drug daunomycin with DNA in solution and at the surface. Bioelectrochem Bioenerg 45:33–40
82. Erdem A, Ozsoz M (2001) Voltammetry of the anticancer drug mitoxantrone and DNA. Turk J Chem 25:469–475
83. Erdem A, Ozsoz M (2001) Interaction of the anticancer drug epirubicin with DNA. Anal Chim Acta 437:107–114
84. Karadeniz H, Alparslan L, Erdem A, Karasulu E (2007) Electrochemical investigation of interaction between mitomycin C and DNA in a novel drug-delivery system. J Pharm Biomed Anal 45:322–326
85. Marrazza G, Chianella I, Mascini M (1999) Disposable DNA electrochemical biosensors for environmental monitoring. Anal Chim Acta 387:297–307
86. Palchetti I, Mascini M (2008) Nucleic acid biosensors for environmental pollution monitoring. Analyst 133:846–854
87. Rogers KR (2006) Recent advances in biosensor techniques for environmental monitoring. Anal Chim Acta 568:222–231
88. Rodriguez-Mozaz S, Lopez de Alda MJ, Marco MP, Damia B (2005) Biosensors for environmental monitoring: a global perspective. Talanta 65:291–297
89. Sassolas A, Leca-Bouvier BD, Blum LJ (2008) DNA biosensors and microarrays. Chem Rev 108:109–139

90. Chiti G, Marrazza G, Mascini M (2001) Electrochemical DNA biosensor for environmental monitoring. Anal Chim Acta 427:15–164
91. Lucarelli F, Kicela A, Palchetti I, Marrazza G, Mascini M (2002) Electrochemical DNA biosensor for electroanalysis of wastewater. Biogeosciences 58:113–118
92. Bettazzi F, Lucarelli F, Palchetti I, Berti F, Marrazza G, Mascini M (2008) Disposable electrochemical DNA-array for PCR amplified detection of hazelnut allergens in foodstuffs. Anal Chim Acta 614:93–102
93. Wang J, Rivas G, Cai X (1997) Screen-printed electrochemical hybridization biosensor for the detection of DNA sequences from the *Escherichia coli* pathogen. Electroanalysis 9:395–398
94. Lucarelli F, Palchetti I, Marrazza G, Mascini M (2002) Electrochemical DNA biosensor as a screening tool for the detection of toxicants in water and wastewater samples. Talanta 56:949–957
95. Wang J, Rivas G, Parrado C, Cai X, Flair MN (1997) Electrochemical biosensor for detecting DNA sequences from pathogenic protozoan Cryptosporidium parvum. Talanta 44:2003–2010
96. Wang J, Rivas G, Luo D, Cai X, Valera FS, Dontha N (1996) DNA modified electrode for the detection of aromatic amines. Anal Chem 68:4365–4369
97. Wang J, Chicharro M, Rivas G, Cai X, Dontha N, Farias PAM, Shiraishi H (1996) DNA biosensor for the detection of hydrazines. Anal Chem 68:2251–2254
98. Wang B, Jansson I, Schenkman JB, Rusling JF (2005) Evaluating enzymes that generate genotoxic benzo[*a*]pyrene metabolites using sensor arrays. Anal Chem 77:1361–1367
99. Shen L, Chen Z, Li Y, Xie S, Xu X, Liang Z, Meng X, Li Q, Zhu Z, Li M, Le XC, Shao Y (2008) Electrochemical DNAzyme sensor for lead based on amplification of DNA-Au bio-bar codes. Anal Chem 80:6323–6328
100. Erdem A, Karadeniz H, Canavar PE, Congur G (2012) Single-use sensor platforms based on carbon nanotubes for electrochemical detection of DNA hybridization related to *Microcystis* spp. Electroanalysis 24:502–511

Chapter 13
Immunosensors

Petr Skládal

Abbreviations

Ab	Antibody
Ag	Antigen
ALP	Alkaline phosphatase
Amp	Amperometry
Cap	Capacitance
CE	Capillary electrophoresis
Comp	Competitive assay
CV	Cyclic voltammetry
DPV	Differential pulse voltammetry
EIS	Electrochemical impedance spectroscopy
ELISA	Enzyme-linked immunosorbent assay
GCE	Glassy carbon electrode
GOPS	Glycidoxypropyltrimethoxysilane
Homo	Homogeneous assay
HRP	Horse radish peroxidase
IDE	Interdigitated array electrode
ITO	Indium tin oxide electrode
MWCNT	Multiwalled carbon nanotube
NP	Nanoparticle
P-homo	Pseudohomogeneous assay
Poten	Potentiometric
QD	Quantum dot
SAM	Self-assembled monolayer
Sandw	Sandwich assay

P. Skládal (✉)
Faculty of Science, Department of Biochemistry, Masaryk University,
Kotlářská 2, Brno 61137, Czech Republic
e-mail: skladal@chemi.muni.cz

L.M. Moretto, K. Kalcher (eds.), *Environmental Analysis by Electrochemical Sensors and Biosensors*, DOI 10.1007/978-1-4939-0676-5_13

SPE	Screen-printed electrode
SWSV	Square wave stripping voltammetry
SWV	Square wave voltammetry

13.1 Introduction

Electrochemical immunosensors combine high sensitivity of electrochemical methods and simple and miniature construction of the required instrumentation with excellent specificity of antibodies as recognition elements. The current status of this approach applied for environmental analysis will be discussed. The various types of biosensors were generally found very suitable for environmental analysis,[1–3] and the subgroup of immunosensors provided numerous attractive applications in this field, too. However, as a relatively novel technology, the biosensors and bioanalytical techniques generally compete with the established methods of classic instrumental analysis.[4]

Historically, the immunoassay[5] variant—the enzyme-linked immunosorbent assay (ELISA)—is a format where the enzyme label is followed optically as a change of absorbance, fluorescence or luminescence. The electrochemical immunoassays employ an electrode to measure the electroactive product released from a biocatalytic reaction of the label enzyme; in this case, the immunoassay and electrode reaction occur at different surfaces. These concepts finally inspired various types of immunosensors where the immunorecognition event proceeds directly at the electrode surface. Thus, the electrochemical immunosensor is obtained when the immunorecognition element (antibody, antigen, hapten) becomes immobilised on the surface of the electrode as a transducer.[6] The assays can be realised in the following formats:

- Heterogeneous (surface-bound immunocomplex, requires separation steps)
- Homogeneous (immunochemical reaction in solution, no separation steps)
- Pseudohomogeneous (immunoreaction at a surface, no separation steps)

The assays can be further arranged in several competitive and sandwich (multilayer) formats (details are shown in Fig. 13.1). The competitive assay is the only choice for small molecules, which are typically analysed in environmental samples. Such analytes possess only one binding epitope which becomes recognised and bound in the active site of the specific antibody. Large molecules providing several epitopes can form immunocomplexes with two antibodies simultaneously (or with even more Ab in case of, e.g. microbes), thus providing sandwich-like structures. For generating a signal, the resulting complex should be labelled with either an enzyme or another electroactive molecule.

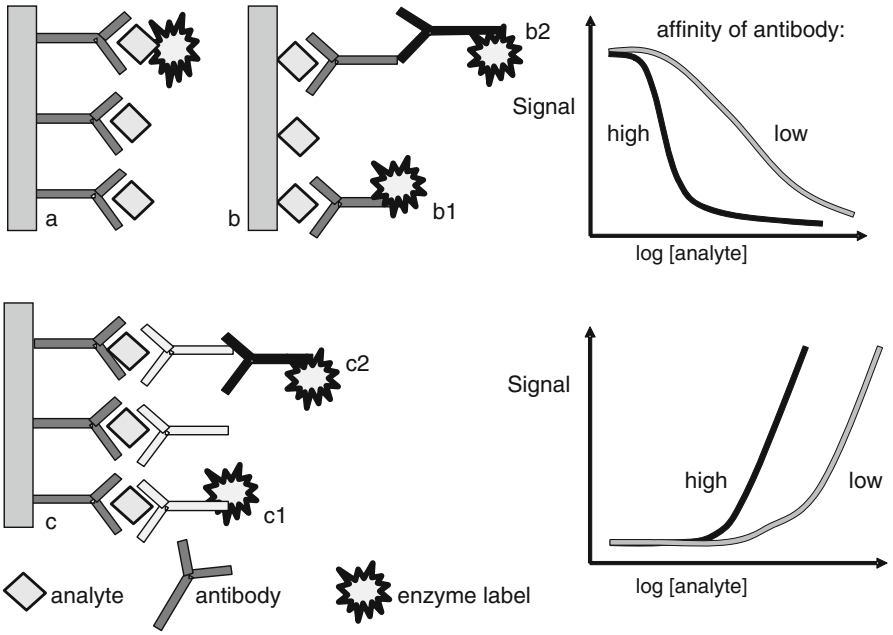

Fig. 13.1 Formats suitable for electrochemical immunosensing include competitive (a, b) and sandwich (c) immunoassays. For competition, the immobilised recognition molecule can be either antibody (a) or antigen (b, antigen, hapten or their derivative); the signal-generating labelled molecule—tracer—includes analyte–enzyme (a) or antibody–enzyme (b1) conjugates. The latter variant can also employ an unlabelled primary antibody and a secondary labelled antibody (b2). For sandwich assays, the capture (primary) antibody is immobilised (c) and the signal is generated using a secondary labelled antibody (c1) or even a tertiary labelled antibody (c2). The general calibration graphs for both competitive and sandwich assays are shown on the *right*

13.2 Immunosensor Technologies

13.2.1 Immunoreagents and Assay Formats

As immunorecognition elements, antibodies, antigens and haptens can be utilised depending on the assay format (Fig. 13.1). Antibodies are mostly immunoglobulins G (IgG) and rarely also IgM; the fragments made from native antibodies by chemical and proteinase-based cleavage (Fab) and recombinant forms of antibodies obtained by gene and protein engineering (single chain variable fragments, scFv) might provide immunosensing surfaces with a higher density of the binding sites.[7] In majority of applications, the molecule of IgG should be immobilised on the electrode, and the covalent linkage should be the preferred option.

Bare metal and carbon electrodes readily adsorb proteins including antibodies, but the resulting immunolayers are not robust enough as slow spontaneous release of proteins occurs; adsorption is perhaps appropriate for single-use immunosensing

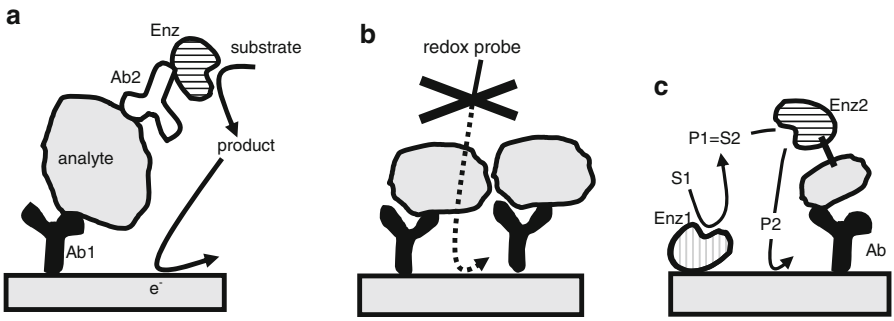

Fig. 13.2 Examples of electrochemical immunosensing assays. (**a**) Sandwich immunoassay where the primary antibody Ab1 captures the target analyte (suitable only for molecules large enough to possess two binding epitopes). This is labelled using the secondary antibody–enzyme conjugate (Ab2–Enz), and finally the added enzyme substrate becomes converted to an electrochemically active product providing a signal at the electrode. (**b**) Direct immunoassay, the captured analyte modifies properties of the sensing surface. For example, blocking of the access to the electrodes decreases the signal of a suitable redox probe. Alternatively, the impedance of the electrode is measured using electrochemical impedance spectroscopy. The tunnelling principle (**c**) employs two complementary enzymes, Enz1 is co-immobilised at the sensing surface and Enz2 becomes bound in the immunocomplex as part of the tracer. In this way, Enz1 and Enz2 are spatially linked and start to collaborate (the generator/acceptor pair) through common reaction intermediates; this does not happen when Enz2 is far away in the bulk solution and no signal enhancement occurs

devices. Noble metal electrodes (gold, platinum, including the screen printed versions) are initially chemically activated using deposition of thiol-based self-assembled monolayers (SAM). The other end of the typically linear molecule of thiol brings a suitable group used for subsequent attachment of antibodies. Thiol modifiers providing amino, carboxyl and hydroxyl groups are widely used; cysteamine, mercaptoundecanoic acid and mercaptodecanol represent example reagents providing these groups. The appropriate conjugation reactions and reagents are described in the literature.[8,9] Special reagents, such as dithiobis(succinimidyl thiopropionic acid), provide thiol groups for the attachment and *N*-hydroxysuccinimide (NHS)-activated carboxyl for immediate and direct binding of proteins. The advanced approaches include mixed SAMs, where active (e.g. biotin) and inactive (hydroxyl, polyethylene glycol, oligosaccharide) end groups allow controlled density of the immobilised binding sites and limit the nonspecific adsorption of either components of the sample matrix or immunoreagents required for the assay. Immunoglobulins become linked directly; the oriented linkage through proteins A and G is the other option; this protein A–IgG affinity complex should be covalently cross-linked for enhanced stability if longer or repeated use of the immunosensor is expected.

The primary immobilised antibody captures the target analyte from the sample, and after washing, the obtained surface-bound immunocomplex should be specifically labelled using the secondary antibody linked to an enzyme label; this conjugate is known as tracer. The final sandwich complex is again washed, the substrate for the enzyme is added and the signal is recorded (Figs. 13.1c and 13.2a).

Alternatively, the free analyte from the sample and the added limited amount of the analyte-enzyme (or other label) conjugate compete for the surface antibody (Fig. 13.1a). Finally (Fig. 13.1b), the analyte might be immobilised and a limited amount of antibody is present in solution. The heterogeneous sensing formats are widely used; the enzyme label amplifies the useful signal which together with the electrochemical measurement provides high sensitivity.

Alternatively, the captured molecules of the analyte can be detected directly; typically, the formation of the immunocomplex on the surface of the electrode blocks access to the surface (Fig. 13.2b). This is measured either using cyclic voltammogram of a suitable redox-active probe (e.g. ferri/ferrocyanide redox pair, signal decreases in case of positive response), or the increased resistance (generally, impedance) of the electrode is determined from electrochemical impedance spectroscopy (EIS). An interesting concept providing pseudohomogeneous assay format is the tunnelling assay (Fig. 13.2c). Formation of the immunocomplex at the sensing surface brings closely together two collaborating enzymes (Enz1 co-immobilised at the electrode, Enz2 bound within the immunocomplex). Afterwards, the signal generated by the enzyme sequence becomes significantly enhanced, thus indicating the extent of the immunointeraction.

13.2.2 Electrochemical Transducers

An electrochemical measuring system is highly sensitive, quite inexpensive and easily miniaturised to portable formats. Progress in electronics allows miniaturising the whole system to a single-chip format; e.g. the embedded digitally controlled potentiostat LMP91000 (Texas Instruments) is programmed through a serial interface (I2C) and consumes minimum power. Amperometric measurement in the three-electrode format is provided. Potentiometric techniques can be simply realised with most digital multimeters. Even the advanced pulsed, voltammetric and galvanostatic techniques are available as hand-held instruments from several companies, PalmSens and EmStat from Palm Instruments, μStat from DropSens, PG581 from Uniscan Instruments and 910 PSTAT mini from Metrohm, and other prototypes have been designed directly in laboratories. EmStat, which plugs directly to the common USB port, is probably the smallest device and the ideal option for OEM applications. An additional board allows multiplexing of several working electrodes, thus providing multichannel measurements.[10] Electrochemistry can also be combined with optical detection providing the highly sensitive electrochemiluminescence (ECL) approach; systems are available from several suppliers (Roche, MesoScale Diagnostics, BioVeris), though portability is not yet simple.

As the measuring element, screen-printed electrodes (SPE) are widely applied due to easy and reproducible fabrication at both laboratory and mass production scales.[11] The low production costs allow a single use of the resulting immunosensors; thus, no complicated regeneration procedures are required. The

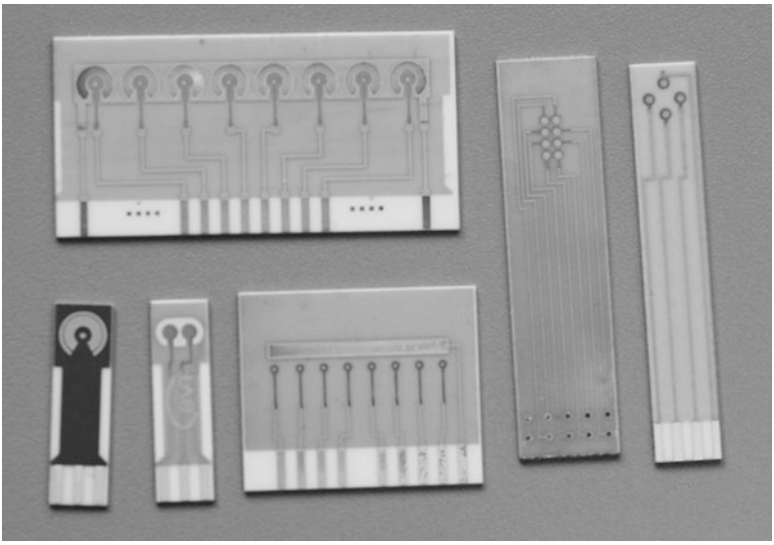

Fig. 13.3 Examples of screen-printed electrochemical sensors suitable for the construction of immunosensors. Options include 1, 2, 4 and 8 working electrodes (available materials Au, Pt, graphite), silver reference (Ag, Ag/AgCl) and auxiliary electrodes. Multichannel sensors produced according to our designs by BVT Technologies

suppliers of SPEs include companies such as BVT Technologies (some multichannel examples are shown in Fig. 13.3), DropSens and Gwent Group. Many researchers prefer to print the desired sensing patterns themselves using commercial inks and pastes or even using custom mixtures often containing carbon nanotubes[12] and metal nanoparticles[13] for improved communication with the labelling biomolecules. Sensing systems are printed on plastics or alumina ceramics, the latter allowing use of high temperatures for manufacturing and providing electrodes quite similar to pure metals or sputtered metal layers. The classic metal rod electrodes are also used, though careful surface preparation is necessary as a disposable use is not possible. The SPE approach allows designing various shapes and arrangement of electrodes; the production of several sensing channels is favourable for detection of several species during one assay.

The measurements are mostly carried out in the simplest amperometric mode with fixed potential applied on the working electrode where the indicating molecule (e.g. product of the enzyme label reaction) becomes converted (either reduced or oxidised). The resulting current followed in time indicates the progress of the reaction. The working potential can also be pulsed in order to improve the signal-to-noise ratio (continuous pulses); alternatively, the accumulated product is converted after applying a single step of potential (chronoamperometry) to achieve higher response. More complex voltammetric techniques are particularly suitable when several different indicating molecules need to be detected; the potential is swept in time and the conversion of individual redox-active molecules occurs

sequentially; this allows multiplexed assays. Alternatively, potentiometric measurements follow the change of potential due to the accumulation of the redox label. The impedimetric measurements either monitor the formation of affinity complexes on the surface of the electrode, when the impedance of the sensing surface becomes significantly affected, or an alternating voltage is applied and the phase and amplitude of the non-faradaic current is interpreted. Optionally, blocking of the electrode with immunocomplexes is probed using an external redox label (ferri/ferrocyanide) and voltammetric measurement.

The electrochemical variant of ELISA employs an external electrode which is sequentially dipped to the working wells, and it quantifies the accumulated indicator molecule. The microwell plates or strips with either bottom-embedded electrochemical systems[14] or top-inserted electrodes[15] significantly profit from parallel processing of multiple samples.

The enzyme labels are typically horse radish peroxidase (HRP, electrochemical detection shown in the scheme) and alkaline phosphatase (ALP). For ALP, the selection of substrates is limited and *p*-aminophenyl phosphate (PAPP) is mostly used as the resulting aminophenol becomes easily and reversibly oxidised at the electrode. A wide choice of substrates (DH_2) generating electroactive products includes hydroquinone, tetramethylbenzidine, aminosalicylic acid and iodide in the case of HRP:

$$\begin{aligned} H_2O_2 + DH_2 &\xrightarrow{\text{peroxidase}} D_{ox} + 2H_2O \\ D_{ox} &\xrightarrow{\text{cathode}} DH_2 \end{aligned}$$

A typical sequence of responses of the heterogeneous amperometric immunosensor for the herbicide 2,4-dichlorophenoxyacetic acid (2,4-D) is shown in Fig. 13.4. The mixture of sample and tracer (antibody-peroxidase conjugate) is added to the sensor with immobilised 2,4-D and allowed to incubate. After a washing step, the surface-bound peroxidase label becomes quantified amperometrically, and the signal is inversely proportional to the amount of herbicide in the sample (as in Fig. 13.1b, plots at the top right corner). The highest response is obtained in the absence of the analyte, when maximum binding of the tracer is achieved, and the blank obtained in the absence of the tracer allows one to correct for nonenzymatic reactions of the substrate mixture.

13.3 Target Compounds

The following part provides examples of electrochemical immunosensors for environmental pollutants published in the last decade. The organisation of text and tables is based on the type of compounds being determined, and besides analytical parameters (limit of detection and total time of analysis), details of the immunosensor construction and assay format are briefly summarised.

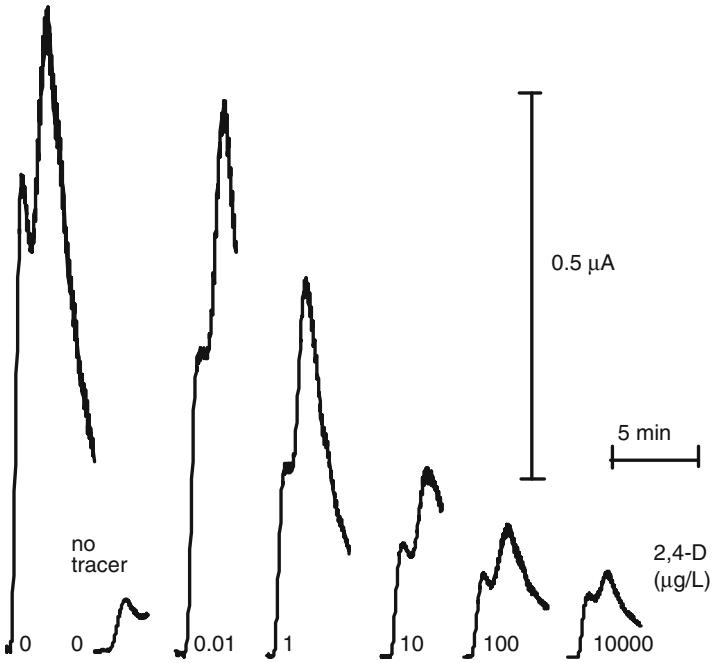

Fig. 13.4 Example of calibration of the immunosensor for the herbicide 2,4-D (2,4-dichlorophenoxyacetic acid). The series of the cathodic current–time recordings was obtained using a Au electrode with covalently bound 2,4-D; an anti-2,4-D Ab-HRP conjugate served as tracer. Measurements were carried out at −50 mV in a flow-through mode with iodide/hydrogen peroxide mixture. The same immunosensor was used repeatedly and regeneration was carried out using pepsin, adapted from reference (16)

13.3.1 Pesticides

The increased use of pesticides for agricultural purposes (control of weeds, insects, fungi and pests) resulted in a wide spread of these contaminants in soils and surface waters and in vegetables and fruits as well. Some pesticides exhibit quite high acute toxicity (organophosphates and carbamates), and on the other hand, residues of the persistent variants are detected in the environment for decades and exhibit bioaccumulation and associated long-term effects in living organisms including humans. The resulting health problems range from asthma, skin rashes and even neurological disorders.[17] Therefore, the public concern about pesticide residues has increased dramatically. The European Community (directive 98/83/EC) sets limits on the concentration of pesticides in water for human consumption at 0.1 µg/L for individual compounds and at 0.5 µg/L for total pesticides. The contents in agricultural products are regulated by national legislations. An extensive review on various types of biosensors for pesticides is available in the literature.[18] Table 13.1 summarises electrochemical immunosensors for pesticides.

Table 13.1 Electrochemical immunosensors for detection of pesticides in environmental samples

Pesticide	LOD (ng/l)	Time (min)	Details of the assay	Ref.
2,4-dichlorophenoxyacetic acid	72	90	Amp, microplate ELISA-Ab, Ag-ALP, 8-channel, tap water	19
2,4-dichlorophenoxyacetic acid	10,000	5	EIS, Au SPE-aminothiophenol SAM-Ab, direct	20
2,4-dichlorophenoxybutyric acid	100	200	EIS, Au/cysteine SAM-GA-Ab, direct, soybean	21
Atrazine	8,300	35	EIS, Au IDE/Ag, comp	22
Atrazine	200	25	Poten pH FET, protein A-Ab, Ag-HRP, comp p-homog, water	23
Atrazine	10	10	EIS, Au-PPy-NTA, Ab-HisTag, direct	24
Atrazine	6	40	Amp, C epoxy composite, protein A-Ab, Ag-HRP, comp, oranges	25
Atrazine	0.2	160	EIS, GCE-conductive polymer-Ag, comp Ab	26
Atrazine	0.01	30	EIS, nanoporous alumina/Au-Ab, direct, water	27
Azinphos-methyl	380	65	Amp, ELISA comp, Ab, Ab2-HRP, water, honeybee	28
Carbofuran	330	30	CV, GCE, Ab in sol-gel, direct, vegetables	29
Carbofuran	60	40	DPV, Au/thiobisbenzenethiol SAM/Au NP-Ab, direct, vegetables	30
Carbofuran	21	60	EIS, Au/Prussian blue, chitosan, Au NP, MWCNT/protein A multilayer, Ab, direct	31
Chlorpyrifos	100	30	DPV, GCE/MWCNT-thionine-chitosan, GA-Ab, direct, vegetables	32
Chlorpyrifos-methyl	400	60	Amp, C SPE/Pt NP/sol-gel, BSA-Ag, Ab-HRP, comp	33
Chlorsulfuron	6.7	180	SWV, C SPE, microplate-Ag, Au NP-Ab, compet, Au dissolved	34
Chlorsulfuron	10	15	Amp, C SPE-HRP/membrane-Ab, Ag-GOD, comp, phomo/tunnelling	35
Coumaphos	0.18	80	Amp, Ab displacement, G-rich ODN, Ru complex	36
Diuron (phenylureas)	5,500		EIS, C SPE/AuNP-Ab, direct	37
Diuron	0.01	30	DPV, SPE-SWCNT-Ab1, Ab2-ALP, sandw, extraction, water	38
Endosulfan	10	60	SWV, GCE/aligned SWCNT-ferrocene-Ag, comp, water	39
Fenthion	10	10	Amp, Pt SPE/dipstick-Ab, Ag-GOD, comp	40
Isoproturon	840	30	Amp, C SPE/membrane-Ag, Ab-HRP, comp, soil	41
Paraoxon	$12 \cdot 10^3$		CV, GCE/Nafion/Au NP-Ab, direct	42
Picloram	100	30	Amp, CPE, magn NP-Ab, Ag-laccase, compet, water	43

(continued)

Table 13.1 (continued)

Pesticide	LOD (ng/l)	Time (min)	Details of the assay	Ref.
Picloram	500	110	Amp, GCE/Au nanoclusters-Ag, Ab-HRP, comp, fruits	[44]
Simazine	0.1	10	Amp, Au-HRP + Ab, Ag-GOD, comp, phomo tunnelling	[45]
Trichloropyridinol	5	35	SWV, GCE/magn beads-Ab, Ag-HRP, comp, river water	[46]

Table 13.2 Electrochemical immunosensors for detection of endocrine disruptors in waters

Compound	LOD (ng/l)	Time (min)	Details of the assay	Ref.
Bisphenol A	600	20	Poten, ISE-Ab, direct	[49]
Bisphenol A	300	25	EIS, GCE-polythiophene-Ab, direct	[50]
17-ß-estradiol	21	40	Amp, ELISA microplate-Ag, Ab-biotin, HRP-avidin, comp, river water	[51]
17-ß-estradiol	6	30	Amp, Au SPE/Au NP-protein A-Ab, Ag-HRP, comp	[52]
17-ß-estradiol	1	65	SWV, C SPE, magn beads-Ag, Ab/Ab2-ALP, comp, surface and waste waters	[53]
17-ß-estradiol	0.25		Amp, C SPE-BSA-Ag, Ab-ALP, comp, river water	[54]
Estrone			CV, Pt/polypyrrole-Ab, direct	[55]
Ethinylestradiol	10	65	SWV, C SPE, magn beads-Ag, Ab/Ab2-ALP, comp, surface and waste waters	[49]
Ethinylestradiol	0.01	25	SWV, GCE/Nafion-MWCNT, magn beads-Ab, direct, river water	[56]

13.3.2 Endocrine Disruptors

This group of pollutants is mimicking the role of sex hormones; negative effects can target also the production of hormones and hormone receptors.[47] The substances exhibiting such effects include hormones of natural human, animal and plant origin (estrogens, phytoestrogens[48]) released to the environment as well as synthetic chemicals as phthalates, polychlorinated biphenyls, alkylphenols, bisphenol A, flame retardants, parabens, polyaromatic hydrocarbons and even some pesticides. The effect on reproductive processes is best known; however, the negative effects can influence the whole endocrine system. The residual levels (ng/L) of estradiol, estrone and ethinylestradiol are found in waters (Table 13.2) with dangerous consequences for the aquatic environment.

13.3.3 Polyaromatic Hydrocarbons, Organochlorine Compounds and Surfactants (Table 13.3)

Polyaromatic hydrocarbons (PAH) originate from combustion processes and are released also during smoking. In living organisms, PAHs undergo oxidative activation in the cytochrome P450 system, and the resulting reactive metabolites (epoxides, diols) attack biomolecules including nucleic acids. The modified nucleotides cause wrong replication and transcription of DNA leading to formation of tumours. The lipophilic character of PAHs is responsible for their binding with the androgenic receptor and consequently nonspecifically induced transcription and translation.

Polychlorinated biphenyls (PCB) were industrial compounds used as dielectrics in capacitors and fluids in transformers; nowadays PCBs became banned in most

Table 13.3 PAHs, PCBs and surfactants compounds determined using electrochemical immunosensors

Compound	LOD (ng/l)	Time (min)	Details of the assay	Ref.
PAHs				
Benzo[a]pyrene	4,000	70	Amp, Au-MUA SAM-Ab, Ag-ALP, comp	57
Benzo[a]pyrene	2,000	180	CV, GCE/SiO_2 NP-BSA-Ag, Ab1, Ab2-HRP, comp, water	58
Benzo[a]pyrene	700	60	CV, GCE/chitosan-graphene-dendrimer-Ag, comp	59
Benzo[a]pyrene	1	60	EIS, Fe_3O_4-Nafion-polyaniline, C NP-Ab-HRP, direct	60
1-Nitropyrene	10^4	20	DPV, GCE-Ab, direct, air, tea	61
PAHs (sum)	20	55	SWV, GCE, magn bead-Ab, Ag-HRP, comp, tap water	62
Phenanthrene	150	40	LSV, C SPE-Ag, Ab-ALP, comp, sea/river water	63
1-Pyrenebutyric acid	30	25	EIS, GCE/Nafion-Au NP-Ab, direct, river water	64
1-Pyrenebutyric acid	10^4	190	SWV, ITO-GOPS-Ab, Ag-Ru(bpy)$_3$, comp	65
PCBs				
PCBs (mixture)	500	30	DPV, C SPE, magn beads-protein G-Ab, Ag-AP, comp, sediments	66
PCBs (mixture)	10	40	SWV, C SPE, magn beads-Ab, Ag-HRP, comp, river water	67
2,4,6-trichlorophenol	200	15	Amp, Au SPE, capillary-protein A separation, Ab, Ag-GAL, comp, surface water	68
Surfactants				
Alkylphenols (ethoxylates)	1,000	60	Amp, C SPE, capillary-Ab, Ag-GAL, comp	69
Nonylphenol	104	30	LSV, C SPE-Nafion-Ab-HRP, signal enhancement, direct, river water	70

developed countries. PCBs are highly persistent and consequently ubiquitous in the environment. Some of the PCB congeners are highly toxic for human health. Dioxins are industrial contaminants resulting from processes involving chlorine (synthesis, production of some plastics, even bleaching). The health risks of dioxins are based on their carcinogenicity; some exhibit endocrinic effects, too. Chlorophenols are released from paper, pulp and dye production and may function as precursors of dioxins. Surfactants and their metabolites—linear alkylbenzene sulphonates (LAS) originate from industrial processes as well as from home washing—are considered as potential endocrine disruptors.

13.3.4 Toxins

Cyanobacteria forming blooms release toxic substances, cyanotoxins, which are hazardous to human health as well as to other organisms in the aquatic environment. The wide group of substances consists of hepatotoxins (microcystins and nodularin), neurotoxins (anatoxins and saxitoxins), cytotoxins (cylindrospermopsins), and dermatotoxins (aplysiatoxins and debromoaplysiatoxins).[71] Most abundant are microcystins (Table 13.4), short cyclic peptides containing strange amino acids synthesised by peptide ligases and released to water after cell lysis of the producer microorganism (*Microcystis*, *Oscillatoria*, *Anabaena* and *Nostoc* species). Seafood products become also contaminated by related saxitoxin and domoic acid.

13.4 Conclusion and Future Prospects

The development of the electrochemical immunosensors considered for the detection of environmental pollutants was briefly reviewed. At present, two types of assays are in focus. The heterogeneous sandwich format is robust and reliable; sensitivity is provided by enzyme labels generating electrochemically measured products. Complications include several incubations and the required washing steps. As alternative, the direct assay formats employ different strategies on how to evaluate the capture of the target compound without any label. This area seems very promising, as novel surface preparation techniques and the use of nanotechnologies (nanoparticles/wires/tubes/...) resulted in very sophisticated devices and assay formats sometimes exhibiting excellent analytical parameters. The affinity of the specific antibody towards the corresponding analyte remains the most important parameter always limiting the other assay steps.

Several enhancement strategies provide significant improvement of performance compared to classic immunoassays. Shortened assay times compared to standard microtitration plate-based ELISA can be achieved through miniaturisation of the working space and enhanced surface-to-volume ratio. Thus, limited diffusion

Table 13.4 Electrochemical immunosensors for marine toxins

Toxin	LOD (ng/l)	Time	Details of the assay	Ref.
Brevetoxin B/dinophysistoxin-1	1.8/2.2	60	SWSV, GCE, magn beads-dual Abs, Cu NP-Ag1, Cd NP-Ag2, comp, seafood	72
Dinophysistoxin-2	70	40	Amp, Ab, Ag-HRP, CE, comp, shellfish	73
Microcystin			Amp, C SPE, microplate ELISA, algae	74
Microcystin-LR	500	60	Amp, C SPE, membrane-Ab, Ag-HRP, comp, river water	75
Microcystin-LR	170	50	Amp, C SPE/PVP-Os/Ag, Ab, Ab2-HRP, comp, water	76
Microcystin-LR	100	11	Amp, Au/membrane/Au-Ab, Ag-GOD, comp, cross-flow, water	77
Microcystin-LR	100		QD-Ab, SWSV	78
Microcystin-LR	50	35	EIS, Si/MWCNT-Ag, Ab, comp.	79
Microcystin-LR	50	15	EIS, Au/Au NP-Ab, direct, water	80
Microcystin-LR	30		Au NP-cysteine SAM/Au, Ab, direct	81
Microcystin-LR	20	25	DPV, Au/Au NP-Ab, direct, algae	81
Microcystin-LR	16	35	DPV, GCE/chitosan/graphene-Ag, Ab-HRP, comp, river water	82
Microcystin-LR	10	130	Amp, GCE-Ab, Ab2-Pt/Ru NP, sandw, river water	83
Microcystin-LR	1.7	40	EIS, GCE/MWCNT/ionic liquid-Ab, direct, water	84
Microcystin-LR	0.007		Cap, Ag NP/Au, thiourea SAM, direct	85
Microcystin-LR	3.7×10^{-5}	50	DPV, GCE/graphene/Au NP/conductive polymer-Ab, direct, river water	86
Okadaic acid	500	70	DPV, Au, magn beads-Ab, Ag-HRP, comp, mussels	87
Okadaic acid	200	70	EIS, C SPE-Ab, direct, mussels	88
Okadaic acid	150	70	Amp, C SPE, magn beads-Ag, Ab, Ab2-ALP, comp, mussels	89
Okadaic acid	19	50	SWV, C SPE/grapheme/Ab, Ag-ovalbumin, comp, shellfish	90
Saxitoxin	800	36	Amp, Ab, Ag-HRP, CE, comp, shellfish	91
Toxin			Cond, SWCNT-Ab on paper	92

pathways allow to establish (or approach) the equilibrium between the immobilised capture partner and the analyte (and tracer) in solution much faster. This happens in microfluidic flow systems with embedded immunosensors, or simply when the immunoassay becomes realised in capillaries. The interface between electrode and the immunorecognition part becomes often modified with the addition of metal nanoparticles or carbon-based nanomaterials (nanotubes, graphene sheets). The benefits include enlarged contact area and enhanced rate of electron transfer; the construction of such systems currently does not seem to be optimised, and configuration or amounts of components mixed together to form the immunolayer

are more or less random and not compared to reference layers. Very often, simple adsorption holds everything together resulting in less robust systems; carefully planned covalent binding stabilising the sensing layers should be introduced. On the other hand, the use of magnetic beads for capture and preconcentration of the target compounds from complex sample matrices seems to be reliable and provides the expected results.

Considering the summarised work reported in the literature, the more complex procedure does not always result in improved analytical procedure—better limit of detection and shortened total time of analysis. Furthermore, the proof of reproducible performance in real life should be addressed more intensively. The transfer of the detector system from laboratory to the real world usually demonstrates several more or less significant problems which associated together make the function of the immunosensing device rather unreliable. However, the experience gained during this phase of testing from purely research approaches to practical evaluations under unpredictable conditions is invaluable and helps to improve weak parts of the immunosensor.

Finally, the conclusion whether the target pollutant was detected or not is presently carried out by the user looking on the measured trace of signals. This evaluation and decision-making should be implemented in the control software, and this might be quite challenging, too. The combination of immunoanalytical devices with chemometrics will in future provide really smart immunosensors suitable for automated measurements and detection of potentially dangerous compounds in the monitored environmental space.

References

1. Rodriguez-Mozaz S, Marco MP, Lopez de Alda MJ, Barcelo D (2004) Biosensors for environmental applications: future development trends. Pure Appl Chem 76:723–752
2. Rodriguez-Mozaz S, Lopez de Alda MJ, Barcelo D (2006) Biosensors as useful tools for environmental analysis and monitoring. Anal Bioanal Chem 386:1025–1041
3. Badihi-Mossberg M, Buchner V, Rishpon J (2007) Electrochemical biosensors for pollutants in the environment. Electroanalysis 19:2015–2028
4. Rodriguez-Mozaz S, Lopez de Alda MJ, Barcelo D (2007) Advantages and limitations of on-line solid phase extraction coupled to liquid chromatography–mass spectrometry technologies versus biosensors for monitoring of emerging contaminants in water. J Chrom 1152:97–115
5. Yalow RS, Berson SA (1959) Assay of plasma insulin in human subjects by immunological methods. Nature 184:1648–1649
6. Skládal P (1997) Advances in electrochemical immunosensors. Electroanalysis 9:737–745
7. Killard AJ, Deasy B, O'Kennedy R, Smyth MR (1996) Antibodies: production, functions and applications in biosensors. Trends Anal Chem 14:257–266
8. Hermanson GT (1996) Bioconjugate techniques. Academic, San Diego, CA
9. Ramírez NB, Salgado AM, Valdman B (2009) The evolution and developments of immunosensors for health and environmental monitoring: problems and perspectives. Braz J Chem Eng 26:227–249

10. Skládal P, Kaláb T (1995) A multichannel immunosensor for 2,4-dichlorophenoxyacetic acid. Anal Chim Acta 316:73–78
11. Hart JP, Crew A, Crouch E, Honeychurch KC, Pemberton RM (2004) Some recent designs and developments of screen-printed carbon electrochemical sensors/biosensors for biomedical, environmental, and industrial analyses. Anal Lett 37:789–830
12. Tran LD, Nguyen DT, Nguyen BH, Do QP, Nguyen HL (2011) Development of interdigitated arrays coated with functional polyaniline/MWCNT for electrochemical biodetection: application for human papilloma virus. Talanta 85:1560–1565
13. Upadhyayula Venkata KK (2012) Functionalized gold nanoparticle supported sensory mechanisms applied in detection of chemical and biological threat agents: a review. Anal Chim Acta 715:1–18
14. Bagel O, Degrand C, Limoges B, Joannes M, Azek F, Brossier P (2000) Enzyme affinity assays involving a single-use electrochemical sensor. Electroanalysis 14:1447–1452
15. Tang TC, Deng A, Huang HJ (2002) Immunoassay with a microtiter plate incorporated multichannel electrochemical detection system. Anal Chem 74:2617–2621
16. Zeravik J, Skládal P (1999) Screen-printed amperometric immunosensor for repeated use in the flow-through mode. Electroanalysis 11:851–856
17. Tankiewicz M, Fenik J, Biziuk M (2010) Determination of organophosphorus and organonitrogen pesticides in water samples. Trends Anal Chem 29:1050–1063
18. Liu S, Zheng Z, Li X (2013) Advances in pesticide biosensors: current status, challenges, and future perspectives. Anal Bioanal Chem 405:63–90
19. Deng AP, Yang H (2007) A multichannel electrochemical detector coupled with an ELISA microtiter plate for the immunoassay of 2,4-dichlorophenoxyacetic acid. Sensor Actuator B Chem 124:202–208
20. Navrátilová I, Skládal P (2004) The immunosensors for measurement of 2,4-dichlorophenoxyacetic acid based on electrochemical impedance spectroscopy. Bioelectrochemistry 62:11–18
21. Zhang L, Wang M, Wang C, Hu X, Wang G (2012) Label-free impedimetric immunosensor for sensitive detection of 2,4-dichlorophenoxybutyric acid (2,4-DB) in soybean. Talanta 101:226–232
22. Valera E, Azcon JR, Rodriguez A, Castanera LM, Sanchez FJ, Marco MP (2007) Impedimetric immunosensor for atrazine detection using interdigitated μ-electrodes (IDμE's). Sensor Actuator B 125:526–537
23. Plekhanova YV, Reshetilov AN, Yazynina EV, Zherdev AV, Dzantiev BB (2003) A new assay format for electrochemical immunosensors: polyelectrolyte-based separation on membrane carriers combined with detection of peroxidase activity by pH-sensitive field-effect transistor. Biosens Bioelectron 19:109–114
24. Ionescu RE, Gondran C, Bouffier L, Jaffrezic-Renault N, Martelet C, Cosnier S (2010) Label-free impedimetric immunosensor for sensitive detection of atrazine. Electrochim Acta 55:6228–6232
25. Zacco E, Galve R, Marco MP, Alegret S, Pividori MI (2007) Electrochemical biosensing of pesticide residues based on affinity biocomposite platforms. Biosens Bioelectron 22:1707–1715
26. Tran HV, Reisberg S, Piro B, Nguyen TD, Pham MC (2013) Label-free electrochemical immunoaffinity sensor based on impedimetric method for pesticide detection. Electroanalysis 25:664–670
27. Pichetsurnthorn P, Vattipalli K, Prasad S (2012) Nanoporous impedemetric biosensor for detection of trace atrazine from water samples. Biosens Bioelectron 32:156–162
28. Ivanov A, Evtugyn A, Budnikov H, Girotti S, Ghini S, Ferri E, Montoya A, Mercader JV (2008) Amperometric immunoassay of azinphos-methyl in water and honeybees based on indirect competitive ELISA. Anal Lett 41:392–405
29. Sun X, Du S, Wang X, Zhao W, Li Q (2011) A label-free electrochemical immunosensor for carbofuran detection based on a sol-gel entrapped antibody. Sensors 11:9520–9531

30. Sun X, Zhu Y, Wang X (2012) Amperometric immunosensor based on deposited gold nanocrystals/4,4′-thiobisbenzenethiol for determination of carbofuran. Food Control 28:184–191
31. Sun X, Du S, Wang X (2012) Amperometric immunosensor for carbofuran detection based on gold nanoparticles and PB-MWCNTs-CTS composite film. Eur Food Res Technol 235:469–477
32. Sun Y, Cao Y, Gong Z, Wang X, Zhang Y, Gao J (2012) An amperometric immunosensor based on multi-walled carbon nanotubes-thionine-chitosan nanocomposite film for chlorpyrifos detection. Sensors 12:17247–17261
33. Wei W, Zhong XM, Wang X, Yin LH, Pu YP, Liu SQ (2012) A disposable amperometric immunosensor for chlorpyrifos-methyl based on immunogen/platinum doped silica sol-gel film modified screen-printed carbon electrode. Food Chem 135:888–892
34. Nangia Y, Bhalla Y, Kumar B, Suri CR (2012) Electrochemical stripping voltammetry of gold ions for development of ultra-sensitive immunoassay for chlorsulfuron. Electrochem Commun 14:51–54
35. Dzantiev BB, Yazynina EV, Zherdev AV, Plekhanova YV, Reshetilov AN, Chang SC, McNeil CJ (2004) Determination of the herbicide chlorsulfuron by amperometric sensor based on separation-free bienzyme immunoassay. Sensor Actuator B 98:254–261
36. Dai Z, Liu H, Shen YD, Su XP, Xu ZL, Sun YM, Zou XY (2012) Attomolar determination of coumaphos by electrochemical displacement immunoassay coupled with oligonucleotide sensing. Anal Chem 84:8157–8163
37. Bhalla V, Sharma P, Pandey SK, Suri CR (2012) Impedimetric label-free immunodetection of phenylurea class of herbicides. Sensor Actuator B 171:1231–1237
38. Sharma P, Bhalla V, Tuteia S, Kukar M, Suri CR (2012) Rapid extraction and quantitative detection of the herbicide diuron in surface water by a hapten-functionalized carbon nanotubes based electrochemical analyzer. Analyst 137:2495–2502
39. Liu G, Wang S, Liu J, Song D (2012) An electrochemical immunosensor based on chemical assembly of vertically aligned carbon nanotubes on carbon substrates for direct detection of the pesticide endosulfan in environmental water. Anal Chem 84:3921–3928
40. Cho YA, Cha GS, Lee YT, Lee HS (2005) A dipstick-type electrochemical immunosensor for the detection of the organophosphorus insecticide fenthion. Food Sci Biotechnol 14:743–746
41. Baskeyfield DEH, Davis F, Magan N, Tothill IE (2011) A membrane-based immunosensor for the analysis of the herbicide isoproturon. Anal Chim Acta 699:223–231
42. Hu SQ, Xie JW, Xu QH, Rong KT, Shen GL, Yu RQ (2003) A label-free electrochemical immunosensor based on gold nanoparticles for detection of paraoxon. Talanta 61:769–777
43. Zeng GM, Zhang Y, Tang L, Chen LJ, Pang Y, Feng CL, Huang GH, Niu CG (2012) Sensitive and renewable picloram immunosensor based on paramagnetic immobilisation. Int J Environ Anal Chem 92:729–741
44. Chen L, Zeng G, Zhang Y, Tang L, Huang D, Liu C, Pang Y, Luo Y (2010) Trace detection of picloram using an electrochemical immunosensor based on three-dimensional gold nanoclusters. Anal Biochem 407:172–179
45. Zeravik J, Ruzgas T, Fránek M (2003) A highly sensitive flow-through amperometric immunosensor based on the peroxidase chip and enzyme-channeling principle. Biosens Bioelectron 18:1321–1327
46. Liu G, Timchalk C, Lin Y (2006) Bioelectrochemical magnetic immunosensing of trichlor-opyridinol: a potential insecticide biomarker. Electroanalysis 18:1605–1613
47. Rodriguez-Mozaz S, Marco MP, Lopez de Alda MJ, Barceló D (2004) Biosensors for environmental monitoring of endocrine disruptors: a review article. Anal Bioanal Chem 378:588–598
48. Yadava SK, Chandrab P, Goyal RN, Shim YB (2013) A review on determination of steroids in biological samples exploiting nanobio-electroanalytical methods. Anal Chim Acta 762:14–24
49. Piao MH, Noh HB, Rahman MA, Won MS, Shim YB (2008) Label-free detection of bisphenol A using a potentiometric immunosensor. Electroanalysis 20:30–37

50. Rahman MA, Shiddiky MJA, Park JS, Shim YB (2007) An impedimetric immunosensor for the label-free detection of bisphenol A. Biosens Bioelectron 11:2464–2470
51. Wang S, Zhuang H, Du L, Lin S, Wang C (2007) Determination of estradiol by biotin-avidin-amplified electrochemical enzyme immunoassay. Anal Lett 40:887–896
52. Liu X, Deng DKY (2009) Picogram-detection of estradiol at an electrochemical immunosensor with a gold nanoparticle-protein G-(LC-SPDP)-scaffold. Talanta 77:1437–1443
53. Kanso H, Barthelmebs L, Inguimbert N, Noguer T (2013) Immunosensors for estradiol and ethinylestradiol based on new synthetic estrogen derivatives: application to wastewater analysis. Anal Chem 85:2397–2404
54. Butler D, Guilbault GG (2006) Disposable amperometric immunosensor for the detection of 17-β-estradiol using screen-printed electrodes. Sensor Actuator B 113:692–699
55. Gao H, Lu JY, Cui YR, Zhang XX (2006) Electrochemical immunoassay of estrone at an antibody-modified conducting polymer electrode towards immunobiosensors. J Electroanal Chem 592:88–94
56. Martinez NA, Pereira SV, Bertolino FA, Schneider RJ, Messina GA, Raba J (2012) Electrochemical detection of a powerful estrogenic endocrine disruptor: ethinylestradiol in water samples through bioseparation procedure. Anal Chim Acta 723:27–32
57. Ahma A, Moore E (2012) Electrochemical immunosensor modified with self-assembled monolayer of 11-mercaptoundecanoic acid on gold electrodes for detection of benzo [a pyrene in water. Analyst 137:5839–5844
58. Wang C, Lin M, Liu Y, Lei H (2011) A dendritic nanosilica-functionalized electrochemical immunosensor with sensitive enhancement for the rapid screening of benzo[a pyrene. Electrochim Acta 56:88–1994
59. Lin MH, Liu YJ, Yang ZH, Huang YB, Sun ZH, He Y, Ni CL (2012) Construction of sensitive amperometric immunosensor based on poly(amidoamine) dendrimer and one-step ionic-liquid-assisted graphene/chitosan platform for benzo[a pyrene detection. Int J Electrochem Sci 7:965–978
60. Lin MH, Liu YJ, Sun ZH, Zhang SL, Yang ZH, Ni CL (2012) Electrochemical immunoassay of benzo[a pyrene based on dual amplification strategy of electron-accelerated Fe_3O_4/polyaniline platform and multi-enzyme-functionalized carbon sphere label. Anal Chim Acta 722:100–106
61. Stoppacher N, Pittner F, Sontag G (2009) Design of a voltammetric immunosensor for determination of 1-nitropyrene. Monatsh Chem 140:909–914
62. Lin YY, Liu GD, Wai CM, Lin YH (2007) Magnetic beads-based bioelectrochemical immunoassay of polycyclic aromatic hydrocarbons. Electrochem Commun 9:1547–1552
63. Moore EJ, Kreuzer MP, Pravda M, Guilbault GG (2004) Development of a rapid single-drop analysis biosensor for screening of phenanthrene in water samples. Electroanalysis 16:1653–1659
64. Yang P, Zheng QL, Xu H, Liu JS, Jin LT (2012) A highly sensitive electrochemical impedance spectroscopy immunosensor for determination of 1-pyrenebutyric acid based on the bifunctionality of Nafion/gold nanoparticles composite electrode. Chin J Chem 30:1155–1162
65. Wei MY, Wen SD, Yang XQ, Guo LH (2009) Development of redox-labeled electrochemical immunoassay for polycyclic aromatic hydrocarbons with controlled surface modification and catalytic voltammetric detection. Biosens Bioelectron 24:2909–2914
66. Centi S, Laschi S, Mascini M (2007) Improvement of analytical performances of a disposable electrochemical immunosensor by using magnetic beads. Talanta 73:394–399
67. Lin YY, Liu GD, Wai CM, Lin YH (2008) Bioelectrochemical immunoassay of polychlorinated biphenyl. Anal Chim Acta 612:23–28
68. Nistor C, Emneus J (2003) A capillary-based amperometric flow immunoassay for 2,4,6-trichlorophenol. Anal Bioanal Chem 375:125–132

69. Rose A, Nistor C, Emneus J, Pfeiffer D, Wollenberger U (2002) GDH biosensor based off-line capillary immunoassay for alkylphenols and their ethoxylates. Biosens Bioelectron 17:1033–1043
70. Evtugyn GA, Eremin SA, Shaljamova RP, Ismagilova AR, Budnikov HC (2006) Amperometric immunosensor for nonylphenol determination based on peroxidase indicating reaction. Biosens Bioelectron 22:56–62
71. Singh S, Srivastava A, Oh HM, Ahn CY, Choi GG, Asthana RK (2012) Recent trends in development of biosensors for detection of microcystin. Toxicon 60:878–894
72. Zhang B, Hou L, Tang DP, Liu BQ, Li JR, Chen GN (2012) Simultaneous multiplexed stripping voltammetric monitoring of marine toxins in seafood based on distinguishable metal nanocluster-labelled molecular tags. J Agric Food Chem 60:8974–8982
73. Zhang XW, Zhang ZX (2012) Development of a capillary electrophoresis-based enzyme immunoassay with electrochemical detection for the determination of okadaic acid and dinophysistoxin2 in shellfish samples. Anal Lett 45:1365–1376
74. Campas M, Marty JL (2007) Highly sensitive amperometric immunosensors for microcystin detection in algae. Biosens Bioelectron 22:1034–1040
75. Lotierzo M, Abuknesha R, Davis F, Tothill IE (2012) A membrane-based ELISA assay and electrochemical immunosensor for microcystin-lr in water samples. Environ Sci Technol 46:5504–5510
76. Chen XQ, He M, Shi HC, Cai Q (2011) An amperometric immunosensor for microcystin-(leucine-arginine) based on screen-printed carbon electrode. Chin J Anal Chem 39:443–448
77. Zhang FH, Yang SH, Kang TY, Cha GS, Nam H, Meyerhoff ME (2007) A rapid competitive binding nonseparation electrochemical enzyme immunoassay (NEEIA) test strip for microcystin-LR (MCLR) determination. Biosens Bioelectron 22:1419–1425
78. Yu HW, Lee J, Kim S, Nguyen GH, Kim IS (2009) Electrochemical immunoassay using quantum dot/antibody probe for identification of cyanobacterial hepatotoxin microcystin-LR. Anal Bioanal Chem 394:2173–2181
79. Han C, Doepke A, Cho W, Likodimos V, de la Cruz AA, Back T, Heineman WR, Halsall HB, Shanov VN, Schulz MJ, Falaras P, Dionysiou DD (2013) A multiwalled-carbon-nanotube-based biosensor for monitoring microcystin-lr in sources of drinking water supplies. Adv Funct Mater 23:1807–1816
80. Sun XL, Shi H, Wang HX, Xiao LW, Li LN (2010) A simple, highly sensitive, and label-free impedimetric immunosensor for detection of microcystin-LR in water. Anal Lett 43:533–544
81. Tong P, Tang S, He Y, Shao Y, Zhang L, Chen G (2011) Label-free immunosensing of microcystin-LR using a gold electrode modified with gold nanoparticles. Microchim Acta 173:299–305
82. Zhao HM, Tian JP, Quan X (2013) A graphene and multienzyme functionalized carbon nanosphere-based electrochemical immunosensor for microcystin-LR detection. Colloids Surf B Biointerfaces 103:38–44
83. Wei Q, Zhao YF, Du B, Wu D, Cai YY, Mao KX, Li H, Xu CX (2011) Nanoporous PtRu alloy enhanced nonenzymatic immunosensor for ultrasensitive detection of microcystin-LR. Adv Funct Mat 21:4193–4198
84. Sun XL, Guan L, Shi H, Ji J, Zhang YZ, Li ZJ (2013) Determination of microcystin-LR with a glassy carbon impedimetric immunoelectrode modified with an ionic liquid and multiwalled carbon nanotubes. Microchim Acta 180:75–83
85. Loyprasert S, Thavarungkul P, Aswatreratanakul P, Wongkittisuka B, Limsakul C, Kanatharana P (2008) Label-free capacitive immunosensor for microcystin-LR using self-assembled thiourea monolayer incorporated with Ag nanoparticles on gold electrode. Biosens Bioelectron 24:78–86
86. Li R, Xia Q, Li Z, Sun X, Liu J (2013) Electrochemical immunosensor for ultrasensitive detection of microcystin-LR based on graphene-gold nanocomposite/functional conducting polymer/gold nanoparticle/ionic liquid composite film with electrodeposition. Biosens Bioelectron 44:235–240

87. Hayat A, Barthelmebs L, Sassolas A, Marty JL (2012) Development of a novel label-free amperometric immunosensor for the detection of okadaic acid. Anal Chim Acta 724:92–97
88. Hayat A, Barthelmebs L, Marty JL (2012) Electrochemical impedimetric immunosensor for the detection of okadaic acid in mussel sample. Sensor Actuator B 171:810–815
89. Dominguez RB, Hayat A, Sassolas A, Alonso GA, Munoz R, Marty JL (2012) Automated flow-through amperometric immunosensor for highly sensitive and on-line detection of okadaic acid in mussel sample. Talanta 99:232–237
90. Eissa S, Zourob M (2012) A graphene-based electrochemical competitive immunosensor for the sensitive detection of okadaic acid in shellfish. Nanoscale 4:7593–7599
91. Zhang X, Zhang Z (2012) Capillary electrophoresis-based immunoassay with electrochemical detection as rapid method for determination of saxitoxin and decarbamoylsaxitoxin in shellfish samples. J Food Compos Anal 28:61–69
92. Wang L, Chen W, Xu D, Shim BS, Zhu Y, Sun F, Liu L, Peng C, Jin Z, Xu C, Kotov NA (2009) Simple, rapid, sensitive, and versatile SWNT-paper sensor for environmental toxin detection competitive with ELISA. Nano Lett 9:4147–4152

Chapter 14
Other Types of Sensors: Impedance-Based Sensors, FET Sensors, Acoustic Sensors

Christopher Brett

14.1 Introduction

In this chapter, types of electrochemical sensor or biosensor which are based on electrical properties and which cannot be grouped into normal voltammetric or potentiometric sensors will be addressed, giving the fundamental principles and selected examples to show how they are implemented for characterisation and for analysis. This will concern sensors based on impedance, solid-state miniaturised sensors and piezoelectric transducer-based sensors.

14.2 Sensors Based on Impedance

The impedance of an electrode–solution or modified electrode–solution interface can be measured directly by appropriate instrumentation, and the impedance can be simplified in some cases to a resistance (conductance) or capacitance. Some of the more common modes of implementation of impedance will be presented in this section. It should be noted that data from impedance experiments contain more information than from voltammetric experiments owing to, amongst other factors, the large range of timescales which is probed. This means it is a more sensitive technique for probing changes to the electrode surface but, at the same time, can make interpretation more difficult.

C. Brett (✉)
Faculdade de Ciências e Tecnologia, Departamento de Química, Universidade de Coimbra, 3004-535 Coimbra, Portugal
e-mail: cbrett@ci.uc.pt

L.M. Moretto, K. Kalcher (eds.), *Environmental Analysis by Electrochemical Sensors and Biosensors*, DOI 10.1007/978-1-4939-0676-5_14

14.2.1 Fundamentals of Electrochemical Impedance

In any electrochemical cell, there is separation of charge, movement of charge or, at high frequency, induction due to the electric field. Thus, the cell can be modelled by an electrical equivalent circuit containing capacitors, resistors or inductors, respectively. Induction phenomena only need to be invoked at very high frequency or in relaxation phenomena at low frequency. Normally, in the case of sensors, owing to the way the electrochemical cell is constructed and in the presence of a large quantity of electrolyte to carry the current, all important interfacial phenomena are concentrated close to the electrode–solution or modified electrode–solution interface. In such cases, modelling of the impedance characteristics has to consider this region alone, the rest of the cell being represented by a cell resistance.[1]

The measurement of electrochemical impedance usually involves applying a small sinusoidal voltage perturbation superimposed on a fixed value of applied potential at frequencies which typically vary from 100 kHz down to 1 mHz. The current response to this perturbation is measured in terms of its amplitude and change in phase which leads to the impedance.

The excitation signal, expressed as a function of time, normally has the form

$$E_t = E_0 \sin(\omega t)$$

where E_t is the potential at time t, E_0 is the amplitude of the signal and ω is the radial frequency. The relationship between radial frequency ω (expressed in radians/second) and frequency f (expressed in Hertz) is $\omega = 2\pi f$.

In a linear system, the response signal, I_t, is shifted in phase (φ):

$$I_t = I_0 \sin(\omega t + \varphi)$$

The impedance is thus

$$Z_t = \frac{E_t}{I_t} = \frac{E_0 \sin(\omega t)}{I_0 \sin(\omega t + \varphi)} = Z_0 \frac{\sin(\omega t)}{\sin(\omega t + \varphi)}$$

and can be expressed in terms of a magnitude, Z_0, and a phase shift, φ.

Furthermore, considering Euler's equation ($\exp(ix) = \cos(x) + i\sin(x)$), the impedance can be expressed as

$$Z_t = Z_0(cos\varphi + i sin\varphi)$$

so that the impedance can be decomposed into a real part and an imaginary part.

For sensor applications, the data presentation is usually as a complex plane plot, with the real part (Z') plotted on the x-axis and the imaginary part (Z'') plotted on the y-axis, which is also referred to as a "Nyquist plot". An alternative representation is of impedance magnitude and phase angle as a function of the logarithm of frequency—this Bode representation is most used in corrosion studies.

Normally, amplitudes of 5–10 mV are used to ensure that the response is linear and to avoid the occurrence of harmonic signals. Different frequencies are used to obtain the impedance response as a function of frequency, usually between 100 kHz and 0.01 Hz, as mentioned previously, which gives rise to a frequency spectrum. For this reason, the technique is often known as electrochemical impedance spectroscopy (EIS).

14.2.2 Model of the Electrochemical Cell and Electrical Equivalent Circuits

As explained above, conditions are usually created in electrochemical cells so that the response is due to processes occurring at the electrode–solution or modified electrode–solution interface. Thus, the rest of the cell can often be represented by a resistance R_Ω.

We now consider three simple but increasingly complex circuits, at an inert electrode immersed in electrolyte solution with electroactive species. All of them are important for electrochemical sensors.

1. At potentials where no electrode process occurs, there is an ordering of charge in the solution at the electrode–solution interface, the double layer. This is conveniently represented by a capacitor, and, in such a case, the equivalent circuit is R_Ω in series with the double-layer capacitance, C_{dl}. The impedance plot is a vertical straight line, as shown in Fig. 14.1a, the components of the impedance being given by

$$Z' = R_\Omega \quad Z'' = -1/(\omega C_{dl})$$

2. If, at a different applied potential, an electrode process occurs, that is, charge transfer controlled over the whole frequency range, then this charge transfer can be represented by a charge-transfer resistance, R_{ct}. The resistance R_{ct} is placed in parallel with the double-layer capacity, C_{dl}, since charge movement and charge separation happen at different sites on the electrode surface. Analysis of the spectrum gives a semicircle of diameter R_{ct}

$$Z' = R_\Omega + \frac{R_{ct}}{1 + (\omega R_{ct} C_{dl})^2} \quad Z'' = -\frac{R_{ct}^2 C_{dl}}{1 + (\omega R_{ct} C_{dl})^2}$$

   as shown in Fig. 14.1b. The maximum of the semicircle corresponds to $\omega R_{ct} C_{dl} = 1$. Naturally, the value of R_{ct} depends on the rate of charge transfer but also on analyte concentration.
3. Finally, the situation can occur where there is kinetic control at high frequencies, but at lower frequencies, owing to the longer timescale of the voltage perturbation, the charge transfer is governed by diffusional mass transport from the

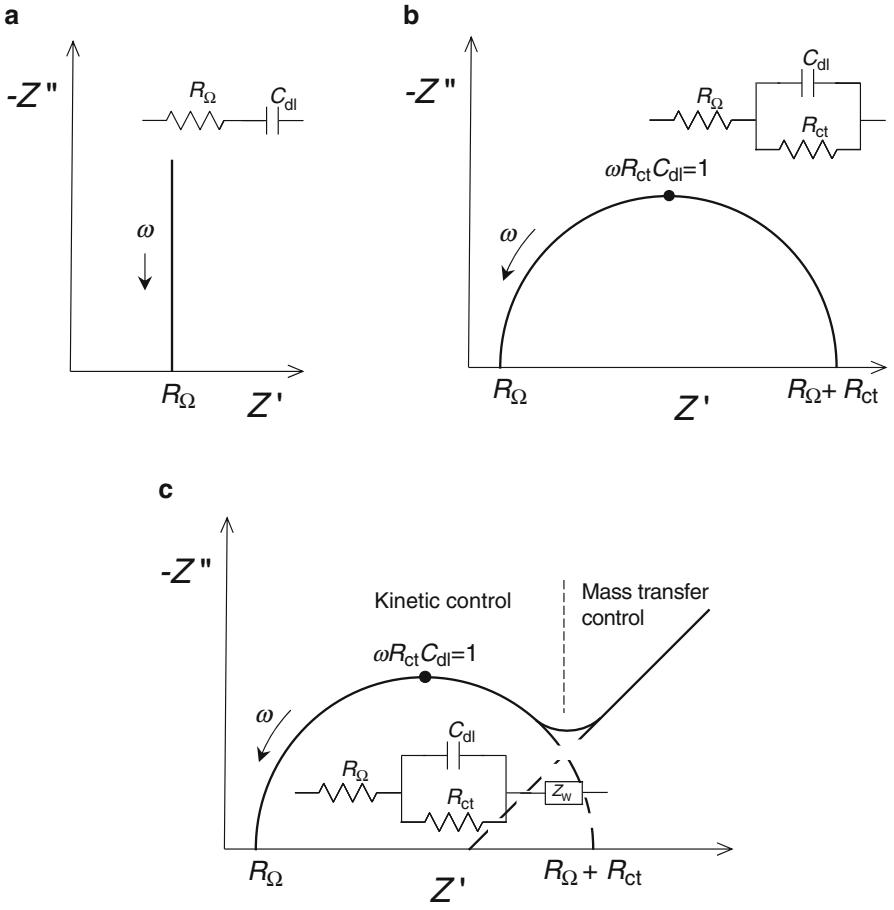

Fig. 14.1 Complex plane impedance plots at electrodes for the shown selected electrical equivalent circuits: (**a**) purely capacitive interfacial response, (**b**) faradaic electron-transfer reaction controlled by kinetics, (**c**) electron-transfer reaction with mass transfer control at low frequencies. R_Ω cell resistance, R_{ct} electron-transfer resistance, C_{dl} double-layer capacitance, Z_W Warburg impedance

interior of the solution. Diffusion control of solution species is represented by a Warburg impedance, Z_W, and corresponds to a line of slope 45° in the complex plane plots. The generic complex plane spectrum has the form shown in Fig. 14.1c. This is often seen when model electroactive species are used, for example, to probe to what extent a modifier film covers the electrode surface, the impedance values becoming larger the more that the surface is covered.

More complex equivalent circuits often need to be invoked for modified electrodes. For example, a film-modified electrode can itself have a resistance and charge

separation that could be represented by another *RC* parallel combination in series with the circuits above.

It is often found that the complex plane plots do not give perfect semicircles, they are depressed, and the vertical straight lines for capacitors appear at lower angles. The reason for this can be attributed to surface nonuniformity and roughness in that each local area has its own *RC* combination, but what is observed macroscopically is the sum of all these contributions. This is often referred to as frequency dispersion and can be taken into account in the modelling by using a constant phase element (CPE). For a nonideal capacitor, this has the form

$$\mathrm{CPE} = -1/(\mathrm{i}\omega C)^{\alpha}$$

where α is called the CPE exponent that varies between 1.0 for a pure capacitor and 0.5 for a porous electrode. It should be noted that values of 1.0 are, in practice, uncommon—for example, a bare glassy carbon electrode in its capacitive region usually gives an exponent of between 0.85 and 0.90.

Thus, experimental impedance data are commonly analysed by fitting them to an appropriate electrical equivalent electrical circuit. A physical model of the electrode–solution or modified electrode–solution process that can be justified should first be constructed and used for parameter fitting together with careful examination of the fitting errors.

Further details on representation and analysis of impedance spectra, especially in more complicated situations, may be found in references (1,2).

14.2.3 Characterisation of Sensors Using Electrochemical Impedance

Electrochemical impedance spectroscopy is excellent for the characterisation of electrodes, modified electrodes and the changes of the interfacial region with time and during use. The impedance response is subject to variations in the characteristics of the modification and substrate electrode surface which are not evident in voltammetric experiments. This is also the case for ion-selective electrodes. Thus, the main application of electrochemical impedance spectra is for system characterisation and as a diagnostic for changes which occur as a result of exposure to the analyte, degradation of response with time and so forth.[3] This begins with a full characterisation of the substrate electrode, in which impedance characterisation should be carried out together with voltammetric characterisation and surface analysis, as in reference (4) for carbon film electrodes. Using impedance spectra as an analytical tool, given their complexity in most situations, can make the obtaining of reproducible analytical data rather difficult.

A summary of several ways in which impedance may be applied to sensor characterisation is given in reference (5). This includes the probing of self-

assembled monolayers to examine for pinholes without using a redox probe by showing that the CPE exponent is 1.0 when a gold electrode surface is completely covered by alkanethiols,[6] characterisation of Nafion-modified electrodes for stripping analysis in the presence of surfactant,[7] recording impedance spectra during ultrasound irradiation to obtain rate constants for guanine and adenine electrooxidation without the complications of adsorption blocking of the surface[8] and characterising redox-mediated electrochemical biosensors.[9] In all of these cases, EIS is an extremely powerful tool and can complement the information obtained by voltammetric techniques.

Application of EIS to characterisation of stripping analysis in the environmental context will now be described in more detail, as an example of how impedance characterisation can be successfully employed. EIS was used to examine Nafion-coated electrodes prepared for the analysis of trace concentrations of cadmium and lead cations by anodic stripping voltammetry at potentials used during such experiments. It was found that irreversible changes to the Nafion film occur after the first stripping experiment, but that the modifier layer is then stable and no further changes occur, which is often seen but without demonstration of the reason.[10] Spectra also showed that the measurement of very high concentrations of metal ions is deleterious for the Nafion film. The effect of Triton-X surfactant was also examined,[11] and some of the impedance results obtained are shown in Fig. 14.2, here plotting the imaginary part of the impedance as a function of frequency. There is clear diagnostic information that at low surfactant concentrations, the polymer film and interfacial region is hardly influenced during the process examined, the influence becoming greater as the Triton concentration is increased and then decreasing to almost zero by 500 mg^{-1} of Triton. In this last case, which is above the critical micelle concentration, the surfactant molecules prefer to form micelles rather than stay close to the Nafion surface. The case of co-deposition of bismuth ions to improve the quality of the response was also examined, with the same conclusions.[12] Also, it was shown by EIS that organofunctionalisation of a graphite/polyurethane composite electrode with incorporated mesoporous silica was beneficial for facilitating heavy metal deposition.[13]

EIS can be used to demonstrate how electrodes or modified electrodes behave after the carrying out of other different types of experiment. For example, one of the difficulties in the analysis of pharmaceutical compounds or pesticides by oxidation is electrode blocking by adsorption of products of the electrode reaction. EIS is a convenient probe of such phenomena, since adsorption alters the shape of the spectra as well as the magnitude of the impedance. For example, in the analysis of the pharmaceutical compound verapamil, it was shown, using a graphite/polyurethane composite electrode, that there is no adsorption so that the same electrode can be used for a long period without any cleaning or surface regeneration.[14] Multilayer self-assembled layer-by-layer structures can also be conveniently probed, for example, of polyoxometalates (−) with poly(ethylamine)(+),[15] such modified electrodes being used for analysis of nitrite and other oxyanions.

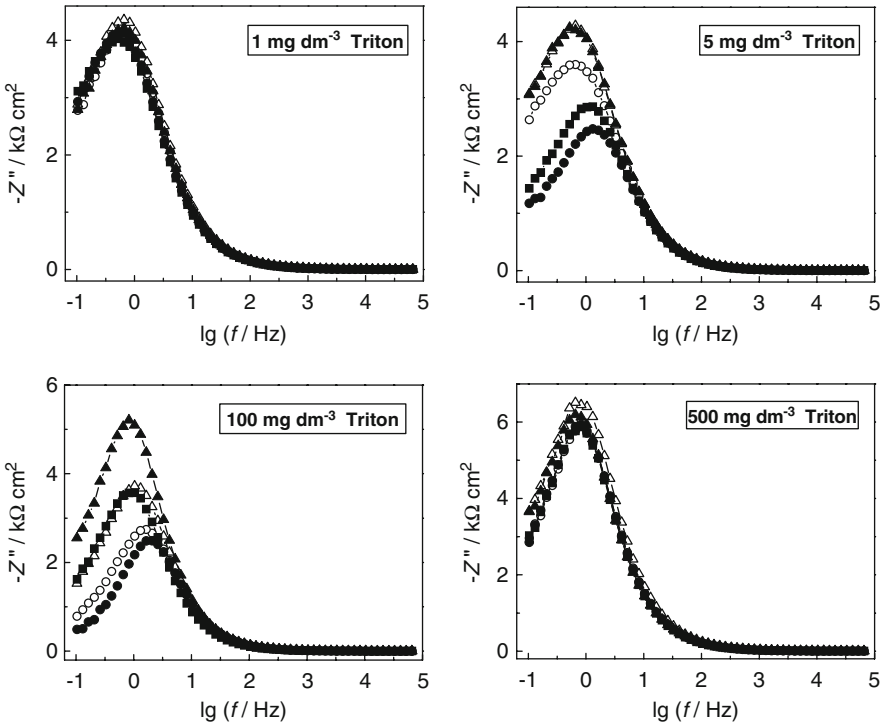

Fig. 14.2 Plots of $-Z''$ vs. lg (f/Hz) for Nafion-coated carbon film electrodes in pH 4.3 acetate buffer solution for different concentrations of Triton-X-100 at −0.5 V vs. SCE at different stages during the SWASV of lead and cadmium ions. Sequential spectra: (*filled square*) buffer electrolyte; (*filled circle*) after deposition during 120 s of 10^{-7} M Pb^{2+} and Cd^{2+}; (*open circle*) after SWASV; (*filled triangle*) with Triton and (*open triangle*) after electrochemical cleaning. From reference (11) with permission of Elsevier

Regarding applications involving surface modification with carbon nanotubes or other nanomaterials, similar considerations can be applied, for example, with chitosan/carbon nanotube-modified electrodes for hydrogen peroxide sensing or glucose biosensing.[16]

Enzyme inhibition sensors are of interest in the environmental context, the most used being those involving acetylcholinesterase inhibited by pesticides; e.g. these can involve rather complex architectures, and characterisation of such systems by EIS is becoming more widespread.[17] Complex sensor architectures have been used for endocrine disruptors, with similar characterisation by electrochemical impedance.[18] Recently, EIS was used for the first time to characterise the response of glucose biosensors in the presence of heavy metal ion inhibition.[19]

14.2.4 Applications of Electrochemical Impedance Spectroscopy in Analysis

Applications of electrochemical impedance spectroscopy as a direct sensing strategy are not common. Sensors which rely on the recording of an impedance spectrum are termed impedimetric sensors. The reasons that they are not in widespread use are, first, as mentioned above, because the spectra are often complex and can easily reflect subtle changes in the interfacial region which are not seen by other electrochemical techniques, thus compromising the analytical precision, and, second, the recording of a spectrum requires at the very least some minutes and commonly up to 30 min if low frequencies (less than 1 Hz) are to be applied. Even given such limitations, impedance spectroscopy can be used to periodically perform self-diagnostics of remotely deployed chemical sensors to decide if calibration is needed, for example, in ion-selective electrodes.[20]

One possible solution to the problem of recording a full impedance spectrum is, if there is full confidence in the impedance characteristics, to choose a smaller number of frequencies and make the spectrum recording take less time. If there is always a semi-circular (or depressed semi-circular) complex plane spectrum, then three or four carefully chosen frequencies should be sufficient to fit the data to the model. Other special cases are:

- If the response is purely capacitive, then use of one frequency is sufficient—capacitive sensors. These are mostly used in the context of physical measurements, such as humidity at miniaturised sensors.
- If the response is almost purely resistive, owing to the high resistance of a dielectric film modifier on the electrode surface, which dominates the response, then a conductance measurement can be made—conductometric sensors or, in a miniature form (see below), chemiresistors.

Examples of successful impedimetric sensors (rather than conductivity or capacitance) are few. One example involved the fabrication of lignin-modified glassy carbon electrodes which are sensitive to ozone. Exposing the sensor electrodes to various ozone concentrations resulted in proportional changes in the charge-transfer resistance in the impedance spectrum.[21] More recently, microelectrochemical sensors were prepared which are suitable for use in marine environments and were tailored to voltammetric and impedimetric or conductivity measurements.[22]

A review of impedimetric biosensors was made, concentrating on impedimetric immunosensors, which rely on antibody–antigen interactions.[23] The necessity of having a marker of the interaction, such as an enzyme, is thus unnecessary. These are exceptionally specific systems where the attachment of the antibody gives a large change in the impedance spectrum. Another area in expansion is application of impedimetric biosensors to foodborne pathogenic bacteria.[24]

With respect to conductometric measurements, recent research has been carried out with conductometric microbiosensors, summarised in reference (25), where careful studies of the impedance obtained at different frequencies were first done in

order to conclude that a minimum frequency of 10 kHz normally needs to be used so that the response is essentially conductive and surface effects can be neglected.

14.3 Solid-State Miniaturised Sensors

The use of microsensors for in-field monitoring of environmental parameters is gaining interest. Amongst them, microsensors based on semiconductor technology offer additional advantages such as small size, robustness, low output impedance and rapid response. The technology used allows integration of circuitry and multiple sensors in the same substrate, and accordingly they can be implemented in compact probes for particular applications, e.g. in situ monitoring and/or on-line measurements.

Miniaturised sensors have been made which are able to be placed in small spaces using semiconductor technology. The various kinds of sensors include ion-selective field-effect transistors (ISFETs) and chemical field-effect transistors (ChemFETs), as well as chemiresistors.

14.3.1 Electrolyte–Insulator–Semiconductor-Based Sensors

Electrolyte–insulator–semiconductors are the basis for silicon field-effect chemical sensors and include ISFETs/ChemFETs,[26] light-addressable potentiometric sensors (LAPSs)[27] and capacitive sensors.[28] The first ISFET was invented in 1970.[29]

Advantages are their small size, possibility of on-chip circuitry and potential for mass production at low cost. They rely on chemical sensitivity of the potential drop at the electrolyte–insulator interface that can be explained by ion exchange or by adsorption of potential-determining ions. Thin insulating oxide and nitride films are produced by conventional methods of microelectronics to provide pH-sensitive gate dielectrics. For example, chalcogenide films have promising potential for the detection of heavy metal ions in solutions, including in multisensor arrays for multicomponent analysis.[30]

All these sensors, in the simplest implementation, are based on a modified *n*-channel metal oxide semiconductor field-effect transistor (*n*-channel MOSFET). A *p*-type silicon substrate (bulk) contains two *n*-type diffusion regions (source and drain), the structure of which is covered with a silicon dioxide insulating layer on top of which a metal gate electrode is deposited. The application of a positive voltage to the gate electrode with respect to the *p*-type silicon creates a conducting channel between the source and the drain. The conductivity of this channel can be modulated by adjusting the strength of the electrical field between the silicon and the gate electrode (V_{gs}), perpendicular to the substrate surface. At the same time, a voltage can be applied between the drain and the source (V_{ds}), which results in a drain current between the *n*-regions and that is measured.

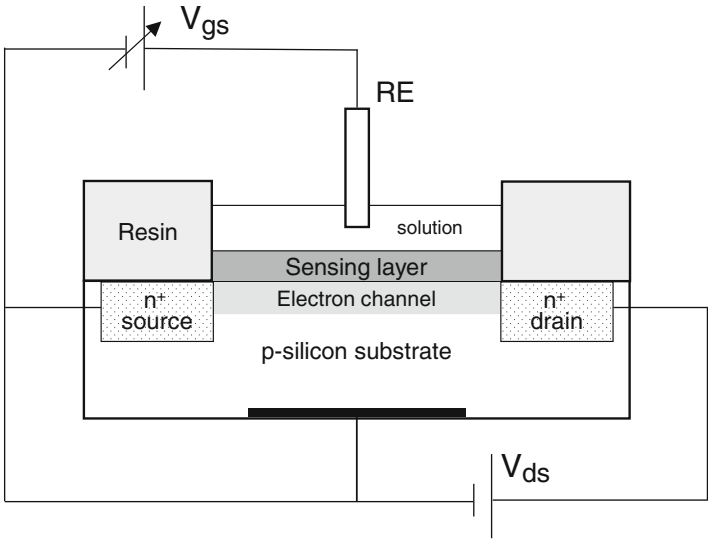

Fig. 14.3 Principle of operation of an ISFET sensor

14.3.1.1 ISFETs and ChemFETs

In ISFETs and ChemFETs, the transistor metal gate electrode is replaced by an electrolyte solution, in the case of ChemFETs probably with a modifier film being placed on top of the gate region to condition access of the species which can influence the source-drain current (see Fig. 14.3).

Thus, an ISFET is an ion-sensitive field-effect transistor used for measuring ion concentrations in solution; when the ion concentration (such as H^+) changes, the current through the transistor will change and the solution is used as the gate electrode. There are practical limitations owing to the necessity of using a separate reference electrode, so much effort has been devoted to making good, stable reference electrodes that can be placed on the same chip. Transistor encapsulation is needed to prevent attack on the electronics by the solution.

In order to improve performance, inorganic oxides other than SiO_2 for pH sensors such as Al_2O_3, Si_3N_4 and Ta_2O_5 have been deposited on top of the SiO_2 by chemical vapour deposition, in order to increase sensitivity and decrease the hysteresis and drift of SiO_2-based ISFETs.

A ChemFET, a chemical field-effect transistor, is a type of FET that is a chemical sensor where the charge on the gate electrode is due to a chemical process. In principle, it may be used to detect atoms, molecules and ions in liquids and gases. For example, the SiO_2 gate material has Si–OH groups on the surface, which can be used for covalent attachment of organic molecules and polymers.

Solid-state potentiometric sensors that are based on the chemical modulation of the work function of organic semiconductors were reviewed. These include the chemically sensitive field-effect transistor in which the conventional gate of

the silicon-based transistor was replaced by an organic semiconductor.[31] A comprehensive review of the ISFET and its applications in biomolecular sensing and characterisation of electrochemical interfaces was given, together with a survey of the different uses of the ISFET in biomedical and environmental applications.[32]

Recently, a review of the role of ISFETs and ChemFETs in the environmental field was presented, emphasising the way in which the measurement of pH and various ions is important in environmental water monitoring.[33] Besides pH, the concentrations of nitrate and ammonium ion are described, and of chloride in swimming pool waters. Regarding waste waters, anionic and cationic surfactants have been developed as well as enzyme ISFETs for measuring pollutants, by enzyme inhibition. A good example of this is modification by acetylcholinesterase for measuring pesticides, proposed as early as 1981,[34] but widespread use of this approach has not occurred owing to practical difficulties. The control of drainage waters in soils and crops is another area where ISFETS have potential application, e.g. in soil analysis[35] as well as in flow injection analysis (FIA) methods for real-time soil analysis, with emphasis on nitrate ions.[36]

A pH ISFET was used to monitor biofilm formation from *Micrococcus luteus* cells in microfluidic channels, the importance of using ISFETs being their small size, access obviously being impossible for larger sensors. Alkalinisation promotes biofilm formation, so detection of this by ISFETS can be used as a preventive measure in clinical and industrial environments.[37]

The use of ChemFETs as recognition devices for environmental application was recognised early on in the 1990s, as documented in,[38] one application being to measure low concentrations of copper, cadmium and silver ions in water.

In enzyme FETs (ENFETs), the detection layer is of enzymes. They are promising tools in medicine, biotechnology, environmental control, agriculture and the food industry, limitations to their use being mainly linked to retention of enzyme activity on immobilisation. Biosensors for the determination of concentrations of toxic substances (organophosphorus pesticides, heavy metal ions, hypochlorite, glycoalkaloids, etc.) can be designed, exploiting the enzyme inhibition effect.[39]

14.3.1.2 Light-Addressable Potentiometric Sensors (LAPS)

The light-addressable potentiometric sensor (LAPS) was first developed by Hafeman in 1988.[27] The LAPS principle is based on semiconductor activation by a light-emitting diode (LED) or a laser. A LAPS usually consists of a metal–insulator–semiconductor or electrolyte–insulator–semiconductor structure. The hetero-structure of $Si/SiO_2/Si_3N_4$ can be excited by a modulated light source, producing a photocurrent, the amplitude of which is sensitive to the surface potential, LAPS thus being able to detect the potential variation caused by an electrochemical event. The normal function of LAPS is for pH detection, via the H^+-sensitive Si_3N_4 layer fabricated on the LAPS surface. The encapsulation of LAPS is much less critical than with ISFETs since no metal contact is formed on the surface and the extremely flat surface makes it possible to incorporate it into a very

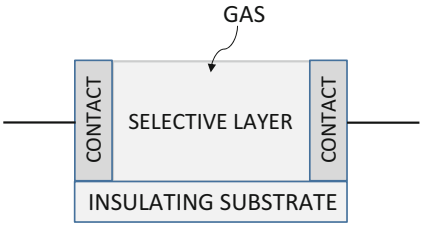

Fig. 14.4 Basic design of a chemiresistor for gas sensing

small volume chamber. Beside pH detection, it has been used for the detection of heavy metals. An integrated electronic tongue device including a multiple LAPS (MLAPS) and two groups of electrochemical electrodes was developed. The MLAPS used a chalcogenide thin film for simultaneous detection of Fe(III) and Cr(VI) ions, detecting other heavy metal ions in wastewater or seawater by stripping voltammetry.[40]

14.3.1.3 Capacitive Sensors

Capacitive miniaturised sensors are based on the charge carrier distribution at an insulator–semiconductor interface, which is controlled by an external voltage (V_{ds}), with a superimposed voltage (V_{gs}), the capacity of the space-charge-layer then being measured and leading to an integral capacitance–voltage (C–V) curve.

Electrochemical interaction at the phase boundary between electrolyte and sensing layer leads to a shift of the C–V characteristic, which can be used as a quantitative sensor signal. Dielectric oxide materials such as Al_2O_3 and Ta_2O_5 can be utilised as pH-sensitive gate insulators for such capacitive electrolyte–insulator–semiconductor structures.[28] Two examples from the literature are as follows. First, a cyanide biosensor based on a pH-sensitive structure with immobilised cyanidase enzyme was prepared and successfully applied.[41] Secondly, a capacitive enzyme sensor using organophosphorus hydrolase was developed for the direct determination of organophosphate pesticides.[42]

14.3.2 Chemiresistors

As their name suggests, chemiresistors involve making a measurement of change of resistance as a result of a chemical reaction. Traditionally MOS are used as the selective layer for gas adsorption and reaction (see Fig. 14.4).

The operating principle is as follows. Gas adsorption on the surface of the metal oxide changes its electrical resistance, and if these gases are oxidising or reducing, the electron transfer at the surface also changes the resistance. Such surface interactions occur at elevated temperatures. Under the best conditions, the change in sensor resistance is a linear function of analyte concentration. If a correct sensing

surface can be made, then application can be made to environmentally dangerous pollutants as well as other species. There is clearly a relation between the fabrication and some characteristics of chemiresistors with the MOSFETs used in ChemFETs. A comparison of the potentialities of the two techniques is thus possible, as reviewed in reference (43)

Within a review on applications of sensors in environmental analysis, the current situation in 2007 was examined with respect to applications of chemiresistors.[44] It was pointed out that the measurement of ppb concentrations of gases was needed, requiring sensitivity enhancement as well as the ability to measure several species simultaneously. This implicitly means the change of the selective layer from a MOS to another material. Some of these challenges have been addressed, and in recent years, since 2011, there has been an increase in the number of publications on chemiresistors, some of them relying on the use of single-walled carbon nanotubes (SWCNT) to increase surface area and thence sensitivity as well as modifying with biological receptors to increase selectivity.[45] Some of these recent examples are now indicated.

Low concentrations of ammonia in urban environments were measured, at room temperature, using chemiresistor gas sensors modified by SWCNT; concentrations of 20 ppb were measured and the detection limit was estimated as 3 ppb.[46] Trace amines in the vapour phase at sub-ppb levels were measured by a robust *p*-type organic nanofibril composite material obtained by surface doping.[47]

Nanometre-thick polyaniline films were used in the fabrication of chemiresistors, with a highly accessible surface geometry that enhanced ammonia and nitrogen dioxide gas adsorption and promoted surface reaction/interaction.[48] Conducting polymers in chemiresistor sensors for sensing hazardous hypergolic liquid propellant vapours and toxic exhaust plume acidic vapours of solid rocket motors (nitrogen oxides, hydrazines and toxic HCl vapours) at explosive, toxic and threshold limit value concentration levels have been reviewed.[49]

The problem of selective, multicomponent analysis in complex samples has also been addressed. Spectral analysis in the frequency domain with quadratic discriminant analysis was used to improve signal recognition in relation to simple steady-state amplitude analysis and was applied to recognise combustible analytes such as acetone, toluene and ethanol.[50]

14.4 Piezoelectric Transducer-Based Sensors

The piezoelectric effect is the generation of an electrical charge in a material as the result of a mechanical force exerted on it. Many materials exhibit the piezoelectric effect, for example, quartz, synthetic ceramics such as lead titanate, poly(vinylidene fluoride) and sucrose; the opposite is called the reverse piezoelectric effect. If an alternating voltage of the required frequency is applied to a piezoelectric material, then a mechanical resonance occurs that emits an electrical signal at a very precise frequency. Such crystal oscillators, nowadays nearly all based on

quartz, have a stable clock signal and are used in watches and clocks, radios, computers and cellphones and in signal generators, oscilloscopes, etc. Extensive details of the theory and applications of piezoelectric transducers can be found in reference (51).

The resonance phenomenon can also be used for chemical sensors, where species are deposited, adsorbed or absorbed within a sensor layer on the surface of the quartz crystal. This is the basis of the quartz crystal microbalance, bulk acoustic wave (BAW) sensors and surface acoustic wave (SAW) sensors. Normally, for chemical sensing applications, an AT-cut quartz crystal is employed at resonance frequencies varying between 1 and 10 MHz.

14.4.1 Quartz Crystal Microbalance (QCM)

If mass is deposited on the surface of a quartz crystal and leads to a rigid deposit, then the shift (reduction) in resonant frequency is given by the Sauerbrey equation[52]:

$$\Delta f = -\frac{2f_0^2}{A\sqrt{\mu_q \rho_q}}\Delta m$$

where f_0 is the resonant frequency (Hz), Δf the frequency change (Hz), Δm the mass change (g), and A the piezoelectrically active crystal area. For AT-cut quartz, ρ_q is the density of quartz (2.648 g cm^{-3}) and μ_q is the shear modulus of quartz for AT-cut crystals (2.947×10^{11} g cm^{-1} s^{-2}) which leads to $\Delta f = -2.91 \times 10^8\ \Delta m$.

If the quartz crystal is put in contact with a viscous liquid (Newtonian liquid) at one of its surfaces, then the Kanazawa equation[53] applies:

$$\Delta f = -f_0^{3/2}\left(\frac{\rho_{liq}\eta_{liq}}{\pi\mu_q\rho_q}\right)^{1/2}$$

where ρ_{liq} is the density of the liquid of viscosity η_{liq}. Thus, immersion of a quartz crystal in solution from air will lead to a reduction in frequency, as will further interaction on the surface with a non-rigid medium (a viscoelastic effect) such as a polymer, protein or other biological molecule. This demonstrates that it is not correct in such circumstances to assume a direct proportionality between frequency and mass changes, as given by the Sauerbrey equation, and this must be investigated. If deposition leads to a rigid film, then the QCM can be used directly as a mass sensor.

For a 10 MHz crystal, a frequency change of 1 Hz corresponds to approximately 4 ng cm^{-2} and the crystal thickness is around 0.16 mm. Crystals are normally supplied in the form of discs of diameter approximately 1 cm. Usually they are coated on both sides with gold by sputtering and connected to the oscillator

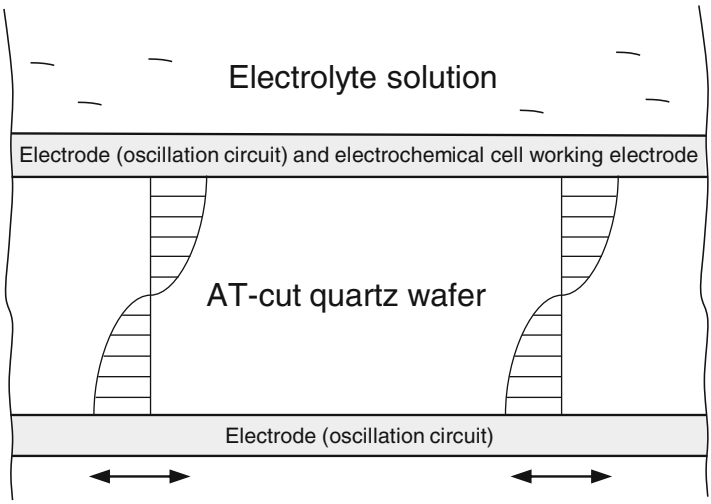

Fig. 14.5 Design principle of the electrochemical quartz crystal microbalance. The electrodes are most commonly of gold

electrical circuit (see Fig. 14.5). The back side is isolated from the exterior and the front side is exposed to the environment. The external gold layer is used to anchor modifier layers, particularly through thiol groups; other metals can be used as electrodes, but are less common.

The potentialities of the surface of the QCM as a sensitive way of interacting with the environment either directly or after modification was realised early on, see reference (54), particularly in a biosensor context. Several more recent examples of the QCM sensors and biosensors will illustrate the types of application. Sometimes the designation bulk acoustic wave (BAW) sensors is employed to refer to the QCM sensing principle.

Phthalocyanine coatings on QCM sensors were used for the detection of low ppm levels of organic compounds in waters.[55] Gold nanoparticles were self-assembled onto the QCM surface leading to a micromolar detection limit, the QCM sensor then being applied to the analysis of copper contamination in drinking water.[56]

Piezoelectric biosensor arrays for dioxins have been reported, the sensor surfaces using different pentapeptides as biomimetic traps (receptors) and measuring the changes in mass.[57] Recently, a protocol to fabricate acoustic micro-immunosensors based on a QCM was described and used to measure carbofuran or atrazine as antigens on a surface functionalised with monoclonal anti-carbofuran or with anti-atrazine IgG antibodies.[58] A similar antibody–antigen approach for parathion is described in reference (59).

In the electrochemical quartz crystal microbalance (EQCM), the QCM surface in contact with the external medium is simultaneously used as a working electrode in an electrochemical circuit (see Fig. 14.5). This enables frequency changes and

voltammetric data to be acquired at the same time, helping the elucidation of complex electrode processes.[60] Modifying the electrode surface leads to interesting possibilities and higher selectivity[61] and is particularly interesting for following the formation of conducting polymers by potential cycling.[62] Another interesting example is following the formation of self-assembled layer-by-layer structures where the voltammetric, electrochemical impedance and frequency change data can all be correlated to enable conclusions to be made concerning monolayer reorganisation while the multilayer build-up process is occurring, e.g. with myoglobin and hyaluronic acid.[63]

Examples of the direct use of EQCM in analysis are not many, most of the reports being devoted to use for characterisation of the analytical process which is then carried out voltammetrically. For example, the growth of thermally responsive surface-attached hydrogels for amperometric glucose biosensors was investigated by EQCM.[64] An EQCM was used to investigate the mass changes accompanying phenol oxidation catalysed by a lutetium bisphthalocyanine (LuPc2) film-modified Pt/quartz electrode, with a view to application in wine analysis.[65] Finally, zinc porphyrins were electropolymerised on an EQCM which was then used to determine the alkaloids nicotine, cotinine and myosmine under flowing conditions.[66]

14.4.2 Surface Acoustic Wave (SAW) Sensors

QCM sensors (or BAW sensors) concern probing alterations to the bulk properties of the piezoelectric crystal. If an acoustic wave is made to travel along the surface of the substrate, then a surface acoustic wave (SAW) sensor can be produced.

The operation of a SAW device is based on acoustic wave propagation near the surface of a piezoelectric solid, which implies that the wave can be trapped or otherwise modified while propagating.[67] Since the displacements decay exponentially away from the surface, most of the wave energy (usually more than 95 %) is confined within a depth equal to one wavelength. A basic SAW device consists of two interdigital transducers (IDT) on a piezoelectric substrate such as quartz. The input IDT launches and the output IDT receives the waves. The width of the electrodes usually equals the width of the interelectrode gaps giving the maximum conversion of electrical to mechanical signal, and vice versa. The minimum electrode width achieved is around 0.3 μm, which determines the highest frequency of around 3 GHz: frequencies can vary between 10 MHz and 3 GHz.

SAW devices are very widespread and just two recent examples in the chemical context will be given. First, a novel analytical sensing system was designed using a SAW device for the characterisation and discrimination of different detergents in water with possible future application in environmental management.[68] Second, a new phthalocyanine chemoselective material was coated on a 300 MHz SAW device using cyclic voltammetry for the selective and sensitive detection of sarin vapour.[69] The field of SAW physical and chemical sensors is large both commercially and in terms of new research.

14.5 Conclusions

In this chapter, the basis of techniques based on the measurement of electrical properties of electrode–solution, modified electrode–solution or solid–solution interfaces has been discussed. It has been demonstrated how they can be employed for characterisation of chemical systems and for analysis through selected examples. There has been an upward trend in the use of all the types of sensor and sensing techniques described, which can be expected to continue in the future.

References

1. Brett CMA, Oliveira-Brett AM (1993) Electrochemistry. Principles, methods and applications (chapter 11). Oxford University Press, Oxford, UK
2. Orazem ME, Tribollet B (2008) Electrochemical impedance spectroscopy. Wiley, Hoboken, NJ
3. Brett CMA, Oliveira-Brett AM (2011) Electrochemical sensing in solution – origins, applications and future perspectives. J Solid State Electrochem 15:1487–1494
4. Gouveia-Caridade C, Soares DM, Liess H-D, Brett CMA (2008) Electrochemical, morphological and microstructural characterization of carbon film resistor electrodes for application in electrochemical sensors. Appl Surf Sci 254:6380–6389
5. Brett CMA (2008) Electrochemical impedance spectroscopy for characterization of electrochemical sensors and biosensors. ECS Trans 13(13):67–80
6. Brett CMA, Kresak S, Hianik T, Oliveira-Brett AM (2003) Studies on self-assembled alkanethiol monolayers formed at applied potential on polycrystalline gold electrodes. Electroanalysis 15:557–565
7. Oliveira Brett AM, da Silva LA, Brett CMA (2002) Adsorption of guanine, guanosine and adenine at electrodes studied by differential pulse voltammetry and electrochemical impedance. Langmuir 18:2326–2330
8. Gouveia-Caridade C, Brett CMA (2008) Strategies, development and applications of polymer-modified electrodes for stripping analysis. Curr Anal Chem 4:206–214
9. Pauliukaite R, Ghica ME, Barsan M, Brett CMA (2007) Characterisation of poly(neutral red) modified carbon film electrodes; application as a redox mediator for biosensors. J Solid State Electrochem 11:899–908
10. Gouveia-Caridade C, Brett CMA (2005) Electrochemical impedance characterisation of Nafion-coated carbon film resistor electrodes for electroanalysis. Electroanalysis 17:549–555
11. Gouveia-Caridade C, Brett CMA (2006) The influence of Triton-X-100 surfactant on the electroanalysis of lead and cadmium at carbon film electrodes – an electrochemical impedance study. J Electroanal Chem 592:113–120
12. Gouveia-Caridade C, Pauliukaite R, Brett CMA (2006) Influence of Nafion coatings and surfactant on the stripping voltammetry of heavy metals at bismuth-film modified carbon film electrodes. Electroanalysis 18:854–861
13. Cesarino I, Cavalheiro ETG, Brett CMA (2011) Simultaneous determination of cadmium, lead, copper and mercury ions using organofunctionalised SBA-15 nanostructured silica modified graphite–polyurethane composite electrode. Electroanalysis 22:61–68
14. Semaan FS, Cavalheiro ETG, Brett CMA (2009) Electrochemical behaviour of verapamil at graphite-polyurethane composite electrodes. Determination of release profiles in pharmaceutical samples. Anal Lett 42:1119–1135
15. Fernandes DM, Ghica ME, Cavaleiro AMV, Brett CMA (2011) Electrochemical impedance study of self-assembled layer-by-layer iron-silicotungstate/poly(ethylenimine) modified electrodes. Electrochim Acta 56:7940–7945

16. Pauliukaite R, Ghica ME, Fatibello-Filho O, Brett CMA (2010) Electrochemical impedance studies of chitosan-modified electrodes for application in electrochemical sensors and biosensors. Electrochim Acta 55:6239–6247
17. Zhai C, Sun X, Zhao WP, Gong ZL, Wang XY (2013) Acetylcholinesterase biosensor based on chitosan/Prussian blue/multiwall carbon nanotubes/hollow gold nanospheres nanocomposite film by one-step electrodeposition. Biosens Bioelectron 42:124–130
18. Rather JA, De Wael K (2012) C-60-functionalized MWCNT based sensor for sensitive detection of endocrine disruptor vinclozolin in solubilized system and wastewater. Sensor Actuator B 171:907–915
19. Ghica ME, Carvalho RC, Amine A, Brett CMA (2013) Glucose oxidase enzyme inhibition sensors for heavy metals at carbon film electrodes modified with cobalt or copper hexacyanoferrate. Sensor Actuator B 178:270–278
20. Radu A, Anastasova-Ivanova S, Paczosa-Bator B, Danielewski M, Bobacka J, Lewenstam A, Diamond D (2010) Diagnostic of functionality of polymer membrane – based ion selective electrodes by impedance spectroscopy. Anal Methods 2:1490–1498
21. Stergiou DV, Veltsistas PG, Prodromidis MI (2008) An electrochemical study of lignin films degradation: proof-of-concept for an impedimetric ozone sensor. Sensor Actuator B 129:903–908
22. Herzog G, Moujahid W, Twomey K, Lyons C, Ogurtsov VI (2013) On-chip electrochemical microsystems for measurements of copper and conductivity in artificial seawater. Talanta 116:26–32
23. Prodromidis MI (2010) Impedimetric immunosensors – a review. Electrochim Acta 55:4227–4233
24. Wang Y, Ye Z, Ying Y (2012) New trends in impedimetric biosensors for the detection of foodborne pathogenic bacteria. Sensors 12:3449–3471
25. Jaffrezic-Renault N, Dzyadevych NV (2008) Conductometric microbiosensors for environmental monitoring. Sensors 8:2569–2588
26. Bergveld P, Sibbald A (1988) Analytical and biomedical applications of ion-selective field-effect transistors. Elsevier, Amsterdam
27. Hafeman DG, Parce JW, McConnell HM (1988) Light-addressable potentiometric sensor for biochemical systems. Science 240:1182–1185
28. Schöning MJ, Luth H (2001) Novel concepts for silicon-based biosensors. Phys Status Solidi A 185:65–77
29. Bergveld P (1970) Development of an ion-sensitive solid-state device for neurophysiological measurements. IEEE Trans Biomed Eng BME 17:70–71
30. Vlasov YG, Tarantov YA, Bobrov PV (2003) Analytical characteristics and sensitivity mechanisms of electrolyte-insulator-semiconductor system-based chemical sensors - a critical review. Anal Bioanal Chem 376:788–796
31. Janata J, Josowicz M (2009) Organic semiconductors in potentiometric gas sensors. J Solid State Electrochem 13:41–49
32. Shinwari MW, Deen MJ, Landheer D (2007) Study of the electrolyte-insulator-semiconductor field-effect transistor (EISFET) with applications in biosensor design. Microelectron Reliab 47:2025–2057
33. Jimenez-Jorquera C, Orozco J, Baldi A (2010) ISFET based microsensors for environmental monitoring. Sensors 10:61–83
34. Janata J, Huber RJ, Cohen R, Kolesar ES (1981) Chemically sensitive field-effect transistor to detect organophosphorous compounds and pesticides. Aviat Space Environ Med 52:666–671
35. Artigas J, Beltran A, Jimenez C, Baldi A, Mas R, Dominguez C, Alonso J (2001) Application of ion sensitive field effect transistor based sensors to soil analysis. Comput Electron Agric 31:281–293
36. Birrell SJ, Hummel JW (2001) Real-time multi ISFET/FIA soil analysis system with automatic sample extraction. Comput Electron Agric 32:45–67

37. Matsuura K, Asano Y, Yamada A, Narus K (2013) Detection of *Micrococcus Luteus* biofilm formation in microfluidic environments by pH measurement using an ion-sensitive field-effect transistor. Sensors 13:2484–2493
38. Barbaro A, Colapicchioni C, Davini E, Mazzamurro G, Piotto A, Porcelli F (1992) CHEMFET devices for biomedical and environmental applications. Adv Mater 4:402–408
39. Dzyadevych SV, Soldatkin AP, Korpan YI, Arkhypova VN, Elskaya AV, Chovelon JM, Martelet C, Jaffrezic-Renault N ((2003) Biosensors based on enzyme field-effect transistors for determination of some substrates and inhibitors. Anal Bioanal Chem 377:496–506
40. Men H, Zou SF, Li Y, Wang YP, Ye XS, Wang P (2005) A novel electronic tongue combined MLAPS with stripping voltammetry for environmental detection. Sensor Actuator B 110:350–355
41. Turek M, Ketterer L, Claßen M, Berndt HK, Elbers G, Krüger P, Keusgen M, Schöning MJ (2007) Development and electrochemical investigations of an EIS-(electrolyte-insulator-semiconductor) based biosensor for cyanide detection. Sensors 7:1415–1426
42. Schoning MJ, Arzdorf M, Mulchandani P, Chen W, Mulchandani A (2003) Towards a capacitive enzyme sensor for direct determination of organophosphorus pesticides: fundamental studies and aspects of development. Sensors 3:119–127
43. Katz HE (2004) Chemically sensitive field-effect transistors and chemiresistors: new materials and device structures. Electroanalysis 16:1837–1842
44. Lieberzeit PA, Dickert FL (2007) Sensor technology and its application in environmental analysis. Anal Bioanal Chem 387:237–247
45. Sarkar T, Gao Y, Mulchandani A (2013) Carbon nanotubes-based label-free affinity sensors for environmental monitoring. Appl Biochem Biotechnol 170:1011–1025
46. Rigoni F, Tognolini S, Borghetti P, Drera G, Pagliara S, Goldoni A, Sangaletti L (2013) Enhancing the sensitivity of chemiresistor gas sensors based on pristine carbon nanotubes to detect low-ppb ammonia concentrations in the environment. Analyst 138:7392–7399
47. Huang H, Gross DE, Yang X, Moore JS, Zang L (2013) One-step surface doping of organic nanofibers to achieve high dark conductivity and chemiresistor sensing of amines. ACS Appl Mater Interfaces 5:7704–7708
48. Srinives S, Sarkar T, Mulchandani A (2013) Nanothin polyaniline film for highly sensitive chemiresistive gas sensing. Electroanalysis 25:1439–1445
49. Selvakumar S, Somanathan N, Reddy KA (2013) Chemiresistor sensors based on conducting polymers for hypergolic propellants and acidic vapors of rocket exhaust plumes – a review. Prop Explos Pyrotech 38:176–189
50. Dobrokhotov V, Larin A, Sowell D (2013) Vapor trace recognition using a single nonspecific chemiresistor. Sensors 13:9016–9028
51. Arnau A (ed) (2008) Piezoelectric transducers and applications , 2nd edn. Springer, Heidelberg
52. Sauerbrey G (1959) Verwendung von schwingquarzen zur wägung dünner schichten und zur mikrowägung. Z Phys 155:206–212
53. Reed CE, Kanazawa KK, Kaufmann JH (1990) Physical description of a viscoelastically loaded AT-cut quartz resonator. J Appl Phys 68:1993–2001
54. Minunni M, Mascini M, Guibault GG, Hock B (1995) The quartz-crystal microbalance as biosensor – a status-report on its future. Anal Lett 28:749–764
55. Harbeck M, Erbahar DD, Gurol I, Musluoglu E, Ahsen V, Ozturk ZZ (2010) Phthalocyanines as sensitive coatings for QCM sensors operating in liquids for the detection of organic compounds. Sensor Actuator B 150:346–354
56. Jin YL, Huang YY, Liu GQ, Zhao R (2013) Gold nanoparticle-sensitized quartz crystal microbalance sensor for rapid and highly selective determination of Cu(II) ions. Analyst 138:5479–5485
57. Mascini M, Macagnano A, Monti D, Del Carlo M, Paolesse R, Chen B, Warner P, D'Amico A, Di Natale C, Compagnone D (2004) Piezoelectric sensors for dioxins: a biomimetic approach. Biosens Bioelectron 20:1203–1210

58. Jia K, Adam PM, Ionescu RE (2013) Sequential acoustic detection of atrazine herbicide and carbofuran insecticide using a single micro-structured gold quartz crystal micro balance. Sensor Actuator B 188:400–404
59. Funari R, Della Ventura B, Schiavo L, Esposito R, Altucci C, Velotta R (2013) Detection of parathion pesticide by quartz crystal microbalance functionalized with UV-activated antibodies. Anal Chem 85:6392–6397
60. Hillman AR (2011) The EQCM: electrogravimetry with a light touch. J Solid State Electrochem 15:1647–1660
61. Perrot H, Calvo E, Brett CMA (2008) Modified piezoelectric surfaces. In: Arnau A (ed) Piezoelectric transducers and applications, 2nd edn. Springer, Heidelberg, Chapter 11
62. Inzelt G (2011) Rise and rise of conducting polymers. J Solid State Electrochem 15:1711–1718
63. Pinto EM, Barsan MM, Brett CMA (2010) Mechanism of formation and construction of self-assembled myoglobin/hyaluronic acid multilayer films – an electrochemical QCM, impedance and AFM study. J Phys Chem B 114:15354–15361
64. Bunsow J, Enzenberg A, Pohl K, Schuhmann W, Johannsmann D (2010) Electrochemically induced formation of surface-attached temperature-responsive hydrogels. amperometric glucose sensors with tunable sensor characteristics. Electroanalysis 22:978–984
65. Gay-Martin M, Diez-Arevalo E, Rodriguez-Mendez ML, Saez JAD (2013) Electrochemical quartz crystal microbalance analysis of the oxidation reaction of phenols found in wines at lutetium bisphthalocyanine electrodes. Sensor Actuator B 185:24–31
66. Noworyta K, Kutner W, Wijesinghe CA, Srour SG, D'Souza F (2012) Nicotine, cotinine, and myosmine determination using polymer films of tailor-designed zinc porphyrins as recognition units for piezoelectric microgravimetry chemosensors. Anal Chem 84:2154–2163
67. Ballantine DA, White RM, Martin SJ, Ricco AJ, Zellers ET, Frye GC, Wohltjen H (1997) Acoustic wave sensors: theory, design and physicochemical applications. Academic, San Diego, USA
68. Vivancos JL, Racz Z, Cole M, Gardner JW (2012) Surface acoustic wave based analytical system for the detection of liquid detergents. Sensor Actuator B 171:469–477
69. Wang P-H, Yu J-H, Li Z-J, Ding Z-J, Guo L, Du B (2013) Synthesis and evaluation of a new phthalocyanine as sensor material for sarin detection. Sensor Actuator B 188:1306–1311

Part III
Sensor Electrodes and Practical Concepts

Chapter 15
From Macroelectrodes to Microelectrodes: Theory and Electrode Properties

Salvatore Daniele and Carlo Bragato

15.1 Introduction

Voltammetry involves the application of a potential that varies with time and the measurement of a current that flows between a working and a reference electrode. Voltammetry can therefore be defined as the exploration of the three-dimensional space that relates to potential, current, and time.[1] However, under suitable circumstances, simplified conditions can lead to a unique relation, not involving time, between current and potential; such situation provides the so-called steady-state voltammetry.[2]

Voltammetric techniques date back to the early of nineteenth century, following the experiments made by Heyrovsky in 1922, and when, for the first time, he showed that by measuring the current while the potential of a dropping mercury electrode (DME) was changed, it was possible to obtain information on the nature of the species in the solution that were reduced at the electrode surface. This technique, called polarography, was used for analytical applications, especially of metal ions. The term voltammetry was first introduced in 1940 to describe experiments, similar to those made at a DME, performed at a solid working electrode.[1] Many variations of the basic polarography were developed during the 1940s and early 1950s. Pulsed waveforms in conjunction with DMEs or static mercury electrodes have been developed and largely applied for analytical investigations.[1] The pulsed techniques were aimed at decreasing the contribution of the capacitive current, which originates from charging the electrical double-layer capacitance that exists at the interface between the electrode and the solution. The charging current is non-faradaic and produces baseline current that must be subtracted in

S. Daniele (✉) • C. Bragato
Department of Molecular Sciences and Nanosystems, University Ca' Foscari of Venice, Dorsoduro 2137, 30123 Venice, Italy
e-mail: sig@unive.it

L.M. Moretto, K. Kalcher (eds.), *Environmental Analysis by Electrochemical Sensors and Biosensors*, DOI 10.1007/978-1-4939-0676-5_15

voltammetric measurements to improve the sensitivity, especially for trace species analysis.[3]

A further impetus in the development of voltammetric techniques has been recorded during the 1980s with the advent of much smaller, than previously employed, electrodes, which were of millimeter size. The smaller electrodes have micrometer size and are commonly referred to as either ultramicroelectrodes (UMEs) or, simply, microelectrodes (MEs).[4–13] Since then, the field of MEs has generated enormous excitement and has seen a huge increase in popularity with the rapid developments in nanofabrication capable of preparing well-defined electrodes of sub-micrometer size down to a few nanometers.[14, 15] Such very small electrodes are nowadays defined nanoelectrodes (NEs). The latter category, normally, includes all electrodes that possess at least one dimension less than 100 nm.[15] It must be considered that the main properties of both MEs and NEs come from a common operational characteristic. It involves the circumstance that under given experimental conditions, the diffusion layer thickness is thicker than the characteristic length of the electrode.[12]

This chapter is concerned with methods in which a constant potential or a potential varied with time is applied to either millimeter sized (called conventional electrodes) or MEs and the ensuing current response as a function of time or potential is measured.

15.2 Mass Transport and Electrode Geometry

A typical electrode reaction involves the transfer of charge between an electrode and a species in solution. The whole process involves a series of steps, including the electron transfer at the electrode surface and the movement of reactant in and out of the interface, that is, the mass transport within the solution. Both phenomena are important in predicting the current flowing in the electrochemical cell. The model of the electrode kinetics predicts that the rate of the electron transfer is affected by the electrode voltage through an exponential relationship.[3] The current therefore, over a potential region, also increases exponentially by increasing the electrode potential. The current increase is limited by the mass transport of both reactant and electrode reaction product (see Chap. 10 for details).

There are three forms of mass transport which can influence an electrolysis process:

- Diffusion
- Convection
- Migration

Diffusion occurs in all solutions and arises from local uneven concentrations of reagents. It is particularly significant in an electrolysis experiment since the conversion reaction only occurs at the electrode surface. Consequently, there will be a lower reactant concentration at the electrode than in bulk solution. Similarly, a

higher concentration of product will exist near to the electrode than further out into the solution.

Convection originates from the action of a force on the solution. There are two forms of convection. The first is termed *natural convection* and is present in any solution. This natural convection is generated by small thermal or density differences and acts to mix the solution in a random and therefore unpredictable manner. In the case of electrochemical measurements, these effects tend to cause problems if the measurement time for the experiment exceeds 20 s.[3] The second type is termed *forced convection*. It is typically several orders of magnitude greater than any natural convection and therefore effectively removes the random aspect, due to natural convection, from the experimental measurements. This of course is only true if the convection is introduced in a well-defined and quantitative manner.[3]

Migration is essentially an electrostatic effect which arises due the application of a voltage at the electrodes. Any charged species near that interface will either be attracted or repelled from it by electrostatic forces.

Due to ion solvation effects and diffuse layer interactions in solution, migration is usually difficult to calculate accurately for real solutions. Most electrochemical measurements, therefore, are performed in solutions which contain a background electrolyte that does not undergo electrolysis itself but helps to shield the reactants from migratory effects. By adding a large quantity of the electrolyte (relative to the reactants), it is possible to ensure that the electrolysis reaction is not significantly effected by migration.

On the above basis, it is evident that to gain a quantitative model of the current flowing at the electrode, one must account for the electrode kinetics, the three-dimensional diffusion, convection, and migration contributions of all the species involved.

The total mass transport of a given species i is given by the flux, J_i (mol s^{-1} cm^{-2}), to an electrode and is described by the Nernst-Planck equation[3]:

$$J_i = -D_i \nabla C_i - \frac{Z_i F}{RT} D_i C_i \nabla \phi + v C_i \tag{15.1}$$

The flux is related to the current through

$$J_i = \frac{i}{nFA} \tag{15.2}$$

The solution of Eq. (15.1) is difficult and currently is beyond the capacity of even the fastest computers. However, electrochemical experiments can be designed to eliminate the contributions of electrostatic potential and hydrodynamic velocity to the overall flux of electroactive species, limiting mass transport to the contribution from *diffusion*. The currents resulting from these experiments can then be classified as *diffusion controlled*.[3]

Contributions from migration can be effectively eliminated by adding an inert electrolyte to the solution at a 10–100-fold excess with respect to the redox couple

Table 15.1 Diffusion equations for different electrode geometries

Electrode geometry	Diffusion equation	
Planar	$\frac{\partial c}{\partial t} = D\left(\frac{\partial^2 c}{\partial x^2}\right)$	$T_{1,1}$
Sphere, hemisphere	$\frac{\partial c}{\partial t} = D\left(\frac{\partial^2 c}{\partial r^2} + \frac{2}{r}\frac{\partial c}{\partial r}\right)$	$T_{1,2}$
Cylinder	$\frac{\partial c}{\partial t} = D\left(\frac{\partial^2 c}{\partial r^2} + \frac{1}{r}\frac{\partial c}{\partial r}\right)$	$T_{1,3}$
Microdisk	$\frac{\partial c}{\partial t} = D\left(\frac{\partial^2 c}{\partial r^2} + \frac{1}{r}\frac{\partial c}{\partial r} + \frac{\partial^2 c}{\partial z^2}\right)$	$T_{1,4}$
Band	$\frac{\partial c}{\partial t} = D\left(\frac{\partial^2 c}{\partial x^2} + \frac{\partial^2 c}{\partial z^2}\right)$	$T_{1,5}$

of interest. The electric field between the two electrodes involved in the measurement is dissipated over all of the ions in solution and not just the electroactive material. Under these conditions, the contribution of migration to the observed current is <1 %. Contributions from convection can be reduced or eliminated by working in quiescent solutions. With careful control of external vibration and temperature, diffusion controlled measurements for up to 20 s or close can be made without significant convective effects.[3]

In the following section how the diffusion mass transport will control the current at electrodes of different sizes and geometries will be described.

15.3 Diffusion Equations and Current Responses

Fick's first and second laws describe the flux of a species and its concentration as functions of time and position, respectively. The general formulations of Fick's laws for the species O at any geometry are:

$$J_O = -D_O \nabla C_O \tag{15.3}$$

$$\frac{\partial C_O}{\partial t} = D_O \nabla^2 C_O \tag{15.4}$$

Although the diffusion equations require, in general, three spatial coordinates to describe the mass transport, in the cases of an infinite plane, a sphere, and an infinitely long cylinder, the boundary allows a reduction from three to one of the number of spatial coordinates. These geometries simplify the Laplace operator so that Eqs. (15.3) and (15.4) acquire simpler forms. The concentration gradient at the electrode surface is obtained by solving Fick's second law, and Table 15.1 shows the simplified forms of the diffusion equations for such electrode geometries. For planar diffusion x is the spatial coordinate directed to the boundary ad having its origin at the boundary surface (Fig. 15.1a). In the case of spherical (Fig. 15.1b) and cylindrical geometries, r represents the radial distance from the electrode center. The solution of these equations, under appropriate boundary conditions, yields the

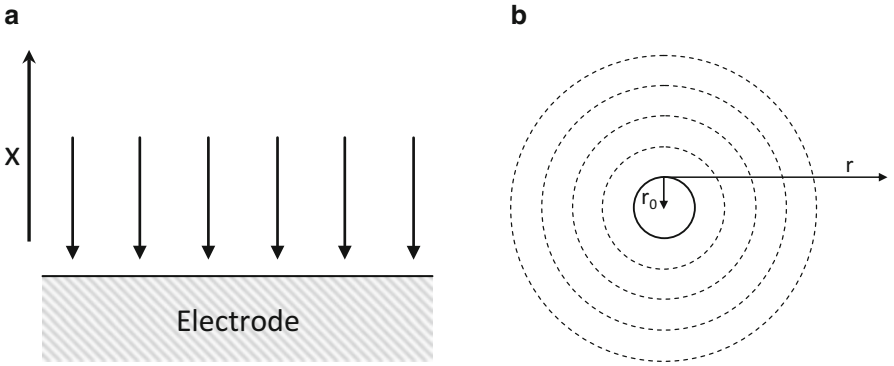

Fig. 15.1 Diffusion mass transport to: (**a**) planar electrode; (**b**) spherical electrode

concentration profiles, $C(x,t)$, i.e., the change of concentration of that species as functions of the distance and time. Boundary conditions, in turn, depend on the electrochemical experiments performed.

15.3.1 Application of a Potential Step

The experiment of interest involves stepping the potential from an initial value, where no electrode reaction occurs, to one at which electrolysis proceeds at diffusion controlled rate. The general reaction considered is:

$$O + ne \leftrightarrows R \tag{15.5}$$

and the electrode is placed in a semi-infinite solution containing only the electroactive species O of concentration C_O^*. The semi-infinite condition highlights the fact the volume of the electrolytic solution is much larger than the electrode size. It is also assumed that a sufficient negative potential is applied at the working electrode so that the surface concentration of O becomes equal to zero, regardless of whether the kinetics of the process is facile or sluggish. Examples of boundary conditions, which are valid under the electrochemical experiment outlined above, are

$$\begin{array}{lll} C_O(x,0) = C_O^* & (\text{for all } x) & \text{Initial conditions} \\ C_R(x,0) = 0 & (\text{for all } x) & \text{Initial conditions} \\ \lim\limits_{x\to\infty} C_O(x,t) = C_O^* & (\text{at all } t) & \text{Semi-infinite conditions} \\ \lim\limits_{x\to\infty} C_R(x,t) = C_R^* & (\text{at all } t) & \text{Semi-infinite conditions} \end{array}$$

Equations for planar ($T_{1,1}$ in Table 15.1) and spherical ($T_{1,2}$ in Table 15.1) electrodes can be solved using the Laplace transform technique to give, after considering Eq. (15.2), the time evolution of the current (i_t).

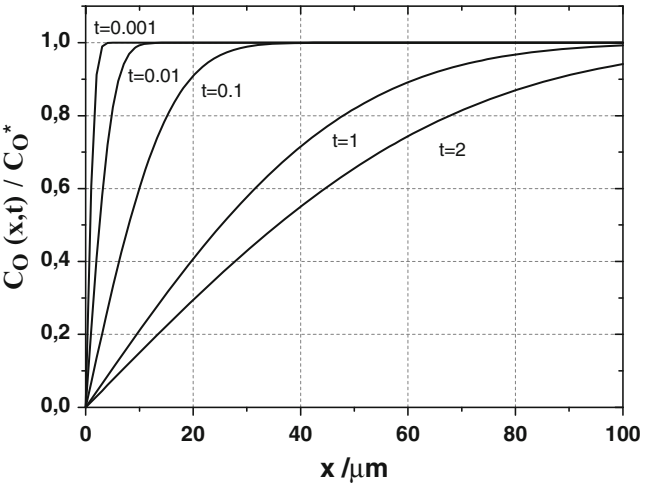

Fig. 15.2 Concentration profiles for a potential step experiments at different step times. Calculations refer to a species having $D_O = 7 \times 10^{-6}$ cm^2 s^{-1}

For a planar electrode, the solution is known as the Cottrell equation and predicts that the current is inversely proportional to $t^{1/2}$

$$i_t = \frac{nFAD_O^{\frac{1}{2}}C_O^*}{\pi^{\frac{1}{2}}t^{\frac{1}{2}}} \tag{15.6}$$

The reason for the current decay can be explained considering how the concentration profile of the reagent species, near to the electrode surface, varies with time. The concentration profiles are given by

$$C_O(x,t) = C_O^* erf\left[\frac{x}{2\sqrt{D_O t}}\right] \tag{15.7}$$

where *erf* is the error function. Figure 15.2 displays several plots of the normalized concentration C_O/C_O^* against distance for various times. It is evident that in the zone near the electrode, the concentration differs from that in the bulk and approaches the latter value asymptotically. It occurs at a distance from the electrode surface, and is defined diffusion layer thickness (δ). As is also evident from Fig. 15.2, δ spreads gradually into the solution as the time increases; the concentration gradient at the electrode surface decreases and overall the current decreases as the time lapses and, theoretically, falls to zero for $t \to \infty$.

The distance at which the species O can diffuse in time t can be predicted by $\delta = (D_O\, t)^{1/2}$ [1] and the distance from the electrode at which the diffusion layer thickness is completely contained is within about $6(D_O\, t)^{1/2}$.[3]

[1] In the literature, δ is also estimated as $(2D_O t)^{1/2}$ and $(\pi D_O t)^{1/2}$.

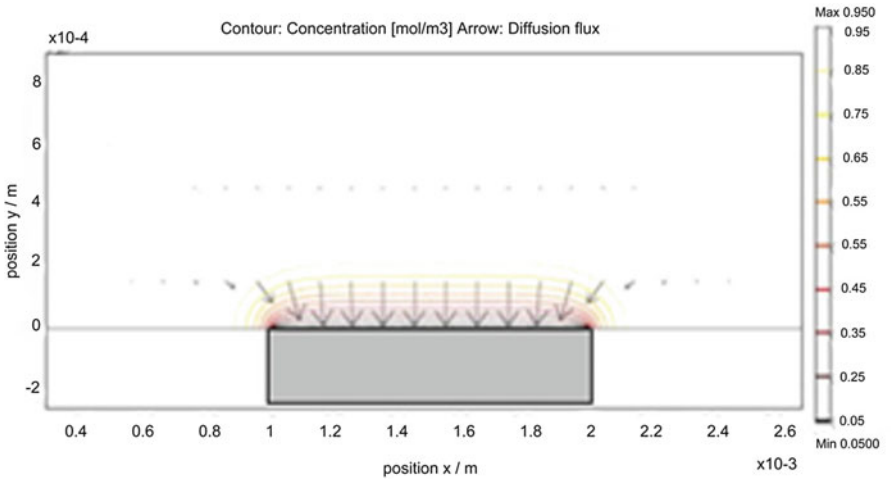

Fig. 15.3 Diffusion flux and concentration profiles at a conventional disk electrode 2 mm diameter. Simulated by the use of COMSOL Multiphysics 3.5

The conditions for planar diffusion are theoretically fulfilled only if the electrode surface is very large. In case of finite disk electrodes, edge effects arise and linear diffusion is no longer linear overall the electrode surface (Fig. 15.3). Diffusion also develops parallel to the electrode surface in the radial direction. However, if the radius of the disk electrode is large enough with respect to the diffusion layer thickness (as is the case of common employed disk electrode of millimeter size), edge effects can be neglected and Cottrell equation accurately accounts for the current profile at the electrode surface. These electrodes are nowadays called either conventional or macroelectrodes.[3–12]

Returning to a spherical electrode, the solution of the diffusion equation $T_{1,2}$ provides[3]

$$i(t) = \frac{nFAC_O^*\sqrt{D_O}}{\sqrt{\pi \cdot t}} + \frac{nFAD_OC_O^*}{r_0} \tag{15.8}$$

which contains both a time-dependent term and a time-independent term. Thus, contrary to the planar electrode, the diffusion current at a spherical electrode approaches a constant value for $t \to 0$. The time-dependent term is prevailing at short times, where the constant term contributes negligibly to the overall current, and Eq. (15.8) reduces to the Cottrell relationship (15.6). At long times, the transient term has decayed to a negligible value and the overall current is steady state and is given by the equation:

$$i = 4\pi nFD_OC_O^*r_0 \tag{15.9}$$

The reason for such behavior can be understood by considering the concentration profile that establishes to the surface of a sphere given by[3]

$$C_O(r,t) = C_O^* \left[1 - \frac{r_0}{r} erfc\left(\frac{r - r_0}{2\sqrt{D_O t}} \right) \right] \tag{15.10}$$

The main difference between the latter and Eq. (15.7) is the factor r_0/r, while $(r-r_0)$ is the distance from the electrode surface, similar to x for a planar electrode. When the diffusion layer is very thin, r is small compared to r_0; the linear and spherical diffusion situations are practically indistinguishable. On the other hand, when the diffusion layer grows and becomes much larger than r_0 (i.e., $(r-r_0) \ll 2(D_O t)^{1/2}$), it can be shown that the concentration profile is given by[3]

$$C_O(r,t) = C_O^*(1 - r_0/r)$$

and the concentration gradient at the electrode surface is proportional to C_O^*/r_0; this provides the steady-state current.

From a practical point of view, the use of Eq. (15.8), or one of its limiting forms, depends on the electrode size. In fact, linear diffusion describes adequately the mass transport at the electrode surface provided that the radius of the sphere is large enough and the time is relatively short. If, for instance, we consider the case of a hanging mercury electrode (i.e., an almost spherical electrode) 0.1 cm radius, immersed in a solution containing an electroactive species having a diffusion coefficient value of 1×10^{-5} cm^2 s^{-1}, Cottrell equation predicts, with 10 % accuracy, the current recorded within 3 s. For longer electrolysis times, the steady-state term starts to contribute significantly. Instead, the prevailing of the steady-state term for such large electrode would require much longer times, so that natural convection would prevent its fully achievement.[3] The achievement of both short-time and long-time limits at spherical electrodes is made possible with the use of MEs (*vide infra*).

The third type of electrode that involves only a single dimension of diffusion is the cylindrical electrode, and the diffusion equation is shown in Table 15.1 (equation $T_{1,3}$). Practical electrodes with such a geometry are made by fine metal or carbon wires connected to a conducting bigger wire with silver epoxy.[3, 8–11] Their behavior, therefore, falls within the category of MEs. Theoretical relationships for predicting current responses at such geometry will be considered in more detail in the MEs section.

15.3.2 Linear Sweep (LSV) and Cyclic Voltammetry (CV)

In voltammetry, the potential changes linearly with time (Fig. 15.4a), starting from an initial potential E_i (usually, where no electrode reaction occurs). Eventually, after reaching a potential E_λ, the sweep is reversed and the potential returns linearly to its initial value (Fig. 15.4b). Thus, in LSV or in the forward scan in CV, the potential at any time is given by $E(t) = E_i \pm v\,t$, where v is the sweep rate (or scan

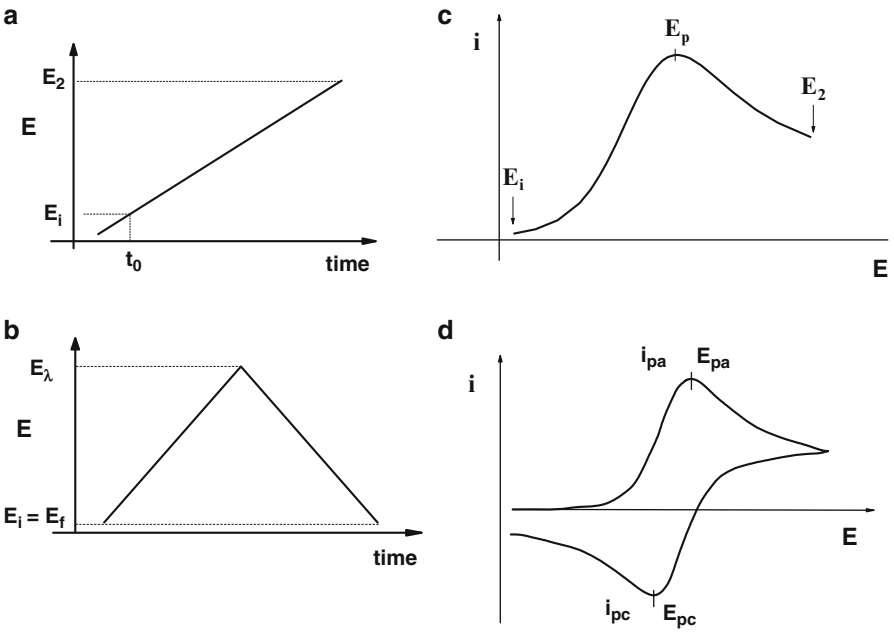

Fig. 15.4 Waveforms for (**a**) LSV and (**b**) CV; current against potential profiles for (**c**) LSV and (**d**) CV (for an oxidation process)

rate) in V s^{-1}. The experiment is considered for reaction (15.5), and it is assumed to be Nernstian (i.e., reversible) in character. For planar and spherical electrodes, the solution of the diffusion equations $T_{1,1}$ and $T_{1,2}$, with the appropriate boundary conditions and the applications of numerical methods,[3] provides the Eqs. (15.11) and (15.12), respectively:

$$i = nFAC_O^*(\pi D_O \sigma)^{1/2}\chi(\sigma t) \tag{15.11}$$

$$i = nFAC_O^*(\pi D_O \sigma)^{1/2}\chi(\sigma t) + \frac{nFAD_O C_O^* \phi(\sigma t)}{r_0} \tag{15.12}$$

where:

$\sigma = \left(\frac{nF}{RT}\right)v$; $\chi(\sigma t)$ and $\phi(\sigma t)$ are tabulated values.[3]

Equation (15.11) indicates that the current depends on $v^{1/2}$ (and consequently on time) in case of the planar electrode; whereas, again, for the spherical electrode, there are two terms: the first is the same as for the planar electrode and the second represents the spherical correction. For conventional spherical electrodes (i.e., hanging mercury electrodes) and values of v relatively large, the planar contribution is much larger than the spherical correction. Under these conditions the spherical

electrode can be consider planar. The current against potential curves for such cases under LSV and CV conditions is shown in Fig. 15.4, which displays the typical peak-shaped profiles both for the forward and backward scans.

The peak current of the LSV (or that of the forward scan in CV) is given by:

$$i_p = 0.4463\left(\frac{F^3}{RT}\right)^{1/2} n^{3/2} A D_O^{1/2} C_O^* v^{1/2} \tag{15.13}$$

and the backward (i_{pc}) to forward (i_{pa}) peak current ratio, i_{pc}/i_{pa}, is equal to 1 for a Nernstian wave with a stable product.

15.4 Diffusion at MEs

Microelectrodes, as mentioned in Introduction, are electrodes with characteristic dimensions on the micrometer or sub-micrometer scale.[4–15] An operational definition of ME has been recommended by IUPAC in 2000s in Pure and Applied Chemistry.[12] Practically, it includes any electrode with at least a linear dimension, called critical dimension, that falls in the micrometer and sub-micrometer size. Thus, microelectrodes can be of different geometries, and Fig. 15.5 shows schemes of some of those for which theoretical treatment exists and equations of current as a function of time or potential have been derived.

The experiments using MEs are similar to those described above in the previous section, which essentially hold for conventional or millimeter-sized electrodes. However, as an electrode is miniaturized to micrometer or even sub-micrometer size, semi-infinite planar diffusion gradually transforms into semi-infinite radial diffusion (Fig. 15.6). Longer experiments produce the same phenomenon. Because of the time-dependent change of the diffusion profile, the solid angle developed by the diffusion layer in front of the electrode increases and grows considerably relative to the electrode surface. For this reason, more electroactive species per unit of time and area reach the electrode surface with respect to the planar electrode. Moreover, the flux in and out of the volume eventually becomes stationary and the diffusion layer stops growing. This implies the achievement of a steady-state current at long times.[4–15] The time needed to reach a steady state depends, however, on the geometry and size of the microelectrode.

From the above qualitative considerations, it appears that the mass transport to microelectrodes, apart from a few cases, is complicated theoretically, and in the next sections, we describe the current-time and current-potential equations, which have been derived by using either analytical solutions or simulation procedures for MEs having the geometries depicted in the scheme of Fig. 15.5, which have been largely employed for practical applications. Detailed information on how MEs and NEs can be fabricated can be found in several reports and reviews.[9, 10, 13–16]

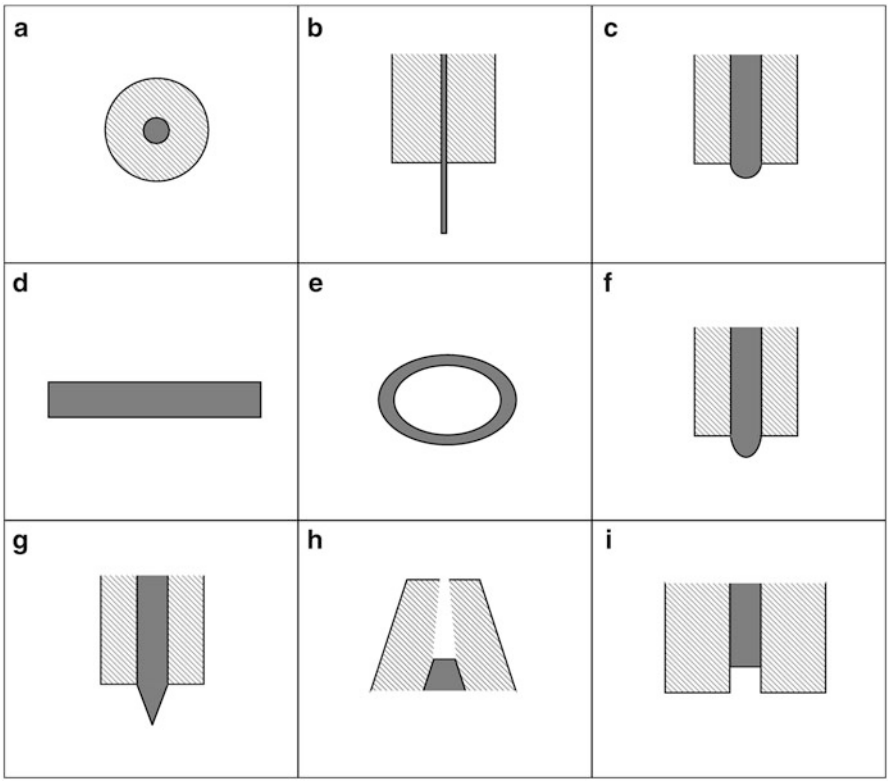

Fig. 15.5 Microelectrode configurations: (**a**) disk, (**b**) cylinder, (**c**) hemisphere, (**d**) band, (**e**) ring, (**f**) sphere cap, (**g**) cone, (**h**) nanopore, and (**i**) recessed microelectrode

15.4.1 Diffusion-Controlled Current-Time Responses for Application of a Potential Step

Spherical and hemispherical microelectrodes are the simplest cases, as the diffusion equation is $T_{1,2}$, i.e., same as that described for conventional spherical electrodes. Thus, the first term (i.e., the Cottrell equation) dominates at short times, where the diffusion layer is thin with respect to the electrode radius. At longer times, the second term dominates and the diffusion layer grows much larger than r_0.

Many applications of MEs are based on steady-state currents, and therefore Table 15.2 shows the equations that predict steady-state currents for both spherical and hemispherical MEs ($T_{2,2}$ and $T_{2,3}$, respectively). Moreover, an equation has been derived that allows establishing the time (t_ε) needed to achieve a steady state within a ε % closeness for a spherical ME[2]:

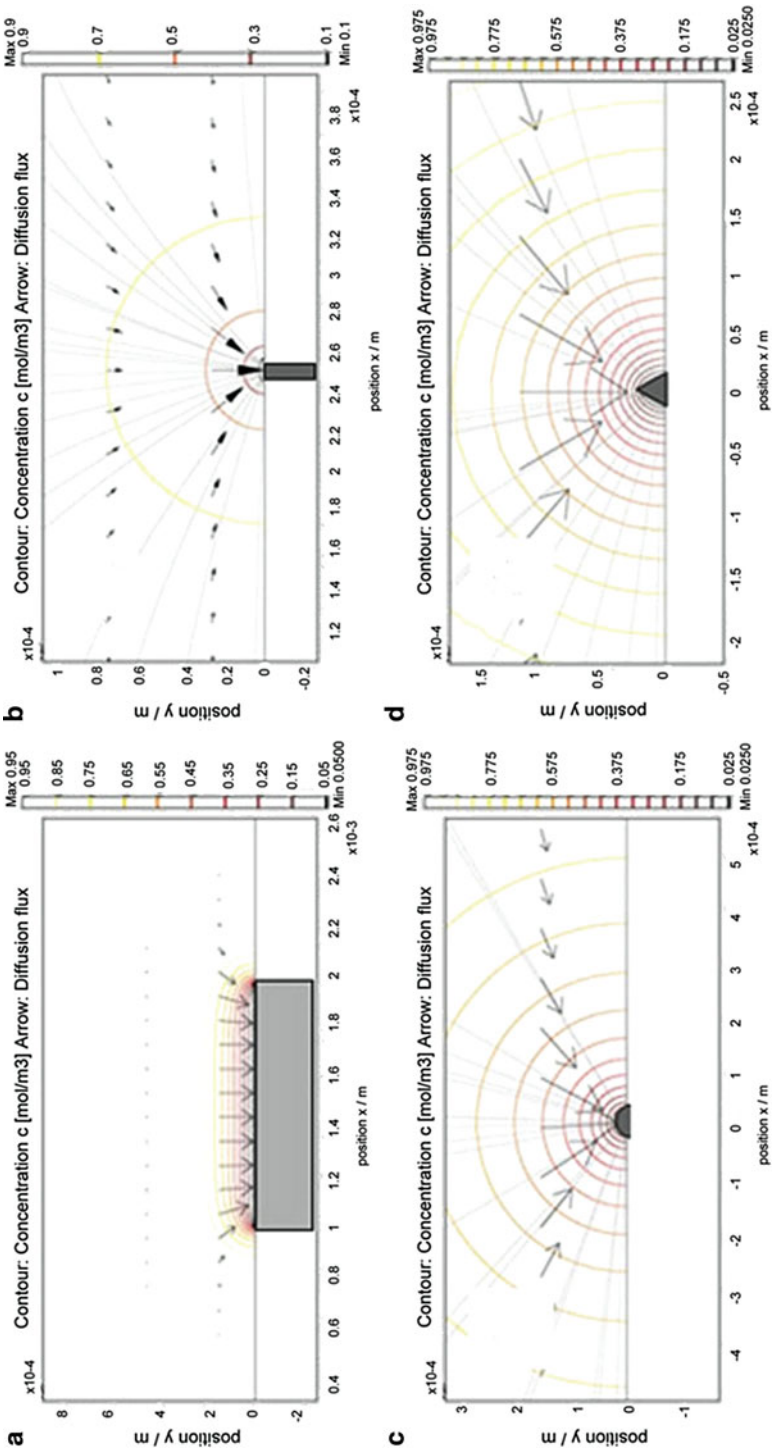

Fig. 15.6 Diffusion fields and concentration profiles at: (**a**) conventional and various microelectrodes, (**b**) disk, (**c**) hemisphere, and (**d**) cone. Simulated by the use of COMSOL Multiphysics 3.5

Table 15.2 Current-time and long-time equations for different geometries

Microelectrode geometry	Current-time equation		Long time	
Sphere, hemisphere	$i = \frac{nFAD_O^{1/2} \cdot C_O^*}{\pi^{1/2} t^{1/2}} + \frac{nFAD_O C_O^*}{r_0}$	$T_{2,1}$	$i = 4\pi nFD_O C_O^* r_O$	$T_{2,2}$
			$i = 2\pi nFD_O C_O^* r_O$	$T_{2,3}$
Microdisk	$i(\tau) = \frac{4nFAD_O C_O^*}{\pi \cdot a} f(\tau)$	$T_{2,4}$	$i = 4nFD_O C_O^* a$	$T_{2,8}$
	$\lim_{t \to 0} f(\tau) = \sqrt{\frac{\pi}{4\tau}} + \frac{\pi}{4} + \frac{3 \cdot \pi \cdot \tau}{2^{10}} + \ldots \quad \tau < 1$	$T_{2,5}$		
	$\lim_{t \to \infty} f(\tau) = 1 + \sqrt{\frac{16}{\pi^3 \cdot \tau}} + \ldots \quad \tau > 1$	$T_{2,6}$		
	$f(\tau) = 0.7854 + 0.8862 \cdot \tau^{-1/2} + 0.2146 \cdot e^{-0.7823 \cdot \tau^{-1/2}}$	$T_{2,7}$		
Cylinder	$i = \frac{nFAD_O C_O^*}{r_0} \left[\frac{2\exp(-0.05\pi^{1/2}\tau^{1/2})}{\pi^{1/2}\tau^{1/2}} + \frac{1}{\ln(5.2945 + 0.7493\tau^{1/2})} \right]$	$T_{2,9}$	$i = \frac{2nFAD_O C_O^*}{r_0 \ln(4D_O t / r_0^2)}$	$T_{2,11}$
	$\tau = 4D_O t / r_0^2$			
	$i = \frac{nFAD_O C_O^*}{r_0} \left[\frac{1}{\sqrt{\pi\theta}} + 0.422 - 0.0675\log(\theta) \pm 0.0058 \left[\log(\theta) - 1.47\right]^2 \right]$	$T_{2,10}$		
	$\theta = D_O t / r_0^2$			
Band	$i = nFD_O C_O^* l \left\{ (\pi\theta)^{-1/2} + 0.97 - 1.10\exp\left[\frac{-9.90}{\lvert\ln(12.37\theta)\rvert} \right] \right\}$	$T_{2,12}$	$i = \frac{2\pi nFAD_O C_O^*}{w \ln(64D_O t / w^2)}$	$T_{2,13}$
	$\theta = D_O t / w^2$			
Ring			$i = nFC_O^* D_O \frac{\pi(a+d)}{\ln 16(d+a)/(d-a)}$	$T_{2,14}$
Recessed electrode			$i = \frac{4\pi nFC_O^* D_O a^2}{4L + \pi a}$	$T_{2,15}$
Pore electrode			$i = 4nFaD_O C_O^* \left[\frac{(1 + (d/a)\tan\vartheta)}{(4d/a\pi) + (1 + (d/a)\tan\vartheta)} \right]$	$T_{2,16}$

Table 15.3 Estimate of the timescales where a pure Cottrell (a) behavior or a steady-state (b) response for various microsized spheres is attained

Diameter/μm	(a) Cottrell response	(b) Steady-state response
0.05	<2.5 ns	>0.4 ms
0.5	<0.25 ms	>40 ms
5	<25 μs	>4 s
50	<2.5 ms	>400 s

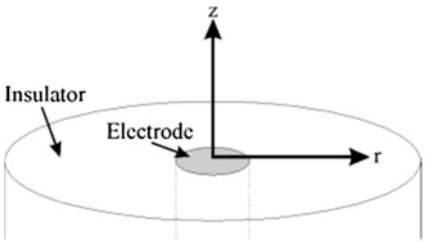

Fig. 15.7 Geometry of diffusion at a microdisk electrode

$$t_\varepsilon = 10^4 d^2/\left(\pi^3 D\varepsilon\right) \tag{15.14}$$

where d is the electrode diameter and D is the diffusion coefficient of the electroactive species. Table 15.3 shows examples of timescales estimated with an error of 5 % for various spherical MEs of different sizes, where the current follows the Cottrell or the steady-state behavior (Table 15.3).

The microdisk (Fig. 15.7) is the most popular electrode for practical applications, as it can be fabricated easily, for instance, by encapsulating carbon fibers or metal wires in glass capillaries and then polishing the tips to expose the microdisk surfaces.[9, 13] However, theory is complicated because diffusion occurs in two dimensions, either normal to the electrode plane (z-axis) or radially (r direction) with respect to the axis of symmetry (Fig. 15.7). As a consequence, the current density is not uniform across the electrode surface, it being larger at the edge. The diffusion equation for this geometry is written in cylindrical coordinates ($T_{1,4}$ in Table 15.1). This choice allows to account for the behavior of the disk ME either at short times, where the diffusion layer is almost parallel to the electrode surface, except to the edge, and z becomes the predominant variable, or at long times, where the diffusion layer grows to a hemi-circle, and it is accounted for the radial coordinate that becomes predominant.

The solution of equation $T_{1,4}$ is not easy and, therefore, approximate analytical solutions have been derived. The analytical expressions derived by Aoki and Osteryoung and, later on, by Shoup and Szabo (equations $T_{2,4–6}$ and $T_{2,7}$, respectively, in Table 15.2) are commonly employed for practical applications. They contain the parameter, τ, that can be regarded as a dimensionless time:

$$\tau = \frac{4D_O t}{a^2}$$

where a is the microdisk radius. The function $f(\tau)$ in equation $T_{2,4}$ assumes two forms for large (i.e., $\tau > 1$) or small (i.e., $\tau < 1$) values of τ and corresponds to long or short times, respectively. It was also verified that the two curves overlap in the domain: $0.82 < \tau < 1.44$. More convenient is the single expression $T_{2,7}$, which covers the entire range of τ. From these equations two limiting forms, as for spherical microelectrodes, can be derived for t (or τ) $\rightarrow 0$ and t (or τ) $\rightarrow \infty$. At short times equations $T_{2,5}$ and $T_{2,7}$, along with $T_{2,4}$, reduce to the Cottrell relationship, while at long times, equations $T_{2,5}$ and $T_{2,7}$, along with $T_{2,4}$, converge to a steady-state current given by $T_{2,8}$. It is useful to mention that the latter result for the microdisk was derived first by Saito by the method of the Bessel expansion.[17]

By analogy to the rigorous result for the spherical microelectrodes and in view of the same functional form, it is possible to estimate the current at microdisks, over a large timescale range, as the combination of the Cottrell and the steady-state terms:

$$i_t = \frac{nFAD_O^{\frac{1}{2}} \cdot C_O^*}{\pi^{\frac{1}{2}} t^{\frac{1}{2}}} + 4nFD_O C_O^* a \tag{15.15}$$

This approximate relationship is accurate at the short- and long-time regimes, while it deviates from the results reported by Aoki and Osteryoung by only a few percent at intermediate-time regimes. The largest error of 7 % occurs for electrolysis time corresponding at $\tau = 1$.

The cylindrical ME, as for the microsphere, involves only a single dimension of diffusion. The corresponding expression of Fick's second law is equation $T_{1,3}$ (in Table 15.1), and its solution, with the boundary conditions as those employed for the spherical electrode, provides an integral that can be evaluated analytically for short and long times, whereas it must be integrated numerically for intermediate times[18] (Table 15.2, $T_{2,10}$). This equation contains the parameter $\theta = Dt/r_0$ and is valid within 1 % error for $\theta < 10^6$. The $\pm$ in $T_{2,10}$ denotes + for $log(\theta) \geq 1.47$ and − for $log(\theta) < 1.47$.[18] A more practical approximate equation, which is valid within 1.3 % error at any time, has also been derived (equation $T_{2,9}$ in Table 15.2).[19] This equation contains the parameter $\tau = 4Dt/r_0^2$ and, as it occurs for a sphere, it displays two limiting situations. In the short-time limit, $T_{2,9}$ reduces to the Cottrell expression, as in this situation, the diffusion layer thickness is small compared to the curvature of the electrode. In particular, for τ not larger than circa 0.01, the diffusion layer is not greater than ~10 % of r_0. In the long-time limit, the current can be predicted by equation $T_{2,11}$, which still contains the parameter τ. Therefore, it is not a steady state. However, the current shows a logarithmic dependence of the time and declines rather slowly, so that it assumes a quasi-steady state.

A band microelectrode is a two-dimensional diffusion system in which the length of the electrode is very much larger than the width. The coordinate system used to treat the diffusion problem at this geometry is shown in Fig. 15.8 and

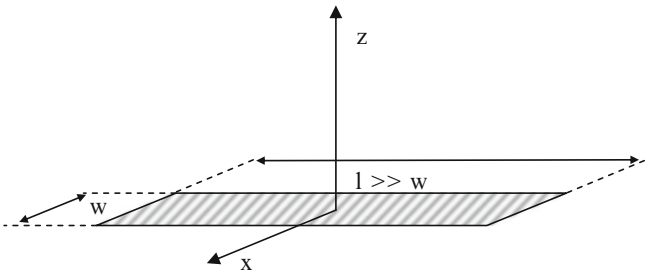

Fig. 15.8 Geometry of diffusion at a microband

highlights that diffusion essentially occurs only along the *x*- and *z*-axes. This, as for the microdisks, causes the current density to be distributed nonuniformly and is especially infinite at the edge of the electrode.

Analytical expressions for the current-time curves have been derived for long and short times.[11] These are in the form of a series expansion, difficult to handle. A more convenient relationship that represents the two expansions as a closed form has also been derived (Table 15.2, $T_{2,12}$). It contains the dimensionless parameter $\theta = Dt/w^2$, where w is the band width and is valid for $\theta < 10^8$.[20, 21] Again, as it can now be expected, at short times, the current converges to the Cottrell equation; at long times the current approaches a limiting form, which, as for the cylindrical electrodes, contains the logarithmic dependence on t. Thus, also the band ME does not provide a true steady-state current at long times. An approximate, but simple, relationship for the long-time current has been derived by applying to the band ME an analogous treatment as for a hemicylinder.[19] In particular, it was noted that the current at a band of length l and width w was identical to that of a hemicylinder of length l and basal radius $r_0 = w/4$. This correspondence has provided the relationship $T_{2,13}$ included in Table 15.2.

15.4.2 Mass Transfer Coefficient

As it has been discussed above, MEs display common features in the response of a potential step experiment, regardless of the geometry. At short times, where the diffusion layer is thin compared to the critical dimension of the ME, the current can be predicted by the Cottrell equation and planar diffusion is prevailing. At long times, where the diffusion layer is large compared to the critical dimension, the current is steady state or quasi-steady state. Under the latter conditions, the current at the MEs is related to the mass transport coefficient, m_O, through

$$i = nFm_O C_O^*$$

Table 15.4 Mass transfer coefficient for some microelectrodes of different geometry

Band		Cylinder		Disk		Hemisphere		Sphere	
$\frac{2\pi D_O}{wln(64D_O\tau/w^2)}$	$T_{4,1}$	$\frac{2D_O}{r_0 ln\tau}$	$T_{4,2}$	$\frac{4D_O}{\pi a}$	$T_{4,3}$	$\frac{D_O}{r_0}$	$T_{4,4}$	$\frac{D_O}{r_0}$	$T_{4,5}$

The mass transfer coefficient m_O represents the diffusion rate at the electrode surface and depends on the geometry as is shown in Table 15.4 for some of the MEs considered above. Thus, as can be easily inferred from the latter in the table, for extremely small electrodes, as is the case of NEs, the diffusion rate, and consequently, the current density, can be extraordinarily high.

15.4.3 Current-Potential Responses at MEs

MEs in LSV or CV produce the same phenomena as in the potential step experiments. In these techniques, the transition from planar to radial diffusion, for a given ME and electrode geometry, is achieved by reducing the scan rate. The faster the transition, the smaller the characteristic length of the ME. Figure 15.9 shows, for instance, a series of CVs obtained at a microdisk electrode at different scan rates. It is evident that at high v, the CV displays the peak-shaped voltammogram as for planar electrodes; as the scan rate decreases, the CV becomes sigmoidal with the forward and backward curves retracing one another. This is caused by the formation of a stationary diffusion layer that is due to the high diffusion mass transport. The current at the stationary state is essentially independent of scan rate and the diffusion-limited current corresponds to that evaluated by a large potential step experiment described above. Theoretical modeling of the current-potential profiles at microelectrodes is usually difficult, and because of the complexity of the task, numerical solutions or digital simulation procedures have often been used. The only exception is the case of the spherical microelectrodes for which Eq. (15.12) (or $T_{2,1}$ in Table 15.2) can be applied.[3]

For disk,[22] cylinder,[23] and band[24] microelectrode geometries, theoretical expressions of the voltammograms have been derived as a function of the parameter, p, which contains the characteristic dimension of the specific ME. Since the peak or maximum current characterizes quantitatively the voltammograms, relevant expressions are given and shown in Table 15.5. In general, for large values of p, the equations $T_{5,1–3}$ are identical with the equation for planar diffusion. For small values of p, the latter equations approach those for the steady-state current displayed in Table 15.2 for the corresponding ME geometry.

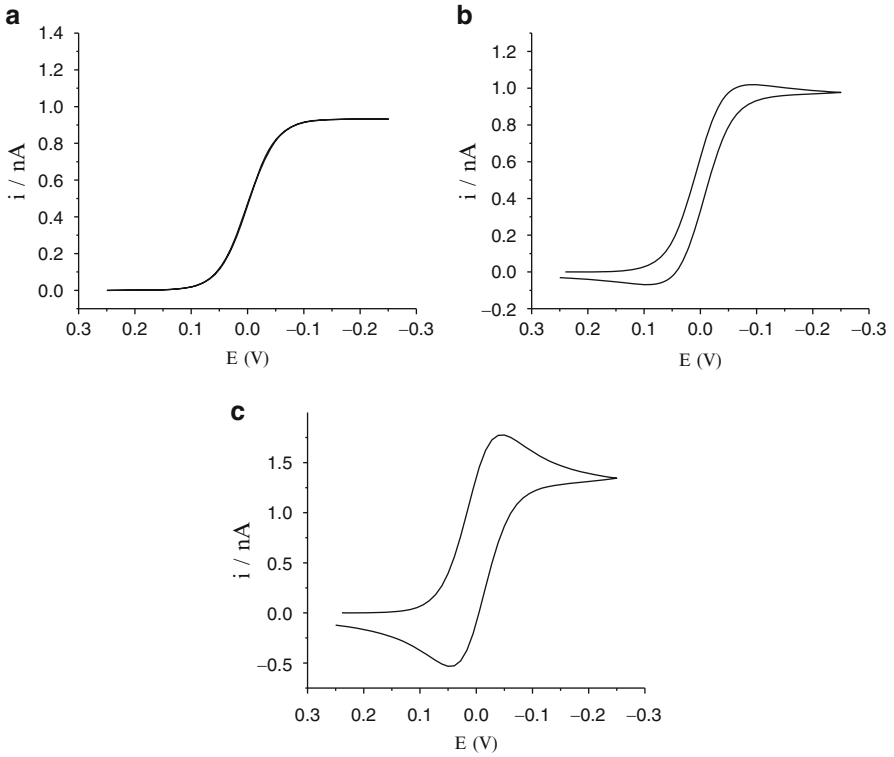

Fig. 15.9 Simulated CVs for a microdisk 4 μm radius at different scan rates: (**a**) $1 mVs^{-1}$; (**b**) $200\ mVs^{-1}$; (**c**) $2\ Vs^{-1}$

Table 15.5 Voltammetric peak current for different electrode geometries

Electrode geometry	Peak (or maximum) current	
Microdisk	$i = 4nFD_O C_O^* a \left[0.34\exp(-0.66p) + 0.66 - 0.13\exp\left(-\frac{11}{p}\right) + 0.351p\right]$ $p = (nFa^2 v/RTD_O)^{1/2}$	$T_{5,1}$
Microcylinder	$i = \frac{n^2F^2C_O^* A r_0 v}{RT}\left(\frac{0.446}{p} + \frac{0.335}{p^{1.85}}\right)$ $p = (nFr_0^2 v/RTD_O)^{1/2}$	$T_{5,2}$
Microband	$i = nFC_O^* D_O \left[0.439p + 0.713p^{0.108} + \frac{0.614p}{1 + 10.9p^2}\right]$ $p = (nFw^2 v/RTD_O)^{1/2}$	$T_{5,3}$

15.4.4 Steady-State Current at Miscellaneous ME

In this section the relationships for steady-state current of various microelectrode of more complicated shapes are briefly described.

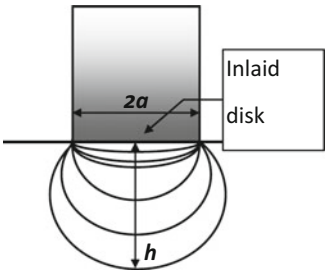

Fig. 15.10 Schematic view of a sphere-cap family of microelectrodes

15.4.4.1 Sphere Caps

Sphere caps are a family of microelectrodes that share a common basal plane of radius a and differ for the sphere-cap heights h (Fig. 15.10). A general expression that predicts the steady-state limiting current has been derived by numerical results and assumes the following form[25–27]:

$$i_d = \alpha(a,h)nFDC_O^* a \tag{15.16}$$

where $\alpha(a,h)$ is a shape-dependent factor that can be calculated by[25–27]

$$\alpha(a,h) = 2\pi \int_0^\infty \frac{\cosh[x\arctan(h/a)]}{\cosh[x\arctan(a/h)]\cosh(\pi x/2)}dx \tag{15.17}$$

Because the latter equation is not easy to handle, an algebraic equation that fits Eq. (15.17) with good accuracy was sought. It was found the following simple relationship[28]:

$$\alpha(a,h) = 4 + \ln 10\left(\frac{h}{a}\right)^{1.36} \tag{15.18}$$

Equations (15.17) and (15.18) assume the values of 4 and 2π for the cases $h = 0$ (i.e., a microdisk) and $h = a$ (i.e., a hemisphere)[25–27], and, therefore, the steady-state limiting current exactly acquires the forms $T_{2,8}$ and $T_{2,3}$ for the microdisk and microhemisphere, respectively.

These kinds of microelectrodes can be prepared by cathodic deposition of mercury onto the surface of metal microdisks that are wettable by mercury. Details on their preparation and characterization can be found in references (25, 28).

15.4.4.2 Microring

The ring electrode can be fabricated as a cross section of an insulating rod on which metal is deposited in ultrathin film. The ring microelectrode can also achieve a

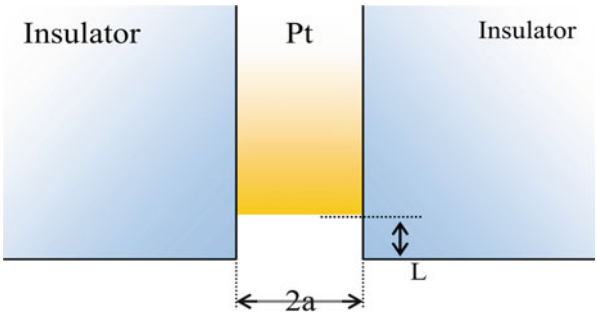

Fig. 15.11 Schematic view of a recessed microelectrode

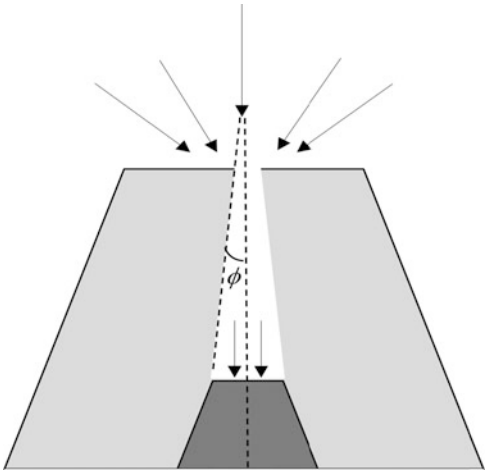

Fig. 15.12 Schematic view of a nanopore electrode

steady state and supports large average current densities. However, as for the disk, it is characterized by nonuniform current density.[29–31] The steady-state current at the ring with an inner radius a and outer radius d is given by equation $T_{2,14}$ in Table 15.2. Since the current varies slightly with the thickness of the ring, it depends almost on the radii rather than on the electrode area.

15.4.4.3 Recessed Microelectrodes and Nanopore Electrodes

In the recessed electrode, the active surface is located at the bottom of a hole. Simple geometry of the electrode is a disk as is shown in Fig. 15.11. These electrodes can be fabricated by etching the metal wires. The steady-state current for such geometry is expressed by equation $T_{2,15}$.[32]

A geometry that is somewhat similar to a recessed ME is that of the nanopore electrode (Fig. 15.12). This electrode geometry is characterized by the small pore orifice, whose radius, a, can be varied between 5 nm and 1 μm; the pore depth, d; and the half-cone angle ϕ. An approximate analytical expression for the steady-state limiting current is given by equation $T_{2,16}$ in Table 15.2.[33]

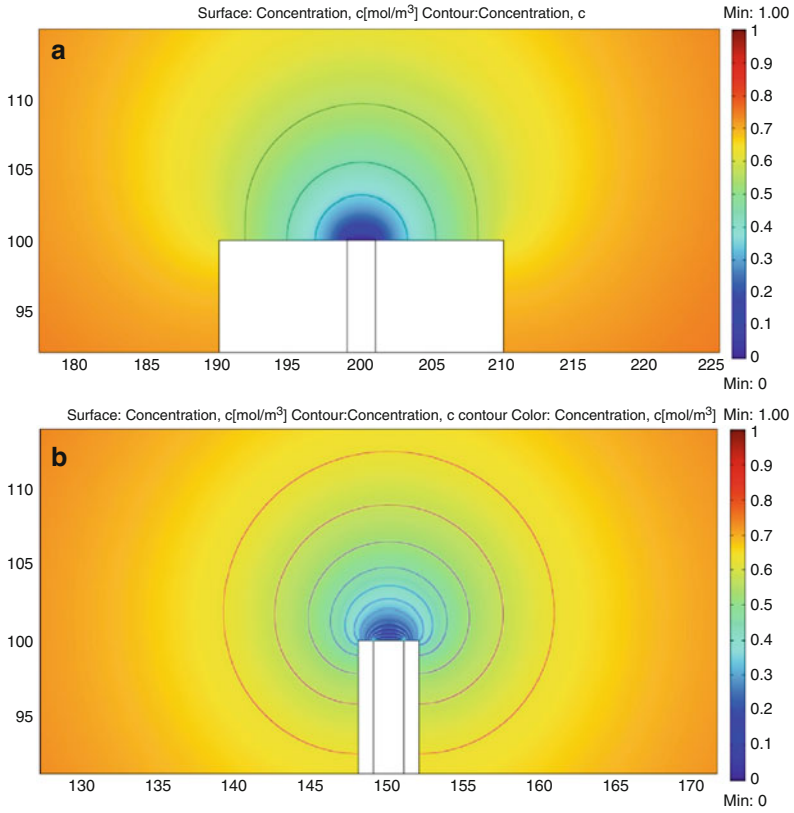

Fig. 15.13 Diffusion fields and concentration profiles at: (**a**) disk microelectrode RG → ∞; (**b**) RG → 1. Simulated by the use of COMSOL Multiphysics 3.5

15.4.4.4 Microelectrodes with Thin Shields

The interest for microelectrodes in which the insulating shields is of thickness comparable to the electrode radius is largely driven by the use of microelectrodes as tips in scanning electrochemical microscopy (SECM).[34, 35] One of the characteristic features of a thin-shielded microelectrode (TSM), with respect to microelectrodes that rest on an infinite insulating plane (as those previously described), is that, on the timescale of standard voltammetric measurements, the radial diffusion is also established behind the plane of the electrode and shield (for instance, contrasts the case of a microdisk in Fig. 15.13). Under these conditions, the flux, and consequently the current, is enhanced to an extent that depends on the relative size of insulating shield and electrode radius (normally referred to as *RG*).

Table 15.6 Steady-state limiting equations for microdisk electrodes with thin shields

Equation	Reference	I_{ss} for RG → *1*
$I_{ss}/I_l = 1.000 + 0.234\ (RG)^{-1} + 0.255\ (RG)^{-2}$	[39]	1.489
$I_{ss}/I_l = 1.000 + 0.379\ (RG)^{2.342}]$	[40]	1.379
$I_{ss}/I_l = 1.000 + 0.1380\ (RG - 0.6723)^{-0.8686}$	[38]	1.364

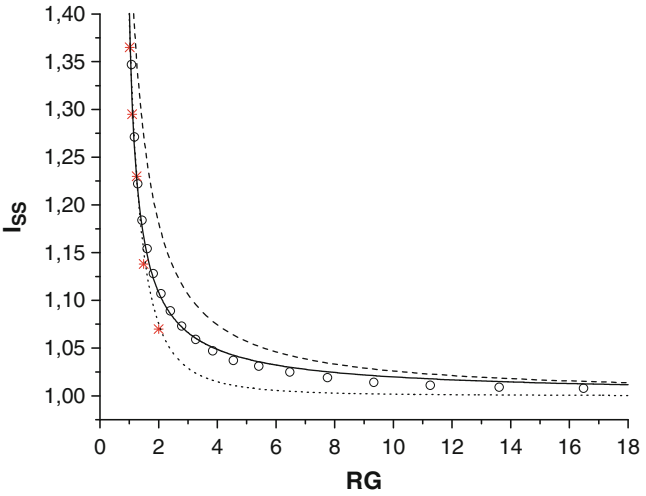

Fig. 15.14 Current against RG plot for a disk TMS: (*dashed lines*) from Ref. (39), (*dotted lines*) from Ref. (40), (*continuous line*) from Ref. (38), (*asterisk*) calculated from Ref. (36), (*open circle*) simulated from Ref. (41)

Equations for the steady-state limiting currents for such geometry are described in this section for the case of the disk (Fig. 15.5a), sphere caps (Fig. 15.5f), and cone (Fig. 15.5g).

Shoup and Szabo were the first to demonstrate, from a theoretical point of view, that at TSMs diffusion from behind the plane of the electrode enhances the flux to the inlaid disk.[36] This has also been confirmed by other researchers, who employed different digital simulation procedures to obtain either steady-state limiting currents[37, 38] or cyclic voltammograms[39] for TSMs with a range of *RG*. From the simulation data, approximate analytical expressions for the steady-state limiting current (i_{ss}) as a function of *RG* have also been derived.[38–41] Table 15.6 summarizes such equations (in a dimensionless form, i.e., $I_{ss} = i_{ss}/i_d$) and the limiting current values calculated for $RG \rightarrow 1$, while Fig. 15.14 displays either the graphical form of the latter equations over a wide *RG* range or currents at discrete *RG* values (36).

For the sphere caps and cone geometries, more complex equations apply. The diffusion problems to these geometries have been addressed by digital simulations, and, therefore, only approximate solutions have been provided. Figure 15.15 shows the parameters involved in the sphere-cap electrode. A general equation that links all parameters involved in this geometry is[41]

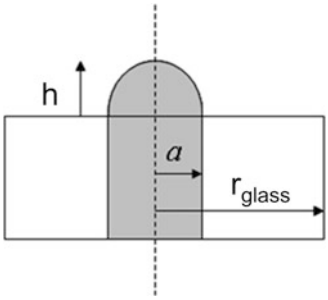

Fig. 15.15 Scheme of a sphere-cap geometry, $RG = r_{glass}/a$

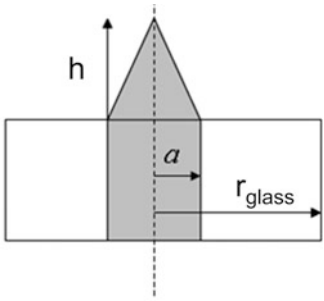

Fig. 15.16 Scheme of a cone geometry. $RG = r_{glass}/a$

$$I_{ss}^{sph} = \frac{1}{4}\Big[4 + 0.5780(RG - 0.6734)^{-0.8348} + \\ + \left(2.2832 + 9.3279(RG + 1.0321)^{-2-2979}\right) \cdot \left(\frac{h^{sph}}{a}\right)^{1.3590}\Big] \tag{15.19}$$

where

$$I_{ss}^{sph} = \frac{i_{ss}}{i_d} \tag{15.20}$$

and i_d stands for steady-state limiting current at a microdisk (i.e., equation $T_{2,8}$ in Table 15.2)

For the micro-cone (see scheme of the geometry in Fig. 15.16), the following relationship has been derived[38]:

$$I_{ss}{}^{cone} = A + B(RG - C)^D \tag{15.21}$$

where the parameters A, B, C, and D are numerical constants which depend on the h/a ratio, as indicated in the Table 15.7.

Table 15.7 Numerical constants corresponding to the analytical equation (15.21)

	$h^{cone}/a = 0.5$	$h^{cone}/a = 1$	$h^{cone}/a = 2$	$h^{cone}/a = 3$
A	1.1270	1.2979	1.6769	2.0585
B	0.1972	0.2795	0.5240	0.8910
C	0.5667	0.4506	0.1794	−0.1900
D	−0.9025	−0.9436	−0.9857	−1.0280

15.5 Applications of Microelectrodes

The unique properties of microelectrodes such as low ohmic drop, high faradaic to capacitive current ratios, rapid achievement of steady-state currents, requirements of only two-electrode electrochemical cells, and small volume samples[4–10, 42–65] are exploited in many fields, including environmental,[56, 57] food,[58] biomedical,[59–61] and material science areas.[62]

In electroanalysis, the majority of measurements with microelectrodes are taken under steady-state conditions by using either chronoamperometry (CA), linear sweep (LSV), or cyclic voltammetry (CV).[13–15, 17] Moreover, to enhance sensitivity in the measurements, fast-scan voltammetry (FSV)[64–68] or accumulation of analytes onto the electrode surface is also performed in conjunction with stripping analysis (SA).[62, 69, 70] FSV has largely been developed for biological applications[61, 64, 65] and employs scan rates up to kV s^{-1}. FSV is also used for the detection of various anions and cations on sub-millisecond timescales.[50, 66–68]

SA is probably one of the fields where microelectrodes find the largest number of applications.[42, 45–47, 64, 68–70] With this regard, the enhanced mass transport to the microelectrode surface by diffusion can obviate, in general, the need for convective mass transport during the pre-concentration step before stripping, while making current responses less affected by convective forces in flowing systems.[62] In fact, in quiescent solutions, a steady-state current is established in a relatively short time for microelectrodes with disk, shrouded hemisphere, and sphere-cap geometries.[7–9, 12] As is illustrated in the previous sections, at microelectrodes which are not small enough in all their dimensions, as is the case for cylinders and bands, the current response attains only a quasi-steady state, as the equations for their currents contain time-dependent terms, even at long times.[7–9, 12] The mass transport properties need to be considered when optimizing analytical procedures in order to achieve the best performance in terms of reproducibility and pre-concentration efficiency for trace element analysis.[62] Natural convection, which may arise during relatively lengthy pre-concentration step experiments, does not affect the stripping responses at disk and sphere-cap microelectrodes[62], whereas some effects were observed with microwires.[62]

Because ohmic drop has little influence on voltammetric responses, additional supporting electrolytes in the solutions are often unnecessary.[7–9, 12, 71–77] This largely avoids contamination of real samples with external chemicals when

ultra-trace element analysis has to be performed thereby leaving existing chemical equilibria unaltered. Therefore, direct measurements of low-ionic-strength samples or resistive media and speciation measurements can be performed straightforwardly without the need for pretreatment.[71, 72]

The lack of sufficient electrolyte in the media, however, makes the dependence of current on the concentration of electroactive species nonlinear, and the interpretation of the results requires that the migrational component in the transport be considered[7]; several reports and reviews deal with the theoretical problems related to the modeling of steady-state voltammograms at microelectrodes without or with dilute supporting electrolyte.[74–78] Fundamental studies describing the combined effects of diffusion and migration at microelectrodes have provided greater understanding and facilitated the prediction of amperometric experimental responses in complex systems such as solutions of polyelectrolytes, large polymer molecules with one or more ionic groups per monomer unit, colloidal suspensions, and polymeric gels.[71] Moreover, migration coupled with homogenous equilibrium and voltammetry in undiluted liquid organic substances has also been investigated from both a theoretical and experimental point of view.[71, 76–78]

List of Symbols (not specified in the text)

A	Area
D_i	Diffusion coefficient of the species (i)
erfc	Error inverse function
F	Faraday constant
n	Stoichiometric number of electrons involved in an electrode reaction
R	Gas constant
Z_i	Charge on species i
∇	Vector operator
ϕ	Electrostatic potential

References

1. Bard AJ, Zoski CG (2000) Voltammetry retrospective. Anal Chem 72:346A–352A
2. Bond AM, Oldham KB, Zoski CG (1989) Steady-state voltammetry. Anal Chim Acta 216:177–230
3. Bard AJ, Faulkner LR (2001) Electrochemical methods. Fundamentals and applications. Wiley, New York, NY
4. Dayton MA, Brown JC, Stutts KJ, Wightman RM (1980) Faradaic electrochemistry at microvoltammetric electrodes. Anal Chem 52:946–950
5. Wightman RM (1981) Microvoltammetric electrodes. Anal Chem 53:1125A–1134A

6. Bond AB, Fleischmann M, Robinson J (1984) The construction and behavior of ultramicroelectrodes – investigations of novel electrochemical systems. J Electrochem Soc 131:C109–C109
7. Deakin MR, Wipf D, Wightman RM (1986) Ultramicroelectrodes. J Electrochem Soc 133: C135–C135
8. Fleischmann M, Pons S, Rolison DR, Schmidt PP (1987) Ultramicroelectrodes. Datatech Systems Inc., Morganton, NC, p 363
9. Montenegro MI, Queirós MA, Daschbach JL (1991) Microelectrodes: theory and applications. Kluwer, The Netherlands
10. Heinze J (1993) Ultramicroelectrodes in electrochemistry. Angew Chem Int Ed Engl 32:1268–1288
11. Aoki K (1993) Theory of ultramicroelectrodes. Electroanalysis 5:627–639
12. Stulik K, Amatore C, Holub K, Marecek V, Kutner W (2000) Microelectrodes. Definitions, characterization, and applications (technical report). Pure Appl Chem 72:1483–1492
13. Zoski CG (2002) Ultramicroelectrodes: design, fabrication, and characterization. Electroanalysis 14:1041–1051
14. Arrigan DWM (2004) Nanoelectrodes, nanoelectrode arrays and their applications. Analyst 129:1157–1165
15. Oja SM, Wood M, Zhang B (2013) Nanoscale electrochemistry. Anal Chem 85:473–486
16. Forster RG, Keyes TE (2007) Ultramicroelectrodes. In: Zoski CG (ed) Handbook of electrochemistry, cap. 6, Elsevier, Amsterdam
17. Saito Y (1968) Theoretical study on the diffusion current at the stationary electrode of circular and narrow band types. Rev Polarogr 15:177–187
18. Aoki K, Honda K, Tokuda K, Matsuda H (1985) Voltammetry at microcylinder electrodes. Part (II): chronoamperometry. J Electroanal Chem 186:79–86
19. Szabo A, Cope DK, Tallan DE, Kovack PM, Wightman RM (1987) Chronoamperometric current at hemicylinder and band microelectrodes: theory and experiments. J Electroanal Chem 217:417–423
20. Aoki K, Honda K, Tokuda K, Matsuda H (1987) Derivation of an approximate equation for chronoamperometric curves at microband electrodes and its experimental verification. J Electroanal Chem 230:61–67
21. Coen S, Cope DK, Tallan DE (1986) Diffusion current at a band electrode by an integral equation method. J Electroanal Chem 215:29–48
22. Aoki K, Akimoto K, Tokuda K, Osteryoung J (1984) Linear sweep voltammetry at very small stationary disk electrodes. J Electroanal Chem 171:219–230
23. Aoki K, Honda K, Tokuda K, Matsuda K (1985) Voltammetry at microcylinder electrodes: part I. Linear sweep voltammetry. J Electroanal Chem 182:267–279
24. Aoki K, Tokuda K (1987) Linear sweep voltammetry at microband electrodes. J Electroanal Chem 237:163–170
25. Baldo MA, Daniele S, Corbetta M, Mazzocchin GA (1995) Performance of platinum-based spherical mercury microelectrodes in cyclic voltammetry and stripping analysis. Electroanalysis 7:980–986
26. Myland JC, Oldham KB (1990) Diffusion-limited currents at hemispheroidal microelectrode. J Electroanal Chem 288:1–14
27. Alfred LCR, Oldham KB (1996) Steady-state currents at sphere-cap microelectrodes and electrodes of related geometry. J Phys Chem 100:2170–2177
28. Daniele S, Bragato C, Baldo MA, Mazzocchin GA (2002) Effects of mercury ion concentration on the preparation of mercury deposits on platinum microdisk electrodes. Ann Chim 92:203–215
29. Szabo AJ (1987) Theory of the current at microelectrodes: application to ring electrodes. J Phys Chem 91:3108–3111
30. Fleishmann M, Pons S (1987) The behavior of microdisk and microring electrodes. J Electroanal Chem 222:107–115

31. Cope DK, Scott CH, Tallman DE (1990) Transient behavior at planar microelectrodes: diffusion current at ring electrodes by the integral equation method. J Electroanal Chem 285:49–69
32. Bond AM, Luscombe D, Oldham KB, Zoski CG (1988) A comparison of the chronoamperometric response at inlaid and recessed disc microelectrodes. J Electroanal Chem 249:1–14
33. Zhang B, Zhang Y, White HS (2006) Steady-state voltammetric response of the nanopore electrode. Anal Chem 78:477–483
34. Bard AJ, Fan FRF, Mirkin MV (1994) Scanning electrochemical microscopy. In: Bard AJ, Rubistein I (eds) Electroanalytical chemistry, Marcel Dekker, New York, 18:243–373
35. Bard AJ, Mirkin MV (eds) (2001) Scanning electrochemical microscopy. Marcel Dekker, NewYork
36. Shoup D, Szabo A (1984) Influence of insulation geometry on the current at microdisk electrodes. J Electroanal Chem 160:27–31
37. Amphlett JL, Denuault G (1998) Scanning electrochemical microscopy (SECM): an investigation of the effects of tip geometry on amperometric tip response. J Phys Chem B 102:9946–9951
38. Zoski CG, Mirkin MV (2002) Steady-state limiting currents at finite conical microelectrodes. Anal Chem 74:1986–1992
39. Fang Y, Leddy J (1995) Cyclic voltammetric responses for inlaid microdisks with shields of thickness comparable to the electrode radius: a simulation of reversible electrode kinetics. Anal Chem 67:1259–1270
40. Zhao G, Giolando DM, Kirchoff JR (1995) Chemical vapor deposition fabrication and characterization of silica-coated carbon fiber ultramicroelectrodes. Anal Chem 67:2592–2598
41. Daniele S, Ciani I, Batistel D (2008) Effect of the insulating shield thickness on the steady-state diffusion-limiting current of sphere cap microelectrodes. Anal Chem 80:253–259
42. Wehmeyer KR, Wightman RM (1985) Cyclic voltammetry and anodic stripping voltammetry with mercury ultramicroelectrodes. Anal Chem 57:1989–1993
43. Li LJ, Fleischmann M, Peter LM (1987) *In-situ* measurements of Pb^{2+} concentration in the lead-acid battery using mercury ultramicroelectrodes. Electrochim Acta 32:1585–1587
44. Daniele S, Baldo MA, Ugo P, Mazzocchin GA (1989) Determination of heavy metals in real samples by anodic strypping voltammetry with mercury microelectrodes. Part 1. Application to wine. Anal Chim Acta 219:9–18
45. Daniele S, Baldo MA, Ugo P, Mazzocchin GA (1989) Determination of heavy metals in real samples by anodic stripping voltammetry with mercury microelectrodes. Part 2. Application to rain and sea waters. Anal Chim Acta 219:19–25
46. Daniele S, Baldo MA, Ugo P, Mazzocchin GA (1990) Voltammetric probe of milk samples by using a platinum microelectrode. Anal Chim Acta 238:357–366
47. Wojciechowski M, Balcerzak J (1991) Square-wave anodic stripping voltammetry of lead and cadmium at cylindrical graphite fiber microelectrodes with in situ plated mercury films. Anal Chim Acta 249:433–445
48. Stulik K (1989) Some aspects of flow electroanalysis. Analyst 114:1519–1525
49. La Course WR, Modi SJ (2005) Microelectrode applications of pulsed electrochemical detection. Electroanalysis 17:1141–1152
50. Harman AR, Baranski AS (1990) Fast cathodic stripping analysis with ultramicroelectrodes. Anal Chim Acta 239:35–44
51. Craston DH, Jones CP, Williams DE (1991) Microband electrodes fabricated by screen printing processes: applications in electroanalysis. Talanta 38:17–26
52. Farrington AM, Jagota N, Slater JM (1994) Simple solid wire microdisk electrodes for the determination of vitamin-C in fruit juices. Analyst 119:233–238
53. Bixler JW, Bond AM (1986) Amperometric detection of picomole samples in a microdisk electrochemical flow-jet cell with dilute supporting electrolyte. Anal Chem 58:2859–2863
54. Davis F, Higson SPJ (2013) Arrays of microelectrodes: technologies for environmental investigations. Environ Sci Process Impacts 15:1477–1489

55. Tan F, Metters JP, Banks CE (2013) Electroanalytical applications of screen printed microelectrode arrays. Sensor Actuator B 181:454–462
56. Pecková K, Barek J (2011) Boron doped diamond microelectrodes and microelectrode arrays in organic electrochemistry. Curr Org Chem 15:3014–3028
57. Marinesco S, Frey O (2013) Microelectrode designs for oxidase-based biosensors. NeuroMethods 80:3–25
58. Sun X, Luo Y, Liao F, Lu W, Chang G (2011) Novel nanotextured microelectrodes: electrodeposition-based fabrication and their application to ultrasensitive nucleic acid detection. Electrochim Acta 56:2832–2836
59. Ordeig O, Del Campo J, Muñoz FX, Banks CE, Compton RG (2007) Electroanalysis utilizing amperometric microdisk electrode arrays. Electroanalysis 19:1973–1986
60. Li CM, Hu W (2013) Electroanalysis in micro- and nano-scales. J Electroanal Chem 688:20–31
61. Bunin MA, Wightman RM (1998) Quantitative evaluation of 5-hydroxytryptamine (serotonin) neuronal release and uptake: an investigation of extrasynaptic transmission. J Neurosci 18:4854–4860
62. Daniele S, Baldo MA, Bragato C (2008) Recent developments in stripping analysis. Curr Anal Chem 4:215–228
63. Molina A, Laborda E, Martínez-Ortiz F, Bradley DF, Schiffrin DJ, Compton RG (2011) Comparison between double pulse and multipulse differential techniques. J Electroanal Chem 659:12–24
64. Takmakov P, McKinney CJ, Carelli RM, Wightman RM (2011) Instrumentation for fast-scan cyclic voltammetry combined with electrophysiology for behavioral experiments in freely moving animals. Rev Sci Instrum 82 art 074302
65. Wood KM, Hashemi P (2013) Fast-scan cyclic voltammetry analysis of dynamic serotonin responses to acute escitalopram. ACS Chem Neurosci 4:715–720
66. Apulche-Aviles MA, Baur JE, Wipf DO (2008) Imaging of metal ion dissolution and electrodeposition by anodic stripping voltammetry-scanning electrochemical microscopy. Anal Chem 80:3612–3621
67. Munteanu G, Munteanu S, Wipf DO (2009) Rapid determination of zeptomole quantities of Pb^{2+} with the mercury monolayer carbon fiber electrode. J Electroanal Chem 632:177–183
68. Yang Y, Pathirathna P, Siriwardhane T, McElmurry SP, Hashemi P (2013) Real-time subsecond voltammetric analysis of Pb in aqueous environmental samples. Anal Chem 85:7535–7541
69. Sigg L, Black F, Buffle J, Cao J, Cleven R, Davison W, Galceran J, Gunkel P, Kalis E, Kistler D, Martin M, Noel S, Nur Y, Odzak N, Puy J, van Riemsdijk W, Temminghoff E, Tercier-Waeber ML, Toepperwien S, Town RM, Unsworth E, Warnken KW, Weng L, Xue H, Zhang H (2006) Comparison of analytical techniques for dynamic trace metal speciation in natural freshwaters. Environ Sci Technol 40:1934–1941
70. Buffle J, Tercier-Waeber ML (2005) Voltammetric environmental trace-metal analysis and speciation: from laboratory to in situ. Trends Anal Chem 24:172–191
71. Ciszkowska M, Stojek Z (1999) Voltammetry in solutions of low ionic strength. Electrochemical and analytical aspects. J Electroanal Chem 466:129–143
72. Daniele S, Mazzocchin GA (1993) Stripping analysis at mercury microelectrodes in the absence of supporting electrolyte. Anal Chim Acta 273:3–11
73. Peña MJ, Fleischmann M, Garrard N (1987) Voltammetric measurements with microelectrodes in low-conductivity systems. J Electroanal Chem 220:31–40
74. Oldham KB (1988) Theory of microelectrode voltammetry with little electrolyte. J Electroanal Chem 250:1–21
75. Oldham KB (1997) Limiting currents for steady-state electrolysis of an equilibrium mixture, with and without supporting inert electrolyte. Anal Chem 69:446–453

76. Daniele S, Baldo MA, Bragato C, Abdelsalam ME, Denuault G (2002) Steady-state voltammetry of hydroxide ion oxidation in aqueous solutions containing ammonia. Anal Chem 74:3290–3296
77. Xu X, Zhang S, Chen H, Kong J (2009) Integration of electrochemistry in micro-total analysis systems for biochemical assays: recent developments. Talanta 80:8–18
78. Zhang DA, Rand E, Marsh M, Andrews RJ, Lee KH, Meyyappan M, Koehne JE (2013) Carbon nanofiber electrode for neurochemical monitoring. Mol Neurobiol 48:380–385

Chapter 16
Electrode Materials (Bulk Materials and Modification)

Alain Walcarius, Mathieu Etienne, Grégoire Herzog, Veronika Urbanova, and Neus Vilà

Electrochemical sensors have a long history and they found an important place in analytical chemistry and environmental monitoring thanks to the attractive properties and huge developments in electrode materials. Some key historical steps[1–20] are gathered in Table 16.1. Hereafter, the electrode materials used for environmental sensing purposes are presented in the form of two successive parts dealing respectively with unmodified and chemically modified electrodes.

16.1 Electrode Types and Configurations

Working electrodes are usually made of conductive materials exhibiting ideal polarization properties over a wide potential window (i.e., ensuring low currents in an electrolyte solution, free of any redox species, over several volts of applied potential). The main classes of materials offering a priori such qualities are: (1) mercury and noble metals (Pt, Pd, Au), (2) some allotropic forms of carbon (graphite, glassy carbon, carbon fibers, or carbon black), and (3) some metal oxides (e.g., indium-tin oxide, ITO), or (4) boron-doped diamond. More recently, in the goal to replace mercury (and especially mercury film electrodes), one has witnessed the development of metal films plated onto solid electrode surfaces. Even more recently, in attempting to increase the electroactive surface area of the conventional electrodes, strategies to build nanostructured electrode surfaces have been proposed. These various aspects are briefly described below.

A. Walcarius (✉) • M. Etienne • G. Herzog • V. Urbanova • N. Vilà
Laboratoire de Chimie Physique et Microbiologie pour l'Environnement, UMR 7564, CNRS – Université de Lorraine, 405 rue de Vandoeuvre, 54600 Villers-les-Nancy, France
e-mail: alain.walcarius@univ-lorraine.fr

L.M. Moretto, K. Kalcher (eds.), *Environmental Analysis by Electrochemical Sensors and Biosensors*, DOI 10.1007/978-1-4939-0676-5_16

Table 16.1 Some historical milestones in the development of electrochemical environmental sensors based on bare and chemically modified electrodes

Year	Historical milestones	References
1922	Polarography at a mercury drop electrode	[1]
1931	Stripping voltammetry of Cu^{2+} at a platinum electrode	[2]
1958	Carbon paste electrodes	[3]
1961	Mercury film electrodes	[4]
1962	Enzyme-modified electrodes	[5]
1973	Adsorption of alkenes on platinum electrodes	[6,7]
1978	Deposition of polymers on electrodes	[8,9]
1981	Chemically modified carbon paste electrodes	[10]
1983	Formation of thiol self-assembled monolayer on gold	[11]
1986	Biosensor based on electropolymerized conducting film	[12,13]
1987	Nafion adsorption for surface protection and metal detection	[14,15]
1987	Sol–gel-derived silica film deposited on an electrode surface	[16]
1992	Electrochemical grafting of diazonium salts on carbon electrode	[17]
1997	Metal detection at a thiol self-assembled monolayer	[18]
1997	Mesostructured metal electrode generated by surfactant templating	[19]
2000	Bismuth film electrode as an alternative to mercury film electrodes	[20]

16.1.1 Bulk "Conventional" Electrode Materials

The emergence of modern electroanalytical sciences is tightly bound to the implication of specific conductive materials as electrode material. Lubert and Kalcher recently provided a history of electroanalytical methods in which the reader could find a wider view of the field.[21] First electroanalytical determination of copper in copper-nickel coins was accomplished by electrogravimetric method on platinum electrodes in the nineteenth century. Later, polagraphy, rewarded by a Nobel Prize for J. Heyrovsky, was developed with dropping mercury electrode and important developments have been then conducted on both analytical methods and materials.

The performance of an electrochemical analysis depends notably on the working electrode material that should allow high signal-to-noise ratio and reproducible response. The choice of this material depends primarily on the redox behavior of the species to be analyzed and the background current resulting from the conditions of analysis in the suitable potential range. It also depends on the accessible potential window, electrical conductivity, surface renewal, mechanical properties, cost, availability, and toxicity. The most popular materials are those involving mercury, carbon, or noble metals (particularly platinum and gold), but silver, nickel, or copper were also considered for specific applications.[22] The range of analytes that can be determined with electrochemical reaction on bulk electrodes is large and comprised both metal ions and organic compounds. The possibility to preconcentrate the species to be detected by simple adsorption or electrochemical concentration before stripping analysis permits to reach very low detection limits, i.e., down to 10^{-10} M. Moreover, several species (e.g., metal ions) can be detected

simultaneously. A large overview of analytical electrochemistry has been given by Wang.[23]

One major advantage of mercury versus other electrodes, e.g., platinum, is the very high overpotential for hydrogen evolution allowing the electrochemical reduction of metal cations even at low potentials. On the contrary, the electrochemistry with this metal is limited on the oxidation side because of the oxidation of mercury. Mercury electrodes were used in various configurations, i.e., dropping mercury, hanging mercury drop, static mercury drop, streaming mercury, and mercury film.[24] But the mechanical instability of the liquid mercury electrode was found limiting for the development of modified electrodes surfaces considered in sensors. Moreover, the toxicity of mercury triggered the search for alternative metals. Bulk bismuth was thereby considered as it displays a very similar behavior as mercury for the stripping analysis of heavy metals.[25]

What one can consider as the first electrochemical sensor, i.e., a modified electrode surface dedicated to a specific target analyte, was a platinum electrode, covered by a protective membrane, the Clark electrode, for the determination of O_2 in blood.[26] The first biosensor was based on the determination with such Clark electrode of O_2 depletion induced by glucose oxidase activity in the presence of glucose.[27] These two examples show the importance of platinum as electrode material. It will be seen below that gold was also widely used for the development of chemically modified electrodes, especially due to the strong interaction with thiol-functionalized organic molecules allowing the formation of self-assembled monolayers (SAM).[11,28]

In the same period, carbon-based materials, i.e., carbon paste,[3] wax-impregnated graphite,[29] pyrolytic graphite[30] and glassy carbon[31] were introduced. This latter electrode was then applied to the anodic stripping analysis of metals.[32] These various materials display different advantages and limitations considering the background current, the potential limits, the electron transfer kinetics, the reproducibility, the stability, and the adsorption properties that must be considered depending on the analytical application.[24] Among these various carbon-based electrodes, one can highlight the importance of carbon paste electrodes for the development of chemically modified electrodes (see below)[33] and the subsequent emergence of screen-printed electrodes allowing numerous applications for decentralized analysis.[34] Another class of carbon-based material, i.e., boron-doped diamond (BDD) was introduced in the 1990s by Swain and Ramesham.[35] The interest of such material is related to the larger potential window accessible in conventional media for environmental analysis and the good resistance to surface fouling, which is of major importance for application in complex matrices.

An important breakthrough in the development of electrochemical sensors was the miniaturization of electrodes, as introduced during the 1970s for O_2 measurement (microcathode) or in vivo analysis of neurotransmitters,[36] and then largely developed in the 1980s.[37,38] The steady state current that can be observed at microelectrodes served later as a basement for the important development in scanning electrochemical microscopy allowing electroanalysis of complex interfaces, with using carbon fiber or metal (Pt, Au) micro- or nanoelectrodes.[39]

Arrays of micro- or nanoelectrodes were also developed, notably for application in environmental monitoring.[40]

Nanomaterials, i.e., metal nanoparticles, carbon nanotubes (multi- and single-walled) and nanofibers, fullerene, and more recently graphene have been and are strongly investigated for analytical purposes.[41–43] The reasons of this enthusiasm for such materials arise from their high electroactive surface area and in some cases their electrocatalytic properties. Specific applications to electroanalysis with these nanomaterials are covered by other chapters of this book (see Chaps. 17 and 20). Increasing the surface area is also possible with using mesostructured or macrostructured carbon electrodes (see below), allowing significant improvement in analytical features of potentiometric and amperometric sensors.[44]

A final class of materials is the optically transparent electrodes based on metal oxides (e.g., indium-tin oxide, ITO). These materials are very popular in the field of energy conversion, as a support for Dye-Sensitive Solar Cells, but the group of Heinemann developed at the end of the 1990s a spectroelectrochemical sensing method based on such transparent electrodes. The method is defined as the coupling of an electrochemical detection with a spectroscopic analysis.[45,46] This approach allows for multimode selectivity and is usually applied in the presence of surface modification for preconcentration of the analyte. More recently, porous and optically transparent electrodes have been prepared and applied for combined spectroscopic and electrochemical analysis[47–51] which should lead in a near future to further developments in analytical sciences applied to the environment.

Electrode modification of these bulk materials is the major topic to be treated in the next sections. We will see that the range of modification that has been considered is quite large, with the deposition of metal film electrodes, the electrode texturation (for increasing the electrode surface area with respect to the geometric one), the functionalization with organic monolayers or polymeric multilayers, or the elaboration of composite electrode materials for the development of sensors for possible application in the field of environmental analysis.

16.1.2 Metal Film Electrodes

Metal film electrodes have been introduced in electrochemical stripping analysis mainly because they were promising alternative to the commonly used electrodes (e.g., less toxic than the mercury drop electrode and easier to regenerate than bulk gold or platinum electrodes). Metal film electrodes offer reliable analytical tools since they are relatively simple to fabricate and consequently easy to reproduce as new surfaces.[23,25,52] Metallic films on electrodes represent a very thin layer of a metal deposited onto a suitable support. The thickness of this layer ranges from micrometric dimensions to ultrathin films whose thickness can be down to tens of nanometers. With respect to the material used for film electrode preparation, one can distinguish three main groups: gold film electrodes (AuFEs),[53–57] mercury film electrodes (MFEs)[58] and bismuth film electrodes (BiFEs).[20,25,59] Other metallic

compounds were also used but more rarely, however they can be traced up in the literature: lead film electrodes,[60–62] silver and silver amalgam film electrodes,[63,64] tin film electrodes,[65] antimony film electrodes,[66–68] cobalt film,[69] gallium[70] or even selenium film plated electrodes.[71]

16.1.2.1 Gold Film Electrodes (AuFEs)

In electrochemistry, gold belongs to traditional materials used for the fabrication of working electrodes. These electrodes offer relatively large anodic potential range and favorable electron transfer kinetics, but they have a limited cathodic potential range in aqueous solution compared to mercury.[72] More problematic are high background currents associated with the formation of surface oxides or adsorbed hydrogen layers and it is rather difficult to keep electrode surfaces free of them. It is noteworthy that oxide layers on the electrode surface can influence/restrict the rate of electron transfer reactions, or they are likely to react with the analyte, giving rise to undesirable responses, which may result in various complications during electrochemical measurements and poor reproducibility.[72,73] For this reason, the surface has to be regenerated by mechanical or electrochemical polishing, which is usually a time-consuming procedure, such additional operation making gold electrodes less attractive for routine analysis.[74] In this context, gold film electrodes (AuFEs) have been shown to be a useful alternative to solid gold electrodes because their active surface can be easily renewed (i.e., by depositing a new gold film between each measurement).

The preparation of AuFEs is commonly carried out via electrochemical deposition from a gold ions solution, although some other procedures have also been reported.[75] Electrochemical deposition, plating, and renewal of Au films are rather simple and can be done as frequently as needed. The film is deposited either ex-situ, from a separate plating solution,[54] or by in situ plating, as common for stripping analyses, which involves the formation of the gold film directly during the reductive accumulation of the analyte from solutions spiked with trivalent gold.[76] Electroless (or chemical) deposition techniques have also been reported in literature. The first autocatalytic, electroless gold plating bath was developed in 1970 at Bell Laboratories to plate thick, pure soft gold on semiconductors and circuit boards without employing an external source of electric current.[77] The original baths did not contain stabilizing additives and they were sensitive to impurities, which tended to lead to spontaneous decomposition. For this reason, some efforts have been made to improve the original borohydride and dimethylamine borane baths, especially in their stability and plating rate, and such improved baths are now commercially available.[78] Generally, the methods of electroplating have advantages over the electroless plating ones in terms of easier control of the film thickness. On the other hand, electroless plating can minimize the number of processing steps when gold is needed in areas which are electrically isolated from each other.[78] Gold film electrodes prepared by vacuum evaporation can also show poor operational and mechanical stability, i.e., the film is likely to peel off from the substrate, implying

Table 16.2 Typical applications of gold film electrodes (AuFEs) in electrochemical stripping analysis

Analyte	Type of sample	Method[a]	Substrate for AuFEs	Ref.
As(III)	Natural water	LSV	Glassy carbon electrodes	85
As	Air filters, biological samples	ASV	Pyrolytic graphite electrode	86
As(III), As(V)	River water	DPASV	Boron-doped diamond electrode	84
As(III), As(V)	River water	CCSA	Carbon paste electrodes	87
Hg(II), Pb(II)	Tap water	ASV	Screen-printed electrodes	89
Cu(II), Bi(III), Sb(III), Pb(II)	Water, fruit, leaves	PSA	Glassy carbon electrodes	90
As(III), As(V)	Groundwater	ASV	Glassy carbon electrodes	88
Hg(II)	Electroplating waste water	SWASV	Glassy carbon electrodes	91

[a]*LSV* linear sweep voltammetry, *ASV* anodic stripping voltammetry, *DPASV* differential pulse stripping voltammetry, *CCSA* constant current stripping amperometry, *PSA* potentiometric stripping amperometry, *SWASV* square wave stripping voltammetry

thereby great care in assembling the electrochemical cell and in introducing solutions into the cell.[79] Other ways employed to prepare AuFEs include thermal evaporation in a tungsten basket used as a hot filament,[80] high-speed selective jet deposition,[81,82] or ionized cluster beam techniques.[83]

Typical applications of AuFEs in stripping voltammetry are summarized in Table 16.2. AuFEs have been extensively exploited for inorganic arsenic analysis,[84–88] among other analytes such as heavy metal species.[89–91] The widespread use of arsenical compound in industry and the concern over arsenic toxicity which can cause several health problems, including pigmentation, hyperkeratosis, and various cancers (e.g., skin, lung, urinary bladder, and kidney),[92] has induced development of methods for quantitative arsenic analysis. In this context, electrochemical methods have been found highly sensitive, low cost, and in addition can distinguish different oxidation states of arsenic. This determination is based on the interaction of As with Au during the deposition step and by the fact that As can be selectively oxidized from Au-As intermetallic during the following stripping step.[84,93]

16.1.2.2 Mercury Film Electrodes (MFEs)

Generally, the hanging mercury drop electrode (HMDE) is the most suitable electrode for anodic stripping voltammetry (ASV) and adsorptive stripping voltammetry (AdSV) analyses because such electrode allows fast and reproducible surface renewal and provides high adsorptivity for organic compounds.[94,95] Nevertheless, even HMDE has some drawbacks that limited its use particularly for automatic or on-site voltammetry analysis as well as analysis in flow conditions since it requires a mercury reservoir and regular maintenance of the capillary and

mechanics used for precise drop generation.[96] Potential risks of poisoning, contamination, and disposal associated with the use of mercury also limited HMDE from an environmental point of view. Moreover, HMDE is not ideal for modification by chemical reagents or coatings for improving its selectivity or sensitivity. Some of these disadvantages can be successfully overcome by using MFEs, prepared by coating a suitable substrate with a thin film of metallic mercury.[58] MFEs provide a larger surface-to-volume ratio, they are mechanically more stable than mercury drops, they can be of fairly small size and thus they offer possibility to be easily incorporated to different cell configurations (e.g., rotating electrodes, flow-through designs) and they can undergo different type of modification as well. In addition, consumption of metallic mercury is minimized since the preparation of MFEs requires only small quantities of mercury.[97]

Ideally smooth mercury films can be prepared only at conductive surfaces that can be wetted by mercury, e.g., carbonaceous materials. Glassy carbon is the preferred support in most cases due to its useful analytical properties.[98,99] Impregnated graphite (i.e., carbon impregnated with wax or paraffin)[100] or carbon fibres[101] have also been used. Pyrolytic graphite,[102] sprayed carbon layers[103] or carbon paste[104] belong to less commonly used carbon-based materials. Noble metals such as gold,[105] platinum,[4] silver[106] or iridium[107] have also been used as support for MFEs plating, but in this case, deposition of mercury leads to so-called metal-mercury amalgam electrodes.[108] On most substrates, mercury hardly deposits as a film of uniform thickness but rather as randomly dispersed mercury droplets.[97]

Mercury film is usually plated electrochemically from a solution containing Hg(II) species by reduction to metallic mercury under convective transport and negative polarization of the substrate.[109] One can consider two main methods for coating an electrode with a mercury film: preplating, involving an initial coating step in which the mercury film is formed on the electrode surface, and in situ plating in which the mercury film formation and the analyte accumulation are carried out simultaneously.[58] Recently, modification of the electrode surface with a mercury precursor (e.g., HgO, $HgCl_2$, or mercury acetate) which undergoes reduction in the course of the experimental procedure, thus producing the mercury film, has been proposed.[110,111] Deposition of mercury by vaporization under vacuum has not found widespread acceptance.[112] In all cases, cleaning of the old film can be carried out by chemical treatment (e.g., with iodine or tetraethylenepentamine), mechanically or by electrochemical oxidation of mercury at a positive potential.[97,113,114]

MFEs found widespread applications in environmental and food trace analysis by stripping voltammetry.[115] The theory and practice of MFE in ASV for the detection of easily amalgamated metals (such as Cd, Pb, Cu, Zn, Bi, Sn) have been well documented in literature.[116] Less common are reports of cathodic stripping voltammetry (CSV) on MFEs after either electrolytic or adsorptive preconcentration. Among species determined by CSV after electrolytic preconcentration are, e.g., selenium,[117] arsenic,[118] or thiocyanate.[119] Applications dealing with the determination of aluminum,[120] titanium,[121] germanium[122] or chlorhexidine[123] have also been reported. As already mentioned, a strong advantage of MFEs over to HDME, is that they offer great scope for variation in cell and

electrode design. In this context, MFEs have found applications in flow injection analysis (FIA),[124] batch injection analysis (BIA)[125] and sequential injection analysis.[126] Portable commercially available analyzers featuring MFEs are already offered with conditioning tablets for the sample and automatic measurement and calibration routines.[97]

16.1.2.3 Bismuth Film Electrodes (BiFEs)

Bismuth film electrodes have undoubtedly been the most promising sensors, exhibiting analytical properties similar to MFEs and thus being very interesting in the field of electrochemical analysis.[20,25,127] The advantageous analytical properties of BiFEs in voltammetric analysis, roughly comparable to those of MFEs (see illustration in Fig. 16.1), are attributed to the property of bismuth to form "fused alloys" with numerous heavy metals, which is analogous to the amalgams that mercury forms.[128]

The most significant advantage of BiFEs is that they are environmentally friendly because bismuth is considered to be safe, as it is much less toxic than mercury and a noncarcinogenic element. This is illustrated by the fact that bismuth and its compounds have been used in medical preparations for over 400 years.[129]

BiFEs are typically prepared by electroplating a thin bismuth layer on an appropriate substrate; in principle, it can be plated on the same substrates as for mercury films. Different forms of carbon, such as glassy carbon,[20,130–133] carbon paste,[59,134,135] graphite-epoxy composite,[136] pencil lead,[137] carbon-based screen-printed

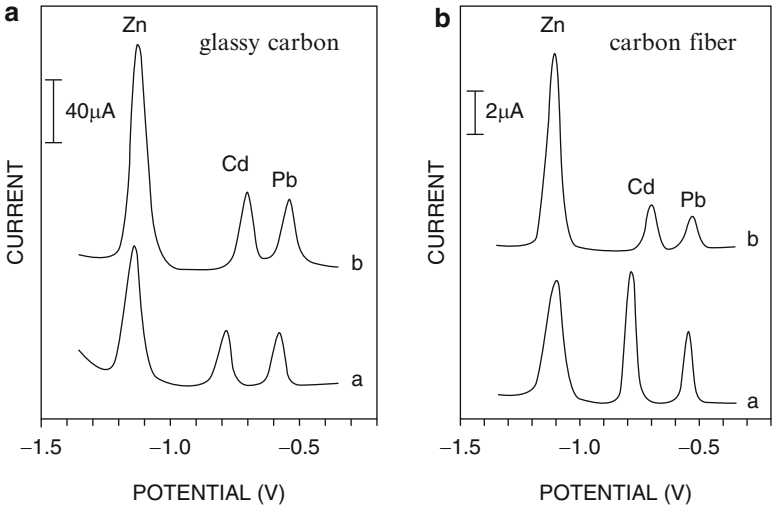

Fig. 16.1 Stripping voltammograms of zinc, cadmium, and lead recorded at glassy carbon and carbon fiber electrodes coated with (**a**) bismuth or (**b**) mercury films. Reprinted with permission from reference (20) Copyright (2000) American Chemical Society

electrodes,[138,139] electrically heated carbon paste electrodes,[140] carbon film resistor electrodes[135] or carbon fibers[134,141] have been used for bismuth film plating. Besides, substrates such as copper,[142,143] boron-doped diamond electrodes,[144] platinum electrodes,[145,146] carbon nanotubes[147–150] or graphene nanosheets[151] have also been used.

The method of coating the conducting substrate with a bismuth film is critical to get satisfactory performance of the resulting BiFEs. There are three methods for BiFE fabrication. The first method, ex-situ plating, involves electroplating the bismuth film before transferring the electrode to the sample solution for analysis. The reported conditions for ex-situ BiFEs plating are variable. In general, an acidic media is always recommended since Bi(III) is easily hydrolyzed at higher pH. Typical conditions are 5–200 mg L^{-1} Bi(III) with a deposition potential in the range from −0.5 to −1.2 V and a deposition time of 1–8 min under conditions of forced convection.[25,152,153] In the second method, in-situ plating, Bi(III) ions are added directly into the sample solution and the bismuth film is deposited on the electrode surface during the analysis. A general practical rule is that the Bi(III) concentration has to be at least 10 times higher than the expected analyte concentration to avoid saturation effects.[154,155] Typical Bi(III) concentrations are in the range of 400–1,000 μg L^{-1}.[20] The plating conditions (plating potential and time) are then dependent on the conditions used for the actual analysis. In-situ plating simplifies and shortens the experimental procedure as no separated bismuth plating step is required, but it is basically limited to anodic stripping analysis where negative polarization of the electrode is employed for the electrolytic preconcentration of metal ions.[127] This method of plating has some limitations in the accessible pH range of the sample solution. Bi(III) ions are very susceptible to hydrolysis in neutral and alkaline media according to Eq. (16.1) and thus in-situ plating is essentially useful for acidic samples.[156]

$$Bi^{3+} + 3H_2O \rightarrow Bi(OH)_3 + 3H^+ \tag{16.1}$$

On the other hand, it was shown that operating in alkaline media is also possible, providing conditions to maintain Bi(III) species in the form of water-soluble stable complexes with OH^- ions (e.g., $Bi(OH)_4^-$) are met, so that they can undergo electrochemical reduction on the electrode surface.[156] It has to be mentioned that under similar highly alkaline conditions, Hg(II) ions hydrolyze and thus MFEs are also inoperative. The third plating method is based on modifying the bulk of an electrode with a bismuth precursor such as Bi_2O_3. This method of bismuth film formation is essentially confined to carbon paste electrodes[157] as the Bi_2O_3 can be readily incorporated into the composite electrode by mixing it with the carbon paste. These modified sensors are easy to prepare and simplify the experimental procedure by providing a means of generating a bismuth film in situ without using Bi(III) salts. However, they exhibit some problems in anodic stripping voltammetry of metal ions such as low linearity and shifts in the stripping peak potential.[127,158]

Bismuth film electrodes have been employed for a wide range of analytical determinations of various analytes in different types of sample. Environmental samples are the predominant ones, followed by food, medical, pharmaceutical,

and various industrial samples.[152] Great diversity exists in the use of BiFEs for the determination of heavy metals (such as Pb, Cd, Co, Zn, Ni, Tl, Sn etc.) in food samples such as wine,[145] potato,[159] garlic,[160] meat,[161] tea leaves[162] or tobacco.[163] BiFEs have also been applied to complex sewage samples,[164] number of soil samples,[163,165] fertilizer samples.[166] Even if the vast majority of practical applications of BiFEs has been focused on the determination of inorganic ions, increasing effort towards organic compounds determination has merged.[152] Fundamental studies are notably dealing with model organic compounds such as nitrophenols,[167,168] picric acid[169] pharmaceutical substances[170–172] and some biological important compounds.[172–174] Finally, the implementation of BiFEs for advanced instrumentation was illustrated, for example, by using a robotic system to monitor continually the release of metal ions during corrosion process,[175] or analyzing non pretreated sea water samples by on-line combination with inductively-coupled plasma-mass spectrometry.[176]

16.1.3 Nanostructured Electrode Surfaces

Structuring electrode surfaces to provide better control of their behavior with their environment has been one of the most active areas of research interest in electrochemistry within the last 30 years.[177] In recent years this revolution in tailoring electrode surfaces has continued at an even greater rate due to the advances in nanofabrication. Nanostructuring electrodes can be regarded as controlling the architecture of an electrode at the nanoscale whether using nanomaterials, templating methods, organic or hybrid modification monolayers (these latter being mainly described in the section below).[178–181] Many of excellent properties that can be achieved by nanostructuration are due to the unique properties of the employed nanomaterials and the ability to tailor the size and architecture of the electrode interface.[182]

In general there are two distinct paths that can be taken toward nanometer scale structure: the top-down approach that employs lithographic tools (such as photolithography, electron beam lithography, X-ray lithography, etc.) to pattern nanostructures on a substrate and the bottom-up approach that takes advantage of the interactions between molecules to assemble them into nanoscale structures in a solution phase.[183–185] Top-down techniques are derived mainly from the methods applied to the production of microstructures in the semiconductor industry and this approach is based on a number of tools and methodologies which consist of three major steps: (1) the deposition of thin films/coatings on a substrate; (2) designing of desired shapes via lithography; (3) pattern transfer using either a lift-off process or selective etching of the films.[183,186,187] The bottom-up approach, starting from atoms or molecules, uses the methods like self-assembly of nanoparticles or monomer/polymer molecules, chemical or electrochemical reactions or sol–gel processing to create porous nanostructures, most often based on templating approaches.[188]

The template synthesis for electrochemical applications was first explored by Martin.[189,190] He introduced membrane-based synthesis by which the desired materials were prepared within the pores of a nanoporous membrane called "template". More recently, other templating methods have been developed and one can distinguish hard or soft templating routes. Hard templating, usually based on colloidal crystals assemblies, is straightforward and highly effective method to prepare periodic macroporous structures that mimic the original shape of template.[191–193] Soft templates, such as molecular or supramolecular aggregates,[194] constitute a powerful tool for nanomaterials fabrication, in particular mesoporous inorganic solids such as silicates,[195] metal oxides[196] or mesoporous polymers or carbons.[197] More details concerning both pathways will be described in following.

16.1.3.1 Porous Membranes as Hard Templates

One of the most popular hard templates is anodic aluminum oxide (AAO) that can be prepared by following two-step anodic process.[198] Typically, a clean aluminum sheet is electropolished and then first anodized in an oxalic acid solution for several hours. After removing the barrier oxide layer in a chromic acid and phosphorus acid, a second anodization is applied for a short time period in the same oxalic acid solution used for first anodization process.[199] As a consequence of their preparation methods, AAO membranes are characterized by high density (10^9–10^{11} per cm^2) of cylindrical pores with uniform diameter between 10 and 200 nm, which can be accurately tuned by the process parameters.[200] Track-etched polymeric membranes are characterized by much smaller pore densities (up to millions pores per cm^2) compared to AAO, with pore diameters ranging from 10 to 2,000 nm. The most commonly used material to prepare membranes of this type is polycarbonate.[201] The track-etched process involves irradiation of a polymer membrane by heavy ions and subsequent chemical etching, resulting in a membrane with pores of predicted geometry.[202]

Figure 16.2 schematically illustrates the most common ways for preparation of nanostructures using porous membrane as template. Several methods have been tested to grow nanomaterials inside the pores of AAO.[203–206] Vapor deposition methods (chemical vapor deposition and molecular beam deposition) generally suffer from the nucleation occurring on the pore walls. Therefore, the deposited materials decorate the pore walls randomly rather than growing into nanotubes, nanowires, or nanorods with controlled morphologies.[207] For this reason, electrochemical deposition method is advantageous in that the mechanism enforces the growth to occur from the bottom to the top. Regardless of the type of the materials to be deposited, the AAO template-assisted electrodeposition of nanostructures follows the same general scheme. Firstly, a thin layer of metal (gold, silver, …) is deposited on one side of the AAO template, which will serve as the working electrode. After electrodeposition under the proper conditions resulting nanostructures may be nanowires or nanotubes and their shape, diameter, and surface roughness are directly determined by the AAO template.[208] Finally, if

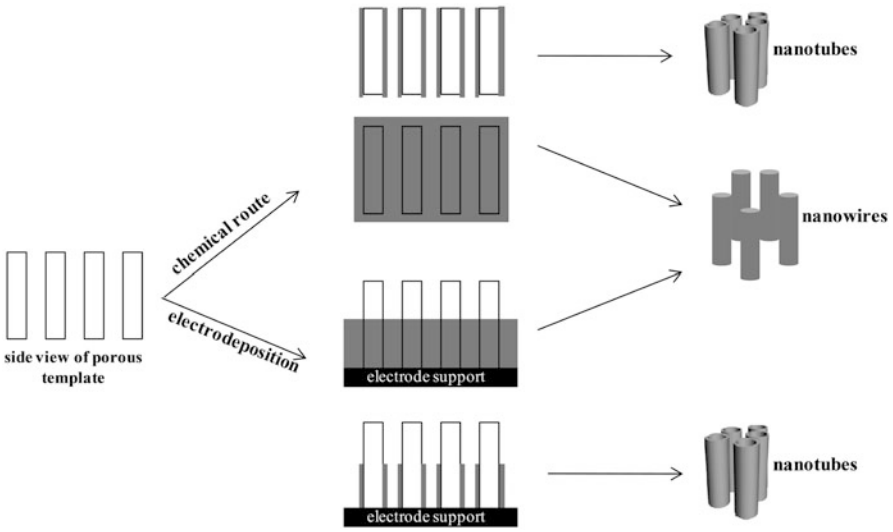

Fig. 16.2 Schematic illustration of nanostructures fabrication using a porous membrane as template

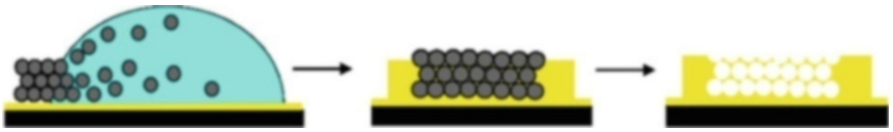

Fig. 16.3 Schematic illustration of template-directed chemical or electrochemical deposition through a colloidal crystal assembly

desired, the AAO template can be removed by dissolving it in an acidic or alkaline solution or the membrane is not removed and resulting devices are ascribed as "nanoelectrodes ensembles" (NEEs). Through this method, various materials, including Au, Ag, Pt, Ni, Fe, Co, ZnO, and Pd have been fabricated as nanorods and nanowires.[207] In addition, nanorods composed of two different materials such as gold-nickel have been described.[209,210]

16.1.3.2 Colloidal Crystal Templating

The general scheme (Fig. 16.3) of a synthesis by colloidal crystal templating (CCT) is relatively straightforward and contains the following steps: (1) self-assembly of colloidal spheres into close-packed arrangements; (2) infiltration of the interstitial space of the template with a fluid and its conversion into a solid; and (3) removing the original template leaving behind ordered interconnected macroporous structures.[191,192,211]

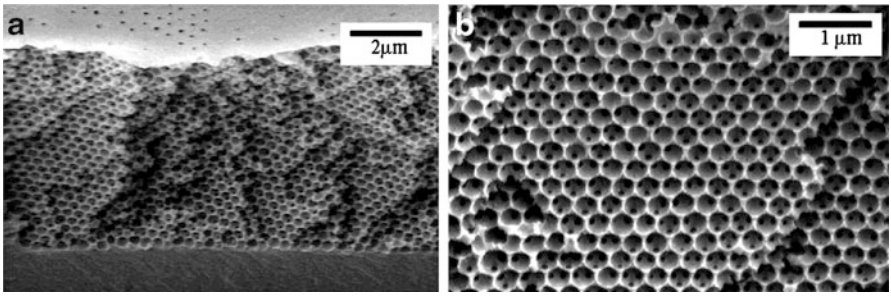

Fig. 16.4 SEM images of macroporous TiO_2 prepared with 351 nm diameter silica spheres. Reprinted with permission from reference (225) Copyright (2001) Wiley-VCH

The colloidal particles of interest for material engineering have usually spherical shape and they are often made of silica[212] or polymers such as poly(methyl methacrylate) (PMMA)[213] or polystyrene (PS).[214] Silica spheres employed in CCT undergoes less shrinkage (ca. 10 % in linear dimensions) than in typical reactions with polymer spheres (often 20–30 %).[211] Moreover, silica particles withstand relatively high processing temperatures in subsequent steps. Disadvantage of silica spheres is associated with template removal, which requires treatment with hydrofluoric acid (toxic and caustic) or hot alkali solution while polymer spheres are usually removed by calcination or extraction with organic solvent. Generally, the spheres self-organize into hexagonally close-packed layers in two dimensions (2D) and into predominantly face-centered cubic arrays in three dimensions (3D).[215,216] However, the resulting CCTs are usually not defect free. They contain point defects, line defects, stacking defects, dislocations, and cracks.[217] Commonly used methods for assembly are based on gravitational, electrostatic and capillary forces[218–220] or on the use of physical confinement in combination with pressure and flow.[221]

After preparation of the colloidal crystal template (CCT) as a thin film, the next steps involve infiltration of template with precursor material and processed to form a composite with the CCT. Because incomplete infiltration may lead to the collapse of the colloidal crystal structure, complete and uniform infiltration is thus of essential importance. Based on the properties of the target materials, different methods for infiltration have been proposed.[192] Infiltration can be conducted with solid, liquid, or gas phase precursors. Of these, infiltration with solid nanoparticles is less common, except for films consisting of monolayers or very few layers of the template.[222] Liquid-phase infiltration applies to sol–gel and solution precursors for the target materials as well as melts. To increase the loading amount of the precursor, the template is often soaked repeatedly in the precursor solution with optimum dilution.[223] This approach is especially suitable for preparation of macroporous metal oxides (such as TiO_2, ZrO_2, or CeO_2) by using metal alkoxide precursor[224–226] (see an illustrative example in Fig. 16.4).

Nevertheless, this method has some limitations (such as a loss of solvent during sol–gel processing or decomposition of the precursor) leading to incomplete filling of interstitial spaces of colloidal crystal. Template-directed electrochemical

deposition is an elegant method that can overcome these problems.[227–230] This technique typically starts with assembling of colloidal crystals onto a conductive substrate. The substrate is then immersed into an electroplating solution along with counter electrode and a potential is applied. Electrodeposition fills CCT sequentially from the bottom to the top, allowing the film thickness to be tailored by altering the electrodeposition time.[231] Electrodeposition methods have been applied to prepared macroporous chalcogenides (CdS, CdSe),[232] metals (such as Pt, Pd, Co, Au, Bi, Sb),[67,153,192,230] metal oxides[233] or conducting polymers.[234]

16.1.3.3 Soft Templating Routes

Soft templates have received more attention over the last decade because they are more versatile and therefore more advantageous than hard templates. Surfactant templating strategy through self-assembly of inorganic species and surfactant is a basic synthetic powerful approach to fabricate ordered mesostructured materials.[235,236] Surfactants, generally known as detergents, can assemble thanks to hydrophobic interactions into spherical, prolate, or cylindrical micelles at a concentration slightly higher than their critical micelle concentration (CMC), and further aggregate into stable 2D or 3D ordered mesostructures of liquid crystalline phases with long-range ordering.[237] One of the first liquid crystal phases that micelles are expected to form is a structure similar to a face-centered or a body-centered cubic crystal lattice. In the case of a body-centered cubic structure, micelles take place of individual atoms, ions, or molecules. Rod-shaped micelles often form into hexagonal arrays made out of six rods grouped around a central one for a total number of seven (see Fig. 16.5 for illustration). At even higher concentration the molecules move into lamellar phase. This structure has a double layer of molecules arranged a bit like a sandwich with polar heads outside and nonpolar tails inside. In principle, increasing the amphiphile concentration beyond the point where lamellar phases are formed would lead to the formation of the inverse topology lyotropic phases, namely the inverse micellar phase, the inverse hexagonal or cubic phases.[238,239]

Actually, the pioneering approaches to mesoporous materials using soft templates are the synthesis of ordered mesoporous silicates based on a liquid crystal (LC)-template mechanism, which was reported in early 1992.[240] In this approach, the inorganic material occupies the continuous solvent (water) region to create inorganic walls between the surfactants cylinders. The stable mesoporous molecular sieve was produced after removal of the organic template by calcinations. In order to support the LC template mechanism, it was demonstrated that the structures and pore dimensions of mesoporous material were intimately linked to the properties of the surfactants, such as surfactant chain length and solution chemistry.[241] Preparation of mesoporous silica using LC templates affords the remarkable advantages owing to precise control over the structure of the resulting inorganic solid due to the knowledge of LC structures. Such mesoporous silicates (and other metal oxides) can be generated as thin films on solid supports,[242] including

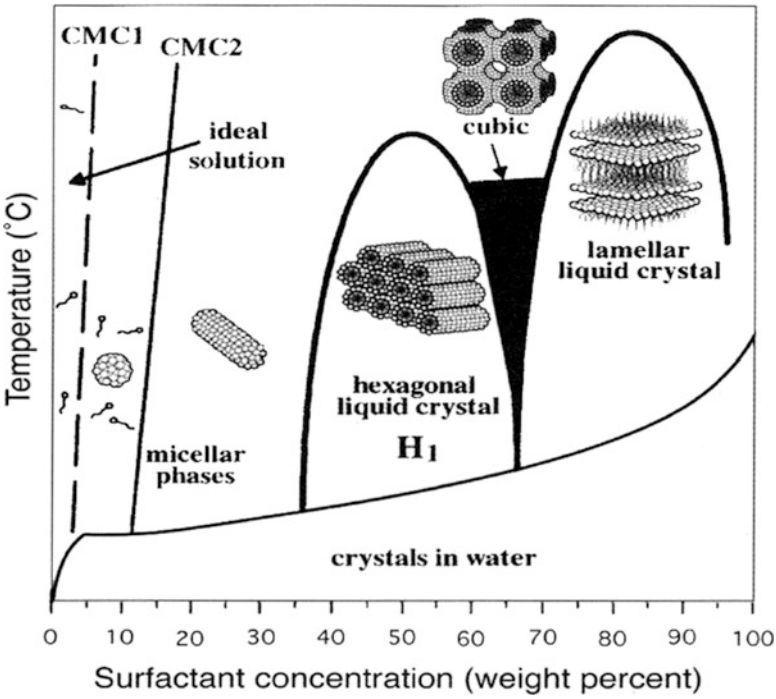

Fig. 16.5 Illustration of liquid crystalline mesostructures that are expected to form as a function of temperature and surfactant concentration. Adapted from reference (239) Copyright (2006) Elsevier

electrodes,[243] but this will be discussed below. Later on, other methods for mesoporous structure fabrication, originating from the observation that surface aggregation of surfactants at electrode surfaces can be controlled by the applied potential (even in dilute surfactant solutions),[244] have been proposed.[245,246] In such a way, there is no need to preform an organized lyotropic mesophase onto the electrode surface (no direct physical cast), the mesoporous film formation results from a self-assembly co-electrodeposition process under fine potential control.[245,246] From the electrochemical point of view, two families of mesoporous conductive electrode materials have been developed: the mesoporous metals (and alloys) and mesoporous carbons.

Mesoporous Metals and Alloys

Traditionally, mesoporous metals have been elaborated by using mesoporous silica as a hard template. In 1997, Attard's research group first reported that mesoporous platinum can be produced by the chemical or electrochemical reduction of metal salts dissolved in the aqueous domains of a hexagonal lyotropic liquid crystal (LLC) phase architecture.[19,247] They have shown that the reduction of platinum salts in this system led to platinum whose nanostructure was a cast of the LLC

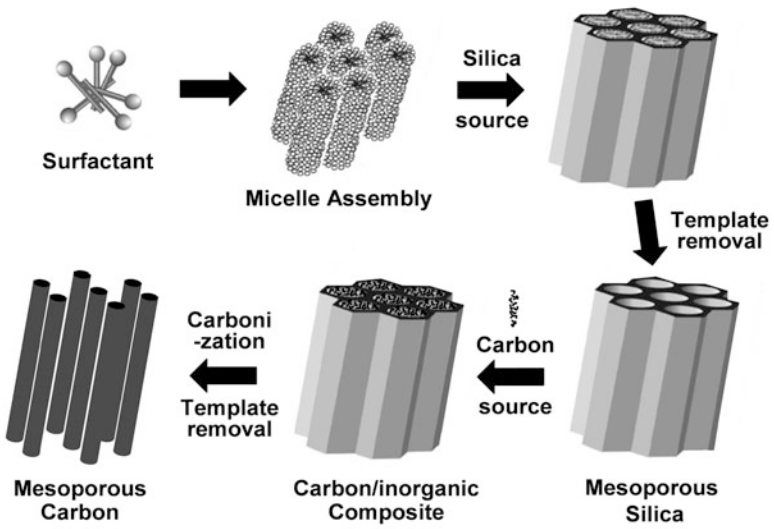

Fig. 16.6 Schematic illustration of the different steps applied to prepare mesostructured carbon through the hard template route

phase. Besides this initial work with mesoporous platinum films, the same group prepared variety of mesostructured materials such as Sn films, Ni/NiO_2, Pt/Ru, or Pd/Pt alloys.[248–250] Bartlett and Marwan extended the idea of LLC templating of mesoporous metals and demonstrated that they could electrochemically deposit the mesoporous film of two metals, one on the top of the other.[251] Although the metals from some groups of elements (such as groups 9 and 10) can be readily templated, the liquid crystal templating mechanism failed to produce mesoporous structures of some important noble metals such as gold, silver, or copper. For example, for copper films made from a mixture of the surfactant Brij 56 and an aqueous solution of $CuCl_2{\cdot}2H_2O$, the authors found that the final materials did not show any mesoporous structures or significant increase in surface area and, if mesostructure was obtained, it did not survive post treatment steps; the mesoporous structure corroded and subsequently collapsed.[252]

Mesoporous Carbon Materials

Recently, attention has been paid to porous carbon materials, owing to their large surface area, large pore volume, chemical inertness, and electrical conducting properties.[253] Porous carbon materials with controlled architecture, morphology, and relatively narrow pore size distribution are usually prepared by a templating (hard or soft) method followed by carbonization processes.[197] The main synthetic way to produce ordered mesoporous carbons relies on the use of ordered mesoporous silica with interconnected pore structures as a hard template.[254] This synthetic route (see Fig. 16.6 for the hard template route) requires (1) preparation of

an ordered mesoporous silica template, (2) impregnation of mesopores with an appropriate carbon source, (3) carbonization, and (4) subsequent selective removal of the silica framework (by dissolution, using HF or NaOH).[255,256]

Often, this time-consuming, and costly process requires multiple infiltrations to complete the filling of the template pores. It is difficult to perform pore filling of the carbon precursors into the mesopores of silica with low accessible pore systems, such as silica thin films with cylindrical mesopores oriented parallel to the substrate.[253] For this reason, recent progress has been achieved in implementing direct soft template approaches, which are mainly based on using supramolecular aggregates as templates (e.g., self-assembled surfactants or block copolymers and thermosetting resins, and in some cases copolymerization of carbon precursors with metal alkoxides).[197,246]

16.1.3.4 Interest of Nanostructured Electrodes for Electrochemical Sensing

The quest for increasing sensitivity and selectivity, as well as long-term durability of electrochemical sensors and biosensors has generated huge amounts of research work in past decades. One of the characteristics of porous materials is their high area surface/volume ratio, favoring thereby the interaction with external reagents. If they are electrically conducting, such materials deposited as thin films on electrode surfaces can contribute to increasing the electroactive surface by several orders of magnitude and thus also the sensitivity of the resulting device.[180,246,257,258] In addition, large surface area and the widely open, ordered macrostructure or mesostructure are expected to offer high preconcentration efficiency and fast diffusion processes, which should lead to very sensitive amperometric or voltammetric detection[44] and thus most applications deal with chemical sensors.

Macroporous and mesoporous metal electrodes have been used for various types of electrochemical sensing and biosensing. For example, an amperometric, nonenzymatic glucose sensor system based on three-dimensional ordered platinum films has been reported to display improved electrocatalytic activity toward glucose oxidation compared to directly deposited Pt, as a result of the large effective surface area and interconnectivity of pores in the macroporous metal.[259] A gold macroporous electrode modified with a nitrofluorenone monolayer has been used as a model system for studying the electrochemical oxidation of NADH.[260] Mesoporous Pt and Pd microelectrodes have been used as an efficient amperometric sensor for hydrogen peroxide and, after loading the huge internal Pd surface with hydrogen, these devices could be used successfully as very stable pH sensors.[261] Macroporous electrodes provide superior conductivities and interconnected pores that are likely to host large amounts of (bio)molecules at the monolayer level. Several redox proteins (hemoglobin, cytochrome *c*, D-sorbitol dehydrogenase etc.) have thus been adsorbed in various conducting and/or electroactive macrostructures and direct electron communication between the biomolecules and the electrode material has been reported.[262–264] Finally, heavy metal ions can be electrochemically detected at

macroporous metal electrodes, as exemplified for the anodic stripping determination of lead and cadmium at macroporous bismuth[153] or antimony[67] electrodes, or the amperometric analysis of mercury at a gold macroporous electrode modified with hexanedithiol.[265]

Mesoporous metal oxide electrodes, i.e., TiO_2, WO_3, Nb_2O_5, or Al_2O_3 films, have been utilized as attractive matrices for the immobilization of high levels of heme proteins without loss in the biomolecule structure or activity.[266–268] Direct electrochemistry of the proteins was claimed in all cases and this was exploited for the electrocatalytic detection of hydrogen peroxide, nitrite species, or nitric oxide. Mesostructured SnO_2 films were found to be sensitive to adsorbed ethanol and molecular hydrogen, leading to the development of selective sensors for these gases.[269] Applications of ordered mesoporous silica-based materials in electrochemistry have been reviewed,[270] but most of them are based on functionalized materials and thus belong to the modified electrodes section (see below). Finally, gas sensors designed from mesoporous thin silica films have been developed and they exhibit fast resistive-type response to relative humidity changes or alcohol vapors.[271–273] The nature of the surfactant template had noticeable impact on the resulting sensor performance.

Ordered macroporous and mesoporous carbon materials deposited as thin films on carbon electrodes have been applied as chemical sensors based on direct electrochemical detection (by amperometry or potentiometry), preconcentration electroanalysis, or electrocatalytic detection, OMC in addition to electrochemical biosensors.[258,274–276] Among selected analytes that have been detected using mesoporous carbon belong dihydroxybenzene or nitrotoluene and nitrobenzene derivatives,[277,278] methyl parathion,[279] L-cysteine and glutathione[275] or NADH.[280] In comparison to carbon nanotubes (CNTs) or graphite powder and glassy carbon, the electrocatalytic performance of mesoporous carbon was often claimed to be superior (better sensitivity, extended linear range, and lower detection limit), due to improved electron transfer kinetics and catalytic capabilities.[188,246,258] In addition, sorption properties of OMC can be exploited to accumulate the analyte prior to electrochemical detection. This has been applied, for example, for determination of hydroquinone,[281] ultra trace of nitroaromatic compounds or nitrobenzene.[282] The anodic stripping voltammetry determination of metal ions, such as Pb^{2+} at Nafion-OMC[283] or Cu^{2+} and Pb^{2+} at polyaniline-OMC.[284] Ordered macroporous carbon monoliths prepared by the colloidal crystal templating have been used as novel and effective solid contacts in ion-selective electrodes.[285] By selecting appropriate ionophores, they were successfully applied to the highly sensitive detection of K^+ and Ag^+ cations. Contrary to the conventional ion-selective electrodes, they also offer the advantage of not requiring an optimization of the inner filling solution, and exhibited excellent long-term stability and good resistance to oxygen interference.[188]

16.2 Modification of Electrode Surfaces

Chemically modified electrodes (CMEs) are part of the so-called integrated chemical systems,[286] gathering assemblies of a number of different chemical components, each specially selected to carry out a particular function, put together in a well-defined way in order to produce a functional structure. Compared with the "conventional" electrodes, the distinguishing feature of a CME is that a modifier is intelligently combined to an electrode surface to endow the electrode with the chemical, electrochemical, optical, electrical, transport, and other desirable properties of the modifier in a rational way, most often determined by the target application.

From the historical point of view, in early 1973, Lane and Hubbard studied by electrochemistry the irreversible chemisorption of a monolayer of alkenes on platinum electrodes.[6,7] They were the first to suggest the possibility of modifying the electrode surface to achieve a desired functionality. In 1976, Elliott and Murray had foreseen the potential of chemically modified electrodes as they described "this line of research as leading to a wide array of chemically modified electrode surfaces with unusual analytical, chemical, catalytic, and optical properties".[287] In the two decades that followed this initial breakthrough, the research field of chemically modified electrodes has boomed, leading the International Union of Pure and Applied Chemistry (IUPAC) to publish two sets of recommendations in 1997 and 1998.[288,289] The IUPAC defines a chemically modified electrode as "an electrode made of conducting or semiconducting material that is coated with a selected monomolecular, multimolecular, ionic, or polymeric film of a chemical modifier and that by means of faradaic reactions or interfacial potential differences exhibits chemical, electrochemical and/or optical properties of the film".[288] Seven classes of chemically modified electrodes for analytical applications were then defined: accumulation, chemical transformation, electrocatalysis, permeability, ionic equilibria, controlled release, and change of mass.[289] Among these seven classes, chemically modified electrodes based on accumulation, electrocatalysis, and permeability are the most documented in the literature. The surface of electrodes for accumulation is designed for the selective binding of target analytes during a nonelectrolytic preconcentration step. Analogously to stripping voltammetry, the preconcentration step is followed by a detection step. This class of chemically modified electrodes has been widely developed over the years[290,291] and has been used for the detection of a wide range of target analytes (heavy metals, organic molecules, proteins...). The electrode surface can also be modified to amplify catalytically the detection signal of the target analyte, resulting in the improvement of limits of detection, sensitivity, and selectivity. Such electrocatalytic sensors include biosensors based on enzyme immobilization. Electrochemical sensors based on permeability operate on discriminative transport through a coating, which lets the target analytes reach the electrode surface while fouling and interfering species are kept away from the surface. Most of the electrochemical sensors and biosensors are operating under one of these three principles.

CMEs have been classified into three categories: (1) monolayers, (2) homogeneous multimolecular layers, and (3) heterogeneous multimolecular layers.[292–294] The first category involves electrode surfaces prepared by the formation of a single monolayer that bears the desired functions. These include self-assembled monolayers (made from thiols, silanes and diazonium salts), and also adsorbed materials. The second category gathers all homogeneous multimolecular layers of organic and inorganic nature that can be deposited onto electrodes. These coatings include organic polymers and inorganic films; which can be generated chemically or electrochemically onto the electrode surface. Thirdly, heterogeneous multimolecular layers or bulk composite-modified electrodes can be prepared and used as electrode materials. The following sections will describe these three approaches for electrode modification, with special focus on CMEs used for environmental analysis purposes.

16.2.1 Monolayers

The formation of a single monolayer on the surface of an electrode relies on the chemisorption or the formation of a covalent bond between a molecule and surface atoms. Three molecule families are reported for the development of electrodes modified in the view of analytical applications: thiols, silanes, and diazonium salts. These monolayers are called self-assembled when organization of the molecules constituting the monolayer present a degree of self-organization achieved during the modification process.

16.2.1.1 Self-Assembled Monolayers: Thiol Monolayers

Preparation and Characterization Methods of Thiol-Based Sensors

Thiol molecules present a high affinity for metal (e.g., mercury, gold, silver, platinum, palladium, copper) and semiconductor (e.g., InAs and GaAs) surfaces on which they spontaneously adsorb to form a monolayer.[28] Gold has been very popular for the preparation of electrodes modified with a densely packed thiol monolayer since the early work by Nuzzo and Allara.[11] The formation of a thiol self-assembled monolayer is described as a two-step process (Fig. 16.7). During the first step, thiols adsorb spontaneously through the cleavage of the H–S bond to form a bond between the gold atoms of the surface and the sulfur atom. This step is relatively fast and the surface of an electrode can be covered within minutes. Spontaneous adsorption of thiols occurs when the electrode is immersed in an aqueous or ethanolic solution. Potentiometric studies suggest that thiol adsorption results in a drop of the open-circuit potential, indicating that a negative charge is transferred to the electrode surface, inducing the reduction of the proton of the thiol group to hydrogen.[295,296] Once adsorbed on the surface of the electrode, thiol

Fig. 16.7 Schematic representation of the two-step process leading to the formation of a complete monolayer

molecules can move around the surface despite a reasonably strong Au–S interaction. This mobility allows self-assembly of the thiol molecules to form a densely packed monolayer covering the entirety of the surface with limited defects. It is a much slower process than adsorption and it may require up to 16 h to form a dense self-assembled monolayer. The quality of the self-assembly is very much dependent on the alkyl chain length and of the terminating group of the thiol considered. Relatively defect-free self-assembled monolayers are usually formed with thiols with octyl chains or longer. The closely packed structure of a self-assembled monolayer is the result of van der Waals forces and electrostatic interactions between adjacent thiol molecules. As the alkyl chain increases, these interactions between neighboring molecules grow stronger conferring to the modified electrode a blocking behavior. Indeed, underpotential deposition of metals (Tl, Pb, Ag, Cd, Cu, and Bi) was possible at a gold electrode modified with a self-assembled monolayer of propanethiol, whereas it was strongly inhibited at octanethiol- and hexadecanethiol-modified electrodes.[297]

The stability of thiol self-assembled monolayers was investigated by electrochemistry.[298–300] Electrodes modified with thiols have a limited potential window for which the Au–S bond is stable. Thiols can be desorbed by either reduction or oxidation. The stability of the Au–S bond depends on the nature of the functional group and of the length of the alkyl chain. The desorption peak potential is linearly dependent on the alkyl chain length.[299] On the other hand self-assembled monolayers of thiol with a long alkyl chain were desorbed at more negative potentials than the ones with short alkyl chain. This increased stability is due to stronger lateral interactions between adjacent molecules as the alkyl chain increased.[300] It was also shown that crystallinity and quality of the electrode surface also influenced the desorption potential as well as the number of desorption peaks. Scanning tunneling microscopy studies have shown that the terminating group has an effect on the monolayer structure.[301] For thiol with different functional groups (–CH_3, –OH, –COOH, –SO_3H) and of same alkyl chain length, Esplandiú et al. have calculated that ethanethiol and mercaptoethanol formed a densely packed structure with an area per molecule of 21.6 $Å^2$ whereas the surface area per molecule in the case of monolayers of mercaptopropionic acid or mercaptosulfonic acid increased to 43 $Å^2$, suggesting a less compact layer. These differences of structure of the self-assembled monolayers have led to the formation of mixed monolayers of two different thiols: one spacer molecule (e.g., alkanethiol, alcohol thiol or amine

thiol), whose role is to form a densely packed monolayer, and a functional molecule (e.g., amino-terminated thiol, carboxylate-terminated thiol, or azide-terminated thiol), which provides reactivity to the modified surface.[28] This strategy is particularly useful in the case of the attachment of large molecules such as proteins[302] and DNA probes.[303] Finally, the stability of self-assembled monolayers was investigated over a period of several weeks of immersion in a variety of biological media.[304] It was shown that the desorption of the thiol monolayer was observed after 35 days probably due to the oxidation of the thiolate group.

Accumulation Sensors

Accumulation sensors are based on the recognition of the target analytes by the selective monolayer formed at the surface of the electrode. Such chemically modified electrodes can be prepared by the immobilization of commercially available thiols, forming a monolayer generally used for the detection of metal ions and small organic molecules.[28] Detection of certain kinds of target analyte requires the engineering of more complex electrode surfaces. In these cases, the electrode surface is further modified by a series of chemical steps leading to the attachment of a recognition element (ligand, antibody, aptamer. . .) which provides selectivity and specificity to the electrode surface.[305] In these cases, the thiol self-assembled monolayer is used as an anchor to attach the recognition element. One of the most common attachment methods involves the formation of a carboxylic acid-terminated self-assembled monolayer, which reacts with 1-(3-dimethylaminopropyl)-3-ethyl-carbodiimide (EDC) and *N*-hydroxysuccinimide (NHS).[306–313] Another option is based on an amine-terminated self-assembled monolayer, which reacts with glutaraldehyde.[314,315] Biomolecules can then be immobilized on the surface of the electrode through the reaction of terminal $–NH_2$ group. A vast number of strategies, protocols and methods exist for the controlled immobilization of biomolecules onto surfaces. We invite the readers to consult existing reviews on the topic for more details.[316,317] Accumulation sensors for the detection of heavy metals are among the most present in the literature. In 1997, Turyan and Mandler used an electrode modified with a self-assembled monolayer bearing a pyridinium group known to form complexes with CrO_4^{2-} and $Cr_2O_7^{2-}$.[18] Cr(VI) ions were accumulated at the surface of the modified electrode by immersion in a Cr(VI)-containing solution for 5 min under stirring. The electrode was then transferred to a Cr(VI)-free for the detection by linear sweep voltammetry (Fig. 16.8). The sensor thus prepared reached a limit of detection of 0.31 nM and was highly selective towards Cr(VI) as 0.1 ppb of Cr(VI) could be detected in the presence of 1,000-fold excess of Cr(III) without significant interferences. This milestone paper has triggered an interest for the development of thiol-based sensors for the detection of heavy metals in water samples.[310,313,318–330] A variety of thiols have been used to confer selectivity; 3-mercaptopropionic acid,[318,324] cysteine[319–321] are among the most common. The metals detected were Cu(II)[310,313,318–321,324,326,327,331] Pb(II)[313,318] Cd(II)[313,325] Hg(II),[330] CH_3Hg^+,[329] La(III),[322,323] uranyl[332] and Fe(III).[328] Gooding and coworkers covalently immobilized oligopeptides onto a

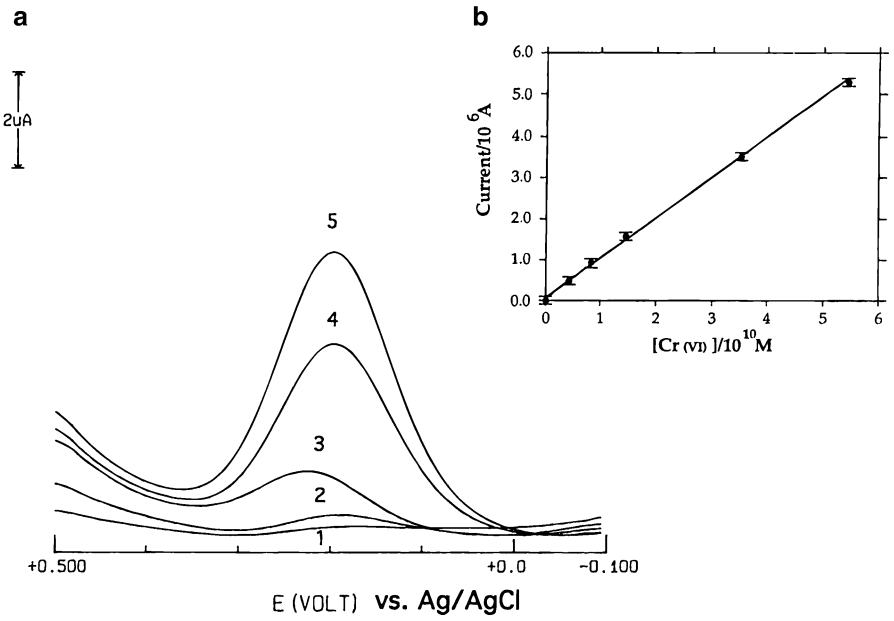

Fig. 16.8 (**a**) Square wave voltammograms of a 4-(2-mercaptoethyl)pyridinium-modified gold electrode after preconcentration of increasing concentrations of Cr(VI): (*1*) 0, (*2*) 0.42, (*3*) 0.83, (*4*) 3.53 and (*5*) 5.44×10^{-10} M; (**b**) Calibration curve for Cr(VI). Reprinted with permission from reference (18) Copyright (1997) American Chemical Society

self-assembled monolayer for the simultaneous detection of Cu^{2+}, Pb^{2+}, and Cd^{2+}.[313] They applied partial least squares regression with an array of sensors modified with four different peptides to determine simultaneously Cu^{2+}, Pb^{2+} and Cd^{2+}. The challenge here mainly resides in the overlap of the voltammetric signal of Pb^{2+} and Cd^{2+}, which was overcome by the statistical analysis given by the four different chemically modified electrodes.[313]

Electrodes modified with thiol self-assembled monolayers were also used for the detection of small organic molecules such as pesticides and toxins,[311,333–337] drugs[309,338] and explosives.[339,340] Proteins[341–344] and bacteria[306,312,314,345–348] can also be detected using electrodes modified with a thiol monolayer. The target analyte is accumulated at the surface of the chemically modified electrode at open-circuit potential. This preconcentration step is followed by a detection step which consists of running a voltammogram for the accumulated redox active analytes or an electrochemical impedance spectrum in the case of non-redox active proteins and bacteria. Electrochemical impedance spectroscopy is particularly well-suited to the detection of bulky molecules and biological entities as this technique is based on current variations caused by disturbances at the electrode solution interface.

Electrocatalytic Sensors

The electrode surface can be modified to allow a reaction to happen or to improve its kinetics. The most common electrocatalytic sensors are based on the immobilization of enzymes onto an electrode surface, taking advantage of the selectivity and efficiency of the biomolecule. Immobilized enzymes biocatalyze a reaction that consume the target analyte. As for sensors based on specific antigen—antibody or aptamer—protein interactions (described in the previous section), a thiol monolayer serves as an attachment layer to immobilize the enzyme. The immobilized enzyme has been selected for its sensitivity to the target analyte and its specificity against interferents. Nevertheless, attachment of the enzyme is not trivial and a special care must be taken for its orientation on the electrode surface to remain active.[316] As for accumulation sensors, enzymes are often immobilized through EDC-NHS[349–352] or glutaraldehyde.[353,354] Two main mechanisms are available for the electrochemical transduction. In the first case, the product of the enzymatic reaction is electrochemically active and is detected by amperometry. Inhibition sensors can also be used for the detection of pesticides. In this case, the presence of the pesticide inhibits the enzymatic reaction by slowing down its kinetics. Chemically modified electrodes based on horseradish peroxidase, tyrosinase, and acetylcholinesterase are using this approach for the detection of pesticides and phenolic compounds.[349–352] Enzymatic biosensors for the environment have been widely developed for the detection of small organic pollutants (e.g., phenol derivatives) and pesticides.[349–355]

Permeability Sensors

Although the vast majority of thiol-based electrochemical sensors are using electrodes modified with a densely packed self-assembled monolayer,[28] Markovich and Mandler introduced the notion that disorganized monolayers might present some properties beneficial from the analytical viewpoint.[356] They have demonstrated that they could control the level of organization of a decanethiol self-assembled monolayer by maintaining short spontaneous adsorption times, obtaining a “brush” type of monolayer with a large number of small pinholes and defects in the monolayer. These findings are in good agreement with previous work by Calvente et al.,[357] in which the impossibility to form a densely packed monolayer with mercaptoethane sulfonate was highlighted. The reasons for the disorganized nature of a mercaptoethane sulfonate monolayer were attributed to (1) the short alkyl chain limiting van der Waals lateral interactions, (2) steric repulsion between adjacent thiols due to the presence of the bulky and charged sulfonate groups, (3) incorporation of solvent molecules facilitated by the high water solubility of the sulfonate group. Herzog and Arrigan harnessed the disorganized monolayer approach to the detection of Cu and Pb via underpotential deposition in the presence of surface-fouling compounds.[358–360] Gold electrodes modified with mercaptoethane sulfonate and mercaptoacetic acid allowed underpotential deposition of Cu^{2+} ions at the surface of the electrode while surfactant molecules were maintained away from the

electrode surface, preventing its fouling. The disorganized monolayer approach offered a simple surface protection method for the detection of copper in soil extracts[361] and wine,[362] whereas bare gold electrodes were not operating properly. This method also bypasses any sample pretreatment normally necessary to remove dissolved organic matter susceptible to foul the electrode surface. Huang and Lin formed a disorganized monolayer on a nanoporous gold electrode reaching better sensitivities and limits of detection than with a smooth gold electrode.[363] The nanoporous aspect of the electrode surface increased the surface area of the electrode while a disorganized monolayer of (3-mercaptopropyl)sulfonate prevented the adsorption of surfactants. These nanostructured chemically modified electrodes were successfully used for the detection of Cu^{2+} in lake waters.

16.2.1.2 Electrode Modification by Electroreduction or Electrooxidation

Among the numerous methods commonly used for the formation of organic coatings on surfaces (plasma deposition of polymers, spin coating, vapor deposition usually employed for inorganic coatings, electrodeposition for coating conducting surfaces with metals, self-assembly. . .), electrografting is a powerful technique that allows the chemical modification of conducting and/or semiconducting surfaces with organic matter by formation of thin films (typically between one monolayer and 50 nm) via very strong substrate-molecule links. Several electrografting methods and their corresponding mechanisms of grafting have been described involving either electrochemical reduction or oxidation processes and eventually leading to the formation of covalent bonds of different nature.[364–368] The formation of a covalent bond between the electrode surface and the electrografted species should contribute to a major stability of the modified surfaces and would lead to an increasing number of applications, for example by providing a novel way to confine biomolecules on electrode surfaces.[369] Electrografting techniques are often separated in oxidative and reductive processes since the first ones can only be performed on nonoxidizable substrates. Among the most commonly employed reagents it should be highlighted the use of aliphatic amines, carboxylates, alcohols, Grignard reagents, vinylics, diazonium salts and halides as well.

Electrografting by Reduction of Diazonium Salts

A first sign of the formation of an organic layer on metallic surfaces by electrochemical reduction of aryl diazonium salts is the disappearance of the expected characteristic broad and irreversible cathodic wave observed by cyclic voltammetry upon an initial scan towards negative potentials. Such "blocking effect" of the electrochemical response was firstly pointed out by Parker and coworkers.[370] The different steps that take place along the electrografting process were established later on.[17,371] It has been demonstrated that the electron transfer concerted with the loss of

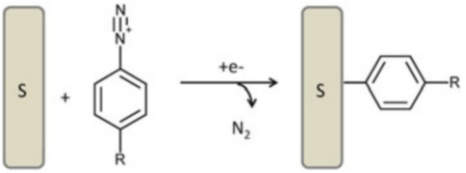

Fig. 16.9 Surface modification by electroreduction of aryldiazonium species

a nitrogen molecule leads to the formation of an aryl radical which is responsible of the organic layer covalently attached to the electrode surface (Fig. 16.9).[372]

The formation of the covalent bond is strongly supported by the long stability of the organic layer formed and its resistance to ultrasonication. The electrochemical modification is due to the reaction of some of the electrogenerated aryl radicals with the surface whereas the aryl radicals remaining in solution can undergo hydrogen abstraction from the solvent, further reduction, dimerization or even decomposition depending on the nature of the solvent. Some of the products formed following these alternative routes can be deposited on the surface and readily removed by rinsing. Even if they are described here in the monolayer section, the organic layers usually obtained can have thicknesses ranging from monolayers to multilayers that can be simply modulated by controlling the charge consumed during the electrografting process. Tuning both the potential and the electrolysis time allows a careful control of the charge during the electrografting process leading to the formation of a monolayer.[373] AFM measurements have been used to determine the thickness of the layers growing on glassy carbon[374] and highly ordered pyrolytic graphite[375] surfaces respectively. Several mechanistic approaches have been proposed to rationalize the formation of multilayers[366] and the formation of azo bonds growing from the first layer obtained on the electrode surface as well. The formation of a multilayer has been explained starting with the electrochemical reduction of two molecules of a diazonium salt as a first step. One of the aryl radicals formed close to the electrode surface would be able to bind the substrate whereas the other one would react with the phenyl group already grafted on the surface. The mechanism proposed for the formation of multilayers on carbon and metals is outlined in Fig. 16.10. Two routes, *A* and *B*, must be considered with a common first step consisting of the monoelectronic reduction of the diazonium salts (R1). Considering the reduction of two molecules, one of them will react with the substrate (R2) while the second one will be able to attack the phenyl group already grafted on the electrode surface leading to a grafted cyclohexadienyl radical (R3). According to route A, the attached radical can react with an aryl radical leading, through reaction R4 and R5, to a pure polyphenyl layer. The reaction of the cyclohexadienyl radical with a diazonium cation (route B) would be also possible leading to the formation of azo bonds in the polymeric chains (R6). Reaction R6 leads to a radical cation that should be easily reduced (R7). The re-oxidation (R8) of the cyclohexadiene obtained through R7 is favored, being the driving force for this reaction the re-aromatization and higher degree of conjugation of the two substituents. This mechanism explains both the growth of polyphenyl layers during the electrografting process and the presence of azo bonds in these multilayers.

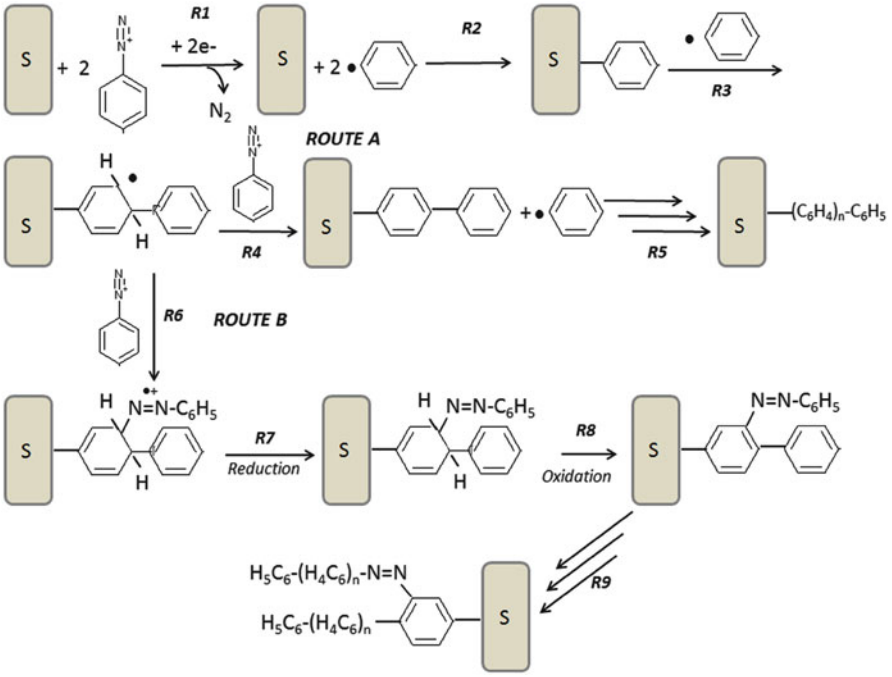

Fig. 16.10 Schematic mechanism of formation of multilayers during electroreduction of aryldiazonium species. Reprinted with permission from reference (366) Copyright (2007) American Chemical Society

Diazonium salts have been electrografted on a variety of substrates: various forms of carbon such as highly ordered pyrolytic graphite (HOPG),[376,377] graphene,[378–380] glassy carbon plates,[17,371,381] carbon fibers[382] and nanofibers,[383] carbon felts,[384] carbon blacks,[385–387] ordered mesoporous carbons,[388–390] carbon nanotubes[391,392] and/or diamond,[393–396] silicon,[397–400] AsGa[401] and InAs/GaAs quantum dots,[402] noble,[403–405] coinage[406] or industrial metals[407–409] and nanoparticles,[410–413] and oxidized surfaces such as indium tin oxide (ITO),[414] SnO_2[415] and TiO_2.[416] Inorganic substrates such as SiO_2, SiOC and SiC[417] can also be derivatized. The electrochemical modification can be carried out either in acidic aqueous media when a protic solvent is required or mainly in acetonitrile when an aprotic organic media is used.

Alternatively to the electrochemical reduction, spontaneous formation of a covalent bond has been also observed on carbon,[418–426] gold,[427] Si, Ga, As and Pd[401] and/or metallic surfaces such as Ni, Cu, Zn or Fe, which are able to reduce the diazonium cation,[428] avoiding the electrochemical step.

An important number of chemical sensors exist based on diazonium electrochemically grafted surfaces.[424,429–436] These modified surfaces have been used to detect ions and a variety of molecules of pharmaceutical, toxicological, environmental, or biological interest. A first example dealing with sensing applications of

Table 16.3 Examples of chemical sensors based on diazonium chemistry-modified surfaces and their applications

Substrate	Diazonium salt (DS)	Application
Carbon, gold	• Dimethoxy hydroquinone DS • Phenyl acetic DS bonded to glucose oxidase • 4-Carboxyphenyl DS • 4-Nitrobenzene DS followed by the reduction of the nitro functional group and attachment of the EDTA • Aminophenyl DS attached to horseradish peroxidase • 4-Nitrobenzene DS followed by the reduction of the nitro functional group to aminophenyl and pyrroloquinolinequinone	• pH sensor[429] • Selective detection of dopamine in the presence of ascorbic acid[424,430] • Accumulation of Cu(II) with no interference of Pb (II) in tap waters; detection of uranium[431,432] • Detection of Pb(II)[433] • Detection of levetiracetam (antiepileptic drug)[434] • Detection of NADH[435,436]

the monolayers obtained by electrochemical reduction of aryl diazonium salts was based on the use of a glassy carbon electrode modified with 4-phenyl acetic acid diazonium tetrafluoroborate to which glucose oxidase was covalently bound to the modified electrode surface.[437] Table 16.3 summarizes some examples of the modified electrodes as chemical sensors.

The electrochemical reduction of diazonium salts has been also used for the development of DNA biosensors.[438] In this sense, DNA oligonucleotides have been attached to carbon,[439,440] diamond[441,442] and silicon.[443] Two strategies have been developed to this aim. A first strategy is based on the attachment of the activated nucleotides to diazonium-modified substrates[439,443] whereas a second approach involves the diazotization of the aminophenyl groups of the analyte which is electrochemically addressed to the substrate.[444]

Analogous procedures have been employed for the development of other biosensors, mainly based on the attachment of proteins and enzymes to surfaces. For instance, 4-aminophenylnitrilotriacetic acid-modified screen-printed carbon electrodes that can chelate Cu(II) and Ni(II) ions, were used to bind a histidine tagged horseradish peroxidase or a green fluorescent protein.[445] In addition, a lot of enzymes such as monoamine oxidase,[446] glucosidase,[447] hydrogenase[448] and cytochrome[449] have been attached to different carbon surfaces, gold and polymers. Fast electron transfer,[450] and full activity of the enzymes[451] are among some of the requirements that must be accomplished in order to use the attachment of these biomolecules for electrochemical detection purposes.

Electrografting by Reduction of Vinylics

The electrochemical reduction of acrylonitrile was the first example of the formation of a covalent bond from vinylic compounds leading to the formation of thin polymeric layers on metallic cathode surfaces.[449–451] The formation of a chemical

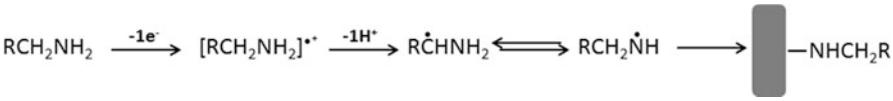

Fig. 16.11 Electrochemical oxidation of alkyl amines and their grafting mechanism

bond has been proved between the surface and the polymer. The electrografting mechanism has been rationalized according to a first flat adsorption of the vinylic monomer[452–457] on the surface followed by an electron transfer process which leads to a radical anion responsible of the formation of the covalent bond. The negative charged species bonded can be stabilized by the attack of a new monomer that creates a bonded dimer anion with a negative charge further away from the electrode. The polymerization can continue along an anionic mechanism. It should be noted that only the initiation step involves an electrochemical process, the growth of the polymeric layer being a purely sequence of chemical reactions.

Vinylic compounds have been attached by electrochemical reduction to an important number of oxidizable materials such as Fe, Ni, Cu, Au, Pt or stainless steel, but also carbon, silicon, CdSe and Teflon.[450–465] Most of metals can be covered with oxides which could be reduced by the application of negative potentials during the electrografting process. However, the possibility that the electrografting occurs also on oxidized sites cannot be ruled out.

The electrografted polymeric films can be loaded with different substances allowing the development of new composite materials.[466,467] To obtain modified surfaces with specific properties, more complex polymers have been electrografted. For instance, an acrylate with a *N*-succinimidyl group, highly reactive with nucleophiles, has been substituted by a ferrocene group or even by biotin-avidine moieties.[468,469] The electrografted layers possessing appropriate functional groups have been further modified by performing chemical reactions leading to additional derivatization of the layers with biomolecules and other targets.

Electrografting by Oxidation of Aliphatic Amines

Aliphatic amines are electrochemically oxidized by an irreversible and slow electron transfer followed by a chemical step consisting of the deprotonation of the corresponding radical cation leading to the formation of radical species capable to form a covalent bond with the electrode surface (Fig. 16.11).[470] The formation of an organic layer on an electrode surface by electrochemical oxidation of an alkyl amine was firstly described on carbon surfaces[471–474] and then on Au, Pt,[475] and p-Si.[476] A large variety of amino derivatives have been electrografted (simple alkyl amines, amines substituted with ferrocene and thiazole groups, different amino acids, benzylic amines with nitro and phosphonic groups and so on).

The organic layers obtained have been characterized by electrochemical techniques when the alkyl amines employed contained electroactive groups such as nitro groups, and also by X-Ray Photoelectron Spectroscopy (XPS),[470–472,477,478]

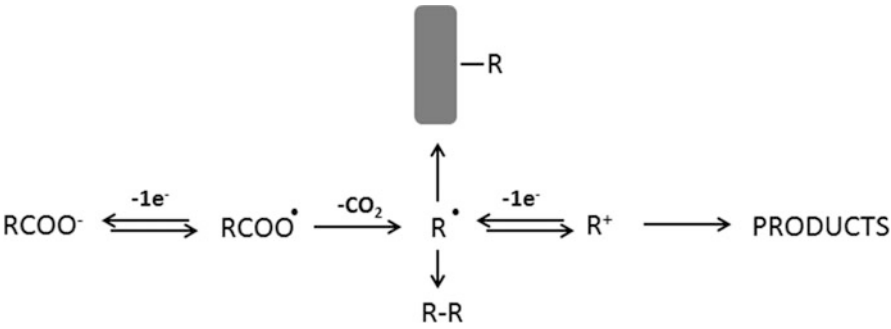

Fig. 16.12 Electrochemical oxidation of carboxylate and subsequent grafting of generated radical

infrared spectroscopy,[470,478] quartz crystal microbalance,[375,376] atomic force microscopy (AFM), scanning electron microscopy (SEM)[479] and electrochemical impedance spectroscopy (EIS).[473,477,479,480] The characterization carried out by IR using partially deuterated amines and the XPS measurements[470] made possible to conclude that the covalent bond is formed through the N atom of the amino group (Fig. 16.11).

These modified surfaces have been used for chemical analysis, attachment of biomolecules, catalysis and electrocatalysis. For instance, electrodes modified by oxidation of amino acids have been used for the determination of dopamine in the presence of ascorbic or uric acids,[481,482] a biosensor has been developed by electrochemical oxidation of thionine where multilayers of horseradish peroxidase were growth by employing glutaraldehyde as a coupling reagent displaying a fast response and low detection limit.[481] Redox catalysts have been also grafted to electrode surfaces by means of the electrochemical oxidation of alkyl amines. In this sense, a histamine-coordinated Os complex has been synthesized as a model redox amine attached to a carbon surface by electrografting and used as an electron transfer mediator between the electrode and a model enzyme.[483] In addition, these N-modified surfaces have been used to prevent the adsorption of biomolecules on the electrode surfaces. In this sense, the electrografting of tetraethyleneglycoldiamine contributes to the reduction of the adsorption of several proteins on surfaces.[484,485] Such modified surfaces have been also used to develop pH sensors,[486] H_2O_2 biosensors,[481] or to immobilize DNA by oxidation of ethylenediamine on carbon nanotubes.[487]

Electrografting by Oxidation of Carboxylates

The electrochemical oxidation mechanism of carboxylates is closely related to the Kolbe reaction.[488,489] The mechanism (Fig. 16.12),[490] consists of a first oxidation leading to the formation of $RCOO^{\bullet}$ type radical species which upon decarboxylation will lead to the formation of $R^{\bullet}$. The rate of the decarboxylation process is

quite fast, so that the formation of such radical species takes place close to the electrode surface and they could react with it. Simultaneously, these radical species $R^{\bullet}$ are much easier to oxidize than the starting material, $RCOO^{-}$, and at the applied potential some of them could be also oxidized to the carbocation R^{+}. The formation of carbocationic species has been proved since compounds coming from their reaction with nucleophilic species have been detected. A competitive mechanism is proposed but the electrografting mechanism should be favored when the radical is formed close to the electrode surface. The film thickness corresponds to 3–4 molecular layers (from 2.0 to 3.3 nm) and has been estimated by AFM.[491] This electrografting process has found application mainly in the field of catalysis and electrocatalysis.[492–494]

16.2.1.3 Other Types of Monolayers on Electrodes

Self-assembled monolayers can also be formed by the covalent attachment of a silane molecule onto a surface made of SiO_2, TiO_2 or indium tin oxide.[28] The first example of self-assembled monolayer was presented by the early work of Jacob Sagiv in 1980.[495] Silane functional groups react with hydroxyl surface groups to form a covalent bond between the substrate and the Si atoms. Monolayers thus formed are more chemically and mechanically stable than thiol self-assembled monolayers.[496] Nevertheless, they are more difficult to form as a more stringent control of the experimental conditions (solvent nature, water content, reaction time, temperature) is needed. Indeed, the ability of silane to undergo hydrolysis in the presence of water and condensate to form multilayers is an hindrance to the formation of self-assembled monolayers. The quality of the self-assembly also depends on the alkyl chain length and on the functional group nature as it has been seen for thiol monolayers. The difficulty to form a silane monolayer, compared to the simplicity of thiol chemisorption on gold, has limited the number of electrochemical sensors based on silane self-assembled monolayers.[497–500] Silane monolayers have found more applications in the domains of molecular electronics[501] or of sensors whose transduction mechanism is based on physical principles (e.g., surface acoustic wave) rather than on electrochemical ones.[502,503] The electrode surface can be modified by silanes via the sol–gel chemistry route, which leads to the formation of multimolecular layers. The environmental applications of such chemically modified electrodes will be presented in a following section. Organophosphonic acids are another family of molecules known to form a self-assembled monolayer onto indium tin oxide substrates.[504,505] Although no chemically modified electrodes based on organophosphonic acids monolayers have been developed for sensor applications, the transparent nature of the indium tin oxide electrode might spark some interest for sensing applications.

16.2.2 Homogeneous Multimolecular Layers

16.2.2.1 Organic Polymers

In the late seventies, the work of two different groups reported the electrochemistry of electroactive polymers (poly-*p*-nitrostyrene and polyvinylferrocene) adsorbed on platinum electrodes.[8,9] Since, polymers have been used to provide new functionalities to electrode surfaces. The next subsection will present briefly the different methods described in the literature for the preparation of polymer-based electrodes for environmental applications. As for the monolayer-modified electrodes, three main classes of electrochemical sensors (accumulation, permeability and electrocatalytic) have been developed for environmental analysis as they are described by the IUPAC.[289]

Preparation of Polymer-Based Sensors

Polymer-modified electrodes can be prepared either by direct deposition of polymer onto the surface (via drop-, dip- or spin-coating methods) or by polymerization onto the electrode surface (via chemical, electrochemical or photochemical routes).[290] The simplest method to prepare a polymer-based sensor is by drop-coating a small volume of polymer dissolved in a solvent. With time, the solvent evaporates leaving the polymer adsorbed onto the electrode surface. Dip- and spin-coating methods have also been used to obtain more uniform films. These methods are used when polymers are already synthesized and need to be immobilized as they are. In situ polymerization is another effective method to prepare polymer-modified electrodes. For electropolymerization, the electrode is immersed in a monomer solution (e.g., pyrrole, thiophene, phenol, aniline. . .) and a suitable potential (either cathodic or anodic) is applied to allow the formation of the polymer film on the electrode surface. Photopolymerization is rarer in the case of electrochemical sensors. Nevertheless, poly(vinyl alcohol) functionalized with styrylpyridinium and acrylated polyurethane have been used for the development of electrochemical sensors.[506]

Secondary Modifications

Modification of electrode surfaces with polymer is seeking the same objective as with monolayers, i.e., the improvement of the analytical performances in terms of selectivity and sensitivity. These improved performances can be achieved by the nature of the polymer itself (e.g., perfluorinated cation-exchanger Nafion®) or by the incorporation of chemical functionalities. Recognition elements (e.g., biomolecules, ligands) can be entrapped during the polymerization process (electro- or photopolymerization) or attached after polymerization by chemical grafting or by

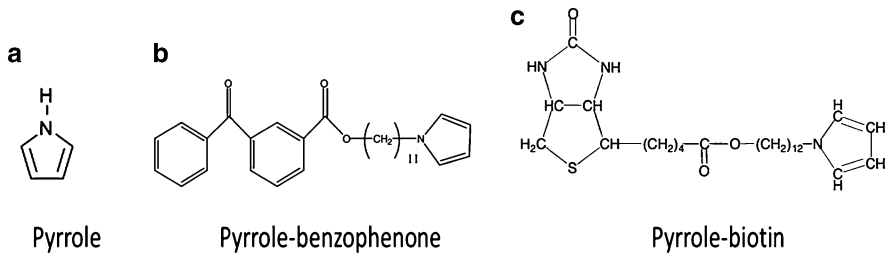

Fig. 16.13 Examples of electropolymerizable monomers for the immobilization of biomolecules by entrapment (**a**), covalent attachment by photografting (**b**) and affinity interactions (**c**)

affinity interactions (e.g., biotin-avidin interaction or nitrilotriacetic acid—metal ions—histidine) (Fig. 16.13).[506–508]

Biomolecules such as enzymes can be physically trapped in the polymer matrix during the electropolymerization process as it was first demonstrated in 1986 for glucose oxidase.[12,13] In theory, this method takes advantage of a 3D bulk polymer matrix, which allows a higher enzyme loading per unit area than a 2D monolayer. However, this implies that all the enzymes trapped remain accessible, the polymer matrix allowing the diffusion of the analyte, which is not necessarily true. The strength of the physical entrapment method resides in its simplicity as it is a one-step procedure, although leaching of the biomolecules into the solution implies a decay of the sensor performances over time. This loss of biomolecules and the difficulty to access trapped biomolecules have encouraged research efforts towards the attachment of biomolecules to the polymer matrix by either covalent bond or by affinity interactions. In 1990, glucose oxidase was covalently attached to a polypyrrole-modified electrode by EDC-NHS chemistry.[509] Since, a number of covalent attachment strategies have been developed using polymer films bearing surface active groups such as amine, aldehyde, *N*-hydroxinaphalimide or benzophenone groups.[508] Although, covalent attachment of biomolecules improves the overall stability of the sensor, it is not necessarily optimum as the biomolecule orientation is not controlled, which eventually lead to a loss of selectivity and sensitivity. The immobilization of biomolecules by affinity interactions can circumvent this drawback. Avidin was used as a bridge between biotinylated polymer films and biotinylated molecules. The possibility to use such polymer-based electrodes for sensing applications was demonstrated by the immobilization of galactose oxidase[510] and glucose oxidase,[511] both enzymes were biotinylated before immobilization. Biomolecules can also be immobilized by the formation of a complex between nitrilotriacetic acid—metal ions—histidine-tagged biomolecule.[512,513] Finally, molecularly imprinted polymers are a specific branch of polymers for which the recognition element is imprinted in the matrix during the polymerization process.[514–516] Molecularly imprinted polymers are prepared from a mixture containing the monomer and the target analyte, whose role is to act as template (Fig. 16.14). After polymerization, the target analyte molecule is extracted, leaving its imprint in the polymeric membrane. Unlike the other types

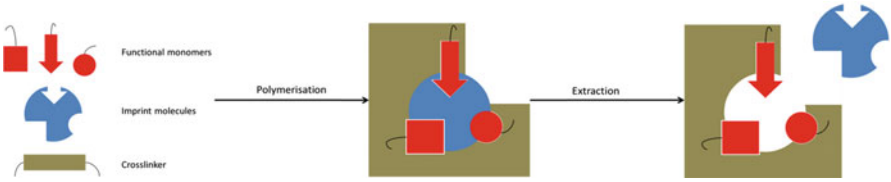

Fig. 16.14 Schematic representation of the molecularly imprinting principle

of chemically modified electrodes, the recognition element is not a molecule added to the polymer matrix but is imprinted with the 3D polymer matrix.

Accumulation and Permeability Sensors

As for other types of chemically modified electrodes, heavy metal ions have been a target of choice, this topic being well-documented by an abundant literature. Typically, Cu(II), Pb(II), Cd(II), Ag(I) and Hg(II) are among the most common analytes.[517–527] The role of the polymer layer on the electrode can either provide protection from surface fouling or selectivity toward the target analyte. In 1987, Florence and coworkers demonstrated the use of Nafion films as a permselective layer that allowed the diffusion of metals to reach the electrode surface while organic substances and proteins were maintained away, avoiding surface fouling.[14,15] Nafion serves a dual role as it is a cation-exchange polymer and hence was favorable to the detection of heavy metals by anodic stripping voltammetry as it was protecting the surface. A number of chemically modified electrodes were developed for the detection of heavy metals based on Nafion films.[528–531] Originally used to protect mercury-film electrodes, the interest for Nafion in environmental applications has seen a resurgence with the development of bismuth film electrodes.[532–536] Electrodes modified with conducting polymers have also been used for the heavy metals detection. Their selectivity was assured by the entrapment of ligands in the polymer matrix,[517–519] polymers functionalized with ligands (EDTA, malonic acid. . .).[520–527] Heavy metals are generally detected by pulsed voltammetry techniques with detection limits in the nM range. Molecularly imprinted polymers have been developed for the detection of small organic molecules relevant to environmental applications.[537–559] These include pesticides,[537–546] polycyclic aromatic hydrocarbons,[547–549] industrial pollutants,[550] antibacterial agents[551] and drugs.[552–559] The target analyte is detected by pulsed voltammetry after an accumulation at open-circuit potential for up to 20 min. The detection limit usually ranges from μM concentrations down to nM concentrations.

Electrocatalytic Sensors

Although the vast majority of enzymatic biosensors based on polymers is developed for the detection of glucose and other biologically relevant molecules, there are some examples of biosensors for environmental applications.[506–508] One of the most common example is the use of tyrosinase (also known as polyphenol oxidase) for the detection of phenol derivatives.[560–565] The enzyme can be immobilized in a polypyrrole or polyaniline matrix by either entrapment, covalent attachment or biotin—avidin interactions. Limits of detection between 10 nM and 1 μM have been reached by amperometry. Biosensors for the detection of pesticides have been based on the immobilization of acetylcholinesterase enzymes in polymer matrix.[566–571] These biosensors are based on the inhibition of acetylcholinesterase activity by the presence of pesticides. The enzymes are immobilized by entrapment, cross-linking or covalent immobilization. Detection by potentiometry or amperometry has led to limits of detection in the picomolar range whereas potentiometric limits of detection were in the submicromolar range. Higson and colleagues have reached an astonishing limit of detection of 10^{-17} M, which they attributed to the benefit of three factors.[570] A highly sensitive recombinant enzyme is immobilized on the electrode, the enzyme inhibition is amplified and finally, the hemispherical diffusion to the microscopic protusion of acetylcholinesterase—polyaniline protusions they observed on the surface of the chemically modified electrode improves the mass transport. Such surprisingly low limits of detection have been obtained in laboratory solutions and have not been repeated on real samples. In recent years, nano-objects such as metal nanoparticles and carbon nanotubes, have been incorporated inside the polymer matrix to boost the sensitivity and limits of detection achieved.[572]

16.2.2.2 Inorganic Thin Films

The interest for inorganic matrices, e.g., metal oxides, in electroanalysis arises from their properties, basically different from organic polymers, because of the nature of the material.[573] For instance, a metal oxide can be either conductive, semiconductive or insulating depending on its composition and the process used for its fabrication, which corresponds to a very wide range of materials, from pure inorganic materials to organic–inorganic hybrids.[258,574,575]

Conductive electrodes based on metal oxide, e.g., indium-tin oxide (ITO), are widely used in electrochemistry as a support for surface modification with the goal to develop sensors with electrochemical transduction or combined spectroscopic and electrochemical responses[45,46,576–580] or electrochemiluminescence.[581,582]

Inorganic thin films can also be prepared from the assembly of two-dimensional layered inorganic solids, such as cationic clays and layered double hydroxides (LDHs, also defined as anionic clays).[583–585] These materials can be used to preconcentrate species on the basis of ion-exchange reactions and applied to heavy metal determination or for the detection of organic pollutants,

e.g., endosulfan.[584] Such inorganic particles have also been used for protein immobilization, the layered material being also able to intercalate redox mediators useful to the operation of bioelectrochemical sensors.[585] The inhibition of activity of the protein in the presence of a pollutant, e.g., Hg(II), can also be advantageously exploited for the detection of this pollutant.[585]

Metal oxides with controlled porosity and reactivity constitute another class of materials for which large developments have been performed in the past 20 years.[241,586] The preparation of thin films has been thoroughly investigated notably for electrochemical applications, including energy conversion[246] or electroanalysis.[188,573] A large overview on the preparation and properties of inorganic and hybrid mesoporous films has been published some years ago.[196] More recently, a review appeared on the electrochemical approaches for the fabrication and/or characterization of pure and hybrid templated mesoporous oxide thin films.[245]

The purpose of this section is to provide some information about the preparation of inorganic thin films with controlled porosity and reactivity on electrodes. Then, their interest for environmental analysis is briefly discussed.

Preparation of Mesoporous Thin Films on Electrode

Inorganic thin films can be deposited onto an electrode surface by controlled evaporation of a starting sol.[587–589] Gelification and templating are induced by the solvent evaporation occurring in the course of deposition (usually made by dip-coating, spin-coating or any other process involving evaporation[590]). Various organic templates have been used (i.e., CTAB, pluronic F127, P123, Brij56, ...), leading to mesostructured films with distinct symmetry (cubic, hexagonal, double gyroid, rhombohedral, ...).[242] The deposition of inorganic films can also be achieved electrochemically by electrolysis, inducing a pH change at the electrode/solution interface. This local pH modulation leads to a precipitation (OH^- species are likely to react with metal ions)[591,592] or a gelification (acceleration of the polycondensation step in the sol–gel process)[593,594] of the metal oxide onto the electrode surface. These particular methods of electro-assisted deposition can be advantageously combined with soft templating to prepare mesostructured films.[595–601]

Functionalization to Get Organic–Inorganic Hybrid Films

The interest of mesoporous oxides for electroanalysis is related to their high specific surface area available for preconcentration of the analytes (typically heavy metals or organics).[575] In this respect, their properties can be tuned/extended by durable functionalization of the inorganic framework with selected organic moieties.[602] Two main routes, i.e., grafting or cocondensation, have been described to get mesoporous organic–inorganic hybrid films bearing organic functionalities that are linked through strong covalent or iono-covalent bonds. Grafting the surface of

the inorganic porous film can be obtained by using appropriate reagents, i.e., organo-alkoxysilanes or organo-chlorosilanes on silica-based materials,[603,604] or other binding groups such as phosphate, phosphonate, carboxylate, and polyphenol, which are likely to bind strongly the metal centers of TiO_2- or ZrO_2-based mesostructured metal oxides.[605,606] The cocondensation is obtained in one-step by the reaction of tetraalkoxysilane ($(RO)_4Si$) and organo-trialkoxysilane ($(RO)_3Si\text{-}R'$) reagents via the sol–gel route.[607,608] Bridged silsesquioxanes, $(RO)_3Si\text{-}R'\text{-}Si(OR)_3$, can also be used to form so-called periodic mesoporous organosilica (PMO) displaying a full integration of the organic groups into the mesopore walls.[609–611]

Biomolecule Immobilization

Mesoporous materials with controlled porosity and functionality have been used to immobilize biomolecules, e.g., proteins.[612] Enzymes of small or medium size such as cytochromes, oxidases, peroxidases, lipases or proteases, can be immobilized via physical adsorption, encapsulation, or chemical binding. Such immobilization was found to maintain some activity of the biomolecule, with applications in the biosensor field.[613] Recently, some developments have been reported in the immobilization of redox proteins in mesoporous transparent electrodes for spectroelectrochemistry.[47–51]

Electroanalysis of Heavy Metals or Organics

Imprinting has been reported using sol–gel-derived thin films prepared from various monomers to produce hybrid films with specific binding sites for parathion. Such films could be deposited on glassy carbon electrodes for application in aqueous solutions. The imprinted films showed high selectivity toward parathion in comparison to similar organophosphates.[614] Nanoengineering the surface of templated materials using selected functions (thiol,[615] amine,[616] acetamide phosphonic acid,[617] cyclam,[618,619] 5-mercapto-1-methyltetrazole[620]...) was found important for improving both the capacity and the selectivity of the accumulation process, which can be exploited for environmental sensing.[621] Examples of electroanalysis using electrodes modified by mesoporous hybrid films have been reported for the detection of various metal species, such as Ag(I),[622] Hg(II),[623] Pb(II)[624] or Cu(II).[599] The typical experiment involves the preconcentration of the analyte in the mesostructured hybrid material, before its desorption/reduction in an appropriate detection medium, and subsequent electroanalysis, most often by stripping voltammetry. The selectivity of the adsorption allows in principle to preconcentrate preferentially the target metal from a complex solution containing potentially-interfering species.[619,621]

16.2.3 Heterogeneous Multimolecular Layers: Bulk Composites

This last category of CMEs gathers all systems that cannot be classified into the above homogeneous layers. It mainly includes composite electrodes based on multicomponent heterogeneous matrices constituted by either (bio)organic[625–630] or inorganic[631–633] modifiers (including notably clays,[584,585,634,635] zeolites[575,636–638] and silica-based and related organic–inorganic hybrid materials[246,291,575,639–649]). As most of these species/materials are electronically insulating, their use in connection to electrochemistry requires a close contact to a conductive electrode material. Besides the above monolayers and homogeneous multimolecular layers made of modifier species/materials deposited as thin films onto electrode surfaces, the heterogeneous multimolecular systems are mostly based on the incorporation of these modifiers into composite conductive matrices such as carbon paste electrodes or, alternatively, screen-printed carbon electrodes (i.e., their thick film homologues in the heterogeneous carbon electrochemical sensors family[650]). The modifier is most often mixed with the basic carbon paste constituents (graphite particles and a binder such as mineral oil or solid paraffin) or a carbon ink (for screen-printed electrodes). The primary role of the modifier is to bring new/additional features and notwithstanding the very high number of modifiers used to date to modify carbon paste or screen-printed electrode, most of them have been selected for their accumulation capability and/or electrocatalytic properties.

16.2.3.1 Modifier Species/Materials for Carbon Paste Electrochemical Sensors

A huge amount of organic, inorganic, and organic–inorganic hybrid materials and species have been dispersed into carbon paste electrodes, CPEs, (or carbon-based screen-printed electrodes) for being used as electrochemical sensors. They are briefly listed below, category by category.

Various types of *inorganic compounds and materials*, existing mainly in the form of powders, have been embedded into carbon composite matrices. They include:

Polyoxometallates and Prussian Blue Derivatives

Polyoxometallates (POMs) are heteropolyanions exhibiting electrocatalytic properties,[651] which are existing in the form of Keggin-type ($XM_{12}O_{40}^{n-}$), Dawson-type ($X_2M_{18}O_{62}^{n-}$), mixed-addenda, or transition metal-substituted structures. Following some pioneering works on POM-modified CPEs,[652,653] the most widely used systems were the Keggin-type phosphomolybdate (PMo_{12}[654,655]) and silicomolybdate ($SiMo_{12}$[655,656]) compounds. The attractive electrocatalytic and ion exchange properties of Prussian Blue ($Fe_4^{III}[Fe^{II}(CN)_6]_3$) and related metal

hexacyanoferrates (with Fe^{III} replaced by another transition metal ion) have been advantageously exploited in electrochemistry.[631] The field was pioneered by Kalcher's group,[657] and metal hexacyanoferrates mostly incorporated in CPEs were Prussian Blue itself,[658–660] copper hexacyanoferrate,[661–663] cobalt hexacyanoferrate,[664] or hybrids based on copper and cobalt hexacyanoferrates.[665]

Clays and Layered Double Hydroxides

Clays are layered aluminosilicates that exhibit cation exchange capabilities and adsorption properties, while layered double hydroxides are anion exchangers with a hydrotalcite-like structure. Both have been incorporated in CPEs and exploited in electroanalysis, mostly to preconcentrate target analytes (usually by ion exchange or organic compounds by adsorption) prior to their voltammetric detection.[584,666] Wang and Martinez acted as pioneers by reporting the first clay-modified CPE.[667] Afterwards, many other works were based on the use of montmorillonites[668–671] and sepiolite,[672–674] but also bentonites,[675–677] vermiculites,[678–680] kaolinites,[681,682] kaolin,[683] (fluoro)hectorites,[672,684] muscovite,[685] and some other natural smectite clays.[686–688]

Zeolites

Zeolites are microporous crystalline aluminosilicates characterized by a regular spatial arrangement of TO_4 tetrahedra (T = Si, Al), leading to well-defined structures made of uniform cages, cavities or channels of defined dimensions (typically in the 4–15 Å range), whose substitution of Si^{+IV} by Al^{+III} in the framework generates negative charges that are compensated by extraframework cations to maintain electroneutrality. Zeolites thus exhibit both size selectivity and ion exchange capacity. This unique feature is probably at the origin of the great development of zeolite-modified electrodes[689] and, because of its powdered form and insulating character, most investigations were based on the dispersion of zeolite particles into CPEs[575,636–638] or screen-printed carbon electrodes.[690] The large-pore (8 Å in diameter) faujasite type zeolites Y[691–694] and X,[694–696] as well as the small-pore (4 Å in diameter) zeolite A[697,698] were mainly used to modify CPEs. Though less commonly used, other zeolite types include mordenite,[699] clinoptilolite,[700–702] ZSM-5,[690] some natural zeolites,[703–705] or zeolite mixtures.[706]

Silica, Functionalized Silica, Nonsiliceous Metal Oxides, and Sol–Gel-Derived Inorganic and Hybrid Materials

Silica gels (or fumed silicas) were historically the first materials of this family to be exploited in CPEs[257,645] due to their adsorption and/or catalytic properties associated

to large specific surface areas (>100 m^2 g^{-1}), leading to enhanced electroanalytical performance.[707–709] They were notably used for the preconcentration and detection of organic pollutants[707,710] or for the accumulation of heavy metal cations prior to their voltammetric detection.[708,709] The properties of silica gels exploited in electroanalysis were then extended by surface modification with very thin reactive layers of metal oxides (i.e., M_xO_y monolayers which could eventually be further transformed into corresponding metal phosphates),[711] or with organo-functional groups covalently attached to the inorganic matrix.[257,645–649] This second category was the most interesting one with respect to environmental analysis as it enabled the selective recognition of analytes (heavy metal ions, for instance) by selected binding sites. Examples are available for organo-functional groups such as propylamine,[616,712,713] a wide range of functions exhibiting high affinity for Hg(II) species (i.e., mercaptopropyl,[615,714] benzothiazolethiol,[715] 3-(2-thiobenzimidazoyl)propyl,[716] 2,5-dimercapto-1,3,4-thiadiazole,[717] or 2-aminothiazole[718]), several groups binding preferably Cu (II) species (i.e., aminopropyl,[616] 2-aminothiazole,[719] the carnosine dipeptide,[720] propylsulfonate,[721] salicylidine,[722] or cyclam derivatives[618]), some functions leading to Pb(II) detection (mercaptopropyl,[714] cyclam-acetamide[619] or 2-aminopyridine[723]), as well as some others likely to recognize other metal ions, alone or in mixture.[724,725] Finally, nonsiliceous metal oxides have been also used to modify CPEs[726] because of their attractive catalytic properties, such as ruthenium oxides (mainly RuO_2),[727] copper oxides (Cu_2O, CuO),[728,729] and to less extent cobalt and nickel oxides.[730]

Nanomaterials

Two main categories of nanomaterials have been introduced into CPEs: the porous materials ordered at the nanoscale and nanoparticles. Ordered mesoporous materials, prepared by the sol–gel process in the presence of a supramolecular template (surfactant or water-soluble polymer), are highly porous solids (pore volume >0.7 mL g^{-1}) exhibiting high specific surface areas (500–1,500 m^2 g^{-1}) due to a periodic and regular arrangement of well-defined mesopores defined by amorphous inorganic walls. The attractiveness of these materials for electroanalysis purposes results from their regular channels, high specific surface areas, and consequently high number of easily accessible active sites, enabled to improve the performance of silica-modified electrodes,[246,575,647] as reported for the detection of metal ions[731,732] or organic pollutants[733] at mesoporous silica-modified CPEs. They can also be functionalized while maintaining an easier access to binding sites and faster mass transfer processes in comparison to their nonordered homologues, inducing dramatic increases in sensitivity of the resulting modified CPEs (see illustrative example for Hg (II) detection at thiol-functionalized silicas in Fig. 16.15).[734] Other examples are mesoporous silica functionalized with aminopropyl,[712,735] carbamoylphosphonic acid,[724,736] 2-benzothiazolethiol,[737] 5-mercapto-1-methyltetrazole,[738] propylsulfonic acid,[721] thiomorpholine,[739] carnosine,[720] acetylacetone,[740] 2-acetylpyridine,[741] thiourea derivatives,[742] or cyclam.[618,619] More recently, ordered mesoporous carbon electrodes have been developed with great promise in electroanalysis,[44] these

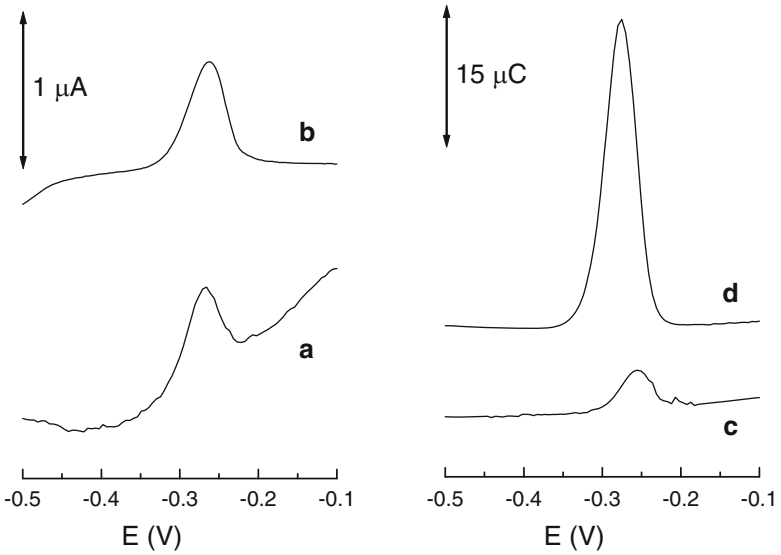

Fig. 16.15 Comparison between thiol-functionalized silica gels and ordered mesoporous silicas (MCM-41 and SBA-15 types) in CPEs applied to preconcentration electroanalysis of Hg^{II} species: electrochemical curves obtained after 2 min accumulation in 1 μM Hg^{II}, with various mercaptopropyl-grafted silica samples incorporated in carbon paste electrodes, (**a**) small pore (~4 nm) silica gel, (**b**) large pore (~6 nm) silica gel, (**c**) small pore (~3 nm) MCM-41, and (**d**) large pore (~6 nm) SBA-15. The curves were recorded after transfer to an analyte-free electrolyte solution (5 % thiourea in 0.1 M HCl), by applying anodic stripping voltammetry in the differential pulse mode. Reprinted with permission from reference (734) Copyright (2003) Wiley-VCH

materials being most often deposited as particulate films onto solid electrodes but an example of OMC-modified CPEs has been also described.[743] The second category of "nano" additives to CPEs concerns the nanoparticles (NPs) for which the physicochemical properties can differ from the bulk materials. Gold nanoparticles in CPEs have been exploited for the detection of metal ions.[744,745] Other nanoparticles with electrocatalytic properties are metal oxides, some of them being used for environmental sensing (i.e., SiO_2[746] or ZrO_2[747]). Note that the particular case of nanosized materials will be treated in the next chapter.

Sparingly Soluble or Insoluble Complexes and Salts

Zirconium phosphate particles have been used as support for a wide range of redox mediators commonly used in bioelectrochemistry, such as the phenothiazines and phenoxazines family,[748–750] and dispersed into CPEs mainly for biosensor applications. Calcium phosphates (especially apatite, $Ca_{10}(PO_4)_6(OH)_2$) were largely used as CPE modifier for the analysis of pollutants subsequent to preconcentration by adsorptive extraction.[751–754] Other sparingly soluble CPE modifiers for heavy metal sensors are aluminophosphates,[755] mercury oxalate,[756] as well as some organometallic complexes.[757]

A great variety of *organic and organometallic compounds*, such as organic ligands and catalysts as well as organometallic catalysts, but also organic polymers and amphiphilic/lipophilic compounds, has been incorporated into carbon paste electrodes for sensor applications. They are briefly presented hereafter.

Molecular Ligands

Numerous N- and/or S-containing molecular ligands have been used to modify CPEs and exploited to accumulate target metal species analytes via complex formation. This family is extraordinary wide so that only some examples are given hereafter, as cited with respect to the target analyte: 2-mercapto-4(3H)-quinazolinone[758] or the Schiff bases glyoxal bis(2-hydroxyanil)[759] and benzylbisthiosemicarbazone[760] for Hg(II); 2,9-dimethyl-1,10-phenanthroline,[761] 1,2-bismethyl(2-aminocyclopentene-carbodithiolate)ethane,[762] salicylaldoxime[763] and naphthazarin (5,8-dihydroxy-1,4-naphthoquinone)[764] for Cu(II); 2,2-′-dithiodipyridine,[765] 2-mercaptoimidazole[766] and 3-amino-2-mercaptoquinazolin-4(3H)-one,[767] for Ag(I); benzoin oxime,[768] diphenylthiocarbazone[769] and *p*-phenylenediamine[770] for Pb(II); 1-(2-pyridylazo)-2-naphthol[771] and 2,4,6-tri (3,5-dimethylpyrazoyl)-1,3,5-triazine[772] for Co(II); dimethylglyoxime[773] for Ni (II); Phenanthroline and 2,2′-bipyridyl derivatives for total iron[774]; Rhodamine B for Au(III)[775]; 1,5-diphenylcarbazide for chromium species[776]; 1-(2-pyridylazo)-2-naphthol for Mn(II) and Mn(VII)[777]; 8-hydroxyquinoline for Tl(III)[778]; 1-furoylthioureas for Cd(II)[779]; propyl gallate for uranium.[780] Note that simultaneous determinations of several cations at an electrode modified with the same ligand is also possible, as illustrated for Hg(II), Co(II), Ni(II), and Pd(II) at CPE containing dimethylglyoxime[781] or Mn(II), Cu(II), and Fe(III) using CPE modified with 2-(5′-bromo-2′-pyridylazo)-5-diethylaminophenol.[782]

Macrocyclic Compounds

Molecular macrocyclic derivatives with "more or less planar geometries" or cage or cup-like shape structures molecules (see some examples in Fig. 16.16) have been used to modify CPEs with the goal to improve the selectivity of their accumulation/recognition properties. Examples of macrocyclic CPE modifiers with "more or less planar geometries" are: crown ethers (18-crown-6[783–785] or dibenzo-18-crown-6[783,785]), thiacrown compounds,[786] macrocyclic thiohydrazone,[787] or tetra-azamacrocyclic compounds of the cyclam family[788]; CPEs modified with such macrocyclic derivatives were used for various purposes such as electrocatalytic, voltammetric or potentiometric detection of metal ions or organics. In addition, cyclodextrins[789–791] or calixarenes,[792–794] both exhibiting very rich host-guest chemistry, have been incorporated into CPEs and subsequently used as sensors for metal ions and organic pollutants.

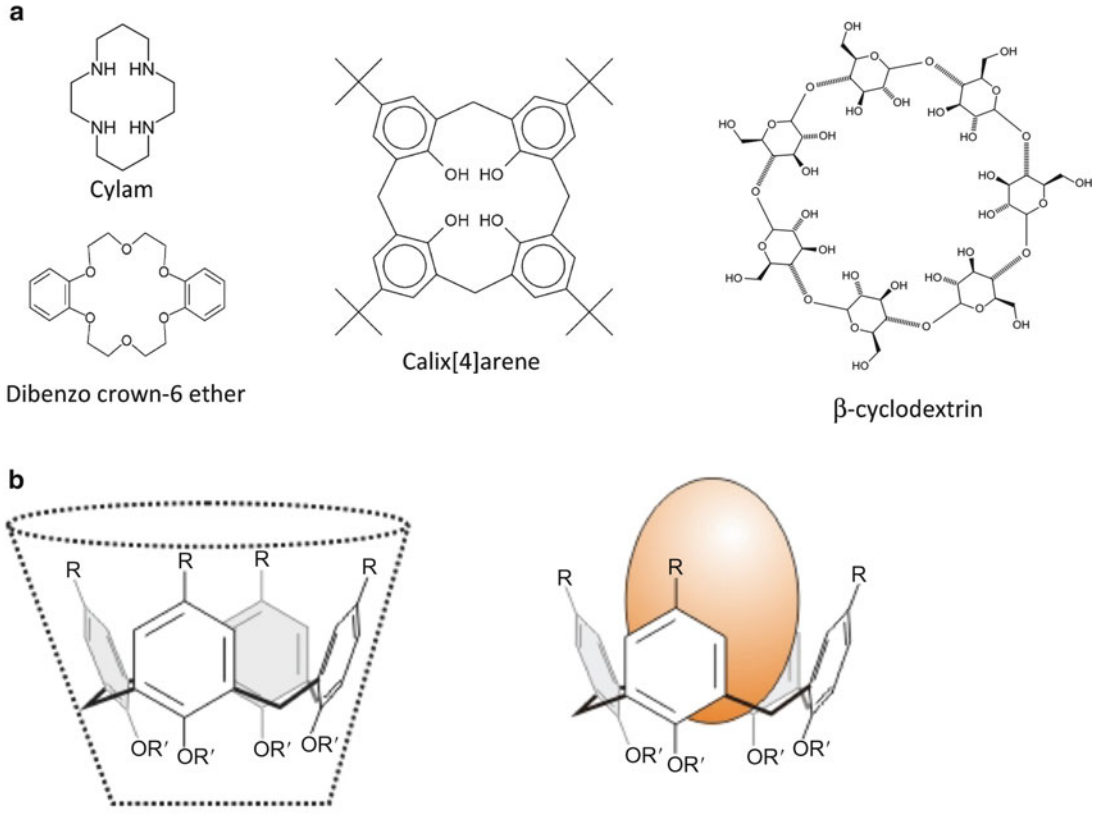

Fig. 16.16 (**a**) Examples of macrocyclic compounds used to modify CPEs. (**b**) Example highlighting the chemical structure of a simple calixarene from which it is easy to see the cup shape of the molecule likely to act as a host for guest species. The symbol R is not a single element but represents a "group" of atoms. The structure of the R group can be varied to give the basic calixarene structure a more selective action rather than simply working on the basis of size

Organic (Electro)Catalysts

Charge transfer mediators are extremely important in electroanalysis since they contribute to increase the sensitivity of the electrochemical detection as well as to enhance the selectivity by lowering the overpotentials usually observed for numerous electroactive analytes, limiting thereby the effect of many interferences. It is however important to immobilize the mediator at the electrode surface to get practically usable, reagent-free sensing devices, and CPE is a particularly valuable host to reach this goal. This is easily made by mixing small amounts (typically a few w:w %) of such (electro)catalysts to carbon paste to get the correspondingly modified CPE (actually, the first example of chemically modified CPE was reported on the basis of quinone derivatives introduced in carbon paste[10]). Although they have almost exclusively found tremendous interest in the field of amperometric biosensors,[625] some applications as electrochemical sensors for environmentally important species have been also reported. Examples involve quinone for nitrite detection[795] or $[Fe(CN)_5L]^{3-}$ (L = 4-aminopyridine) for aromatic aldehydes.[796] On the other hand, the extremely popular class of electrocatalysts including the redox-active dyes phenothiazines, phenoxazines and phenazines, which have found many applications as CPE modifiers applied to the electrocatalytic detection of biologically relevant molecules and in the field of electrochemical biosensors,[33,650] did not encounter to date the same success for applications as environmental sensors.

Organometallic Complexes

Another important family of charge transfer mediators that have been immobilized in heterogeneous carbon-based electrochemical sensors and biosensors is that of organometallic complexes (Fig. 16.17), such as ferrocene and ferrocene derivatives, metal phthalocyanines, metal porphyrins, Schiff bases, and some others. Again, they were mostly applied in the biosensing field or to detect biologically relevant molecules by electrocatalysis, but various examples of environmental applications can be found in the literature. For instance, CPEs comprising ferrocene and ferrocene derivatives have been applied to the electrocatalytic detection of phenol,[797] sulfite,[798] nitric oxide,[799] or hydrazine,[800] while ferrocene can be also used as an electrochemical probe to detect surfactants.[801] Phthalocyanines are intensely colored macrocyclic compounds that form coordination complexes with many elements of the periodic table, but mainly cobalt phthalocyanine (CoPc) has been widely used as CPE modifier for the electrocatalytic determination of environmentally relevant species. This has been notably applied to the detection of thiol compounds,[802,803] pesticides (organophosphates,[804] carbamates,[804,805] dithiocarbamates[806]), herbicides,[807] hydrazine,[808,809] or bisphenol A.[810] Besides CoPc, other metal complexes of phthalocyanine macrocycles have been introduced into CPEs for sensing purposes, including complexes of iron,[811] copper,[812] or manganese.[813] On the other hand, the electrocatalytic properties of metal porphyrins were also exploited, such as copper porphyrin immobilized on zeolite-modified CPE for

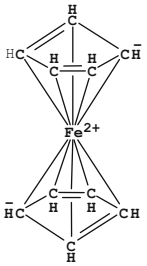

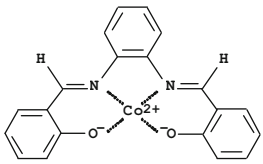

Cobalt salophen (Schiff base)

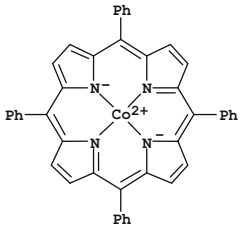

Cobalt porphyrin

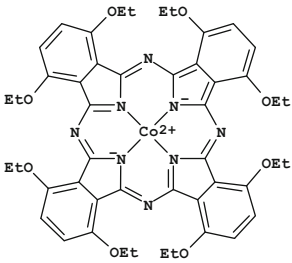

Cobalt phthalocyanine

Fig. 16.17 Commonly used organometallic complexes as mediators in carbon paste electrodes

hydrazine sensing[814] or CPE modified with silica gels covered with metal oxide thin films supporting iron[815] or cobalt[816] porphyrins for the electrocatalytic detection of molecular oxygen. Some Schiff base complexes were also used for similar purposes.[817,818] Finally, other organometallic electrocatalysts have been reported as CPE modifiers, such as rhodium acetamide,[819] iron(II)-nitroprusside,[820] or Co(II)-1-alkyl-1H-benzo[d][1–3]triazole derivatives[821] for sensing of some pollutants.

Organic Polymers

As aforementioned, functional macromolecular compounds such as organic and organometallic polymers or organic–inorganic hybrid copolymers have been widely applied to the chemical modification of electrode surfaces in the form of films deposited on solid electrodes.[294] They have been also directly incorporated as powder in the bulk of CPE matrices and subsequently exploited for their intrinsic properties (ion exchange, adsorption, redox/mediator activity, electronic conductivity, ...). CPEs were modified with a wide range of chelating resins (i.e., containing N- and/or S-based functional groups) likely to bind metal ions prior to their electrochemical detection.[822–826] Molecularly imprinted polymers (i.e., macromolecular compounds formed in the presence of a molecule that is extracted afterwards, thus leaving complementary cavities behind, which can then be exploited to the selective accumulation of the original molecule) were also exploited for their selective recognition properties (e.g., towards pesticides, phenol derivatives or explosives[827–829]). Several natural macromolecular compounds (humic substances,[830–832] lichens,[833,834] or keratin[835]) were modifiers of CPEs

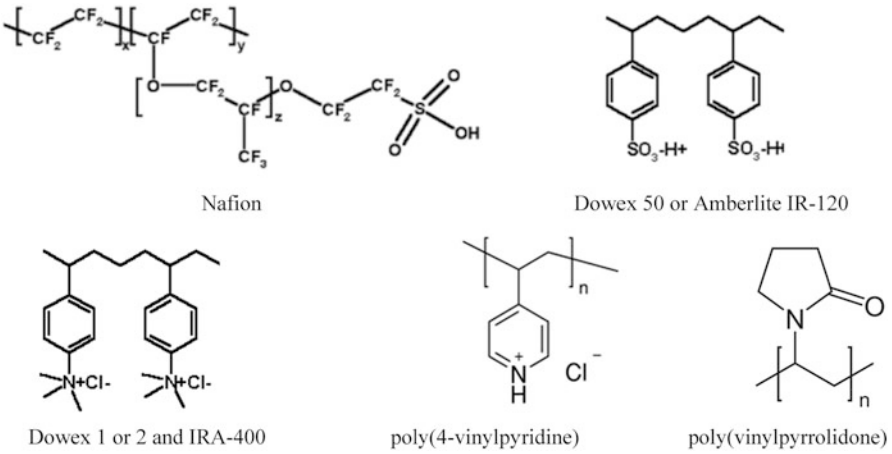

Fig. 16.18 Some examples of polymeric materials (especially ion exchangers) used to modify carbon paste or screen-printed carbon electrodes

and applied to preconcentration electroanalysis of heavy metals. The second category of polymeric modifiers gathers both cation exchangers (polymeric support functionalized with sulfonate or carboxylate groups, such as the perfluorinated-sulfonate ionomer, Nafion) and anion exchange resins, which have been used for electroanalytical purposes. Cations exchangers involve most often a polymeric support functionalized with sulfonate or carboxylate groups (first example in early 1984[836]), such as the perfluorinated-sulfonate ionomer, Nafion, mostly applied for adsorptive stripping voltammetry of cationic analytes such as metal ions,[837–839] the Dowex 50W-X8 resin,[840,841] and several Amberlite resins (e.g., IR-120,[842,843] IRC-718,[844] or XAD-2[845]). The anion exchange resins were essentially nitrogen-bearing polymers, i.e., quaternized poly(4-vinylpyridine)[846,847] and Amberlite LA2.[848–850] Some examples are illustrated in Fig. 16.18. Finally, it is noteworthy that redox polymers and related electrocatalytic systems (i.e., macromolecules containing redox centers which support the electron transfer by electron hopping), or conducting polymers, have been largely used as CPE modifiers (most often applied for bioelectrocatalytic purposes[33]) but only few examples are dealing with environmental electroanalysis; one example is the electrocatalytic detection of nitrite with a ruthenium-based polymer.[851]

Surfactants and Lipids

The interest of amphiphilic and lipophilic compounds as CPE modifiers relies on their preferable interaction with the hydrophobic matrix and, once immobilized in/on the composite electrode, thereby opening the door to further applications to either adsorptive stripping voltammetry of organic compounds (via favorable hydrophobic interactions) or to the preconcentration analysis of ionic species via open-circuit

accumulation by ion-pair formation. Various kinds of cationic, anionic and nonionic surfactants[852] and some lipids[853] have been exploited for those purposes. Numerous examples are available for cationic surfactants: cetyltrimetylammonium bromide (CTAB, or its chloride homologue CTAC),[854–859] cetylpyridinium,[860,861] or Septonex (1-ethoxycarbonylpentadecyltrimethylammonium),[862–864] which have been notably used to detect anionic forms or complexes of metal species. CPEs modified with anionic (e.g., sodium dodecyl sulfate) and nonionic surfactants were mainly applied to the detection of drugs or pharmaceuticals.[33] This was also the case of lipid-based CPEs (stearic and lauric acids), which were directed to pharmaceuticals electroanalysis.[33]

Finally, some *biological materials*, mainly enzymes, have been introduced into carbon composite matrices and the resulting electrodes used as environmental biosensors (in addition to numerous other biosensing applications[33,625,650]). The main examples are based on tyrosinase (or polyphenol oxidase) for the detection of phenolic compounds[865–869] or thiols,[870] acetylcholinesterase for organophosphate and carbamate pesticides,[804,805,811] organophosphorous hydrolase for pesticides,[871] or bienzymatic systems for amperometric immunosensor for polycyclic aromatic hydrocarbons.[872]

16.2.3.2 Detection Mechanisms at Modified Carbon-Based Electrochemical Sensors

The two main detection schemes at chemically modified carbon-based electrodes are preconcentration electroanalysis and electrocatalysis, even if some other processes (potentiometric detection, amperometric biosensors) have been also applied.

Preconcentration Electroanalysis

This technique involves the accumulation of the analyte at the electrode surface from diluted solutions, via favorable interaction with the electrode modifier, and its subsequent electrochemical detection. This enables to lower the detection limit and to increase the sensor sensitivity owing to effective concentration of the analyte. This is especially useful to enable quantitative determinations when they are not achievable by direct electrochemical measurement performed in the native medium. Compared to stripping voltammetric techniques, this one is based on *chemical accumulation* rather than on an electrolytic one, thus being basically independent on potentials. The typical experimental procedure involves successive steps (Fig. 16.19a) that must be optimized to get the best performance. The analyte is first accumulated at open-circuit under constant stirring (to enhance mass transport rates). The electrode is then removed from the preconcentration medium, rinsed with pure water, and immersed into the analysis cell containing an appropriate electrolyte, where the electrochemical quantification is carried out (analyte desorption is usually required, especially when the electrode modifier is an

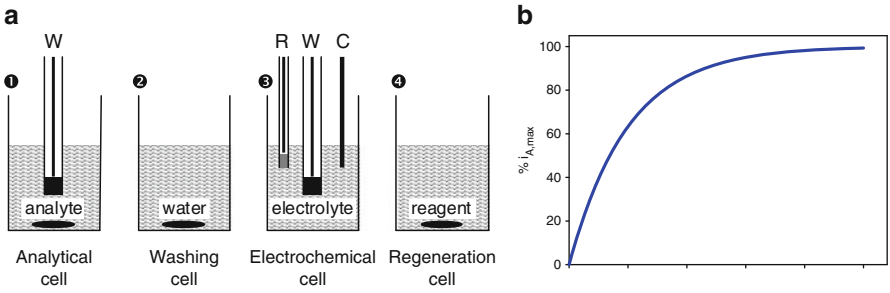

Fig. 16.19 (**a**) Schematic illustration of the four successive steps usually involved in a typical voltammetric analysis performed at a chemically modified electrode after preconcentration. *W*, *R*, and *C* refer to the working electrode, the reference electrode, and the counter-electrode, respectively. (**b**) Dependence of the voltammetric signal on the accumulation or reaction time for a 1:1 reaction between a modifier and an analyte (x-axis = time in arbitrary units)

insulating material). Medium exchange between accumulation and detection steps is often performed but not obligatorily. An additional regeneration step can be necessary when performing successive experiments, which is ideally achieved chemically (by immersing the electrode in an appropriate medium containing a regeneration reagent). Mechanical renewal of modified carbon paste surfaces might be also useful to avoid any memory effects, which is evidently not required for single-use screen-printed electrodes. Various pathways for analyte accumulation at chemically modified CPEs have been described, including physical or chemical adsorption, ion exchange or ion pairing, complexation, hydrophobic interactions, or even the formation of sparingly soluble compounds (by reaction of the analyte with a reagent immobilized in the carbon paste matrix). The performance of the modified electrode is directly related to the modifier properties, especially its binding capacity and selectivity for the target analyte, and to the kinetics of the preconcentration reaction. Actually a general model, taking into account the modifier capacity and the recognition reaction order and equilibrium constant, has been established[678] and, without entering into the details, the typical dependence of the voltammetric current on the accumulation/reaction time can be mathematically derived (see an illustration on Fig. 16.19b). As shown, it represents an exponential curve with a quasi-linear range at short times because in this case the analyte diffusion to the binding sites is rate-determining whereas, after long interaction time between analyte and modifier, chemical equilibrium is attained and currents values tend to level off.

Electrocatalytic Detections

The analyte can be directly detected on the electrode surface (i.e., without preconcentration) but this usually suffers from rather high overpotentials. Indeed, in case of slow heterogeneous electron transfer kinetics, the direct oxidation or

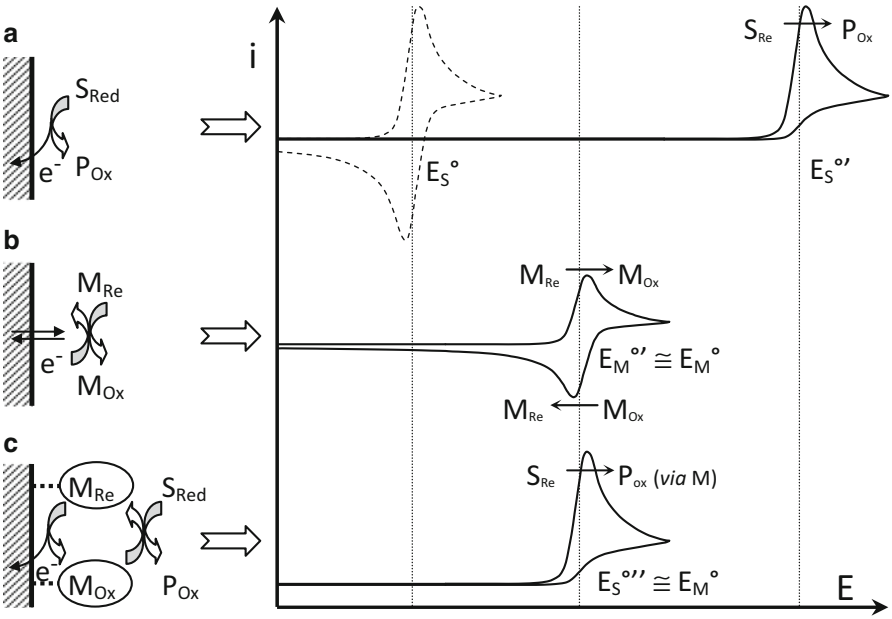

Fig. 16.20 Scheme illustrating the general principle of mediated electrocatalysis at a mediator-modified electrode: (**a**) overpotential observed for the direct oxidation of a reductant substrate S_{Red} into an oxidized product P_{Ox} (*dotted line* represents the curve that would have been obtained in the absence of kinetic limitations); (**b**) electrochemical behavior of a redox mediator couple (M_{Red}/M_{Ox}) characterized by fast electron transfer kinetics; (**c**) electrocatalytic transformation of S_{Red} into P_{Ox} by means of the mediator immobilized at the electrode surface

reduction of a redox-active species at the electrode surface might be inhibited, thus requiring the application of significant overpotentials to overcome the activation energy barrier at the interface. Several strategies have been developed to circumvent this limitation and mediated electrocatalysis is an elegant one (largely applied with modified CPEs thanks to the (electro)catalytic properties of the modifier immobilized on/in the electrode surface). The general principle of mediated electrocatalysis (Fig. 16.20) is described by Eqs. (16.2–16.4) using oxidation of a substrate S_{Red} into a product P_{Ox} as an example. Assuming a high overpotential for the electrochemical oxidation of S_{Red} ($E_S^{\circ\prime} \gg E_S^{\circ}$, Eq. (16.2); the subscript S indicates the substrate, M the mediator; the prime symbol designates the observed signal with the corresponding overpotential), the addition of a mediator M_{Red} (from a fast M_{Ox}/M_{Red} redox couple) enables to lower the overpotential barrier by electrogeneration of M_{Ox} at $E_M^{\circ\prime} = E_M^{\circ}$ (Eq. 16.4), which then reacts chemically with S_{Red} to produce P_{Ox} with concomitant regeneration of the catalyst M_{Red} (Eq. 16.3). The overall process results therefore in the electrochemical transformation of S_{Red} at a much lower overpotential than the initial substrate in the absence of mediator ($E_M^{\circ\prime} \gg E_S^{\circ\prime}$).

$$S_{Red} - ne^- \rightarrow P_{Ox} \qquad (E_S^{\circ\prime} >> E_S^{\circ}) \tag{16.2}$$

$$S_{Red} + M_{Ox} \rightarrow P_{Ox} + M_{Red} \qquad (\text{occurring if } E_S^{\circ} < E_M^{\circ}) \tag{16.3}$$

$$M_{Red} - ne^- \rightarrow M_{Ox} \qquad (E_M^{\circ\prime} \cong E_M^{\circ}) \tag{16.4}$$

There is a strong interest in immobilizing the mediator at the electrode surface to get reagent-free devices (also requiring less amount of mediator as compared to the soluble ones). It is however important that the mediator is attached strongly enough to the electrode surface to avoid any leaching into the solution, but also mobile enough or, as in the case of particulate modifiers, in close contact to carbon particles to properly act as an efficient electron shuttle between the electrode surface and the electroactive analyte. The result of the electron shuttling is a lowering of the overvoltage to the formal potential of the mediator couple (as described above), with concomitant improvements in both sensitivity and selectivity of the electrochemical sensor. In such case, detection is usually made voltammetrically or amperometrically.

Other Detection Modes

Though not so widely applied to heterogeneous multimolecular modified electrodes, potentiometry was sometimes used for the direct detection of analytes likely to interact with the electrode modifier (e.g., organic ligands,[873–876] metal oxides,[877,878] surfactants[879]). In such case, the electrode response was proportional to the logarithm of the analyte concentration contrary to the direct proportionality between the analyte concentration and the sampled current in amperometric or voltammetric analysis. Stripping potentiometry (or potentiometric stripping analysis) was also reported.[880,881] Finally, electrogenerated chemiluminescence was exploited at modified CPEs for the detection of drugs or organic pollutants.[882–884]

References

1. Heyrovsky J (1922) Elektrolysa se rtutovou kapkovou kathodou. Chem Listy 16:256–264
2. Zbinden C (1931) Nouvelle méthode de microdétermination de l'ion cuivre. Bull Soc Chim Biol 13:35–38
3. Adams RN (1958) Carbon paste electrodes. Anal Chem 30:1576
4. Bruckenstein S, Nagai T (1961) The rotated, mercury-coated platinum electrode. Anal Chem 33:1201–1209
5. Clark LC, Lyons C (1962) Electrode systems for monitoring cardiovascular surgery. Ann N Y Acad Sci 102:29–45
6. Lane RF, Hubbard AT (1973) Electrochemistry of chemisorbed molecules. II. Influence of charged chemisorbed molecules on the electrode reactions of platinum complexes. J Phys Chem 77:1401–1410
7. Lane RF, Hubbard AT (1973) Electrochemistry of chemisorbed molecules. I. Reactants connected to electrodes through olefinic substituents. J Phys Chem 77:1411–1421

8. Miller LL, Van den Mark MR (1978) A poly-p-nitrostyrene electrode surface. Potential dependent conductivity and electrocatalytic properties. J Am Chem Soc 100:3223–3225
9. Merz A, Bard AJ (1978) A stable surface modified platinum electrode prepared by coating with electroactive polymer. J Am Chem Soc 100:3222–3223
10. Ravichandran K, Baldwin RP (1981) Chemically modified carbon paste electrodes. J Electroanal Chem 126:293–300
11. Nuzzo RG, Allara DL (1983) Adsorption of bifunctional organic disulfides on gold surfaces. J Am Chem Soc 105:4481–4483
12. Foulds NC, Lowe CR (1986) Enzyme entrapment in electrically conducting polymers. Immobilisation of glucose oxidase in polypyrrole and its application in amperometric glucose sensors. J Chem Soc Faraday Trans 82:1259–1264
13. Umaña M, Waller J (1986) Protein-modified electrodes. The glucose oxidase/polypyrrole system. Anal Chem 58:2979–2983
14. Hoyer B, Florence TM (1987) Application of polymer-coated glassy carbon electrodes to the direct determination of trace metals in body fluids by anodic stripping voltammetry. Anal Chem 59:2839–2842
15. Hoyer B, Florence TM, Batley GE (1987) Application of polymer-coated glassy carbon electrodes in anodic stripping voltammetry. Anal Chem 24:1608–1614
16. Lundgren CA, Murray RW (1987) Microporous glass films as support media for electroactive films on electrodes. J Electroanal Chem 227:287–292
17. Delamar M, Hitomi J, Pinson J, Savéant JM (1992) Covalent modification of carbon surfaces by grafting of functionalized aryl radicals produced from electrochemical reduction of diazonium salts. J Am Chem Soc 114:5883
18. Turyan I, Mandler D (1997) Selective determination of Cr(VI) by a self-assembled monolayer-based electrode. Anal Chem 69:894–897
19. Attard GS, Bartlett PN, Coleman NRB, Elliott JM, Owen JR, Wang JH (1997) Mesoporous platinum films from lyotropic liquid crystalline phases. Science 278:838–840
20. Wang J, Lu J, Hočevar SB, Farias PAM, Ogorevc B (2000) Bismuth-coated carbon electrodes for anodic stripping voltammetry. Anal Chem 72:3218–3222
21. Lubert KH, Kalcher K (2010) History of electroanalytical methods. Electroanalysis 22:1937–1946
22. Adams RN (1969) Electrochemistry at solid electrodes. Dekker, New York, NY
23. Wang J (2006) Analytical electrochemistry, 3rd edn. John Wiley & Sons, New York, NY
24. Kissinger PT, Heineman WR (1996) Laboratory techniques in electroanalytical chemistry, 2nd edn. Dekker, New York, NY
25. Wang J (2005) Stripping analysis at bismuth electrodes: a review. Electroanalysis 17:1341–1346
26. Clark LC, Wold R, Granger D, Taylor Z (1953) Continuous recording of blood oxygen tensions by polarography. J Appl Physiol 6:189–193
27. Clark LC (1993) How the first enzyme electrode was invented. Biosens Bioelectron 8(1):iii–vii
28. Mandler D, Kraus-Ophir S (2011) Self-assembled monolayers (SAMs) for electrochemical sensing. J Solid State Electrochem 15:1535–1558
29. Perone SP (1963) The application of stripping analysis to the determination of silver(I) using graphite electrodes. Anal Chem 35:2091–2094
30. Miller FJ, Zittel HE (1963) Fabrication and use of pyrolytic graphite electrode for voltammetry in aqueous solutions. Anal Chem 35:1866–1869
31. Zittel HE, Miller FJ (1965) A glassy-carbon electrode for voltammetry. Anal Chem 37:200–203
32. Yoshimori T, Arakawa M, Takeuchi T (1965) Anodic stripping coulometry of gold using the glassy carbon electrode. Talanta 12:147–152
33. Švancara I, Kalcher K, Walcarius A, Vytřas K (2012) Electroanalysis with carbon paste electrodes. CRC Press, Taylor & Francis Group, Boca Raton, FL
34. Wang J, Tian B (1992) Screen-printed stripping voltammetric/potentiometric electrodes for decentralized testing of trace lead. Anal Chem 64:1706–1709

35. Swain GM, Ramesham R (1993) The electrochemical activity of boron-doped polycrystalline diamond thin film electrodes. Anal Chem 65:345–351
36. Ponchon JL, Cespuglio R, Gonon F, Jouvet M, Pujol JF (1979) Normal pulse polarography with carbon fiber electrodes for in vitro and in vivo determination of catecholamines. Anal Chem 51:1483–1486
37. Dayton MA, Brown JC, Stutts KJ, Wightman RM (1980) Faradaic electrochemistry at microvoltammetric electrodes. Anal Chem 52:946–950
38. Wightman RM (1981) Microvoltammetric electrodes. Anal Chem 53:1125A–1134A
39. Bard AJ, Mirkin MV (2001) Scanning electrochemical microscopy. Marcel Dekker, Inc., New York, NY
40. Beni V, Arrigan DWM (2008) Microelectrode arrays and microfabricated devices in electrochemical stripping analysis. Curr Anal Chem 4:229–241
41. Yáñez-Sedeño P, Pingarrón JM, Riu J, Rius FX (2010) Electrochemical sensing based on carbon nanotubes. Trends Anal Chem 29:939–953
42. Agüí L, Yáñez-Sedeño P, Pingarrón JM (2008) Role of carbon nanotubes in electroanalytical chemistry: a review. Anal Chim Acta 622:11–47
43. Rivas GA, Rubianes MD, Rodríguez MC, Ferreyra NF, Luque GL, Pedano ML, Miscoria SA, Parrado C (2007) Carbon nanotubes for electrochemical biosensing. Talanta 74:291–307
44. Walcarius A (2012) Electrocatalysis, sensors and biosensors in analytical chemistry based on ordered mesoporous and macroporous carbon-modified electrodes. Trends Anal Chem 38:79–97
45. Shi Y, Slaterbeck AF, Seliskar CJ, Heineman WR (1997) Spectroelectrochemical sensing based on multimode selectivity simultaneously achievable in a single device. 1. Demonstration of concept with ferricyanide. Anal Chem 69:3679–3686
46. Ross SE, Shi Y, Seliskar CJ, Heineman WR (2003) Spectroelectrochemical sensing: planar waveguides. Electrochim Acta 48:3313–3323
47. Schaming D, Renault C, Tucker RT, Lau-Truong S, Aubard T, Brett MJ, Balland V, Limoges B (2012) Spectroelectrochemical characterization of small hemoproteins adsorbed within nanostructured mesoporous ITO electrodes. Langmuir 28:14065–14072
48. Renault C, Balland V, Martinez-Ferrero E, Nicole L, Sanchez C, Limoges B (2009) Highly ordered transparent mesoporous TiO_2 thin films: an attractive matrix for efficient immobilization and spectroelectrochemical characterization of cytochrome c. Chem Commun 7494–7496
49. Renault C, Harris KD, Brett MJ, Balland V, Limoges B (2011) Time-resolved UV-visible spectroelectrochemistry using transparent 3D-mesoporous nanocrystalline ITO electrodes. Chem Commun 47:1863–1865
50. Frasca S, Von Graberg T, Feng J, Thomas A, Smarsly BM, Weidinger IM, Scheller FW, Hildebrandt P, Wollenberger U (2010) Mesoporous indium tin oxide as a novel platform for bioelectronics. ChemCatChem 2:839–845
51. Frasca S, Richter C, Von Graberg T, Smarsly BM, Wollenberger U (2011) Electrochemical switchable protein-based optical device. Eng Life Sci 11:554–558
52. Wang J (2007) Stripping analysis. In: Bard AJ, Stratmann M (eds) Encyclopedia of electrochemistry. Wiley-VCH Verlag GmbH & Co. KGaA, Weinheim
53. Hamilton TW, Ellis J, Florence TM (1980) Determination of arsenic and antimony in electrolytic cooper by anodic stripping voltammetry at a gold film electrode. Anal Chim Acta 119:225–233
54. Pinilla Gil E, Ostapczuk P (1994) Potentiometric stripping determination of mercury (II), selenium (IV), copper (II) and lead (II) at a gold film electrode in water samples. Anal Chim Acta 293:55–65
55. Sun YC, Mierzwa J, Yang MH (1997) New method of gold-film electrode preparation for anodic stripping voltammetric determination of arsenic (III and V) in seawater. Talanta 44:1379–1387

56. Viltchinskaia EA, Zeigman LL, Garcia DM, Santos PF (1997) Simultaneous determination of mercury and arsenic by anodic stripping voltammetry. Electroanalysis 9:633–640
57. Chadim P, Švancara I, Pihlar B, Vytřas K (2000) Gold-plated carbon paste electrodes for anodic stripping determination of arsenic. Collect Czech Chem Commun 65:1035–1046
58. Economou A, Fielden PR (1997) Applications, potentialities and limitations of adsorptive stripping analysis on mercury film electrodes. Trends Anal Chem 16:286–292
59. Vytřas K, Švancara I, Metelka R (2002) A novelty in potentiometric stripping analysis: total replacement of mercury by bismuth. Electroanalysis 14:1359–1364
60. Tyszczuk K, Korolczuk M (2007) Fast simultaneous adsorptive stripping voltammetric determination of Ni (II) and Co (II) at lead film electrode plated on gold substrate. Electroanalysis 19:1539–1542
61. Korolczuk M, Tyszczuk K, Grabarczyk M (2005) Adsorptive stripping voltammetry of nickel and cobalt at in situ plated lead film electrode. Electrochem Commun 7:1185–1189
62. Bobrowski A, Kalcher K, Kurowska K (2009) Microscopic and electrochemical characterization of lead film electrode applied in adsorptive stripping analysis. Electrochim Acta 54:7214–7221
63. Baś B, Kowalski Z (2002) Preparation of silver surface for mercury film electrode of prolonged analytical application. Electroanalysis 14:1067–1071
64. Kapturski P, Bobrowski A (2007) Silver amalgam film electrode of prolonged application in stripping chronopotentiometry. Electroanalysis 19:1863–1868
65. Czop E, Economou A, Bobrowski A (2011) A study of in situ plated tin-film electrodes for the determination of trace metals by means of square-wave anodic stripping voltammetry. Electrochim Acta 56:2206–2212
66. Tesařová E, Vytřas K (2009) Potentiometric stripping analysis at antimony film electrodes. Electroanalysis 21:1075–1080
67. Urbanová V, Vytřas K, Kuhn A (2010) Macroporous antimony film electrodes for stripping analysis of trace heavy metals. Electrochem Commun 12:114–117
68. Hočevar SB, Švancara I, Ogorevc B, Vytřas K (2007) Antimony film electrode for electrochemical stripping analysis. Anal Chem 79:8639–8643
69. Soropogui K, Sigaud M, Vittori O (2007) A cobalt film electrode for nitrite determination in natural water. Electroanalysis 19:2559–2564
70. Tyszczuk K, Korolczuk M, Grabarczyk M (2007) Application of gallium film electrode for elimination of copper interferences in anodic stripping voltammetry of zinc. Talanta 71:2098–2101
71. Nagaosa Y, Zong P, Kamio A (2009) Selenium coated carbon electrode for anodic stripping voltammetric determination of copper (II). Microchim Acta 167:241–246
72. Oesch U, Janata J (1983) Electrochemical study of gold electrodes with anodic oxide films – II. Inhibition of electrochemical redox reactions by monolayers of surface oxides. Electrochim Acta 28:1237–1246
73. Forsberg G, O'Laughlin JW, Megargle RG, Koirtyihann SR (1975) Determination of arsenic by anodic stripping voltammetry and differential pulse anodic astripping voltammetry. Anal Chem 47:1586–1592
74. Švancara I, Matoušek M, Sikora E, Schachl K, Kalcher K, Vytřas K (1997) Carbon paste electrode plated with a gold film for the voltammetric determination of mercury (II). Electroanalysis 9:827–833
75. Netterfield RP, Martin PJ (1986) Nucleation and growth studies of gold films prepared by evaporation and ion-assisted deposition. Appl Surf Sci 25:265–278
76. Švancara I, Pravda M, Hvizdalová M, Vytřas K, Kalcher K (1994) Voltammetric investigations on carbon paste electrodes as support for mercury films. Electroanalysis 6:663–671
77. Okinaka Y (1970) Electroless gold deposition using borohydride of dimethylamine borane as reducing agent. Plating 57:914–920
78. Okinaka Y, Kato M (2010) Electroless deposition of gold. In: Schlesinger M, Paunovic M (eds) Modern electroplating, 5th edn. John Wiley & Sons, Inc., New York, NY, pp 483–498

79. Golan Y, Margulis L, Rubinstein I (1992) Vacuum deposited gold films. 1. Factors affecting the film morphology. Surf Sci 264:312–326
80. Barnes MC, Kim DY, Ahn HS, Lee CO, Hwang NM (2000) Deposition mechanism of gold by thermal evaporation: approach by charged cluster model. J Cryst Growth 213:83–92
81. Bocking C (1994) High speed selective jet electrodeposition of gold and gold alloys using single circular jets. Trans Inst Met Finish 72:133–140
82. Gelchinski MH, Romankiw LT, Vigliotti DR, von Gutfeld RJ (1985) Electrochemical and metallurgical aspects of laser-enhanced jet plating of gold. J Electrochem Soc 132:2575–2581
83. Feng SW, Nainaparampil JJ, Tabet MF, Urban FK (1994) Gold and zinc thin films deposited by the ionized cluster beam technique. Thin Solid Films 253:402–406
84. Song Y, Swain GM (2007) Development of a method for total inorganic arsenic analysis using anodic stripping voltammetry and a Au-coated, diamond thin-film electrodes. Anal Chem 79:2412–2420
85. Dai X, Nekrassova O, Hyde ME, Compton RG (2004) Anodic stripping voltammetry of arsenic (III) using gold nanoparticle-modified electrodes. Anal Chem 76:5924–5929
86. Davis PH, Dulude GR, Griffin RM, Matson WR, Zink EW (1978) Determination of total arsenic at the nanogram level by speed-anodic stripping voltammetry. Anal Chem 50:137–143
87. Švancara I, Vytřas K, Bobrowski A, Kalcher K (2002) Determination of arsenic at a gold-plated carbon paste electrode using constant current stripping analysis. Talanta 58:45–55
88. Rasul SB, Munir AKM, Hossain ZA, Khan AH, Alauddin M, Hussam A (2002) Electrochemical measurements and speciation of inorganic arsenic in groundwater of Bangladesh. Talanta 58:33–43
89. Mandil A, Idrissi L, Amine A (2010) Stripping voltammetric determination of mercury (II) and lead (II) using screen-printed electrodes modified with gold films, and metal ion preconcentration with thiol-modified magnetic particles. Microchim Acta 170:299–305
90. Wang E, Sun W, Yang Y (1984) Potentiometric stripping analysis with a thin-film gold electrode for determination of copper, bismuth, antimony, and lead. Anal Chem 56:1903–1906
91. Zen JM, Chung MJ (1995) Square-wave voltammetric stripping analysis of mercury (II) at a poly(4-vinylpyridine)/gold film electrode. Anal Chem 67:3571–3577
92. WHO (2001) Arsenic in drinking water. WHO fact sheet No. 210. Bull World Health Organ 78:1096
93. Song Y, Swain GM (2007) Total inorganic arsenic detection in real water samples using anodic stripping voltammetry and a gold-coated diamond thin-film electrode. Anal Chim Acta 593:7–12
94. Diederich HJ, Meyer S, Scholz F (1994) Automatic adsorptive stripping voltammetry at thin-mercury film electrodes (TMFE). Fresenius J Anal Chem 349:670–675
95. Zuman P (2000) Role of mercury electrodes in contemporary analytical chemistry. Electroanalysis 12:1187–1194
96. Vyskočil V, Barek J (2009) Mercury electrodes - possibilities and limitations in environmental electroanalysis. Crit Rev Anal Chem 39:173–188
97. Economou A, Fiedel PR (2003) Mercury film electrodes: developments, trends and potentialities for electroanalysis. Analyst 128:205–212
98. Sahlin E, Jagner D, Ratana-Ohpas R (1997) Mercury nucleation on glassy carbon electrodes. Anal Chim Acta 346:157–164
99. Frenzel W (1993) Mercury films on a glassy carbon support: attributes and problems. Anal Chim Acta 273:123–137
100. Copeland TR, Christie JH, Osteryoung RA, Skogerboe RK (1973) Analytical application of pulsed voltammetric stripping at thin film mercury electrodes. Anal Chem 45:2171–2174
101. Cushman MR, Bennet BG, Anderson CW (1981) Electrochemistry at carbon fibers: Part 1. Characteristics of the mercury film carbon fiber electrode in differential pulse anodic stripping voltammetry. Anal Chim Acta 130:323–327

102. Gustavsson I, Lundstrom K (1983) A pyrolitic carbon film electrode for voltammetry - III: application to anodic-stripping voltammetry. Talanta 30:959–962
103. Kaufmann JM, Laudet A, Christian GD, Patriarche GJ (1982) Preparation and characterization of graphite-coated metallic electrodes: the graphite-sprayed electrode. Talanta 29:1077–1082
104. Farghaly OA (2004) A novel method for determination of magnesium in urine and water samples with mercury film-plated carbon paste electrode. Talanta 63:497–501
105. Shea D, MacCrehan WA (1988) Determination of hydrophilic thiols in sediment pore water using ion-pair liquid chromatography coupled to electrochemical detection. Anal Chem 60:1449–1454
106. Lexa J, Stulik K (1985) Preparation of a mercury film electrode modified by tri-n-octylphosphine oxide and the electrochemical properties of this electrode. Talanta 32:1027–1033
107. Kounaves SP, Deng W (1993) Analytical utility of the iridium-based mercury ultramicroelectrode with square-wave anodic stripping voltammetry. Anal Chem 65:375–379
108. Yosypchuk B, Fojta M, Barek J (2010) Preparation and properties of mercury film electrodes on solid amalgam surface. Electroanalysis 22:1967–1973
109. Armalis S, Pockeviciute D, Atolyte O (1996) Influence of hydrodynamic conditions of the solution on the sensitivity of stripping analysis of trace metals. Fresenius J Anal Chem 354:696–698
110. Brainina KZ, Ivanov AV, Khanina RM (2001) Long-lived sensors with replaceable surface for stripping voltammetric analysis: Part I. Anal Chim Acta 436:129–137
111. Metelka R, Vytřas K, Bobrowski A (2000) Effect of the modification of mercuric oxide on the properties of mercury films at HgO-modified carbon paste electrodes. J Solid State Electrochem 4:348–352
112. Zou M, Yang H, Huang G (1984) Fenxi Huaxue 12:1011–1015
113. Eskilsson H, Haraldsson C, Jagner D (1985) Determination of nickel and cobalt in natural waters and biological material by reductive chronopotentiometric stripping analysis in a flow system without sample deoxygenation. Anal Chim Acta 175:79–88
114. Wasberg M, Ivaska A (1986) A computer-controlled voltammetric flow-injection system. Anal Chim Acta 179:433–438
115. Brainina KZ, Malakhova NA, Stojko NY (2000) Stripping voltammetry in environmental and food analysis. Fresenius J Anal Chem 368:307–325
116. Brainina KZ, Neyman E (1993) Electrochemical stripping methods, vol 26 (Series Ed Winefordner JD). John Wiley & Sons, Inc., New York
117. Eskilsson H, Haraldsson C (1987) Reductive stripping chronopotentiometry for selenium in biological materials in flow system. Anal Chim Acta 198:231–237
118. Adeloju SB, Young TM, Jagner D, Batley GE (1999) Constant current cathodic stripping potentiometric determination of arsenic on a mercury film electrode in the presence of copper ions. Anal Chim Acta 381:207–213
119. Donten M, Kublik Z (1986) Application of a copper-based mercury film electrode in cathodic stripping voltammetry. Anal Chim Acta 185:209–218
120. Lo Balbo A, Dall'Orto VC, Sobral S, Rezzano I (1998) Linear scan stripping voltammetry at glassy-carbon base on thin-mercury film electrodes for determination of trace aluminium in dialysis fluids. Anal Lett 31:2717–2728
121. Pereira MC, Pereira ML (1999) Application of adsorptive stripping voltammetry to the determination of trace levels of titanium in mice organs. Electroanalysis 11:1207–1210
122. Feng D, Yang P, Yang Z (1991) Determination of germanium by potentiometric stripping analysis and adsorption potentiometric stripping analysis. Talanta 38:1493–1498
123. Wang LH, Tsai SJ (2001) Voltammetric behavior of chlorhexidine at a film mercury electrodes and its determination in cosmetics and oral hygiene products. Anal Chim Acta 441:107–116
124. Martinotti W, Queirazza G, Guarinoni A, Mori G (1995) In-flow speciation of copper, zinc, lead and cadmium in fresh waters by square wave anodic stripping voltammetry Part II. Optimization of measurement step. Anal Chim Acta 305:183–191

125. Brett CMA, Brett AMO, Tugulea A (1996) Anodic stripping voltammetry of trace metals by batch injection analysis. Anal Chim Acta 322:151–157
126. Ivaska A, Kubiak WW (1997) Application of sequential injection analysis to anodic stripping voltammetry. Talanta 44:713–723
127. Economou A (2005) Bismuth-film electrodes: recent developments and potentialities for electroanalysis. Trends Anal Chem 24:334–340
128. Long GG, Freedman LD, Doak GO (1978) Bismuth and bismuth alloys. In: Grayson M (ed) Encyclopedia of Chemical Technology, vol 3. Wiley, New York, pp 912–937
129. Yang N, Sun H (2007) Biocoordination chemistry of bismuth: recent advances. Chem Rev 251:2354–2366
130. Krolicka A, Pauliukaite R, Švancara I, Metelka R, Bobrowski A, Norkus E, Kalcher K, Vytřas K (2002) Bismuth-film-plated carbon paste electrode. Electrochem Commun 4:193–196
131. Banks CE, Kruusma J, Hyde ME, Salimi A, Compton RG (2004) Sonoelectroanalysis: investigation of bismuth-film-modified glassy carbon electrodes. Anal Bioanal Chem 379:277–282
132. Wang J, Lu J, Kirgöz ÜA, Hočevar SB, Ogorevc B (2001) Insights into the anodic stripping voltammetric behavior of bismuth film electrodes. Anal Chim Acta 434:29–34
133. Pierini GD, Granero AM, Di Nezio MS, Centurión ME, Zon MA, Fernández H (2013) Development of an electroanalytical method for the determination of lead in Argentina raw propolis based on bismuth electrodes. Microchem J 106:102–106
134. Hočevar SB, Ogorevc B, Wang J, Pihlar B (2002) A study on operational parameters for avanced use of bismuth film electrode in anodic stripping voltammetry. Electroanalysis 14:1707–1712
135. Pauliukaitė R, Brett CMA (2005) Characterization and application of bismuth-film modified carbon electrodes. Electroanalysis 17:1354–1359
136. Kırgöz ÜA, Marín S, Pumera M, Merkoçi A, Alegret S (2005) Stripping voltammetry with bismuth modified graphite-epoxy composite electrodes. Electroanalysis 17:881–886
137. Demetriades D, Economou A, Voulgaropoulos A (2004) Study of pencil-lead bismuth-film electrodes for the determination of trace metals by anodic stripping voltammetry. Anal Chim Acta 519:167–172
138. Wang J, Lu J, Hočevar SB, Ogorevc B (2001) Bismuth-coated screen-printed electrodes for stripping voltammetric measurements of trace lead. Electroanalysis 13:13–16
139. Calvo Quintana J, Arduini F, Amine A, van Velzen K, Palleschi G, Moscone D (2012) Part two: analytical optimisation of a procedure for lead detection in milk by means of bismuth-modified screen-printed electrodes. Anal Chim Acta 736:92–99
140. Flechsig GU, Korbout O, Hočevar SB, Thongngamdee S, Ogorevc B, Gründler P, Wang J (2002) Electrically heated bismuth-film electrode for voltammetric stripping measurements of trace metals. Electroanalysis 14:192–196
141. Lin L, Thongngamdee S, Wang J, Lin Y, Sadik OA, Ly SY (2005) Adsorptive stripping voltammetric measurements of trace uranium at the bismuth film electrode. Anal Chim Acta 535:9–13
142. Legeai S, Vittori O (2006) A Cu/Nafion/Bi electrode for on-site monitoring of trace heavy metals in natural waters using anodic stripping voltammetry: an alternative to mercury-based electrodes. Anal Chim Acta 560:184–190
143. Legeai S, Bois S, Vittori O (2006) A copper bismuth film electrode for adsorptive cathodic stripping analysis of trace nickel using square wave voltammetry. J Electroanal Chem 591:93–98
144. Banks CE, Kruusma J, Moore RR, Tomcík P, Peters J, Davis J, Komorsky-Lovrić S, Compton RG (2005) Manganese detection in marine sediments: anodic vs. cathodic stripping voltammetry. Talanta 65:423–429
145. Baldo MA, Daniele S, Bragato C (2003) Bismuth film microelectrodes for heavy metals monitoring by anodic stripping voltammetry. J Phys IV 107:103–106

146. Mercado E, Rodríguez-López M, López O, Rodríguez G, Fachini ER, Blanco PT, Carrasquillo A Jr (2007) Effect of bismuth surface coverage on the kinetics of quinone–hydroquinone at polycrystalline platinum electrodes. J Electroanal Chem 604:26–32
147. Wang N, Dong X (2008) Stripping voltammetric determination of Pb(II) and Cd(II) based on the multiwalled carbon nanotubes-nafion-bismuth modified glassy carbon electrodes. Anal Lett 41:1267–1278
148. Deng W, Tan Y, Fang Z, Xie Q, Li Y, Liang X, Yao S (2009) ABTS-multiwalled carbon nanotubes nanocomposite/Bi film electrode for sensitive determination of Cd and Pb by differential pulse stripping voltammetry. Electroanalysis 21:2477–2485
149. Jia X, Li J, Wang E (2010) High sensitivity determination of lead (II) and cadmium (II) based on the CNTs-PS/Bi composite film electrode. Electroanalysis 22:1682–1687
150. Mandil A, Pauliukaite R, Amine A, Brett CMA (2012) Electrochemical characterization of and stripping voltammetry at screen printed electrodes modified with different brands of multiwall carbon nanotubes and bismuth films. Anal Lett 45:395–407
151. Li J, Guo S, Zhai Y, Wang E (2009) High-sensitivity determination of lead and cadmium based on the nafion-graphene composite film. Anal Chim Acta 649:196–201
152. Švancara I, Prior C, Hočevar SB, Wang J (2010) A decade with bismuth-based electrodes in electroanalysis. Electroanalysis 22:1405–1420
153. Urbanová V, Bartoš M, Vytřas K, Kuhn A (2010) Porous bismuth film electrodes for signal increase in anodic stripping voltammetry. Electroanalysis 22:1524–1530
154. Królicka A, Bobrowski A, Kowal A (2006) Effects of electroplating variables on the voltammetric properties of bismuth deposits plated potentiostatically. Electroanalysis 18:1649–1657
155. Baldrianova L, Švancara I, Vlček M, Economou A, Sotiropoulous S (2006) Effect of Bi(III) concentration on the stripping voltammetric response of in situ bismuth-coated carbon paste and gold electrodes. Electrochim Acta 52:481–490
156. Švancara I, Vytřas K, Kalcher K (1997) Solid electrodes plated with metallic films. Sci Pap Univ Pardubice Ser A 3:207–225
157. Švancara I, Baldrianová L, Tesařová E, Hočevar SB, Elsuccary SAA, Economou A, Sotiropoulos S, Ogorevc B, Vytřas K (2006) Recent advances in anodic stripping voltammetry with bismuth-modified carbon paste electrodes. Electroanalysis 18:177–185
158. Pauliukaite R, Metelka R, Švancara I, Królicka A, Bobrowski A, Vytřas K, Norkus E, Kalcher K (2002) Carbon paste electrodes modified with Bi_2O_3 as sensor for the determination of Cd and Pb. Anal Bioanal Chem 374:1155–1158
159. Guzsvány V, Kádár M, Gaál F, Bjelica L, Tóth K (2006) Bismuth film electrode for the cathodic electrochemical determination of thiamethoxam. Electroanalysis 18:1363–1371
160. Du D, Ye X, Zhang J, Liu D (2008) Cathodic electrochemical analysis of methyl parathion at bismuth-film-modified glassy carbon electrode. Electrochim Acta 53:4478–4484
161. Ghanjaoui MEA, Srij M, El Rhazi M (2009) Assessment of lead and cadmium in canned foods by square-wave stripping voltammetry. Anal Lett 42:1294–1309
162. Korolczuk M, Moroziewicz A, Grabarczyk M (2005) Determination of subnanomolar concentrations of cobalt by adsorptive stripping voltammetry at a bismuth film electrode. Anal Bioanal Chem 382:1678–1682
163. Chatzitheodorou E, Economou A, Voulgaropoulos A (2004) Trace determination of chromium by square-wave adsorptive stripping voltammetry on bismuth film electrodes. Electroanalysis 16:1745–1754
164. Li J, Zhang J, Wei H, Wang E (2009) Combining chemical reduction with an electrochemical technique for the simultaneous detection of Cr(VI), Pb(II) and Cd(II). Analyst 134:273–277
165. Kadara RO, Tothill IE (2004) Stripping chronopotentiometric measurements of lead (II) and cadmium (II) in soils extracts and wastewaters using a bismuth film screen-printed electrode assembly. Anal Bioanal Chem 378:770–775

166. Kokkinos C, Economou A, Raptis I, Efstathiou CE (2008) Lithographically fabricated disposable bismuth-film electrodes for the trace determination of Pb(II) and Cd(II) by anodic stripping voltammetry. Electrochim Acta 53:5294–5299
167. Hutton EA, Hočevar SB, Ogorevc B, Smyth MR (2003) Bismuth film electrode for simultaneous adsorptive stripping analysis of trace cobalt and nickel using constant current chronopotentiometric and voltammetric protocol. Electrochem Commun 5:765–769
168. Hutton EA, Ogorevc B, Smyth MR (2004) Cathodic electrochemical detection of nitrophenols at a bismuth film electrode for use in flow analysis. Electroanalysis 16:1616–1621
169. Adamovski M, Zając A, Gründler P, Flechsig GU (2006) Self-assembled monolayers on bismuth electrodes. Electrochem Commun 8:932–936
170. Rodríguez JA, Barrado E, Castrillejo Y, Santos JR, Lima JLFC (2007) Validation of a tubular bismuth film amperometric detector: determination of diclofenac sodium by multisyringe flow injection analysis. J Pharm Biomed Anal 45:47–53
171. Sattayasamitsathit S, Thavarungkul P, Kanatharana P (2007) Bismuth film electrode for analysis of tetracycline in flow injection system. Electroanalysis 19:502–505
172. Bučková M, Gründler P, Flechsig GU (2005) Adsorptive stripping voltammetric detection of daunomycin at a bismuth bulk electrode. Electroanalysis 17:440–444
173. Timur S, Anik U (2007) α-Glucosidase based bismuth film electrode for inhibitor detection. Anal Chim Acta 598:143–146
174. Xu M, Wu Y, Wang J, Zhou F (2006) Electrochemistry of and redox-induced metal release from metallothioneins at a nafion-coated bismuth film electrode. Electroanalysis 18:2099–2105
175. Ruhling D, Schulte A, Schuhmann W (2006) An electrochemical robotic system for routine cathodic adsorptive stripping analysis of Ni^{2+} ion release from corroding NiTi shape memory alloys. Electroanalysis 18:53–58
176. Cao GX, Jimenéz O, Zhou F, Xu M (2006) Nafion-coated bismuth film and nafion-coated mercury film electrodes for anodic stripping voltammetry combined on-line with ICP-mass spectrometry. J Am Soc Mass Spectrom 17:945–952
177. Martin CR, Foss CA Jr (1996) Chemically Modified Electrodes. In: Kissinger PT, Heineman WR (eds) Laboratory Techniques in Electroanalytical Chemistry. Marcel Dekker Inc., New York, pp 403–442
178. Gooding JJ, Lai LMH, Goon IY (2009) Nanostructured electrodes with unique for biological and other applications. In: Alkire RC, Kolb DM, Lipkowski J, Ross PN (eds) Chemically Modified Electrodes, vol 11. Wiley-VCH Verlag GmbH & Co. KGaA, Weinheim, Germany
179. Love JC, Estroff LA, Kriebel JK, Nuzzo RG, Whitesides GM (2005) Self-assembled monolayers of thiolates on metals as a form of nanotechnology. Chem Rev 105:1103–1169
180. Walcarius A (2010) Template-directed porous electrodes in electroanalysis. Anal Bioanal Chem 396:261–272
181. Guo YG, Hu JS, Wan LJ (2008) Nanostructured materials for electrochemical energy conversion and storage devices. Adv Mater 20:2878–2887
182. Wang J (2005) Nanomaterial-based electrochemical biosensors. Analyst 130:421–426
183. Liu M, Ji Z, Shang L (2010) Top-Down Fabrication of Nanostructures. In: Chi L (ed) Nanotechnology, vol 8, Wiley-VCH Verlag GmbH & Co. KGaA, Weinheim, pp 3–47
184. Qin D, Riggs BA (2012) Nanotechnology: top-down approach. In: Atwood JL, Steed JW (eds) Encyclopedia of supramolecular chemistry. CRC Press, Taylor & Francis, Boca Raton, FL
185. Geissler M, Xia Y (2004) Patterning: principles and some new developments. Adv Mater 16:1249–1269
186. Mijatovic D, Eijkel JCT, Van den Berg A (2005) Technologies for nanofluidic systems: top-down vs. bottom-up- a review. Lab Chip 5:492–500
187. Gates BD, Xu Q, Stewart M, Ryan M, Willson CG, Whitesides GM (2005) New approaches to nanofabrication: molding, printing, and other techniques. Chem Rev 105:1171–1196
188. Etienne M, Walcarius A (2012) Electrochemistry within template nanosystems. In: Wadhawan JD, Compton RG (eds) Electrochemistry, vol 11, Nanosystems electrochemistry. RSC Publishing, Cambridge

189. Martin CR (1994) Nanomaterials – a membrane-based synthetic approach. Science 266:1961–1966
190. Martin CR (1996) Membrane-based synthesis of nanomaterials. Chem Mater 8:1739–1746
191. Velev OD, Kaler EW (2000) Structured porous materials via colloidal crystal templating: from inorganic oxides to metals. Adv Mater 12:531–534
192. Velev OD, Lenhoff AM (2000) Colloidal crystals as templates for porous materials. Curr Opin Colloid Interface Sci 5:56–63
193. Lytle JC, Stein A (2006) Recent progress in syntheses and applications of inverse opals and related macroporous materials prepared by colloidal crystal templating. Annu Rev Anal Chem 1:1–79
194. Hamley IW (2003) Nanotechnology with soft materials. Angew Chem Int Ed 42:1692–1712
195. Wan Y, Zhao D (2007) On the controllable soft-templating approach to mesoporous silicate. Chem Rev 107:2821–2860
196. Sanchez C, Boissière C, Grosso D, Laberty C, Nicole L (2008) Design, synthesis, and properties of inorganic and hybrid thin films having periodically organized nanoporosity. Chem Mater 20:682–737
197. Wan Y, Shi Y, Zhao D (2008) Supramolecular aggregates as templates: ordered mesoporous polymers and carbons. Chem Mater 20:932–945
198. Diggle JW, Downie TC, Goulding CW (1969) Anodic oxide films on aluminum. Chem Rev 69:365–405
199. She G, Mu L, Shi W (2009) Electrodeposition of one-dimensional nanostructures. Recent Patent Nanotechnol 3:182–191
200. Masuda H, Yamada H, Satoh M, Asoh H, Nakao M, Tamamura T (1997) Highly ordered nanochannel-array architecture in anodic alumina. Appl Phys Lett 71:2770–2773
201. Martin CR (1995) Template synthesis of electronically conductive polymer nanostructures. Acc Chem Res 28:61–68
202. Fleisher RL, Price PB, Walker RM (1975) Nuclear tracks in solids: principles and applications. University of California Press, Berkeley, CA
203. Cao G, Liu D (2008) Template-based synthesis of nanorod, nanowire, and nanotube arrays. Adv Colloid Interface Sci 136:45–64
204. Zhang J, Kielbasa JE, Carrol DL (2010) Controllable fabrication of porous alumina templates for nanostructures synthesis. Mater Chem Phys 122:295–300
205. Lakshmi BB, Dorhout PK, Martin CR (1997) Sol–gel template synthesis of semiconductor nanostructures. Chem Mater 9:857–862
206. Schmuki P, Virtanen S (2009) Electrochemistry at the nanoscale. Springer, New York
207. Lee KR, Kwon YU (2010) Hard templates for fabrication of nanostructured films. Nano 5:75–87
208. Zhang LY, Fen J, Hue DS (2007) An investigation of thermal decomposition of β-FeOOH nanowire arrays assembled in AAO templates. Mater Lett 61:1363–1367
209. Bok HM, Shuford KL, Kim S, Kim SK, Park S (2008) Multiple surface plasmon modes for a colloidal solution of nanoporous gold nanorods and their comparison to smooth gold nanorods. Nano Lett 8:2265–2270
210. Kim S, Shuford KL, Bok HM, Kim SK, Park S (2008) Intraparticle surface plasmon coupling in quasi-one-dimensional nanostructures. Nano Lett 8:800–804
211. Stein A, Wilson BE, Rudisill SG (2012) Design and functionality of colloidal-crystal-templated materials-chemical applications of inverse opals. Chem Soc Rev 42:2763–2803
212. Stöber W, Fink A, Bohn E (1968) Controlled growth of monodisperse silica spheres in the micron size range. J Colloid Interface Sci 26:62–69
213. Antl L, Goodwin JW, Hill RD, Ottewill RH, Owens SM, Papworth S (1986) The preparation of poly(methyl methacrylate) latices in non-aqueous media. Colloids Surf 17:67–78
214. Goodwin JW, Hearn J, Ho CC, Ottewill RH (1974) Studies on the preparation and characterisation of monodisperse polystyrene latices. Kolloid Z Z Polym 252:464–471

215. Hornig DF, Plumb RC (1957) Vibrational spectra of molecules and complex ions in crystals. IX. Boric acid. Journal Chem Phys 26:637–642
216. López C (2003) Materials aspects of photonic crystals. Adv Mater 15:1679–1704
217. Lozano G, Míguez H (2008) Relation between growth dynamics and the spatial distribution of intrinsic defects in self-assembled colloidal crystal films. Appl Phys Lett 92:091904–091906
218. Bevan MA, Lewis JA, Braun PV, Wiltzius P (2004) Structural evolution of colloidal crystals with increasing ionic strength. Langmuir 20:7045–7052
219. Tien J, Terfort A, Whitesides GM (1997) Microfabrication through electrostatic self-assembly. Langmuir 13:5349–5355
220. Denkov N, Velev O, Kralchevski P, Ivanov I, Yoshimura H, Nagayama K (1992) Mechanism of formation of two-dimensional crystals from latex particles on substrates. Langmuir 8:3183–3190
221. Trau M, Saville DA, Aksay IA (1997) Assembly of colloidal crystals at electrode interfaces. Langmuir 13:6375–6381
222. Shimmin RG, Vajtai R, Siegel RW, Braun PV (2007) Room-temperature assembly of germanium photonic crystals through colloidal crystal templating. Chem Mater 19:2102–2107
223. Chen X, Li Z, Ye J, Zou Z (2010) Forced impregnation approach to fabrication of large-area, three-dimensionally ordered macroporous metal oxides. Chem Mater 22:3583–3585
224. Aoi Y, Kobayashi S, Kamijo E, Deki S (2005) Fabrication of three-dimensional ordered macroporous titanium oxide by the liquid-phase deposition method using colloidal template. J Mater Sci 40:5561–5563
225. Turner ME, Trentler TJ, Colvin VL (2001) Thin films of macroporous metal oxides. Adv Mater 13:180–183
226. Blanford CF, Yan H, Schroden RC, Al-Daous M, Stein A (2001) Gems of chemistry and physics: macroporous metal oxides with 3D order. Adv Mater 13:401–407
227. Plowman BJ, Bhargava SK, O'Mullane AP (2011) Electrochemical fabrication of metallic nanostructured electrodes for electroanalytical applications. Analyst 136:5107–5119
228. Bartlett PN, Baumberg JJ, Birkin PR, Ghanem MA, Netti MC (2002) Highly ordered macroporous gold and platinum films formed by electrochemical deposition through templates assembled from submicron diameter monodisperse polystyrene spheres. Chem Mater 14:2199–2208
229. Szamocki R, Reculusa S, Ravaine S, Bartlett PN, Kuhn A, Hempelmann R (2006) Tailored mesostructuring and biofunctionalization of gold for increased electroactivity. Angew Chem Int Ed 45:1317–1321
230. Bartlett PN, Birkin PR, Ghanem MA (2000) Electrochemical deposition of macroporous platinum, palladium and cobalt films using polystyrene latex sphere templates. Chem Commun 17:1671–1672
231. Tauer K (2004) Latex particles. In: Caruso F (ed) Colloids and colloid assemblies: synthesis, modification, organization and utilization of colloidal particles. Wiley-VCH Verlag GmbH & Co. KGaA, Weinheim
232. Braun PV, Wiltzius P (1999) Electrochemically grown photonic crystals. Nature 402:603–604
233. Lenz J, Trieu V, Hempelmann R, Kuhn A (2011) Ordered macroporous ruthenium oxide electrodes for potentiometric and amperometric sensing applications. Electroanalysis 23:1186–1192
234. Bartlett PN, Birkin PR, Ghanem MA, Toh CS (2001) Electrochemical syntheses of highly ordered macroporous conducting polymers grown around self-assembled colloidal templates. J Mater Chem 11:849–853
235. Lu Y (2006) Surfactant-templated mesoporous materials: from inorganic to hybrid to organic. Angew Chem Int Ed 45:7664–7667
236. Fendler JH (1987) Atomic and molecular clusters in membrane mimetic chemistry. Chem Rev 87:877–899

237. Deng Y, Wei J, Sun Z, Zhao D (2013) Large-pore ordered mesoporous materials templated from non-Pluronic amphiphilic block copolymers. Chem Soc Rev 42:4054–4070
238. Neto AMF, Salinas SRA (2005) The physics of lyotropic liquid crystals: phase transition and structural properties. Oxford University Press, New York, NY
239. Yan F, Texter J (2006) Polymerization of and in mesophases. Adv Colloid Interface Sci 128–130:27–35
240. Kresge CT, Leonowicz ME, Roth WJ, Vartuli JC, Beck JS (1992) Ordered mesoporous molecular sieves synthesized by a liquid-crystal template mechanism. Nature 359:710–712
241. Beck JS, Vartuli JC, Roth WJ, Leonowicz ME, Kresge CT, Schmitt KD, Chu CTW, Olson DH, Sheppard EW (1992) A new family of mesoporous molecular sieves prepared with liquid crystal templates. J Am Chem Soc 114:10834–10843
242. Grosso D, Cagnol F, Soler-Illia GJAA, Crepaldi EL, Amenitsch H, Brunet-Bruneau A, Bourgeois A, Sanchez C (2004) Fundamentals of mesostructuring through evaporation-induced self-assembly. Adv Funct Mater 14:309–322
243. Etienne M, Quach A, Grosso D, Nicole L, Sanchez C, Walcarius A (2007) Molecular transport into mesostructured silica thin films: electrochemical monitoring and comparison between p6m. P6(3)/mmc, and Pm3n structures. Chem Mater 19:844–856
244. Chen M, Burgess I, Lipkowski J (2009) Potential controlled surface aggregation of surfactants at electrode surfaces - a molecular view. Surf Sci 603:1878–1891
245. Etienne M, Guillemin Y, Grosso D, Walcarius A (2013) Electrochemical approaches for the fabrication and/or characterization of pure and hybrid templated mesoporous oxide thin films: a review. Anal Bioanal Chem 405:1497–1512
246. Walcarius A (2013) Mesoporous materials and electrochemistry. Chem Soc Rev 42:4098–4140
247. Attard GS, Glyde JC, Göltner CG (1995) Liquid-crystalline phases as templates for the synthesis of mesoporous silica. Nature 378:366–368
248. Attard GS, Corker JM, Göltner CG, Henke S, Templer RH (1997) Liquid-crystal templates for nanostructured metals. Angew Chem Int Ed 36:1315–1317
249. Whitehead AH, Elliott JM, Owen JR, Attard GS (1999) Electrodeposition of mesoporous tin films. Chem Commun 331–332
250. Nelson PA, Elliott JM, Attard GS, Owen JR (2002) Mesoporous nickel/nickel oxide nanoarchitectured electrode. Chem Mater 14:524–529
251. Bartlett PN, Marwan J (2003) Electrochemical deposition of nanostructured (H 1 -e) layers of two metals in which pores within the two layers interconnect. Chem Mater 15:2962–2968
252. Bender F, Mankelow RK, Hibbert DB, Gooding JJ (2006) Lyotropic liquid crystal templating of roups 11 and 12 metal films. Electroanalysis 18:1558–1563
253. Tanaka S, Doi A, Nakatani N, Katayama Y, Miyake Y (2009) Synthesis of ordered mesoporous carbon films, powders, and fibers by direct triblock-copolymer-templating method using an ethanol/water system. Carbon 47:2688–2698
254. Jun S, Joo SH, Ryoo R, Kruk M, Jaroniec M, Liu Z, Ohsuna T, Terasaki O (2000) Synthesis of new, nanoporous carbon with hexagonally ordered mesostructure. J Am Chem Soc 122:10712–10713
255. Lee JS, Joo SH, Ryoo R (2002) Synthesis of mesoporous silicas of controlled pore wall thickness and their replication to ordered nanoporous carbons with various pore diameters. J Am Chem Soc 124:1156–1157
256. Ryoo R, Joo SH, Jun S (1999) Synthesis of highly ordered carbon molecular sieves via template-mediated structural transformation. J Phys Chem B 103:7743–7746
257. Walcarius A (1998) Analytical applications of silica-modified electrodes- a comprehensive review. Electroanalysis 10:1217–1235
258. Walcarius A, Kuhn A (2008) Ordered porous thin films in electrochemical analysis. Trends Anal Chem 27:593–603
259. Song YY, Zhang D, Gao W, Xia XH (2005) Nonenzymatic glucose detection by using a three-dimensionally ordered, macroporous platinum template. Chem Eur J 11:2177–2182

260. Ben-Ali S, Cook DA, Evans SAG, Thienpont A, Bartlett PN, Kuhn A (2003) Electrocatalysis with monolayer modified highly organized macroporous electrodes. Electrochem Commun 5:747–751
261. Evans SAG, Elliott JM, Andrews LM, Bartlett PN, Doyle PJ, Denuault G (2002) Detection of hydrogen peroxide at mesoporous platinum microelectrodes. Anal Chem 74:1322–1326
262. Wang CH, Yang C, Song YY, Gao W, Xia XH (2005) Adsorption and direct electron transfer from hemoglobin into a three-dimensionally ordered macroporous gold film. Adv Funct Mater 15:1267–1275
263. Bon Saint Côme Y, Lalo H, Wang Z, Etienne M, Gajdzik J, Kohring GW, Walcarius A, Helpelmann R, Kuhn A (2011) Multiscale-tailored bioelectrode surfaces for optimized catalytic conversion efficiency. Langmuir 27:12737–12744
264. Chen HH, Suzuki H, Sato O, Gu ZZ (2005) Biosensing capability of gold-nanoparticles – immobilized three-dimensionally ordered macroporous film. Appl Phys A 81:1127–1130
265. Oh CS, Kim H, Rengaraj S, Kim Y (2012) In situ detection and removal of metal ion by porous gold electrode. Microporous Mesoporous Mater 147:1–4
266. Xu X, Tian B, Zhang S, Kong J, Zhao D, Liu B (2004) Electrochemistry and biosensing reactivity of heme proteins adsorbed on the structure-tailored mesoporous Nb_2O_5 matrix. Anal Chim Acta 519:31–38
267. Topoglidis E, Campbell CJ, Cass AEG, Durrant JR (2006) Nitric oxide biosensors based on the immobilization of hemoglobin on mesoporous titania electrodes. Electroanalysis 18:882–888
268. Feng JJ, Xu JJ, Chen HY (2006) Direct electron transfer and electrocatalysis of hemoglobin adsorbed onto electrodeposited mesoporous tungsten oxide. Electrochem Commun 8:77–82
269. Wang Y, Wu X, Li Y, Zhou Z (2004) Meso-structured SnO_2 as sensing materials for gas sensors. Solid State Elect 48:627–632
270. Walcarius A (2005) Impact of mesoporous silica-based materials on electrochemistry and feedback from electrochemical science to the characterization of these ordered materials. C R Chim 8:693–712
271. Falcaro P, Bertolo JM, Innocenzi P, Heinz A, Bearzotti A (2004) Ordered mesostructured silica films: effect of pore surface on its sensing properties. J Sol Gel Sci Technol 32:107–110
272. Innocenzi P, Falcaro P, Bertolo JM, Bearzotti A, Heinz A (2005) Electrical responses of silica mesostructured films to changes in environmental humidity and processing conditions. J Non Cryst Solids 351:1980–1986
273. Innocenzi P, Martucci A, Guglielmi M, Bearzotti A, Traversa E (2001) Electrical and structural characterisation of mesoporous silica thin films as humidity sensors. Sensor Actuat B 76:299–303
274. Jia N, Wang Z, Yang G, Shen H, Zhu L (2007) Electrochemical properties of ordered mesoporous carbon and its electroanalytical application for selective determination of dopamine. Electrochem Commun 9:233–238
275. Ndamanisha JC, Bai J, Qi B, Guo L (2009) Application of electrochemical properties of ordered mesoporous carbon to the determination of glutathione and cysteine. Anal Biochem 386:79–84
276. Zhu L, Tian C, Yang D, Jiang X, Yang R (2008) Bioanalytical applications of the ordered mesoporous carbon modified electrodes. Electroanalysis 20:2518–2525
277. Nie D, Li P, Zhang D, Zhou T, Liang Y (2010) Simultaneous determination of nitroaromatic compounds in water using capillary electrophoresis with amperometric detection on an electrode modified with a mesoporous nano-structured carbon material. Electrophoresis 31:2981–2988
278. Bai J, Guo L, Ndamanisha JC, Qi B (2009) Electrochemical properties and simultaneous determination of dihydroxybenzene isomers at ordered mesoporous carbon-modified electrode. J Appl Electrochem 39:2497–2503
279. Pan D, Ma S, Bo X, Guo L (2011) Electrochemical behavior of methyl parathion and its sensitive determination at a glassy carbon electrode modified with ordered mesoporous carbon. Microchim Acta 173:215–221

280. Zhu L, Yang R, Jiang X, Yang D (2009) Amperometric determination of NADH at a Nile blue/ordered mesoporous carbon composite electrode. Electrochem Commun 11:530–533
281. Yu J, Du W, Zhao F, Zeng B (2009) High sensitive simultaneous determination of catechol and hydroquinone at mesoporous carbon CMK-3 electrode in comparison with multi-walled carbon nanotubes and Vulcan XC-72 carbon electrodes. Electrochim Acta 54:984–988
282. Zang J, Guo CX, Hu F, Yu L, Li CM (2011) Electrochemical detection of ultratrace nitroaromatic explosives using ordered mesoporous carbon. Anal Chim Acta 683:187–191
283. Zhu L, Tian C, Yang R, Zhai J (2008) Anodic stripping voltammetric determination of lead in tap water at an ordered mesoporous carbon/nafion composite film electrode. Electroanalysis 20:527–533
284. Guo Z, Li S, Liu XM, Gao YP, Zhang WW, Ding XP (2011) Mesoporous carbon-polyaniline electrode: characterization and application to determination of copper and lead by anodic stripping voltammetry. Mater Chem Phys 128:238–242
285. Lai CZ, Fierke MA, Stein A, Bühlmann P (2007) Ion-selective electrodes with three-dimensionally ordered macroporous carbon as the solid contact. Anal Chem 79:4621–4626
286. Bard AJ (1994) Integrated chemical systems: a chemical approach to nanotechnology, vol 7. John Wiley & Sons, New York, NY
287. Elliott CM, Murray RW (1976) Chemically modified carbon electrodes. Anal Chem 48:1247–1254
288. Durst RA, Bäumer AJ, Murray RW, Buck RP, Andrieux CP (1997) Chemically modified electrodes: recommended terminology and definitions. Pure Appl Chem 69:1317–1323
289. Kutner W, Wang J, L'Her M, Buck RP (1998) Analytical aspects of chemically modified electrodes: classification, critical evaluation and recommendations. Pure Appl Chem 70:1301–1318
290. Arrigan DWM (1994) Voltammetric determination of trace metals and organics after accumulation at modified electrodes. Analyst 119:1953–1966
291. Walcarius A (2001) Electrochemical applications of silica-based organic–inorganic hybrid materials. Chem Mater 13:3351–3372
292. Murray RW (1984) Chemically modified electrodes. In: Bard AJ (ed) Electroanalytical chemistry, vol 13. Marcel Dekker Inc., New York, NY
293. Murray RW, Ewing AG, Durst RA (1987) Chemically modified electrodes: molecular design for electroanalysis. Anal Chem 59:379A–390A
294. Murray RW (ed) (1984) Molecular design of electrode surfaces, techniques of chemistry. John Wiley and Sons, New York, NY
295. Zhong CJ, Woods NT, Dawson GB, Porter MD (1999) Formation of thiol-based monolayers on gold: implications from open circuit potential measurements. Electrochem Commun 1:17–21
296. Cohen-Atiya M, Mandler D (2003) Studying thiol adsorption on Au, Ag and Hg surfaces by potentiometric measurements. J Electroanal Chem 550–551:267–276
297. Oyamatsu D, Kuwabata S, Yoneyama H (1999) Underpotential deposition behavior of metals onto gold electrodes coated with self-assembled monolayers of alkanethiols. J Electroanal Chem 473:59–67
298. Beulen MWJ, Kastenberg MI, Van Veggel FCJM, Reinhoudt DN (1998) Electrochemical stability of self-assembled monolayers on gold. Langmuir 14:7463–7467
299. Widrig AC, Chung C, Porter MD (1991) The electrochemical desorption of n-alkanethiol from polycrystalline Au and Ag electrodes monolayers. J Electroanal Chem 310:335–359
300. Porter MD, Bright TB, Allara DL, Chidsey CED (1987) Spontaneously organized molecular assemblies. 4. Structural characterization of n-alkyl thiol monolayers on gold by optical ellipsometry, infrared spectroscopy, and electrochemistry. J Am Chem Soc 109:3559–3568
301. Esplandiú MJ, Hagenström H, Kolb DM (2001) Functionalized self-assembled alkanethiol monolayers on Au (111) electrodes: 1. Surface structure and electrochemistry. Langmuir 17:828–838
302. Ji X, Ren J, Jin J, Nakamura T (2007) A sensor for superoxide in aqueous and organic/aqueous media based on immobilized cytochrome c on binary self-assembled monolayers. Biosens Bioelectron 23:241–247

303. Lai RY, Seferos DS, Heeger AJ, Bazan GC, Plaxco KW (2006) Comparison of the signaling and stability of electrochemical DNA sensors fabricated from 6- or 11-carbon self-assembled monolayers. Langmuir 22:10796–10800
304. Flynn NT, Tran TNT, Cima MJ, Langer R (2003) Long-term stability of self-assembled monolayers in biological media. Langmuir 19:10909–10915
305. Gooding JJ, Darwish N (2012) The rise of self-assembled monolayers for fabricating electrochemical biosensors–an interfacial perspective. Chem Rec 12:92–105
306. Geng P, Zhang X, Meng W, Wang Q, Zhang W, Jin L, Feng Z, Wu Z (2008) Self-assembled monolayers-based immunosensor for detection of Escherichia coli using electrochemical impedance spectroscopy. Electrochim Acta 53:4663–4668
307. Chow E, Wong ELS, Pascoe O, Hibbert DB, Gooding JJ (2007) Extending the dynamic range of electrochemical sensors using multiple modified electrodes. Anal Bioanal Chem 387:1489–1498
308. Mena ML, Carralero V, González-Cortés A, Yáñez-Sedeño P, Pingarrón JM (2005) Laccase biosensor based on N-succinimidyl-3-thiopropionate-functionalized gold electrodes. Electroanalysis 17:2147–2155
309. Thavarungkul P, Dawan S, Kanatharana P, Asawatreratanakul P (2007) Detecting penicillin G in milk with impedimetric label-free immunosensor. Biosens Bioelectron 23:688–694
310. Chow E, Wong ELS, Böcking T, Nguyen QT, Hibbert DB, Gooding JJ (2005) Analytical performance and characterization of MPA-Gly-Gly-His modified sensors. Sensor Actuat B 111–112:540–548
311. Liu XP, Deng YJ, Jin XY (2009) Ultrasensitive electrochemical immunosensor for ochratoxin A using gold colloid-mediated hapten immobilization. Anal Biochem 389:63–68
312. Tolba M, Ahmed MU, Tlili C, Eichenseher F, Loessner MJ, Zourob M (2012) A bacteriophage endolysin-based electrochemical impedance biosensor for the rapid detection of Listeria cells. Analyst 137:5749–5756
313. Chow E, Ebrahimi D, Gooding JJ, Hibbert DB (2006) Application of N-PLS calibration to the simultaneous determination of Cu(2+), Cd(2+) and Pb(2+) using peptide modified electrochemical sensors. Analyst 131:1051–1057
314. Escamilla-Gómez V, Campuzano S, Pedrero M, Pingarrón JM (2008) Immunosensor for the determination of Staphylococcus aureus using a tyrosinase-mercaptopropionic acid modified electrode as an amperometric transducer. Anal Bioanal Chem 391:837–845
315. Navrátilová I, Skládal P (2004) The immunosensors for measurement of 2,4-dichlorophenoxyacetic acid based on electrochemical impedance spectroscopy. Bioelectrochemistry 62:11–18
316. Hanefeld U, Gardossi L, Magner E (2009) Understanding enzyme immobilisation. Chem Soc Rev 38:453–468
317. Samanta D, Sarkar A (2011) Immobilization of bio-macromolecules on self-assembled monolayers: methods and sensor applications. Chem Soc Rev 40:2567–2592
318. Shen H, Mark E, Seliskar CJ, Mark HB Jr, Heineman WR (1997) Stripping voltammetry of copper and lead using gold electrodes modified with self-assembled monolayers. J Solid State Electrochem 1:241–247
319. Liu A, Chen D, Lin C, Chou HH, Chen C (1999) Application of cysteine monolayers for electrochemical determination of sub-ppb copper(II). Anal Chem 13:1549–1552
320. Arrigan DWM, Le Bihan L (1999) A study of L-cysteine adsorption on gold via electrochemical desorption and copper(II) ion complexation. Analyst 124:1645–1649
321. Yang W, Gooding JJ, Hibbert DB (2001) Characterisation of gold electrodes modified with self-assembled monolayers of L -cysteine for the adsorptive stripping analysis of copper. J Electroanal Chem 516:10–16
322. Aihara M, Tanaka F, Miyazaki Y, Takehara K (2002) Adsorption of lanthanide (III) ions from aqueous solutions by self-assembled monolayers of glutathione on gold. Anal Lett 35:759–765
323. Zugle R, Kambo-Dorsa J, Gadzekpo VPY (2003) Detection of metal ions using ion-channel sensor based on self-assembled monolayer of thioctic acid. Talanta 61:837–848

324. Freire RS, Kubota LT (2004) Application of self-assembled monolayer-based electrode for voltammetric determination of copper. Electrochim Acta 49:3795–3800
325. Burshtain D, Mandler D (2005) Studying the binding of Cd2+ by ω-mercaptoalkanoic acid self assembled monolayers by cyclic voltammetry and scanning electrochemical microscopy (SECM). J Electroanal Chem 581:310–319
326. Mohadesi A, Taher MA (2007) Voltammetric determination of Cu(II) in natural waters and human hair at a meso-2,3-dimercaptosuccinic acid self-assembled gold electrode. Talanta 72:95–100
327. Chow E, Gooding JJ (2006) Peptide modified electrodes as electrochemical metal ion sensors. Electroanalysis 18:1437–1448
328. Shervedani RK, Hatefi-Mehrjardi A, Asadi-Farsani A (2007) Sensitive determination of iron (III) by gold electrode modified with 2-mercaptosuccinic acid self-assembled monolayer. Anal Chim Acta 601:164–171
329. Ji HF, Zhang Y, Purushotham VV, Kondu S, Ramachandran B, Thundat T, Haynie DT (2005) 1,6-Hexanedithiol monolayer as a receptor for specific recognition of alkylmercury. Analyst 130:1577–1579
330. Berchmans S, Arivukkodi S, Yegnaraman V (2000) Self-assembled monolayers of 2-mercaptobenzimidazole on gold: stripping voltammetric determination of Hg(II). Electrochem Commun 2:226–229
331. Liu G, Nguyen QT, Chow E, Böcking T, Hibbert DB, Gooding JJ (2006) Study of factors affecting the performance of voltammetric copper sensors based on Gly-Gly-His modified glassy carbon and gold electrodes. Electroanalysis 18:1141–1151
332. Becker A, Tobias H, Mandler D (2009) Electrochemical determination of uranyl ions using a self-assembled monolayer. Anal Chem 81:8627–8631
333. Moressi MB, Andreu R, Calvente JJ, Fernández H, Zón MA (2004) Electro-oxidation of altertoxin I (ATX-I) at gold electrodes modified by dodecanethiol self-assembled monolayers. J Electroanal Chem 570:209–217
334. Moressi MB, Calvente JJ, Andreu R, Fernández H, Zón MA (2007) Improvement of alternariol monomethyl ether detection at gold electrodes modified with a dodecanethiol self-assembled monolayer. J Electroanal Chem 605:118–124
335. Ozoemena KI, Nyokong T (2005) Surface electrochemistry of iron phthalocyanine axially ligated to 4-mercaptopyridine self-assembled monolayers at gold electrode: applications to electrocatalytic oxidation and detection of thiocyanate. J Electroanal Chem 579:283–289
336. Hleli S, Martelet C, Abdelghani A, Burais N, Jaffrezic-Renault N (2006) Atrazine analysis using an impedimetric immunosensor based on mixed biotinylated self-assembled monolayer. Sensor Actuat B 113:711–717
337. Ahmad A, Moore E (2012) Electrochemical immunosensor modified with self-assembled monolayer of 11-mercaptoundecanoic acid on gold electrodes for detection of benzo[a] pyrene in water. Analyst 137:5839–5844
338. Arya SK, Chornokur G, Venugopal M, Bhansali S (2010) Dithiobis(succinimidyl propionate) modified gold microarray electrode based electrochemical immunosensor for ultrasensitive detection of cortisol. Biosens Bioelectron 25:2296–2301
339. Bozic RG, West AC, Levicky R (2008) Square wave voltammetric detection of 2,4,6-trinitrotoluene and 2,4-dinitrotoluene on a gold electrode modified with self-assembled monolayers. Sensor Actuat B 133:509–515
340. Tredici I, Merli D, Zavarise F, Profumo A (2010) α-Cyclodextrins chemically modified gold electrode for the determination of nitroaromatic compounds. J Electroanal Chem 645:22–27
341. Zhang S, Sun W, Zhang W (1998) Direct electrochemistry of hemoglobin at silver electrode modified by lipoic acid monolayer. Anal Lett 31:2159–2171
342. Bart M, Stigter ECA, Stapert HR, de Jong GJ, van Bennekom WP (2005) On the response of a label-free interferon-gamma immunosensor utilizing electrochemical impedance spectroscopy. Biosens Bioelectron 21:49–59

343. Billah M, Hays HCW, Millner PA (2007) Development of a myoglobin impedimetric immunosensor based on mixed self-assembled monolayer onto gold. Microchim Acta 160:447–454
344. Chen J, Zhang J, Li J, Yang HH, Fu F, Chen G (2010) An ultrasensitive signal-on electrochemical aptasensor via target-induced conjunction of split aptamer fragments. Biosens Bioelectron 25:996–1000
345. Guo X, Kulkarni A, Doepke A, Halsall HB, Iyer S, Heineman WR (2012) Carbohydrate-based label-free detection of Escherichia coli ORN 178 using electrochemical impedance spectroscopy. Anal Chem 84:241–246
346. Xi F, Gao J, Wang J, Wang Z (2011) Discrimination and detection of bacteria with a label-free impedimetric biosensor based on self-assembled lectin monolayer. J Electroanal Chem 656:252–257
347. Labib M, Zamay AS, Kolovskaya OS, Reshetneva IT, Zamay GS, Kibbee RJ, Sattar SA, Zamay TN, Berezovski MV (2012) Aptamer-based viability impedimetric sensor for bacteria. Anal Chem 84:8966–8969
348. Escamilla-Gómez V, Campuzano S, Pedrero M, Pingarrón JM (2009) Gold screen-printed-based impedimetric immunobiosensors for direct and sensitive. Biosens Bioelectron 24:3365–3371
349. Vidal JC, Esteban S, Gil J, Castillo JR (2006) A comparative study of immobilization methods of a tyrosinase enzyme on electrodes and their application to the detection of dichlorvos organophosphorus insecticide. Talanta 68:791–799
350. Pedrosa VA, Caetano J, Machado SAS, Freire RS, Bertotti M (2007) Acetylcholinesterase immobilization on 3-mercaptopropionic acid self assembled monolayer for determination of pesticides. Electroanalysis 19:1415–1420
351. Yang S, Li Y, Jiang X, Chen Z, Lin X (2006) Horseradish peroxidase biosensor based on layer-by-layer technique for the determination of phenolic compounds. Sensor Actuat B 114:774–780
352. Yang S, Chen Z, Jin X, Lin X (2006) HRP biosensor based on sugar-lectin biospecific interactions for the determination of phenolic compounds. Electrochim Acta 52:200–205
353. Schöning MJ, Krause R, Block K, Musameh M, Mulchandani A, Wang J (2003) A dual amperometric/potentiometric FIA-based biosensor for the distinctive detection of organophosphorus pesticides. Sensor Actuat B 95:291–296
354. Wang J, Krause R, Block K, Musameh M, Mulchandani A, Schöning MJ (2003) Flow injection amperometric detection of OP nerve agents based on an organophosphorus-hydrolase biosensor detector. Biosens Bioelectron 18:255–260
355. Du D, Ding J, Tao Y, Chen X (2008) Application of chemisorption/desorption process of thiocholine for pesticide detection based on acetylcholinesterase biosensor. Sensor Actuat B 134:908–912
356. Markovich I, Mandler D (2001) Disorganised self-assembled monolayers (SAMs): the incorporation of amphiphilic molecules. Analyst 126:1850–1856
357. Calvente JJ, Kovacova Z, Sanchez MD, Andreu R, Fawcett WR (1996) Desorption of spontaneously adsorbed and electrochemically readsorbed 2-mercaptoethanesulfonate on Au (111). Langmuir 12:5696–5703
358. Herzog G, Arrigan DWM (2003) Application of disorganized monolayer films on gold electrodes to the prevention of surfactant inhibition of the voltammetric detection of trace metals via anodic stripping of underpotential deposits: detection of copper. Anal Chem 75:319–323
359. Herzog G, Arrigan DWM (2003) Comparison of 2-mercaptoethane sulfonate and mercaptoacetic acid disorganized monolayer-coated electrodes for the detection of copper via underpotential deposition-stripping voltammetry. Electroanalysis 15:1302–1306
360. Herzog G, Arrigan DWM (2005) Underpotential deposition and stripping of lead at disorganized monolayer-modified gold electrodes. Electroanalysis 17:1816–1821

361. Herzog G, Beni V, Dillon PH, Barry T, Arrigan DWM (2004) Effect of humic acid on the underpotential deposition-stripping voltammetry of copper in acetic acid soil extract solutions at mercaptoacetic acid-modified gold electrodes. Anal Chim Acta 511:137–143
362. Herzog G, Arrigan DWM (2005) Application of the disorganized monolayer gold electrode to copper determination in white wine. Anal Lett 37:591–602
363. Huang JF, Lin BT (2009) Application of a nanoporous gold electrode for the sensitive detection of copper via mercury-free anodic stripping voltammetry. Analyst 134:2306–2313
364. Downard AJ (2000) Electrochemically assisted covalent modification of carbon electrodes. Electroanalysis 12:1085–1096
365. Pinson J, Podvorica F (2005) Attachment of organic layers to conductive or semiconductive surfaces by reduction of diazonium salts. Chem Soc Rev 34:429–439
366. Doppelt P, Hallais G, Pinson J, Podvorica F, Verneyre S (2007) Surface modification of conducting substrates. Existence of azo bonds in the structure of organic layers obtained from diazonium salts. Chem Mater 19:4570–4575
367. Allongue P, Pinson J (2009) Organic functionalization of surfaces by electrografting: methods and applications. Actual Chim 327–328:98–103
368. Bélanger D, Pinson J (2011) Electrografting: a powerful method for surface modification. Chem Soc Rev 40:3995–4048
369. Abdellaoui S, Corgier BC, Mandon CA, Doumeche B, Marquette CA, Blum LJ (2013) Biomolecules immobilization using the aryldiazonium electrografting. Electroanalysis 25:671–684
370. Ahlberg E, Helgée B, Parker BD (1980) The reaction of aryl radicals with metallic electrodes. Acta Chem Scand B 34:181–186
371. Allongue P, Delamar M, Desbat O, Fagebaume R, Hitmi J, Pinson J, Savéant JM (1997) Covalent modification of carbon surfaces by aryl radicals generated from the electrochemical reduction of diazonium salts. J Am Chem Soc 119:201–207
372. Andrieux CP, Pinson J (2003) The standard redox potential of the phenyl radical/anion couple. J Am Chem Soc 125:14801–14806
373. Allongue P, Henry de Villeneuve C, Cherouvrier G, Cortes R, Bernard MC (2003) Phenyl layers on H-Si(111) by electrochemical reduction of diazonium salts: monolayer versus multilayer formation. J Electroanal Chem 550–551:161–174
374. Kariuki JK, McDermott MT (2001) Formation of multilayers on glassy carbon electrodes via the reduction of diazonium salts. Langmuir 17:5947–5951
375. Belmont JA, Amici R, Galloway M, Collin P (1998) Reaction of carbon black with diazonium salts, resultant carbon black products and their uses. US Patent, US 19985851280
376. Kariuki JK, McDermott MT (1999) Nucleation and growth of functionalized aryl films on graphite electrodes. Langmuir 15:6534–6540
377. Ray K, McCreery RL (1997) Spatially resolved raman spectroscopy of carbon electrode surfaces: observations of structural and chemical heterogeneity. Anal Chem 69:4680–4687
378. Lomeda JR, Doyle CD, Kosynkin DV, Hwang WF, Tour JM (2008) Diazonium functionalization of surfactant-wrapped chemically converted grapheme sheets. J Am Chem Soc 130:16021–16030
379. Sinitskii A, Dimiev A, Corley DA, Fursina AA, Kosynkin DV, Tour JM (2010) Kinetics od diazonium functionalization of chemically converted grapheme nanoribbons. ACS Nano 4:1949–1954
380. Sharma R, Baik JH, Perera CJ, Strano MS (2010) Anomalously large reactivity of single grapheme layers and edges toward electron transfer chemistries. Nano Lett 10:398–405
381. Saby C, Ortiz B, Champagne GY, Bélanger D (1997) Electrochemical modification of glassy carbon electrode using aromatic diazonium salts. 1. Blocking effect of 4-nitrophenyl and 4-carboxyphenyl groups. Langmuir 13:6805–6813
382. Delamar M, Desarmot G, Fagebaume O, Hitmi R, Pinson J, Savéant JM (1997) Modification of carbon fiber surfaces by electrochemical reduction of aryl diazonium salts: application to carbon epoxy composites. Carbon 35:801–807

383. Barroso-Bujans F, Fierro JLG, Rojas S, Sanchez-Cortes S, Arroyo M, Lopez-Manchado MA (2007) Degree of functionalization of carbon nanofibers with benzenesulfonic groups in acid medium. Carbon 45:1669–1678
384. Coulon E, Pinson J, Bourzat JD, Commerçon A, Pulicani JP (2001) Electrochemical attachment of organic groups to carbon felt surfaces. Langmuir 17:7102–7106
385. Lyskawa J, Grondein A, Bélanger D (2010) Chemical modification of carbon powders with aminophenyl and cyanophenyl groups and a study of their reactivity. Carbon 48:1271–1278
386. Cooke JM, Galloway CP, Bissell MA, Adams CE, Yu MC, Belmont JA, Amici, RM (2000) Polymeric products containing modified carbon products and methods of making and using the same. US Patent 6 110 9994 A (to Cabot Corp.).
387. Smith RDL, Pickup PG (2009) Voltammetric quantification of the spontaneous chemical modification of carbon black by diazonium coupling. Electrochim Acta 54:2305–2311
388. Li Z, Dai S (2005) Surface functionalization and pore size manipulation for carbons of ordered structure. Chem Mater 17:1717–1721
389. Li Z, Yan W, Dai S (2005) Surface functionalization of ordered mesoporous carbons. A comparative study. Langmuir 21:11999–12006
390. Wang X, Liu R, Waje MM, Chen Z, Yan Y, Bozhilov KN, Feng P (2007) Sulfonated ordered mesoporous carbon as stable and highly active protonic acid catalyst. Chem Mater 19:2395–2397
391. Bahr JL, Yang J, Kosynkin DV, Bronikowski MJ, Smalley RE, Tour JM (2001) Functionalization of carbon nanotubes by electrochemical reduction of aryl diazonium salts: a bucky paper electrode. J Am Chem Soc 123:6536–6542
392. Marcoux PR, Hapiot P, Batail P, Pinson J (2004) Electrochemical functionalization of nanotube films: growth of aryl chains on single-walled carbon nanotubes. New J Chem 28:302–307
393. Kuo TC, McCreery RL, Swain GM (1999) Electrochemical modification of boron-doped chemical vapor diamond surfaces with covalently bonded monolayers articles. Electrochem Solid State Lett 2:288–290
394. Szunerits S, Boukherroub R (2008) Different strategies for functionalization of diamond surfaces. J Solid State Electrochem 12:1205–1218
395. Yang W, Baker SE, Butler JE, Lee CS, Russell JN, Shang L, Sun B, Hamers RJ (2005) Electrically addressable biomolecular functionalization of conductive nanocrystalline diamond thin films. Chem Mater 17:938–940
396. Uetsuka H, Shin D, Tokuda N, Sacki K, Nebel CE (2007) Electrochemical grafting of boron-doped single crystalline chemical vapor deposition diamond with nitrophenyl molecules. Langmuir 23:3466–3472
397. Rappich J, Hinrichs K (2009) In situ study of nitrobenzene grafting on Si(111)-H surfaces by infrared spectroscopic ellipsometry. Electrochem Commun 11:2316–2319
398. Henry de Villeneuve C, Pinson J, Bernard MC, Allongue P (1997) Electrochemical formation of close-packed phenyl layers on Si(111). J Phys Chem B 101:2415–2420
399. Pandey D, Zemlyanov DY, Bevan K, Reifenberger RG, Dirk SM, Howell SW, Wheeler DR (2007) UHV STM I(V) and XPS studies of aryl diazonium molecules assembled on Si(111). Langmuir 23:4700–4708
400. Wang D, Buriak JM (2006) Trapping silicon surface-based radicals. Langmuir 22:6214–6221
401. Stewart MP, Maya F, Kosynkin DV, Dirk SM, Stapleton JJ, McGuiness CL, Allara DL, Tour JM (2004) Direct covalent grafting of conjugated molecules onto Si, GaAs, and Pd surfaces from aryldiazonium salts. J Am Chem Soc 126:370–378
402. Chen M, Kobashi K, Chen B, Lu M, Tour JM (2010) Functionalized self-assembled InAs/GaAs quantum-dot structures hybridized with organic molecules. Adv Funct Mater 20:469–475
403. Lehr J, Williamson BE, Flavel BS, Downard A (2009) Reaction of gold substrates with diazonium salts in acidic solution at open-circuit potential. Langmuir 25:13503–13509
404. Ghilane J, Delamar M, Guilloux-Viry M, Lagrost C, Mangeney C, Hapiot P (2005) Indirect reduction of aryldiazonium salts onto cathodically activated platinum surfaces: formation of metal-organic structures. Langmuir 21:6422–6429

405. Janin M, Ghilane J, Randriamahazaka H, Lacroix JC (2009) Microelectrodes modification through the reduction of aryl diazonium and their use in scanning electrochemical microscopy (SECM). Electrochem Commun 11:647–650
406. Bernard MC, Chaussé A, Cabet-Deliry E, Chehimi MM, Pinson J, Podvorica F, Vautrin-Ul C (2003) Organic layers bonded to industrial, coinage, and noble metals through electrochemical reduction of diazonium salts. Chem Mater 15:3450–3462
407. Hinge M, Ceccato M, Kingshott P, Besenbacher F, Pedersen SU, Daasbjerg K (2009) Electrochemical modification of chromium surfaces using 4-nitro- and 4-fluorobenzenediazonium salts. New J Chem 33:2405–2408
408. Adenier A, Bernard MC, Chehimi MM, Cabet-Deliry E, Desbat B, Fagebaume O, Pinson J, Podvorica FC (2001) Covalent modification iron surfaces by electrochemical reduction of aryldiazonium salts. J Am Chem Soc 123:4541–4549
409. Kullapere M, Matisen L, Saar A, Sammelselg V, Tammeveski K (2007) Electrochemical behavior of nickel electrodes modified with nitrophenyl groups. Electrochem Commun 9:2412–2417
410. Mirkhalaf F, Paprotny J, Schiffrin DJ (2006) Synthesis of metal nanoparticles stabilized by metal-carbon bonds. J Am Chem Soc 128:7400–7401
411. Ghosh D, Pradhan S, Chen W (2008) Titanium nanoparticles stabilized by Ti-C covalent bonds. Chem Mater 20:1248–1250
412. Ghosh D, Chen W (2008) Palladium nanoparticles passivated by metal-carbon covalent linkages. J Mater Chem 18:755–762
413. Kumar VKR, Gopidas KR (2010) Synthesis and characterization of gold-nanoparticle-cored dendrimers stabilized by metal-carbon bonds. Chem Asian J 5:887–896
414. Maldonado S, Smith TJ, Williams RD, Morin S, Barton E, Stevenson KJ (2006) Surface modification of indium tin oxide via electrochemical reduction of aryldiazonium cations. Langmuir 22:2884–2891
415. Adenier A, Barré N, Cabet-Deliry E, Chaussé A, Griveau S, Mercier F, Pinson J, Vautrin-Ul C (2006) Study of the spontaneous formation of organic layers on carbon and metal surfaces from diazonium salts. Surf Sci 600:4801–4812
416. Bureau C, Pinson J, French (2007) Process of modification of insulating, semiconductor, or metal surfaces, and such products obtained. Patent FR2892325 European Patent EP1948720.
417. Belmont JA, Amici RM, Galloway P (1996) Manufacture and use of diazonium salt-modified carbon black. Patent PCT Int Appl WO 96 18688 A1 (to Cabot Corp.).
418. Belmont JA Patent (1996) Manufacture of carbon products containing an attached organic group formed by reaction with diazonium salts, and the carbon products obtained. Patent PCT Int. Appl WO 96 18690 A1 (to Cabot Corp.).
419. Belmont JA, Reed TFP (1996) EPDM, hydrogenated NBR and butyl rubber compositions containing carbon black products. Patent PCT Int Appl WO 96 18674 A1 (to Cabot Corp.).
420. Bahr JL, Tour JM (2001) Highly functionalized carbon nanotubes using in situ generated diazonium compounds. Chem Mater 13:3823–3824
421. Dyke CA, Tour JM (2003) Solvent-free functionalization of carbon nanotubes. J Am Chem Soc 125:1156–1157
422. Dyke CA, Tour JM (2003) Unbundled and highly functionalized carbon nanotubes from aqueous reactions. Nano Lett 3:1215–1218
423. Strano MC, Dyke CA, Ursa ML, Barone PW, Allen MJ, Shan H, Kittrell C, Hauge RH, Tour JM, Smalley RE (2003) Electronic structure control of single-walled carbon nanotube functionalization. Science 301:1519–1522
424. Fan FRF, Yang J, Lintao C, Price DW, Dirk SM, Kosynkin DV, Yao Y, Rawlett AM, Tour JM, Bard AJ (2002) Charge transport through self-assembled monolayers of compounds of interest in molecular electronics. J Am Chem Soc 124:5550–5560
425. Adenier A, Cabet-Deliry E, Chaussé A, Griveau S, Mercier F, Pinson J, Vautrin-Ul C (2005) Grafting of nitrophenyl groups on carbon and metallic surfaces without electrochemical induction. Chem Mater 17:491–501

426. Bourdillon C, Delamar M, Demaille C, Hitmi R, Moiroux J, Pinson J (1992) Immobilisation of glucose oxidase on a carbon surface by electrochemical reduction of diazonium salts. J Electroanal Chem 336:113–123
427. Yang XH, Hall SB, Burrell AK, Officer DL (2001) A pH-responsive hydroquinone functionalized glassy carbon electrode. Chem Commun 2628–2629
428. Downard AJ, Roddick AD, Bond AM (1995) Covalent modification of carbon electrodes for voltammetric differentiation of dopamine and ascorbic acid. Anal Chim Acta 317:303–310
429. Betelu S, Vautrin-Ul C, Ly J, Chaussé A (2009) Screen-printed electrografted electrode for trace uranium analysis. Talanta 80:372–376
430. Uestuendag Z, Solak AO (2009) EDTA modified glassy carbon electrode: preparation and characterization. Electrochim Acta 54:6426–6432
431. Alonso-Lomillo MA, Dominguez-Renedo O, Hernandez-Martin A, Arcos-Martinez M (2009) Horseradish peroxidase covalent grafting onto screen-printed carbon electrodes for levetiracetam chronoamperometric determination. Anal Biochem 395:86–90
432. Harper JC, Polsky R, Dirk SM, Wheeler DR, Brozik SM (2007) Electroaddressable selective functionalization of electrode arrays catalytic NADH detection using aryl diazonium modified gold electrodes. Electroanalysis 19:1268–1274
433. Ghanem MA, Chrétien JM, Kilburn JD, Bartlett PN (2009) Electrochemical and solid-phase synthetic modification of glassy carbon electrodes with dihydroxybenzene compounds and the electrocatalytic oxidation of NADH. Bioelectrochemistry 76:115–125
434. Harnisch JA, Pris AD, Porter MD (2001) Attachment of gold naoparticles to glassy carbon electrodes via a mercaptobenzene film. J Am Chem Soc 123:5829–5830
435. Urchaga P, Weissmann M, Baranton S, Girardeau T, Coutanceau C (2009) Improvement of the platinum nanoparticles-carbon substrate interaction by insertion of a thiophenol molecular bridge. Langmuir 25:6543–6550
436. Sassolas A, Leca-Bouvier BD, Blum LJ (2008) DNA biosensors and microarrays. Chem Rev 108:109–139
437. Betelu S, Vautrin-Ul C, Chaussé A (2009) Novel 4-carboxyphenyl-grafted screen-printed electrode for trace Cu(II) determination. Electrochem Commun 11:383–386
438. Rezek B, Shin D, Nebel CE (2007) Properties of hybridized DNA arrays on single-crystalline undoped and boron-doped (100) diamonds studied by atomic force microscopy in electrolytes. Langmuir 23:7626–7633
439. Yang N, Uetsuka H, Nebel CE (2009) DNA-sensing with nano-textured diamond electrodes. Diamond Relat Mater 18:592–595
440. Shabani A, Mak AWH, Gerges I, Cuccia LA, Lawrence MF (2006) DNA immobilization onto electrochemically functionalized Si(100) surfaces. Talanta 70:615–623
441. Corgier BP, Laurent A, Perriat P, Blum LJ, Marquette CA (2007) A versatile method for direct and covalent immobilization of DNA proteins on biochips. Angew Chem Int Ed 46:4108–4110
442. Blankespoor R, Limoges B, Schoellhorn B, Syssa-Magale JL, Yazidi D (2005) Dense monolayers of metal-chelating ligands covalently attached to carbon electrodes electrochemically and their useful application in affinity binding of histidine-tagged proteins. Langmuir 21:3362–3375
443. Alonso-Lomillo MA, Dominguez-Renedo O, Matos P, Arcos-Martinez MJ (2010) Disposable biosensors for determination of biogenic amines. Anal Chim Acta 665:26–31
444. Xinyang L, Xiaolin W, Gang Y, Weijuan J, Xiaogong W (2010) Polystyrene-based diazonium salt as adhesive: a new approach for enzyme immobilization on polymeric supports. Polymer 51:860–867
445. Ruediger O, Abad JM, Hatchikian EC, Fernandez VM, De Laccy AL (2005) Oriented immobilization of Desulfovibrio gigas hydrogenase onto carbon electrodes by covalent bonds for nonmediated oxidation of H_2. J Am Chem Soc 127:16008–16009
446. Alonso-Lomillo MA, Yardimci C, Dominguez-Renedo O, Hernandez-Martin A, Arcos-Martinez MJ (2009) CYP450 2B4 covalently attached to carbon and gold screen printed electrodes by diazonium salt and thiols. Anal Chim Acta 633:51–56

447. Polsky R, Harper JC, Dirk SM, Arango DC, Wheeler DR, Brozik SM (2007) Diazonium-functionalized horseradish peroxidase immobilized via addressable electrodeposition: direct electron transfer and electrochemical detection. Langmuir 23:364–366
448. Pellissier M, Zigah D, Barriere F, Hapiot P (2008) Optimized preparation and scanning electrochemical microscopy analysis in feedback mode of glucose oxidase layers grafted onto conducting carbon surfaces. Langmuir 24:9089–9095
449. Lécayon G, Bouizem Y, Le Gressus C, Reynaud C, Juret C (1982) Grafting and growing mechanisms of polymerized organic films onto metallic surfaces. Chem Phys Lett 91:506–510
450. Leroy C, Boiziau C, Perreau J, Reynaud C, Zalezer G, Lécayon G, Le Gressus C (1985) Molecular structure of an electropolymerized polyacrylonitrile film and its pyrolyzed derivatives. J Mol Struct 128:269–281
451. Lécayon G, Viel P, Auge C, Le Gressus C, Reynaud C, Boiziau C, Leroy C, Perreau J (1986) Modification of the surface of an oxidizable metal cathode by grafting and gowth of a poly (acrylonitrile). Ann Phys 11:27–30
452. Baute N, Teyssié P, Martinot L, Mertens M, Dubois P, Jerôme R (1998) Electrografting of acrylic and methacrylic monomers onto metals. Influence of the relative polarity and donor-acceptor properties of the monomer and the solvent. Eur J Inorg Chem 1998:1711–1720
453. Geskin VM, Lazzaroni R, Mertens M, Jerôme R, Brédas JL (1996) Acrylonitrile on Cu(100): a density functional theoretical study of adsorption and electrochemical grafting. J Chem Phys 105:3278–3289
454. Crispin X, Lazzaroni R, Geskin VM, Baute N, Dubois P, Jerôme R, Brédas JL (1999) Controlling the electrografting of polymers onto transition metal surfaces through solvent versus monomer adsorption. J Am Chem Soc 121:176–187
455. Bureau C, Delhalle J (1999) Synthesis and structure of polymer/metal interfaces: a convergence of views between theory and experiment. J Surf Anal 6:159–170
456. Palacin S, Bureau C, Charlier J, Deniau G, Mouanda B, Viel P (2004) Molecule-to-metal bonds: electrografting polymers on conducting surfaces. ChemPhysChem 5:1468–1481
457. Deniau G, Azoulay L, Jegou P, Le Chevallier G, Palacin S (2006) Carbon-to-metal bonds: electrochemical reduction of 2-butenenitrile. Surf Sci 600:675–684
458. Baute N, Martinot L, Jerôme R (1999) Investigation of the cathodic electropolymerization of acrylonitrile, ethyl acrylate and methyl methacrylate by coupled quartz crystal microbalance analysis and cyclic voltammetry. J Electroanal Chem 472:83–90
459. Cuenot S, Gabriel S, Jerôme C, Jerôme R, Duwez AS (2005) Are electrografted polymers chemisorbed or physisorbed onto their substrate? Macromol Chem Phys 206:1216–1220
460. Labaye A, Jerôme C, Geskin VM, Louette P, Lazzaroni R, Martinot L, Jerôme R (2002) Full electrochemical synthesis of conducting polymer films chemically grafted to conducting surfaces. Langmuir 18:5222–5230
461. Ignatova M, Voccia S, Gilbert B, Markova N, Mercuri PS, Galleni M, Sciannamea V, Lenoir S, Cossement D, Gouttebaron R, Jerôme R, Jerôme C (2004) Synthesis of copolymer brushes endowed with adhesion to stainless steel surfaces and antibacterial properties by controlled nitroxide-mediated radical polymerization. Langmuir 20:10718–10726
462. Gabriel S, Dubruel P, Schacht E, Jonas AM, Alain M, Gilbert B, Jerôme R, Jerôme C (2005) Electrografting of poly(ethylene glycol) acrylate: a one-step strategy for the synthesis of protein-repellent surfaces. Angew Chem Int Ed 44:5505–5509
463. Petrov P, Lou X, Pagnoulle C, Jerôme C, Calberg C, Jerôme R (2004) Functionalization of multi-walled carbon nanotubes by electrografting of polyacrylonitrile. Macromol Rapid Commun 25:987–990
464. Defever T, Deniau G, Palacin S, Goux-Capes L, Barrau S, Mayne-l'Hermite M, Bourgoin JP (2006) Cathodic electropolymerization on the surface of carbon nanotubes. J Electroanal Chem 589:46–51
465. Benedetto A, Viel P, Noel S, Izard N, Chenevier P, Palacin S (2007) Carbon nanotubes/fluorinated polymers nanocomposite thin films for electrical contacts lubrication. Surf Sci 601:3687–3692

466. Mertens M, Martinot L, Calberg C, Jerôme R, Schrijnemackers J (1994) Depositing doped coatings on electrically conducting surfaces by electropolymerization. European Patent EP0618276
467. Viel P, Ameur S, Bureau C (2004) Process for coating a surface. French Patent FR2851181
468. Jerôme C, Gabriel S, Voccia S, Detrembleur C, Ignatova M, Gouttebaron R, Jerôme R (2003) Preparation of reactive surfaces by electrografting. Chem Commun 2500–2501
469. Bureau C, Mouanda B, Ameur S, Charlier J, Palacin S (2002) Solid support comprising a functionalized conducting or semiconducting surface of electricity, its preparation process, and its uses. French Patent FR2841908.
470. Adenier A, Chehimi MM, Gallardo I, Pinson J, Vilà N (2004) Electrochemical oxidation of aliphatic amines and their attachment to carbon and metal surfaces. Langmuir 20:8243–8253
471. Barbier B, Pinson J, Desarmot G, Sanchez M (1990) Electrochemical bonding of amines to carbon fiber surfaces toward improved carbon-epoxy composites. J Electrochem Soc 137:1757–1764
472. Deinhammer RS, Ho M, Anderegg JW, Porter MD (1994) Electrochemical oxidation of amine-containing compounds: a route to the surface modification of glassy carbon electrodes. Langmuir 10:1306–1313
473. Antoniadou S, Jannakoudakis AD, Jannakaudokis PD, Theodoridou E (1992) Anion exchange activity of electrochemically bonded ethylenediamine on carbon fibers. J Appl Electrochem 22:1060–1064
474. Geneste F, Moinet C (2005) Electrochemically linking TEMPO to carbon via amine bridges. New J Chem 29:269–271
475. Herlem G, Goux C, Fahys B, Gonçalves AM, Mathieu M, Sutter E, Penneau JF (1997) Surface modification of platinum and gold electrodes by anodic oxidation of pure ethylenediamine. J Electroanal Chem 435:259–265
476. Herlem G, Reybier K, Trokourey A, Fahys B (2000) Electrochemical oxidation of ethylenediamine: new way to make ployethyleneimine-like coatings on metallic or semiconducting materials. J Electrochem Soc 147:597–601
477. Yang G, Shen Y, Wang M, Chen H, Liu B, Dong S (2006) Copper hexacyanoferrate multilayer films on glassy carbon electrode modified with 4-aminobenzoic acid in aqueous solution. Talanta 68:741–747
478. Lakard B, Herlem G, Herlem M, Etcheberry A, Morvan J, Fahys B (2002) Spectroscopic and ab initio study of polymeric films used as chemical sensors. Surf Sci 502–503:296–303
479. Herlem M, Fahys B, Herlem G, Lakard B, Reybier K, Trokourey A, Diaco T, Zairi S, Jaffrezic-Renault N (2002) Surface modification of p-Si by a polyethylenimine coating: influence of the surface pre-treatment. Application to a potentiometric transducer as a pH sensor. Electrochim Acta 47:2597–2602
480. Li X, Wan Y, Sun C (2004) Covalent modification of a glassy carbon surface by electrochemical oxidation of p-aminobenzenesulfonic acid in aqueous solution. J Electroanal Chem 569:79–87
481. Zhang L (2008) Covalent modification of glassy carbon electrode with cysteine fort he determination of dopamine in the presence of ascorbic acid. Michrochim Acta 161:191–200
482. Zhang L, Lin X (2001) Covalent modification of glassy carbon electrodes with glutamic acid for simultaneous determination of uric acid and ascorbic acid. Analyst 126:367–370
483. Tsujimura S, Katayama A, Kano K (2006) Osmium complex grafted on a carbon electrode surface as a mediator for a bioelectrocatalytic reaction. Chem Lett 35:1244–1245
484. Downard AJ, Bin Mohamed A (1999) Suppression of protein adsorption at glassy carbon electrodes covalently modified with tetraethylene glycol diamine. Electroanalysis 11:418–423
485. Downard AJ, Jackson SL, Tan ESQ (2005) Fluorescence microscopy study of protein adsorption at modified glassy carbon surfaces. Aust J Chem 58:275–279
486. Herlem G, Lakard B, Herlem M, Fahys B (2001) pH sensing at Pt electrode surfaces coated with linear polyethylenimine from anodic polymerization of ethylenediamine. J Electrochem Soc 148:E435–E438

487. Tang H, Chen J, Cui K, Nie L, Kuang Y, Yao S (2006) Immobilisation and electro-oxidation of calf thymus deoxyribonucleic acid at alkylamine modified carbon nanotube electrode and its interaction with promethazine hydrochloride. J Electroanal Chem 587:269–275
488. Kolbe H (1849) Darstellung des reinen Kobaltoxyd's. Justus Liebigs Ann Chem 69:257–294
489. Wurtz CA (1855) Sur une nouvelle classe de radicaux organiques. Ann Chim Phys 44:275–312
490. Andrieux CP, Gonzalez F, Savéant JM (2001) Homolytic and heterolytic radical cleavage in the Kolbe reaction. Electrochemical oxidation of arylmethyl carboxylate ions. J Electroanal Chem 498:171–180
491. Brooksby PA, Downard AJ, Yu SSC (2005) Effect of applied potential on arylmethyl films oxidatively grafted to carbon surfaces. Langmuir 21:11304–11311
492. Geneste F, Cadoret M, Moinet C, Jézequel G (2002) Cyclic voltammetry and XPS analyses of graphite felt derivatized by non-Kolbe reactions in aqueous media. New J Chem 26:1261–1266
493. Maia G, Maschion FC, Tanimoto ST, Vaik K, Mäeorg U, Tammeveski K (2007) Attachment of anthraquinone derivatives to glassy carbon and the electrocatalytic behavior oft he modified electrodes toward oxygen reduction. J Solid State Electrochem 11:1411–1420
494. Vaik K, Mäeorg U, Maschion FC, Maia G, Schiffrin DJ, Tammeveski K (2005) Electrocatalytic oxygen reduction on glassy carbon grafted with anthraquinone by anodic oxidation of a carboxylate substituent. Electrochim Acta 50:5126–5131
495. Sagiv J (1980) Organized monolayers by adsorption. 1. Formation and structure of oleophobic mixed monolayers on solid surfaces. J Am Chem Soc 102:92–98
496. Haensch C, Hoeppener S, Schubert US (2010) Chemical modification of self-assembled silane based monolayers by surface reactions. Chem Soc Rev 39:2323–2334
497. Hao C, Yan F, Ding L, Xue Y, Ju H (2007) A self-assembled monolayer based electrochemical immunosensor for detection of leukemia K562A cells. Electrochem Commun 9:1359–1364
498. Mantzila AG, Prodromidis MI (2005) Performance of impedimetric biosensors based on anodically formed Ti/TiO2 electrodes. Electroanalysis 17:1878–1885
499. Fang X, Tan OK, Tse MS, Ooi EE (2010) A label-free immunosensor for diagnosis of Dengue infection with simple electrical measurements. Biosens Bioelectron 25:1137–1142
500. Wei MY, Wen SD, Yang XQ, Guo LH (2009) Development of redox-labeled electrochemical immunoassay for polycyclic aromatic hydrocarbons with controlled surface modification and catalytic voltammetric detection. Biosens Bioelectron 24:2909–2914
501. Onclin S, Mulder A, Huskens J, Ravoo BJ, Reinhoudt DN (2004) Molecular printboards: monolayers of beta-cyclodextrins on silicon oxide surfaces. Langmuir 20:5460–5466
502. Sheikh S, Blaszykowski C, Thompson M (2008) Acoustic wave-based detection in bioanalytical chemistry: competition for surface plasmon resonance? Anal Lett 41:2525–2538
503. Länge K, Rapp BE, Rapp M (2008) Surface acoustic wave biosensors: a review. Anal Bioanal Chem 391:1509–1519
504. Chockalingam M, Darwish N, Le Saux G, Gooding JJ (2011) Importance of the indium tin oxide substrate on the quality of self-assembled monolayers formed from organophosphonic acids. Langmuir 27(6):2545–2552
505. Chen X, Luais E, Darwish N, Ciampi S, Thodarson P, Gooding JJ (2012) Studies on the effect of solvents on self-assembled monolayers formed from organophosphonic acids on indium tin oxide. Langmuir 28:9487–9495
506. Sassolas A, Blum LJ, Leca-Bouvier BD (2012) Immobilization strategies to develop enzymatic biosensors. Biotechnol Adv 30:489–511
507. Cosnier S (2005) Affinity biosensors based on electropolymerized films. Electroanalysis 17:1701–1715

508. Cosnier S, Holzinger M (2011) Electrosynthesized polymers for biosensing. Chem Soc Rev 40:2146–2156
509. Schuhmann W, Lammert R, Uhe B, Schmidt HL (1990) Polypyrrole, a new possibility for covalent binding of oxidoreductases to electrode surfaces as a base for stable biosensors. Sensor Actuat B 1:537–541
510. Yang S, Witkowski A, Hutchins RS, Scott DL, Bachas LG (1998) Biotin-modified surfaces by electrochemical polymerization of biotinyl-tyramide. Electroanalysis 10:58–60
511. Cosnier S, Galland B, Gondran C, Le Pellec A (1998) Electrogeneration of biotinylated functionalized polypyrroles for the simple immobilization of enzymes. Electroanalysis 10:808–813
512. Davis J, Glidle A, Cass AEG, Zhang J, Cooper JM (1999) Spectroscopic evaluation of protein affinity binding at polymeric biosensor films. J Am Chem Soc 121:4302–4303
513. Haddour N, Cosnier S, Gondran C (2005) Electrogeneration of a poly(pyrrole)-NTA chelator film for a reversible oriented immobilization of histidine-tagged proteins. J Am Chem Soc 127:5752–5753
514. Haupt K (2001) Molecularly imprinted polymers in analytical chemistry. Analyst 126:747–756
515. Haupt K, Mosbach K (2000) Molecularly imprinted polymers and their use in biomimetic sensors. Chem Rev 100:2495–2504
516. Suryanarayanan V, Wu CT, Ho KC (2010) Molecularly imprinted electrochemical sensors. Electroanalysis 22:1795–1811
517. Wanekaya A, Sadik OA (2002) Electrochemical detection of lead using overoxidized polypyrrole films. J Electroanal Chem 537:135–143
518. Mohadesi A, Taher MA (2007) Overoxidized polypyrrole doped with 4,5-dihydroxy-3-(p-sulfophenylazo)-2,7-naphthalene disulfonic acid as a selective and regenerable film for the stripping detection of copper(II). Anal Sci 23:969–974
519. Zanganeh AR, Amini MK (2007) A potentiometric and voltammetric sensor based on polypyrrole film with electrochemically induced recognition sites for detection of silver ion. Electrochim Acta 52:3822–3830
520. Rahman A, Won M, Shim Y (2003) Characterization of an EDTA bonded conducting polymer modified electrode: its application for the simultaneous determination of heavy metal ions. Anal Chem 75:2828–2834
521. Yoo K, Woo S, Jyoung J (2003) Trace mercury determination by differential pulse anodic stripping voltammetry using polythiophene-quinoline / glassy carbon modified electrode. Bull Kr Chem Soc 24:27–31
522. Rahman MA, Park DS, Won MS, Park SM, Shim YB (2004) Selective electrochemical analysis of various metal ions at an EDTA bonded conducting polymer modified electrode. Electroanalysis 16:1366–1370
523. Heitzmann M, Basaez L, Brovelli F, Bucher C, Limosin D, Pereira E, Rivas BL, Royal G, Saint-Aman E, Moutet JC (2005) Voltammetric sensing of trace metals at a poly(pyrrole-malonic acid) film modified carbon electrode. Electroanalysis 17:1970–1976
524. Rivas BL, Pooley SA, Brovelli F, Pereira E, Basaez L, Puentes J, Moutet JC, Saint-Aman E (2006) Synthesis and properties of styrene copolymers. Preparation of film-modified electrodes to detect Pb2+ ions. J Appl Polym Sci 100:2380–2385
525. Zhang L, Li W, Shi M, Kong J (2006) Probing trace Pb(2+) using electrodeposited N, N'-(o-phenylene)-bis-benzenesulfonamide polymer as a novel selective ion capturing film. Talanta 70:432–436
526. Heitzmann M, Bucher C, Moutet JC, Pereira E, Rivas BL, Royal G, Saint-Aman E (2007) Complexation of poly(pyrrole-EDTA like) film modified electrodes: application to metal cations electroanalysis. Electrochim Acta 52:3082–3087

527. Nateghi MR, Fallahian MH (2007) Self-doped anthranilic acid-pyrrole copolymer / gold electrodes for selective preconcentration and determination of Cu (I) by differential pulse anodic stripping voltammetry. Anal Sci 23:563–567
528. Ugo P, Moretto LM (1995) Ion-exchange voltammetry at polymer-coated electrodes: principles and analytical prospects. Electroanalysis 7:1105–1113
529. Gouveia-Caridade C, Brett CMA (2006) The influence of Triton-X-100 surfactant on the electroanalysis of lead and cadmium at carbon film electrodes – an electrochemical impedance study. J Electroanal Chem 592:113–120
530. Ugo P, Moretto LM, Rudello D, Birriel E, Chevalet J (2001) Trace iron determination by cyclic and multiple square-wave voltammetry at nafion coated electrodes. Application to pore-water analysis. Electroanalysis 13:661–668
531. Strasunske K, Mikkelsen Ø, Billon G (2010) Nafion coated silver amalgam electrode for determination of trace metals by anodic stripping voltammetry. Electroanalysis 22:501–507
532. Gouveia-Caridade C, Pauliukaite R, Brett CMA (2006) Influence of nafion coatings and surfactant on the stripping voltammetry of heavy metals at bismuth-film modified carbon film electrodes. Electroanalysis 18:854–861
533. Xu H, Zeng L, Xing S, Xian Y, Shi G, Jin L (2008) Ultrasensitive voltammetric detection of trace lead(II) and cadmium(II) using MWCNTs-nafion/bismuth composite electrodes. Electroanalysis 20:2655–2662
534. Torma F, Kádár M, Tóth K, Tatár E (2008) Nafion/2,2'-bipyridyl-modified bismuth film electrode for anodic stripping voltammetry. Anal Chim Acta 619:173–182
535. Wang Y, Liu Z, Yao G, Zhu P, Hu X, Xu Q, Yang C (2010) Determination of cadmium with a sequential injection lab-on-valve by anodic stripping voltammetry using a nafion coated bismuth film electrode. Talanta 80:1959–1963
536. Jia J, Cao L, Wang Z (2007) Nafion/poly(sodium 4-styrenesulfonate) mixed coating modified bismuth film electrode for the determination of trace metals by anodic stripping voltammetry. Electroanalysis 19:1845–1849
537. Kröger S, Turner APF, Mosbach K, Haupt K (1999) Imprinted polymer-based sensor system for herbicides using differential-pulse voltammetry on screen-printed electrodes. Anal Chem 71:3698–3702
538. Shoji R, Takeuchi T, Kubo I (2003) Atrazine sensor based on molecularly imprinted polymer-modified gold electrode. Anal Chem 75:4882–4886
539. Weetall HH, Hatchett DW, Rogers KR (2005) Electrochemically deposited polymer-coated gold electrodes selective for 2,4-dichlorophenoxyacetic acid. Electroanalysis 17:1789–1794
540. Pardieu E, Cheap H, Vedrine C, Lazerges M, Lattach Y, Garnier F, Remita S, Pernelle C (2009) Molecularly imprinted conducting polymer based electrochemical sensor for detection of atrazine. Anal Chim Acta 649:236–245
541. Xie C, Gao S, Guo Q, Xu K (2010) Electrochemical sensor for 2,4-dichlorophenoxy acetic acid using molecularly imprinted polypyrrole membrane as recognition element. Microchim Acta 169:145–152
542. Gómez-Caballero A, Unceta N, Goicolea MA, Barrio RJ (2007) Voltammetric determination of metamitron with an electrogenerated molecularly imprinted polymer microsensor. Electroanalysis 19:356–363
543. Pan MF, Fang GZ, Liu B, Qian K, Wang S (2011) Novel amperometric sensor using metolcarb-imprinted film as the recognition element on a gold electrode and its application. Anal Chim Acta 690:175–181
544. Gómez-Caballero A, Unceta N, Aranzazu Goicolea M, Barrio RJ (2008) Evaluation of the selective detection of 4,6-dinitro-o-cresol by a molecularly imprinted polymer based microsensor electrosynthesized in a semiorganic media. Sensor Actuat B 130:713–722
545. Weetall HH, Rogers KR (2004) Preparation and characterization of molecularly imprinted electropolymerized carbon electrodes. Talanta 62:329–335

546. Luo N, Hatchett DW, Rogers KR (2007) Recognition of pyrene using molecularly imprinted electrochemically deposited poly(2-mercaptobenzimidazole) or poly(resorcinol) on gold electrodes. Electroanalysis 19:2117–2124
547. Kirsch N, Honeychurch KC, Hart JP, Whitcombe MJ (2005) Voltammetric determination of urinary 1-hydroxypyrene using molecularly imprinted polymer-modified screen-printed carbon electrodes. Electroanalysis 17:571–578
548. Kirsch N, Hart JP, Bird DJ, Luxton RW, McCalley DV (2001) Towards the development of molecularly imprinted polymer based screen-printed sensors for metabolites of PAHs. Analyst 126:1936–1941
549. Huan S, Hu S, Shen G, Yu R (2003) Au microelectrode based on molecularly imprinted oligomer film for rapid electrochemical sensing. Anal Lett 36:2401–2416
550. Liu Y, Song QJ, Wang L (2009) Development and characterization of an amperometric sensor for triclosan detection based on electropolymerized molecularly imprinted polymer. Microchem J 91:222–226
551. Liao H, Zhang Z, Li H, Nie L, Yao S (2004) Preparation of the molecularly imprinted polymers-based capacitive sensor specific for tegafur and its characterization by electrochemical impedance and piezoelectric quartz crystal microbalance. Electrochim Acta 49:4101–4107
552. Özcan L, Şahin Y (2007) Determination of paracetamol based on electropolymerized-molecularly imprinted polypyrrole modified pencil graphite electrode. Sensor Actuat B 127:362–369
553. Blanco-López MC, Gutiérrez-Fernández S, Lobo-Castañón MJ, Miranda-Ordieres AJ, Tuñon-Blancó P (2004) Electrochemical sensing with electrodes modified with molecularly imprinted polymer films. Anal Bioanal Chem 378:1922–1928
554. Gómez-Caballero A, Goicolea MA, Barrio RJ (2005) Paracetamol voltammetric microsensors based on electrocopolymerized-molecularly imprinted film modified carbon fiber microelectrodes. Analyst 130:1012–1018
555. Li J, Jiang F, Wei X (2010) Molecularly imprinted sensor based on an enzyme amplifier for ultratrace oxytetracycline determination. Anal Chem 82:6074–6078
556. Kang J, Zhang H, Wang Z, Wu G, Lu X (2009) A novel amperometric sensor for salicylic acid based on molecularly imprinted polymer-modified electrodes. Polym Plast Technol Eng 48:639–645
557. Ozkorucuklu SP, Sahin Y, Alsancak G (2008) Voltammetric behaviour of sulfamethoxazole on electropolymerized-molecularly imprinted overoxidized polypyrrole. Sensors 8:8463–8478
558. Yeh WM, Ho KC (2005) Amperometric morphine sensing using a molecularly imprinted polymer-modified electrode. Anal Chim Acta 542:76–82
559. Cosnier S, Fombon JJ, Labbé P, Limosin D (1999) Development of a PPO-poly(amphiphilic pyrrole) electrode for on site monitoring of phenol in aqueous effluents. Sensor Actuat B 59:134–139
560. Mousty C, Lepellec A, Cosnier S, Novoa A, Marks RS (2001) Fabrication of organic phase biosensors based on multilayered polyphenol oxidase protected by an alginate coating. Electrochem Commun 3:727–732
561. Arslan A, Kiralp S, Toppare L, Yagci Y (2005) Immobilization of tyrosinase in polysiloxane/polypyrrole copolymer matrices. Int J Biol Macromol 35:163–167
562. Rajesh KK (2005) A new tyrosinase biosensor based on covalent immobilization of enzyme on N-(3-aminopropyl) pyrrole polymer film. Curr Appl Phys 5:178–183
563. Wang P, Liu M, Kan J (2009) Amperometric phenol biosensor based on polyaniline. Sensor Actuat B 140:577–584
564. Yildiz HB, Castillo J, Guschin DA, Toppare L, Schuhmann W (2007) Phenol biosensor based on electrochemically controlled integration of tyrosinase in a redox polymer. Microchim Acta 159:27–34

565. Stein K, Schwedt G (1993) Comparison of immobilization methods for the development of an acetylcholinesterase biosensor. Anal Chim Acta 272:73–81
566. Ivanov AN, Evtugyn GA, Gyurcsányi RE, Tóth K, Budnikov HC (2000) Comparative investigation of electrochemical cholinesterase biosensors for pesticide determination. Anal Chim Acta 404:55–65
567. Pritchard J, Law K, Vakurov A, Millner P, Higson SPJ (2004) Sonochemically fabricated enzyme microelectrode arrays for the environmental monitoring of pesticides. Biosens Bioelectron 20:765–772
568. Snejdarkova M, Svobodova L, Evtugyn G, Budnikov H, Karyakin A, Nikolelis DP, Hianik T (2004) Acetylcholinesterase sensors based on gold electrodes modified with dendrimer and polyaniline. Anal Chim Acta 514:79–88
569. Law KA, Higson SPJ (2005) Sonochemically fabricated acetylcholinesterase micro-electrode arrays within a flow injection analyser for the determination of organophosphate pesticides. Biosens Bioelectron 20:1914–1924
570. Du D, Ye X, Cai J, Liu J, Zhang A (2010) Acetylcholinesterase biosensor design based on carbon nanotube-encapsulated polypyrrole and polyaniline copolymer for amperometric detection of organophosphates. Biosens Bioelectron 25:2503–2508
571. Prakash S, Chakrabarty T, Singh AK, Shahi VK (2013) Polymer thin films embedded with metal nanoparticles for electrochemical biosensors applications. Biosens Bioelectron 41:43–53
572. Lahiff E, Lynam C, Gilmartin N, O'Kennedy R, Diamond D (2010) The increasing importance of carbon nanotubes and nanostructured conducting polymers in biosensors. Anal Bioanal Chem 398:1575–1589
573. Cox JA, Jaworski R, Kulesza PJ (1991) Electroanalysis with electrodes modified by inorganic films. Electroanalysis 3:869–877
574. Walcarius A, Etienne M (2009) Electrochemistry and electrochemical sensors based on mesoporous silica. In: Lin Y, Nalwa HS (eds) Handbook of electrochemical nanotechnology, vol 2. American Scientific Publishers, Stevenson Ranch, CA, pp 1–38
575. Walcarius A (2008) Electroanalytical applications of microporous zeolites and mesoporous (organo)silicas: recent trends. Electroanalysis 20:711–738
576. Shi Y, Seliskar CJ, Heineman WR (1997) Spectroelectrochemical sensing based on multimode selectivity simultaneously achievable in a single device. 2. Demonstration of selectivity in the presence of direct interferences. Anal Chem 69:4819–4827
577. Conklin SD, Heineman WR, Seliskar CJ (2007) Spectroelectrochemical sensing based on multimode selectivity simultaneously achievable in a single device. 19. Preparation and characterization of films of quaternized poly (4-vinylpyridine) – silica. Electroanalysis 19:523–529
578. Maizels M, Seliskar C, Heineman W, Bryan SA (2002) Spectroelectrochemical sensing based on multimode selectivity simultaneously achievable in a single device. Electroanalysis 14:1345–1352
579. Zudans I, Heineman WR, Seliskar CJ (2004) In situ dynamic measurements of sol–gel processed thin chemically selective PDMDAAC–silica films by spectroscopic ellipsometry. Chem Mater 16:3339–3347
580. Zudans I, Paddock JR, Kuramitz H, Maghasi AT, Wansapura CM, Conklin SD, Kaval N, Shtoyko T, Monk DJ, Bryan SA, Hubler TL, Richardson JN, Seliskar CJ, Heineman WR (2004) Electrochemical and optical evaluation of noble metal- and carbon-ITO hybrid optically transparent electrodes. J Electroanal Chem 565:311–320
581. Miao W (2008) Electrogenerated chemiluminescence and its biorelated applications. Chem Rev 108:2506–2553
582. Fähnrich KA, Pravda M, Guilbault GG (2001) Recent applications of electrogenerated chemiluminescence in chemical analysis. Talanta 54:531–559
583. Tonelli D, Scavetta E, Giorgetti M (2013) Layered-double-hydroxide-modified electrodes: electroanalytical applications. Anal Bioanal Chem 405:603–614

584. Navrátilová Z, Kula P (2003) Clay modified electrodes: present applications and prospects. Electroanalysis 15:837–846
585. Mousty C (2010) Biosensing applications of clay-modified electrodes: a review. Anal Bioanal Chem 396:315–325
586. Soler-Illia GJAA, Sanchez C, Lebeau B, Patarin J (2002) Chemical strategies to design textured materials: from microporous and mesoporous oxides to nanonetworks and hierarchical structures. Chem Rev 102:4093–4138
587. Brinker CJ, Lu Y, Sellinger A, Fan H (1999) Evaporation-induced self-assembly: nanostructures made easy. Adv Mater 11:579–585
588. Lu Y, Ganguli R, Drewien CA, Anderson MT, Brinker CJ, Gong W, Guo Y, Soyez H, Dunn B, Huang MH, Zink JI (1997) Continuous formation of supported cubic and hexagonal mesoporous films by sol–gel dip-coating. Nature 389:364–368
589. Brinker JC, Scherer GW (1990) Sol-gel science: the physics and chemistry of sol-gel processing. Academic Press, Inc., San Diego, CA
590. Boissière C, Grosso D, Chaumonnot A, Nicole L, Sanchez C (2011) Aerosol route to functional nanostructured inorganic and hybrid porous materials. Adv Mater 23:599–623
591. Therese G, Kamath PV (2000) Electrochemical synthesis of metal oxides and hydroxides. Chem Mater 12:1195–1204
592. Tench D, Warren LF (1983) Electrodeposition of conducting transition metal oxide/hydroxide films from aqueous solution. J Electrochem Soc 130:869–872
593. Shacham R, Avnir D, Mandler D (1999) Electrodeposition of methylated sol-gel films on conducting surfaces. Adv Mater 11:384–388
594. Sibottier E, Sayen S, Gaboriaud F, Walcarius A (2006) Factors affecting the preparation and properties of electrodeposited silica thin films functionalized with amine or thiol groups. Langmuir 22:8366–8373
595. Choi KS, Lichtenegger HC, Stucky GD, McFarland EW (2002) Electrochemical synthesis of nanostructured ZnO films utilizing self-assembly of surfactant molecules at solid–liquid interfaces. J Am Chem Soc 124:12402–12403
596. Tan Y, Srinivasan S, Choi KS (2005) Electrochemical deposition of mesoporous nickel hydroxide films from dilute surfactant solutions. J Am Chem Soc 127:3596–3604
597. Etienne M, Sallard S, Schröder M, Guillemin Y, Mascotto S, Smarsly BM, Walcarius A (2010) Electrochemical generation of thin silica films with hierarchical porosity. Chem Mater 22:3426–3432
598. Goux A, Etienne M, Aubert E, Lecomte C, Ghanbaja J, Walcarius A (2009) Oriented mesoporous silica films obtained by electro-assisted self-assembly (EASA). Chem Mater 21:731–741
599. Etienne M, Goux A, Sibottier E, Walcarius A (2009) Oriented mesoporous organosilica films on electrode: a new class of nanomaterials for sensing. J Nanosci Nanotechnol 9:2398–2406
600. Goux A, Ghanbaja J, Walcarius A (2009) Prussian Blue electrodeposition within an oriented mesoporous silica film: preliminary observations. J Mater Sci 44:6601–6607
601. Walcarius A, Sibottier E, Etienne M, Ghanbaja J (2007) Electrochemically assisted self-assembly of mesoporous silica thin films. Nature Mater 6:602–608
602. Nicole L, Boissière C, Grosso D, Quach A, Sanchez C (2005) Mesostructured hybrid organic–inorganic thin films. J Mater Chem 15:3598–3627
603. Impens NRE, Van der Voort P, Vansant E (1999) Silylation of micro-, meso- and non-porous oxides: a review. Microporous Mesoporous Mater 28:217–232
604. Moller K, Bein T (1998) Inclusion chemistry in periodic mesoporous hosts. Chem Mater 10:2950–2963
605. Angelomé PC, Aldabe-Bilmes S, Calvo ME, Crepaldi EL, Grosso D, Sanchez C, Soler-Illia GJAA (2005) Hybrid non-silica mesoporous thin films. New J Chem 29:59–63

606. Angelomé PC, Soler-Illia GJAA (2005) Organically modified transition-metal oxide mesoporous thin films and xerogels. Chem Mater 17:322–331
607. Burkett SL, Sims SD, Mann S (1996) Synthesis of hybrid inorganic-organic mesoporous silica by co-condensation of siloxane and organosiloxane precursors. Chem Commun 1367–1368
608. Macquarrie DJ (1996) Direct preparation of organically modified MCM-type materials. Preparation and characterisation of aminopropyl-MCM and 2-cyanoethyl-MCM. Chem Commun 1961–1962.
609. Asefa T, MacLachlan M, Coombs N, Ozin GA (1999) Periodic mesoporous organosilicas with organic groups inside the channel walls. Nature 402:867–871
610. Melde BJ, Holland BT, Blanford CF, Stein A (1999) Mesoporous sieves with unified hybrid inorganic/organic frameworks. Chem Mater 11:3302–3308
611. Inagaki S, Guan S, Fukushima Y, Ohsuna T, Terasaki O (1999) Self-assembly of biphenylene-bridged hybrid mesoporous solid with molecular-scale periodicity in the pore walls. J Am Chem Soc 121:9611–9614
612. Zhou Z, Hartmann M (2012) Recent progress in biocatalysis with enzymes immobilized on mesoporous hosts. Top Catal 55:1081–1100
613. Hasanzadeh M, Shadjou N, De la Guardia M, Eskandani M, Sheikhzadeh P (2012) Mesoporous silica-based materials for use in biosensors. Trends Anal Chem 33:117–129
614. Marx S, Zaltsman A, Turyan I, Mandler D (2004) Parathion sensor based on molecularly imprinted sol-gel films. Anal Chem 76:120–126
615. Sayen S, Etienne M, Bessière J, Walcarius A (2002) Tuning the sensitivity of electrodes modified with an organic-inorganic hybrid by tailoring the structure of the nanocomposite material. Electroanalysis 14:1521–1525
616. Etienne M, Bessière J, Walcarius A (2001) Voltammetric detection of copper(II) at a carbon paste electrode containing an organically modified silica. Sensor Actuat B 76:531–538
617. Yantasee W, Deibler LA, Fryxell GE, Timchalk C, Lin Y (2005) Screen-printed electrodes modified with functionalized mesoporous silica for voltammetric analysis of toxic metal ions. Electrochem Commun 7:1170–1176
618. Goubert-Renaudin S, Etienne M, Rousselin Y, Denat F, Lebeau B, Walcarius A (2009) Cyclam-functionalized silica-modified electrodes for selective determination of Cu(II). Electroanalysis 21:280–289
619. Goubert-Renaudin S, Moreau M, Despas C, Meyer M, Denat F, Lebeau B, Walcarius A (2009) Voltammetric detection of lead(II) using amide-cyclam-functionalized silica-modified carbon paste electrodes. Electroanalysis 21:1731–1742
620. Sánchez A, Morante-Zarcero S, Pérez-Quintanilla D, Sierra I, del Hierro I (2010) Development of screen-printed carbon electrodes modified with functionalized mesoporous silica nanoparticles: application to voltammetric stripping determination of Pb(II) in non-pretreated natural waters. Electrochim Acta 55:6983–6990
621. Yantasee W, Lin Y, Hongsirikarn K, Fryxell GE, Addleman R, Timchalk C (2007) Electrochemical sensors for the detection of lead and other toxic heavy metals: the next generation of personal exposure biomonitors. Environ Health Perspect 115:1683–1690
622. Etienne M, Cortot J, Walcarius A (2007) Preconcentration electroanalysis at surfactant-templated thiol-functionalized silica thin films. Electroanalysis 19:129–138
623. Sanchez A, Walcarius A (2010) Surfactant-templated sol–gel silica thin films bearing 5-mercapto-1-methyl-tetrazole on carbon electrode for Hg(II) detection. Electrochim Acta 55:4201–4207
624. Yantasee W, Lin Y, Li X, Fryxell GE, Zemanian TS, Viswanathan VV (2003) Nanoengineered electrochemical sensor based on mesoporous silica thin-film functionalized with thiol-terminated monolayer. Analyst 128:899–904

625. Gorton L (1995) Carbon paste electrodes modified with enzymes, tissues, and cells (a review). Electroanalysis 7:23–45
626. Kauffmann JM, Guest Ed. (1997) Bioelectrochem Bioenerg 42(1).
627. Buehlmann P, Aoki H, Xiao KP, Anemiya S, Tohda K, Umezawa Y (1998) Chemical sensing with chemically modified electrodes that mimic gating at biomembranes incorporating ion-channel receptors. Electroanalysis 10:1149–1158
628. Chung TD, Kim H (1998) Electrochemistry of calixarene and its analytical applications. J Incl Phenom Mol Recognit Chem 32:179–193
629. Echegoyen L, Echegoyen LE (1998) Electrochemistry of fullerenes and their derivatives. Acc Chem Res 31:593–601
630. Ferancova A, Labuda J (2001) Cyclodextrins as electrode modifiers. Fresenius J Anal Chem 370:1–10
631. Itaya K, Uchida I, Neff VD (1986) Electrochemistry of polynuclear transition metal cyanides: Prussian blue and its analogues. Acc Chem Res 19:162–168
632. Alber KS, Cox JA, Kulesza PJ (1997) Solid-state amperometric sensors for gas phase analytes: a review of recent advances. Electroanalysis 9:97–101
633. Kulesza PJ, Cox JA (1998) Solid-state voltammetry—analytical prospects. Electroanalysis 10:73–80
634. Macha SM, Fitch A (1998) Clays as architectural units at modified-electrodes. Mikrochim Acta 128:1–18
635. Mousty C (2004) Sensors and biosensors based on clay-modified electrodes-new trends. Appl Clay Sci 27:159–177
636. Walcarius A (1996) Zeolite modified electrodes: analytical applications and prospects. Electroanalysis 8:971–986
637. Walcarius A (1999) Zeolite-modified electrodes in electroanalytical chemistry. Anal Chim Acta 384:1–16
638. Walcarius A (2003) Implication of zeolite chemistry in electrochemical science and applications of zeolite-modified electrodes. In: Auerbach SM, Carrado KA, Dutta PK (eds) Handbook of zeolite science and technology. Marcel Dekker Inc., New York, NY, pp 721–783
639. Lev O, Wu Z, Bharathi S, Glezer V, Modestov A, Gun J, Rabinovich L, Sampath S (1997) Sol-gel materials in electrochemistry. Chem Mater 9:2354–2375
640. Alber KS, Cox JA (1997) Electrochemistry in solids prepared by sol-gel processes. Mikrochim Acta 127:131–147
641. Lin J, Brown CW (1997) Sol-gel glass as a matrix for chemical and biochemical sensing. Trends Anal Chem 16:200–211
642. Collinson MM (1998) Analytical applications of organically modified silicates. Mikrochim Acta 129:149–165
643. Wang J (1999) Sol-gel materials for electrochemical biosensors. Anal Chim Acta 399:21–27
644. Rabinovich L, Lev O (2001) Sol-gel derived composite ceramic carbon electrodes. Electroanalysis 13:265–275
645. Walcarius A (2001) Electroanalysis with pure, chemically-modified, and sol-gel-derived silica-based materials. Electroanalysis 13:701–718
646. Collinson MM (2002) Recent trends in analytical applications of organically modified silicate materials. Trends Anal Chem 21:30–38
647. Walcarius A, Mandler D, Cox J, Collinson MM, Lev O (2005) Exciting new directions in the intersection of functionalized sol-gel materials with electrochemistry. J Mater Chem 15:3663–3689
648. Walcarius A, Collinson MM (2009) Analytical chemistry with silica sol gels: traditional routes to new materials for chemical analysis. Annu Rev Anal Chem 2:121–143
649. Lev O, Sampath S (2010) Sol-gel electrochemistry. Electroanal Chem 23:301–390

650. Kalcher K, Švancara I, Metelka R, Vytřas K, Walcarius A (2006) Heterogeneous carbon electrochemical sensors. In: Dickey EC, Pishko MV (eds) Encyclopedia of sensors, vol 4. American Scientific Publishers, Stevenson Ranch, CA, pp 283–430
651. Sadakane M, Steckhan E (1998) Electrochemical properties of polyoxometalates as electrocatalysts. Chem Rev 98:219–237
652. Lu G, Wu X, Lan Y, Yao S (1999) Studies on 1:12 phosphomolybdic heteropoly anion film modified carbon paste electrode. Talanta 49:511–515
653. Wang XL, Wang EB, Lan Y, Hu CW (2002) Renewable PMo12-based inorganic-organic hybrid material bulk-modified carbon paste electrode: preparation, electrochemistry and electrocatalysis. Electroanalysis 14:1116–1121
654. Liu H, He P, Li Z, Sun C, Shi L, Liu Y, Zhu G, Li J (2005) An ionic liquid-type carbon paste electrode and its polyoxometalate-modified properties. Electrochem Commun 7:1357–1363
655. Han Z, Zhao Y, Peng J, Feng Y, Yin J, Liu Q (2005) The electrochemical behavior of Keggin polyoxometalate modified by tricyclic, aromatic entity. Electroanalysis 17:1097–1102
656. Han Z, Zhao Y, Peng J, Liu Q, Wang E (2005) Inorganic-organic hybrid polyoxometalate containing supramolecular helical chains: preparation, characterization and application in chemically bulk-modified electrode. Electrochim Acta 51:218–224
657. Boyer A, Kalcher K, Pietsch R (1990) Voltammetric behavior of perborate on Prussian blue-modified carbon paste electrodes. Electroanalysis 2:155–161
658. Moscone D, D'Ottavi D, Compagnone D, Palleschi G, Amine A (2001) Construction and analytical characterization of Prussian blue-based carbon paste electrodes and their assembly as oxidase enzyme sensors. Anal Chem 73:2529–2535
659. Gomez del Rio MI, De La Fuente C, Acuna JA, Vazquez MD, Tascon ML, Vicente Perez S, Sanchez BP (1995) Determination of nitrites by using an electrocatalytic method on Prussian Blue chemically carbon paste electrode. Quim Anal 14:108–111
660. Li J, Wei X, Yuan Y (2009) Synthesis of magnetic nanoparticles composed by Prussian blue and glucose oxidase for preparing highly sensitive and selective glucose biosensor. Sensor Actuat B 139:400–406
661. Toito Suarez W, Marcolino LH Jr, Fatibello-Filho O (2006) Voltammetric determination of N-acetylcysteine using a carbon paste electrode modified with copper(II) hexacyanoferrate (III). Microchem J 82:163–167
662. Ojani R, Raoof JB, Norouzi B (2008) Cu(II) hexacyanoferrate(III) modified carbon paste electrode; application for electrocatalytic detection of nitrite. Electroanalysis 20:1996–2002
663. Alamo LS, Tangkuaram T, Satienperakul S (2010) Determination of sulfite by pervaporation-flow injection with amperometric detection using copper hexacyanoferrate-carbon nanotube modified carbon paste electrode. Talanta 81:1793–1799
664. Abbaspour A, Mehrgardi MA (2004) Electrocatalytic oxidation of guanine and DNA on a carbon paste electrode modified by cobalt hexacyanoferrate films. Anal Chem 76:5690–5696
665. Siroueinejad A, Abbaspour A, Shamsipur M (2009) Electrocatalytic oxidation and determination of sulfite with a novel copper-cobalt hexacyanoferrate modified carbon paste electrode. Electroanalysis 21:1387–1393
666. Thérias S, Mousty C (1995) Electrodes modified with synthetic anionic clays. Appl Clay Sci 10:147–162
667. Wang J, Martinez T (1989) Trace analysis at clay-modified carbon paste electrodes. Electroanalysis 1:167–172
668. Raber G, Kalcher K, Stadlober M (1998) New voltammetric methods for the determination of heavy metals using a montmorillonite modified carbon paste electrode. Sci Pap Univ Pardubice Ser A 3:163–193
669. Kula P, Navratilova Z, Kulova P, Kotoucek M (1999) Sorption and determination of Hg (II) on clay modified carbon paste electrodes. Anal Chim Acta 385:91–101
670. Huang W (2004) Voltammetric determination of bismuth in water and nickel metal samples with a sodium montmorillonite (SWy-2) modified carbon paste electrode. Microchim Acta 144:125–129

671. Sun D, Wan C, Li G, Wu K (2007) Electrochemical determination of lead(II) using a montmorillonite calcium-modified carbon paste electrode. Microchim Acta 158:255–260
672. Hernandez L, Hernandez P, Lorenzo E, Sosa Ferrera Z (1988) Comparative study of the electrochemical behavior of sepiolite- and hectorite-modified carbon paste electrodes in the determination of dinocap. Analyst 113:621–623
673. Hernandez L, Hernandez P, Sosa Z (1988) Determination of phenol by differential-pulse voltammetry with a sepiolite-modified carbon paste electrode. Fresenius Z Anal Chem 331:525–527
674. Hernandez P, Vicente J, Gonzalez M, Hernandez L (1990) Voltammetric determination of linuron at a carbon-paste electrode modified with sepiolite. Talanta 37:789–794
675. Naranjo-Rodriguez I, Munoz-Leyva JA, de Cisneros JLH (1997) Use of a bentonite-modified carbon paste electrode for the determination of some phenols in a flow system by differential-pulse voltammetry. Analyst 122:601–604
676. Marchal V, Barbier F, Plassard F, Faure R, Vittori O (1999) Determination of cadmium in bentonite clay mineral using a carbon paste electrode. Fresenius J Anal Chem 363:710–712
677. Rezaei B, Ghiaci M, Sedaghat ME (2008) A selective modified bentonite-porphyrin carbon paste electrode for determination of Mn(II) by using anodic stripping voltammetry. Sensor Actuat B 131:439–447
678. Kalcher K, Grabec I, Raber G, Cai X, Tavcar G, Ogorevc B (1995) The vermiculite-modified carbon paste electrode as a model system for preconcentrating mono- and divalent cations. J Electroanal Chem 386:149–156
679. Svegl IG, Ogorevc B, Hudnik V (1996) A methodological approach to the application of a vermiculite-modified carbon paste electrode in interaction studies: influence of some pesticides on the uptake of Cu(II) from a solution to the solid phase. Fresenius J Anal Chem 354:770–773
680. Svegl IG, Kolar M, Ogorevc B, Pihlar B (1998) Vermiculite clay mineral as an effective carbon paste electrode modifier for the preconcentration and voltammetric determination of Hg(II) and Ag(I) ions. Fresenius J Anal Chem 361:358–362
681. Oropeza MT, Gonzalez I, Teutli-Leon MM, Chazaro LF (2005) Voltammetric study of cadmium-kaolinite system using modified carbon paste electrodes. In: Applications of analytical chemistry in environmental research. Research Signpost, Trivandrum, pp 67–77
682. Tonlé IK, Letaief S, Ngameni E, Walcarius A, Detellier C (2011) Square wave voltammetric determination of lead(II) ions using a carbon paste electrode modified by a thiol-functionalized kaolinite. Electroanalysis 23:245–252
683. El Mhammedi MA, Bakasse M, Najih R, Chtaini A (2009) A carbon paste electrode modified with kaolin for the detection of diquat. Appl Clay Sci 43:130–134
684. Ozkan D, Kerman K, Meric B, Kara P, Demirkan H, Polverejan M, Pinnavaia TJ, Ozsoz M (2002) Heterostructured fluorohectorite clay as an electrochemical sensor for the detection of 2,4-dichlorophenol and the herbicide 2,4-D. Chem Mater 14:1755–1761
685. Dilgin Y, Dursun Z, Nisli G (2003) Flow injection amperometric determination of ascorbic acid using a photoelectrochemical reaction after immobilization of methylene blue on muscovite. Turkish J Chem 27:167–180
686. Tonlé IK, Ngameni E, Walcarius A (2005) Preconcentration and voltammetric analysis of mercury(II) at a carbon paste electrode modified with natural smectite-type clays grafted with organic chelating groups. Sensor Actuat B 110:195–203
687. Tonlé IK, Ngameni E, Tcheumi HL, Tchieda V, Carteret C, Walcarius A (2008) Sorption of methylene blue on an organoclay bearing thiol groups and application to electrochemical sensing of the dye. Talanta 74:489–497
688. Tcheumi HL, Tonlé IK, Ngameni E, Walcarius A (2010) Electrochemical analysis of methylparathion pesticide by a gemini surfactant intercalated clay modified electrode. Talanta 81:972–979

689. Rolison DR (1990) Zeolite-modified electrodes and electrode-modified zeolites. Chem Rev 90:867–878
690. Walcarius A, Rozanska S, Bessière J, Wang J (1999) Screen-printed zeolite-modified carbon electrodes. Analyst 124:1185–1190
691. Walcarius A, Lamberts L, Derouane EG (1993) The methyl viologen incorporated zeolite modified carbon paste electrode – Part 1 – electrochemical behaviour in aqueous media – effects of supporting electrolyte and immersion time. Electrochim Acta 38:2257–2266
692. Ardakani MM, Akrami Z, Kazemian H, Zare HR (2008) Accumulation and voltammetric determination of cobalt at zeolite-modified electrodes. J Anal Chem 63:184–191
693. Senthilkumar S, Saraswathi R (2009) Electrochemical sensing of cadmium and lead ions at zeolite-modified electrodes: optimization and field measurements. Sensor Actuat B 141:65–75
694. Walcarius A, Barbaise T, Bessière J (1997) Factors affecting the analytical applications of zeolite modified electrodes: preconcentration of electroactive species. Anal Chim Acta 340:61–76
695. Chen B, Goh NK, Chia LS (1996) Determination of copper by zeolite molecular sieve modified electrode. Electrochim Acta 42:595–604
696. Walcarius A (1999) Factors affecting the analytical applications of zeolite modified electrodes: indirect detection of non-electroactive cations. Anal Chim Acta 388:79–91
697. Walcarius A, Mariaulle P, Louis C, Lamberts L (1999) Amperometric detection of nonelectroactive cations in electrolyte-free flow systems at zeolite modified electrodes. Electroanalysis 11:393–400
698. Wang J, Martinez T (1988) Accumulation and voltammetric measurement of silver at zeolite-containing carbon-paste electrodes. Anal Chim Acta 207:95–102
699. El Murr N, Kerkeni M, Sellami A, Ben Taarit Y (1988) The zeolite-modified carbon paste electrode. J Electroanal Chem 246:461–465
700. Walcarius A, Vromman V, Bessière J (1999) Flow injection indirect amperometric detection of ammonium ions using a clinoptilolite-modified electrode. Sensor Actuat B 56:136–143
701. Ardakani MM, Karimi MA, Mashhadizadeh MH, Pesteh M, Azimi MS, Kazemian H (2007) Potentiometric determination of monohydrogen arsenate by zeolite-modified carbon-paste electrode. Int J Environ Anal Chem 87:285–294
702. Saiapina OY, Pyeshkova VM, Soldatkin OO, Melnik VG, Akata Kurç B, Walcarius A, Dzyadevych SV, Jaffrezic-Renault N (2011) Conductometric enzyme biosensors based on natural zeolite clinoptilolite for urea determination. Mater Sci Eng C 31:1490–1497
703. Hernandez P, Alda E, Hernandez L (1987) Determination of mercury(II) using a modified electrode with zeolite. Fresenius Z Anal Chem 327:676–678
704. Kilinc Alpat S, Yuksel U, Akcay H (2005) Development of a novel carbon paste electrode containing a natural zeolite for the voltammetric determination of copper. Electrochem Commun 7:130–134
705. Gligor D, Maicaneanu A, Walcarius A (2010) Iron-enriched natural zeolite modified carbon paste electrode for H_2O_2 detection. Electrochim Acta 55:4050–4056
706. Naranjo-Rodriguez I, Munoz-Leyva JA, de Cisneros JLH (2003) Flow injection study of 2,4,6-trichlorophenol by differential pulse voltammetry at a zeolite-modified carbon paste electrode. Bull Electrochem 19:289–294
707. Arranz A, De Betono SF, Moreda JM, Cid A, Arranz JF (1997) Preconcentration and voltammetric determination of the herbicide metamitron with a silica-modified carbon paste electrode. Mikrochim Acta 127:273–279
708. Walcarius A, Bessière J (1997) Silica-modified carbon paste electrode for copper determination in ammoniacal medium. Electroanalysis 9:707–713
709. Walcarius A, Devoy J, Bessière J (2000) Silica-modified electrode for the selective detection of mercury. J Solid State Electrochem 4:330–336

710. Ruiz Barrio MA, Pingarrón Carrazon JM (1992) Voltammetric determination of pentachlorophenol with a silica gel-modified carbon paste electrode. Fresenius J Anal Chem 344:34–38
711. Gushikem Y, Rosatto SS (2001) Metal oxide thin films grafted on silica gel surfaces: recent advances on the analytical application of these materials. J Braz Chem Soc 12:695–705
712. Walcarius A, Luthi N, Blin JL, Su BL, Lamberts L (1999) Electrochemical evaluation of polysiloxane-immobilized amine ligands for the accumulation of copper(II) species. Electrochim Acta 44:4601–4610
713. Walcarius A, Etienne M, Delacote C (2004) Uptake of inorganic HgII by organically modified silicates: influence of pH and chloride concentration on the binding pathways and electrochemical monitoring of the processes. Anal Chim Acta 508:87–98
714. Yantasee W, Lin Y, Zemanian TS, Fryxell GE (2003) Voltammetric detection of lead(II) and mercury(II) using a carbon paste electrode modified with thiol self-assembled monolayer on mesoporous silica (SAMMS). Analyst 128:467–472
715. Cavalheiro ETG, Marino G, Cesarino I (2006) Differential pulse anodic stripping voltammetric determination of mercury(II) in natural water at a carbon paste electrode modified with organofunctionalized amorphous silica. Anal Chem Indian J 2:37–44
716. Aleixo LM, de Fatima BS, Godinho OES, Oliveira Neto G, Gushikem Y, Moreira JC (1992) Development of a chemically modified electrode based on carbon paste and functionalized silica gel for preconcentration and voltammetric determination of mercury(II). Anal Chim Acta 271:143–148
717. Dias Filho NL, do Carmo DR (2005) Stripping voltammetry of mercury(II) with a chemically modified carbon paste electrode containing silica gel functionalized with 2,5-dimercapto-1,3,4-thiadiazole. Electroanalysis 17:1540–1546
718. Dias Filho NL, do Carmo DR, Rosa AH (2006) An electroanalytical application of 2-aminothiazole-modified silica gel after adsorption and separation of Hg(II) from heavy metals in aqueous solution. Electrochim Acta 52:965–972
719. Takeuchi RM, Santos AL, Padilha PM, Stradiotto NR (2007) Copper determination in ethanol fuel by differential pulse anodic stripping voltammetry at a solid paraffin-based carbon paste electrode modified with 2-aminothiazole organofunctionalized silica. Talanta 71:771–777
720. Sayen S, Gerardin C, Rodehuser L, Walcarius A (2003) Electrochemical detection of copper (II) at an electrode modified by a carnosine - silica hybrid material. Electroanalysis 15:422–430
721. Ganesan V, Walcarius A (2004) Surfactant templated sulfonic acid functionalized silica microspheres as new efficient ion exchangers and electrode modifiers. Langmuir 20:3632–3640
722. Abu-Shawish HM, Saadeh SM, Hussien AR (2008) Enhanced sensitivity for Cu(II) by a salicylidine -functionalized polysiloxane carbon paste electrode. Talanta 76:941–948
723. Torabi R, Shams E, Zolfigol MA, Afshar S (2006) Anodic stripping voltammetric determination of lead(II) with a 2-aminopyridinated-silica modified carbon paste electrode. Anal Lett 39:2643–2655
724. Yantasee W, Lin Y, Fryxell GE, Busche BJ (2004) Simultaneous detection of cadmium, copper, and lead using a carbon paste electrode modified with carbamoylphosphonic acid self-assembled monolayer on mesoporous silica (SAMMS). Anal Chim Acta 502:207–212
725. Dias Filho NL, Caetano L, do Carmo DR, Rosa AH (2006) Preparation of a silica gel modified with 2-amino-1,3,4-thiadiazole for adsorption of metal ions and electroanalytical application. J Braz Chem Soc 17:473–481
726. Labuda J, Meister A, Glaeser P, Werner G (1998) Metal oxide-modified carbon paste electrodes and microelectrodes for the detection of amino acids and their application to capillary electrophoresis. Fresenius J Anal Chem 360:654–658
727. Wang J, Lin Y (1994) Electrocatalytic flow detection of amino acids at ruthenium dioxide-modified carbon electrodes. Electroanalysis 6:125–129

728. Lefèvre G, Bessière J, Walcarius A (1999) Cuprite-modified electrode for the detection of iodide species. Sensor Actuat B 59:113–117
729. Carjonyte R, Malinauskas A (1998) Amperometric sensor for hydrogen peroxide, based on Cu_2O or CuO modified carbon paste electrodes. Fresenius J Anal Chem 360:122–123
730. Mannino S, Cosio MS, Ratti S (1993) Cobalt(II, III) oxide chemically modified electrode as amperometric detector in flow-injection systems. Electroanalysis 5:145–148
731. Walcarius A, Despas C, Trens P, Hudson MJ, Bessière J (1998) Voltammetric in situ investigation of a MCM-41-modified carbon paste electrode - a new sensor. J Electroanal Chem 453:249–252
732. Walcarius A, Bessière J (1999) Electrochemistry with mesoporous silica: selective mercury (II) binding. Chem Mater 11:3009–3011
733. Zhou C, Liu Z, Dong Y, Li D (2009) Electrochemical behavior of o-nitrophenol at hexagonal mesoporous silica modified carbon paste electrodes. Electroanalysis 21:853–858
734. Walcarius A, Etienne M, Sayen S, Lebeau B (2003) Grafted silicas in electroanalysis: amorphous versus ordered mesoporous materials. Electroanalysis 15:414–421
735. Ojani R, Ahmadi E, Raoof JB, Mohamadnia F (2009) Characterization of a carbon paste electrode containing organically modified nanostructure silica: application to voltammetric detection of ferricyanide. J Electroanal Chem 626:23–29
736. Yantasee W, Lin Y, Fryxell GE, Wang Z (2004) Carbon paste electrode modified with carbamoylphosphonic acid functionalized mesoporous silica: a new mercury-free sensor for uranium detection. Electroanalysis 16:870–873
737. Cesarino I, Marino G, Matos JR, Cavalheiro ETG (2008) Evaluation of a carbon paste electrode modified with organofunctionalised SBA-15 nanostructured silica in the simultaneous determination of divalent lead, copper and mercury ions. Talanta 75:15–21
738. Morante-Zarcero S, Sanchez A, Fajardo M, Hierro I, Sierra I (2010) Voltammetric analysis of Pb(II) in natural waters using a carbon paste electrode modified with 5-mercapto-1-methyltetrazol grafted on hexagonal mesoporous silica. Microchim Acta 169:57–64
739. Ganjali MR, Asgari M, Faridbod F, Norouzi P, Badiei A, Gholami J (2010) Thiomorpholine-functionalized nanoporous mesopore as a sensing material for Cd^{2+} carbon paste electrode. Solid State Electrochem 14:1359–1366
740. Popa DE, Buleandra M, Mureseanu M, Ionica M, Tanase IG (2010) Carbon paste electrode modified with organofunctionalized mesoporous silica for electrochemical detection and quantitative determination of cadmium(II) using square wave anodic stripping voltammetry. Rev Chim 61:162–167
741. Zhou W, Chai Y, Yuan R, Guo J, Wu X (2009) Organically nanoporous silica gel based on carbon paste electrode for potentiometric detection of trace Cr(III). Anal Chim Acta 647:210–214
742. Javanbakht M, Divsar F, Badiei A, Fatollahi F, Khaniani Y, Ganjali MR, Norouzi P, Chaloosi M, Ziarani GM (2009) Determination of picomolar silver concentrations by differential pulse anodic stripping voltammetry at a carbon paste electrode modified with phenylthiourea-functionalized high ordered nanoporous silica gel. Electrochim Acta 54:5381–5386
743. Zhu L, Tian C, Zhu D, Yang R (2008) Ordered mesoporous carbon paste electrodes for electrochemical sensing and biosensing. Electroanalysis 20:1128–1134
744. Mashhadizadeh MH, Eskandari K, Foroumadi A, Shafiee A (2008) Self-assembled mercapto-compound-gold-nanoparticle-modified carbon paste electrode for potentiometric determination of cadmium(II). Electroanalysis 20:1891–1896
745. Mashhadizadeh MH, Khani H (2010) Sol-gel-Au nanoparticle modified carbon paste electrode for potentiometric determination of sub ppb level of Al(III). Anal Methods 2:24–31
746. Ganjali MR, Motakef-Kazemi N, Norouzi P, Khoee S (2009) A modified Ho^{3+} carbon paste electrode based on multi-walled carbon nanotubes (MWCNTs) and nanosilica. Int J Electrochem Sci 4:906–913

747. Parham H, Rahbar N (2010) Square wave voltammetric determination of methyl parathion using ZrO_2-nanoparticles modified carbon paste electrode. J Hazard Mater 177:1077–1084
748. Pessoa CA, Gushikem Y, Kubota LT, Gorton L (1997) Preliminary electrochemical study of phenothiazines and phenoxazines immobilized on zirconium phosphate. J Electroanal Chem 431:23–27
749. Malinauskas A, Ruzgas T, Gorton L (2000) Electrochemical study of the redox dyes Nile Blue and Toluidine Blue adsorbed on graphite and zirconium phosphate modified graphite. J Electroanal Chem 484:55–63
750. Munteanu FD, Mosbach M, Schulte A, Schuhmann W, Gorton L (2002) Fast-scan cyclic voltammetry and scanning electrochemical microscopy studies of the pH-dependent dissolution of 2-electron mediators immobilized on zirconium phosphate containing carbon pastes. Electroanalysis 14:1479–1487
751. El Mhammedi MA, Bakasse M, Chtaini A (2007) Square-wave voltammetric determination of paraquat at carbon paste electrode modified with hydroxyapatite. Electroanalysis 19:1727–1733
752. El Mhammedi MA, Achak M, Bakasse M, Chtaini A (2009) Electrochemical determination of para-nitrophenol at apatite-modified carbon paste electrode: application in river water samples. J Hazard Mater 163:323–328
753. El Mhammedi MA, Achak M, Chtaini A (2009) $Ca_{10}(PO_4)_6(OH)_2$-modified carbon-paste electrode for the determination of trace lead(II) by square-wave voltammetry. J Hazard Mater 161:55–61
754. El Mhammedi MA, Achak M, Najih R, Bakasse M, Chtaini A (2009) Microextraction and trace determination of cadmium by square wave voltammetry at the carbon paste electrode impregnated with $Ca_{10}(PO_4)_6(OH)_2$. Mater Chem Phys 115:567–571
755. Abdollahi S (1995) Preconcentration and determination of Pb^{2+} at an $AlPO_4$ containing carbon paste electrode. Anal Chim Acta 304:381–388
756. Mascarenhas RJ, Satpati AK, Yellappa S, Sherigara BS, Bopiah AK (2006) Wax-impregnated carbon paste electrode modified with mercuric oxalate for the simultaneous determination of heavy metal ions in medicinal plants and ayurvedic tablets. Anal Sci 22:871–875
757. Abbas MN, Mostafa GAE (2003) New triiodomercurate-modified carbon paste electrode for the potentiometric determination of mercury. Anal Chim Acta 478:329–335
758. Cai X, Kalcher K, Lintschinger J, Neuhold C (1993) Stripping voltammetric determination of trace amounts of mercury using a carbon paste electrode modified with 2-mercapto-4(3H)-quinazolinone. Mikrochim Acta 112:135–146
759. Won MS, Moon DW, Shim YB (1995) Determination of mercury and silver at a modified carbon paste electrode containing glyoxal bis(2-hydroxyanil). Electroanalysis 7:1171–1176
760. Colilla M, Mendiola MA, Procopio JR, Sevilla MT (2005) Application of a carbon paste electrode modified with a Schiff base ligand to mercury speciation in water. Electroanalysis 17:933–940
761. Prabhu SV, Baldwin RP, Kryger L (1987) Chemical preconcentration and determination of copper at a chemically modified carbon-paste electrode containing 2,9-dimethyl-1,10-phenanthroline. Anal Chem 59:1074–1078
762. Safavi A, Pakniat M, Maleki N (1996) Design and construction of a flow system for determination of Cu(II) ions in water by means of a chemically modified carbon paste electrode. Anal Chim Acta 335:275–282
763. Danet AF, Neagu D, Dondoi MP, Iliescu N (2004) Anodic stripping voltammetric determination of copper(II) with salicylaldoxime carbon paste electrodes. Rev Chim 55:1–4
764. Chaisuksant R, Pattanarat L, Grudpan K (2008) Naphthazarin modified carbon paste electrode for determination of copper(II). Microchim Acta 162:181–188
765. Sugawara K, Tanaka S, Taga M (1991) Voltammetry of silver(I) using a carbon-paste electrode modified with 2,2'-dithiodipyridine. J Electroanal Chem 304:249–255

766. Cai X, Kalcher K, Neuhold C, Goessler W, Grabec I, Ogorevc B (1994) Studies on the voltammetric behavior of a 2-mercaptoimidazole containing carbon paste electrode: determination of traces of silver. Fresenius J Anal Chem 348:736–741
767. Mohadesi A, Taher MA (2007) Stripping voltammetric determination of silver(I) at carbon paste electrode modified with 3-amino-2-mercaptoquinazolin-4(3H)-one. Talanta 71:615–619
768. Peng T, Zhe T, Wang G, Shen B (1994) Differential pulse voltammetric determination of lead (II) with benzoin oxime-modified carbon paste electrodes. Electroanalysis 6:597–603
769. Molina-Holgado T, Pinilla-Macias JM, Hernandez-Hernandez L (1995) Voltammetric determination of lead with a chemically modified carbon paste electrode with diphenylthiocarbazone. Anal Chim Acta 309:117–122
770. Adraoui I, El Rhazi M, Amine A, Idrissi L, Curulli A, Palleschi G (2005) Lead determination by anodic stripping voltammetry using a p-phenylenediamine modified carbon paste electrode. Electroanalysis 17:685–693
771. Khan MR (1998) 1-(2-Pyridylazo)-2-naphthol modified carbon paste electrode for trace cobalt(II) determination by differential pulse cathodic voltammetry. Analyst 123:1351–1357
772. Lu X, Wang Z, Geng Z, Kang J, Gao J (2000) 2,4,6-tri(3,5-Dimethylpyrazoyl)-1,3,5-triazine modified carbon paste electrode for trace Cobalt(II) determination by differential pulse anodic stripping voltammetry. Talanta 52:411–416
773. Thomsen KN, Kryger L, Baldwin RP (1988) Voltammetric determination of traces of nickel (II) with a medium exchange flow system and a chemically modified carbon paste electrode containing dimethylglyoxime. Anal Chem 60:151–155
774. Mattos CS, do Carmo DR, de Oliveira MF, Stradiotto NR (2008) Voltammetric determination of total iron in fuel ethanol using a 1,10 phenantroline/Nafion carbon paste-modified electrode. Int J Electrochem Sci 3:338–345
775. Koelbl G, Kalcher K, Voulgaropoulos A (1992) Voltammetric determination of gold with a Rhodamine B-modified carbon paste electrode. Fresenius J Anal Chem 342:83–86
776. Paniagua AR, Vazquez MD, Tascon ML, Sanchez Batanero P (1993) Determination of chromium(VI) and chromium(III) by using a diphenylcarbazide-modified carbon paste electrode. Electroanalysis 5:155–163
777. Khoo SB, Soh MK, Cai Q, Khan MR, Guo SX (1997) Differential pulse cathodic stripping voltammetric determination of manganese(II) and manganese(VII) at the 1-(2-pyridylazo)-2-naphthol-modified carbon paste electrode. Electroanalysis 9:45–51
778. Cai Q, Khoo SB (1995) Determination of trace thallium after accumulation of thallium(III) at a 8-hydroxyquinoline-modified carbon paste electrode. Analyst 120:1047–1053
779. Estevez-Hernandez O, Naranjo-Rodriguez I, de Cisneros JLH, Reguera E (2007) Evaluation of carbon paste electrodes modified with 1-furoylthioureas for the analysis of cadmium by differential pulse anodic stripping voltammetry. Sensor Actuat B 123:488–494
780. Wang J, Lu J, Larson DD, Olsen K (1995) Voltammetric sensor for uranium based on the propyl gallate-modified carbon paste electrode. Electroanalysis 7:247–250
781. Zhang ZQ, Liu H, Zhang H, Li YF (1996) Simultaneous cathodic stripping voltammetric determination of mercury, cobalt, nickel and palladium by mixed binder carbon paste electrode containing dimethylglyoxime. Anal Chim Acta 333:119–124
782. Ghoneim EM (2010) Simultaneous determination of Mn(II), Cu(II) and Fe(III) as 2-(5'-bromo-2'-pyridylazo)-5-diethylaminophenol complexes by adsorptive cathodic stripping voltammetry at a carbon paste electrode. Talanta 82:646–652
783. Prabhu SV, Baldwin RP, Kryger L (1989) Preconcentration and determination of lead (II) at crown ether and cryptand containing chemically modified electrodes. Electroanalysis 1:13–21
784. Ijeri VS, Srivastava AK (2001) Voltammetric determination of lead at chemically modified electrodes based on crown ethers. Anal Sci 17:605–608

785. Srivastava AK, Gaichore RR (2010) Macrocyclic compounds based chemically modified electrodes for voltammetric determination of L-tryptophan using electrocatalytic oxidation. Anal Lett 43:1933–1950
786. Tanaka S, Yoshida H (1989) Stripping voltammetry of silver(I) with a carbon-paste electrode modified with thiacrown compounds. Talanta 36:1044–1046
787. Ruiperez J, Mendiola MA, Sevilla MT, Procopio JR, Hernandez L (2002) Application of a macrocyclic thiohydrazone modified carbon paste electrode to copper speciation in water samples. Electroanalysis 14:532–539
788. Pouretedal HR, Keshavarz MH (2005) Cyclam modified carbon paste electrode as a potentiometric sensor for determination of cobalt(II) ions. Chem Res Chin Univ 21:28–31
789. Ferancova A, Korgova E, Labuda J, Zima J, Barek J (2002) Cyclodextrin modified carbon paste based electrodes as sensors for the determination of carcinogenic polycyclic aromatic amines. Electroanalysis 14:1668–1673
790. Roa Morales G, Ramirez-Silva MT, Romero-Romo MA, Galicia L (2003) Determination of lead and cadmium using a polycyclodextrin-modified carbon paste electrode with anodic stripping voltammetry. Anal Bioanal Chem 377:763–769
791. Roa Morales G, Ramirez Silva MT, Romero Romo MM, Galicia L (2005) Heavy metal determination by anodic stripping voltammetry with a carbon paste electrode modified with alpha -cyclodextrin. In: Palomar M (ed) Applications of Analytical Chemistry in Environmental Research, Research Signpost, Trivandrum, India
792. Arrigan DWM, Svehla G, Harris SJ, McKervey MA (1994) Use of calixarenes as modifiers of carbon paste electrodes for voltammetric analysis. Electroanalysis 6:97–106
793. Canpolat EC, Sar E, Coskun NY, Cankurtaran H (2007) Determination of trace amounts of copper in tap water samples with a calix[4]arene modified carbon paste electrode by differential pulse anodic stripping voltammetry. Electroanalysis 19:1109–1115
794. Raoof JB, Ojani R, Alinezhad A, Rezaie SZ (2010) Differential pulse anodic stripping voltammetry of silver(I) using p-isopropylcalix[6]arene modified carbon paste electrode. Monatsh Chem 141:279–284
795. Raoof JB, Ojani R, Ramine M (2009) Voltammetric sensor for nitrite determination based on its electrocatalytic reduction at the surface of p-duroquinone modified carbon paste electrode. J Solid State Electrochem 13:1311–1319
796. Liu KE, Abruna HD (1989) Electroanalysis of aromatic aldehydes with modified carbon paste electrodes. Anal Chem 61:2599–2602
797. Kong YT, Imabayashi SI, Kano K, Ikeda T, Kakiuchi T (2001) Peroxidase-based amperometric sensor for the determination of total phenols using two-stage peroxidase reactions. Am J Enol Viticult 52:381–385
798. Raoof JB, Ojani R, Karimi-Maleh H (2008) Electrocatalytic determination of sulfite using 1-[4-(ferrocenylethynyl)phenyl]-1-ethanone modified carbon paste electrode. Asian J Chem 20:483–494
799. Casero E, Pariente F, Lorenzo E, Beyer L, Losada J (2001) Electrocatalytic oxidation of nitric oxide at 6,17-diferrocenyldibenzo[b, i]5,9,14,18-tetraaza[14]annulen-nickel(II) modified electrodes. Electroanalysis 13:1411–1416
800. Ojani R, Raoof JB, Norouzi B (2008) Acetylferrocene modified carbon paste electrode; a sensor for electrocatalytic determination of hydrazine. Electroanalysis 20:1378–1382
801. Hattori T, Kato M, Tanaka S, Hara M (1997) Adsorptive stripping voltammetry of anionic surfactants on a carbon paste electrode using ferrocenyl cationic surfactant as an analytical electrochemical probe. Electroanalysis 9:722–725
802. Halbert MK, Baldwin RP (1985) Electrocatalytic and analytical response of cobalt phthalocyanine containing carbon paste electrodes toward sulfhydryl compounds. Anal Chem 57:591–595

803. Cookeas EG, Efstathiou CE (1994) Flow injection amperometric determination of thiocyanate and selenocyanate at a cobalt phthalocyanine modified carbon paste electrode. Analyst 119:1607–1612
804. Skladal P (1991) Determination of organophosphate and carbamate pesticides using a cobalt phthalocyanine-modified carbon paste electrode and a cholinesterase enzyme membrane. Anal Chim Acta 252:11–15
805. Nunes GS, Barcelo D, Grabaric BS, Diaz-Cruz JM, Ribeiro ML (1999) Evaluation of a highly sensitive amperometric biosensor with low cholinesterase charge immobilized on a chemically modified carbon paste electrode for trace determination of carbamates in fruit, vegetable and water samples. Anal Chim Acta 399:37–49
806. Shaidarova LG, Budnikov GK, Zaripova SA (2001) Electrocatalytic determination of dithiocarbamate-based pesticides using electrodes modified with metal phthalocyanines. J Anal Chem 56:748–753
807. Fernandez C, Reviejo AJ, Pingarrón JM (1995) Voltammetric determination of the herbicides thiram and disulfiram with a cobalt phthalocyanine modified carbon paste electrode. Analysis 23:319–324
808. Siangproh W, Chailapakul O, Laocharoensuk R, Wang J (2005) Microchip capillary electrophoresis/electrochemical detection of hydrazine compounds at a cobalt phthalocyanine modified electrochemical detector. Talanta 67:903–907
809. Conceicao CD, Faria RC, Fatibello-Filho O, Tanaka AA (2008) Electrocatalytic oxidation and voltammetric determination of hydrazine in industrial boiler feed water using a cobalt phthalocyanine-modified electrode. Anal Lett 41:1010–1021
810. Yin HS, Zhou YL, Ai SY (2009) Preparation and characteristic of cobalt phthalocyanine modified carbon paste electrode for bisphenol A detection. J Electroanal Chem 626:80–88
811. Ciucu AA, Negulescu C, Baldwin RP (2003) Detection of pesticides using an amperometric biosensor based on ferrophthalocyanine chemically modified carbon paste electrode and immobilized bienzymatic system. Biosens Bioelectron 18:303–310
812. Sotomayor MDPT, Tanaka AA, Kubota LT (2002) Development of an enzymeless biosensor for the determination of phenolic compounds. Anal Chim Acta 455:215–223
813. Santos WJ, Sousa AL, Sotomayor MP, Damos FS, Tanaka SM, Kubota LT, Tanaka AA (2009) Manganese phthalocyanine as a biomimetic electrocatalyst for phenols in the development of an amperometric sensor. J Braz Chem Soc 20:1180–1187
814. Guerra SV, Xavier CR, Nakagaki S, Kubota LT (1998) Electrochemical behavior of copper porphyrin synthesized into zeolite cavity. A sensor for hydrazine. Electroanalysis 10:462–466
815. Ribeiro ES, Gushikem Y, Biazzotto JC, Serra OA (2002) Electrochemical properties and dissolved oxygen reduction study on an iron(III)-tetra(o-ureaphenyl)porphyrinosilica matrix surface. J Porphyr Phthalocyan 6:527–532
816. Pessoa CA, Gushikem Y (2001) Cobalt porphyrins immobilized on niobium(V) oxide grafted on a silica gel surface: study of the catalytic reduction of dissolved dioxygen. J Porphyr Phthalocyan 5:537–544
817. Shamsipur M, Najafi M, Hosseini MRM, Sharghi H (2007) Electrocatalytic reduction of dioxygen at carbon paste electrode modified with a novel cobalt(III) Schiff's base complex. Electroanalysis 19:1661–1667
818. Kamyabi MA, Shahabi S, Hosseini-Monfared H (2007) Electrocatalytic oxidation of hydrazine at a cobalt(II) Schiff-base-modified carbon paste electrode. J Electrochem Soc 155:F8–F12
819. Gil ED, Kubota LT (2000) Electrochemical behavior of rhodium acetamidate immobilized on a carbon paste electrode: a hydrazine sensor. J Braz Chem Soc 11:304–310
820. do Carmo DR, de Oliveira MF, Stradiotto NR (2003) Electrocatalytic and voltammetric determination of sulfhydryl compounds through iron nitroprusside modified graphite paste electrode. J Braz Chem Soc 14:616–620

821. Zhuang RR, Jian FF, Wang KF (2010) An electrochemical sensing platform based on a new zinc complex for the determination of hydrogen peroxide and nitrite. Sens Lett 8:228–232
822. Compagnone D, Bannister JV, Federici G (1992) Electrochemical sensors for the determination of metal ions. Sensor Actuat B 7:549–552
823. Agraz R, Sevilla MT, Hernandez L (1995) Voltammetric quantification and speciation of mercury compounds. J Electroanal Chem 390:47–57
824. Agraz R, de Miguel J, Sevilla MT, Hernandez L (1996) Application of a Chelite P modified carbon paste electrode to copper determination and speciation. Electroanalysis 8:565–570
825. Mikysek T, Švancara I, Vytřas K, Banica FG (2008) Functionalised resin-modified carbon paste sensor for the voltammetric determination of Pb(II) within a wide concentration range. Electrochem Commun 10:242–245
826. Sar E, Berber H, Asci B, Cankurtaran H (2008) Determination of some heavy metal ions with a carbon paste electrode modified by poly(glycidyl methacrylate-methylmethacrylate-divinylbenzene) microspheres functionalized by 2-aminothiazole. Electroanalysis 20:1533–1541
827. Alizadeh T (2009) High selective parathion voltammetric sensor development by using an acrylic based molecularly imprinted polymer-carbon paste electrode. Electroanalysis 21:1490–1498
828. Alizadeh T, Ganjali MR, Norouzi P, Zare M, Zeraatkar A (2009) A novel high selective and sensitive para-nitrophenol voltammetric sensor, based on a molecularly imprinted polymer-carbon paste electrode. Talanta 79:1197–1203
829. Alizadeh T, Zare M, Ganjali MR, Norouzi P, Tavana B (2010) A new molecularly imprinted polymer (MIP)-based electrochemical sensor for monitoring 2,4,6-trinitrotoluene (TNT) in natural waters and soil samples. Biosens Bioelectron 25:1166–1172
830. Navratilova Z, Kula P (1992) Determination of mercury on a carbon paste electrode modified with humic acid. Electroanalysis 4:683–687
831. Sun QY, Wang CM, Li LX, Li HL (1999) Preconcentration and voltammetric determination of palladium(II) at sodium humate modified carbon paste electrodes. Fresenius J Anal Chem 363:114–117
832. Thobie-Gautier C, Lopes da Silva WT, Rezende MOO, El Murr N (2003) Sensitive and reproducible quantification of Cu^{2+} by stripping with a carbon paste electrode modified with humic acid. J Environ Sci Health A 38:1811–1823
833. Connor M, Dempsey E, Smyth MR, Richardson DH (1991) Determination of some metal ions using lichen-modified carbon paste electrodes. Electroanalysis 3:331–336
834. Dempsey E, Smyth MR, Richardson DH (1992) Application of lichen-modified carbon paste electrodes to the voltammetric determination of metal ions in multielement and speciation studies. Analyst 117:1467–1470
835. Sugawara K, Matsui H, Hoshi S, Akatsuka K (1998) Voltammetric detection of silver(I) using a carbon paste electrode modified with keratin. Analyst 123:2013–2016
836. Wang J, Greene B, Morgan C (1984) Carbon paste electrodes modified with cation-exchange resin in differential pulse voltammetry. Anal Chim Acta 158:15–22
837. Gao Z, Wang G, Li P, Zhao Z (1991) Differential pulse voltammetric determination of cobalt with a perfluorinated sulfonated polymer-2,2-bipyridyl modified carbon paste electrode. Anal Chem 63:953–957
838. Gao Z, Li P, Wang G, Zhao Z (1990) Preconcentration and differential-pulse voltammetric determination of iron(II) with Nafion-1,10-phenanthroline-modified carbon paste electrodes. Anal Chim Acta 241:137–146
839. Lee GJ, Kim CK, Lee MK, Rhee CK (2010) Advanced Use of Nanobismuth/Nafion electrode for trace analyses of zinc, cadmium, and lead. J Electrochem Soc 157:J241–J244
840. Hernandez L, Melguizo JM, Blanco MH, Hernandez P (1989) Determination of cadmium (II) with a carbon paste electrode modified with an ion-exchange resin. Analyst 114:397–399

841. Gonzalez P, Cortinez VA, Fontan CA (2002) Determination of nickel by anodic adsorptive stripping voltammetry with a cation exchanger-modified carbon paste electrode. Talanta 58:679–690
842. Wu WS, Uddin MS, Chi H, Hidajat K (1994) Electrochemically assisted metal uptake by cation exchange based chemically modified electrodes. J Appl Electrochem 24:548–553
843. Mariaulle P, Sinapi F, Lamberts L, Walcarius A (2001) Application of electrodes modified with ion-exchange polymers for the amperometric detection of non-redox cations and anions in combination to ion chromatography. Electrochim Acta 46:3543–3553
844. Agraz R, Sevilla MT, Hernandez L (1993) Chemically modified electrode for the simultaneous determination of trace metals and speciation analysis. Anal Chim Acta 273:205–212
845. Alvarez E, Sevilla MT, Pinilla JM, Hernandez L (1992) Cathodic stripping voltammetry of paraquat on a carbon paste electrode modified with Amberlite XAD-2 resin. Anal Chim Acta 260:19–23
846. Guadalupe AR, Jhaveri SS, Liu KE, Abruna HD (1987) Electroanalysis of primary amines with chemically modified carbon paste electrodes. Anal Chem 59:2436–2438
847. Biryol I, Uslu B, Kucukyavuz Z (1998) Voltammetric determination of amoxicillin using a carbon paste electrode modified with poly(4-vinyl pyridine). S T P Pharma Sci 8:383–386
848. Kalcher K (1985) Voltammetric determination of trace amounts of gold with a chemically modified carbon paste electrode. Anal Chim Acta 177:175–182
849. Cai X, Kalcher K, Diewald W, Neuhold C, Magee RJ (1993) Voltammetric determination of trace amounts of mercury with a carbon paste electrode modified with an anion-exchanger. Fresenius J Anal Chem 345:25–31
850. Neuhold C, Kalcher K, Diewald W, Cai X, Raber G (1994) Voltammetric determination of nitrate with a modified carbon paste electrode. Electroanalysis 6:227–236
851. O'Shea TJ, Leech D, Smyth MR, Vos JG (1992) Determination of nitrite based on mediated oxidation at a carbon paste electrode modified with a ruthenium polymer. Talanta 39:443–447
852. Wang LH, Tseng SW (2001) Direct determination of d-panthenol and salt of pantothenic acid in cosmetic and pharmaceutical preparations by differential pulse voltammetry. Anal Chim Acta 432:39–48
853. Kauffmann JM (1997) Lipid based enzyme electrodes for environmental pollution control. NATO ASI Ser Ser 2(38):107–114
854. Stadlober M, Kalcher K, Raber G, Neuhold C (1996) Anodic stripping voltammetric determination of titanium(IV) using a carbon paste electrode modified with cetyltrimethylammonium bromide. Talanta 43:1915–1924
855. Stadlober M, Kalcher K, Raber G (1997) A new method for the voltammetric determination of molybdenum(VI) using carbon paste electrodes modified in situ with cetyltrimethylammonium bromide. Anal Chim Acta 350:319–328
856. Stadlober M, Kalcher K, Raber G (1997) Anodic stripping voltammetric determination of vanadium(V) using a carbon paste electrode modified in situ with cetyltrimethylammonium bromide. Electroanalysis 9:225–230
857. Stadlober M, Kalcher K, Raber G (1998) Voltammetric determination of titanium, vanadium, and molybdenum using a carbon paste electrode modified with cetyltrimethylammonium bromide. Sci Pap Univ Pardubice Ser A 3:103–137
858. Huang W (2005) Voltammetric determination of bisphenol A using a carbon paste electrode based on the enhancement effect of cetyltrimethylammonium bromide (CTAB). Bull Kr Chem Soc 26:1560–1564
859. Liu S, Li J, Zhang S, Zhao J (2005) Study on the adsorptive stripping voltammetric determination of trace cerium at a carbon paste electrode modified in situ with cetyltrimethylammonium bromide. Appl Surf Sci 252:2078–2084
860. Jezkova J, Musilova J, Vytřas K (1997) Potentiometry with perchlorate and fluoroborate ion-selective carbon paste electrodes. Electroanalysis 9:1433–1436

861. Vytřas K, Khaled E, Jezkova J, Hassan HNA, Barsoum BN (2000) Studies on the potentiometric thallium(III)-selective carbon paste electrode and its possible applications. Fresenius J Anal Chem 367:203–207
862. Švancara I, Foret P, Vytřas K (2004) A study on the determination of chromium as chromate at a carbon paste electrode modified with surfactants. Talanta 64:844–852
863. Galik M, Cholota M, Švancara I, Bobrowski A, Vytřas K (2006) A study on stripping voltammetric determination of osmium(IV) at a carbon paste electrode modified in situ with cationic surfactants. Electroanalysis 18:2218–2224
864. Švancara I, Galik M, Vytřas K (2007) Stripping voltammetric determination of platinum metals at a carbon paste electrode modified with cationic surfactants. Talanta 72:512–518
865. Wang J, Chen L (1995) Hydrazine detection using a tyrosinase-based inhibition biosensor. Anal Chem 67:3824–3827
866. Lutz M, Burestedt E, Emneus J, Liden H, Gobhadi S, Gorton L, Marko-Varga G (1995) Effects of different additives on a tyrosinase based carbon paste electrode. Anal Chim Acta 305:8–17
867. Wang J, Lu F, Kane SA, Choi YK, Smyth MR, Rogers K (1997) Hydrocarbon pasting liquids for improved tyrosinase-based carbon-paste phenol biosensors. Electroanalysis 9:1102–1109
868. Liu S, Yu J, Ju H (2003) Renewable phenol biosensor based on a tyrosinase-colloidal gold modified carbon paste electrode. J Electroanal Chem 540:61–67
869. Liu Z, Liu Y, Yang H, Yang Y, Shen G, Yu R (2005) A phenol biosensor based on immobilizing tyrosinase to modified core-shell magnetic nanoparticles supported at a carbon paste electrode. Anal Chim Acta 533:3–9
870. Huang TH, Kuwana T, Warsinke A (2002) Analysis of thiols with tyrosinase-modified carbon paste electrodes based on blocking of substrate recycling. Biosens Bioelectron 17:1107–1113
871. Chough SH, Mulchandani A, Mulchandani P, Chen W, Wang J, Rogers KR (2002) Electroanalysis 14:273–276
872. Fähnrich KA, Pravda M, Guilbault GG (2003) Disposable amperometric immunosensor for the detection of polycyclic aromatic hydrocarbons (PAHs) using screen-printed electrodes. Biosens Bioelectron 18:73–82
873. Abbaspour A, Moosavi SMM (2002) Chemically modified carbon paste electrode for determination of copper(II) by potentiometric method. Talanta 56:91–96
874. Mashhadizadeh MH, Talakesh M, Peste M, Momeni A, Hamidian H, Mazlum M (2006) A novel modified carbon paste electrode for potentiometric determination of mercury(II) ion. Electroanalysis 18:2174–2179
875. Ortega DR, Silva MTR, Pardave MP, Alarcon-Angeles G, Hernandez AR, Romo MR (2009) Development a boron potentiometric determination methodology using a carbon paste electrode modified with a beta -cyclodextrin-azomethine-H inclusion complex. ECS Trans 20:13–19
876. Javanbakht M, Divsar F, Badiei A, Ganjali MR, Norouzi P, Ziarani GM, Chaloosi M, Jahangir AA (2009) Potentiometric detection of mercury(II) ions using a carbon paste electrode modified with substituted thiourea-functionalized highly ordered nanoporous silica. Anal Sci 25:789–794
877. Zheng X, Guo Z (2000) Potentiometric determination of hydrogen peroxide at MnO_2-doped carbon paste electrode. Talanta 50:1157–1162
878. Teixeira MFS, Cavalheiro ETG, Bergamini MF, Moraes FC, Bocchi N (2004) Use of carbon paste electrode modified with spinel-type manganese oxide as potentiometric sensor for lithium ions in flow injection analysis. Electroanalysis 16:633–639
879. Ejhieh AN, Masoudipour N (2010) Application of a new potentiometric method for determination of phosphate based on a surfactant-modified zeolite carbon-paste electrode (SMZ-CPE). Anal Chim Acta 658:68–74
880. Trojanowicz M, Matuszewski W (1989) Potentiometric stripping determination of nickel at a dimethylglyoxime-containing graphite paste electrode. Talanta 36:680–682

881. Švancara I, Ogorevc B, Novic M, Vytřas K (2002) Simple and rapid determination of iodide in table salt by stripping potentiometry at a carbon-paste electrode. Anal Bioanal Chem 372:795–800
882. Xu GB, Dong SJ (1999) Chemiluminescent determination of luminol and hydrogen peroxide using hematin immobilized in the bulk of a carbon paste electrode. Electroanalysis 11:1180–1184
883. Xu G, Dong S (2000) Electrochemiluminescent detection of chlorpromazine by selective preconcentration at a Lauric acid-modified carbon paste electrode using tris(2,2'-bipyridine) ruthenium(II). Anal Chem 72:5308–5312
884. Zhuang Y, Zhang D, Ju H (2005) Sensitive determination of heroin based on electrogenerated chemiluminescence of tris(2,2'-bipyridyl)ruthenium(II) immobilized in zeolite Y modified carbon paste electrode. Analyst 130:534–540

Chapter 17
Nanosized Materials in Amperometric Sensors

Fabio Terzi and Chiara Zanardi

During the last 20 years, the scientific community has witnessed the diffusion of a large number of different nanosized materials in many different applications.[1–5] Following an analogous trend, their use in electroanalysis has found so wide diffusion that, nowadays, electrode modifications based on these materials constitute the preferred approach for the development of amperometric sensors; quite spontaneously, this trend has also involved the field of environmental monitoring.

The main advantages ascribable to the use of nanosized materials in electroanalysis directly derive from their nanometric dimensions:

1. The high number of atoms localised in the correspondence to defects, such as vertexes and corners, that confer the material peculiar reactivity in electrocatalytic processes.
2. The high surface to volume ratio that induces an enormous enlargement of the electroactive area when nano-objects are deposited on the electrode surface.
3. The small spatial dimension that allows a direct electrical connection with the biological recognition element.
4. The possibility to stably fix, onto the electrode surface, a large number of molecules possessing functional groups capable to selectively interact with the analyte in solution.

Due to the outstanding properties of these materials, the number of reviews and books published so far is so high that even a mere list of them is almost impossible to compile.[5–32] However, it should be admitted that the term "nano" is sometimes used also to indicate objects whose size is often in the "micro regime." Actually, the distinction between nano- and micro-objects is not univocal and depends on the nature of the material. Most properly, it is based on the characteristics exhibited by the material, as we will try to explain in this chapter.

F. Terzi • C. Zanardi (✉)
Department of Chemical and Geological Sciences, University of Modena and Reggio Emilia, Modena, Italy
e-mail: chiara.zanardi@unimore.it

L.M. Moretto, K. Kalcher (eds.), *Environmental Analysis by Electrochemical Sensors and Biosensors*, DOI 10.1007/978-1-4939-0676-5_17

Although many aspects discussed hereafter are also valid in a variety of disciplines, specific applications in the field of electroanalysis will be treated. For this reason, only electrically conductive nanosized materials will be considered. They mainly consist of metal nanoparticles (NPs), carbon nanotubes (CNTs), graphene, and, to a lesser extent, metal oxides, quantum dots (QDs), metal clusters, and fullerenes.

17.1 Classification of Nanosized Materials

The classification of nanosized materials is quite challenging, due to the extreme heterogeneity of compositions and shapes reported so far. A tentative classification may be based on dimensionality of the structures, as shown in Table 17.1.[33]

The classification scheme reported above can not be applied rigidly: as an example, NPs can be considered 3D objects when compared to much smaller structures such as 0D clusters, which consist of aggregates of few tens of atoms characterised by a well-defined structure.[34] At the same time, Transmission Electron Microscopy (TEM) images show that carbon black grains possess a spherical shape, i.e. they can be considered a 0D object, but actually consist of disordered graphene sheets.

In most cases, nanostructures consist of an inorganic core of metals, carbon or semiconductors. Relatively few examples of organic nanosized materials have been reported; in the majority of cases, they are based on conductive polymers.[35]

Metal nanomaterials are generally based on noble metals, although the use of Ag and Cu has been also reported.[8, 11, 13–15, 17–20, 23, 24, 26–28] NPs constitute the most common nanostructure reported in electroanalytical applications; although their shape can be approximated to a sphere, more properly they consist of polyhedrons (Fig. 17.1). Among the other reported metal nanostructures, nanowires are most popular.[36, 37]

Carbon nanostructures (Fig. 17.2) constitute a variety of materials mainly based on carbon atoms possessing sp^2 hybridisation. The most important similar materials in electroanalysis are CNTs[1, 25, 29, 30, 40, 41] and graphene,[1, 7, 9, 12, 21, 22, 42–46] even though applicative examples involving fullerenes[47] and carbon blacks[48] are also reported. Both CNTs and graphene can be considered graphite derivatives, consisting

Table 17.1 Tentative classification of the nanosized materials

Nanostructures	Number of dimensions in the nanoscale	Examples
Zero-dimensional (0D)	3	Nanoparticles, clusters, carbon black, diamondoids, fullerenes
One-dimensional (1D)	2	Nanowires, nanotubes
Two-dimensional (2D)	1	Graphene
Three-dimensional (3D)	3	Tetrapodal structures, nanoporous systems

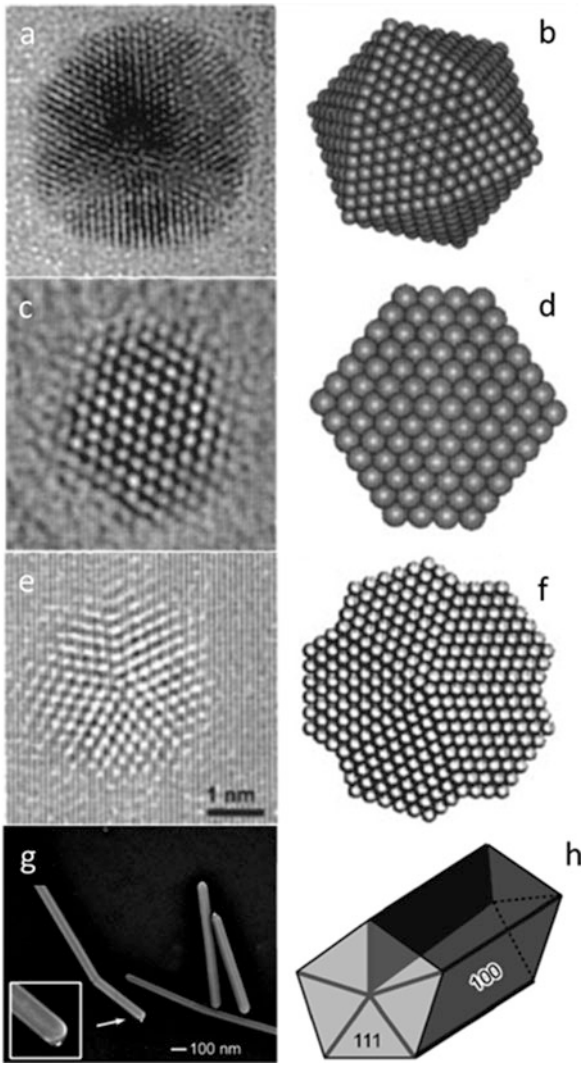

Fig. 17.1 Images of Au NPs at atomic resolution level registered by means of TEM. NPs possessing icosahedral (**a**), cubo-octahedral (**c**) and truncated decahedral (**e**) shapes are shown, together with the relevant hardball models of the NPs (**b**, **d**, **f**, respectively). (**g**, **h**) are scanning electron microscopy (SEM) image of Ag nanowires and relevant geometrical model, respectively. Adapted with permission from refs. [38, 39]

of rolled up or planar sheets, respectively. In the specific case of CNTs both single- and multi-wall tubes have been employed, although a precise assessment of the analytical performances of the two systems has not been reported. Although CNTs are often considered to exhibit uniform sp^2 structures, they possess a number of structural defects, such as vacancies and interstitials[49, 50]; their role in conditioning the electrocatalytic properties of the material still constitutes a debated aspect.

As to semiconductors, they mainly consist of metal oxide NPs, e.g. TiO_2, MnO_2 and CuO_x, or of QDs, e.g. CdSe and CdS. They are only occasionally used in electroanalysis, even though the number of literature reports has been increasing for the last few years.[14, 15, 54, 55]

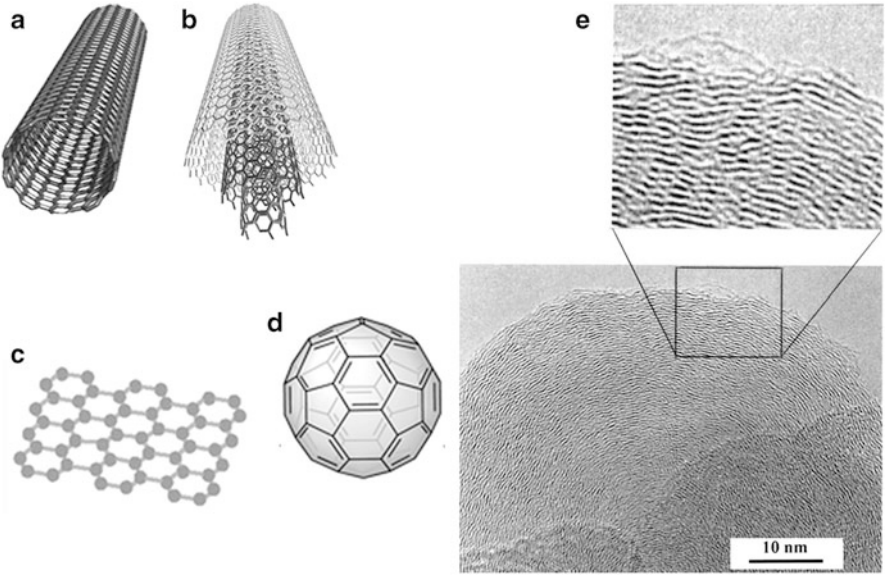

Fig. 17.2 Different carbon-based materials used in electroanalysis: schemes for single- (**a**) and multi- (**b**) wall CNTs, graphene (**c**), C_{60} fullerene (**d**); TEM images of carbon black particles (**e**). Adapted with permission from refs. [42, 51–53]

17.2 Synthesis of Nanosized Materials

The strict control of size and shape of the nanosized material is extremely important for the performances exhibited by the resulting sensor. For the same reason, the full comprehension of the relation between properties and structure is only possible when using nano-objects characterised by similar shape and narrow size distribution, i.e. characterised by a relative standard deviation lower than 20 %. A large number of synthetic parameters affects the size, size distribution and shape of the nano-objects.

Two different strategies can be followed for the synthesis of nanosized materials, i.e. either a top-down or a bottom-up methodology. The former one is based on the subdivision of bulk material into finely divided particles that can be collected as solid powder, suspended inside a liquid or directly deposited onto the electrode surface. The minute particles are usually obtained by physical methods, such as thermal evaporation, sputtering, or laser ablation. In addition, nanosized particles of metallic nature can be also obtained by electrochemical synthesis, exploiting the dissolution of a sacrificial anode.[56]

The bottom-up strategy is based on wet chemical or gas phase methods. In particular, at least four families of methods can be identified in the case of solution-based methods[56, 57]:

1. Chemical reduction of metal salts.
2. Electrochemical deposition onto a substrate.
3. Decomposition of organometallic compounds.
4. Biosynthesis through living organisms.

In the case of methods in gas phase, different procedures, such as chemical vapour deposition, condensation of metal vapours and laser pyrolysis, have been proposed.[58, 59]

Many synthetic procedures, such as the major part of wet chemical methods, are relatively simple; hence, the researchers often prefer synthesising the nanosized material on their own. This choice allows one to tune the properties of the materials by changing the details of the preparation procedure. On the contrary, procedures based on complex and expensive instrumentation, such as those required to prepare CNTs, force one to buy the nanosized materials on the market. It is worth noticing that for the last 20 years the number of firms commercialising nanomaterials, and the variety of products offered, have increased enormously, following the trend of diffusion of these materials in many applications. The major drawback affecting some of the commercial products, in particular CNTs, lies in the presence of significant amounts of impurities originating from the synthesis. For this reason, different purification protocols have been developed, aiming at obtaining materials characterised by a more exactly defined chemical composition. In particular, the dispersion of CNTs in strong acidic media represents one of the most popular procedures adopted to remove metallic impurities, although a number of defects and a significant shortening of the CNT length have been observed at the end of this chemical treatment.[60]

Sometimes, further treatments are necessary to obtain more efficiently performing materials, following one of the methods previously described. As an example, the highly conductive graphene is generally obtained through (electro) reduction of graphene oxide[61, 62]; the last material, simply prepared by exfoliation of graphite flakes, is stable in water but poorly conductive in absence of (electro) chemical pre-treatments.

17.3 Stability of the Nanosized Materials in Solution

The majority of synthetic procedures previously described, consisting of both top-down and bottom-up approaches, require nanosized materials to be stably dispersed in solution. To this aim, the inorganic core has to be surrounded by an external shell (Fig. 17.3), generally consisting of a more or less ordered and dense organic monolayer. It constitutes the interface between the nano-object and the solution. In the case of a bottom-up approach, it also plays a key role in controlling the growth of the inorganic cores.

The stability of nanosized materials in solution can be predicted on the basis of Derjaguin and Landau, Verwey and Overbeek (DLVO) theory, and relevant extensions.[63] Among the different processes occurring in charge of nano-objects in

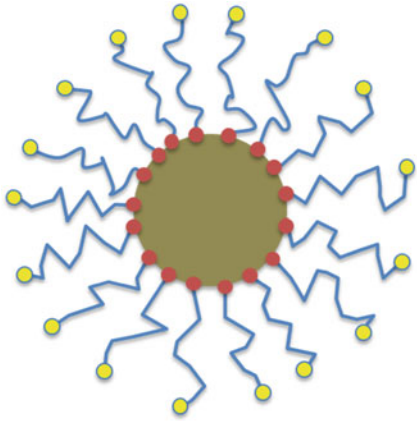

Fig. 17.3 Simplified scheme showing an inorganic core surrounded by an encapsulating shell; the main chemical functionalities of the organic molecules are evidenced. For the sake of simplicity, the case of NPs is reported

solution, it is important to consider that finely divided powder spontaneously tends to reduce the surface/volume ratio, leading to an increase of the dimensions of the cores and ultimately to lose the peculiarities proper of nanomaterials. Two main processes may be operative: aggregation and coalescence.[64, 65] Aggregation consists in the formation of ensembles of nano-objects due to the interaction among the cores or among the encapsulating layers of adjacent nano-objects. After aggregation, the cores still retain their own individuality, so that the properties typical of nanosized materials are preserved. On the other hand, coalescence consists in the formation of nanostructures characterised by a different shape and by core dimensions larger than those of the starting nano-objects, so that they may lose the characteristics of true nanosized materials.

The stable dispersion of nano-objects in solution is generally achieved by exploiting repulsive forces between encapsulating clouds. Different mechanisms can be actually activated[66, 67]:

1. Electrostatic stabilisation (Fig. 17.4a), which takes advantage of electrostatic repulsion among nano-objects, thanks to net positive or negative charges possessed by the capping layer (e.g. citrate or chloride ions surrounding Au NPs or carboxylic groups formed on the surface of CNTs through acid treatment).
2. Steric stabilisation (Fig. 17.4b), which is based on the steric repulsion between the organic layers of neighbouring nano-objects approaching to each other (e.g. alkylthiols or polymers surrounding Au NPs).
3. Electrosteric stabilisation, which implies both the previously described mechanisms (e.g. Au NPs surrounded by ionic surfactants, such as tetraalkylammonium salts: the alkyl chains generate steric repulsion, while the charged head groups induce coulombic repulsion).

Some authors claim that nano-objects can be dispersed in solution without the addition of any encapsulating agent; in this case, the solvent itself acts as the capping agent[56] and the impurities present in the solvent media may play a role in the stabilisation. In addition, the precursors of the nano-objects may release capping species during the synthesis; as an example, Au NPs can be prepared in solution

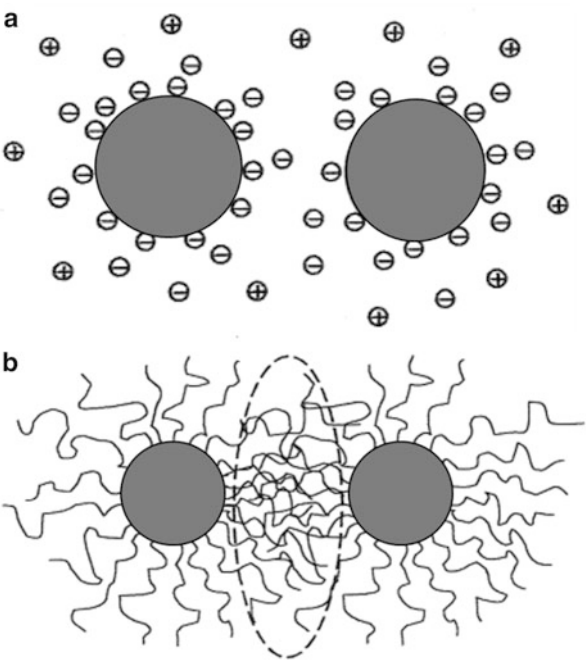

Fig. 17.4 Electrostatic (**a**) and steric (**b**) forces induce stable dispersion of nano-objects in solution. For the sake of simplicity, the case of NPs is reported. Adapted with permission from ref. [66]

Table 17.2 Some examples of encapsulating agents acting on given nanosized particles

Encapsulating agent	Nanomaterials	Reference
Thiols	Au NPs encapsulated by 1-dodecanethiol	69
Amines	Pt NPs encapsulated by 1-dodecylamine	70
Tetraalkylammonium salts	Ni, Cu, and Au NPs encapsulated by tetraoctylammonium bromide	67
Inorganic anions	Au NPs encapsulated by chloride anions	68
Carboxylic acids	Au NPs encapsulated by citrate anions CNTs treated with strong acidic solutions	60, 71
Phosphines	Pd NPs encapsulated by triphenylphosphine	72
Solvent molecules	Ti, Zr, V, Nb and Mn NPs encapsulated by tetrahydrofurane molecules; adsorbed chloride ions can contribute to the stabilisation of the NPs	67

phase without the addition of any additional encapsulating agent, since the precursor, namely $AuCl_4^-$, releases Cl^- anions during the reduction process[68]: Cl^- anions act as labile, though effective, encapsulating species. Some examples of encapsulating agents are reported in Table 17.2.

Alternatively, more or less rigid enclosures acting as templates can be also used. A typical example in electroanalysis is given by the electroless deposition of noble metal nanostructures in polycarbonate membranes.[73] The template can be

subsequently retained in order to keep the nano-objects well separated from each other, e.g. when the aim is to obtain a nano-electrode array. Alternatively, it can be removed, e.g. in order to disperse the nano-objects in solution.

17.4 Reactivity of the Layer of Encapsulating Agent

Since the encapsulating shell constitutes the interface between the inorganic core and the surrounding environment, the properties of the whole nanosized material are strongly conditioned by the chemical nature of the capping species.[74–81] The most important aspects to take into account are:

1. The strength of the interaction between the organic cloud and the inorganic core.
2. The permeability of the organic shell to species in solution.
3. The reactivity of the outermost portion of the organic layer.

In particular, encapsulating agents can be more or less strongly anchored to the core. Strong chemical bonds are generally preferred when specific organic functionalities, acting as the effective site of interaction with the analyte, have to be anchored on the outermost surface of the inorganic core. This is, for instance, the case of DNA strands stably anchored on Au NPs by means of thiol moieties. On the other hand, when well-packed organic layers are formed, the inorganic core results insulated with respect to species in solution. Labile encapsulating agents are generally preferred when the interaction between the analyte and the inorganic core is essential to the effectiveness of the sensing system, e.g. to activate electrocatalytic processes. Moreover, when the synthesis of the nano-objects is part of a more complex process leading to modified electrodes, the use of labile capping molecules is crucial in order to easily substitute them by more strongly adsorbed species. As an example, in the case of the formation of composite materials, the interaction of the core with the second component, e.g. with polymeric chains, is essential in order to reach a stable anchoring.[82, 83] A further application requiring the use of labile encapsulating agents concerns two-step synthetic procedures: in a first step nano-objects encapsulated by a labile surrounding cloud are formed, and in a second step the labile encapsulating system is substituted by more strongly grafted molecules, which represent the final capping agents. As an example, Au NPs surrounded by nucleic acid strands can be prepared through the synthesis of Au cores capped by citrate ions, which are subsequently substituted by DNA[84] or Peptide Nucleic Acid (PNA)[85] molecules.

As already mentioned, the outermost portion of the organic layer conditions the interaction of the nano-objects with the external environment. Organic moieties can induce selective interactions with the analyte in solution; for instance, carboxylic groups on the surface of CNTs form complexes with heavy metals.[86] Alternatively, as it happens in the example reported in Fig. 17.5, specific functional groups can activate chemical reactions leading to the anchorage of a second layer on the outermost portion of the nano-object, which may bear the actual receptors for the

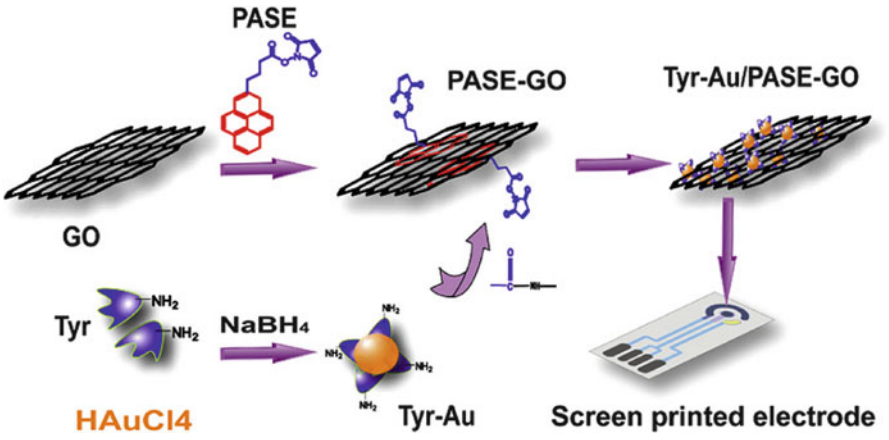

Fig. 17.5 Assembling process of tyrosinase (Tyr) modified Au NPs on chemically functionalysed graphene oxide (GO) sheets, and subsequent deposition onto screen-printed electrodes. Reprinted with permission from ref. [87]

target analyte. On the other hand, the outermost portion of the organic shell can induce stable anchoring of the nano-objects on the electrode surface; this aspect will be detailed in the following.

It is well evident that the investigations on the reactivity of organic molecules anchored on the inorganic core surface are essential to predict the properties of the nanosized materials.[75–79] However, these studies constitute a challenging task: molecules anchored on the surface of nanosized materials exhibit peculiar behaviour with respect to the analogous molecules in solution. One of the most notable examples is the change of the acidity character of the molecules undergoing adsorption, as reported by many authors.[79]

17.5 Multicomponent Nanosized Materials

Many multicomponent materials, conventionally called "hybrids," have been proposed so far, taking advantage of the nature of nanosized materials. Their use is very appealing from a scientific and technological point of view, particularly with respect to catalysis and electrocatalysis, since the properties of these systems often do not derive from the mere sum of those of the single components: in most cases, a synergic action notably improve the performance.[88]

Despite an univocal definition of the term "hybrid" is still missing in the literature, a possible general classification has been reported by Gomez-Romero in the case of bicomponent systems, which represent the most frequently reported materials.[89] Figure 17.6 reports a similar classification scheme, suitably adapted to the nanosized materials that are most commonly reported in electroanalytical applications. Composites constitute a family of hybrid materials that play major

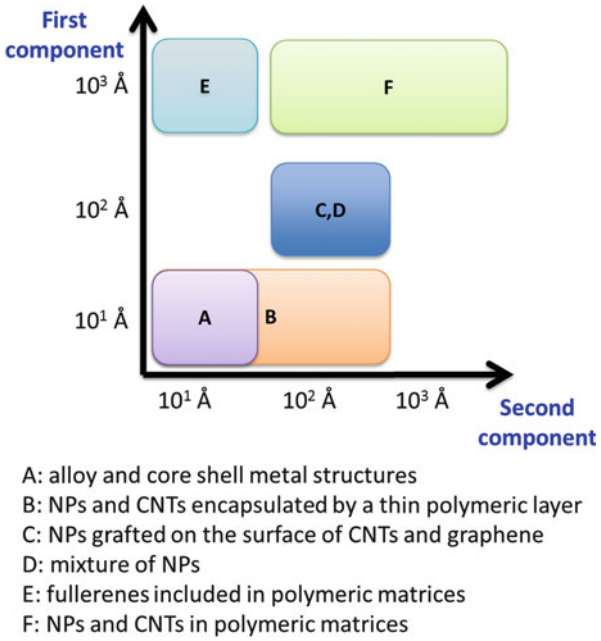

Fig. 17.6 Tentative classification of bicomponent hybrids most commonly reported in electroanalytical applications

role in electroanalysis; according to IUPAC they are defined as «multicomponent materials comprising multiple, different (non-gaseous) phase domains in which at least one type of phase domain is a continuous phase».[90]

Many materials reported in Fig. 17.6 have been widely applied in electroanalysis. Metal NPs deposited on CNTs and conductive polymers including NPs, graphene or CNTs[52, 91–99] constitute typical examples. On the contrary, several quite interesting multicomponent materials (Fig. 17.7a–d)[34, 100, 101] are still poorly investigated in the frame of electroanalysis. In the case of bicomponent materials, they mainly consist of:

a. Alloy structures.
b. Core-shell structures.
c. Small NPs of a first component segregated inside a bicomponent nanostructure; the term "segregation" indicates the formation of small ensembles of atoms of a first component inside shells of a second component, acting as a sort of "adhesive."
d. One component partially segregated on the surface of a nano-object made of a second component.

Similar structures usually consist either of metals or of semiconductors such as in the case of QDs. Although the synthesis of these multicomponent nanosized materials is based on strategies similar to those employed for monocomponent materials, important experimental modifications should be adopted.[34] As an example, in the case of bimetallic nano-objects, if the synthetic procedure starts from the

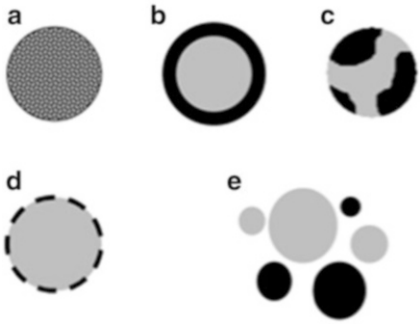

Fig. 17.7 Main bicomponent nanosized materials: alloy (**a**) and core-shell (**b**) structures; segregation of small NPs (**c**) and partial surface segregation (**d**). A mixture of nano-objects possessing different composition is also shown (**e**). For the sake of simplicity the case of NPs is reported

relevant metal salts, the order according to which the components are reduced constitutes the most important synthetic variable. The simplest method lies in the contemporary reduction of two different metal salts. Alternatively, it is possible to perform a two-step reduction: one metal salt is reduced in the first step, forming monocomponent metal nanostructures and the second metal salt is reduced in a following step, generating a coating on the surface of the first metal. It is worthy to note that some authors[102] report that intimate contact between structures possessing different composition, possessed by mixtures of different nanosized materials (Fig. 17.7e), may lead to properties very similar to those of the relevant alloys.

17.6 Grafting the Nanosized Materials on a Substrate

The grafting of nanosized materials onto a substrate is a very important topic for practical applications,[103] also including electroanalysis. The deposition procedure should be carefully chosen and controlled, aiming at conferring the surface the properties sought. In particular, the morphology of the resulting nanostructure, the access of species in solution to the inorganic cores and the spatial arrangement of the nano-objects on the electrode surface constitute the most important aspects to take into account in choosing the most suitable deposition approach to adopt.

Due to many constrains previously discussed when dealing with the preparation of nano-objects, these are generally synthesised in advance with respect to the anchoring on the surface. In this respect, the main strategies reported in the literature consist of grafting pre-synthesised nano-objects through a monolayer or a thicker film, i.e. in the form of a hybrid material. Alternatively, the synthesis and the deposition can be carried out concomitantly; as an example, metal and metal oxide nanostructures can be obtained through electrodeposition of the relevant precursors.

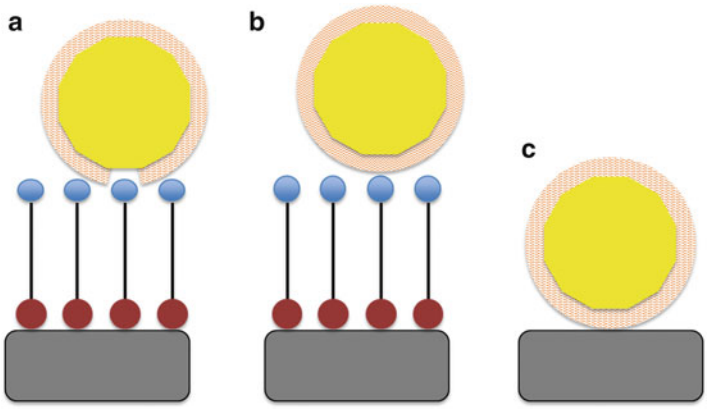

Fig. 17.8 Some deposition strategies followed in the deposition of nano-objects onto electrode surfaces through monolayers. For the sake of simplicity, the case of an ordered monolayer is shown

17.6.1 Grafting of Pre-formed Nano-objects Through Monolayers

Pre-synthesised nano-objects can be deposited onto electrode substrates through a more or less ordered monomolecular organic layer, possessing a thickness up to few nanometres.[74, 75, 81] The main strategies reported in the literature are schematised in Fig. 17.8.[104, 105]

Monolayers suitable to anchor nano-objects on electrode surfaces are based on organic species possessing two functional groups. The groups at the outermost portion of the monolayer can form strong chemical bonds either with the inorganic core (Fig. 17.8a) or with the capping organic layer (Fig. 17.8b); typical examples are thiols or amines for the grafting of noble metal NP cores, or carboxylic acids for the anchoring of amine functionalised CNTs or NPs. The portion of the molecules located between the two functional groups affects the charge transmission through the electrode coating and conditions the final structure and stability of the monolayer. It is evident that the chemical and physical properties of such a thin film can be widely tuned by changing the chemical composition of the organic molecule forming the monolayer.[1–8, 106]

Self-Assembled Monolayers (SAMs) actually constitute peculiar cases of monolayers[1–8] consisting of adsorbed or covalently anchored molecules on a substrate surface, that undergo a self-organisation process: after adsorption on the substrate, the final structure of the SAM consists of a packed well-ordered thin film. Hence, the relation between the properties of the coating and its structure can be established. Unfortunately, the term "SAM" is sometimes used also to indicate what is actually a disordered monolayer, so that misleading information can be extracted from the literature.

Organosulfur compounds represent the most common class of molecules exploited for formation of monolayers.[1–8] Among the possible systems, the most extensively studied ones are based on thiols adsorbed on Au.

When considering electroanalytical applications, monolayer depositions are commonly prepared in liquid phase, by simply dipping the substrate into a dilute solution of the organic molecules, in the millimolar concentration range.

A peculiar case consists of deposition of nano-objects by exploiting the organic shell surrounding the inorganic core; in this case, a functional group suitable to achieve direct anchoring of the nano-object on a bare substrate should be present in the outermost portion of the encapsulating cloud (Fig. 17.8c).

17.6.2 Grafting of Pre-formed Nano-Objects in the Form of a Hybrid Material

Hybrid materials can be synthesised in solution and subsequently deposited on electrode surfaces, as in the case reported in Fig. 17.5. In many cases, the deposition is simply carried out by means of drop casting, even though more complex procedures can be adopted. Alternatively, the deposition of nano-objects on the electrode surface may require the formation of a hybrid material on the substrate. At variance with the grafting through monolayers, thicker films are generally obtained in this case.

Since a precise classification of the different preparation methods is not straightforward,[97, 99] only some of the most important deposition methods exploited in electroanalysis are listed in Table 17.3.

In most cases, the stable anchoring of nano-objects on electrode surfaces is achieved thanks to inclusion in an organic matrix. It can simply act as a support for the nano-objects or improve the performances of the sensing system taking advantage of synergic effects. When the organic matrix possesses an insulating nature, the amount of conducting nanosized materials included has to be suitably chosen in order to exceed the charge percolation threshold; on the other hand, in case of conducting matrices the fraction of nano-objects can be varied in a wider range.

17.6.3 Concurrent Synthesis and Deposition of Nano-Objects

A number of procedures allow the contemporary formation of metal and metal oxide nano-objects and their deposition onto electrode surfaces.[117–120] In the case of metal nanostructures, the processes involve chemical or cathodic reduction of the relevant metal salts (Fig. 17.9).

Table 17.3 Most important methods used to graft nano-objects on electrode surfaces leading to formation of hybrid materials

Method	Example	Reference
Dispersion of nano-objects and polymers in solution and subsequent deposition by means of drop casting or spin coating	Ag NPs encapsulated by hexadecyl ammine mixed with poly (3-hexylthiophene) in chloroform	[107]
	Single wall CNTs mixed with polyaniline in *N*-methyl-2-pyrrolidinone	[108]
Inclusion in sol-gel	Embedding of Au NPs encapsulated by citrate ions in a (3-mercatopropyl)-3-methoxysilane sol	[109]
Electrogeneration of polymers on a substrate in the presence of nanostructures	Inclusion of Au NPs encapsulated by *N*-dodecyl-*N*,*N*-dimethyl-3-ammonium-1-propanesulphonate during the electrogeneration of poly (3,4-ethylenedioxythiophene) films	[110]
Chemical synthesis of a soluble polymer in the presence of nano-objects and subsequent deposition by means of drop casting or spin coating	Chemical polymerisation of pyrrole in the presence of CNTs in acidic aqueous solution containing an oxidising species, namely persulphate ions	[111]
Adsorption of nano-objects on a preformed polymeric film	Au NPs encapsulated by tetraoctylammonium bromide adsorbed on poly (3,4-ethylenedioxythiophene) film surface	[112]
Layer-by-layer deposition	Alternate deposition of anionic Au NPs encapsulated by 11-mercaptoundecanonate and a cationic polythiophene	[113, 114]
Langmuir-Blodgett and Langmuir-Schaeffer deposition	Co-deposition of poly (3-hexylthiophene) and Au NPs encapsulated by dodecanethiol	[115, 116]

Nanostructures deposition can be carried out on bare substrates (Fig. 17.9a) or on polymeric films pre-synthesised on electrode surfaces (Fig. 17.9b). Alternatively, the formation of the nano-objects and of the polymer matrix can occur concurrently on the electrode surface (Fig. 17.9c); in this case, the relevant monomer molecules can constitute the reducing agent. The presence of the monomeric precursor or of the already synthesised polymeric component during the formation of the nano-objects may lower the extent of aggregation: the organic chains may act as seeds for the formation of nanostructures or as encapsulating agents.

As to metal oxide nanostructures, a number of different procedures have been proposed. The most adopted one consists in the variation of the pH value in the close proximity of the electrode surface, induced by an electrochemical process; the local increment of the pH value leads to precipitation of oxide/hydroxide species onto the electrode surface.[121]

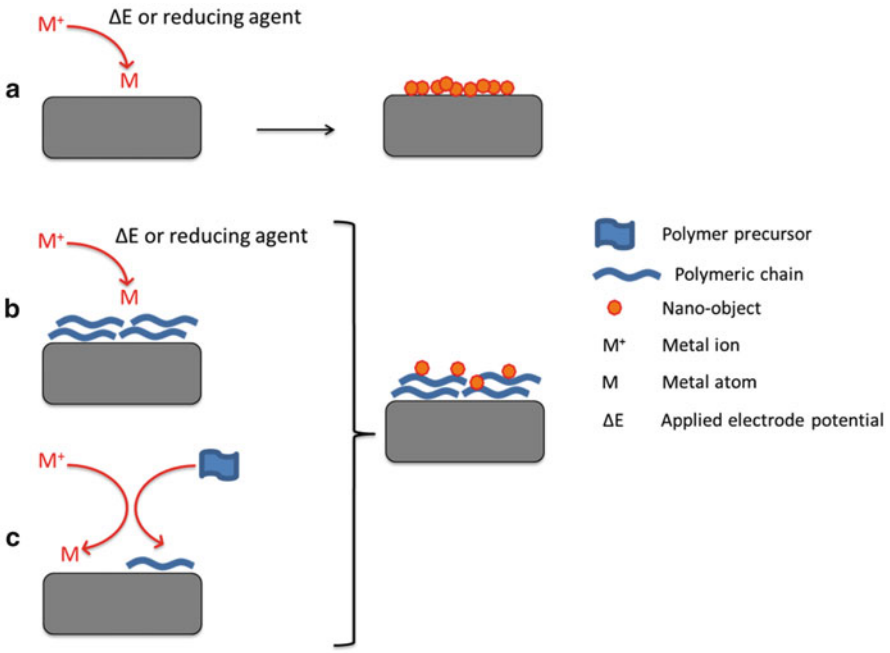

Fig. 17.9 Formation of metal nanostructures on surfaces, through different reduction processes of the relevant metal salts

The synthesis of nano-objects concurrent to their deposition onto electrode surface allows the formation of nanostructured surfaces in a very rapid and easy way, without the addition to the solution of any other chemical species, except for the supporting electrolyte or the reducing agent. However, although many authors claim that the size of the resulting nanostructure can be controlled by suitable choice of the deposition parameters, the size distribution of the obtained nanostructures is generally quite broad.

17.7 Electroanalytical Applications of Nanosized Materials

As already mentioned, many amperometric sensors have been developed with one or more of the nanosized materials previously described.[1–32] In the following sections, we will try to highlight how the performances of many amperometric sensors, in terms of sensitivity, limit of detection and selectivity, can be significantly improved by the use of materials under the different "nano" forms, critically analysing systems that are most often encountered in environmental context.

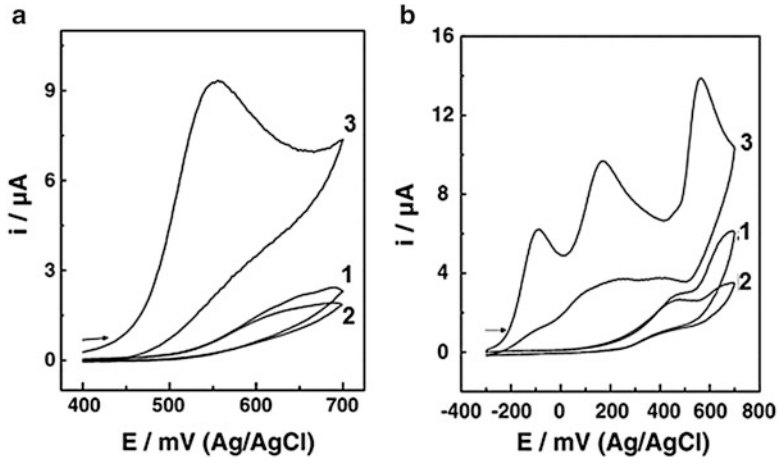

Fig. 17.10 Cyclic voltammograms recorded on 0.25 mM NO_2^-, 0.1 M phosphate buffer solution (pH 7.2) in the absence (**a**) and in the presence (**b**) of 0.25 mM N_2H_4 and SO_3^{2-}. The responses collected at bare (**1**), sol-gel (**2**) and sol-gel/Au NPs (**3**) modified glassy carbon electrodes are reported; 0.02 V s^{-1} scan rate. Adapted with permission from ref. [122]

17.7.1 Nanosized Materials in Electrocatalytic Reactions

Many species of interest in the environmental monitoring are electroactive, e.g. NO_2^-, NO_3^-, (poly)phenols and nitroaromatic derivatives. However, a number of drawbacks limit the use of bare conventional electrodes in the determination of these species by means of amperometric sensors: (1) evident electrode fouling, mainly due to products of the electrochemical reaction, (2) low selectivity, due to overlapping of electrochemical signals coming from different species in solution, (3) scarce sensitivity that often raises the limit of detection. Finally, it should be noticed that there are situations in which the overpotential involved in the charge transfer in charge of the analyte is so high that the relevant signal is overlapped to the solvent discharge. In many similar cases, the properties of nanosized materials allow the amperometric sensors to exhibit performances considerably superior with respect to those of bare electrodes. Indeed, nanostructured surfaces induce peculiar interaction with the analyte in solution, finally leading to voltammetric responses usually located at less extreme potential values and characterised by higher and sharper current peaks and by higher repeatability (Fig. 17.10).

The general term "electrocatalysis" is many times invoked to give account for the peculiar behaviour of nanostructured surfaces with respect to bare ones. Due to the character of these electrode materials, electrocatalysis is meant here to refer to a lowering of the activation energy of the charge transfer, rather than to the involvement of a redox mediator. However, a clear definition of the mechanisms involved in the analyte/surface interaction is often challenging. The frequent occurrence of complex electrode mechanisms and the necessity to complement electrochemical investigations with microscopic and spectroscopic studies constitute main constrains

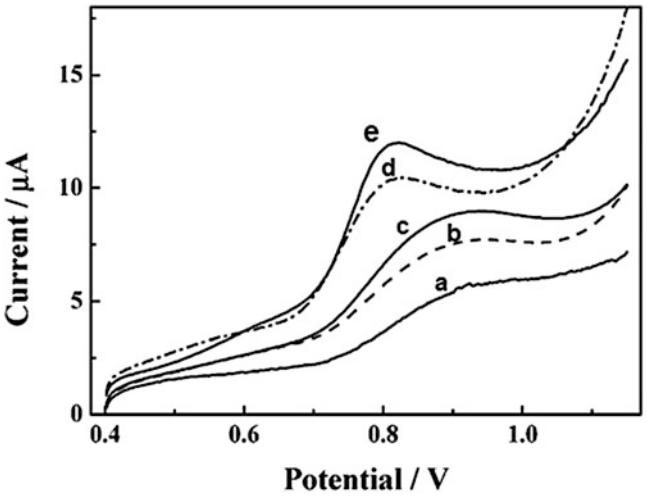

Fig. 17.11 Linear sweep voltammograms recorded at modified glassy carbon electrodes in 5.0 nM NO_2^-, 0.1 M phosphate buffer solution; 0.1 V s^{-1}. Different electrode coatings have been considered: CNTs (**a**), CNTs-Chit (**b**), $OMIMPF_6$-CNT-Chi (**c**), ($OMIMPF_6$-CNT) gel (**d**), ($OMIMPF_6$-CNT) gel-Chi (**e**). (*Chit* chitosan, *OMIMPF*$_6$ 1-octyl-3-methylimidazolium hexafluorophosphate). Adapted with permission from ref. (124)

in preventing from a precise definition of the system. Some clues can be extrapolated from electrocatalytic studies carried out in the frame of investigations on fuel cells. In particular, it has been proved that the electro-oxidation of different species, such as alcohols and carbohydrates on the surface of noble metals takes advantage of the formation of surface hydrated oxides.[123]

In the case of nanosized materials, electrocatalytic properties may arise from a combination of many different peculiarities. They mainly take origin from the presence of a number of atoms possessing a low coordination number, localised in correspondence of vertexes and corners of the nano-objects. This may induce significant decrease of the overpotential involved in charge transfer processes of the target analyte, leading to voltammetric signals significantly different with respect to those recorded at bare electrode surfaces.

The comprehension of the mechanisms involved in surface/analyte interaction becomes even more challenging when the performances of the sensor can take advantage of co-catalytic effects arising from the formation of a hybrid material. In these cases, the electrode coatings may exhibit electro-catalytic performances superior to those of the two single components, so that electrochemical processes involving the analyte occur at less extreme potential values (Fig. 17.11). However, only few papers have studied the mechanisms involved in electro co-catalysis.

Besides electrocatalysis, different effects also need to be taken into account to explain the improvement of sensor sensitivity when using nanosized materials, e.g. the increase of electroactive surface area and the reduced fouling. As a matter of fact, although only very rarely considered, electrode fouling broadens

the voltammetric peaks as a consequence of the progressive modification of the electroactive sites during the voltammetric scan; in this respect, antifouling effects induced by the nanostructured surface not only result in more repeatable signals, but also in sharper peaks.

17.7.2 Nanosized Materials in Stripping Voltammetric Techniques

As described in Chap. 10, sect. 10.4.6, the term "stripping voltammetry" refers to a series of electrochemical techniques based on a two-step procedure involving (1) pre-concentration of the analyte at the electrode surface and (2) potential sweep, according to different possible waveforms, inducing analyte re-dissolution. In particular, anodic stripping voltammetry constitutes the electrochemical technique of choice for the detection of heavy metals at the trace level. Although this analysis has constituted one of the oldest applications of electrochemistry in analytical chemistry, it still represents an open problem in the environmental control. The main advantage arising from the use of nanostructured surfaces should be ascribed to the notable increase of the electroactive area, which induces a higher amount of analyte molecules to be pre-concentrated on the electrode surface (Fig. 17.12); this aspect positively affects both the sensitivity and the detection limit of the analysis.

Moreover, sharp voltammetric peaks are generally recorded when using nanostructured electrode coatings, resulting in resolution of signals of different metals in solution and further increase of peak heights. In this respect, the differences between bare and nanostructured surfaces are supposed to be due to a different interaction of the resulting zero-valence metals with the electrode surface: the presence of atoms possessing a low coordination number in the nanostructured surface may induce less strong chemical interactions, favouring the stripping step.

Among the different nanostructured surfaces proposed for such an application,[11] those based on Bi and Sb represent good alternatives to Hg. Noble metal NPs are also widely used, especially for As and Hg determination, due to the affinity of these materials for the zero-valence metals.

Many amperometric sensors developed for heavy metal quantification are based on carbon nanostructured surfaces, mainly consisting of CNTs and graphene. The interaction of these nanosized materials with the analytes involves carboxyl groups localised in correspondence to the defects of the nanostructure. However, the possible involvement of metal impurities normally present in CNTs, as well as the capability of sp^2 hybridised carbon sites to adsorb species from the solution, should be also taken into account. On the other hand, the adsorption of many organic and inorganic species present in the solution constitutes the main drawback that limits the actual applications of carbon-based electrode materials in real matrices. Some strategies have been proposed to reduce this effect, e.g. the

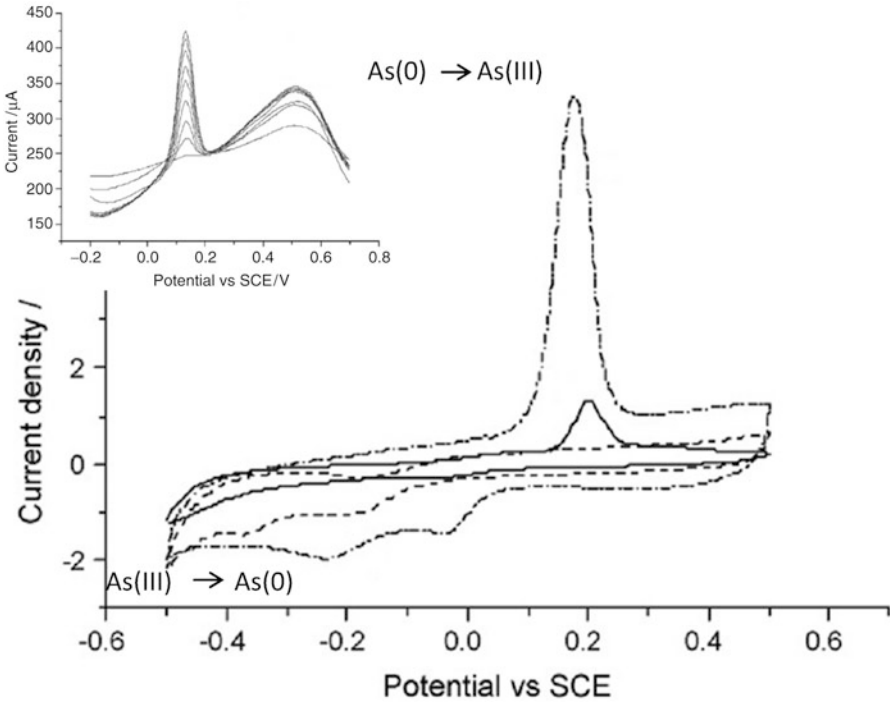

Fig. 17.12 Cyclic voltammetric responses of 0.5 mM As(III) in 0.1 M HCl at bare Au electrode (*solid line*), at CNTs (*dashed line*) and at Au NPs/CNTs (*dash dotted line*) modified glassy carbon electrodes; 0.1 V s^{-1} potential scan rate. Inset reports square wave anodic stripping voltammetric responses in 10–70 nM As(III) solutions (pre-deposition: −0.4 V vs. SCE for 120 s; stripping: $f = 50$ Hz, $E_{sw} = 20$ mV, $\Delta E_s = 2$ mV). Adapted with permission from ref. (125)

deposition of CNTs on a Nafion coating acting as an electrostatic filter. A step forward in this direction is represented by the use of hybrid materials consisting of metal NPs supported on CNTs.[126] Electrodes consisting of similar hybrids take advantage of (1) the enormous enlargement of the electroactive surface area induced by the use of CNTs and (2) the electrocatalytic properties of metal NPs; the presence of this component at the solution/electrode interface limits the adsorption of interfering organic species at the CNT surfaces.

The strong adsorption of organic molecules occurring at carbon surfaces can be exploited to improve the sensitivity of the sensor response toward several organic species: analytes can be pre-concentrated at carbon nanostructured surfaces in advance to the actual voltammetric detection, following an approach very similar to Solid Phase MicroExtraction (SPME). This analytical procedure, called "Adsorptive Stripping Voltammetry" (AdSV) has been applied for the detection of electroactive species of interest in the environmental field, such as herbicides[127] or nitro-derivatives.[128] Thanks to the occurrence of mechanisms similar to those

described in the previous section, voltammetric peaks often result very sharp and located at less extreme potentials.

Independently of the stripping strategy adopted, the selectivity of the sensor can be enhanced by the functionalization of the nanosized material with organic moieties, which induce selective adsorption of the target analyte. As an example, this strategy has been widely exploited for the analysis of heavy metals[11] by stably fixing carboxylic, amino or thiol groups on the surface of the inorganic core.

As it is well evident from the mechanisms described, the proper choice of morphology of the nanostructured surface plays a key role in defining the properties of the sensor. As a general consideration, electroactive surfaces possessing as high as possible roughness are generally preferred, in order to increase the sensor sensitivity. To such a purpose, pre-synthesised nano-objects are generally linked to the underlying electrode surface by means of organic[83] or inorganic[129] polymeric films: when compared to monolayers, the porous polymer binder allows a higher number of nano-objects to be finally present at the electrode/solution interface. Moreover, this second component can also play an active role in the electrochemical process involving the analyte, so that a synergic effect between the two components can be finally invoked.

As already cited, metal nanostructured surfaces characterised by a high surface/volume ratio can be also obtained by electrochemical approaches.

17.7.3 Nanosized Materials in Bio-Catalytic Sensors

The selectivity of many amperometric sensors takes advantage of the involvement of a biological element. When considering the environmental monitoring, several chemical species are detected through the use of bio-catalytic sensors, i.e. sensors requiring the mediation of a specific enzyme; a few examples include phenol-pesticides by means of tyrosinase, nitrate by means of nitrate reductase and organophosphorous-pesticide by inhibition of acetyl cholinesterase. Furthermore, redox active proteins can also be involved, such as in the case of haemoglobin in the catalytic reduction of nitrite.

The advantages arising from the use of a biological element also include the possibility to reach very low detection limits.

The co-presence of nanosized materials in these electrode coatings appears promising to further improve the performances of bio-catalytic sensors. The advantages are not merely related to the possibility of significantly increasing the number of biological receptors at the solution/electrode interface. Two further important properties of nanosized materials, in fact, can positively affect the performances of these biosensors, namely their nano dimension and their electrocatalytic properties.

The nano dimension of the material allows the enzyme to adapt its three-dimensional configuration to the morphology of the underlying nanostructure, without undergoing protein denaturation. This process induces an intimate contact between the nano-objects fixed at the electrode surface and the redox active sites of

the enzyme, often located well inside the protein. Nano-objects finally act as electrical bridges providing effective charge transfer between the substrate transducer and the bio-receptor; hence, the addition of a suitable redox mediator in solution is unnecessary. As a direct consequence the charge transfer rate is not limited by the diffusion of the redox mediator to the electrode surface and unaffected by ohmic drops due to the insulating nature of the polypeptide shell surrounding the active site of the enzyme.

Several bio-catalytic sensors take advantage of the electrocatalytic properties of the nanosized materials previously underlined. This aspect is particularly meaningful for enzymes requiring the presence of NAD^+ as the cofactor or leading to H_2O_2 production: as previously highlighted, the use of nanostructured surfaces allows the detection of the analyte at less extreme potential values, and leads to voltammetric peaks characterised by higher repeatability and leading to high sensitivity detection.

Among different nanosized materials, Au NPs and CNTs are most widely used to obtain stable anchoring of proteins on electrode surfaces. The strategy most frequently adopted consists in the formation of amide bonds between amino groups of the peptide chains and carboxylic groups in the outermost portion of the nanosized material. Alternatively, deposition procedures can be based on electrostatic attraction between positively or negatively charged encapsulating shells and enzymes possessing opposite charge, as a function of the relevant isoelectric point and of the solution pH value. This last deposition process can be also reiterated in a so-called layer-by-layer deposition technique, to increase the number of biological element on the electrode surface. Due to the hydrophilic nature of the deposit, even proteins in the internal part of the coating are in close contact with the solution, so that interactions between the biological element and the analyte are well possible.

17.7.4 Nanosized Materials in Affinity Biosensors

Affinity biosensors, namely genosensors, immunosensors and aptasensors, can be suitably developed to quantify the amount of many biohazard agents in environment. The list of the species possibly detectable by one of these sensor systems is quite wide. It ranges from simple chemical species, e.g. heavy metal ions,[130] to more complex pathogenic microorganisms.[131]

Many sensor systems take advantage of the stable deposition of bio-receptors on nanostructured surfaces. Although many papers simply ascribe the improvement of the sensor sensitivity to the higher amount of biological elements that can be anchored on such a surface, only a few papers discuss the correlation between sensor performances and morphology of the nanostructure.[132–134] The authors conclude that the marked curvature of NPs affects the spatial disposition of bio-receptor molecules on the surface, inducing a poorly packed structure that facilitates the access of the complementary bio-molecule to form the receptor-analyte adduct. This result indicates that the careful control of the substrate morphology constitutes the basis for the obtainment of particularly sensitive sensors.

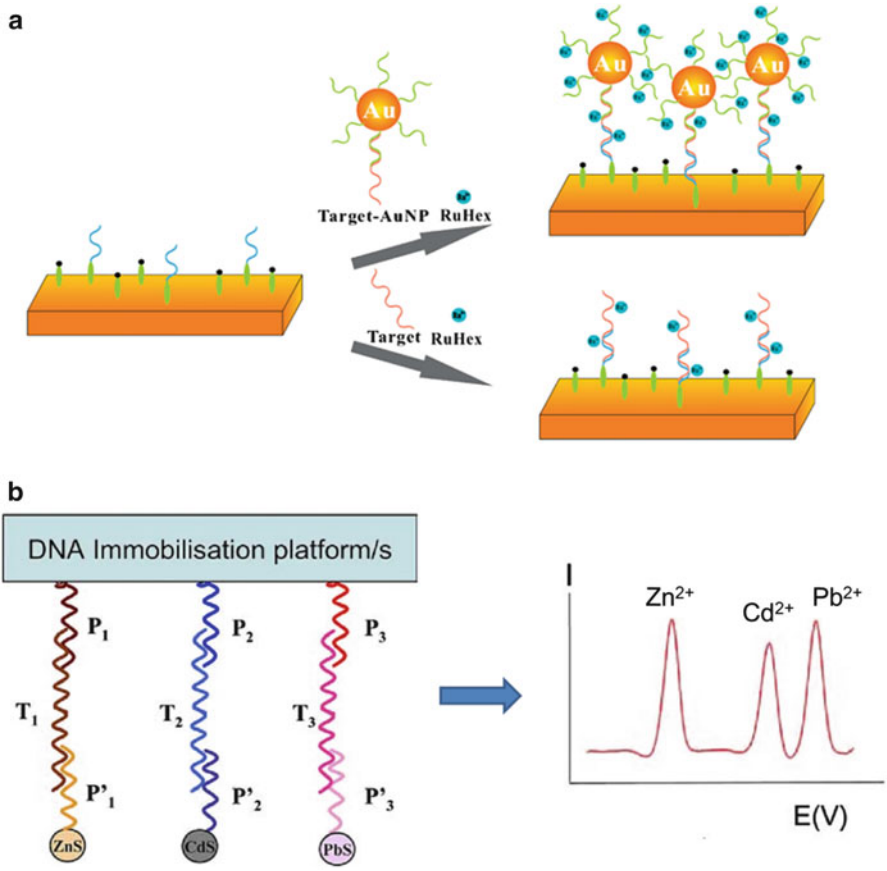

Fig. 17.13 Schematic representation of two strategies involving nanosized materials in genosensors. (**a**) Amplified detection of DNA by means of Au NPs functionalised with the complementary oligonucleotide sequence. The anchoring of DNA on the electrode surface is detected by exploiting a positively charged redox probe, namely $[Ru(NH_3)_6]^{3+}$, interacting with negatively charged phosphoric groups of DNA. A higher amount of electroactive species is present in the close proximity of the electrode surface when using NP functionalised strands. Adapted with permission from ref. (135). (**b**) Multiple detection of three DNA sequences by means of labelling with different QDs, namely ZnS, CdS, and PbS; after hybridisation, QDs are dissolved and the relevant metal ions are quantified by anodic stripping voltammetry. Adapted with permission from ref. (31)

The performance of affinity sensors can be also improved by the involvement of nanosized materials, in particular Au NPs and QDs, acting as labels for the actual formation of the receptor-analyte adduct. Actually, the amperometric signal of many affinity sensors derives from an electrochemical process directly involving the analyte. Most often, redox active species need being added in solution and many different strategies can be adopted to indirectly collect the amperometric signal. Among the many different approaches proposed in the literature that involve

nanosized materials, Fig. 17.13 reports only a couple of examples, trying to show the main advantages arising from the use of nanosized tags. For the sake of simplicity, the case of genosensors is reported; similar strategies can be also exploited in different affinity sensors.

17.8 Characterisation of the Nanosized Materials

As it is well evident from the description of electroanalytical applications of nanosized materials, the strict control of the chemical composition, size and shape of the nanostructured coating is of primary importance for the obtainment of a sensor possessing the properties sought. To such a purpose, the use of a number of characterisation techniques is fundamental in order to establish precise relationships between the properties of the material and its structure. The most important investigative approaches are based on microscopic, spectroscopic and electrochemical techniques.[136]

As to microscopic techniques, TEM and SEM play a key role in the definition of the size of the nano-objects and of the morphology of the nanostructures on the electrode surface. Scanning probe microscopic techniques include a number of different experimental setups that can also give important morphological information. Atomic Force Microscopy (AFM) constitutes the most popular experimental setup, although a number of different scanning probe configurations are nowadays possible in order to obtain additional information concerning composition, electrical conductivity, optical and mechanical properties; they include conducting AFM, phase imaging AFM, Kelvin probe microscopy, electric force microscopy, scanning near field optical microscopy and photocurrent imaging.[136, 137]

As to spectroscopic techniques, Energy Dispersive Spectroscopy (EDS) is usually coupled with electron microscopies, aiming at determining qualitative and quantitative composition of the nanostructures on the surfaces. To this same aim, photoemission spectroscopy and vibrational spectroscopies, in particular IR absorption and Raman scattering, are also very popular.[136, 137]

As to purely electrochemical techniques, also "simple" voltammetric techniques in the presence of reversible redox couples in solution can give a clear indication of the actual deposition of the nanostructure on the electrode surface and of the effects on the charge transfer resistance. This information can be complemented by impedance spectroscopy (EIS) investigations, which evidence changes in charge transfer process at the electrode/solution interface before and after electrode modification.

Although the major part of the reported instrumental investigations are carried out in the dry state, in the frame of amperometric sensing the most proper characterisation setup should allow the analysis of the electrode coating in the solution phase and under polarisation at given potential values. To this aim, microscopic and spectroscopic techniques should be coupled to electrochemical ones[138]; the most meaningful examples include AFM[137, 139] and absorption spectroscopies in the UV-

Vis-NIR and IR spectral ranges.[136, 137] The main problem that limits the diffusion of these hyphenated techniques consists of the time resolution required to follow evolving electrochemical systems in real time.

A number of attempts have been also carried out to characterise these electrode coatings by coupling optical and microscopic techniques. As an example, optical spectroscopic techniques coupled to microscopes can be used to perform hyperspectral imaging, easily reaching a resolution down to few tens of microns.

Some of the previously described techniques, such as TEM and photoemission spectroscopy, require to be carried out in vacuum; this environment may introduce artefacts due to the complete desolvation of the electrode coating. Luckily, some modern experimental setups, such as environmental SEM, allow the characterisation of samples at relatively high pressure values.

17.9 Conclusions and Perspectives

As pointed out in the Introduction section, the number of literature reports dealing with nanostructures in amperometric sensing is increasing rapidly. In many cases, the nanosized materials involved and techniques proposed for their deposition onto electrode surfaces are actually variants of already known systems. On the contrary, some of the more innovative experimental approaches are so complex to be realised or require so much expensive instrumentation that they are very rarely adopted. Moreover, novel systems, such as multimetallic nano-objects and some multicomponent composite materials, are still poorly investigated. In addition, some nano-objects developed in the frame of different contexts, e.g. organic electronics and catalysis, could be exploited in amperometric sensors.

Some of the most popular nano-objects, e.g. Au NPs encapsulated by thiol molecules or citrate ions, can be synthesised in the laboratory, even in large quantity. Actually, the possibility to employ commercial products is often one of the most important factors in conditioning the popularity of some nano-objects; as an example, it is undoubted that the number of applications involving CNTs are significantly higher with respect to those involving non-commercial carbon nanostructures. Difficult or even impossible access on the market constitutes an even worse obstacle when nano-objects suitably functionalised with organic moieties are required: custom syntheses are usually time-consuming and not trivial at all. Fortunately, the number of different commercial precursors for the preparation of the nano-objects and for their grafting is continuously increasing.

Computational analyses of the responses are also very challenging and rare in the case of amperometric sensing on modified electrodes, due to the complexity of most of the systems. The superior performances of new computers will possibly allow unprecedented simulations; in the case of composites based on nano-sized materials, studies of the diffusion to micro- and nano-electrode systems may be exploited.[140] Similarly, calculations regarding the reaction mechanisms based on

Density Functional Theory (DFT) have been exploited to give a rational to the performance of different electrocatalysts.[141]

As to characterisation techniques, recent advances in electronics and software lead to a continuous increase of both spatial and time resolution. Some experimental setups that were impossible to realise few years ago are now well possible and even diffused. Nevertheless, the correlation between the performance of sensing systems and the nature of the electrode coating is often poorly investigated; in particular, systematic investigations on key aspects of the nanomaterials, such as the influence of the size and shape on electrochemical properties, are lacking. Furthermore, precise reaction mechanisms of the different analytes are almost always unknown. It is worth noticing that combinatorial approaches, which can give a rationale to the structure–properties relationship, are very rare in amperometric sensing.[142]

The combination of different analytical techniques will allow the development of novel approaches to sensing. In particular, the coupling between optics and electrochemistry seems to be very promising. In this respect, only few examples of light addressable electrodes and photoelectrochemical sensors have been reported.[143, 144] Finally, increase of the sensitivity of the sensing system has been achieved by irradiating the electrochemical cell with microwaves or ultrasounds.[145–147]

In conclusion, it is well evident from what discussed in this chapter that, despite the enormous scientific activity concerning nano-sized materials, there is still wide room to exploit at best their properties in electroanalysis.

References

1. Perez-Lopez B, Merkoci A (2012) Carbon nanotubes and graphene in analytical sciences. Microchim Acta 179:1–16
2. Bigall NC, Parak WJ, Dorfs D (2012) Fluorescent, magnetic and plasmonic–hybrid multifunctional colloidal nano objects. Nano Today 7:282–296
3. Guo S, Wang E (2011) Noble metal nanomaterials: controllable synthesis and application in fuel cells and analytical sensors. Nano Today 6:240–264
4. Bera D, Qian L, Tseng TK, Holloway PH (2010) Quantum dots and their multimodal applications: a review. Materials 3:2260–2345
5. Huang XJ, Choi YK (2007) Chemical sensors based on nanostructured materials. Sens Act B 122:659–671
6. Wieckowski A, Savinova ER, Vayenas CG (2003) Catalysis and electrocatalysis at nanoparticle surface. Marcel Dekker, New York, USA
7. Wu S, He Q, Tan C, Wang Y, Zhang H (2013) Graphene-based electrochemical sensors. Small 9:1160–1172
8. Dey RS, Bera RK, Raj CR (2013) Nanomaterial-based functional scaffolds for amperometric sensing of bioanalytes. Anal Bioanal Chem 405:3431–3448
9. Kochmann S, Hirsch T, Wolfbeis OS (2012) Graphenes in chemical sensors and biosensors. Trends Anal Chem 39:87–113
10. Su S, Wu W, Gao J, Lu J, Fan C (2012) Nanomaterials-based sensors for applications in environmental monitoring. J Mater Chem 22:18101–18110

11. Aragay G, Merkoçi A (2012) Nanomaterials application in electrochemical detection of heavy metals. Electrochim Acta 84:49–61
12. Chen D, Feng H, Li J (2012) Graphene oxide: preparation, functionalization, and electrochemical applications. Chem Rev 112:6027–6053
13. Saha K, Agasti SS, Kim C, Li X, Rotello VM (2012) Gold nanoparticles in chemical and biological sensing. Chem Rev 112:2739–2779
14. Marin S, Merkoçi A (2012) Nanomaterials based electrochemical sensing applications for safety and security. Electroanalysis 24:459–469
15. Aragay G, Pino F, Merkoci A (2012) Nanomaterials for sensing and destroying pesticides. Chem Rev 112:5317–5338
16. Zhang J, Li CM (2012) Nanoporous metals: fabrication strategies and advanced electrochemical applications in catalysis, sensing and energy systems. Chem Soc Rev 41:7016–7031
17. Katz E, Willner I, Wang J (2004) Electroanalytical and bioelectroanalytical systems based on metal and semiconductor nanoparticles. Electroanalysis 16:19–44
18. Siangproh W, Dungchai W, Rattanarat P, Chailapakul O (2011) Nanoparticle-based electrochemical detection in conventional and miniaturized systems and their bioanalytical applications: a review. Anal Chim Acta 690:10–25
19. Rassaei L, Marken F, Sillanpaa M, Amiri M, Cirtiu CM, Sillanpaa M (2011) Nanoparticles in electrochemical sensors for environmental monitoring. Trends Anal Chem 30:1704–1715
20. Campbell FW, Compton RG (2010) The use of nanoparticles in electroanalysis: an updated review. Anal Bioanal Chem 396:241–259
21. Chen D, Tang L, Li J (2010) Graphene-based materials in electrochemistry. Chem Soc Rev 39:3157–3180
22. Shao Y, Wang J, Wu H, Liu J, Aksay IA, Lina Y (2010) Graphene based electrochemical sensors and biosensors: a review. Electroanalysis 22:1027–1036
23. Li H, Liu S, Dai Z, Bao J, Yang X (2009) Applications of nanomaterials in electrochemical enzyme biosensors. Sensors 9:8547–8561
24. Xiao Y, Li CM (2008) Nanocomposites: from fabrications to electrochemical bioapplications. Electroanalysis 20:648–662
25. Wang J, Lin Y (2008) Functionalized carbon nanotubes and nanofibers for biosensing applications. Trends Anal Chem 27:619–626
26. de la Escosura-Muñiz A, Ambrosi A, Merkoçi A (2008) Electrochemical analysis with nanoparticle-based biosystems. Trends Anal Chem 27:568–584
27. Guo S, Wang E (2007) Synthesis and electrochemical applications of gold nanoparticles. Anal Chim Acta 598:181–192
28. Welch CM, Compton RG (2006) The use of nanoparticles in electroanalysis: a review. Anal Bioanal Chem 384:601–619
29. Balasubramanian K, Burghard M (2006) Biosensors based on carbon nanotubes. Anal Bioanal Chem 385:452–468
30. Wang J (2005) Carbon-nanotube based electrochemical biosensors: a review. Electroanalysis 17:7–14
31. Merkoçi A, Aldavert M, Markín S, Alegret S (2005) New materials for electrochemical sensing V: nanoparticles for DNA labelling. Trends Anal Chem 24:341–349
32. Zen JM, Kumar AS, Tsai DM (2003) Recent updates of chemically modified electrodes in analytical chemistry. Electroanalysis 15:1073–1087
33. Pokropivny VV, Skorokhod VV (2007) Classification of nanostructures by dimensionality and concept of surface forms engineering in nanomaterial science. Mater Sci Eng C 27:990–993
34. Toshima N, Yonezawa T (1998) Bimetallic nanoparticles-novel materials for chemical and physical applications. New J Chem 22:1179–1201
35. Eftekhari A (2010) Nanostructured conductive polymers. Wiley, Chichester, UK
36. Yogeswaran U, Chen SM (2008) A review on the electrochemical sensors and biosensors composed of nanowires as sensing material. Sensors 8:290–313

37. Wanekaya AK, Chen W, Myung NV, Mulchandani A (2006) Nanowire-based electrochemical biosensors. Electroanalysis 18:533–550
38. Yacaman MY, Ascencio JA, Kiu HB, Gardea-Torresdey J (2001) Structure shape and stability of nanometric sized particles. J Vac Sci Technol B 19:1091–1103
39. Chen J, Wiley BJ, Xia Y (2007) One-dimensional nanostructures of metals: large-scale synthesis and some potential applications. Langmuir 23:4120–4129
40. Yanez-Sedeno P, Riu J, Pingarron JM, Rius FX (2010) Electrochemical sensing based on carbon nanotubes. Trends Anal Chem 29:939–953
41. Pumera M (2012) Voltammetry of carbon nanotubes and graphenes: excitement, disappointment, and reality. Chem Rec 12:201–213
42. Gan T, Hu S (2011) Electrochemical sensors based on graphene materials. Microchim Acta 175:1–19
43. Hernandez FJ, Ozalp VC (2012) Graphene and other nanomaterial-based electrochemical aptasensors. Biosensors 2:1–14
44. Brownson DAC, Kampouris DK, Banks CE (2012) Graphene electrochemistry: fundamental concepts through to prominent applications. Chem Soc Rev 41:6944–6976
45. Artiles MS, Rout CS, Fisher TS (2011) Graphene-based hybrid materials and devices for biosensing. Adv Drug Deliv Rev 63:1352–1360
46. Kuila T, Bose S, Khanra P, Mishra AK, Kim NH, Lee JH (2012) Recent advances in graphene-based biosensors. Biosens Bioelectron 26:4637–4648
47. Griese S, Kampouris DK, Kadara RO, Banks CE (2008) A critical review of the electrocatalysis reported at C60 modified electrodes. Electroanalysis 20:1507–1512
48. Zhang X, Cui Y, Lv X, Li M, Ma S, Cui Z, Kong Q (2011) Carbon nanotubes, conductive carbon black and graphite powder based paste electrodes. Int J Electrochem Sci 6:6063–6073
49. Charlier JC (2002) Defects in carbon nanotubes. Acc Chem Res 35:1063–1069
50. Collins PG (2009) In: Narlikar AV, Fu YY (eds) Oxford handbook of nanoscience and technology: frontiers and advances. Oxford University Press, Oxford
51. Tzirakis MSD, Orfanopoulos M (2013) Radical reactions of fullerenes: from synthetic organic chemistry to materials science and biology. Chem Rev 113:5262–5321
52. Choudhary V, Gupta A (2011) In: Yellampalli S (ed) Polymer/carbon nanotube nanocomposites, carbon nanotubes – polymer nanocomposites. InTech, Rijeka
53. Harris PJF (2005) New perspectives on the structure of graphitic carbons. Crit Rev Solid State Mat Sci 30:235–253
54. Rahman MM, Saleh Ahammad AJ, Jin JH, Ahn SJ, Lee JJ (2010) A comprehensive review of glucose biosensors based on nanostructured metal-oxides. Sensors 10:4855–4886
55. Liu A (2008) Towards development of chemosensors and biosensors with metal-oxide-based nanowires or nanotubes. Biosens Bioelectron 24:167–177
56. Bonnemann H, Richards RM (2001) Nanoscopic metal particles – synthetic methods and potential applications. Eur J Inorg Chem 2001:2455–2480
57. Narayanan KB, Sakthivel N (2010) Biological synthesis of metal nanoparticles by microbes. Adv Colloid Interf Sci 156:1–13
58. Swihart MT (2003) Vapor-phase synthesis of nanoparticles. Curr Opin Colloid Interface 8:127–133
59. Kruis FE, Fissan H, Peled A (1998) Synthesis of nanoparticles in the gas phase for electronic, optical and magnetic applications – a review. J Aerosol Sci 29:511–535
60. Hou PX, Liu C, Cheng HM (2008) Single-walled carbon nanotubes as anisotropic relaxation probes for magnetic resonance imaging. Carbon 46:2003–2025
61. Mao S, Pu H, Chen J (2012) Graphene oxide and its reduction: modeling and experimental progress. RSC Adv 2:2643–2662
62. Compton C, Nguyen ST (2010) Graphene oxide, highly reduced graphene oxide, and graphene: versatile building blocks for carbon-based materials. Small 6:711–723
63. Pashley R, Karaman M (2004) Applied colloid and surface chemistry. Wiley, Berlin
64. Schmid G (2004) Nanoparticles – from theory to application. Wiley-VCH, Weinheim

65. Duncan S (1992) Introduction to colloid and surface chemistry. Butterworth-Heinemann, Oxford
66. Roucoux A, Schulz J, Patin H (2002) Reduced transition metal colloids: a novel family of reusable catalysts? Chem Rev 102:3757–3778
67. Aiken JD III, Finke RG (1999) A review of modern transition-metal nanoclusters: their synthesis, characterization, and applications in catalysis. J Mol Cat A 145:1–44
68. Zanardi C, Terzi F, Zanfrognini B, Pigani L, Seeber R, Lukkari J, Ääritalo T (2010) Composite electrode coatings in amperometric sensors. Effects of differently encapsulated gold nanoparticles in poly(3,4-ethylendioxythiophene) system. Sens Act B 144:92–98
69. Brust M, Walker M, Bethell D, Schiffrin DJ, Whyman R (1994) Synthesis of thiol-derivatised gold nanoparticles in a two-phase liquid–liquid system. J Chem Soc Chem Commun 1994:801–802
70. Bayindir Z, Duchesne PN, Cook SC, MacDonald MA, Zhang P (2009) X-ray spectroscopy studies on the surface structural characteristics and electronic properties of platinum nanoparticles. J Chem Phys 131:244716
71. Kumar S, Gandhi KS, Kumar R (2007) Ind Eng Chem Res 46:3128–3136
72. Son SU, Jang Y, Yoon KY, Kang E, Hyeon T (2004) Nano Lett 4:1147–1151
73. De Leo M, Pereira FC, Moretto LM, Scopece P, Polizzi S, Ugo P (2007) Chem Mater 19:5955–5964
74. Schreiber F (2000) Structure and growth of self-assembling monolayers. Progr Surf Sci 65:151–256
75. Ulman A (1996) Formation and structure of self-assembled monolayers. Chem Rev 96:1533–1554
76. Haensch C, Hoeppener S, Schubert US (2010) Chemical modification of self-assembled silane based monolayers by surface reactions. Chem Soc Rev 39:2323–2334
77. Ma Z, Zaera F (2006) Organic chemistry on solid surfaces. Surf Sci Rep 61:229–281
78. Sullivan TP, Huck WTS (2003) Reactions on monolayers: organic synthesis in two dimensions. Eur J Org Chem 2003:17–29
79. Chechik V, Crooks RM, Stirling CJM (2000) Reactions and reactivity in self-assembled monolayers. Adv Mater 12:1161–1171
80. Barteau MA (1996) Organic reactions at well-defined oxide surfaces. Chem Rev 96:1413–1430
81. Mandler D, Kraus-Ophir S (2011) Self-assembled monolayers (SAMs) for electrochemical sensing. J Solid State Electrochem 15:1535–1558
82. Terzi F, Zanfrognini B, Zanardi C, Pigani L, Seeber R (2011) Poly(3,4-ethylenedioxythiophene)/Au-nanoparticles composite as electrode coating suitable for electrocatalytic oxidation. Electrochim Acta 56:3575–3579
83. Giannetto M, Mori G, Terzi F, Zanardi C, Seeber R (2011) Composite PEDOT/Au nanoparticles modified electrodes for determination of mercury at trace levels by anodic stripping voltammetry. Electroanalysis 23:456–462
84. Cutler JI, Auyeung E, Mirkin CA (2012) Spherical nucleic acids. J Am Chem Soc 134:1376–1391
85. Anstaett P, Zheng Y, Thai T, Funston AM, Bach U, Gasser G (2013) Synthesis of stable peptide nucleic acid-modified gold nanoparticles and their assembly onto gold surfaces. Angew Chem Int Ed 52:4217–4220
86. Gao C, Guo Z, Liu JH, Huang XJ (2012) Highly efficient and completely flexible fiber-shaped dye-sensitized solar cell based on TiO_2 nanotube array. Nanoscale 4:1948–1963
87. Song W, Li DW, Li JT, Li Y, Long YT (2011) Disposable biosensor based on graphene oxide conjugated with tyrosinase assembled gold nanoparticles. Biosens Bioelectron 26:3181–3186
88. Jiang HL, Xu O (2011) Recent progress in synergistic catalysis over heterometallic nanoparticles. J Mater Chem 21:13705–13725

89. Gómez-Romero P, Sanchez C (2004) Hybrid materials, functional applications. An introduction. In: Gómez-Romero P, Sanchez C (eds) Functional hybrid materials. Wiley-VCH, Weinheim
90. International Union of Pure and Applied Chemistry (2013) IUPAC goldbook. http://goldbook.iupac.org
91. Wu B, Zheng N (2013) Surface and interface control of noble metal nanocrystals for catalytic and electrocatalytic applications. Nano Today 8:168–197
92. Chu H, Wei L, Cui R, Wang J, Li Y (2010) Carbon nanotubes combined with inorganic nanomaterials: preparations and applications. Coord Chem Rev 254:1117–1134
93. Kumar Vashist S, Zheng D, Al-Rubeaan K, Luong JHT, Sheu FS (2011) Advances in carbon nanotube based electrochemical sensors for bioanalytical applications. Biotechnol Adv 29:169–188
94. Lu X, Zhang W, Wang C, Wen TC, Wei Y (2011) One-dimensional conducting polymer nanocomposites: synthesis, properties and applications. Progr Polym Sci 36:671–712
95. Gajendran P, Saraswathi R (2008) Polyaniline-carbon nanotube composites. Pure Appl Chem 80:2377–2395
96. Huang X, Qi X, Boey F, Zhang H (2012) Graphene-based composites. Chem Soc Rev 41:666–686
97. Zanardi C, Terzi F, Seeber R (2013) Polythiophenes and polythiophene-based composites in amperometric sensing. Anal Bioanal Chem 405:509–531
98. Janáky C, Visy C (2013) Conducting polymer-based hybrid assemblies for electrochemical sensing: a materials science perspective. Anal Bioanal Chem 405:3489–3511
99. Zanardi C, Terzi F, Pigani L, Seeber R (2011) Electrode coatings consisting of polythiophene-based composites containing metal centre. In: Lechkov M, Prandzheva S (eds) Encyclopedia of polymer composites: properties, performance and applications. Nova, New York
100. Chaudhuri RG, Paria S (2012) Core/shell nanoparticles: classes, properties, synthesis mechanisms, characterization, and applications. Chem Rev 112:2373–2433
101. Walther A, Muller AHE (2013) Janus particles: synthesis, self-assembly, physical properties, and applications. Chem Rev 113:5194–5261
102. Terzi F, Zanardi C, Daolio S, Fabrizio M, Seeber R (2011) Au/Pt nanoparticle systems in methanol and carbon monoxide electroxidation. Electrochim Acta 56:3673–3678
103. Rao CNR, Kulkarni GU, Thomas PJ, Edwards PP (2000) Metal nanoparticles and their assemblies. Chem Soc Rev 29:27–35
104. Daniel MC, Astruc D (2004) Gold nanoparticles: assembly, supramolecular chemistry, quantum-size-related properties, and applications toward biology, catalysis, and nanotechnology. Chem Rev 104:293–346
105. Shipway A, Katz E, Willner I (2000) Nanoparticle arrays on surfaces for electronic, optical, and sensor applications. Chem Phys Chem 1:18–52
106. Fernandes de Farias R (2009) Chemistry on modified oxide and phosphate surfaces: fundamentals and applications. Academic, Amsterdam
107. Kuila BK, Garai A, Nandi AK (2007) Synthesis, optical, and electrical characterization of organically soluble silver nanoparticles and their poly(3-hexylthiophene) nanocomposites: enhanced luminescence property in the nanocomposite thin films. Chem Mater 19:5443–5452
108. Baibarac M, Batlog I, Lefrant S, Mavellec JY, Chauvet O (2003) Polyaniline and carbon nanotubes based composites containing whole units and fragments of nanotubes. Chem Mater 15:4149–4156
109. Jena BK, Ray CR (2006) Enzyme-free amperometric sensing of glucose by using gold nanoparticles. Chem Eur J 12:2702–2708
110. Zanardi C, Terzi F, Pigani L, Heras A, Colina A, Lopez-Palacios J, Seeber R (2008) Development and characterisation of a novel composite electrode material consisting of poly (3,4-ethylenedioxythiophene) including Au nanoparticles. Electrochim Acta 53:3916–3923
111. Fan J, Wan M, Zhu D, Chang B, Pan Z, Xie S (1999) Synthesis and properties of carbon nanotube-polypyrrole composites. Synth Metals 102:1266–1267

112. Zotti G, Vercelli B, Berlin A (2008) Gold nanoparticle linking to polypyrrole and polythiophene: monolayers and multilayers. Chem Mater 20:6509–6516
113. Kotov NA (2002) In: Decher G, Schlenoff JB (eds) Multilayer thin films: sequential assembly of nanocomposite materials. Wiley-VCH, Weinheim, Germany
114. Wang S, Li C, Chen F, Shi G (2007) Layer-by-layer deposited multilayer films of water soluble polythiophene derivative and gold nanoparticles exhibiting photoresponsive properties. Nanotechnology 18:185707(1)–185707(6)
115. Ruiz V, Nicholson PG, Jollands S, Thomas PA, Macpherson JV, Unwin PRJ (2005) Molecular ordering and 2D conductivity in ultrathin poly(3-hexylthiophene)/gold nanoparticle composite films. J Phys Chem B 109:19335–19344
116. Nicholson PG, Ruiz V, Macpherson JV, Unwin PR (2006) Effect of composition on the conductivity and morphology of poly(3-hexylthiophene)/gold nanoparticle composite Langmuir-Schaeffer films. Phys Chem Chem Phys 8:5096–5105
117. Kim BY, Cho MS, Kim YS, Son Y, Lee Y (2005) Fabrication and characterization of poly (3,4-ethylenedioxythiophene)/gold nanocomposite via in-situ redox cycle system. Synth Met 153:149–152
118. Panda BR, Chattopadhyay AJ (2007) A water-soluble polythiophene–Au nanoparticle composite for pH sensing. Colloid Interf Sci 316:962–967
119. Cho MS, Kim SY, Nam JD, Lee Y (2008) Preparation of PEDOT/Cu composite film by in situ redox reaction between EDOT and copper(II) chloride. Synth Met 158:865–869
120. Millan MD, Taranekar P, Waenkaew P, Advincula RC (2005) Formation of gold nanoparticles stabilized by a star block copolymer and simultaneous polymerization of a dithiophenylpyrrole monomer. Polymer Preprints 46:652–653
121. Zhitomirsky I (2002) Cathodic electrodeposition of ceramic and organoceramic materials. Fundamental aspects. Adv Coll Interf Sci 97:279–317
122. Maduraiveeran G, Ramaraj R (2007) A facile electrochemical sensor designed from gold nanoparticles embedded in three-dimensional sol-gel network for concurrent detection of toxic chemicals. Electrochem Commun 9:2051–2055
123. Burke LD (2004) Scope for new applications for gold arising from the electrocatalytic behaviour of its metastable surface states. Gold Bull 37:125–135
124. Xiao F, Liu L, Li J, Zeng J, Zeng B (2008) Electrocatalytic oxidation and voltammetric determination of nitrite on hydrophobic ionic liquid-carbon nanotube gel-chitosan composite modified electrodes. Electroanalysis 20:2047–2054
125. Xiao L, Wildgoose GG, Compton RG (2009) Sensitive electrochemical detection of arsenic (III) using gold nanoparticle modified carbon nanotubes via anodic stripping voltammetry. Anal Chim Acta 620:44–49
126. Wildgoose GG, Banks CE, Compton RG (2006) Metal nanoparticles and related materials supported on carbon nanotubes: methods and applications. Small 2:182–193
127. Chicharro M, Bermejo E, Moreno M, Sanchez A, Zapardiel A, Rivas G (2005) Adsorptive stripping voltammetric determination of amitrole at a multi-wall carbon nanotubes paste electrode. Electroanalysis 17:476–482
128. Hrapovic S, Majid E, Liu Y, Male K, Luong JHT (2006) Metallic nanoparticle–carbon nanotube composites for electrochemical determination of explosive nitroaromatic compounds. Anal Chem 78:5504–5512
129. Jena BK, Raj CR (2008) Gold nanoelectrode ensembles for the simultaneous electrochemical detection of ultratrace arsenic, mercury and copper. Anal Chem 80:4836–4844
130. Zhu Z, Su Y, Li J, Li D, Zhang J, Song S, Zhao Y, Li G, Fan C (2009) Highly sensitive electrochemical sensor for mercury(II) ions by using a mercury-specific oligonucleotide probe and gold nanoparticle-based amplification. Anal Chem 81:7660–7666
131. Pedrero M, Campuzano S, Pingarrón JM (2011) Magnetic beads-based electrochemical sensors applied to the detection and quantification of bioterrorism/biohazard agents. Electroanalysis 24:470–482

132. Cederquist KB, Keating CD (2009) Curvature effects in DNA: Au nanoparticle conjugates. ACSNano 3:256–260
133. Hill HD, Millstone JE, Banholzer MJ, Mirkin CA (2009) The role radius of curvature plays in thiolated oligonucleotide loading on gold nanoparticles. ACSNano 3:418–424
134. Zanardi C, Baldoli C, Licandro E, Terzi F, Seeber R (2012) Development of a gold-nanostructured surface for amperometric genosensors. J Nanopart Res 14:1148–1159
135. Li D, Song S, Fan C (2010) Target-responsive structural switching for nucleic acid-based sensors. Acc Chem Res 43:631–641
136. Holze R (2009) Surface and interface analysis – an electrochemists toolbox, vol 74, Springer series in chemical physics. Springer, Berlin
137. Terzi F, Pasquali L, Seeber R (2013) Studies of the interface of conducting polymers with inorganic surfaces. Anal Bioanal Chem 405:1513–1535
138. Alkire RC, Kolb DM, Lipkowski J, Ross PN (2008) Diffraction and spectroscopic methods in electrochemistry, advances in electrochemical science and engineering, vol 4. Wiley-VCH, Weinheim
139. Innocenti M, Loglio F, Pigani L, Seeber R, Terzi F, Udisti R (2005) In situ atomic force microscopy in the study of electrogeneration of polybithiophene on Pt electrode. Electrochim Acta 50:1497–1503
140. Streeter I, Compton RG (2007) Diffusion-limited currents to nanoparticles of various shapes supported on an electrode; Spheres, hemispheres, and distorted spheres and hemispheres. J Phys Chem C 111:18049–18054
141. Hammer B, Noeskov JK (2000) In: Gates BC, Knozinger H (eds) Advances in catalysis, vol 45. Elsevier, New York
142. Mustera TH, Trinchi A, Markleya TA, Lau D, Martin P, Bradbury A, Bendavid A, Dligatch S (2011) A review of high throughput and combinatorial electrochemistry. Electrochim Acta 56:9679–9699
143. Wang GL, Xu JJ, Chen HY (2009) Progress in the studies of photoelectrochemical sensors. Sci China Ser B Chem 52:1789–1800
144. Farrell ST, Breslin CB (2004) Oxidation and photo-induced oxidation of glucose at a polyaniline film modified by copper particles. Electrochim Acta 49:4497–4503
145. Cutress IJ, Marken F, Compton RG (2009) Microwave-assisted electroanalysis: a review. Electroanalysis 21:113–123
146. Banks CE, Compton RG (2003) Ultrasonically enhanced voltammetric analysis and applications: an overview. Electroanalysis 15:329–346
147. Compton RG, Eklund JC, Marken F (1997) Sonoelectrochemical processes: a review. Electroanalysis 9:509–522

Chapter 18
Electrochemical Sensors: Practical Approaches

Anchalee Samphao and Kurt Kalcher

18.1 Introduction

The design and manufacturing of sensors is an important issue for both fields, sensor research and application.

For commercialization sensors need to be of constant, reproducible quality and characteristics which is of particular interest for mass-produced one-shot sensors. Apart from these requirements a sufficiently long shelf-lifetime is necessary in order to guarantee the logistic supply with the devices.

Sensor research starts usually with laboratory-made or commercially available simple electrodes which are tailored and modified according to the needs and intentions.

An important aspect is the miniaturization of sensing devices, which can be achieved by either a diminishing of the dimension of macrosensors, or by new concepts of placing micro- and nanosized systems directly on semiconductors and integrating them in the electronic circuits on chips, such as SoC (system on a chip, lab on a chip) and μTAS (micro total analytical system) approaches. In such cases, combination with microsystems and micromachines, also known as MEMS or MOEMS (micro-electro-mechanical systems, micro-optoelectro-mechanical systems), allows the realization of mechanical tasks in more complex analytical approaches, such as pumping, and valve-splitting, in a single microsized chip.[1–3] Thus, also theoretical considerations concerning micro- and ultramicro-electrodes gain increasing importance.[4,5]

In the chapter here a brief overview will be given on the basic transducers and on preparation techniques to create electrochemical sensors. Due to the huge amount of literature in this field, only characteristic examples and review articles will be cited.

A. Samphao
Chemistry Department, Ubon Ratchathani University, Ubon Ratchathani, Thailand

K. Kalcher (✉)
Institute of Chemistry – Analytical Chemistry, Karl-Franzens University, Graz, Austria
e-mail: kurt.kalcher@uni-graz.at

L.M. Moretto, K. Kalcher (eds.), *Environmental Analysis by Electrochemical Sensors and Biosensors*, DOI 10.1007/978-1-4939-0676-5_18

18.2 Sensor Preparation Technologies

18.2.1 Bulk Macroelectrodes

18.2.1.1 Disc Electrodes

The most common form of solid macrosized bulk working electrodes for electrochemical measurements is a circular disc shape embedded in a usually round holder. Contact is made on the back of the electrode either simply mechanically or by soldering. Older approaches with mercury contacts are getting out of fashion due to a worldwide mercuriphobia. In fact any shape other than a circular disc is possible, but care has to be taken that there is a good electric contact with the electrode material and that the insulation is sufficient in order to avoid resistive and parasitic effects.

Concentric symmetry of the working electrode and its housing is applied with rotating disc (RDE) and rotating ring disc electrodes (RRDE) where an axial rotation of the electrode sustains a convective transport of the solution to the electrode surface.[6–8] In order to reduce electric noise of the current due to wiper contacts with brushes mercury can be still a good medium to establish electric contact between the moving working electrode and the static measuring contact point.

Most of the disc electrodes require polishing before their use (commonly with a slurry of alumina with particle sizes of 0.2 and 0.05 μm in water) because due to impurities and oxide formation at the surface the background current may be high and noisy.

The shape of the electrode may vary significantly from the disc type if the sensor is used as a detector in flow systems, e.g., ring or tubular-shaped metal sheets; nevertheless the most common form is the wall-jet configuration (the effluent stream hits the surface with a perpendicular angle) with a disc shaped detector.

Electrode materials for disc electrodes in electroanalysis are glassy carbon (GC), gold, platinum, silver, and other metals, mainly noble metals; but also graphite, semiconductors, or solid heterogeneous carbon composites can be used (see next Sect. 18.2.1.3).

18.2.1.2 Film Electrodes

Film electrodes are usually prepared from a film precursor (solution, mono- or oligomers, which is either cast or printed on the electrode support or deposited in another way (chemical deposition by oxidation, reduction, electrochemical deposition, electropolymerization, etc.). The corresponding methods will be discussed in the following chapter.

Somehow uniformly in literature thick and thin film electrodes are distinguished: The first comprises film thicknesses in the micrometer range, the second below.

18.2.1.3 Paste Electrodes

Paste electrodes are heterogeneous electrodes where conductive particles are embedded in a liquid binder which can be electroactive or not. The concept was basically designed by Adams with carbon paste electrodes (CPEs)[9–11] and has been extremely successful due to the facility of direct modification under very mild conditions.[12–16] In fact, any conductive pastes may be used as the particulate matter, a subject which is of high interest with research and production of capacitors, solar cells, and batteries, but only of little attention in electroanalysis. The binder can be hydrophobic (paraffin oil, silicon oil, etc.) or hydrophilic (electroactive, ionic liquid, etc.).[11] Heterogeneous electrodes with solid binders behave similar to CPEs, but are more robust against mechanic and other stresses; the solids may be polymers (e.g., 17) or low-melting organic compounds (e.g., 18,19). The formers may be created from monomers after inducing polymerization (e.g., with UV-light), or from polymeric solutions by evaporation of the solvent.

Holders for carbon pastes can be very simple, such as pipette tips, glass, or polymer tubes, but may be designed also as piston-driven devices facilitating the extrusion of paste and generation of a new surface.[11] In the latter case attention must be paid to the heterogeneous composition of the electrode material because particular a tapering shape may squeeze out more liquid at the beginning leading to more dry pastes in subsequent measurements.

Pretreatment of the surface is simpler than with solid electrodes, consisting of only wiping off excess paste and smoothing on a wet filter paper, Teflon, or glass sheet to provide similar conditions of the surface (mainly similar roughness) for comparable measurements.

18.2.1.4 Liquid Electrodes

Mercury is the classical electrode material for voltammetric measurements; it was used by Heyrovsky already.[20] Due to a globally increasing ban of mercury its use has been reduced drastically in the past decades though its properties for electrochemical measurements in the negative potential range are unequaled in many respects. In electrochemical analysis it is still present in the form of metal film and metal solid amalgam electrodes (MeSAE with Ag, Cu, Bi, Cd; e.g., 21). Silver amalgam is often applied in a renewable form with a silver contact moving through a small Hg-reservoir,[22–31] but it is also useful as a paste electrode with organic binders.[32]

The classical electrode setup is the dropping mercury electrode (DME) with a mercury container and a glass capillary through which the metal is running continuously; a further improvement is the static mercury drop electrode (SMDE introduced by Princeton Applied Research, PAR) where with the aid of a valve a drop is set at the tip of the capillary and is mechanically dislodged with a small hammer allowing a precise control of the drop time. A further development is the controlled

growth mercury electrode (CGME by BioAnalyticalSystems Incorporated, BASi) with a fast-response valve which controls incrementally the growth of a drop by many very short opening-closing cycles. The dynamic approach of a dropping electrode provides quasi-continuously a new electrode surface at practically all times of the measurement combined with the disadvantage of a periodically changing surface area which produces oscillating currents.

Static assays of mercury electrodes include the pool electrode and the hanging mercury drop electrode (HMDE developed by Kemula[33]). With the latter a mercury drop is placed on the tip of a capillary by squeezing the metal out of the reservoir with a micrometer screw-controlled piston.

18.2.2 Micro- and Nanosized Electrodes

Apart from the necessity to scaling down sensors for special applications, such as small sample volumes, topical and surface scanning electroanalysis, in vivo measurements (e.g., in the brain), the electrochemical behavior (particularly the mass transfer characteristics) changes drastically when diminishing the surface area in a way that the electrode diameter becomes significantly smaller than the diffusion layer thickness. The consequences are an increase in the mass transport rate, a decrease in the capacitance of the double layer along with a decrease of Ohmic losses (product of current and solution resistance). Thus the presence of a counter electrode and a supporting electrolyte is obsolete in many cases.[34] Whereas with macroelectrodes the faradaic current (diffusion current) vanishes to zero with sufficiently long time according to the Cottrell equation, it drops to a constant value only with microelectrodes which is proportional to the inverse of the electrode radius (spherical correction). Typical dimensions of microelectrodes are in the low micrometer range (1–10 μm); smaller dimensions are often classified as ultramicroelectrodes[35] though authors are not strict with dimensioning and classification.

The shape of microelectrodes can be spherical, hemispherical, cylindrical, or disc shape, but also microrings, lines, bands, and irregular shapes were fabricated. Traditional approaches rely on potting or sealing the conductive electrode material with an insulating shroud. Fibers with thin diameters can be sealed with glass or polymers and cut afterwards. Other approaches employ more sophisticated techniques, such as microlithography or similar. More details can be found in the corresponding Chaps. 15 and 20.

Nanosized electrodes are even more difficult to prepare as single electrodes. Nevertheless, ensembles of them are easier to realize when using templates onto which the electrodes are deposited. Due to cross talk effects and high electrode surfaces combined with regular assemblies and arrangements improved effects are sometimes observed when compared to classical macrosized electrodes. The subject is discussed in Chap. 15.

18.2.3 Casting and Coating Techniques

Many sensors are based on films and membranes, often a combination of more of them to perform certain tasks. Thus, the generation of films or the attachment of membranes on surfaces during the sensor preparation is often a crucial step.

Films and membranes can act as:

precursors or actual electrode materials;
protective layers with size exclusion effects;
charge or diffusion barrier;
immobilization and anchoring structures for modifiers;
catalysts;
preconcentrators of analytes;
modifiers of surface characteristics;
wetting aids;
adhesion layers;
insulation layers.

The number of layer should be kept to a minimum; each one can be the source of irregularities during production, and each is a diffusion barrier for the analyte decreasing mass transport, as a consequence, decreases the signal and increases the response time.

In the following paragraphs a short overview will be given on the most convenient techniques for creating films and membranes on supports will be discussed.

18.2.3.1 Drop-Coating

This simple procedure requires a micropipette with which a small volume (a few microliters or less) is directly dropped on the support either once or repetitively to obtain thicker membranes. The drop-coated surface is then dried at ambient conditions or cured at elevated temperatures. Important for the quality and uniformity of the cast layer is the surface roughness and its wettability with the membrane solution which can be estimated via hydrophilicity-lipophilicity considerations or contact angle measurements. Chromatographic and capillary migration effects can be the reason for inhomogenities as well.

18.2.3.2 Dip-Coating

The surface where the membrane should be placed is submerged in the precursor solution and pulled out from it with some constant and repeatable speed. Higher velocity produces thicker films because more solution will remain at the surface. Immediately after the removal from the solution the liquid layer is unequally thick, a disadvantage which can be somehow overcome by careful drying or curing.

Nevertheless, due to evaporation effects the thickness differs between brim and centered areas of the covered surface. Dip-coating is frequently used to prepare thin films (thickness in the nm range).

18.2.3.3 Spin-Coating

The support is rotated and at the rotational center the precursor solution (a few microliters) is applied. Due to the centrifugal forces it is swept over the surface creating a thin liquid film which is converted to solid by drying or curing.

18.2.3.4 Spray-Coating

With spray-coating the precursor solution is nebulized into small aerosol droplets which are deposited on the support surface. The droplet formation is influenced by the geometry of the spray chamber (capillary thickness, air jet velocity) and by the viscosity of the solution.

18.2.3.5 Membrane Coverage

In most sensor designs receptors biocomponents, mediators, etc., should be located directly at the sensing area (electrode surface). This is often done by sorption or by integrating the components into a polymeric structure; sometimes the consequence is a decreased activity of the reactive principle or insufficient immobilization leading to a poor or varying performance of the sensor. In simple cases immobilization can be simply achieved by putting a size-exclusion membrane (dialysis membrane) over the electrode and thus forcing larger molecules (e.g., enzymes) to stay at the sensor surface. Nevertheless, it is necessary to choose a proper cut-off molecular size of the membrane pores in order to allow penetration of the analyte on one hand and to prevent depletion of the surface compounds on the other. Coverage with dialysis membranes is usually applied to biosensors.

18.2.4 Printing Techniques

18.2.4.1 Screen Printing

Screen printing is a very versatile technique which is employed for the production of all forms of commercially available strip-type chemical sensors (e.g., glucose test strips).

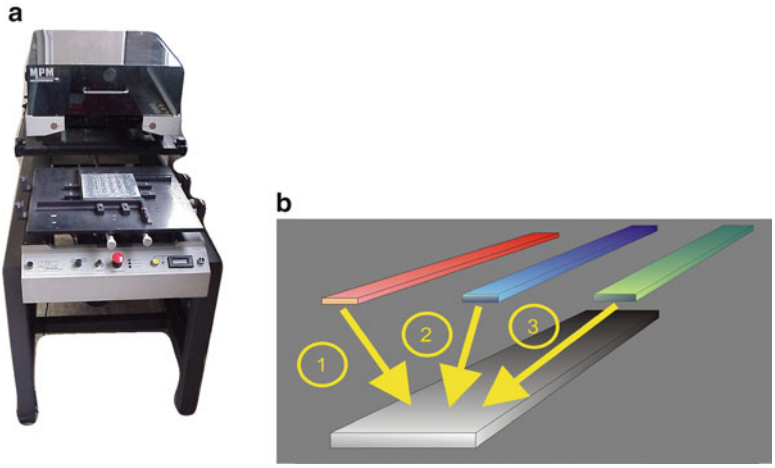

Fig. 18.1 Screen printing; (**a**) MPM semiautomatic printer; (**b**) screen printing of an electrochemical sensor: printing of the working (*1*), reference (*2*) and counter (*3*) electrodes

A screen (a woven mesh or a thin metal foil) with a stencil reflecting the patterns to be printed is put as a mask on the support; a filling blade (squeegee) moves the precursor solution ("ink") over the screen and fills the openings of the stencil, thus printing on the support.[15,36–48]

Printing can be done with automatic or semi-automatic devices, but also manually. It facilitates printing of working (Au, Ag, Pt, C), reference (Ag/AgCl) and auxiliary electrodes, reactive and insulating layers as well as contacts and leads with structuring down to 50 µm (Fig. 18.1). Thus, whole electrochemical cells can be realized on one strip requiring only a few µL of test solution. Typical nonconductive supports are sintered alumina or resins.

18.2.4.2 Inkjet Printing

An alternative to screen printing is inkjet printing where nanoliter amounts of an ink are printed onto a support as a single spot. Microsized patterns can be realized by combining spots (pixels). Inks can contain nanoparticles (usually with particle sizes significantly less than 200 nm to avoid obstruction of the nozzle) or precursors; layers can be printed repeatedly to obtain thicker films.[49–51] Supports are ceramic materials or heat-resistant polymers if thermal curing is required (e.g., Teflon®, Kapton®). Apart from commercial mass products used for printing with personal computers, industrial printers with heatable work-benches, camera-control of droplet formation, pixelwise movement control in combination with CAD-designed printing shapes allow to correspond to the high technical requirements for sensor and biosensor production (Fig. 18.2).

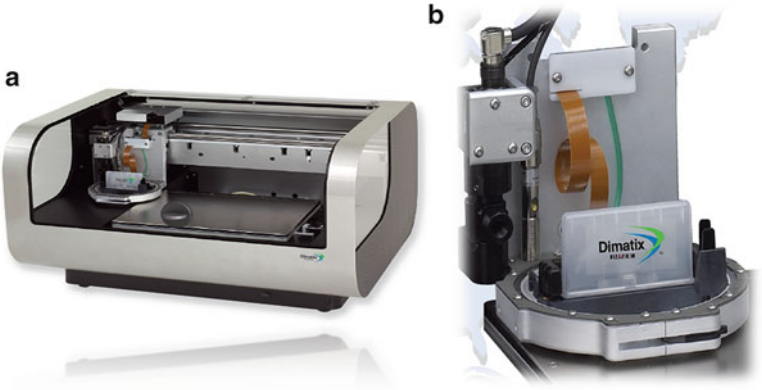

Fig. 18.2 Technical inkjet printer Dimatix Materials Printer DMP-2800; (**a**) printer with controllable x/y pixeling, (**b**) cartridge

18.2.4.3 Lithography

Lithography, originally performed with flat and smooth stone surfaces and nowadays with polymer-covered plates, is a printing technique for inks where the surface of the plate is structured into lipophilic and hydrophilic areas, from which the former ones show adhesion tendencies towards a greasy ink which is then printed onto the support.

Photolithography. This is one of the most frequently used techniques for creating micro- and nanostructured patterns on a base (e.g., a wafer or a resin plate covered with a metal layer). A thin photosensitive layer (photoresist) is cast onto the support, frequently by spin-coating, and is exposed to electromagnetic radiation after putting a mask over it with the structure to be printed as light-permeable and impermeable pattern.[52,53] With "positive" photoresists (e.g., diazides) the photons cause degradation to products which can be washed off by alkali hydroxides and giving access to the underlying base. With "negative" ones (monomers, oligomers) the light induces polymerization making the photoresist insoluble in the subsequent washing procedure to remove the layer from the unexposed areas (Fig. 18.3). For the fabrication of small-sized electrode arrays with photolithography see chapter 20, sect. 20.2.2.

Using short wavelengths (UV, X-rays) results in micro- and nanolithography where structures down to 10 nm can be reproduced.[54,55] A variant invented by Chou, nanoimprint lithography (NIL) presses the master nanostructure against a polymer surface which can be replicated by heating (thermoplastic NIL)[56,57] or by cold welding.[58] In magnetolithography magnetic nanoparticles cover areas of the support with magnetic fields (magnetic masks) in analogy to photoresists.

18.2.4.4 Soft Lithography

This technique developed by G.M. Whitesides employs elastomeric stamps, molds, and conformable photomasks to produce repetitive micro- and nanostructures.[54,55]

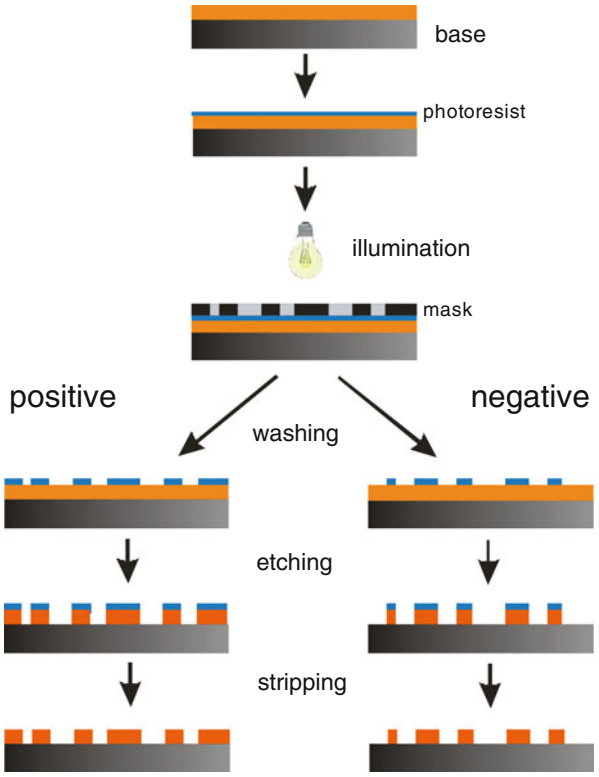

Fig. 18.3 Photolithography; in positive mode the illuminated areas are etched away and the nonilluminated remain; in negative mode vice versa

Stamps and molds are usually prepared from a master with relief structure on its surface by replica molding where the elastomer precursor is cast onto the master and is peeled off after polymerization. As elastomer most notably polydimethylsiloxane (PDMS) is used. With micro-contact printing, a nonphotolithographic technique, the stamp prints the replica information onto a support, often in the form of self-assembling monolayers changing the surface characteristics to lipophilic on the contact spots (Fig. 18.4). The noncontacted area can be etched off or plated by deposition in an ensuing step.[54,59–63]

18.2.5 Other Film Preparation Technologies

18.2.5.1 Electrodeposition

Electrodeposition is the precipitation of a product of electrochemical oxidation or reduction on an electrically conductive surface.

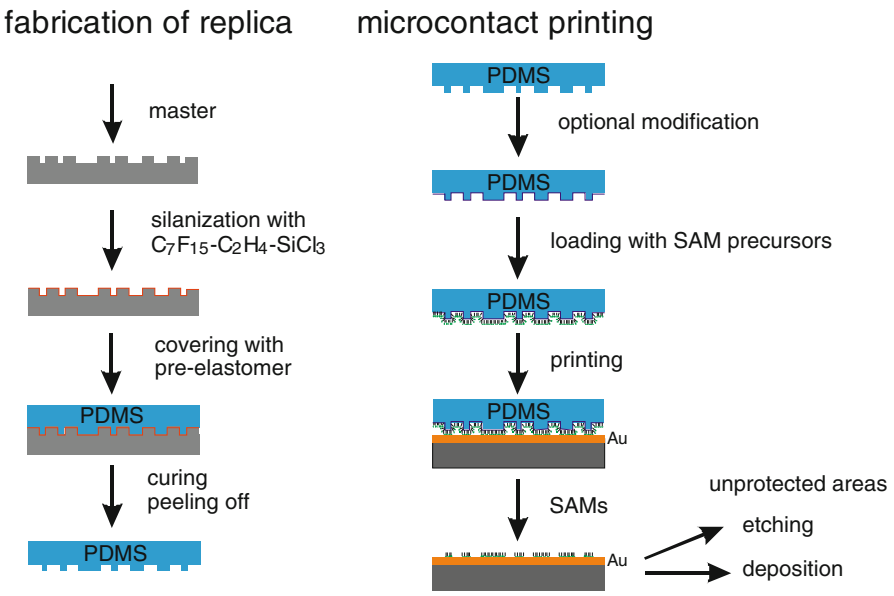

Fig. 18.4 Soft Lithography: preparation of the replica (*left*) and microcontact printing (*right*)

The classical form is the deposition of thin metal layers on support electrode surfaces, called metal film electrodes (MFEs). The precursor is a solution of the metal ion which is reduced to the element at the support, usually a glassy carbon electrode. First electrodes of this type were mercury film electrodes, which can be modeled as an ensemble of small droplets with high surface-to-volume ratio. Other films can be represented as compact thin layer of metals. Compared to disc electrodes metal film electrodes are highly attractive for many reasons: the amount of deposited metal is very small which may be decisive for toxicity and cost considerations; due to the creation of a film at the time of need, polishing of the film surface is superfluous (but in fact not for the support); in situ (during the measurement step) and ex situ (in a preceding separate step) are possible. One main reason for the use of MFEs is the preconcentration of the analyte; currently there are trends to substitute toxic mercury by other metals, such bismuth,[64] antimony,[65] or even lead and others.[66] Other purposes are exploitations of specific properties of the metal as a sensor component, such as sorptive, catalytic, electric, or optic effects. With heterogeneous electrodes, e.g., carbon pastes, extrinsic or intrinsic film formation is possible depending if the precursor is located outside (in solution) or inside the electrode bulk material (as a dispersion).[11]

Electrodeposition is also possible for electrically insulation films which may have catalytic or other functions, e.g., deposition of Prussian Blue[67] or MnO_2-films.[68] In any case care must be taken that the resulting film corresponds to the required properties with respect to stability, adhesion, and porosity depending on its envisaged function.

18.2.5.2 Electropolymerization

Electropolymerization is the electrochemically induced polymerization of monomers on a conductive surface.[69–77] This is achieved by usually cyclically polarizing the electrode surface which is at the same time exposed to a solution of the monomer. The electrochemical reaction is rather irreversible; the film formation can be followed by the current response. The best known example is probably poly (aniline), but also poly(pyrrole) or poly(thiophene) are popular (Fig. 18.5).

The outcome of electropolymerization is often an electrically conductive thin layer the polymer which can be exploited for its functional groups (e.g., protonizable–deprotonizable), as a trap for biomacromolecules or as an anchoring structure for other modifiers.

18.2.5.3 Sputter Deposition

With sputtering a noble gas (usually argon) under low pressure in a vacuum chamber is ionized and the positive particles are accelerated towards the target. Upon collision atom clusters of the target material are bombarded out from the surface and deposited anywhere in the chamber, also on the surface of a substrate which is intended to be covered with a thin layer (Fig. 18.6).

The deposition proceeds at low temperatures; typical target materials are gold, platinum, or graphite. Even carbides can be deposited in a controlled way.[78] Often magnetic fields are superimposed in a magnetron to keep the released and ionizing electrons close to the target surface.[79] Sputtering ions from noble gases can be used also for etching purposes (sputter etching) for removing surface layers of a sample for cleaning reasons or for recording depth profiles if the ion-generating device is designed in a gun-like fashion.

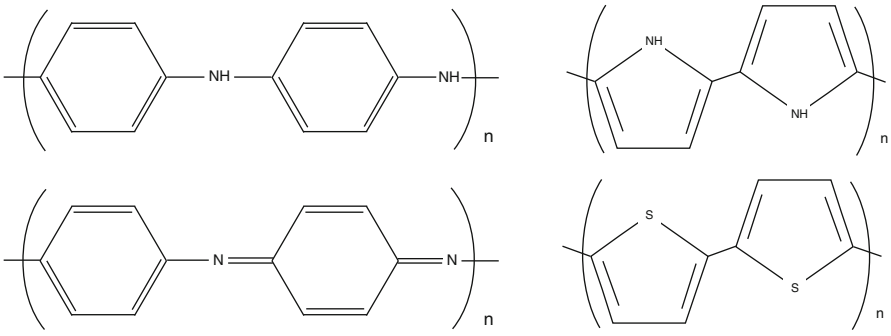

Fig. 18.5 Poly(aniline) in different oxidation states, poly(pyrrole) and poly(thiophene)

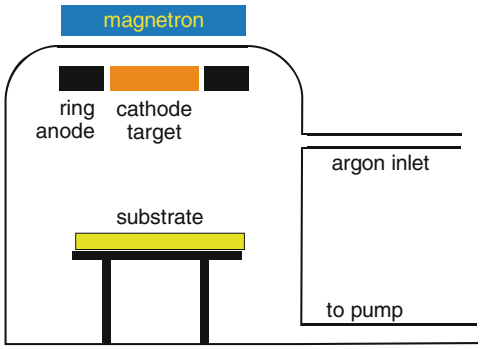

Fig. 18.6 Schematics of a sputtering device with a magnetron

18.2.5.4 Chemical Vapor Deposition (CVD)

CVD is a process where the substrate (in electronic industry frequently a wafer) is covered with a thin layer using the vapors of a compound as a precursor, which is basically pyrolized and deposited. Pyrolization in the simplest case may occur simply thermally by heating up the substrate (hot walls) at atmospheric pressure (APCVD), low pressure (LPCVD), or ultrahigh vacuum (UHVCVD); in the latter cases gas phase reactions inferring unwanted products are minimized. The deposition process may be assisted by a plasma, called plasma-enhanced (PECVD) or microwave plasma assisted chemical vapor deposition (MPCVD).[80] Here the vapors are subdued to plasma discharge during the deposition, and the substrate is placed at one discharge electrode. CVD is important for the synthesis of carbonaceous materials like carbon nanotubes,[81–85] graphenes[86] and boron-doped diamond,[87–91] but also for other compounds based on silicon[92] or ceramics.[93] A special form is the organometallic chemical vapor deposition with organometallics as the precursor.

A related technique is the organic metal deposition (OMD) where the organometallic compound is not applied as a vapor, but in another form directly on the surface.[94,95]

Another variant, the atomic layer deposition (ALD), formerly called atomic layer epitaxy, is a process similar to CVD, but the deposition is split into two half-reactions by sequential use of usually two precursors. The first one is typically an organometallic compound; after its application and subsequent purging the second precursor, e.g., a plasma, is applied, and any by-products are purged off again. ALD is applied to deposit oxide or nitride films, occasionally sulfides.[96–98] The layers may be also electrochemically deposited (E-ALD), usually with underpotential deposition to restrict reactions to a single layer at the surface and alternating reduction–oxidation cycles. In case of cadmium sulfide a monoatomic layer of cadmium is deposited from Cd^{2+}; after solution exchange sulfide is deposited as CdS by underpotential oxidation of the reduced Cd^0. The cycles can be repeated.

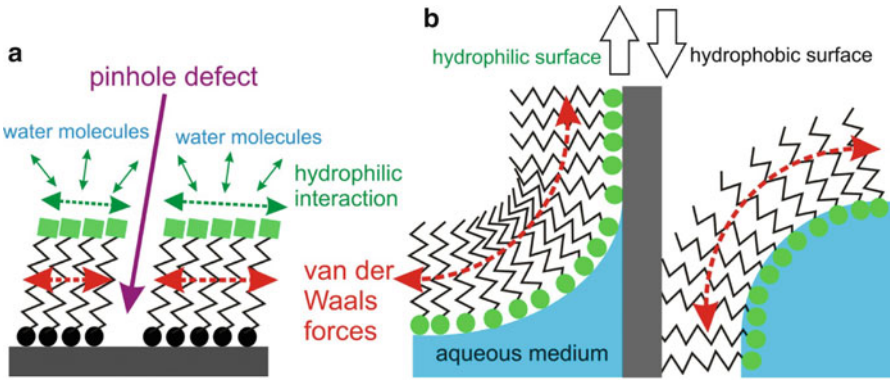

Fig. 18.7 Self-assembled monolayer (SAM, **a**) and Langmuir-Blodgett-layer (LBL) on a hydrophilic and a hydrophobic surface (**b**)

18.2.6 Monolayers and Multistacked Monolayers

Monolayers are a single layer of molecules, in sensor designs usually placed on a surface of a substrate. Monolayers differ from normal sorption layers by showing a regular repetitive structure which results from two phenomenons: (1) specific interaction between molecule and surface, and (2) specific interaction among the sorbing molecules. Monolayer-forming molecules exhibit surfactant character with some hydrophilic and lipophilic character. Thus, they often used as models for biological membranes.[99–101] All the thin film formation techniques discussed briefly in the following section rely on self assembling and self-organization, either by hydrophilic-hydrophobic or by electrostatic properties.

18.2.6.1 Self-Assembled Monolayers (SAMs)

Self-assembled monolayers form spontaneously when certain surfaces are exposed to solutions containing SAM-precursors (Fig. 18.7a).[102–104]

The reason for the self-assembly is the sorption of a certain end on the surface, usually some specific affinity of a molecule group to the surface material. The off-standing rests of the molecules, e.g., some hydrocarbon chain, interact with each other (van-der-Waals-interaction); additional stability of the overall structure may be achieved by corresponding end-heads of the molecules away from the substrate surface. The films are quite compact, but pin-hole imperfections may be deteriorating the surface characteristics. Self-assembling behavior is quite frequently employed for generating sensing surfaces.[105–107]

The best-known example for SAM formation and consequently the most exploited system is the chemisorptions of thiols on gold,[108–110] but also other systems are possible, such as carboxylates on metal oxides or silicates on glass,

but even formation of more complex aggretates is possible.[105–107,111,112] SAMs are usually stable at room temperature, but multidentate adsorbates may improve their stability.[113,114]

18.2.6.2 Langmuir-Blodgett Layers (LB Films)

Langmuir-Blodgett layers, going back to pioneering work of Irving Langmuir and Katherine Burr Blodgett in the General Electric laboratories, are monolayers formed by sorption of a surfactant layer established at a liquid–gas interface after immersion or emersion (Fig. 18.7b).

Formation of the monolayer is usually done with a Langmuir-Blodgett trough. With the aid of a moveable barrier a dense monomolecular layer of the surfactant on the liquid phase is maintained and controlled with a thin Wilhelmy plate, the force on which is proportional to the surface tensions. A dipping device provides the application of the layer on the substrate. Depending on its quality (hydro- or lipophilic) the nature of the surface is reversed after sorption. Multiple immersions and emersions allow stacking of the layers.[115–121]

18.2.6.3 Layer-by-Layer (LbL) Deposition of Multistacked Thin Films

In the LbL technique the driving force for self-assembling and organization of monolmolecular films is not specific sorption and/or amphiphilic hydrophilicity–hydrophobicity diversities within molecules, but electrical charges. Thus, on a negatively charged surface a monolayer of R^+ or a bilayer of R^+S^- can be regularly attached with charge attraction as the ordering force. The layer formation is typically controlled by ellipsometry or with quartz crystal microbalances; typical layer thicknesses are in the low nm-range. LbL-deposition is simple and inexpensive allowing the deposition of a wide range of materials, such as biological molecules, polyelectrolytes, metals and nanoparticles.[122–132]

18.2.7 Special Films and Techniques

18.2.7.1 Xerogels, Aerogels, and Sol–Gel Route

Sols and gels are usually prepared from precursors (often metal alkoxylates) by controlled partial hydrolysis which initiates polymerization. Upon normal drying the fluffy structure collapses forming a xerogel, which can be transferred into a compact and dense form by curing at higher temperatures (Fig. 18.8).[133–137] The preparation parameters such as hydrolysis conditions, aging time etc. are crucial. Application of sols or gels on surfaces is commonly done by film casting techniques

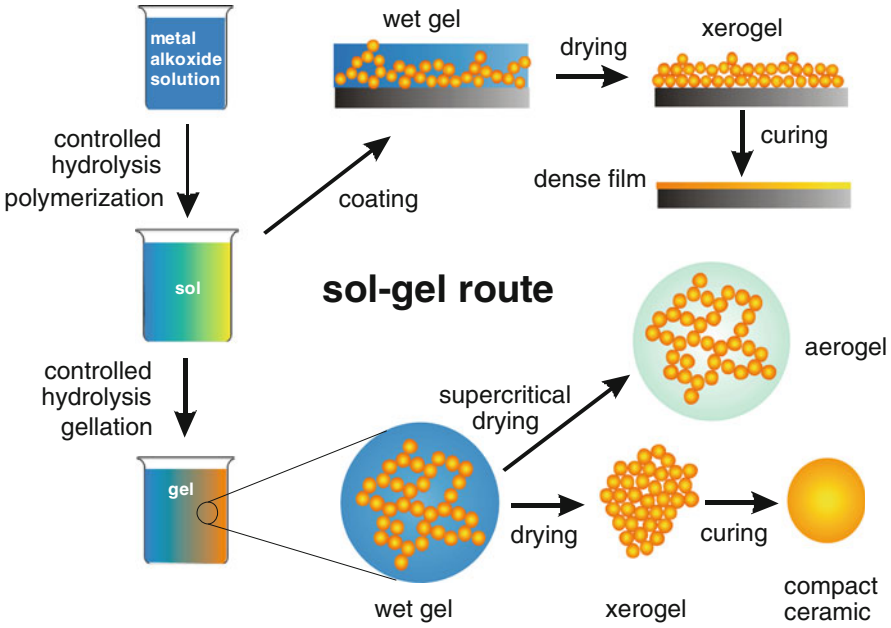

Fig. 18.8 Sol–gel route, aerogels, xerogels, and compact ceramics

like spin or dip coating. This process can be exploited for creating thin dense films on surfaces.

When the solvent is carefully removed from the gel structure (e.g., by extraction with alcohol under supercritical conditions) materials with interesting properties are obtained, .i.e., aerogels.[138–141] They are ultralight, made up to 99.98 % of air, and extremely insulating against heat and cold. Aerogels can be of silica, metal oxide, polymer, or carbon type, the latter being prepared by sintering gelled polymers; they may be interesting electrode materials because they have an enormous void volume and they are electrically conductive.

18.2.7.2 Hydrogels

Hydrogels are hydrophilic polymers containing entrapped water, but insoluble in water by themselves.[142–163] They are usually rich in oxygen or hydroxyl groups, such as poly(vinyl alcohol), poly(ethylene glycol), poly (2-hydroxyethyl methacrylate), or derivatives of chitosan and are highly biocompatible. Of particular interest are smart hydrogels where the swelling is dependent on a stimulus (stimuli-responsive hydrogels); relevant stimuli can be temperature, pH value, solvent composition, low molecular mass solutes etc.

18.2.7.3 Enzyme Immobilization and Biosensors

With enzyme electrodes it is important to fix the biocomponent to the surface of the electrode, because in this way the formed electrochemically active products and intermediates can be detected best, immediately after their generation. Various immobilization techniques are commonly in use.[164]

Membrane Coverage

After application of the enzyme a membrane (size exclusion dialysis membrane) is put over the electrode surface and prevents the diffusion of the protein and/or other components into the test solution. This way seems the simplest method for immobilization of enzymes and has been frequently employed.[165,166] Nevertheless, any membrane at the surface hinders the mass transport of the analyte to some extent resulting in decreased signals and longer response times.

Adsorption

Some enzymes may be sorbed on certain surfaces, such as carbon, gold, or ZnO. The latter can be also present as nanostructured material (layer, nanoparticles) attached to the electrode.[167–177]

Electrostatic Binding

Biopolymers usually contain a lot of protonizable–deprotonizable functional groups, so that a net charge occurs if the pH of the ambient medium is below or above the isoelectric point. Thus it is possible to attach proteins by means of electrostatic binding, which can be also done layer-by-layer.[178–183]

Attachment to SAMs

If SAM-precursors are functionalized at their non-sorbing end enzymes may be bound there for immobilization purposes.[184,185]

Entrapment

Macromolecules, such as polymers in solution (e.g., Nafion®, chitosan), gels, and hydrogels, or electrogenerated polymers may be used to immobilize enzymes where the three-dimensional structure acts as a kind of host for the protein;

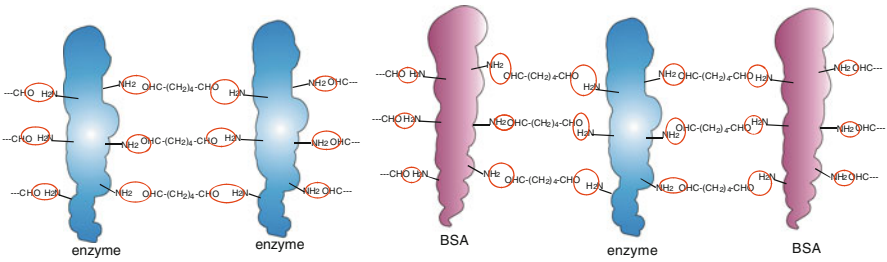

Fig. 18.9 Cross-linking of an enzyme without (*left*) and with (*right*) bovine serum albumin (BSA) using glutar aldehyde and Schiff base-formation

nevertheless, catalysts or mediators may be integrated as well.[186–194] The membrane can perform also other tasks like repulsion of interferents. Polymeric networks can be even created from monomers by inducing polymerization in the solution containing the enzyme.[195]

Cross-linking

One very conventional method for the immobilization of enzymes (and other proteins) is cross-linking. The principle is straight forward: Polymeric structures are made more insoluble by cross-linking them with each other.[196–199] To do so, typical functional groups on the outside of the polymeric molecule are covalently bound to a bi-functional linker, which possesses two reactive groups on each end. The most frequently used cross-linking agent for proteins and enzymes is glutaraldehyde which reacts easily with amino-groups forming Schiff's bases. In this way the molecules are interconnected with each other forming an insoluble network. As the concentration of enzymes is rather low cross-linking can be improved by adding an inactive protein, usually bovine serum albumin (BSA; Fig. 18.9).

Covalent Attachment

Covalent attachment provides usually the most stable biocomponent immobilization from all attachment procedures. A functional group of the biomolecule is covalently attached to a functional group of the support, either directly or with the aid of a bifunctional spacer; in case of enzymes the active center should not be affected.[200–209] Covalent attachment is possible not only for the biocomponent, but also for cofactors and coenzymes or mediators. The support can be the functionalized electrode surface itself, or nanostructured materials which will be integrated in immobilization layers, or precipitated or electropolymerized layers on the sensor surface.

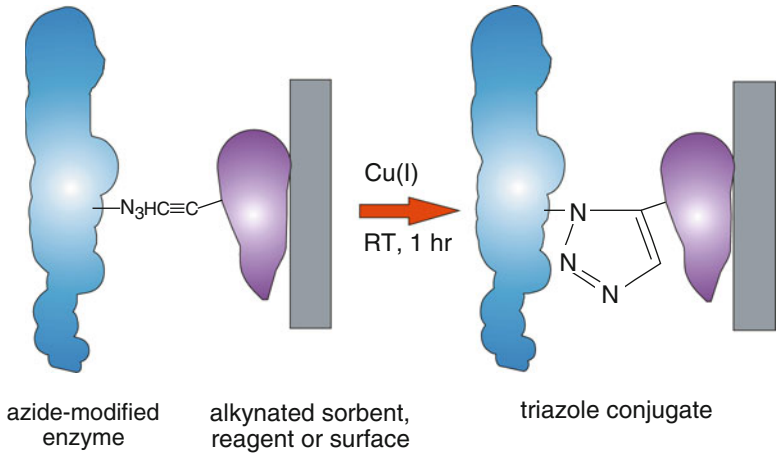

Fig. 18.10 Click chemistry with azide-modified enzyme and alkyne forming a stable triazole conjugate

A special form is the covalent immobilization by "click chemistry" described first by Sharpless.[210] The concept relies on easily proceeding, rather spontaneous chemical reactions between functional groups of smaller units to form bigger structures under mild (ambient) conditions; it can be applied to the immobilization of bioreceptors.[211–222] Often the reactive azide group is introduced in one partner, which undergoes reaction with a functional group of the target; e.g., formation of a triazole ring with arinyl derivatives (azide-alkyne Huisgen cycloaddition, Fig. 18.10).

Immobilization via Affinity Binding

Avidin (occurring in eggs) or streptavidin (produced by *Streptomyces avidinii*) are usually tetrameric proteins, where each subunit has very high affinity to bind biotin (vitamin B7). The formation constants lie between 10^{14} and 10^{16} which can be classified as the strongest noncovalent bonds. Thus, biotinylated conjugates can be easily bound to avidin-modified counter-partners and surfaces.[128,223–244]

18.2.7.4 Molecular Imprinting

With molecular imprinting a polymer is formed from monomers in the presence of a template molecule for which the monomers may contain affinity groups. After polymerization the template is removed (e.g., by extraction), and the remaining cavities present artificial receptors which show affinity to the template molecules either by size and shape or by the presence of affinity groups (see Chap. 16, sect. 16.2.2.1).

The principle can be used for accumulating the target species, or to immobilize it by self assembling. Often molecular imprints exhibit poor specificity towards the target particularly if size and shape are the selective criterions.[245–259]

18.3 Electrochemical Cells

In the following paragraphs the basic setups for the measurements are described; more details can be found in the various chapters dealing with specific measurement arrangements, such as potentiometry (Chap. 9) or controlled potential techniques (Chap. 10). Numerous books on electroanalytical chemistry may provide deeper insight into the problematic; thus, citations here are arbitrary and incomplete.[260–263]

18.3.1 Electrodes

Electrodes in electrochemical measurements are classified according to their function or task in the electrochemical cell. The most important type is the working electrode because it is the location where the most important process for the measurement (recognition) takes place. Reference electrodes provide a well-defined potential reference point in the solution, whereas counter and auxiliary electrodes serve to establish a closed circuit or to take over other tasks of the measurement.

18.3.1.1 Working Electrodes (WE)

All sensors used for electroanalytical purposes are working electrodes.

For potentiometric measurements the working electrodes consist of electrodes of first and second order (redox couple) or of membranes containing insoluble salts, ionophores, or complexes (see Chap. 9). In the classical arrangement the ion-sensitive membrane (glass, solid, or liquid) is placed between the sample solution and the inner reference electrode which is in many cases a second order electrode in order to avoid polarization effects. The membrane can also be placed directly on solid supports like in coated wire electrodes, or may be formed by the binder of carbon paste electrodes. The potential of the working electrode (potential of the redox couple or membrane potential) follows more or less the Nernst equation and is measured against the well-defined potential of a reference electrode as a potential difference (voltage). The measuring device (voltmeter) for potentiometric measurements should have a high input impedance to avoid significant current flows which would deteriorate or even impair the measurements. High input impedance can be easily achieved with corresponding operational amplifiers

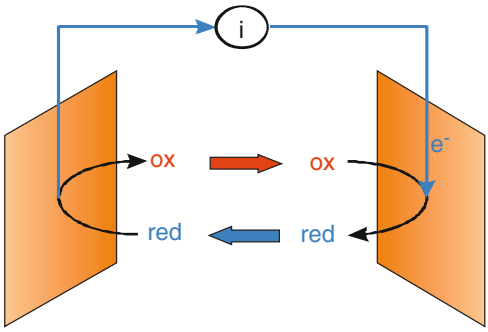

Fig. 18.11 Principle of biamperometry. A current can be monitored if both partners of a redox couple, ox and red, are present in the solution

configured as voltage followers which are installed in series with the measurement circuit before the voltmeter.

Whereas potentiometry uses an experimental approach with a minimum current flow, the voltametric setup involves a galvanostat and measures potential differences with a predefined constant current. In this case electrochemical processes at the electrode surface provide the generation of electric charge; thus the working electrodes are basically the same as the ones for voltammetric and amperometric measurements (see below). Depletion of an electroactive species causes the galvanostat to increase the potential to keep up a constant current flow.

In voltammetric and amperometric setups the working electrode represents an interface with (usually) a solution, where the analyte (or some follow-up products) is electrochemically converted (oxidized or reduced) producing a current flow. In the simples case another electrode exposed to the solution guarantees a closed electric circuit. Such types of electrodes are designated as counter electrodes. Voltammetric and amperometric methods are controlled potential techniques, where the potential applied at the working electrode defines the essential electrochemical reaction occurring there. Therefore, a precise control of the potential at the working electrode is necessary in order to monitor electrochemical reactions under well-defined conditions.

In context with voltammetry and amperometry, the term polarization must be mentioned. Polarization is the effect that, unlike with Ohm's law, application or change of a potential does not change the current flow. In solutions with the absence of electroactive species the potential regime where polarization occurs is the potential window where amperometric measurements are possible. On the cathodic side the window is limited by the reduction of the cation of the supporting electrolyte or by hydrogen evolution (aqueous media), on the anodic side by the oxidation of the electrode material, of the anion of the supporting electrolyte or by oxygen evolution. Working electrodes are polarizable electrodes, and electrochemically active species, which produce a current flow, are often called depolarizers.

Most electrochemical measurements involve one working electrode with exception of biamperometry, where two working electrodes are employed (Fig. 18.11). In this experimental setup a potential high enough to provoke the oxidation and reduction of both partners of a redox couple is applied and a current can be

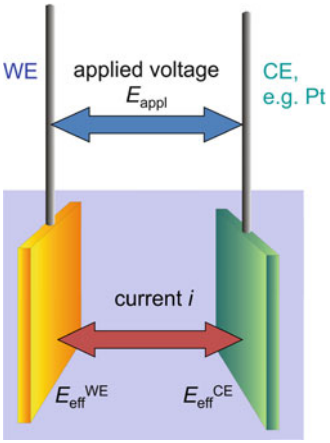

Fig. 18.12 Two-electrode arrangement with external potential control using a working and a counter electrode

monitored, because the extents of oxidation and reduction of a partner of the couple at the anode and the cathode are equal. If one of the partners is completely removed from the solution by a chemical reaction, the current drops to zero. This is the principle of the classical dead-stop titration.

18.3.1.2 Counter Electrodes (CE)

A closed electric circuit is an essential prerequisite to measure an electric entity. In the simplest case an inert counter electrode, e.g., noble metals or graphite, beside the working electrode performs this task resulting in a two-electrode assay (Fig. 18.12). This basic setup was also used by Heyrovsky in the early times of polarography. The main problem in this arrangement is polarization of the counter electrode in case that potential control is important. The effective potential at the working electrode, $E_{\text{eff}}{}^{\text{WE}}$, which defined the electrochemical reaction, is the external potential, E_{appl} diminished by the potential drop due to the current flow (i—current, R_s—resistivity of the solution) and by the polarization potential of the counter electrode, $E_{\text{eff}}{}^{\text{CE}}$ (Eq. 18.1).

$$E_{\text{eff}}{}^{\text{WE}} = E_{\text{appl}} - E_{\text{eff}}{}^{\text{CE}} - iR_s \tag{18.1}$$

As the polarization potential of the counter electrode and the ohmic drop are in principle unknown (the latter which is proportional to the current flow can be estimated and compensated) the effective potential at the working electrode may differ significantly from the applied potential, thus deteriorating or even impairing potential control. This problem can be circumvented by using a reference electrode and a three-electrode setup.

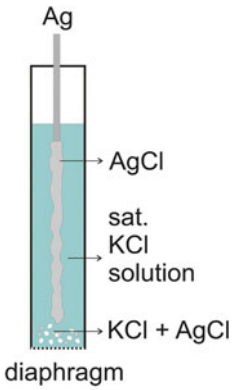

Fig. 18.13 Sketch of an Ag/AgCl reference electrode with saturated KCl electrolyte

18.3.1.3 Reference Electrodes (RE)

These electrodes are electrochemical half cells providing a constant potential; they are basically nonpolarizable, which means that their potential is independent from a current flow through the cell, or at least they follow Ohm's law. They contain a redox couple where both partners are present in well-defined concentrations (in fact, activities). Basically it is possible to realize a normal hydrogen electrode (NHE) as a potential reference with 0.000 V (per definition) but the practical efforts are enormous (proton activity 1.000 mol/L, hydrogen gas pressure 1.000 atm using a specially activated platinum electrode); additionally the potential is not very robust because small current flows or temperature changes may cause significant deviations already.

Thus, usually more robust systems are practically employed, such as the Ag/AgCl and the saturated calomel electrode (SCE). They contain redox couples consisting of the metal (Ag^0 or Hg^0, activity = 1) and its monovalent cation (Ag^+ and Hg_2^{2+}, resp.) in a well-defined and practically easily reproducible concentration. The latter is achieved by the presence of an anion (commonly chloride from potassium chloride) which forms a sparingly soluble salt with the cation, whose free concentration in solution is determined by the solubility product. Potassium chloride is present in high concentration because it also acts as a supporting electrolyte in the reference electrode. As it is a half cell only, it must have contact with the measurement solution in order to provide a closed circuit with the working electrode. Contact between the reference electrode filling (defined concentration of potassium chloride saturated with the sparingly soluble salt) and the measurement solution is made via a diaphragm, capillary, grind joint, or gel in order to avoid mixing; such an interface can be the cause of the appearance of junction potentials (Fig. 18.13). Occasionally open reference electrodes are in use, but in this case it must be guaranteed that the concentration of the counter ion of the slightly soluble (chloride) is present at a constant concentration in the sample solution in order to avoid potential shifts. The most common reference electrode is the silver/silver chloride electrode due to an increasing ban of mercury from the lab and to the ease

Table 18.1 Potentials of silver–silver chloride reference electrodes in mV

	c(KCl)			
Temp (°C)	1 mol/kg	1 mol/L	3 mol/L	sat
0	236.6	249.3	224.2	220.5
5	234.1	246.9	220.9	216.1
10	231.4	244.4	217.4	211.5
15	228.6	241.8	214.0	206.8
20	225.6	239.6	210.5	201.9
25	222.3	236.3	207.0	197.0
30	219.0	233.4	203.4	191.9
35	215.7	230.4	199.0	186.7
40	212.1	227.3	196.1	181.4
45	208.4	224.1	192.3	176.1
50	204.5	220.8	188.4	170.7

of preparation: simply, a silver wire is electrolyzed in hydrochloric acid for a short time which provides a porous coverage of the metal with AgCl; afterwards the wire is immersed in the potassium chloride solution.

The potentials of silver–silver chloride reference electrodes are summarized in Table 18.1.

According to Bard et al.[264] the standard potential of Ag/AgCl electrodes (with an activity of chloride of 1 mol/kg) can be approximated by Eq. (18.2).

$$\mathrm{E}^0(\mathrm{V}) = 0.23695 - 4.8564 \times 10^{-4} \times \mathrm{t} - 3.4205 \times 10^{-6} \times \mathrm{t}^2 - 5.869 \times 10^{-9} \times \mathrm{t}^3 \quad \text{for } 0 < \mathrm{t} < 95^\circ\mathrm{C} \tag{18.2}$$

In potentiometric measurements the reference electrode is combined with the working electrode as second half cell.

If the counter electrode is replaced by a reference electrode in the two-electrode setup for amperometric measurements, polarization of the RE is avoided (Fig. 18.14). Thus, the applied potential becomes better controllable.

Still apart from small junction potentials and ohmic shifts of the reference electrode potential under current flow the iR-drop diminishes the applied potential at the working electrode in dependence on the current (Eq. 18.3). E_{appl} is shifted by the (constant) potential of the reference electrode, E_{RE}.

$$E_{\mathrm{eff}}{}^{\mathrm{WE}} = E_{\mathrm{appl}} - E_{\mathrm{RE}} - iR_{\mathrm{s}} \tag{18.3}$$

Potential drops can be estimated and ruled out; many instruments offer such possibilities. Nevertheless, it sometimes requires some efforts, and wrong handling may cause peak distortions or oscillations.

Quasi-reference electrodes are frequently used for measurements in nonaqueous media; also here a redox couple is present in solution, but the electrolyte has to be somehow lipophilic to be soluble in sufficiently high concentration (e.g.,

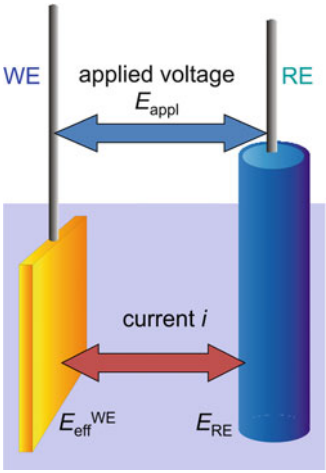

Fig. 18.14 Two-electrode setup for potential control using a working and a reference electrode

tetrabutylammonium salts rather than potassium chloride). The exact potential should be determined by measuring a standard compound (e.g., ferrocene).

Pseudo reference electrodes are in fact counter electrodes made of an inert electrode material (platinum, graphite) and usually employed for nonaqueous measurements. The main problem is its polarization (see counter electrode); therefore a standard compound (e.g., ferrocene) must be measured either under identical conditions or better even in the sample solution to find the effective potential applied to the working electrode.

18.3.1.4 Auxiliary Electrodes (AE)

They are used as additional electrode together with a working and reference electrode in three-electrode setups (Fig. 18.15). Their task is to provide the current flow from the working electrode, whereas the reference electrode still establishes the potential which is determining the electrochemical reaction occurring at the working electrode. As the current between reference and working electrode becomes negligible small, the potential is well controllable (Eq. 18.4).

$$E_{\text{eff}}{}^{\text{WE}} = E_{\text{appl}} - E_{\text{RE}} \tag{18.4}$$

The auxiliary electrode should have a high surface compared to the working electrode to avoid complications with the corresponding electrochemical counter reactions occurring at it. Typically, they are from platinum or graphite.

For measurements with microelectrodes the reference electrode can be omitted due to very small polarization effects only.

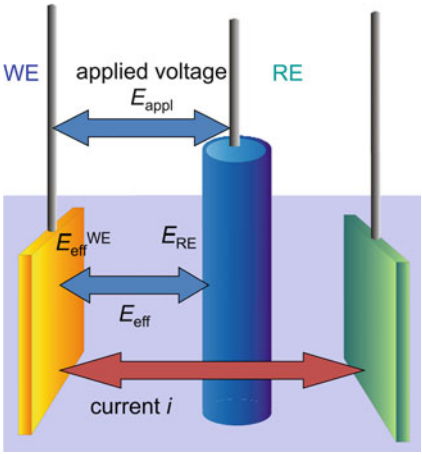

Fig. 18.15 Three-electrode setup for potential-controlled techniques

18.4 Practical Assays

Electrochemical measurements with solutions may be basically classified in stationary and hydrodynamic approaches, depending on the relative movement of electrode surface and test solution towards each other.

Hydrostatic measurements are usually batch measurements with stationary electrodes where neither the solution nor the electrode surface are moved against each other during by stirring, flowing, or rotating. The volumes may range from milliliters via microliters (popular technique with sensors using drop-sized samples such as blood or other biological fluids) even to nanoliters in chip assays.

Hydrodynamic techniques include measurements with stirred solutions or electrodes (rotated electrode and rotated ring-disc electrode) and measurements in flowing streams of a carrier.

Rotated electrodes are used for studies of the character of electrode reactions and their kinetics and for the estimation of electroanalytical parameters. Convection provides a constant mass transport of the analyte to the electrode surface with changed diffusion characteristics compared to quiescent liquids. The effect is similar to a stirring of the solution, but the rotation of an electrode can be controlled much more precisely than of a solution. Rotating ring-disc electrodes are practically used only for elucidating electrochemical reaction mechanisms where oxidation or reduction on the disc creates (collection experiment) or consumes (shielding experiment) electroactive substances which are monitored with the ring electrode.

Most hydrodynamic measurements are performed with electrodes which are use as detectors in flow systems. Different geometric arrangements are possible: thin layer cells with parallel flow or with wall jet configuration, tubular or needle electrodes in contact with the effluent, or even highly porous electrodes (reticulated vitreous carbon) where the carrier passes through the electrode itself.

Flowing carriers may arise from dynamic separation systems, such as chromatography of capillary electrophoresis, but they may be also used to speed up batch analysis and to improve its performance and sample throughput rate. They are often referred to as injection analysis because the sample and optionally also other reactants are injected into a flowing stream of carrier which finally passes the detector.

Flow injection analysis (FIA) was conceptually designed by Ruzicka and Hansen in 1974[265–267] based on the ideas of continuous flow analysis (CFA) which had been introduced by Skeggs in 1957.[268] In the latter technique plugs of samples are separated with air bubbles in capillaries in order to avoid cross-over reactions and contaminations. FIA uses a continuous flow of a carrier, and a sample plug is injected into the stream where eventually dispersion occurs. In the simplest assay the sample plug is transported over the detector. Reagents which are added to the carrier or in a separate stream as well as reactors containing enzymes provide a wide spectrum for practical applications. So far (2013) over 22,000 scientific articles have been published dealing with FIA.

A more sophisticated and versatile variety of FIA is sequential injection analysis (SIA) developed by Ruzicka and Marshall in 1990.[269,270] Here plugs of samples and reagents are injected into a carrier stream and can be moved forward or reverse, mixed etc. The core is a multiposition valve which distributes and directs the various fluid plugs in combination with a pump; the final reaction cocktail is transported to the detector. The valve may even control the determination of a whole set of analytical parameters which is realized in the so-called valve-on-lab (VOL).[271]

A hybride form between hydrodynamic measurement and batch analysis is batch-injection-analysis (BIA) developed by Wang.[272] In this case the detector is placed in a big volume of basic solution, and the sample is injected onto it producing a transient signal which returns back to the baseline after dilution. The advantage is a simplification over FIA by eliminating the carrier flow, but reproducibility may be poor when injecting manually.

18.5 Future Aspects

Electrochemical sensors are intrinsically dependent on electrochemical conversions and/or electrical properties of the analyte. In this respect it seems almost self-evident that within the past few years new materials and integration of nanosized materials in the receptor layer of the sensor have gained enormous, almost exponentially increasing attention. Nanosized materials facilitate electrochemical sensing in two ways: due to the enormous surface-to-volume ratio new material properties with respect to either increased signals or catalytic effects improve the analytical situations substantially. Another aspect is miniaturization: in contrast to optical devices a miniaturization and multiplication of sensors to form arrays does not infer particular problems, particularly because the technology may be directly taken from electronic industry where the production of extremely miniaturized printed circuit boards is routine technique already. Miniaturization stimulates also

further developments of micro- and, particularly, nanosized electrodes which will unfold their full performance in combination with micromechanic systems (MEMS technology), such as pumps and valves; as an example it will be possible in the future to combine implanted microsized sensors (e.g., glucose) with actuators to launch the release of a therapeutic agent (e.g., insulin) from implanted reservoirs, with control and surveillance systems, also implanted, supplied by biofuel cells using as energy source blood glucose.

Interesting new materials, such as grapheme, have found quite a few applications already with electrochemical sensors, a trend which is likely to continue in an increased rate in the next few years. Thus, new materials and new physical and physicochemical techniques will also stimulate the emergence of new coating, modification, and detecting methods.

With respect to analytes it can be stated that electrochemical sensors hardly will be designed for elemental analysis as batch laboratory techniques; here, electromagnetic and mass spectrometric methods offer so many advantages over electroanalysis that their performance is hardly reached by the latter one. Nevertheless, sensors which can be applied in the field may be advantageous in this respect because they may help in an early stage of the entire sampling and analytical protocol to decide, if it is necessary to analyze a sample in more details in the laboratory or not.

However, the main application of electrochemical will be in molecular analysis, and particularly in highly specific and sensitive applications. This is reflected by the current situation of electrochemical sensor research already: most applications are dealing with biosensors, because bio-mimetic receptors can detect their targets with high specificity at low occurrence levels.

References

1. Wang J (2002) On-chip enzymatic assays. Electrophoresis 23(5):713–718
2. Korvink JG, Paul O (2005) MEMS – a practical guide to design, analysis and applications. William Andrew, Burlington, MA
3. Geschke O, Klank H, Tellemann P (2008) Microsystem engineering of lab-on-a-chip devices, 2nd edn. Wiley-VCH, New York, NY
4. Bond AM (1994) Past, present and future contributions of microelectrodes to analytical studies employing voltammetric detection. Analyst 119(11):R1–R21
5. Aoki K (1993) Theory of ultramicroelectrodes. Electroanalysis 5(8):627–639
6. Penar J (1995) Application of the rotating disk and rotating ring-disk electrodes for studies of the kinetics and of mechanism of electrode reactions. Theoretical basis. Annales Universitatis Mariae Curie Sklodowska AA Chemia 46–47:119–172, Volume Date 1991–1992
7. Deslouis C, Tribollet B (1992) Flow modulation techniques in electrochemistry. Adv Electrochem Sci Eng 2:205–264
8. Albery WJ, Hitchman ML (1971) Ring-disk electrodes, 1st edn. Clarendon, Oxford, Oxford Science Research Papers
9. Adams RN (1958) Carbon paste electrodes. Anal Chem 30:1576
10. Adams RN (1963) Carbon paste electrodes. A review. Rev Polarogr 11:71–78

11. Svancara I, Kalcher K, Walcarius A, Vytras K (2012) Electroanalysis with carbon paste electrodes. CRC Press, Francis & Taylor, Boca Raton, FL, 666 pp
12. Kalcher K (1990) Chemically modified carbon paste electrodes in voltammetric analysis. Electroanalysis 2:419–433
13. Kalcher K, Wang J, Kauffmann J-M, Svancara I, Vytras K, Neuhold C, Zhongping Y (1995) Sensors based on carbon paste in electrochemical analysis: a review with particular emphasis on the period 1990-1993. Electroanalysis 7:5–22
14. Gordon L (1995) Carbon paste electrodes modified with enzymes, tissues and cells. Electroanalysis 7:23–45
15. Kalcher K, Svancara I, Metelka R, Vytras K, Walcarius A (2006) Heterogeneous carbon electrochemical sensors. In: Grimes CA, Dickey EC, Pishko MV (eds) Encyclopedia of sensors, vol 4. American Scientific Publishers, Stevenson Ranch, CA, pp 283–430
16. Svancara I, Vytras K, Kalcher K, Walcarius A, Wang J (2009) Carbon paste electrodes in facts, numbers, and notes: a review on the occasion of the 50-years jubilee of carbon paste in electrochemistry and electroanalysis. Electroanalysis 21:7–28
17. Merkoci A, Alegret S (2007) G5raphite-epoxy electrodes for stripping analysis. Compr Anal Chem 49:143–161
18. Diewald W, Kalcher K, Neuhold C, Svancara I, Cai X (1994) Voltammetric behaviour of thallium(III) at a solid heterogeneous carbon electrode using ion pair formation. Analyst 119:299–304
19. Compagnone D, Schweicher P, Kauffmann J-M, Guilbault GG (1998) Sub-micromolar detection of hydrogen peroxide at a peroxidise/tetramethylbenzidine solid carbon paste electrode. Anal Lett 31(7):1107–1120
20. Heyrovsky J (1922) Elektrolysa rtutovou kapkovou kathodou. Chem List 16:256–264
21. Josypcuk B, Fojta M, Yosypchuk O (2013) Thiolate monolayers formed on different amalgam electrodes. Part II: properties and application. J Electroanal Chem 694:84–93
22. Piech R (2013) Sensitive voltammetric determination of titanium(IV) in catalytic adsorptive mandelic acid-chlorate(V) system on renewable silver amalgam film electrode. Electroanalysis 25(3):716–722
23. Guzsvany V, Petrovic J, Krstic J, Papp Z, Putek M, Bjelica L, Bobrowski A, Abramovic B (2013) Renewable silver-amalgam film electrode for voltammetric monitoring of solar photodegradation of imidacloprid in the presence of Fe/TiO2 and TiO2 catalysts. J Electroanal Chem 699:33–39
24. Brycht M, Vajdle O, Zbiljic J, Papp Z, Guzsvany V, Skrzypek S (2012) Renewable silver-amalgam film electrode for direct cathodic SWV determination of clothianidin, nitenpyram and thiacloprid neonicotinoid insecticides reducible in a fairly negative potential range. Int J Electrochem Sci 7(11):10652–10665
25. Guziejewsk D, Brycht M, Skrzypek S, Nosal-Wiercinska A, Ciesielski W (2012) Voltammetric determination of acibenzolar-s-methyl using a renewable silver amalgam film electrode. Electroanalysis 24(12):2303–2308
26. Putek M, Guzsvany V, Tasic B, Zarebski J, Bobrowski A (2012) Renewable silver-amalgam film electrode for rapid square-wave voltammetric determination of thiamethoxam insecticide in selected samples. Electroanalysis 24(12):2258–2266
27. Bas B, Bugajna A, Jakubowska M, Niewiara E (2012) Normal pulse voltammetric determination of subnanomolar concentrations of chromium(VI) with continuous wavelet transformation. Electroanalysis 24(11):2157–2164
28. Bas B, Jakubowska M, Gorski Ł (2011) Application of renewable silver amalgam annular band electrode to voltammetric determination of vitamins C, B1 and B2. Talanta 84 (4):1032–1037
29. Piech R, Bas B (2011) Sensitive voltammetric determination of gallium in aluminum materials using renewable mercury film silver based electrode. Int J Environ Anal Chem 91 (5):410–420

30. Bas B, Bas S (2010) Rapidly renewable silver amalgam annular band electrode for voltammetry and polarography. Electrochem Commun 12(6):816–819
31. Piech R, Bas B, Niewiara E, Kubiak WW (2008) Renewable copper and silver amalgam film electrodes of prolonged application for the determination of elemental sulfur using stripping voltammetry. Electroanalysis 20(7):809–815
32. Danhel A, Yosypchuk B, Vyskocil V, Zima J, Barek J (2011) A novel paste electrode based on a silver solid amalgam and an organic pasting liquid. J Electroanal Chem 656 (1–2):218–222
33. Kemula W, Zawadowska J (1980) New model of the hanging mercury drop electrode and its application in aqueous and non-aqueous media. Fresenius' Z Anal Chem 300:39–43
34. Montenegro MI, Queiros MA, Daschbach JL (1991) Microelectrodes: theory and applications, vol 197, NATO science series E: applied sciences. Springer Science + Business Media, Dordrecht, Softcover Reprint
35. Fleischmann M, Pons S, Rolison DR, Schmidt PP (1987) Ultramicroelectrodes. Datatech Systems Inc., Morganton, NC
36. Prudenziati M, Hormadaly J (2012) Technologies for printed films, vol 26, Woodhead publishing series in electronic and optical materials: printed films. Woodhead Publishing Limited, Cambridge, UK, pp 3–29
37. Honeychurch KC (2012) Screen-printed electrochemical sensors and biosensors for monitoring metal pollutants. Insci J 2(1):1–51
38. Gonzalez-Macia L, Morrin A, Smyth MR, Killard AJ (2010) Advanced printing and deposition methodologies for the fabrication of biosensors and biodevices. Analyst 135 (5):845–867
39. Zen J-M, Kumar AS (2006) Screen-printed electrochemical sensor. In: Grimes CA, Dickey EC, Pishko MV (eds) Encyclopedia of sensors, vol 9. American Scientific Publishers, Stevenson Ranch, CA, pp 33–52
40. Huang X-J, O'Mahony AM, Compton RG (2009) Microelectrode arrays for electrochemistry: approaches to fabrication. Small 5(7):776–788
41. Hart JP, Crew A, Crouch E, Honeychurch KC, Pemberton RM (2007) Screen-printed electrochemical (bio)sensors in biomedical, environmental and industrial applications. Compr Anal Chem 49:497–557
42. Tudorache M, Bala C (2007) Biosensors based on screen-printing technology, and their applications in environmental and food analysis. Anal Bioanal Chem 388:565–578
43. Galan-Vidal CA, Paez-Hernandez ME (2005) Screen-printing electrochemical sensors for environmental studies. In: Palomar M (ed) Applications of analytical chemistry in environmental research. Research Signpost, Trivandrum, pp 23–36
44. Hart JP, Crew A, Crouch E, Honeychurch KC, Pemberton RM (2004) Recent designs and developments of screen-printed carbon electrochemical sensors/biosensors for biomedical, environmental, and industrial analyses. Anal Lett 37(5):789–830
45. Honeychurch KC, Hart JP (2003) Screen-printed electrochemical sensors for monitoring metal pollutants. Trends Anal Chem 22(7):456–469
46. Pilloton R, Mela J, Marradini L (1999) Screen printed electrochemical biosensors on ceramic and polymeric substrates. Advances in science and technology: solid state chemical and biochemical sensors, vol. 26, pp. 501-507.
47. Bouchard RJ (1999) Thick film technology: an historical perspective, vol 100, Ceramic transactions: dielectric ceramic materials. Wiley, Rochester, NY, pp 429–442
48. Hart JP, Wring SA (1994) Screen-printed voltammetric and amperometric electrochemical sensors for decentralized testing. Electroanalysis 6(8):617–624
49. Loffredo F, De Girolamo Del Mauro A, Burrasca G, La Ferrara V, Quercia L, Massera E, Di Francia G, Della Sala D (2009) Ink-jet printing technique in polymer/carbon black sensing device fabrication. Sens Actuators B B143(1):421–429

50. Teichler A, Perelaer J, Schubert US (2013) Ink-jet printing of organic electronics - comparison of deposition techniques and state-of-the-art developments. J Mater Chem C Mater Opt Elect Dev 1(10):1910–1925
51. Lopez FV, Diez A, Odriozola A (2007) Inkjet printing of conductive and resistive coatings. Int Polym Process 22(1):27–32
52. Suzuki K, Smith BW (eds) (2007) Microlithography: science and technology, 2nd edn. Taylor & Francis, New York, NY
53. Naulleau P (2012) Optical lithography. In: Cabrini S, Kawata S (eds) Nanofabrication handbook. CRC Press Taylor & Francis, New York, NY, pp 127–139
54. Xia Y, Whitesides GM (1998) Soft lithography. Annu Rev Mater Sci 28:153–184
55. Gates BD, Xu Q, Stewart M, Ryan D, Willson CG, Whitesides GM (2005) New approaches to nanofabrication: molding, printing, and other techniques. Chem Rev 105(4):1171–1196
56. Chou SY, Krauss PR, Renstrom PJ (1996) Imprint lithography with 25-nanometer resolution. Science 272:85–87
57. Sotomayor Torres CM, Zankovych S, Seekamp J, Kam AP, Clavijo Cedeno C, Hoffmann T, Ahopelto J, Reuther F, Pfeiffer K, Bleidiessel G (2003) Nanoimprint lithography: an alternative nanofabrication approach. Mater Sci Eng C 23(1–2):23–31
58. Lu Y, Huang JY, Wang C, Sun S, Lou J (2010) Cold welding of ultrathin gold nanowires. Nat Nanotechnol 5:213–224
59. Alois A, Rinaldi R (2012) Nanotechnology for diagnostic and sensing: soft and advanced imaging/sensing approaches to analyze biomolecules, vol 10, Springer series on chemical sensors and biosensors: optical nano- and microsystems for bioanalytics. Springer, New York, NY, pp 83–99
60. Martinez E, Samitier J (2011) Soft lithography and variants. In: Del Campo A, Arzt E (eds) Generating micro- and nanopatterns on polymeric materials. Wiley-VCH, Weinheim, pp 57–68
61. Duan X, Reinhoudt DN, Huskens J (2011) Soft lithography for patterning self-assembling systems. In: Samori P, Cacialli F (eds) Functional supramolecular architectures, vol 1. Wiley, New York, NY, pp 343–369
62. Wolfe DB, Qin D, Whitesides GM (2010) Rapid prototyping of microstructures by soft lithography for biotechnology, vol 583, Methods in molecular biology: microengineering in biotechnology. Humana Press, Totowa, NJ, pp 81–107
63. Mele E, Pisignano D (2009) Nanobiotechnology: soft lithography, vol 47, Progress in molecular and subcellular biology: biosilica in evolution, morphogenesis, and nanobiotechnology. Springer, Berlin, pp 341–358
64. Svancara I, Prior C, Hocevar SB, Wang J (2010) A decade with bismuth-based electrodes in electroanalysis. Electroanalysis 22:1405–1420
65. Pauliukaite R, Metelka R, Svancara I, Krolicka A, Bobrowski A, Norkus E, Kalcher K, Vytras K (2004) Screen-printed carbon electrodes bulk-modified with Bi_2O_3 or Sb_2O_3 for trace determination of some heavy metals. Sci Pap Univ Pardubice A10:47–58
66. Bobrowski A, Kalcher K, Kurowska K (2009) Microscopic and electrochemical characterization of lead film electrode applied in adsorptive stripping analysis. Electrochim Acta 54:7214–7221
67. Boyer A, Kalcher K, Pietsch R (1990) Voltammetric behavior of perborate on Prussian blue modified carbon paste electrodes. Electroanalysis 2:155–161
68. Schachl K, Alemu H, Kalcher K, Jezkova J, Svancara I, Vytras K (1997) Flow-injection determination of hydrogen peroxide using a carbon paste electrode modified with a manganese dioxide film. Anal Lett 30:2655–2673
69. Schab-Balcerzak E (ed) (2011) Electropolymerization. InTech Open, Rijeka, Croatia, Open access book
70. Li H-L, Zhang X-G (2012) Electropolymerization at metal surfaces. In: Somasundaran P (ed) Encyclopedia of surface and colloid science, 2nd edn. CRC Press, Taylor & Francis, Boca Raton, FL, pp 2385–2401

71. Harris PJF (2011) Carbon nanotube science: synthesis, properties and applications. Cambridge University Press, Cambridge
72. Vorotyntsev MA, Zinovyeva VA, Konev DV (2010) Mechanisms of electropolymerization and redox activity: fundamental aspects. In: Cosnier S, Karyakin A (eds) Electropolymerization. InTech Open, Rijeka, Croatia, pp 27–50
73. Nicolas M (2008) Fabrication of superhydrophobic surfaces by electropolymerization of thiophene and pyrrole derivatives. J Adhes Sci Technol 22(3–4):365–377
74. Advincula R, Xia C, Onishi K, Tarenekar P, Deng S, Baba A, Knoll W (2002) Conjugated polymer network ultrathin films by electropolymerization of precursor polymers: polymer design, characterization strategies, and devices. Polym Prepr 43(2):514–515
75. Sabouraud G, Sadki S, Brodie N (2000) The mechanisms of pyrrole electropolymerization. Chem Soc Rev 29(5):283–293
76. Imisides MD, John R, Riley PJ, Wallace GG (1991) The use of electropolymerization to produce new sensing surfaces: a review emphasizing electrodeposition of heteroaromatic compounds. Electroanalysis 3(9):879–889
77. Adamcova Z, Dempirova L (1989) Film-forming electropolymerization. Prog Org Coat 16(4):295–320
78. Jansson U, Lewin E (2013) Sputter deposition of transition-metal carbide films - a critical review from a chemical perspective. Thin Solid Films 536:1–24
79. Kelly PJ, Arnell RD (2000) Magnetron sputtering: a review of recent developments and applications. Vacuum 56:159–172
80. Vasudev MC, Anderson KD, Bunning TJ, Tsukruk VV, Naik RR (2013) Exploration of plasma-enhanced chemical vapor deposition as a method for thin-film fabrication with biological applications. ACS Appl Mater Interfaces 5(10):3983–3994
81. Jourdain V, Bichara C (2013) Current understanding of the growth of carbon nanotubes in catalytic chemical vapour deposition. Carbon 58:2–39
82. Nguyen JJ, Turano S, Ready WJ (2012) The synthesis of carbon nanotubes grown on metal substrates. Nanosci Nanotechnol Lett 4(12):1123–1131
83. Lubej M, Plazl I (2012) Theoretical descriptions of carbon nanotubes synthesis in a chemical vapor deposition reactor. Chem Biochem Eng Q 26(3):277–284
84. Ayre GN, Uchino T, Mazumder B, Hector AL, Smith DC, Ashburn P, de Groot CH, Hutchison JL (2010) Chemical vapour deposition of CNTs using structural nanoparticle catalysts. In: Marulanda JM (ed) Carbon nanotubes, 1st edn. InTech Open, Rijeka, Croatia, pp 19–38, online book
85. Robertson J, Zhong G, Esconjauregui S, Zhang C, Fouquet M, Hofmann S (2012) Chemical vapor deposition of carbon nanotube forests. Phys Stat Sol B Bas Sol State Phys 249 (12):2315–2322
86. Zhang Y, Zhang L, Zhou C (2013) Review of chemical vapor deposition of graphene and related applications. Acc Chem Res 46(10):2329–2339
87. Chen X, Chen G (2011) Fabrication and application of Ti/BDD for wastewater treatment. In: Brillas E, Martinez-Huitle CA (eds) Synthetic diamond films, 1st edn. Wiley, Weinheim, pp 353–371
88. Luong JHT, Male KB, Glennon JD (2009) Boron-doped diamond electrode: synthesis, characterization, functionalization and analytical applications. Analyst 134(10):1965–1979
89. Pinault M-A, Barjon J, Kociniewski T, Jomard F, Chevallier J (2007) The n-type doping of diamond: present status and pending questions. Phys B Condens Matter 401–402:51–56
90. Nebel CE, Rezek B, Shin D, Uetsuka H, Yang N (2007) Diamond for bio-sensor applications. J Phys D Appl Phys 40(20):6443–6466
91. Kraft A (2007) Doped diamond electrodes. New trends and developments. Jahrbuch Oberflaechentechnik 63:85–95
92. Goto T (2012) Chemical vapor deposition of structural ceramics and composites. In: Bansal NP, Boccaccini AR (eds) Ceramics and composites processing methods, 1st edn. Wiley, Hoboken, NJ, pp 271–312

93. Bekermann D, Barreca D, Gasparotto A, Maccato C (2012) Multi-component oxide nanosystems by chemical vapor deposition and related routes: challenges and perspectives. CrystEngComm 14(20):6347–6358
94. Jackson TJ, Palmer SB (1994) Oxide superconductor and magnetic metal thin film deposition by pulsed laser ablation: a review. J Phys D Appl Phys 27:1581
95. Izumi T (2007) Metal organic deposition of YBCO films; high Ic and long-length results. In: Paranthaman MP, Selvamanickam V (eds) Flux pinning and ac loss studies on YBCO coated conductors, 1st edn. Nova Publishers, Hauppauge, NY, pp 153–169
96. Miikkulainen V, Leskela M, Ritala M, Puurunen RL (2013) Crystallinity of inorganic films grown by atomic layer deposition: overview and general trends. J Appl Phys 113(2):021301/1–021301/101
97. Lee BH, Yoon B, Abdulagatov AI, Hall RA, George SM (2013) Growth and properties of hybrid organic-inorganic metalcone films using molecular layer deposition techniques. Adv Func Mater 23(5):532–546
98. Pinna N, Knez M (eds) (2011) Atomic layer deposition of nanostructured materials, 1st edn. Wiley-VCH, Weinheim
99. Pulsipher A, Yousaf MN (2011) Self-assembled monolayers as dynamic model substrates for cell biology, vol 240, Advances in polymer science: bioactive surfaces. Springer, Berlin, pp 103–134
100. Koepsel JT, Murphy WL (2012) Patterned self-assembled monolayers: efficient, chemically defined tools for cell biology. ChemBioChem 13(12):1717–1724
101. Hudalla GA, Murphy WL (2011) Chemically well-defined self-assembled monolayers for cell culture: toward mimicking the natural ECM. Soft Matter 7(20):9561–9571
102. Prashar D (2012) Self assembled monolayers - a review. Int J ChemTech Res 4(1):258–265
103. Hagelberg F (2011) Self-assembled monolayers. In: Sattler KD (ed) Handbook of nanophysics, vol 5, 1st edn. CRC Press, Boca Raton, FL, pp 17/1–17/20
104. Jamison AC, Chinwangso P, Lee TR (2011) Self-assembled monolayers: the development of functional nanoscale films. In: Knoll W, Advincula RC (eds) Functional polymer films, vol 1, 1st edn. Wiley-VCH, Weinheim, pp 151–217
105. Mandler D, Kraus-Ophir S (2011) Self-assembled monolayers (SAMs) for electrochemical sensing. J Solid State Electrochem 15(7–8):1535–1558
106. Weddemann A, Ennen I, Regtmeier A, Albon C, Wolff A, Eckstaedt K, Mill N, Peter MK-H, Mattay J, Plattner C, Sewald N, Hütten A (2010) Review and outlook: from single nanoparticles to self-assembled monolayers and granular GMR sensors. Beilstein J Nanotechnol 1:75–93
107. Samanta D, Sarkar A (2011) Immobilization of bio-macromolecules on self-assembled monolayers: methods and sensor applications. Chem Soc Rev 40(5):567–2592
108. Azzaroni O, Salvarezza RC (2012) Chemisorbed self-assembled monolayers. In: Gale PA, Steed JW (eds) Supramolecular chemistry: from molecules to nanomaterials, vol 7, 1st edn. Wiley, London, pp 3445–3461
109. Pensa E, Cortes E, Corthey G, Carro P, Vericat C, Fonticelli MH, Benitez G, Rubert AAA, Salvarezza RC (2012) The chemistry of the sulfur-gold interface: in search of a unified model. Acc Chem Res 45(8):1183–1192
110. Pieters G, Prins LJ (2012) Catalytic self-assembled monolayers on gold nanoparticles. New J Chem 36(10):1931–1939
111. Jadhav SA (2011) Self-assembled monolayers (SAMs) of carboxylic acids: an overview. Cent Eur J Chem 9(3):369–378
112. Gooding JJ, Ciampi S (2011) The molecular level modification of surfaces: from self-assembled monolayers to complex molecular assemblies. Chem Soc Rev 40(5):2704–2718
113. Srisombat L, Jamison AC, Lee TR (2011) Stability: a key issue for self-assembled monolayers on gold as thin-film coatings and nanoparticle protectants. Colloids Surf A Physicochem Eng Asp 390(1–3):1–19

114. Chinwangso P, Jamison AC, Lee TR (2011) Multidentate adsorbates for self-assembled monolayer films. Acc Chem Res 44(7):511–519
115. Ammam M (2013) Polyoxometalates: formation, structures, principal properties, main deposition methods and application in sensing. J Mater Chem A Mater Energ Sust 1(21):6291–6312
116. Yakhmi JV, Saxena V, Aswal DK (2012) Conducting polymer sensors, actuators and field-effect transistors. In: Banerjee S, Tyagi AK (eds) Functional materials: preparation, processing and applications, 1st edn. Elsevier, Amsterdam, pp 61–110
117. Giancane G, Valli L (2012) State of art in porphyrin Langmuir-Blodgett films as chemical sensors. Adv Colloid Interface Sci 171–172:17–35
118. Singh A, Debnath AK, Aswal DK, Joshi A, Samanta S, Saxena V, Gupta SK, Yakhmi JV (2010) Organic semiconductor films for chemiresistor sensors. In: Aswal DK, Yakhmi JV (eds) Molecular and organic electronics devices, 1st edn. Nova Science Pub Inc., Hauppauge, NY, pp 367–402
119. Pavinatto FJ, Caseli L, Oliveira ON Jr (2010) Chitosan in nanostructured thin films. Biomacromolecules 11(8):1897–1908
120. Ram MK, Yavuz O, Aldissi M (2010) Conducting polymer nanocomposite membrane as chemical sensors. In: Ram MK, Bhethanabotla VR (eds) Sensors for chemical and biological applications, 1st edn. CRC Press, Boca Raton, FL, pp 43–72
121. Pastorino L, Erokhina S (2011) Protein thin films: sensing elements for sensors. In: Lim T-K (ed) Nanosensors, 1st edn. CRC Press, Boca Raton, FL, pp 97–168
122. Seshan K (2012) Handbook of thin film deposition, 3rd edn. Elsevier, Amsterdam
123. Sato K, Takahashi S, Anzai J (2012) Layer-by-layer thin films and microcapsules for biosensors and controlled release. Anal Sci 28(10):929–938
124. Oliveira ON Jr, Aoki PHB, Pavinatto FJ, Constantino CJL (2012) Controlled architectures in LbL films for sensing and biosensing. In: Decher G, Schlenoff JB (eds) Multilayer thin films, vol 2, 2nd edn. Wiley, Weinheim, pp 951–983
125. Ariga K, Ji Q, Hill JP (2012) Novel multilayer thin films: hierarchic layer-by-layer (Hi-LbL) assemblies. In: Decher G, Schlenoff JB (eds) Multilayer thin films, vol 1, 2nd edn. Wiley, Weinheim, pp 69–81
126. Du N, Zhang H, Yang D (2012) One-dimensional hybrid nanostructures: synthesis via layer-by-layer assembly and applications. Nanoscale 4(18):5517–5526
127. Ariga K, Ji Q, McShane MJ, Lvov YM, Vinu A, Hill JP (2012) Inorganic nanoarchitectonics for biological applications. Chem Mater 24(5):728–737
128. Takahashi S, Sato K, Anzai J (2012) Layer-by-layer construction of protein architectures through avidin-biotin and lectin-sugar interactions for biosensor applications. Anal Bioanal Chem 402(5):1749–1758
129. Zhou M, Dong S (2011) Bioelectrochemical interface engineering: toward the fabrication of electrochemical biosensors, biofuel cells, and self-powered logic biosensors. Acc Chem Res 44(11):1232–1243
130. de Villiers MM, Otto DP, Strydom SJ, Lvov YM (2011) Introduction to nanocoatings produced by layer-by-layer (LbL) self-assembly. Adv Drug Deliv Rev 63(9):701–715
131. Evtugyn GA, Hianik T (2011) Layer-by-layer polyelectrolyte assembles involving DNA as a platform for DNA sensors. Curr Anal Chem 7(1):8–34
132. Kotov N (2011) Tunable nanocomposites: combining properties for ultrastrong materials and environmental sensors to neural implants. PMSE Prepr 104:178
133. Aurobind SV, Amirthalingam KP, Gomathi H (2006) Sol-gel based surface modification of electrodes for electro analysis. Adv Colloid Interface Sci 121(1–3):1–7
134. Livage J (2004) Basic principles of sol-gel chemistry. In: Aegerter MA, Mennig M (eds) Sol-gel technologies for glass producers and users. Kluwer Academic Publishers, Boston, MA, pp 3–14
135. Mentruit MP, Palomino GT, Arean CO (2001) The alkoxide sol-gel route to high-surface-area metal oxides. Trend Inorg Chem 7:1–14

136. Francis LF (1999) Sol-gel methods for oxide coatings, vol 13, Materials engineering: intermetallic and ceramic coatings. CRC Press, Boca Raton, FL, pp 31–82
137. Livage J (1998) Smart thin films via the sol-gel route. In: Prasad PN (ed) Science and technology of polymers and advanced materials: emerging technologies and business opportunities. Plenum Press, New York, NY, pp 649–662, Proceedings of the International Conference on Frontiers of Polymers and Advanced Materials, 4th, Cairo
138. Han Y-L (2013) Aerogel materials for aerospace. In: Zhang S, Zhao D (eds) Aerospace materials handbook, 1st edn. CRC Press, Boca Raton, FL, pp 699–743
139. Riffat SB, Qiu G (2013) A review of state-of-the-art aerogel applications in buildings. Int J Low Carbon Tech 8(1):1–6
140. Tian HY, Buckley CE, Paskevicius M, Sheppard DA (2013) Hydrogen storage in carbon aerogels. In: Terranova ML, Orlanducci S, Rossi M (eds) Carbon nanomaterials for gas adsorption, 1st edn. Pan Stanford Publishing, Singapore, pp 131–160
141. Aegerter MA, Leventis N, Koebel MM (eds) (2011) Aerogels handbook, 1st edn. Springer, New York, NY
142. Gerlach G, Arndt KF (eds) (2012) Hydrogel sensors and actuators: engineering and technology, vol 6, 1st edn, Springer series on chemical sensors and biosensors. Springer, New York, NY
143. Luh XJ, Scherman OA (eds) (2013) Polymeric and self assembled hydrogels: from fundamentals understanding to applications, 1st edn. RSC Publishing, Cambridge
144. Stein DB (ed) (2010) Handbook of hydrogels: properties, preparation & applications, 1st edn. Nova Science Pub, Inc., Hauppauge, NY
145. Hapiot F, Menuel S, Monflier E (2013) Thermoresponsive hydrogels in catalysis. ACS Catal 3(5):1006–1010
146. Passauer L (2012) Highly swellable lignin hydrogels: novel materials with interesting properties, vol 1107, ACS symposium series: functional materials from renewable sources. ACS, Washington, DC, pp 211–228
147. Fujiwara T (2012) Thermo-responsive gels: biodegradable hydrogels from enantiomeric copolymers of poly(lactide) and poly(ethylene glycol), vol 1114, ACS symposium series: degradable polymers and materials. ACS, Washington, DC, pp 287–311
148. Lyon LA, Serpe MJ (eds) (2012) Hydrogel micro and nanoparticles, 1st edn. Wiley-VCH, Weinheim
149. Zhang H, Zhang F, Wu J (2013) Physically crosslinked hydrogels from polysaccharides prepared by freeze-thaw technique. React Funct Polym 73(7):923–928
150. Buenger D, Topuz F, Groll J (2012) Hydrogels in sensing applications. Prog Polym Sci 37 (12):1678–1719
151. Roy N, Saha N, Jelinkova L, Saha P, Saha T (2012) Smart hydrogels. Plasty a Kaucuk 49 (3–4):73–80
152. Appel EA, del Barrio J, Loh X, Jun S, Oren A (2012) Supramolecular polymeric hydrogels. Chem Soc Rev 41(18):6195–6214
153. Uliniuc A, Popa M, Hamaide T, Dobromir M (2012) New approaches in hydrogel synthesis-click chemistry: a review. Cell Chem Technol 46(1–2):1–11
154. Hu J, Zhang G, Liu S (2012) Enzyme-responsive polymeric assemblies, nanoparticles and hydrogels. Chem Soc Rev 41(18):5933–5949
155. Egawa Y, Seki T, Takahashi S, Anzai J (2011) Electrochemical and optical sugar sensors based on phenylboronic acid and its derivatives. Mater Sci Eng C Mater Biol Appl 31 (7):1257–1264
156. Liu J (2011) Oligonucleotide-functionalized hydrogels as stimuli responsive materials and biosensors. Soft Matter 7(15):6757–6767
157. Khaleque T, Abu-Salih S, Saunders JR, Moussa W (2011) Experimental methods of actuation, characterization and prototyping of hydrogels for BioMEMS/NEMS applications. J Nanosci Nanotechnol 11(3):2470–2479

158. Yang Q, Adrus N, Tomicki F, Ulbricht M (2011) Composites of functional polymeric hydrogels and porous membranes. J Mater Chem 21(9):2783–2811
159. Minko S (2010) Stimuli-responsive thin hydrogel films and membranes. Smart polymer systems 2010, 1st International Conference, Atlanta, GA, May 5–6, 2010
160. Ikeda M, Ochi R, Hamachi I (2010) Supramolecular hydrogel-based protein and chemosensor array. Lab Chip 10(24):3325–3334
161. Lin D, Che J (2010) Hydrogel-modified bio-electrodes. Huaxue Jinzhan 22(6):1195–1202
162. Ju XJ, Chu LY (2009) Temperature-sensitive hydrogels with molecule-recognition properties. Handbook of Hydrogels. Nova Science Pub, Inc., Hauppauge, NY, pp 649–662
163. Richter A (2009) Hydrogels for actuators, vol 6, Springer series on chemical sensors and biosensors: hydrogel sensors and actuators. Springer, New York, NY, pp 221–248
164. Urban GA, Weiss T (2009) Hydrogels for biosensors, vol 6, Springer series on chemical sensors and biosensors: hydrogel sensors and actuators. Springer, New York, NY, pp 197–220
165. Bianco P (2002) Protein modified- and membrane electrodes: strategies for the development of biomolecular sensors. Rev Mol Biotechnol 82(4):393–409
166. Lobo-Castanon MJ, Alvarez-Crespo SL, Alvarez-Gonzalez MI, Saidman SB, Miranda-Ordieres AJ, Tunon-Blanco P (1998) Biosensors based on carbon paste electrodes using immobilized dehydrogenase enzymes. an overview and trends. Sci Pap Univ Pardubice Ser A Fac Chem Tech 3:17–29
167. Zhiwei Z, Helong J (2010). Enzyme-based electrochemical biosensors, biosensors. In: Serra PA (ed.), ISBN: 978-953-7619-99-2, InTech, available from: http://www.intechopen.com/books/biosensors/enzyme-based-electrochemical-biosensors
168. Chen LY, Gu BX, Zhu GP, Wu YF, Liu SQ, Xu CX (2008) Electron transfer properties and electrocatalytic behavior of tyrosinase on ZnO nanorod. J Electroanal Chem 617:7–13
169. Lu XB, Zhang HJ, Ni YW, Zhang Q, Chen JP (2008) Porous nanosheet-based ZnO microspheres for the construction of direct electrochemical biosensors. Biosens Bioelectron 24:93–98
170. Umar A, Rahman MM, Al-Hajry A, Hahn YB (2009) Highly-sensitive cholesterol biosensor based on well-crystallized flower-shaped ZnO nanostructures. Talanta 78:284–289
171. Umar A, Rahman MM, Kim SH, Hahn YB (2008) ZnO nanonails: synthesis and their application as glucose biosensor. J Nanosci Nanotechnol 8:3216–3221
172. Umar A, Rahman MM, Vaseem M, Hahn YB (2009) Ultra-sensitive cholesterol biosensor based on low-temperature grown ZnO nanoparticles. Electrochem Commun 11:118–121
173. Wang JX, Sun XW, Wei A, Lei Y, Cai XP, Li CM, Dong ZL (2006) Zinc oxide nanocomb biosensor for glucose detection. Appl Phys Lett 88:233106
174. Wang YT, Yu L, Zhu ZQ, Zhang J, Zhu JZ (2009) Novel uric acid sensor based on enzyme electrode modified by ZnO nanoparticles and multiwall carbon nanotubes. Anal Lett 42:775–789
175. Weber J, Jeedigunta S, Kumar A (2008) Fabrication and characterization of ZnO nanowire arrays with an investigation into electrochemical sensing capabilities. J Nanomater 2008:638523
176. Wei A, Sun XW, Wang JX, Lei Y, Cai XP, Li CM, Dong ZL, Huang W (2006) Enzymatic glucose biosensor based on ZnO nanorod array grown by hydrothermal decomposition. Appl Phys Lett 89:123902
177. Zhang FF, Wang XL, Ai SY, Sun ZD, Wan Q, Zhu ZQ, Xian YZ, Jin LT, Yamamoto K (2004) Immobilization of uricase on ZnO nanorods for a reagentless uric acid biosensor. Anal Chim Acta 519:155–160
178. Caruso F, Niikura K, Furlong DN, Okahata Y (1997) Assembly of alternating polyelectrolyte and protein multilayer films for immune sensing. Langmuir 13:3427–3433
179. Decher G, Hong JD, Schmitt J (1992) Buildup of ultrathin multilayer films by a self assembly process: III. Consecutively alternating adsorption of anionic and cationic polyelectrolytes on charged surfaces. Thin Solid Films 210–211:831–835

180. Du D, Chen SZ, Cai J, Zhang AD (2008) Electrochemical pesticide sensitivity test using acetylcholinesterase biosensor based on colloidal gold nanoparticle modified sol-gel interface. Talanta 74:766–772
181. He JA, Samuelson L, Li L, Kumar J, Tripathi SK (1998) Oriented bacteriorhodopsin/polycation multilayers by electrostatic layer-by-layer assembly. Langmuir 14:1674–1679
182. Lvov Y, Decher G, Moehwald H (1993) Assembly, structural characterization, and thermal behavior of layer-by-layer deposited ultrathin films of poly(vinyl sulfate) and poly (allylamine). Langmuir 9:481–486
183. Yang WW, Wang JX, Zhao S, Sun YY, Sun CQ (2006) Multilayered construction of glucose oxidase and gold nanoparticles on Au electrodes based on layer-by-layer covalent attachment. Electrochem Commun 8:665–672
184. Mendes RK, Carvalhal RF, Kubota LT (2008) Effects of different self-assembled monolayers on enzymeimmobilization procedures in peroxidase-based biosensor development. J Electroanal Chem 612(2):164–172
185. Ferretti S, Paynter S, Russell DA, Sapsford KE, Richardson DJ (2000) Self-assembled monolayers: a versatile tool for the formulation of bio-surfaces. TrAC Trends Anal Chem 19(9):530–540
186. Lin Y, Yantasee W, Wang J (2005) Carbon nanotubes (CNTs) for the development of electrochemical biosensors. Front Biosci 10(1):492–505
187. Karra S, Zhang M, Gorski W (2013) Electrochemistry and current control in surface films based on silica-azure redox nanoparticles, carbon nanotubes, enzymes, and polyelectrolytes. Anal Chem 85(2):1208–1214
188. Noroozifar M, Khorasani-Motlagh M, Tavakkoli H (2013) Electrochemical determination of ascorbic acid using modified glassy carbon electrode by multiwall carbon nanotube-nafion in chloroacetic acid media. Asian J Chem 25(1):119–124
189. Marzuki N, Abu Bakar F, Salleh AB, Heng LY, Yusof NA, Siddiquee S (2012) Electrochemical biosensor immobilization of formaldehyde dehydrogenase with nafion for determination of formaldehyde from Indian mackerel (Rastrelliger kanagurta) fish. Curr Anal Chem 8(4):534–542
190. Rather JA, Pilehvar S, De Wael K (2013) A biosensor fabricated by incorporation of a redox mediator into a carbon nanotube/nafion composite for tyrosinase immobilization: detection of matairesinol, an endocrine disruptor. Analyst 138(1):204–210
191. Ruan C, Li T, Ju X, Liu H, Lou J, Gao W, Sun W (2012) Nafion-ZrO_2 nanoparticle-ionic liquid nanobiocomposite for the direct electrochemistry of myoglobin. J Solid State Electrochem 16(11):3661–3666
192. Atta NF, Galal A, Azab SM (2012) Novel sensor based on carbon paste/nafion modified with gold nanoparticles for the determination of glutathione. Anal Bioanal Chem 404 (6–7):1661–1672
193. Marzuki NI, Abu Bakar F, Salleh AB, Heng LY, Yusof NA, Siddiquee S (2012) Development of electrochemical biosensor for formaldehyde determination based on immobilized enzyme. Int J Electrochem Sci 7(7):6070–6083
194. Teles FRR, Fonseca LP (2008) Applications of polymers for biomolecule immobilization in electrochemical biosensors. Mater Sci Eng C Biomim Supramol Syst 28:1530–1543
195. William RH (1993) Biosensors based on polymer networks formed gamma irradiation crosslinking. Appl Biochem Biotechnol 41(1–2):87–97
196. Gade VK, Shirale DJ, Gaikwad PD, Savale PA, Kakde KP, Kharat HJ, Shirsat MD (2006) Immobilization of GOD on electrochemically synthesized Ppy-PVS composite film by crosslinking via glutaraldehyde for determination of glucose. React Funct Polym 66:1420–1426
197. Sassolas A, Blum LJ, Leca-Bouvier BD (2012) Immobilization strategies to develop enzymatic biosensors. Biotechnol Adv 30(3):489–511
198. Gao Y, Fu X, Wu D (2008) Immobilization method of enzyme in biosensor. Shandong Huagong 37(4):21–22

199. Wang J (2006) Electrochemical biosensors: towards point-of-care cancer diagnostics. Biosens Bioelectron 21(10):1887–1892
200. Khezrian S, Salimi A, Teymourian H, Hallaj R (2013) Label-free electrochemical IgE aptasensor based on covalent attachment of aptamer onto multiwalled carbon nanotubes/ionic liquid/chitosan nanocomposite modified electrode. Biosens Bioelectron 43:218–225
201. Kim JH, Jin J-H, Lee J-Y, Park EJ, Min NK (2012) Covalent attachment of biomacromolecules to plasma-patterned and functionalized carbon nanotube-based devices for electrochemical biosensing. Bioconjug Chem 23(10):2078–2086
202. Matsumura H, Ortiz R, Ludwig R, Igarashi K, Samejima M, Gorton L (2012) Direct electrochemistry of phanerochaete chrysosporium cellobiose dehydrogenase covalently attached onto gold nanoparticle modified solid gold electrodes. Langmuir 28 (29):10925–10933
203. Yusof NA (2012) Electrochemical DNA biosensor based on poly(allylamine hydrochloride) modified screen printed electrode. Asian J Chem 24(2):518–522
204. Dursun F, Ozoner SK, Demirci A, Gorur M, Yilmaz F, Erhan E (2012) Vinylferrocene copolymers based biosensors for phenol derivatives. J Chem Technol Biotechnol 87(1):95–104
205. Santiago-Rodriguez L, Mendez J, Flores-Fernandez GM, Pagan M, Rodriguez-Martinez JA, Cabrera CR, Griebenow K (2011) Enhanced stability of a nanostructured cytochrome c biosensor by PEGylation. J Electroanal Chem 663(1):1–7
206. Uygun ZO, Sezgintuerk MK (2011) A novel, ultra sensible biosensor built by layer-by-layer covalent attachment of a receptor for diagnosis of tumor growth. Anal Chim Acta 706 (2):343–348
207. Makowski MS, Zemlyanov DY, Lindsey JA, Bernhard JC, Hagen EM, Chan BK, Petersohn AA, Medow MR, Wendel LE, Chen D (2011) Covalent attachment of a peptide to the surface of gallium nitride. Surf Sci 605(15–16):1466–1475
208. Sun Y, Ren Q, Qin Y, Shang Z (2011) Amino-functionalization of multi-wall carbon nanotubes and their used in electrochemical glucose sensors. Huaxue Yanjiu Yu Yingyong 23(2):165–172
209. Kim BC, Zhao X, Ahn H-K, Kim JH, Lee H-J, Kim KW, Nair S, Hsiao E, Jia H, Oh M-K (2011) Highly stable enzyme precipitate coatings and their electrochemical applications. Biosens Bioelectron 26(5):1980–1986
210. Kolb HC, Finn MG, Sharpless KB (2001) Click chemistry: diverse chemical function from a few good reactions. Angew Chem Int Ed 40(11):2004–2021
211. Palomo JM (2013) Click-chemistry in biocatalysis. Curr Org Chem 17(7):691–700
212. Wu M, Zhang H, Wang Z, Shen S, Le XC, Li X-F (2013) "One-pot" fabrication of clickable monoliths for enzyme reactors. Chem Commun 49(14):1407–1409
213. Celebi B, Bayraktar A, Tuncel A (2012) Synthesis of a monolithic, micro-immobilized enzyme reactor via click-chemistry. Anal Bioanal Chem 403(9):2655–2663
214. Hayat A, Marty J-L, Radi A-E (2012) Novel amperometric hydrogen peroxide biosensor based on horseradish peroxidase azide covalently immbilized on ethynyl-modified screen-printed carbon electrode via click chemistry. Electroanalysis 24(6):1446–1452
215. Ansari SA, Husain Q (2012) Potential applications of enzymes immobilized on/in nano materials: a review. Biotechnol Adv 30(3):512–523
216. Chen Y, Wu M, Wang K, Chen B, Yao S, Zou H, Nie L (2011) Vinyl functionalized silica hybrid monolith-based trypsin microreactor for on line digestion and separation via thiol-ene "click" strategy. J Chromatogr A 1218(44):7982–7988
217. Ran Q, Peng R, Liang C, Ye S, Xian Y, Zhang W, Jin L (2011) Direct electrochemistry of horseradish peroxidase immobilized on electrografted 4-ethynylphenyl film via click chemistry. Anal Chim Acta 697(1–2):27–31

218. Ran Q, Peng R, Liang C, Ye S, Xian Y, Zhang W, Jin L (2011) Covalent immobilization of horseradish peroxidase via click chemistry and its direct electrochemistry. Talanta 83(5):1381–1385
219. Xie T, Wang A, Huang L, Li H, Chen Z, Wang Q, Yin X (2009) Recent advance in the support and technology used in enzyme immobilization. Afr J Biotechnol 8(19):4724–4733
220. Gole A, Murphy CJ (2008) Azide-derivatized gold nanorods: functional materials for "click" chemistry. Langmuir 24(1):266–272
221. Shoichet MS, Yuan Y, Shi M, Wosnick, Jordan (2007) Method of biomolecule immobilization on polymers using click-type chemistry. PCT Int. Appl. (2007), WO 2007003054 A1 20070111
222. Canalle LA, Vong T, Adams P, Hans HM, van Delft FL, Raats Jos MH, Chirivi Renato GS, van Hest Jan CM (2011) Clickable enzyme-linked immunosorbent assay. Biomacromolecules 12(10):3692–3697
223. Heineman WR, Seliskar CJ, Morris LK, Bryan SA (2012) Proceedings of SPIE, 8545, Optical materials and biomaterials in security and defence systems technology IX, 26–27 September 2012, Edinburgh, UK, ISBN: 854509/1-854509/13
224. Wan Y, Xu H, Su Y, Zhu X, Song S, Fan C (2013) A surface-initiated enzymatic polymerization strategy for electrochemical DNA sensors. Biosens Bioelectron 41:526–531
225. Mehenni H (2012) Development of an avidin sensor based on the poly(methoxy amino-β-styryl terthiophene)-coated glassy carbon electrode. Can J Chem 90(3):271–277
226. Mehenni H, Dao LH (2012) Towards the development of a direct electrochemical biodetector of avidin based on the poly(chloro amino-β-styryl terthiophene)-coated glassy carbon electrode. Aust J Chem 65(4):395–401
227. Kuramitz H, Mawatari Y, Ikeuchi M, Kutomi O, Hata N, Taguchi S, Sugawara K (2012) Multiplexed assay for proteins based on sequestration electrochemistry using the protein binding electroactive magnetic microbeads. Anal Sci 28(1):77–81
228. Hong C, Yuan R, Chai Y, Zhuo Y, Yang X (2012) A strategy for signal amplification using an amperometric enzyme immunosensor based on HRP modified platinum nanoparticles. J Electroanal Chem 664:20–25
229. Deng T, Cao Z, Shen G (2011) A novel electrochemical impedance biosensor based on plasma-polymerized films for detection of biotin, vol 239–242, Advanced materials research: Pt. 2, Advanced materials. Trans Tech, Switzerland, pp 1653–1656
230. Chung D-J, Kim K-C, Choi S-H (2011) Electrochemical DNA biosensor based on avidin-biotin conjugation for influenza virus (type A) detection. Appl Surf Sci 257(22):9390–9396
231. Timalsina YP, Branen J, Aston DE, Noren K, Corti G, Schumacher RM, David N (2011) Alternating current impedance spectroscopic analysis of biofunctionalized vertically-aligned silica nanospring surface for biosensor applications. J Appl Phys 110(1):014901/1–014901/8
232. Olowu RA, Ndangili PM, Baleg AA, Ikpo CO, Njomo N, Baker P, Iwuoha E (2011) Spectroelectrochemical dynamics of dendritic poly(propyleneimine)-polythiophene star copolymer aptameric 17β-estradiol biosensor. Int J Electrochem Sci 6(5):1686–1708
233. Dubuisson E, Chibane A, Grangeat P, Mailley P (2009) Electrochemical DNA-hybridisation detection via enzymatic amplification at microelectrode array modified with polypyrrole-oligonucleotide films. Sens Lett 7(5):880–887
234. Haddad R, Cosnier S, Maaref A, Holzinger M (2009) Non-covalent biofunctionalization of single-walled carbon nanotubes via biotin attachment by π-stacking interactions and pyrrole polymerization. Analyst 134(12):2412–2418
235. Kuramitz H, Piruska A, Halsall HB, Seliskar CJ, Heineman WR (2008) Simultaneous multiselective spectroelectrochemical sensing of the interaction between protein and its ligand using the redox dye nile blue as a label. Anal Chem 80(24):9642–9648
236. Suprun E, Shumyantseva V, Bulko T, Rachmetova S, Rad'ko S, Bodoev N, Archakov A (2008) Au-nanoparticles as an electrochemical sensing platform for aptamer-thrombin interaction. Biosens Bioelectron 24(4):825–830

237. Shiddiky MJA, Rahman MA, Cheol CS, Shim YB (2008) Fabrication of disposable sensors for biomolecule detection using hydrazine electrocatalyst. Anal Biochem 379(2):170–175
238. Fang L, Lue Z, Wei H, Wang E (2008) Quantitative electrochemiluminescence detection of proteins: avidin-based sensor and tris(2,2′-bipyridine) ruthenium(II) label. Biosens Bioelectron 23(11):1645–1651
239. Huang X, Du D, Gong X, Cai J, Tu H, Xu X, Zhang A (2008) Composite assembly of silver nanoparticles with avidin and biotinylated AChE on gold for the pesticidal electrochemical sensing. Electroanalysis 20(4):402–409
240. Wang B, Du X, Zheng J, Jin B (2005) Electrochemical sensor based on immobilization of single stranded deoxyribonucleic acid on Pt electrode surface by avidin-biotin system. Fenxi Huaxue 33(6):789–792
241. Hoshi T, Hiwatashi Y, Anzai JI (2004) Electrochemical deposition of avidin with ascorbate oxidase on the surface of platinum electrodes for amperometric glucose sensors. ITE Lett Batt New Technol Med 5(6):552–555
242. Kizek R, Vacek J, Trnkova L, Klejdus B, Kuban V (2003) Electrochemical biosensors in agricultural and environment. Chem List 97(10):1003–1006
243. Hoshi T, Anzai JI, Osa T (1994) Electrochemical deposition of avidin on the surface of a platinum electrode for enzyme sensor applications. Anal Chim Acta 289(3):321–327
244. Anzai JI, Hoshi T, Osa T (1993) Electrochemical preparation of active avidin films for enzyme sensor applications. Chem Lett 7:1231–1234
245. Iqbal N, Lieberzeit PA (2012) Artificial receptors for mass-sensitive sensors: targeting analytes from surfaces, nanoparticles, and bioanalytes by molecular imprinting. In: Li S (ed) Molecularly imprinted sensors: overview and applications, 1st edn. Elsevier, Amsterdam, pp 195–235
246. Tan J, Yan XP (2012) Discrimination of analytes with fluorescent molecular imprinting sensor arrays. In: Li S (ed) Molecularly Imprinted sensors: overview and applications, 1st edn. Elsevier, Amsterdam, pp 161–173
247. Salian VD, Byrne ME (2013) Living radical polymerization and molecular imprinting: improving polymer morphology in imprinted polymers. Macromol Mater Eng 298(4):379–390
248. Sharma PS, D'Souza F, Kutner W (2012) Molecular imprinting for selective chemical sensing of hazardous compounds and drugs of abuse. TrAC Trends Anal Chem 34:59–77
249. Diaz-Diaz G, Antuna-Jimenez D, Carmen B-LM, Jesus L-CM, Miranda-Ordieres AJ, Tunon-Blanco P (2012) New materials for analytical biomimetic assays based on affinity and catalytic receptors prepared by molecular imprinting. TrAC Trends Anal Chem 33:68–80
250. Sharma PS, Pietrzyk-Le A, D'Souza F, Kutner W (2012) Electrochemically synthesized polymers in molecular imprinting for chemical sensing. Anal Bioanal Chem 402 (10):3177–3204
251. Wu X (2012) Molecular imprinting for anion recognition in aqueous media. Microchim Acta 176(1–2):23–47
252. Zhang Y, Shimizu KD (2011) Molecular imprinting and sensor development. In: Wang B, Anslyn EV (eds) Chemosensors: principles, strategies and applications, 1st edn. Wiley, Hoboken, NJ, pp 107–120
253. Balamurugan S, Spivak DA (2011) Molecular imprinting in monolayer surfaces. J Mol Recognit 24(6):915–929
254. Chen L, Xu S, Li J (2011) Recent advances in molecular imprinting technology: current status, challenges and highlighted applications. Chem Soc Rev 40(5):2922–2942
255. Verheyen E, Schillemans JP, van Wijk M, Demeniex M-A, Hennink WE, van Nostrum CF (2011) Challenges for the effective molecular imprinting of proteins. Biomaterials 32 (11):3008–3020
256. Li S, Li W, Tiwari A, Prabaharan M (2010) Molecular imprinting: a biomimetic tool for highly selective separation, sensing and catalysis. In: Li S, Tiwari A, Prabaharan M, Aryal A (eds) Smart polymer materials for biomedical applications, 1st edn. Nova, Hauppauge, NY, pp 1–16

257. Flavin K, Resmini M (2010) Molecular imprinting with nanomaterials. In: Geckeler KE, Nishide H (eds) Advanced nanomaterials, vol 2, 1st edn. Wiley-VCH, Weinheim, pp 651–675
258. Wu X, Shimizu KD (2008) Molecular imprinting for sensor applications. In: Rotello VM, Thayumanavan S (eds) Molecular recognition and polymers: control of polymer structure and self-assembly, 1st edn. Wiley, Weinheim, pp 395–429
259. Gupta R, Kumar A (2008) Molecular imprinting in sol-gel matrix. Biotechnol Adv 26 (6):533–547
260. Zoski CG (ed) (2007) Handbook of electrochemistry, 1st edn. Wiley, Weinheim
261. Smyth MR, Vos JG (eds) (1992) Analytical voltammetry, Wilson & Wilson's comprehensive analytical chemistry, vol XXVII, 1st edn. Elsevier, Amsterdam
262. Bagotsky VS (2006) Fundamentals of electrochemistry, 2nd edn. Wiley, Hoboken, NJ
263. Monk PMS (2001) Fundamentals of electroanalytical chemistry, 1st edn. Wiley-VCH, Weinheim
264. Bard AJ, Parson R, Jordan J (1985) Standard potentials in aqueous solution, 1st edn. Marcel Dekker, New York, NY
265. Ruzicka J, Hansen EH (1988) Flow injection analysis, 2nd edn. Wiley, New York
266. Trojanovicz M (ed) (2008) Advances in flow analysis, 1st edn. Wiley, Weinheim
267. Kolev S, McKelvie ID (eds) (2008) Advances in flow injection analysis and related techniques, 1st edn, Comprehensive analytical chemistry: Wilson & Wilson's comprehensive analytical chemistry. Elsevier, Amsterdam
268. Skeggs LT Jr (1957) An automatic method for colorimetric analysis. Am J Clin Pathol 28 (3):311–322
269. Ruzicka J, Marshall GD (1990) Sequential injection: a new concept for chemical sensors, process analysis and laboratory assays. Anal Chim Acta 237:329–343
270. Economou A (2005) Sequential-injection analysis (SIA): a useful tool for on-line sample-handling and pre-treatment. TrAC Trends Anal Chem 24(5):416–425
271. Luque de Castro MD, Ruiz-Jimenez J, Perez-Seradilla JA (2008) Lab-on-Valve: a useful tool in biochemical analysis. TrAC Trends Anal Chem 27(2):118–126
272. Wang J (1992) Injection analysis – from flow injection analysis to batch-injection analysis. Microchem J 45:219–224

Chapter 19
Gas Sensors

Ulrich Guth, Winfried Vonau, and Wolfram Oelßner

19.1 General Considerations

Gas analysis in the environment is a broad field and includes emission and immission evaluation and control. Furthermore, the determination of gases dissolved in water, such as oxygen and carbon dioxide, is a main task for environmental gas analysis. Depending on the matrix to be analysed, the gas concentration and the volume of gases which can be used for sampling and analysis have to be selected. In the environment the direct measurement in air or in water is preferred because sampling and transport of the gaseous analyte to the lab include a lot of possible sources of mistakes. For example, changes in temperature of the sampled gas must be avoided because water vapour can condense and gases can be dissolved in the water films. Additionally, the solubility of gases in water depends on the temperature. These mistakes caused by sampling cannot be compensated by the best analytical method. The majority of gas analyses are performed in special labs mostly by gas chromatography. For these analyses special knowledge is required. Depending on the amount of gas which is available for sampling either containers are used in flowing gas or small amounts of gas samples are taken by the so-called gas mouse. Electrochemical gas sensors offer an alternative concept especially due to the opportunity to measure directly in the matrix to be analysed, e.g. in field applications.

U. Guth (✉)
Department of Chemistry and Food Chemistry, Dresden University of Technology, 01062 Dresden, Germany
e-mail: guth@ksi-meinsberg.de

W. Vonau • W. Oelßner
Kurt-Schwabe-Institute for Measuring and Sensor Technology Meinsberg, 04736 Waldheim, Germany
e-mail: vonau@ksi-meinsberg.de; oelssner@ksi-meinsberg.de

L.M. Moretto, K. Kalcher (eds.), *Environmental Analysis by Electrochemical Sensors and Biosensors*, DOI 10.1007/978-1-4939-0676-5_19

19.2 Principles of Electrochemical Gas Sensors

Therefore, electrochemical gas sensors are widely spread in many fields of environmental monitoring, for the investigation of metabolisms and the control of biological processes. They are well established to gain real-time information for process control by in situ measurements of the chemical composition without sampling. Electrochemical sensors are small and inexpensive and do not require a sophisticated knowledge in their application.[1]

Every electrochemical reaction, e.g. the reduction of oxygen, is connected with the flow of an ionic charge carrier and a turnover of mass. Electrochemical reactions can occur spontaneously only to a very small extent (10^{-12} mol). After the establishment of the electrochemical equilibrium an equilibrium voltage or the electromotive force (emf) can be measured. On the other hand, the reaction can be pushed by means of an external polarisation voltage. In that case a current is flowing due to the reaction turnover.

Depending on the used electrolyte and the working temperature, electrochemical gas sensors can be applied in real matrices at temperatures from −30 °C up to 1,600 °C. The so-called conventional electrochemical gas sensors, which work with aqueous or liquid electrolytes, are usually applied up to about 50 °C, whereas solid electrolyte-based sensors operate in the temperature range >500 °C. Both types of sensors work according to electrochemical measuring principles, like potentiometry, amperometry or impedimetry. Due to the cheap equipment also dynamic methods like cyclovoltammetry, linear sweep voltammetry and their differential modes are suited for field application. Sensitivity, selectivity and stability (reliability and durability) of sensors are mainly influenced by the measuring conditions with respect to temperature, pressure and chemical environment. In the low-temperature range, electrochemical gas sensors are used to measure O_2, NO and CO in the gas phase as well as dissolved in water. NH_3 and CO_2 in gaseous as well as in aqueous matrices can be determined indirectly via pH changes of an inner electrolyte. For measurements of oxygen and combustibles like hydrogen, CO and hydrocarbons at high temperatures in exhausts (emission control) solid electrolyte sensors are commonly utilised. Sensors for the determination of free oxygen and equilibrium oxygen in reducing gases are also commercially available. The main advantage of high-temperature sensors is the very short response time in the ms range. Generally it is possible to measure most gases by normal temperature sensors as well as with high-temperature sensors. In Fig. 19.1 a general overview on the different electrochemical gas sensors und their operation mode is given. The preferably used gas sensor principles are marked in red.

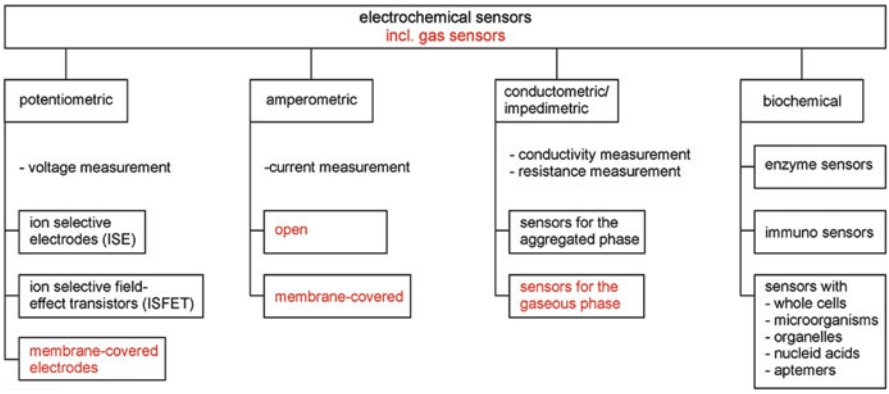

Fig. 19.1 Overview on the principles of electrochemical gas sensors

19.3 High-Temperature Gas Sensors

Electrochemical cells with solid electrolytes are widely used as gas sensors for emission monitoring in exhausts and fermentation plants. As a solid electrolyte gas-tight sintered ceramics in form of tubes, discs, planar substrates or thick films consisting of stabilised zirconia (e.g. YSZ means the most common solid electrolyte yttria-stabilised zirconia) are utilised. With increasing temperature the electrolytical conductivity increases exponentially.

Potentiometric sensors (Fig. 19.2, left) are able to measure free oxygen and oxygen in an established thermodynamically equilibrium, e.g. the ratio of partial pressures of burnt and non-burnt components.[2,3] They are oxygen concentration cells which can be symbolised by

$$O_2\left(\varphi'_{o_2}\right), Pt\left|(ZrO_2)_{0.84}(Y_2O_3)_{0.08}\right|Pt, O_2\left(\varphi''_{o_2}\right)$$

$$1/2O_2(g) + 2e^-(Pt) \leftrightarrows O^{2-}(YSZ)$$

Oxygen cannot penetrate the gas-tight ceramic. Under electrochemical equilibrium it takes up two electrons from the metal (platinum) and is incorporated in the solid electrolyte as an oxide ion O^{2-} (cathodic reaction, arrow in the right direction). In the opposite direction oxide ions are removed from the solid electrolytes, electrons remain in the platinum and oxygen is formed (anodic reaction, left direction). The cell reaction is the electrochemical transfer of oxygen from the side of higher partial pressure to the other with lower one. According to the Nernst's equation the open-circuit voltage depends logarithmically on the gas partial pressure p_{O_2} on both sides:

$$O_2\left(\varphi'_{o_2}\right), Pt\left|(ZrO_2)_{0.84}(Y_2O_3)_{0.08}\right|Pt, O_2\left(\varphi''_{o_2}\right)$$

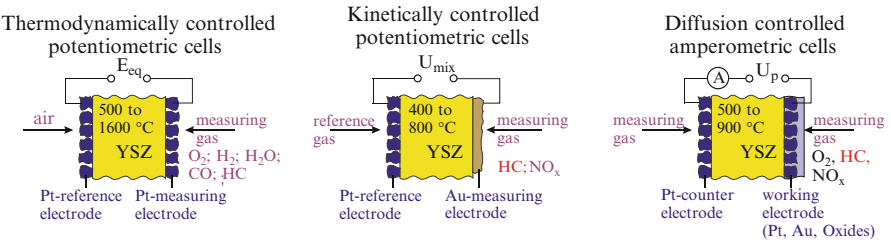

Fig. 19.2 Basic principles of gas sensors based on solid electrolytes[2]

$$E = -U_{eq} = \frac{RT}{4F} ln \frac{p''_{O_2}}{p'_{O_2}}$$

If the total pressure on both sides is equal and nearly 1 bar the partial pressure can be expressed by the volume concentration φ_{O_2}

$$E = -U_{eq} = \frac{RT}{4F} ln \frac{\varphi''_{O_2}}{\varphi'_{O_2}}$$

with R = 8.314 V A s/(mol K) and F = 96,485 A s/mol, on one side air with 50 % r. h. the following results (quantity equation is used):

$$\varphi(O_2)/vol\% = \exp\left(3.025 - \frac{U_{eq}/mV}{0.0215T/K}\right)$$

In *amperometric sensors* (Fig. 19.2 right)[1,4] one electrode is covered by a diffusion-limiting layer (also a chamber with small holes can be used) so that the transport of oxygen to the electrode is the rate-limiting step. This is schematically shown in Fig. 19.3. When the electrode is polarised by an external voltage, the current increases as long as enough electrochemically active species are present.

In the plateau phase the electrochemical turnover only depends on the transport rate (diffusion rate) of active species. In case of an oxygen electrode all oxygen that reaches the electrode is reduced electrochemically. The rate-limiting current is proportional to the gas concentration. Therefore these sensors exhibit a linear sensor function and can be calibrated with air.

With the area A and the length L of the hole and the diffusion coefficient of oxygen D_{O_2} the current measured is proportional to the oxygen partial pressure:

$$I_{\text{lim}} = -\frac{4FD_{O_2}A}{RTL} p_{O_2}$$

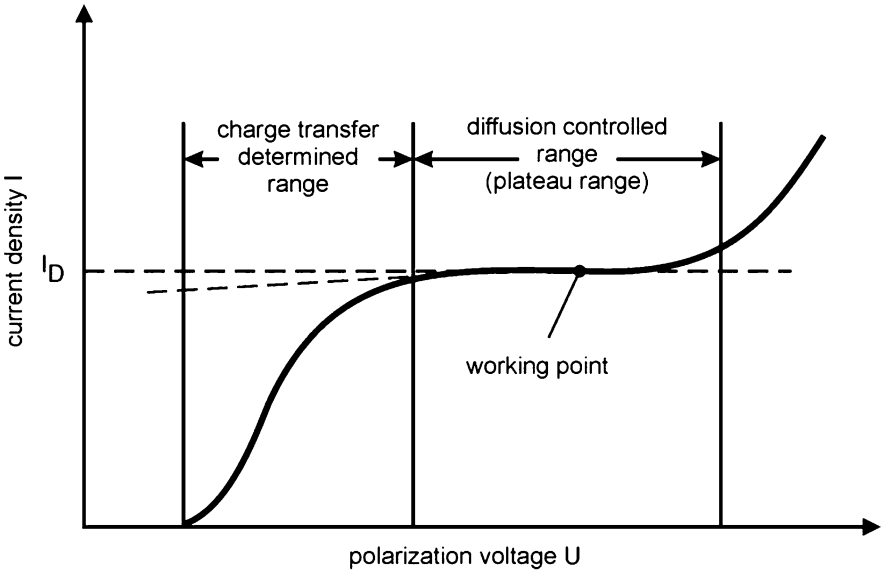

Fig. 19.3 Behaviour of a polarised electrode

For the measurement of gas components like hydrocarbons (HC) or nitric oxides (NO_x) in non-equilibrated gas phases kinetically determined sensors are used (Fig. 19.2 middle).[5,6] Depending on the electrode material, the gas components do not equilibrate on the measuring electrode at temperatures <700 °C. Thus gas components which are not thermodynamically stable are electrochemically active. In an HC- and O_2-containing gas, for example, at least two electrode reactions can take place: the electrochemical reduction of oxygen and the electrochemical oxidation of hydrocarbons. The measured open-circuit voltage does not obey the Nernst equation. Therefore such electrode behaviour is often referred to non-Nernstian electrodes (or *mixed potential sensors*). The cell voltage depends logarithmically on the concentrations of the hydrocarbons:

$$U_{mix} = U_O - A \cdot ln(\varphi_{HC})$$

The mixed potential of such solid electrolyte electrodes is, in contrary to that of electrodes in aqueous solution, very stable and reproducible.

Sensors based on solid electrolytes are also known for CO_2.[7] The general setup of a thick film sensor is given in Fig. 19.4. As a solid electrolyte sodium ion conductors like ß-alumina or Nasicon together with sodium carbonate are used. The electrochemical reactions take place at temperatures between 350 and 550 °C. The electrode reactions of the measuring and reference electrode are

$$Na_2CO_3 \leftrightarrows 2Na^+ + 1/2O_2(g) + CO_2(g) + 2e^-(Au) \qquad \text{measuring electrode}$$

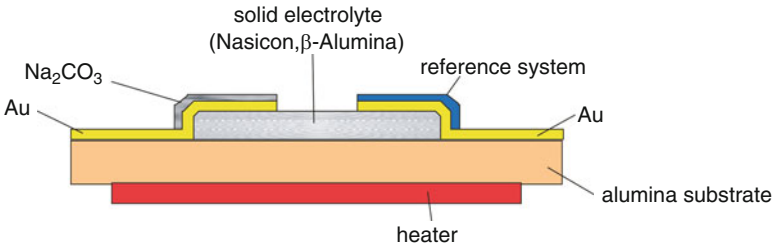

Fig. 19.4 Schematic cross section of a solid-state CO_2 sensor

$$2SiO_2(s) + 2Na^+ + ½O_2(g) + 2e^-(Au) \leftrightarrows Na_2Si_2O_5(s) \qquad \text{reference electrode}$$

In the cell reaction sodium silicate and CO_2 react to sodium carbonate and silica:

$$Na_2CO_3(s) + 2SiO_2(s) \leftrightarrows Na_2Si_2O_5(s) + CO_2(g)$$

If the solid components are pure the cell emf depends only on the CO_2 partial pressure:

$$E = Const + \frac{RT}{2F} ln p_{CO_2}$$

Such sensors show long-term stability without cross sensitivity vs. water vapour. Organic compounds are oxidised by oxygen on the surface of hot electrodes.

19.4 Normal-Temperature Gas Sensors

19.4.1 Amperometric Gas Sensors

Amperometric gas sensors are the second most important group of electrochemical gas sensors. The development of these sensors can be traced back to the introduction of the Clark-electrode in the mid-1950s, which is well known for the determination of dissolved oxygen. Amperometric gas sensors consist of a working electrode mostly covered by a membrane, a counter and a reference electrode which are in connection with a liquid electrolyte solution. These sensors have been designed in different forms and are significant also in commercial terms. The schematic setup is shown in Fig. 19.5.[8]

The electrolyte phase has to carry the cell current by enabling the transport of charge carriers in the form of ions and often it has to provide co-reactants (usually water, protons or hydroxide ions) to the electrode as well as to allow the removal of ionic products from the reaction site. That is the main reason for aging and limiting life time. Counter and reference electrodes may be combined into a single electrode

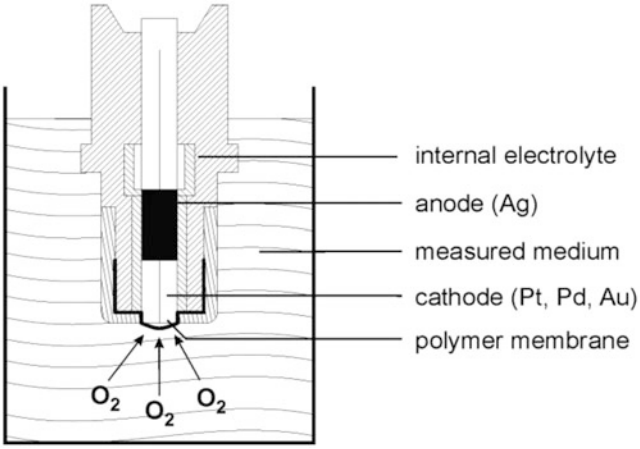

Fig. 19.5 Cross section of the Clark cell

for non-critical applications. For gas sensors the most important challenge consists in the development of a working electrode which is accessible for the sample gas while still being in contact with the usually liquid internal electrolyte solution. Either, the gas must be dissolved in the electrolyte solution before coming in contact with the electrode, or the so-called triple points are required where the gas, liquid and solid electrode phases meet. The electrochemical cell is separated from the medium to be analysed by a gas-permeable membrane. This is pressed against a flat electrode leaving only a thin layer of electrolyte solution between electrode and membrane. The membrane has the important role of eliminating the interference of redox-active substances other than the measured gas which might be present in the sample and to avoid fouling of the working electrode. The membrane also allows the internal use of a high concentration of an electrolyte in the electrochemical cell without having to modify the sample itself, thus eliminating errors due to the $i \cdot R$ drop which would otherwise be present. Chloride ions in the electrolyte solution are involved in the counter electrode mechanism and also establish a constant reference potential. Modern Clark electrodes are equipped with a porous poly(tetrafluoroethylene) (PTFE) membrane. Due to the hydrophobic behaviour of the material the pores (typical diameter 10 μm) are not wetted but allow the transport of dissolved gases. As the mass-transfer rate of the analyte is slow, the faradaic current is controlled by diffusion rather than the kinetics of the electrode reaction and this assures a linear dependence of the current on the concentration of the dissolved oxygen (see Fig. 19.3). The layer of the electrolyte solution between membrane and electrode is kept thin in order not to compromise sensitivity and response time.

The selectivity to a certain gas species can be ensured not only by the kind of membrane but also by the polarisation voltage which is necessary to promote a certain electrochemical reaction. The voltage which has to be applied between the working and the reference electrode must be higher than the equilibrium emf.

Table 19.1 Reactions of gas electrodes

Gas	Cathodic reactions	Anodic reactions
CO	$½O_2 + 2H^+ + 2e^- \rightarrow H_2O$	$CO + H_2O \rightarrow CO_2 + H^+ + 2e^-$
NO	$O_2 + 4H^+ + 4e^- \rightarrow 2H_2O$	$NO + H_2O \rightarrow NO_2 + 2H^+ + 2e^-$
NO_2	$O_2 + 4H^+ + 4e^- \rightarrow 2H_2O$	$NO_2 + H_2O \rightarrow HNO_3 + H^+ + e^-$
O_3	$O_3 + 2H^+ + 2e^- \rightarrow O_2 + H_2O$	

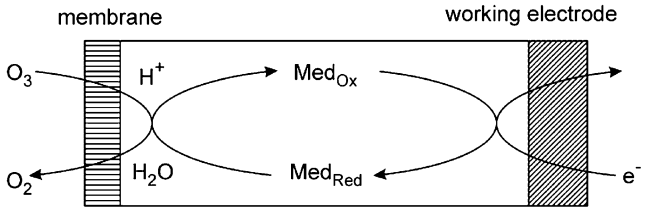

Fig. 19.6 Working principle of an ozone sensor

In Table 19.1 electrode reactions in which gases are involved are listed.

The cell reaction consists of an oxidation of the gas which is to be measured and the reduction of molecular oxygen. Such sensors can be applied at temperatures from −20 to +50 °C, with a usual recommendation between 5 and 25 °C. According to the special shape and the size of the electrodes these sensors have typically a sensitivity of 0.1 µA/ppm ± 0.02 µA/ppm. These sensors are available on the market from several companies, e.g. City Technology, London, UK; EnviteC Wismar, Germany; and IT Dr. Gambert, Wismar, Germany. Depending on the gas, its concentration and the expected life time the response time is between 5 and 25 s and the lifetime in air <3 years. Generally, these sensors are not so robust and the lifetime is limited, but they have a higher selectivity as the resistive semiconductor sensors.

The determination of ozone can be carried out directly in an irreversible reaction at +2.07 V which leads to a poisoning of the electrode surface and a shortening of the lifetime. The better way is to use an indirect reaction via a redox mediator. Ozone reacts with the reduced mediator and the oxidised mediator in turn is reduced on the working electrode (Fig. 19.6). The flowing current is proportional to the ozone concentration. As mediators inorganic redox couples like Br^-, OBr^-; AsO_3^{3-}, AsO_3^{3-}; and Fe^{2+}, Fe^{3+} are used. Amperometric ozone sensors are broadly available on the market as well for measuring in air as for monitoring of cleaning processes.

19.4.2 Fuel Cell Principle

In a more simple design the fuel cell principle without an external voltage is used to measure oxygen (Fig. 19.7). The voltage is generated between the oxygen cathode

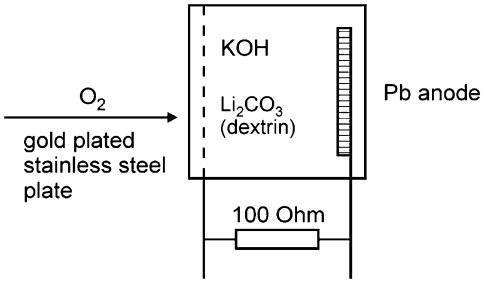

Fig. 19.7 Oxygen sensor (fuel cell principle)

and an anode made of lead. According to the oxygen concentration the cathode may be metallic or covered by a polymer membrane. At present such bare electrodes are only rarely used; an exception is the determination of oxygen in sewage and in beverages with electrodes which are regularly abraded mechanically for cleaning.

Oxygen is reduced in alkaline solution at a voltage of +0.401 V according to the cathodic reaction

$$O_2 + 2H_2O + 4e^- \rightarrow 4OH^- \qquad +0.401\ \text{V}$$

As an anode reaction lead is oxidised:

$$4OH^- + 2Pb \rightarrow 2PbO + 2H_2O + 4e^- \qquad -0.58\ \text{V}$$

For the overall cell reaction results,

$$O_2 + 2Pb \rightarrow 2PbO$$

Therefore the cell voltage is 0.981 V. The current which is proportional to the oxygen partial pressure is measured by means of a 100 Ω resistor.

19.4.3 Severinghaus Sensors (Electrodes)

Unlike other gases such as oxygen the determination of dissolved CO_2 is more difficult due to its chemical reactions with water. This is partly true for measuring CO_2 in ambient air which contains more or less water especially under condensing conditions. CO_2 cannot be reduced electrochemically in aqueous solution so that a simple sensor setup like for the determination of oxygen is not possible. This is important for interpreting analytical results as well as for understanding the measurement principle applied, as for example in the Severinghaus electrode. The concentration of CO_2 is only reasonable with the knowledge of the pH of the analysed medium.[9]

In Fig. 19.8 the interaction of CO_2 and water is shown in terms of the pH dependence of the equilibrium concentration of the formed components. At pH

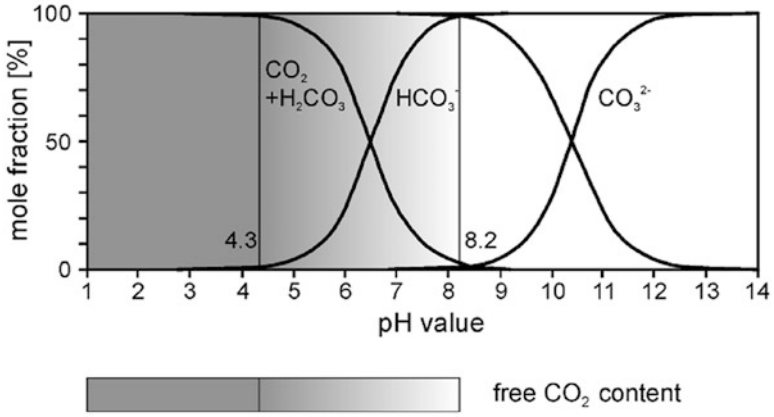

Fig. 19.8 pH dependence of the carbonate system

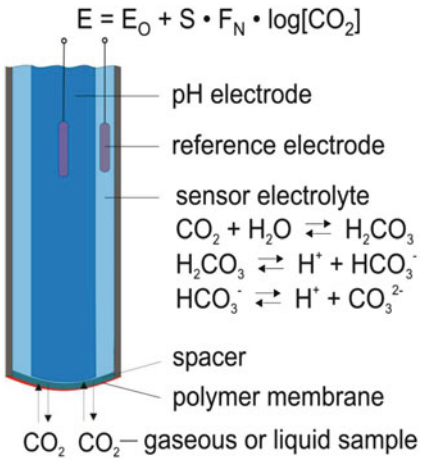

Fig. 19.9 Basic principle of a Severinghaus sensor (electrode)

values below 4.3 nearly the total carbonate exists as free dissolved CO_2 in the solution. It should be mentioned that the values depend slightly on the temperature and on the alkalinity and salinity of the solution. The same arguments apply to the determination of ammonia (NH_3).

Figure 19.9 shows schematically the so-called Severinghaus carbon dioxide sensor (sometimes also called electrode) and illustrates its mode of operation. Main constituents of the sensor are a thin polymer membrane, the hydrogen carbonate containing electrolyte solution, a thin hydrophilic spacer sheet soaked with the electrolyte solution and a pH sensor. CO_2 permeates from the gaseous or liquid specimen through the membrane into the electrolyte film in the spacer until equilibrium between the CO_2 partial pressure on both sides of the membrane has been established. During measurement virtually no CO_2 is consumed.

Table 19.2 Application of electrochemical gas sensors according to the gas to be analysed

Kind of gas	Sensor principle (high temperature)	Sensor principle (normal temperature)
O_2	Potentiometric, amperometric	Amperometric fuel cell principle
O_2, dissolved		Amperometric Fuel cell principle
O_3		Amperometric
CO, NO, NO_2	Mixed potential (potentiometric)	Amperometric
Combustibles HC, H_2	Mixed potential (potentiometric)	
CO_2	Potentiometric	Severinghaus
CO_2 dissolved		Severinghaus

Whereas CO_2 sensors for measurements in gases can simply be calibrated by using commercially available test gases, the calibration of electrochemical CO_2 sensors for measurements in liquids is not trivial. Contrary to standardised, long-term stable buffer solutions with defined pH values, which are generally used in pH measuring technique, solutions with defined CO_2 content are not long-term stable and therefore commercially not available. For this reason, calibration solutions with defined CO_2 concentration must be prepared immediately before starting the calibration procedure.

Since the sensitivity of electrochemical CO_2 sensors changes only slightly in the course of time, it is sufficient to carry out regularly one-point calibrations in order to correct the zero-point drift. Two-point calibrations are only necessary in longer time intervals or after the sensor had been out of use for a longer period. If the sensor is continuously in use, as a rule, one-point calibrations at least once per week and two-point calibrations at least once per month are recommended. For two-point calibrations two calibration solutions with different CO_2 concentrations are needed.

19.4.4 Application

As discussed in the former paragraphs there are high- and low-temperature gas sensors (Table 19.2). Which sensor for which application can be recommended is a question of expected information, response time and lifetime. This depends on the matrix to be analysed and on the temperature. For long-term applications at high as well as low temperatures with a short response time high-temperature sensors based on solid electrolytes are preferred. They can be used for the most part maintenance free. On the other hand, the price of those sensors is mostly much higher than that of normal-temperature sensors. Normal-temperature sensors need calibrations from time to time.

References

1. Gründler P (2004) Chemische Sensoren (in German). Springer, Berlin
2. Guth U (2012) Gas sensors. In: Bard A, Inzelt G, Scholtz F (eds) Electrochemical dictionary. Springer, Heidelberg, pp 400–406, 595–596, 2nd extended edition
3. Kleitz M, Siebert E, Fabry P, Fouletier J (1992) Solid-state electrochemical sensors. In: Göpel W, Hesse J, Zemel JN (eds) Sensors. A comprehensive survey, vol 2. Weinheim, Wiley-VCH, p 413
4. Moos R, Sahner K, Fleischer M, Guth U, Barsan N, Weimar U (2009) Solid state gas sensor research in Germany - a status report. Sensors 9:4323–4365. doi:10.3390/s90604323
5. Guth U, Zosel J (2004) Electrochemical solid electrolyte gas sensors – hydrocarbon and NO_x analysis in exhaust gases. Ionics 10:366–377
6. Fergus JW (2007) Solid electrolyte based sensors for the measurement of CO and hydrocarbon gases. Sensors Actuators B 122:683–693
7. Fergus JW (2008) A review of electrolyte and electrode materials for high temperature electrochemical CO_2 and SO_2 gas sensors. Sensors Actuators B 134:1034–1041
8. Guth U, Vonau W, Zosel J (2009) Recent developments in electrochemical sensor application and technology - a review. Meas Sci Technol 20: 1–14, 042002
9. Zosel J, Oelßner W, Decker M, Gerlach G, Guth U (2011) The measurement of dissolved and gaseous carbon dioxide concentration. Meas Sci Technol 22, 072001, doi: 10.1088/0957-0233/22/7/072001

Part IV
Sensors with Advanced Concepts

Chapter 20
Sensor Arrays: Arrays of Micro- and Nanoelectrodes

Michael Ongaro and Paolo Ugo

20.1 Introduction

It is long known that geometry, surface structure, and material constituting an electrode have a profound effect on the electrochemical behavior of electroactive species and, as a consequence influence the electrochemical response. The size of working electrodes also affects the response of the electrode, due to mass transport effects of the active species to and from the electrode. Electrodes miniaturization is one of the main trends in the field of electrochemistry of the last decades. Electrodes can be classified, according to their dimensions as: macroelectrodes (having dimensions greater than 100 μm and commonly on the order of millimeters),[1] microelectrodes (ME) (having at least one dimension below 100 μm),[1] ultramicroelectrodes (UME) (having one dimension less than the diffusion layer, therefore below to 25 μm).[1] When such miniaturization is taken to the extreme, nanoelectrodes (NE) can be obtained. A nanoelectrode has one dimension less than 100 nm, or following a more rigorous definition, one dimension which is in the same range-scale of the charging double layer, therefore less than 50 nm.[1] Although IUPAC defines microelectrodes as electrodes with at least one dimension less than tens of micrometers, down to submicrometer range,[2] we find the classification proposed by Compton more convenient for the purposes of this chapter. For this reason, in the following we will address electrodes according to Compton's classification.

Besides the obvious practical advantage of the small size, allowing smaller sample volumes to be used and application to in vivo measurements, microelectrodes offer a number of advantages such as high current density, low background charging current, and enhanced mass transport efficiency. For an in-depth discussion about macro- micro- and nanoelectrodes see Chap. 15.

M. Ongaro • P. Ugo (✉)
Department of Molecular Sciences and Nanosystems, University Ca' Foscari of Venice, S. Marta 2137, Venice, Italy
e-mail: ugo@unive.it

L.M. Moretto, K. Kalcher (eds.), *Environmental Analysis by Electrochemical Sensors and Biosensors*, DOI 10.1007/978-1-4939-0676-5_20

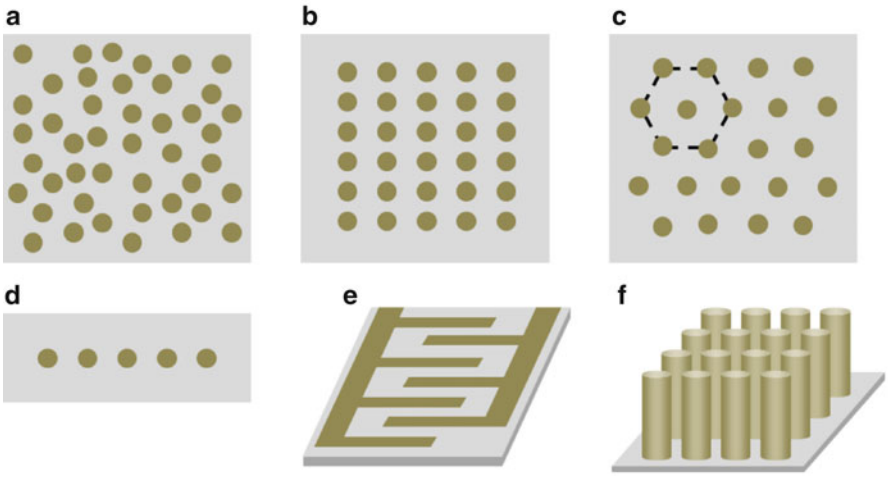

Fig. 20.1 Different array designs: (**a**) random array (ensemble), (**b**) square array, (**c**) hexagonal array, (**d**) linear array,(**e**) interdigitated array, (**f**) three dimensional array. Figure adapted from ref. (6)

A drawback in the use of microelectrodes (as well as smaller sized electrode) is related to the extremely low currents obtained. One way to overcome this problem is to use arrays of micro- or nanoelectrodes (MEA and NEA, respectively), whereby multiple electrodes are operated in parallel. The shapes and the geometry of the MEA/NEA are mainly limited by their fabrication technique and can be conveniently classified according to the design and application they are designed for. Individual electrodes in the array may assume random arrangements (Fig. 20.1a), in this case the array is more properly defined as an ensemble of micro or nanoelectrodes (MEE and NEE, respectively) as first termed by Martin and coworkers.[3] Note that Walt[4] uses the term ensemble to mean a grouping of sensor elements that respond collectively, and therefore each element cannot provide its own signal for detection. However, in this chapter we will use the term ensemble as defined by Martin. The main advantage of random configurations is their easy fabrication, since usually it does not require expensive and technologically demanding instrumentation. The main drawback is the random geometry of the electrode, which makes difficult a clear comparison with theoretical models. Moreover, the random spacing between the individual electrodes can lead to different diffusion mechanisms on the same ensemble. The design of arrays with well defined geometry and inter-electrodic spacing is highly preferred as far as electroanalytical applications are concerned, nonetheless the fabrication of such arrays is not always practical and requires special equipments which are not always present in chemistry laboratories. The most common geometries of regular arrays consist of disks electrodes in a square- or hexagonal-shaped arrangements (Fig. 20.1b, c) or parallel band electrodes, a special configuration of the latter geometry being interdigitated arrays (Fig. 20.1e); in another popular design, micro- or nanodisks are arranged in a linear fashion (Fig. 20.1d). All these configurations exploit planar electrodic

surfaces, which are not advantageous for acute tissue slice experiments. However, by using three-dimensional electrodes, it is possible to monitor the electrochemical activity of the tissue directly after placing the electrode onto the tissue, the geometry of the array reduces the distance between the electrode and the active cells.[5] Such three-dimensional arrays are usually made of cylindrical structures and may be conveniently fabricated by etching the insulating material in which the micro- or nanoelectrodes are embedded in; therefore 3D ordered, random or linear arrays can be obtained (Fig. 20.1f).

All these array geometries show peculiar electrochemical behavior which can be properly exploited for electroanalytical purposes. The goal of this chapter is to give an overview of the different types of micro- and nanoelectrodes arrays (ensembles, ordered, interdigitated, etc.) as well as a brief description of the main techniques used for their fabrication. Note that in most cases the fabrication of nanoelectrodes arrays requires more specialized fabrication techniques with respect to microelectrode arrays, and therefore they will be presented separately. Specific electrochemical properties of micro and nanoelectrodes arrays will be described in relation to the specific diffusion mechanisms observed in such electrochemical sensors.

20.2 MEAs Fabrication Techniques

20.2.1 Assembly Techniques

In the following paragraph we will present selected examples of microfabrication techniques which do not require any special equipment and therefore are accessible to almost every laboratory. Giving a complete list of all the microfabrication techniques described in the literature, for preparing MEAs is out of our goals; further information is indeed available in other recent reviews.[1, 7, 8] Literature descriptions of these "easy" fabrication techniques can be categorized into two designations which are: assembly of electrode materials (microwires or microbands) and self-assembly of molecules. The former is based on physical techniques, while for the latter chemical principles dominate.

20.2.1.1 Assemblies of Electrodic Materials

Obtaining MEAs by assembling electrode materials has some advantages such as: ready use of available materials, low cost, easy fabrication, and robustness of the array.

The simplest approaches involve the embedding of microsized electrodic materials in insulating matrices. Wu et al.[9] fabricated a gold circular microarray by wrapping a gold mini-grid around precast cylinders. Bond and coworkers[10] made a 10×10 MEA by embedding gold wires in epoxy resin layer-by-layer.

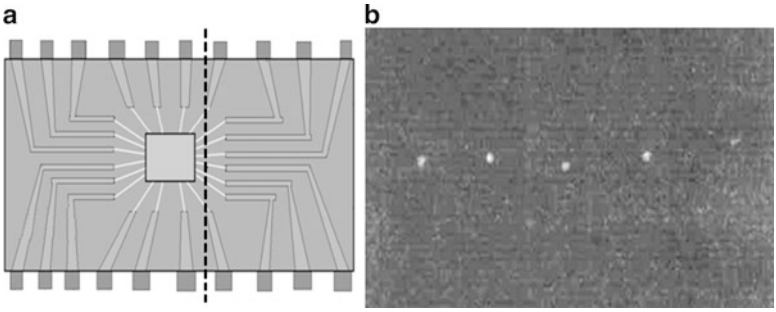

Fig. 20.2 (**a**) Schematic representation of the cutting sections (*dashed lines*) in the chip. *Thin lines* represent the gold wires. (**b**) Picture of five ME obtained from a chip, showing inter-electrode distance and electrode diameter. (Adapted with permission from ref. (11))

Angnes et al.[11] developed a method to transform inexpensive electronic chips into a MEA. In this procedure, the chips are sawed through their middle, as shown by the dashed line in Fig. 20.2a, leading to the destruction of the silicon circuit and to the cutting of the gold wires that connect it with the external terminals. By embedding in resin and polishing the surface of the sawed chip it is possible to obtain a linear array where the tips of the gold wires (typically 25 μm in diameter), are the electrodes of the array. In Fig. 20.2b, a picture of five ME, from a set of twelve, obtained by this method, is shown.

More recently, Szunerits and coworkers[12] described the fabrication of an ordered microelectrode array based on an etched optical fiber bundle. The tip of an optical fiber bundle, comprising 6,000 fibers with a mean diameter of 4 μm, is etched using a mixture of HF an NH_4F aqueous solution. The etched surface and the sides of the bundle were sputter coated with 1 μm thick gold layer. Silver paste was used to grant electrical contact among the sides of the bundle and a copper wire, and subsequently insulated by using a varnish, so that only the etched surface is electrochemically active. In the final step, the surface of the etched bundle is partially covered with an electrophoretic paint, so that only the tip apex of the fibers is exposed. By controlling the electrophoretic paint deposition conditions, it is possible to define the exposed surface of the fibers and therefore define the radius of the ME. Such devices present an interesting combination of optical and electrochemical properties. In Fig. 20.3 SEM images of the bundle before (a) and after (b) electrophoretic paint deposition and a schematic representation of the MEA are reported (c).

Not only metallic MEA were prepared by electrode assembly methods. Martin et al. reported a procedure for preparing a carbon microdiscs array by filling the pores of a microporous membrane (3, 8, and 13 μm pores diameter) with carbon paste.[13, 14] Jin and coworkers[15, 16] proposed another procedure to produce carbon MEA. A small amount of mercury was first inserted into a glass capillary (Fig. 20.4a). Then about 90 carbon fibers were carefully inserted into the other end of the glass capillary (Fig. 20.4b). The carbon fiber array was sealed to the tip of

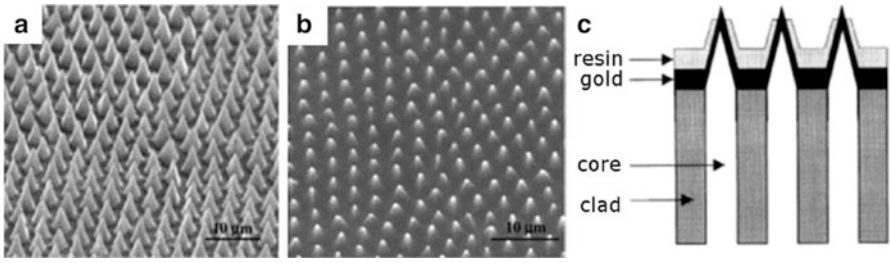

Fig. 20.3 SEM picture of a metalized optical fiber bundle (**a**) and of resin-coated fiber bundle (**b**). Schematic representation of a optical fiber MEA cross section (**c**). (Reprinted with permission from ref. (12))

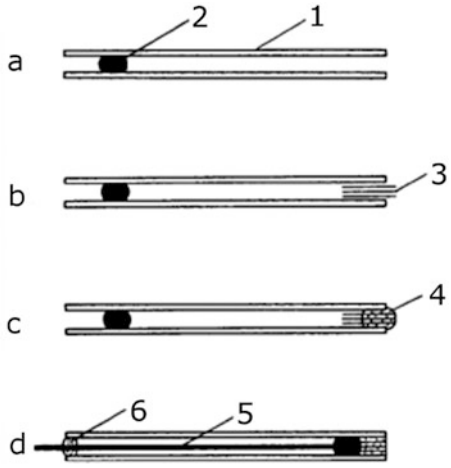

Fig. 20.4 Process of manufacturing the carbon fiber microdisk array electrode. (1) glass capillary; (2) mercury; (3) carbon fiber array; (4) low-viscosity adhesive; (5) copper wire; (6) epoxy resin. (Reprinted with permission from ref. (15))

the glass capillary by using a low viscosity adhesive (Fig. 20.4c). The carbon fiber array was polished with emery paper and connected to a copper wire via the mercury junction by pushing a copper wire down (Fig. 20.4d).

20.2.1.2 Self-Assembly of Monolayers

It is possible to exploit the well-known property of alkanethiols for forming very stable and well-organized self-assembled monolayers (SAM) on gold substrate[17–19] for the fabrication of MEE and MEA. Indeed, such monolayers can effectively block electron transfer between the gold substrate and the redox species in the solution.[20] For example, a SAM of a mixture of 3-mercaptoprotic acid (MPA) and hexadecanethiol (HDT) was prepared on a gold macro electrode by coadsorption in an ethanolic solution. MPA can be selectively removed from the mixed SAM in 0.5 M KOH at scan rate of 0.1 V/s, leaving small bare gold dots on the surface of the

electrode.[21] Patterned SAM were produced on gold substrate either by micro-contact printing technique[22] or by inkjet printing technique.[23, 24] In the former case, the stamp is inked with a thiolic solution and brought into contact with the gold substrate, transferring the thiols from the stamp to the gold; in the latter, the thiolic solution is printed on the surface of the electrode by using a modified inkjet desktop printer.

20.2.2 Photolithography

Photolithography is the most diffused technique for the fabrication of regular arrays of microelectrodes. Photolithography is a microfabrication technique which is based on the selective removal of parts of thin films (photoresist) exposed to UV light. This procedure allows one to obtain regular arrays of micro electrodes with high spatial resolution, nonetheless this technique requires special and expensive equipments; besides, the photolithographic process requires access to a clean room. The simplest photolithographic procedure[25] for the fabrication of a MEA is summarized below:

1. Starting substrate material: silicon wafers.
2. Thermal oxidation of silicon in order to obtain a SiO_2 layer for electrical isolation between the substrate and the surface.
3. Sputtering deposition of 100 nm layer of Ni/Cr followed by 100 nm layer of Au. Ni/Cr alloy, necessary to enhance the Au adherence.
4. Photolithographic definition of metal tracks (patterning of designed layout).
5. Photoresist deposition.
6. Photolithographic definition of the openings of microelectrodes and external contact pads. The photoresist is used here for electrical isolation of the metal tracks.
7. Hardening of photoresist by heating the MEA up to 450 °C for 1 h, in order to improve the device's chemical resistance.

In Fig. 20.5, a schematic representation of the lateral view of a microelectrode obtained by photolithography is reported.

A number of different photolithographic procedures for the production of gold microelectrode arrays were reported.[26–28] Besides gold, platinum,[29–33] iridium[34–38] carbon[39, 40] and boron-doped diamond[41, 42] were also used as metal electrode

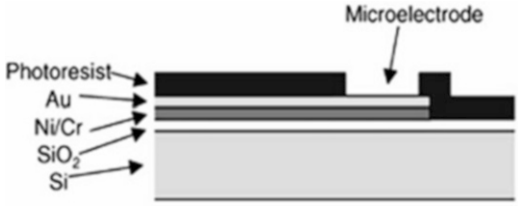

Fig. 20.5 Lateral view of a photolithographted MEA. (Reprinted with permission from ref. (25))

material. The most important advantage of this technique is that the size, shape, and inter-electrode spacing can be designed according to the requirements of the final application.

20.3 Templated Synthesis of Nanoelectrode Ensembles

The membrane templated synthesis is based on the idea that the pores of a host material can be used as a template to direct the growth of new materials. Historically, the template synthesis in track-etched materials was introduced by Possin[43] and Williams and Giordano,[44] who prepared different metallic wires with diameter as small as 10 nm within the pores of etched nuclear damaged tracks in mica. The first synthesis of NEEs prepared by using nanoporous membranes as templating material, was described by Menon and Martin[45] who deposited gold nanofibres with a diameter as small as 10 nm within the pores of track etched polycarbonate (PC) membranes by chemical (electroless) method, obtaining a random ensemble of metal nanodisks surrounded by the insulating polymer. All the nanoelectrodes were interconnected each other so that they all experienced the same electrochemical potential. The scheme of the structure of a NEE is shown in Fig. 20.6.

Afterwards, various examples of membrane-templated electrochemical deposition of nanowires of semiconductors,[47] metals (e.g. Ni and Co),[48] oxides, and conducting polymers[49] appeared in the literature.

In the template synthesis of nanoelectrodes, each pore of the membrane is filled with a metal nanowire or nanofiber. The metal fibers growth can be performed both using electrochemical[4, 48] or electroless[45, 50, 51] deposition methods.

In both deposition methods, the pore density in the template, determines the number of metal nanoelectrode elements on the NEE surface and, correspondingly,

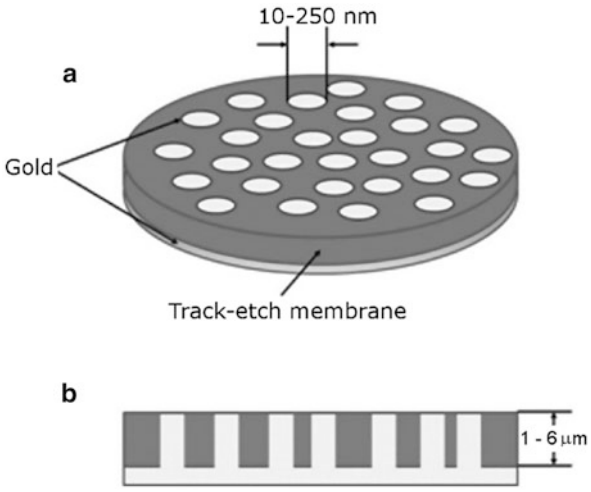

Fig. 20.6 Scheme of a nanoelectrode ensemble in a template membrane (**a**) overall view; (**b**) lateral section. (Reprinted with permission from ref. (46))

the average distance between them; while the diameter of the pores in the template determines the diameter of the individual nanoelectrodes. Since track-etched membranes are characterized by randomly distributed pores, unless special procedures are applied,[52] by this method it is only possible to obtain random ensembles of nanoelectrodes, i.e. NEE.

20.3.1 Template Electrochemical Deposition of Metals

The electrochemical deposition inside the pores of a nanoporous membrane requires that one side of the membrane is made conductive. This can be done by plasma or vacuum deposition of a thin layer of metal (typically 100–200 nm) on one side of the membrane. The metal layer can be the same or different from the metal which will be electrodeposited inside the pores and the membrane should be robust enough to tolerate this kind of treatment. In electrochemical template deposition, the coated membrane is placed in an electrochemical cell, acting as the cathode and a counter electrode is the anode. As an alternative, it is possible to place the membrane directly in contact with a solid electrode. Figure 20.7 shows the interesting cell setup recently proposed by Gambirasi et al.[53] in which the membrane is placed between a solid electrode and a sponge drenched in the electrolyte; the pressure made by the electrode on the sponge keeps the membrane tightly fixed to the electrode for the time of the deposition.

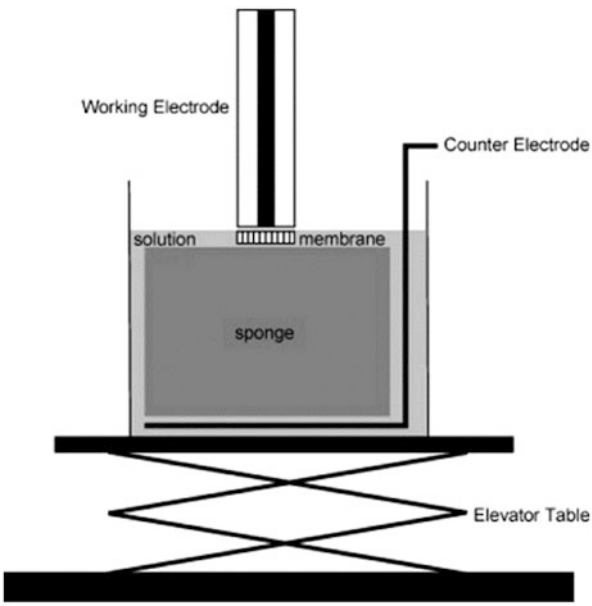

Fig. 20.7 Schematic representation of the cell setup. By rising the elevator the membrane lying over the sponge, soaked with the electrolyte, is pressed on the surface of the electrode. (Reprinted with permission from ref. (53))

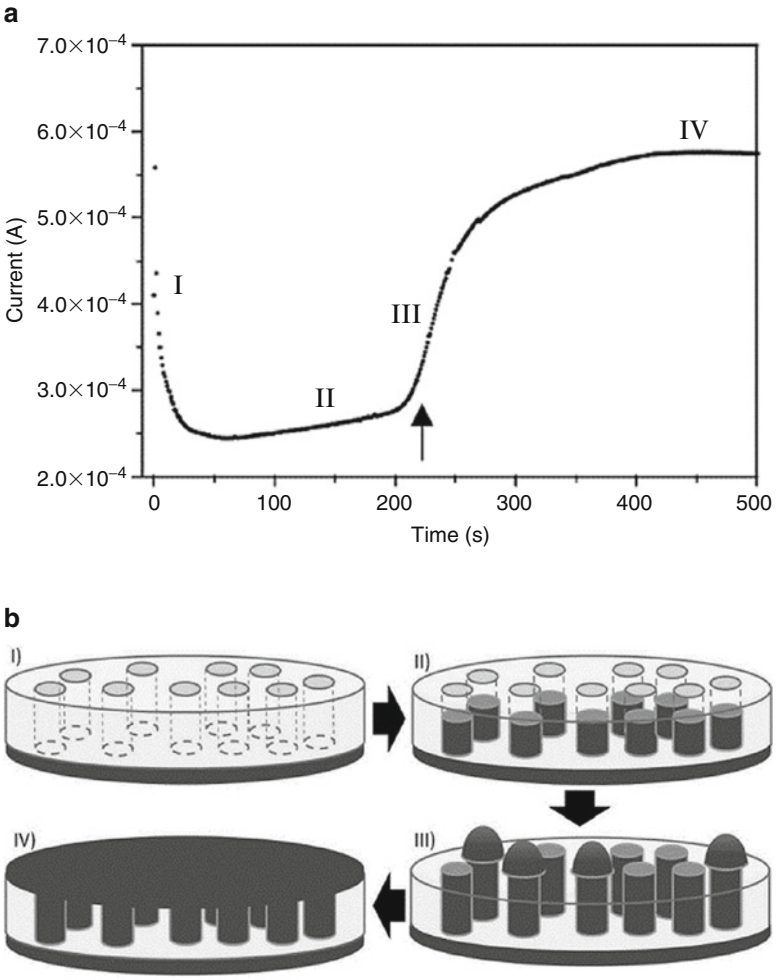

Fig. 20.8 (**a**) Dependence of the reduction current on time for the potentiostatic deposition of gold in a nanoporous membrane, and (**b**) sketched representation of the four deposition phases: I) double layer charging current; II) slight current increase which corresponds to the pores' filling with gold; III) steep current increase which corresponds to the formation of hemispheric caps; IV) constant current which correspond to the formation of a planar layer

The deposition can be conducted in potentiostatic or in galvanostatic conditions. In the former case, it is possible to monitor the time course of the deposition and the progressive filling of the pores by analyzing the time transient current. As shown in Fig. 20.8a, the deposition curve can be divided in four parts[48, 54–56] (denoted I-IV, Fig. 20.8a) associated to the four steps of deposition, sketched in Fig. 20.8b. Immediately after closing the circuit (phase I), the current shows an intense peak and a fast decay due to the depletion of metal ions following the fast initial deposition and the increase of resistance inside the pores of the membrane.

Subsequently, the current slowly decreases to reach a plateau (phase II) while the deposition proceeds and the pores are filled. At the beginning of phase III, the current increases again due to the increase of the electrode area subsequent to the emersion of the metal from the pores. In this phase it is possible to observe caps on the tips of the nanowires with a typical mushroom shape.[48] Finally, the overgrown caps merge together into an almost flat surface leading to a plateau in the current transient (phase IV). For the sake of NEE preparation, it is essential to stop the electrodeposition at the end of stage II, before the "mushroom caps" start to grow.

Since the process is based on the progressive growth and filling of the pores from the bottom metallic layer toward the open end of the pores, final products are nanowires and not hollow structures (e.g. nanotubes).

Electrodeposition of metals has been studied to obtain gold nanowires, but also other materials, such as, for instance, metals (Co[48, 57, 58] Ni[48, 54, 59] Cu[48, 54] Pt and Pd[60]), alloys (NiFe,[58] FeSiB[59]) or salts (Bi_2Te_3,[61] CdS[47]).

20.3.2 Template Electroless Deposition

The electroless deposition involves the chemical reduction of a metal salt from the solution to a surface. Noncatalytic surfaces, such as insulating polymers, have to be activated (made catalytic) prior to the electroless deposition. Usually, this is performed by generating metal nuclei on the surface of the noncatalytic material. In this way, the metal ion is preferentially reduced at the sensitized surface so that only this surface is plated with the desired metal.[62]

The principles of electroless deposition on nanoporous membranes are exemplified by the Au deposition method developed in Charles Martin's laboratory[45, 49] for the template fabrication of NEEs, nanotubes, and other shaped gold materials. The electroless deposition of gold can be divided in three steps:

(1)"Sensitization" of the membrane, adsorbing Sn^{2+} ions on the substrate; (2) the Sn^{2+} ions act as reducing agent on the surface of the membrane for the formation of Ag nanoparticles; (3) galvanic displacement of Ag particles by reduction of gold, followed by the catalytic reduction of more gold, after addition of a reducing agent (formaldehyde).

A detailed description of the gold electroless deposition process may be found in the first original papers.[45, 63]

In contrast to the electrochemical template deposition, in the electroless method the metal layer grows from the catalytic nuclei, which are located on the pore walls, towards the center of the pores. For this reason it is possible to stop the deposition at short times in order to obtain hollow tubes instead of nanowires. This procedure allows to obtain microfiltration membranes with golden pores.[64, 65] Also other metals, such as Cu,[66] Pd[67] and Ni-P[68] can be deposited in polycarbonate templates by electroless deposition. In this case a suitable procedure for the desired metal has to be applied.

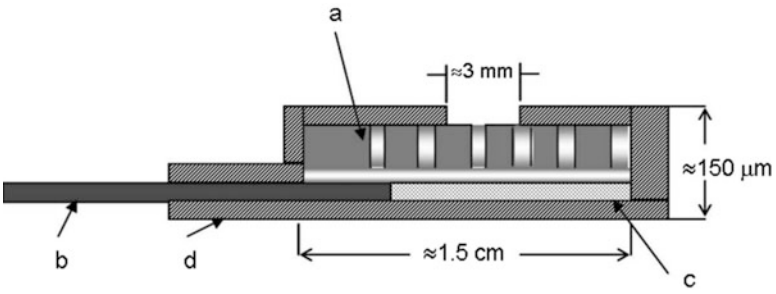

Fig. 20.9 Schematic representation of a NEE section, prepared using a track-etched polycarbonate membrane as template. (**a**) Track-etched golden membrane; (**b**) copper adhesive tape with conductive glue to connect to instrumentation; (**c**) aluminum adhesive foil with nonconductive glue; d: insulating tape. Note: the dimensions of the pores (nanofibers) are only indicative and not in scale. (Reprinted with permission from ref. (74))

When the goal of the deposition is to obtain metallic fibers protruding from the insulating matrix, e.g. 3D-NEEs, it is possible to partly etch the template. Polycarbonate can be dissolved by organic solvents, such as CH_2Cl_2/C_2H_5OH mixtures[69, 70] or, as an alternative, by etching with oxygen plasma.[71]

For fabricating from a metalized membrane a handable electrode system, the following procedure is typically followed[45, 50, 64, 70, 72–74]:

1. The starting material for the NEE preparation is a piece of a golden polycarbonate membrane, with the both faces covered and the pores filled with gold. The smooth side of the membrane is peeled off with adhesive tape 3 M (scotch Magic™) so that the tips of the nanowires remain exposed on one side.
2. A piece of copper adhesive tape (5×60 mm) with conductive glue (Ted Pella, Inc.) is first affixed on a small adhesive nonconductive aluminum square and then to the lower Au coated surface of a 5×5 mm piece of peeled membrane, so that only a small part is in contact with the copper tape. (This is because the conductive glue on the copper tape contains Ni particles which could damage the gold layer[45]).
3. Strips of nonconductive tape are applied to the lower and upper sides of the assembly in order to insulate the aluminum and copper tape, this can be done using both a piece of adhesive insulating tape, or heat shrinkable adhesive polymer films, such as Top Flite Monokote or similar.
4. A circular hole with an area typically of 0.07 cm^2 is punched into the upper piece of insulator prior to its placement on the assembly. The surface of the ensemble exposed to the solution defines the geometric area (A_{geom}) and can indeed be changed at pleasure, e.g. from 0.03 to 3 cm^2 [75] without influencing the signal/noise (S/N) ratio which is typical of NEEs.
5. As a final step, the NEE assembly is heat-treated at 150 °C for 15 min. This procedure produces a water-tight seal between the gold nanowires and the surrounding polycarbonate.

Figure 20.9 shows a side view of a NEE ready to be used in an electrochemical experiment.

20.4 Ordered Arrays of Nanoelectrodes by Nanolithography

Top down techniques, such as ion beam lithography,[76–78] electron beam lithography (EBL),[79] nanoimprint[80] or scanning probe lithography[81, 82] allow one to achieve high resolution nanostructuring, providing a precise positioning and sizing down to a scale of a few nanometers, which can be used to obtain ordered arrays of nanoelectrodes. A recent advance on the use of PC for preparing arrays of nanoelectrodes (NEA), comes from the demonstration that polycarbonate can be successfully used as high resolution resist for e-beam lithography. The method is based on the implementation of e-beam lithography, for the production of the pores on the polymeric membrane with a higher resolution with regard to photolithography.[83]

The nanoelectrodes are fabricated by patterning arrays of holes in a thin film of PC spin-coated on a gold layer on Si/Si_3N_4 substrate. In order to improve adhesion of the Au film a thin Cr or Ti layer is previously evaporated. The PC surface is exposed to the e-beam and the tracks developed (etched) in KOH. As shown in Fig. 20.10, thanks to the good properties of PC, as a high resolution e-beam resist, by this way it is possible to obtain perfectly ordered array of nano-holes with controlled diameter, as small as 50 nm.[83]

These holes can already be used as gold recessed nanoelectrodes, however by further electrochemical deposition of gold, it is possible to fill partially or totally the holes up to obtain arrays of inlaid nanodisk electrodes (Fig. 20.11).

The perfect control of the geometry of the array allows the full control of the diffusion regime at the NEA. Note that similar procedures have been developed also using polymers different from PC, as well as different nanolithographic tools.[77–79]

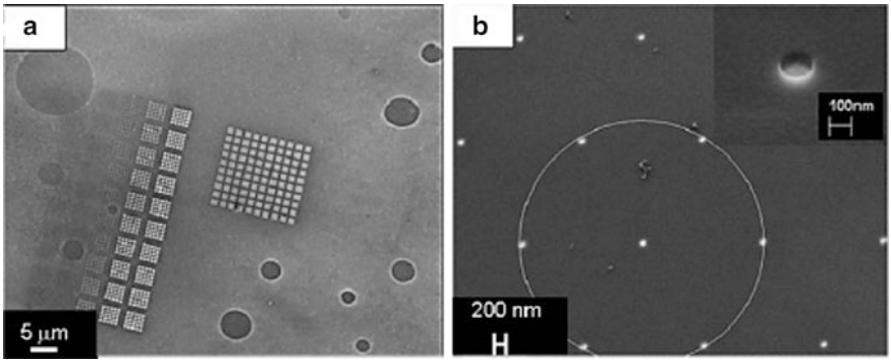

Fig. 20.10 (**a**) SEM micrograph of a nanohole matrix on PC membrane, obtained by e-beam lithography, development at 70 °C for 60 s and subsequent electrochemical gold deposition. (**b**) Top view of 75 nm radius dots in a hexagonal array on PC film; *inset*: higher magnification detail. (Reprinted with permission from ref. (83))

The advantages of using PC are in its good quality and easy use as high resolution e-beam resist and on the possibility to functionalize it with biomolecules, using already known functionalization methods.[84, 85]

20.5 Electrochemistry with Ensembles and Arrays of Micro and Nanoelectrodes

From a voltammetric view point, micro- and nanoelectrode arrays con be considered as an assembly of very small electrodes separated by a nonconductive substrate. The size of the electrode affects the mass transport of redox species to and from the electrode surface, and, as a consequence, affects the observed electrochemical response. In this paragraph, we will only take into consideration voltammetric experiments performed in stagnant solutions, in the presence of excess supporting electrolyte, so that the only relevant mode of mass transport is diffusion. Let us consider a monoelectronic electrochemically reversible reaction in which the electroactive species Ox is reduced at the electrode to Red, as shown below in reaction (20.1).

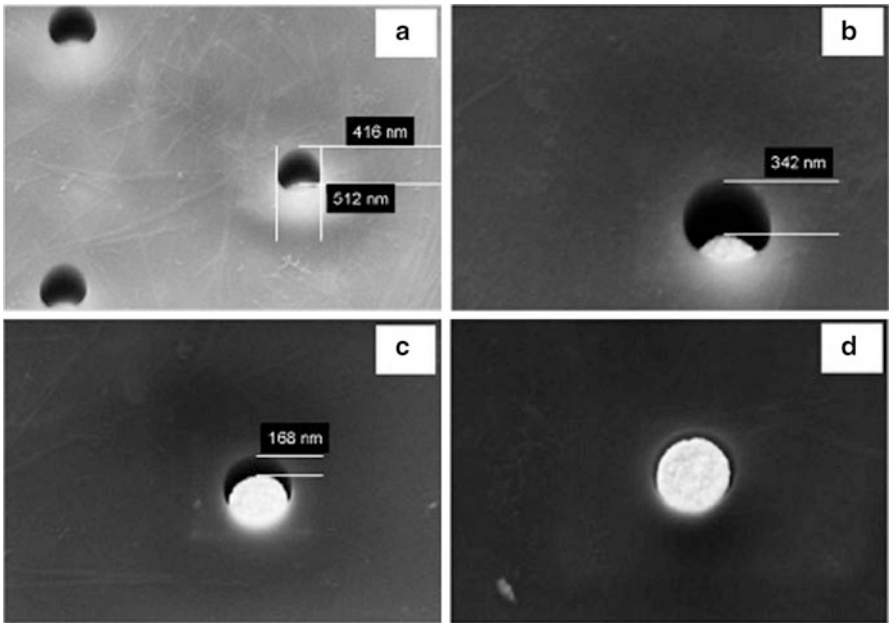

Fig. 20.11 SEM images of NEAs with holes of 500 nm in diameter with gold electrochemically deposited inside for 0 s (**a**), 10 s (**b**), 20 s (**c**) and 30 s (**d**). Estimated recession depths: (**a**) 450 nm; (**b**) 300 nm; (**c**) 150 nm; (**d**) 0 nm. (Reprinted with permission from ref. (83))

$$\mathrm{Ox} + \mathrm{e}^- \rightleftharpoons \mathrm{Red} \tag{20.1}$$

As the reduction of Ox progresses, a depletion of Ox in the vicinity of the electrode surface is observed. This sets up a concentration gradient so that Ox diffuses from the bulk of the solution towards the electrode surface. The layer through which this gradient extends, defines the diffusion layer thickness.[86]

At a macroelectrode, the reduction of Ox occurs across the entire electrode surface so that the diffusion of Ox to the electrode is planar and the current response gives rise to a peak-shaped voltammetric curve.[87] However, at the edge of the electrode, i.e. where the conductive material meets the insulating substrate, the diffusion layer becomes convergent, since the diffusion is effectively to a point. Such edge effect is negligible at macroelectrodes since the contribution of convergent diffusion at the edges is overwhelmed by planar diffusion towards the entire electrode area.

When a ME is used in the same experiment, edge effects become relevant and the diffusion from the bulk of the solution should be described by a radial geometry instead of a linear one. In radial diffusion regime the voltammograms are defined by a sigmoidal shape, where the limiting current (I_{lim}), and not the peak current, is the key parameter directly related to the analyte concentration.

For ultramicroelectrodes, the thickness of the diffusion layer, δ, is given as the summation of planar and radial contribution by Eq. (20.2)[87]:

$$1/\delta(t) = \left[1/(\pi Dt)^{1/2}\right] + 1/r \tag{20.2}$$

where r is the radius of the electrode, D is the diffusion coefficient of the species and t is the timescale of the experiment. From Eq. (20.2) it is evident that the diffusion layer grows with time.

One can conclude that, as the electrode decreases in size, the diffusion layer thickness approaches the size of the electrode dimension.

The steady-state diffusion-controlled limiting current, $I(t \to \infty)$, is proportional to the inverse of the diffusion layer thickness, according to Eq. (20.3)[87]:

$$I(t \to \infty) = nFAC^{\circ}/\delta(t \to \infty) \tag{20.3}$$

where n is the number of electrons exchanged, F is the faraday constant, A is the electrode surface area, and C° is the bulk concentration of the redox species. Dividing Eq. (20.3) by A, it is evident that smaller electrodes provide higher current densities as a consequence of the enhanced mass transport.

For electrodes with dimensions in the tens of nm range, the diffusion layer is decreased to achieve dimensions comparable with the thickness of the electrical double layer. Electrostatic forces within the double layer can accelerate the flux of oppositely charged redox species, so generating the conditions for a further enhancement of the mass transport to the nanoelectrodes surface. Dickinson and Compton[88] presented numerical solution of the Poisson-Boltzman equation, for

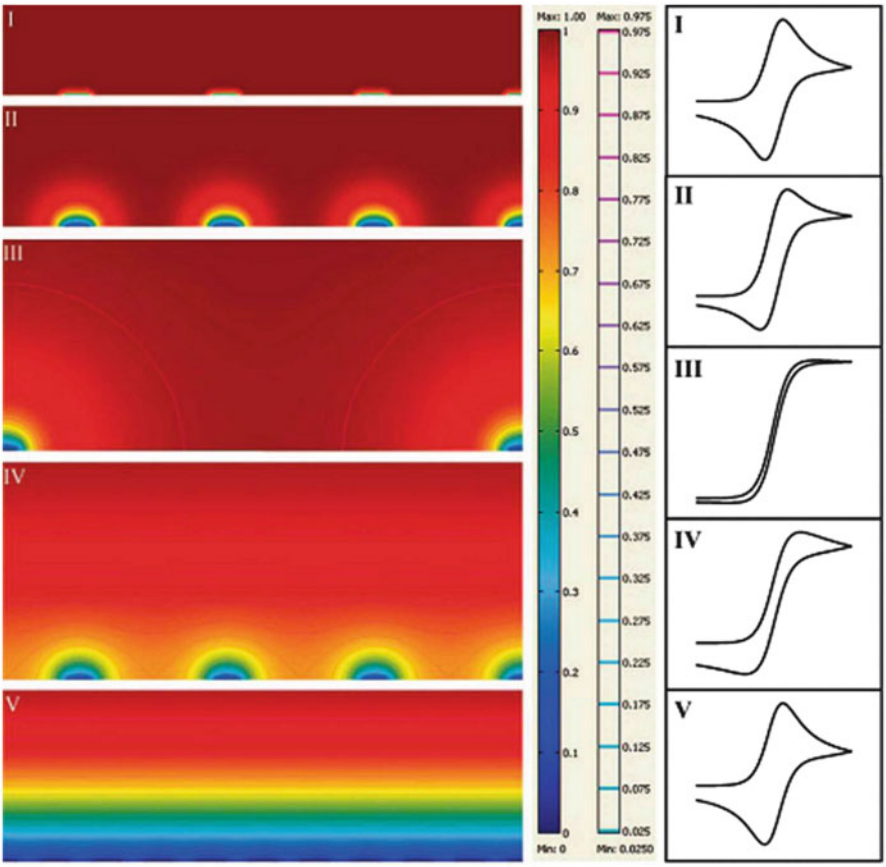

Fig. 20.12 Simulated concentration profiles with isoconcentration contour lines, over a microelectrode array representing the five main categories of diffusion modes (form I to V). In the scale bar next to the figure, the red color represents the bulk concentration and the blue color represents zero concentration. The second scale bar represents a relative concentration scale for the contour lines. Typical CVs of the each category are shown at the right (Reprinted with permission from ref. (92))

hemispherical nanoelectrodes of vanishing size, revealing that the effects of curvature on the diffuse double layer become significant for electrodes with radii less than 50 nm. An enhanced driving force is therefore expected for nanoelectrodes as compared to electrodes larger than 50–100 nm, especially at low concentrations of supporting electrolyte.[88] Further studies, to go deeper into the theoretical modeling of electrochemical processes at nanoelectrodes, are strongly required.[89]

Micro/nanoelectrode arrays can exhibit different voltammetric responses depending on the scan rate (i.e. time scale of the experiment) and the reciprocal distance among the nanoelectrodes.[14, 90, 91]

Different situations are summarized in Fig. 20.12. When radial diffusion boundary layers totally overlap, i.e. when the diffusion hemisphere is larger than the mean

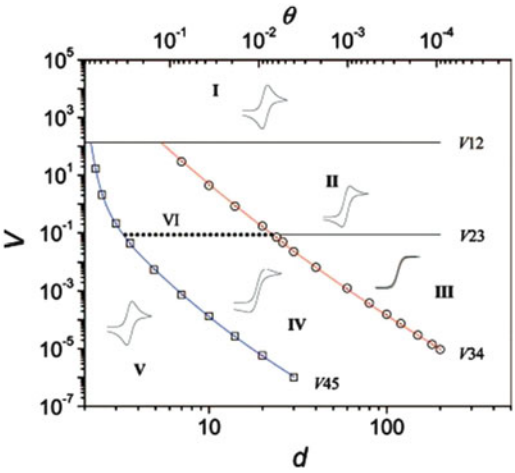

Fig. 20.13 Zone diagram of cyclic voltammetric behavior at microelectrode arrays. *d* is the center-to center distance of individual electrodes in the array (measured in units of a), *V* is the dimensionless scan rate, and θ is the fraction of electrochemically active area in the array. (Reprinted with permission from ref. (92))

hemidistance among the nanoelectrodes, the arrays behave as macroelectrodes with respect to the Faradic current (total overlap regime, peak shape voltammograms, case V). When the diffusion hemisphere becomes shorter (higher scan rates) or the hemidistance among nanodisks is larger, the voltammetric response is dominated by radial diffusion conditions at each element (pure radial regime, sigmoidally shaped voltammograms, case III). At very high scan rates, the linear active state is reached, where linear diffusion is predominant at each electrode (peak-shaped voltammograms, but with peak currents much smaller than case V, case I). Obviously, intermediate situations can be observed (case IV and II).

Recent theoretical studies,[7, 90, 92–94] examined in detail the role of the different diffusion regimes on the voltammetric responses recorded at arrays of micro- and nanoelectrodes. Guo and Lindner[92] introduced a very useful zone-diagram where the combination of suitable dimensionless parameters allows one to determine the diffusion regime (and kind of voltammetric response) operative at a certain kind of array, at a specific voltammetric scan rate (see Fig. 20.13).

Note that such a simulation was developed for arrays in which the effect at the border of the array are negligible; that is for array including a very large number of electrodes.[75, 83]

This condition can be achieved for arrays of small size only if the size of the individual electrodes is very small, i.e. at the nanoscale level. The following example can help in understanding this concept. If one builds an array of 100 electrodes ordered according to a square geometry, 36 of them will be on the periphery. This means that at least 36 % of the electrodes will experience border effects. If one wants to make this border effects negligible, it is necessary to increase the overall number of electrodes in the array of 2 orders of magnitude; e.g. in a 10^4 electrodes squared array only 3.96 % of them will be in the perimeter. If the array is built to operate under pure radial condition, the distance between the electrodes should be at least $10r$,[90] where *r* is the radius of the individual electrodes, which means, that if

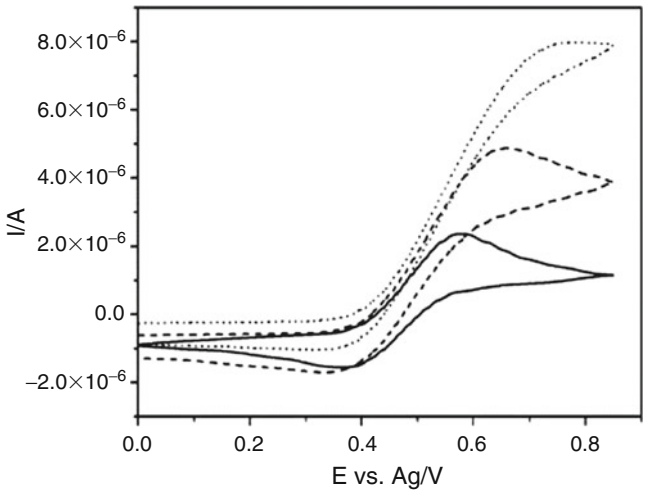

Fig. 20.14 Cyclic voltammograms recorded at different scan rates at a NEE (geometric area 0.07 cm^2; active area 0.004 cm^2), 50 mM ferrocene in [tris(*n*-hexyl)tetradecylphosphonium] [bis (trifluoromethylsulfonyl)amide]. Scan rates: *full line* 5 mV/s; *dashed line* 50 mV/s; *dotted line* 500 mV/s. (Reprinted with permission from ref. (96))

$r = 10$ μm, the side of a 10^4 electrodes-array will be as large as 1 cm. If $r = 0.1$ μm, the side of the array, (with the same number of electrodes), will be only 1 mm. This is an aspect to be taken into account when miniaturization is a must.

On the other hand, in the case of arrays composed by a small number of nanoelectrodes, border effects play a relevant role.[95] Note that, under these conditions, when the overall size of the array is in the μm range, even for arrays operating in total overlap condition, sigmoidally shaped voltammograms are observed.[95]

20.5.1 Current Signals at NEEs

The diffusion regime usually observed at NEEs, fabricated from commercially available track-etched membrane, is the total overlap regime,[45] nevertheless, transition from one regime as a function of the nanoelements distance has been experimentally demonstrated using specially-made membranes.[91] It was recently shown that, for NEE, the transition from the total overlap to the pure radial regime can be observed by increasing the electrolyte viscosity.[96] The voltammetric patterns recorded at NEEs in high-viscosity ionic liquids are indeed peak-shaped CV at low scan rates, while they become sigmoidally shaped at high scan rate (see Fig. 20.14). Note that the diffusion coefficient, D, decreases at increasing viscosity, so that diffusion hemispheres around each nanoelectrodes are smaller in a high-viscosity medium.

Coming back to the more common situation of the voltammetric use of NEEs in aqueous media, it is worth stressing that, for electroanalytical purposes, the main advantage of the total overlap regime is the enhanced detection limit with respect to conventional electrodes with the same surface area. This is because at NEEs operating under total overlap diffusion conditions, the faradaic current (I_F) is proportional to the total geometric area of the ensemble exposed to the sample solution (A_{geom}, area of the nanodisks plus the insulator area), while the double layer capacitive current (I_C), which is the main component of the noise in electroanalytical chemistry, is proportional only to the nanodisks area (active area, A_{act}).[45]

Typical values for the geometric area range from 0.008 to 0.580 cm^2 [75]. Note that this parameter is defined at the moment of the NEE fabrication, by the dimension of the hole punched in the insulator. The active area can be easily calculated by the pore density (q) and mean pore radius (r), using the equation reported below:

$$A_{act} = \pi r^2 q A_{geom} \tag{20.4}$$

The ratio between the active and the geometric area defines a key parameter named fractional electrode area (f):

$$f = A_{act}/A_{geom} \tag{20.5}$$

Faradic-to-capacitive currents at NEEs and conventional electrodes with the same geometric area are related by Eq. (20.6)[97]:

$$(I_F/I_C)_{NEE} = (I_F/I_C)_{conv} f \tag{20.6}$$

Being typical f values for NEEs between 10^{-3} and 10^{-2}, I_F/I_C ratios at NEEs can be 2–3 orders of magnitude higher than for conventional electrodes with the same geometric area. Such an improvement in the faradaic to capacitive currents ratio explains why detection limits (DLs) at NEEs can be 2–3 order of magnitude lower than with conventional electrodes.[45, 98, 99] Since the improvement in S/N ratios are strictly related to the fractional area, the electroanalytical performances of NEEs are not affected by any variation in the geometric area as long as the active area changes accordingly, i.e. the f parameter is kept constant.[75]

Since the main advantage of NEEs over conventional macro (mm-sized) or even ultramicro- (μm-sized) electrodes is a dramatic lowering of double layer capacitive currents[45, 98]; in case of inability to directly characterize the morphology of the electrodes, the lack of this characteristic should be taken into account as a diagnostic parameter to discriminate well-prepared from defective NEEs.

For example, voltammograms affected by a large capacitive current, are indicative of poor sealing between the nanowires and the surrounding PC insulator and/or heavy scratching of the PC membrane caused by improper handling of the NEE. On the other hand, a radial diffusive contribution to the overall signal

suggests a larger distance between the nanoelectrodes, possibly due to a only partial filling of the pores with gold.[74]

20.5.2 Electron Transfer Kinetics at NEEs

An important feature characterizing NEEs and NEAs is that their responses are very sensitive to the electron transfer kinetics.[45] According to model proposed by Amatore et al.,[100] as well as to more recent theoretical studies,[7, 92, 93] NEEs behave as partially blocked surface electrodes (PBEs), whose current responses are identical to those of naked electrodes with the same overall geometric area, but with a smaller apparent rate constant (k°_{app}) for the electron transfer which decreases as the coverage of the surface increases. According to this model, the nanodisks electrodes are the unblocked surface and the template membrane is the blocking material.

The apparent rate constant (k°_{app}) is related to the true standard rate constant by the following equation:

$$k^\circ_{app} = k^\circ(1 - \vartheta) = k^\circ f \tag{20.7}$$

where $\vartheta = (A_{geom} - A_{act})/A_{geom}$ and f is the fractional electrode area (see Eq. 20.5).

From an analytical viewpoint, the operativity of Eq. (20.7) means that high faradic currents can be achieved on redox couples with "very reversible" behavior. In cyclic voltammetry (CV) in fact, the reversibility of a redox system depends on the k° value and on the scan rate (v). Using conventional electrodes, reversible patterns are obtained when:

$$v^{1/2} \leq (k^\circ/0.3) \tag{20.8}$$

but if NEEs are used, k° is substituted by k°_{app}, and the previous relation becomes:

$$v^{1/2} \leq [(k^\circ f)/0.3] \tag{20.9}$$

Considering that mean f values range from 10^{-2} to 10^{-3}, from Eq. (20.9) we can conclude that, for a certain redox couple, the scan rate value that defines the transition between reversible and quasi-reversible behavior will be placed at 2–3 orders of magnitude lower than those at conventional electrodes. Note that such a boundary scan rate will decrease with decreasing f. This is a limitation to be seriously taken into account when trying to optimize NEEs for analytical applications, since it is important to consider the contrasting effect both of the increased I_F/I_C value and the apparent slowing down of the electron transfer kinetics. On the other hand, from a mechanistic viewpoint, it is an advantage since it means that with NEEs it is easier to measure experimentally very large k° values.[45,99] By the analysis of ΔE_p dependence on the scan rate,[101] and using suitable working curves,[102] smaller k°_{app} values are obtained and converted to larger k° by Eq. (20.7).[99]

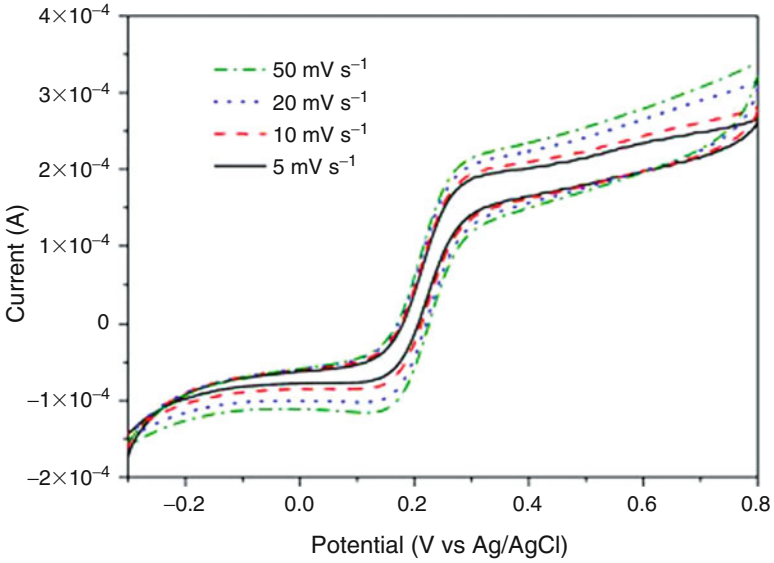

Fig. 20.15 CVs recorded in 10^{-4} M ferrocene methanol and 0.5 M $NaNO_3$. Scan rates: 5 (*full line*), 10 (*dash line*), 20 (*dot line*), and 50 mV s^{-1} (*dash-dot line*). Geometrical characteristics: nanodisk radius = 75 nm, distance centre to centre = 3 μm, estimated number of nanoelectrodes in the array = 1.1×10^4. (Reprinted with permission from ref. (83))

20.5.3 Current Signals at Nanolithographated NEAs

As explained previously, the use of advanced nanolithographic methods allows one to obtain ordered arrays of nanoelectrodes with controlled geometry. The role of the distance/radius of the nanoelectrodes, as well as of their number (with respect to the negligibility of border effects) has been explained earlier in this chapter. For NEA, the possibility to control the geometry of the electrodes in the array allows one to obtain, at pleasure electrode array which operate under pure radial control rather than under total overlap conditions (see Fig. 20.15).

However, it is worth to stress that, because of the nanolithographic process itself, quite often, the nanoelectrodes obtained are slightly recessed, so that theoretical model for such geometries must be taken into account.[78, 83]

20.6 Complex Operating Modes

In the arrays and ensembles presented in the previous paragraphs, all the micro- and nanoelectrodes are polarized at the same potential, and their geometry were designed to amplify the current signal (if the micro- and nanoelectrodes are diffusionally independent) or to minimize the signal-to-noise ratio (if the diffusion

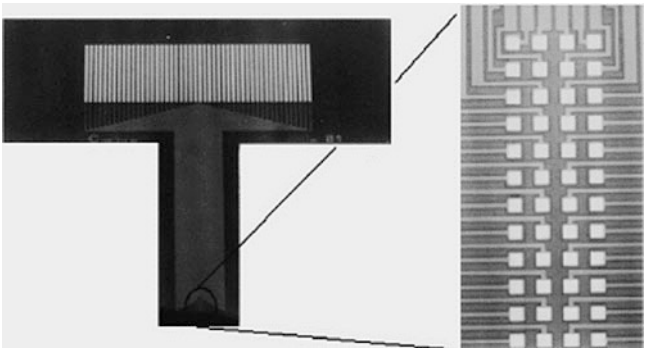

Fig. 20.16 View of silicon chip device which includes 48 connection pads for 48 gold microelectrode. (Reprinted with permission from ref. (106))

layers at the micro- and nanoelectrodes overlap). In this paragraph, we will present arrays with different geometries designed for fast multiparametric analysis, i.e. individually addressable array, or which exploit a peculiar cross-talking diffusion mechanism to enhance the current signal recorded at the array, such as in interdigitated arrays of microelectrodes (IAM).

20.6.1 Individually Addressable Micro- and Nanoelectrode Arrays

At individually addressable arrays, identical or different potentials can be applied to each microelectrode; by this way, as long as diffusional cross-talk between the microelectrodes is avoided, multiple analyte determination can be achieved.

Until now, arrays of individually addressable microelectrodes have been produced very rarely, mainly because their fabrication heavily relies on sophisticated technology. There are two different ways of realizing individually addressable microelectrodes arrays: (1) each electrode may be connected by its own line to a corresponding bond pad on the chip border, therefore each microelectrode of the array has its own connection[103–105] (see Fig. 20.16), or alternatively, (2) in a multiplexed design, in which individual addressing of array electrodes is realized on the chip by an integrated circuit (IC). In this case the addressing hardware is built onto each microelectrode array chip[106–109] (see Fig. 20.17). For obvious reason, the former way of realization is easier from a technological view point, but only a limited number of individually addressable microelectrodes can be located on the array because of the limited space on the chip border available for bond pads.

The electrochemical measurements can be performed sequentially or simultaneously; however, recording sequentially cyclic voltammograms with a large number of individually addressed microelectrodes can be time consuming.[110]

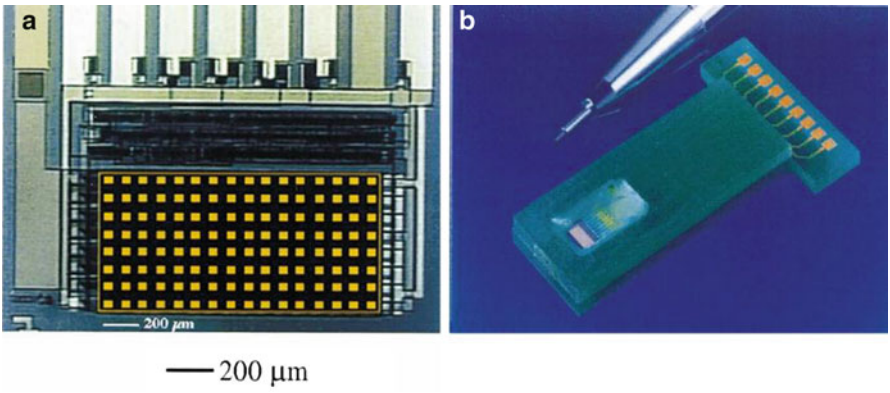

Fig. 20.17 (**a**) Multiplexed chip bearing 128 microelectrodes (16 × 8) for 9 inlets/outlets pads. The addressing hardware is built onto the microelectrode array chip. (**b**) View of the packaged chip. (Reprinted with permission from ref. (106))

Although individually addressable microelectrode arrays require sophisticated technology and electronic circuitry, they found application in a number of field such as: high spatial resolution concentration profile,[107] extracellular signal recording,[103] multiplexed peptide and DNA analysis.[106]

Addressable electrodes arrays functionalized with biomolecules, were successfully commercialized as electrochemical sensors for immunoassays. An example is the CombiMatrix 98001 chip. This array was, at first, developed for the synthesis of different nucleic acid sequences, by using electrochemical placement of nucleic acids at specific locations.[111] The CombiMatrix method allows to drive the building of oligonucleotides on single elements of the array by a software-controlled turning on and off of the synthetic reaction. DNA arrays, at first, found applications in gene expression levels,[112, 113] resequencing genes to identify mutations[114–116] analysis of sequence polymorphism on a large scale[117] and analyzing DNA–protein interactions.[118] Anyway, the possibility to individually functionalize each electrode of the array allowed the application of the sensor to multiplexed immunoassay analysis, by exploiting antigen–antibody interactions. By functionalizing antibodies with specific oligonucleotides, it is possible to direct the adsorption of the antibodies on specific microelectrodes where complementary oligonucleotides were synthesized. The key feature of this system is the exploitation of biological sensing elements for antigen recognition and the ability to screen those antigens against a vast array of probes. This mechanism was further developed in applications such as: detection of pathogens,[119–121] proteomic and protein detection,[122, 123] oncologic diagnostic.[124, 125]

Although being desirable, the preparation of individually addressable nanoelectrode arrays is still at an early development level.[126] The further miniaturization of addressable arrays would allow to increase the number of electrodes in the arrays, as well as to enhance the mass transport and therefore the current density achieved by the sensor.

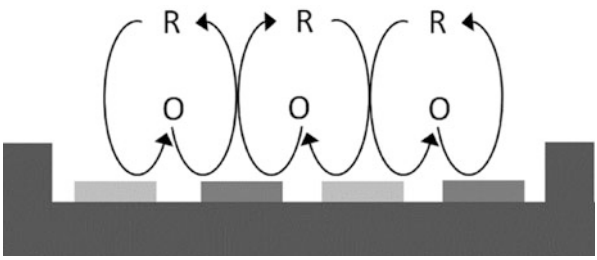

Fig. 20.18 Illustration of the current enhancement mechanism of redox cycling on an IAM electrode. *R* reduced molecule, *O* oxidized molecule

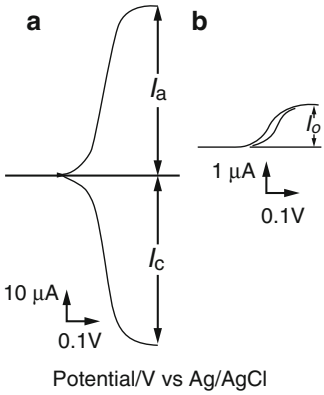

Fig. 20.19 Cyclic voltammogram of 1 mM ferrocene in acetonitrile solution at IAM. (**a**) Dual mode; (**b**) single mode. (Reprinted with permission from ref. (131))

20.6.2 Interdigitated Arrays

The interdigitated arrays of microelectrodes (IAM) consist of a multiple pairs of microband electrodes which are separated by a small gap. Each set of microband electrodes in the IAM can be potentiostated individually, so that a redox species generated at a microband electrode (generator) can diffuse through a small gap towards a second microband electrode (collector) where the reverse reaction takes place. This peculiar feature gives to such electrode-specific electrochemical behavior which can be exploited for analytical purposes.[127] In fact, such redox cycling mechanism greatly enhances the current output[128]; moreover the narrow gap between generator and collector microband electrodes is advantageous for measuring diffusion coefficients of redox species in highly resistive media[129, 130] because enhanced electric signal and fast response time can be achieved.[131] In Fig. 20.18, the redox cycling mechanism on a IAM electrode is reported.

The redox cycling mechanism described above is achieved when IAM are operated in dual mode. In dual mode, the collector electrodes are held at a constant potential, while the generator electrodes are scanned. As the generator electrode potential approaches the redox potential, both collector and generator current increases by the same magnitude but with opposite sign ($I_a = -I_c$). When the generator potential overcomes the redox potential, both generator and collector currents reach a plateau. In Fig. 20.19a a voltammogram recorded with IAM operating in dual mode is reported.

When IAM is operated in single mode (Fig. 20.19b), the collector electrodes are not potentiostated, and the current recorded at the generator electrodes give a sigmoidal curve. Note that the current recorded in dual mode is about 50 times higher than that recorded in single mode.

Dual mode, not only enhances the current signal, but the absence of a capacitive charging current at the collector electrode also enhances the signal-to-noise ratio. In fact, in conventional cyclic voltammetry the magnitude of the charging current is linearly proportional to the scan rate, the Faradic current, instead, is proportional to the square root of the scan rate. Therefore, a higher scan rate gives a lower signal-to-noise ratio. When the IAM electrode is operated in dual mode, there is no charging current at the collector because the potential is fixed. Even when the potential scan rate is high and redox cycling becomes inefficient, the collector current is not affected by double layer charging currents. Therefore, the IAM electrode is also suitable for high scanning speed voltammetry.

The diffusion-controlled limiting current at IAM operating in dual mode is given by Eq. (20.10)[132]:

$$\left|I_{lim}\right| = mbnFc * D\left[0.637\ln\left\{2.25\left(1 + W_b/W_g\right)\right\} - 0.19/\left(1 + W_b/W_g\right)^2\right] \quad (20.10)$$

Where m is number of microband electrode pairs, b is the band length and W_b and W_g are the microband and the gap width, respectively. From this equation, it is evident that the smaller the gap between the microelectrodes, the higher the redox cycle number obtained and, as a consequence, the higher the current enhancement. Narrow-gap IAM offers high sensitivity and short response time. The IAM electrode also has a small sample volume requirement for practical measurements. These characteristics make IAM suitable for the detection of biological substances and for detection in liquid chromatography (LC) or flow injection analysis (FIA).[133]

20.7 Conclusion

Micro and nanoelectrodes arrays can be obtained both by bottom-up and top-down nanotechnologies. In both cases, the final result is a composite material in which micro or nanoelements of a metal conductor are embedded into an insulating matrix. The control of the geometry of the composite allows one to obtain functional materials with unique electroanalytical characteristics. MEE and NEE can be obtained by rather simple and cheap techniques, the main drawback being the random geometry of the array, which leads to a less precise description of the array behavior by modeling. On the other hand the fabrication of MEA and NEA with high spatial resolution requires expensive and technological demanding instrumentations.

Arrays show enhanced mass fluxes and are characterized by a dramatic enhancement of the signal to background current ratio with respect to other electrode

systems. Since the mass flux enhancement scales inversely with the electrode dimensions, fabrication of arrays/ensembles of electrodes in the nanometer scale (NEA/NEE) allows to further increase the current density recorded at the arrays. A drawback is their extreme sensitivity to the electron transfer kinetics.

The possibility to move from present NEE/NEA (where all nanoelectrodes are interconnected each other) to more sophisticated nanoelectrodes systems, where multiple analyte determination is achieved, as well as the extreme miniaturization of such devices, are obvious for environmental or food analyses and for materials testing as well.

Finally, it is worth stressing that further advantages can be pointed out due to the composite nature of micro and nanoelectrode arrays. They are indeed composed of metal nanoelements surrounded by a (relatively) wide surface of a suitable polymer. Recent studies showed that a wide polymer surface can be exploited for functionalization process, by immobilizing on it molecule layers with biorecognition capabilities, which can be coupled, by a suitable redox cycle, with the electrochemical transduction capabilities of the metal nanoelectrodes.[84, 85, 134]

Future research efforts should be devoted to the development of singly addressable nanoelectrodes where multiple analyte determination can be achieved. Furthermore, studies to go deeper into the theoretical modeling of electrochemical processes at nanoelectrodes are strongly required, in order to gain a better understanding of their electrochemical behavior.

Acknowledgements The authors would like to thank MIUR (Rome) (project: PRIN 2010AXENJ8) for the partial financial support.

References

1. Compton RG, Wildgoose GG, Rees NV, Streeter I, Baron R (2008) Design, fabrication, characterisation and application of nanoelectrode arrays. Chem Phys Lett 459:1–17
2. Štulík K, Amatore C, Holub K, Mareček V, Kutner W (2000) Microelectrodes. Definitions, characterization, and applications. Pure Appl Chem 72:1483–1492
3. Penner RM, Martin CR (1987) Preparation and electrochemical characterization of ultramicroelectrode ensembles. Anal Chem 59:2625–2630
4. LaFratta CN, Walt DR (2008) Very high density sensing arrays. Chem Rev 108:614–637
5. Szunertis S, Walt DR (2003) The use of optical fiber bundles combined with electrochemistry for chemical imaging. Chem Phys Chem 4:186–192
6. Szunertis S, Thouin L (2007) Microelectrode arrays. In: Zoski CG (ed) Handbook of electrochemistry. Elsevier, Amsterdam
7. Huang X-J, O'Mahony AM, Compton RG (2009) Microelectrode arrays for electrochemistry: approaches to fabrication. Small 5:776–788
8. Beni V, Arrigan DWM (2008) Microelectrode arrays and microfabricated devices in electrochemical stripping analysis. Curr Anal Chem 4:229–241
9. Wu P (1993) Fabrication and characterization of a new class of microelectrodes arrays exhibiting steady-state current behavior. Anal Chem 65:1643–1646

10. Lee CY, Tan YJ, Bond AM (2008) Identification of surface heterogeneity effects in cyclic voltammograms derived from analysis of an individually addressable gold array electrode. Anal Chem 80:3873–3881
11. Nascimento VB, Augelli MA, Pedrotti JJ, Gutz IGR, Angnes L (1997) Arrays of gold microelectrodes made from split integratedcircuit chips. Electroanal 9:335–339
12. Szunerits S, Garrigue P, Bruneel J-L, Servant L, Sojic N (2003) Fabrication of a sub-micrometer electrode array: electrochemical characterisation and mapping of an electroactive species by confocal raman microspectroscopy. Electroanal 15:548–555
13. Cheng IF, Martin CR (1988) Ultramicrodisk electrode ensembles prepared by incorporating carbon paste into a microporous host membrane. Anal Chem 60:2163–2165
14. Cheng IF, Whiteley LD, Martin CR (1989) Ultramicroelectrode ensembles. comparison of experimental and theoretical responses and evaluation of electroanalytical detection limits. Anal Chem 61:762–766
15. Jin WR, Weng QF, Wu JR (1997) Determination of bovine serum albumin by capillary zone electrophoresis with end-column amperometric detection at the carbon fiber microdisk array electrode. Anal Chim Acta 342:67–74
16. Jin WR, Wei HY, Zhao X (1997) Determination of adenine and guanine by capillary zone electrophoresis with end-column amperometric detection at a carbon fiber microdisk array electrode. Electroanal 9:770–774
17. Cheng Q, Brajter-Toth A (1992) Selectivity and sensitivity of self-assembled thioctic acid electrodes. Anal Chem 64:1998–2002
18. Cheng Q, Brajter-Toth A (1995) Permselectivity and high sensitivity at ultrathin monolayers. Effect of film hydrophobicity. Anal Chem 67:2767–2775
19. Cheng Q, Brajter-Toth A (1996) Permselectivity, sensitivity, and amperometric pH sensing at thioctic acid monolayer microelectrodes. Anal Chem 68:4180–4185
20. Ulman A (1996) Formation and structure of self-assembled monolayers. Chem Rev 96:1533–1554
21. Nishizawa M, Sunagawa T, Yoneyama H (1997) Selective desorption of 3-mercaptopropionic acid from a mixed monolayer with hexadecanethiol assembled on a gold electrode. J Electroanal Chem 436:213–218
22. He HX, Li QG, Zhou ZY, Zhang H, Li SFY, Liu ZF (2000) Fabrication of microelectrode arrays using microcontact printing. Langmuir 16:9683–9686
23. Sankhe AY, Booth BD, Wiker NJ, Kilbey SM (2005) Inkjet-printed monolayers as platforms for tethered polymers. Langmuir 21:5332–5336
24. Rianasari I, Walder L, Burchardt M, Zawisza I, Wittstock G (2008) Inkjet-printed thiol self-assembled monolayer structures on gold: quality control and microarray electrode fabrication. Langmuir 24:9110–9117
25. Lowinsohn D, Peres HEM, Kosminsky L, Paixao TRLC, Ferreira TL, Ramirez-Fernandez F-J, Bertotti M (2006) Design and fabrication of a microelectrode array for iodate quantification in small sample volumes. Sensor Actuat B Chem 113:80–87
26. Aguiar FA, Gallant AJ, Rosamond MC, Rhodes A, Wood D, Kataky R (2007) Conical recessed gold microelectrode arrays produced during photolithographic methods: characterization and causes. Electrochem Commun 9:879–885
27. Ordeig O, Godino N, del Campo J, Munoz FX, Nikolajeff F, Nyholm L (2008) On-chip electric field driven electrochemical detection using a poly(dimethylsiloxane) microchannel with gold microband electrodes. Anal Chem 80:3622–3632
28. Varshney M, Li Y (2008) Double interdigitated array microelectrode-based impedance biosensor for detection of viable *Escherichia coli* O157:H7 in growth medium. Talanta 74:518–525
29. Ojima H, Umeda M, Mohamedi M, Uhida I (2003) Electrochemical detection of protons produced in an electrode reaction using interdigitated microarray electrodes. Electroanal 15:1677–1681

30. Gavin PF, Ewing EG (1996) Continuous separations with microfabricated electrophoresis-electrochemical array detection. J Am Chem Soc 118:8932–8936
31. Orozco J, Suarez G, Fernandez-Sanchez C, McNeil C, Jimenez-Jorquera C (2007) Characterization of ultramicroelectrode arrays combining electrochemical techniques and optical microscopy imaging. Electrochim Acta 53:729–736
32. Koster O, Schumann W, Vogt H, Mokwa W (2001) Quality control of ultra-microelectrode arrays using cyclic voltammetry, electrochemical impedance spectroscopy and scanning electrochemical microscopy. Sensor Actuat B Chem 76:573–581
33. Berduque A, Lanyon YH, Beni V, Herzog G, Watson YE, Rodgers K, Stam F, Alderman J, Arrigan DWM (2007) Voltammetric characterisation of silicon-based microelectrode arrays and their application to mercury-free stripping voltammetry of copper ions. Talanta 71:1022–1030
34. Nolan MA, Kouvanes SP (1999) Microfabricated array of iridium microdisks as a substrate for direct determination of Cu^{2+} or Hg^{2+} using square-wave anodic stripping voltammetry. Anal Chem 71:3567–3573
35. Silva PRM, El Khakani MA, Le Drogoff B, Chaker M, Vijh AK (1999) Mercury-electroplated-iridium microelectrode array based sensors for the detection of heavy metal ultratraces: optimization of the mercury charge. Sensor Actuat B Chem 60:161–167
36. Tercier-Weaber M- L, Buffle J, Ficcabrino GC, Koudelka-Hep M, Riccardi G, Confalonieri F, Sina A, Graziottin F (2000) A novel probe with individually addressable gel-integrated microsensor arrays for real-time high spatial resolution concentration profile measurements. Electroanal 12:27–34
37. Kouvanes SP, Deng W, Hallock PR, Kovacs GT, Storment C (1994) Iridium-based ultramicroelectrode array fabricated by microlithography. Anal Chem 66:418–423
38. Noel S, Tercier-Waeber M-L, Lin L, Buffle J, Guenat O, Koudelka-Hep M (2006) Integrated microelectroanalytical system for direct simultaneous voltammetric measurements of free meta ion concentrations in natural waters. Electroanal 18:2061–2069
39. Wang J, Luo D-B, Horiuchi T (1998) Anodic stripping with collection at interdigitated carbon film microelectrode arrays. Electroanal 10:107–110
40. Heo JI, Shim DS, Teixidor GT, Oh S, Madou MJ, Shin H (2011) Carbon interdigitated array nanoelectrodes for electrochemical applications. J Electrochem Soc 158:J76–J80
41. Lawrence NS, Pagels M, Meredith A, Jones TGJ, Hall CE, Pickles CSJ, Godfried HP, Banks CE, Compton RG, Jiang L (2006) Electroanalytical applications of boron-doped diamond microelectrode arrays. Talanta 69:829–834
42. Simm AO, Banks CE, Ward-Jones S, Davies TJ, Lawrence NS, Jones TGJ, Jiang L, Compton RG (2005) Boron-doped diamond microdisc arrays: electrochemical characterisation and their use as a substrate for the production of microelectrode arrays of diverse metals (Ag, Au, Cu) via electrodeposition. Analyst 130:1303–1311
43. Possin GE (1970) A method for forming very small diameter wires. Rev Sci Instrum 41:772–774
44. Williams WD, Giordano N (1984) Fabrication of 80Å metal wires. Rev Sci Instrum 55:410–412
45. Menon VP, Martin CR (1995) Fabrication and evaluation of nanoelectrode ensembles. Anal Chem 67:1920–1928
46. Ongaro M, Ugo P (2013) Bioelectroanalysis with nanoelectrode ensembles and arrays. Anal Bioanal Chem 405:3715–3729
47. Routkevitch D, Bigioni T, Moskovits M, Xu J-M (1996) Electrochemical fabrication of CdS nanowire arrays in porous anodic aluminum oxide templates. J Phys Chem 100:14037–14047
48. Schoenberger C, van der Zande BMI, Fokkink LGJ, Henny M, Schmid C, Kruger M, Bachtold A, Huber R, Birk H, Staufer U (1997) Template synthesis of nanowires in porous polycarbonate membranes: electrochemistry and morphology. J Phys Chem B 101:5497–5505
49. Martin CR (1999) In: Bard AJ, Rubinstein I (eds) Electroanalytical chemistry. Marcel Dekker, New York

50. De Leo M, Pereira FC, Moretto LM, Scopece P, Polizzi S, Ugo P (2007) Towards a better understanding of gold electroless deposition in track-etched templates. Chem Mater 19:5955–5964
51. Gilliam RJ, Thorpe SJ, Kirk DJW (2006) A nucleation and growth study of gold nanowires and nanotubes in polymeric membranes. Appl Electrochem 37:233–239
52. Pra LD-D, Ferain E, Legras R, Demoustier-Champagne S (2002) Beam interactions with materials and atoms. Nucl Instrum Methods Phys Res B 196:81–88
53. Gambirasi A, Cattarin S, Musiani M, Vázquez-Gómez L, Verlato E (2011) Direct electrodeposition of metal nanowires on electrode surface. Electrochim Acta 56:8582–8588
54. Konishi Y, Motoyama M, Matsushima H, Fukunaka Y, Ishii R, Ito Y (2003) Electrodeposition of Cu nanowire arrays with a template. J Electroanal Chem 559:149–153
55. Motoyama M, Fukunaka Y, Sakka T, Ogata YH, Kikuchi S (2005) Electrochemical processing of Cu and Ni nanowire arrays. J Electroanal Chem 584:84–91
56. De Leo M (2006) Nanoelectrode ensembles for electrochemical sensing purposes. PhD thesis, University Ca' Foscari of Venice, Université de Bordeaux 1, doi: http://hdl.handle.net/10579/766
57. Piraux L, Duboix S, Champagne S (1997) Template synthesis of nanoscale materials using the membrane porosity. Nucl Inst Methods Phys Res B 131:357–363
58. Chiriac H, Moga AE, Urse M, Ovari T-A (2003) Preparation and magnetic properties of electrodeposited magnetic nanowires. Sensors Actuat A Phys 106:348–351
59. Pirota KR, Navas D, Hernandez-Vélez M, Nielsch K, Vasquez M (2004) Novel magnetic materials prepared by electrodeposition techniques: arrays of nanowires and multi-layered microwires. J Alloy Compd 369:18–26
60. Platt M, Dryfeand RAW, Robaerts EPL (2004) Structural and electrochemical characterisation of Pt and Pd nanoparticles electrodeposited at the liquid/liquid interface. Electrochim Acta 49:3937–3945
61. Prieto AL, Sander MS, Gonzalez MSM, Gronsky R, Sands T, Stacy AM (2001) Electrodeposition of ordered Bi_2Te_3 nanowire arrays. J Am Chem Soc 123:7160–7161
62. Paunovic M, Schlesinger M (2000) Modern electroplating. Wiley, New York
63. Pereira FC, Moretto LM, De Leo M, Boldrin Zanoni MV, Ugo P (2006) Gold nanoelectrode ensembles for direct trace electroanalysis of iodide. Anal Chim Acta 575:16–24
64. Jirage KB, Hulteen JC, Martin CR (1997) Nanotubule-based molecular-filtration membranes. Science 278:655–658
65. Hulteen JC, Jirage KB, Martin CR (1998) Introducing chemical transport selectivity into gold nanotubule membranes. J Am Chem Soc 120:6603–6604
66. Bercu B, Enculescu I, Spohr R (2004) Copper tubes prepared by electroless deposition in ion track templates. Nucl Inst Methods B 225:497–502
67. Dryfe RAW, Simm AO, Kralj B (2003) Electroless deposition of palladium at bare and templated liquid/liquid interfaces. J Am Chem Soc 125:13014–13015
68. Tai Y-L, Teng H (2004) Template synthesis and electrochemical characterization of Nickel-based tubule electrode arrays. Chem Mater 16:338–342
69. Krishnamoorthy K, Zoski CG (2005) Fabrication of 3D gold nanoelectrode ensembles by chemical etching. Anal Chem 77:5068–5071
70. De Leo M, Kuhn A, Ugo P (2007) Ionomer-coated electrodes and nanoelectrode ensembles as electrochemical environmental sensors: recent advances and prospects. Electroanal 19:227–236
71. Yu S, Li N, Wharton J, Martin CR (2003) Nano wheat fields prepared by plasma-etching gold nanowire-containing membranes. Nano Lett 3:815–818
72. Ugo P, Moretto LM, Vezzà F (2002) Ionomer-coated electrodes and nanoelectrode ensembles as electrochemical environmental sensors: recent advances and prospects. Chem Phys Chem 3:917–925
73. Ugo P (2005) Polymer based voltammetric sensors. In: Grimes CA, Dickey EC, Pishko MV (eds) Encyclopedia of sensors. American Scientific Publishers, Stevenson Ranch

74. Ugo P, Moretto LM (2007) Template depositions of metals. In: Zoski C (ed) Handbook of electrochemistry. Elsevier, Amsterdam
75. Moretto LM, Pepe N, Ugo P (2004) Voltammetry of redox analytes at trace concentrations with nanoelectrodes ensembles. Talanta 62:1055–1060
76. Arrigan DWM (2004) Nanoelectrods, nanoelectrode arrays and their application. Analyst 129:1157–1165
77. Errachid A, Mills CA, Pla-Roca M, Lopez MJ, Villanueva G, Bausells J, Crespo E, Teixidor F, Samitier J (2008) Focused ion beam production of nanoelectrode arrays. Mater Sci Eng C 28:777–780
78. Lanyon YH, De Marzi G, Watson YE, Quinn AJ, Gleeson JP, Redmond G, Arrigan DWM (2007) Fabrication of nanopore array electrodes by focused ion beam milling. Anal Chem 79:3048–3055
79. Sandison ME, Cooper JM (2006) Nanofabrication of electrode arrays by electron-beam and nanoimprint lithographies. Lab Chip 6:1020–1025
80. Losilia NS, Martinez J, Garcia R (2009) Large area nanoscale patterning of silicon surfaces by parallel local oxidation. Nanotechnology 20:475304
81. Losilia NS, Oxtoby NS, Martinez J, Garcia F, Garcia R, Mas-Torrent M, Vecciana J, Rovia C (2008) Sub-50 nm positioning of organic compounds onto silicon oxide patterns fabricated by local oxidation nanolithography. Nanotechnology 19:455308
82. Albonetti C, Martinez J, Losilia NS, Greco P, Cavallini M, Borgatti F, Montecchi M, Pasquali L, Garcia R, Biscarini F (2008) Parallel-local anodic oxidation of silicon surfaces by soft stamps. Nanotechnology 19:435303
83. Moretto LM, Tormen M, De Leo M, Carpentiero A, Ugo P (2011) Polycarbonate-based ordered arrays of electrochemical nanoelectrodes obtained by e-beam lithography. Nanotechnology 22:185305
84. Pozzi Mucelli S, Zamuner M, Tormen M, Stanta G, Ugo P (2008) Nanoelectrode ensembles as recognition platform for electrochemical immunosensors. Biosens Bioelectron 23:1900–1903
85. Zamuner M, Pozzi Mucelli S, Tormen M, Stanta G, Ugo P (2008) Electrochemical nanobiosensors and protein detection. Eur J Nanomed 1:33–36
86. Compton RG, Banks CE (2007) Understanding voltammetry. World Scientific, Singapore
87. Bard AJ, Faulkner L (2000) Electrochemical methods. Wiley, New York
88. Dickinson EJF, Compton RG (2009) Diffuse double layer at nanoelectrodes. Phys Chem Lett C 113:17585–17589
89. Henstridge MC, Compton RG (2011) Mass transport to micro- and nanoelectrodes and their arrays: a review. Chem Rec 12:63–71
90. Lee HJ, Beriet C, Ferrigno R, Girault HH (2001) Cyclic voltammetry at a regular microdisc electrode array. J Electroanal Chem 502:138–145
91. Hulteen JC, Menon VP, Martin CR (1996) Template preparation of nanoelectrode ensembles achieving the "pure-radial" electrochemical-response limiting case. J Chem Soc Faraday T 92:4029–4032
92. Guo J, Lindner E (2009) Cyclic voltammograms at coplanar and shallow recessed microdisk electrode arrays: guidelines for design and experiment. Anal Chem 81:130–138
93. Davies TJ, Compton RG (2005) The cyclic and linear sweep voltammetry of regular and random arrays of microdisc electrodes: theory. J Electroanal Chem 585:63–82
94. Amatore C, Oleinik AI, Svir I (2009) Numerical simulation of diffusion processes at recessed disk microelectrode arrays using the quasi-conformal mapping approach. Anal Chem 81:4397–4405
95. Godino N, Borrise X, Munoz FX, del Campo FJ, Compton RG (2009) Mass transport to nanoelectrode arrays and limitations of the diffusion domain approach: theory and experiment. J Phys Chem C 113:11119–11125
96. Ugo P, Moretto LM, De Leo M, Doherty AP, Vallese C, Pentlavalli S (2010) Diffusion regimes at nanoelectrode ensembles in different ionic liquids. Electrochim Acta 55:2865–2872

97. Ugo P, Moretto LM, Vezzà F (2003) In: Baltes H, Fedder GK, Korvink JG (eds) Sensors update. Wiley-VCH, Weinheim
98. Ugo P, Moretto LM, Bellomi S, Menon VP, Martin CR (1996) Ion exchange voltammetry at polymer film coated nanoelectrode ensembles. Anal Chem 68:4160–4165
99. Brunetti B, Ugo P, Moretto LM, Martin CR (2000) Electrochemistry of phenothiazine and methylviologen biosensor electron-transfer mediators at nanoelectrode ensembles. J Electroanal Chem 491:166–174
100. Amatore C, Saveant JM, Tessier D (1983) Charge transfer at partially blocked surfaces. A model for the case of microscopic active and inactive sites. J Electroanal Chem 147:39–51
101. Greef R, Pea R, Peter LM, Pletcher D, Robinson J (1985) Instrumental methods in electrochemistry. Ellis Horwood Ltd., Chester
102. Nicholson RS (1965) Theory and application of cyclic voltammetry for measurement of electrode reaction kinetics. Anal Chem 37:1351–1355
103. Ecken H, Ingebrandt S, Krause M, Richter D, Hara M, Offenhausser A (2003) 64-Channel extended gate electrode arrays for extracellular signal recording. Electrochim Acta 48:3355–3362
104. Zoski C, Simjee N, Guenat O, Koudelka-Hep M (2004) Addressable microelectrode arrays: characterization by imaging with scanning electrochemical microscopy. Anal Chem 76:62–72
105. Connolly P, Moores GR, Monaghan W, Shen J, Britland S, Clark P (1992) Microelectronic and nanoelectronic interfacing techniques for biological systems. Sensor Actuat B Chem 6:113–121
106. Livache T, Bazin H, Caillat P, Roget A (1998) Electroconducting polymers for the construction of DNA or peptide arrays on silicon chips. Biosens Bioelectron 13:629–634
107. Pei J, Tercier-Waeber M-L, Buffle J, Fiaccabrino GC, Koudelka-Hep M (2001) Individually addressable gel-integrated voltammetric microelectrode array for high-resolution measurement of concentration profiles at interfaces. Anal Chem 73:2273–2281
108. Meyer H, Drewer H, Ortindig B, Cammann K, Kakerow R, Manoli Y, Mokwa W, Rospert M (1995) Two-dimensional imaging of O_2, H_2O_2, and glucose distributions by an array of 400 individually addressable microelectrodes. Anal Chem 67:1164–1170
109. Ficcabrino GC, Koudelka-Hep M, Jeanneret S, Vandenberg A, Derooij NF (1994) Array of individually addressable microelectrodes. Sensor Actuat B Chem 19:675–677
110. Sullivan MG, Utomo H, Fagan PJ, Ward MD (1999) Automated electrochemical analysis with combinatorial electrode arrays. Anal Chem 71:4369–4375
111. Montgomery DD (2000) Electrochemical solid phase synthesis. US Patent 6,093,302, 25 July 2000
112. Lockhart DJ, Dong HL, Byrne MC, Follettie MT, Gallo MV, Chee MS, Mittmann M, Wang CW, Kobayashi M, Horton H, Brown EL (1996) Expression monitoring by hybridization to high-density oligonucleotides arrays. Nat Biotechnol 14:1675–1680
113. Schena M, Shalon D, Davis RW, Brown PO (1995) Quantitative monitoring of gene expression patterns with a complementary DNA microarray. Nature 270:467–470
114. Chee M, Yang R, Hubbell E, Berno A, Huang XC, Stern D, Winkler J, Lockhardt DJ, Morris MS, Fodor SPA (1996) Accessing genetic information with high-density DNA arrays. Science 274:610–614
115. Cargill M, Altshuler D, Ireland J, Sklar P, Ardlie K, Patil N, Shaw N, Lane CR, Lim EP, Kalyanaraman N et al (1999) Characterization of a single-nucleotide polymorphisms in coding regions of human genes. Nat Genet 22:231–238
116. Halushka MK, Fan JB, Bentley K, Hsie L, Shen N, Weder A, Cooper R, Lipshutz R, Chakravarti A (1999) Patterns of a single-nucleotide polymorphisms in candidate genes for blood-pressure homeostasis. Nat Genet 22:239–247
117. Wang DG, Fan JB, Siao CJ, Berno A, Young P, Sapolsky R, Ghandour G, Perkins N, Winchester E, Spencer J et al (1998) Large-scale identification, mapping and genotyping of single-nucleotide polymorphisms in the human genome. Science 180:1077–1082
118. Bulyk ML, Gentalen E, Lockhart DJ, Church GM (1999) Quantifying DNA–protein interactions by double-stranded DNA arrays. Nat Biotechnol 17:573–577

119. Wojciechowski J, Danley D, Cooper J, Yazvenko N, Rowe Taitt C (2010) Multiplexed electrochemical detection of yersinia pestis and staphylococcal enterotoxin B using an antibody microarray. Sensors 10:3351–3362
120. Yoo SM, Lee SY (2008) Diagnosis of pathogens using DNA microarray. Recent Pat Biotechnol 2:124–129
121. Aguilar ZP, Fritsch I (2003) Immobilized enzyme linked DNA-hybridization assay with electrochemical detection for cryptosporidium parvum hsp70 mRNA. Anal Chem 75:3890–3897
122. MacBeath G (2002) Protein microarrays and proteomics. Nat Genet 32:526–532
123. Stoevesandt O, Taussig MJ, He M (2009) Protein microarrays: high-throughput tools for proteomics. Expert Rev Proteomics 6:145–157
124. Mischel PS, Cloughesy TF, Nelson SF (2004) DNA-microarray analysis of brain cancer: molecular classification for therapy. Nat Rev Neurosci 10:782–792
125. Macgregor PF, Squire JA (2002) Application of microarrays to the analysis of gene expression in cancer. Clin Chem 48:1170–1177
126. Zoski CG, Yang N, He P, Berdondini L, Koudelka-Hep M (2007) Addressable Nanoelectrode Membrane Arrays: Fabrication and Steady-State Behavior. Anal Chem 79:1474–1484
127. Sanderson DG, Anderson LB (1985) Filar electrodes: steady-state currents and spectroelectrochemistry at twin interdigitated electrodes. Anal Chem 57:2388–2393
128. Amatore C, Fosset B, Bartlet J, Deakin MR, Wighman RM (1988) Electrochemical kinetics at microelectrodes: part V. Migrational effects on steady or quasi-steady-state voltammograms. J Electroanal Chem 256:255–268
129. Nishihara H, Dalton F, Murray RW (1991) Interdigitated array electrode diffusion measurements in donor-acceptor solutions in polyether electrolyte solvents. Anal Chem 63:2955–2960
130. Goss CA, Majda M (1991) Lateral diffusion in organized bilayer assemblies of electroactive amphiphiles influence of the oxidation state of the amphiphile investigated by steady-state methods involving an interdigitated micro-electrode array device. J Electroanal Chem 300:377–405
131. Niwa O (1995) Electroanalysis with interdigitated array microelectrodes. Electroanal 7:606–613
132. Aoki K, Morita M, Niwa O, Tabei H (1988) Quantitative analysis of reversible diffusion-controlled currents of redox soluble species at interdigitated array electrodes under steady-state conditions. J Electroanal Chem 256:269–282
133. Iwasaki Y, Morita M (1995) Electrochemical measurements with interdigitated array microelectrodes. Curr Sep 14:2–8
134. Silvestrini M, Fruck L, Ugo P (2013) Functionalized ensembles of nanoelectrodes as affinity biosensors for DNA hybridization detection. Biosens Bioelectron 40:265–270

Chapter 21
Sensors and Lab-on-a-Chip

Alberto Escarpa and Miguel A. López

21.1 Introduction

Fields like miniaturization and nanotechnology have been greatly developed in the last years. Like other fields, analytical chemistry has also been affected by this new technology. In this sense, the possibility to carry out laboratory operations on a small scale using miniaturized devices is very appealing. From the analytical point of view, small scale reduces the required time to analyze a product, as greater control of molecular interactions is achieved at the microscale level; makes easier automation and simplification; and provides additional advantages such as the speed of result generation (high throughput), the amount of information (simultaneous or multiparametric), the autonomy allowing field test (portability), reduction of reagent cost, or the amount of chemical waste. The tremendous potential of miniaturized analytical systems is clear in fields as medicine, facilitating the development of new diagnostic abilities, and significantly improving their applications in food analysis or environmental monitoring.

The final aim of analytical miniaturized systems is represented by the *micro total analysis systems*.[1] μ-TAS concept was developed from the modification of the TAS by downsizing and integrating the analytical process steps onto single monolithic devices. In essence, a μ-TAS is a device that improves the performance of an analysis by virtue of its reduced size. Besides analytical tasks can be performed into a miniaturized system, other chemical functions such as synthesis can be also performed. For this reason, today, μ-TAS concept has also been called by "lab-on-a-chip". On the other hand, it has to be pointed out that miniaturization is more than simply the scaling down of well-known systems since the relative importance of forces and processes changes with scale. One of the most relevant characteristics of analytical microsystems is the omnipresence of laminar flow (Reynold's number

A. Escarpa (✉) • M.A. López
Dpto. Química Analítica, Química Física e Ingeniería Química,
Universidad de Alcalá, Madrid, Spain
e-mail: alberto.escarpa@uah.es

L.M. Moretto, K. Kalcher (eds.), *Environmental Analysis by Electrochemical Sensors and Biosensors*, DOI 10.1007/978-1-4939-0676-5_21

are typically very low), in which viscous forces dominate over inertia. This means that turbulence is often unattainable and that molecule transportation only occurs through diffusion, which has direct consequences on the designs of this type of microsystem. In addition to its small size, the key feature derived from the micro-TAS or lab-on-a-chip concepts is the possibility of handling fluidics on a nanoliter and even picoliter scale, widening the scope of micro-TAS to now be labeled microfluidics. Therefore, microfluidics is the science and technology of systems that process or manipulate small amounts of fluidics (10^{-9}–10^{-18} L) using channels measuring from tens to hundredths of micrometers. For this reason, the term microfluidics emphasizes the strong impact that miniaturization and integration have on the fluidics and chemical engineering of analytical microsystems.[2,3]

Micro-TAS, lab-on-a-chip devices or *microfluidics* in Analytical Chemistry can be seen as different analytical microsystems comprising: (1) the direct measurement of one or a few components with little or no sample preparation (μ-sensors); (2) the measurement of one or a few components which require some treatment of the sample (μFIA); (3) the analysis of more complex samples involving the separation of their components (μ-HPLC and μ-CE).[4] In all cases, one of the oldest and most important challenges in analytical chemistry is chased: the accurate measurement of a specific compound in a complex matrix. Taking in consideration these principles, the aim of this chapter would be mainly focus on the integration of sensors or sensor-like systems in microfluidic systems as platforms for electrochemical sensing in the environmental field.

Microfluidic platforms on a microchip format (microfluidic chips) are made up of a network of channels to perform multiple operations involving at least one injector (where a sample plug is loaded) and pumping microchannels (where the transport of analytes is performed) that are suitably interfaced to reservoirs (where different solution/samples are deposited). Microchannels and reservoirs are fabricated on microchips using mainly photolithography or micromolding to form channels for sample injection, transport, and analyte detection on planar substrates. Once all of the solutions, including those of the samples, are loaded, the samples are typically transferred hydrodynamically or electrokinetically into an injector region. Then their components are pumped by applying either high voltage or pressure and are afterwards detected with a suitable detection system.

In the following sections a general overview of the different aspects related to microfluidic analytical systems will be presented, followed by specific applications of electrochemical microfluidic platforms to environmental analysis.

21.2 Microfabrication

A microfluidic platform provides a set of unit operations (fluidic handling), which are designed for easy combination within a well-defined fabrication technology, where the monolithic approach is the most commonly used. The platform allows the implementation of different application-specific systems (assays) in an easy and

flexible way, based on the same fabrication technology. In consequence, a microfluidic platform cleverly integrates the required operations during the analysis. These units are metering, mixing, incubating, and so on: in other words, all physical and chemical operations for the performance of sample introduction, preparation, separation and detection.[5]

In this sense, a relevant key of these miniaturized analytical systems is the necessity of the development of microfabrication techniques. The accurate and deep description of the microfabrication techniques is obviously outside of the scope of this chapter (readers can find more information in excellent books[6]). However, a brief description of materials properties and the most important aspects involved in both, glass and polymer microfabrication technologies for microfluidic platforms, in the microchip format, will be described.

It is clear that material substrate used for microchip fabrication is a key factor since the performance of the microfluidic platform will be strongly dependant of this material. Glass, polymers, and in lower extension silicon are the three main types of materials used for microfluidic devices fabrication.

Silicon was the first material used due to the well-established microfabrication processes developed for semiconductor microelectronics industry. The chemical and physical properties of silicon are well characterized. It possesses good thermal conductivity, it is resistant to high temperatures and structurally strong, and can be produced virtually in any geometrical microstructure with high precision, and its surface chemistry has been studied extensively giving the capability to attach molecules to its surface easily. However, it has some important limitations[7]: (1) It is not optically transparent in the wavelength range for optical detection; (2) It is electrically conductive, so it is unsuitable for electrochemical detection or electrokinetic flow transport or reagents; (3) Proteins and other biomolecules tend to bind to silicon surface groups, reducing the sensitivity; (4) The microchip construction is relatively expensive, time consuming and (5) The wet etching process typically used in fabrication produces a low aspect ratio.

Although silicon has been a significant material in microfluidic devices, these drawbacks have made it replaced or combined with glass or polymer substrates for most analytical applications.

Besides, the use of glass as material substrate can overcome some of the problems associated to silicon. Glass is less expensive, it presents good chemical resistance and it is optically transparent through the visible spectrum allowing LIF detection. Furthermore, thanks to be none electrically conductive, glass is compatible with electrokinetic fluid transport. However, glass also has some drawbacks. As with silicon substrates, the wet-etching method used for fabrication does not produce a high aspect ratio, toxic chemicals are involved, and this material is more fragile.

Structures on glass substrates are usually generated using standard photolithographic technologies.[8–10] Figure 21.1a presents an example diagram of such procedure. Briefly, first a layer of photoresist is spin-coated on top of the sacrificial mask layer (Cr/Al) (*deposition*). Photoresist is a polymer that becomes soluble (positive) or insoluble (negative) in developer solutions after exposure to light (*exposition light*). In the next step the photoresist spun on the microchip is exposed

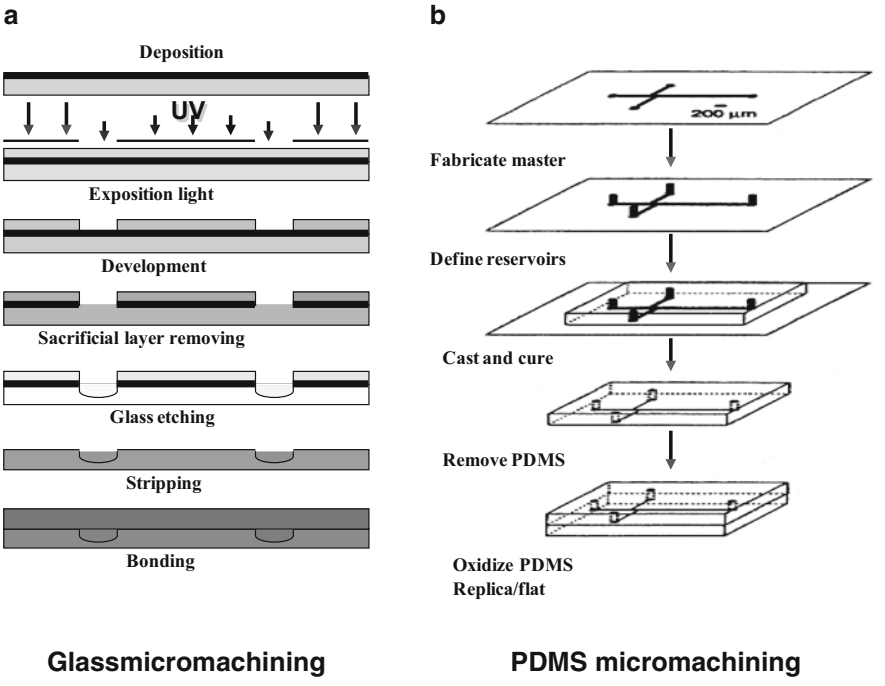

Fig. 21.1 (**a**) Microfabrication of glass microchips. (Adapted from reference (10)). (**b**) Microfabrication of PDMS microchips. (Adapted from reference (12))

in the region defined by a photomask, typically using an aligner. The photomask is a plate with a user-designed pattern that is transparent while the background is opaque (or vice versa) to the exposition light. After the microchip is baked to harden unexposed resist, the exposed photoresist is dissolved with a developer solution (*development*). The sacrificial mask layer (Cr/Al) of the exposed region is removed using the appropriate etchants (*sacrificial layer removing*). During this time, the sacrificial layer underneath the unexposed photoresist remains intact. After pattern transfer and development, the portions of the microchip that are to be etched have been unmasked and are now ready for chemical etching (*glass etching*). HF is used as the primary etchant and can be prepared in various solutions including HF/NH_4F, HF/HNO_3, and concentrated HF. The etching rate of HF for glass is readily controllable if the temperature is controlled. Following etching of the microchannels, the photoresist and sacrificial mask layer are stripped (*stripping*), and the access holes drilled. The access holes can be drilled on the etched substrate or on another blank glass wafer. When holes are drilled on the etched substrate, aligning two substrates for bonding is much easier. Finally, the substrate is bonded to another piece of substrate to form a finished microchip (*bonding*).

In the last years, polymers have emerged as an interesting alternative to glass and silicon in the microfluidic platforms fabrication. Polymers offers the advantage of being low cost and easily produced since microfabrication techniques (e.g., injection

molding, compression molding, extrusion, hot embossing, soft lithography, laser photoablation, screen printing, and replication) are highly reproducible; while expensive patterning procedures are only required for constructing the mold. In addition, polymers have good chemical resistance, optical transparency, low auto fluorescence, none toxic, and do not absorb UV. Moreover a variety of surface modification methods are availably improving the efficiency of these devices. There are a variety of materials (e.g., plexiglas, cyclic olefin copolymers, polyester, polycarbonate, polymethyl methacrylate (PMMA)), each with specific properties offering the possibility of tailoring a material to a specific application. However, without any doubt poly(dimethylsiloxane) (PDMS) has emerged as the most used polymer material. PDMS is flexible, optically transparent, impermeable to water and permeable to gases, and very compatible with biological studies. Nevertheless due to its hydrophobic surface, this material presents some limitations as poor wettability, forming bubbles in aqueous solutions, lower durability, and the tendency to adsorb proteins and other molecules. However, due to the elastomeric nature of PDMS that allows an easy seal with smooth and flat surfaces, hybrid devices using mainly PDMS and other different type of material as glass, polyester have been reported.

Related to polymer microfabrication microchips, the two major ways are replication from a master (moulding methods) and direct machining.[11,13,14] Replication methods often produce a microstructure by allowing a polymer workpiece to form an inverse copy of a mould. These methods are: hot embossing, injection moulding, and casting. The formation of microchannels and other structures using moulding methods generally involves two primary steps: (1) moulder (also known as master) fabrication, and (2) channel pattern transfer from that moulders to polymer substrates. These methods have in common that a very soft or even liquid form of polymer is poured or pressed into a mould, after which the material is hardened and removed from the mould. On the other hand, direct machining methods remove small amounts of polymer in places where the microstructures (microchannels, reservoirs) should be located. This type of micromachining is laser ablation.

Hot embossing is the process of pressing a mould into heated, softened thermoplastic, followed by cooling, thereby producing an inverted replicate of the mould. The first step in hot embossing consists of heating the mould and the polymer to glass transition temperature. Once the polymer begins to soften it takes on the form and the shape of the mould. The mould and the polymer are then cooled below the glass transition temperature to harden the polymer, and afterwards the polymer is removed from the mold. Embossing can take several minutes per device and can be a useful tool in rapid prototyping devices.

In the injection moulding technique the molten polymer material is injected into the mould. For microinjection moulding, the mould is heated to the softening temperature of the polymer to prevent the injected polymer material from hardening too early. After injection of molten polymer into the mould, this is slowly cooled, so that the polymer hardens and then, the polymer microstructure can be removed from the mould. Injection moulding allows very high-throughput production with low production costs (moulded devices are released every 5–10 s).

On the other hand, laser micromachining (such as photoablation) is a direct machining method based on the removal of polymer material by using intense UV or infrared radiation provided by a laser. The photoablation process involves absorption of a short-wavelength laser pulse to break covalent bonds in long chain polymer molecules with production of a shock wave that ejects decomposed polymer fragments.[6] Many commercially available polymers can be photoablated, including polycarbonate, poly(methylmethacrylate) (PMMA), polystyrene, nitrocellulose, and poly (tetrafluoroethylene). The laser energy can be specially patterned using a mask with the subsequent generation of microcavities and channels in various geometries or controlling position of the laser with x-y stages. The resulting structures are generally characterized as having little thermal damage, straight vertical walls, and well-defined depth. However, laser ablation does not lend itself well to mass production.

A particular example of polymer machining of great significance is the PDMS microchip.[12] PDMS is a widely used polymer substrate for soft lithography-based microfabrication and nowadays has a relevant role in the miniaturization scene not only as microchip material but as ideal material to build "lab-on-a-chip" systems (soft lithography). Apart of the features described before, the major advantage of this material is the ability of rapid prototyping of complex structures.

Casting uses a chemical process to harden the polymer.[6] Two components, a base and a hardener or cure, are mixed just prior to use. Immediately upon mixing, the chemical curing process starts. After some time, this process results in hardening of the polymer (at atmospheric pressure and temperature). The liquid mixture is poured in the mould and as the polymer sets it takes the shape of the mould. The polymer structure can then be removed from the mould. This technique is very popular with elastomers such as PDMS because they form hermetic, reversible seals and smooth surfaces like glass or silicon by adhesion. Casting is the simplest among these three moulding processes, but requires contact with the mould for minutes or hours. A schematic representation of this type of replica moulding is shown in Fig. 21.1b.[12] Channels in PDMS are easily formed by replica moulding, which is simply the generation of a negative replica of the master in PDMS by pouring the prepolymer over the master and subsequent curing at atmospheric pressure at somewhat elevated temperatures. In the last step, the PDMS replica containing the channel network was sealed irreversibly with a second flat slab of PDMS. In the example shown, this is due to oxidation of both surfaces in an oxygen plasma discharge. Oxidation results in a stronger seal than with untreated PDMS, and it seems to be easier to fill oxidized PDMS channels with liquids, and as we explained before, higher cathodic EOFs were generated which is consistent with a more negatively charged surface of PDMS after oxidation. However, instead of irreversible oxidation, glass plates are usually used for sealing the channels, also physically supporting certain integrated elements like electrodes. When the PDMS and glass parts are ready and cleaned with methanol, the two surfaces are brought into contact by a reversible seal. For irreversible bonding, as is described in the example shown before the two surfaces are placed under plasma and brought into contact after appropriate surface activation.

Apart from these more established materials, a low-temperature co-fired ceramic (LTCC) has also been used for constructing electrochemical microfluidic devices. Using this material, highly intricate three-dimensional structures can be designed, integrating fluid networks, embedded passives and electronic circuits by means of unfired flexible sheets. After firing, the LTCC becomes rigid with very good thermal, mechanical, and electrical properties.

21.3 Standard Operation on Microfluidic Platforms

21.3.1 Sample Preparation

Due to the complexity of environmental real samples and the low relative abundance of pollutants, preparative cleanup and preconcentration steps are usually required. Although sample preparation techniques are widely developed in conventional formats and off-line, it is important to point out that from the different steps related to the analytical process, sample preparation is notably the least developed in miniaturized devices. However, very exciting unique opportunities could be expected because of (1) the intrinsic possibilities of microfabrication technology to create sophisticated designs and microstructures in connection with sample preparation requirements; (2) the natural possibilities offered by microfluidics: the presence of laminar flow and diffusion; and (3) the ease of using electrokinetic phenomena to move fluidics into the network channels with accuracy (focusing on flow techniques). The integration of sample pretreatment in microfluidic systems can eliminate sample handling loss or contamination problems arising from off-line sample manipulation.[15]

The main sub-categories of sample pre-treatment include isolation/clean-up and sample pre-concentration, which will be discussed in the following paragraphs. Excellent literature is proposed for further reading.[5,16–22]

21.3.1.1 Isolation/Clean-up from the Sample Matrix

A challenging task faced by the analytical chemist when dealing with raw samples is extracting/isolating the analyte of interest from the sample matrix. It is fair to say that the majority of nonideal samples arrive in a format incompatible with most analytical instrumentation, and requires some degree of clean-up. Even well-defined samples (e.g. aqueous solutions) require basic filtration prior to analysis. Other desirable techniques may include liquid/liquid extraction and solid phase extraction.

Filtration Approaches

Possibly the most essential step when performing analysis in microfluidic systems, especially in environmental field, is the filtration of sample prior to processing. Due

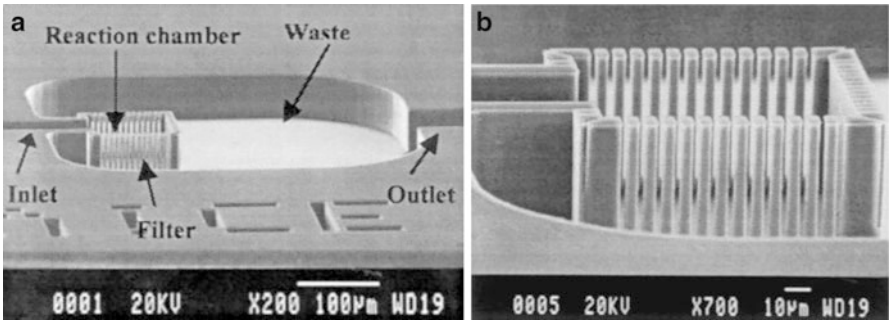

Fig. 21.2 (**a**) A SEM overview of the single filter-chamber device. (**b**) SEM image of the filter-chamber (side view). The pillars are 3 µm wide and 50 µm high with a spacing of 2 µm. From (23) reproduced by permission of John Wiley and Sons

to the typical small dimensions in microstructures, particulates can cause serious operational problems, providing sites for nucleation or blockage. The simplest solution is to filter all reagents and sample *on-chip* prior to analysis.

Related to filtration, two approaches have been employed: structurally-based filters (filtering and retention by integrated flow restrictions and controlled by manufacturing process) and diffusion based filtration (filtering by diffusion in laminar flows). Structurally-based or microfabricated filters have been proposed in popular architectures like frits, pillar structures, or flow restrictions within fluidic channels to mimic conventional filters.[19] Figure 21.2 shows a scanning electron microscope (SEM) of a typical example where it can be observed the single filter-chamber device (A) and the filter chamber (B) (side view). In this case, the pillars are 3 µm wide and 50 µm high with spacing of 2 µm. The effectiveness and application of these filter structures is determined by the resolution limits of the manufacturing process. Consequently, filtering of sub-micron sized particulates using physical structures puts stringent demands on device fabrication. To fabricate microfiltering devices more easily, sandwiching a thin polycarbonate track-etched membrane between cover and bottom plates or the photopolymerization of a membrane into a channel has also been introduced.[24–26]

By other hand, filtration can be induced by allowing the analytes of interest to migrate across a laminar boundary between two adjacent layers (sample and solvent stream) where material transport only occurs by diffusion due to the predominance of laminar flow in microfluidc systems.[27,28] An interesting quality of laminar flow is that material transport between two adjacent streamlines only takes place by diffusion, and not by turbulent mixing as it is done in a test tube. This inherent feature of microfluidics is conceptually despite in Fig. 21.3 towards two classic designs: T and H-designs. Since species of low molecular mass have greater mobility (larger diffusion coefficients) than large molecular species, the process can be further controlled by altering the time in which the two fluids come into contact. The approach is highly configurable since the time allowed for diffusional transfer between streams is directly controlled by fluid velocity and the length of the

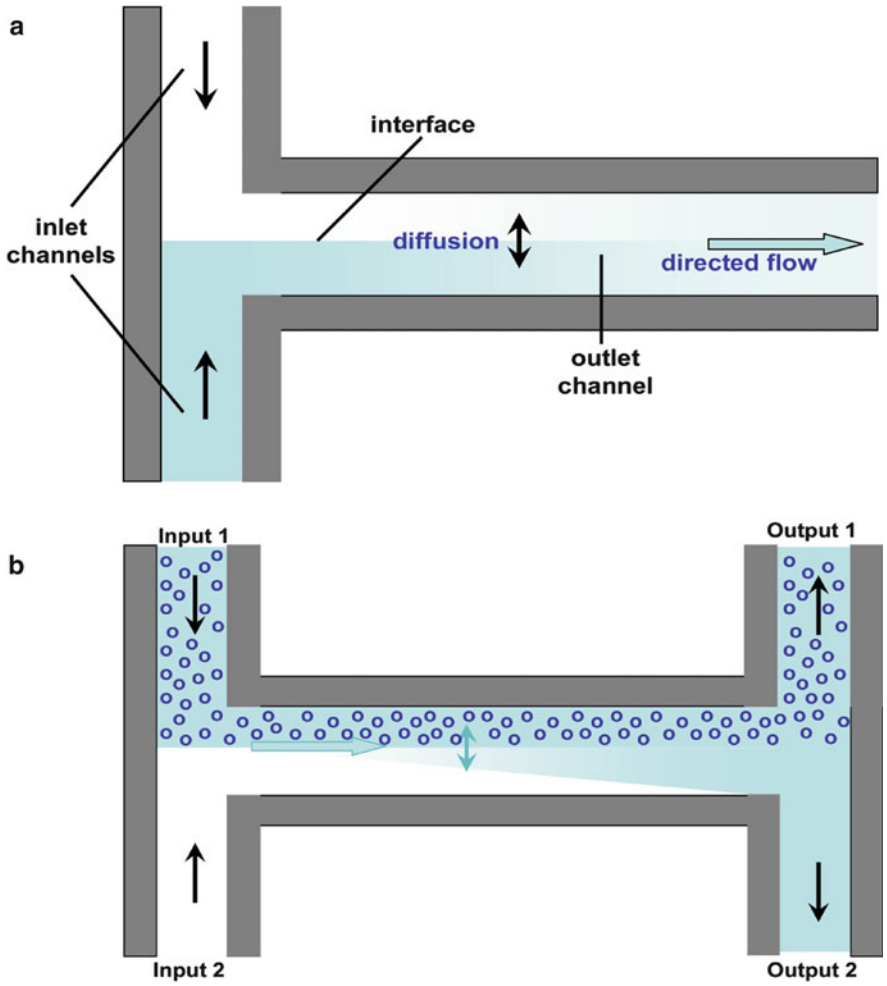

Fig. 21.3 Conceptual drawing of two filtering microdevices based on laminar flow and diffusion principles. (**a**) A junction where two liquids meet and flow downstream side by side. (**b**) H-filter. From (5) reproduced by permission of John Wiley and Sons

channel. Importantly, this approach addresses many of the problems associated with structurally-based filters, since its operation is reliant on the control of molecular diffusion rather that the resolution of the manufacturing process.

Both approaches fix perfectly to microfabrication and microfluidic technologies. The first one because of the well-known integration technology of multiple micropieces into a single microdevice; whereas the second one works on the basis of an inherent property in microfluidics: presence of laminar flow and diffusion.

Extraction Approaches

Liquid/liquid extraction, technique widely used in conventional sample pretreatment methodologies, describes the physical process by which a compound (or a mixture of compounds) is transferred from one liquid phase to another, and could play a predominant role in miniaturized systems. The high surface-to-volume ratio and the short diffusion distances, typically within microfluidic environments, combined with laminar flow conditions, offer the possibility of performing liquid-liquid extraction within micro channels without shaking. Different ions as Fe (II) or Ni (II) have been extracted and analyzed in microdevices.[29,30] Although a potential drawback could be the low unit throughput (normally between 1 and 100 μL min^{-1}), this problem can be obviated by operating arrays of parallel channels concurrently.

Solid phase extraction is a broadly used technique in which a target molecule is retained by a chromatographic stationary phase material and subsequently eluted in an appropriate (and selective) solvent. SPE functions either as a sample clean-up method and a pre-concentration method. This fact is due not only that the target analyte is retained within the stationary phase and the unwanted components of the sample matrix flow to waste, but also after elution in the desired volume entails pre-concentration of the analyte. Several and creative approaches for performing solid-phase extraction in microfluidics have been proposed. A first approach entails to coat channel walls with a high affinity stationary phase, although this methodology is less common. Since coating channel approaches depend on the available surface area for interaction, into micron-size channels the contact surface is very small. A simpler way to increase the surface area is to pack the microchannels with stationary phase; however, packing process is not easy, and sometimes this alternative is also avoided. The group of Ramsey integrated filtration, concentration, and separation onto a microchip device for determination of PAHs. After filtration on an array of thin channels, sample concentration and separation was performed in a C-18 coated separation channel.[31] Korenaga et al. presented the on-chip cleanup of benzo[a]pyrene and benzo[k]fluoranthene from diesel exhaust particles using silica gel beads packed into the microchannel.[32] Tennico and Remcho have recently used iron oxide nanoparticles as solid-phase extraction support in a microchip device. The NPs functionalized with octadecylsilane were used for extraction of parabens and nonsteroidal anti-inflammatory drugs in water. The packing, removal, and replenishment of extraction bed are performed straightforward by the aid of a magnet.[33] A very attractive possibility, compatible with miniaturized dimensions, is to replace conventional stationary phase materials by a continuous porous bed in situ formed from polymerization of organic monomers. The process of bed formation is easy, since a low-viscosity monomer solution can be introduced by vacuum or pressure into the microfluidic channel prior to initiation. In this sense, Augustin et al. reported a monolithic stationary phase synthesized by the polymerization of acrylate monomers for enrichment and successive separation of PAHs by SPE-MCEC.[34] Similar works have been reported for in-situ monolithic fabrication in a microfluidic device.[35,36]

21.3.1.2 Preconcentration: Electrokinetic Approaches

In addition to the complexity of environmental samples, analytes may be present at extremely low concentrations. This combined with the ultrasmall detection volumes encountered in microfluidic systems (pL–nL) makes often desirable to incorporate sample pre-concentration prior to detection within microfluidic systems.

Electrokinetic flow-driven systems have a relevant role in microfluidic devices due to their inherent and easy miniaturization, simplicity of fabrication, and high-controlled fluidic manipulation. Although this fluidic motion will be discussed more detailed in a next section, this principle has shown very useful to analyte preconcentration in microchips. These techniques have been studied for several decades and are commonly used in CE conventional systems as a single-step preconcentration method for achieving high sensitivity. Two different strategies, the first one, based on the velocity change of the analytes between the sample and separation solution zones (stacking), together with "focusing" techniques where the analytes are focused at the points where the migrating velocities become zero will be presented briefly.

In *field amplified stacking* (FAS), a background solution (BGS) with a high conductivity and a sample solution (S) with a low conductivity are prepared. The S is introduced into the capillary filled with the BGS, and then an appropriate voltage is applied to both ends of a capillary. The local electric field in the sample zone is higher than that in the BGS as the electric current in the capillary is constant. Therefore, the electrophoretic velocity of the analytes in the sample zone is faster than that in the BGS. This difference in the electrophoretic velocities between the S and BGS zones generates the "stacking" effect at the S/BGS boundary, so that the analytes are concentrated around the boundary. From the first application of FAS in MCE reported by Jacobson and Ramsey[37] different approaches have been reported. In the work of Noh et al.,[38] FAS and FASI (field amplified sample injection) methods are uniquely combined with a background electrolyte modified with gold nanoparticles to enhance preconcentration and separation performance. The presence of nanoparticles in the background electrolyte provides additional sites for solute interaction and has the ability to alter the apparent mobility of analytes as well as electrosmotic flow. A 200-fold increase in sensitivity in the determination of phenolic endocrine disruptors in water samples was reported.

However, in FAS there is a major problem, that neutral analytes cannot be concentrated. To improve this low applicability in FAS, *electrokinetic chromatography* (EKC) conditions on a microchip have been introduced for concentrating neutral analytes.[39] Also, the adsorption of analytes onto the inner PDMS microchannel wall was prevented using ionic liquids (ILs), while the EOF is increased due to the charge of the ILs.[40]

Another difficulty usually observed in FAS is to concentrate a sample solution containing high-concentration salts, e.g., sea water, because a high conductivity in the sample matrix provides a smaller difference in the electric field at the BGS/S boundary. Trying to solve this trouble, Isotacophoresis (ITP) can be used where an

ionic sample solution is introduced between leading (LE) and terminating electrolyte (TE) solutions. The electrophoretic mobilities of the electrolytes are in the order of LE > S > TE. When the voltage is applied to a separation column, the sample ions are separated in the order of the electrophoretic mobilities, and then all the divided zones migrate with a uniform velocity toward a detection point. Up to a million-fold sample stacking have been reported using ITP method integrated on a CE microchip.[41]

Related to "focusing" techniques, different possibilities are available for the preconcentration and separation in electrophoretic analysis. In these techniques, the migration direction of analytes is inversed in a separation channel. Thus, the analytes are "focused" at the points where the migrating velocities become zero. For a better understanding of these techniques some selected examples based on electric field gradient focusing (EFGF), and temperature gradient focusing (TGF) will be discussed.

In *electric field gradient focusing*, sample molecules migrate in a channel applied as an electric field gradient. In the microchannel, a hydrodynamic counterflow is also introduced with a constant velocity. When the electric field at the inlet is higher than that at the outlet and the counterflow is introduced from the outlet, a faster electrophoretic migration of the sample overcomes the hydrodynamic flow. Thus, the sample moves toward the outlet. With decrease in the electric field along the microchannel, the electrophoretic velocity of the sample is gradually decreased and finally inversed due to the counterflow, so that the sample is focused and separated in the order of their electrophoretic mobilities. EFGF on planar microchips have been first reported by Humble et al.[42]

Ross et al.[43] have developed a novel technique using a *temperature gradient focusing* (TGF). The electrophoretic velocity of the sample is gradually changed by the variation of the ionic strength of the BGS which is dependent on the temperature. TGF is more advantageous than EFGF in respect of easier operation and the applicability to a wide range of analytes.

In addition to chemical preconcentration methods, some relevant applications make use of biological reagents. In this sense, antibody modified surfaces such as microchannel walls or micro/nano particles allow the specific enrichment and determination of selected analytes. The use of antibodies in microfluidic platforms for environmental analysis will be more deeply discussed below. An interesting application is the bacterial enrichment for selective enumeration of bacterial species and sensitive detection from environmental samples.[44] This process is time-consuming in which a species-selective growth medium is inoculated with a sample containing the target species allowing the bacteria to multiply over a period of several hours to days.[45] In the work of Dharmasiri et al.[46] selective antibodies are immobilized on the surface of a PMMA microchannel where enrichment takes places. Beyor et al.[47] makes use of specific antibody modified superparamagnetic polystyrene beads within the microchannels for isolation and preconcentration of *E. coli* cells. In both cases, off-chip PCR detection was performed with recoveries of 70 %.

21.3.2 Fluid Transport

Different strategies for liquid-transport within a microfluidic platform have been reported in the literature, and mainly categorized as pressure, electric, and passive fluid handling forces. The difference lies mainly in the nature of the driving agent behind the transport. When flow is generated mechanically by a pump is called pressure-driven flow; when flow is driven by a voltage is called electro-osmotic flow; and when not external power sources are required to drive liquids, it is called passive flow. In a general sense, in the miniaturization scene, electrokinetic flow-driven systems are clearly dominant versus hydrodynamic ones. The reason for this dominance lies partially in the inherent simplicity of fabrication and operation combined with unique features with respect to separation speed, sample injection, and reagent consumption. Although a deeply discussion of fluid motion on microfluidic platforms is out of the scope of this chapter, a brief description of these systems will be overviewed.

In pressure-driven (*or hydrodynamic*) *microfluidic systems*, a pump is used to set fluids into motion. A large variety of principles have been developed and wider information can be found in interesting reviews.[5,48–50] Within these microsystems, the pumping mechanism is based on the use of mechanical displacement micropumps. They can be defined as those that exert oscillatory or rotational pressure forces on the working fluid through a moving solid–fluid (vibrating diaphragm, peristaltic, rotary pumps) or fluid–fluid (ferrofluid, phase change, gas permeation pumps) boundary. There are a large combination of actuators for pumping and valves (electrostatic, piezoelectric, thermopneumatic, electromagnetic, etc.) which determine de overall performance, in terms of generated pressure, stroke displacement, response time, and reliability. By other hand, one of the most used pumping methods includes the use of syringe or piston micropump, although it is increasingly difficult to use in micro/nanochannels due to the hydrodynamic resistance increases with the reduction in dimension. An important drawback of pressure driven flow systems, especially when separation has to be performed, is the presence of a parabolic velocity flow profile. This causes sample plug dispersion and peak broadening, rendering less attractive for separations. Furthermore, the flow behavior is usually nonlinear, which may be a problem for this kind of device. However, pressure-driven flow can be used for both aqueous and nonaqueous liquids.

Electro-osmotic flow (EOF) is the liquid flow originating in the presence of an electric field when an ionic solution is in contact with a charged solid phase. Oppositely charged ions in the fluid shield the surface charge and can be manipulated with a DC or AC electric field. DC electro-osmotic pumping is normally used, particularly for electrophoretic separations. As a well-known example, in silica material in contact with an aqueous electrolytic solution, the solid surface has an excess of negative charge due to their ionization of the surface's silanol groups. A high number of counterions of these anions are found on the interphase between the capillary wall and the solution originating the electric double layer, which is formed by a stagnant layer adjacent to the capillary wall (Stern layer) and a mobile diffuse

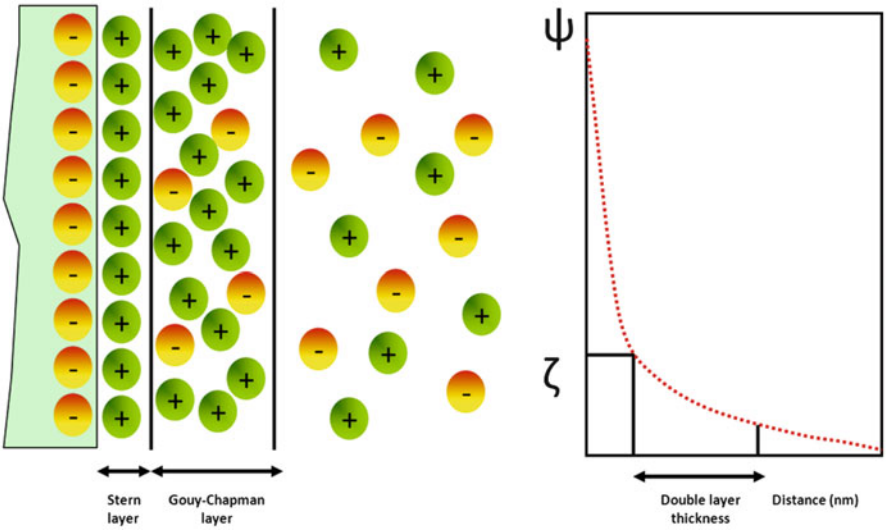

Fig. 21.4 Formation of the double layer and generation of the Electro-osmotic flow (EOF). Adapted from reference (5)

layer (Gouy-Chapman layer). The cationic counterions in the diffuse layer migrate toward the cathode. As they are solvated, they drag solvent with them, originating the EOF (Fig. 21.4). The linear velocity of the EOF depends on the potential originated across the double layer and the zeta potential. The flow is simply created by filling a microchannel with a buffer solution and applying a suitable voltage at the channel ends. Some advantages with respect to hydrodynamic flow systems are the absence of mobile parts such as valves, actuators, and also the particular flow profile. Contrary to hydrodynamic flows, where one finds a parabolic distribution of the flow velocities which the largest velocity at the center of the channel and zero velocity at the walls, in elelctrokinetics, EOF is generated close to the wall and therefore, it produces a flat profile with a very uniform velocity distribution across the entire cross-section of the channel. Furthermore, EOF is pulse free and there is no back pressure (as there is with mechanical pumps). The main problem arises from the strong dependence on the chemical factors involved in the microsystems as the pH values. This dependency makes electro-osmotic flow hard to control, since every change in pH, dielectric constant or concentration, due to reactions or the mixing process, has an immediate effect on the magnitude of the EOF. On the other hand, this strong dependency also means that there are many parameters that can be exploited to control and manipulate the EOF. Furthermore, other mayor limitations are the high voltage and the electrically conductive solution required.

Other liquid-transport strategy involves wettability change due to applied electric potential. In *Electrowetting*, discrete liquid droplets are manipulated in the presence of programmed voltage sequences applied to an electrode array. By applying sequences of AC or DC electric potentials between ground and actuation

electrodes, droplets of reagents or samples can be drive to move, to merge, to divide and to dispense from reservoirs by combining electrostatic and dielectrophoresis forces. In electrowetting, the fluid is transported using surface tension (an interfacial force which dominates at microscale). Voltage is applied on the dielectric layer, decreasing the interfacial energy of the solid and liquid surface, which results in fluid flow. Thus, when applying the electric potential along the interface of a liquid metal droplet in an electrolyte, charge redistribution occurs, resulting in a gradient in surface tension at the interface, which causes movement of the droplet to regions of lower surface tension. Switching the direction of the applied potential also changes the direction motion.[51–53]

Passive forces that do not require external power sources to drive liquids have been also reported for microfluidic devices. In these cases, only gravity and capillary forces are used to drive fluidics within the microchannels.[54]

21.3.3 Sample Introduction

In microfluidics, injection of small and well-defined amounts of sample solutions is a key function. Introduction of samples to a microfluidic chip requires an interfacing system between samples with volumes in the mL-μL range from the macro world, and microfluidic systems handling volumes in the nL-pL range.[5] Without any doubt, world-to-chip interfacing is considered a major challenge. In most cases, this problem is brilliantly resolved using microchips, where electrokinetic fluid manipulations allows aliquoting or injection function. This arrangement is mainly devoted to microchip capillary electrophoresis where electrokinetic motion and injection is well established. Three injection methodologies have been employed in MCE: no-pinched, pinched, and gated injections, being the first one the easiest and most widely used. As an example, the nonpinched approach will be briefly described.

As can be observed in Fig. 21.5, the microchip in CE design includes integrated injectors which are usually either cross-channel pieces, formed by orthogonally intersecting the separation channel with a channel connecting the sample to waste (T injectors) or twin-T injectors, where the two arms of the sample-to-waste channel are offset to form a large injector region. These performances allow volume-defined electrokinetic sample injection of short injection plugs with reproducibility. In the no-pinched approach, which is shown in Fig. 21.6, the principle can be carried out using just a single power supply. A high voltage is applied to the sample reservoir for a short time with the detection reservoir held at ground (injection). Sample is introduced directly into the separation channel by electrokinetic injection. After the injection is completed, the high voltage is switched back to the buffer reservoir and the separation is initiated (run/separation). This injection procedure becomes the easies but least reproducible scheme, although good relative standard deviations (less than 5 %) are reported.

In lower extension, other approaches have been proposed such as micro and nanodispensing, microrotary-injection valves, pressure injection. Fang et al.

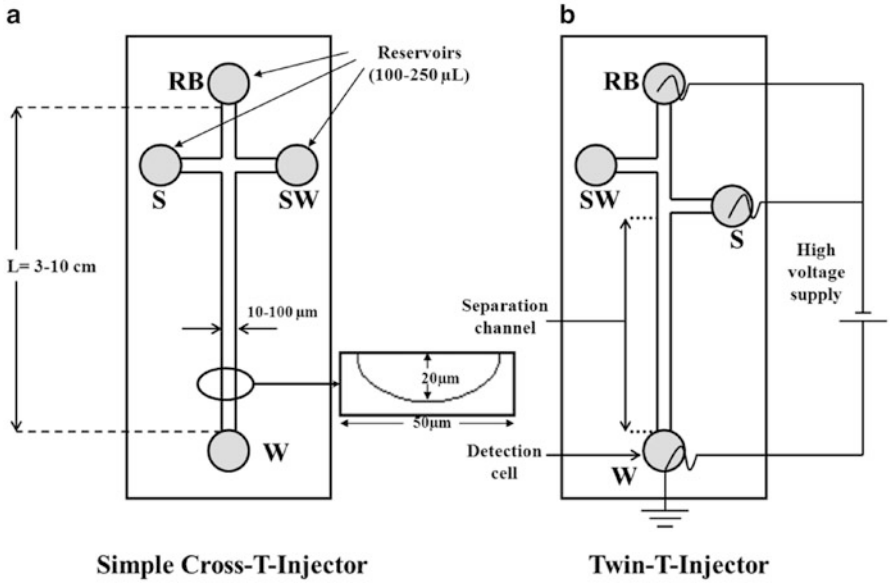

Fig. 21.5 Microchip layouts. From (5) reproduced by permission of John Wiley and Sons

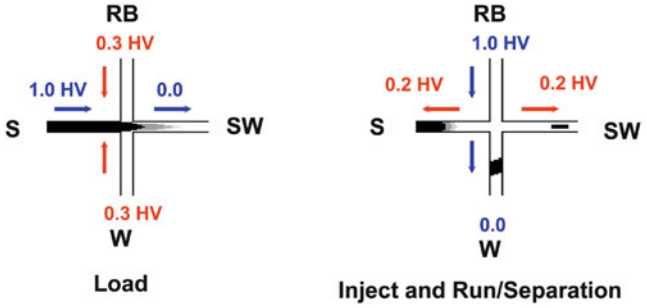

Fig. 21.6 Schematics of pinched injection protocol. *Arrows* depict direction of flow of the sample and separation buffers. Adapted from reference (55)

summarize the different possible modes of sample introduction for microfluidic chips where different integration and automation grades are reported.[56]

21.3.4 Separation

Analytical separation techniques play a prominent role in analytical science since reliable analyses usually require their participation. Separation techniques can be classified as those involved in the treatment of samples, the so-called

nonchromatographic separation tehcniques (without instrumental detection) and those involved in the detection of analytes after chromatographic or electrophoretic separation. The implication of the first ones in the microfluidic domain has already been studied above. Below, a brief introduction to miniaturization tendencies in both chromatographic (HPLC chips) and electrophoretic separation (MCE) techniques and their integration in microfluidic platforms will be presented.

The replacement of microcolumns by capillaries has led to the development of very interesting modern alternatives in analytical separation science. Thus, capillary liquid chromatographies (CLC), through so-called micro and nano-HPLC, and capillary electrophoresis (CE), have introduced a true revolution in instrumental separation techniques. However, despite the clear improvement and possibilities these modes represent, miniaturization of the equipment as a whole is not truly evident. Miniaturization affects many of the components and devices integrated in the commercialized equipment, but the equipment itself is not considered miniaturized at all. The true pass to miniaturization is given when chromatographic or electrophoretic separations are carried out on chips.

In this sense, MCE was one of the earliest examples of μTAS, and it constitutes one of the most representative examples of analytical microsystems.[1] Using this performance, analysis times can be reduced to seconds and extremely high separation efficiencies can be achieved. The easy microfabrication of a network of channels using materials of well-known chemistry, and the possibility of using the electrokinetic phenomena to move fluids are among the most important factors to understand the relevance of CE microchips to miniaturization. Due to its relevance, even in the environmental monitoring field, a wider description of the foundations and specific examples on environmental MCE will be provided below.

Many of the benefits already discussed for micro-CE could equally be applied to downsized chromatographic techniques. However, relatively few examples of chip-based chromatographic instruments are covered in the literature compared with chip-based CE devices, and most of them carried out nonelectrochemical detection (mainly MS detection) which is out of the scope of this chapter. This fact is not surprising since CE is almost perfectly suited to miniaturization. Also, the miniaturization of chromatographic systems involves a number of technical challenges, such as the microfabrication of valves and pumps, which are generally not encountered in MCE.[5] Besides, hybrid methodologies with electrophoretic and chromatographic foundations such as micellar electrokinetic chromatography (MEKC) and capillary electrokinetic chromatography (CEC) provide a wide analytical potential.

21.3.5 Detection

From the beginning, detection has been one of the main challenges for analytical microsystems, since very sensitive techniques are needed as a consequence of the ultrasmall sample volumes used in micron-sized environments. In principle, a wide variety of detection alternatives can be used in *microfluidic* systems, but Laser-Induced

Fluorescence (LIF) and electrochemical detection (ED), are the routes most commonly used. LIF was the original detection technique and it is the most often used detection scheme because of its inherent sensitivity.[57] However, the high cost and the large size of the instrumental set-up for LIF are sometimes incompatible with the concept of μTAS. In addition, tedious derivatization schemes are needed to use LIF with nonfluorescent compounds. The principal alternative to LIF detection is, without any doubt, ED. Electrochemical detection is very important because presents the inherent ability for miniaturization without loss of performance and its high compatibility with microfabrication techniques. Likewise, it possesses high sensitivity, its responses are not dependent on the optical path length or sample turbidity, and it has low power supply requirements which are additional advantages.[58–60]

Amperometry, the simplest voltammetric technique, have been the most widely used in electrochemical sensors. The data is provided as a current generated by an electrode reaction. A three-electrode system consisting of a working electrode, a reference, and an auxiliary electrode is the basic configuration. By applying the desired potential to the working electrode with respect to the reference electrode, the current is prompted to flow between the working electrode and the auxiliary to be measured. The conditions are fixed to be the diffusion of the analyte to the surface of the working electrode, which is the limiting factor. This way, the current changes linearly with respect to analyte concentration. The miniaturization and integration of this type of sensors is easily achieved by creating a three-electrode system in the form of thin- or thick-film patterns.[61,62] As the electrode diameter is decreased into the low micrometer range, a shift to nonplanar diffusion occurs (compared to planar diffusion in conventional macroelectrodes) causing an increase in the collection efficiency of the electroactive species at the surface. The practical result is an increase in the signal-to-noise ratio which generally translates into a lower detection limit. The disadvantages are that the decreased current that accompanies miniaturization can require improved electronics/shielding for it to be measured accurately, and that a stable reference electrode is necessary.[63] The combination of electrodes often seen in these microsensors is platinum used for the working electrode, Ag/AgCl for the reference electrode, and a platinum auxiliary electrode. Depending on the purpose, other materials, such as gold, carbon, iridium, or the use of nanoparticles such as CNTs or nanowires can be used for the working electrode. The shape, size, and position of the electrodes are precisely defined and this system can be formed in a network of microchannels. This technique presents good detection limits but is restricted to electroactive analytes. Selectivity is achieved through a judicious choice of the detection potential.

The coupling of electrochemical sensors onto microfluidic platforms can be adapted from those previously reported for MCE. In this sense, and according to the relative position between both working electrode—separation channel, the configurations can be classified as: *end-channel*, *in-channel* and *off-channel* detection.[64] This configuration is especially important in case of MCE since minimal band broadening and electrical isolation (decoupling) from the high separation voltage must be ensured. In *end-channel* detection, the electrode is placed just

outside the separation channel. For *in-channel* detection, the electrode is placed directly into the separation channel, and *off-channel* detection involves grounding the driving voltage before it reaches the detector by means of a decoupler.

On the other hand, *conductometric* detection is a less sensible, but universal detection technique that has been applied as a detection mode in CE-microchips and microfluidic platforms in general. Conductometry can be, either in the galvanic (a pair of electrodes is placed in the separation channel for liquid impedance measurement) or the contactless mode (no contact between the pair of electrodes and separation channel solution). Contactless detection (CCD) is preferred for different reasons: (1) in case of MCE the electronic circuit is decoupled from the high-voltage applied for separation (no direct DC coupling between the electronics and the liquid in the channel), (2) the formation of glass bubbles at the metal electrodes is prevented, and (3) electrochemical modification or degradation of the electrode surface is prevented; (4) can be used with a wide range of background electrolytes and can take place at any location along a channel.

21.4 Environmental Analysis on Board of Electrochemical Microfluidic Platforms

It is clear that environmental monitoring is crucial to understand how the natural processes occur and to implement and regulate existing directives concerning chemical species in the environment. In this sense, the development of portable, robust, and accurate analytical systems to monitor a plethora of environmental compounds such as contaminants, explosives, chemical warfare agents, and inorganic and organic ions is highly demanded. Portability is a key feature in environmental analysis techniques, since allows analysis to be carried out outside of the laboratory, preventing or minimizing the risk of contaminating the sample and leading to a faster response time and lower cost. The ability to use portable equipment is an intrinsic characteristic of microfluidic systems, giving response to this analytical demand. Furthermore, the special needs for sample introduction, complexity of the sample matrix, low concentration of the chemical species; together with the necessity of real-time measurements in the field (in a large quantity and quality), and in autonomous, robust, and self-sufficient manner, are additional challenges of using microfluidic devices for environmental analysis. Excellent reviews have been reported about microfluidic devices and its applications on environmental monitoring.[15,45,65–67]

Remarkable developments on microfluidic devices have been made over the last decade and a promising future for this technology is expected. Furthermore, new electrochemical techniques for microfluidic applications have been presented over the last few years. The detection of single or multiple analytes on the same device making use of different electrochemical techniques (amperometric, potentiometric, conductimetric, or electrochemiluminiscence); microfluidic transport based on

electrokinetic flow, electrowetting, or the volume change of bubbles; together with the broad extended CE microchip separations are some of the most relevant approaches applied to microfluidic platforms.

The accurate measurement of a specific compound in a complex matrix, that is known as one of the oldest and most important challenges in analytical chemistry, can be carried out by following two main approaches: (1) improving selectivity toward the detection system by using selective (bio)sensors, or (2) improving selectivity toward separation systems with nonspecific detectors coupled after the separation of sample mixture. In this section, according to this principle, an overview of the utilization of microfluidic platforms with electrochemical detection for environmental analysis will be presented. First, selected examples of those microfluidic platforms used as separation systems will be reported, followed by the implementation of (bio)sensors in microfluidic platforms for the analysis of species of environmental interest.

21.4.1 Microfluidic Platforms as Separation Systems

Both chromatography and electrophoresis separation techniques are implemented in analytical microdevices. However, without any doubt, microchip capillary electrophoresis is still the most used method within microfluidic platforms for environmental analysis.[68] In this section, an overview of the fundamentals and applications of CE microchips to environmental analysis will be presented and, in lower extension, some aspects related to electrochromatography and HPLC on chip.

21.4.1.1 Microchip Electrophoresis

Different parts constitute a CE microchip: injector (where a sample plug is critically loaded), separation microchannels (where electrophoretic separation of analytes is performed) reservoirs (where different solutions/samples are deposited). Once all solutions, including those of the samples, are loaded, the samples are typically transferred into an injector region. Then their components are separated by application of high voltage and afterwards detected.

Microchip platform (monolithic approach) eliminates the necessity of most fluidic connections that otherwise link microfluidic components. Avoiding such connections greatly reduces sample dispersion, delay times, and dead volumes between the different microchip compartments, and therefore, significantly increasing the separation power of such integrated miniaturized systems.

The typical layout of a microchip electrophoresis (both a simple cross T-injector (*A*), and a twin-T injector (*B*)) has been already depicted in Fig. 21.5. It has a network of channels with widths varying from 10 to 100 μm with typical straight separation channels between 3 and 10 cm. In a typical set-up, buffer solutions are introduced on sample (S), running buffer (RB), and waste (W) reservoirs. The

reservoir volume is often defined by their capacities (100–250 μL). Electric fields are applied to the reservoirs by high voltage power supplies (1–5 kV), and platinum electrodes are placed in the reservoirs for injection and separation because samples are normally electrokinetically driven into the network channels.

Capillary zone electrophoresis (CZE) is the most commonly used separation mode in CE microchip due to its versatility, ease of operation, and separation power. This electrophoretic mode is based on the theory and mechanism of action directly transferred from the conventional CE. In CZE the channel contains only a buffered medium and the electrophoretic mobilities of the analytes depend on their charge/mass ratio, acting as separation mechanism. These different velocities make possible to separate cations and anions if the EOF is strong, in order to lead anionic substances to the detector located usually at the cathode. It has the limitation of being useful only for separation of charged species.

Most of the key features of MCE are common for the different types of microfluidic platforms. Thus, very fast analysis without loss of performance (high efficiency), the possibility of performing several assays simultaneously (parallelization of analysis), very low sample consumption and waste generation, sometime low cost due to the use of inexpensive materials (plastics) in single-use microsystems (disposability), integration of the different analytical steps are among the most attractive characteristics. Some selected examples of environmental analysis are discussed.

Wang and coworkers have developed a method for determining thiol-containing degradation products of V-type nerve agents in water samples.[69] The detection of three of these compounds was achieved in only 4 min in a water sample spiked with its corresponding standards. The microsystem consists of a glass capillary electrophoresis microchip with amperometric detection (screen-printed carbon ink electrode). A derivatization of the compounds with *o*-phthaldialdehyde was necessary, which was developed both *on*- and *off-chip*. When the process was performed *on-chip*, the complete reaction between derivatization agent and compounds was not achieved, resulting in decreased sensitivity. With the same microsystem,[70] three organophosphate nerve agents were detected in 140 s from a river water sample spiked with those analytes. In both cases, the LODs were in micromolar range, but this seems to be insufficient for real applications. Better LODs were obtained by the same research group using contactless conductivity as its detection mode.[71] A detection limit within the nanomolar range was achieved for the determination of three organophosphonate nerve agent degradation products from a river water sample (spiked with standards). In this work, a disposable PMMA microchip with integrated electrodes was used with excellent results (analysis time 130 s).

Wang and coworkers have also separated and detected three different groups of pollutants (nitrophenols, aromatic amines, and chlorophenols) by capillary electrophoresis on a glass microchip with amperometric detection using river and groundwater samples. In this case, the detected compounds were previously added. Five nitrophenol derivates were detected in 120 s with a glassy carbon electrode,[72] three aromatic amines (4-aminophenol, 2-aminonaphthalene, and *o*-aminobenzoic acid) in 150 s with a boron-doped diamond thin-film detector,[73] and phenol and three

chlorophenols in 120 s with a carbon SPE modified with gold.[74] In these papers, the LODs were within the micromolar range and accuracy was not evaluated. The samples were filtered before the analysis.

Hilmi et al.[75] demonstrated a CE chip with direct amperometric detection for five nitroaromatic explosives, including trinitrotoluene (TNT), in ground water and soil extracts. The microfluidic device achieved rapid separation and detection of explosive compounds with LODs of 100–200 μg/L.

Also using amperometric detection, Chen, et al.[76,77] developed a three-dimensionally adjustable amperometric detector for MCE and applied to separate aromatic amines and nitroaromatic pollutants. Amperometry, and related pulse amperometric detection modes, are very attractive because provide enhanced selectivity related to conductimetric detection.

Garcia et al. obtained good results in their analysis of environmental samples using a PDMS microchip with pulse amperometric detection (PAD). Levoglucosan (the largest single component of the water extractable organics in smoke particles) was determined in smoke particles in only 1 min.[78] The results obtained with this method are in accordance with those obtained with GC/MS. The aerosol particles were collected and extracted *off-chip* and *off-line*. The LOD achieved (17 μM) was adequate for the analysis of smoke samples but insufficient for atmospheric samples. In another paper from the same group,[79] three of the most important pollutants (phenol, 4,6-dinitro-*o*-cresol, and pentachlorophenol) were detected in a city water sample spiked with the corresponding standards. The LODs were within the micromolar range and accuracy was evaluated by determining phenol in two medicines with labeled content. Sample treatment was not necessary.

In the work of Ha et al.,[80] a MCE for monitoring endocrine disrupting species was used with amperometric detection. Thin film electrodes fabricated from Prussian Blue-modified indium tin oxide were incorporated into a serpentine microchannel configuration. Four endocrine disruptors were separated and detected in 2 min with LOD of 59 nM.

Conductivity detection is also used, both in contact and contactless mode, in microchip electrophoresis. As previously commented, some advantages of this technique are the simplification in the construction of the device, avoiding the electrode fouling and high sensitivity. Bodor et al. have determined three anions (NO_2^-, F^-, PO_4^{3-}) in river, tap, and mineral water on a PMMA column-coupling microchip with conductivity detection.[81] The microchip consists of two coupled columns: The first is used as an isotachophoresis (ITP) column and the second as a CZE column. In the ITP stage, the sample was preconcentrated and cleaned up and, in the CZE stage, the anions were separated. Minimal sample treatment *off-chip* was needed (filtration and degassing). LODs were within the micromolar range and the accuracy of the method was not evaluated.

Isotachophoresis was also utilized by Prest et al. with a PMMA microfluidic device coupled to conductimetric detection, for both selenium and arsenic species obtaining good LODs.[82,83]

Tanyayiwa et al.[84] also used contactless conductimetric detection utilizing external electrodes independent from the electrophoretic separation part of the

device. This microfluidic device was used for multi-analysis of small inorganic and organic ions with LODs in the micromolar range.

Recently, Liu et al. developed a MCE with contactless detection for inorganics ions and heavy metals.[85] Using this device, an average LOD of 0.4 μM for inorganics cations in water was obtained.

In the work of Rogers and Ding,[86] a MCE method for the determination of holacetic acids using contactless CD was used. In this case, an *off-chip* solid-phase extraction step was implemented prior to MCE analysis. These products, a class of disinfectant by-products generated during the water chlorination treatment process, were determined in swimming pool water with LODs ranging from 38 to 500 ppb.

Besides, Pumera et al.[87] used of contactless conductivity detection for a PMMA microchip CE device. Separation of potassium, sodium, barium and lithium cations and chloride, sulfate, fluoride, acetate, and phosphate anions was achieved, producing LODs of 2.8 μmol/L for potassium and 6.4 μmol/L for chloride. In a similar way, this detection technique was also used by Lichtenberg et al.[88] for a glass microchip CE device. Potassium, sodium, and lithium cations were separated using the device, producing an LOD of 18 μmol/L for potassium. In order to improve this LOD, sample-preconcentration by field-amplified sample stacking (FASS) was suggested as a method to make the LOD comparable with other contact conductivity detection methods previously reported. The differences in LODs are attributed to the difference in geometrical parameters of the electrodes used in the device manifold.

21.4.1.2 Electrokinetic Chromatography

On the other hand, electrokinetic chromatography has also been transferred to microchip format. Micellar electrokinetic chromatography (MEKC) is characterized by the use of micelles as pseudo phase. Micelles are aggregates that are formed by adding the surfactants to the separation buffer at a concentration above their critic micellar concentration. Ionic surfactants form micelles that move at a different velocity to the EOF. In this case, the separation of neutral molecules is produced by their distribution between the aqueous and the micellar phases. When the micellar phase moves to the detector, the elution range is between the time corresponding to EOF and the migration time of the micelles, and all analytes will migrate between these two limits depending on their distribution between the two phases.

Luong et al. were able to determine trinitrotoluene, 2,4-dinitrotoluene, and 2,6-dinitrotoluene in soil and groundwater samples by MEKC-EC on a glass microchip and using a gold wire as electrode.[89] The analysis time was 4 min and LODs were below the micromolar range. The accuracy of the method was validated by comparison with the LC procedure of the US EPA (method 8330). For the soil sample, an extraction step *off-chip* was necessary.

Gertsch et al.[90] reported a MCE with contact conductivity detection for the determination of perchlorate in water at the ppb level. Separation of this compound

from competing anions in drinking water was achieved using a micellar pseudostatinary phase containing a zwitterionic surfactant to selectively retain perchlorate. Using this method a total analysis time of 60 s and a LOD of 5.6 ppb in drinking water was obtained.

21.4.1.3 Microchip HPLC

HPLC in Lab-on-a-chip includes the integration of individual operations such as reaction, preconcentration, separation, and the corresponding detection into mass-produced and low-cost device development. This methodology is of particular interest for the on-line coupling to mass spectrometry analysis, because of its compatibility with the flow-rate requirements of a nano-electrospray interface. However, few examples are reported with electrochemical detection. A. Ishida et al.[91] have developed a microchip for reversed phase LC using porous monolithic silica. The chip layout consists of a double T-shaped injector and a 40 cm separation channel in a serpentine configuration. The microchip is constructed in glass with overall dimensions of 35 mm × 35 mm. The molotithic stationary phase is created by introducing reactant solutions by syringes. By other hand, different valves connected to syringes allow the introduction of the mobile phase and sample. The end of the separation channel is connected to an electrochemical detector using conventional amperometric detection. Different catechin compounds can be separated with good resolution, although long analysis times are required.

21.4.2 Microfluidic Platforms for Electrochemical Sensing

Microfluidic platforms can be considered as an ideal tool for electrochemical sensing. One of the main reasons lies in is capability to perform microscale flow-injection analysis.[92,93] This concept includes electrokinetic or hydrodymanic injection, pumping, and analyte detection using the microfluidic platform as a microchip format to prevent interconnections and dead volumes. This approach is clearly advantageous since it allows accurate, ultrasmall sample volumes (loop-size variable) to be introduced and has accurate fluid-control and manipulation capabilities.

Fluidic manipulation in conjunction with the high compatibility of ED with microfabrication techniques is crucial to understand the next step towards new designs for electrochemical sensors based on microfluidic chips. In consequence, at this stage, we need to realize that sensor platforms are the new approach to understanding the classic view of sensors: a more complicated layout of channels where fluidic motion is produced and where detection systems are also integrated.

The history of miniaturizing bio/chemical sensors is over 30 years old, as is represented by the development of ion-sensitive field-effect transistors (ISFETs).[94,95] Stimulated by the current trend of μTAS and lab-on-a-chip technologies, they are currently being incorporated in microfluidic systems for the

realization of highly sophisticated systems.[96–98] However, as we have already mentioned before, the miniaturization of microfluidic devices depends on micromachining technology. The integration of different components such as pumps and valves on a chip is possible but tends to be complicated. In conducting highly sophisticated microsystems, electrochemical principles provide more realistic solutions.[99] As previously stated for MCE, basic structures used in microfabricated electrochemical devices are patterns of electrodes formed using thin- or thick-film processes. Therefore, the structure and function of each component can be made very simple. Moreover, microfabrication makes batch fabrication possible, simultaneously reducing costs.

As in the case of large-scale bio/chemical sensors, different classifications according to multiple criteria can be used. The most common way to group sensors is to consider their transducing mechanism (electrical, optical, mass, thermal, piezoelectric, etc.), and their recognition principle (enzymatic, DNA, molecular recognition, etc.). Although the volume of published works is not as extensive as in the case of microchip capillary electrophoresis, an overview of electrochemical microfluidic platforms for sensing in environmental analysis is reported. They will be classified depending on the nature of the biological molecule and selected examples will be described from different approaches such as the use of antibodies, enzymes, DNA, or directly chemical sensors.

21.4.2.1 Microfluidic Immunosensors

Immunological methods make use of antibodies as analytical tool for detecting a plethora of clinical, environmental, and food-relevant analytes. The special features that had made immunoassay widely increased in the last decades are the highly sensitivity and specificity of the antibody-antigen interaction. Although enzyme-linked immunosorbent assay (ELISA), currently performed in microtiter plates is the most common technique, a variety of assay types can be performed depending of the analytes or samples.

Combination of both techniques explodes the selectivity and sensitivity from immunoassays with the remarkable features from microfluidic platforms. Microfluidic immunosensors make use of a network of microchannels and/or immunoreactor chambers usually built in a monolithic platform with part or all the necessary components for immunoassay procedures.

Some of the features that make microfluidic platforms especially suitable for immunoassays are described next:

1. Firstly, the long-time associated to incubation in normal immunoassay can be attributed to the inefficient mass transport for the immunoreagents to move from the bulk solution to the wall surface where interaction takes places. In microchannels, the surface area to volume ratio is higher and that makes the diffusional distances dramatically reduced and produces lower analysis times.

2. Furthermore, the miniaturization reduces drastically the consumption of the expensive reagents as well as those special samples.
3. Procedures can be automated, since different steps and fluid movement can be easily controlled, especially with electrokinetic fluidic motion, through the control of applied electric fields, or in a more complicated ways (e.g., using pumps, valves, and mixers).

All these advantages have made microfluidic immunoassays platforms as emergent, powerful option for the analysis of a broad variety of analytes in different fields. Although still it is in its infancy, microfluidic immunosensors reveal as very promising tool in environmental applications. For supplementary information, the reader is guided to excellent review articles.[7,63,100–103]

Electrochemical microfluidics immunoassay can be conducted either in homogeneous and heterogeneous configurations. In homogeneous assays, both unbound antibody and antigen–antibody complex are freely placed in the solution. Discrimination of both species in microfluidic devices is usually accomplished by their electrophoretic mobility differences in microchannels. In heterogeneous assays, either antibody or antigen are immobilized on a solid surface and a separation step is performed to isolate the desired analyte from any other potential interferences. Heterogeneous assays benefit from the high surface area/volume ratio that rend higher sensitivity while homogeneous format take advantage from the possibility of multiplexing format and fast electrophoretic separations Heterogenous immunoassays are predominantly used in microfluidics and different strategies have been implemented based on where the antibodies are immobilized: on microchannel walls, on microbeads, or on the electrode surfaces positioned within the microchannels.

The use of microbeads as immobilization support entails some advantages such as the surface to volume ratio is highly increased even in comparison with microchannel wall surface immobilization. When the beads are dispersed, diffusion distances are reduced and the higher efficiency of interactions between samples and reagents rend better sensitivity. Furthermore, the antibodies or antigens attached onto the beads can be easily transported in a fluidic system. A highly control of the antibody load into the channel and fast replacement of the beads between assays are added benefits. By other hand, the high variability of surface modification available on these microbeads introduces multiple functionalities to a single microfluidic design. However, microbeads have the risk of adsorbing to channels and electrodes, clogging channels, or increasing the flow resistance.

When beads are magnetics, the main advantage comes from its easy manipulation by magnetic fields. This fact eliminates the need for physical retention microstructures allowing the beads to be immobilized and released at different stages and desired areas of the assay. In the work of Martinez et al.[104] a microfluidic immunoassay (ELISA) for rapid and sensitive quantification of ethinylestadiol (EE2) in river water samples was developed. The assay was conducted by immobilization of the specific antibodies onto the surface of magnetic particles. These modified beads were allowed to react with the samples outside of the microfluidic devices before injection and retention in the channel for subsequent assay steps. Electrochemical

detection was performed on the surface of a gold electrode within the channel. The total assay time was 30 min and the LOD of 0.09 ng/L.

Another possibility to immobilize the antibodies implies their direct attach onto electrode surfaces usually located as the walls of the microchannels. Different substrates can be used as electrode material. However, carbon derivatives, platinum, and mainly gold are the most used in microfluidic devices. An interesting possibility to immobilize biomolecules on the gold electrode surfaces within microchannels is through the use of monolayer of poly dendrimers. In the work or Park et al.[105,106] the antigen 2,4-dinitrophenylacetic acid (DNP) modified surface is constructed onto a gold electrode for microfluidic immunosensing of anti DNP antibodies. In a first step, an amine-reactive SAM is produced where a poly(amidoamine) G4 dendrimer is attached. Subsequently, a succinimidyl ester of DNP is allowed to react. *N*-Hydroxysuccinimide (NHS) groups, which located at the end of activated-DNP, react with the plenty of amine groups on the dendrimer for its immobilization. As a proof of concept of this microfluidic device, GOX tagged anti-DNP antibodies were used as analyte. After loading the sample into the reaction channel and interaction with the antigen-functionalized electrodes, the electrochemical signal was produced by the GOX enzyme using ferrocennemethanol as the electron mediator and glucose as the substrate. This work is also an example where the transport of multiple liquids is performed without any external equipment. The hydraulic pressure caused by the elastic deformation of the liquid reservoir can be used as the driving force to transfer the multiple liquids into the device. This is achieved using elastic PDMS cover caps with a reversed mushroom-shaped locking component to retain the internal pressure, which acts as the latch.[106]

21.4.2.2 Microfluidic Enzyme-Sensors

Enzymes have also been used as selective biorecognition elements to determine a specific substrate in environmental microfluidic biosensors. Amperometric biosensors, which have proven to have great potential since the 1980s, can be incorporated into microfluidic devices transferring their benefits to lower dimension devices.

Exploiting the benefits of using magnetic beads as immobilization support for biological material, Llopis et al.[107] presented a microfluidic biosensor for carbofuran determination. The pesticide was determined in a microfluidic system by means of the enzymatic inhibition of acetylcholinesterase immobilized on magnetic beads. The enzyme, coupled to magnetic beads, is immobilized in the capture region of a single cross-microfluidic device with the aid of a magnetic field. The presence of the pesticide inhibits the enzyme activity; hence, a smaller amount of thiocholine, which is the electrochemically active product of catalyzed hydrolysis when acetylcholinesterase is used as the substrate, can be amperometrically detected on the surface of a platinum disk working electrode with off-channel configuration. Easy renewal of the biosensing material after each determination can be accomplished with highly reproducible leading sensitivity and a stable response to the pesticide.

Analogous strategy for this type of integrated microfluidic enzyme-biosensors is presented by Monty et al.[108] A dual microchannel device with a gas-liquid interface is used as an amperometric biosensor to determine organophosphate chemicals based on acetylcholinesterase inhibition. Rapid diffusion of the vapor sample into the liquid microchannel where the enzyme is immobilized allows pesticides to be detected with a lower detection limit and shorter detection time. The electrochemical cell is constructed by using a nanoporous polycarbonate membrane which is used to separate both the gas and the liquid microchannels, and where a thick sputtered gold layer acts as the working and counter electrodes. A conventional Ag/AgCl reference electrode is immersed in a small vial which is electrokinetically connected to the liquid microchannel.

In another example, Chikkaveeraiah et al.[109] developed a single microfluidic device for the determination of hydrogen peroxide at nanomolar concentrations. The design, based on a single microfluidic channel, incorporates a biocatalytic sensing electrode, an Ag/AgCl reference and Pt wire counter electrodes. The sensing electrode was a gold wire coated with 5 nm glutathione-decorated gold nanoparticles, and horseradish peroxidase was covalently linked to the glutathione nanoparticles. Detection of H_2O_2 based on direct bioelectrocatalysis using HRP was performed with high sensitivity, and an unprecedented detection limit was obtained for an unmediated enzyme electrode.

21.4.2.3 Microfluidic DNA-Sensors

Despite the great and well-known advantages of miniaturization, today an ideal sensor platform is required to not only be miniaturized and cost-efficient but also capable to simultaneously detect multiple analytes. Most likely, DNA analysis is the area in which multiplexed devices are most extensively applied, mainly based on the concept of DNA microarrays or DNA chips and usually associated to the microfabrication of diagnostic kits by screen-printed technology.

DNA biosensors such as conventional DNA microarrays make use of sequence-specific DNA detection. They consist of an immobilized DNA strand to detect the complimentary sequences by DNA-DNA hybridization. The newly developed “lab on a chip” concept is essentially an adaptation of DNA chips to content channels and chambers for flowing liquids, thus avoiding its limitations. They integrate, on a single chip, modules for DNA extraction, purification, amplification, and detection, most of them using microfluidic capillary electrophoresis devices.[22]

One of the main applications of microfluidic DNA-sensing platforms on environmental analysis lies on its utilization as high-throughput systems for the rapid detection of nucleic acids that identify specific bacterial pathogens. Nowadays, a serious attention is needed in the evaluation of microbial cells in water, soil, and environment. These platforms are feasible to incorporate all the functional components of a macro-scale instrument into the restricted spatial domains of a microchannel for the identification of pathogens within minutes with a single-cell sensitivity level.[110,111]

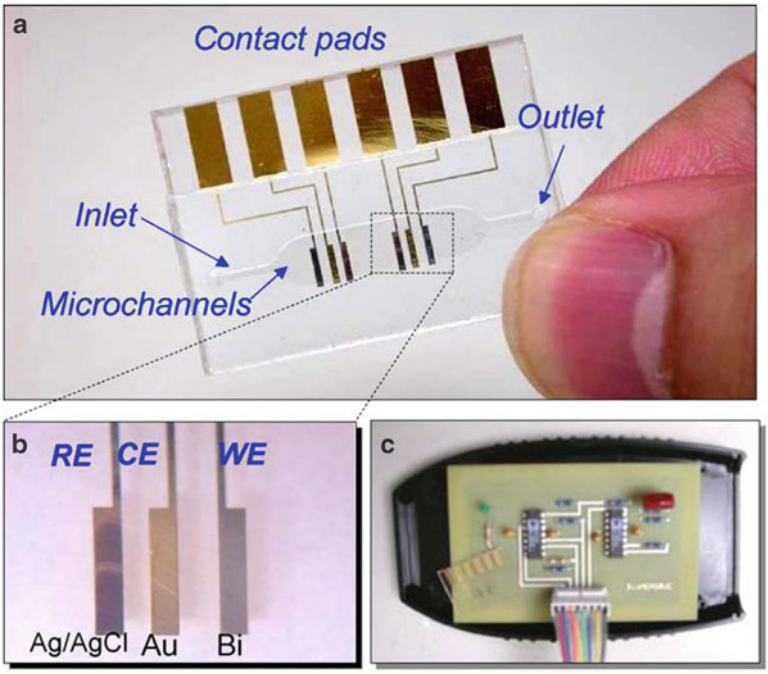

Fig. 21.7 Device pictures: (**a**) the entire chip including the sensor array and the microfluidic channels, (**b**) the magnified picture of the 3-electrode sensor, and (**c**) the customized detection circuits along with the chip. From (113) reproduced by permission of Elsevier

As an example of this methodology, Nugen et al.[112] reported an electrochemical magnetic genosensor to determine mRNA amplified sequences from *Cryptosporidium parvum*. This is protozoal infectious agent that can be found in contaminated water. A sandwich hybridization assay with capture probe-coated paramagnetic beads and tagged liposomes entrapped with potassium ferro/ferrihexacyanide is used for amperometric detection in a gold interdigitated ultramicroelectrode array (IDUA). The assay is performed in the chamber of a single microchannel and, after hybridization, magnetic beads are retained on the IDUA where liposomal amplification is used for electrochemical detection.

21.4.2.4 Microfluidic Chemical Sensors

Direct voltammetric and potentiometric detection of various analytes of environmental interest have also been reported in microfluidic devices.

A miniaturized sensor for heavy-metal ions consisting of a nontoxic bismuth working electrode, an integrated Ag/AgCl reference electrode, and a gold counter electrode, has been proposed by Zou et al.[113] Pb(II) and Cd(II) are positioned in a microchamber of 4.5 μL in which a planar array of multiple sensors can be located for multiple measurements using different sensor son one chip (Fig. 21.7).

Anodic stripping voltammetry is used to determine various heavy-metal ions in situ without the undesirable presence of Hg. This group also presents a similar device for continuous and on-site heavy metal monitoring (Pb(II)).[114] This polymer lab chip sensor allows 43 consecutive measurements in nondeoxygenating standard solutions inside the microchannels using square-wave anodic stripping voltammetry. Pb concentrations range 1–1,000 ppb with a LOD of 0.55 ppb and 300 s deposition time.

In another work from the same group,[115] an on-chip dual pH and nitrate ion-selective sensor chip has been realized using self-assembly nanobead-packed hetero columns, which provides an easy sample loading with hydrophilic silica nanobead-packed column and an ion-selective sensor with hydrophobic PS nanobeads, respectively. The nanobead-packed hetero columns provide a new electrochemical sensing platform with a high sensitivity and excellent ion selectivity with easy sampling for environmental monitoring. The potentiometric response of the nitrate ion-selective sensor chip was linear with a Nernstian slope of −61.369 (mV decade^{-1}) within the NO_3^- concentration range of 10^{-5}–10^{-1}. The response times of the pH and nitrate sensors were less than 5 s and 7 s, respectively.

Masadome et al.[116] developed a microfluidic polymer chip containing a nitrate ion-selective electrode for determination of nitrate ion in environmental water samples such as tap water, well-water, and water for agricultural use. The electrode is based on tetradodecylammonium bromide as an anion exchanger. Using Na^+ −ISE as reference electrode, the detector showed an almost Nernstian response to nitrate ion over a concentration range between 1.0×10^{-5} and 1.0×10^{-1} M, with an anionic slope of -54.3 ± 1.3 mV/decade.

A nitrate sensor has been also reported by Kim et al..[117] This sensor uses a simple electrochemical system composed of a silver sensing electrode, a silver oxide reference electrode, and a platinum counter electrode in 0.01 M NaOH concentrically distributed electrolyte. These micro-electrodes are microfabricated on a silicon substrate, providing an electrochemical microcell ion which a single microfluidic channel is used to deliver the reagents. Nitrate concentration is detected using double-potential step chronocoulometry in which the current accrued from nitrate reduction to nitrite is integrated.

21.5 Conclusions and Future Trends

Microfluidic platforms can be considered as an emergent and new approach for high selective and sensitivity sensing. Within these devices, planar monolithic microchip format is the most common arrangement. Also electrochemical detection, due to its inherent miniaturization and high compatibility with microfabrication techniques, appears as natural detection principle in these platforms. This detection principle is not expensive and compatible with the disposability of microfluidic platforms after its use. Although both electrokinetic and hydrodynamic flows are performed in microfluidic platforms, the first approach is clearly dominant in miniaturized

analytical separation science (i.e. Capillary electrophoresis microchip technology). However, when microfluidics is used as new platform sensing, hydrodynamic approach is also widely used. The probable reason is because hydrodynamic pumping is more reproducible, and since no separation is strictly required; the high efficiency separation given by electrophoretic approaches is not needed. However, electrokinetics has a prominent and unique role in microfluidoc platforms because of flow in multiple channels on a microchip can be easily controlled with a few electrodes.

Although a growing number of articles recognize the utility of microfluidic platforms for environmental analysis, some challenges must be achieved. Even though, a revolution in technology and microfabrication techniques takes places, integration of components into complete and functional systems, small and thus potentially portable, and simple to be used by nonexperts are features required. Especially in environmental samples, it is clearly showed the enormous difficulties that the analysis of real samples presents on a microscale. Important efforts have to be done in handling complex and highly variable sample matrices integrating sample treatment on microfluidic devices, the possibility to operate for days to months in the field, or improving sensitivity and selectivity through the use of ultrasensitive detectors. Moreover, additional efforts have to be made towards the validation of the methods to demonstrate the reliability of microfluidic systems.

No doubt exists that performing novel ultrasensitive detection routes, new devices materials, and systematically using smart bioreactives and nanotechnology are the keys to defining the success and incorporation of microfluidic devices in environmental analysis.

References

1. Manz A, Graber N, Widmer HM (1990) Miniaturized total chemical analysis systems: a novel concept for chemical sensing. Sens Actuat B 1:244–248
2. Whitesides GW (2006) The origin and the future of microfluidics. Nature 442:368–373
3. Janasek D, Franzke J, Manz A (2006) Scaling and design of miniaturized chemical-analysis systems. Nature 442:374–380
4. Gerschke O, Klank H, Tellesmann P (eds) (2004) Mycrosystem engineering of lab-on-a-chip devices. Wiley, Weinheim
5. Ríos A, Escarpa A, Simonet B (2009) Miniaturization of analytical systems. Principles, designs and applications. Wiley, Weinheim
6. Madou MJ (ed) (2000) Fundamentals of microfabrication (The science of miniaturization). CRC Press LLC., Boca Raton, FL
7. Hervás M, López MA, Escarpa A (2012) Electrochemical immunosensing on board microfluidic chip platforms. Trends Anal Chem 31:109–128
8. Gardieneers JG, Oosterbroek RE, Van der Berg A (2003) Silicon and glass micromachining for μ-TAS. In: Oosterbroek RE, Van der Berg A (eds) Lab-on-a-chip: miniaturized systems for (bio) Chemical analysis and synthesis. Elsevier, Amsterdam, pp 37–64
9. Jorgensen AM, Mogensen KB (2004) Silicon and cleanroom processing. In: Geschke O, Klank H, Telleman P (eds) Microsystem engineering of lab-on-a-chip devices. Wiley-VCH, Weinheim, pp 117–160

10. Petersen D, Mogensen KB, Klank H (2004) Glass micromachining. In: Geschke O, Klank H, Telleman P (eds) Microsystem engineering of lab-on-a-chip devices. Wiley-VCH, Weinheim, pp 161–168
11. Klank H (2004) Polymer micromachining. In: Geschke O, Klank H, Telleman P (eds) Microsystem engineering of lab-on-a-chip devices. Wiley-VCH, Weinheim, pp 169–182
12. Duffy DC, Schueller OJA, Whitesides GM (1998) Rapid prototyping of microfluidic systems in poly(dimethylsiloxane). Anal Chem 70:4974–4984
13. Becker H, Gärtener C (2003) Microreplication technologies for polymer-base μ-TAS application. In: Oosterbroek RE, van der Berg A (eds) Lab-on-a-chip: miniaturized systems for (bio) Chemical analysis and synthesis. Elsevier, Amsterdam, pp 21–35
14. Binyamin G, Boone TD, Lackritz HS, Ricco AJ, Sassi AP, Williams SJ (2003) Plastic microfluidic devices: electrokinetic manipulations, life science applications, and production technologies. In: van der Oosterbroek RE, Berg A (eds) Lab-on-a-chip: miniaturized systems for (bio) Chemical analysis and synthesis. Elsevier, Amsterdam, pp 83–112
15. Li HF, Lin JM (2009) Applications of microfluidic systems in environmental analysis. Anal Bioanal Chem 393:555–567
16. Ramos L, López MA, Escarpa A (2012) Miniaturization in sample preparation. In: Guardia M, Garrigues S (eds) Handbook of green analytical chemistry. Wiley, Chichester
17. Rios A, Escarpa A, Gonzalez MC, Crevillén AG (2006) Challenges of analytical microsystems. Trends Anal Chem 25:467–479
18. de Mello AJ, Beard N (2003) Dealing with "real" samples: sample pre-treatment in microfluidic systems. Lab Chip 3:11N–19N
19. Lichtenberg J, de Rooij N, Veerporte E (2002) Sample pretreatment on microfabricated devices. Talanta 56:233–266
20. Sueyoshi K, Kitagawa F, Otsuka K (2008) Recent progress of online sample preconcentration techniques in microchip electrophoresis. J Sep Sci 31:2650–2666
21. Chen X, Cui DF (2009) Microfluidic devices for sample pretreatment and applications. Mycrosyst Technol 15:667–676
22. Crevillén AG, Hervás M, López MA, González MC, Escarpa A (2007) Real samples analysis on microfluidic devices. Talanta 74:342–357
23. Andersson H, van der Wijngaart W, Stemme G (2001) Micromachined filter-chamber array with passive valves for biochemical assays on beads. Electrophoresis 22:249–257
24. Long Z, Liu D, Ye N, Qin J, Lin B (2006) Integration of nanoporous membranes for sample filtration/preconcentration in microchip electrophoresis. Electrophoresis 27:4927–4934
25. Hatch AV, Herr AE, Throckmorton J, Brennan JS, Singh AK (2006) Integrated preconcentration SDS-PAGE of proteins inmicrochips using photopatterned cross-linked polyacrylamide gels. Anal Chem 78:4976–4984
26. Noblitt SD, Kraly JR, VanBuren JM, Hering SV, Colett JL, Henry CS (2007) Integrated membrane filters for minimizing hydrodynamic flow and filtering in microfluidic devices. Anal Chem 79:6249–6254
27. Brody JP, Yager P (1997) Diffusion-based extraction in a microfabricated device. Sens Actuat A 58:13–18
28. Weigl BH, Yager P (1999) Microfluidic diffusion-based separation and detection. Science 283:346–347
29. Tokeshi M, Minagawa T, Kitamori T (2000) Integration of a microextraction system on a glass chip: ion-pair solvent extraction of Fe(II) with 4,7-Diphenyl-1,10-phenantrolinedisulfonic acid and tri-n-octylmethylammonium choride. Anal Chem 72:1711–1714
30. Sato K, Tokeshi M, Sawada T, Kitamori T (2000) Molecular transport between two phases in a microchannel. Anal Sci 16:455–456
31. Broyles BS, Jacobson SC, Ramsey JM (2003) Sample filtration, concentration, and separation integrated on microfluidic devices. Anal Chem 75:2761–2767
32. Masaki H, Hoshi J, Amano S, Sasaki Y, Korenaga T (2006) Integration of the cleanup process: pretreatment of polycyclic aromatic hydrocarbons from diesel exhaust particles on silica gel beads in a microchannel. Anal Sci 22:345–348

33. Tennico YH, Remcho VT (2010) In-line extraction employing functionalized magnetic particles for capillary and microchip electrophoresis. Electrophoresis 31:2548–2557
34. Augustin V, Proczek G, Dugay J, Descroix S, Hennion MC (2007) Online preconcentration using monoliths in electrochromatography capillary format and microchips. J Sep Sci 30:2858–2865
35. Yu C, Davey MH, Svec F, Frechet JMJ (2001) Monolithic porous polymer for on-chip solid-phase extraction and preconcentration prepared by photoinitiated in situ polymerization within a microfluidic device. Anal Chem 73:5088–5096
36. Yu C, Xu MC, Svec F, Fréchet JMJ (2002) Preparation of monolithic polymers with controlled porous properties for microfluidic chip applications using photoinitiated free-radical polymerization. J Polym Sci A Polym Chem 40:755–769
37. Jacobson SC, Ramsey JM (1995) Microchip electrophoresis with sample stacking. Electrophoresis 16:481–486
38. Noh HB, Lee KS, Lim BS, Kim SJ, Shim YB (2010) Total analysis of endocrine disruptors in a microchip with gold nanoparticles. Electrophoresis 31:3053–3060
39. Palmer J, Burgi DS, Munro NJ, Landers JP (2001) Electrokinetic injection for stacking neutral analytes in capillary and microchip electrophoresis. Anal Chem 73:725–731
40. Xu Y, Jiang H, Wang E (2007) Ionic liquid-assisted PDMS microchannel modification for efficiently resolving fluorescent dye and protein adsorption. Electrophoresis 28:4597–4605
41. Jung B, Bharadwaj R, Santiago JG (2006) On-chip million fold sample stacking using transient isotachophoresis. Anal Chem 78:2319–2327
42. Humble PH, Kelly RT, Woolley AT, Tolley HD, Lee ML (2004) Electric field gradient focusing of proteins based on shaped ionically conductive acrylic polymer. Anal Chem 76:5641–5648
43. Ross D, Locascio LE (2002) Microfluidic temperature gradient focusing. Anal Chem 74:2556–2564
44. Ramadan Q, Gijs MAM (2012) Microfluidic applications of functionalized magnetic particles for environmental analysis: focus on waterborne pathogen detection. Microfluid Nanofluid 13:529–542
45. Jokerst JC, Emori JM, Henry CS (2012) Advances in microfluidics for environmental analysis. Analyst 137:24–34
46. Dharmasiri U, Witek MA, Adams AA, Osiri JK, Hupert ML, Bianchi TS, Roelke DL, Soper SA (2010) Enrichment and detection of Escherichia coli 0157:H7 from water samples using an antibody modified microfluidic chip. Anal Chem 82:2844–2849
47. Beyor N, Seo T, Liu P, Mathies RA (2008) Immunomagnetic bead-based cell concentration microdevice for dilute pathogen detection. Biomed Microdevices 10:909–917
48. Woias P (2005) Micropumps - past, progress and future prospects. Sens Actuat B 105:28–38
49. Iverson BD, Garimella SV (2008) Recent advances in microscale pumping technologies: a review and evaluation. Microfluid Nanofluid 5:145–174
50. Nisar A, Afzulpurkar N, Mahaisavariya B, Tuantranont A (2008) MEMS-based micropumps in drug delivery and biomedical applications. Sens Actuat B 130:917–942
51. Mugele F, Baret JC (2005) Electrowetting: from basics to applications. J Phys Condens Matter 17:R705–R774
52. Bahadur V, Garimella SVJ (2006) An energy-based model for electrowetting-induced droplet actuation. J Micromech Microeng 16:1494–1503
53. Bahadur V, Garimella SV (2007) Electrowetting-based control of static droplet states on rough surfaces. Langmuir 23:4918–4924
54. Li X, Ballerini DR, Shen W (2012) A perspective on paper-based microfluidics: current status and future trends. Biomicrofluidics 6:011301–011313
55. Kutter JP, Mogensen KB, Klank H (2004) Microfluidics components. In: Gescheke O, Klank H, Telleman P (eds) Microsystem engineering of lab-on-a-chip devices. Wiley-VCH, Weinheim, pp 39–76

56. Fang Q, Shi XT, Du WB, He QH, Shen H, Fang ZL (2008) High-throughput microfluidic sample-introduction systems. Trends Anal Chem 27:521–532
57. Schwarz MA, Hauser PC (2001) Recent developments in detection methods for microfabricated analytical devices. Lab Chip 1:1–6
58. Vandaveer WR, Pasas SA, Martin RS, Lunte SM (2002) Recent developments in ampeometric detection for microchip capillary electrophoresis. Electrophoresis 23:3667–3677
59. Wang J (2005) Electrochemical detection for capillary electrophoresis microchips: a review. Electroanalysis 17:1133–1140
60. Pumera M, Merkoci A, Alegret S (2006) New materials for electrochemical sensing VII. Microfluidic chip platforms. Trends Anal Chem 25:219–235
61. De Mello A (2002) Miniaturization. Anal Bioanal Chem 372:12–13
62. Suzuki H (2000) Advances in the microfabrication of electrochemical sensors and systems. Electroanalysis 12:703–715
63. Bange A, Halsall HB, Heineman WR (2005) Microfluidic immunosensor systems. Biosens Bioelectron 20:2488–2503
64. Vandaveer WR, Pasas-Farmer SA, Fischer DU, Frankenfeld CN, Lunte SM (2004) Recent developments in electrochemical detection for microchip capillary electrophoresis. Electrophoresis 25:3528–3549
65. Marle L, Greenway G (2005) Microfluidic devices for environmental monitoring. Trends Anal Chem 24:795–802
66. Miró M, Hansen EH (2007) Miniaturization of environmental chemical assays in flowing systems: the lab-on-a-valve approach vis-a-vis lab-on-a-chip microfluidic devices. Anal Chim Acta 600:46–57
67. West J, Becker M, Tombrink S, Manz A (2008) Micro total analysis systems: latest achievements. Anal Chem 80:4403–4419
68. Chen G, Lin Y, Wang J (2006) Monitoring environmental pollutants by microchip capillary electrophoresis with electrochemical detection. Talanta 68:497–503
69. Wang J, Zima J, Lawrence NS, Chatrathi MP, Mulchandani A, Collins GE (2004) Microchip capillary electrophoresis with electrochemical detection of thiol-containing degradation products of V-Type nerve agents. Anal Chem 76:4721–4726
70. Wang J, Chatrathi MP, Mulchandani A, Chen W (2001) Capillary electrophoresis microchips for separation and detection of organosphosphate nerve agents. Anal Chem 73:1804–1808
71. Wang J, Pumera M, Collins GE, Mulchandani A (2002) Measurements of chemical warfare agent degradation products using an electrophoresis microchip with contactless conductivity detector. Anal Chem 74:6121–6125
72. Fischer J, Barek J, Wang J (2006) Separation and detection of nitrophenols at capillary electrophoresis microchips with amperometric detection. Electroanalysis 18:195–199
73. Shin D, Tryk DA, Fujishima A, Muck A Jr, Chen G, Wang J (2004) Microchip capillary electrophoresis with a boron-doped diamond electrochemical detector for analysis of aromatic amines. Electrophoresis 25:3017–3023
74. Wang J, Chatrathi MP, Tian B (2000) Capillary electrophoresis microchips with thick-film amperometric detectors: separation and detection of phenolic compounds. Anal Chim Acta 416:9–14
75. Hilmi A, Luong JHT (2000) Electrochemical detectors prepared by electroless deposition for microfabricated electrophoresis chips. Anal Chem 72:4677–4682
76. Yao X, Wang J, Zhang L, Yang P, Chen G (2006) A three-dimensionally adjustable amperometric detector for microchip electrophoretic measurement of nitroaromatic pollutants. Talanta 69:1285–1291
77. Chen G, Bao H, Yang P (2005) Fabrication and performance of a three-dimensionally adjustable device for the amperometric detection of microchip capillary electrophoresis. Electrophoresis 26:4632–4640

78. García CD, Engling G, Herckes P, Collett J Jr, Henry C (2005) Determination of levoglucosan from smoke sample using microchip capillary electrophoresis with pulsed amperometric detection. Environ Sci Technol 39:618–623
79. Ding Y, García CD (2006) Pulsed amperometric detection with poly(dimethylsiloxane)-fabricated capillary electrophoresis microchips for the determination of priority pollutants. Analyst 131:208–214
80. Ha K, Joo GS, Jha SK, Kim YS (2009) Monitoring of endocrine disruptors by capillary electrophoresis amperometric detector. Microeelctron Eng 86:1407–1410
81. Bodor R, Madajova V, Kaniansky D, Masar M, Johnck M, Stanislawski B (2001) Isotachophoresis and isotachophoresis - zone electrophoresis separations of inorganic, anions present in water samples on a planar chip with column-coupling separation channels and conductivity detection. J Chromatogr A 916:155–165
82. Prest JE, Baldock SJ, Fielden PR, Goddard NJ, Brown BJT (2003) Determination of inorganic selenium species by miniaturised isotachophoresis on a planar polymer chip. Anal Bioanal Chem 376:78–84
83. Prest JE, Baldock SJ, Fielden PR, Goddard NJ, Brown BJT (2003) Miniaturised isotachophoretic analysis of inorganic arsenic speciation using a planar polymer chip with integrated conductivity detection. J Chromatogr A 990:325–334
84. Tanyanyiwa J, Abad-Villar EM, Fernandez-Abedul MT, Costa-Garcia A, Hoffman W, Guber AE, Herrmann D, Gerlach A, Gottschlich N, Hauser PC (2003) High-voltage contactless conductivity-detection for lab-on-chip devices using external electrodes on the holder. Analyst 128:1019–1022
85. Liu B, Zhang Y, Mayer D, Krause H-J, Jin Q, Zhao J, Offenhäusser A (2011) A simplified poly(dimethylsiloxane) capillary electrophoresis microchip integrated with a low-noise contactless conductivity detector. Electrophoresis 32:699–704
86. Ding YS, Rogers K (2010) Determination of haloacetic acids in water using solid-phase extraction/microchip capillary electrophoresis with capacitively coupled contactless conductivity detection. Electrophoresis 31:2602–2607
87. Pumera M, Wang J, Opekar F, Jelinek I, Feldman J, Lowe H, Hardt S (2002) Contactless conductivity detector for microchip capillary electrophoresis. Anal Chem 74:1968–1971
88. Lichtenberg J, de Rooij NF, Verpoorte E (2002) A microchip electrophoresis system with a integrated in-plane electrodes for contactless conductivity detection. Electrophoresis 23:37693780
89. Hilmi A, Luong JHT (2000) Micromachined electrophoresis chips with electrochemical detectors for analysis of explosive compounds in soil groundwater. Environ Sci Technol 34:3046–3050
90. Gertsch JC, Noblitt SD, Cropek DM, Henry CS (2010) Rapid analysis of perchlorate in drinking water at parts per billion levels using microchip electrophoresis. Anal Chem 82:3426–3429
91. Ishida A, Yoshikawa T, Natsume M, Kamidate T (2006) Reverse-phase liquid chromatography on a microchip with sample injector and monolithic silica column. J Chromatogr A 1132:90–98
92. Blasco AJ, Crevillén AG, Fuente P, González MC, Escarpa A (2007) Electrochemical valveless flow microsystems for ultra fast and accurate analysis of total isoflavones with integrated calibration. Analyst 132:323–329
93. Crevillén AG, Pumera M, González MC, Escarpa A (2009) Microfluidic chips with electrochemical detectors based on multiwalled carbon nanotubes as flow injection and separation electrokinetic driven systems. Lab Chip 9:346–353
94. Janata J (1990) Potentiometric microsensors. Chem Rev 90:691–703
95. Bergveld P (2003) Thirty years of ISFETOLOGY – what happened in the past 30 years and what may happen in the next 30 years? Sens Actuat B 88:1–20
96. Wang J (2002) Electrochemical nucleic acid biosensors. Trends Anal Chem 21:226–232

97. Wang J (2006) Electrochemical biosensors: towards point-of-care cancer diagnostics. Biosens Bioelectron 21:1887–1892
98. Nyholm L (2005) Electrochemical techniques for lab-on-a-chip applications. Analyst 130:599–605
99. Sassa F, Morimoto K, Satoh W, Suzuki H (2008) Electrochemical techniques for microfluidic applications. Electrophoresis 29:1787–1800
100. Lim CT, Zhang Y (2007) Bead-based microfluidic immunoassays: the next generation. Biosens Bioelectron 22:1197–1204
101. Henares TG, Mizutani F, Hisamoto H (2008) Current development in microfluidic immunosensing chip. Anal Chim Acta 611:17–30
102. Lin C, Wang JH, Wu HW, Lee GB (2010) Microfluidic immunoassays. J Assoc Lab Automat 15:253–274
103. Ng AHC, Uddayasankar U, Wheeler AR (2010) Immunoassays in microfluidic systems. Anal Bioanal Chem 397:991–1007
104. Martíinez NA, Schneider RJ, Messina GA, Raba J (2010) Modified paramagnetic beads in a microfluidic system for the determination of ethinylestradiol (EE2) in river water samples. Biosens Bioelectron 25:1376–1381
105. Park SW, Lee JH, Yoon HC, Kim BW, Sim SJ, Chae H, Yang SS (2008) Fabrication and testing of a PDMS multi-stacked hand-operated LOC for use in portable immunosensing systems. Biomed Microdevices 10:859–868
106. Park SW, Lee JH, Kim K, Yoon HC, Yang SS (2009) An electrochemical immunosensing lab-on-a-chip integrated with latch mechanism for hand operation. J Micromech Microeng 19:025024
107. Llopis X, Pumera M, Alegret S, Merkoci A (2009) Lab-on-a-chip for ultrasensitive detection of carbofuran by enzymatic inhibition with replacement of enzyme using magnetic beads. Lab Chip 9:213–218
108. Monty CN, Oh I, Masel RI (2008) Enzyme-based electrochemical multiphase microreactor for detection of trace toxic vapors. IEEE Sensors J 8:580–586
109. Chikkaveeraiah BV, Liu H, Mani V, Papadimitrakopoulus F, Rusling JF (2009) A microfluidic electrochemical device for high sensitivity biosensing: detection of nanomolar hydrogen peroxide. Electrochem Commun 11:819–822
110. Teles FRR, Fonseca LP (2008) Trends in DNA biosensors. Talanta 77:606–623
111. Dutse SW, Yusof NA (2011) Microfluidic-based lab-on-a-chip systems in DNA-based biosensing: an overview. Sensors 11:5754–5768
112. Nugen SR, Asiello PJ, Connelly JT, Baeumner AJ (2009) PMMA biosensor for nucleic acids with integrated mixer and electrochemical detection. Biosens Bioelectron 24:2428–2433
113. Zou Z, Jang A, Macknight E, Wu PM, Do J, Bishop PL PL, Ahn CH (2008) Environmentally friendly disposable sensors with microfabricated on-chip planar bismuth electrode for *in situ* heavy metal ions measurements. Sens Actuators B 134:18–24
114. Jung W, Jang A, Bishop P, Ahn CH (2011) A polymer lab chip sensor with microfabricated planar silver electrode for continuous and on-site heavy metal measurement. Sens Actuat B 155:145–153
115. Jang A, Zou Z, Lee KK, Ahn CH, Bishop P (2010) Potentiometric and voltammetric polymer lab chip sensor for determination of nitrate, pH and Cd(ii) in water. Talanta 83:1–8
116. Masadome T, Nakamura K, Iijima D, Horiuchi O, Tossanaitada B, Wakida S, Imato T (2010) Microfluidic polymer chip with an embedded ion-selective electrode detector for nitrate-ion assay in environmental samples. Anal Sci 26:417–423
117. Kim D, Goldberg IB, Judy JW (2009) Microfabricated electrochemical nitrate sensor using double-potential-step chronocoulometry. Sens Actuat B 135:618–624

Chapter 22
Electronic Noses

Corrado Di Natale

22.1 Introduction

The investigation of olfaction physiology progressed considerably in the last decades improving the understanding of olfactory receptors mechanisms and explaining the sensitivity to volatile compounds. In 2004, the identification of the genetic repertoire expressing the olfactory receptors has been awarded with the Nobel prize.[1] More recent studies begin also to unveil the signal pathways leading from the generation of olfactory neuron signal to the cognitive identification of the odours.[2] Nonetheless, olfaction is still considered as the most mysterious of the natural senses basically because of its strong association with unconscious perceptions at which corresponds an unusual scarcity of semantic expressions limiting the communication of olfactory experiences. With respect to other senses (vision, hearing, and touch), for which technological correspondent exists since more than one century, the attempts to endow artificial systems with odour recognition features have been thwarted for a long time.

The most important element of an artificial olfaction system is the ensemble of sensors translating the primary stimuli into a measurable signal, usually electric.

Attempts to relate the signal of sensors to olfaction sensations episodically appeared in the 1960s.[3,4] But the advent of artificial olfaction is associated to the development of solid-state gas sensors and interestingly it involves a sensors feature that has been traditionally considered as a negative property of these devices.

Indeed, most of the solid-state sensors developed since the 1970s are intrinsically non-selective, making them unsuitable for analytical purposes. The non-selectivity of chemical sensors were considered as one of the main problems limiting their diffusion for practical applications. Nonetheless, physiological investigations about olfaction receptors show that Nature strategy for odour recognition

C. Di Natale (✉)
Department of Electronic Engineering, University of Rome Tor Vergata,
via del Politecnico 1, 00133 Rome, Italy
e-mail: dinatale@uniroma2.it

L.M. Moretto, K. Kalcher (eds.), *Environmental Analysis by Electrochemical Sensors and Biosensors*, DOI 10.1007/978-1-4939-0676-5_22

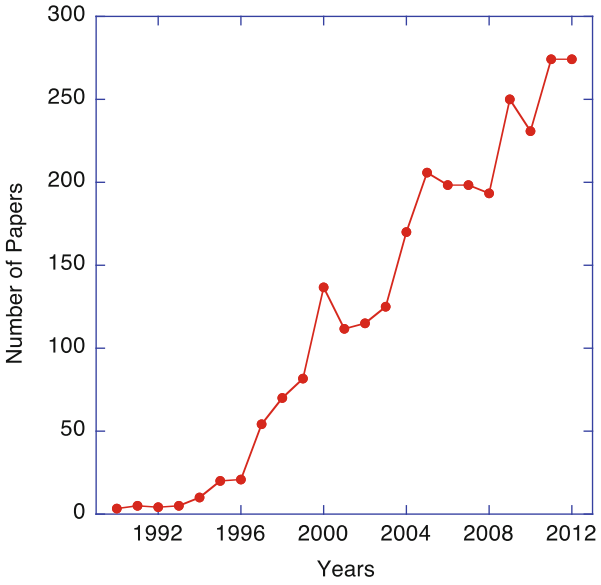

Fig. 22.1 Time distribution of papers identified with the keyword "electronic nose" in the Scopus database

is completely different from the analytical approach. Receptors were found to be rather unselective, namely each receptor senses several kinds of molecules and each molecule is sensed by many receptors.[5] This behaviour was first found in amphibians[6] and then in insect[7] and mammals.[8] Following this discovery, it was proposed that arrays of non-selective chemical sensors might show properties similar to that of natural olfaction.[9] On the basis of this conjecture, the development of artificial olfaction became possible. Such systems were dubbed as "electronic noses", and this denomination is currently given to any array of unselective chemical sensor coupled with some multicomponent classifier. Since the 1980s almost all sensor technologies were used to assemble electronic noses. Odour classification properties of artificial systems were tested on several different fields proving that electronic noses could be in principle used to replace human olfaction in practical applications such as food quality and medical diagnosis.[10] The research on electronic nose has been rapidly growing and it moved from development of sensor systems to diverse subject areas. A search on Scopus database with the keyword "electronic nose" returned 2,864 documents whose time distribution of papers is shown in Fig. 22.1.

22.2 Introduction to Chemical Sensors

A sensor is an electronic device whose parameters depend on some external quantity of whatever nature.[11] As an example, according to this definition there are resistors whose resistance is a function of external temperature (thermistors) or

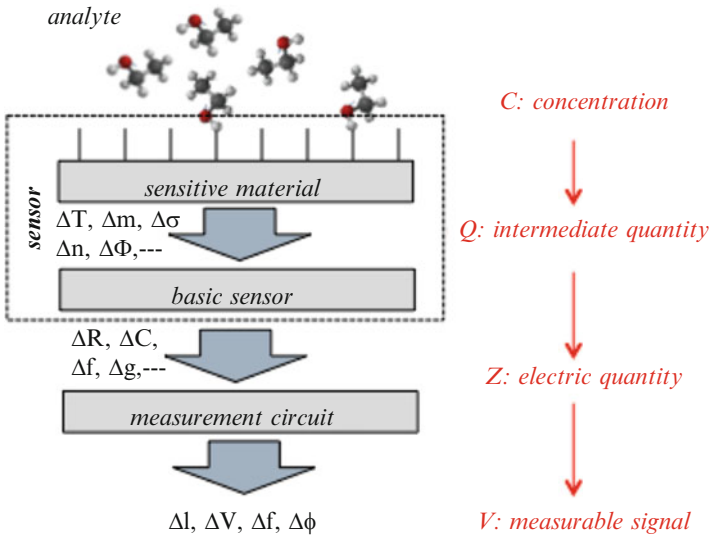

Fig. 22.2 Schematic representation of a generic chemical sensor. Targeted molecules interact with a chemically interactive material. As a consequence of the interaction, one or more, physical properties of the interactive material change. These quantities can be the temperature (ΔT), the mass (Δm), the electric conductance (ΔC), the refraction index (Δn) or the work function (ΔΦ). For each, and many others, of these quantities there are a number of devices that, once properly connected in an electric circuit, provide an electrical signal that is a function of the quantity of interactions occurring at the interface between the sensor and the environment

diodes whose current–voltage relationship is strongly altered once they are illuminated by light (photodiodes). In the same way there are devices that from the electronic point of view are resistors, capacitors, or even field effect transistors whose electrical parameters may depend on the chemical composition of the environment at which they are in contact.

Electronics properties of materials may hardly be directly influenced by the environmental chemistry, and then in order to achieve chemical sensors a composite structure is necessary.

Figure 22.2 shows the general structure of a chemical sensor. The device is composed by two parts. The first is a chemically interactive material, namely a solid-state layer of molecules that can interact with the molecules in the environment. These interactions can be of different nature, and the more utilised are adsorption and reaction phenomena. The interaction with a target molecule (hereafter called analyte) and a solid-state layer is a chemical event that, as a consequence, can modify the physical properties of the sensing layer. Properties such as conductivity, work function, mass or optical absorbance are among those that can be transduced into an electric signal by suitable transducers. These transducers are the second component of chemical sensors, and they are sometimes called "basic devices". An example of the whole chain of transduction translating the presence of a volatile compound into an electric signal is given in Fig. 22.3.

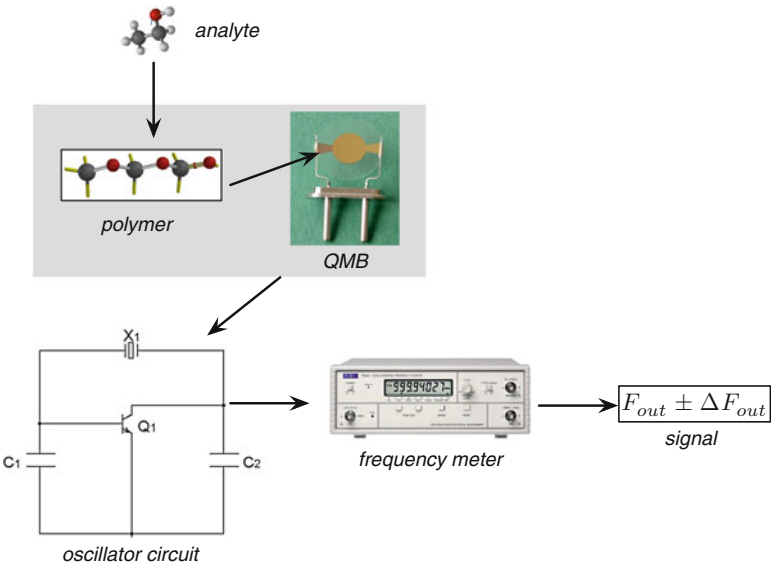

Fig. 22.3 Example of a complete transduction chain from the analyte to the measured signal. An airborne volatile compound is absorbed into a polymer layer coating a quartz microbalance. The quartz microbalance is connected to an oscillator circuit and the frequency of the output signal is proportional to the absorbed amount of molecules. The frequency of the output signal is measured by a frequency counter and the measure value is then provided

The matching between sensitive material and transducer is not univocal: a single sensitive material can be coupled with many different transducers and vice versa. In practice, there are many possibilities to assemble a chemical sensor. The optimal matching between sensitive layer and transducer is than fundamental to achieve a well performing sensor.

Before to illustrate the technological basis of chemical sensors it is important to introduce the fundamental parameters that allow a correct interpretation of the performance of any sensor. These parameters are sensitivity, resolution and selectivity.

The fundamental action of a chemical sensor is the conversion of the information about the concentration of a chemical species into an electric signal. The relationship between the signal and the chemical concentration can be represented by an analytical function that embodies the sensor operation.

$$v = f(c)$$

where V is a generic signal, and c is the analyte concentration. The knowledge of the response function is necessary to estimate from the sensor signal the amount of concentration. This estimation is straightforward if the response function is linear, and in more general cases the estimation may require the solution of a non-linear equation.

Beside response function, there are other important quantities that are necessary to be known to appreciate sensor performances.[12] One of these quantities is the

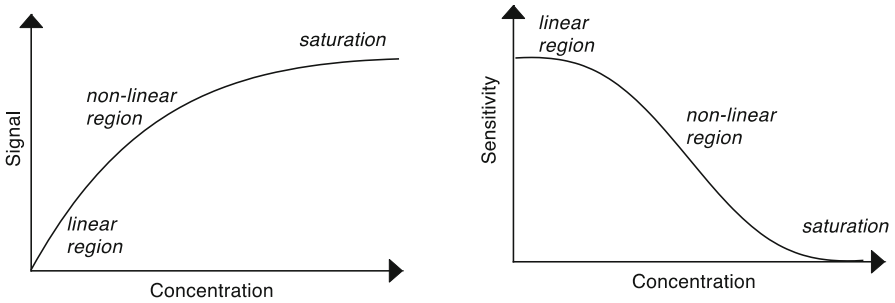

Fig. 22.4 Typical response curve (*left*) and sensitivity (*right*) of a generic chemical sensor based on adsorption of target molecules in a sensing layer characterised by a limited amount of adsorption sites

sensitivity. The sensitivity expresses the capability of a sensor to modify its signal as a consequence of a change of concentration. Analytically, it is the first derivative of the response function

$$S = \frac{dv}{dc} = \frac{df(c)}{dc}$$

Only in case of a linear response function, the sensitivity is a constant quantity. In all the other cases it is a function of the concentration.

Let us consider a common case of a chemical sensor based on a sensitive material characterised by a limited number of adsorption sites. The amount of adsorbed molecules as a function of the concentration is ruled by the Langmuir isotherm. The response curve is almost linear at low concentration and tends to the saturation corresponding to the complete occupation of available adsorption sites. A sensor containing such a sensing material and a basic transducer simply providing a signal proportional to the number of adsorbed molecules is represented by the response curve shown in Fig. 22.4 (left). In Fig. 22.4 (right) the corresponding sensitivity is shown. The sensitivity is larger at low concentrations, and it tends gradually to zero as the sensor response reaches the saturation. In order to fully appreciate the importance of sensitivity it is necessary to evaluate the influence of measurement errors. The knowledge of the signal v is affected by an error and this error is propagated in an error on the estimation of the concentration. Simple mathematical considerations leads to the conclusion that given an error ΔV_{err} affecting the signal V, the error Δc on the estimated concentration is given by the following relationship:

$$\Delta c_{res} = \frac{\Delta V_{err}}{S}$$

The error in concentration is then inversely proportional to the sensitivity. It is worth to mention that in case of electrical signals, the error Δv is limited by the electronic noise that determines the ultimate uncertainty of any electric signal.

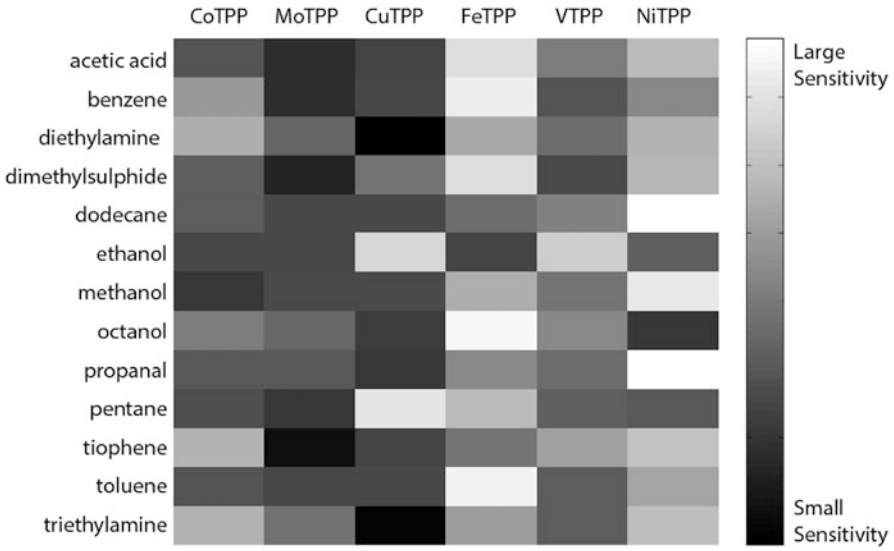

Fig. 22.5 Sensitivity map of an array of metalloporphyrins-coated quartz microbalances

The previously mentioned quantities are completely general, and their importance holds for any kind of sensor. For chemical sensors an additional parameter of great importance is the selectivity. The selectivity defines the capability of a sensor to be sensitive only to one quantity rejecting all the others. In case of physical sensors, the number of quantities is limited to a dozen and the selectivity can be achieved in many practical applications. For chemical sensors, it is important to consider that the number of chemical compounds is of millions and that the structural differences among them may be extremely subtle. With these conditions the selectivity of chemical sensor can be obtained only in very limited conditions. Lack of selectivity means that the sensor responds with comparable intensity to different species and with such a sensor it is not possible to deduce any reliable information about the chemical composition of the measured sample. Selectivity is a straightforward requisite for analytical systems where sensors and its related measurement technique are addressed to the detection of individual compounds. As mentioned in the previous section, selectivity is not found in olfactory receptors. As a consequence, artificial olfaction systems are not based on individual selective sensors, but on sensors whose selectivity can be oriented towards molecular families, or better, towards interaction mechanisms. Figure 22.5 shows a typical selectivity map related to an array of quartz microbalances (see next section) coated with different metalloporphyrins based on the same macrocycle (tetraphenylporphyrin) but with different metal atoms. Figure 22.5 depicts well the concept of combinatorial selectivity, namely each compounds is identified by a unique sensitivity pattern that makes possible the identification.

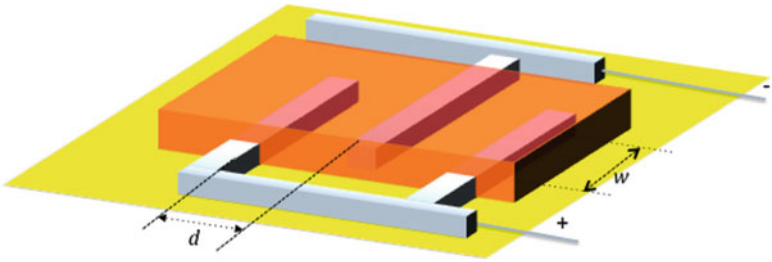

Fig. 22.6 Structure of a conductance transducer based on an interdigitated electrode is coated by a thick sensing layer. The relationship between the resistivity of the sensing layer and the actual resistance measured at the terminal contacts can be calculated by a Schwartz-Christoffel transform

22.3 Chemical Sensor Technologies

In this section the basic principles of the most popular categories of chemical sensors are illustrated. Sensors are here classified according to the physical intermediate quantity.

22.3.1 Sensors Based on Conductance Changes

In order to measure the conductance change a suitable transducer is necessary. The most widely used configuration is based on interdigitated electrodes deposited on an insulating substrate as shown in Fig. 22.6. The sensitive film is then deposited over the electrodes pattern. Usually, and in particular for organic conductive materials, the film thickness is larger than the electrode thickness. In this condition the total resistance of the sensor can be calculated applying the Schwartz-Christoffel coordinate change.[13] Anyway, the expected behaviour of resistance as an inverse function of the number of finger electrode is found.

22.3.2 Metal Oxide Semiconductors

Changes of conductance become appreciable in materials characterised by a limited number of mobile charge carriers. In practical, semiconductors are subjected to large changes of conductance also in presence of a modest variation of the number of conductance electrons or holes. The most popular materials undergoing a conductance change upon the interaction with gases are the metal-oxide semiconductors. These are oxides of transition metals, whose the most known and studied is SnO_2.[14] This is a wide band gap n-type semiconductor whose main sensitivity mechanism is related to the role played by oxygen.[15] At sufficiently

high temperature (e.g. above 200 °C) dissociative adsorption sites of molecular oxygen are activated on the oxide surface. A charge transfer occurs between the material and the adsorbed oxygen atom with the consequence that the conductance band in proximity of the surface becomes depleted and a surface potential barrier is formed. The amount of depletion and the barrier height are proportional to the number of adsorbed molecules. Since the material is a semiconductor, the number of conductance electrons is limited and then it is also limited the amount of oxygen molecules that can be adsorbed at the surface. The consequence of the exposure to oxygen is a reduction of the surface conductance. The exposure to any molecule interacting on the sensor surface with adsorbed oxygen atoms may result in a release of electrons back to the conductance band and in a reduction of the surface conductance band depletion and in a lowering of the potential barrier. Paradigmatic, to this regard, is the case of carbon monoxide that reacts with the bounded oxygen to form carbon dioxide releasing an electron back to the conductance band. This is only one of the many interactions taking place on the surface of metal oxides, and the sensitivity of these devices is extended to many different kinds of volatile compounds. The sensitivity can be further modified adding tiny layers of catalytic metal atoms on the surface. It is important to remark that this kind of sensors request to be operated at high temperature, and as a consequence an electrically actuated heater is integrated in the device. Since the sensitivity depends on temperature it can be modulated changing the working temperature. On this basis, a single sensor operated at different temperatures can behave as a set of virtual sensors. Then, the concept of combinatorial selectivity illustrated in Fig. 22.4 can be obtained with only one sensor device.[16,17]

Metal oxide semiconductor sensors can be prepared in many different ways, in any case the general advice is to produce a nano crystalline material in such a way the modulation of the surface conductance band population becomes dominant in the whole sensor providing the maximum sensitivity. Recently metal oxides growth in regular shapes such as nanosized belts and rods[18] has shown peculiar properties. The characteristics of these structures, although interesting, have not yet resulted in practical improvements of performances.

Arrays of metal oxide semiconductor chemiresistors have been frequently used as electronic noses. Example of results are concerned with the detection of tea cultivars,[19] the freshness of fishes,[20] and the detection of toxigenic fungi in cereals.[21]

22.3.3 Conducting Polymers and Molecular Aggregates

The conductance properties of organic materials based either on polymers or molecular aggregates are studied since several years with broader scopes related to the possibility to develop a novel sort of electronics based on carbon chemistry.[22] Chemical sensors based on conducting polymer may be considered as a lateral result of these studies. Indeed, aggregates of polypyrrole or polytiophene have a semiconducting character and their conductance can change after the exposure to

volatile compounds. With respect to metal oxides these sensors have two important advantages: they are operated at room temperature and, most important, their chemical sensitivity can be changed at synthesis level modifying the chemical structure of the monomer.[23] One of the drawbacks of these sensors is the instability mainly due to the degradation of doping radicals that are added to increase the conductance.

Conducting polymers have been demonstrated to be an important material for electronic nose application. Demonstration of their properties has been provide in the assessment of seafood freshness,[24] the detection of streptomyces in potable water,[25] and the quality of olive oils.[26]

22.3.4 Carbon Black-Embedded Non-conducting Polymers

Polymers are excellent absorbant materials whose selectivity can be tailored through chemical synthesis. Since only few polymers are conductive their use for gas sensing is usually associated to mass transducers (see later). An ingenious method to transduce the absorption into a layer of non-conductive polymer into a change of electric resistance was introduced some years ago.[27] It consists in embedding a precise quota of carbon black grains in the polymer matrix. The conductivity of carbon black ensures the charge transfer between the carbon black grains suspended in the polymer. As a consequence of the absorption of volatile compounds the polymer swells and the mean distance between the carbon black grains increases. This leads to an increase of resistivity that can be adequately detected. These sensors were soon patented and they were used in a commercial electronic nose (Cyranose) that was used for many applications in particular in breath analysis for medical diagnosis. In this field demonstrations of sensitivity and discrimination properties have been provided for diseases such as asthma,[28] and chronic obstructive pulmonary disease.[29]

22.3.5 Mass Transducers

The adsorption of molecules into a sorbent layer (e.g. a polymer or a molecular film) produces a change of mass and the measurement of these mass shifts can allow the evaluation of the amount of adsorbed molecules. The measure of small mass changes is made possible by piezoelectric resonators. A piezoelectric resonator is a piezoelectric crystal properly cut along a well specified crystalline axis. Due to the piezoelectric effect, the mechanical resonance of the crystal is coupled with an electric resonance. Since crystal resonance is extremely efficient the electric resonance is characterised by a very large quality factor. This property is largely exploited in electronics to build stable oscillators as clock references. The same effect is exploited for chemical sensing adopting particularly shaped crystals such

as in quartz microbalances (QMB).[30] These are thin slabs of AT cut quartz oscillating at a frequency between 5 and 50 MHz approximately. The frequency of the mechanical oscillation decreases almost linearly with the mass on the quartz surface. If the quartz is connected to an oscillator circuit, the electric frequency decreases linearly with the mass. A typical QMB has a limit of detection around 1 ng. Such an amount is sufficient in many practical applications.

QMB-based electronic layers were used for many applications. As an example, metalloporphyrins-coated QMB were used in a large variety of application in the fields of food analysis and medical diagnosis. Examples in food analysis fish freshness,[31] food aroma detection,[32] and microbiological contamination of cereals.[33] Noteworthy results in medical diagnosis have been obtained for lung cancer[34] and asthma diagnosis.[35]

Piezoelectric effect can also be exploited with other configurations such as those based on surface acoustic waves (SAW).[36] These devices are operated at larger frequencies and since the mass sensitivity is proportional to the square of the resonant frequency they are supposed to be largely sensitive with respect to QMB. However, as discussed in a previous section, resolution is the key parameter of a sensor and resolution is limited by signal noise. Since SAW signals are at large frequency (hundreds of MHz) the noise of SAW is larger than the noise of QMB so the increase of performance is rather reduced with respect to what it is supposed to be.

More sophisticated mass transducers were proposed by using resonant cantilevers similar to those adopted in atomic force microscopy.[37] In spite of the claimed properties, these sensors were never demonstrated in practical applications.

22.3.6 Field Effect Transistors

Most of the properties of field effect transistors (FET) depend on the difference between the work function of electrons in the metal gate and in the semiconductor. This difference can be modulated by a layer of electric dipoles at the metal–oxide interface. The principle was adequately exploited with a palladium gate FET exposed to hydrogen gas.[38] H_2 molecules dissociate into atomic hydrogen at the palladium surface, and hydrogen atoms can diffuse through the palladium film until to reach the oxide surface where they form an ordered dipoles layer. As a result, although under constant bias, the current flowing in the FET changes revealing the chemical interaction.

Arrays of catalytic metal gated FET were used to assemble electronic noses. Main results were obtained in the detection of different microbiological processes such as the fermentation of meat[39] and the infection mammalian cells.[40]

This basic structure was successively modified changing the gate metal and thickness in order to extend the range of measured gases. In this way sensitivity to ammonia, an important gas for fish freshness and quality was also obtained.[41] FET structures were also modified to accommodate, as sensing part, organic molecular layers, such as metalloporphyrins.[42,43]

22.3.7 Colour Indicators

Chemical sensing based on optical sensitive layers is a captivating strategy due to the strong influence of target chemicals on the absorption and fluorescence spectra of chosen indicators.[44] Nonetheless, the chemical practice of this approach is badly balanced by the transducer counterpart. Indeed, standard optical instrumentations are usually expensive.

On the other hand in the last decade the performance of consumer electronics was steadily growing. This gave rise to a number of low-cost advanced optical equipments such as digital scanners, cameras, and screens whose characteristics largely fit the requirements necessary to capture changes of optical properties of sensitive layers in many practical applications.

The first demonstration in this direction was given by Suslick and colleagues when they showed that a digital scanner has enough sensitivity to detect the colour changes in chemical dyes due to the adsorption of volatile compounds.[45]

Furthermore, Lundström and Filippini proved that it is possible to assemble a sort of spectrophotometer using the computer screen monitor as a programmable source and a web cam as detector.[46] This last technique, known as Computer Screen Photo assisted Technique (CSPT) is based on the fact that a computer screen can be easily programmed to display millions of colours, combining wavelengths in the optical range. Compared with the use of digital scanners, to probe the sample with a variable combination of wavelengths instead of use the white light of scanners, gives the possibility to perform an optical fingerprint measurement allowing a simultaneous evaluation of absorbance and fluorescence of samples. Due to the large diffusion of portable computers, PDAs, and cellular phones all endowed with colour screen, camera, and an even more extended computation capabilities, the application of the CSPT concept may be foreseen as to greatly extend the analytical capacity worldwide. CSPT has demonstrated its utility in particular to classify airborne chemicals reading absorbance and fluorescence changes in chemical dyes such as metalloporphyrins.[47] Standard opto-chemical sensors are based either on absorbance or on fluorescence while CSPT arrangement gives the possibility to evaluate at the same both the effects.[48,49]

A typical CSPT arrangement is shown in Fig. 22.7 and an example of signals from a single spot is shown in Fig. 22.8. This arrangement can adequately work as an electronic nose.[50]

The use of image sensors, such as in CSPT, offers also the possibility to largely increase the size of the sensor array approaching the large number of olfactory receptors. This was first demonstrated several years ago using a CCD camera to measure, at once, the optical changes occurring in a large number of fluorescent indicators deposited on the tips in a bundle of optical fibres.[51]

The basic property of an image sensor is the segmentation of a whole scene into a number of elementary units, called pixels. Each pixel corresponds to one photo detector measuring the light intensity shining from a section of the whole scene. Eventually, when an image sensor captures a sensitive surface coated by a

Fig. 22.7 Arrangement of a CSPT-based electronic nose. The screen is the light source used to probe the sensing layer that is imaged by a webcam. In the *inset* the imaged sensing layer. *Circles* indicate the region of interest whose pixels intensities are averaged and considered as the sensor array response

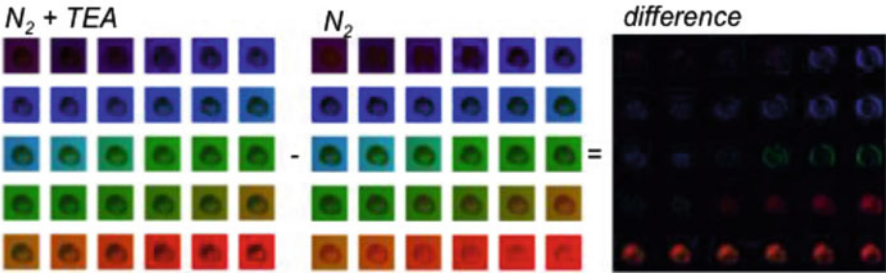

Fig. 22.8 Example of CSPT data signals. A sequence of multicolour images is taken when the sensing layer is exposed to the sample and to the reference atmosphere. The difference shows that changes occurs under blue and red colour illuminations

continuous layer of chemical indicators, the sensing layer is segmented into a number of elementary units corresponding to the pixels of the image. Then, since it is possible to evaluate the optical properties of single pixels, each pixel of the image may correspond to an individual sensor. To this end, even low-resolution images may result in thousands of independent sensing units, then under the

hypotheses that different types of indicators are optically different (this trivially means that each indicator has a different colour) it is possible to cluster the camera evaluation of the colour of individual pixels in abstract classes each containing pixels carrying the same chemical indicator.[52] In this architecture, individual pixels play the role of individual olfactory receptor neurons and the abstract classes gathering together pixels carrying similar indicators are analogous to the glomeruli units observed in natural olfaction.[53] This platform can then efficiently mimic the dynamics between signals of single receptors and how these are transformed by the convergence into the glomeruli. Hardware development is limited to the receptor units (the colour indicators) while glomeruli are a software implementation. Post-glomeruli processing can be easily accomplished via software and results can be strongly connected to the physical and chemical properties of the interaction of volatile compounds with the receptor layer. The platform can then allow the investigation of the properties of biologically derived processing paradigms extending the similarities between artificial and natural olfaction.[54]

22.4 Conclusions

The conversion of chemical information into electric signals that can be measured, stored, analysed, transmitted and integrated with other data can be performed by several different technologies. These technologies are sometimes equivalent in terms of performances and for some specific applications one technology may outperform the others. It is important in any application to design the optimal sensor array in order to determine the quality and the quantity of the relevant chemical species.

Chemical sensors are an almost mature technology for many practical applications. For this scope it is necessary a strong co-operation between sensors developers and end-users in order to optimise practical solutions. At this level it is important a correct and careful analysis of user needs and expectations and an education effort towards the users in order to disseminate the intrinsic novelty carried by sensors systems such as those widely belonging to the class of artificial olfaction.

It is also important that developers and users are aware of the intrinsic limit of information that is carried by the volatile part of a sample. For instance, in food analysis it is important to consider that sensory analysis is almost never confined to the only olfactory perception. Actually, synesthetic action among the senses is required to form a full judgement over a certain food sample. As an example, in fish analysis quality index, linearly correlated with the days in ice, is calculated considering at the same time visual, tactile, and olfactory perceptions. This suggests that in order to fully reproduce the perceptions of humans with artificial sensors the electronic nose has to be compared and integrated with instruments providing information about visual aspects, texture, and firmness. This opens a further novel investigation direction involving again researchers from different areas confirming that an interdisciplinary approach is the most strong added value for the analysis of any kind of sample.

References

1. Buck L, Axel R (1991) A novel multigene family may encode odorant receptors: a molecular basis for odor recognition. Cell 65:175–187
2. Korsching S (2002) Olfactory maps and odor images. Curr Opin Neurobiol 12:387–392
3. Moncrieff R (1961) An instrument for measuring and classifying odours. J Appl Physiol 16(1):742–749
4. Wilkens WF, Hatman AD (1964) An electronic analogue for the olfactory process. Ann NY Acad Sci 116:608–620
5. Imai T, Suzuki M, Sakano H (2006) Odorant receptor derived cAMP signals direct axonal targeting. Science 314:657–661
6. Sicard G, Holley A (1984) Receptor cell responses to odorants: similarities and differences among odorants. Brain Res 292:283–296
7. Hallem E, Ho M, Carlson J (2004) The molecular basis of odor coding in the drosophila antenna. Cell 117:965–979
8. Malnic B, Hirono J, Sato T, Buck L (1999) Combinatorial receptor codes for odors. Cell 96:713–723
9. Persaud K, Dodds G (1982) Analysis of discrimination mechanisms in the mammalian olfactory system using a model nose. Nature 299:352–355
10. Röck F, Barsan N, Weimar U (2008) Electronic nose: current status and future trends. Chem Rev 108:705–725
11. Fraden J (2004) Handbook of modern sensors. AIP Press, New York, NY
12. D'Amico A, Di Natale C (2001) A contribution on some basic definitions of sensors properties. IEEE Sens J 1:183–190
13. Gardner J, Bartlett P, Pratt K (1995) Modelling of gas-sensitive conducting polymer devices. IEE Proc Circ Dev Syst 142:321–333
14. Barsan N, Koziej D, Weimar U (2007) Metal oxide based gas sensor research: how to? Sens Actuat B 121:18–35
15. Barsan N, Weimar U (2001) Conduction model of metal oxide gas sensors. J Electroceram 7:143–167
16. Heilig A, Bârsan N, Weimar U, Schweizer-Berberich M, Gardner JW, Göpel W (1997) Gas identification by modulating temperatures of SnO2-based thick film sensors. Sens Actuat B 43:45–51
17. Martinelli E, Polese D, Catini A, D'Amico A, Di Natale C (2012) Self-adapted temperature modulation in metal-oxide semiconductor gas sensors. Sens Actuat B 161:534–541
18. Comini E, Baratto C, Faglia G, Ferroni M, Vomiero A, Sberveglieri G (2009) Quasi one dimensionale metal oxide semiconductors: preparation, characterization and application as chemical sensors. Prog Mat Sci 54:1–67
19. Dutta R, Kashwan K, Bhuyan M, Hines E, Gardner J (2003) Electronic nose based tea quality standardization. Neural Netw 16:847–853
20. El Barbri N, Mirhisse J, Ionescu R, El Bari N, Correig X, Bouchikhi B, Llobet E (2009) An electronic nose system based on a micromachined gas sensor array to assess the freshness of sardines. Sens Actuat B 141:538–543
21. Falasconi M, Gobbi E, Pardo M, Della Torre M, Bresciani A, Sberveglieri G (2005) Detection of toxigenic strains of Fusarium verticilloides in corn by electronic olfactory system. Sens Actuat B 108:250–257
22. Heeger AJ (2001) Semiconducting and metallic polymers (Nobel lecture). Angew Chemie Int Ed 40:2591–2611
23. Persaud K (2005) Polymers for chemical sensing. Mater Today 8:38–44
24. Gonzalez-Martin A, Lewis B, Raducanu M, Kim J (2010) An array based sensor for seafood freshness assessment. Bull Korean Chem Soc 31:3084
25. Bastos A, Magan N (2006) Potential of an electronic nose for the early detection and differentiation between streptomyces in potable water. Sens Actuat B Chem 116:151–155

26. Guadarrama A, Rodriguez-Mendez M, Sanz C, Rios J, de Saja J (2001) Electronic nose based on conducting polymers for the quality control of the olive oil aroma. Anal Chim Acta 432:283–292
27. Lonergan M, Severin E, Doleman B, Beaber S, Grubbs R, Lewis N (1996) Array-based vapor sensing using chemically sensitive carbon black-polymer resistor. Chem Mater 8:2298–2312
28. Dragonieri S, Schot R, Mertens B, Cessie S, Gauw S, Spanevello A, Resta O, Willard N, Vink T, Rabe K, Bel E, Sterk P (2007) An electronic nose in the discrimination of patients with asthma and controls. J Allergy Clin Immunol 120:856–862
29. Hattesohl AD, Jörres RA, Dressel H, Schmid S, Vogelmeier C, Greulich T, Noeske S, Bals R, Koczulla AR (2011) Discrimination between COPD patients with and without alpha 1-antitrypsin deficiency using an electronic nose. Respirology 16:1258–1264
30. Ballantine D, White R, Martin S, Ricco A, Frye G, Wohltien H, Zellers E (1997) Acoustic wave sensors. Academic, San Diego, CA
31. Di Natale C, Brunink J, Bungaro F, Davide F, D'Amico A, Paolesse R, Boschi T, Faccio M, Ferri G (1996) Recognition of fish storage time by a metalloporphyrins-coated QMB sensor array. Meas Sci Technol 7:1103–1114
32. Santonico M, Pittia P, Pennazza G, Martinelli E, Bernabei M, Paolesse R, D'Amico A, Compagnone D, Di Natale C (2008) Study of the aroma of artificially flavoured custards by chemical sensor array fingerprinting. Sens Actuat B 133:345–351
33. Eifler J, Martinelli E, Santonico M, Capuano R, Schild D, Di Natale C (2011) Differential detection of potentially hazardous Fusarium Species in wheat grains by an electronic nose. PLoS One 6:e21026
34. Di Natale C, Macagnano A, Martinelli E, Paolesse R, D'Arcangelo G, Roscioni C, Finazzi A, D'Amico A (2003) Lung cancer identification by the analysis of breath by means of an array of non-selective gas sensors. Bios Bioelectron 18:1209–1218
35. Montuschi P, Santonico M, Mondino C, Penazza G, Mantini G, Martinelli E, Capuano R, Ciabattoni G, Paolesse R, Di Natale C, Barnes P, D'Amico A (2010) Diagnostic performance of an electronic nose, fractional exhaled nitric oxide, and lung function testing in asthma. Chest 137:790–796
36. Gan H, Che Man Y, Tan C, Norami I, Nazimah S (2005) Characterization of vegetable oils by surface acoustic wave sensing electronic nose. Food Chem 89:507–518
37. Yoo Y, Chae M, Kang J, Kim T, Hwang K, Lee J (2012) Multifunctionalized cantilever systems for electronic nose applications. Anal Chem 84:8240–8245
38. Lundstrom I, Shivaram S, Svensson C, Lundkvist L (1975) A hydrogen sensitive MOS field effect transistor. Appl Phys Lett 26:55–57
39. Eklov T, Johannson G, Winquist F, Lundstrom I (1998) Monitoring sausage fermentation using an electronic nose. J Sci Food Agric 76:525–532
40. Bachinger T, Riese U, Eriksson R, Mandenius C (2002) Gas sensor arrays for early detection of infection in mammalian cell culture. Bios Bioelectron 17:395–403
41. Winquist F, Spetz A, Armgarth M, Nylander C, Lundstrom I (1983) Modified palladium metal-oxide semiconductor structure with increased ammonia gas sensitivity. Appl Phys Lett 43:839–841
42. Takulapalli B, Laws G, Liddell P, Andreasson J, Erno Z, Gust D, Thornton T (2008) Electrical detection of amine ligation to a metalloporphyrin via a hybrid SOI-MOSFET. J Am Chem Soc 130:2226–2233
43. Di Natale C, Buchholt K, Martinelli E, Paolesse R, Pomarico G, D'Amico A, Lundström I, Lloyd Spetz A (2009) Investigation of quartz microbalance and ChemFET transduction of molecular recognition events in a metalloporphyrin film. Sens Actuators B 135:560–567
44. Gauglitz G (2006) Optical sensing looks to new field. Trends Anal Chem 25:748–750
45. Rakow N, Suslick K (2000) A colorimetric sensor array for odour visualization. Nature 406:710–713
46. Filippini D, Svensson S, Lundström I (2003) Computer screen as a programmable light source for visible absorption characterization of (bio)chemical assays. Chem Commun 9:240–241

47. Filippini D, Alimelli A, Di Natale C, Paolesse R, D'Amico A, Lundström I (2006) Chemical sensing with familiar devices. Angew Chem Int Ed 45:3800–3803
48. Gatto E, Malik MA, Di Natale C, Paolesse R, D'Amico A, Lundström I, Filippini D (2008) Polychromatic fingerprinting of excitation emission matrices. Chem Eur J 14:6057–6060
49. Malik MA, Gatto E, Macken S, DiNatale C, Paolesse R, D'Amico A, Lundström I, Filippini D (2009) Imaging fingerprinting of excitation emission matrices. Anal Chim Acta 635:196–201
50. Alimelli A, Pennazza G, Santonico M, Paolesse R, Filippini D, D'Amico A, Lundström I, Di Natale C (2006) Fish freshness detection by a computer screen photoassisted based gas sensor array. Anal Chim Acta 582:320–328
51. Dickinson T, Michael K, Kauer J, Walt D (1999) Convergent self encoded bead sensor arrays in the design of an artificial nose. Anal Chem 71:2192–2198
52. Di Natale C, Santonico M, Paolesse R, Filippini D, D'Amico A, Lundstrom I (2010) Evaluation of the performance of sensors based on optical imaging of a chemically sensitive layer. Anal Bioanal Chem 397:613–621
53. Di Natale C, Martinelli E, Paolesse R, D'Amico A, Filippini D, Lundström I (2008) An experimental biomimetic platform for artificial olfaction. PLoS One 3:e3139
54. Martinelli E, Polese D, Dini F, Paolesse R, Filippini D, Lundström I, Di Natale C (2011) An investigation on the role of spike latency in an artificial olfactory system. Front Neuroeng 4:16

Chapter 23
Remote Sensing

Tomer Noyhouzer and Daniel Mandler

Remote sensing is the ability to acquire information about an object or phenomenon without physically contacting the object or the place from which this information is obtained. Remote sensing is a fast developing field, which makes it possible to monitor secluded or inaccessible areas. Sensing can be passive, where energy is collected or active whereby energy is emitted by the sensor and perturbs the sensing environment. Remote sensing is of particular interest and importance in monitoring the environment. It is worth mentioning that remote sensing has two quite different aspects (see Fig. 23.1); the first is to sense from the distance, typically from satellite. This approach is commonly applied for assessing and mapping large areas and providing information about biodiversity, physical changes, and threats and identification of global variations such as temperature, haze, etc. In this case, the sensors (mostly optical) are located far from the analyte. On the other hand, remote sensing (or monitoring) refers also to deploying the sensing devices on-site where sampling and analysis is carried out locally (mostly of aquatic systems) and the data are transmitted to the control unit that is located remotely. This approach, which is termed *remote environmental monitoring*, allows, in principle, collecting data simultaneously from different locations, monitoring on-site at real-time physical, chemical, (micro)biological, and radiological parameters, and therefore can be used as the basis of early alarm systems.

Remote electrochemical sensing has many advantages since the electrochemical sensors can be made relatively small and cheap, nevertheless, they can be highly sensitive and in many cases possess also high selectivity and robustness. Transduction of the electrochemical response into an electrical signal that can be transmitted over long distances is an inherent part of the electrochemical sensor. Electrochemical sensors are often categorized into potentiometric, amperometric, or conductometric devices. Potentiometric sensors measure the changes in the electrochemical potential between two electrodes, where the potential of one of them is designed to

T. Noyhouzer • D. Mandler (✉)
Institute of Chemistry, The Hebrew University of Jerusalem, Jerusalem 91904, Israel
e-mail: daniel.mandler@mail.huji.ac.il

L.M. Moretto, K. Kalcher (eds.), *Environmental Analysis by Electrochemical Sensors and Biosensors*, DOI 10.1007/978-1-4939-0676-5_23

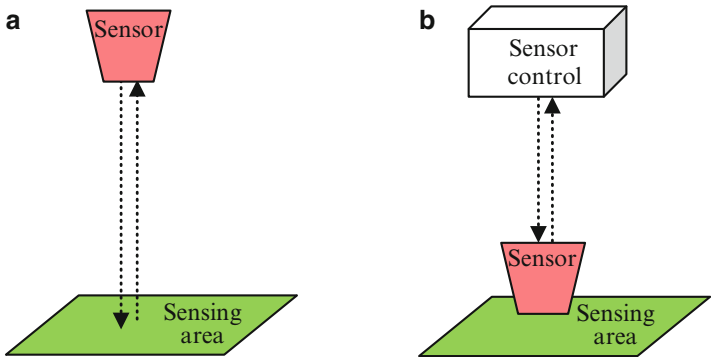

Fig. 23.1 Schematics of both approaches termed "remote sensing": (**a**) Remote sensing by a sensor that is located far from the analyte. (**b**) Remote environmental sensing by a sensor that is in contact with the analyte but transmits the data

be highly selective towards the activity of the analyte while the other electrode potential is kept constant (a reference electrode). Ion selective electrodes (ISE) as well as the pH electrode belong to this family. Although the potentiometric measurement is the simplest it usually lacks sensitivity. Amperometric or voltammetric sensors are highly sensitive due to the accumulation of the analyte on the electrode surface. Selectivity is achieved by either scanning the potential where the analyte is oxidized or reduced or as a result of modifying the electrode surface with a layer that selectively interacts with the analyte. The current that is measured is proportional to the concentration of the analyte in the sample. The last group, conductometric sensors, is based on modulation of the resistivity of a selective layer by the analyte. This is also a two-electrode system (such as used for potentiometry). All three types of electrochemical sensors can be miniaturized and therefore can be incorporated in remote electrochemical sensing systems.

23.1 Basic Concepts and Setup in Remote Electrochemical Sensing

23.1.1 The Flow System

Constructing a device that works well for remote environmental sensing requires not only developing the recognition element but integrating it in an autonomous system. Hence, in addition to the challenges in constructing the sensing and transduction parts of the sensor, one faces with the challenge of developing a sampling and delivery system. This usually requires introducing of a flow system. The utilization of flow systems not only enables the automation of the measurement and relatively easy data collection,[1] but also simplifies the entire process in comparison with a static process, which contains various stages of liquid replacements

and mixing.[2] Another advantage of coupling is the versatility of the flow system, which enables easy and simple adjustment of the chemicals, tubing, and speed and volume of the various solutions. This increases the precision and accuracy of the measurements since it allows better control and optimization of the process. Moreover, electrochemical methods are known for their inherent high sensitivity, thus, allowing the measurement of very low concentration by employing small volumes. All these make coupling between electrochemical measurements and flow systems ideal for remote sensing.[3] The advantages of an automated electrochemical flow system are well documented in remote environmental sensing where the collected data are in far, problematic, or inaccessible areas.

Coupling between electrochemical sensors and flow systems is the key element which makes remote electrochemical sensing feasible. The majority of the flow systems employ stripping methodology, which is based on a continuous flow. This approach utilizes a valve selector and one or more pumps. The different solutions are selected by the valve selector, and can be channeled to the electrochemical flow cell. A flow system which employs a continuous flow approach can be based on simple apparatus (which can be controlled by a microprocessor or manually). The downside of this approach is the use of relatively large volumes of sample and reagents. In order to overcome this disadvantage, one can employ a bidirectional pump that flows the same volume through the cell several times.[4,5]

The development of Flow Injection Analysis (FIA) caused a revolution in the field of on-line electrochemical analysis, and nowadays most of the systems are still based on FIA. In FIA the sample is introduced (injected) into an eluent flow, which transfers the sample to the detection area or measuring cell. The most known example of a FIA system is high performance liquid chromatography (HPLC). FIA has many advantages, such as simplicity and low consumption of sample and reagents, yet it does not lack of disadvantages. From the location were the analyte is introduced into the system until it reaches the measuring cell it undergoes tailored dispersion. The dispersion dilutes the analyte until it reaches the working electrode in the measuring cell and therefore reduces the sensitivity. To improve the FIA an alternative methodology based on Sequential Injection Analysis (SIA) was developed.[6] The heart of the SIA is a multioptional valve selector.[7] The solutions are suck and pumped in a sequence of segments using a bidirectional pump. Figure 23.2 depicts the major differences between FIA and SIA systems. The fundamental difference is the way the analyte is pumped through the system. In FIA the analyte is pumped using the eluent flow towards the detection cell, while in SIA the analyte is first withdrawn from its container and then pumped towards the detection cell. This difference causes also a differences in the profile of the flow.[8]

FIA systems are better for specific cases, while SIA systems are more modular. The adjustment of a SIA system to an experimental scenario can take some time, but once the system is optimized it can run autonomously. This advantage and the substantial reduction in the volume of reagents consumed and waste produced, as well as the ability to utilize several chemicals (which is limited only by the number of valves in the valve selector) make SIA an attracting platform for remote environmental sensing.

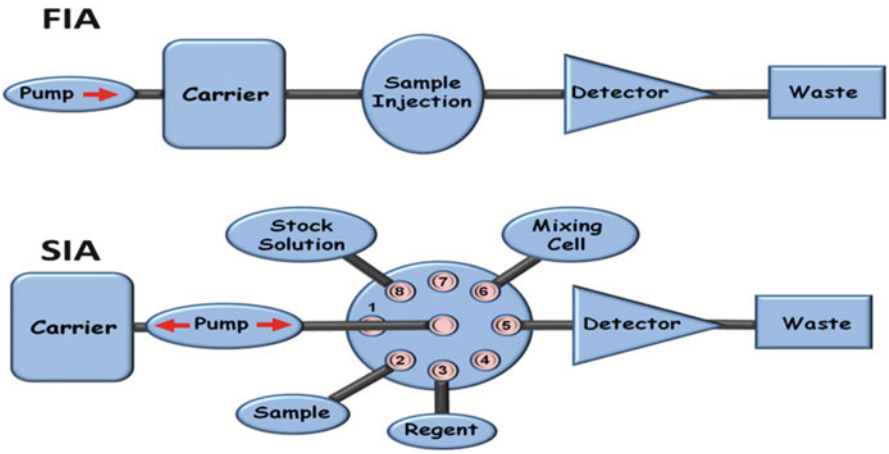

Fig. 23.2 Schematics of FIA and SIA systems

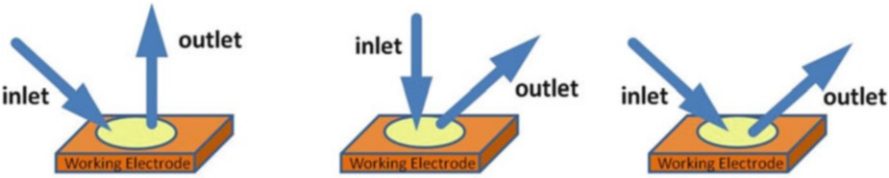

Fig. 23.3 Different types of electrochemical cells based on wall-jet methodology

23.1.2 The Electrochemical Cell

Flow systems can be divided into two categories, not only according to the flow regime (FIA and SIA) but by the nature of the electrochemical cell as well. Although there are a few types of cells, most of the systems can be divided into wall-jet and thin-layer cells.

Electrochemical cells based on a wall-jet pattern are very common in systems that utilize disposable electrodes. The basic principle behind these cells is to increase mass transfer towards the electrode surface both by using a flow system and manipulating the flow profile.

The liquid is driven in a specific angle, usually 90°, which causes it to collide with the electrode surface. The wall-jet arrangement requires that the diameter of the solution jet is much smaller than that of the working electrode disk.[9] Figure 23.3 illustrates different types of wall-jet cells; the solution flows towards the electrode colliding with its surface and then continues in a vertical or diagonal tube. The counter electrode can be either part of the cell itself or a hollow inlet tube.

From an hydrodynamic point of view the behavior of an electrode in a wall-jet flow cell is similar to the most common electrochemical hydrodynamic tool, i.e.,

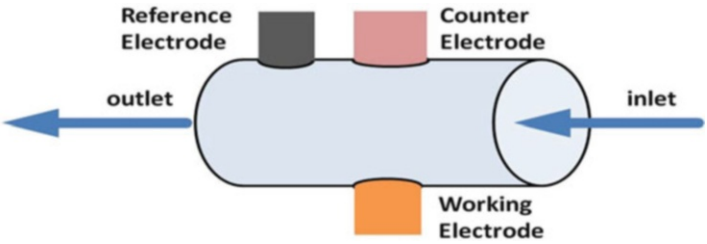

Fig. 23.4 Electrochemical flow-by cell

the rotating disc electrodes, as the limiting current depends on the diffusion coefficient of the depolarizer similarly between both systems.[10]

The other type of cells is based on a thin-layer configuration, where the liquid flows parallel to the electrode surface as illustrated in Fig. 23.4. These cells, which are also called channel cells, are characterized by their simplicity and the fact that the electrical field between the working and the counter electrode is more symmetrical, hence the background noise is reduced, which can be very critical when measuring trace elements.

Most of the thin-layer commercial flow cells utilize a gasket. In this approach, a gasket is used to separate the electrodes. The shape of the gasket determines the shape and size of the measuring chamber. The use of a gasket enables more flexibility in the design of the cell; moreover, the same system can be used for different purposes and different volumes by simply changing the gasket. This approach allows a simple adjustment of the shape of the cell and the working electrode. Moreover, by changing the shape of the cell one controls the flow regime.

Figure 23.5 shows the commercial flow cell manufactured by Bioanalytical Instruments[11] (BASi, USA) that employs a gasket. The working electrode shape is controlled by the shape of the different gaskets. Figure 23.6 shows three types of commercially available gaskets, where the shape of the cell determines the flow pattern inside the measuring chamber.

Figure 23.7 shows side and top views of a cross and radial flow gaskets and how the electrode configuration determines the choice of the gasket and the suitable flow pattern. If a dual electrodes configuration, where the electrodes are parallel, is chosen then the cross flow gasket will give the optimum results. On the other hand, if a single electrode configuration is used the radial flow gasket is preferred. When the electrodes are side by side an arc flow gasket usually performs better.

The two fundamental flow cell designs that were discussed differ essentially in the position of the working electrode relative to the direction of the eluent flow. The thin-layer cell exhibit laminar flow parallel to the electrode surface, while the wall-jet design exhibits a flow direction perpendicular to the electrode surface. Comparative studies between the different cell designs were conducted. In spite of the fact that equations that describe the current as a function of the cell-type and geometries have been derived, comparison between the theoretical and experimental results was not satisfactory. The difference between the calculated and experimental was

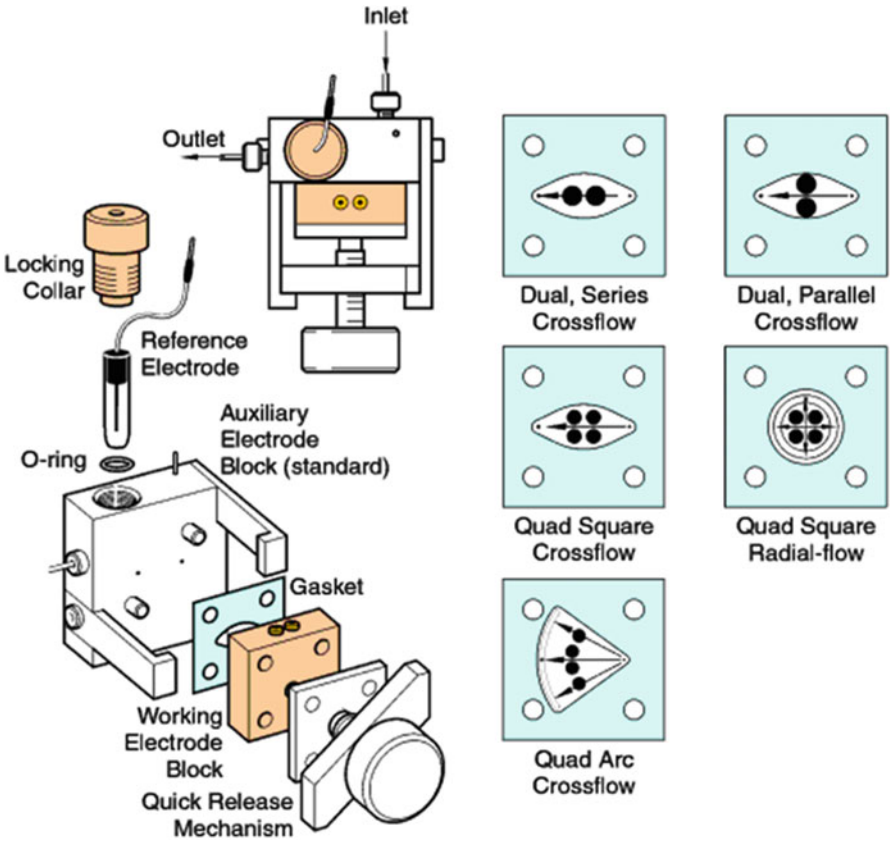

Fig. 23.5 A commercially available flow cell, which uses gaskets of different shapes[11] (designed by BASi), with permission from BASi Bioanalytical Systems, Inc. Further reproduction prohibited without permission. Copyright 2014

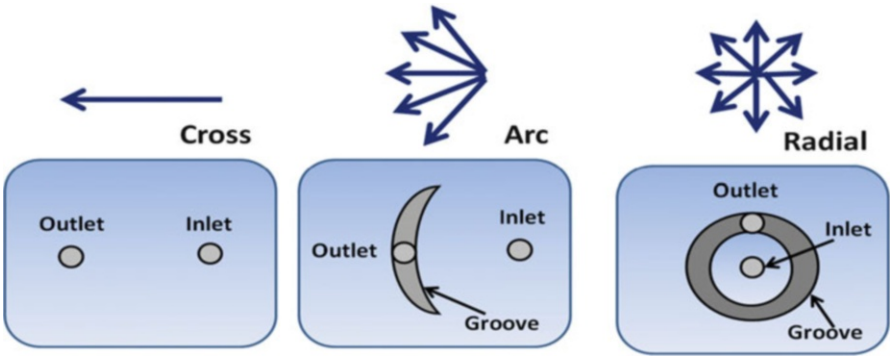

Fig. 23.6 Gaskets designed by BASi for electrochemical flow cell, with permission from BASi Bioanalytical Systems, Inc. Further reproduction prohibited without permission. Copyright 2014

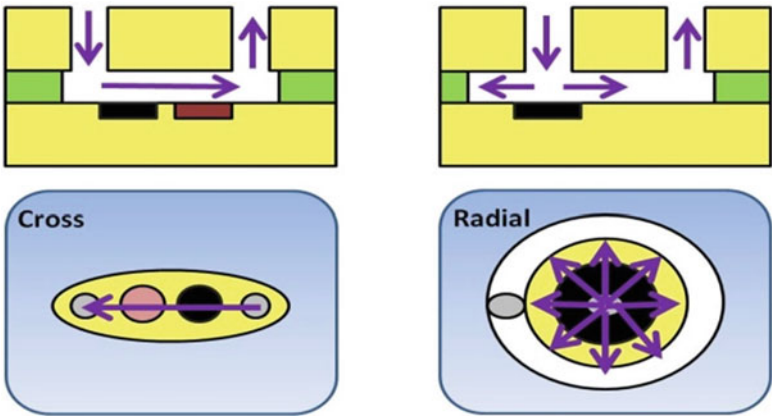

Fig. 23.7 Side and top views of a cross and radial gaskets

attributed to effects that arose from the electrode material, deviations in fluid flow, and inadequacies in the theory that was due to different operating conditions.[12,13]

There are several reports that although the thin-layer cell suffers from reduced mass transfer and higher uncompensated resistance through the flow cell, it is more sensitive and showed better reproducibility than the wall-jet cell.[9,14–17] On the other hand, it was argued on other reports that wall-jet is superior to other designs in terms of current sensitivity and improved signal to noise (S/N) ratio.[17–22] In general a thin-layer design is preferred for potentiometric measurements, while voltammetric measurements will yield better sensitivity in wall-jet design. Furthermore, most commercially available wall-jet cells are designed for use with disposable electrodes.

23.1.3 Frequency of Sampling

The traditional approach of environmental monitoring is based on discrete sampling followed by laboratory analysis. This concept suffers from one major disadvantage, namely, the time that passes between sampling and analysis through which the species can undergo different biological, physical, and chemical transformations leading to changes in concentration and chemical speciation.[23] Furthermore, when the measurements are carried out in the laboratory after sampling, numerous precautions must be taken to avoid artifacts bound to sample contamination, adsorption processes, and evolution of the sample before the analysis.[24] Discrete sampling methods are also expensive and time consuming. Moreover, discrete sampling does not provide accurate, real-time information about changes accruing in the concentrations or relations of the chemical species, which govern different processes in the environment. For example, Ouddane et al.[25] showed that the concentrations of Zn, Fe, and Cu measured in the Vorma River not only alter daily, but vary dramatically

during a 24 h course. Evidently, understanding the dynamics of trace metals (and other species) in aquatic systems can be accomplished only when the frequency of sampling is sufficient, i.e., is higher than the changes. Moreover, small changes may have a large impact on the dynamics of processes in aquatic systems.[26] For example, it has already been shown that the concentrations of total dissolved metals and/or their labile fractions evolve quickly with time. This could be attributed to the variation of phytoplankton activity or the temperature fluctuation during daily cycles.[27,28] Local perturbations and particularly the resuspension of contaminated sediments can also have a transitional effect on the concentrations and speciation of trace elements.[29–31] These phenomena when occurring frequently can be of great importance to the aquatic organisms and the interpretation of the acquired data.

Hence, the frequency of sampling and measurement must be determined by the necessity, that is, by the expected changes in the environment that might have an important effect. This must be very often compromised by the technological limitations. For example, while monitoring pH can be performed at intervals of seconds or less, it is presently impossible to monitor the levels of heavy metals at their natural abundance at the same frequency.

The interaction between the urban-industrialized region and the environment has very often a negative impact and poses a threat to the environment.[32,33] In order to reduce this threat and prevent the health hazard resulting from the pollution of water bodies, such as rivers and lagoons, international and national laws are constantly legislated.[34] These laws impose the frequency of monitoring in order to ensure water, air, and soil quality. The use of a remote-on-line system enables not only the enforcement of the regulations but also an immediate on-line warning in the case of detecting abnormalities in the form of concentrations or levels of the monitored species.[25,35,36]

23.2 Types of Electrochemical Sensors for Remote Sensing

23.2.1 Stationary Remote Electrochemical Sensing

Monitoring is basically of at least two dimensions; space and time. In many cases there is a need to monitor a constant location, which means that the sensor is fixed in space and monitoring becomes only time-dependent. For this mission, a stationary remote environmental sensor is the evident option. A stationary sensor is more flexible in terms of dimensions, weight, and power supply. This flexibility also lowers the cost of the sensor. Stationary sensors are quite common, less common are stationary sensors that are controlled remotely.

Heavy metals are of clear monitoring interest due to the role they play in geological processes and their environmental and toxicological effects. Many of the heavy metals, e.g., lead, mercury, and cadmium, are highly toxic, which makes them a target for remote environmental monitoring in particular in aquatic systems.

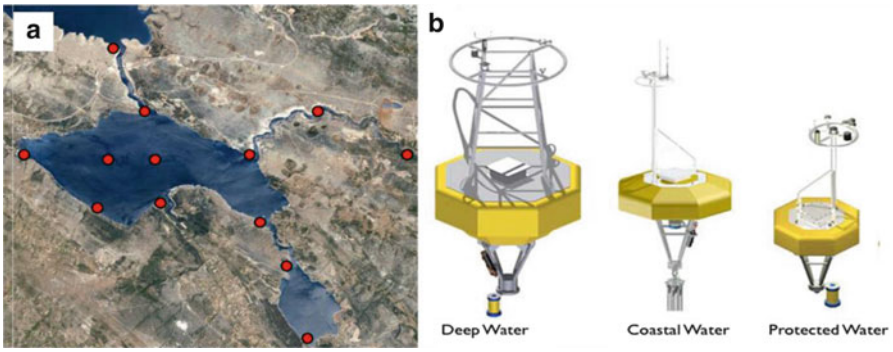

Fig. 23.8 (**a**) Illustration of monitoring station distribution in an aquatic environment. (**b**) Buoys that are designed by Sound Ocean System Inc. for deep, coastal, and protected water[47]

Furthermore, several of these heavy metals tend to bioaccumulate[37] in various organisms, which complicates their monitoring significantly. Automatic trace metal monitoring systems (ATMS)[25] are one example of an important tool in monitoring these elements using a stationary remote sensing device. ATMS, are a family of systems that can be placed in different locations and provide continuous (time dependent) monitoring.[1,38–40] Billon and coworkers applied the ATMS for voltammetric detection of Cu, Fe, Pb, Mn, and Zn in the Deûle River (France).[41] They showed, using differential pulse anodic stripping voltammetry (DP-ASV) that the concentrations of Zn, Cu and Fe vary, and is a function of the pH and turbidity.[25,29] ATMS can also be used as part of a sensor network.[42] The information that is collected by such network can be utilized in order to obtain a 2D or 3D models of the contaminant distribution in the environment.[24,43,44] The sensor network offers a powerful combination of distributed sensing capacity, computational tools together with internet or satellite communication, which are applicable in numerous research fields, such as ecological studies. Moreover, new designs of sensor networks allow for the observation of systems in near real-time, based on incoming data not only from local sources, but also from nearby networks, and from remote sensing data streams.[24,45] These advances are providing new and better understanding of our ecological systems by revealing previously unobservable phenomena and also raising questions and insights.[46] Figure 23.8a shows a schematic distribution of a sensor network. The ATMS (which are marked by the red dots) are placed in strategically points that are determined by a previous geological survey, simulations, or a potential contamination source. The ATMS are placed not only in the estuaries (entering or exiting the water body) but can also be positioned along the river or lake in order to provide a better insight on the measured parameters. Buoys are used in order to position a station and acquire information regarding phenomenon that occurs not near the shore, but also in the middle of the water body. Buoys can also be used to supply power to the sensor via solar panels and make an ideal platform for numerous sensors for monitoring atmospheric and hydrodynamic environments as well as for speciation. Figure 23.8b shows three

types of buoys that are manufactured by Sound System Ocean Inc (SOSI).[47] These buoys are designed for different conditions, i.e., deep, costal, and protected waters.

During the last decades there has been an extensive use of aquatic sensors and monitoring stations for monitoring basic water parameters, such as temperature and conductivity (salinity). Physical sensors are very often used for monitoring aquatic systems. They are usually very robust and reliable and can be used for long time without or with minimal maintenance. Mead et al. used a network of gas sensors for measuring ppb levels of toxic gases (CO, NO, and NO_2) in urban environments.[48] Coloso and coworkers used a sensor network to measure temperature and dissolved oxygen (DO) in various habitats and at multiple depths for a more complete estimate of whole lake metabolism and better understanding of the spatial and temporal complexity of lakes.[49] Other chemical aquatic sensors such as used for measuring total suspended solids (TSS), nutrients (N, P), and dissolved organic matter, are constantly developed and improved. Yet, depending on local biofouling, they require very frequent maintenance, that is, after a period of 2 weeks up to 1 month a cleaning procedure or other services are crucial for their reliable operation. Electrochemical sensors for monitoring the oxidation–reduction potential (ORP) or ion selective electrodes (ISEs) had been considered the most problematic for long-term autonomous deployment within networks, as their response tended to drift excessively over time in the absence of frequent servicing. However, major developments in sensor technology, such as better LOD or stability due to new membrane materials, especially in electrochemical sensors[50–52] enable the long term use of sensors in remote locations as part of a sensor network.[41] Evidently, as more aquatic sensors are becoming accessible, models can be readily examined and refined.

23.2.2 Mobile Remote Electrochemical Sensing

In the period between 1975 and 1977 three scientists from the San-Diego Naval Ocean Systems Center went on a sampling campaign in the San-Diego bay. The sampling and measurements were conducted from a small vessel. This was not the first off-shore sampling campaign, but it was the first one that utilized an automated electrochemical system for the measurement of heavy metals.[53] In the previous sections we described the aspects of remote environmental monitoring using different technologies. We emphasized the advantages of placing the sensor at a remote or unreachable location. These sensors are usually deployed at a stationary location, which can be by river estuaries, factories, or even in the middle of the water body positioned inside a special buoy (Fig. 23.8b). The use of stationary sensors are very common for monitoring fresh water sources, such as ground and surface water, however monitoring a marine environment is more challenging. Positioning of a permanent sensor at the estuary can monitor the diversity and speciation flowing into the bay, but not the entire large area of the bay or the ocean. Furthermore, one needs to consider the fact that some water bodies exhibit complex

currents and coastal systems. Tides, for example, influence the local measured concentrations and may also cause salinity shifts.[54] From a biological point of view, heavy metals will undergo dilution when entering a large water body and appear very low but may still be of biologically significance. Hence, it is evident that monitoring must allow time as well as space dependence of the target analytes.

The application of an automated-mobile system that is controlled from a boat or the shore can solve some of these issues. The sensors can travel to a required area and perform the measurements and continue to their next location. A major limitation of the traditional sensor network is the generally fixed sampling locations. The fact that the sensor is not permanent like a station or a buoy gives the user more flexibility in planning the monitoring strategy. This type of sensing can help covering a large area with a small number of sensors. In fact, one sensor can perform as an entire network and produce results from several locations, thus contributing valuable insight on the entire system. Another advantage is the ability of the sensor to access problematic areas in complex environments, for example under arctic ice sheets.[55] Nevertheless, assembling an autonomous-mobile device has numerous demands spanning from power supply to a wireless control unit. Several approaches have been considered in order to fulfill all the requirements from such robotic device also referred to as a robotic fish or "robofish".[56]

One of the first devices was the "RoboTuna" project.[57] A group from MIT demonstrated that a long robotic fish that mimics the motion of a fish can be used for aquatic monitoring. Several versions of this prototype were made; the latest was developed in order to monitor the 2010 oil spill in the gulf oil Mexico. The robot was equipped with an on-board crude oil sensor to detect and track oil plumes and a salinity sensor based on conductometry. Monitoring and tracking these two elements was critical for clean-up effort, the protection of sensitive areas and understanding the spill's environmental and ecological impacts.

There were a number of attempts to construct robotic fish for oceanographic investigations; most of them were battery-powered equipped with a CTD (Conductivity, Temperature, and Depth) detector leading to relatively short operation time. This was a major set-back for the early systems such as Remus (remote environmental monitoring units)[58] and AutoSub[59] which could operate for 7 and 12 h, respectively. The use of solar-powered robots was just a matter of time, and led to the next anticipated progress in this field. RiverNet was the first project aimed to develop a sensors network for water monitoring based on a solar-powered underwater robot (SAUV or solar-powered autonomous underwater vehicle).[60] A production version of the robot is now commercially available from Falmouth Scientific, Inc., the "SAUV II" (see Fig. 23.9). The SAUV is equipped with a standard CTD sensor as well as dissolved oxygen and pH sensors. The SAUV can also be used as a platform for other environmental sensors such as nitrate, heavy metals, etc.[61,62]

Robotic and autonomous underwater vehicles (AUVs) are playing a crucial role in improving our understanding of the oceans. Oceanographers are employing an increasing number (and variety) of in situ autonomous sensing systems.[63] One example of a widely used system is the autonomous underwater gliders that are

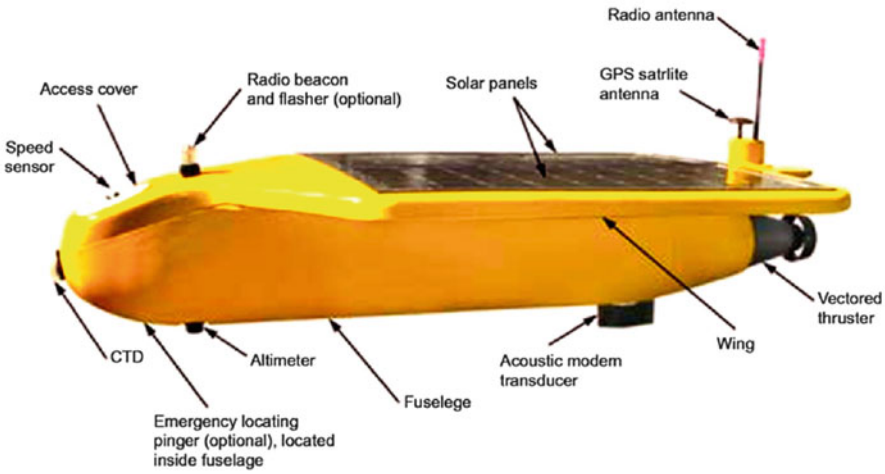

Fig. 23.9 SAUV II a solar-powered robot. Reproduced with permission from Falmouth Scientific Inc

sent to sample and monitor specific phenomena. The gliders are equipped with wings that are designed for steering the vehicles horizontally while a buoyancy engine is used to conduct the vertical profiles.[64]

Although a mobile system has some advantages compared to a fixed system such as a buoy, it still suffers from some drawbacks. The mobile sensor has a larger power consumption that cannot always be solved by using solar energy leading to a shorter operation time. Radical changes in the flow or environment can cause damage to the mobile sensor or change the models it is programmed to follow, leading to a reduced functionality of the sensor. A typical environmental change that can disrupt the operation of the sensor is the blossoming of algae on the water surface. Commonwealth Scientific and Industrial Research Organization (CSIRO)[65] tried to exploit all the advantages of the autonomous mobile sensor while using a network of fixed sensors to overcome the disadvantages. The main interest was monitoring pathogens and pesticides especially organophosphates and carbamates. In order to monitor these substances, the inventors used the enzyme, acetylcholinesterase (AChE) as a biomarker. The measurement was based on the amperometric detection using carbon nanotubes (CNT) modified electrodes.[66] They constructed two types of mobile robots; an AUV (autonomous underwater vehicles or autonomous Unmanned Vehicle) for shallow waters or small reservoirs and a Catamaran-based vehicle equipped with solar panels for other scenarios. To reduce the power consumption the inventors used cellular communication and added an option whereby the robots change their operation and reduce the amount or type of sampling/sensing based on the amount of the energy power that is left. They also constructed a large sensor network based on stationary sensors that were reinforced with mobile sensors. This network could produce online information and utilizes

the mobile sensors in case further data are needed in a certain area or for monitoring special phenomenon.

There are numerous groups that develop AUVs and other robotic platforms most of them are aimed at increasing the data collection efficiencies, particularly in unreachable and hostile environments. Despite the fast growing interest and demand for remote sensing for both regulatory and scientific purposes, more efforts that will contribute directly to the quality of remote environmental monitoring are required. For example, underwater communication, biomimetics (robotics that mimics the function or structure of a biological system) and other propulsion mechanism, power sources, sensing, autonomous navigation , artificial intelligence and hydrodynamic.[56] The technology is progressing rapidly and it is evident that autonomous robotic sensing is the future of oceanography and pollution monitoring.

23.2.3 Submersible Remote Electrochemical Sensing

Automatic monitoring is essential for recording large sets of temporal and spatial information from a water body (river, lake, lagoon, and even ocean), and is also required for rigorous biogeochemical interpretation.[67] In the previous section we described the general concept of a remote station for environmental monitoring. These systems are usually based on a sampling system that can withdraw the water from different depths and a flow system that can transfer it to the electrochemical measuring cell (detector). Another type of measurement is the submersible electrode (sensor), which is also known as an on-cable electrode. This is a different concept were instead of using a sampling system and bringing the sample to the electrode, the electrode is brought to the sample. The basic idea of the submersible electrode is shown in Fig. 23.10. The electrode which comprises of a complete three-electrode cell is connected by a long shielded cable to a potentiostat and a recording device.

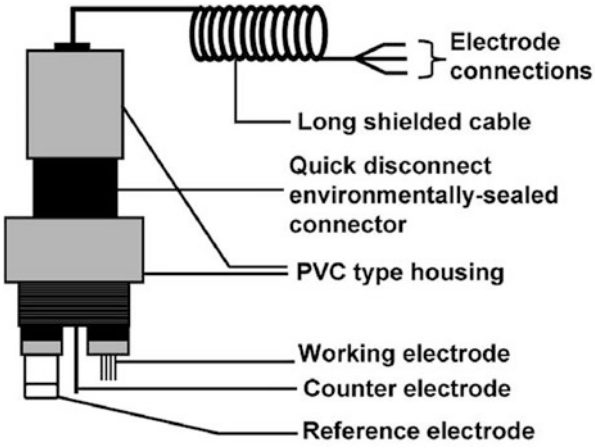

Fig. 23.10 Schematics of the remote electrochemical sensor for remote sensing. Reproduced with permission from reference (68)

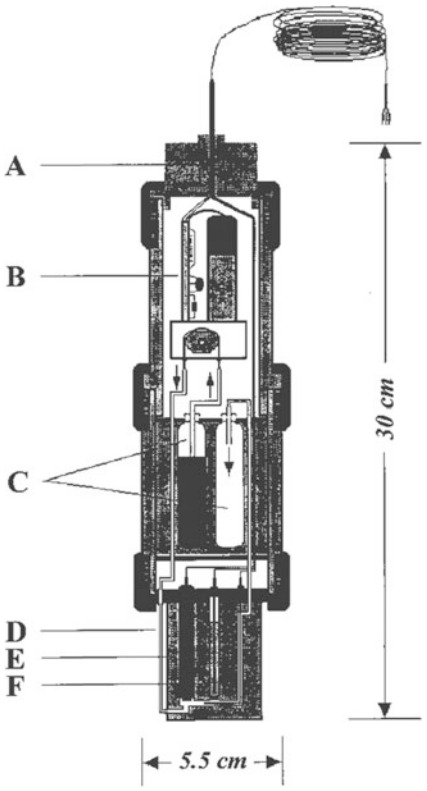

Fig. 23.11 Schematic diagram of a submersible electrode that can serve as a complete system. A, cable connection; B, micropump; C, reservoirs for reagent and waste solutions; D, microdialysis sampling tube and an electrochemical flow detector; E and F, working and reference electrodes, respectively. Reproduced with permission from reference (77)

The first submersible device was designed by Trecier and Zirino in the early 1990s.[69] They designed a submersible flow trough cell that was based on either a mercury film or a mercury drop electrode. Since this early development, most of the work in this filed was carried out by Wang and his coworkers.[70] They developed electrodes for monitoring different species from heavy metals[71–73] to organic compounds, such as phenols, peroxides and explosives.[68,74–76] The approach was usually similar and involved a submersible stripping sensor for in situ monitoring of the "total" content of dissolved species. They also successfully integrated the submersible voltammetric TNT electrode with the Remus AUV creating an autonomous submersible electrode.[68]

In the beginning of the twenty-first century there have been a few major advancements in this field including the first step in the incorporation of all the protocol steps of the measuring system: sampling, sample pretreatment, calibration, measurement, and cleaning, into one sealed electrode.[40,77,78] A schematic diagram of a submersible electrode that can serve as complete system or a lab-on cable system can be seen in Fig. 23.11.

Although the vast progress in this field and the clear advantages, there are only few commercially available submersible electrochemical sensors for marine-specification. Most of the sensors that are developed in the lab show a lesser

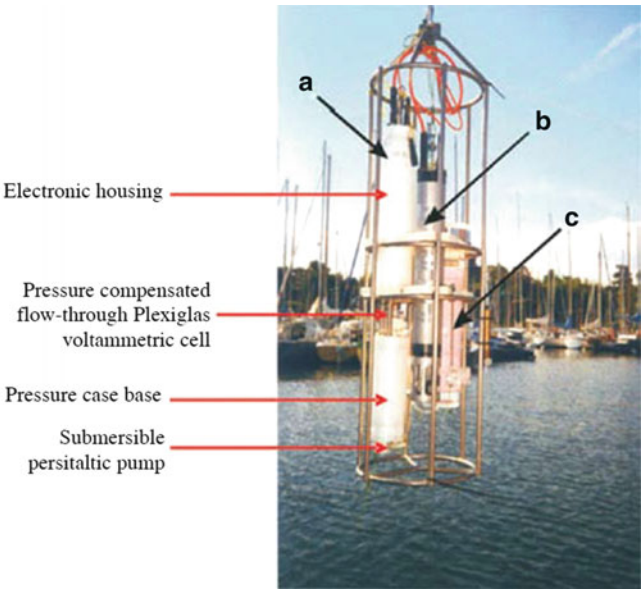

Fig. 23.12 Standard version of the VIP system for in-situ monitoring and profiling. (**a**) Voltammetric probe, (**b**) multiparameter probe, and (**c**) online O_2 removal system. Reproduced with permission from reference (54)

sensitivity in the field. There are a few examples of submersible electrodes, which showed good results in the lab as well as under real conditions. These electrodes were tested not only for sensitivity and accuracy but also for their reproducibility and stability as a function of time. The major setback in the validation of the electrode is the fact that the electrodes are exposed to various species (organic and inorganic) that can cause fouling even in the presence of an automated cleaning protocol. Even electrodes that pass all of these strict tests such as the electrodes developed for nitrate[50] or trace metals[79] not always succeed in the transition to the next step. One of the very few commercially available systems is the voltammetric in situ profiling system (VIP). The first prototype of the VIP system was developed by Tracier in collaboration with Idronaut in 1998.[1] This system later underwent further improvements and was commercialized by Idronaut (Fig. 23.12). The VIP is made of several units, such as on-line oxygen removal module, a multiparameter probe, and a calibration unit. The system has the capability of monitoring trace metals down to a depth of 500 m with a subnanomolar sensitivity.[80,78]

VIP systems may demonstrate the next step in the evolution of the submersible electrode. In 2009 the VIP system was tested by four of the leading labs in aquatic metal speciation in Europe.[78] The system was simultaneously tested in Sweden, Italy, Switzerland, and the UK. They preformed measurements of Cu(II), Pb(II), and Cd(II) in natural waters at a frequency of 2–3 analyses per hour. The results were compared to the standard methods: inductively coupled plasma mass spectrometry (ICP-MS) and voltammetry using mercury electrodes. The results were almost

identical to those obtained by the standard methods and showed that the VIP system is a reliable solution for remote environmental sensing. The system can provide information about the different geochemical behavior of dissolved metals and enables to distinguish between a variety of metal fractions. To show a the possible use of the VIP system as part of a sensor network, two systems were placed a few meters apart and preformed sampling at a depth of 1.5 m every 50 min for a couple of days. The systems successfully measured dynamic concentrations of Cd and Pb as well as the salinity of the sampling site. While this and similarly developed systems hold a great promise for possible sensor networks they still suffer from a few fundamental problems. These systems require skilled operators, preferably with good background in electrochemistry. Unlike the ISE, the VIP system can measure the open circuit potential (OCP) for a period of up to 3 weeks without constant maintenance. It is also worth mentioning that the VIP system has a size and weight limitation, which is not ideal for an autonomous remote device. In summary, the most significant advantage of the submersible electrode is the fact that no sampling system is needed, which is also its biggest disadvantage. A sampling system makes the remote system more complicated in terms of weight, size, and power supply but can also be used to filter the water and protect the electrode surface from fouling. Although some submersible electrode can utilize a special filter it can also be fouled and requires maintenance. Another type of a mobile environmental sensor, which does not utilize a flow system is the hybrid robot developed by the Brazilian oil company Petrobras S.A.[81] This hybrid robot was developed not only to replace manual sampling but also to conduct continuous monitoring of water quality and gas emission near oil pipe lines. The robot is designed to operate on a wide variety of terrains, including water, land, marshes, swamps, and sand.

23.3 Environmentally Monitoring Platforms

The previous sections described the different parameters involved in the fabrication of a remote environmental sensor and the different types of sensor, which were developed. This section focuses on some of the more ambitious projects, which attempted to construct an environmentally monitoring platform. The idea behind a platform is a combination of several sensors from the same or different types in order to obtain a complete prospective of the inspected area. During the last decade several projects were mostly funded by the European Union (EU) or the US, but despite several successful trials, so far they all have remained as scientific projects and to the best of our knowledge none of them has been commercialized or is constantly operating.

HydroNet was a project funded by the EU framework 7th program. The project began in 2008 and ended in the beginning of 2012. Partners from ten countries participated in the project. It was aimed at designing, developing, and testing a new technological platform for improving the monitoring of water bodies based on a network of sensors and autonomous, floating, and sensorized robots, embedded in an Ambient Intelligence infrastructure. A network of sensors was designed to

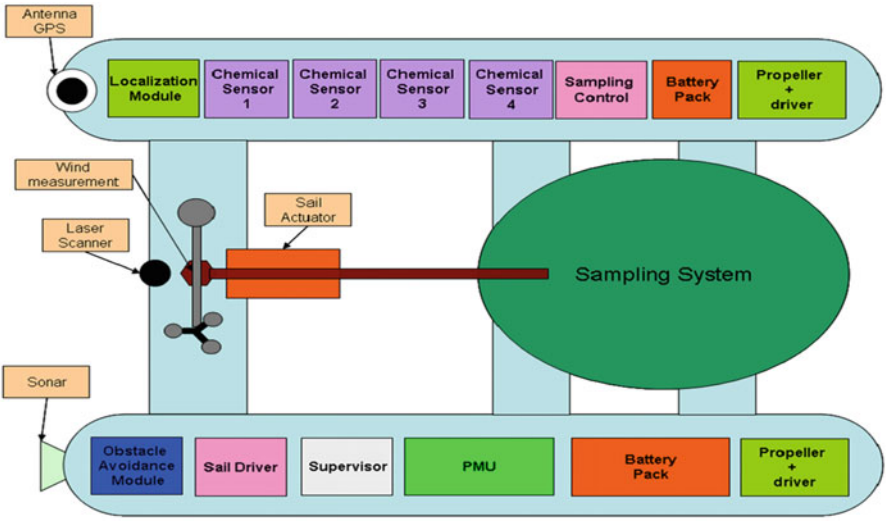

Fig. 23.13 Schematics of the HydroNet robot. All the sensors are connected to the main sampling system

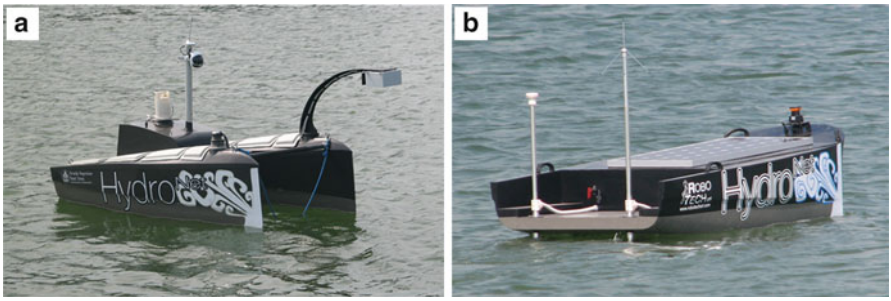

Fig. 23.14 The HydroNet robots that were developed for: (**a**) costal water, (**b**) rivers.

sample and analyze several chemical and physical parameters in water in real-time and continuously monitor the well-being status of water bodies. (Electro)chemical,[52,82,83] optical and biological[66] sensors were developed and used for monitoring of physical parameters and pollutants in water such as chromate, cadmium, mercury, oil, and chlorophyll. Enhanced mathematical models were also developed for simulating the pollutants transport and processes in rivers, lakes, and coastal waters. The sensors were planned also to be embedded into fixed stations (buoys) and mobile robots that are able to navigate, as part of a network, in diverse water scenarios, from coastal sea waters, to creeks and rivers (both at the head and mouth of the rivers) to natural and artificial lakes and lagoons. The scheme of the Hydronet robot is shown in Fig. 23.13, while Fig. 23.14 shows the actual Hydronet robot that was developed.

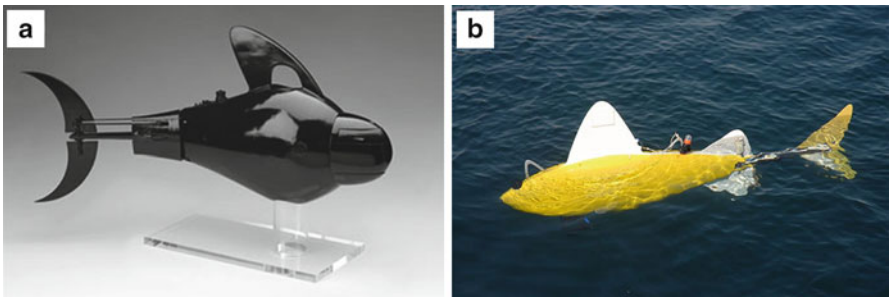

Fig. 23.15 (**a**) Prototype of SHOAL-1 that was shown in the London Science Museum. (**b**) The prototype of SHOAL-2 during a live test

The robot and sensors were part of an Ambient Intelligence platform, which integrated not only sensors for water monitoring and robot tasks execution, but also communication backhaul systems, databases technologies, and knowledge discovery in databases (KDD) processes for extracting and increasing knowledge on water management. From a scientific point of view the project was a big success, new technologies were developed and a significant contribution was made is several fields. Yet, the project did not result in a prototype that could be easily commercialized.

SHOAL[84] is another example of an ambitious project that was developed under the EU 7th framework program. The SHOAL project began in 2009 and involved partners from France, UK, Spain, and Ireland. SHOAL aimed to develop a number of robotic fish that will operate together in order to monitor and search for pollution in ports and other aquatic areas. The swarms of autonomously controlled robots were equipped with an array of chemical sensors that were able to locate pollution and identify its source. The robot was equipped with various sensors for phenols, dissolved oxygen (DO), nutrients, and heavy metals (Cu and Pb). The chemical sensors were based on an array of microelectrodes. Moreover, the robots were also given intelligence so that in case that significant amount of pollution is detected, the robots operate together communicating via ultrasonic communications to find the source of the pollution. In other words, the fleet of sensors aimed to provide early alarms and to determine the source of the pollution. The data from the robots were to be used for creating a real-time map of the pollutants present in the water and their concentration and location on a 3D map of the port. The robots were constructed to mimic real fish so as not to alarm other marine inhabitants. Two prototypes were constructed SHOAL-1 (Fig. 23.15a) and SHOAL-2 (Fig. 23.15b). The project officially ended in may 2012 after a successful test in port of Gijon, Spain.

SHOAL was not the first project to develop a robot that mimics the behavior of fish. Unlike the other projects, which are based on a sophisticated robotic platform, the Bayen group from UC Berkley designed a simpler system (see Fig. 23.16). They based their system on a mobile floating sensor network.[85] The sensors were put into a floating device equipped with a cellular device (smart-phone) which served as the microprocessor. The devices were then scattered in estuarine environments and rivers and were carried by the current trough the area of interest. The data from the

Fig. 23.16 The two main types of floating sensors. On the *left*, the passive sensors that are driven by the flow. On the *right*, the sensors that have a propeller to maneuver them when encountering obstacles. Reproduced with permission from reference (85)

sensors were transmitted via the cellular phone network using a special application or a short-range wireless radio. The movement of the sensors was tracked by GPS providing a virtual map of the current and the different measured parameters. This information helped to track the movement of the contaminants in real time. Since they used a large number of these sensors, and recorded the combined data, they gathered enough information to get a reliable picture about how contaminated the area was. This approach is characterized by its simplicity and low-power consumption; on the other hand, the devices lack any real navigational abilities. Although there was developed a more advanced model that has a propeller, which can assist the sensor to avoid obstacles once the sensors are deployed, no route adjustment can be made, and it is hard to repeat a measurement. To solve this issue a large number of sensors must be deployed. Furthermore since the device cannot navigate back to its base, a collection mechanism needs to be established. Today the researches are waiting at the end of the route to collect each device.

These projects are just the tip of the iceberg. Organization such as GEOTRACES[86] which are interested in the distribution of the different elements in the environment under different conditions, as well as environmental agencies such as EPA, which are more interested in mapping and preventing pollution, are pushing all the time for more sophisticated platforms and more accurate sensors. These demands help to push science into its limits and beyond. We believe that with time more collaborations will lead to significant improvements making an autonomous remote sensing a common daily routine.

23.4 Conclusions and Perspectives

Clearly remote environmental sensing is going to play an increasing role in our attempts to understand anthropogenic and natural processes. The ability to monitor the environment in space and time in not only crucial for understanding processes but also as a measure of protection, that could serve as early alarm in cases of sudden pollution or environmental changes. Surveying the development of remote

environmental monitoring is fascinating and reveals tremendous efforts usually funded by governmental and legislation agencies. Clearly, the progress in this area lags behind the need. At the same time, the lack of commercial systems also inhibits legislation, which has also an effect on commercialization of new products.

Remote environmental sensing systems, which will be able to eventually make it to the market, require the development of an entire platform, which includes an autonomous vehicle and miniaturized sensors. This, in fact, requires assembling many subunits such as power, control, and navigation systems as well as sampling and flow systems for the sensors. Recently and mostly by the support of the EU we have witnessed such efforts to bring together under one umbrella the various expertise and skills that are needed to develop such systems. A major challenge still lies in constructing the sensors. There is a very large gap between a prototype that is developed in the laboratory and a final device that can be called a sensor. Measuring continuously a signal (especially of low concentration) in the environment by a sensor poses some challenges such as calibration, cleaning, and others, which are very often underestimated by scientists. It seems that much more efforts are required before durable, reliable, yet relatively cheap and robust sensors could be easily integrated in remote environmental monitoring units. Clearly, there is still to be accomplished in this important and challenging field.

References

1. Tercier ML, Buffle J, Graziottin F (1998) Novel voltammetric in-situ profiling system for continuous real-time monitoring of trace elements in natural waters. Electroanalysis 10:355–363
2. Zagatto EAG, Carneiro JMT, Vicente S, Fortes PR, Santos JLM, Lima J (2009) Mixing chambers in flow analysis: a review. J Anal Chem 64:524–532
3. Johnson DC, Weber SG, Bond AM, Wightman RM, Shoup RE, Krull IS (1986) Electroanalytical voltammetry in flowing solutions. Anal Chim Acta 180:187–250
4. Volikakis GJ, Efstathiou CE (2000) Determination of rutin and other flavonoids by flow-injection/adsorptive stripping voltammetry using nujol-graphite and diphenylether-graphite paste electrodes. Talanta 51:775–785
5. Volikakis GJ, Efstathiou CE (2005) Fast screening of total flavonols in wines, tea-infusions and tomato juice by flow injection/adsorptive stripping voltammetry. Anal Chim Acta 551:124–131
6. Lenehan CE, Barnett NW, Lewis SW (2002) Sequential injection analysis. Analyst 127:997–1020
7. Ivaska A, Kubiak WW (1997) Application of sequential injection analysis to anodic stripping voltammetry. Talanta 44:713–723
8. Ruzicka J, Gubeli T (1991) Principles of stopped-flow sequential injection-analysis and its application to the kinetic determination of traces of a proteolytic-enzyme. Anal Chem 63:1680–1685
9. Soucaze Guillous B, Kutner W (1997) Flow characteristics of a versatile wall-jet or radial-flow thin-layer large-volume cell for electrochemical detection in flow-through analytical systems. Electroanalysis 9:32–39
10. Karyakin AA, Karyakina EE, Gorton L (1996) Prussian-Blue-based amperometric biosensors in flow-injection analysis. Talanta 43:1597–1606

11. BASi (2013) http://www.basinc.com/
12. Morgan DM, Weber SG (1984) Noise and signal-to-noise ratio in electrochemical detectors. Anal Chem 56:2560–2567
13. Stulik K, Pacakova V (1986) Some aspects of design, performance and applications of electrochemical detectors in HPLC and FIA. Ann Chim 76:315–332
14. Ryan MD, Bowden EF, Chambers JQ (1994) Dynamic electrochemistry—methodology and application. Anal Chem 66:R360–R427
15. Danhel A, Shiu KK, Yosypchuk B, Barek J, Peckova K, Vyskocil V (2009) The use of silver solid amalgam working electrode for determination of nitrophenols by HPLC with electrochemical detection. Electroanalysis 21:303–308
16. Davey DE, Mulcahy DE, Oconnell GR (1993) comparison of detector cell configurations in flow-injection potentiometry. Electroanalysis 5:581–588
17. Patthy M, Gyenge R, Salat J (1982) comparison of the design and performance-characteristics of the wall-jet type and thin-layer type electrochemical detectors—separation of catecholamines and phenothiazines. J Chromatogr 241:131–139
18. Hanekamp HB, Dejong HG (1982) Theoretical comparison of the performance of electrochemical flow-through detectors. Anal Chim Acta 135:351–354
19. Yamada J, Matsuda H (1973) Limiting diffusion currents in hydrodynamic voltammetry. 3. Wall jet electrodes. J Electroanal Chem 44:189–198
20. Stojanovic RS, Bond AM, Butler ECV (1992) A comparative-study of the cylindrical wire, thin-layer, and wall-jet detector cells for the determination of inorganic arsenic by ion exclusion chromatography with constant and pulsed amperometric detection. Electroanalysis 4:453–461
21. Maixnerova L, Barek J, Peckova K (2012) Thin-layer and wall-jet arrangement of amperometric detector with boron-doped diamond electrode: comparison of amperometric determination of aminobiphenyls in HPLC-ED. Electroanalysis 24:649–658
22. Maccarthy P, Klusman RW, Cowling SW, Rice JA (1993) water analysis. Anal Chem 65: R244–R292
23. Sole S, Alegret S (2001) Environmental toxicity monitoring using electrochemical biosensing systems. Environ Sci Poll Res 8:256–264
24. Rundel PW, Graham EA, Allen MF, Fisher JC, Harmon TC (2009) Environmental sensor networks in ecological research. New Phytol 182:589–607
25. Lourino-Cabana B, Iftekhar S, Billon G, Mikkelsen O, Ouddane B (2010) Automatic trace metal monitoring station use for early warning and short term events in polluted rivers: application to streams loaded by mining tailing. J Environ Monit 12:1898–1906
26. Hanrahan G, Patil DG, Wang J (2004) Electrochemical sensors for environmental monitoring: design, development and applications. J Environ Monit 6:657–664
27. Nimick DA, Gammons CH, Cleasby TE, Madison JP, Skaar D, Brick CM (2003) Diel cycles in dissolved metal concentrations in streams: Occurrence and possible causes. Water Resourc Res 39. doi:10.1029/2002WR001571
28. McKnight D, Bencala KE (1988) Diel variations in iron chemistry in an acidic stream in the Colorado Rocky-Mountains, USA. Arctic Alpine Res 20:492–500
29. Lourino-Cabana B, Billon G, Magnier A, Prygiel E, Baeyens W, Prygiel J et al (2011) Evidence of highly dynamic geochemical behaviour of zinc in the Deule river (northern France). J Environ Monit 13:2124–2133
30. Saulnier I, Mucci A (2000) Trace metal remobilization following the resuspension of estuarine sediments: Saguenay Fjord, Canada. Appl Geochem 15:191–210
31. Van den Berg GA, Meijers GGA, Van der Heijdt LM, Zwolsman JJG (2001) Dredging-related mobilisation of trace metals: a case study in the Netherlands. Water Res 35:1979–1986
32. Inano S, Yamazaki H, Yoshikawa S (2004) The history of heavy metal pollution during the last 100 years, recorded in sediment cores from Osaka castle moat, southwestern Japan. Quaternary Res (Tokyo) 43:275–286

33. Watanabe T, Ohe T, Hirayama T (2005) Occurrence and origin of mutagenicity in soil and water environment. Environ Sci 12:325–346
34. EPA (2013) http://www.epa.gov/lawsregs/
35. Diamond D, Lau KT, Brady S, Cleary J (2008) Integration of analytical measurements and wireless communications—current issues and future strategies. Talanta 75:606–612
36. LaGier MJ, Fell JW, Goodwin KD (2007) Electrochemical detection of harmful algae and other microbial contaminants in coastal waters using hand-held biosensors. Mar Pollut Bull 54:757–770
37. DeForest DK, Brix KV, Adams WJ (2007) Assessing metal bioaccumulation in aquatic environments: the inverse relationship between bioaccumulation factors, trophic transfer factors and exposure concentration. Aquat Toxicol 84:236–246
38. Mikkelsen O, Strasunskiene K, Skogvold S, Schroder KH, Johnsen CC, Rydningen M et al (2007) Automatic voltammetric system for continuous trace metal monitoring in various environmental samples. Electroanalysis 19:2085–2092
39. Miro M, Jimoh M, Frenzel W (2005) A novel dynamic approach for automatic microsampling and continuous monitoring of metal ion release from soils exploiting a dedicated flow-through microdialyser. Anal Bioanal Chem 382:396–404
40. Tercier-Waeber ML, Confalonieri F, Riccardi G, Sina A, Noel S, Buffle J et al (2005) Multi physical-chemical profiler for real-time in situ monitoring of trace metal speciation and master variables: development, validation and field applications. Mar Chem 97:216–235
41. Superville P-J, Louis Y, Billon G, Prygiel J, Omanovic D, Pizeta I (2011) An adaptable automatic trace metal monitoring system for on line measuring in natural waters. Talanta 87:85–92
42. Jang A, Zou Z, Lee KK, Ahn CH, Bishop PL (2011) State-of-the-art lab chip sensors for environmental water monitoring. Meas Sci Technol 22:032001
43. Rajar R, Zagar D, Cetina M, Akagi H, Yano S, Tomiyasu T et al (2004) Application of three-dimensional mercury cycling model to coastal seas. Ecol Model 171:139–155
44. Rajar R, Zagar D, Sirca A, Horvat M (2000) Three-dimensional modelling of mercury cycling in the Gulf of Trieste. Sci Tot Environ 260:109–123
45. Pastorello GZ, Sanchez-Azofeifa GA, Nascimento MA (2011) Enviro-Net: from networks of ground-based sensor systems to a web platform for sensor data management. Sensors 11:6454–6479
46. Porter J, Arzberger P, Braun HW, Bryant P, Gage S, Hansen T et al (2005) Wireless sensor networks for ecology. Bioscience 55:561–572
47. SOSI http://www.soundocean.com/home
48. Mead MI, Popoola OAM, Stewart GB, Landshoff P, Calleja M, Hayes M et al (2013) The use of electrochemical sensors for monitoring urban air quality in low-cost, high-density networks. Atmos Environ 70:186–203
49. Coloso JJ, Cole JJ, Hanson PC, Pace ML (2008) Depth-integrated, continuous estimates of metabolism in a clear-water lake. Can J Fish Aquat Sci 65:712–722
50. Le Goff T, Braven J, Ebdon L, Scholefield D (2003) Automatic continuous river monitoring of nitrate using a novel ion-selective electrode. J Environ Monit 5:353–358
51. Scholefield D, Le Goff T, Braven J, Ebdon L, Long T, Butler M (2005) Concerted diurnal patterns in riverine nutrient concentrations and physical conditions. Sci Tot Environ 344:201–210
52. Noyhouzer T, Mandler D (2013) A new electrochemical flow cell for the remote sensing of heavy metals. Electroanalysis 25:109–115
53. Zirino A, Lieberman SH, Clavell C (1978) measurement of Cu and Zn in San Diego bay by automated anodic-stripping voltammetry. Environ Sci Technol 12:73–79
54. Mills G, Fones G (2012) A review of in situ methods and sensors for monitoring the marine environment. Sensor Rev 32:17–28
55. Wadhams P, Wilkinson JP, McPhail SD (2006) A new view of the underside of Arctic sea ice. Geophys Res Lett 33, L04501

56. Bogue R (2011) Robots for monitoring the environment. Ind Robot 38:560–566
57. Stix G (1994) ROBOTUNA. Sci Am 270:142–142
58. Stokey R, Allen B, Austin T, Goldsborough R, Forrester N, Purcell M et al (2001) Enabling technologies for REMUS docking: an integral component of an autonomous ocean-sampling network. IEEE J Ocean Eng 26:487–497
59. Collar PG, McPhail SD (1995) Autosub—an autonomous unmanned submersible for ocean data-collection. Electron Commun Eng J 7:105–114
60. Dickey TD, Bidigare RR (2005) Interdisciplinary oceanographic observations: the wave of the future. Sci Mar 69:23–42
61. Montgomery JL, Harmon T, Kaiser W, Sanderson A, Haas CN, Hooper R et al (2007) The WATERS network: an integrated environmental observatory network for water research. Environ Sci Technol 41:6642–6647
62. Wegehenkel M, Kersebaum KC (2005) The validation of a modeling system for calculating water balance and catchment discharge using simple techniques based on field data and remote sensing data. Phys Chem Earth 30:171–179
63. Williams SB, Pizarro OR, Jakuba MV, Johnson CR, Barrett NS, Babcock RC et al (2012) Monitoring of benthic reference sites using an autonomous underwater vehicle. IEEE Robot Automat Mag 19:73–84
64. Rudnick DL, Davis RE, Eriksen CC, Fratantoni DM, Perry MJ (2004) Underwater gliders for ocean research. Mar Technol Soc J 38:73–84
65. CISRO (2013) http://www.csiro.au/
66. Musameh MM, Gao Y, Hickey M, Kyratzis IL (2012) Application of carbon nanotubes in the extraction and electrochemical detection of organophosphate pesticides: a review. Anal Lett 45:783–803
67. Florence TM (1982) The speciation of trace-elements in waters. Talanta 29:345–364
68. Wang J (2007) Electrochemical sensing of explosives. Electroanalysis 19:415–423
69. Tercier ML, Buffle J, Zirino A, Devitre RR (1990) In situ voltammetric measurement of trace-elements in lakes and oceans. Anal Chim Acta 237:429–437
70. Wang J (2000) In situ electrochemical monitoring: from remote sensors to submersible microlaboratories. Lab Robot Automat 12:178–182
71. Wang J, Foster N, Armalis S, Larson D, Zirino A, Olsen K (1995) Remote stripping electrode for in-situ monitoring of labile copper in the marine-environment. Anal Chim Acta 310:223–231
72. Wang J, Tian BM, Wang JY (1998) Electrochemical flow sensor for in-situ monitoring of total metal concentrations. Anal Commun 35:241–243
73. Wang J, Wang JY, Lu JM, Tian BM, MacDonald D, Olsen K (1999) Flow probe for in situ electrochemical monitoring of trace chromium. Analyst 124:349–352
74. Wang J, Cepria G, Chen Q (1996) Submersible bioprobe for continuous monitoring of peroxide species. Electroanalysis 8:124–127
75. Wang J, Chen Q, Cepria G (1996) Electrocatalytic modified electrode for remote monitoring of hydrazines. Talanta 43:1387–1391
76. Wang J, Chen QA (1995) Remote electrochemical biosensor for field monitoring of phenolic-compounds. Anal Chim Acta 312:39–44
77. Wang J, Tian BM, Wang JY, Lu JM, Olsen C, Yarnitzky C et al (1999) Stripping analysis into the 21st century: faster, smaller, cheaper, simpler and better. Anal Chim Acta 385:429–435
78. Braungardt CB, Achterberg EP, Axelsson B, Buffle J, Graziottin F, Howell KA et al (2009) Analysis of dissolved metal fractions in coastal waters: an inter-comparison of five voltammetric in situ profiling (VIP) systems. Mar Chem 114:47–55
79. Tercier-Waeber ML, Buffle J, Confalonieri F, Riccardi G, Sina A, Graziottin F et al (1999) Submersible voltammetric probes for in situ real-time trace element measurements in surface water, groundwater and sediment-water interface. Meas Sci Technol 10:1202–1213

80. Chapin TP, Nimick DA, Gammons CH, Wanty RB (2007) Diel cycling of zinc in a stream impacted by acid rock drainage: initial results from a new in situ Zn analyzer. Environ Monit Assess 133:161–167
81. Freitas G, Gleizer G, Lizarralde F, Hsu L, Salvi dos Reis NR (2010) Kinematic reconfigurability control for an environmental mobile robot operating in the Amazon Rain Forest. J Field Robot 27:197–216
82. Noyhouzer T, Mandler D (2011) Determination of low levels of cadmium ions by the under potential deposition on a self-assembled monolayer on gold electrode. Anal Chim Acta 684:1–7
83. Fink L, Mandler D (2010) Thin functionalized films on cylindrical microelectrodes for electrochemical determination of Hg(II). J Electroanal Chem 649:153–158
84. SHOAL (2012) http://www.roboshoal.com/
85. Flow System Network (2013) http://float.berkeley.edu/
86. Geotraces (2013) http://www.geotraces.org/

Index

L.M. Moretto, K. Kalcher (eds.), *Environmental Analysis by Electrochemical Sensors and Biosensors*, DOI 10.1007/978-1-4939-0676-5

N

Q

R

T